Handbook of Elemental Speciation II – Species in the Environment, Food, Medicine and Occupational Health

Handbook of Elemental Speciation II: Species in the Environment, Food, Medicine & Occupational Health
Edited by R. Cornelis, H. Crews, J. Caruso and K. G. Heumann
 ISBN: 0-470-85598-3 (HB)

Handbook of Elemental Speciation II – Species in the Environment, Food, Medicine and Occupational Health

Editor-in-Chief

Rita Cornelis

Ghent University, Belgium

Associate Editors

Joe Caruso

University of Cincinnati, USA

Helen Crews

Central Science Laboratory, UK

Klaus Heumann

Johannes Gutenberg-University Mainz, Germany

John Wiley & Sons, Ltd

John Wiley & Sons Ltd, The Atrium, Southern Gate, Chichester,
West Sussex PO19 8SQ, England

Telephone (+44) 1243 779777

E-mail (for orders and customer service enquiries): cs-books@wiley.co.uk
Visit our Home Page on www.wiley.com

Other Wiley Editorial Offices

John Wiley & Sons Inc., 111 River Street, Hoboken, NJ 07030, USA

Jossey-Bass, 989 Market Street, San Francisco, CA 94103-1741, USA

Wiley-VCH Verlag GmbH, Boschstr. 12, D-69469 Weinheim, Germany

John Wiley & Sons Australia Ltd, 33 Park Road, Milton, Queensland 4064, Australia

John Wiley & Sons (Asia) Pte Ltd, 2 Clementi Loop #02-01, Jin Xing Distripark, Singapore 129809

John Wiley & Sons Canada Ltd, 22 Worcester Road, Etobicoke, Ontario, Canada M9W 1L1

Wiley also publishes its books in a variety of electronic formats. Some content that appears in print may not be available in electronic books.

Library of Congress Cataloging-in-Publication Data:

Handbook of elemental speciation II: species in the environment, food, medicine & occupational health / editor-in-chief Rita Cornelis. . . [*et al.*].
p. cm.
Includes bibliographical references and index.
ISBN-13 978-0-470-85598-0 (cloth : alk. paper)
ISBN-10 0-470-85598-3 (cloth : alk. paper)
1. Speciation (Chemistry) 2. Analytical toxicology. I. Cornelis, Rita.
RA1221.H365 2005
543′.1 – dc22

2004028293

British Library Cataloguing in Publication Data

A catalogue record for this book is available from the British Library

ISBN-13 978-0-470-85598-0 (HB)
ISBN-10 0-470-85598-3 (HB)

Typeset in 10/12pt Times by Laserwords Private Limited, Chennai, India
Printed and bound in Great Britain by Antony Rowe Ltd, Chippenham, Wiltshire
This book is printed on acid-free paper responsibly manufactured from sustainable forestry in which at least two trees are planted for each one used for paper production.

Contents

List of Contributors

J. C. Altamirano
Forensic Chemistry Center, Cincinnati, Ohio, USA

J. F. Artiola
The University of Arizona, Tucson, Arizona, USA

W. Bal
Polish Academy of Sciences, Warsaw, Poland

H.-K. Biesalski
University of Hohenheim, Stuttgart, Germany

J. P. Buchet
Université catholique de Louvain, Brussels, Belgium

W. Buscher
University of Münster, Münster, Germany

J. Byczkowski
JZB Consulting, Fairborn, Ohio, USA

R. Cornelis
Ghent University, Ghent, Belgium

H. M. Crews
Central Science Laboratory, Sand Hutton, UK

J. R. Dainty
Institute of Food Research, Norwich, UK

K. De Cremer
Ghent University, Ghent, Belgium

J. Feldmann
University of Aberdeen, Old Aberdeen, UK

D. Flaßbeck
University of Duisburg-Essen, Essen, Germany

T. E. Fox
Institute of Food Research, Norwich, UK

G. Geipel
Institute of Radiochemistry, Dresden, Germany

D. Gibičar
Jožef Stefan Institute, Ljubljana, Slovenia

K. Günther
Institute for Chemistry and Dynamics of the Geosphere, Juelich, Germany

K. G. Heumann
Johannes Gutenberg-University Mainz, Mainz, Germany

S. J. Hill
University of Plymouth, Plymouth, UK

A. V. Hirner
University of Duisburg-Essen, Essen, Germany

P. Hoet
Université catholique de Louvain, Brussels, Belgium

P. Hoffmann
Darmstadt Technical University, Darmstadt, Germany

M. Horvat
Jožef Stefan Institute, Ljubljana, Slovenia

N. Jakubowski
Institute of Spectrochemistry and Applied Spectroscopy (ISAS), Dortmund, Germany

K. Kasprzak
National Cancer Institute at Frederick, Frederick, Maryland, USA

B. Kastenholz
Institute for Chemistry and Dynamics of the Geosphere, Juelich, Germany

M. Kersten
Johannes Gutenberg-University, Mainz, Germany

D. Klockow
International Association of Environmental Analytical Chemistry, Allschwil, Switzerland

D. A. Kulik
Paul Scherrer Institute, Villigen-PSI, Switzerland

W. D. Lehmann
German Cancer Research Center, Heidelberg, Germany

D. Lison
Université catholique de Louvain, Brussels, Belgium

S. Mann
AnalytikSupport, Niederkassel, Germany

D. Metze
North Rhine Westphalia State Environment Agency, Essen, Germany

N. Mihalopoulos
University of Crete, Heraklion, Greece

R. Milačič
Jožef Stefan Institute, Ljubljana, Slovenia

G. M. Morrison
Chalmers University of Technology, Göteborg, Sweden

D. Nohr
University of Hohenheim, Stuttgart, Germany

O. Nygren
National Institute for Working Life, Umeå, Sweden

N. Proust
THALES Research and Technology France, Orsay, France

T. Prohaska
University of Natural Resources and Applied Life Sciences, Vienna, Austria

S. Rauch
Chalmers University of Technology, Göteborg, Sweden

V. Riihimäki
Finnish Institute of Occupational Health, Helsinki, Finland

E. Rosenberg
Vienna University of Technology, Vienna, Austria

D. Schaumlöffel
Centre National de la Recherche Scientifique, Pau, France

M. Sperling
University of Münster, Münster, Germany

G. Stingeder
University of Natural Resources and Applied Life Sciences, Vienna, Austria

D. M. Templeton
University of Toronto, Toronto, Canada

P. C. Uden
University of Massachusetts, Amherst, Massachusetts, USA

N. Ulrich
University of Hannover, Hannover, Germany

S. Valkonen
Finnish Institute of Occupational Health, Helsinki, Finland

V. Verougstraete
Université catholique de Louvain, Brussels, Belgium

T. Walczyk
Swiss Federal Institute of Technology, Zurich, Switzerland

R. G. Wuilloud
University of Cincinnati, Cincinnati, Ohio, USA

Preface

Speciation has evolved over the past two (or is it three?) decades into an important sub-discipline of analytical chemistry having considerable impact on environmental monitoring and the life sciences. In its embryonic phase, elemental speciation was an academic curiosity, "a rebel without a cause", straddling the boundary between the two large and well-developed areas of inorganic and organic analytical chemistry. Gradually, it became apparent that elemental speciation bridged the gap between both fields as it borrowed and combined the major methodologies and techniques, notably chromatography in its various modes and sensitive spectroscopic detection methods that coalesced into hyphenated techniques. It is now clear that the incremental development of speciation analysis was not born as a trivial academic pursuit but as the solution to major problems in environmental chemical measurement. I mention just a few examples: challenges due to massive worldwide emission of organolead compounds in the atmosphere through the extensive use of tetra-alkyl lead compounds in automobile fuel; several mercury pollution incidents connected with the indiscriminate use and disposal of methylmercury compounds, without recognising its extreme toxicity; severe disruptions of the marine environment with effects on aquaculture, connected with the use of organotin compounds, for example, as anti-fouling agents in the marine environment and agricultural applications.

Currently, elemental speciation is well respected and has established itself as a real bridge, the paranymph between organic and inorganic analytical chemistry, utilising the best of both fields for its development, specific methodology and fundamental paradigms.

Despite many potential application areas, speciation analysis, at least until recently, seemed rather slow in finding practical exploitation. This is not surprising. There is a definite induction period needed for any new development before it finds its place in technology and society. We cannot force the pace. Despite scientific achievements, ultimately the applications need to be triggered by societal needs, pushed from practice rather than pulled from science.

A handbook such as this one is a welcome compendium of information that would otherwise be scattered throughout the scientific literature. It can serve as a reference book for those interested in the subject in academe, government and industry and those involved with important questions related to the differences in behaviour between atoms and molecules.

The first volume of the Handbook of Elemental Speciation with the subtitle "Techniques and Methodology" appeared in mid-2003. It deals with the experimental basis and contains chapters on the collection and storage of samples and their problems, on the various methods used in sample preparation and sample preseparation for analysis, the full range of different separation and detection techniques that together provide the necessary sensitivity and selectivity for trace and ultra-trace analysis with a number of hyphenated techniques from solution, the important topic of calibration and quality assurance/quality control. The work also provides a detailed description of the actual status of direct speciation methods in solid samples on the basis of, on one side, different beam methods of analysis based on electrons and X-rays and, on the other side, with solid or solution applications using new possibilities offered by synchrotron X-ray methods through the exploitation of the fine structure of the X-ray absorption edge. The first volume is concluded with an overview of rapid screening methods and risk assessment/regulatory issues concerned with

speciation. It provides the necessary background material and a thorough description of the practice of elemental speciation.

If the first volume deals with the analytical chemistry of *elemental speciation*, according to the IUPAC definition, and, as such, is a basic scientific discipline, this accompanying second volume deals largely with *speciation* and *chemical species* as defined by the IUPAC. The material belongs to applied science and, as far as its routine application of scientific concepts is concerned, can even be considered as technology.

What follows in this volume of the Handbook of Elemental Speciation, as a welcome and practical complement to Volume I, is a thorough survey of chemical speciation of the different elements, treated systematically, more or less from alpha to omega, within sequence: the compounds of aluminium, antimony, arsenic, cadmium, chromium, cobalt, copper, iron, lead, manganese, mercury, molybdenum, nickel, platinum (and the other noble metals), selenium, silicon, sulphur, thallium, tin vanadium and finally, zinc. This systematic survey of the different relevant elements for speciation is followed by a review of groups of elemental species, the actinide elements, halogens as present in the atmosphere, the volatile metals and, finally, a chapter on proteins and one on the metals' behaviour in humic/fulvic acids and their implications for elemental bio-availability in the soil/water environment. For all these topics, the analytical chemistry aspects are completed with data on the physical and chemical properties, environmental, toxicological, health and legislative aspects of the species of interest, in short everything important for the issues in hand. The text concludes with chapters on various modelling aspects connected with speciation issues.

It is obvious that for a complex topic such as this one, the preferable way to deal with the rather disparate contents is through assembling the experience of a number of different expert authors, as no single person would master in sufficient detail all the topics to be developed. As in the previously published volume, the editors selected experts carefully, to provide overall a high-quality work.

Is this volume going to be the end of the series and the collaboration among the four editors? I sincerely hope not! The present and previous volume, as comprehensive as they are, still leave numerous gaps in the field. The two volumes are heavily centred on the environmental and health sciences, evidently the most important areas of application up to now. However, it is clear that as the subdiscipline develops, a myriad of new analytical challenges will arise in other areas. We can only hope that the present two volumes will become the start of further complements in a continuing series of handbooks. Speciation analysis in materials science and especially in the microscopic and nano-size spatial domains, the pursuit of speciation analysis and its exploitation in speciation in solid samples, the growing applications and the challenges of elemental speciation of metal-containing proteins in the bio-sciences (metalloproteomics) and the global issues connected with elemental speciation in bio-geochemistry will be further areas of expansion for this important methodology.

Freddy Adams

Antwerp, Belgium, October 2004

Acknowledgments

The editors express their sincere appreciation and gratitude to all the contributors for writing outstanding chapters. The idea for this Handbook came from Katya Vines, who was then Managing Editor at Wiley. Jenny Cossham became Managing Editor at the start of the actual writing. The editors thank her for her support and friendly cooperation throughout the project.

Rita Cornelis
Helen Crews
Joe Caruso
Klaus Heumann

Technical Abbreviations and Acronyms

Abbreviations

AAS	atomic absorption spectrometry
ACD	allergic contact dermatitis
ACGIH	American Conference of Governmental Industrial Hygienists
ACSL	Advanced Continuous Simulation Language
ACSV	adsorptive cathodic stripping voltammetry
ACW	artificial cement water
ADI	acceptable daily intake
ADME	absorption distribution metabolism and excretion
ADP	adenosine diphosphate
AE	acrodermatitis enteropathica
AED	atomic emission detection
AEM	analytical electron microscopy
AFS	atomic fluorescence spectrometry
ALA	aminolevulinic acid
ALA-D	delta aminolevulinic acid dehydratase activity
ALA-U	delta aminolevulinic acid (urine)
ALS	amyothrophic lateral sclerosis
AMP	adenosine monophosphate
AMS	accelerator mass spectrometry
AOAC	Association of Official Agricultural Chemists
AOS	activated oxygen species
APCI	atmospheric pressure chemical ionisation
APDC	ammonium pyrrolidine dithiocarbamate
API-MS	atmospheric pressure ionization-mass spectrometry
APP	amyloid precursor protein
APXS	alpha proton X-ray spectrometry
AROI	acceptable range of oral intake
ASV	anode stripping voltammetry
ATCUN	amino terminal Cu(II) and Ni(II)-binding
ATN	acute tubular necrosis
ATP	adenosine triphosphate
ATR	attenuated total reflectance
ATR-FTIR	attenuated total reflection Fourier transform infrared
ATSDR	Agency for Toxic Substances and Disease Registry
AUC	area under the curve
AWQC	ambient water quality criteria
BBM	brush border membrane
BCM-ESR	blood circulation monitoring-electron spin resonance
BCR	Community Bureau of Reference (Commission of the European Communities)
BDE	bromodiphenyl ether
BLM	biotic ligand model
BMD	bench mark dose
BRHS	British Regional Heart Study
BSE	back scattered electrons
BW	body weight
CA	cellulose acetate
CAC	Codex Alimentarius Commission
CAPD	continuous ambulatory peritoneal dialysis
CCA	chromium(VI) trioxide – copper oxide – arsenic trioxide
CCD	charge coupled device
CCFAC	Codex Committee for Food Additives and Contaminants
CCP	capacitively coupled plasma
CCS	copper chaperone for superoxide dismutase

CE	capillary electrophoresis
CFC	chlorinated and fluorinated carbon
CGC	capillary gas chromatography
CHD	coronary heart disease
CI	chemical ionisation
CIEF	capillary isoelectric focusing
CIMS	chemical ionization mass spectrometry
CJD	Creutzfeldt-Jacob disease
CMT	cylcopentadienyl manganese tricarbonyl
CNS	central nervous system
CONSAAM	Conversational Simulation Analysis and Modeling
COX	cytochrome oxidase
CP	caeruloplasmin
CPVC	chlorinated PVC
CRM	certified reference material
CSF	cerebrospinal fluid
CSV	cathodic stripping voltammetry
CV	cold vapor
Cys	cysteine
CZE	capillary zone electrophoresis
DAD	diode array detector
D-DDC	diethylammonium diethyl dithiocarbamate
DAO	diamine oxidase
DBT	dibutyltin
DCI	desorption chemical ionisation
DCP	direct-current plasma
DDT	dichlorodiphenyltrichloroethane
DEAE	diethylaminoethyl
DEGS-PS	diethylene glycol succinate
DFG	German Research Community
DFO	desferroxiamine
DGE	The German Society for Nutrition
DI	deiodinases
DIHEN	direct injection high efficiency nebulizer
DIN	direct injection nebulizer
DIT	diiodothyrosine
DL-AAS	diode laser atomic absorption spectrometry
DMA	dimethylarsinic acid
DMDSe	dimethyl diselenide
DMPS	2,3-dimercapto-1-propane sulfonate
DMS	dimethyl sulfide
DMSA	dimercaptosuccinic acid
DMSD	dimethyl silanediol
DMSe	dimethyl selenide
DMSeP	dimethylselenonium propionate
DMSO	dimethyl sulfoxide
DMSP	dimethylsulfoniopropionate
DMT	divalent metal transporter
DNA	deoxyribonucleic acid
DOC	dissolved organic carbon
DOM	dissolved organic matter
DPASV	differential pulse anodic stripping voltammetry
DPC	diphenyl carbazide
DPCSV	differential pulse cathodic stripping voltammetry
DRC	dynamic reaction cell
DTPA	diethylenetriamine-pentaacetic acid
DTPA-TEA	diethylenetriamine-pentaacetic acid-triethanolamine
DTT	dithiothreitol
DV	Daily Value
ECD	electron capture detector
EDS	energy dispersive spectrometry
EDTA	ethylenedinitrilotetraacetic acid or ethylenediaminetetraacetic acid
EDXA	energy-dispersive X-ray analysis
EELS	electron energy loss spectroscopy
EFSA	European Food Safety Authority
EHMA	ethylhexylmercaptoacetate
EIA	enzyme immunoassay
EI-MS	electron impact mass spectrometry
ELISA	enzyme linked immunosorbent assay
ELNES	energy loss near-edge structure
ELSD	evaporative light-scattering detection
EMPA	electron micro probe analysis
ENDOR	electron nuclear double resonance

EP	erythrocyte porphyrin
EPA	Environmental Protection Agency
EPR	electron paramagnetic resonance
EPXRS	electron-probe X-ray spectrometry
EQA	external quality assurance
ES	electrospray
ESADDI	estimated safe and adequate daily dietary intakes
ESCA	electron spectroscopy for chemical analysis
ESEEM	electron spin echo envelope modulation
ESI MS-MS	electrospray ionisation tandem mass spectrometry
ESI	electrospray ionisation
ESI-MS	electrospray ionization mass spectrometry
ESR	electron spin resonance
ET-AAS	electrothermal atomic absorption spectrometry
EtSH	ethyl mercaptan
EXAFS	extended X-ray absorption fine structure spectroscopy
EZP	exchangeable zinc pool
FA	fulvic acid
FAAS	flame atomic absorption spectrometry
FCAW	flux-cored arc welding
FDA	Food and Drug Administration
FEP	fluoroethylene polymer
FIA	flow-injection analysis
FIA	fluorescence immunoassay
FPD	flame photometric detector
FPLC	fast protein liquid chromatography
FR	flame retardants
FT-IR	Fourier-transform infrared radiation
FVC	forced vital capacity
GABA	gamma-aminobutyric acid
GC	gas chromatography
GC-AAS	gas chromatography-atomic absorption spectrometry
GC-AED	gas chromatography-atomic emission detection
GC-ECD	gas chromatography – electron capture detection
GC-MS	gas chromatography mass spectrometry
GEM	Gibbs energy minimisation
GF	graphite furnace
GFAAS	graphite furnace atomic absorption spectrometry
gHb	glycated hemoglobin
GI	gastrointestinal
GIME	gel-integrated microelectrode array
GLC	gas–liquid chromatography
GMAW	gas metal arc welding
GMP	guanosine monophosphate
GPC	gel permeation chromatography
GPEC	gradient polymer elution chromatography
GPX	glutathione peroxidase
GSGD	gas sampling glow discharge
GSH	glutathione (reduced form)
GT	gammaglutamyl-transpeptidase
GTAW	gas tungsten arc welding
GTF	glucose tolerance factor
HA	humic acids
HbA	hemoglobin A
HbF	fetal hemoglobin
HDEHP	bis(2-ethyl-hexyl)-hydrogen-phosphate
HDL	high density lipoprotein
HEDP	1-hydroxyethane-1,1-diphosphonic acid
HEPA	high efficiency particulate air
HFBA	heptafluorobutanoic acid
HFO	hydrous ferric oxide
HG	hydride generation
HG-AAS	hydride generation-atomic absorption spectrometry
HG-AFS	hydride generation – atomic fluorescence spectrometry
HG-GC	hydride generation gas chromatography

HG-ICP AES	hydride generation – inductively coupled plasma – atomic emission spectrometry
HHPN	hydraulic high pressure nebulizer
HKF	Helgeson-Kirkham-Flowers
HLA	human lymphocyte antigens
HMM	high molecular mass
HPLC	high performance liquid chromatography
HPLC-ICP	high performance liquid chromatography-inductively coupled plasma
HRIDMS	high resolution isotope dilution mass spectrometry
HRSEM	high resolution scanning electron microscopy
HS	humic substances
IAP	ion activity product
IARC	International Agency for Research on Cancer
IBMK	isobutyl methyl ketone
IC	ion chromatography
ICNCM	International Committee on Nickel Carcinogesis in Man
ICP	inductively coupled plasma
ICP-AES	inductively coupled plasma-atomic emission spectrometry
ICP-MS	inductively coupled plasma-mass spectrometry
ICP-OES	inductively coupled plasma optical emission spectroscopy
ICT	idiopathic copper toxicosis
IDLH	immediately dangerous to life or health
IDMS	isotope dilution mass spectrometry
IEF	isoelectric focusing
IEUBK	integrated exposure uptake biokinetic
IFCC	International Federation of Clinical Chemistry
IgE	immunoglobulin E
IMO	International Maritime Organisations
INAA	instrumental neutron activation analysis
IOMA	isooctyl mercaptoacetate
IPM	interior points method
IQC	internal quality control
IRMA	immunoradiometric assay
IUPAC	International Union of Pure and Applied Chemistry
JECFA	Joint Expert Committee on Food Additives
K_{sp}	solubility constant
K-XRF	K-shell X-ray fluorescence
LA	laser ablation
LA-ICP-MS	laser ablation inductively coupled plasma mass spectrometry
LC	liquid chromatography
LC-MS	liquid chromatography-mass spectrometry
LDH	lactate dehydrogenase
LDL	low density lipoprotein
LDR	linear dynamic range
LFER	linear free-energy relationships
LI TOF	laser-induced time of flight
LIA	luminescence immunoassay
LIBD	laser-induced breakdown detection
LIBS	laser-induced breakdown spectroscopy
LIPAS	laser-induced photo acoustic spectroscopy
LMA	law of mass action
LMM	low molecular mass
LOAEL	lowest-observed-adverse-effect level
LOD	limit of detection
LPAS	laser-induced photoacoustic spectroscopy
LP/RP-ICP-MS	low pressure/reduced pressure-ICP-MS
LT	low temperature
LT-GC	low temperature – gas chromatography
L-XRF	L-shell X-ray fluorescence
MAC	maximum allowable concentration

MALDI	matrix assisted laser desorption ionization
MALDI-MS	matrix assisted laser desorption ionization mass spectrometry
MBT	monobutyltin
MCH	mean corpuscular hemoglobin
MCHC	mean corpuscular hemoglobin concentration
MCLG	maximum contamination level goal
MEKC	micellar electrokinetic chromatography
MEPC	Marine Environment Protection Committee
MeSH	methyl mercaptan
Met	methionine
MIBK	methyl isobutyl ketone
MIC	minimal inhibitory concentrations
MIG	metal inert gas
MIP	microwave-induced plasma
MIP-AED	microwave-induced plasma-atomic emission detector
MIP-AES	microwave-induced plasma atomic emission spectrometry
MIT	monoiodothyrosine
ML	one ligand complexes
ML_2	two-ligand complexes
μLC	liquid chromatography of micro-scale
MLs	maximum limits
MMA	manual metal arc
MMA	monomethylarsonic acid
MMM	medium molecular mass
MMT	methylcyclopentadienyl manganese tricarbonyl
MNK	Menkes protein (P-type ATPase)
MnSOD	manganese superoxide dismutase
MRL	maximum residue limit
MS	mass spectrometry
MSA	methanesulfonic acid
MSIA	methanesulfinic acid
MT	metallothionein
NAA	neutron activation analysis
NAC	*N*-acetyl cysteine
NaDDTC	sodium diethyldithiocarbamate
NAG	*N*-acetyl-β-D-glucosaminidase
NASA	National Aeronautic and Space Administration
NCOMP	noncompartmental programs
NCV	nerve conduction velocity
NEM	non-electrostatic model
NEQAS	national external quality assurance system
NHANES	national health and nutrition examination surveys
NIES	National Institute of Environmental Studies
NIOSH	National Institute for Occupational Safety and Health
NIR	near infra-red
NIST	National Institute of Standards and Technology
NMR	nuclear magnetic resonance
NN	1-nitroso-2-naphthol
NOEL	no-observed-effect level
NOM	natural organic matter
NPDES	national pollution discharge regulations
NTA	nitrilotriacetic acid
NTBI	nontransferrin-bound Fe
OEL	occupational exposure limit
OMCTS	octamethylcyclotetrasiloxane
ORNL	Oak Ridge National Laboratory
OSHA	Occupational Safety and Health Administration
OTC	organotin compounds
PAA	proton activation analysis
PAD	pulse amperometric detection
PAGE	polyacrylamide gel electrophoresis
PAR	4-(2-pyridylazo)resorcin
PBDE	polybrominated diphenyl ethers
PBPK	physiologically based pharmacokinetic
PC	polycarbonate
PCA	principal component analysis
PCB	polychlorinated biphenyl
PDMS	polydimethylsiloxanes

PEC	predicted environmental concentration
PEL	permissible exposure limit
PES	polyethersulfon
P-FPD	pulsed flame photometric detector
PGC	packed-column gas chromatography
PGE	platinum group element(s)
PIXE	proton induced X-ray emission
PKC	protein kinase C
PNC-PAGE	preparative native continuous polyacrylamide gel electrophoresis
PNEC	predicted no effect concentration
PNS	peripheral nervous systems
PP	polypropylene
PrP	prion protein
PSA	potentiometric stripping analysis
pTDI	predicted tolerable daily intake
PTFE	polytetrafluoroethylene
PTI-IDMS	Positive thermal ionisation isotope dilution mass spectrometry
PTWI	provisional tolerable weekly intake
PVC	polyvinylchloride
PVDF	poly(vinylidene fluoride)
QMS	quadrupole mass spectrometry
RA	relative area
RBC	red blood cell
RBP	retinol-binding protein
RC	regenerated cellulose
RDF	radial distribution function
RDI	recommended daily intakes
REACH	registration evaluation and authorization of chemicals
RfC	reference concentration
RI	refractive index
RIA	radioimmunological assays
RoHS	restriction of the use of certain hazardous substances
ROS	reactive oxygen species
SAAM	simulation analysis and modeling
SAE-SPE	strong anion exchange solid phase extraction
SAT	salinities and temperatures
SAW	submerged arc welding
SAX	strong anion exchange
SBI	silicone breast implant
SBSE	stir bar sorptive extraction
SCF	Scientific Committee for Food
SCOEL	Scientific Committee on Occupational Exposure Limits
SDDC	sodium dimethyl dithiocarbamate
SDS	sodium dodecyl sulfate
SDS-PAGE	sodium dodecyl sulfate polyacrylamide gel electrophoresis
SE	secondary electrons
SEC	size exclusion chromatography
SEM	scanning electron microscopy
SeP	selenoprotein-P
SFC	supercritical fluid chromatography
SFE	supercritical fluid extraction
SFMS	sector field mass spectrometer
SIDMS	speciated isotope dilution mass spectrometry
SIDS	sudden infant death syndrome
SIMS	secondary ion mass spectrometry
SIT	specific ion interaction theory
SMAW	shielded metal arc welding
SOD	superoxide dismutase
SOP	standard operation procedure
SPARC	secreted protein acidic rich in cysteine
SPE	solid phase extraction
SPME	solid-phase microextraction
SSAS	solid solution-aqueous solution
SVD	singular value decomposition
TARL	tolerable average residue level
TBG	thyroid hormone binding globulin
TBP	tributylphosphate
TBT	tributyltin
TBTO	bis tri-n-butyloxide
TCyT	tricyclohexyltin

TDI	tolerable daily intake
TEL	tetraethyl lead
TEM	transmission electron microscopy
TEP	total exchangeable pool
TFA	trifluoroacetic acid
TGN	trans-golgi network
THF	tetrahydrofurane
TIBC	total iron binding capacity
TIG	tungsten inert gas
TIMS	thermal ionisation mass spectrometry
TLC	thin layer chromatography
TLV	threshold limit value
TLV-TWA	threshold limit value-time-weighted average
TML	tetramethyl lead
TMSOL	trimethyl silanol
TOC	total organic carbon
TOF-MS	time of flight-mass spectrometry
TOF-SIMS	time-of-flight secondary ion mass spectrometry
TPhT	triphenyltin
TPTZ	tripyridyl-triazine
TR	thioredoxin reductase
TRLFS	time-resolved laser-induced fluorescence spectroscopy
TRW	Technical Review Workgroup
TTA	α-thenoyltrifluoroacetone
TWA	time weighted average
TXRF	total reflection X-ray fluorescence
UHT	ultra high temperature
UIBC	unsaturated iron-binding capacity
UNEP	United Nations Environmental Programme
USEPA	US Environmental Protection Agency
UV-VIS	ultraviolet-visible
VC	vital capacity
VLDL	very low density lipoprotein
VLMM	very low molecular mass
VMC	volatile metal compounds
VMS	volatile methylsiloxanes
VOC	volatile organic compounds
VSC	volatile sulfur compound
WEEE	waste from electrical and electronic equipment
WFD	water framework directive
WHO	World Health Organization
WIPP	waste isolation pilot plant
WND	Wilson disease protein
WQC	water quality criteria
WWTP	wastewater treatment plant
XAFS	X-ray absorption fine structure spectroscopy
XANES	X-ray absorption near edge structure
XAS	X-ray absorption spectroscopy
XPS	X-ray photoelectron spectroscopy
XRD	X-Ray Diffraction
XRF	X-ray fluorescence
XRFS	X-Ray fluorescence spectroscopy
ZnPP	zinc protoporphyrin

CHAPTER 1
Introduction

Wolfgang Buscher
Institut für Anorganische und Analytische Chemie, University of Münster, Münster, Germany

Michael Sperling
Institut für Anorganische und Analytische Chemie, University of Münster, Münster, Germany

Elemental Speciation has become a challenging part of analytical chemistry. The short-, medium-, and long-term perspectives are far-reaching, and it may be interesting to dwell upon the ways the scientific community will continue its progress. It is to be expected that a renewed legal framework will come into effect, in which essentiality and toxicity of the elemental species, instead of total trace element concentration, becomes the key issue.

During the past 20 to 30 years, elemental speciation has grown into a full-fledged analytical discipline. The technological and methodological achievements in recent years have considerably increased the possibilities of analytical chemistry. Today, it is possible to determine numerous element species accurately at concentration levels that were inconceivable some 10 years ago.

The first volume of this Handbook gave a comprehensive overview of the analytical possibilities and the general technical and methodological aspects of speciation analysis [1].

The present – second – volume will cover the species by element or group of compounds (actinides, halogens, volatile metals, proteins, and humic acids) describing the state of the art for the sections environment, food, clinical, and occupational health and hygiene. Special chapters on the possibilities of modeling will introduce the reader to the modern way of predicting chemical situations through theoretical calculations, made possible by the availability of modern high-performance computers.

Newcomers in the field will appreciate the total overview that this Handbook provides. Experienced analysts will value the comprehensive detailing of the most current developments in the different sectors of elemental speciation.

The current situation in Speciation Analysis is complex. On the one hand, there is a group of elemental species that has been thoroughly investigated and described (e.g. methylmercury, organotin compounds, and organoarsenicals). On the other hand, there are those compounds for which only preliminary scientific knowledge has

Handbook of Elemental Speciation II: Species in the Environment, Food, Medicine & Occupational Health
Edited by R. Cornelis, H. Crews, J. Caruso and K. G. Heumann
 ISBN: 0-470-85598-3 (HB)

been gained (e.g. elements bound to proteins, to humic acids, etc.).

For the first group, the technological progress in instrumental analysis has reached a level of performance that enables analysts to determine elemental species accurately at picogram levels and below. In principle, these procedures already allow comprehensive survey measurements. Unfortunately, the number of laboratories with the necessary skills and analytical instrumentation is still much too limited for routine control activities.

Although in research laboratories there exist reliable analytical instrumentation and validated standard operation procedures (SOPs), almost every analytical approach turns out to be only applicable to a few elemental species, in a narrow range of matrices. While it would not be too difficult for instrument manufacturers to transfer such know-how into routinely usable analytical instruments, such instrumentation would lack in general applicability and would therefore only appeal to a limited market segment. As long as laws, regulations, and directives do not force industrial and governmental controlling bodies to systematically analyze elemental species, the size of the market will remain too small to guarantee a reasonable return on investment for routine-instrument development.

The support for scientific research through universities and research institutions must increasingly be justified on the basis of the relevance decided by external funding bodies. Many traditional fields of application such as environmental sciences do not offer a promising outlook in this respect. As a consequence, analytical research groups face a substantial reduction of support because of the reallocation of funds to more "fashionable" sciences such as molecular biology or nanotechnology. To adjust to this situation, analytical scientists need to use their creativity in finding ways to participate by creating their niche in, for example, nanotechnology, cancer research, or proteomics. This requires an open mind in terms of new opportunities, evaluating strengths and weaknesses of existing techniques and methodologies and a departure from technique-oriented toward problem-oriented research. Analytical chemistry provides basic information about the status of humans and their environment and about the characteristics of materials, its cycling, and interactions. There is little doubt that the role of speciation analysis is crucial in answering questions about the bioavailability, biological activity, toxicity, or nutritional value and metabolism of trace elements. The important role of speciation analysis is evident from the more than 500 publications every year on the subject and from the gradual introduction of chemical species, rather than total amounts, in rules and regulations. These developments were possible only because different scientific disciplines have crossed their respective borderlines.

Analytical chemistry

More and more sensitive analytical techniques have reached a detection power limited only by mere contamination problems. At the same time, the risk of contamination has been drastically reduced by on-line coupling of separation and detection into a closed system. There remain, however, limitations imposed by the presence of contaminants in the reagents and the release of impurities by the packing material and many utensils through contact with the sample. Nevertheless, the quality of the information obtained through these techniques has been enhanced drastically by the increased sensitivity gained through hyphenation [2]. Modern mass spectrometric techniques allow to collect information on the atomic as well as the molecular species [3, 4]. Fast separation techniques such as Flow Injection [5], Fast Protein Liquid Chromatography (FPLC) [6], Capillary Electrophoresis [7], and Multicapillary Gas Chromatography [8] reduce the analysis time and therefore the possibilities for species transformation during analysis. Sample preparation has also been made instrumental, benefiting from automation and feedback control (e.g. microwave extraction with temperature and pressure control [9]). Solvent-less extraction [10] and other soft enzymatic extraction methods try to keep fragile species intact. Some X-ray spectroscopic and microbeam techniques are available for direct elemental speciation analysis in the solid state, thus bypassing sample

preparation [11]. Additionally, increasing Quality Management has caused the comparability and traceability of analytical measurements to get possible even for trace and ultra-trace analyses. Manufacturers of certified reference materials (CRMs) have started to market CRMs for speciation analysis [12, 13]. Research groups have established the state of the art in speciation analysis and discussed shortcomings and artifacts during intercomparison studies and workshops. Species-specific isotope dilution analysis has been proven to be a very versatile tool for studying species transformation even during the analysis and enables accurate determination even under dynamic conditions [14, 15].

Toxicology

The toxicologists have developed increasingly reliable investigation and calculation models to determine the toxicity of chemical species. These data form the basis for comprehensive characterization and description of chemical species to be used in legislation.

Chemometrics

Analytical chemistry, toxicology, and other disciplines can be improved significantly by using chemometrical methods. The continuing development in data processing techniques allows the use of highly complex algorithms suited to improve the quality and quantity of information extractable from huge sets of data. Accordingly, this discipline offers valuable support tools.

Medicine, biology, and food science

The assessment of the effect of elemental species in medicine, biology, and food science depends heavily on the quality of the analytical and toxicological input. The most recent developments in this connection are coming from the field of proteomics and metallomics, dealing with the determination of trace metals in biomolecules. These new scientific fields will hopefully provide a more fundamental understanding of the essential role of trace metals in life processes and enhance our knowledge of their physiological effect on different organisms. Although this research field has only recently emerged, the very first results are already exciting.

It is obvious from this list of disciplines and their interactions that only interdisciplinary, targeted approaches will be able to generate the momentum for further development in elemental speciation analysis. This supposes well-coordinated research aimed at answering complex and important questions. It will be interesting to see whether initiatives such as the European Virtual Institute for Speciation Analysis (http://www.speciation.net) can provide an efficient platform for such activities [16].

1 REFERENCES

1. Cornelis, R., Crews, H., Caruso, J. and Heumann, K. (Eds.), *Handbook of Elemental Speciation: Techniques and Methodology*, John Wiley & Sons, Chichester, 2003.
2. Szpunar, J. and Łobiński, R., Hyphenated techniques in speciation analysis, in *RSC Chromatography Monographs*, Smith, R. M. (Ed.), Royal Society of Chemistry, Cambridge, MA, 2003.
3. Vanhaecke, F. and Köllensperger, G., Detection by ICP-MS spectrometry, in *Handbook of Elemental Speciation: Techniques and Methodology*, Cornelis, R., Crews, H., Caruso, J. and Heumann, K. (Eds.), John Wiley & Sons, Chichester, 2003, Chapter 5.3, pp. 281–312.
4. Wind, M. and Lehmann, W. D., *J. Anal. At. Spectrom.*, **19**, 20 (2004).
5. Tyson, J. F., Flow injection atomic spectrometry for speciation, in *Handbook of Elemental Speciation: Techniques and Methodology*, Cornelis, R., Crews, H., Caruso, J. and Heumann, K. (Eds.), John Wiley & Sons, Chichester, 2003, Chapter 5.2, pp. 261–280.
6. Ferrarello, C. N., Fernández de la Campa, M. R. and Sanz-Medel, A., *Anal. Bioanal. Chem.*, **373**, 412 (2002).
7. Michalke, B., Capillary electrophoresis in speciation analysis, in *Handbook of Elemental Speciation: Techniques and Methodology*, Cornelis, R., Crews, H., Caruso, J. and Heumann, K. (Eds.), John Wiley & Sons, Chichester, 2003, Chapter 4.3, pp. 201–223.
8. Feldhaus, R., Buscher, W., Kleine-Benne, E. and Quevauviller, Ph., *Trends Anal. Chem.*, **21**, 356 (2002).
9. Bouyssiere, B., Szpunar, J., Potin-Gautier, M. and Lobinski, R., Sample preparation techniques for elemental speciation studies, in *Handbook of Elemental Speciation: Techniques and Methodology*, Cornelis, R., Crews, H., Caruso, J. and Heumann, K. (Eds.), John Wiley & Sons, Chichester, 2003, Chapter 3.2, pp. 95–118.
10. Szpunar, J. and Łobiński, R., Sample preparation techniques for elemental speciation studies, in *Elemental Speciation: New Approaches for Trace element Analysis*, Vol. XXXIII, *Comprehensive Analytical Chemistry*, Caruso,

J. A., Sutton, K. L. and Ackley K. L. (Eds.), Elsevier, Chapter 2, pp. 7–40 (2000).

11. Ortner, H. M., Characterization of individual aerosol particles with special reference to speciation techniques, in *Handbook of Elemental Speciation: Techniques and Methodology*, Cornelis, R., Crews, H., Caruso, J. and Heumann, K. (Eds.), John Wiley & Sons, Chichester, 2003, Chapter 6.1, pp. 505–525.
12. Quevauviller, Ph., Reference materials, in *Handbook of Elemental Speciation: Techniques and Methodology*, Cornelis, R., Crews, H., Caruso, J. and Heumann, K., John Wiley & Sons, Chichester, 2003, Chapter 7.2, pp. 563–590.
13. Cornelis, R., Crews, H., Donard, O. F. X., Ebdon, L. and Quevauviller, Ph., *Fresenius' J. Anal. Chem.*, **370**, 120 (2001).
14. Heumann, K. G., Calibration in elemental speciation analysis, in *Handbook of Elemental Speciation: Techniques and Methodology*, Cornelis, R., Crews, H., Caruso, J. and Heumann, K. (Eds.), John Wiley & Sons, Chichester, 2003, Chapter 7.1, pp. 547–562.
15. Huo, D. W., Kingston, H. M. and Larget, B., Application of isotope dilution in elemental speciation: speciated isotope dilution mass spectrometry (SIDMS), in *Elemental Speciation: New Approaches for Trace element Analysis*, Vol. XXXIII, *Comprehensive Analytical Chemistry*, Caruso, J. A., Sutton, K. L. and Ackley, K. L. (Eds.), Elsevier, 2000, Chapter 10, pp. 277–314.
16. Cornelis, R., Buscher, W., Sperling, M., Donard, O. X. F., Proust, N., Rosenberg, E. and Milačič, R., *Accred. Qual. Assur.*, **9**, 268 (2004).

CHAPTER 2

Element by Element Review

2.1 Introduction

Rita Cornelis

Laboratory for Analytical Chemistry, Ghent University, Ghent, Belgium

Volume 2 of the Handbook of Elemental Speciation endeavors to compile the state of the art in elemental speciation for a large number of chemical elements. The reader will clearly see why it is important to measure chemical species rather than total element concentrations, especially in relation to environment and living organisms, in health or disease.

Roughly 90 elements are present on earth in an as yet unknown number of chemical species.

Our interest went to those species that occur in low concentrations in environmental matrices and in living systems. Left out are the abundant elements, carbon, hydrogen, oxygen, nitrogen and phosphor, and calcium, lithium, sodium, potassium, magnesium, chlorine and fluorine and those elements for which the elemental species have not yet been substantially investigated and little or no speciation knowledge is available. It is expected that our knowledge in chemical species will expand greatly during the coming decades, in line with the increasing analytical competence. The analytical methodology is the subject of Volume 1 of this Handbook [1]. This second volume covers in detail the various species of 21 elements, of the actinides, and of four groups of compounds (halogens, volatile metal compounds of biogenic origin, metal complexes of humic substances and metal complexes of proteins). Chapters on modeling of trace element species in the environment, food, health and disease illustrate the power of modern chemometric techniques in describing the behavior of elemental species in complicated systems.

The chapters intend to provide basic knowledge about the chemical species of each element or group of compounds. The general structure of each chapter aims at following a logical progression, starting with the elemental species as they occur naturally in the environment, in many cases upset by dumping practices and further worsened by input of synthetic species and their derivatives of purely anthropogenic origin. (The organotin compounds are undoubtedly one of the worst examples.) The next step deals with the chemical form under which they end up in the life cycle, including the food chain. The study is complete

Handbook of Elemental Speciation II: Species in the Environment, Food, Medicine & Occupational Health
Edited by R. Cornelis, H. Crews, J. Caruso and K. G. Heumann
 ISBN: 0-470-85598-3 (HB)

when it is known which elemental species are being inhaled or ingested by man, how they are incorporated, excreted and, last but not least, how they have either been beneficial to the health of the subjects or, on the contrary, posed a health risk.

The rudimentary depth of fundamental knowledge in this relatively young discipline made it impossible to impose a strict organization of the chapters. Each contribution has been written by specialists in the field, who have aimed at being as informative as possible. The individual style of each author plays, however, a decisive role in the way the existing knowledge is presented. It is inevitable that every author be conditioned by his or her personal focus and academic background in either analytical chemistry, medical sciences, occupational medicine or environmental sciences.

We hope that the knowledge contained in the two volumes of this Handbook will provide a stimulus for further research in this young and exciting scientific domain.

1 REFERENCES

1. Cornelis, R., Crews, H., Caruso, J. and Heumann, K., *Handbook of Elemental Speciation. Techniques and Methodology*, John Wiley & Sons, Chichester, (2003).

2.2 Speciation of Aluminum

2.2.1 Speciation of Aluminum in the Environment

Radmila Milačič

Jožef Stefan Institute, Ljubljana, Slovenia

1 INTRODUCTION

Aluminum (Al) is the most abundant metal in the lithosphere. It is bound predominantly in sparingly soluble oxides (bauxite) and complex alumosilicates, comprising 8% of the Earth's crust. Its chemistry depends strongly on pH. In contrast, because Al is very insoluble in the neutral pH range, its abundance in the oceans is much less, the Al concentration being below 1 $\mu g\,dm^{-3}$. Nevertheless, its solubility is significantly increased under acidic ($pH < 6.0$) or alkaline ($pH > 8.0$) conditions and/or in the presence of inorganic and organic complexing ligands. Acid rain may substantially mobilize and release Al into soil solution, and into underground and surface waters. This effect is observed especially in poorly buffered soils [1, 2]. Al solubility in soil also increases as a response to elevated nitrification that causes an increase in acidity and consequently mobilizes Al into soil solution [3]. The released mononuclear ionic Al species may undergo polymerization or may be complexed by available inorganic or organic ligands [4]. Al^{3+} is a very reactive species. It reacts 10^7 times faster than Cr^{3+}. In the environment and in biological systems, Al exists only in Al^{3+} oxidation state. Al is too reactive to be found free in nature. It is widely used in the industry, representing an additional burden to the environment. $Al_2(SO_4)_3$ is added to drinking water as a coagulant to clarify turbid drinking waters. Alums, double sulfate salts of Al^{3+} and Na^+, K^+ or $NH_4{}^+$ such as $KAl(SO_4)_2{\cdot}12H_2O$ are used in the paper industry for tanning (to replace Cr^{3+} salts) and dyeing. Alums are also added to foods, and $Al(OH)_3$ can be found in pharmaceutical products, such as antacids [5]. With the increased release of

Handbook of Elemental Speciation II: Species in the Environment, Food, Medicine & Occupational Health
Edited by R. Cornelis, H. Crews, J. Caruso and K. G. Heumann
 ISBN: 0-470-85598-3 (HB)

Al to the environment, its toxic effects on humans, animals and plants have been observed.

2 THE AQUEOUS CHEMISTRY OF ALUMINUM

Al is a small, highly charged ion. The effective ionic radius of Al^{3+} is 0.054 nm. Because of its charge, in aqueous solutions at low pH values, Al^{3+} is coordinated by six water molecules in an octahedral configuration. In solutions more acidic than pH 5.0, $Al(H_2O)_6{}^{3+}$ exists (abbreviated as Al^{3+}). In less acidic solution, $Al(H_2O)_6{}^{3+}$ undergoes hydrolysis to yield $Al(H_2O)_5(OH)^{2+}$ (abbreviated as $Al(OH)^{2+}$) and $Al(H_2O)_4(OH)_2{}^{+}$ (abbreviated as $Al(OH)_2{}^{+}$) species. In the neutral pH range, Al is mainly precipitated as $Al(OH)_3$. In basic solutions, the precipitate redissolves, resulting in formation of tetrahedral $Al(OH)_4{}^{-}$. The equilibria among mononuclear Al species in aqueous solutions may be expressed by the following reactions with corresponding equilibrium constants [5]:

$$Al(H_2O)_6{}^{3+} + H_2O \rightleftarrows Al(H_2O)_5(OH)^{2+} + H_3O^+$$

$$K_1a = 10^{-5.5} \qquad (2.2.1.1)$$

$$Al(H_2O)_5(OH)^{2+} + H_2O \rightleftarrows Al(H_2O)_4(OH)_2{}^{+} + H_3O^+$$

$$K_2a = 10^{-5.6} \qquad (2.2.1.2)$$

Significant amounts of soluble $Al(OH)_3$ are not formed in solution, but deprotonation from two more $Al(H_2O)_4(OH)_2{}^{+}$ bound waters yields the soluble tetrahydroxy aluminum species.

$$Al(H_2O)_4(OH)_2{}^{+} + 2H_2O \rightleftarrows Al(H_2O)_2(OH)_4{}^{-} + 2H_3O^+$$

$$K_4a = 10^{-12.1} \qquad (2.2.1.3)$$

Martin [5] reported the distribution of soluble mononuclear Al species in aqueous solutions at various pH values, calculated on the basis of thermodynamic equilibrium constants at 25 °C and an ionic strength of 0.16. Al^{3+} is the prevailing species below pH 5.0. In the pH range between 5.0 and 6.2, there is a mixture of Al^{3+}, $Al(OH)^{2+}$, $Al(OH)_2{}^{+}$ and colloidal $Al(OH)_3$ species. At a pH higher than 6.2, the dominant species is $Al(OH)_4{}^{-}$.

When the pH of an acidic aqueous solution increases, the charge density of Al, due to hydrolysis, decreases and Al begins to polymerize [4]. Polynuclear Al species represent important metastable dissolved constituents that may remain in solution for many years. The smallest polynuclear Al complex in solution is the Al dimer, which is linked by a dihydroxide bridge $(Al_2(OH)_2(H_2O)_8)^{4+}$. This Al dimer is not a stable species. The ring structure of six aluminum hydroxide octahedra $(Al_6(OH)_{12})^{6+}$, the double-ring $(Al_{10}(OH)_{22}{}^{8+})$ and the triple-ring $(Al_{13}(OH)_{30}{}^{9+})$ structures are more stable Al polymers [4]. The most widely used method for direct observation of polynuclear Al species is nuclear magnetic resonance (NMR) spectroscopy. Various polynuclear Al complexes with the general formula $[Al_2(OH)_3]_n{}^{3+}$ and other polynuclear structures of Al have been proposed in the literature [6]. The extent of polymerization and the distribution of polymers depend on the degree of oversaturation, pH, temperature and age of the solution. Elevated concentrations of polynuclear species are found only in highly saturated solutions that are not in contact with adsorbing surfaces. Higher temperatures and aging of solutions favor the polymerization process. It was demonstrated that Al also tends to hydrolyze at clay surfaces, resulting in polymer formation in soil solution and aquatic systems. Coalescing of polymers increases the molecular mass, leading to precipitation of Al from solution as amorphous $Al(OH)_3$. If suspended particulate matter is present in natural water samples, it will readily adsorb polynuclear Al species [6].

3 THE DISTRIBUTION OF ALUMINUM IN ENVIRONMENTAL SOLUTIONS

In environmental solutions, F^-, $SO_4{}^{2-}$ and organic ligands compete with OH^- for formation of Al complexes. Al^{3+} forms stronger complexes with F^- than $SO_4{}^{2-}$. In acidic solutions, containing more fluoride than Al, almost all Al^{3+} exists in the form of fluoride complexes. Unless there are very high concentrations of sulfate present, fluoride is the most important inorganic ligand that complexes Al in acidic environmental solutions. However, under alkaline conditions, F^- or $SO_4{}^{2-}$ are displaced by the OH^- ion [7]. There is evidence of interactions between

Al and silica. Recently, hydroxyaluminosilicates have been directly identified in acidic solutions by atomic force microscopy [8]. Interactions of Al with HCO_3^- are rather weak. With PO_4^{3-}, Al forms sparingly soluble species that are precipitated as $AlPO_4$. Other inorganic anions that can be found in natural waters, that is, Cl^-, Br^-, I^-, S^{2-} and NO_3^-, do not form significant complexes with Al [9].

Naturally occurring organic substances of various types play an important role in the binding of Al in soils, sediments, plants and in natural waters. Most soils are composed of mineral fraction and organic matter. Organic ligands originate either from plants or are synthesized by microorganisms. The soil organic compounds that form stable complexes with Al are low molecular mass (LMM) substances such as simple aliphatic acids, phenols and phenolic acids, sugar acids and complex polynuclear phenols. High molecular mass (HMM) organic compounds that also form stable complexes with Al are yellow- to dark-colored humic and fulvic acids. The formation of complexes occurs by the reaction of Al^{3+} with carboxyl and phenolic groups [10]. A particular role in complexation of Al in the soil solution is played by carboxylic LMM organic acids, that is, formic, acetic, propionic, butyric, oxalic, succinic and fumaric, as well as hydroxycarboxylic LMM organic acids, that is, lactic, tartaric and citric. Although their concentration in soil solution is normally very low, in the concentration range of 10^{-3} mol dm^{-3}, higher quantities can be found in the rhizosphere of crop plants. The leaves of plants often contain high concentrations of citric and malic and to a lesser extent succinic, fumaric and oxalic acids [10]. Some of these organic ligands can form strong complexes with Al^{3+} and may therefore compete for complex formation with inorganic

Table 2.2.1.1. Critical stability constants of some mononuclear Al(III) complexes ($\mu = 0.10$, T = 25 °C).

Ligand	Quotient Q	Log Q	Source: reference no.
HOH, HL	$[AlL^{2+}]/[Al^{3+}][L^-]$	8.47	12, 13
	$[AlL_2^+]/[Al^{3+}][L^-]^2$	16.8	
($\mu = 0$)	$[AlL_3]/[Al^{3+}][L^-]^3$	24.7	
($\mu = 0$)	$[AlL^{4-}]/[Al^{3+}][L^-]^4$	31.5	
HF, HL	$[AlL^{2+}]/[Al^{3+}][L^-]$	6.42	12
	$[AlL_2^+]/[Al^{3+}][L^-]^2$	11.63	
	$[AlL_3]/[Al^{3+}][L^-]^3$	15.5	
	$[AlL^{4-}]/[Al^{3+}][L^-]^4$	18.1	
H_2SO_4, H_2L ($\mu = 0$)	$[AlL^+]/[Al^{3+}][L^{2-}]$	3.5	14
EDTA, H_4L	$[AlL^-]/[Al^{3+}][L^{4-}]$	16.5	12
	$[AlHL]/[AlL^-][H^+]$	2.5	
	$[AlL^-]/[AlOHL^{2-}][H^+]$	5.83	
	$[AlOHL^{2-}]/[Al(OH)_2L^{3-}][H^+]$	10.31	
Lactic acid, HL ($\mu = 6$)	$[AlL^{2+}]/[Al^{3+}][L^-]$	2.36	12
	$[AlL_2^+]/[Al^{3+}][L^-]^2$	4.42	
	$[AlL_3]/[Al^{3+}][L^-]^3$	5.8	
Oxalic acid, H_2L ($\mu = 1.0$)	$[AlL^+]/[Al^{3+}][L^{2-}]$	6.1	15
	$[AlL_2^-]/[Al^{3+}][L^{2-}]^2$	11.09	
	$[AlL_3^{2-}]/[Al^{3+}][L^{2-}]^3$	15.12	
Malic acid, H_2L (T = 37 °C, $\mu = 0.15$)	$[AlL^+]/[Al^{3+}][L^{2-}]$	4.60	12
	$[AlL_2^-]/[Al^{3+}][L^{2-}]^2$	7.62	
	$[AlHL^{2+}]/[AlL^+][H^+]$	2.27	
	$[AlHL_2]/[AlL_2^-][H^+]$	3.69	
	$[AlL_2^-]/[AlOHL_2^{2-}][H^+]$	3.31	
Citric acid, H_3L	$[AlL]/[Al^{3+}][L^{3-}]$	7.98	12
	$[AlHL^+]/[AlL][H^+]$	2.94	
	$[AlL]/[AlH_{-1}L^-][H^+]$	3.31	
	$[AlH_{-1}L^-]/[Al(OH)(H_{-1}L)^2][H^+]$	6.23	

Note: EDTA = ethylenedinitrilotetraacetic acid, μ = ionic strength, T = temperature

ligands, or may even, like citrate, solubilize Al from precipitates (hydroxide, phosphate) [5, 11].

In environmental solutions, an equilibrium exists among the various Al species. The distribution of Al species depends on the concentration of Al, the concentration of inorganic and organic ligands and their corresponding stability constants with Al. Temperature and, in particular, the pH of the solution also play important roles. Stability constants for some typical inorganic and organic ligands that can bind Al in environmental solutions [12–15] are presented in Table 2.2.1.1.

4 THE TOXICITY OF ALUMINUM

Elevated concentrations of soluble Al species in the environment cause toxic effects to living organisms. The toxicity of Al depends primarily on its chemical forms. Labile positively charged aqua- and hydroxy mononuclear complexes have been recognized as the most toxic Al species. Harmful effects of Al were observed on organisms of aquatic [16, 17] and terrestrial [18–21] habitats. Al exhibited severe toxic effects on fish exposed to 2.8 μmol dm^{-3} concentrations of aqua- and hydroxy aluminum complexes in the pH range from 4.0 to 6.5. Responses to Al were the most severe at pH 6.1 since $Al(OH)_3$ stuck to fish gills and at pH 4.5 due to electrolyte loss [16]. Toxic effects of Al on amphibians were also observed [17]. Investigations on the influence of Al on red spruce root growth indicated that chronic exposure to mononuclear positively charged aqua- and hydroxy aluminum species in concentrations greater than 180 to 250 μmol dm^{-3} of Al inhibited root growth [19]. Al toxicity is also the major factor limiting crop productivity on acid soils, which comprise up to 40% of the world's arable lands. The major symptom of Al toxicity is a rapid inhibition of root growth and root branching [21].

In order to understand the phenomena of Al toxicity, intensive investigations have been carried out in the last two decades on speciation of Al by computer modeling and by the use of experimental analytical techniques. However, speciation of Al is still a difficult task because of the complexity of chemical compounds present in environmental solutions and the great influence of pH on the distribution of Al species.

5 SPECIATION OF ALUMINUM IN ENVIRONMENTAL SAMPLES

5.1 Computer modeling

Computer modeling is a widely used approach to elemental speciation and can be readily accomplished using one of the many available computer programs for speciation. Among numerous applications, computer simulation was employed in speciation of Al in soil solution, taking into consideration dissolved silica [22]. The proposed model demonstrated that dissolved silica has a remarkable influence on Al speciation. Increasing concentrations of silicic acid may effectively inhibit the formation of toxic Al^{3+}, $Al(OH)^{2+}$, $Al(OH)_2{}^{+}$ as well as polynuclear Al hydroxy species, and, furthermore prevent Al toxicity to plants. Al binding to humic substances in acid soils [23] and acid surface waters [24] has also been investigated by computer modeling. Investigation of the factors influencing Al speciation in natural water equilibria with the mineral phase gibbsite was also carried out with the aid of computer programs [25]. These theoretical predictions have been successful for well-defined solutions with known total metal concentrations, ligand concentrations and known corresponding stability constants but tend not to predict accurately the metal species in soil solutions owing to the very complex matrix. Because of uncertainty in thermodynamic data, particularly involving naturally occurring organic solutes, it is useful to distinguish analytically among various forms of Al. The need for the experimental determination of the Al compounds present in environmental solutions resulted in the development of numerous analytical techniques for speciation of Al.

5.2 Analytical techniques for speciation of Al in environmental water samples and soil solutions

In speciation analysis of Al, it is of great importance to avoid extraneous contamination

Table 2.2.1.2. Driscoll's scheme for fractionation of Al [34].

← Total reactive Al, acid digestion →		
← Labile Al measured by rapid reaction with 8-hydroxyquinoline →		
← Al in strong cation-exchange column effluent →		
Nonlabile mononuclear Al organic complexes	Labile mononuclear inorganic Al species aqua Al^{3+}, hydroxy aluminum complexes, fluoro aluminum complexes, sulfato aluminum complexes	Acid-soluble Al colloidal Al, polynuclear Al species, strong Al organic complexes

during sampling and speciation procedures. Samples should be collected in high-density polyethylene or Teflon ware, previously soaked in 10% HNO_3 for 48 h and rinsed with high-purity water (MiliQ, water doubly distilled in quartz) [26]. In order to prevent chemical transformation of Al species, samples should be analyzed immediately after sampling or stored in the dark and cold. When the concentrations of Al in the samples are low (ng cm^{-3} concentration level), the speciation analysis should be carried out under clean room conditions (at least class 10,000).

Numerous fractionation procedures have been developed to operationally determine labile, quickly reacting mononuclear Al species, based on the rates of reaction with complexing agents such as 8-hydroxyquinoline [27], ferron [28] or pyrocatechol violet [29]. Ion-exchange [30] and chelating ion-exchange [31] chromatography also allow the determination of mononuclear Al species. Miller and Andelman [31] reported the speciation of Al in acidic waters using a Chelex-100 preconditioned resin. A batch procedure was applied at various time intervals to distinguish among rapidly, moderately and slowly exchangeable as well as inert Al forms. Kožuh *et al*. modified a batch Chelex-100 technique to a column procedure with inductively coupled plasma atomic emission spectrometry (ICP-AES) detection [32] and a microcolumn system with electrothermal atomic absorption spectrometry (ETAAS) detection [33] for the determination of mononuclear Al species in aqueous soil extracts [32] and environmental water samples [33]. The authors also optimized the parameters influencing the efficiency of the extraction procedure for the determination of the total water-soluble Al in soil samples [32]. In pure aqueous solutions, all these techniques enable determination of the sum of positively charged aqua- and hydroxy Al species in the acidic and neutral pH range. In environmental samples, various inorganic and organic ligands are present that compete for Al. The resulting Al complexes could also contribute to the measurement signal of total mononuclear Al. In order to distinguish between various groups of Al species, Driscoll proposed an analytical scheme [34] that combines three techniques for speciation of Al in natural waters. Rapid reaction of Al with 8-hydroxyquinoline complexing agent, column ion-exchange and acid digestion were applied to differentiate among labile mononuclear Al species, nonlabile mononuclear Al species and the acid soluble Al fraction, see Table 2.2.1.2.

Many investigators used Driscoll's scheme and applied it with minor modifications to the determination of Al species in environmental water samples [26, 35, 36]. Selective procedures have also been developed for the speciation of Al^{3+} in environmental samples based on reaction with the fluorescent chelating agent morin [37], using a fluoride ion-selective electrode [38] and isotachophoresis [39].

In the last decade, investigations were directed at the development of analytical methods for simultaneous determination of different Al species by a single procedure. For this purpose, ion chromatography in combination with postcolumn derivatization using Ultraviolet Visible spectroscopy (UV–VIS) [40, 41] or fluorescence detection [42, 43] was employed. The method developed by Willet

[41], which was able to distinguish among free Al (Al^{3+}, $Al(OH)^{2+}$, $Al(OH)_2{}^+$ and $Al(SO_4)^+$), doubly charged Al-containing ions, that is, $(AlF)^{2+}$ and singly charged Al-containing ions, that is, $AlF_2{}^+$, $Al(ox)^+$, $Al(cit)^+$ was successfully applied to the speciation of Al in soil solutions [42]. Neutral and negatively charged species did not influence the determination of positively charged Al species. Jones and Paull [43] developed an ion chromatographic procedure for the direct determination of Al species in waters over a wide pH range, including the alkaline region. Inorganic mononuclear Al species were separated from AlF^{2+}, $AlF_2{}^+$ and Al bound to organic molecules. Sutheimer and Cabaniss [44] reported the separation of soluble complexes of aluminum fluoride, aluminum citrate, aluminum acetate and aluminum silicate from Al^{3+}, $Al(OH)^{2+}$, $Al(OH)_2{}^+$ and $Al(OH)_4{}^-$ (which appeared as a single peak) by the use of cation-exchange high performance liquid chromatography (HPLC) with fluorescence detection of the aluminum lumogallion complex.

One of the reasons why ion-exchange HPLC systems were not frequently applied to the speciation of Al lies in the common use of halide solutions as eluents. These eluents lead to corrosion problems with the stainless steel components of HPLC systems and are subject to matrix interference effects with conventional detection systems, that is, optical spectrometric methods. Mitrović *et al*. [45] developed a cation-exchange fast protein liquid chromatography (FPLC) procedure with ICP-AES detection for speciation of mononuclear Al species. By employing aqueous 8 mol dm^{-3} $NaNO_3$ linear gradient elution quantitative determination of individual Al species (Al^{3+}, $Al(OH)^{2+}$, $Al(OH)_2{}^+$ and $Al(OH)_4{}^-$) in the pH range from 3.0 to 11.0 was obtained in synthetic aqueous solutions containing Al. The increasing ionic strength of the eluent during the chromatographic run (gradient elution) allowed the separation of positively charged Al species. The charge of the separated Al species was deduced from the retention times. The experimental data agreed well with Martin's predictions [5] calculated on the basis of the thermodynamic equilibrium constants at 25 °C and an ionic strength of 0.16. The possibility of distinguishing between aqua- and hydroxy Al species is of great importance in studies of Al toxicity. However, in complex sample matrices positively charged $Al(SO_4)^+$ and $AlF_2{}^+$ species as well as negatively charged oxalato- and citrato-Al complexes coeluted with $Al(OH)_2{}^+$ species, and AlF^{2+} coeluted with $Al(OH)^{2+}$ species. The technique was successfully employed for speciation of Al in soil extracts in which concentrations of total Al were higher than 0.5 $\mu g\,cm^{-3}$. Since most natural water samples and some soil extracts contain very low Al concentrations, the same investigators appreciably improved the sensitivity of the technique down to low $ng\,cm^{-3}$ concentrations by employing a cation-exchange FPLC-ETAAS procedure, using aqueous 8 mol dm^{-3} NH_4NO_3 linear gradient elution [46]. The influence of some typical inorganic and organic ligands on the distribution of Al species at pH 4.0 and 6.0 was investigated as well and is presented in Figure 2.2.1.1.

Speciation of Al in soil extracts and environmental water samples was performed using the improved technique [46]. On the basis of the retention times and data comparison with those in Figure 2.2.1.1, it was possible to determine particular Al species or estimate groups of Al species present in the samples analyzed.

The sensitivities of most analytical techniques developed are adequate for speciation of Al in environmental samples. On the basis of the specific selectivity of a particular technique, single Al species or different groups of Al species may be determined. In order to obtain more comprehensive information on the Al species present in environmental samples, comparison of analytical data from complementary procedures needs to be performed. Borrmann and Seubert [47] combined ion chromatography with size-exclusion and cation-exchange columns using "on line" detection via postcolumn UV photometry and atomic spectrometry. The proposed analytical system enabled determination of Al^{3+} and complexed Al (fluoro-, oxalato- and citrato aluminum complexes) in the pH range from 3 to 5. Cation-exchange HPLC and size-exclusion HPLC with

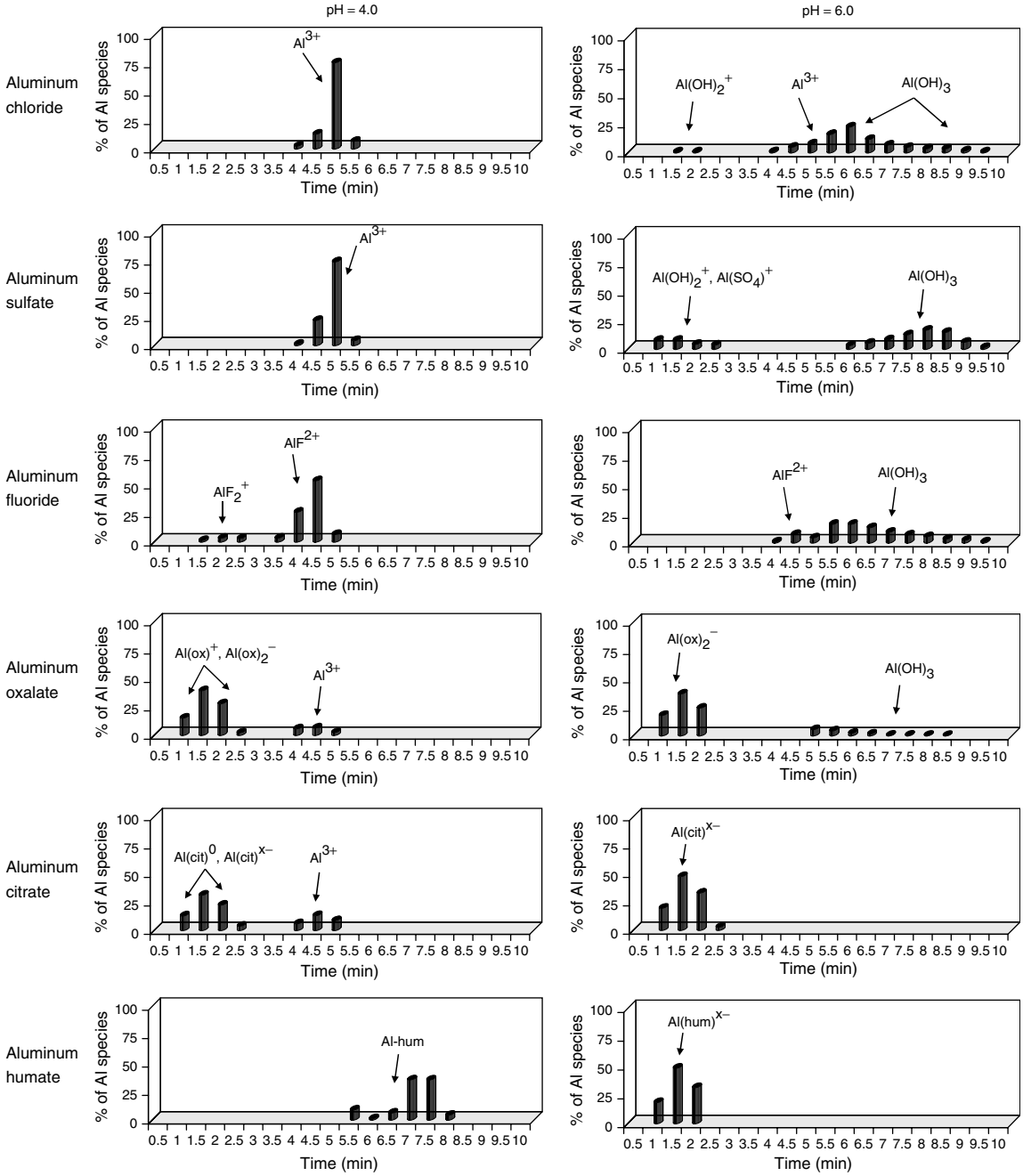

Figure 2.2.1.1. Influence of some inorganic and organic ligands on the distribution of aluminum species (250 ng cm^{-3} Al) at pH 4.0 and 6.0 employing cation-exchange FPLC with ETAAS detection (fraction collection 0.5 cm^3). The percentage of mononuclear aluminum species in filtered (0.1 μm) synthetic samples was determined using a Mono S HR 5/5 column, a sample volume of 1 cm^3, aqueous-NH_4NO_3 (8 mol dm^{-3}) linear gradient elution in 10 min, and at flow rate of 1 cm^3 min^{-1}, $n = 2$. (Reproduced from Reference [46] by permission of Wiley VCH.)

fluorescence detection were also used for determination of Al^{3+} and complexed Al (fluoro-, oxalato- and citrato aluminum complexes) [48]. The two techniques were employed in Al speciation in soil extracts. Milačič *et al*. [49] combined three analytical techniques: cation-exchange FPLC-ICP-AES [45], microcolumn chelating ion-exchange chromatography – ETAAS [33] and 8-hydroxyquinoline spectrometry [27] for determination of Al species in aqueous soil extracts and percolating water samples. Taking into consideration the specific selectivity of the technique and by comparison of the analytical data, it was demonstrated that in aqueous extracts of forest soils and in percolating water samples of forest soils Al exists predominately as mononuclear species bound to organic molecules, partially in complexes with humic acids and to a smaller extent as aluminum sulfato species. The prevalent mononuclear Al species in clay and sandy soils were estimated to be aluminum fluoro complexes, and the dominant Al mononuclear species in acid soils were presumed to be aluminum sulfato complexes.

Since humic and fulvic acids play an important role in the environment, many investigations were oriented to the development of analytical techniques for determination of aluminum fulvic and humic complexes. Some procedures were based on kinetic discrimination of quickly reacting Al species with oxine in a flow system [50, 51], whereas others were directed to determination of the individual concentrations of Al species. Sutheimer and Cabaniss [52] applied high-performance cation-exchange chromatography for quantification of free Al and Al complexed by fulvic acids. Size-exclusion chromatography was used for speciation of Al in natural waters [53]. The data indicated that Al was bound to a broad size range of humic substances and that inorganic Al was present in polynuclear form. Mitrović and Milačič [54] studied Al speciation in forest soil extracts by size-exclusion chromatography with UV and ICP-AES detection and cation-exchange FPLC with ETAAS detection. An example of such speciation analysis of deciduous forest soils by two techniques is presented in Figure 2.2.1.2.

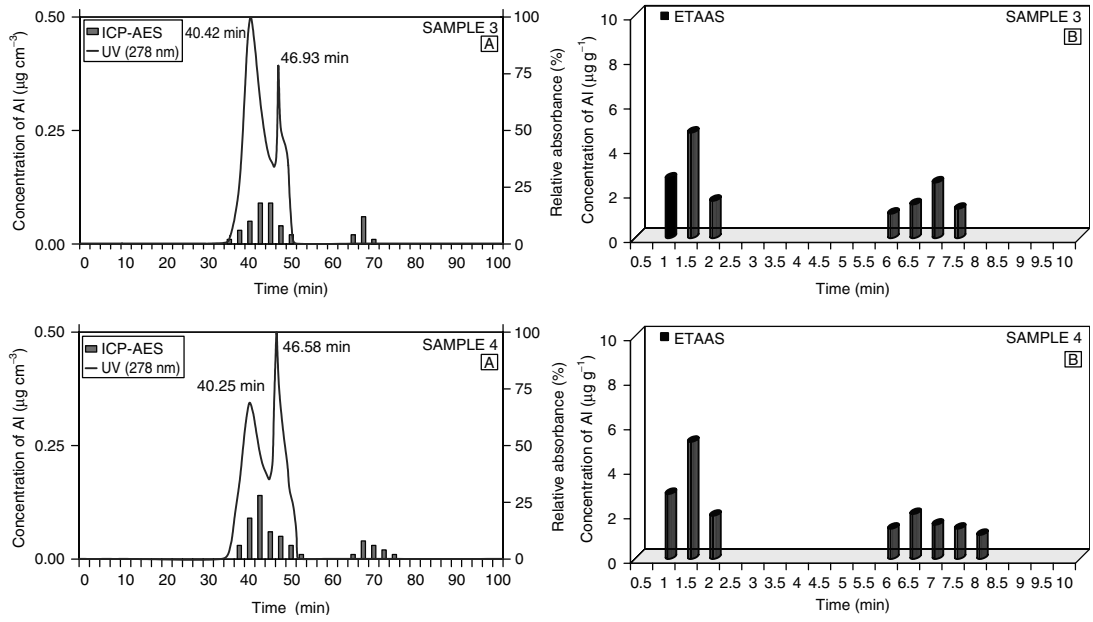

Figure 2.2.1.2. Determination of Al species in filtered (0.45 μm) aqueous extracts of deciduous forest soils (samples 3 and 4) by size-exclusion ICP-AES-UV (a) and FPLC-ETAAS (b) techniques. (Reprinted from *Sci. Total Environ.*, 258, Mitrović, B. and Milačič, Speciation of aluminum in forest soil extracts by size exclusion chromatography with UV and ICP-AES detection and cation exchange fast protein liquid chromatography with ETAAS detection, 183, (2000), wih permission from Elsevier.)

The FPLC chromatograms of samples No. 3 and 4 represent elution of mononuclear Al species. The LMM complexes of AlF_2^+, aluminum citrate and aluminum oxalate are eluted with the solvent front, whereas Al-humic complexes are eluted at a retention time from 6.0 to 8.0 min. The size-exclusion chromatographic peaks of samples No. 3 and 4 indicate that the molecular mass of Al bound to humic acids in both samples ranges from 7200 to 13,500 Da. Species eluted from 65 to 75 min represent the LMM-Al fraction. Combination of the two techniques indicated that 80–95% of total water-soluble Al in the samples exists in the form of mononuclear Al species. 45–55% of total water-soluble Al corresponds to LMM complexes of AlF_2^+, aluminum citrate and aluminum oxalate, and 30–40% of total water-soluble Al exists in the form of Al bound to humic substances with molecular masses ranging from 6400 to 9000 Da (conifer forest soils) and 7200 to 13,500 Da (deciduous forest soils). Comparison of the data from size-exclusion ICP-AES-UV and FPLC-ETAAS techniques for determination of aluminum humate complexes indicated good agreement of results (94–104%). Combination of the proposed complementary speciation techniques enables a reliable interpretation of the analytical data. It also provides more comprehensive information on the Al species present in forest soil extracts. This is very important when the toxicity of particular Al species is studied and when the consequences of acid rain are investigated in the terrestrial environment.

5.3 Analytical techniques for speciation of Al in plants

Al toxicity is a well-known limiting factor in plants growing in acid soils. Nevertheless, some plants are able to tolerate even phytotoxic concentrations of Al. They have developed special tolerance mechanisms, among which external and internal tolerance mechanisms are most frequently mentioned [21]. It was presumed that LMM organic acids (citric, oxalic, malic, succinic) are involved in both tolerance mechanisms [55]. The detoxification of Al proceeds through complexation reactions either outside or inside the roots. Investigations of Al-tolerance mechanisms, the uptake, the kinetics and the spatial distribution of Al in Al-tolerant and Al-sensitive plants have been based on the determination of total Al [56, 57]. Since Al toxicity depends appreciably on its chemical form, there was a need to apply reliable analytical techniques for determination of Al species in plant sap. Al speciation is also necessary in the investigations of Al uptake, transformations and translocation into the upper parts of plants.

There are only a few analytical techniques for identification and quantification of mononuclear aqua- and hydroxy aluminum species [45, 46]. Until recently, there was also a lack of reliable analytical techniques for quantitative determination of LMM-Al complexes. Bantan *et al.* developed an analytical procedure for quantitative determination of aluminum citrate and some other negatively charged Al complexes in the pH range from 3.0 to 11.0 by the use of anion-exchange FPLC with ICP-AES [58] or ETAAS [59] detection. For this purpose, aqueous 4 mol dm^{-3} $NaNO_3$ linear gradient elution [58] or aqueous 4 mol dm^{-3} NH_4NO_3 linear gradient elution [59] was applied. The possibilities for speciation of LMM-Al organic acid complexes in plant sap were investigated by applying cation-exchange and anion-exchange FPLC techniques in combination with optical atomic spectrometric methods [60]. The behavior of different LMM-Al complexes was investigated in synthetic aqueous solutions. Speciation analysis of plant sap of *Sempervivum tectorum* with a high concentration of total Al (9.3 $\mu g\,cm^{-3}$) and *Sansevieria trifasciata* with an appreciably lower concentration of total Al (0.065 $\mu g\,cm^{-3}$) indicated that the species present in these samples exist as negatively charged LMM-Al complexes, which were eluted at the retention time typical of aluminum citrate and Aluminum aconitate. In order to identify Al-binding ligands eluted under the chromatographic peaks, analysis by the electrospray ionization ES-MS technique using a Z spray ion source was also applied. It was proved that the predominant LMM-Al negatively charged complexes in the samples analyzed were aluminum citrate and aluminum aconitate. In addition, it was demonstrated that other LMM organic acids do

not form complexes with Al in these samples. Bantan Polak *et al*. [61] also performed an investigation on the uptake of various Al species in Al-tolerant Chinese cabbage (*Brassica rapa L. ssp. pekinensis*). Plants were exposed to 10 $\mu g\,cm^{-3}$ of Al in the nutrient solution (pH 4.2), containing Al^{3+}, aluminum citrate or aluminum malate in a time span from 1 up to 24 h. In each experiment, the nutrient solution and stem sap were analyzed by a combination of cation- and anion-exchange FPLC-ICP-AES techniques. Identification of Al binding ligands eluted under the chromatographic peaks was performed by the ES-MS-MS technique. Typical distributions of Al^{3+}, aluminum citrate and aluminum malate on cation-exchange (Mono S) and anion-exchange (Mono Q) FPLC columns at pH 4.2 are presented in Figure 2.2.1.3, and the corresponding electrospray ionization tandem mass spectrometry (ES-MS-MS) spectra are shown in Figure 2.2.1.4.

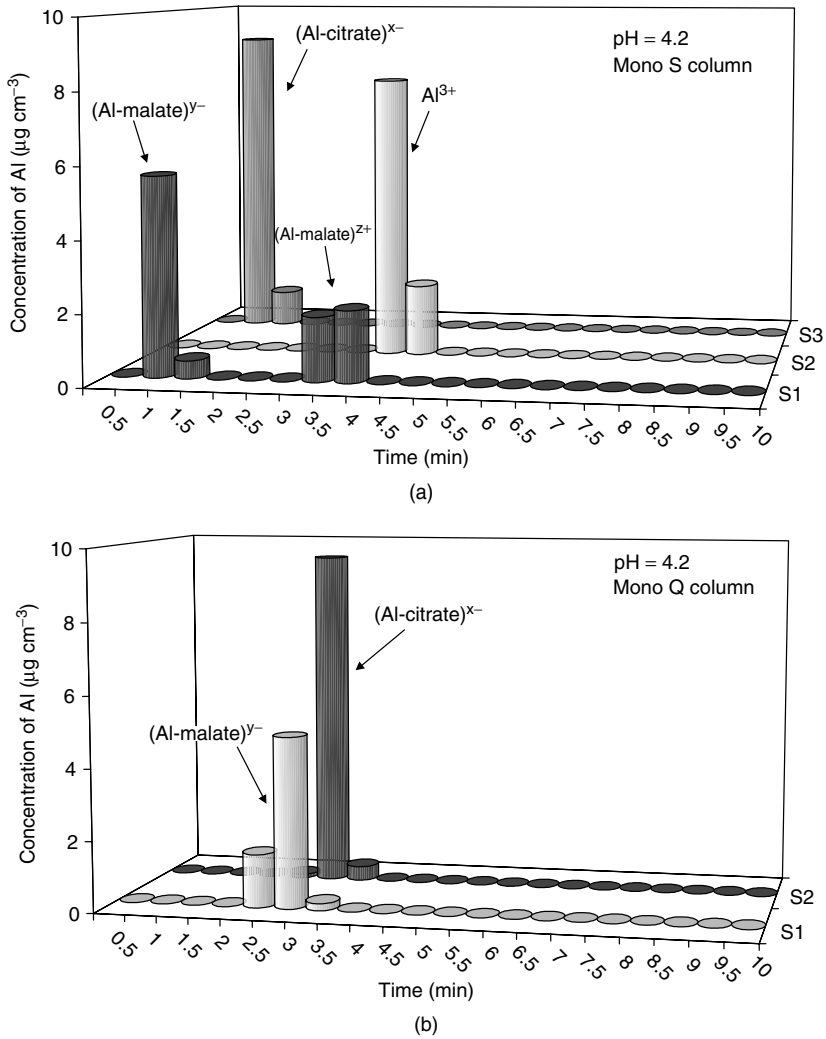

Figure 2.2.1.3. Typical distribution of Al^{3+}, aluminum citrate and aluminum malate at pH 4.2 on a cation-exchange Mono S column (a) and on an anion-exchange Mono Q column (b) using ICP-AES detection, $n = 3$. (Reprinted from *Phytochemistry*, 57, Bantan Polak, T., Milačič, R., Pihlar, B. and Mitrović B., The uptake and speciation of various Al species in the Brassica rapa pekinensis, 189, (2001), with permission from Elsevier.)

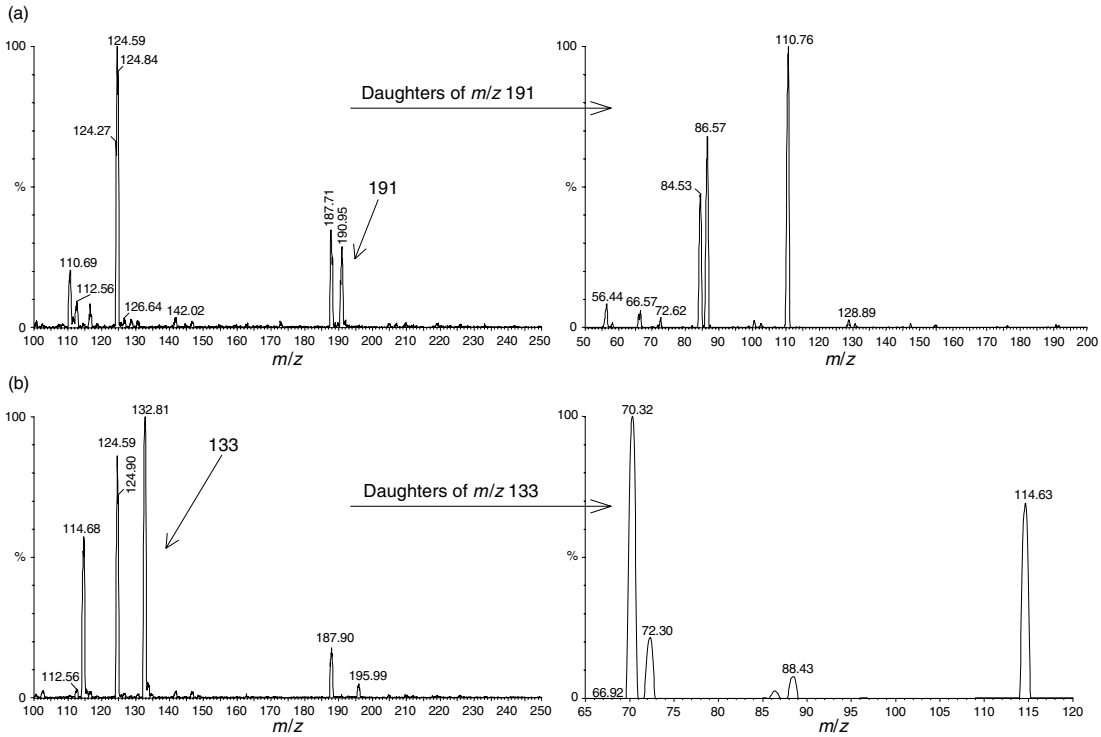

Figure 2.2.1.4. ES mass spectra and corresponding daughter ion mass spectra for synthetic solutions of aluminum citrate (a) and aluminum malate (b). (Reprinted from *Phytochemistry*, 57, Bantan Polak, T., Milačič, R., Pihlar, B. and Mitrović B., The uptake and speciation of various Al species in the Brassica rapa pekinensis, 189, (2001), with permission from Elsevier.)

The applied combination of speciation techniques enabled determination of particular chemical forms of Al present in the nutrient solution or in stem sap. The results demonstrated that Al^{3+} added to the nutrient solution was not transformed in the growth media during the course of the experiments, but in the roots transformation to aluminum malate occurred. Al was transported from roots to the upper parts of the plant as aluminum malate (70%) and Al^{3+} (30%). Aluminum citrate or aluminum malate added to the nutrient solution was transferred to the upper parts of the plant without transformation of their chemical forms.

6 CONCLUSIONS

Because of its toxic effects on living beings, Al may represent an environmental hazard, particularly under increased acidic conditions. Growing environmental concern over the presence of increased Al concentrations in soil solutions and fresh waters resulted in the development of numerous analytical techniques for the determination of Al species. Owing to the complex chemistry of Al, the variety of Al species present in environmental solutions and the great influence of pH on Al speciation, quantitative determination of particular chemical forms of Al is still a very difficult task for analytical chemists. Numerous analytical techniques are based on the rate of reaction among various Al species and different complexing agents and specific reactions with various chelating and ion-exchange resins. These techniques in general enable the determination of quickly reactive chemical forms of Al, mainly the sum of aqua- and hydroxy aluminum species that have been recognized as the most toxic Al species to living organisms. However, in the presence of other inorganic and organic ligands that also form complexes with Al, these techniques are not selective enough. In

recent years, more selective analytical techniques have been developed for speciation of Al by applying ion chromatography, cation-exchange HPLC, cation- and anion-exchange FPLC techniques and size-exclusion chromatography. These separation procedures were combined with different detection techniques (atomic spectrometric methods, specific reactions with chelating agents) for determination of separated Al species. For instance, cation-exchange (FPLC) with ICP-AES or ETAAS detection in pure aqueous solutions enabled quantitative determination of individual Al species (Al^{3+}, $Al(OH)^{2+}$, $Al(OH)_2{}^+$ and $Al(OH)_4{}^-$), which is of great importance in studies of Al toxicity.

In complex matrices such as environmental solutions, a combination of complementary speciation techniques is necessary for reliable interpretation of analytical data to be made. It is also important that after chromatographic separation, Al species are determined not only on the basis of the retention time but also that the Al complex, eluted under a chromatographic peak, be characterized. ES-MS-MS provides a powerful tool for postcolumn characterization of Al-binding ligands.

7 REFERENCES

1. Matzner, E. and Prenzel, J., *Water, Air, Soil Pollut.*, **61**, 221 (1992).
2. Mulder, J. and Stein, A., *Geochim. Cosmochim. Acta*, **58**, 85 (1994).
3. Lawrence, G. B. and David, M. B., *Environ. Sci. Technol.*, **31**, 825 (1997).
4. Driscoll, C. T. and Schecher, W. D., Aluminum in the Environment, in *Metal Ions in Biological Systems, Vol. 24, Aluminum and its role in Biology*, Sigel, S. and Sigel, A. (Eds.), Marcel Dekker, New York, 1988, Chapter 2, pp. 59–122.
5. Martin, R. B., *Clin. Chem.*, **32**, 1797 (1986).
6. Bertch, P. M., Aqueous Polynuclear Aluminum Species, in *The Environmental Chemistry of Aluminum*, Sposito, G. (Ed.), CCR Press, Boca Raton, FL, 1989, Chapter 4, pp. 87–115
7. Smith, R. W., *Coord. Chem. Rev.*, **149**, 81 (1996).
8. Doucet, F. J., Rotov, M. E. and Exley, C., *J. Inorg. Biochem.*, **87**, 71 (2001).
9. Kiss, T. and Farkas, E., The Bioinorganic Chemistry of Aluminum, in *Perspectives on Bioinorganic Chemistry, Vol 3*, Hay, R. K., Dilworth, J. R. and Nolan, K. B., (Eds). JAI Press, London, 1996, pp. 199–250.
10. Stevenson, F. J. and Vance, G. F., Naturally Occurring Aluminum-Organic Complexes, in *The Environmental Chemistry of Aluminum*, Sposito, G. (Ed.), CCR Press, Boca Raton, FL, 1989, Chapter 5, pp. 117–145.
11. Martin, R. B., *J. Inorg. Biochem.*, **28**, 181 (1986).
12. Martell, A. E., Hancock, R. D., Smith, R. M. and Motekaitis, R. J., *Coord. Chem. Rev.*, **149**, 311 (1996).
13. Smith, R. M. and Martell, A. E., *Critical Stability Constants, Volume 4: Inorganic complexes*, Plenum Press, New York, 1976.
14. Nordstrom, D. K. and May, H. M., Aqueous Equilibrium Data for Mononuclear Aluminum Species, in *The Environmental Chemistry of Aluminum*, Sposito, G. (Ed.), CCR Press, Boca Raton, FL, 1989, Chapter 2, pp. 30–53.
15. Martell, A. E. and Smith, R. M. *Critical Stability Constants, Volume 3: Other Organic Ligands*, Plenum Press, New York, 1977.
16. Nevile, C. M. and Campbell, P. G. C., *Water, Air, Soil Pollut.*, **42**, 311 (1988).
17. Freda, J., *J. Environ. Pollut.*, **71**, 305 (1991).
18. Alva, A. K. and Summer, M. E., *Water, Air, Soil Pollut.*, 57–58, **121** (1991).
19. Miller, E. K., Huntington, T. G., Johnson, A. H. and Friedland, A. J., *J. Environ. Qual.*, **21**, 345 (1991).
20. Kuo, S., Brauen, S. E. and Jellum, E. J., *Soil Sci.*, **153**, 365 (1992).
21. Kochian, L. V., *Annu. Rev. Plant. Physiol. Plant Mol. Biol.*, **46**, 237 (1995).
22. Bi, S., An, S., Tang, W., Xue, R., Wen, L. and Liu, F., *J. Inorg. Biochem.*, **87**, 97 (2001).
23. Tipping, E., Berggren, D., Mulder, J. and Woof, C., *Eur. J. Soil Sci.*, **46**, 77 (1995).
24. Tipping, E., Woof, C. and Hurley, M. A., *Water Res.*, **25**, 425 (1991).
25. Bi, S., *Analyst*, **120**, 2033 (1995).
26. Fairman, B., Sanz-Medel, A., Galleo, M., José Quintela, M., Jonea, P. and Benson, R., *Anal. Chim. Acta*, **286**, 401 (1994).
27. James, B. R., Clark, C. J. and Riha, S. J., *Soil Sci. Soc. Am. J.*, **47**, 893 (1983).
28. Jardine, P. M. and Zelazny, L. W., *Soil Sci. Soc. Am. J.*, **50**, 895 (1986).
29. Samaritin, J. M., Wehr, J. D., Buccafuri, A. and Sahn, M., *Int. J. Environ. Anal. Chem.*, **50**, 173 (1993).
30. Lawrence, G. B. and Driscoll, C. T., *Environ. Sci. Technol.*, **22**, 1293 (1988).
31. Miller, J. R. and Andelman, B., *Water Res.*, **21**, 999 (1987).
32. Kožuh, N., Milačič, R. and Gorenc, B., *Ann. Chim.*, **86**, 99 (1996).
33. Kožuh, N., Milačič, R., Gorenc, B., Abollino, O. and Sarzanini, C., *Int. J. Environ. Anal. Chem.*, **67**, 27 (1997).
34. Driscoll, C. T., *Int. J. Environ. Anal. Chem.*, **16**, 267 (1984).
35. Fairman, B. and Sanz-Medel, A., *Int. J. Environ. Anal. Chem.*, **50**, 161 (1993).

36. Canizares, P. and Luque de Castro, M. D., *Anal. Chim. Acta*, **295**, 59 (1994).
37. Browne, B. A., Driscoll, C. T. and McColl, J. G., *J. Environ. Qual.*, **19**, 73 (1990).
38. Moore, C. S. and Ritchie, G. S. P., *Soil Sci.*, **39**, 1, (1988).
39. Smid, S., Kordel, W., Kloppel, H. and Klein, W., *J. Chromatogr.*, **470**, 289 (1989).
40. Bertsch, P. M. and Anderson, M. A., *Anal. Chem.*, **61**, 535 (1989).
41. Willet, I. R., *Soil Sci. Am. J.*, **53**, 1385 (1989).
42. Gibson, J. A. E. and Willet, I. R., *Commun. Soil Sci. Plant Anal.*, **22**, 1303 (1991).
43. Jones, P. and Paull, B., *Anal. Proc.*, **29**, 402 (1992).
44. Sutheimer, S. H. and Cabaniss, S. E., *Anal. Chem.*, **67**, 2342 (1995).
45. Mitrović, B., Milačič, R. and Pihlar, B., *Analyst*, **121**, 627 (1996).
46. Mitrović, B., Milačič, R., Pihlar, B. and Simončič, P., *Analusis*, **26**, 381 (1998).
47. Borrmann, G. and Seubert, A., *Anal. Chim. Acta*, **332**, 233 (1996).
48. Tsunoda, K., Yagasaki, T., Aziawa, S, Akaiwa, H. and Satake, K., *Anal. Sci.*, **13**, 757 (1997).
49. Milačič, R., Kožuh, N. and Mitrović, B., *Mikrochim. Acta*, **129**, 139 (1998).
50. Clarke, N., Danielsson, L. G. and Sparén, A., *Water, Air, Soil Pollut.*, **84**, 103 (1995).
51. Downard, A. J., Powell, K. J. and Money, S. D., *Anal. Chim. Acta*, **120**, 111 (1997).
52. Sutheimer, S. H. and Cabaniss, S. E., *Geochim. Cosmochim. Acta*, **61**, 1 (1997).
53. Zernichow, L. and Lund, W., *Anal. Chim. Acta*, **300**, 167 (1995).
54. Mitrović, B. and Milačič, R., *Sci. Total Environ.*, **258**, 183 (2000).
55. Jones, D. L., *Plant Soil*, **205**, 25 (1998).
56. Zhang, G. and Taylor, G. J., *Plant Physiol.*, **91**, 1094 (1989).
57. Lazof, D. B., Goldsmith, J. G., Rufty, T. W. and Linton, R. W., *Plant Physiol.*, **106**, 1107 (1994).
58. Bantan, T., Milačič, R. and Pihlar, B., *Talanta*, **46**, 227 (1998).
59. Bantan, T., Milačič, R. and Pihlar, B., *Talanta*, **47**, 929 (1998).
60. Bantan, T., Milačič, R., Mitrović, B. and Pihlar, B., *Fresenius' J. Anal. Chem.*, **365**, 545 (1999).
61. Bantan Polak, T., Milačič, R., Pihlar, B. and Mitrović, B., *Phytochemistry*, **57**, 189 (2001).

2.2.2 Speciation of Aluminum in Food: Sources, Including Potable Water

Radmila Milačič

Jožef Stefan Institute, Ljubljana, Slovenia

1 INTRODUCTION

Food is the main source of the essential major and minor elements for humans. Na, Mg, P, K and Ca are recognized as the major and Fe, Zn, Cu, Co, Cr, Se, Mo and I are considered to be the minor essential elements. There are some additional trace elements such as B, F, Li, Si, V, Ni, As, Sn and Pb that may be potentially essential to humans [1]. Aluminum (Al) is not considered to be an essential element in human beings, but its toxic effects are well known, particularly in patients with chronic renal failure [2, 3]. The bioavailability of Al from food depends on its chemical forms and the presence of Al-binding ligands. For instance, consuming black tea with milk would appreciably decrease Al bioavailability because of the formation of sparingly soluble aluminum-phosphato species, whereas drinking tea with lemon would drastically increase bioavailability of Al owing to formation of aluminum citrate complexes. Concern over the possible relation between environmental Al exposure and Alzheimer's disease [4] encouraged investigations of the potential intake of Al into the human body, including foods. Foodstuffs and drinking water represent the potential oral Al exposure. The concentration of Al in foodstuffs may increase during food processing by the use of Al-containing food additives. Al may also migrate into foodstuffs via leaching from kitchenware or from food packing. Parenterally administered nutrients, contaminated with Al, represent a risk for Al intoxication, particularly in infants with reduced kidney function. Infants fed with nutrition formulae may also be exposed to elevated Al concentrations.

In order to estimate the total dietary intake of Al in human beings, it is first necessary to determine the total Al concentrations in different foodstuffs and then afterwards to determine the chemical species of Al present in foodstuffs, particularly those high in Al.

Handbook of Elemental Speciation II: Species in the Environment, Food, Medicine & Occupational Health
Edited by R. Cornelis, H. Crews, J. Caruso and K. G. Heumann
 ISBN: 0-470-85598-3 (HB)

2 TOTAL ALUMINUM CONCENTRATIONS IN FOODS AND BEVERAGES

Numerous studies have been carried out on determining total Al concentrations in various foodstuffs [5–22]. Müller *et al*. intensively investigated the Al content in foods and beverages typical of German nutritional habits [5]. A total of 128 items were included in this investigation. Concentrations of Al in typical representative items obtained by Müller *et al*. [5] and data reported by other investigators [6, 7] are summarized in Table 2.2.2.1.

The data of Table 2.2.2.1 indicate that Al concentrations in rice, flour and bread ranged from 0.7 to 38 $\mu g\,g^{-1}$ Al. In some biscuits, higher Al concentrations (up to 60 $\mu g\,g^{-1}$) were observed, probably due to the use of Al-containing food additives. These additives are used to perform various functions in food. Sodium aluminum phosphate is used as a source of acid in raising agents, and aluminum sodium silicate is used as an anticaking agent to prevent particles of food adhering to each other [5, 8]. Data from Table 2.2.2.1 further indicate that meat and fish contain from 0.5 to 30 $\mu g\,g^{-1}$ Al, while higher concentrations of up to 80 $\mu g\,g^{-1}$ Al are found in liver and kidneys. Concentrations of Al in various vegetables and pulses in general range between 2 and 90 $\mu g\,g^{-1}$ Al. However, various sorts of lettuce may contain up to 1,000 $\mu g\,g^{-1}$ Al. Considering that in lettuce the dry matter represents only about 10%, the latter concentration is not so extremely high. In the group of Milačič [7], it was demonstrated that the concentration of Al in lamb's lettuce was not influenced by the total and water-soluble Al content in soil. Lamb's lettuce growing on clay soil (pH 6.2) high in total and water-soluble Al (40,700 and 7.70 $\mu g\,g^{-1}$ Al, respectively) contained 332 $\mu g\,g^{-1}$ Al, whereas lamb's lettuce growing on peat soil (pH 6.5) low in total and water-soluble Al (6,800 and 0.62 $\mu g\,g^{-1}$ Al, respectively) contained 413 $\mu g\,g^{-1}$ Al. On the basis of these observations, it can be concluded that lamb's lettuce may accumulate Al even from soils low in Al. Herbs and spices (Table 2.2.2.1) contain higher concentrations of Al, as well. Marjoram with Al concentrations up to 1,186 $\mu g\,g^{-1}$ also seems to be an Al accumulator. Sugar, sugar products and fruits are in general low in Al content. Milk is also low in Al, but dairy products, especially some types of cheese, contain up to 70 $\mu g\,g^{-1}$ Al, due to additives used in cheese processing. Cocoa and cocoa products may contain slightly elevated Al concentrations, but coffee powder is low in Al content. Consequently,

Table 2.2.2.1. Total Al concentrations in various foods in $\mu g\,g^{-1}$ expressed on dry weight basis and in beverages[a] in $\mu g\,cm^{-3}$, reported by different authors.

Food	Range ($\mu g\,g^{-1}$ Al) ($\mu g\,cm^{-3}$ Al)[a]	Reference
Rice	2.5–21	[5]
	0.7–1.6	[6]
Flour	1.5–38	[5]
	9.8–20.2	[6]
Bread	2.4–22	[5]
	13.5–22.0	[6]
	24–37	[9]
Biscuits	7.9–60	[5]
Meat	3.7–29	[5]
	0.5–1.8	[6]
	4.0–10.0	[9]
Liver, kidneys	9.3–82	[5]
Fish	2.5–30	[5]
	0.5–4.0	[6]
Vegetables	2.3–81	[5]
	3.6–92	[7]
	17.5–79.0	[6]
Lettuce	201–1011	[5]
	27–412	[7]
Pulses	2.4–33	[5]
	3.6–8.6	[6]
Herbs	29–300	[5]
Spices	5.7–1186	[5]
Table salt	0.2–22	[5]
Fruits	2.1–68	[5]
	1.1–9.7	[6]
Sugar and sugar products	3.0–36	[5]
Milk	2.5–6.1	[5]
Dairy products	2.2–70	[5]
	1.3–6.3	[6]
	6.0–13.0	[9]
Cocoa	21–161	[5]
Cocoa products	4.5–75	[5]
Black tea leaves	607–1291	[5]
	684–1192	[7]
Coffee (powder)	9–29	[5]
Black tea infusions[a]	4.2	[5]
	2.5–4.2	[7]
Coffee infusions[a]	0.1	[5]
	0.35	[7]
Beverages[a]	0.2–8.2	[5]
	3.3–7.3	[6]
Red wine[a]	0.5–4.5	[9]
	1.5–38	[5]

[a] concentration in beverage.

coffee infusions also contain low Al concentrations (0.1 to 0.35 $\mu g\,cm^{-3}$). Black tea leaves are the foodstuffs with the highest concentrations of Al, ranging from 600 up to 1,300 $\mu g\,g^{-1}$. Elevated Al concentrations (2.5–4.2 $\mu g\,cm^{-3}$) are also found in black tea infusions. Beverages in general contain below 8 $\mu g\,cm^{-3}$ Al, though exceptions are some types of red wine with Al concentrations up to 38 $\mu g\,cm^{-3}$. However, our results indicated that Slovenian red wines contained appreciably lower Al concentrations (0.1 to 0.2 $\mu g\,cm^{-3}$).

From the data of Table 2.2.2.1, it is also evident that different authors in general obtained comparable results for various foodstuff items. Comparable Al concentrations in foodstuffs were also reported by other investigators in Germany [10], Taiwan [11], Hungary [12], China [13] and Finland [14–19]. In the United Kingdom, comparable concentrations of Al were found in bread, fish, several vegetables, refreshing drinks and dairy products, but much lower Al concentrations were found in milk, meat and lettuce [20]. Variations in Al concentrations in various sorts of lettuce ranging from 11 up to 413 $\mu g\,g^{-1}$ were observed in a study of the Al content of vegetables, carried out in Slovenia [7]. Since some sorts of lettuce may contain very low concentrations of Al, and the others seem to be Al accumulators, this is probably the reason why in the United Kingdom lettuce in general contained lower Al concentrations. Monitoring studies in the United States of America revealed similar Al concentrations to those in Table 2.2.2.1 for bread, cakes, various vegetables, chocolate and spices. However, food of animal origin contained considerably lower Al concentrations [21, 22].

On the basis of the reported data, it may be concluded that the Al content of frequently consumed foods increases in the following order: beverages, food of animal origin and food of plant origin. The concentration of Al in different foodstuffs sometimes depends on the region of food production. Concentrations of Al in foodstuffs are in general lower than 30 $\mu g\,g^{-1}$. Higher concentrations of Al can be found in processed foodstuffs, some dairy products, some sorts of lettuce, cocoa and cocoa products and in spices. The highest concentrations of Al are found in black tea leaves (up to 1,300 $\mu g\,g^{-1}$). However, studies performed on the average Al concentration in 24-h diets [9] indicated that the average dietary intake of Al is about 6 mg/day [8, 9]. This value is very low compared to the Provisional Tolerable Weekly Intake of Al, which for an adult man is 60 mg/day and was established by the joint FAO/WHO Expert Committee on Food Additives [23].

3 TOTAL ALUMINUM CONCENTRATIONS IN DRINKING WATERS

One of the main routes of entry of Al into the human body is through the consumption of drinking water with high Al concentrations. Important sources of elevated Al concentrations in drinking water are the use of Al-based flocculating agents such as $Al_2(SO_4)_3$ and the release of soluble Al species into surface, ground and drinking waters because of soil acidification. For this reason, concentrations of Al in drinking water may considerably vary between different water supplies. Monitoring of Al concentrations performed for the 54 municipality water supplies in Quebec, Canada [4], indicated that total Al concentrations ranged between 5 and 260 $ng\,cm^{-3}$, with an average concentration of 40 $ng\,cm^{-3}$ Al. Variations in Al concentrations in tap water were also observed in regular monitoring in 12 municipality water supplies in Slovenia [24]. Total Al concentrations ranged between 1 and 200 $ng\,cm^{-3}$, with an average concentration of 37 $ng\,cm^{-3}$ Al. Higher Al concentrations in drinking water ranging from 200 to 500 $ng\,cm^{-3}$, were observed in Kenya [6]. Since water is used not only for drinking but also in preparation of food, such high concentrations of Al in drinking water may contribute to increased intake of Al into the human body.

4 TOTAL ALUMINUM CONCENTRATIONS IN PARENTERAL SOLUTIONS, NUTRITION FORMULAE AND BREAST MILK

Parenteral exposure to Al can occur via total parenteral nutrition [25]. Contamination may appear

because of the use of calcium salts and additives for parenteral nutrition, containing concentrations higher than 100 $\mu g\,cm^{-3}$ Al [26]. Intensive studies on contamination of parenteral nutrition solutions with Al indicate different concentrations of this contaminant [25–32]. Lower concentrations from 0.007 to 0.018 $\mu g\,cm^{-3}$ Al [27], moderate Al concentrations from 0.004 to 0.07 $\mu g\,cm^{-3}$ [26] and higher Al concentrations from 0.06 to 1.23 $\mu g\,cm^{-3}$ Al [32] were reported in parenteral solutions. Despite highly elevated renal Al excretion, the median serum Al concentrations in patients on parenteral nutrition were slightly increased [26]. Therefore, parenteral nutrition solutions may represent a risk of Al intoxication in infants with reduced kidney function and in patients with impaired renal function.

Concentrations of Al in infant formulae made up ready for consumption exhibited lower concentrations in cow's milk–based formulae of 0.02 to 0.57 $\mu g\,cm^{-3}$ Al, than in soya-based formulae of 0.42 to 2.35 $\mu g\,cm^{-3}$ Al [33]. A similar range of Al concentrations in infant formulae of 0.06–1.23 $\mu g\,cm^{-3}$ Al was reported by Baydar *et al*. [32]. The Al content in baby food samples was also determined. In slurried baby food samples, Al concentrations ranged between 0.4 and 3.0 $\mu g\,g^{-1}$ Al [34].

Reports on concentrations of Al in breast milk indicate a wide range of Al concentrations from 0.004 to 2.67 $\mu g\,cm^{-3}$ Al [8, 34, 35].

5 MIGRATION OF ALUMINUM FROM FOOD PACKING INTO FOODSTUFFS AND LEACHABILITY OF ALUMINUM FROM KITCHENWARE INTO FOODSTUFFS

Al foils are frequently used for packing, and foil containers are used for chilled and frozen food. Investigations of the Al content in foods after being frozen, refrigerated and cooked or baked in Al foil containers showed a very small increase of Al concentrations, compared to the natural Al content in food [36]. Foodstuffs with neutral pH and low salt content such as milk and dairy products, edible fats and oil do not significantly leach Al from Al food packing.

Most Al in packing is used in converted form. This means that the packed goods do not come in contact with the Al itself, since there is a layer of plastic (epoxy-phenolic resin, vinyls) that covers the Al packing. An experiment was carried out in order to evaluate the influence of storage of apple juice on leaching of Al from coated Al cans. The results indicate only a slight increase in Al concentration in apple juice stored for 22 months in coated Al cans [36].

Numerous investigations have been carried out to estimate the extent of leaching from Al utensils. Rajwanshi *et al*. investigated the leaching of Al with organic acids and fluoride [37]. Oxalic acid leached Al more efficiently than acetic, tartaric and citric acids. Fluoride alone was not able to leach Al significantly from utensils, but assisted in leaching Al in the presence of acids. Gramiccioni *et al*. [9] compared the Al content in selected foodstuffs after cooking in Al cookware or in glassware and stainless steel. The data indicated that in general normally salted foods (pasta, beans) did not leach appreciable concentrations of Al from Al cookware during cooking. Tomato sauce leached moderate Al concentrations, which increased after cooking from 2.84 to 5.53 $\mu g\,g^{-1}$ Al. Coffee also leached some Al from cookware. The concentration increased from 0.37 prepared in stainless steel containers to 0.93 $\mu g\,g^{-1}$ Al prepared in Al containers. Similar observations for espresso coffee made in stainless steel (0.35 $\mu g\,cm^{-3}$ Al) and in Al containers (1.1 $\mu g\,cm^{-3}$ Al) were also reported by other investigators [7]. Pickles significantly leached Al during cooking in Al utensils [9]. The concentration of Al after cooking in stainless steel was 0.37 $\mu g\,g^{-1}$ Al, and in Al cookware it was found to be 19.30 $\mu g\,g^{-1}$ Al. Ivanova *et al*. [7] observed similar effects after cooking sauerkraut and sour turnip in Al cookware. The concentrations of Al in the sauce of sauerkraut and sour turnip found after cooking in stainless steel cookware were 0.2 and 0.1 $\mu g\,cm^{-3}$ but after cooking in Al cookware were appreciably higher, 31.3 and 26.0 $\mu g\,cm^{-3}$ Al, respectively.

It can be therefore concluded that Al does not migrate significantly from Al food packings into foodstuffs when food of normal salinity and neutral pH is stored. However, appreciably

high concentrations of Al may be leached during storage or cooking of acidic foodstuffs such as tomato sauce and pickles, containing low molecular mass organic acids. Considering the increased bioavailability of Al complexes with low molecular mass organic acids, the use of Al utensils for such kinds of foods is not recommended.

6 SPECIATION OF ALUMINUM IN FOODSTUFFS

Al speciation has not been frequently applied in the analysis of foodstuffs. The main reason lies in difficulties related to efficient extraction of Al species from solid foods without transformation of these species before analysis. The other reasons are the complexity and variability of the Al species present in foodstuff samples and the lack of reliable speciation techniques for the determination of the variety of Al species. However, there are some reports of speciation of Al in drinking waters and tea infusions.

6.1 Speciation of Al in drinking waters

There are numerous reports on speciation of Al in environmental water samples, but data on Al speciation in tap water are rather scarce. Mitrović *et al*. applied cation-exchange fast protein liquid chromatography (FPLC) – electrothermal atomic absorption spectrometry (ETAAS) for speciation of Al in environmental water samples and in tap water [38]. Al present in tap water of pH 7.6 and a total Al concentration 5.2 $ng\,cm^{-3}$ was eluted from the column with the solvent front, indicating the presence of $Al(OH)_4^-$ species. Gauthier *et al*. [4] investigated the chemical speciation of Al in four drinking water supplies that underwent complete treatment in water purification, including a flocculation step with Al sulfate. The mean total Al concentration in these tap waters was 37 $ng\,cm^{-3}$. The proportion of organic monomeric Al was determined experimentally, and inorganic forms of Al (Al^{3+}, Al-hydroxy species, aluminum fluoro, aluminum silicato and aluminum sulfato species) were estimated using the AL-CHEMI speciation model. Because of the high pH of these waters, the prevailing monomeric Al form was found to be aluminum-hydroxy species.

6.2 Speciation of Al in tea infusions

Flaten and Lund [39] investigated Al speciation in black tea infusions of different origin. The total Al concentrations in tea infusions were about 5 $\mu g\,cm^{-3}$. Speciation of Al was studied by size-exclusion chromatography using postcolumn reaction with pyrocatechol violet and a UV-visible spectrophotometric liquid chromatography (LC) detector for the detection of Al at 580 nm, and organic molecules at 280 nm. A representative chromatogram is presented in Figure 2.2.2.1.

Data from Figure 2.2.2.1 indicate that the Al peak was eluted at 28 min and coeluted with organic molecules. The size of the Al species eluted was estimated on the basis of the calibration of the size exclusion chromatography (SEC) column and was presumed to range from 4,000 to 6,500 Da. The analysis of tea infusions of different origin indicated that Al is bound in the

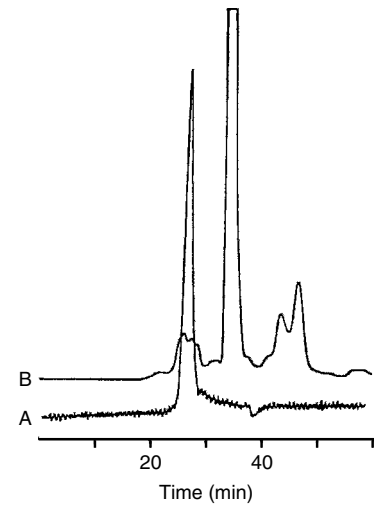

Figure 2.2.2.1. Size-exclusion chromatograms of a tea infusion prepared from a Twinings Earl Gray tea bag, mobile phase 0.12 mol l^{-1} Tris at pH 5.5. (A) Aluminum detected at 580 nm after postcolumn reaction with pyrocatechol violet; (B) organic material detected at 280 nm. (Reprinted from *Sci. Total Environ.,* **207,** Flaten A. K and Lund W, Speciation of aluminum in tea infusions studied by size exclusion chromatography with detection by post-column reaction, 21, (1997) with permission of Elsevier.)

same size-range of organic molecules, irrespective of the origin of the tea. It was estimated that Al-binding ligands in tea infusions might correspond to polyphenolic compounds. Erdemodlu *et al*. [40] investigated the speciation of Al in black tea infusions by a combination of Amberlite XAD-7 and Chelex-100 resins. Al in eluents was determined by flame atomic absorption spectrometry (FAAS). Hydrolyzable polyphenols were retained on an XAD-7 resin, while Chelex-100 resin was used to separate cationic Al species. On the basis of the results, they concluded that about 20% of total Al in black tea infusions corresponds to cationic Al species, and about 30% of Al exists in the form of hydrolyzable polyphenols.

7 CONCLUSIONS

Foodstuffs and drinking water represent potential routes of intake of Al into the human body. Extensive investigations on the total Al concentrations in various foodstuffs indicated that under normal circumstances the average dietary intake of Al is about 6 mg/day. This value is low compared to the recommended upper limit of 60 mg/day for an adult man established by the joint FAO/WHO Expert Committee on Food Additives [23]. The concentration of Al in foodstuffs may increase during the food processing by the use of Al-containing food additives. Al may also migrate to foodstuffs via leaching from kitchenware, particularly when acidic food is prepared in such containers. Al foils and coated Al cans used in food packing do not represent an appreciable source of migration of Al from packing material into foodstuffs. Parenterally administered nutrients, contaminated with Al, may represent a risk of Al intoxication, particularly in infants with reduced kidney function. Infants fed with nutrition formulae may also be exposed to elevated Al concentrations. Drinking water contaminated with Al can represent a potential body burden especially for subjects with impaired renal function.

There is a lack of speciation data on the Al compounds present in foodstuffs. There are only a few reports on the speciation of Al in black tea infusions, indicating that Al may be bound to polyphenolic compounds. There are also some speciation data on the distribution of Al species in tap water, suggesting that Al-hydroxy complexes are the prevailing species.

In order to better understand Al accumulation in the human body, speciation data on representative foodstuffs, especially those with elevated Al concentrations, are needed. There is an open field for scientists to develop new analytical techniques for speciation of Al in such complex matrices as foodstuffs.

8 REFERENCES

1. Fairweather-Tait, S. J. and Hurrell, R. F., *Nutr. Res. Rev.*, **9**, 295 (1996).
2. Alfrey, A. C., Aluminum intoxication in renal failure: a historic overview, in *Aluminum in Chemistry, Biology and Medicine, Vol. 2*, Nicolini, M., Zatta, P. F. and Corain, B. (Eds.), Harwood Academic Publishers GmbH, Switzerland; *Life Chem. Rep.*, **11**, 197 (1994).
3. D'Haese, P. C. and De Broe, M. E., Recent insights in the monitoring, diagnosis and treatment of aluminum-overload in dialysis patients, in *Aluminum in Chemistry, Biology and Medicine*, Vol. 2, Nicolini, M., Zatta, P. F. and Corain, B. (Eds.), Harwood Academic Publishers GmbH, Switzerland; *Life Chem. Rep.*, **11**, 215 (1994).
4. Gauthier, E., Fortier, I., Courchesne, F., Pepin, P., Mortimer, J. and Gauvreau, D., *Environ. Res. Sec. A*, **84**, 234 (2000).
5. Müller, M., Anke, M. and Illing Günther, H., *Food Chem.*, **61**, 419 (1998).
6. Oniawa, P. C., Ikadeh, G. C. and Nweze, S. E., *Food Chem.*, **58**, 351 (1997).
7. Ivanova, S., Šalehar, A., Milačič, R. and Požek-Novak, T., *Kemija v Šoli*, **9/1**, 22 (1997).
8. Sherlock, J. C., Aluminum in foods and the diet, in *Aluminum in Food and the Environment*, Massey, R. C. and Taylor, D. (Eds.), The Royal Society of Chemistry, Cambridge, UK, 1989, pp. 68–76.
9. Gramiccioni, L., Ingrao, G., Milana, M. R., Santaroni, P. and Tomassi, G., *Food Additives Contam.*, **13**, 767 (1996).
10. Trier, S. and Kluthe, R., *Ernährungs-Umschau*, **35**, 307 (1988).
11. Hsu, G. S. W. and Wu, J. Y., *Fu Jen Stud.*, **24**, 69 (1990).
12. Schamschula, R. G., Sugar, E., Un, P. S. H., Duppenthaler, J. L., Toth, K. and Barmes, D. E., *Acta Physiol. Hung.*, **72**, 237 (1988).
13. Wang, L., Su, D. Z. and Wang, Y. F., *Biomed. Environ. Sci.*, **7**, 91 (1994).
14. Nuurtamo, M., Varo, P., Saari, E. and Koivistoinen, P., *Acta Agric. Scand.*, **22**, 57 (1980).
15. Nuurtamo, M., Varo, P., Saari, E. and Koivistoinen, P., *Acta Agric. Scand.*, **22**, 77 (1980).

16. Varo, P., Nuurtamo, M., Saari, E. and Koivistoinen, P., *Acta Agric. Scand.*, **22**, 37 (1980).
17. Varo, P., Lähelmä, O., Nuurtamo, M., Saari, E. and Koivistoinen, P., *Acta Agric. Scand.*, **22**, 89 (1980).
18. Varo, P., Nuurtamo, M., Saari, E. and Koivistoinen, P., *Acta Agric. Scand.*, **22**, 115 (1980).
19. Varo, P., Nuurtamo, M., Saari, E. and Koivistoinen, P., *Acta Agric. Scand.*, **22**, 127 (1980).
20. Ward, N. I. and Savage, J. M., *Sci. Total Environ.*, **146/147**, 309 (1994).
21. Sullivan, D. M., Kehoe, D. F. and Smith, R. L., *J. Assoc. Off. Anal. Chem. Int.*, **70**, 118 (1978).
22. Pennington, J. A. T. and Jones, J. W., Dietary intake of aluminum, in *Aluminum and Health*, Gitelman, H. J. (Ed.), Marcel Dekker, New York, Basel, 1989, pp. 67–100.
23. World Health Organization, Evaluation of Certain Food Additives and Contaminants; Thirty-third Report of the Joint FAO/WHO Expert Committee on Food Additives, WHO Technical Report Series No. 776, WHO, Geneva, 1989, pp. 26–27.
24. Benedik, M. and Milačič, R., Monitoring of Al, Cr, Pb, Cu and Zn in water and dialysis fluid in Haeomodialysis centers in Slovenia, in *Trace Elements in Man and Animals*, Fosher, P. W. F., L'Abbe, M. R., Cockell, K. A. and Gibson, R. S. (Eds.), NCR Research Press, Ottawa, Canada, 1997, pp. 286–287.
25. Greger, J. L. and Sutherland, J. E., *Crit. Rev. Clin. Lab. Sci.*, **34**, 439 (1997).
26. Wilhelm, M., Hoelzer, J., Luebbers, K., Stoehr, G. and Ohmann, C., *J. Trace Elem. Med. Biol.*, **14**, 223 (2001).
27. Sombra, L., Luconi, M., Silva, M. F., Olsina, R. A. and Fernandez, L., *Analyst*, **126**, 1172 (2001).
28. Allwood, M. C., *Nutrition*, **15**, 958 (1999).
29. Klein, G. L., *Am. J. Clin. Nutr.*, **61**, 449 (1995).
30. Klein, G. L., Leichtner, A. M. and Heyman, M. B., *J. Pediatr. Gastroenterol. Nutr.*, **27**, 457 (1998).
31. Bishop, N. J., Morley, R., Day, P. J. and Lucas, A., *N. Engl. J. Med.*, **336**, 1557 (1997).
32. Baydar, T., Aydin, A., Duru, S., Isimer, A. and Sahin, G., *J. Toxicol. Clin. Toxicol.*, **35**, 277 (1997).
33. Baxter, M. J., Burrel, A. A., Crews, H. M. and Massey, R. C., Aluminum in infant formulae and tea and leaching during cooking, in *Aluminum in Food and the Environment*, Massey, R. C. and Taylor, D. (Eds.), The Royal Society of Chemistry, Cambridge, UK, 1989, pp. 77–87.
34. Vinas, P., Padro-Martínez, M. and Hernández-Córdoba, M., *J. AOAC Int.*, **84**, 1187 (2001).
35. Mandić, M., Grgić, J., Grgić, Z., Seruga, M. and Hasenay, D., *Sci. Total Environ.*, **170**, 165 (1995).
36. Severus, H., The use of aluminum – especially as packaging material – in the food industry, in *Aluminum in Food and the Environment*, Massey, R. C. and Taylor, D. (Eds.), The Royal Society of Chemistry, Cambridge, UK, 1989, pp. 88–101.
37. Rajwanshi, P., Singh, V., Gupta, M. K., Shrivastav, R., Subramanian, V., Parkash, S. and Dass, S., *Bull. Environ. Contam. Toxicol.*, **63**, 271 (1999).
38. Mitrović, B., Milačič, R., Pihlar, B. and Simončič, P., *Analusis*, **26**, 381 (1998).
39. Flaten, A. K. and Lund, W., *Sci. Total Environ.*, **207**, 21 (1997).
40. Erdemodlu, S. E., Pyrzyniska, K. and Gücer, S., *Anal. Chim. Acta*, **411**, 81 (2000).

2.2.3 Speciation of Aluminum in Clinical Aspects (Health & Disease)

Radmila Milačič

Jožef Stefan Institute, Ljubljana, Slovenia

1 INTRODUCTION

Aluminum (Al) has no known biological function in living cells but exhibits biological toxicity in experimental models [1–4] and, in particular, in patients undergoing regular dialysis [5, 6]. Al is related to many clinical disorders such as renal osteodystrophy [7], microcytic anemia [8] and dialysis encephalopathy [9]. Al accumulation in brain has also been related to the neurodegenerative process in Alzheimer's disease [10, 11], but it is still a matter of debate whether Al is deposited in the brain compartments as the result of or as the inducer of Alzheimer's disease.

Although Al is the most abundant metal in the environment, the sparingly soluble nature of most Al compounds considerably decreases the probability of an Al body burden in humans from environmental sources. Therefore, the normal body burden of Al is rather low, less than 35 mg, distributed, with the exception of the lung, in all human tissues at concentration levels of 2–3 $mg\,kg^{-1}$ dry mass [5]. The reported normal serum Al concentrations are also low, ranging from 0.5 to 8 $ng\,cm^{-3}$ Al [12], and a recent report from Sanz Medel's group indicated even lower normal Al concentrations, around 2 $ng\,cm^{-3}$ Al or less [13]. The main route of entry of Al into the human body is through consuming drinking water with high Al concentrations. The sources of elevated Al concentrations in drinking water are either owing to the use of flocculating agents

Handbook of Elemental Speciation II: Species in the Environment, Food, Medicine & Occupational Health
Edited by R. Cornelis, H. Crews, J. Caruso and K. G. Heumann
 ISBN: 0-470-85598-3 (HB)

such as $Al_2(SO_4)_3$ or to soil acidification and consequential release of soluble Al species into surface, ground and drinking waters. Al overload in patients with chronic renal failure has been largely prevented by eliminating aluminum-containing phosphate-binding agents and by the use of high-purity water for preparation of dialysis fluids [14]. However, Al may still enter the body of dialysis patients via consumption of food and beverages and, in particular, by consumption of Al-based drugs and antacids [15]. Several epidemiological studies also indicated a connection between an increased risk of various mental disorders, including Alzheimer's disease, and elevated Al levels in drinking water [16, 17].

In order to better understand Al transportation in the human body, it is necessary to know the chemical species in which Al is present in body fluids and tissues [18]. Among a variety of biological samples, Al speciation was most frequently investigated in human serum. Progress was made in the development of analytical techniques for the determination of the amount and composition of high molecular mass Al (HMM-Al) as well as low molecular mass Al (LMM-Al) species in human serum. However, because of the complex chemistry of Al in serum, its low total concentration and the high risk of contamination by extraneous Al, speciation of Al in biological fluids is still a difficult task for analytical chemists.

2 ALUMINUM-BINDING LIGANDS IN HUMAN SERUM

2.1 Potential high molecular mass Al-binding ligands

There is a broad consensus that most Al in human serum is bound to proteins. This fraction is considered to be the HMM-Al fraction. Although albumin (M_w 66,000) is present in human serum at concentrations of about 40 $g\,dm^{-3}$, it is too weak as a metal ion binder at physiological pH values (7.4) to be able to effectively compete for Al^{3+} with other much stronger Al^{3+} carriers such as citrate and transferrin [19, 20].

The concentration of transferrin (M_w 77,000) in normal human serum is about 3 $g\,dm^{-3}$. Transferrin has two metal-ion-binding sites per molecule. Since it is only 30% saturated with Fe^{3+}, it has available about 50 $\mu mol\,dm^{-3}$ of unoccupied metal binding sites. So it can be regarded as a potential binding ligand for Al^{3+} under physiological conditions [19–21]. Because of the unique involvement of the synergistic bicarbonate anion in the formation of metal-transferrin complexes, metals are only bound as a ternary complex between the metal, the protein and a carbonate anion. The Al^{3+} binding constants to transferrin are high; Log K_1 is 12.9 and Log K_2 12.3. Since the corresponding Fe^{3+} binding constants are much higher (Log K_1 22.7 and Log K_2 22.1), Al^{3+} is not competitive with Fe^{3+} in binding transferrin [20]. It is possible that Al^{3+} and other toxic metals that strongly bind to transferrin enter the brain by this pathway [19].

2.2 Potential low molecular mass Al-binding ligands

Citrate occurs in human serum at a concentration of about 0.1 $mmol\,dm^{-3}$ [19, 22] and is considered to be one of the major LMM-Al binding ligands in mammalian serum [19]. Martin [23, 24] and Venturini and Berthon [25] calculated the distribution of Al^{3+} species in the presence of 0.1 $mmol\,dm^{-3}$ of citrate in a wide pH range. At pH < 3, the prevailing species is Al^{3+}. At pH values near 3, the positively charged citrate complex $AlLH^+$ coexists with Al^{3+}. At pH 3–5, the prevailing species is neutral AlL°. As the pH increases, AlL° undergoes deprotonation with $pK_b = 3.4$. The resulting $AlLH_{-1}^-$ species contains three anionic carboxylate groups and a deprotonated citrate hydroxy group. The $AlLH_{-1}^-$ species prevails in the pH range from 4 to 7.5. At pH > 7.5, water-derived $Al(OH)_4^-$ occurs and dominates at pH > 8. Although most of the citrate in serum is present as the Ca^{2+} complex, Al^{3+} easily displaces Ca^{2+} from citrate. Citrate solubilizes Al^{3+} from insoluble $Al(OH)_3$ and $AlPO_4$. It is therefore strongly recommended that citrate compounds are avoided in the diet of dialysis patients [22].

In human serum, the total concentration of phosphate is about 2 mmol dm^{-3} [22]. Al^{3+} readily forms sparingly soluble species with PO_4^{3-}, which may precipitate from body fluids as a mixed phosphato-hydroxy complex and under serum conditions may be described as $Al(PO_4)_{0.2}(OH)_{2.4}$. Because of precipitation reactions, the solution chemistry of the phosphate system may be directly studied only at pH < 4, so it was scarcely investigated [26]. In many investigations, soluble Al-phosphate species were not involved in speciation models, and citrate was considered as the prevailing LMM-Al species in human serum [22–25]. In order to estimate the binding constants of Al-phosphate species at physiological pH, linear free-energy relationships (LFER) have been used. Stability constants estimated by LFER calculations were then used in computer modeling of Al-phosphate at physiological pH. The prevailing LMM-Al species in human serum was deduced to be the mixed hydroxy complex $Al(PO_4)(OH)^-$ [27, 28].

Proposed models for biological speciation considered only binary species of Al^{3+} with LMM ligands. Since biological systems contain various potential LMM-Al binding ligands, the formation of ternary Al complexes is also possible. In the group of Kiss [29], a comprehensive investigation was carried out on the main potential LMM-Al binders in blood serum. The species distribution of binary aluminum citrate (A) and aluminum phosphate (B) and ternary aluminum citrate phosphate systems was calculated in a pH range from 2 to 8. The stability constants for the neutral and slightly alkaline pH range were estimated on the basis of LFER calculations. The data clearly demonstrated that at physiological pH, the LMM-Al species present in serum are binary citrate $(AlAH_{-2})^{2-}$ and phosphate $(AlBH_{-1})^-$ complexes, and ternary species $(AlAB)^{3-}$ and $(AlABH_{-1})^{4-}$. The percentage of particular LMM-Al species varies with the total concentration of Al in serum.

Other LMM constituents of blood serum such as lactate, oxalate and amino acids have significantly lower affinities for Al^{3+} than citrate and phosphate and were therefore not considered in modeling calculations [29]. The presence of $Al(OH)_4^-$ was predicted in human serum but at a very low concentration, representing only about 3% of total LMM-Al species [27].

3 ANALYTICAL TECHNIQUES AND CHEMICAL SPECIATION OF ALUMINUM IN HUMAN SERUM

The main problem in chemical speciation of Al in the serum of healthy subjects is the very low Al concentration (a few ng cm^{-3}) [12, 13] and contamination by extraneous Al. The speciation of Al in healthy subjects was therefore in general possible only in spiked samples. To avoid contamination with extraneous Al, high-density polyethylene or Teflon ware should be used, previously soaked with 10% HNO_3 for 48 h and rinsed with high-purity water (MiliQ, water doubly distilled in quartz) [30]. Speciation analysis should be carried out under clean room conditions (at least class 10,000). In order to remove Al from eluents used in chromatographic procedures, Van Landeghem *et al.* [31] applied an on-line silica-based C_{18} scavenger column that had a strong affinity to adsorb Al. Similarly, Soldado *et al.* [32] used an Al scavenger column containing Chelex 100 chelating agent adsorbed on C_{18} bonded silica. Bantan *et al.* [33] treated the chromatographic eluent first with the chelating resin Chelex 100 (batch procedure). After decanting and filtering, the eluent was passed through a silica-based high performance liquid chromatography (HPLC) LiChrosorb RP-18 column to remove traces of Al. Since the fast protein liquid chromatography (FPLC) columns used in the speciation procedure also contained trace amounts of Al, cleaning of the resin column was performed by passing 10 cm^3 of 5 mol dm^{-3} citric acid through the column. A similar cleaning procedure was also applied to remove traces of Al efficiently from microultrafiltration membranes Centricon 30 [33].

To obtain reliable analytical data in speciation of Al in biological samples, it is extremely important to avoid all possible sources of contamination and to apply appropriate cleaning procedures for removing traces of Al from the eluents,

reagents, columns and filtering devices used in the speciation procedure.

3.1 Determination of HMM-Al species in human serum

In order to determine the percentage of Al bound to the protein serum fraction, HMM-Al species were separated from LMM-Al species by ultrafiltration procedures. The quantification and characterization of Al-binding protein was performed by using different chromatographic procedures in combination with various detection techniques. The most intensive investigations in the area of determination of HMM-Al species were carried out in the group of Sanz Medel [32, 34–39].

3.1.1 Fractionation of Al in human serum

Pérez Parajón *et al*. [34] critically appraised the speciation of Al in serum by ultrafiltration and highlighted the problems of contamination that led to controversial results reported by previous investigators. The authors compared ultrafiltration and microultrafiltration procedures. Al in filtrates was determined by electrothermal atomic absorption spectrometry (ETAAS). Since the classical ultrafiltration procedure was more liable to the contamination with extraneous Al, microultrafiltration, which minimized contamination risk, gave more reliable results. Data indicated that in spiked serum of healthy subjects, about 8% of total Al was ultrafiltrable, while in renal patients this percentage was about 13%. From these data, it was concluded that most Al (about 90%) is bound to the HMM protein fraction and was in agreement with data from some other investigators [40, 41]. Pérez Parajón *et al*. [34] also found that after desferroxiamine (DFO) chelation therapy in renal patients, total serum Al and the ultrafiltrable fraction increased significantly. The reason was most probably the mobilization of Al by DFO from body tissues and serum proteins. Wróbel *et al*. [35] reported that about 11% of total serum Al was ultrafiltrable. They found that the percentage was influenced neither by the individual renal pathology of the patients nor by kidney transplantation. In patients undergoing DFO chelation therapy, the total Al was significantly increased. In one patient, the serum Al concentration was increased from 60 ng cm^{-3} before DFO treatment to 180 ng cm^{-3} after DFO treatment. In another patient, an increase in Al concentration from 15 to 150 ng cm^{-3} was observed. The ultrafiltrable fraction that represented about 11% of total Al before DFO treatment was increased to almost 80% of total serum Al after DFO treatment. In further investigations, Wróbel *et al*. [36] reported that ultrafiltrable Al in spiked human serum was found to be $12 \pm 5\%$. Fractionation data obtained by other investigators indicated that in normal, nonexposed subjects the percentage of microultrafiltrable Al was about 20% [33, 42]. It was also experimentally demonstrated [33] that the percentage of LMM-Al in spiked serum was the same, regardless of the total Al concentration in the spiked serum, when samples were spiked with 50 to 150 ng cm^{-3} of Al^{3+}. However, it was found that the percentage of ultrafiltrable Al varied among different pooled serum samples and ranged from 15 to 19% [33].

Fractionation of serum by the microultrafiltration procedure gives information on the ratio between HMM-Al and LMM-Al in human serum. It can also provide a useful analytical tool in the estimation of the efficiency of the chelation therapy.

3.1.2 Chromatographic procedures for the determination of HMM-Al species in human serum

In order to quantify and characterize the Al-binding proteins in serum, chromatographic procedures in combination with various specific detection techniques are required. Many investigators used size-exclusion chromatography (SEC). The SEC analysis of protein-bound Al in serum is rather complicated because of the critical role of bicarbonate in the binding of Al by transferrin [21]. In the absence of bicarbonate in the eluting buffer, more peaks and a greater proportion of LMM-Al fraction were observed [43]. In contrast, when bicarbonate was added to the eluting buffer, fewer peaks

were observed in the SEC chromatogram, and the largest peak appeared in the transferrin/albumin region [44]. Because of the poor resolution between transferrin and albumin, it was not possible to identify the Al-binding protein in serum by SEC procedures. To obtain higher resolution in separation of serum proteins, anion-exchange chromatographic columns were applied. Blanco González *et al*. [37] and Garciá Alonso *et al*. [38] used a TSK DEAE-3SW silica-based ion-exchange column and 0.05 mol dm^{-3} tris(hydroxymethyl)-aminomethane (TRIS-HCl) buffer with "off-line" detection of separated species by ETAAS [37], or "on-line" Al derivatization with 8-hydroxiquinoline-5-sulfonic acid and molecular fluorimetric detection [38]. Their investigations indicated that Al was bound only to transferrin, but a significant amount of Al was retained by the silica-based column support. To prevent Al adsorption on the column, Wróbel *et al*. [36] used a polymeric anion-exchange (Protein Pak DEAE-5-PW) column for separation of serum proteins. Linear gradient elution was applied in 30 min, using (0–1.0 mol dm^{-3}) NaCl in TRIS-HCl buffer (pH 7.4) containing 0.01 mol dm^{-3} of $NaHCO_3$. The elution profile was detected with a UV detector at 280 nm and Al determined in 600 μL fractions "off-line" by ETAAS. The fraction containing Al-binding protein was also characterized by SDS-PAGE electrophoresis. The results again confirmed that transferrin was the only serum protein that binds Al. To exclude the risk of displacement of Al from the protein during the chromatographic procedure, Soldado Cabezuelo *et al*. [32] used faster separation columns. An anion-exchange FPLC Mono Q HR 5/5 column was applied in speciation of spiked human serum and serum of uremic subjects. Linear gradient elution was applied in 20 min using (0–0.25 mol dm^{-3}) NaCl in TRIS-HCl buffer (pH 7.4) containing 0.01 mol dm^{-3} of $NaHCO_3$. A Chelex 100 scavenger column was used "on-line" to clean up the eluents (<1.5 μg cm^{-3} Al) before they entered the analytical column. UV detection at 280 nm was used to characterize the serum proteins, and Al was determined in 500 μL fractions "off-line" by ETAAS. An example of such speciation analysis of serum from a dialysis patient is presented in Figures 2.2.3.1 and 2.2.3.2.

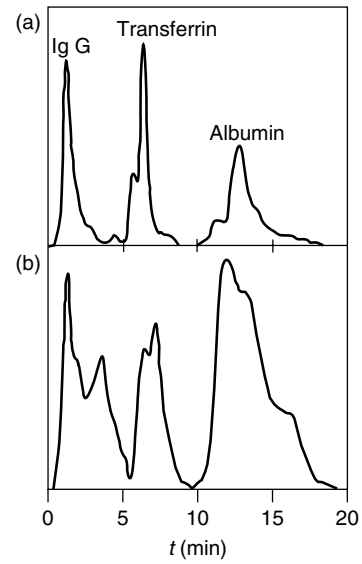

Figure 2.2.3.1. Anion-exchange FPLC separation of human serum proteins: (a) standard solution (0.5 g L^{-1} transferrin, 5 g L^{-1} albumin and 1 g L^{-1} immunoglobulin G); and (b) diluted (1 + 4) uremic serum. Detection at 280 nm. (Reproduced from Reference [32] by permission of the Royal Society of Chemistry.)

These data demonstrate that both Al and transferrin are eluted from 6 to 8 min, confirming that Al is bound to transferrin. To obtain lower limits of detection enabling speciation of Al in unspiked serum of normal subjects on an anion-exchange Mono Q HR 5/5 column, Soldado Cabezuelo *et al*. [39] used "on-line" quadrupole inductively coupled plasma mass spectrometry (ICP-MS) and high-resolution ICP-MS systems in detection of separated Al species. Proteins were detected by UV spectrophotometry at 295 nm. Linear gradient elution was applied in 15 min using (0–0.25 mol dm^{-3}) ammonium acetate in TRIS-HCl buffer (pH 7.4). Traces of Al in eluents were removed by using a Chelex 100 scavenger column. The high-resolution ICP-MS detection system enabled "on-line" speciation of unspiked human serum containing 2.5 ng cm^{-3} of total Al. In the eluting volume typical of transferrin, two distinct peaks were obtained, presumably indicating two binding sites of Al in transferrin [19–21]. Nagaoka and Maitani [45] used the same FPLC Mono Q HR 5/5 column and the same buffer as

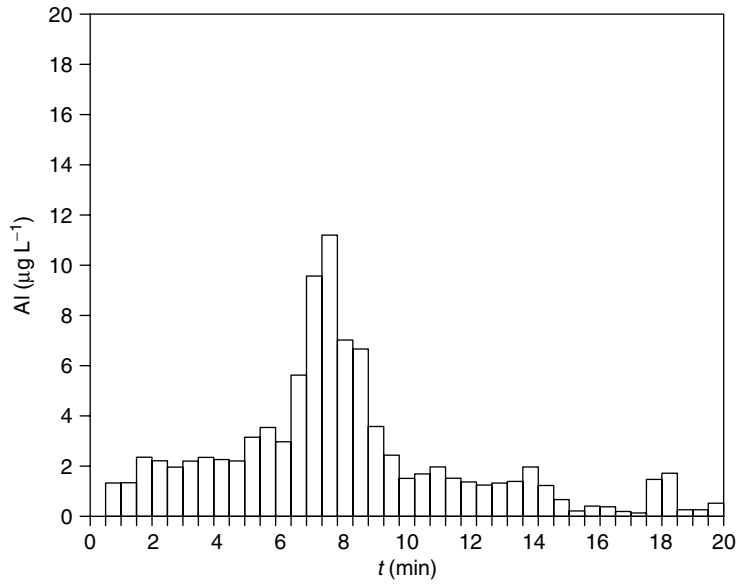

Figure 2.2.3.2. Aluminum elution profile, as detected by ETAAS, of a representative undiluted serum sample (total Al content 92 $\mu g L^{-1}$) from a dialysis patient. (Reproduced from Reference [32] by permission of the Royal Society of Chemistry.)

Soldado Cabezuelo *et al*. [39] but different gradient elution conditions in 50 min. By combining UV (280 nm) detection of eluting proteins and high-resolution ICP-MS detection of Fe and Al, they concluded that Al is selectively bound to the N-lobe site of transferrin.

The above experimental data obtained by chromatographic and various detection techniques demonstrated that the HMM-Al binding ligand in human serum is transferrin. These conclusions agree with theoretical predictions that transferrin is a potential protein-binding ligand for Al^{3+} at physiological conditions [19–21]. The experimental microultrafiltration data indicate that the HMM-Al protein fraction represents 80 to 90% of total serum Al.

3.2 Determination of LMM-Al species in human serum

To complete information on modeling of LMM-Al complexes in human serum [22–29], it is also necessary to determine the amount and the composition of these species. This requirement was also pointed out in investigations of Al toxicity in humans. As described above (Section 3.1.1.), first attempts were made to fractionate HMM-Al from LMM-Al complexes by microultraltrafiltration. Reported data indicated that 8–20% of total Al in serum of healthy subjects corresponded to ultrafiltrable LMM-Al species [33–36, 40–42]. With the exception of one report [42], all experiments on serum of healthy subjects have been performed using spiked samples.

The composition of LMM-Al species in human serum was investigated by different chromatographic procedures in combination with various detection techniques. Keirsse *et al*. [46] applied SEC analysis with ETAAS detection for speciation of Al species in spiked serum of a healthy volunteer and the spiked hemofiltrate of a uremic patient. Besides the HMM fraction, which represented 40% of total Al in the spiked serum, two unidentified LMM fractions of Al were separated on a P10 Bio-gel column. Two unidentified LMM fractions of Al were also observed in the spiked hemofiltrate sample separated on a P4 gel. Favarato *et al*. [47] employed a TSK-GEL HW 55S SEC column for separation of Al species present in the serum of normal and occupationally exposed

subjects. Separated Al species were determined by ETAAS. In addition to one HMM-Al fraction, three to five separated LMM fractions that contained Al were also found but not identified. Leung *et al*. [48] examined the *in vitro* effect of citrate and DFO on Al-binding constituents in serum from a patient with chronic renal failure by gel filtration chromatography on a Bio-gel P-2 column and by FPLC chromatography using Superose-6 HR 10/30 and HR 15/50 columns. Separated Al species were determined by ETAAS. It was found that after addition of an excess of citric acid to serum, the chromatographic peak that was presumed to correspond to aluminum citrate was significantly increased.

In order to determine the composition of LMM-Al species present in human serum, there was a need for the development of more powerful speciation techniques. Since aluminum citrate has been theoretically predicted as one of the important LMM-Al binding ligands in human serum [22–25, 29], efforts were directed to the development of a reliable analytical procedure for speciation of this biologically important molecule.

3.2.1 Analytical techniques for the speciation of aluminum citrate and some other LMM-Al species

An intensive study of the possibilities of aluminum citrate speciation by HPLC with ETAAS detection was reported by Datta *et al*. [49]. The potential for separation of aluminum citrate from other Al species was investigated by the use of normal, reversed-phase and mixed-phase (ODS/NH_2) columns and various mobile phases. The best results for synthetic standard solutions of aluminum citrate were obtained when cyclobonded and cyanobonded phase columns were employed using a mobile phase composed of $MeOH : H_2O$ (1 : 1, v/v) with TEA and glacial acetic acid (pH 4.0). However, the retention characteristics were not reproducible and aluminum citrate recoveries were moderate and did not exceed 65%, most probably due to adsorption of Al on the silica-based columns. For that reason, the technique was not recommended for routine quantification of aluminum citrate in biological samples. In the group of Milačič, first data on quantitative determination of aluminum citrate in synthetic solutions [50] and the application of the technique developed to speciation of LMM-Al species in serum samples [33, 51, 52] were reported. Bantan *et al*. [50] applied separation on a Mono Q HR 5/5 strong anion-exchange column with ICP-AES detection, using aqueous 0 to 4 mol dm^{-3} $NaNO_3$ gradient elution in 10 min. The hydrophilic polyether resin-based column substituted with quaternary amine groups enabled quantitative determination of synthetic solutions of aluminum citrate over a wide pH range from 3.5 to 11.0. Data from this study are presented in Figure 2.2.3.3.

It can be seen that in the pH range from 6.5 to 7.4, negatively charged aluminum citrate complexes were quantitatively eluted from 5.0 to 6.0 min with a maximum peak at 5.5 min. At pH values lower than 6.0, the percentage of negatively charged species decreased, presumably due to a neutral aluminum citrate complex appearing in the solution. At pH 3.5, a broad peak was observed for the positively charged citrate complex at an elution time from 1.0 to 3.0 min, and a small peak also occurred at the retention time of negatively charged aluminum citrate complexes. It was proven that species that were not eluted at pH values lower than 6.0 (neutral aluminum citrate, Al^{3+}) were strongly adsorbed on the resin column and did not influence subsequent separations. On increasing pH values above 7.4, the percentage of negatively charged aluminum citrate species decreased since the predominant species becomes $Al(OH)_4^-$, which was eluted from 2.0 to 3.0 min. Because of its high tendency to adsorb strongly on the column, this species was quantitatively determined only at pH 11.0. The distribution of Al species versus pH, in the presence of an excess of 3 mol dm^{-3} citric acid (Figure 2.2.3.3), in general agree with the calculated data reported by Martin [23, 24] and Venturini and Berthon [25]. The experimental data with other LMM-Al complexes indicated that at physiological pH negatively charged Al-EDTA and aluminum oxalate complexes were also separated from aluminum citrate. Although the repeatability of measurement was very good (RSD 2%), the applicability of the

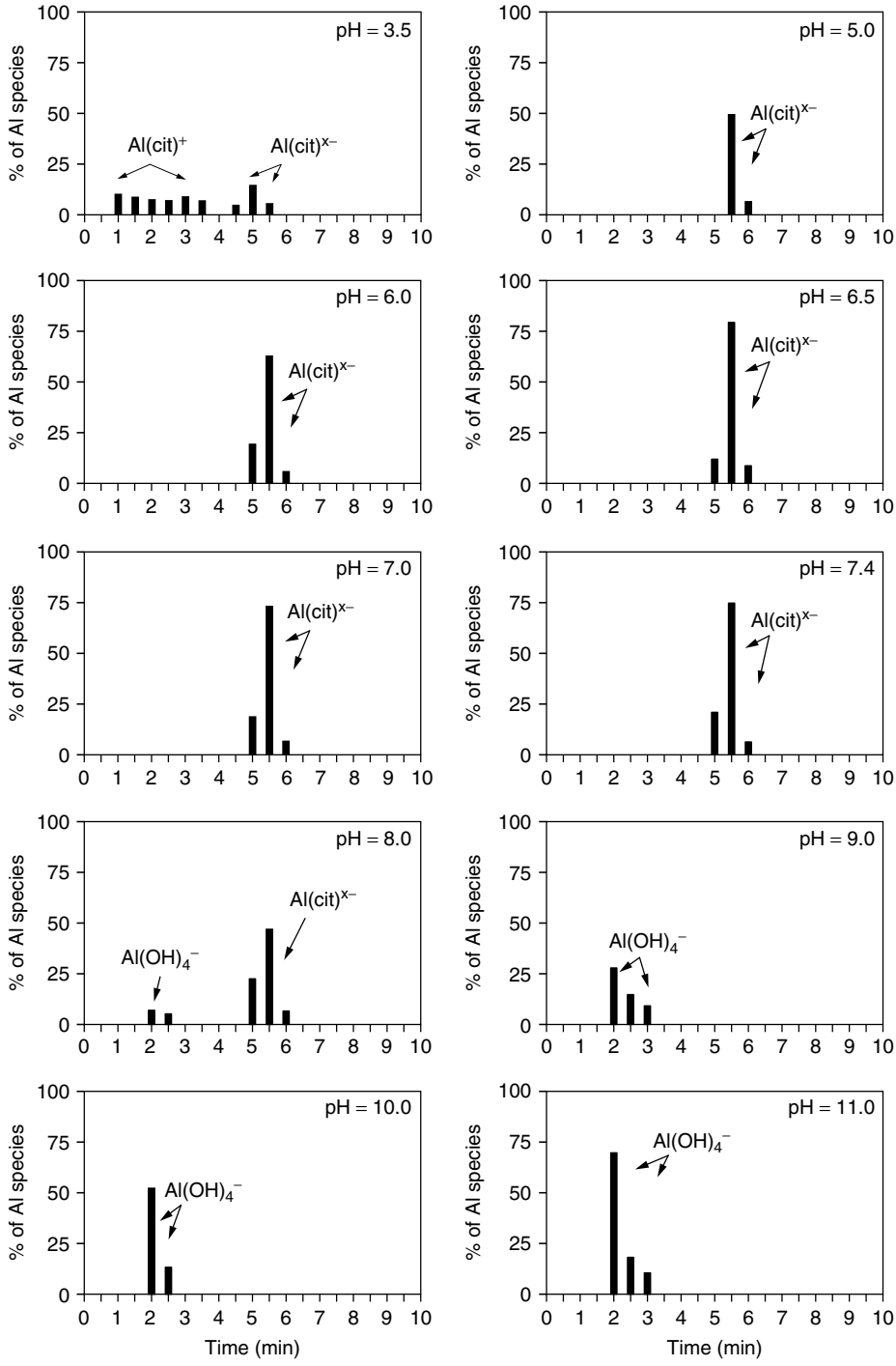

Figure 2.2.3.3. Influence of pH on the distribution of Al species (2.5 μg Al cm^{-3}, 3 M excess of citric acid) employing anion-exchange FPLC with ICP-AES detection (fraction collection 0.5 cm^3). The percentage of monomeric Al species in synthetic samples of aluminum citrate. Mono Q HR 5/5 column, sample volume 0.5 cm^3, aqueous-$NaNO_3$ (4 mol dm^{-3}) linear gradient elution, flow rate 1 cm^3 min^{-1}, $n = 3$. (Reference 50).

developed technique to most biological samples was limited because of its moderate sensitivity (LOD 0.1 $\mu g\,cm^{-3}$ of separated Al species).

3.2.2 Determination of LMM-Al species in human serum: an analytical approach

Because of the very low total concentration of Al in human serum [12, 13], speciation of LMM-Al in healthy subjects was possible only in spiked samples. Most investigators spiked serum with Al^{3+} so that the concentration of total Al in serum after spiking ranged between 100 and 200 $ng\,cm^{-3}$ and was similar to concentrations that could be found in serum of some dialysis patients. Since reported concentrations of ultrafiltrable Al in serum represented only 10–20% of total Al [33–36, 40–42], it was necessary to apply very sensitive analytical procedures in order to identify and quantify the LMM-Al complexes present in spiked serum and serum of dialysis patients.

A previously developed anion-exchange FPLC-ICP-AES procedure [50] using $NaNO_3$ as eluent was not sensitive enough. To lower the detection limits for speciation of aluminum citrate to the low $ng\,cm^{-3}$ concentration level, the choice of an appropriate eluent that enabled quantitative separation of aluminum citrate on a Mono Q HR 5/5 strong anion-exchange column and reliable determination of separated Al species by ETAAS played a critical role. For this purpose, Bantan *et al.* [33] examined the capability of various eluent solutions. Aqueous 0–4 $mol\,dm^{-3}$ NH_4NO_3 gradient elution was found to separate quantitatively aluminum citrate on a strong anion-exchange Mono Q HR 5/5 FPLC column in the pH range 6.5 to 7.4. The main advantage of NH_4NO_3 eluent lies in its ability to decompose quantitatively in the graphite tube during the ashing step. This enabled quantitative and very reproducible (RSD 2%) determinations of separated Al species by ETAAS in 0.5 cm^3 fractions collected throughout the chromatographic procedure. Negatively charged aluminum citrate was quantitatively eluted from 4.5 to 5.5 min. The low limit of detection for separated species (2 ng aluminum citrate cm^{-3}) provided the possibility of applying the technique for the analysis of LMM-Al species in spiked human serum. An investigation was performed in spiked (50–150 ng Al^{3+}, nitrate salt) pooled serum of healthy volunteers. All the necessary steps to avoid contamination as described above in Section 3 were considered [33]. Samples were first microultrafiltered. Speciation analysis of the microultrafiltrable fraction representing 15–19% of total Al indicated that LMM-Al species were quantitatively eluted under the elution time typical of aluminum citrate. On the basis of these observations, it was presumed that LMM-Al corresponded to aluminum citrate.

In addition to citrate [22–25], phosphate [27, 28] and ternary citrate-phosphate complexes [29] have also been considered to be important LMM-Al species present in human serum. So it was necessary to provide more detailed information on the identity of the Al species eluted under the chromatographic peak [33]. For this purpose, Bantan *et al.* [51] characterized LMM-Al species in spiked serum not only on the basis of the retention time but also by ES-MS-MS analysis of the LMM ligands eluted under the chromatographic peak. The study was performed on the spiked serum of eight healthy subjects in order to estimate individual variability in the percentage and composition of LMM-Al species. Separation and determination of Al was performed as described previously [33]. To obtain better selectivity, 0.2 cm^3 fractions were collected throughout the chromatographic run and in the fractions containing Al, ES-MS-MS analysis was performed. Two examples of such analysis (two different spiked samples, No. I and IV) are presented in Figures 2.2.3.4 and 2.2.3.5.

The mass spectra in Figure 2.2.3.4 (sample No. I) indicated that in the fraction eluted from 2.4 to 2.6 min a phosphate-binding ligand (peak m/z 97 and corresponding daughter ion spectra with m/z 97 and 79) was present, whereas in the fraction eluted 3.0 to 3.2 min the presence of a citrate binding ligand was confirmed (peak m/z 191 and the corresponding daughter ion spectra with m/z 111, 87 and 85). Mass spectra from Figure 2.2.3.5 (sample No. IV) indicated that in the fraction eluted from 2.4 to 2.6 min a phosphate-binding ligand (peak m/z 97 and the corresponding

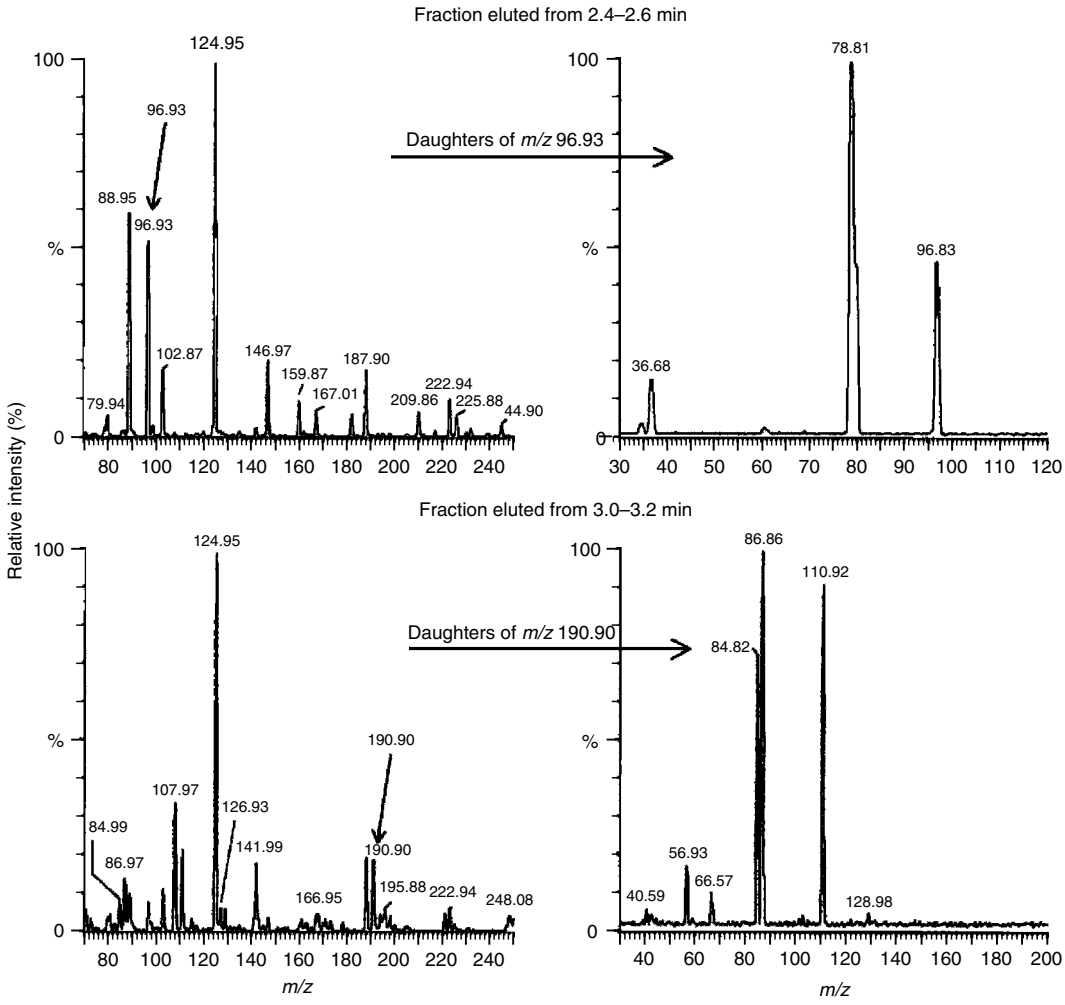

Figure 2.2.3.4. ES-mass spectra and corresponding daughter ion mass spectra of m/z 191 and 97 for eluted fractions from 2.4 to 2.6 min and 3.0 to 3.2 min, respectively, on an anion-exchange FPLC column for serum sample No. I. (Reproduced from Reference [51] by permission of The Royal Society of Chemistry.)

daughter ion spectra with m/z 97 and 79) was present, whereas in the fraction eluted from 3.0 to 3.2 min the presence of both phosphate (peak m/z 97 and corresponding daughter ion spectra with m/z 97 and 79) and citrate (peak m/z 191 and corresponding daughter ion spectra with m/z 111, 87 and 85) binding ligands was confirmed. On the basis of these analyses, aluminum citrate and aluminum phosphate were identified in sample No. I, whereas in sample No. IV aluminum phosphate and ternary aluminum citrate phosphate species were present. These data are in agreement with the computer-aided speciation calculations in human serum performed in the group of Kiss [29]. (See Figure 2.2.3.6 and compare data at pH 7.4).

The experimental data of Bantan *et al.* [51] further indicate that the distribution of LMM-Al species varied among particular individuals. Individual variability was also observed in the percentage of LMM-Al species in spiked serum, which ranged from 14 up to 55%. The same analytical procedure was also applied by the same group to an

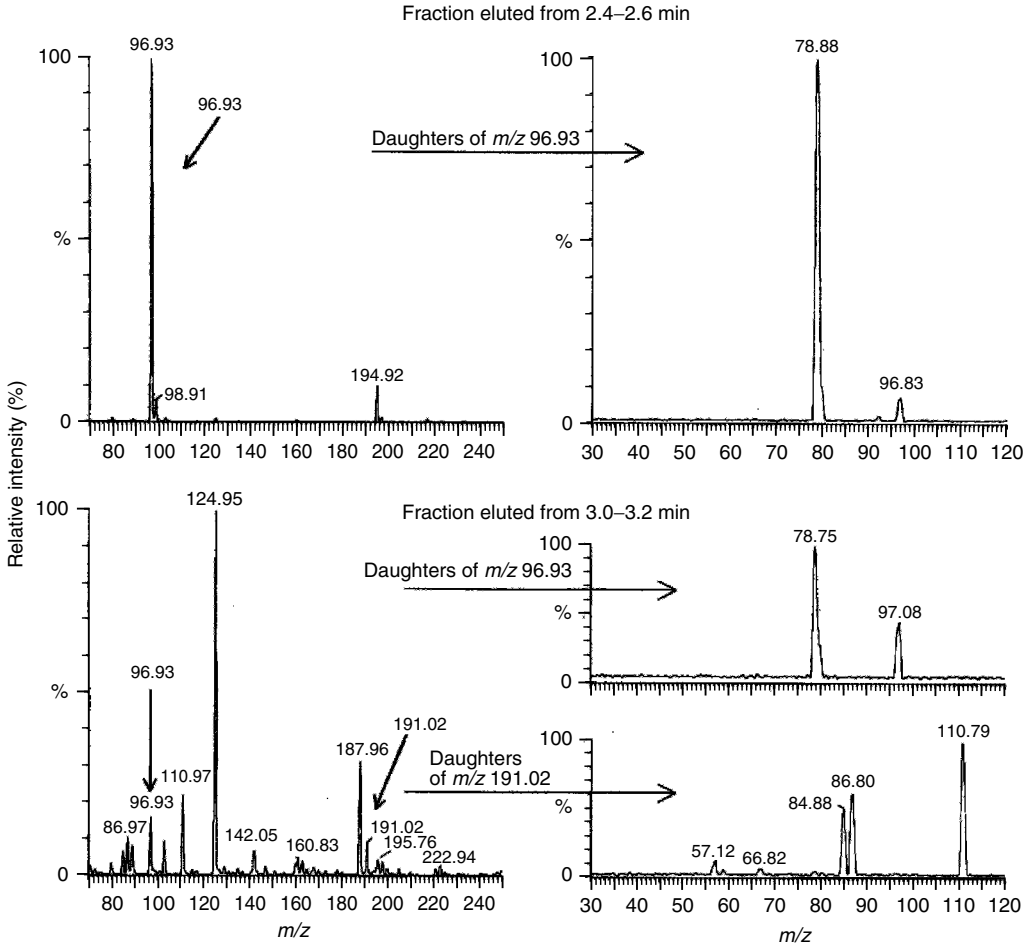

Figure 2.2.3.5. ES-mass spectra and corresponding daughter ion mass spectra of m/z 191 and 97 for eluted fractions from 2.4 to 2.6 min and 3.0 to 3.2 min, respectively, on an anion-exchange FPLC column for serum sample No. IV. (Reproduced from Reference [51] by permission of The Royal Society of Chemistry.)

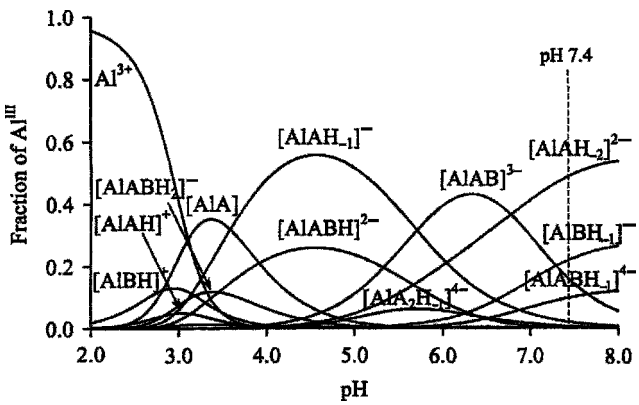

Figure 2.2.3.6. Species distribution curves for complexes formed in the Al^{III}-citrate-phosphate system at serum concentrations ($c_{Al} = 6 \times 10^{-7}$ M, $c_{citrate} = 99 \times 10^{-6}$ M, $c_{phosphate} = 1.1 \times 10^{-3}$ M). (Reproduced from Reference [29] by permission of Wiley VCH.)

investigation of the speciation of LMM-Al species in the serum of six continuous peritoneal dialysis patients [52]. Three serum samples with low total Al concentrations (below 12 ng cm^{-3}) were spiked before speciation analysis, whereas the high total Al concentrations in serum of three patients who consumed Al-based drugs (80 to 130 ng cm^{-3} Al) enabled determination of the percentage and for the first time also the distribution of LMM-Al complexes in nonspiked samples. It was demonstrated that the percentage of LMM-Al species in the serum of continuous ambulatory peritoneal dialysis (CAPD) patients in spiked and nonspiked samples ranged from 24 to 53% and in one nonspiked sample was even 100%. The authors did not find a reason for such a high content of LMM-Al species in this particular sample. LMM-Al species in spiked and nonspiked samples corresponded to Al-phosphate, aluminum citrate and ternary aluminum citrate phosphate complexes. It was also demonstrated that spiking of serum with Al^{3+} did not influence the distribution of LMM-Al species. Therefore, spiking may be applied in the investigations of the distribution of LMM-Al complexes in serum, when the total concentration of Al is too low to perform reliable speciation analysis.

4 CONCLUSIONS

Al is involved in many health disorders. In order to understand the mechanisms of Al toxicity, its transport through the human body and its accumulation in target organs, speciation analysis may contribute important information. In the last two decades, numerous investigations have been carried out on computer modeling and on the development of reliable analytical techniques for speciation of Al in biological samples. Human serum was the most intensively investigated. Because of the very low concentrations of Al in serum of normal subjects (a few ng cm^{-3}) and the environmental abundance of Al, there is a high risk of contamination during speciation analysis. Appropriate handling of samples and cleaning procedures should be applied in order to avoid contamination by extraneous Al. In addition, analysis should be performed under clean room conditions. Anion-exchange FPLC with UV and ETAAS or high-resolution ICP-MS detection were found to be the most convenient analytical techniques for the determination of HMM-Al binding ligands. In combination with SDS-PAGE electrophoretic analysis of separated protein fractions containing Al, it was confirmed that transferrin is the Al-binding protein in human serum. The percentage of this HMM-Al species ranged between 80 and 90% of total serum Al. The combination of microultrafiltration and speciation analysis of ultrafiltrable Al by anion-exchange FPLC and ES-MS-MS techniques demonstrated that the LMM-Al fraction is composed of aluminum citrate, aluminum phosphate and ternary aluminum citrate-phosphate complexes. The percentage and the composition of LMM-Al species is individually variable. In general, it was found that sera of dialysis patients contain higher percentages of LMM-Al complexes (up to 50%). The composition of HMM-Al species and LMM-Al species determined by the analytical techniques developed agrees with the data calculated by computer modeling reported in the literature.

5 REFERENCES

1. Zatta, P., Cervellin, D. and Zambenedetti, P., *Toxicol. In vitro*, **12**, 287 (1998).
2. Zatta, P., Taylor, A., Zambenedetti, P., Milačič, R. and Dell'Antone, P., *Life Sci.*, **66**, 2261 (1999).
3. Sargazi, M., Roberts, N. B. and Shenkin, A., *J. Inorg. Biochem.*, **87**, 37 (2001).
4. Ward, R. J., Zhang, Y. and Crichton, R. R., *J. Inorg. Biochem.*, **87**, 9 (2001).
5. Alfrey, A. C., Aluminum intoxication in renal failure: a historic overview, in *Aluminum in Chemistry, Biology and Medicine*, Vol. 2, Nicolini, M., Zatta, P. F. and Corain, B. (Eds.), Harwood Academic Publishers GmbH, Switzerland; *Life Chem. Rep.*, **11**, 197 (1994).
6. D'Haese, P. C. and De Broe, M. E., Recent insights in the monitoring, diagnosis and treatment of aluminum-overload in dialysis patients, in *Aluminum in Chemistry, Biology and Medicine*, Vol. 2, Nicolini, M., Zatta, P. F. and Corain, B. (Eds.), Harwood Academic Publishers GmbH, Switzerland; *Life Chem. Rep.*, **11**, 215 (1994).
7. Kausz, A. T., Antonsen, J. E., Hercz, G., Pei, Y., Weiss, N. S., Emerson, S. and Sherrard, D. J., *Am. J. Kidney Dis.*, **34**, 688 (1999).
8. Vittori, D., Nesse, A., Perez, G. and Garbossa, G., *J. Inorg. Biochem.*, **76**, 113 (1999).
9. Reusche, E., *Acta Neuropathol. (Berl.)*, **94**, 612 (1997).

10. Harrington, C. R., Vischik, C. M., McArthur, F. K., Taylor, G. A., Edwardson, J. A. and Candy, J. M., *Lancet*, 993 (1994).
11. Zatta, P., *Med. Hypoth.*, **44**, 169 (1995).
12. Caroli, S., Alimonti, A., Coni, E., Petrucci, F., Senofonte, O. and Violante, N., *Crit. Rev. Anal. Chem.*, **24**, 363 (1994).
13. Sariego Muñiz, C., Fernández Martín, J. L., Marchante Gayón, J. M., García Alonso, J. I., Cannata, J. B. and Sanz-Medel, A., *Biol. Trace Elem. Res.*, **82**, 259 (2001).
14. De Broe, M. E., D'Haese, P. C., Couttenye, M. M., Van Landeghem, G. F. and Lamberts, L. V., *Nephrol. Dial. Transplant.*, Suppl. 1, 47 (1993).
15. Jeffery, E. H., Abreo, K., Burgess, E., Cannata, J. and Greger, J. L., *J. Toxicol. Environ. Health*, **48**, 649 (1996).
16. McLachlan, D. R. C., *Environmetrics*, **6** 233 (1995).
17. Gauthier, E., Fortier, I., Courchesne, F., Pepin, P., Mortimer, J. and Gauvreau, D., *Environ. Res. Sec. A*, **84**, 234 (2000).
18. Zatta, P., Zambenedetti, P. and Milačič, R., *Analusis*, **26**, M72 (1998).
19. Zatta, P. F., Nicolini, M. and Corain, B., Aluminum(III) toxicity and blood-brain barrier permeability, in *Aluminum in Chemistry, Biology and Medicine*, Vol. 1, Nicolini, M., Zatta, P. F. and Corain, B. (Eds.), Cortina International, Verona, 1991, pp. 97–112.
20. Martin, R. B., Savory, J., Brown, S. Bertholf, R. L. and Willis, M. R., *Clin. Chem.*, **33/3**, 405 (1987).
21. Harris, W. R., *Coord. Chem. Rev.*, **149**, 347 (1996).
22. Martin, R. B., Aluminum in biological systems, in *Aluminum in Chemistry, Biology and Medicine*, Vol. 1, Nicolini, M., Zatta, P. F. and Corain, B. (Eds.), Cortina International, Verona, 1991, pp. 3–20.
23. Martin, R. B., *Clin. Chem.*, **32**, 1797 (1986).
24. Martin, R. B., *J. Inorg. Biochem.*, **28**, 181 (1986).
25. Venturini, M. and Berthon, G., *J. Inorg. Biochem.*, **37**, 69 (1989).
26. Kiss, T. and Farkas, E., The bioinorganic chemistry of aluminum, in *Perspectives on Bioinorganic Chemistry*, Vol. 3, Hay, R. K., Dilworth, J. R. and Nolan, K. B. (Eds.), JAI Press, London, 1996, pp. 199–250.
27. Harris, R. W., *Clin. Chem.*, **38**, 1809 (1992).
28. Atkári, K., Kiss, T., Bertani, R. and Martin, R. B., *Inorg. Chem.*, **35**, 7089 (1996).
29. Lakatos, A., Evanics, F., Dombi, Gy., Bertani, R. and Kiss, T., *Eur. J. Inorg. Chem.*, 3079 (2001).
30. Fairman, B., Sanz-Medel, A., Galleo, M., José Quintela, M., Jonea, P. and Benson, R., *Anal. Chim. Acta*, **286**, 401 (1994).
31. Van Landeghem, G. F., D'Haese, P. C., Lamberts, L. V. and De Broe, M. E., *Anal. Chem.*, **66**, 216 (1994).
32. Soldado Cabezuelo, A., Blanco González, E. and Sanz-Medel, A., *Analyst*, **122**, 573 (1997).
33. Bantan, T., Milačič, R. and Pihlar, B., *Talanta*, **47**, 929 (1998).
34. Pérez Parajón, J., Blanco González, E., Cannata, J. B. and Sanz-Medel, A., *Trace Elem. Med*, **6**, 41 (1989).
35. Wróbel, K., Blanco González, E. and Sanz-Medel, A., *J. Anal. Atom. Spectrom.*, **9**, 281 (1994).
36. Wróbel, K., Blanco González, E., Wróbel, Kz. and Sanz-Medel, A., *Analyst*, **120**, 809 (1995).
37. Blanco González, E., Pérez Parajón, J., García Alonso, J. I. and Sanz-Medel, A., *J. Anal. At. Spectrom.*, **4**, 175 (1989).
38. García Alonso, J. I., López García, A., Sanz-Medel, A. and Blanco González, E., *Anal. Chim. Acta*, **225**, 339 (1989).
39. Soldado Cabezuelo, A., Montes Bayón, M., Blanco González, E., García Alonso, J. I. and Sanz-Medel, A., *Analyst*, **123**, 865 (1998).
40. Leung, F. Y., Hodsman, A. B., Muirhead, N. and Henderson, A. R., *Clin. Chem.*, **31**, 20 (1985).
41. Khalil-Manesh, F., Agness, C. and Gonick, H. C., *Nephron*, **52**, 329 (1989).
42. Röllin, H. B. and Nogueira, C. M. C. A, *Eur. J. Clin. Chem. Clin. Biochem.*, **35**, 215 (1997).
43. van Ginkel, M. F., van der Voet, G. B., van Eijk, H. G. and de Wolff, F. A., *J. Clin. Chem. Clin. Biochem.*, **28**, 459 (1990).
44. Leung, F. Y., Niblock, A. E., Bradley, C. and Henderson, A. R., *Sci. Total Environ.*, **71**, 49 (1988).
45. Nagaoka, M. H. and Maitani, T., *Analyst*, **125**, 1962 (2000).
46. Keirsse, H., Smeyers-Verbeke, J., Verbeelen, D. and Massart, D. L., *Anal. Chim. Acta*, **196**, 103 (1987).
47. Favarato, M., Mizzen, C. A. and McLachlan, D. R., *J. Chromatogr.*, **576**, 271 (1992).
48. Leung, F. Y., Niblock, A. E., Bradley, C. and Henderson, A. R., *Sci. Total Environ.*, **71**, 49 (1988).
49. Datta, A. K., Wedlund, P. W. and Yokel, R. A., *J. Trace Elem. Electrolytes Health Dis.*, **4**, 107 (1990).
50. Bantan, T., Milačič, R. and Pihlar, B., *Talanta*, **46**, 227 (1998).
51. Bantan, T., Milačič, R., Mitrović, B. and Pihlar, B., *J. Anal. At. Spectrom.*, **14**, 1743 (1999).
52. Bantan Polak, T., Milačič, R., Mitrović, B. and Pihlar, B., *J. Pharm. Biomed. Anal.*, **26**, 189 (2001).

2.2.4 Speciation of Aluminum in Occupational Health

Sinikka Valkonen and Vesa Riihimäki
Finnish Institute of Occupational Health, Helsinki, Finland

1 ALUMINUM SPECIES IN OCCUPATIONAL EXPOSURE

Occupational exposure to aluminum or aluminum compounds may be encountered in primary or secondary aluminum production, cryolite (Na_3AlF_6) refining, in aluminum foundries, in the production of aluminum flake powder, corundum (Al_2O_3), aluminum fluoride (AlF_3), or aluminum sulfate ($Al_2(SO_4)_3$), and when working on aluminum such as grinding, extruding or welding [1].

On the basis of measurements of aluminum in serum and urine, increased internal loads have sometimes been detected in workers engaged in primary aluminum production [2], melting and foundry [3], and in the production of cryolite [4], corundum [5], or aluminum sulfate [6]. However, a recent review of studies on health effects in workers exposed to different aluminum compounds [7] suggested that increased body burdens are presently of concern only in aluminum powder production and in certain types of aluminum welding.

Aluminum flake powder was produced either by melting solid aluminum and "atomizing" by means of compressed air to form powder, which was then ball-milled with white spirit, or by direct ball-milling of shredded aluminum foil to give the same end product [8]. After drying, the powder consisted of flakes 10 to 200 μm in diameter and 0.05 to 1 μm in thickness. Another company produced pyro-powder, which was made of aluminum particles of less than 5 μm in diameter with a fine layer of aluminum oxide on the surface [9]. Some powder workers have exhibited 30 times higher serum aluminum and 100 times higher urinary aluminum levels than occupationally nonexposed persons [6, 10].

Aluminum is welded either with the metal inert gas (MIG) or tungsten inert gas (TIG) method. MIG welding produces plenty of metal fume (in the authors' study, up to 14 mg m^{-3} of aluminum was found in the breathing zone), whereas TIG welding produces little fume. In the high temperatures of the arc welding process, aluminum is vaporized

Handbook of Elemental Speciation II: Species in the Environment, Food, Medicine & Occupational Health
Edited by R. Cornelis, H. Crews, J. Caruso and K. G. Heumann
 ISBN: 0-470-85598-3 (HB)

and then quickly condensed, largely reacting with oxygen, into chains of submicrometer particles that may agglomerate and form larger spheres or rafts (still below 1 μm is size and thus respirable) [11]. The composition of the microparticles is mainly aluminum oxide (Al_2O_3). Grinding and polishing accompany welding. Grinding dusts contain particles of metallic aluminum larger than the welding fume particles. Depending on the grinding and polishing tools used, a variable fraction of the dust is expected to be respirable. Among MIG welders, serum and urinary aluminum levels can, in extreme cases, exceed normal values by 20- and 100-fold, respectively [12].

2 PARTICLE CHARACTERISTICS AND TOXICOKINETICS

The occupationally important aluminum species are the fine particulate aluminum and its oxide in the form of powder or freshly generated welding fume. The physical dimensions of the particles have been described above. Aluminum is insoluble in water, and aluminum oxide is very slightly soluble. Aluminum sulfate, which is widely used as a flocculant for the treatment of raw and waste water, is a water soluble salt. Opposite to what is known for aluminum powder workers and aluminum MIG welders, these authors noted no significant increase of aluminum body burden among aluminum sulfate production workers in spite of long-term exposure to the dust, especially in bagging, and Sjögren *et al*. [6] also observed only slight increases of serum and urinary aluminum. The authors believe that this discrepancy can be explained on the basis of differences in particle characteristics and consequent dissimilarities in inhalation toxicokinetics.

Sjögren *et al*. [12] exposed three previously unexposed volunteers to the MIG welding fumes of aluminum for one day, and six professional aluminum welders to similar welding fumes over one workweek. Their remarkable observations were that among the unexposed volunteers, urinary aluminum concentration rose from the preexposure level (0.1 $\mu mol\,L^{-1}$) up to 15 $\mu mol\,L^{-1}$, peaking soon after the end of exposure, and then declined with a half-time of about 8 h. Among the professional welders, those who had a working history of two years or more and had the highest nonexposure urinary aluminum levels (1.6–13.6 $\mu mol\,L^{-1}$) did not show any consistent increase of urinary aluminum during or immediately after exposures, and neither did they show any decline during the following weekend. Hence, aluminum in urine depended partly on the current exposure as indicated by the previously unexposed volunteers and partly on the duration of past exposure (and accumulated body burden thereof) as indicated by the long-term welders.

A subsequent study by the same authors demonstrated that among welders exposed for less than one year, the elimination half-time for aluminum in urine was about nine days, whereas among welders exposed for more than 10 years the urinary half-time was calculated to be six months or longer [13]. Riihimäki *et al*. [14] studied aluminum welders who had been occupationally active for four years and found that whilst the serum aluminum concentration declined right after a workday to about a half in 16 h, later on and some months after a total stop of welding, serum aluminum decreased with an apparent half-time of about 137 days (4 subsequent weekly samples). It should be noted that there was no obvious corresponding decline in urinary aluminum over the same period.

Among active flake powder workers, urinary aluminum declined over a four- to five-week holiday with a half-time of 35 to 42 days, whereas among retired workers the half-times varied from less than one up to eight years and were related to the number of years since retirement [8].

Because of the very small particle size, aluminum welding fume is breathed deep into the lungs, where about 30% is expected to be deposited, and an additional 20% is deposited in the airways [15]. Although the previous data show that part of the deposited aluminum is rapidly absorbed and excreted, it can be assumed from the inhalation toxicokinetic model for sparingly soluble particles [15] that part will be retained in the lungs over months or years with gradual

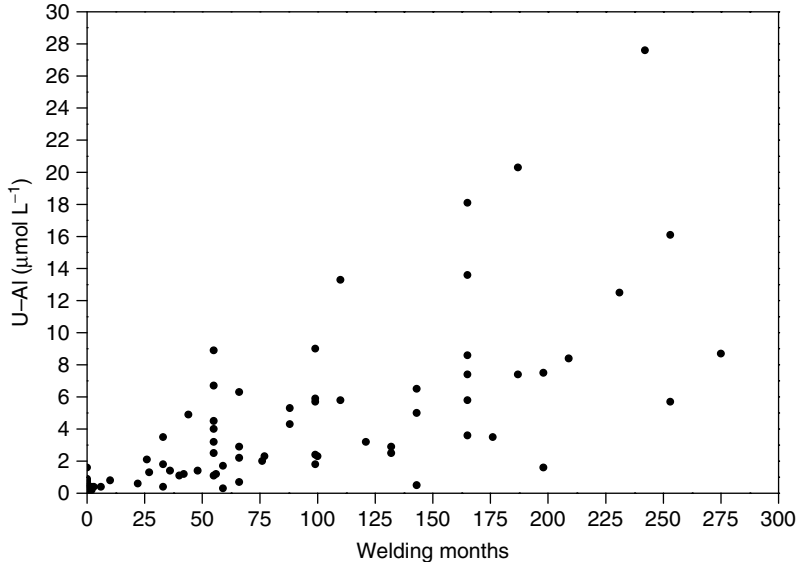

Figure 2.2.4.1. Correlation between the duration of welding history with aluminum (months) and urinary aluminum concentration in a morning sample voided after an interval of two days away from exposure. (Reproduced by permission of Finnish Institute of Occupational Health from Riihimäki, V., Hänninen, H., Akila, R., Kovala, T., Kuosma, E., Paakkulainen, H., Valkonen, S. and Engström, B., *Scand. J. Work Environ. Health*, **26**, 118 (2000).)

dissolution and absorption. The main part of the particulate substance is expected to be cleared by the mucociliary escalator to the gastrointestinal tract where absorption of aluminum is low [16]. Nevertheless, on the basis of the assumptions that welding of aluminum over four years had resulted in a steady state (daily uptake equals daily excretion) and that all excretion of aluminum takes place via urine, about 1.4% of the inhaled and deposited aluminum was estimated to be absorbed [1].

Apparently, aluminum powders are handled in the respiratory system rather similarly to the welding fume particles because aluminum in blood and urine of the exposed workers exhibit much the same features as among welders. Differences in particle size, shape and the different technologies used in particle generation, however, raise suspicions that also specific toxicokinetic properties may be involved. These authors found that aluminum sulfate particles in the premises of production and bagging tended to be large (10 μm or more in diameter). In the humid respiratory system, this water soluble and hygroscopic substance is expected to grow even larger and become quantitatively deposited in the airways. On the airway mucosa aluminum sulfate dissolved in water is transformed to less soluble species or is bound to mucus [17], and is presumably cleared to the gastrointestinal tract where only little is taken up.

The critical toxicokinetic characteristic of the sparingly soluble, small inhaled aluminum particles is accumulation in the lungs and, after dissolution and transport, in other organs, notably the bones. What is feared most is that it could also accumulate in the brain, which, like the bone tissue, is a known target of aluminum toxicity [16]. Figure 2.2.4.1 illustrates the concern. Urinary aluminum (as well as serum aluminum, which is not shown) among MIG welders increased with the number of months at work [18]. The study population was drawn from 10 different places of work: in some of them, the slope of increase in urinary aluminum was steep because of intensive exposure, in some it was not because, for example, personal respiratory protection was used.

3 COMBINED OCCUPATIONAL AND NONOCCUPATIONAL EXPOSURE

Intake and uptake of aluminum for the healthy general population from various sources such as food, water, community air, antiperspirants and vaccines have been recently reviewed [16, 19]. The intake may vary markedly, from 1 to 30 mg or even more per day, especially depending on the use of food products containing aluminum in food additives. However, absorption of dietary aluminum under normal circumstances causes minor changes in serum or urinary aluminum levels and will not confuse biological monitoring of workers. In contrast, the use of antiacid drugs (aluminum hydroxide) and antiulcer agents (sucralfate) may result in ingestion of up to several grams of aluminum per day and absorption of up to 5 mg per day [16]. This large dose of aluminum is reflected in clearly increased levels of both serum and urinary aluminum [20, 21]. In individual cases, urinary aluminum can reach 10 μmol L^{-1}. After the drug use was stopped, aluminum concentrations in plasma and urine declined rapidly, but slightly increased levels in urine could be observed during some weeks. Ingestion of acid food cooked in utensils made of aluminum can in exceptional cases increase aluminum concentration in urine [22].

4 OBJECTIVES OF BIOLOGICAL MONITORING

The purpose of biological monitoring of occupational exposure to aluminum is to prevent hazardous accumulation in the body and thus any potential systemic toxicity. There have been different views as to whether plasma/serum or urine best reflects aluminum body burden. Several authors [2, 23] have pointed out that urinary excretion of aluminum is more sensitive than the serum aluminum value to occupational aluminum exposure. Whilst significant increases in urinary aluminum were observed already at low levels of exposure, increases of serum aluminum were only marginal and remained within the range of normally encountered values. Figure 2.2.4.2 depicts the correlation between serum and urinary aluminum (for the timing of sampling, see later) among 84 welders [18]. There is a fair correlation between the two parameters (note the logarithmic scale) with a tendency

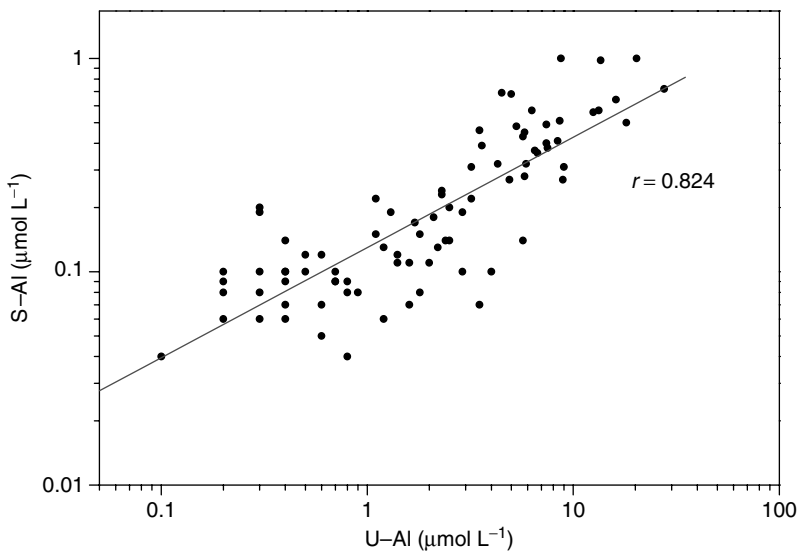

Figure 2.2.4.2. Correlation of the serum (S–Al) and urinary (U–Al) aluminum concentrations. (Reproduced by permission of Finnish Institute of Occupational Health from Riihimäki, V., Hänninen, H., Akila, R., Kovala, T., Kuosma, E., Paakkulainen, H., Valkonen, S. and Engström, B., *Scand. J. Work Environ. Health*, **26**, 118 (2000).)

for the serum aluminum to follow more closely the rise in urinary aluminum only at higher levels.

Urinary and serum aluminum concentration of aluminum welders in samples taken at the end of the shift depend both on the current exposure and the body burden. Which one of the two plays the dominant role in any actual measurement is determined by the duration and intensity of the preceding work history. In order to uncover the body burden, some time needs to be allowed for the elimination of the most recent uptake. In search for the ideal timing for sampling, the authors have found it both useful and practical to use the serum sample obtained in the morning before work (and entering the contaminated premises), and to use the urine sample voided in the morning after a normal two-day rest period [18, 22].

Other important biological monitoring objectives that concern the health significance of the biological measurements, or aspects of method validity, for example, physiological variability in serum binding or in renal handling, are more elusive. In particular, the relationships between serum or urinary aluminum and aluminum in the brain are not known. During continuing exposure, serum and urinary aluminum could be predictive of metal accumulation in the brain since rabbits exposed via inhalation to fine aluminum oxide dust for five months exhibited almost doubling of the serum aluminum concentration and more than doubling of the brain aluminum level [24]. The situation can be completely different after the exposure has ceased.

5 DETERMINATION OF ALUMINUM IN SERUM AND URINE

Standardized sampling time, contamination-free sample collection, storage and analysis together with reliable analytical methods of aluminum in serum and urine are required for the purposes of biological monitoring. Serum is preferred over plasma for aluminum analysis because anticoagulants, such as heparin and citrate, may contain Al. Urine is obtained as a spot sample. Standardization of aluminum concentration for excretion rate of urine is normally used, although it is not clear whether correction to a common relative density or creatinine excretion is the more appropriate method [25, 26].

Electrothermal atomic absorption spectrometry (ETAAS) is the most common, suitable and cost-effective instrumental technique for the determination of aluminum in serum and urine. Other techniques, for example, inductively coupled plasma atomic emission spectrometry (ICP-AES) or inductively coupled plasma mass spectrometry (ICP-MS), are less used for occupational samples. These methods alone provide no information about aluminum speciation in serum and urine. Chromatographic separation techniques coupled with spectrometric detection have recently been reviewed for the speciation of aluminum both in environmental and biological samples [27]. Internal quality control (IQC) and external quality assurance (EQA) procedures should be used to monitor and review the validity of the analytical performance [26, 28].

5.1 Collection and storage

Dust from the workplace constitutes a major contamination hazard. The specimen has to be collected outside the working area, and after washing the hands. To avoid contamination from clothing and skin, urine is voided before (preshift sample) or after (postshift sample) changing the clothes, preferably after a shower, directly into acid-washed polyethylene vials. Whole blood is collected into an acid-washed glass tube or an Al-free evacuated collection tube and centrifuged. Serum is transferred using an Al-free plastic pipette into an acid-washed plastic tube. Stainless steel needles and vinyl gloves free of talc have to be used. No commercially available plastic containers or glass tubes should be used before acid cleaning. Recommendations and guidelines for sampling and storage have been reviewed [26, 29, 30].

Glass should not be used for storage of the samples for aluminum measurement, whereas polypropylene or polystyrene tubes were found to be suitable. Acidification by, for example, nitric acid does not seem necessary for urine specimens

to prevent adsorption of aluminum onto containers. Serum and urine are stable in plastic vials for several days at room temperature and can be stored in the refrigerator at $<5\,^{\circ}C$ for one to two weeks; for longer storage, freezing at $-20\,^{\circ}C$ is recommended [31].

5.2 Analytical determination

The use of ETAAS for analysis of aluminum in serum and urine provides contamination-free, accurate and sensitive measurements from a small sample size. The limit of determination around 1 $\mu g\,L^{-1}$ (0.04 $\mu mol\,L^{-1}$) has been regularly reviewed [32]. Stabilized temperature platform facilities and matrix modification may be used to reduce the loss of volatile aluminum and gas interference effects. Several ETAAS methods that are based on relatively simple preparation with matrix-matched calibration, using nitric acid, Triton X-100, magnesium nitrate alone or together with Triton X-100 as matrix modifiers have been published for aluminum in occupational samples [22, 33–35]. Analytical methods for aluminum in serum and urine have been reviewed [25, 32].

Absence of contamination in analysis should be verified by repeated analyses of blanks in each series. Preparation is performed under reasonably particulate-free conditions in a high efficiency particulate air (HEPA) filtered laminar flow hood. Powder-free gloves are worn throughout. All laboratory equipment should be acid washed or acid rinsed and the reagents must be of Al-free high-purity grade.

5.3 Internal quality control and external quality assurance

IQC and EQA procedures provide regular use of control or reference materials and participation in EQA schemes. Commercial reference materials useful for quality control of aluminum in occupational samples are available with noncertified reference values for human serum or freeze-dried urine from SERO AS, Billingstad, Norway, and from Bio-Rad, QSD, Irvine, USA, as well as from NIST (National Institute of Standards and Technology), Gaithersburg, USA.

EQA schemes relevant in biological monitoring are operated for aluminum in serum and urine by the German Society of Occupational Medicine [36] and the Centre de Toxicologie du Quebec in Canada [37]. Additionally, worldwide schemes for aluminum in plasma or serum are operated by the University of Surrey in Great Britain (UK NEQAS for Trace Elements) [38] and by the Laboratoire de Biochimie-Toxicologie in France [39].

6 ASSESSMENT OF RESULTS

The upper reference limit of aluminum in occupationally nonexposed people who do not consume antacid drugs is estimated to be approximately 16.2 $\mu g\,L^{-1}$ (0.6 $\mu mol\,L^{-1}$) for urine and below 5.4 $\mu g\,L^{-1}$ (0.2 $\mu mol\,L^{-1}$) for serum [25, 33]. The German biological tolerance value for occupational exposures (BAT value) for urinary aluminum is 200 $\mu g\,L^{-1}$ (7.4 $\mu mol\,L^{-1}$) (not corrected to relative density) in an after-shift specimen [40]. Interpretation of the result is not unambiguous. A high urinary aluminum level combined with a short work history is predictive of intensive current exposure, whereas in the context of a long work history it may also indicate a high body burden.

The concentration of aluminum in specimens collected in the morning after two days away from work is less affected by exposure of the preceding days and is more reflective of the body burden. On the basis of adverse effects of aluminum on welders, the Finnish Institute of Occupational Health has recommended 6.0 $\mu mol\,L^{-1}$ (corrected to relative density of 1.024) as the biological action level in a specimen collected in the morning after two days without exposure. Recent findings in welders both in Finland [18] and in Sweden [7] suggest that this action level may be too high to protect the worker from harmful effects in central nervous system functions. No action levels for

aluminum in serum in occupational exposure have been proposed. Measurement of serum aluminum in a preshift sample, or later in the postexposure phase, is capable of detecting remarkably increased body burdens of Al. However, this situation is not typical of the occupational setting and indeed should be prevented with the help of the biological monitoring program. Hence, measurement of urinary Al, which is more sensitive to exposure, is to be preferred.

7 REFERENCES

1. Sjögren, B., Elinder, C.-G., Iregren, A., McLachlan, D. R. C. and Riihimäki, V., Occupational aluminum exposure and its health effect, in *Research Issues in Aluminum Toxicity*, Yokel, R. A. and Golub, M. S. (Eds), Taylor & Francis, Washington, DC, 1997, Chapter 9, pp. 165–183.
2. Röllin, H. B., Theodorou, P. and Cantrell, A. C., *Occup. Environ. Med.*, **53**, 417 (1996).
3. Hosovski, E., Mastelica, Z., Sunderic, D. and Radulovic, D., *Med. Lav.*, **81**, 119 (1990).
4. Grandjean, P., Horder, M. and Thomassen, Y., *J. Occup. Med.*, **32**, 58 (1990).
5. Valentin, H., Preusser, P. and Schaller, K.-H., *Int. Arch. Occup. Environ. Health*, **38**, 1 (1976).
6. Sjögren, B., Lundberg, I. and Lidums, V., *Br. J. Ind. Med.*, **40**, 301 (1983).
7. Iregren, A., Sjögren, B., Gustafsson, K., Hagman, M., Nylén, L., Frech, W., Andersson, M., Ljunggren, K. G. and Wennberg, A., *Occup. Environ. Med.*, **58**, 453 (2001).
8. Ljunggren, K. G., Lidums, V. and Sjögren, B., *Br. J. Ind. Med.*, **48**, 106 (1991).
9. Kraus, T., Schaller, K.-H., Angerer, J. and Letzel, S., *Int. Arch. Occup. Environ. Health*, **73**, 61 (2000).
10. Letzel, S., Schaller, K.-H., Angerer, J., Drexler, H., Weber, A., Schmid, K. and Weltle, D., *Occup. Hyg.*, **3**, 271 (1996).
11. Hewitt, P. J., *Indoor Built Environ.*, **5**, 253 (1996).
12. Sjögren, B., Lidums, V., Håkansson, M. and Hedström, L., *Scand. J. Work Environ. Health*, **11**, 39 (1985).
13. Sjögren, B., Elinder, C.-G., Lidums, V. and Chang, G., *Int. Arch. Occup. Environ. Health*, **60**, 77 (1988).
14. Riihimäki, V., Valkonen, S., Engström, B., Tossavainen, A. and Aitio, A., Kinetics of aluminum among workers and implications for biomonitoring, Presented at *43rd Nordic Work Environment Meeting*, Loen, Norway, Aug. 28–30, 1994.
15. Snipes, M. B., *Crit. Rev. Toxicol.*, **20**, 175 (1989).
16. Yokel, R. A. and McNamara, P. J., *Pharmacol. Toxicol.*, **88**, 150 (2001).
17. Greger, J. L. and Sutherland, J. E., *Crit. Rev. Clin. Lab. Sci.*, **34**, 439 (1997).
18. Riihimäki, V., Hänninen, H., Akila, R., Kovala, T., Kuosma, E., Paakkulainen, H., Valkonen, S. and Engström, B., *Scand. J. Work Environ. Health*, **26**, 118 (2000).
19. Soni, M. G., White, S. M., Flamm, W. G. and Burdock, G. A., *Regul. Toxicol. Pharmacol.*, **33**, 66 (2001).
20. Allain, P., Mauras, Y., Krari, N., Duchier, J., Cournot, A. and Larcheveque, J., *Br. J. Clin. Pharmacol.*, **29**, 391 (1990).
21. Mistry, P., Varghese, Z. and Pounder, R. E., *Aliment. Pharmacol. Ther.*, **5**, 549 (1991).
22. Valkonen, S. and Aitio, A., *Sci. Total Environ.*, **199**, 103 (1997).
23. Gitelman, H. J., Alderman, F. R., Kurs-Lasky, M. and Rockette, H. E., *Ann. Occup. Hyg.*, **39**, 181 (1995).
24. Röllin, H. B., Theodorou, P. and Kilroe-Smith, T. A., *Br. J. Ind. Med.*, **48**, 389 (1991).
25. Aitio, A., Riihimäki, V. and Valkonen, S., Aluminum, in *Biological Monitoring of Chemical Exposure in the Workplace*, Vol. 2, Lehtinen, S. (Ed.), World Health Organization, Geneva, 1996, pp. 1–17.
26. Aitio, A., Quality assurance, in *Biological Monitoring of Chemical Exposure in the Workplace*, Vol. 1, Lehtinen, S. (Ed.), World Health Organization, Geneva, 1996, pp. 20–51.
27. Bi, S. P., Yang, X. D., Zhang, F. P., Wang, X. L. and Zou, G. W., *Fresenius' J. Anal. Chem.*, **370**, 984 (2001).
28. Menditto, A., Apostoli, P. and Aitio, A. *Ann. Ist. Super. Sanità*, **32**, 207 (1996).
29. Cornelis, R., Heinzow, B., Herber, R. F. M., Christensen, J. M., Poulsen, O. M., Sabbioni, E., Templeton, D. M., Thomassen, Y., Vahter, M. and Vesterberg, O., *J. Trace Elem. Med. Biol.*, **10**, 103 (1996).
30. Subramanian, K. S., *Biol. Trace Elem. Res.*, **49**, 187 (1995).
31. Wilhelm, M. and Ohnesorge, F. K., *J. Anal. Toxicol.*, **14**, 206 (1990).
32. Taylor, A. and Walker, A., *Ann. Clin. Biochem.*, **29**, 377 (1992).
33. Schaller, K.-H., Letzel, S. and Angerer, J., Aluminum, in *Handbook of metals in Clinical and Analytical Chemistry*, Seiler, H. G., Sigel, A. and Sigel, H. (Eds), Marcel Dekker, New York, Basel, Hong Kong, 1994, pp. 217–226.
34. Wang, S. T., Pizzolato, S. and Demshar, H. P., *J. Anal. Toxicol.*, **15**, 57 (1991).
35. Johnson, K. E. and Treble, R. G., *J. Clin. Lab. Anal.*, **6**, 264 (1992).
36. Lehnert, G., Schaller, K.-H. and Angerer, J., *Int. Arch. Occup. Environ. Health*, **72**, 60 (1999).
37. Weber, J. P., *Sci. Total Environ.*, **71**, 111 (1988).
38. Taylor, A. and Briggs, R. J. *Ann. Inst. Super. Sanita*, **32**, 271 (1996).
39. Guillard, O., Piriou, A. and Pineau, A., *Ann. Inst. Super. Sanita*, **32**, 241 (1996).
40. *Deutsche Forschungsgemeinschaft (DFG): MAK- und BAT-Werte-Liste 2000*. 36 Mitt., Wiley-VCH, Weinheim BRD, 2000.

2.3 Speciation of Antimony

Nina Ulrich
University of Hannover, Hannover, Germany

Handbook of Elemental Speciation II: Species in the Environment, Food, Medicine & Occupational Health
Edited by R. Cornelis, H. Crews, J. Caruso and K. G. Heumann
 ISBN: 0-470-85598-3 (HB)

1 INTRODUCTION

The investigation of antimony and its compounds is of growing interest in the field of element speciation. They are considered as pollutants of major concern by the Environmental Protection Agency (EPA) of the United States and the European Commission [1, 2]. The German Research Community (DFG) also underlines the importance of the monitoring of antimony [3]. In addition, the maximum admissible concentration of antimony in drinking waters was established at 10 $\mu g\,L^{-1}$ in Europe and recommended at below 2 $\mu g\,L^{-1}$ Sb in Japan.

The speciation of antimony is important especially in the environmental and biomedical field because its toxicity, its bioavailability and its reactivity depend not only on the oxidation state but also on the very nature of the specific compound. Generally, inorganic antimony is more toxic than organic species, with Sb(III) being more toxic than Sb(V).

Antimony, a metalloid in the 5th group of the periodic system, shows similar chemical characteristics as arsenic, so that the early speciation experiments used similar methods for the investigations. The main stratagems include reduction of the antimony compounds and the formation of gaseous hydride or volatile organic species, separation of the species by liquid chromatography to end with a suitable detection system. In addition, extraction techniques (liquid/liquid and liquid/solid), coprecipitation, electrochemical and radiochemical methods are described.

2 GENERAL INFORMATION

2.1 Antimony sources

Antimony (Sb) is a relatively rare element of the 5th main group. Its abundance is as high as that of cadmium, around 0.7 $mg\,kg^{-1}$ in the terrestrial environment. Natural sources of antimony include rock weathering and volcanic activity. Therefore, it is widely distributed and found in low background concentrations in all matrices. In addition, it is obvious that Sb is emitted by anthropogenic sources into the environment.

The natural or background concentrations of Sb in different environmental matrices offer a great variety. In uncontaminated water, the concentration is typically around or below 1 $\mu g\,L^{-1}$. Depending on the rock structure, in soil Sb contents of up to 500 $mg\,kg^{-1}$ have been measured. The concentration of Sb in plants and animals seems to be correlated to the soil content. In mammals, most of the antimony is excreted chemically unchanged in less than 48 h after uptake. Studies showed that even in populations of sheep eating grass grown on highly Sb-rich soils, the Sb concentrations remain rather low.

In addition to the natural sources, there are a great variety of anthropogenic sources of antimony. In Japan, about 20,000 tons of Sb are employed in different industrial processes every year, opposite to only 100 tons of arsenic, well known for its toxicity [4]. Ancient Egyptians used antimony compounds as cosmetics. Alchemists considered antimony an important material and a possible source of gold. More recently, antimony is used as part of letter metals and hardener of soft lead bullets, so that elevated concentrations of Sb can be find around fire ranges. It is a component of break linings and an additive in the vulcanization process of rubber, for example, in the tyre industry. Therefore, it has been suggested that higher concentrations of Sb would be present at high traffic areas, crossings and maybe airports. Sb is used together with organic chemicals as an important constituent in many fire retardants, for example, as part of textiles, carpets and coatings of walls. This practice has lately been questioned because of the toxicity of Sb compounds. Otherwise, Sb compounds are used as clarifying agent and as pigment in the production of ceramics and glassware as well as in metal coatings. Finally, a relatively large amount of Sb is emitted during the combustion of fossil fuels such as coal and oil.

Another important area of the application of Sb compounds is the biomedical field. Sb compounds are used as therapeutic agents mainly in tropical, parasitic diseases such as Leishmaniasis and Bilharziasis with millions of people living at risk. Therefore, some analytical efforts have been made to ensure the quality of the therapeuticals and to investigate the mode of action of the compounds.

2.2 Antimony toxicity

Generally, the toxicity of Sb compounds is ca. 10 times less than that of arsenic, but it depends largely on the oxidation state and chemical structure. Important are the binding partners, potential ligands and the solubility of the compounds. Like arsenic, inorganic antimony species are more toxic than organic species. Elemental Sb is more toxic than its salts. Trivalent Sb has a toxicity that is 10 times higher than that of pentavalent Sb [5]. Sb_2O_3 and $SbCl_3$ are known for their ability to act as inhalative lung carcinogens in female rats and to elevate the sister chromatide exchange rate in cells [6]. There are few data about the toxicity of antimony, predominantly total Sb, in humans. Most antimony species are excreted unchanged after uptake within 48 h. Lead-battery workers, who are exposed to Sb_2O_3 and SbH_3, showed elevated Sb levels in their urine. SbH_3 is highly toxic and can cause injuries of the central nervous system and blood hemolysis.

Sb(V) has only very slight affinity for erythrocytes, whereas Sb(III) reacts with red blood cells and sulfhydryl containing compounds. The toxicity is caused by irreversible binding to thiol-containing enzymes. In contrast to arsenic, Sb(III) and Sb(V) seem not to be detoxified via methylation in mammals, but the mechanism for their genotoxicity remains unclear [7]. Exposure to antimony and its compounds can cause irritation of the respiratory tract, leading to pneumoconiosis. In addition, antimony can induce different forms of health-threatening effects such as dermatitis, keratitis, conjunctivitis, suppuration of the nasal septum and gastritis.

2.3 Preparing for speciation

2.3.1 Species of main interest

Up to now, there is a major gap between the species occurring in the environment and relevant from a biochemical point of view and those investigated by the analytical chemical community. Environmental matrices offer a great variety of different reaction partners and complexing agents for inorganic Sb. In laboratory experiments, Sb show strong interactions with oxygen and sulfur, for example, forming oxides, sulfide and other compounds. Probably, there are many Sb species in matrices such as water or sludge, sediment or soil, which cannot be addressed today. Some of the reasons for this are given in the section "analytical problems with Sb speciation". In biological samples, many reactions of Sb involving enzymes, proteins and other biomolecules could take place leading to Sb compounds with Sb–C bindings and also to molecules with a high molar mass. To the author's knowledge, there is only one study published giving a brief reference to these processes [8].

In speciation analysis, mainly two groups of species have been investigated up to now. First and classically, the examination of inorganic antimony is represented by the oxidation states of trivalent antimony [Sb(III)] and pentavalent antimony [Sb(V)]. Normally, no conclusions are given about the chemical structure of these compounds, although a few authors tried to conclude about the aqueous chemistry of Sb(III) and Sb(V) [9]. Many inorganic compounds are known and commercially available, for example, the halogenides and oxides of both oxidation states, but mostly the sodium antimonyltartrate for Sb(III) and the potassium hexahydroxyantimonate for Sb(V) are used as standards. These two components combine high purity with sufficient solubility in aqueous solutions, which are features that many antimony species do not show.

Second comes the investigation of simple organic antimony compounds in environmental and biomedical samples. In early publications, a relatively broad variety of methylated species has been described [10]. Monomethylated methylstibonic acid [$MeSbO(OH)_2$] and dimethylated dimethylstibinic acid [Me_2SbOOH] as well as monomethylstibine [$MeSbH_2$] and dimethylstibine [Me_2SbH] were proposed, on the analogy of arsenic chemistry. More recent studies showed massive rearrangements of the Sb compounds in the course of the experiments. These artifacts raised serious doubts regarding the correctness of the earlier assumptions. In addition, many groups

tried to synthesize the mono- and dimethylated compounds without success. The products were either not be formed at all, could not be purified or were unstable under environmental conditions. Nowadays, only the presence of trimethylated antimony compounds in nature has been demonstrated beyond doubt. There are four different trimethylated Sb(V) species used for analysis: Me_3SbCl_2, Me_3SbBr_2, $Me_3Sb(OH)_2$ and Me_3SbO, therefore they should be called Me_3SbX_2. All these compounds show similar chemical behavior in the specific experimental conditions. Me_3SbCl_2 appeared to be able to form a single charged cation or anion, depending on the conditions, whereas in case of Me_3SbO only an anionic species was described. Because of the lack of commercially available standards, all methylated compounds are laboratory made and purified, which is described in the following section "synthesis of organic antimony compounds". In addition to the trimethylated Sb(V) compounds, the trimethylated Sb(III) [Me_3Sb] is used for analysis. Some authors applied this species directly as standard to gas chromatographic analysis, whereas others use it for the synthesis of the pentavalent compound. The Me_3Sb is formed during the reduction of Me_3SbX_2 by sodium borohydride, an important step in Sb speciation.

Although +III and +V are the main oxidation states of Sb in all types of samples, the oxidation state −III is of great importance in Sb speciation. Many authors apply the reduction of Sb compounds to Sb(−III) to form the corresponding hydrides for speciation purposes. The SbH_3 is gaseous at room temperature and sufficiently stable during the analysis, although it may be easily oxidized under aerobic conditions and undergo rearrangement reactions in case of methylated Sb compounds.

2.3.2 Synthesis of organic antimony compounds

Most of the literature about the synthesis of environmentally relevant antimony species is rather old, sometimes leading back to the beginning of the twentieth century. These compounds were not described spectrometrically and their purity could not be sufficiently proven. Therefore, up to now only the trimethylated species of antimony have been synthesized and purified as to meet the quality requested for analytical purposes. Dorsk *et al.* described the synthesis of Me_3SbCl_2 [11]. Other species, for example, the mono- and dimethylated compounds, could either not be formed and purified at all or showed chemical characteristics unsuitable for analysis, for example, insolubility, polymerization and sensitivity to air, moisture or light. Meinema *et al.* prepared dimethylated compounds by reaction of Me_3SbCl_2 with natrium in liquid ammonia [12]. Morris *et al.* have studied trimethylstibine oxide and found that, when prepared by oxidation of trimethylstibine with HgO in anhydrous diethyl ether, the compound has a dimeric structure [13]. In addition, they proposed a polymeric structure for dialkylstibinic acids because antimony has in comparison to arsenic a lesser tendency to form double bonds with oxygen.

More recent methods showed differences between the formatted species, depending on the synthesis route. Dodd *et al.* showed that $MeSbO(OH)_2$ and Me_2SbOOH were either polymeric or not accessible under environmental conditions [9]. The synthesis of $Me_3Sb(OH)_2$ was fulfilled by the reduction of Me_3SbCl_2 by potassium borohydrate and subsequent oxidation with mercury oxide. The group achieved dimethylic species of Sb(V) like $Me_2SbCl(O_2H_2)_2$, but no species without hydrogen peroxide. These compounds were not suitable for analysis because they were insoluble in many media and exploded upon heating.

For analysis, mostly Me_3SbCl_2, Me_3SbBr_2, $Me_3Sb(OH)_2$ and Me_3SbO were used. Zheng *et al.* investigated the mass spectra of these compounds and concluded that in aqueous solution exchange of chloride and hydroxide may take place [14]. Deprotonation could lead to a monoanionic species. In addition, they showed the presence of monoanionic Sb(V), for example, $Sb(OH)_6^-$, $H_2SbO_4^-$, and dimeric, dianionic Sb(III) as $[Sb_2(C_4O_6H_2)_2]^{2-}$ in aqueous solution, providing some explanations for the chromatographic behavior of these species.

3 EXPERIMENTAL SETUP

3.1 Speciation analysis

The speciation of antimony is a rising field in analytical chemistry, although in comparison with other metal and metalloid speciation, for example, mercury, lead or arsenic, there are relatively few papers dealing exclusively with speciation of antimony. Many authors combine the speciation of antimony with other metals or metalloids such as lead, tin, arsenic, bismuth, selenium or tellurium. In these methods, the parameters of the separation and the detection had to be optimized in such a way as to allow the investigation of all elements. As a consequence, fewer antimony species are monitored and the detection limits are typically higher than in methods exclusively developed for antimony speciation. In the last five years, there have been more papers solely dealing with Sb speciation in order to get more data about this element in different matrices.

Two main routes have been followed by most of the authors. The classical way is the reduction of the antimony compounds to the corresponding hydride or methylated compounds and the separation with means of gas chromatography. The second path is the separation of the species by liquid chromatography. Some authors applied electrophoresis for the separation. For the detection, mostly element specific detectors were used, including atomic absorption spectrometry (AAS), atomic fluorescence spectrometry (AFS), inductively coupled plasma – atomic emission spectrometry (ICP-AES) or inductively coupled plasma – mass spectrometry (ICP-MS). Some authors used photometric detection or electrospray mass spectrometry (ESI-MS). One group fulfilled the speciation with neutron activation analysis (NAA). A review of the methods is given [15].

Many authors investigate only the oxidation states of Sb, the inorganic Sb(III) and Sb(V). There are numerous publications dealing with procedures to do so. Most often, the total Sb and the Sb(III) contents are measured in a two-step procedure, and the Sb(V) concentration is calculated on the basis of these results. Some studies showed in simple model systems the affinity of Sb to oxygen and sulfur-containing compounds. A major drawback in the development of Sb speciation is the lack of calibrants. As a consequence, many species, for example, showing as peaks in chromatograms, cannot be identified. This problem will be addressed further in the section “problems with speciation”.

3.2 First attempts in speciation

The first attempts of speciation of different antimony compounds were made by Andreae *et al.* in 1981 [10, 16]. They applied techniques already developed for the speciation of arsenic and used the reducibility of antimony compounds by sodium borohydride in acidic solution. Sb(III) and Sb(V) were reduced simultaneously in a highly acidic solution containing iodide as prereducing agent. In a second step, Sb(III) was selectively reduced at near-neutral pH, at which no reduction of Sb(V) takes place. The Sb(V) amount was calculated by subtraction. Methylstibonic acid and dimethylstibinic acid could be reduced without the addition of iodine. The stibines were collected after formation on a cold trap filled with gas chromatographic package. They eluted in the order stibine, methylstibine and dimethylstibine and were detected by quartz furnace AAS with detection limits of 0.3–0.6 $\mathrm{ng\,L^{-1}}$. This was the first report of the analyses of methylated antimony compounds. There is some doubt on the reliability of the data because rearrangements of Sb species have been examined widely.

3.3 Separation by reductive methods

Antimony compounds can be reduced to the corresponding hydrides or organometallic compounds. Sb(III) and Sb(V) are both reduced to stibine, SbH_3, at room temperature a toxic gas with a strong garlic smell. Its stability under the analytical conditions is sufficient for the determination with different element specific detectors.

The methylated Sb(V) species are reduced to the corresponding Sb(III) species: $MeSbO(OH)_2$ to $MeSbH_2$, Me_2SbOOH to Me_2SbH and Me_3SbX_2 to Me_3Sb. These reactions have been used widely for the speciation of antimony. Advantages are the low detection limits even by use of AAS detection and the separation from the matrix, because the analytes are going from liquid to gaseous phase. Drawbacks are the limitation to reducible species, the difference in detector response for different compounds leading to problems in quantification and a great variety of matrix effects on the reduction process. Many authors deal with the parameters of the reduction and the influences, for example, of matrix components on the analytical performance.

Four different setups for the reduction can be found in literature.

1. The classical batch type for speciation of Sb(III) and Sb(V)
2. The classical batch type mainly for speciation of organic species
3. The flow injection
4. The postcolumn reaction after liquid chromatographic separation

The first three strategies will be presented in this section, the latter as part of the liquid chromatographic methods. In addition, the products of the reduction can be collected and preconcentrated in cold traps and afterwards be analyzed with low-temperature gas chromatography (LTGC). In contrast to the differential methods for the determination of Sb(III) and Sb(V), the inorganic Sb gives only one signal because both oxidation states form the same hydride (SbH_3). Therefore, these methods are used for the determination of methylated Sb compounds. They are described below in the section "low-temperature gas chromatography".

Element specific detection is predominant as detection in the reductive type speciation of Sb, for example, hydride generation-atomic absorption spectrometry (HG-AAS), hydride generation – inductively coupled plasma – atomic emission spectrometry (HG-ICP AES) and hydride generation – inductively coupled plasma – mass spectrometry (HG-ICP MS).

3.4 The classical batch type for speciation of Sb(III) and Sb(V)

The knowledge of the oxidation states of antimony is one of the main goals for the speciation. By the reduction of Sb(III) and Sb(V), the same product, SbH_3, is formed, so that no direct speciation is possible. Nevertheless, quite a lot of authors used the hydride formation for the distinction between both oxidation states. Sb(III) is reduced fast and easily at pH-values from strongly acidic to nearly neutral. In contrast, Sb(V) is only reduced at rather a low pH and at much slower rates. Typically, no complete reduction of Sb(V) could be achieved without a prereduction to Sb(IIII) [17]. Preconcentration of the analytes is possible with the batch type reactors. Mostly, the hydride was collected in cold traps, although it is not used as often as in LTGC.

As stipulated before, the speciation of Sb(III) and Sb(V) is fulfilled in a two-step procedure. At first, one part of the sample is reduced at higher pH-values without prereduction, so that only Sb(III) is reduced. After that, a second part of the sample is completely prereduced from Sb(V) to Sb(III) before the reduction step, so that the total amount of antimony is measured. The Sb(V) concentration could now be calculated as the difference between the two measurements [18, 19]. Typical conditions and analytical data for the batch type reduction are given in Table 2.3.1. Detection limits for total Sb and Sb(III) were identical.

3.5 Continuous flow and flow injection methods

Flow injection is often used for the preconcentration of antimony species in cold traps in order to improve the performance of the analytical methods. Compared to the batch reactions, typically lesser concentrated solutions are employed. Figure 2.3.1 shows a schematic diagram of a HG-ICP-MS system and Table 2.3.2 reports the conditions for the on-line reduction of Sb(V) and Sb(III) [19].

Table 2.3.1. Conditions and analytical data for the batch type reduction [19].

Parameter	Value	Parameter	Value
Sample aliquots	3 mL	Detection	AAS
Prereducing agent	3 mL 2% KI	Detection limit	2.97 ng
Acid	5 mL 4 M HCl	Sensitivity	3.03×10^{-3} a.u./ng
Prereducing time	30 s	Precision ($n = 10$)	3.6% at 40 ng
Reducing agent	3 mL 4% $NaBH_4$	Linear range	3.0–95 ng

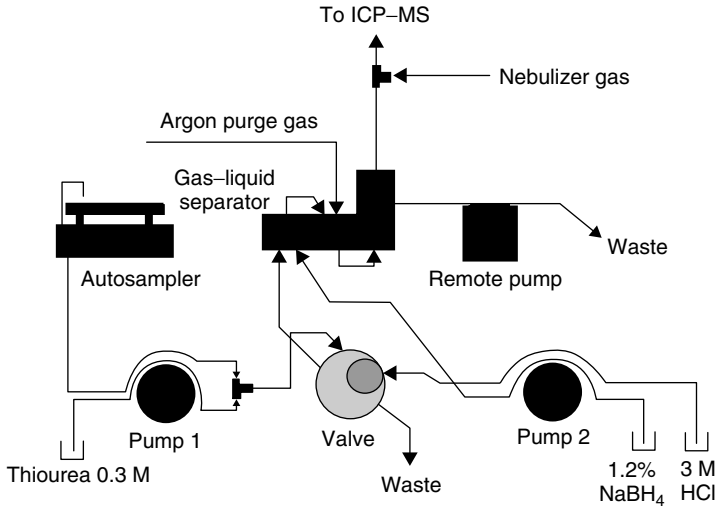

Figure 2.3.1. FI-HG-ICP MS setup used by Bowman *et al*. (Reproduced from Reference [20] by permission of The Royal Society of Chemistry.)

Table 2.3.2. Conditions and analytical data for the on-line-reduction procedure [20].

Parameter	Value	Parameter	Value
Sample aliquots	200 $\mu g\,L$	Detection	ICP MS
Prereducing agent	0.3 M thiourea	Flow rate	0.35 mL
Reaction time	180 s	Detection limit	0.06 $\mu g\,kg^{-1}$
Reducing agent	1.2% $NaBH_4$	Precision ($n = 10$)	10%
Acid	0.12 M HCl	Linearity	Up to 50 $\mu g\,kg^{-1}$

Many authors tried to find reducing parameters suitable not only for antimony but also for the other hydride forming elements like As, Bi, Se, Te [21, 22]. Cabredo *et al*. used a flow injection method for the preconcentration of antimony in a cold trap system for the detection with gas phase molecular absorption spectrometry [23]. A two-step method for the speciation of Sb(III) and Sb(V) is presented by Hou and Narasaki [24]. First, the total Sb was determined by HG-ICP MS after prereduction with potassium iodide and reduction with borohydride. In a second step, the Sb(III) is detected selectively at pH 5.5 without inference of Sb(V). The inductively coupled plasma – atomic emission spectrometry (ICP-AES) has been applied as detector for flow injection hydride generation used by Menendez Garcia *et al*. [25].

One method was presented for the speciation of the two inorganic and the trimethylated Sb-compounds by selective reduction without gas chromatography. The flow injection method was used by Ulrich for the speciation of Sb(III), Sb(V) and Me_3SbO in a three-step procedure [26].

It was stated that fluoride influenced strongly the hydride formation and suppressed it completely for inorganic species in the presence of iodide. Detection limits of 1.1, 1.2 and 1.4 $\mu g\,L^{-1}$ with standard deviations of 2.6–8.1% for Me_3SbO, Sb(III) and Sb(V) were achieved and the time consumption of the analysis was comparable to liquid chromatographic separations.

Continuous flow as technique for sample delivery has been used rarely for antimony speciation. A major drawback of such methods is the large amount of sample needed for a single analysis. Especially in the environmental and biomedical field, the sample size is often limited. Menendez Garcia *et al*. presented a method for a tandem online separation of Sb(III) and Sb(V) with continuous flow and the selective extraction of the Sb(III) dithiocarbamate into methylisobutylketon (MIBK) followed by addition of acid and reducing agent and ICP-AES detection [25]. Risnes and Lund studied the effects of interferences on the hydride formation in a continuous flow setting [27].

3.6 Factors that influence hydride generation

According to the literature, the hydride formation process for antimony species depends on many factors. Important are the concentration of borohydride and the nature and concentration of acid, the reaction time and the presence or absence of prereducing agents like iodide. In addition, many authors deal with the influence of matrix elements or compounds, which in many instances can hinder the reduction process to a large extend. All parameters affect the reduction of the diverse antimony species in different ways. While Sb(III) and even more of the methylated compounds are easily reduced under various circumstances, the reduction of Sb(V) is critical.

3.7 Reduction

Most literature deals with the reduction of antimony with sodium borohydride in acetic solution. Depending of the experimental setup, different concentrations and pH-values were applied. Variation of the pH-value have been used by Alegria *et al*. for the speciation of Sb(III) and Sb(V) because only Sb(III) was reduced in significant amounts by borohydride at pH 5 to 7 [17].

In contrast to that, many authors stated a dependence of reduction on the pH-value of the samples and the Sb(V):Sb(III) ratio. That means there is a significant amount of Sb(V) detected under the conditions of Sb(III) reduction, which causes unreproducible errors in the speciation analysis. Deng *et al*. overcame this problem by adding 8-hydroxyquinoline as masking agent [28].

Some authors describe the electrochemical reaction of antimony [29–31]. This reduction should overcome the problems of contamination and low stability of borohydride solutions and the interferences by transition metals. Nevertheless, the studies showed problems in the stability of the electrodes and the reproducibility of the results.

3.8 Prereducing agents

Pentavalent antimony could not be reduced by sodium borohydride in sufficient amounts in a short time. Especially when flow injection or post-column derivatization are used, the prereduction of Sb(V) is essential for the performance of the methods. Diverse prereducing agents have been applied such as potassium iodide, potassium bromide, L-cysteine or thiourea with different results.

Welz and Sucmanova concluded that L-cysteine was able to reduce Sb(V) in 5 to 30 min similar to the action of potassium iodide [32]. An advantage was the better stability of the L-cysteine solution in comparison to iodide. When simultaneous speciation of different hydride forming elements should be performed, Bowman *et al*. proposed the use of thiourea [20]. This compound was able to reduce Sb(V) to Sb(III) in less than 300 s.

Vuchkova and Arpadjan examined the influence of dithiocarbamates on the hydride generation because these complexing agents could be used for preconcentration and matrix separation of antimony compounds [33]. The reduction was performed with good results in methanolic solution.

3.8.1 Impact of matrix elements

Different studies deal with the problems of matrix components for the reduction of antimony. Two main effects have been described: the reoxidation of antimony by oxidizing compounds such as HNO_3 and the reaction of $NaBH_4$ with matrix elements, leading to a decrease in efficiency of the added sodium borohydride. Risnes and Lund examined the influences of nitric acid and several transition metal elements on the determination of Sb(III) and Sb(V) [27]. Both interferences could be minimized by using a solution containing 10% thiourea as prereducing agent in a continuous flow type procedure with ICP-AES detection.

A 100-fold excess of Cu^{2+}, Cd^{2+}, Ni^{2+}, Pb^{2+} and Fe^{3+} led only to a slight signal suppression [34]. Hou and Narasaki found strong interferences of the hydride formation especially for trivalent or hexavalent chromium and for molybdenum [24].

3.9 Low-temperature gas chromatography

Gas chromatography was used for the separation of the antimony hydrides and methylated compounds. All these are gaseous at room temperature and are often preconcentrated by cold trapping, so that better performance could be achieved by using low-temperature gas chromatography. The mechanism of separation relies on differences in boiling point and interaction of the species with the chromatographic material. Mostly packed columns were applied. Figure 2.3.2 shows a hydride-generation apparatus for LTGC with ICP-MS detection [35].

Krupp *et al*. used low-temperature gas chromatography coupled with inductively coupled plasma mass spectrometry (LTGC-ICP-MS) for the determination of several metal and metalloid species [35]. In a batch reactor, the sample was derivatized by hydrogenation with 5% $NaBH_4$. The reaction products were dried and the species were collected in a packed GC column filled with supelcoport absorption material and cooled in liquid nitrogen. Several organic antimony species could be detected at ^{121}Sb after GC separation. Clark and Craig showed the possibility of an on-column hydride generation [36]. The difficulty of the quantification of the methylated species is described in many publications because no standards are available for the correlation of the signal intensity to the concentration. Therefore, no analytical data regarding detection limits and reproducibilities can be given for this group of methods.

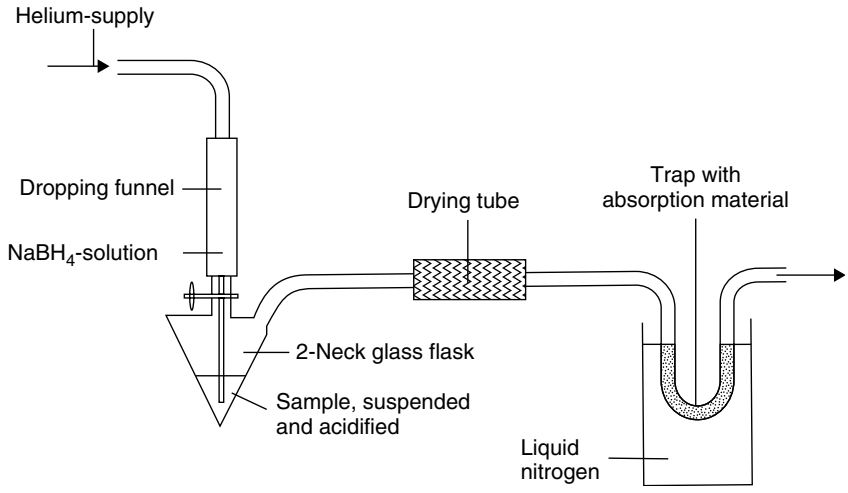

Figure 2.3.2. Hydride-generation apparatus for LTGC with ICP-MS detection. (Reproduced from Reference [35] by permission of Springer Verlag GmbH & Co KG.)

3.10 Separation by liquid chromatographic methods

Liquid chromatography is the second interesting method for antimony speciation. It offers the possibility to overcome some drawbacks of the reduction methods as listed below:

1. Only reducible species can be detected. No other species can be viewed.
2. The reduction for the separation of Sb(III) and Sb(V) employs two steps. The Sb(V) is calculated by subtracting Sb(III) from total Sb. This leads to elevated standard deviations of the methods. In addition, the time of analysis may be shorter for liquid chromatography.
3. It is either possible to investigate Sb(III)/Sb(V) or total inorganic Sb/methylated species by the reduction method. Liquid chromatography offers the possibility to monitor all species in a single run.

These reasons led several groups to work on Sb speciation by liquid chromatography. The species of main interest, Sb(III), Sb(V) and Me_3SbX_2, are anionic in aqueous solution. In addition, a cationic form of Me_3SbX_2 has been described. Therefore, mainly ion chromatography (anion chromatography) has been applied. Two types of methods can be distinguished: The first one uses liquid chromatography directly coupled to an element specific detection, while the latter applies liquid chromatography with postcolumn reduction, to combine the advantages of liquid chromatography with the matrix separation and low detection limits of the reduction methods. Both groups of methods will be described in the next sections.

3.11 Liquid chromatography without hydride generation

The separation of Sb(III) and Sb(V) was fulfilled by Smichowski *et al.* using anion chromatography with phthalic acid as eluent and a Hamilton PRP-X100 column with different element specific detectors [15]. Detection limits were 400 and 80 $\mu g\,L^{-1}$ for Sb(III) and Sb(V) for the detection with HG-ICP MS. The phthalic acid method has been expanded to the detection of Sb(III), Sb(V) and Me_3SbO by Ulrich, as shown in Figure 2.3.3 [37]. Both methods showed extensive peak broadening for the Sb(III) peak at relatively large retention times.

Zheng *et al.* used a silica gel column with phthalic acid eluent, which led to a significant improvement of the retention times, the peak shapes and the detection limits with 0.1 and 0.3 $\mu g\,L^{-1}$ for Sb(V) and Sb(III), but loss of the ability for Me_3SbX_2 separation [14]. Zhang *et al.*

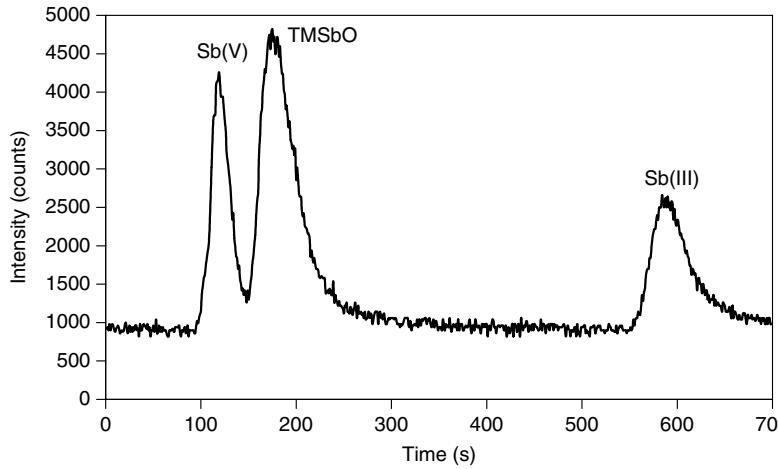

Figure 2.3.3. The ion chromatographic separation of 100 $\mu g\,L^{-1}$ Sb(III), Sb(V) and Me_3SbO (named TMSbO in the figure) with ICP-AES detection. (Reproduced from Reference [37] by permission of Springer Verlag GmbH & Co KG.)

used a 2-cm anion chromatographic column and tartrate eluent and achieved a good separation of Sb(III) and Sb(V) [38]. The short columns minimized the strong interactions between the Sb(III) and the anion-exchange material. Another study showed the applicability of a miniaturized anion-exchange column for the speciation of Sb(III) and Sb(V) with hydride generation – atomic fluorescence detection (HG-AFS) [39].

Guerin *et al.* used anion chromatography with an ammonium phosphate eluent and methanol modifier and ICP-MS detection for the determination of several metalloid species including Sb(V) [40]. The application of ultrasonic nebulization for HPLC-ICP MS has been described by Krachler and Emons with detection limits of 14 ng L^{-1} for Sb(III), 12 ng L^{-1} for Sb(V) and 9 ng L^{-1} for Me_3SbCl_2 [41]. Their procedure covered two steps: in the first one Sb(V) and Sb(III) were separated with ethylenedinitrilotetraacetic acid (EDTA) eluent, whereas in the second Sb(V) and Me_3SbCl_2 were eluted with NH_4HCO_3 and tartaric acid. Figures 2.3.4 and 2.3.5 show these determinations.

The influence of different complexing agents such as citrate and tartrate on anion chromatographic separations was studied by Ulrich [42]. It was concluded that these compounds have a strong influence on the retention times of the species and the performance of the method and that eluents with low complexing tendency should be used.

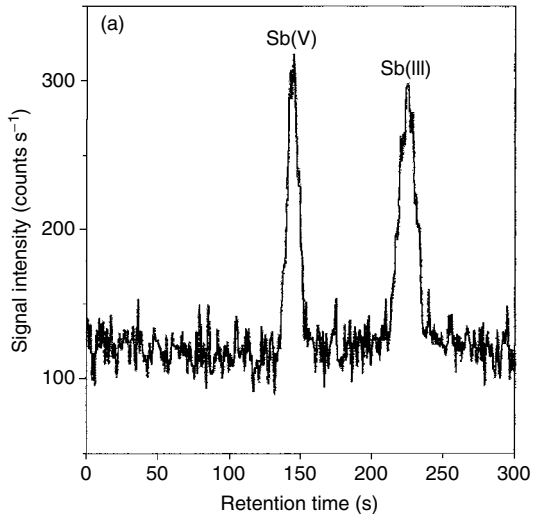

Figure 2.3.4. Chromatogram of the separation of 50 ng L^{-1} Sb(III) and Sb(V). (Reprinted from *Anal. Chim. Acta.* 429, Krachler, M. and Emons, H., Speciation Analysis of Antimony by High Performance Liquid Chromatography Inductively Coupled Plasma Mass Spectrometry Using Ultrasonic Nebulization, 125, Copyright (2001), with permission from Elsevier.)

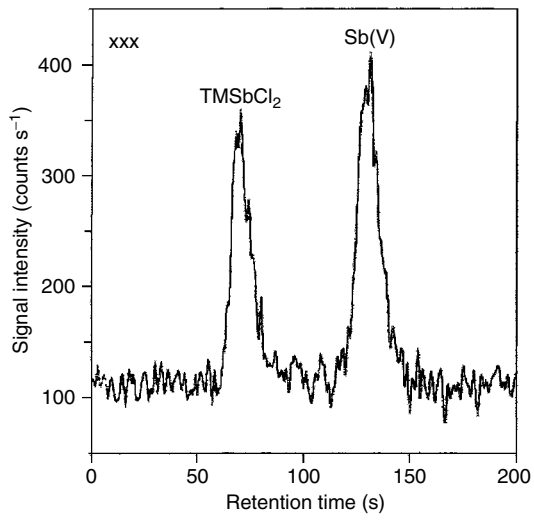

Figure 2.3.5. Chromatogram of the separation of 50 ng L^{-1} Sb(V) and Me_3SbCl_2. (Reprinted from *Anal. Chim. Acta.* 429, Krachler, M. and Emons, H., Speciation Analysis of Antimony by High Performance Liquid Chromatography Inductively Coupled Plasma Mass Spectrometry Using Ultrasonic Nebulization, 125, Copyright (2001), with permission from Elsevier.)

3.12 Liquid chromatography followed by hydride generation

Several authors describe liquid chromatography and postcolumn reduction of the antimony species. Better detection limits could be achieved in comparison to the direct coupling of ion chromatography to an element specific detection. Two reasons have been proposed: The separation from the matrix with lesser background signals and probability of signal overlap and – in case of plasma spectrometry – the use of dry plasma, which can enhance the detection limits significantly. A major drawback is the limitation of the methods to the reducible species, although all antimony species considered in the literature up to now can be reduced with sodium borohydride to gaseous compounds at least at elevated temperatures.

The reduction was mostly done in a flow injection type setting with either one-step addition of acid and sodium borohydride or two-step addition of a first prereducing agent followed by borohydride. Figure 2.3.6 shows a setting for the one-step procedure [38].

Krachler and Emons described the chromatographic behavior and the reduction characteristics for several liquid chromatographic systems coupled to flow injection HG-AAS for the speciation of Sb(III), Sb(V) and Me_3SbCl_2. Detection limits of 0.4, 0.7, and 1 $\mu g\,L^{-1}$ for Me_3SbCl_2, Sb(III) and Sb(V) were obtained. In addition, ICP-AES and ICP-MS have been used as detectors for liquid chromatography.

3.13 Capillary electrophoresis

Only few papers deal with the speciation of antimony with capillary electrophoresis. Michalke and Schramel developed a method with 20 mM Na_2HPO_4/NaH_2PO_4 at pH 5.6 as background electrolyte and NaOH or acetic acid as stacking electrolytes and on-line coupling with an ICP-MS detection system [43]. Detection limits of 0.1–0.7 $\mu g\,L^{-1}$ could be achieved for inorganic and methylated antimony species. Figure 2.3.7 shows an example of an electropherogram of the separation of Sb(V), Sb(III) – here present as $Sb(OH)_3$ – and Me_3SbCl_2.

3.14 Special methods

Only few authors use graphite furnace atomic absorption spectrometry (GF-AAS) for detection in antimony speciation. Garbos *et al.* described differences for the sensitivities of Sb(III) and Sb(V) with palladium as modifier in the graphite furnace, which was connected to the low reducting efficiency for Sb(V) [44]. Thiourea as prereducer was used by Wifladt *et al.* [45]. Moreno *et al.* described the possibility of the usage of AFS for the speciation of Sb(III) and Sb(V) [46]. Deng *et al.* used this technique with 8-hydroxychinoline as masking agent for interferences of Sb(V) and transition metals on the selective determination of Sb(III) [28].

Genetically engineered bacteria were used for the selective analysis of Sb(III) by Scott *et al.* [47]. The bacteria produced β-galactosidase, depending on the amount of Sb(III) present. The β-galactosidase concentration was monitored electrochemically. Several authors used electrochemical techniques for the speciation of antimony. Wagner *et al.* determined Sb(III) and Sb(V) by adsorptive stripping voltammetry [48]. The different electroactivities of Sb(III) and Sb(V) were used for speciation, as Sb(V) is not active at mercury electrodes and has to be reduced first [49].

Garbos *et al.* presented a speciation method involving the measurement of Sb(V) and total antimony with ICP-MS. The Sb(III) was selectively removed by solvent extraction with *N*-benzoyl-*N*-phenylhydroxylamine and its concentration was calculated as the difference between total Sb and Sb(V) with a detection limit of 0.7 ng L^{-1} [44].

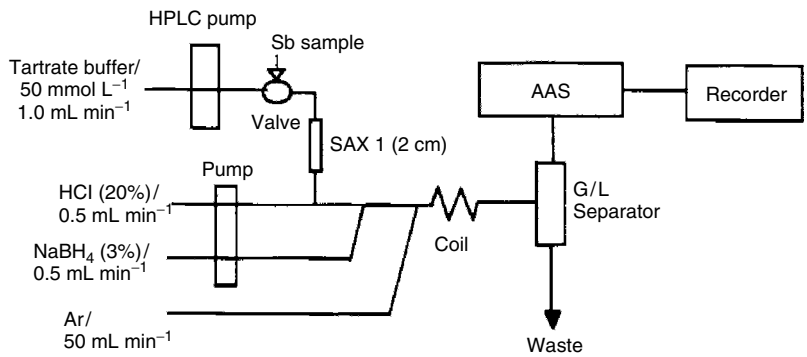

Figure 2.3.6. Schematic diagram of high performance liquid chromatography (HPLC) coupled to HG-AAS for the speciation of Sb. (Reproduced from Reference [20] by permission The Royal Society of Chemistry.)

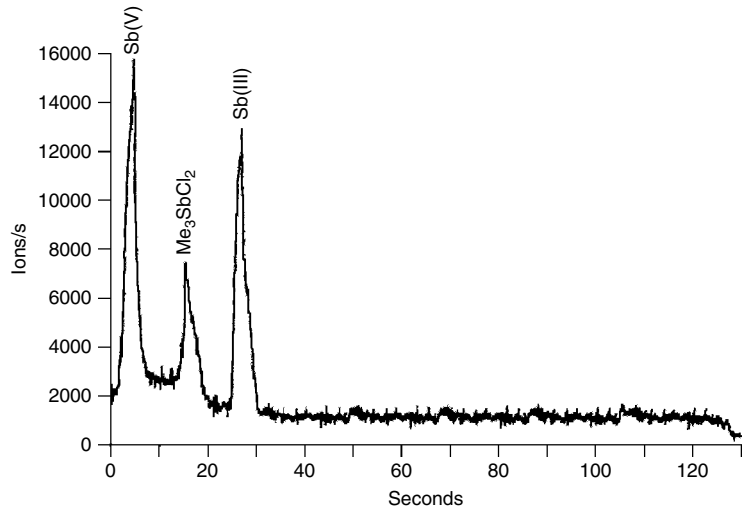

Figure 2.3.7. Electropherogram of the separation of 10 $\mu g\,L^{-1}$ Sb(V), Sb(III) – here present as $Sb(OH)_3$ – and Me_3SbCl_2. (Reprinted from *J. Chromatogr. A,* 834, Michalke, B. and Schramel, P., Antimony speciation in environmental samples by interfacing capillary electrophoresis online to an inductively coupled plasma mass spectrometer, 341, Copyright (1999), with permission from Elsevier.)

A simple photometric method for the speciation of Sb(III) and Sb(V) was developed by Rath *et al.* [50]. They determined the Sb(III) concentration with bromopyrogallol red and the total antimony after reduction of the Sb(V) with iodide. The Sb(V) content could be calculated by the difference of the two measurements. A totally different approach consisted of successive precipitation of antimony species for analysis of both species [51].

4 PROBLEMS LINKED TO ANTIMONY SPECIATION

Sb speciation exhibits a bundle of problems. Some of them are more general in nature and apply to every speciation analysis, whereas some are specific for Sb.

The problems can be separated in the following groups:

- Problems with standards
- Problems with samples
- Chromatographic problems
- Problems of detection

These problems will be addressed next.

4.1 Problems with standards

The stability of standards is critical for the analysis of antimony species, especially for the investigation of the oxidations states Sb(III) and Sb(V). The oxidizability of Sb(III) was reported by Krachler and Emons [41]. They found that freshly made standards of Sb(III) were not stable for more than a few hours, after which peaks of Sb(III) and Sb(V) occurred during the measurements. A better stability of the standards was achieved by thoroughly removing dissolved oxygen by flushing with helium or by complexation of Sb(III) by the addition of 1.25 mM EDTA at pH 4.7.

A special problem for Sb speciation is the synthesis of the necessary standards. There are several compounds that have been proposed for environmental samples but could not be synthesized in appropriate quality. Several signals in the chromatograms could not be identified because no standard compounds were available. In addition, there are no certified reference materials for Sb species in different matrices.

4.2 Problems with samples

The total content of Sb in most matrices is rather low, often in the low $\mu g\ L^{-1}$ or $\mu g\ kg^{-1}$ range.

That means even lower concentrations for the species, especially for the rarer ones. Therefore, there is often only one method suitable and available for the determination of Sb species in this ultra trace region, which leads to problems with the validation of the results.

The extraction efficiencies for Sb are extremely low for many matrices, so that the speciation must deal with fractions very low in Sb and a residue, which contains most of the antimony. Another important problem is the stability of the Sb species in the samples. It has been shown for standards that there is a rapid oxidation of Sb. If such processes took place in the samples, no reliable data of the species distribution can be gathered. Up to now, there are no evaluations on the sample stability in respect to Sb in the literature, a problem that should be addressed as soon as possible.

4.3 Chromatographic problems

The methylated compounds of antimony can, like arsenic species, undergo transformation during gas chromatographic examinations. Dodd *et al*. investigated the reduction process of Me_3SbCl_2 and $Me_3Sb(OH)_2$, which both should react with potassium borohydride to the single product Me_3Sb [9]. Gas chromatographic analysis showed four different peaks presumably representing SbH_3, $MeSbH_2$, Me_2SbH and Me_3Sb, so that obviously molecular rearrangement occurs during the analysis. Figure 2.3.8 shows this rearrangement [9]. As a consequence, there should be some doubts as to the correctness of some older studies on antimony species in which reduction and gas chromatographic separation have been applied.

On the other hand, the presence of mono- and dimethylated species in environmental or biomedical samples is still possible. As there are no standards available of these compounds, standard addition techniques cannot be considered. These species might undergo rearrangements as well, so that similar chromatograms could be achieved with either Sb species.

There are two main problems in liquid chromatography: the first one is the peak broadening especially for Sb(III). The Sb(III) in aqueous solution occurs as double or even higher charged anions that interact strongly with the ion chromatographic resin. On the other hand,

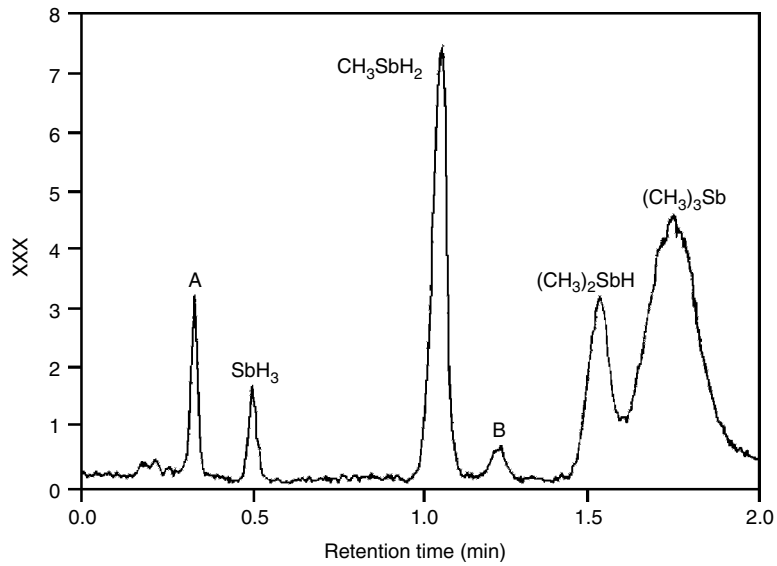

Figure 2.3.8. HG-GC-MS chromatograms of the products from $Me_3Sb(OH)_2$ solution. A and B are unspecified components. (Reproduced from Dodd, M., Grundy, S. L., Reimer, K. J. and Cullen, W. R., (1992) with permission of John Wiley and Sons Limited [9].)

Sb(V) and Me_3SbX_2 have short retention times, so that the separation of all three components in one single chromatographic analysis has been rarely done [42].

4.4 Detection problems

Hutton *et al*. recognized signal suppression in ICP-MS determinations with the presence of refractory elements [52]. The groups of Guy *et al*. and Jakubowski *et al*. showed different behavior of dry aerosols like organometallic gases in comparison to nebulized metal solutions [53, 54]. Feldmann and Hirner described the necessity of internal standards for ICP-MS detection because of the influence of hydrogen on the plasma and the deposition of SiO_2 out of the samples in the nebulizer and the detector during the chromatographic analysis [55].

5 RESULTS OF SPECIATION

Up to now, only few data of antimony species in different matrices exists. One main reason is the low concentrations, especially in uncontaminated environmental samples, which make the speciation a very difficult task. Another reason is the lack of suitable standards. Only few inorganic compounds and gaseous Me_3Sb are available commercially. Different groups made efforts to synthesize organic antimony species such as $MeSbO(OH)_2$ for analytical purposes, but they all failed. Only trimethylated pentavalent antimony species (Me_3SbCl_2, Me_3SbBr_2, Me_3SbO, $Me_3Sb(OH)_2$) have been produced in sufficient amounts and purity. In addition, no standard reference materials are available up to now in which all relevant antimony species have been certificated.

Another important point for the investigation of real world samples and for the understanding of the fate of Sb in biota is the development of gentle and yet efficient extraction processes for different matrices. The efficiencies are still generally low, distinctively lower than for As. Extraction yields from soil with water, methanol/water or 0.2 mol L^{-1} acetic acid are less than 1% [56]. Slightly better results are obtained by enzymatic or alkaline extractions [57]. In addition, often there are no data about the stability of the species during the extraction processes.

Most data are documented for different kinds of water samples, for example, natural water, mineral water, waste water or sea water. A few studies exist about antimony in soil, in sediments, in landfill and sewage gases, in plants and in tissues. But nearly all of them only give selective information about single samples and some general description about the distribution of antimony species in the environment or the food chain. One relatively large area for antimony speciation belongs to the biomedical field because of the use of antimony as therapeutic agent in tropical diseases. Distinctive procedures have been developed for quality insurance in these drugs. In addition, antimony species in cell extracts have been investigated to give insight into mechanisms of drug action.

5.1 Antimony complexes

Complexes of Sb(III) and Sb(V) can influence the chromatographic behavior of this species [42]. Guy *et al*. presented a method for the monitoring of different antimony complexes of citrate, malate and lactate [53]. The structure of these compounds was investigated with nuclear magnetic resonance (NMR). For the separation of the compounds, liquid chromatography with NH_4Cl as eluent and either ICP-AES or ESI-MS as detector was used. Results showed no influence on the chromatographic behavior for Sb(III) species, whereas different Sb(V) complexes could be detected.

5.2 Antimony in the environment

There are not many data available about the speciation of Sb in the environment. Some studies deal with the Sb cycles and the average amount in different kind of samples, but these examinations deal with the total content of Sb. The main pathways of antimony are atmospheric input and the

water cycle. The concentration level of antimony in the earth's crust is ca. 0.2 mg kg^{-1}. In unpolluted waters, the concentration of Sb is typically below 1 $\mu g L^{-1}$. Anthropogenic activity and pollution can lead to concentrations as high as 100 $\mu g L^{-1}$. It has been estimated that around 38 ton of Sb are emitted yearly into the environment by human activities. The dependence of the total Sb concentration in leaves on the amount and the distance to traffic has been established recently [58].

Information about Sb speciation in environmental samples have been documented in a few case studies, for example, one special lake, one special area of needle trees, one special soil. Some of these studies will be described in the next sections about environmental reactions related to the matrices water, sediment, soil, plants and landmill and sewage gases.

5.3 Environmental chemistry of antimony species

Up to now, there are only a few studies that deal with the environmental chemistry of antimony compounds. Because of the low concentration of antimony in typical samples, the monitoring of the species is difficult. Most of the authors stress the similarities between arsenic and antimony and propose similar pathways of biochemical reactions. Parris and Brinckman investigated the methylation and oxidation of trimethylstibine [59] after a possible biological methylation of inorganic antimony compounds. The abiotic oxidation took place rapidly for Me_3Sb with a constant of 10^3 $M^{-1}s^{-1}$. Therefore, they concluded that the concentration of Me_3Sb in any aerobic surroundings in the environment should be limited by this process.

The biomethylation of Sb(III) and Sb(V) to Me_3Sb by microorganisms was first monitored in 1997, although the process had been proposed for many years [60]. One reason could be the low concentration of these compounds in the head space of experimental cultures of microorganisms, especially in respect to arsenic species. The aerobic biomethylation by *Scopulariopsis brevicaulis* was shown under aerobic conditions by Andrewes *et al.* [61]. In anaerobic environments, Me_3Sb was measured above soil-enrichment cultures spiked with Sb(III) [51].

5.4 Antimony in water

Water is the matrix, in which the antimony speciation has been mostly applied. Especially tap, fresh and mineral water sources have been used as test matrices for newly developed methods. Therefore, there is a relatively large amount of data available for this matrix.

Garbos *et al.* examined natural waters in the area of Warsaw [62]. The total antimony concentration was less than 1 $\mu g L^{-1}$, with over 90% of Sb(V) in the samples. This result, similar to other studies, reveals that in natural waters the prevailing chemical form is Sb(V). Problematic is the instability of Sb(III) regarding oxidation, which has been found in other studies. Maybe the predominance of Sb(V) in water samples is caused by species transformation after the sampling. This problem – as for other matrices – has to be addressed further on. Smichowski *et al.* as well as Nash *et al.* give a review on antimony speciation in water [15, 63].

5.5 Antimony in sediments and sludges

Slurry formation-hydride generation AAS was used by de la Calle Guntinas *et al.* for the speciation of Sb(III) and Sb(V) in sediments [18]. The antimony species in the slurry were directly reduced to the hydride, without any further sample preparation. The analysis evolves in two steps as described in the experimental section, first detecting Sb(III), then total Sb, with the calculation of the Sb(V) amount as the difference between the two measurements. In marine sediments, total contents of 0.161 $\mu g g^{-1}$ with a Sb(V) : Sb(III) ratio of 5 : 1 were found. The same group investigated the bioavailability of antimony in sediments with similar methods [19]. They found that less than 50% of the antimony is soluble in aqua regia, which they stated to be a good estimate of the maximum plant-available amount.

Krupp *et al*. investigated sediments in a German river by LTGC-ICP-MS [35]. The samples were freeze-dried, homogenized and stored at $-20\,^{\circ}C$. No statement was made about the influence of sample preparation on the analytical results. The three methylated antimony species were found in concentrations of 0.2 to 9.8 ng g^{-1} for $MeSbH_2$, 0.1 to 1.2 ng g^{-1} for Me_2SbH and 0.1 to 0.9 ng g^{-1} for Me_3Sb. In addition, $SbEt_3$ was postulated in some of the samples. It was identified on the basis of the calculation of the boiling point based on retention time. No standard was available for this species. Eight antimony species have been found in fouling sludge by Michalke and Schramel, but they were only able to identify Sb(V) and Me_3SbCl_2 by standard addition [43]. Nash *et al*. presented in a review mainly focusing on methodologies for total Sb some aspects on antimony speciation in sediments [63].

5.6 Antimony in soil

Only very few data are available about the antimony speciation in soils. One drawback – as for sediments and sludges – is the low extractability of antimony compounds, although the antimony content in soil can reach as much as 100 mg kg^{-1}, for example, due to rock whethering. De la Calle Guntinas *et al*. investigated the bioavailability of antimony in one soil sample and between 44 and 48% of the antimony could be extracted by aqua regia [19]. Ulrich found Sb(V) to be the predominant species in antimony-rich soils. Two unidentified substances were noted [26]. In addition, Me_3SbO could be identified as shown in Figure 2.3.9.

5.7 Antimony in plants

Benson and Cooney proposed a bioalkylation process of antimony by marine algae similar to arsenic [64]. But they did not show analytical proofs for their hypothesis. The biosorption of Sb(III) and Sb(V) of two biological substrates, *spirulina platensis*, a cyanobacterium, and *phaseolus*, derived from a plant were studied by Madrid *et al*. [65]. Both substrates were able to accumulate antimony over a wide range of pH-values, temperatures and incubation times. The accumulation depended on the oxidation state of antimony with a higher rate for Sb(III). The amount of antimony in the plant was monitored with electrothermal AAS after extraction of the plants with nitric or hydrochlorid acid.

Freshwater plants were examined using HG-GC-MS by Dodd *et al*. Organoantimony compounds

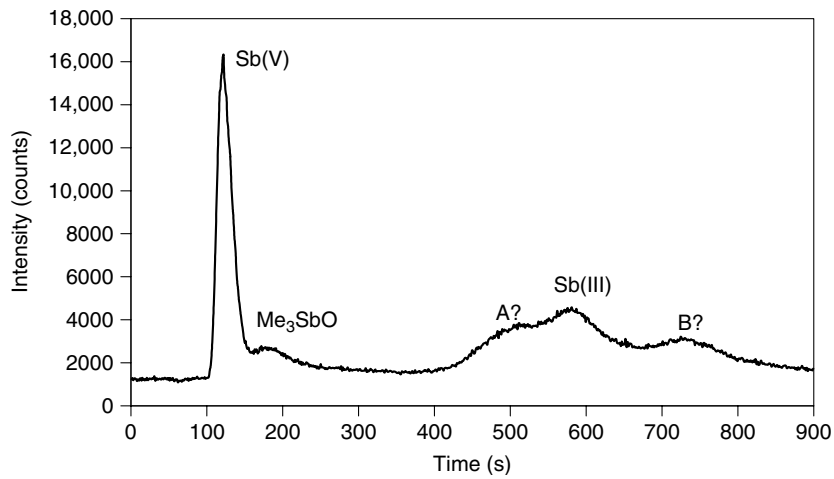

Figure 2.3.9. Chromatogram of a soil sample from eastern part of Germany, measured by IC-ICP MS at ^{121}Sb, where Sb(III), Sb(V) and Me_3SbO (named TMeSbO) were identified and two more species were to be seen.

were identified in pondweed (*potamogetan pectinatus*) on the basis of the retention times and the mass spectral data [66].

5.8 Antimony in landfill and sewage gases

Feldmann and Hirner investigated several metal and metalloid species in landfill and sewage gases [55]. They collected the gases directly by cryogenic trapping cooled by acetone/liquid nitrogen to $-80\,^{\circ}C$. The gases consisted of 45 to 61% methane and less than 1% oxygen. As analytical method, thermodesorption combined with gas chromatography for separation and ICP-MS for detection of ^{121}Sb and ^{123}Sb were used. The standards used for the determination were prepared by Müller, a member of the group of Hirner, as mixture of methylated hydrides [67]. One major component in the chromatogram was detected in concentrations of 0.618 to 71.6 $\mu g\,m^{-3}$ and could be identified as Me_3Sb by comparison of the retention time with that of the standard. SbH_3 was only found in very low concentrations in landfill gases.

5.9 Antimony in the biomedical field

There is a growing interest in the speciation of antimony in the biomedical field because the mechanism of its toxicity to humans is not well understood and Sb is used as an important therapeutic agent in several tropical diseases. The mode of action of these compounds is rather unknown because it cannot be examined unless thorough knowledge of the Sb species in the cells is acquired, which implies speciation analysis. In the last few years, some efforts have been made to investigate these samples, although much more data are needed for the understanding of the complex biological processes.

The analysis of biological samples is rather challenging because matrices such as urine, tissue and cell extracts show a rich variety of complexing agents and salts. In addition, there are biomolecules, for example, enzymes or proteins, able to bind with metalloids and to promote reactions such as oxidation or reduction of Sb. In the next sections, some methods for the Sb speciation in biomedical samples will be described.

5.9.1 Antimony speciation in tissue and cells

Rondon *et al.* presented a method for the selective determination of Sb(III) and Sb(V) in liver tissue [68]. They first extracted selectively Sb(III) with 1 mol L^{-1} acetic acid, then measured the total amount of antimony after microwave-assisted mineralization. Detection was done with HG-AAS. The method was proven with standard materials, but no data for real samples were given.

Several medical studies deal with the specifications of Sb(III) in cells and the metabolization of antimony, although mostly no concrete analytical chemical data are given and the results are derived from cell experiments. Nies described the pathway of Sb(III) in *Escherichia coli* [69]. It enters the cells via the glycerol facilitator. The detoxification of cells from Sb(III) should work similarly to that of arsenite by efflux.

5.9.2 Antimony speciation in urine

Krachler and Emons presented a method for the speciation of Sb(III), Sb(V) and Me_3SbCl_2 in urine by HPLC-ICP MS with detection limits of respectively 8 ng L^{-1}, 20 ng L^{-1} and 12 ng L^{-1} and 8 ng L^{-1} [87]. The method was applied to occupationally exposed and nonexposed individuals. The predominant species was Sb(V) followed by Me_3SbCl_3, and only trace amounts of Sb(III) were found. The sum of these antimony species represented a range of 51–78% of the total Sb in the samples.

5.9.3 Antimony drugs as treatment for leishmaniasis

Leishmaniasis is a parasitical, tropical disease, endemic in 80 countries, with approximately 400,000 new cases per year, which was described first by Leishman and Donovan in 1903 [70, 71].

An emerging risk is Leishmaniasis as HIV-co-infection, for example, in Southern Europe. *Leishmania donovani* and some other leishmanial species are the main causative agents of visceral Leishmaniasis [72]. The parasites exist in two forms, the extracellular promastigote and the amastigotes, which live inside the phagolysosomes of macrophage cells of many host species [73–75]

In the early years of the twentieth century, Sb(III) compounds have been used as therapeutic agents for Leishmaniasis. Because of their high toxicity, they have been exchanged by pentavalent antimony in 1950. Nowadays, mainly sodium stibogluconate (pentostam) and meglumine antimonite (glucantime) are used. Although the antimony drugs have been prescribed over the last decades, their mechanism of action remains unclear [76]. In addition, clinical resistance to the antimony was increasingly reported, uprising the need for new anti-leishmanial drugs [77, 78].

The toxicity of antimony in the parasitic cells depends on the stage of the parasite and the oxidation state of the antimony compounds. As experiments show promastigotes of *L. donovani* are generally more resistant against the antimony than amastigotes, with Sb(III) being far more toxic than Sb(V). Therefore, it has been hypothesized that Sb(V) is accumulated by the macrophage and reduced to Sb(III) either in its phagolysosome or directly in the parasite cell [79, 80]. Cross-resistance between Sb(III) and Sb(V) has been shown in *Leishmania tarentolae*, indicating a major role of trypanothione as complexing agent in the parasitic resistance [81]. However, the mechanism seems to be different in other species of *Leishmania*. An additional possibility is the direct toxicity of Sb(V) for the amastigotes [82, 83]. Recently, some efforts have been made to establish analytical methods for the antimony speciation in extracts of different cell types. Shaked-Mishan *et al*. used ion chromatography ICP-MS to show the direct reduction of antimony within the parasite cells [88]. The same group used selective reduction for antimony speciation in cell samples with similar results [84]. These were the first data showing direct reduction activity in cells and indicating a mechanism involving reduction and toxicity of the Sb(III) compound because Sb(V)-resistant *Leishmania* showed no activity. Several unidentified antimony species have been found in the samples, pointing to more antimony metabolism in the cells. Figure 2.3.10 shows the reduction activity in *Leishmania* cell extracts [84].

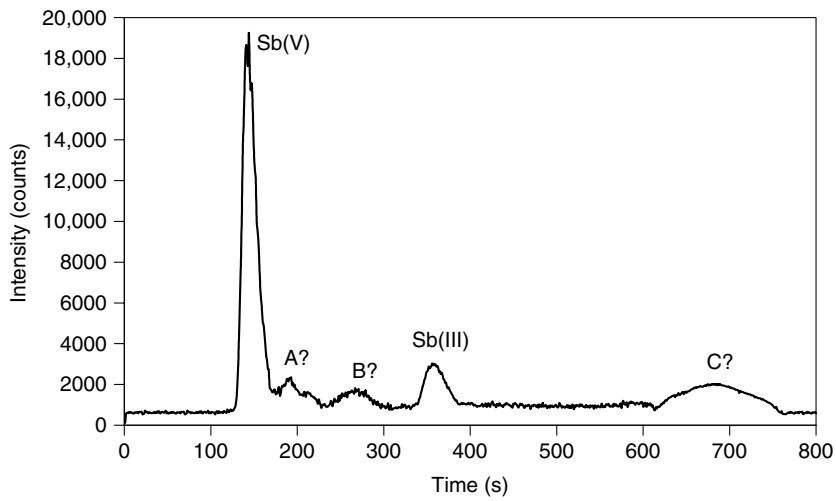

Figure 2.3.10. Indication of reduction activity in cells: cell extracts of amastigotes *Leishmania* incubated with Sb(V), measured with IC-ICP MS and nitric acid as eluent. The components A–C are unidentified compounds. (Reprinted from *Anal. Chim. Acta,* 417, Ulrich, N., Determination of antimony species with fluoride as modifier and flow injection hydride generation inductively coupled plasma emission spectrometry, 201, Copyright (2000), with permission from Elsevier.)

5.9.4 Antimony treatment for bilharziasis

In addition to leishmania, antimony containing drugs are used as therapeuting agents for bilharziasis, the most widespread parasitic disease in Egypt [85]. Compounds such as antimony potassium tartrate, antimony piperazine and antimony lithium thiomaleate could be investigated by extraction and preconcentration of antimony by dithiocarbamates [86]. Belal *et al*. applied the reaction of different Sb(III) antibilharzial compounds with dibromodiethylbarbituric acid for a potentiometric titration procedure [34].

5.9.5 Quality control of pharmaceutical drugs

One of the problems of the treatment of leishmaniasis with antimony drugs is the quality control. The therapeutic agent is Sb(V), whereas Sb(III) is relatively toxic and should not be present in the pharmaceuticals in larger amounts. Therefore, efforts have been made for the determination of Sb(III) in these products. Rath *et al*. used a phometric method [50].

6 CONCLUSION

Antimony speciation is a growing field of analytical chemistry. Two main types of techniques are applied in modern methods. First, there is the selective reduction to distinguish between Sb(III) and Sb(V) or – after gas chromatography – between inorganic Sb and methylated compounds. The other route is the use of liquid chromatography to investigate inorganic and organic Sb species, although up to now from all organic antimony compounds only trimethylated Sb have been clearly identified in environmental or biomedical samples.

Sb speciation is used for gathering data about the environmental distribution of Sb compounds and the Sb cycle in nature. Although some results have been presented, the data are much too anecdotic to draw general conclusions on the species distribution up to now. Another important field is the biomedical speciation. In this field, recent efforts have led to a slightly better understanding of the mode of action of antiparasitic therapeutic agents.

New attempts were made to establish other analytical methods, especially in the biomedical field. Size-exclusion chromatography might be a new pathway for the separation of antimony species. Much effort is needed to overcome the difficulties encountered in Sb speciation: the low concentration, the lack of standards and of reference materials and as a consequence reliability of the data.

7 REFERENCES

1. United States Environmental Protection Agency, *Water Related Fate of the 129 Priority Pollutants*, Vol. 1, USEPA, Washington, DC, 1979, EP-440/4-79-029A.
2. Council of the European Communities, Council Directive to the Quality of Water Intended to Human Consumption, 1980, 80/778/EEC.
3. MAK- und BAT-Werte-Liste, 1996, ed. Deutsche Forschungsgemeinschaft (DFG), VCH, Weinheim, 1996.
4. Zheng, J., Ohata, M. and Furuta, N., *Anal. Sci.*, **16**, 75 (2000).
5. Fowler, B. A. and Goering, P. L. in *Metals and their Components in the Environment*, Merian, E. (Ed.), VCH, Weinheim, 1991, pp. 743–758.
6. Kuroda, K. G., Endo, A., Okamoto, A., Yoo, Y. S. and Horiguchi, S., *Mutat. Res.*, **264**, 163 (1991).
7. International Agency for Research on Cancer (IARG), *IARG Monograph*, Vol. 47, IARC, Lyon, 1989, p. 21.
8. Shaked-Mishan, P., Ulrich, N., Ephros, M. and Zilberstein, D., *J. Bioanal. Chem.*, **276**, 3971 (2001).
9. Dodd, M., Grundy, S. L., Reimer, K. J. and Cullen, W. R., *Appl. Organomet. Chem.*, **6**, 207 (1992).
10. Andreae, M. O., Asmode, J.-F., Foster, P. and Van't dack, L., *Anal. Chem.*, **53**, 1766 (1981).
11. Dorsk, G. O., Long, G. G. and Key, M. E., *Inorg. Synth.*, **9**, 92 (1967).
12. Meinema, H. A., Martens, H. F. and Noltes, J. G., *J. Organomet. Chem.*, **51**, 223 (1973)
13. Morris, W., Zingaro, R. A. and Laane, J., *J. Organomet. Chem.* **91**, 295 (1975).
14. Zheng, J., Takeda, A. and Furuta, N., *J. Anal. At. Spectrom.*, **16**, 62 (2000).
15. Smichowski, P., Madrid, Y. and Camara, C., *Fresenius' J. Anal. Chem.*, **360**, 623 (1998).
16. Andreae, M. O., Determination of the chemical species of some of the "hydride elements" (arsenic, antimony, tin and germanium) in seawater: methodology and results, in *Trace Metals in Seawater*, Wong, C. S., Boyle, E., Bruland, K. W., Berton, J. D. and Goldberg, E. D. (Eds.), Plenum, New York, 1983, pp. 1–19.

17. Alegria, B., Barbera, R. and Farre, R., *Int. J. Environ. Anal. Chem.*, **38**, 65 (1990).
18. de la Calle Guntinas, M. B., Madrid, Y. and Camara, C., *Analyst*, **116**, 1029 (1991).
19. de la Calle Guntinas, M. B., Madrid, Y. and Camara, C., *Microchim. Acta*, **109**, 149 (1992).
20. Bowman, J., Fairman, B. and Catterick, T., *J. Anal. At. Spectrom.*, **12**, 313 (1997).
21. Chen, C.-S. and Jiang, S.-J., *Spectrochim. Acta B*, **51**, 1813 (1996).
22. Chen, H., Brindle, I. D. and Zheng, S., *Analyst*, **117**, 1603 (1992).
23. Cabredo, S., Galban, J. and Sanz, J., *Talanta*, **46**, 631 (1998).
24. Hou, H.-B. and Narasaki, H., *Anal. Sci.*, **15**, 911 (1999).
25. Menendez Garcia, A., Perez Rodiguez, M. C., Sanchez Uria, J. E. and Sanz-Medel, A., *J. Anal. Chem.*, **353**, 128 (1995).
26. Ulrich, N., *Anal. Chim. Acta*, **359**, 245 (1998).
27. Risnes, A. and Lund, W., *J. Anal. At. Spectrom.*, **11**, 943 (1996).
28. Deng, T.-L., Chen, Y.-W. and Belzile, N., *Anal. Chim. Acta*, **432**, 293 (2001).
29. Ding, W.-W. and Sturgeon, R. E., *J. Anal. At. Spectrom.*, **11**, 421 (1996).
30. Brockmann, A., Nonn, C. and Golloch, A., *J. Anal. At. Spectrom.*, **8**, 397 (1993).
31. Ding, W.-W. and Sturgeon, R. E., *J. Anal. At. Spectrom.*, **11**, 225 (1996).
32. Welz, B. and Sucmanova, M., *Analyst*, **118**, 1417 (1993).
33. Vuchkova, L. and Arpadjan, S., *Talanta*, **43**, 479 (1996).
34. Belal, F., Ibrahim, F. A., Sharaf El-Din, M. and El-Tarras, M. F., *Microchem. J.*, **44**, 296 (1991).
35. Krupp, E. M., Grümping, R., Furchtbar, U. R. R. and Hirner, A. V., *Fresenius' J. Anal. Chem.*, **354**, 546 (1996).
36. Clark, S. and Craig, P. J., *Appl. Organomet. Chem.*, **2**, 33 (1988).
37. Ulrich, N., Shaked, P. and Zilberstein, D., *Fresenius' J. Anal. Chem.*, **368**, 62 (2000).
38. Zhang, X., Cornelis, R. and Mees, L., *J. Anal. At. Spectrom.*, **13**, 205 (1998).
39. Sayago, S., Beltran, R. and Gomez-Ariza, J. L., *J. Anal. At. Spectrom.*, **15**, 423 (2000).
40. Guerin, T., Astruc, M., Batel, A. and Borsier, M., *Analyst*, **33**, 188 (2001).
41. Krachler, M. and Emons, H., *Anal. Chim. Acta*, **429**, 125 (2001).
42. Ulrich, N., *Fresenius' J. Anal. Chem.*, **360**, 797 (1998).
43. Michalke, B. and Schramel, P., *J. Chromatogr. A*, **834**, 341 (1999).
44. Garbos, S., Bulska, E. and Hulanicki, A., *Fresenius' J. Anal. Chem.*, **361**, 43 (1998).
45. Wifladt, A.-M., Wibetoe, G. and Lund, W., *Fresenius' J. Anal. Chem.*, **357**, 92 (1997).
46. Moreno, M. E., Perez-Conde, C. and Camara, C., *J. Anal. At. Spectrom.*, **13**, 1181 (1998).
47. Scott, D. L., Ramanathan, S., Shi, W., Rosen, B. P. and Daunert, S., *Anal. Chem.*, **69**, 16 (1997).
48. Wagner, W., Sander, S. and Henze, G., *Fresenius' J. Anal. Chem.*, **354**, 11 (1996).
49. Belzile, N. and Chen, Y. W., *Can. J. Anal. Sci. Spectrosc.*, **44**, 85 (1999).
50. Rath, S., Jardim, W. F. and Dorea, J. G., *Fresenius' J. Anal. Chem.*, **358**, 548 (1997).
51. Sun, Y. C., Yang, J. Y., Lin, Y. F., Yang, M. H. and Alfassi, Z. B., *Anal. Chim. Acta*, **276**, 33 (1993).
52. Hutton, R. C., Bridenne, M., Coffre, E., Marot, Y. and Simondet, F., *J. Anal. At. Spectrom.*, **5**, 463 (1990).
53. Guy, A., Jones, P. and Hill, S. J., *Analyst*, **123**, 1513 (1998).
54. Jakubowski, N., Feldmann, I. and Stuewer, D., *J. Anal. At. Spectrom.*, **8**, 969 (1993).
55. Feldmann, J. and Hirner, A. V., *J. Environ. Chem.*, **60**, 339 (1995).
56. Lintschinger, J., Koch, I., Serves, S., Feldmann, J. and Cullen, W. R., *Fresenius' J. Anal. Chem.*, **359**, 484 (1997).
57. Krachler, M., Emons, H. and Zheng, J., *Trends Anal. Chem.*, **20**, 79 (2001).
58. Krachler, M., Burow, M. and Emons, H., *Analyst*, **124**, 777 (1999).
59. Parris, G. E. and Brinckman, F. E., *Environ. Sci. Technol.*, **10**, 1128 (1976).
60. Gürleytük, G., Van Fleet-Stalder, V. and Chasteen, T. G., *Appl. Organomet. Chem.*, **11**, 471 (1997).
61. Andrewes, P., Cullen, W. R., Feldmann, J., Koch, I., Polishchuk, E. and Reimer, K. J., *Appl. Organomet. Chem.*, **12**, 827 (1998).
62. Garbos, S., Bulska, E., Hulanicki, A., Fijalek, Z. and Soltyk, K., *Spectrochim. Acta B*, **55**, 795 (2000).
63. Nash, M. J., Maskall, J. E. and Hill, S. J., *J. Environ. Monit.*, **2**, 97 (2000).
64. Benson, A. A. and Cooney, R. V., in *The Biological Alkylation of Heavy Metals*, Craig, P. J. and Glocking, F. (Eds.), The Royal Society of Chemistry, 1988, p. 345.
65. Madrid, Y. M., Barrio-Cordoba, E. and Camara, C., *Analyst*, **123**, 1593 (1998).
66. Dodd, M., Pergantis, S. A., Cullen, W. R., Li, H., Eigendorf, G. K. and Reimer, K. J., *Analyst*, **121**, 223 (1996).
67. Müller, L. M., Bestimmung organischer Antimon- und Bismutverbindungen im Deponiegas, Diploma Thesis, University of Essen, 1994.
68. Rondon, C., Burguera, J. L., Brunetto, M. R., Gallignani, M. and Petit de Pena, Y., *Fresenius' J. Anal. Chem.*, **353**, 133 (1995).
69. Nies, D. H., *Appl. Microbiol. Biotechnol.*, **51**, 730 (1999).
70. Herwaldt, B. L., *Lancet*, **354**, 1191 (1999).
71. Ashford, R. P., Desjeux, P. and deRaadt, P., *Parasitol. Today*, **8**, 104 (1992).
72. Ephros, M., Waldman, E. and Zilberstein, D., *Antimicrob. Agents. Chemother.*, **41**, 1064 (1997).
73. Callahan, H., Portal, A. C., Devereaux, R. and Grogl, M., *Antimicrobiol. Agents Chemother.*, **41**, 818 (1997).

74. Chang, K. P. and Dwyer, D. M., *Sciences*, **193**, 678 (1976).
75. Chang, K. P., Fong, D. and Bray, R. S., The biology of *Leishmania* and Leishmaniasis, in *Leishmaniasis*, Chang, K. P. and Bray, D. (Eds.), Elsevier, Amsterdam, 1985.
76. Ephros, M., Bitnun, A., Shaked, P., Waldman, E. and Zilberstein, D., *Antimicrob. Agents Chemother.*, **43**, 278 (1999).
77. Faraut-Gambarelli, F., Pearroux, R., Denau, M., Giusiano, B., Marty, P., Michel, G., Faugere, B. and Dumon, H., *Antimicrob. Agents Chemother.* **41**, 827 (1997).
78. Ibrahim, M. E., Hag-Ali, M., El-Hassan, A. M., Theander, I. G. and Kharazmi, A., *Parasitol. Res.*, **80**, 569 (1994).
79. Borst, P. and Ouellette, M., *Annu. Rev. Microbiol.*, **49**, 427 (1995).
80. Roberts, W. L., Berman, J. D. and Rainey, P. M., *Antimicrob. Agents Chemother.*, **39**, 1234 (1995).
81. Legare, D., Papadopoulou, B., Roy, G., Mukhopadhyay, R., Haimeur, A., Dey, S., Grondin, K., Brochu, C., Rosen, B. P. and Ouellette, M., *Exp. Parasitol.*, **87**, 275 (1997).
82. Dey, S., Papadopoulou, B., Roy, G., Grondin, K., Dou, D., Rosen, B. P., Ouellette, M. and Haimeur, A., *Mol. Biochem. Parasitol.*, **67**, 49 (1994).
83. Haimeur, A. and Ouellette, M., *Antimicrob. Agents Chemother.*, **42**, 1689 (1998).
84. Ulrich, N., *Anal. Chim. Acta*, **417**, 201 (2000).
85. Gustafsson, L. L., Beermann, B. and Abdi, Y. A., *Handbook of Drugs for Tropical Parasitic Infections*, Taylor & Francis, London, 1987.
86. El-Rabbat, N. A., Farag, H. H., El-Kommos, M. E. and Refaat, I. H., *Talanta*, **9**, 951 (1990).
87. Krachler, M. and Emons, H., *J. Anal. At. Spectrom.*, **16**, 20 (2001).
88. Shaked-Mishan, P., Ulrich N., Ephros M. and Zilberstein D., *J. Biol. Chem.,* **276**, 3971 (2001).

2.4 Speciation of Arsenic

2.4.1 Arsenic and Arsenic Species in Environment and Human Nutrition

Thomas Prohaska and Gerhard Stingeder

University of Natural Resources and Applied Life Sciences, Vienna, Austria

1 INTRODUCTION

Realgar, orpiment and other arsenic minerals were already known to the Greeks of Aristotle's time (about 300 BC), even though the element itself was not known. Arsenic was first described by Albertus Magnus in the thirteenth century. It was widely used as a poison and in folk remedies. The element found more and more application in agriculture and industry in the twentieth century. It is only since "Arsenic and Old Lace", the famous play written by Joseph Kesselring in 1941, that arsenic has been known as a toxic element to everyone. Nowadays, the biological and environmental effects of arsenic are studied in detail [1] since serious pollution and numerous cases of poisoning from arsenic in drinking water have been found in the last decades. Many cases occur in poor countries that lack the necessary infrastructure to be able to react promptly. Even though regulations still focus on total arsenic concentrations, the effect of arsenic is dependent on the physical and chemical properties, toxicity, mobility and biotransformation of arsenic species.

Handbook of Elemental Speciation II: Species in the Environment, Food, Medicine & Occupational Health
Edited by R. Cornelis, H. Crews, J. Caruso and K. G. Heumann
 ISBN: 0-470-85598-3 (HB)

2 SOURCES OF ARSENIC

Arsenic is found ubiquitously in the atmosphere, in water, soils and sediments, as well as in organisms. The abundance of arsenic is about 52nd in the earth crust and the element is associated with igneous and sedimentary rocks, particularly with sulfide ores [2]. Arsenic is very mobile, and different mechanisms control mobilization and transformation of arsenic in the environment. Atmospheric arsenic is released by natural phenomena as well as by anthropogenic sources and returned to the earth's surface by dry and wet deposition. Natural and anthropogenic sources contribute 60 : 40 to the atmospheric deposition [3], whereas other estimations report a 30 : 70 split [4]. The element circulates in various forms through the atmosphere, water and soil before entering its ultimate sink in the sediments. Relatively little is known about the fate of arsenic in sediments: Arsenic sulfides are assessed as ultimate arsenic sink in anoxic sediments and the rate of remobilization of arsenic as a function of redox conditions in sediments is under investigation [3].

2.1 Natural sources

Arsenic is found in more than 245 minerals: 60% arsenates, 20% sulfides and sulfosalts, 20% arsenides, arsenites, oxides and elemental As. The most common mineral is arsenopyrite (FeAsS). Table 2.4.1.1 gives an overview of the major arsenic minerals in nature. The earth's crust and rocks contain about 2 to 3 μg As/g (levels range from 0.1 to several hundred $\mu g\,g^{-1}$) [5]. Sedimentary rocks contain in general higher levels of arsenic (0.5–455 $\mu g\,g^{-1}$) than igneous rocks (0.06–113 $\mu g\,g^{-1}$) [6]. Sands and sandstones tend to have the lowest concentration. Concentration levels in coals and bituminous deposits are often high. Samples of organic rich shale have As concentrations up to 900 $\mu g\,g^{-1}$. The usual concentration range in coal is 2.5 to 20 $\mu g\,g^{-1}$ but extremely high concentrations up to 35 $mg\,g^{-1}$ do occur [7]. Most of the arsenic is associated with pyrite.

Table 2.4.1.1. Major arsenic minerals occurring in nature.

Arsenopyrite	Fe[AsS]
	Ni[AsS]
Cobaltite	Co[AsS]
Realgar	As_4S_4
Orpiment	As_2S_3
Proustite	Ag_3AsS_3
Enargite	Cu_3AsS_4
Tennantite	$(Cu, Fe, Zn)_3AsS_{3-4}$
Arsenolite	As_2O_3
Claudedite	As_2O_3
Löllingite	$Fe[As_2]$
Chloanthite	$Ni[As_2]$
Niccolite	Ni[As]
Smaltin	$Co[As_{2-3}]$

Arsenic is mobilized by water and leaching depends on several factors such as pH or the redox potential. The two dominant natural sources of As in the atmosphere are low-temperature volatilization (about 26,000 tons per year) and volcanic activity (about 17,000 tons per year) [3].

2.2 Anthropogenic sources

The world production of arsenic is estimated at 75 to 100×10^3 tons per year. Sweden is the world's leading producer, and the United States uses half of the world's production [8]. In 1990, about 70% was used in wood preservatives, 22% in agricultural chemicals (herbicides and desiccants), 4% in glass, 2% in nonferrous alloys and 2% various.

Main sources of arsenic are copper and lead ores. Raw products are both As_2O_3 and elemental As. Arsenic is released to the environment by various industrial processes, mining or smelting and agricultural activities as well as a by-product of coal combustion. Nriagu and Pacyna estimate a total anthropogenic input between 64,000 and 132,000 tons per year onto land [4]. (see Table 2.4.1.2)

2.2.1 Industry

Elemental As is used as an additive in special alloys. Arsine is used in microelectronics and semiconductor industry. Moreover, arsenic trioxide finds its application as a decolorizing agent in the

Table 2.4.1.2. Main sources of As discharge onto soil (after [4]).

Source	Contribution (%)
Commercial waste	40
Coal ash	22
Atmospheric fallout from steel production	13
Other mining activities	16
Other sources[a]	5

[a] Agricultural and food wastes, animal wastes and manure, logging and other wood wastes

glass and ceramics industries. The main amount of As is released from the metal processing industries (about 1.5 kg As per ton Cu, 0.4 kg As per ton Pb and 0.65 kg As per ton Zn) [3]. The elevated level of As within the gangue mineral together with an economic ore mineral causes risks of wind dispersal and leaching of As during processing, which can lead to very high As concentrations near old dumps. Smelting of Cu is the largest solely anthropogenic input (about 40%) followed by coal combustion (20%). Coal combustion produces fly ash up to 30% of the weight of coal. Arsenic is enriched in fly ash particles as a consequence of the condensation of volatile arsenic species onto the surfaces of the particles. Levels of 6 to 200 μg As per gram can be found in pulverized ash (e.g. fuel ash). Arsenate is the dominant species in fly ash, and arsenite contributes between 3 and 40%. Fly ash is partially used for the production of cement but the main part is disposed of as mine fills or in waste dumps [7].

Solutions, which are used in geothermal power plants to raise steam, can contain high amounts of arsenate and provide a further potential for pollution. Significant contamination of rice fields by inorganic arsenic in wastewater from geothermal electric power stations and mining waste have been reported in Japan [9].

2.2.2 Sewage sludge

The degree of industrialization is reflected in the amount of As in sewage sludge. The As is derived mainly from surface runoff, atmospherically deposited As, residues from pesticides, to a minor degree phosphate detergents and a major impact from industrial effluents. It is reported that arsenic is released as volatile methylated and hydride species from sewage treatment facilities and landfill sites [10].

2.2.3 Agriculture and forestry

Arsenic compounds are widely used in agriculture and forestry as insecticide or herbicide, as growth promoter, as well as in sheep dips (to control ticks, lice and fleas), wood preservative, cotton desiccant and dye reagent. Phosphate fertilizers are another possible source of arsenic, depending on the phosphate rock used (about 8 μg As/g rock), even though no significant increase in the As concentration of soils from this source was detected so far.

The total amount of As in agricultural use is decreasing steadily, even if developing countries are still using large quantities of agents, which are already forbidden in Western Europe. Because of the toxic effects on the environment, the consumption of arsenic in agriculture and forestry has decreased to half from 1980 to 1990. Inorganic As compounds were applied in the early twentieth century (Pb, Ca, Mg and Zn arsenates, Zn arsenite, copper acetoarsenite (Paris green)) but have been largely replaced by organic arsenicals (e.g. mono- and disodium methanoarsenate or cacodylic acid). Sodium arsenite was used in the 1970s in the United States to control aquatic weeds and has led to significant contamination. Already, the production of the compounds is a potential risk. For example, dumping of industrial effluents from the production of Paris green has contaminated the groundwater in the residential area of Calcutta [11]. Pollution from residual As is a major concern, and "replant syndromes" can be observed in young fruit trees as a result of phytotoxic levels of As in soil. Soils treated with pesticides show higher As concentration compared to areas treated with herbicides, which are usually applied at lower rates.

Chromated copper arsenate (CCA) is a commonly used wood preservative against biological decay [12]. Other compounds are arsenic pentoxide, calcium arsenate, lead arsenate and sodium arsenate. The wood preservative industry is the

major market for As in the United States. Long-term problems can be expected when the treated wood needs to be dumped or burnt.

Arsenic (e.g. arsanilic acid or 3-nitro-4-hydroxy-phenylarsonic acid) is furthermore used as feed additive, for example, in poultry feeds to control coccidiosis and as growth promoter [13].

2.2.4 Other applications

Until 1940, inorganic As was used for medication. The best known is Salvarsan (arsphenamine), formerly used extensively for treatment of syphilis and yaws. Nowadays, arsenic is still used as antiparasitic agent in veterinary medicine and in folk remedies. Recently, arsenic trioxide was investigated for the treatment of promyelocytic leukemia [14].

Arsenic (as sulfide realgar) finds further applications as pigment and in fireworks. Paris green, also called *Schweinfurt green*, an extremely poisonous, bright green powder, was used extensively as a pigment in wallpaper in the nineteenth century [15]. Additionally, surface soil contamination is reported by disposal of tannery waste containing sodium arsenite used as pesticides at the tannery [16].

3 ARSENIC SPECIES AND THEIR TRANSFORMATION PATHWAYS

Arsenic can be described as a semi-metal-forming covalent compound or anionic species. The oxidation states are −III, 0, III and V [8]. Elemental As has several allotropic forms (grey, yellow and black arsenic). Grey As is the stable form.

More than 25 different As compounds have been identified in biological samples [17]. The most common arsenic species with environmental importance are listed in Table 2.4.1.3. Arsenic species can undergo transformation via abiotic or biotic processes. Oxidation, reduction, adsorption, desorption, dissolution, precipitation and volatilization of arsenic commonly occur [4, 6]. Figure 2.4.1.1 shows a simplified transformation pathway of arsenic in the environment.

Elemental arsenic and arsenic trioxide are the main particles found in atmospheric deposits. Arsenic trioxide is a product of smelting operations and a raw product for most arsenicals. Arsenate is the thermodynamically more stable form of inorganic As in soils and water. Arsenate and arsenite can be converted easily under oxidizing or reducing condition. Oxidation of arsenite to arsenate in soils is conducted by bacteria or catalytically by Mn(IV) and Fe(III) oxides. As(V) can furthermore be immobilized by coprecipitation with hydrous iron or manganese oxides [20].

$$MnO_2 + HAsO_2 + 2H^+ \leftrightarrows Mn^{2+} + H_3AsO_4$$

$$2Fe^{3+} + HAsO_2 + 2H_2O \leftrightarrows 2Fe^{2+} + H_3AsO_4 + 2H^+$$

The acidic and basic properties of arsenic and arsenous acid influence their environmental and analytical behavior:

Arsenic acid:

$$H_3AsO_4 + H_2O \Leftrightarrow H_2AsO_4^- + H_3O^+ \qquad pK_a = 2.20$$

$$H_2AsO_4^- + H_2O \Leftrightarrow HAsO_4^{2-} + H_3O^+ \qquad pK_a = 6.97$$

$$HAsO_4^{2-} + H_2O \Leftrightarrow AsO_4^{3-} + H_3O^+ \qquad pK_a = 11.53$$

Arsenous acid:

$$H_3AsO_3 + H_2O \Leftrightarrow H_2AsO_3^- + H_3O^+ \qquad pK_a = 9.22$$

$$H_2AsO_3^- + H_2O \Leftrightarrow HAsO_3^{2-} + H_3O^+ \qquad pK_a = 12.13$$

$$HAsO_3^{2-} + H_2O \Leftrightarrow AsO_3^{3-} + H_3O^+ \qquad pK_a = 13.4$$

The most stable species in normal soil within pH 4 to 8 are $H_2AsO_4^-$ (pH 2 to 7), $HAsO_4^{2-}$ (pH > 7) and H_3AsO_3 (pH < 9). A drop of the redox potential (Eh) below +300 mV at pH 4 or below −100 mV at pH 8 leaves H_3AsO_3 as the thermodynamically stable As species in the absence of complexing species and methylating

Table 2.4.1.3. Main arsenic compounds and their LD_{50} values when applicable.

Species	LD_{50} [mg kg^{-1}] [18]	
As (elemental)	763	As
Inorganic arsenic(III) species		
As trioxide	14	As_2O_3
Arsenous acid	14	$HAsO_2$
Arsenite (AsIII)	14	AsO_3^{3-}
As chloride	14	$AsCl_3$
As sulfide	14	As_2S_3
Arsine (AsH_3)	3	AsH_3
Inorganic arsenic(V) species		
As pentoxide	20	As_2O_5
Orthoarsenic acid	20	H_3AsO_4
Metaarsenic acid	20	$HAsO_3$
Arsenate (AsV)	20	AsO_4^{3-}
Organic As species		
Monomethylarsine (MMA)		CH_3AsH_2
Dimethylarsine (DMA)		$(CH_3)_2AsH$
Trimethylarsine (TMA)		$(CH_3)_3As$
Monomethylarsonic acid (MMAA)	1800	$CH_3AsO(OH)_2$
Dimethylarsonic acid (Cacodylic acid)(DMAA)	2600	$(CH_3)_2AsO(OH)$
Trimethylarsine oxide (TMAO)		$(CH_3)_3AsO$
Arsenobetaine		$(CH_3)_3As^+ CH_2COOH$
Arsenocholine		$(CH_3)_3As^+ CH_2CH_2OH$
Dimethylarsinoyl Ethanol		$(CH_3)_2AsOCH_2CH_2OH$
Arsenosugars (R-dimethylarsinoylriboside) 1_6		See structure below[19]

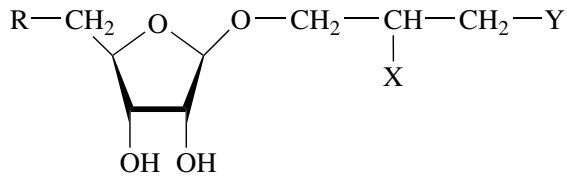

	R	X	Y
1	$(CH_3)_2As(O)$–	–OH	–OH
2	$(CH_3)_2As(O)$–	–OH	$-OPOHCH_2CH(OH)CH_2OH$
3	$(CH_3)_2As(O)$–	–OH	$-SO_3H$
4	$(CH_3)_2As(O)$–	–OH	$-OSO_3H$
5	$(CH_3)_2As(O)$–	$-NH_2$	$-SO_3H$
6	$(CH_3)_2As^+$–	–OH	$-OSO_3H$

organisms [2]. Figure 2.4.1.2 shows the pE/pH diagram for As-H_2O system at 25 °C.

The presence of sulfide and reducing conditions can lead to the precipitation of As_2S_3 in lake, river and marine sediments. The formation of sulfides in a reducing environment accompanies the reduction of As(V) to As(III). On the other hand, geogenic sulfides can undergo oxidation with a release of As into the surrounding environment [21]. Sulfates are formed and leached out because of the high redox potential of sulphur. Subsequently, the amount of arsenic sulfide is low in soils.

Oxidation of arsenite to arsenate is one of the protective mechanisms of microorganisms [2]. There are also well aquatic bacteria, which reduce

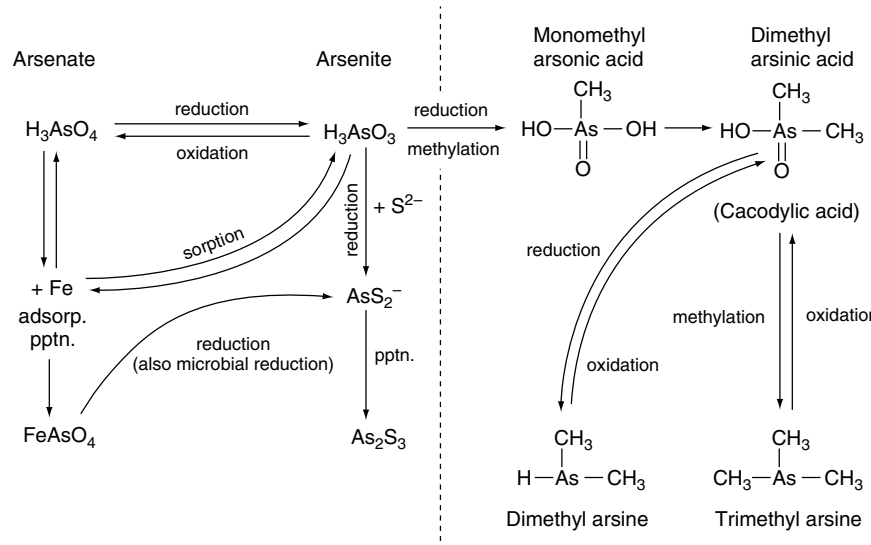

Figure 2.4.1.1. Simplified transformation pathway of arsenic in the environment. (Reprinted from [8] with permission from Springer.)

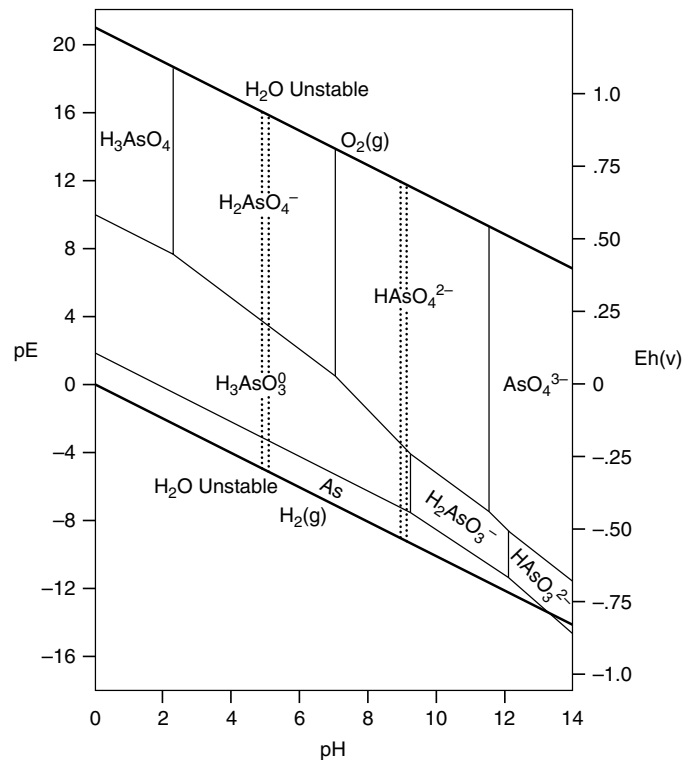

Figure 2.4.1.2. pE – pH diagram for the As-H_2O system at 25 °C. Total dissolved As species set at 50 ng g^{-1}. The area with the vertical bars represent the common pE–pH domain in natural water. (Reprinted from [22] with permission from Elsevier Science Publishing B.V.)

arsenate to arsenite under aerobic conditions. Anaerobic reduction was observed in activated sewage sludge and wine yeast. The reduction of arsenate to arsine is only observed in significant quantities in soils enriched with glucose and urea. Some soils release arsine from arsenite under anaerobic conditions [2].

Originally, inorganic As is incorporated by autotrophic organisms such as algae.

Biotransformation by organisms can be observed throughout the food chain [23]. Methylation is considered as a detoxification process by organisms and degradation of methylated species by photochemical processes can be observed as well. Methylation by fungi or bacteria forms monomethylarsonic acid, dimethylarsinic acid (cacodylic acid), trimethylarsenic acid or trimethylarsine [2]. The formation of toxic trimethylarsine by molds growing on wall paper decorated with As pigments led to a number of poisoning incidents in England and Germany as well as in New York/USA in the nineteenth century.

Challenger described in his review the mechanism of arsenic methylation by fungi and favored the hypothesis that the methylation of arsenic involved the transfer of a methyl group from already methylated compounds [15]. Although arsenic intermediates as described by Challenger are found in cell preparations, the reaction is supposed to be more complex in reality. In his first review, Challenger suggested that bacteria do not methylate arsenic. The first report of arsine produced by bacteria was published 1971 [24]. Since then, a number of bacteria have been identified to produce methylarsine. Cullen and Reimer comprehensively describe different transformation mechanisms by microbiological activities in their review [2]. The methylation of inorganic As has been studied extensively in methanogenic bacteria, which produce methane as their primary metabolic end product under anaerobic conditions. Bacterial reactions usually lead to dimethylarsine, a compound stable in the absence of oxygen.

Arsines and methylarsines are generally volatile and unstable in air. Arsine is a toxic gas with a typical smell of garlic. Arsine decomposes following the reaction:

$$AsH_3 \Leftrightarrow 1/n As_n + 1.5\ H_2 (+66.5\ kJ)$$

Several publications report about the biotransformation of highly toxic inorganic arsenic species to less toxic methylarsonic acid or dimethylarsinic acid [25]. Arsenic compounds are metabolized in animals, plants, algae and mushrooms to even more complex organoarsenicals such as arsenobetaine, arsenocholine, dimethylarsynilribosides (arsenosugars) and tetramethylarsonium ion and to a small extent to some other nonidentified arsenic species [26].

4 ARSENIC IN THE ECOSYSTEM

4.1 Arsenic in soils

The natural level of As in soils depends on the rock type, the normal range being 1 to 40 μg As/g [8]. In general, arsenic levels in uncontaminated and untreated soils seldom exceed 10 $\mu g\, g^{-1}$. The European Community recommended for total arsenic levels in soil not to exceed 20 $\mu g\, g^{-1}$.

Increased concentrations are usually found for acid sulfate soils due to the weathering of pyrite. In agricultural areas, arsenic residues can accumulate up to 600 $\mu g\, g^{-1}$. Highly polluted soils can be localized in the neighborhood of mining plants or coal-fired power plants and concentrations of more than 1000 $\mu g\, g^{-1}$ have been recorded for sites in Australia [27]. Total As contamination in mine spoils in England exceeded 20,000 $\mu g\, g^{-1}$ with its maximum concentration at a depth of 20 to 40 mm [28].

Arsenic mobility is a result of complex interactions between soil and solution. Main factors are the redox potential, pH, particle size, content of organic matter, nature of minerals and competing ions [29]. Inorganic Arsenic species (mainly arsenate) have been known to have a high affinity to oxide surfaces [30]. The level of available As is lower in soils with a high amount of clay, Fe/Al oxides and calcite due to sorption of As. Especially in coarse textured soils, As can move down a profile with leaching

water. The bioavailability of arsenic in soils and sediments is usually reflected by the extractability using a variety of different reagents [20].

Arsenic in soils is mainly present as arsenate. However, arsenous acid is the predominant form under reducing conditions [8]. The soil conditions can also lead to a change in the oxidation state or to methylation by microbial activity. Arsenite is generally more mobile than arsenate, hence immobilization of As can be enhanced by oxidation. Arsenic solubility is low under oxidizing conditions (200–500 mV) and up to 95% of arsenic is present as arsenate. At high pH or under reducing conditions, arsenate is reduced to soluble arsenite. Under moderately reducing conditions (0–100 mV), arsenic solubility is controlled by iron oxy-hydroxides. At strong reducing conditions (−200 mV), the amount of soluble arsenic increases significantly. However, arsenate to arsenite transformation is slow and can be controlled by manganese (MnO_2 is reduced to Mn^{2+}). (See Figure 2.4.1.2 and paragraph 3, as well). Among the competing anions (Cl^-, $NO_3{}^-$, $SO_4{}^{2-}$ and $PO_4{}^{3-}$), $PO_4{}^{3-}$ substantially suppresses arsenate sorption since arsenic shows many chemical similarities to phosphor. Nevertheless, the soil chemistry of As is much more diverse because of the different oxidation states and species and the formation of bonds with S and C. Phosphate, in contrast, is more stable over a wider range of Eh and pH conditions than arsenate. Variable results have been obtained in the reduction of the toxicity of As by adding Al, Fe and Zn compounds, S, lime and organic matter [1]. Currently, there are several methods under investigation for the remediation of contaminated soils, but most methods are expensive, time consuming and risky [31]. Recently, the use of plants, which accumulate arsenic to a high amount (hyperaccumulator), is under research to be applied in phytoremediation of contaminated sites [32].

4.2 Arsenic in water

Concentrations of arsenic in freshwater vary by more than four orders of magnitude, depending on the source of arsenic, the amount available and the local geochemical environment. Under natural conditions, the greatest range and the highest concentrations of arsenic are found in groundwaters as a result of the strong influence of water-rock interactions and the favorable physical and geochemical conditions for arsenic mobilization and accumulation. Distinct seasonal variations in arsenic concentration can be observed. Usual groundwater concentrations range from <0.5 to $10\ \mu g\,L^{-1}$. Concentrations up to $370\ \mu g\,L^{-1}$ have been reported in Wyoming and Montana as a result of geothermal inputs from the Yellowstone geothermal system [33].

Wells in contaminated areas in Bangladesh or Taiwan in some cases show an extremely increased arsenic concentration of up to $2500\ \mu g\,L^{-1}$ and bore waters in Argentina have concentrations of more than $7800\ \mu g\,L^{-1}$. Average values for arsenic in seawater are about $2\ \mu g\,L^{-1}$, whereas in freshwater a wider variation of $0.4–80\ \mu g\,L^{-1}$ can be observed [34].

Increased concentrations are also reported in river waters in arid areas. Surface waters often have a high pH and alkalinity and show concentrations of naturally occurring arsenic ranging between 190 and $21{,}800\ \mu g\,L^{-1}$. Significant increases in arsenic concentration of river water may also occur as a result of pollution from industrial or sewage effluents, from mill tailings or mine wastes, as well. Concentrations up to $556\ \mu g\,L^{-1}$ are reported in streams adjacent to deposits in British Columbia. Only limited data are available for arsenic in oilfield and other brines, but concentrations can be very high (more than $200\ mg\,L^{-1}$) [8].

The most common valence states of arsenic in water are arsenate, which is more prevalent in aerobic surface waters, and arsenite, which is more likely to occur in anaerobic groundwaters [35]. Arsenate is mainly stable as $HAsO_4{}^{2-}$ and $H_2AsO_4{}^-$ in the pH range of seawater. Arsenite is again stable as neutral H_3AsO_3. Organic arsenic forms may be produced mostly in surface waters by biological activity (e.g. as a result of methylation reactions by phytoplankton[2]) but are rarely quantitatively important. Organic forms may, however, occur where waters are significantly affected by industrial pollution or agricultural activities.

4.3 Arsenic in the atmosphere

Natural phenomena (weathering, biological activities and volcanic activities) as well as anthropogenic sources (smelting operations, fossil fuel combustion, pesticides) release arsenic to the atmosphere. Arsenic is present in air mainly in particulate form as arsenic trioxide. The relatively high volatility of some As compounds (both from natural and anthropogenic origin) means that the geochemical cycle contains significant fluxes through the atmosphere. Volatile methylated and hydride species are also released from sewage treatment facilities and landfill sites [10].

Average levels for arsenic in Europe are about 1 $ng\,m^{-3}$ for rural areas, 2 $ng\,m^{-3}$ in urban areas and <50 $ng\,m^{-3}$ in industrial areas [18]. Concentrations of arsenic in rainfall and snow in rural areas are at typically less than 0.03 $\mu g\,L^{-1}$. Smelting and coal burning increase the concentration by one order of magnitude and concentrations up to 16 $\mu g\,L^{-1}$ have been found in rainfall down wind of a copper smelter [36]. Total arsenic deposition rates have been calculated in the range $<1-1000$ $\mu g\,m^{-2}\,yr^{-1}$, depending on the relative proportions of wet and dry deposition and proximity to contamination sources. Values in the range $38-266$ $\mu g\,m^{-2}\,yr^{-1}$ (about half as dry deposition) were estimated for the mid-Atlantic coast [37]. An estimate of the total atmospheric flux suggested 73,540 tons per year with a 60 : 40 or 30 : 70 split between natural and anthropogenic sources [4]. The atmospheric input of arsenic was reported to lead in the upper 5 cm of the soil to a concentration of approx. 5 times higher compared to lower regions [3].

4.4 Arsenic in biological tissues

Arsenic shows no indication of being an essential element in biological processes, even though some organic compounds are reported to stimulate root growth of plants and arsenic compounds have been used as food additives to promote animal growth, as well. Both arsenite and arsenate accumulate in living tissues because of their affinity for proteins, lipids and other cellular compounds [38]. The highest As concentration is found in aquatic life forms because of accumulation of compounds that have been synthesized from arsenate at low trophic levels. Typical concentrations range from 5 to 50 $\mu g\,g^{-1}$ but can go up to 2500 $\mu g\,g^{-1}$ [2, 39]. It is well known that the arsenic concentration in marine animals is usually higher than in the surrounding water and that arsenic is mainly present as organic species [40].

The ability of aquatic organisms to transform inorganic As into complex organoarsenicals appears to be retained along the food chain. Fish retains up to 99% in an organic form [39]. In general, organoarsenical species in aquatic plants are found mainly as dimethylarsenic compounds. The concentration of organoarsenicals is usually lower in freshwater fish. Arsenobetaine and arsenocholine are found as products of marine animals and mushrooms [41]. After its isolation in 1977, arsenobetaine was recognized to be the most abundant arsenic compound in marine animals. Arsenocholine was found in significant concentrations in marine shrimp, and the presence of arsenic-containing sugar derivates is also well established [42]. Trimethylarsine oxide has been found as minor component, as well. More than 25 arsenic species have been reported in biological tissues [17]. Mostly, natural levels in plants are less than 1 $\mu g\,g^{-1}$. Brandstetter *et al.* reported concentration ranges in plant tissues in the Austrian Alp region from 0.03 to 34.5 $\mu g\,g^{-1}$ [43].

A limited number of plants and algae is known to accumulate As to a significantly higher extent or correlate directly with the As concentration of the surroundings. These plants can be used either for phytoremediation of contaminated areas or for bio-monitoring of As contamination [32].

The main route for uptake of inorganic arsenic compounds is through roots, whereas organic compounds enter the plant by absorption through the leaves or bark.

Bioavailable arsenic in soils is usually reflected by the amount of As found in the mobile or easily mobilized fraction of sequential extraction schemes

(see Table 2.4.1.4). The total As content in soils usually does not reflect the phytoavailability and phytotoxicity [8]. As an example, concentrations of arsenic in fruits were directly correlated to HCl extractable arsenic in highly contaminated soils.

Table 2.4.1.4. As fraction as assessed by sequential leaching [44–46].

Fraction	Characterisation
Mobile	Includes the water soluble and easily exchangeable (unspecifically adsorbed) metals and easily soluble metallorganic complexes.
Easily mobilized	Contains the specifically bound, surface-occluded species (sometimes also $CaCO_3$ bound species and metallorganic complexes with low bonding forces).
Carbonate bound	As that is bound on carbonates.
Organically bound	Different methods extract the organically bound fraction before the oxide fraction before the carbonate-bound fraction or directly after the carbonate-bound fraction or after the oxide-bond fraction. The organically bound fraction itself can again be diverted up to three separate fractions.
Mn oxide bound	This fraction is sensitive to drying procedures prior to extraction. They are most susceptible to changes in pE and pH. Trace metals bond to Mn-Ox may be readily mobilized upon changed environmental conditions. This fraction is to be separated prior to Fe- or Al oxides
Fe and Al oxide bound	In this fraction, the Fe-bound fraction can also be distinguished in amorphous Fe-bound and crystalline Fe-bound fraction
Residual fraction	This fraction mainly contains crystalline-bound trace metals and are most commonly dissolved with high concentrated acids and special digestion procedures.
	Also, a sulfide fraction can be distinguished.

5 TOXIC EFFECTS OF ARSENIC

There are great differences in the toxicity of the single species. In general, organo-arsenic compounds are significantly less toxic than inorganic arsenic compounds. Arsenite is reported to be more soluble, mobile and more toxic than arsenate compounds [8]. The toxicity is directly related to mobility in water and body fluids. The toxicity conforms to the following order (highest to lowest toxicity): arsines > inorganic arsenites > organic trivalent compounds (arsenoxides) > inorganic arsenates > organic pentavalent compounds > arsonium compounds > elemental arsenic [1, 8]. Arsenobetaine and arsenocholine are considered as nontoxic. Add to this that the pollutant is usually toxic to plants and soil biota at concentrations that do not affect animal or human health.

5.1 Microbial toxicity

It is reported that arsenic has a direct influence on the microbial activities especially in soils. Many factors influence the inhibitory effect on the microflora. Decrease in population of bacteria, fungi and nematodes were reported to correlate with the concentration of As [47]. Maliszewska *et al*. report that overall arsenite and arsenate had little effect on the development of actinomycetes and fungi flora and suppressed the growth of *Azotobacter sp*. They observed a decrease in dehydrogenase activity, as well [48]. Other investigations report the inhibition of urease activity by As(III) [49].

Cullen and Reimer describe in their review the varying tolerance of microorganisms for arsenic and that arsenite oxidation by an inducible enzyme system is one mechanism of resistance [2]. Marine fungi seem to be more tolerant than nonmarine. The growth of *Dendryphiella Salina* was actually stimulated by arsenic. A variety of fungi has increased tolerance to arsenate in the presence of phosphate. Plasmid-mediated resistance to arsenate can be explained by the synthesis of a highly specific arsenate efflux pump that eliminates intracellular arsenate. A number of bacteria have been

isolated that show resistance to arsenite/arsenate and newly discovered bacteria use arsenic in their energy generation process in much the same way that humans use oxygen to release energy from food [50].

5.2 Effects on plants

No evidence exists that there might be an arsenic species that is an essential nutrient for plants, even if stimulation of root growth and small yield increases at low As levels have been observed [8]. This effect was explained by displacement of adsorbed phosphate by arsenate, releasing phosphate as a nutrient. The concentration, which is necessary to injure plants, ranges from 1 to 10 $\mu g\, g^{-1}$. Crops are very tolerant to soil arsenic, whereas beans, rice and vegetables show a higher sensitivity.

The symptoms in case of toxicity for plants indicate a limitation in the movement of water and a loss of turgor, resulting in wilting [51]. Light activation is inhibited by interference with the pentose phosphate pathway. Symptoms from organoarsenic species (methylarsonic and dimethylarsinic acid) include chlorosis, gradual necrosis, dehydration, cessation of growth and finally death [52].

5.3 Effects of arsenic species on animals

Inorganic arsenic species are known as poison but have also been used as medicine for thousands of years, dating back to the ancient Greeks and Romans.

Even if the element arsenic is reported as an essential nutrient at trace levels for some animals, no comparable data exists for humans [53]. Arsenic deficiency for goats is reported to lead to decreased growth, greater abortion of fetuses during pregnancy and higher mortality rate during the second lactation. Similar events have been reported for rodents and chicken. However, the deficiency signs depend on several other dietary factors as well, such as, for example, zinc, arginine, choline, methionine and guanidoacetic acid status. These substances are interrelated because they affect the methionine metabolism. Inorganic As is reduced by reductive methylation in the liver and excreted in the urine as organic species [54].

6 ARSENIC IN HUMAN NUTRITION

Historically, the use of arsenic trioxide as homicidal and suicidal agent is well known and the poisonous nature has been widely exploited. The currently accepted health limits for human consumption are 1 $\mu g\, g^{-1}$ food (dry weight) [55].

At present, it is inappropriate to give dietary recommendations for arsenic for humans with respect to the essentiality of arsenic since no data are available [56]. On the basis of animal studies, the suggested arsenic requirement for animals is between 25 and 50 ng As/g food (based on diets containing 4000 $kcal\, kg^{-1}$) without any specification of the species. This dietary intake is equal to about 20 μg As per day if extrapolated to the human. Human diets normally contain 12 to 50 μg As per day and thus the postulated arsenic requirement for humans apparently can be met by food and water normally consumed without reaching the health limits.

Today, a number of areas are contaminated with As, resulting in an ecological and a health problem. Recently, the most extensive poisoning has been reported for Bangladesh and West Bengal (India) [8].

6.1 Drinking water

The current WHO provisional level of As in drinking water is 10 $\mu g\, L^{-1}$, the target for the European Union is 10 $\mu g\, L^{-1}$ (current standard in Germany, effective since 1996) and the current level in the United States is 50 $\mu g\, L^{-1}$ [57]. In January 2001, the Environmental Protection Agency (EPA) published a new standard for arsenic in drinking water that requires public water supplies to reduce the total arsenic concentration to 10 $\mu g\, L^{-1}$ by 2006. The current level dates from 1975 and is based on the standard set by

the Public Health Service in 1943. The new rule was withdrawn before it took effect and finally on October 31, 2001 EPA announced again its decision to move forward in implementing a new standard for arsenic in 2006.

Exposure of As by contaminated drinking water has resulted in serious As poisoning [18]. Incidents due to geologically contaminated groundwater are reported from Argentina, Bangladesh, Canada, Chile, China, Hungary, India, Mongolia, Mexico, Romania, Taiwan, Thailand and the United States. In Bangladesh alone, 1/6th of the 120 million population is potentially at risk from drinking As-contaminated water. The problem in Bangladesh was undetected for many years because of the lack of suitable arsenic testing laboratories within the country. Main sources are wells, which are drilled in As-rich geologic areas. Concentration of inorganic As in well water ranges from 95 to 3700 $\mu g\,L^{-1}$ in the affected areas.

Mining-related As problems in water have been identified in many parts of the world, such as Austria, Ghana, Greece, India, Mexico, South Africa, Thailand, the United Kingdom and the United States. Groundwater concentrations between 10 and 5000 $\mu g\,L^{-1}$ are reported. Another main source of arsenic pollution of water is contamination by industrial or agricultural waste.

Several methods are applied for removing inorganic arsenic (mainly arsenate) from drinking water (e.g. coagulation/filtration, lime softening, activated alumina, ion-exchange, reverse osmosis, reversal electrodialysis and nanofiltration). In September 1993, EPA developed, with contractor support, a document entitled "Treatment and Occurrence-Arsenic in Potable Water Supplies" [58]. This document summarized the results of pilot-scale studies examining low-level arsenic removal, from 50 $\mu g\,L^{-1}$ down to 1 $\mu g\,L^{-1}$ or less.

6.2 Dietary exposure

The lowest values of actual daily intake of arsenic are reported for the Netherlands as 12 μg As per day. Nriagu *et al*. report that a typical US adult diet contains about 48 μg As per day [57]. The main sources are dairy products, meat, fish and poultry. Table 2.4.1.5 lists average dietary uptakes in different countries without specifying the chemical species involved. Arsenicals – arsanilic acid and roxarsone – are permitted for nontherapeutic uses as growth promoters in animal feeds in the United States [59].

Data on food indicate that trace concentrations of arsenic are present in all nutrients, but total arsenic concentrations in food vary widely from

Table 2.4.1.5. Estimated average dietary intake of arsenic in various countries. Reproduced from [18] by permission of WHO.

Country	Method of sampling[a]	Intake of total arsenic $\mu g\ day^{-1}$
Australia	MB (adult male)	73.3
	(adult female)	52.8
	(2-year-old)	17.3
Brazil	DD[b](students)	18.7–19.5
	(S. Catarina 1 region)	49.2–52.9
	(Manaus region)	139.6–159.3
		16.5–17.0
Canada	TD (5 cities – adult male)	59.2
	(5 cities – 1 to 4 yrs)	14.9
Croatia	MB	11.7
Japan	DD (adult – male&female)	182
Spain	TD (Basque region – adult)	291
UK	TD (adults)	63
USA	MB (adults)	52.6
	(0.5–2 yrs)	27.6

[a] MB: market basket survey; TD: total diet study; DD: duplicate diet study.
[b] Mean values not reported.

country to country (type of soil, water, geochemical activity, use of arsenical pesticides). The highest concentrations of total arsenic are found in seafood. Typical levels in seafood range from 5 to 50 $\mu g\,kg^{-1}$ even if concentrations up to 2500 $\mu g\,kg^{-1}$ were measured [39]. The concentration in freshwater fish is usually much lower than in marine fish and concentration levels vary with respect to species and locations. These levels found in seafood are not considered as a health hazard because the arsenic species belong to the group of organoarsenicals that are considered as nontoxic.

Seafood is followed by meat and grain with respect to the arsenic concentration. Fruit, vegetables and diary products have generally lower total concentrations. Edible seaweed contains 19 to 172 $\mu g\,kg^{-1}$ As, and similar levels are reported for marine algae from Norway. Concentrations of total arsenic in various food groups in North America are given in Table 2.4.1.6.

Contamination of crops, fruits and vegetables occur through spraying or root uptake. Ordinary crop plants do not accumulate enough As to be toxic to humans. Moreover, the edible parts accumulate less As than the rest of the plant, and accumulation of As residues to toxic levels cannot be expected. Instead, growth reductions and crop failures are the main consequences from As pollution. The accumulation of As in grapes grown in contaminated vineyards remains a problem and over 50% of the wine sold in the United States contains more than 50 μg As/L. The significant reduction of As-containing pesticides has significantly reduced the possibility of As contamination via crops, fruits or vegetables.

Arsenic in food occurs as a mixture of inorganic species and the less toxic organic arsenicals, including trimethyl species such as arsenobetaine. In general, organoarsenic compounds account for 60 to 99%. Studies indicate that inorganic arsenic levels in fish and shellfish are generally low (<1%), but that other foodstuffs (meat, poultry, diary products and cereals) contain higher proportions of inorganic arsenic.

6.3 Other sources of exposure

Arsenic is found in household items, tobacco smoke (estimates are 0.25 μg As per cigarette), laundry detergent and bone meal. Another source of direct As uptake is As inhalation of exhaust fumes of coal, which is burnt inside in open pits and from consumption of foods dried over coal fires. This problem is found especially in southern China. Air levels up to 0.13 $mg\,m^{-3}$ are reported, which is up to 40 times higher than the standard [60, 61].

In addition, there is the potential for significant occupational exposure to arsenic in several industrial areas, in particular, arsenic production, nonferrous smelting, electronics, wood preservation,

Table 2.4.1.6. Total arsenic concentrations in various food groups from Canada. Reproduced from [18] by permission of WHO.

Food category	Mean (μg As/kg wet weight)	Range (μg As/kg wet weight)
Milk and dairy products	3.8	<0.4–26
Meat and poultry	24.3	<1.3–536.0
Fish and shellfish	1662.4	77.0–4830.0
Soups	4.2	<0.2–11.0
Bakery goods and cereals	24.5	<0.1–365.0
Vegetables	7.0	<0.1–84.0
Fruit and fruit juices	4.5	<0.1–37.0
Fats and oils	19.0	<1.0–57.0
Sugar and candies	10.9	1.4–105
Beverages[a]	3.0	0.4–9.0
Miscellaneous[b]	12.5	<0.8–41.0

[a] Includes coffee, tea, soft drinks, wine and canned and bottled beer.
[b] Includes bran muffins, muffins with and without raisins, gelatin desserts, raisins, baked beans, weiners and raw & canned beets.

glass manufacturing and the production and application of arsenical pesticides. Moreover, arsenic inhalation can occur in areas with excessive use of arsenic-containing pesticides. At present, a number of countries have established occupational regulations for arsenic, which set limits in the range from 0.01 to 0.1 $mg\,m^{-3}$ of inorganic arsenic in the workplace.

7 ANALYSIS OF ARSENIC AND ARSENIC SPECIES

There is no shortage of analytical methods for the analysis of total concentration of arsenic as well as for As speciation, but special attention has to be paid to sampling and sample preparation. Sampling is fundamental for a reliable monitoring. Sample removal from its natural environment can already disturb the equilibrium. In water samples, oxidation may take place and arsenate is the only species that is finally analyzed. Sample preparation such as digestion, filtration, preservation and/or prereduction is usually carried out prior to analyses, depending on the analytical procedure. It is evident that sample preparation needs to be done without alteration of the chemical species. This problem is especially relevant in case of geological material, soils and biological tissues that need some kind of processing prior to analysis. Methanol extraction is in most cases sufficient to remove essentially all organoarsenicals into solution. Another example concerns arsenobetaine that is not transformed on storage but is hydrolyzed almost quantitatively by hot alkali digestion.

7.1 Total arsenic concentration

Colorimetric techniques as well as voltammetric techniques have been largely replaced by flame and flameless atomic absorption – and emission spectrometry. Later, the introduction of inductively coupled plasma mass spectrometry reduced the limits of detection significantly ($<1\,pg\,g^{-1}$ in solution). Direct methods are increasingly used to assess the As concentration and the binding states in different types of solid samples: X-ray fluorescence (XRF), X-ray adsorption near edge structure (XANES), secondary electron microscopy (SEM), secondary ion mass spectrometry (SIMS), laser ablation inductively coupled plasma mass spectrometry (LA-ICP-MS), extended X-ray adsorption fine structure (EXAFS) and wide-angle X-Ray scattering as well as infrared spectroscopy and alpha proton X-ray spectrometry (APXS) on board the Mars Pathfinder mission, which measured the composition of six soil samples and five rock samples at the Ares Vallis landing site on Mars.

To investigate As in the field, it is necessary to provide a field test kit, which is easy and safe to use, cheap, robust and reliable. Sensitivity should as an example range from 2 to 1000 $\mu g\,L^{-1}$ for As in drinking water. Most of the current field test kits are based on the Gutzeit method, which involves the reduction of As(III) and As(V) by zinc. Arsine gas is released and produces a stain on mercuric bromide paper. Early kits were particularly tested in India and Bangladesh but showed poor reliability at lower concentrations ($<100\ \mu g\,L^{-1}$). A development of the standard Gutzeit kit is currently under research and should be stable, sensitive and easy to calibrate [18].

7.2 Analysis of arsenic species

An overview is given of current analytical methodologies for arsenic speciation in environmental samples in the article by Taboada-de la Calzada *et al.* [62]. Most of the methods are conventional instrumental methods – mainly chromatographic techniques (high performance liquid chromatography (HPLC), gas chromatography (GC), etc.) coupled with a variety of detectors. Even if chemical speciation has become state of the art in arsenic speciation, analytical problems such as sampling, sample preparation and the availability of certified reference materials are still far from trivial and not yet well established. A main problem is the preservation of species for subsequent laboratory analysis. A number of CRMs have been characterized for their arsenic species [63].

Speciation procedures of inorganic arsenic species are done on the one hand on the basis of different

oxidation/reduction conditions to determine As(III) and As(V), and on the other hand on the basis of selective extraction in different phases. Spectrophotometric methods using SDDC (sodium dimethyl dithiocarbamate) were modified for the determination of arsenite and arsenate by control of pH. Hydride generation is applied for speciation by variation of the pH and coupled to atomic fluorescence chromatography, atomic absorption spectrometry (AAS), atomic emission spectrometry or inductively coupled plasma mass spectrometry [62]. The difference in electrochemical properties enables electrochemical techniques for speciation (differential pulse polarography). Voltammetric methods can be coupled to inductively coupled plasma atomic emission (ICP-AES) or inductively coupled plasma mass spectrometry (ICP-MS).

Nowadays, speciation methods, including the various organoarsenicals, involve an initial separation by a chromatographic technique (e.g. GC, liquid chromatography (LC), size-exclusion chromatography (SEC), capillary zone electrophoreses (CE)), coupled to an element specific detector (e.g. AAS, inductively coupled plasma emission spectrometry (ICP-AES), inductively coupled plasma mass spectrometry (ICP-MS)). Such combinations resulted in powerful speciation techniques with very low detection limits. These different coupling techniques used for arsenic speciation are described comprehensively in various reviews [2, 62, 64–66].

Gas chromatography was applied for the measurements of volatile species using thermal desorption, packed column or open tubular GC. The latter columns show high resolution, which is essential for the analysis of complex environmental and biological samples and offer improved sensitivity. Since many compounds are not volatile or cannot be transformed to volatile derivates without loss of information (e.g. metalloproteins, arsenocholine, As-containing lipids), LC is, however, the most commonly applied separation technique. The coupling to sensitive element specific detectors (ICP-MS) is steadily improving this field of application. Normal and reversed phase partition chromatography, ion interaction chromatography, ion-exchange chromatography as well as SEC are applied as separation techniques. Capillary zone electrophoresis is based on the separation in an electrical field and was applied comprehensively for the speciation of arsenic, even though there is still a lack of "real sample applications" [67].

Recently, arsenic speciation using microorganisms was under discussion [62]. The demand for the determination of arsenic species raises furthermore the need for the development and optimization of multidimensional chromatography for the separation and molecule-specific detection (such as electrospray tandem mass spectrometry (ES-MS-MS) [68].

In soil science, speciation is usually referred to as the characterisation of the phase on which As is bound [44]. This is assessed by applying sequential extraction schemes. A general goal of selective chemical leaching is the accurate determination of the partitioning of elements among different discrete phases of a sample. In practice, some major factors may influence the success in selective leaching, such as (i) the chemical properties of an extractant chosen, (ii) the extraction efficiency, (iii) experimental parameter effects, (iv) the sequence of the individual steps, (v) specific matrix effects such as cross-contamination and reabsorption, (vi) heterogeneity as well as physical associations (e.g. coatings) of the various solid fractions. All these factors have to be critically considered. Several well-established standard procedures can be found in literature [44].

8 REFERENCES

1. Fowler, B. A., *Biological and Environmental Effects of Arsenic*, Elsevier, New York, 1983.
2. Cullen, W. R. and Reimer, K. J., *Chem. Rev.*, **89**, 713 (1989).
3. Hutchinson, T. C. and Meema, K. M. (Eds.), *Lead, Mercury, Cadmium and Arsenic in the Environment*, Wiley & Sons, New York, 1987.
4. Nriagu, J. O. and Pacyna, J. M., *Nature*, **333**, 134 (1988).
5. Ure, A. M. and Berrow, M. L., The elemental constituents of soils, in *Environmental Chemistry*, Vol. 2, Bowen, H. J. M. (Ed.), Royal Society of Chemistry, London, 1982, pp. 94–204.
6. Bhumbla, D. K. and Keefer, R. F., in *Arsenic in the Environment, Part 1: Cycling and Characterization*,

Nriagu, J. O. (Ed.), Wiley & Sons, New York, 1994, p. 51.
7. Smith, E., Naidu, R. and Alston, A. M., *Adv. Agron.*, **64**, 149 (1998).
8. Adriano, D. C., *Metals in the Terrestrial Environment*, Springer, New York, 2001.
9. Takamatsu, T., Aoki, H. and Yoshida, T., *Soil Sci.*, **133**, 239 (1982).
10. Feldmann, J. and Hirner, A. V., *Int. J. Environ. Anal. Chem.*, **60**, 339 (1995).
11. Chatterjee, A., Das, D. and Chakraborti, D., *Environ. Pollut.*, **80**, 57 (1993).
12. Irvine, J. and Jones, E. B. C., *J. Inst. Wood Sci.*, **7**, 20 (1975).
13. Calvert, C. C., in *Arsenical Pesticides*, Woolson, E. A. (Ed.), American Chemical Society, Washington, DC, 1975.
14. Cable News Network, Arsenic found successful in treating leukemia, 14 South 1 CNN Center Atlanta, GA 30303 http://www.cnn.com/HEALTH/9811/07/arsenic.leukemia 1998.
15. Challenger, F., *Chem. Rev.*, **36**, 315 (1945).
16. Sadler, R., Olszowy, H., Shaw, H., Biltoft, R. and Connell, D., *Water, Air, Soil Pollut.*, **78**, 189 (1994).
17. Gallagher, P. A., Wei, X., Shoemaker, J. A., Brockhoff, C. A. and Creed, J. T., *J. Anal. At. Spectrom.*, **14**, 1829 (1999).
18. Water, Sanitation and Health, Department of Protection of the Human Environment, World Health Organization CH-1211 Geneva 27, Switzerland. http://www.who.int/water_sanitation_health/Arsenic/arsenic.htm.
19. Le, X. C., http://www.ualberta.ca/~xcle/arsenic.htm.
20. Wenzel, W. W. and Blum, W. E. H., Assessment of metal mobility in soil-methodological problems, in *Metal Speciation and Contamination of Soil*, Allen, H. E. and Huang, C. P. (Eds.), Lewis Publisher, 1994, Chapter 9.
21. Hallacher, L. E., Kho, E. B., Bernard, N. D., Orcutt, A. M., Dudley, W. C. and Hammond, T. M., *Pac. Sci.*, **39**, 266 (1985).
22. Cherry, J. A., Shaikh, A. U., Tallman, D. E. and Nicholson, R. V., *J. Hydrol.*, **43**, 373 (1979).
23. Goessler, W., Maher, W., Irgolic, K. J., Kuehnelt, D., Schlagenhaufen, C. and Kaise, T., *Fresenius' J. Anal. Chem.*, **359**, 434 (1997).
24. McBride, B. C. and Wolfe, R. S., *Biochemistry*, **10**, 4312 (1971).
25. Le, X. C., Cullen, W. R. and Reimer, K. J., *Talanta*, **40**, 185 (1993).
26. Francesconi, K. A., Hunter, D. A., Bachmann, B., Raber, G. and Goessler, W., *Appl. Organomet. Chem.*, **13**, 669 (1999).
27. Smith, E., Naidu, R. and Alston, A. M., *Adv. Agron.*, **64**, 149 (1998).
28. Peterson, P. J., Benson, L. M. and Porter, E. K., in *Heavy Metals in the Environment, London, September 1979*, CEP Consultants, Edinburgh, 1979, p. 198.
29. Jones, C. A., Langner, H. W., Anderson, K., McDermott, T. R. and Inskeep, W. P., *Soil Sci. Soc. Am. J.*, **64**, 600 (2000).
30. Wenzel, W. W., Kirchbaumer, N., Prohaska, T., Stingeder, G., Lombi, E. and Adriano, D. C., *Anal. Chim. Acta*, **436**, 309 (2001).
31. Wenzel, W. W., Adriano, D. C., Salt, D. and Smith, R., in *Bioremediation of Contaminated Soils*, Agronomy Monograph No. 37, Adriano, D. C., Bollag, J. M., Frankenberger, W. T. Jr. and Sims, R. C. (Eds.), Soil Science Society of America (SSSA) Madison, WI, 1999, p. 456.
32. Ma, L. Q., Komar, K. M., Tu, C., Zhang, W., Cai, Y. and Kennelley, E. D., *Nature*, **409**, 579 (2001).
33. Nimick, D. A., Moore, J. N., Dalby, C. E. and Savka, M. W., *Water Resour. Res.*, **34**, 3051 (1998).
34. Penrose, W. R., *Crit. Rev. Environ. Control*, **4**, 465 (1975).
35. Pettine, M., Camusso, M. and Martinotti, W., *Sci. Total Environ.*, **119**, 253 (1992).
36. Crecelius, E. A., Bothner, M. H. and Carpenter, R., *Environ. Sci. Technol.*, **9**, 325 (1975).
37. Scudlark, J. R. and Church, T. M., *Atmos. Environ.*, **22**, 937 (1988).
38. Ferguson, J. F. and Gavis, J., *Water Res.*, **6**, 1259 (1972).
39. Nriagu, J. O. and Simmons, M. (Eds.), *Food Contamination from Environmental Sources*, Wiley & Sons, New York, 1990.
40. Lunde, G., *Nature*, **224**, 186 (1969).
41. Kuehnelt, D., Goessler, W. and Irgolic, K. J., *Appl. Organomet. Chem.*, **11**, 459 (1997).
42. Edmonds, J. S., Francesconi, K. A., Healy, P. C. and White, A. H., *J. Chem. Soc.*, **1**, 2989 (1982).
43. Brandstetter, A., Lombi, E., Wenzel, W. W. and Adriano, D. C., in *Remediation Engineering of Contaminated Soils*, Wise, D. L., Tarantolo D. J., Cichon E. J., Inyang H. I. and Stottmeister U (Eds.), Marcel Dekker, New York, 2000, p. 715.
44. Wenzel, W. W., Kirchbaumer, N., Prohaska, T., Stingeder, G., Lombi, E. and Adriano, D. C., *Anal. Chim. Acta*, **436**, 309 (2001).
45. Zeien, H., Brümmer, G. W. *Mitteilng. Dtsch. Bodenkundl. Gesellsch.* **59** (1989) 505.
46. Wenzel, W. W. and Blum, W. E. H. Biogeochemistry of trace metals, in: D. C., Adriano, Z.-S., Chen, S.-S., Yang, I.K., Iskandar (Eds.), Advances in Environmental Sciences, Science Reviews, Northwood, 1997, p. 121.
47. Bisessar, S., *Water, Air, Soil Pollut.*, **17**, 305 (1982).
48. Maliszewska, W., Dec, S., Wierzbicka, H. and Wozniakowska, A., *Environ. Pollut. Ser. A*, **37**, 195 (1985).
49. Tabatabai, M. A., *Soil Biol. Biochem.*, **9**, 9 (1977).
50. Oremland, R. S. and Stolz, J. F., *Science*, **300**, 939 (2003).
51. Machlis, L., *Plant Physiol.*, **16**, 521 (1941).
52. Lario, Y., Burló, F., Aracil, P., Martínez-Romero, D., Castillo, S., Valero, D. and Carbonell-Barrachina, A. A., *Food Additives Contam.*, **19**, 417 (2002).

53. Leonard, A., in *Metals and Their Compounds in the Environment. Occurrence, Analysis and Biological Relevance*, E. Merian in cooperation with Clarkson *et al*. (Eds.), VCH, Weinheim, Germany, 1991, p. 751.
54. Goessler, W., Kuehnelt, D. and Irgolic, K. J., *Determination of Arsenic Compounds in Human Urine by HPLC-ICP-MS, in Arsenic: Exposure and Health Effects*, Abernathy, C.O. (Ed.) Chapman & Hall, London, 1997, pp. 33–44.
55. National Food Authority, *Australian Food Standards Code: March 1993*, Australian Government Public Service, Canberra, Australia, 1993.
56. Anke, M., Glei, M., Arnhold, W., Drobner, C. and Seifert, M., in *Handbook of Nutritionally Essential Mineral Elements*, O'Dell, B. L. and Sunde, R. A. (Eds.), Marcel Dekker, New York, 1997.
57. Nriagu, J. O. (Ed.), *Arsenic in the Environment*, Wiley & Sons, New York, 1994.
58. United States Environmental Protection Agency, US, http://www.epa.gov/safewater/ars/treat.html.
59. NRC (National Research Council), *The Use of Drugs in Food Animals: Benefits and Risks*, National Academy Press, Washington, DC, 1999.
60. Finkelmann, R. B. and Gross, P. M., *Int. J. Coal Geol.*, **40**, 91 (1999).
61. Maeda, S., Kumamoto, T., Yonemoto, M., Nakajima, S., Takeshita, T., Higashi, S. and Ueno, K., *Sep. Sci. Technol.*, **18**, 375 (1983).
62. Taboada-de la Calzada, A., Villa-Lojo, M. C., Beceiro-Gonzalez, E., Alonso-Rodriguez, E. and Prada-Rodriguez, D., *Trends Anal. Chem.*, **17**, 167 (1998).
63. Lagarde, F., Amran, M. B., Leroy, M. J. F., Demesmay, C., Olle, M., Lamotte, A., Muntau, H., Michel, P., Thomas, P., Caroli, S., Larsen, E., Bonner, P., Rauret, G. and Maier, E. A., *Fresenius' J. Anal. Chem.*, **363**, 18 (1999).
64. Szpunar-Lobinska, J., Witte, C., Lobinski, R. and Adams, F. C., *Fresenius' J. Anal. Chem.*, **351**, 351 (1995).
65. Irgolic, K. J. and Stockton, R. A., *Mar. Chem.*, **22**, 265 (1987).
66. Szpunar, J., *Analyst*, **125**, 963 (2000).
67. López-Sánchez, F., Amran, M. B., Lakkis, M. D., Lagarde, F., Rauret, G. and Leroy, M. J. F., *Fresenius' J. Anal. Chem.*, **348**, 810 (1994).
68. McSheehy, P. P, Lobinski, R. and Szpunar, J., *Analyst*, **126**, 1055 (2001).

2.4.2 Arsenic Speciation in Human Tissues

Jean-Pierre Buchet

Université catholique de Louvain, Brussels, Belgium

1 EFFECTS OF ARSENIC IN THE HUMAN ORGANISM

The use of inorganic arsenic (As_i) for the treatment of anemia and chronic skin diseases has been discontinued for decades but, at present, As_2O_3 regains interest for the therapeutic management of acute promyelocytic leukemia [1], while several organoarsenicals are used as antiparasitic drugs.

Most often, however, the poison character of arsenic is acknowledged [2–4]. In living organisms, soluble pentavalent inorganic arsenicals can compete with phosphate and lead to the formation of 1-arseno-3-phosphoglycerate that is spontaneously hydrolyzed without ATP production; in addition, they are easily reduced into arsenite, which rapidly binds to biological thiol groups, inhibiting many important enzymes, among which is the activity involved in ATP production by way of oxidative phosphorylation reactions. An impairment of energy production coupled with the inhibition of many other thiol enzymes can affect virtually all cellular functions. Thiol enzymes such as glutathione peroxidase and thioredoxin reductase have been recently shown to be much more sensitive to inhibition by trivalent mono- and dimethylated As than by the inorganic trivalent form of the element [5]; the same compounds, involved in the As_i metabolism (see below) were shown to be able to nick and break phage X174 supercoiled DNA and proved to be 77 and 386 times more potent, respectively, than As^{III} in a Comet assay using human lymphocytes [6].

The strong irritating behavior of As^{III} toward living tissues coupled with its powerful inhibiting properties explains the gastrointestinal symptoms, disturbances of cardiovascular and nervous system functions and eventually death in case of severe acute intoxication.

Several epidemiological studies have shown that chronic exposure to As_i is causally related with cancer in humans. The risk of lung cancer is

Handbook of Elemental Speciation II: Species in the Environment, Food, Medicine & Occupational Health
Edited by R. Cornelis, H. Crews, J. Caruso and K. G. Heumann
 ISBN: 0-470-85598-3 (HB)

increased among workers and populations living near certain As-emitting industries, and it appears that tobacco consumption can further increase that risk. In case of ingestion of As-rich water, risks for skin, lungs, bladder and kidney cancer are increased. Besides these most critical effects, many other disturbances have been causally related with As toxicity. As the element is distributed in all organs, impairments in several systems have been described; they include respiratory, cardiovascular, gastrointestinal, hematological, hepatic, skin, neurological and genotoxic effects [2–4]:

- dusts with inorganic arsenic are irritating for the respiratory tract, but increased frequency of cough, sore throat, sputum and rhinorrhea has also been reported in consumers of contaminated drinking water;
- the contribution of As to 'Blackfoot' disease is disputed but 'Raynaud' syndrome, cyanosis and gangrene of the fingers and toes have been reported not only in Taiwan but also in Germany, Chile, Mexico, Bangladesh;
- inorganic arsenicals are irritating for the gastrointestinal mucosa, causing nausea, vomiting and diarrhea; this is of course more the case after acute exposure but has also been reported after chronic exposure by inhalation and ingestion;
- the toxic action of arsenic on bone marrow cells is probably responsible for red and/or white blood cell depression often observed after exposure by the oral route; it should be recalled that poisoning with arsine gas causes hemolysis probably due to fragilization of the erythrocyte membrane following reduced glutathione depletion caused by arsine;
- reversible liver enlargement has been observed particularly in two episodes of food poisoning by As in Japan, portal hypertension in subjects treated with Fowler's solution for several years and liver cirrhosis in German vintners after heavy consumption of wine contaminated with arsenic-containing pesticides; large elevations in serum enzymes indicating hepatotoxicity are observed only in cases of acute poisoning;
- chronic exposure to inorganic arsenic frequently causes hyperkeratosis of the palms and soles and hyperpigmentation (melanosis speckled with paler spots) in areas of the skin not exposed to the sun;
- chromosome aberrations in cultured lymphocytes and micronuclei in exfoliated buccal and bladder cells have been observed in subjects exposed to the element; the evidence for an effect of As on reproduction and development seems accumulating but needs confirmation because of the limitations of the studies reporting such outcomes;
- in subjects surviving acute poisoning, peripheral nervous disturbances are frequently encountered; the lower extremities are often more severely affected than the upper extremities; exposure to lower levels affects sensory and motor neurons: abnormalities in electromyograms have been reported in subjects consuming contaminated drinking water; the peripheral neuropathy symptoms may progressively disappear when exposure is ended, but recovery is often not complete.

In recent years, evidence has increased that chronic consumption of As-rich drinking water might be associated with an increased risk of high blood pressure and diabetes [4].

2 ARSENIC ABSORPTION AND DISTRIBUTION IN MAN

The bioavailability of inorganic As compounds absorbed through inhalation and ingestion is proportional to their water solubility: As oxides, sodium arsenite and arsenate enter the organism more rapidly and to a greater extent than As sulfides or lead arsenate. The valence state of the element does not influence its absorption rate in hamsters intratracheally instilled with solutions of inorganic soluble salts. Likewise, in man, the gastrointestinal absorption of both tri- and pentavalent inorganic arsenicals is rapid and extensive. Limited data suggest that the percutaneous absorption of arsenate from water is very low (1% in man). Organoarsenicals such as monomethylarsonic acid (MMA) and dimethylarsinic acid (DMA) are efficiently (>80%) absorbed by the oral route.

Because of the matrix complexity, the *total* As concentration in biological tissues is most often reported. In environmentally exposed subjects, As distributes almost equally in internal organs; a slight increased concentration can, however, be observed in tissues with a high keratin content such as hair and nails. As shown in Table 2.4.2.1, quite variable concentrations are found in a same tissue from different individuals, and different environmental exposure levels may be proposed to explain differences among corresponding tissue concentrations observed in different countries (however, an influence of the analytical techniques used cannot be totally excluded). Other data suggest that As accumulates in tissues with age without any sex-linked differences. An increased concentration in blood ($>1\ \mu g\,L^{-1}$) can be observed during a short period only after the absorption step; after a lethal dose, concentrations in liver and kidney are markedly higher than in other organs. Scarce efforts for the speciation of As in biological tissues from environmentally exposed subjects indicate the presence of only very low and barely higher proportions of MMA and DMA, respectively. In tissues of an acutely intoxicated man (Table 2.4.2.1), MMA/DMA ratios ranged between 2.5 and 3 and MMA proportions between 10 and 30% of the total tissue contents.

3 ARSENIC BIOTRANSFORMATIONS AND EXCRETION IN MAN

The knowledge on As biotransformation in mammals is limited to the inorganic forms and, according to observations in human volunteers and laboratory animals, results are similar following absorption by inhalation, ingestion or even intravenous injection of water-soluble compounds. Data on biotransformations chiefly derive from investigations on urinary metabolites because the kidney is the main excretory organ in animals. While in microorganisms inorganic arsenate undergoes successive reductions and oxidative methylations, leading to mono-, di- and trimethylated arsenicals [10], in man and other mammals, however, only the two first steps are observed: they lead to mono- and dimethylated arsenicals identified as monomethylarsonic (MMA^V) and dimethylarsinic (DMA^V) acids (Scheme 2.4.2.1). Several thiols (cystein, dithiothreitol) can reduce pentavalent arsenicals *in vitro* but, *in vivo*, reduced glutathione seems to play the most important role in the reduction steps; methyl groups are supplied by *S*-adenosyl methionine and possibly also by Vit B_{12} and methylated analogs. Arsenic methyltransferases have been located in different organs, but the liver cytosol proved to be the best source of enzymatic activities; arsenite and methylarsonous acid methyltransferases from rabbit [11] and rat [12] liver have been partially purified and characterized.

The speciation of As in urine was long limited to the directly reducible forms of the element, that is, the inorganic tri- and pentavalent derivatives and the methylated compounds MMA and DMA. The latter, determined as arsines, were thought to involve As in the pentavalent state until Le *et al.* [13] demonstrated for the first time the presence of MMA^{III} and DMA^{III} in urine from people in Inner Mongolia who consume drinking water with 510 to 660 $\mu g\ As\ L^{-1}$ and administered 300 mg of the chelator sodium 2,3-dimercapto-1-propane sulfonate (DMPS) after an overnight fasting. That the presence in urine of trivalent methylated arsenicals was not necessarily due to treatment with the chelator was confirmed by the detection of spontaneous MMA^{III} in urine of 17% of Romanian subjects [14] consuming As-rich drinking water. Afterwards, not only MMA^{III} but also DMA^{III} have been observed in urine in 48 and 72%, respectively, of subjects who drink contaminated water in West Bengal [15]. However,

Table 2.4.2.1. Total arsenic concentration in human tissues (ng As g^{-1} wet weight).

Tissue	Environmentally exposed subjects		Fatal poisoning (Reference 9)
	(Reference 7)	(Reference 8)	
Liver	14.5 ± 6.9	129 ± 39.7	147,000
Kidney	12.4 ± 20.7	129 ± 72.3	26,600
Lung	19.9 ± 22.7	104 ± 29.5	1113
Spleen	15.2 ± 16.6	101 ± 49.4	1172
Brain	3.9 ± 1.0	–	833
Cerebellum	–	132 ± 60.2	1095
Skin	–	153 ± 97.7	2900

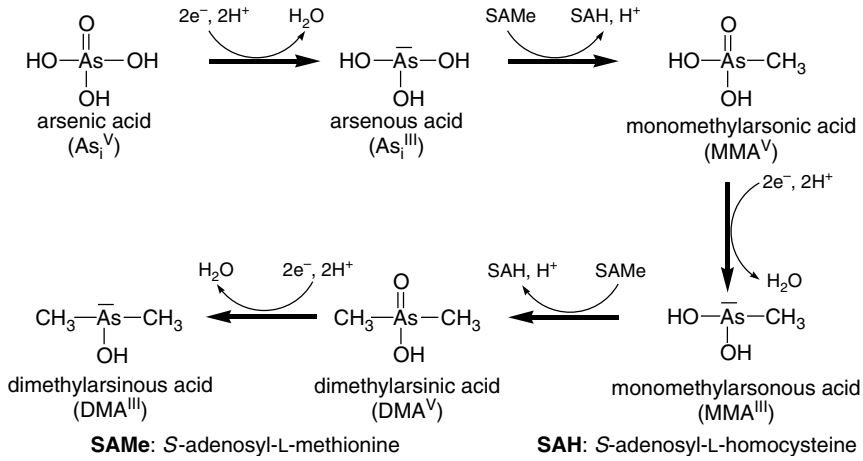

Scheme 2.4.2.1

until now, trivalent methylated As compounds have not (yet?) been shown in urine of control people, that is, nonoccupationally exposed and consuming drinking water with low As level ($<10\ \mu g\ L^{-1}$). In addition, the stability of trivalent inorganic, mono- and dimethylated As added in human urine samples appears to display a considerable variation [16]. Urinary MMA^V and DMA^V concentrations reported previously for control subjects are probably correct and do not underestimate any of the methylated compound; the possible imprecision only relates to the valence state of As in the methylated derivatives, as previous determinations included a reduction step of arsenicals in acid medium effective on both the trivalent and pentavalent species of MMA and DMA.

The methylation of inorganic trivalent As has been studied in man administered 7.14 $\mu g\ As^{III}$/kg either iv or po [17]. Within the 24 h following the absorption, 30 and 22% of the dose was excreted in urine after iv and po administration, respectively. A clear-cut difference in the proportion of As forms was also evidenced: unmetabolized forms and mono and dimethylated metabolites represented 63, 13, 24 and 38, 23, 39% of the urinary excretion after the iv and po administration, respectively. This points to the importance of the liver for As metabolism and to that of the kidney for its excretion. The po administration of 7.14 $\mu g\ As^V$ as MMA or as DMA showed that in man no de-methylation occurs; at the opposite, a limited methylation of MMA($\pm$10%) into DMA was observed. During four days, after a single dose (7.14 μg As/kg) of $NaAsO_2$, MMA or DMA, 46, 78 and 75%, respectively, of the dose are eliminated in urine; the time corresponding to the excretion of half the total amount excreted in four days was below 4 h in the case of MMA, approximately 11 h for DMA and 28 h for $NaAsO_2$.

In one volunteer, five consecutive daily doses of 1 mg inorganic As^{III} were shown to lead to a partial saturation of the As methylation capacity. This observation is consistent with the inhibition at high substrate concentration of As methylation in *in vitro* systems involving a rat liver cytosol preparation as enzyme source [18] or a primary culture of human hepatocytes [19]. Observations in cases of attempted suicide with As trioxide [20] are also in accordance with a possible saturation of the As methylation: during several days after As ingestion, inorganic forms of the element represent the highest proportion of urinary metabolites. Another support to the hypothesis of a possible saturation of inorganic As by excess of substrate is given by the observations of Benramdane *et al*. [9] who measured As in tissues of a subject who died three days after ingestion of 8 g As_2O_3: 80% of As was present as inorganic species (mainly trivalent), 14% as MMA and 6% as DMA.

Arsine gas is readily absorbed by the respiratory route; its metabolism leads to the urinary excretion of the same metabolites [21] as after absorption of other inorganic arsenicals.

Organoarsenicals can be easily absorbed through mushrooms or seafood consumption. They are rapidly excreted in urine, some without transformation (arsenobetaine, arsenocholine), but others may undergo changes leading to DMA excretion [22].

4 FACTORS POTENTIALLY MODIFYING ARSENIC METABOLISM

It should be stressed that most population groups studied so far have on average 10–30% inorganic, 10–20% MMA, and 60–70% DMA in urine but show a considerable interindividual variation. Groups with unusually low or high urinary excretion of MMA have been identified, pointing to the possible existence of a genetic polymorphism in the biomethylation of As [23]. In some studies, age and sex did not influence the relative distribution of the urinary As metabolites; in others, children had a higher percentage of inorganic As and a lower percentage of DMA in urine than adults and, compared with men, a higher relative amount of DMA has been observed in urine in women [4]. A reduced methylation of As and an increased tissue retention of the element possibly leading to increased toxic effects have been observed in animals fed a diet deficient in precursors of *S*-adenosylmethionine [24]. This led several authors to suggest that poor nutrition might increase the toxicity of As, but only slight variations in the percentage of methylated As metabolites have been observed in the urine of populations consuming As-rich drinking water and either enjoying good nutrition or suffering from extensive malnutrition [4]. Experimental studies on As metabolism in man have shown that liver disease did not affect the urinary excretion of an iv injected dose but respectively increased and decreased the proportions of MMA and DMA in urine [25].

A severe nephrectomy leading to a uremic syndrome in rabbits administered a small dose of carrier-free ^{74}As-As(V) strongly reduced the renal excretion of the element; this caused an extensive binding of As_i to insoluble tissue constituents, the more so as the methylation capacity of the uremic rabbit was deeply depressed [26].

Patients with chronic renal insufficiency and without any known exposure to inorganic As showed a threefold increase of the element in serum and a twofold increase in packed cells compared with controls; these increases are related to the degree of renal insufficiency [27] and involve DMA and mainly arsenobetaine [28], which are also the only metabolites found in serum of control subjects [29].

5 ARSENIC LEVELS IN HUMAN BIOLOGICAL SAMPLES

Hair, nail, blood and mainly urine can be analyzed to document an undue absorption of inorganic As. However, matrix complexity often prevents As speciation so that only total As concentration can be determined in nonliquid biological samples. Specific sample pretreatments have been proposed in particular cases, for example, the digestion of hair in 2 M NaOH at 95 °C for 3 hours to reveal DMA [30] and the liberation of protein-bound arsenicals from binding sites on liver cytosolic proteins by CuCl at pH 1 [31] or 2 M HNO_3 at 110 °C for 1 min [32]. As species are more easily identified in blood and urine; nevertheless, for kinetics reasons, the determination of urinary metabolites is preferred for the biomonitoring of exposure to the element. High performance liquid chromatography (HPLC) techniques using ion pair separation on reversed-phase C_{18} or anion and/or cation exchangers have been proposed to separate arsenicals excreted in urine but more than a single chromatographic step is usually necessary to determine all the metabolites identified up to now. Many procedures are used to quantify As compounds: inductive coupled plasma with mass spectrometry (ICP-MS) can detect any As compound and appears to be the most sensitive method. Less expensive techniques include atomic absorption spectrometry (AAS) and atomic fluorescence spectrometry (AFS). This latter technique, however, needs the formation of volatile arsenicals to

be burnt in an air/H_2 flame. Both tri and pentavalent inorganic and methylated arsenicals generate corresponding volatile arsines when treated at pH ≤ 2 with a reducing agent such as $NaBH_4$, but only trivalent compounds do so at pH 6. A strong oxidation step is needed to mineralize trimethylarsonium derivatives such as arsenobetaine before their detection by AFS.

5.1 Hair and nails

Hair and nails concentrate As because of their keratin content, which is believed to bind trivalent As forms, possibly methylated as DMA in human hair [30]. Both tissues are subject to external contamination and can be used to identify As ingestion provided that external contamination can be excluded. While several washing procedures have been proposed, no definitive technique appears to be available to selectively assess absorbed As. As levels in samples from persons not subjected to significant exposure are less than 1 μg As/g but values up to several $\mu g\, g^{-1}$ have been reported after either consumption of As-rich drinking water or exposure to dusts of a coal-fired power plant [33]. To quantify low-level As exposure through drinking water, determinations in toenail samples have also been reported [34].

5.2 Blood

As concentration in blood mainly reflects recent exposure because the element is rapidly cleared from blood following a 3-exponential clearance curve, the first component of which corresponds to the majority of As in blood and has a half-life of about 1 h. In case of severe intoxication, however, a biological half-life of As in blood as long as 60 h has been calculated [20]. Comparing nonexposed subjects, consumers of As-rich drinking water and Black Foot Disease patients, Heydorn [35] found concentrations of 2.5, 15 and 30 μg As/L of plasma and 2.5, 22 and 60 μg As/L of whole blood, respectively. However, more recent techniques lead to lower concentrations in control subjects: 0.38 and 3.2 $\mu g\, L^{-1}$ in serum and packed cells, respectively [36] and 0.96 $\mu g\, L^{-1}$ in whole blood [28]. Because it is influenced by seafood consumption and increases much less and for a shorter duration than in urine, As concentration in blood can actually be considered as an incidental biomarker of exposure to the element.

Table 2.4.2.2. Concentration (μg As/L) of arsenic metabolites in urine of control subjects.

Subject number	Asi	MMA	DMA	Reference
148	1.9 ± 1.2	1.9 ± 1.4	2.1 ± 1.5	[40]
413	1.3 ± 1.8	1.6 ± 2.2	6.1 ± 9.0	[41]
30	1.7 ± 1.1	2.0 ± 1.0	3.3 ± 2.5	[42]
21	3.7 ± 2.0	1.0 ± 0.6	7.7 ± 5.8	[43]

5.3 Urine

A few studies report baseline values of the urinary As metabolites in populations not particularly exposed to the element. Most often, the valence state of As in inorganic and methylated species is not specified, but due attention is paid to the consumption of seafood. Some published values are presented in Table 2.4.2.2. Nonhydride-producing As species are generally assumed to be organic arsenicals of dietary origin; their abundance is highly variable and may be concomitant with an excretion of DMA related to arsenosugar digestion after seaweed or mussels consumption [37, 38]. Depending on the contamination level of drinking water by As, the urinary excretion of the element and its metabolites can range between <10 and 1000 (and more) μg As/L [39]; DMA^V is currently the metabolite present in the highest proportion but has been shown, in some extreme cases, associated with the presence of MMA^{III} and DMA^{III} [14, 15].

6 THE BIOLOGICAL MONITORING OF OCCUPATIONAL EXPOSURE TO INORGANIC ARSENIC

In occupational settings, exposure to inorganic As forms is much more frequent than to the methylated (herbicides) or arylated (pesticides) arsenicals. To monitor occupational exposure, the determination of the urinary metabolites is the preferred biomarker. The relevant urinary arsenicals include the tri- and/or pentavalent inorganic,

mono- and dimethylated As forms; their concentration in urine mainly reflects recent exposure. As the consumption of some seafood can increase the urinary DMA excretion [22, 43], urine sample collection must be performed 2 to 3 days after subjects refrained from eating fish, shellfish or seaweed. The monitoring of an occupational exposure through urine analysis must also take into account a possible inorganic As ingestion through drinking water because the same metabolites as after inorganic As inhalation (or ingestion) at the workplace are produced. Highly significant relationships are reported between exposure to airborne inorganic As compounds and the concentration of As in urine; regression coefficients, however, are varying highly according to the different working exposures, different contributions of oral exposure and different analytical methods adopted [44]. Recent studies in a copper smelter [45], a sulfuric acid plant [46] and glassworks [47], using specific measurement of urinary metabolites report more coherent results: after an 8 h exposure to a mean concentration of 10 $\mu g\,As/m^3$ in air, the mean urinary concentration of inorganic As ranges between 5 and 7 $\mu g\,L^{-1}$, while it remains below 1.5 $\mu g\,L^{-1}$ in nonoccupationally exposed subjects. The value for the sum of As_i, MMA and DMA is below 15 $\mu g\,As/L$ in nonoccupationally exposed subjects without recent seafood consumption [44]. The American Conference of Governmental Industrial Hygienists (ACGIH) biological exposure index for inorganic As is 35 $\mu g\,As/L$ (As_i + MMA + DMA) in urine collected at the end of a workweek [48].

7 REFERENCES

1. Soignet, S. L., Maslak, P., Wang, Z. G., Jhanwar, S., Calleja, E., Dardashti, L. J., Corso, D., Deblasio, A., Gabrilove, J., Scheinberg, D. A., Pandolfi, P. P. and Warrell, R. P., *N. Engl. J. Med.*, **339**, 1341 (1998).
2. WHO, *Environmental Health Criteria 224: Arsenic and Arsenic Compounds*, 2nd ed., IPCS International Programme on Chemical Safety, Geneva, Switzerland, 2001.
3. ATSDR, *Toxicological Profile for Arsenic (update). Agency for Toxic Substances and Disease Registry*, U.S. Department of Health and Human Services, Atlanta, GA, 2001.
4. National Research Council, *Arsenic in Drinking Water (update)*, Committee on Toxicology, National Academy Press, Washington, DC, 2001.
5. Lin, S., Del Razo, L. M., Styblo, M., Wang, C., Cullen, W. R. and Thomas, D. J., *Chem. Res. Toxicol.*, **14**, 305 (2001).
6. Mass, M. J., Tennant, A., Roop, B. C., Cullen, W. R., Styblo, M., Thomas, D. J. and Kligerman, A. D., *Chem. Res. Toxicol.*, **14**, 355 (2001).
7. Dang, H. S., Jaiswal, D. D. and Somasundaram, S., *Sci. Total Environ.*, **29**, 171 (1983).
8. Yamauchi, H. and Yamamura, Y., *Bull. Environ. Contam. Toxicol.*, **31**, 267 (1983).
9. Benramdane, L., Accominotti, M., Fanton, L., Malicier, D. and Vallon, J. J., *Clin. Chem.*, **45**, 301 (1999).
10. Cullen, W. R., McBride, B. C. and Reglinski, J., *J. Inorg. Biochem.*, **21**, 179 (1984).
11. Zakharyan, R. A., Ayala-Fiero, F., Cullen, W. R., Carter, D. M. and Aposhian, H. V., *Toxicol. Appl. Pharmacol.*, **158**, 9 (1999).
12. Lin, S., Shi, Q., Nix, F. B., Styblo, M., Beck, M. A., Herbin-Davis, K. M., Hall, L. L., Simeonsson, J. B. and Thomas, D. J., *J. Biol. Chem.*, **277**, 10795 (2002).
13. Le, X. C., Lu, X., Ma, M., Cullen, W. R., Aposhian, H. V. and Zheng, B., *Anal. Chem.*, **72**, 5172 (2000).
14. Aposhian, H. V., Gurzau, E. S., Le, X. C., Gurzau, A., Healy, S. M., Lu, X., Ma, M., Yip, L., Zakharyan, R. A., Maiorino, R., Dart, R. C., Tircus, M. G., Gonzales-Ramirez, D., Morgan, D. L., Avram, D. and Aposhian, M. M., *Chem. Res. Toxicol.*, **13**, 693 (2000).
15. Mandal, B. K., Ogra, Y. and Suzuki, K. T., *Chem. Res. Toxicol.*, **14**, 371 (2001).
16. Del Razo, L. M., Styblo, M., Cullen, W. R. and Thomas, D. J., *Toxicol. Appl. Pharmacol.*, **174**, 282 (2001).
17. Buchet, J. P. and Lauwerys, R., Inorganic arsenic metabolism in humans, in *Arsenic: Exposure and Health*, Chappell, W. R., Abernathy, C. O. and Cothern, C. R. (Eds.), Science and Technology Letters, Northwood, MI, 1994, pp. 181–189.
18. Buchet, J. P. and Lauwerys, R., *Arch. Toxicol.*, **57**, 125 (1985).
19. Styblo, M., Del Razo, L. M., LeCluyse, E. L., Hamilton, G. A., Wang, C., Cullen, W. R. and Thomas, D. J., *Chem. Res. Toxicol.*, **12**, 560 (1999).
20. Mahieu, P., Buchet, J. P., Roels, H. and Lauwerys, R., *Clin. Toxicol.*, **18**, 1067 (1981).
21. Apostoli, P., Alessio, L., Romeo, L., Buchet, J. P. and Leone, R., *J. Toxicol. Environ. Health*, **52**, 331 (1997).
22. Le, X., Ma, M. and Lai, V., Exposure to arsenosugars from seafood ingestion and speciation of urinary arsenic metabolites, in *Arsenic Exposure and Health Effects*, Chappell, W. R., Abernathy, C. O. and Calderon, R. L. (Eds.), Elsevier Science B.V., Amsterdam, 1999, pp. 69–79.
23. Vahter, M., *Toxicol. Lett.*, **112–113**, 209 (2000).
24. Vahter, M. and Marafante, E., *Toxicol. Lett.*, **37**, 41 (1987).

25. Geubel, A., Mairlot, M., Buchet, J. P., Dive, C. and Lauwerys, R., *Int. J. Clin. Pharm. Res.*, **8**, 117 (1988).
26. De Kimpe, J., Cornelis, R., Mees, L., Vanholder, R. and Verhoeven, G., *J. Trace Elem. Med. Biol.*, **13**, 7 (1999).
27. Zhang, X., Cornelis, R., De Kimpe, J., Mees, L., Vanderbiesen, V. and Vanholder, R., *Fresenius' J. Anal. Chem.*, **353**, 143 (1995).
28. Zhang, X., Cornelis, R., De Kimpe, J., Mees, L., Vanderbiesen, V., De Cubber, A. and Vanholder, R., *Clin. Chem.*, **42**, 1231 (1996).
29. Zhang, X., Cornelis, R., De Kimpe, J. and Mees, L., *Anal. Chim. Acta*, **319**, 177 (1996).
30. Yamato, N., *Bull. Environ. Contam. Toxicol.*, **40**, 633 (1988).
31. Styblo, M., Hughes, M. and Thomas, D., *J. Chromatogr., B*, **677**, 161 (1996).
32. De Kimpe, J. and Cornelis, R., *Toxicol. Environ. Chem.*, **71**, 279 (1999).
33. Hindmarsh, J. T., Dekerkhove, D., Grime, G. and Powell, J., Hair arsenic as an index of toxicity, in *Arsenic Exposure and Health Effects*, Chappell, W. R., Abernathy, C. O. and Calderon, R. L. (Eds.), Elsevier, Amsterdam, 1999, pp. 41–49.
34. Karagas, M. R., Tosteson, T. D., Blum, J., Klaue, B., Weiss, J. E., Stannard, V., Spate, V. and Morris, J. S., *Am. J. Epidemiol.*, **152**, 84 (2000).
35. Heydorn, K., *Clin. Chim. Acta*, **28**, 349 (1970).
36. De Kimpe, J., Cornelis, R., Mees, L., Van Lierde, S. and Vanholder, R., *Am. J. Nephrol.*, **13**, 429 (1993).
37. Le, X. C., Cullen, W. R. and Reimer, K. J., *Clin. Chem.*, **40**, 617 (1994).
38. Heinrich-Ramm, R., Mindt-Prüfert, S. and Szadkowski, D., *Int. J. Hyg. Environ. Health*, **203**, 475 (2001).
39. Buchet, J. P., Hoet, P., Haufroid, V. and Lison, D., Consistency of biomarkers of exposure to inorganic arsenic: review of recent data, in *Arsenic Exposure and Health Effects*, Chappell, W. R., Abernathy, C. O. and Calderon, R. L. (Eds.), Elsevier, Amsterdam, 1999, pp. 31–40.
40. Foa, V., Colombi, A., Maroni, M., Buratti, M. and Calzaferri, G., *Sci. Total Environ.*, **34**, 241 (1984).
41. Kalman, D. A., Hughes, J., van Belle, G., Burbacher, T., Bolgiano, D., Kolbe, K., Mottet, N. K. and Polissar, L., *Environ. Health Perspect.*, **89**, 145 (1990).
42. Lin, T. H. and Huang, Y. L., *Biol. Trace Elem. Res.*, **48**, 251 (1995).
43. Buchet, J. P., Lison, D., Ruggeri, M., Foa, V. and Elia, G., *Arch. Toxicol.*, **70**, 773 (1996).
44. Lauwerys, R. and Hoet, P., Exposure to inorganic and organometallic substances, in *Industrial Chemical Exposure. Guidelines for Biological Monitoring*, Lewis Publishers, CRC Press LLC, Boca Raton, FL, 2001, Chapter 2, pp. 36–49.
45. Hakala, E. and Pyy, L., *Toxicol. Lett.*, **77**, 249 (1995).
46. Offergelt, J. A., Roels, H., Buchet, J. P., Boeckx, M. and Lauwerys, R., *Br. J. Ind. Med.*, **49**, 387 (1992).
47. Apostoli, P., Bartoli, D., Alessio, L. and Buchet, J. P., *Occup. Environ. Med.*, **56**, 825 (1999).
48. ACGIH (American Conference of Governmental Industrial Hygienists), *Threshold Limit Values for Chemical Substances and Physical Agents and Biological Exposures Indices*, Cincinnati, OH, 2001.

2.5 Speciation of Cadmium

2.5.1 Speciation of Cadmium in the Environment and Food

Klaus Günther and Bernd Kastenholz

Institute for Chemistry and Dynamics of the Geosphere, Institute III: Phytosphere, Research Center Juelich, Germany

1 ENVIRONMENT

It is well known that cadmium compounds belong to the most hazardous pollutants in the environment. The intake of even very small amounts of this ubiquitous element already causes severe toxic effects to humans. Therefore, the speciation of cadmium in the different environmentally relevant matrices is absolutely necessary.

1.1 Water

The speciation of cadmium in aquatic matrices is dominated by electrochemical methods. Anodic stripping voltammetry with a rotating disk electrode was used to investigate the kinetic speciation of cadmium in freshwaters [1] and in aqueous solutions containing dissolved organic matter [2]. Another technique like gel-integrated Hg-plated-Ir-based microelectrode array in combination with anodic stripping voltammetry was suitable to discriminate between mobile and colloidal metal species in natural waters at nanomolar or subnanomolar levels [3]. Organic chelates were the dominant chemical ligands of cadmium (73 to 83%) in filtered estuarine water samples from a high-salinity region determined by differential pulse anodic stripping voltammetry (DPASV) [4]. In contrast to this result, 80% of the dissolved cadmium in water from a polluted lake was analyzed as free Cd^{2+} ions measured by the same electrochemical procedure and a technique involving ligand

Handbook of Elemental Speciation II: Species in the Environment, Food, Medicine & Occupational Health
Edited by R. Cornelis, H. Crews, J. Caruso and K. G. Heumann
 ISBN: 0-470-85598-3 (HB)

exchange [5]. The speciation of cadmium in seawater applying DPASV revealed that two different cadmium species were present in the voltammograms obtained. By UV-irradiation experiments, an inorganic and organic cadmium form could be detected. Water column samples exhibited an enrichment of inorganic cadmium by depth [6].

Electrochemical detection was also used to specify Cd^{2+} and monomethyl-Cd^{+} ions in Atlantic Ocean water. The concentrations measured resulted in the range of about 0.5 $\mu g\,L^{-1}$ for monomethylcadmium ions as represented in Figure 2.5.1.1. Thereby, humic acids did not influence the voltammetric determination of monomethylcadmium. It was also discovered that biomethylation was the most probable formation process for this methylated cadmium species [7]. This result was confirmed by another study of Pongratz and Heumann who showed that monomethylcadmium in ocean waters had a maximum concentration in water depths up to 50 m, often correlating well with the chlorophyll-a content represented in Figure 2.5.1.2 [8]. In depths of about 200 m, significant concentrations of methylated metal compounds could be detected by using a voltammetric method, in which no chlorophyll-a was present. The authors concluded that marine bacteria predominantly contributed to methylated metals at deeper water levels [8]. An overview of trace element speciation techniques in waters concerning the relationship between aquatic toxicity and bioaccumulation of dissolved metal compounds like those of cadmium, zinc, and other trace elements was given by Florence, Morrison, and Stauber [9].

The speciation analysis of Cd in biomatrices is mainly applied to microorganisms [10–12], animals [13–17], and phytosystems [18–31].

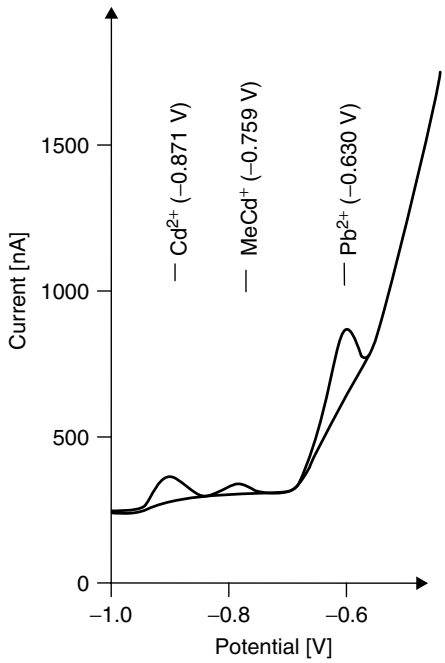

Figure 2.5.1.1. DPASV (differential pulse anodic stripping voltammogram) of a seawater sample from the Atlantic Ocean with a determined $MeCd^{+}$ concentration of 492 $pg\,L^{-1}$. (Reproduced from Reference [7] by permission of American Chemical Society.)

1.2 Microorganisms

In bacteria, a cadmium-binding form was analyzed by high-performance gel permeation liquid chromatography combined with inductively coupled plasma mass spectrometry. Cadmium was bound to a metallothionein (MT)-like protein with a molecular mass of about 10,000 Da [10]. A combined procedure consisting of extraction, gel permeation chromatography (GPC), anion-exchange chromatography, high performance liquid chromatography (HPLC), and sodium dodecyl sulfate polyacrylamide gel electrophoresis (SDS-PAGE) was applied to purify a cadmium-binding protein with a molecular mass of 23,000 Da in bacilli [11]. In bacteria cells of *Escherichia coli*, a cadmium-binding protein with a molecular mass of about 39,000 Da was detected by using Sephadex G-100, metal chelate affinity chromatography, and disc gel electrophoresis in the purification procedure. Cadmium levels were estimated by atomic absorption spectrometry (AAS) [12].

1.3 Animals

Concerning terrestrial cadmium speciation studies, earthworms were investigated using polyacrylamide

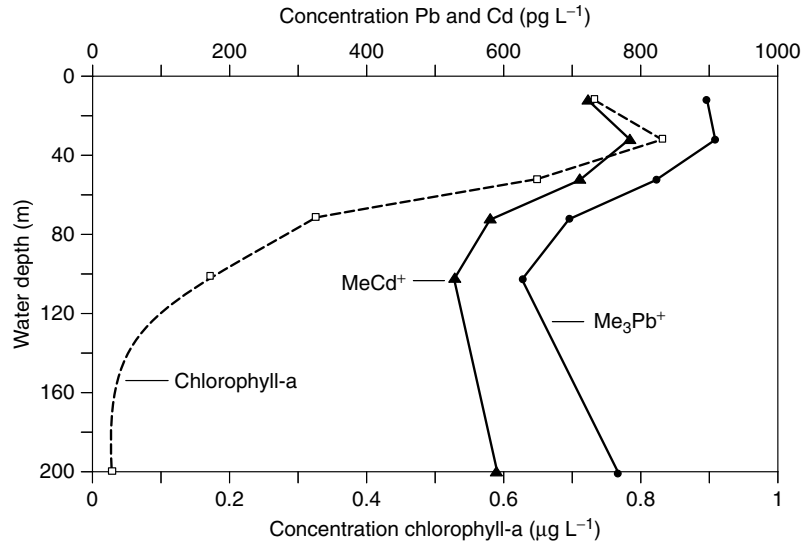

Figure 2.5.1.2. Concentration depth profile of trimethyllead, monomethylcadmium, and chlorophyll-a in the South Atlantic at 47°S, 15°W. (Reproduced from *Chemosphere*, 39, Pongratz, R. and Heumann, K. G., Production of methylated mercury and lead by polar macroalgae – a significant natural source for atmospheric heavy metals in clean room compartments, 89 (1999), with permission of Elsevier.)

gel electrophoresis under nondenaturing conditions [13] and gel filtration chromatography of prepared supernatants [14]. The electrophoretic and chromatographic properties of the detected cadmium-binding proteins were similar to MT used for comparison in both cases. In terrestrial snails taken from polluted land near an industrial complex, a cadmium-binding protein of molecular mass 22,000 Da was found [15]. In aquatic animals, proteins bound to cadmium were detected in worms [16] and zooplankton [17]. In amphipods from polar marine waters, the cytosolic bound cadmium was related to proteins in the molecular mass range of 18,000 Da. After centrifugation of the homogenates, 66% of the total cadmium was found in pellets and 34% in the cytosol. A combination of gel chromatography and flame AAS was applied to analyze the MT-like cadmium proteins [17].

1.4 Phytosystems

Cadmium compounds in vertebrates and fungi are detoxified by the MTs. In highly cadmium-contaminated plant cell cultures, the element was mainly complexed to the phytochelatin peptides. However, small amounts of cadmium were bound to proteins with a molecular mass of greater than 30,000 Da [18]. GPC with inductively coupled plasma mass spectrometry detection was developed for the speciation of cadmium complexes with oligopeptides, known to be biosynthesized by plants exposed to metal stress [19]. Kaneta, Hikichi, Endo, and Sugiyama investigated cadmium-treated rice plants with respect to the existing cadmium bonding states. The plant extracts were separated by GPC. By this method, three cadmium peaks were detected, one species representing an organic compound with a molecular mass of greater than 440,000 Da and another species with a molecular mass of 33,100 Da. The third peak included a cadmium-containing material with a molecular mass of 7000 Da and an inorganic cadmium salt [20]. Cadmium-binding complexes with an apparent molecular mass of 5600 Da were isolated from the roots of cadmium-contaminated rice plants. The purified cadmium species contained 44% cysteine and 39% glutamate and lacked in aromatic amino acids. Spectroscopic measurements indicated the presence of a cadmium-mercaptide bonding [21].

A cadmium-binding protein with a molecular mass of 3100 Da and a cysteine content of 40% was isolated from roots of maize [22]. Other cadmium-binding proteins from roots of tomato were partially characterized by using gel electrophoresis [23, 24]. Guenther and Umland investigated the cadmium species existing in leaves from unpolluted rape. Two cadmium elution ranges were detected in the cytoplasmic fraction, one cadmium species greater than 80,000 Da and two cadmium species with a molecular mass of 4400 Da. No relationship of one of the low-molecular mass cadmium species to the classes of phytochelatins or MTs could be stated [25]. Further cadmium-binding components were detected in pea [26] and soybean plants [27].

In the process of Rhizobium–faba bean symbiosis, two cadmium-binding protein complexes with molecular masses of 200,000 Da and 67,000 Da were formed by the nodules at higher levels of cadmium. This result was thought to be a mechanism by which Rhizobium–faba bean elevated resistance to cadmium toxicity [28]. By conducting gel chromatographic separation at pH 7.5, a cadmium-binding protein in algae was analyzed. This protein was suggested to be a dimer with a molecular mass of 6500 Da [29]. Roots of grass produced a MT-like protein when they were exposed to cadmium for seven days. To purify this protein with a molecular mass of 3700 Da, a combination of anion exchanger and gel filtration was used [30].

Tobacco plants were exposed to nonphytotoxic levels of cadmium to examine the role of the cadmium-binding peptides (CdBPs) in the tobacco leaves. For that, the protoplasts and vacuoles were isolated from leaves of cadmium-exposed seedlings to directly determine the localization of Cd and CdBPs. Thereby, it turned out that the purified vacuoles contained all of the CdBPs and cadmium found in protoplasts. Probably, the CdBPs were synthesized extravacuolarly [31]. A chromatogram of purified CdBPs is presented in Figure 2.5.1.3 and the amino acid composition of this compound is found in Table 2.5.1.1. Amino acid analysis showed that the main components were γ-(Glu-Cys)$_3$-Gly and γ-(Glu-Cys)$_4$-Gly.

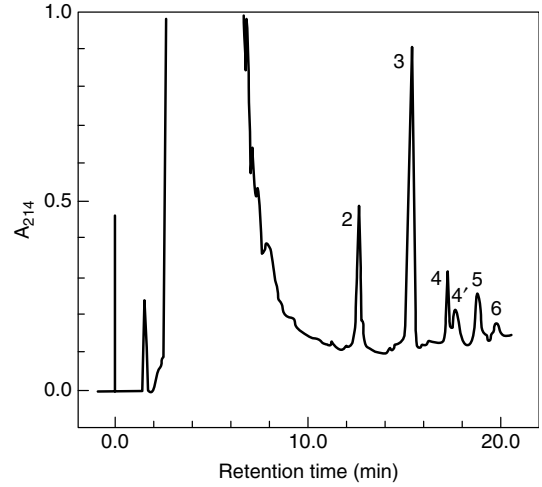

Figure 2.5.1.3. HPLC chromatogram of purified CdBPs (cadmium-binding peptides) from tobacco leaves after acidic extraction, gel filtration on Sephadex G-50, and lyophilization. Detection was in the UV range at 214 nm. Amino acid analysis represented in Table 2.5.1.1 showed that the predominant components in the system, peaks 2 and 3, consisted only of three amino acids, cysteine, glutamate/glutamine, and glycine. Peaks 2 and 3 were identified as γ-(Glu-Cys)$_3$-Gly and γ-(Glu-Cys)$_4$-Gly, respectively. (Reproduced from Reference [31] by permission of American Society of Plant Biologists.)

Table 2.5.1.1. Amino acid composition of purified cadmium-binding peptides from tobacco leaves.

Amino acid	Amino acid composition (residue %)				
	Peak 2	Peak 3	Peak 4	Peak 5	Peak 6
Cys	38.0	38.0	37.7	39.9	35.0
Asp/Asn	0.2	0.1	0.0	0.0	0.0
Thr	0.3	0.2	0.1	0.0	0.0
Ser	0.3	0.3	0.1	0.0	0.0
Glu/Gln	46.2	49.5	48.5	48.6	53.0
Pro	0.0	0.0	0.0	0.0	0.0
Gly	14.2	11.4	10.5	11.1	11.9
Ala	0.3	0.2	0.4	0.1	0.0
Val	0.0	0.0	0.4	0.1	0.1
Ile	0.1	0.0	0.1	0.0	0.0
Leu	0.1	0.0	0.1	0.0	0.0
Tyr	0.0	0.0	0.0	0.1	0.1
Phe	0.0	0.0	0.0	0.0	0.1
His	0.0	0.0	0.0	0.0	0.0
Lys	0.0	0.1	0.0	0.0	0.0
Arg	0.4	0.2	2.3	0.0	0.0
N	3	4	4	4	4

The results of this study suggested that these molecules might be involved in transport of Cd to the vacuole [31].

1.5 Soil and soil solutions

The investigation of the phytoavailability of cadmium in soils is very important to understand the mechanisms of trace metal uptake and transport by the plant root. The speciation of cadmium in soils was performed by using sequential extraction methods for dividing the particulate-bound cadmium into several fractions. Statistical data showed that the two fractions "exchangeable cadmium" and the "metal-fulvic acid-complex-bound cadmium" represented the plant-available cadmium fractions to a great extent [32]. Sequential chemical extraction procedures were applied to the speciation of cadmium in different soils and sediments [33–38]. Thereby, the respective matrices were incubated with special aqueous solutions, like magnesium nitrate solution for simply exchangeable cadmium ions or sodium acetate solution for carbonate-bound cadmium ions under determined conditions. The respectively extracted part of cadmium in the single solutions was analyzed.

In soil solutions, methods based on dialysis and ion exchange as well as special computer programs (e.g. GEOCHEM) to the elucidation of the cadmium-binding proportions were applied [39]. Different chromatographic methods such as exclusion and reversed-phase HPLC as well as ion-exchange chromatography were used to identify the various species of cadmium in the same matrices. Using ion-exchange chromatography, cadmium was found to be mainly in the form of inorganic cationic species, including the free ionic form, Cd^{2+}. Also, some organic and inorganic neutral species were detected, especially in soils of higher pH [40].

The activity of free Cd^{2+}, Zn^{2+}, and other ions in other soil solutions was determined by using a combination of the Donnan equilibrium and graphite furnace AAS method. The principal species of Cd and Zn in these matrices were free metal ions and hydrolyzed ions [41]. In contaminated soils containing between 0.1 and 38 mg Cd kg^{-1}, free Cd^{2+} activity in solution was determined by the use of DPASV, assuming DPASV was sensitive to easily dissociated inorganic ion-pairs and free Cd^{2+} ions while excluding organic complexes [42]. Otto, Carper, and Larive found that Cd^{2+} ions were predominantly bound to the oxygen-containing functional groups of the fulvic acids investigated using cadmium-113 nuclear magnetic resonance spectroscopy. These results are environmentally important because soil and aquatic fulvic acids affect the bioavailability and transport of metal ions [43]. In Figure 2.5.1.4, a well-characterized soil fulvic acid is represented. It contains a mixture of phenol-carboxylate polyelectrolytes and has a molecular mass of about 1000 Da. Light scattering data emphasized the polydisperse character of this mixture. The equilibrium behavior of metal ion binding by this matrix was examined theoretically and experimentally [44].

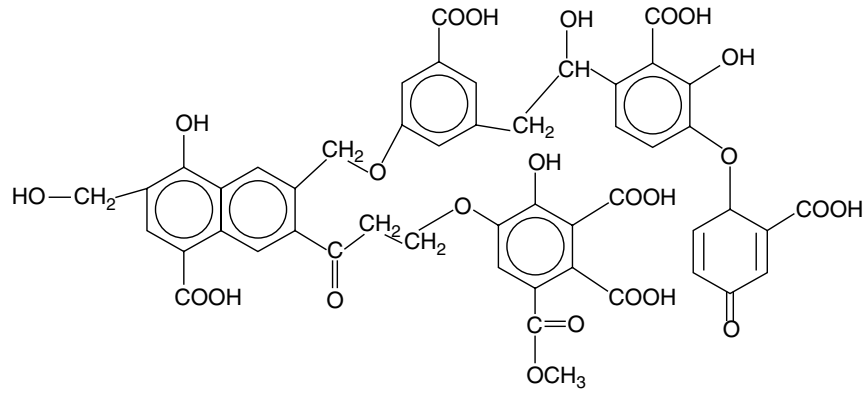

Figure 2.5.1.4. A speculative sketch of a plausible component of a soil fulvic acid mixture. (Reproduced from Reference [44] by permission of Wiley-VCH.)

2 FOOD

It is very important to investigate the effects of long-term, low-level cadmium exposure in the human organism to validate existing risk assessment procedures. The bioavailability and intestinal absorption of cadmium is predominantly determined by the available cadmium-binding forms in food [45]. Therefore, it is urgently demanded to investigate the cadmium species especially in these matrices.

As about 70% of the cadmium intake by human beings can be ascribed to vegetable foodstuffs, it is rather important to investigate the existing cadmium species right in this food category [46]. Many of the examined plants were not analyzed with regard to their eatable parts. For example, in rice [47], pepper [48], and wheat plants [49], the cadmium species in roots were analyzed. Therefore, the results obtained have little significant meaning to questions of nutrition science.

2.1 Fruit and vegetables

Also in the past, the cadmium-binding forms in eatable parts of plants were investigated. For example, in cabbage leaves a cadmium-binding complex with a molecular mass of 10,000 Da was discovered [50, 51]. In other studies, systematical investigations on the cadmium-binding states of several vegetable foodstuffs were realized. The plants were subjected to liquid shearing by treatment with an electrical dispersant (ultra-turrax) in buffer. After that, the centrifugation of the resulted homogenates and the separation in supernatants (cytosols) and pellets followed. After an acid digestion, the cadmium contents of the cytosol and pellet fractions were determined. By this procedure, the distribution of cadmium between the cytosol phase and the solid components of the plant cell was investigated [52, 53]. By this so-called initial step of element speciation [54], consequently, it turned out which percentage of cadmium could be further characterized by GPC. As an example, the percentages of cadmium in the cytosols of 20 commercial vegetable foodstuffs are represented in Figure 2.5.1.5 after the application of the sample preparation above-mentioned. The values obtained range from 28 to 87%. In most plants, the cytosol parts range from 37 to 75%. Very high percentages of cadmium in the cytosol were found in paprika with about 90%. From these results, the authors concluded that nearly all of the cadmium in this foodstuff could be submitted to a speciation analysis [53, 55].

Further characterization of 17 vegetable cytosols by using GPC revealed that cadmium mainly occurred as species of greater than 30,000 Da. In lettuce, paprika, carrot, and Jerusalem artichoke, small amounts of cadmium species with a molecular mass of less than 5000 Da were present. In Chinese cabbage, 100% of the cadmium species were eluted in the range of less than 5000 Da shown in Figure 2.5.1.6 [53].

In order to elucidate the cadmium species in contaminated vegetables, radish and spinach plants were treated with different amounts of cadmium. The eatable parts of these plants were homogenized in a buffer and centrifuged. Cadmium in the resulted fractions was analyzed by graphite furnace AAS [46]. The percentage of cadmium in the cytosol fractions ranged from 28 to 38% for spinach and was about 80% for radish. The resulted cytosols were separated on a Sephacryl S-400 GPC column [46]. In Figure 2.5.1.7, it is obvious that there are two cadmium elution ranges for all spinach groups with an elution maximum of about 200,000 Da for the high molecular mass species. The high molecular mass (150,000–700,000 Da) and the low molecular mass cadmium species ($<$150,000 Da) in all plant cytosols eluted at about the same retention volume by using GPC [46]. Nearly identical results were obtained for the radish cytosols. It was verified that the high molecular mass Cd species in both vegetables were cadmium proteins [46].

The GPC fractions of the high molecular mass Cd species of both plants investigated were further separated by a preparative native continuous polyacrylamide gel electrophoresis (PNC-PAGE) method [46]. The detected cadmium species of both plants showed a very similar elution behavior in all cytosols analyzed. Therefore, it was supposed that the high molecular mass cadmium

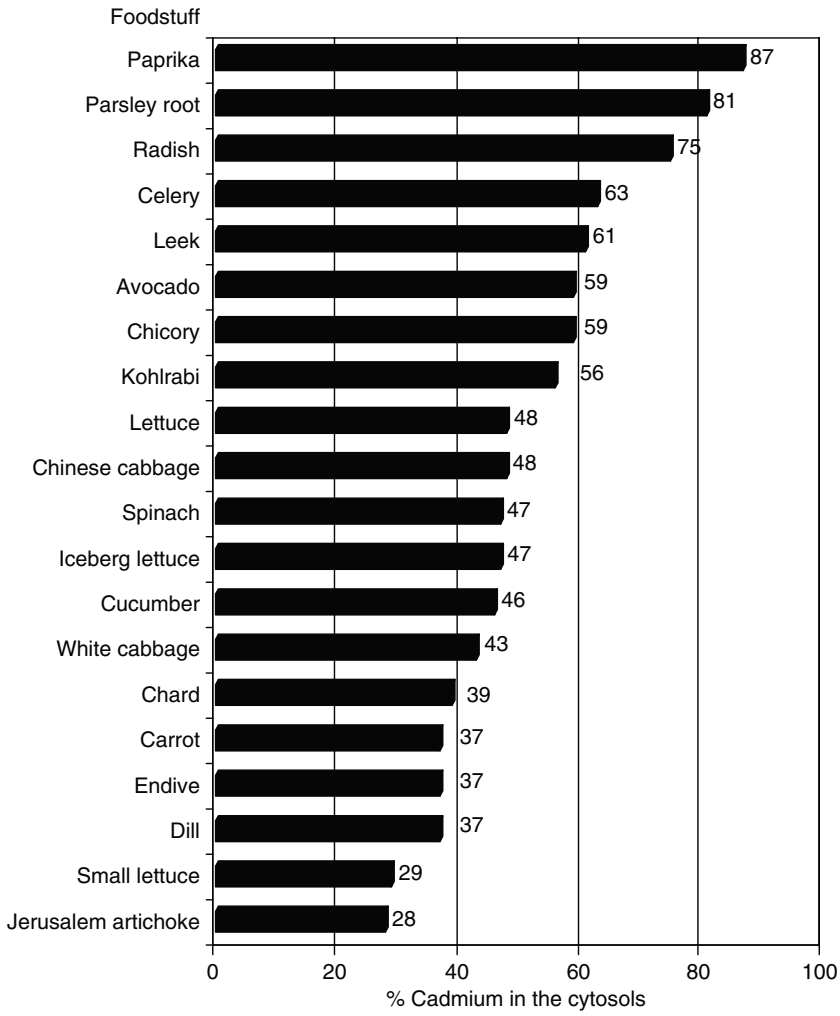

Figure 2.5.1.5. Percentual cadmium in the cytosols (supernatants) of commercial vegetable foodstuffs after ultra-turrax treatment in buffer and centrifugation of the homogenates obtained. The soluble parts are now available to a further speciation analysis. (Reproduced from References [53, 55] by permission of Springer Verlag GmbH & Co KG.)

species of the two different vegetable foodstuffs have a very similar chemical structure [46]. It is very interesting that in the model plant *Arabidopsis thaliana*, cadmium proteins of a similar size range, compared to the high molecular mass cadmium species available in spinach and radish, were detected by using a combination of GPC, PNC-PAGE, and electrothermal atomic absorption spectrometry (ET-AAS) [56].

In native lettuce, the majority of cadmium was bound to a low molecular mass protein of about 3200 Da and to a high molecular mass protein of more than 75,000 Da by using a combination of ultra-turrax homogenization in buffer and subsequent ultracentrifugation and gel filtration of the cytosol [57, 58].

2.2 Legumes and rice

In soybeans harvested in the region where the well-known "Itai–Itai" disease broke out, cadmium species of more than 100,000 Da were detected

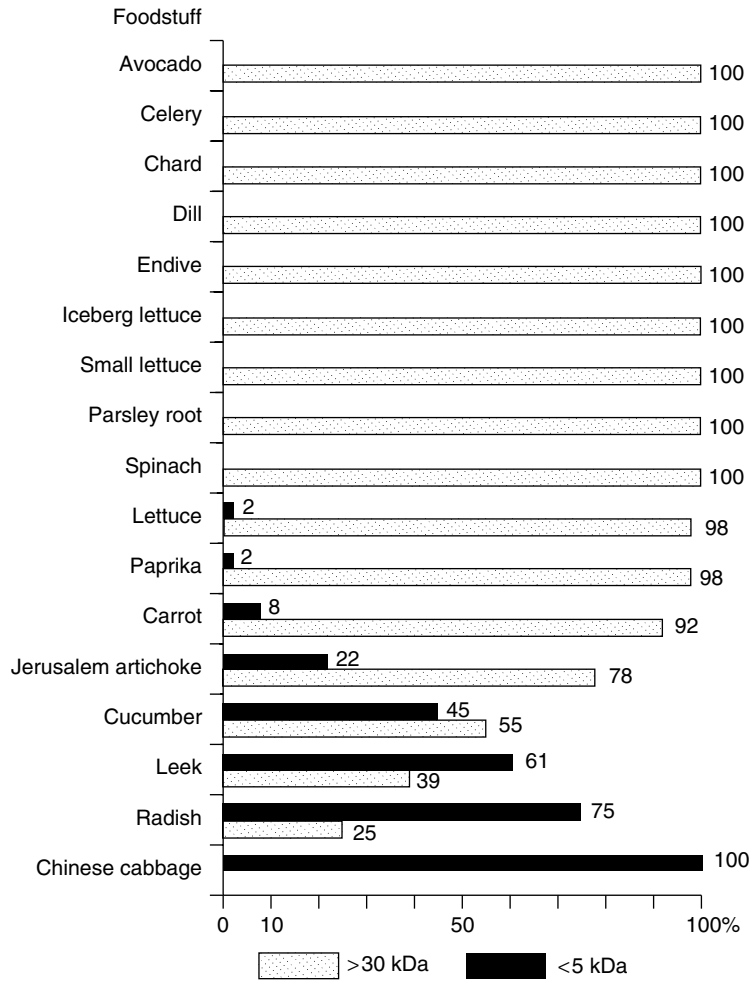

Figure 2.5.1.6. Distribution of the cadmium recovered on low molecular mass (<5000 Da) and high molecular mass (>30,000 Da) species in the cytosols of vegetable foodstuffs after cell breakdown, centrifugation, and gel permeation chromatography on Sephadex G-50. (Reproduced from Reference [53] by permission of Forschungszentrum Juelich GmbH.)

and served as a basis for the toxicological evaluation of the element in food [59–61]. The speciation analysis of cadmium was carried out after extraction by the coupling of liquid chromatographic methods with element analytical procedures in the on-line-mode. In other soybeans harvested from soil treated with cadmium-containing sewage sludge, cadmium species of more than 50,000 Da were analyzed [62]. Another study concerning the bioavailability of metal compounds in food revealed that cadmium in rice grains existed as an insoluble complex with phytic acid and protein by using gel filtration chromatography [63]. After an extraction of polished rice grains grown in cadmium-contaminated rice fields, cadmium was mostly bound to glutelin in soluble fractions. This compound was analyzed by HPLC with on-line detection by inductively coupled plasma mass spectrometry [64]. Bean fruits were investigated by a combined ultra- and diafiltration technique for use in speciation analysis of protein-bound cadmium in plants. The cadmium species detected by these methods were present mainly in the molecular mass range of greater than 30,000 Da [65].

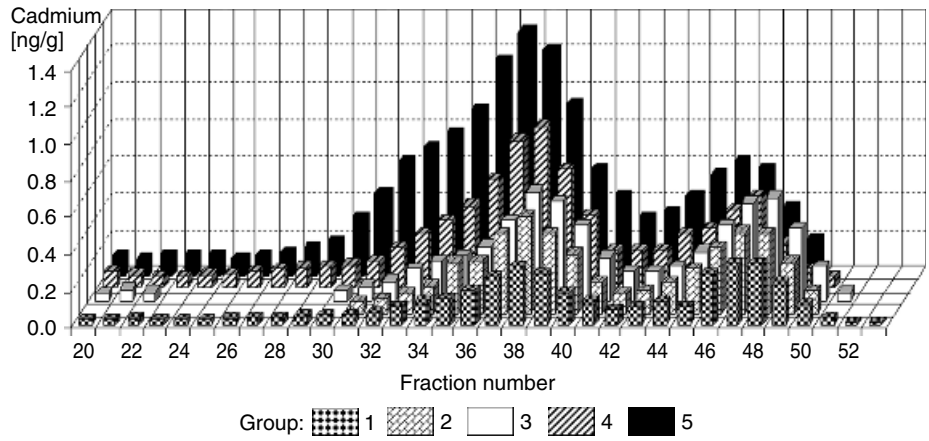

Figure 2.5.1.7. The Cd distributions in uncontaminated (1) and contaminated (2–5) spinach cytosols are shown. Plant groups 2 to 5 were each contaminated with four different amounts of cadmium. The cytosols were separated by Sephacryl S-400 S gel permeation chromatography. The most important Cd-binding form in the cytosols of all spinach plants examined was found to be high molecular weight Cd species (fractions 32–40). The Cd elution maxima were detected in the range of about 200 kDa (fraction 37). (Reproduced from Reference [46] by permission of Springer Verlag GmbH & Co KG.)

2.3 Cereals

A major dietary source of cadmium are cereals [45]. In wheat, three to four cadmium-containing substances were eluted in the range of 4000 to >100,000 Da using GPC [66, 67]. General considerations on cadmium species and other metal-binding forms in corn and cereals were published by Brueggemann and Ocker [68, 69].

2.4 Yeast

In brewers' yeast, *Saccharomyces cerevisiae*, a cadmium-binding protein of 9000 Da, was analyzed. The characteristics of MTs for this protein were proved, and thus these molecules were expected to play a role in cadmium-resistance. The cadmium compound was purified by gel permeation and subsequent ion-exchange column chromatography [70]. Another cadmium-binding protein with a molecular mass of 8000 Da was found in the same organism [71].

2.5 Mushrooms

In the mushroom *Agaricus bisporus*, no MT-like components were detected by applying a combination of gel filtration, ion-exchange, and affinity chromatography [72]. In a cadmium-accumulating mushroom, *Agaricus macrosporus*, a Cd-binding phosphoglycoprotein with a molecular mass of 12,000 Da was isolated. This compound was proposed to bind cadmium by its phospherine groups and furthermore, it was not related to MT [73]. Kruse and Lommel found two cadmium-containing protein fractions in the mushroom *Agaricus arvensis Schff. ex Fr.* with molecular masses of 2000 and 15,000 to 20,000 Da [74].

2.6 Shellfish

In marine animals, mainly the common mussel *Mytilus edulis* was investigated [75–77]. Mussel cytosols were purified by GPC [75–77], revealing cadmium-binding proteins with two molecular masses [75, 76]. Each of the two proteins was further resolved into four subcomponents by ion-exchange chromatography. As a result, small cytosolic cadmium amounts were bound to macromolecules of more than 50,000 Da [75, 76]. Metallothionein-like proteins of the common mussel from natural populations were characterized and partially purified. For that purpose, different coupling techniques consisting of inductively

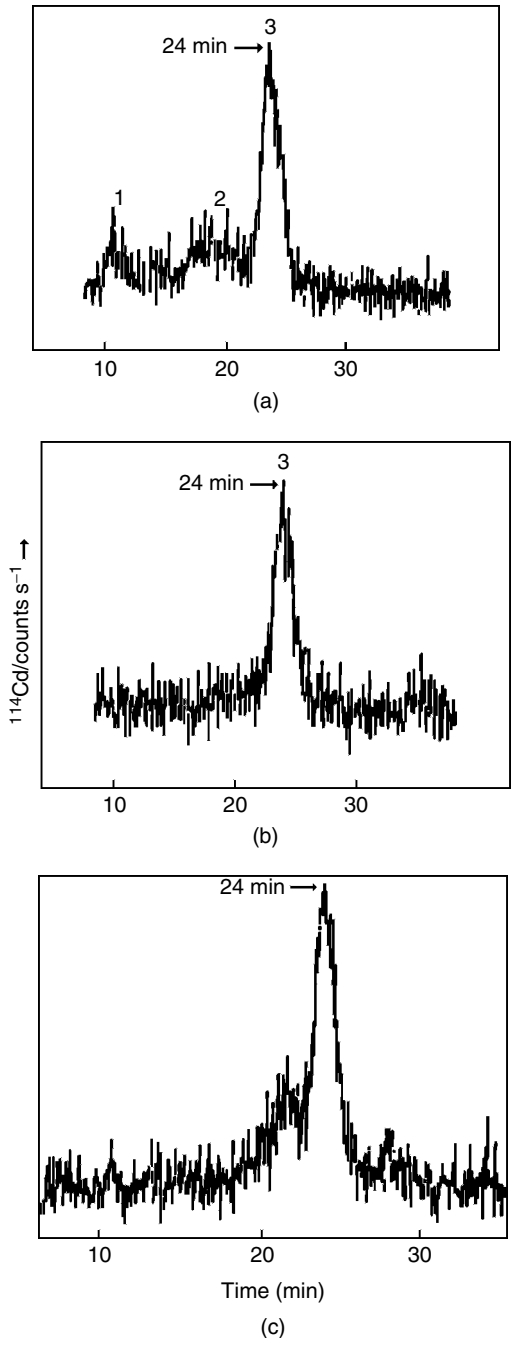

Figure 2.5.1.8. HPLC – ICP mass spectra of the cadmium species from (a) uncooked and (b) cooked pig kidney; (c) equine renal MT (metallothionein). 1, 2, and 3 are high molecular, medium molecular and low molecular mass ^{114}Cd-containing peaks, respectively. (Reproduced from Reference [82] by permission of Royal Society of Chemistry.)

coupled plasma mass spectrometry (ICP-MS) and fast protein liquid chromatography were applied [77]. Oyster extracts were also separated by GPC. In the resulted fractions corresponding to a high molecular mass protein that was heat labile, cadmium and zinc could be detected [78]. In another study, the Cd-binding proteins in American oysters were investigated after exposing these animals to Cd concentrations in a flowing seawater system [79].

2.7 Meat

Predominantly liver and kidney are the critical target organs for cadmium toxicity and accumulation in organisms. Consequently, some methods for characterizing chemical forms of trace metals in animal liver were provided. Metal speciation was applied by a combination of supercritical fluid extraction with on-line detection by AAS [80]. On simulated gastric digestion of cooked pig kidney, all of the cadmium present in solution eluted as one peak that corresponded to ionic cadmium. A subsequent simulated intestinal digestion of the gastric digest under neutral conditions proved that the retention time for the whole cadmium corresponded to that of MT. The authors concluded that the metal had dissociated from the MT binding sites under the acidic conditions and was rebound at pH 7 [81].

In a study of Crews, Dean, Ebdon, and Massey, cooked and uncooked pig kidney was compared

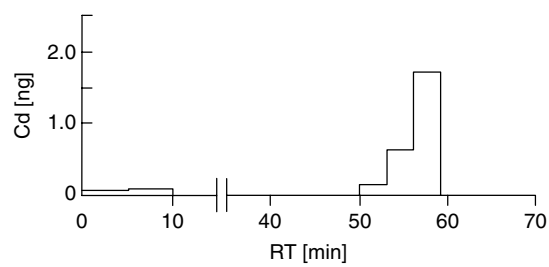

Figure 2.5.1.9. Concentrations of Cd in HPLC fractions of breast milk after sample pretreatment. The collected "MT-fractions" (56–59 min) were run on isoelectric focusing as shown in Figure 2.5.1.10. (Reproduced from Reference [83] by permission of Walter de Gruyter GmbH & Co KG.)

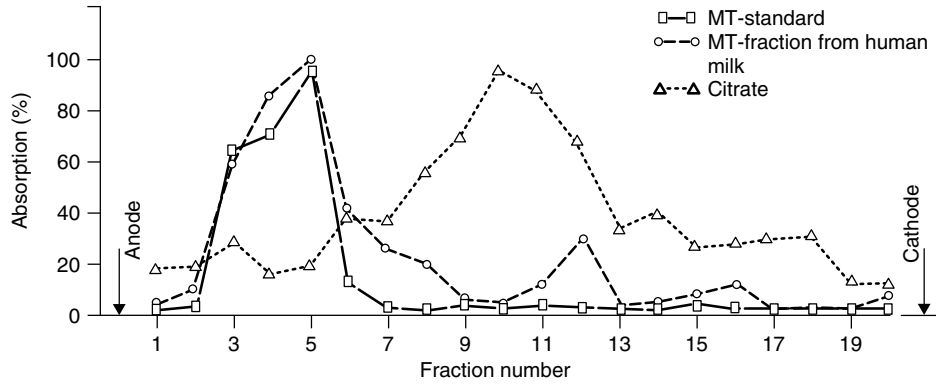

Figure 2.5.1.10. Distribution profile of MT (metallothionein)-standard, accepted MT-fraction (56–59 min, Figure 2.5.1.9) obtained from human milk and citrate in an isoelectric focusing cell. In the resulted electropherogram, good correspondence was obtained by comparing the MT-fraction from human milk with that of the MT-standard. Therefore, cadmium occurring in breast milk is predominantly present as cadmium-metallothionein species. (Reproduced from Reference [83] by permission of Walter de Gruyter GmbH & Co KG.)

with respect to the investigation of cadmium species in these matrices. By a combination of HPLC and inductively coupled plasma mass spectrometry, it was found that the majority of soluble cadmium in retail pig kidney was bound to a MT-like protein that was heat stable and that survived *in vitro* gastrointestinal digestion. In uncooked kidney, three peaks corresponding to molecular masses of 1,200,000 Da, 70,000 Da and 6000 to 9000 Da were detected after aqueous extraction [82]. The small amount of the high molecular and the medium molecular mass cadmium species from this matrix was presumably rendered insoluble during cooking. In Figure 2.5.1.8, mass spectra of the cadmium species of uncooked and cooked pig kidney and equine renal MT are presented. In all cases, the same retention time (24 min) for the low molecular mass cadmium species (6000 to 9000 Da) were measured [82].

2.8 Milk

For the elucidation of the cadmium-binding forms in human milk, a combination of high performance liquid chromatography (HPLC) and voltammetry was applied. The determination of the cadmium in the single HPLC fractions followed after a nitric acid digestion by DPASV [83]. The cadmium elution time was in accordance with the retention of the MT-standard (57 min) verified by this method. In Figure 2.5.1.9, the elution profile of cadmium from human milk is shown. The resulted fraction with the highest cadmium content (57 min), an MT-standard and citrate, were further separated by isoelectric focusing and the following distribution profiles of standards and sample were compared to each other [83]. As a result, in Figure 2.5.1.10 it is shown that good correspondence was achieved between the MT-standard and the accepted "MT-fraction" from human breast milk. Michalke and Schramel concluded that cadmium occurring in human milk was mainly available as MT. Furthermore, as represented in Figure 2.5.1.10, it could be shown that cadmium was not associated with the known zinc binding factor citrate although there is a chemical relationship between Cd and Zn. Both elements are bound to completely different biomolecules in human milk [83] and also in the most vegetable food [53].

3 REFERENCES

1. Lam, M. T., Murimboh, J., Hassan, N. M. and Chakrabarti, C. L., *Electroanalysis*, **13**, 94 (2001).
2. Lam, M. T., Chakrabarti, C. L., Cheng, J. and Pavski, V., *Electroanalysis*, **9**, 1018 (1997).
3. Pei, J., Tercier-Waeber, M.-L. and Buffle, J., *Anal. Chem.*, **72**, 161 (2000).

4. Kozelka, P. B. and Bruland, K. W., *Mar. Chem.*, **60**, 267 (1998).
5. Xue, H. and Sigg, L., *Anal. Chim. Acta*, **363**, 249 (1998).
6. Helmers, E., *Fresenius' J. Anal. Chem.*, **350**, 62 (1994).
7. Pongratz, R. and Heumann, K. G., *Anal. Chem.*, **68**, 1262 (1996).
8. Pongratz, R. and Heumann, K. G., *Chemosphere*, **39**, 89 (1999).
9. Florence, T. M., Morrison, G. M. and Stauber, J. L., *Sci. Total Environ.*, **125**, 1 (1992).
10. Takatera, K. and Watanabe, T., *Anal. Sci.*, **8**, 469 (1992).
11. Capasso, C., Nazzaro, F., Marulli, F., Capasso, A., La Cara, F. and Parisi, E., *Res. Microbiol.*, **147**, 287 (1996).
12. Khazaeli, M. B. and Mitra, R. S., *Appl. Environ. Microbiol.*, **41**, 46 (1981).
13. Ramseier, S., Deshusses, J. and Haerdi, W., *Mol. Cell. Biochem.*, **97**, 137 (1990).
14. Suzuki, K. T., Yamamura, M. and Mori, T., *Arch. Environ. Contam. Toxicol.*, **9**, 415 (1980).
15. Cooke, M., Jackson, A., Nickless, G. and Roberts, D. J., *Bull. Environ. Contam. Toxicol.*, **23**, 445 (1979).
16. Demuynck, S. and Dhainaut-Courtois, N., *Comp. Biochem. Physiol.*, **106C**, 467 (1993).
17. Ritterhoff, J. and Zauke, G.-P., *Mar. Environ. Res.*, **45**, 179 (1998).
18. Grill, E., Winnacker, E.-L. and Zenk, M. H., *Science*, **230**, 674 (1985).
19. Vacchina, V., Polec, K. and Szpunar, J., *J. Anal. At. Spectrom.*, **14**, 1557 (1999).
20. Kaneta, M., Hikichi, H., Endo, S. and Sugiyama, N., *Environ. Health Perspect.*, **65**, 33 (1986).
21. Obata, H. and Umebayashi, M., *Soil Sci. Plant Nutr.*, **32**, 461 (1986).
22. Rauser, W. E. and Glover, J., *Can. J. Bot.*, **62**, 1645 (1984).
23. Bartolf, M., Brennan, E. and Price, C. A., *Plant Physiol.*, **66**, 438 (1980).
24. Lue-Kim, H. and Rauser, W. E., *Plant Physiol.*, **81**, 896 (1986).
25. Guenther, K. and Umland, F., *Fresenius' Z. Anal. Chem.*, **331**, 302 (1988).
26. Gruenhage, L., Weigel, H.-J., Ilge, D. and Jaeger, H.-J., *J. Plant Physiol.*, **119**, 327 (1985).
27. Casterline, J. L. Jr., and Barnett, N. M. *Plant Physiol.*, **69**, 1004 (1982).
28. El-Enany, A.-W. E. and Abd-Alla, M. H., *Phyton*, **35**, 45 (1995).
29. Hart, B. A. and Bertram, P. E., *Environ. Exp. Bot.*, **20**, 175 (1980).
30. Rauser, W. E., *Plant Physiol.*, **74**, 1025 (1984).
31. Voegeli-Lange, R. and Wagner, G. J., *Plant Physiol.*, **92**, 1086 (1990).
32. Krishnamurti, G. S. R. and Naidu, R., *Aust. J. Soil Res.*, **38**, 991 (2000).
33. Krishnamurti, G. S. R., Huang, P. M., Van Rees, K. C. J., Kozak, L. M. and Rostad, H. P. W., *Analyst*, **120**, 659 (1995).
34. Ho, M. D. and Evans, G. J., *Anal. Commun.*, **34**, 363 (1997).
35. Ramachandran, V. and D'Souza, T. J., *Chem. Spec. Bioavail.*, **9**, 121 (1997).
36. Krishnamurti, G. S. R., Huang, P. M., Kozak, L. M., Rostad, H. P. W. and Van Rees, K. C. J., *Can. J. Soil Sci.*, **77**, 613 (1997).
37. Davidson, C. M., Wilson, L. E. and Ure, A. M., *Fresenius' J. Anal. Chem.*, **363**, 134 (1999).
38. Benitez, L. N. and Dubois, J.-P., *Int. J. Environ. Anal. Chem.*, **74**, 289 (1999).
39. Holm, P. E., Andersen, S. and Christensen, T. H., *Water Res.*, **29**, 803 (1995).
40. Tills, A. R. and Alloway, B. J., *J. Soil Sci.*, **34**, 769 (1983).
41. Wu, Q., Hendershot, W. H., Marshall, W. D. and Ge, Y., *Commun. Soil Sci. Plant Anal.*, **31**, 1129 (2000).
42. Sauve, S., Norvell, W. A., McBride, M. and Hendershot, W., *Environ. Sci. Technol.*, **34**, 291 (2000).
43. Otto, W. H., Carper, W. R. and Larive, C. K., *Environ. Sci. Technol.*, **35**, 1463 (2001).
44. Langford, C. H., Gamble, D. S., Underdown, A. W. and Lee, S., Interaction of metal ions with a well characterized fulvic acid, in *Aquatic and Terrestrial Humic Materials*, Christman, R. F. and Gjessing, E. T. (Eds.), Ann Arbor Science, Ann Arbor, MI, 1983, Chapter 11, pp. 219–237.
45. Crews, H. M., *Spectrochim. Acta B*, **53**, 213 (1998).
46. Guenther, K., Ji, G. and Kastenholz, B., *Fresenius' J. Anal. Chem.*, **368**, 281 (2000).
47. Shah, K. and Dubey, R. S., *J. Plant Physiol.*, **152**, 448 (1998).
48. Jemal, F., Didierjean, L., Ghrir, R., Ghorbal, M. H. and Burkard, G., *Plant Sci.*, **137**, 143 (1998).
49. Hart, J. J., Welch, R. M., Norvell, W. A., Sullivan, L. A. and Kochian, L. V., *Plant Physiol.*, **116**, 1413 (1998).
50. Wagner, G. J., *Plant Physiol.*, **76**, 797 (1984).
51. Wagner, G. J. and Trotter, M. M., *Plant Physiol.*, **69**, 804 (1982).
52. Guenther, K. and Waldner, H., *Anal. Chim. Acta*, **259**, 165 (1992).
53. Guenther, K., *Contributions to Multielemental Speciation Analysis in Vegetable Foodstuffs: Investigations on the Binding Forms of Many Elements with Special Regard to Zinc and Cadmium*, Reports of the Research Centre Juelich 3358, ISSN 0944–2952, Juelich (1997).
54. Guenther, K., von Bohlen, A. and Strompen, C., *Anal. Chim. Acta*, **309**, 327 (1995).
55. Guenther, K. and Weber, G., Element speciation analysis: an overview, in *Analytiker-Taschenbuch*, Vol. 20, Guenzler, H., Bahadir, A. M., Danzer, K., Fresenius, W., Galensa, R., Huber, W., Linscheid, M., Schwedt, G. and Toelg, G. (Eds.), Springer, Berlin, Heidelberg, New York, 1998, pp. 71–103.
56. Kastenholz, B., *Anal. Lett.*, **37**, 657 (2004).
57. Henze, W. and Umland, F., *Anal. Sci.*, **3**, 225 (1987).
58. Henze, W. and Umland, F., Speciation of cadmium and copper in lettuce leaves, in *Trace Element Analytical*

Chemistry in Medicine and Biology, Vol. 4, Braetter, P. and Schramel, P. (Eds.), Walter de Gruyter & Co, Berlin, New York, 1987, pp. 501–507.
59. Yoshida, S., Tanaka, R. and Kashimoto, T., *J. Food Hyg. Soc. Jpn.*, **27**, 64 (1986).
60. Yoshida, S., *Agric. Biol. Chem.*, **50**, 2273 (1986).
61. Yoshida, S., Tanaka, R. and Kashimoto, T., *J. Food Hyg. Soc. Jpn.*, **26**, 511 (1985).
62. Casterline, J. L. Jr., and Yip, G. *Arch. Environ. Contam. Toxicol.*, **3**, 319 (1975).
63. Suzuki, T., Takeda, M. and Uchiyama, M., *J. Hyg. Chem.*, **23**, 345 (1977).
64. Suzuki, K. T., Sasakura, C. and Ohmichi, M., *J. Trace Elem. Med. Biol.*, **11**, 71 (1997).
65. Lange-Hesse, K., Dunemann, L. and Schwedt, G., *Fresenius' J. Anal. Chem.*, **339**, 240 (1991).
66. Brueggemann, J., *Getr. Mehl Brot*, **48**, 26 (1994).
67. Brueggemann, J., *Veroeff. Arbeitsgem. Getreideforsch.*, **248**, 93 (1993).
68. Brueggemann, J. and Ocker, H.-D., *Getr. Mehl Brot*, **42**, 108 (1988).
69. Brueggemann, J. and Ocker, H.-D., *Veroeff. Arbeitsgem. Getreideforsch.*, **213**, 98 (1988).
70. Inouhe, M., Hiyama, M., Tohoyama, H., Joho, M. and Murayama, T., *Biochim. Biophys. Acta*, **993**, 51 (1989).
71. Mangir, M. and Ehrlich, W., *Chemosphere*, **19**, 1261 (1989).
72. Esser, J. and Brunnert, H., *Environ. Pol. A*, **41**, 263 (1986).
73. Meisch, H.-U., Beckmann, I. and Schmitt, J. A., *Biochim. Biophys. Acta*, **745**, 259 (1983).
74. Kruse, H. and Lommel, A., *Z. Lebensm. Unters. Forsch.*, **168**, 444 (1979).
75. Frazier, J. M., *Environ. Health Perspect.*, **65**, 39 (1986).
76. Frazier, J. M., George, S. S., Overnell, J., Coombs, T. L. and Kagi, J., *Comp. Biochem. Physiol.*, **80C**, 257 (1985).
77. Ferrarello, C. N., de la Campa, M. D. F, Carrasco, J. F. and Sanz-Medel, A., *Anal. Chem.*, **72**, 5874 (2000).
78. Nordberg, M., Nuottaniemi, I., Cherian, M. G., Nordberg, G. F., Kjellstrom, T. and Garvey, J. S., *Environ. Health Perspect.*, **65**, 57 (1986).
79. Ridlington, J. W. and Fowler, B. A., *Chem.-Biol. Interact.*, **25**, 127 (1979).
80. Wang, J. and Marshall, W. D., *Anal. Chem.*, **66**, 3900 (1994).
81. McWeeny, D. J., Crews, H. M. and Massey, R. C., Speciation chemistry of foods – problems and prospects, *ACS Symposium Series*, Vol. 445, American Chemical Society, 1991, Chapter 19, pp. 248–256.
82. Crews, H. M., Dean, J. R., Ebdon, L. and Massey, R. C., *Analyst*, **114**, 895 (1989).
83. Michalke, B. and Schramel, P., *J. Trace Elem. Electrolytes Health Dis.*, **4**, 163 (1990).

2.5.2 Speciation of Cadmium in Health and Disease

Violaine Verougstraete

Université catholique de Louvain, Brussels, Belgium

1 INTRODUCTION

Various cadmium compounds have found their way into modern society [1–5]. In humans, uptake of cadmium may occur via the inhalation of contaminated air or the ingestion of food and drinking water. Workers may be exposed to the metal or its compounds present as fumes or dust in the air at the workplace. For the nonsmoking general population, food is generally the major source of exposure, the contribution from other pathways (ambient air, drinking water, ingestion of household dust) to total uptake being small. Tobacco smoke is an important additional source of cadmium uptake in smokers, as the plant naturally accumulates relatively high cadmium concentrations in its leaves.

2 METABOLISM OF CADMIUM

2.1 Absorption

2.1.1 Oral route

Most ingested cadmium species pass through the gastrointestinal tract without being absorbed and are eliminated in the feces (Figure 2.5.2.1). Observations in humans indicate that the average gastrointestinal absorption of cadmium is about 3–7% when no specific modifying factors are present. Main factors that potentially affect the absorption rate of the ingested cadmium include the type of cadmium compound, the composition of the diet, interactions with other trace elements in the diet (in particular zinc), iron status, and age [2, 5–8].

Little is known about the mechanism of uptake of the various forms of cadmium and on the transport across the epithelial cells in the intestine. Experimental systems trying to elucidate this have most frequently used high doses of cadmium salts (such as $CdCl_2$) perfused through jejunal loops without the normal intestinal contents. Uptake of ionic cadmium is reported to occur preferentially in the duodenum, where pH is low because of the emptying of the gastric contents into this part of intestine. Distal to the pancreatic duct, pH increases, and the cadmium is chelated by various dietary components and less available for intestinal uptake.

An *in vitro* experiment carried out by Iijima [9] has tested the solubility of various cadmium

Handbook of Elemental Speciation II: Species in the Environment, Food, Medicine & Occupational Health
Edited by R. Cornelis, H. Crews, J. Caruso and K. G. Heumann
 ISBN: 0-470-85598-3 (HB)

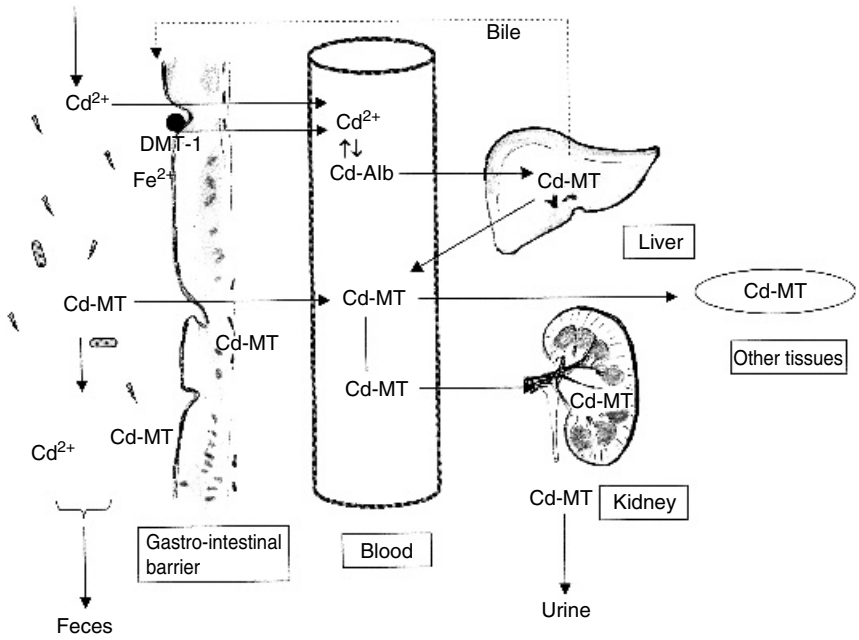

Figure 2.5.2.1. Absorption, distribution, and excretion of cadmium after exposure by the oral route: most of the ingested Cd is not absorbed and is directly eliminated in feces. The intestinal absorption of the Cd ion may proceed by simple diffusion and/or be mediated by a metal-ion transporter (DMT-1). Cd may be present in food as Cd-MT, and these complexes may be absorbed intact. In blood, absorbed Cd^{2+} binds to anionic groups of proteins such as albumin. Liver synthesizes MT that binds Cd^{2+}, and Cd-MT is released in bloodstream. Cd-MT is filtered by the renal glomerulus and may be reabsorbed by the proximal tubule cells. In humans, the main portion of the Cd body burden is found in liver, kidney, and other tissues where it is bound to MT. Absorbed Cd is eliminated from the body in feces and in urine.

compounds in artificial gastric and intestinal juices. The solubility in artificial gastric juice was reported to amount 72–94% for cadmium stearate, carbonate, and oxide. On the contrary, solubility in artificial intestinal juice was low for all tested compounds (2, 0.01, 0.1% for cadmium stearate, carbonate, and oxide, respectively).

It has been reported that metallothionein (MT), a low-molecular weight protein capable of binding as many as seven cadmium atoms per molecule, is usually the principal form of cadmium in foods from animal origin [10–12]. After exposure to such foodstuffs, cadmium may be present in the intestine lumen either as a complex with MT (Cd-MT) or with other dietary constituents. If these complexes are stable at low pH, they are not preferentially absorbed in the duodenum.

Experimental studies have indicated that Cd-MT complexes may be absorbed intact by the intestine, but data on the rate of absorption are contradictory: studies in animals given a single oral dose of cadmium in the form of Cd-MT or $CdCl_2$ have indicated similar absorption of both forms of cadmium, although differences were observed in the tissue distribution, with Cd-MT being distributed preferentially to the kidneys. On the other hand, when animals were given Cd-MT with the diet or via a gastric tube for several weeks, the concentrations of cadmium in liver and kidney were consistently lower than in animals exposed to similar doses of $CdCl_2$, indicating a lower absorption of Cd-MT [13].

Experiments conducted in rats have suggested that the ingested cadmium taken up by the mucosal cells is bound to MT directly in the mucosa. One part of this MT-bound cadmium will be absorbed, whereas the other part will be sequestered for several days and eliminated in feces by desquamation of the mucosal cells [14, 15].

Recently, some of the factors that contribute to metal homeostasis at the molecular level have been identified and appear to include proteins that mediate the import of metals from the extracellular environment, such as the metal-ion transporter DMT1 (also known as *NRAMP2* or *DCT1*). Located in the apical membrane of the enterocytes, this protein is considered to be a major cellular uptake mechanism for the dietary iron ion in the duodenum but appears to also mediate the active cellular uptake of the zinc, manganese, copper, cobalt, nickel, cadmium, and lead divalent ions. The existence of a common mechanism of uptake for a wide range of metals implicates that a potential interplay among these elements may occur at their absorption level [16, 17].

The influence on absorption of the type of diet and deriving from it, of the chemical complexation of cadmium in the ingested food, has been evaluated both in experimental systems and in volunteers. In most of these studies, the cadmium content in diet, blood, urine, or in feces was analyzed either by flame-atomic absorption spectrometry (flame-AAS) or by graphite furnace atomic absorption spectrometry (GFAAS). Experimentally, the bioavailability of cadmium from boiled crab hepatopancreas, in which cadmium is mainly associated with denaturated proteins of low solubility, was reported to be slightly lower than from inorganic cadmium ($CdCl_2$) [18]. In human volunteers who ingested hepatopancreas labeled with radioactive cadmium chloride, whole-body retention was only slightly lower than the values obtained using dissolved cadmium ions (1.2–7.6 vs 4.6–6%) [5, 19, 20]. Dietary intake and uptake of cadmium in nonsmoking women consuming either a mixed diet low in shellfish or with shellfish once a week or more were compared by Vahter *et al*. [13]. The shellfish diet contained twice as much cadmium as the mixed diet. Cadmium in feces corresponded to 100 and 99% of that in shellfish and mixed diets, respectively, indicating both a low absorption of the dietary cadmium (<1%) and no significant difference in uptake despite the differences in the daily intake of cadmium. In two groups that consumed either a vegetarian/high-fiber diet or a mixed diet, fecal cadmium values were in the same range [21]. Overall, these results indicate that in general, cadmium absorption after ingestion of food from animal origin is not dependent on chemical complexation.

Contradictory results have been reported on the bioavailability of plant cadmium compared to inorganic Cd [12]. Experimental data showed that when rats were given either a soil polluted with cadmium or an equal amount of cadmium as $CdCl_2$, the relative oral bioavailability of soil-adsorbed cadmium appeared to be reduced more than twofold as compared to the inorganic cadmium. This suggests that the soil matrix may significantly reduce the absorption of cadmium in the gastrointestinal tract [22].

Beside the chemical complexation of cadmium in food, metal–metal interactions in the body and in food may affect cadmium gastrointestinal absorption. The presence of divalent and trivalent cations such as calcium, chromium, and magnesium in the jejunum lumen has been reported to decrease cadmium uptake in rats, possibly by a nonspecific effect on the charge distribution of the intestinal brush border membrane [23]. Zinc has been reported either to increase the amount of absorbed cadmium or to reduce it [24–28].

Effects of plant zinc on plant cadmium bioavailability have been investigated experimentally by McKenna *et al*. [12] and results indicated (a) that increased plant zinc lowered cadmium retention in kidney, liver, and jejuno-ileum of animals; (b) a lower bioavailability of cadmium from crops grown in zinc-cadmium contaminated sites compared with cadmium-only polluted sites if both metals were absorbed readily in edible plant tissues; (c) plant species differed in cadmium availability for identical concentrations of zinc and cadmium in edible tissues because of differences in plant speciation or plant components that may interfere with absorption in the animal gut, [12, 29–30]. In humans, blood cadmium levels (as a reflection of cadmium uptake) measured in oyster consumers and seal meat eaters were low compared to that in Japanese farmers with similar intakes from cadmium polluted rice (1–3 vs 7–62 $\mu g\,L^{-1}$) [31, 32]. The lower bioavailability of the cadmium from oysters compared to rice

might also be partially explained by differences in intake/status of iron and zinc. The higher absorption of cadmium from contaminated rice has, in particular, been attributed to the fact that rice excludes soil zinc from its grain, which allows increased cadmium exposures without any counteracting increase in food zinc. Cultures and crops such as wheat, lettuce, or others grown in Western countries do not seem to exclude zinc as rice does. Moreover, it has been shown that the iron remaining in polished rice has a very low bioavailability compared with iron in other foods. This may result in an inadequate supply of iron and influence the nutritional status in consumers of a diet where rice is the dominant food [30].

Studies in volunteers have also indicated that cadmium gastrointestinal absorption is significantly and positively influenced by a depleted iron body store. When a breakfast that contained around 25 μg labeled cadmium chloride was given to a group of 22 subjects of whom 66% of the female subjects had a low ferritin, average absorption was $8.9 \pm 2\%$ in 10 subjects with low body iron stores (ferritin $<20\ \mu g\,L^{-1}$) and $2.3 \pm 0.3\%$ in 12 subjects with normal iron stores ($>20\ \mu g\,L^{-1}$) [33]. In the study of Berglund *et al*. [21], a depleted iron store status was associated with, at most, a doubling of cadmium oral absorption. A possible explanation for the higher absorbed levels of cadmium in the case of iron depletion is the existence of a common mechanism of uptake for both elements. The depletion of iron is reported to upregulate the expression of DMT1, a transporter mainly responsible for the active uptake of iron in the mucosal cell but with some affinity for other divalent ions such as cadmium [16, 34].

No influence of age on gastrointestinal absorption of cadmium has been demonstrated in human studies. However, it has been demonstrated that suckling rats absorbed cadmium ($CdCl_2$) to a greater extent than adult rats (25.6% in one-week-old rats vs 7% in six-weeks-old animals on milk diet) [35, 36].

2.1.2 Inhalation route

After inhalation exposure, the amount of absorbed cadmium from the lung will be influenced by several factors, including the type of cadmium compound. In air, cadmium metal and salts exist primarily as fine suspended particulate matter. When inhaled, some fraction of this particulate matter (<10 μm) is deposited in the airways or the lungs and the rest is exhaled. After deposition, the uptake into lung epithelial cells, interstitium, or the systemic circulation depends on physical and biochemical processes in the respiratory tract such as clearance, solubilization, and transport. The deposition pattern of the particles is related to the particle density and size; the larger particles tend to be deposited in the upper part of the respiratory tract, whereas the smaller particles may reach the gas exchange area. Particle size and density may vary according to the compound in presence: for example, cadmium fumes, consisting mainly of cadmium oxide, have a small particle size (0.1 μm), but in an experiment conducted with cadmium sulfide, the median aerodynamic diameter was reported to be 3.1 μm [37]. Studies of the particle size distributions of cadmium in urban aerosols generally show that the metal is associated with particulate matter in the respirable range [2].

Another key determinant for the lung absorption is the solubility of the chemical species present in the respiratory system. Highly water-soluble salts such as chloride, acetate, nitrate, and sulfate would be expected to have the highest absorption; however, the pattern of absorption of the different cadmium compounds does not always correlate with solubility as defined with water as solvent [2, 5, 38, 39].

In 1973, the Task Group on Metal Accumulation [40] made estimates of the respiratory and total absorption after inhalation of an aerosol of a compound with a relatively low solubility, such as CdO. Assuming that ventilation is moderate, that the cadmium aerosol is deposited and cleared from the respiratory tract as are other particles in general and that the particles deposited on the ciliated epithelium will be entirely transferred to the gastrointestinal tract because of the low solubility, it can be estimated that respiratory absorption will vary between 2.5 and 50%, depending on particle size and alveolar deposition (50 or 100%) [40].

Several experimental studies have investigated the influence of speciation on lung absorption of cadmium after single or repeated inhalation exposure, mostly comparing a soluble chloride compound with a compound present either at the workplace (oxide, sulfate, ...) or in cigarette smoke (oxide). Cadmium content in lung tissues, in blood, in urine, or in feces was determined using AAS or GFAAS.

After single inhalation of CdO (dust or fumes), CdS, or $CdCl_2$ through an endotracheal tube, CdO dust exhibited a much longer pulmonary retention in the rat than CdO fumes. According to the authors of the study, this might be explained by the smaller particle size of CdO in fumes compared to dust. $CdCl_2$ and CdS were cleared from the lungs about three times as fast as CdO dust (retention half-time: about 70 days for $CdCl_2$ and CdS vs 215 days for CdO). In monkeys exposed to the same compounds, about 40–60%, >90% and <20% of the total lung cadmium could be lavaged 40 days after exposure to CdO, CdS, and $CdCl_2$, respectively [37, 41].

In rats and rabbits exposed to aerosols of $CdCl_2$ and CdO for two hours, a greater clearance of $CdCl_2$ (58%) than of CdO (46%) was observed, although both compounds had similar total deposition rates [42].

In rats exposed continuously during 30 days to submicron aerosols of $CdCl_2$, CdO (0.1 mg m^{-3}) or CdS (1 mg m^{-3}), most of the cadmium in the $CdCl_2$ and CdO-exposed groups was found in the lung cytosolic compartment, both at the end of the inhalation and after an additional two-month period in fresh air. However, the cadmium content of the lung homogenates, cytosols, and the lung cytosolic MT was found to be twice as much in CdO exposed rats compared to rats exposed to $CdCl_2$. The alveolar lavage analysis also indicated that inhaled CdO, despite a lower solubility, was more available to lung tissue than the soluble $CdCl_2$. In the group exposed to CdS, fecal excretion of cadmium was greater than after CdO exposure, reflecting a greater mucociliary clearance from the lung to the gastrointestinal tract and thus a lower absorption from the lung. Moreover, no detectable transfer of inhaled CdS to liver and kidney was found [38].

In humans, quantitative data on absorption after inhalation exposure to cadmium derive also from comparisons of uptake in smokers and nonsmokers. On the basis of the comparison of the cadmium body burdens, cadmium absorption from cigarette smoke appears to be higher than absorption of cadmium aerosols measured in animals [43].

The chemical form of cadmium in cigarette smoke is likely to be similar to that produced by other combustion processes, primarily cadmium oxide. The greater absorption of cadmium from tobacco smoke is likely due to the very small size of particles in cigarette smoke and the consequent high alveolar deposition [43]. According to Krajnc *et al*. [44], cadmium in ambient air is associated to particles of circa 1 to 2 μm, and a deposition of 20–30% can be assumed. Particles of cigarette smoke being much smaller, a deposition of 50% can be assumed for these particles. On the basis of data from autopsies, it was calculated that 67% of the deposited amount in the lung due to smoking is being absorbed and the same rate can be assumed for ambient air. Hence, Krajnc *et al*. calculated that 14% of the inhaled amount of cadmium from ambient air and 40% from cigarettes is being absorbed [44].

Overall, it is estimated that about 10% of the cadmium present in cigarettes (1–2 μg/cigarette) is inhaled and that 25–50% of the inhaled cadmium by the smokers is absorbed. Thus, smoking a pack of 20 cigarettes daily will result in a net uptake of 0.5–2 μg cadmium [2, 5, 45].

2.1.3 Dermal route

Available information suggests that cadmium is not well absorbed though the skin. Limited penetration of water-soluble cadmium compounds ($CdCl_2$) has been demonstrated when applied as a solution or as ointment to shaved skin of animals. Cadmium was also reported to accumulate in the skin as evidenced directly by the measurement of the element itself but also indirectly by the increased concentration of zinc in the skin, probably reflecting a local induction of MT [46].

No studies conducted in humans on the dermal absorption of the various cadmium compounds

were located. *In vitro*, the percutaneous absorption of cadmium from $CdCl_2$ in water and soil has been measured using human cadaver skin [47]. The bioavailability of ^{109}Cd mixed as the chloride salt with a sample of soil was low: skin penetration was between 0.6 and 0.13% of the applied dose (analysis of the radioactivity by scintillation counting). Application of a water solution of ^{109}Cd resulted in the penetration of about 10% of the applied dose into the skin fragment after 16 h and about 0.5% absorption in the plasma. An additional experiment was carried out to simulate exposure that would be comparable with a swim or bathing by exposure of human skin to $CdCl_2$ in water during 30 min. After 30 min, about 2% of the applied dose was measured in the skin and no cadmium was found in the plasma receptor fluid. These results are, however, not directly extrapolative to other cadmium compounds that may be markedly less water-soluble than the chloride compound.

Following absorption, cadmium is mainly present in the organism as Cd^{2+} ions and the biodisposition of cadmium as ion is assumed to be independent of the chemical form to which exposure occurred.

2.2 Distribution

Once absorbed, cadmium is widely distributed and retained in the body where it accumulates throughout life. Hence, the body burden increases because of the continuous exposure, and the element has a biological half-life of about 20 years. While the newborn baby has a total body burden of less than 1 μg of cadmium, the average total body burden at age 50 has been estimated to range from 5 to 30 mg. After long-term low-level exposure, about half the body burden of cadmium is localized in the kidneys and liver, a third of the total being in the kidneys, with the major portion located in the cortex. The distribution of cadmium in the kidney is of particular importance, as this organ is a critical target after long-term exposure. The ratio between the cadmium concentration in the kidney and that in the liver decreases with the intensity of exposure. High renal burdens have been found in cadmium-exposed workers without functional renal impairment (up to 450 or even 600 $mg\,kg^{-1}$ ww tissue). In nonoccupationally exposed subjects, the cadmium concentration in the kidneys is generally between 10 and 50 $mg\,kg^{-1}$ ww (two- to fivefold increase in smokers) [2, 48, 49].

In blood, most cadmium is found in the erythrocytes (about 90%). The measured value of cadmium in blood is generally below 3 $\mu g\,L^{-1}$ in European subjects not occupationally exposed to cadmium. Concentrations in the order of 5 to 10 $\mu g\,L^{-1}$ are extremely rare, unless in heavily contaminated areas [2, 32]. Reported cadmium concentrations in the blood of exposed workers are generally between 5 and 50 $\mu g\,L^{-1}$, but levels between 100 and 300 $\mu g\,L^{-1}$ have resulted from extreme exposure [50–52]. As tobacco smoking is an additional source of cadmium intake in the general population, values for cadmium in blood are two- to fivefold higher in smokers than in nonsmokers.

Cadmium does not appear to undergo any direct metabolic conversion, such as oxidation, reduction, or alkylation. The Cd^{2+} ion binds to anionic groups in proteins and other molecules [5]. The sulfhydryl groups in albumin and MT have a particularly high affinity for the cadmium ion. In all tissues, cadmium is bound mainly to MT whose production is stimulated by cadmium exposure and also by other metals such as zinc, copper, and mercury. Exact physiologic functions of MT are not known, but it is thought to play an important role in the biological detoxification of metals, including cadmium [5]. It has been reported that pretreatment with metals known to stimulate the synthesis of MT prevents the toxicity of subsequent cadmium exposure [53–55], and a deficiency in MT appears to occur in several mammalian tissues that are highly susceptible to the toxic effects, such as rat, mouse, monkey testes, rat ventral prostate, and hamster ovary [56]. Non-MT-bound cadmium may therefore have a role in the pathogenesis of cadmium-related tissue injury. The speciation of other cadmium complexes in tissue or biological fluids is unknown [5].

Further studies in humans that documented the influence of speciation on the distribution of

cadmium in the body were not located. In animals, it has been reported that after oral administration of cadmium bound to MT, the cadmium is distributed proportionally more to the kidneys, whereas cadmium as chloride administered by the same route distributes primarily to the liver [57–59].

2.3 Excretion

Most of the cadmium that has been absorbed after ingestion or inhalation is excreted slowly, with urinary and fecal excretion being approximately equal. Urinary excretion is related to body burden, recent exposure, and renal damage. In people with low exposures, cadmium in urine is mainly related to body burden, and the extent of excretion increases with age at least until age 50 to 60 and then declines slowly. In exposed people with renal damage, urinary excretion of cadmium increases. Cadmium can also be excreted by other routes (bile, saliva, hair, nails) but to a lesser extent [2, 5, 60]. In urine, cadmium has been reported to be bound to MT [2, 60]. Cadmium is also eliminated in breast milk, and concentrations are reported to be 5–10% of levels in blood [5]. For the elucidation of the cadmium-binding forms in human milk, a combination of high performance liquid chromatography and voltammetry was applied. It could be concluded that the cadmium in human milk is mainly available as MT (see Sections 2.5.1, 2.8).

No further information on the forms of cadmium involved in the excretion of the element was located.

Concerning a possible transplacental transfer, it appears that the placenta provides a relative barrier, protecting the fetus against cadmium exposure. There is some buildup of cadmium in the placenta, and cadmium levels in placenta are significantly higher in smokers than in nonsmokers. The mechanism involved is still unknown, but the most plausible hypothesis is that cadmium is retained by binding to MT in the placenta. Cadmium can cross the placenta but at a low rate. The cadmium concentration in newborn blood is on average 40–50% lower than in maternal blood.

3 TOXICOLOGICAL ASPECTS

Cadmium has no known physiological role.

Cadmium is toxic to a wide range of organs. Primary targets are the kidneys, bone, and the lung, although it is generally accepted that after long-term exposure, either by the inhalation of cadmium compounds at occupational settings or by the ingestion of food and drinking water, the kidney is the critical organ [2, 60].

From the located information, many toxic effects appear to involve the ionic form of cadmium (Cd^{2+}). Following mechanisms of toxicity, frequently evoked, seem to indicate that of importance for the occurrence of toxic effects is the interaction of the cadmium ion with MT or its presence as free, unbound ion. For example, renal damage is believed to occur if there is a localization of free cadmium (Cd^{2+}) or an excessive concentration of cadmium that remains unbound to MT. In rats, cadmium (ion) has been shown to perturb lipid composition and enhance lipid peroxidation in liver tissue [61]. Cadmium ion has also been shown to alter zinc, iron, and copper metabolism, as well as selenium [62]. The ionic radius and charge of the cadmium ion being comparable to those of the calcium ion, it is conceivable that the cadmium ion replaces the calcium at cellular binding sites and may lead to disturbances in cellular calcium homeostasis [1].

3.1 Toxicological aspects for the general population

In nonoccupationally exposed subjects, exposure occurs mainly by ingestion of cadmium-contaminated food. Tobacco smoking is an additional source of uptake, both in the general population and in workers.

Acute intoxication has been observed after food and drink contamination by high concentrations of cadmium from solders in water pipes, taps, cooling, or heating devices, or from dissolution of cadmium from pottery, usually occurring when acid juices and the like are stored in these items [2, 63–65]. The main symptoms of oral

toxicity are nausea, vomiting, diarrhea, abdominal cramps, headache, and salivation, and recovery from mild or moderate poisoning appears to be rapid and complete.

Two fatal cases of self-poisoning with cadmium compounds were reported in the literature. The ingestion of about 150 g cadmium chloride caused hemorraghic necrosis of the stomach, duodenum, and jejunum. Death occurred 30 hours after admission. Necropsy showed also pulmonary edema, pleural effusions and ascites, focal hepatic necrosis, and slight pancreatic hemorrhage. Kidneys appeared normal [66]. Wisniewska-Knypl *et al*. [67] reported that ingestion of 25 $mg\,kg^{-1}$ cadmium iodide resulted in death seven days later; necropsy revealed damage to the heart, liver, and kidneys, besides gastrointestinal damage.

The bone tissue constitutes a target organ for the general population exposed repeatedly to excessive concentrations of cadmium compounds in food or in drinking water. A severe form of bone disease caused by cadmium intoxication is the clinical syndrome referred to as *Itai–Itai disease* reported in aged Japanese women living in the basin of the Jinzu river, characterized by osteomalacia and osteoporosis. The major source of uptake of cadmium was the ingestion of rice and water polluted by a mine located 50 km upstream from the endemic area [2]. Cadmium is believed to exert a negative effect on bone metabolism. The mechanism is, however, not fully understood and types of bone lesions associated with cadmium exposure are not clearly identified. Beside disturbance of bone metabolism, another explanation is that cadmium induces kidney damage and/or hypercalciuria, which might promote osteoporosis and osteoporotic fractures.

Renal effects can be detected in the general population after long-term, low-level oral exposure to cadmium. The reported renal effects of cadmium in environmentally exposed populations mainly consist in tubular proteinuria that may be accompanied by other signs of tubular dysfunction such as enzyme leakage and depressed tubular resorption of amino acids, glucose, calcium, copper, and inorganic phosphate [5]. Until now, mortality studies were not able to detect an excess of end-stage renal disease in populations exposed to cadmium compounds, however, a recent epidemiological study suggests that the incidence of renal replacement therapy is increased in a population with occupational/environmental exposure to cadmium [68].

Other adverse reactions in various organs/systems such as the liver, testes, cardiovascular and hematological systems have been reported in animals exposed to very high doses of cadmium compounds, but the relevance of these observations for human exposure conditions is uncertain.

In *in vitro* and *in vivo* experiments, several cadmium compounds (chloride, sulfate, acetate) appear to have the capability of altering genetic material but no consensus has been reached on the mechanism of action. Studies performed in environmentally exposed populations do not allow to identify the type of cadmium compound(s) to which subjects are precisely exposed, but it cannot be excluded that cadmium might exert genotoxic effects [1, 2].

There is currently no indication or evidence that cadmium acts as a carcinogen in the general population exposed by the oral route.

With regard to reprotoxicity, epidemiological studies do not speak for an association between exposure to cadmium and relevant effects on fertility or reproductive organs in the general population. No clear evidence indicates that cadmium has adverse effects on the development of the offspring of women exposed indirectly via the environment. Some effects on birth mass and motor and perceptual abilities of offspring have been reported related to cadmium measured in hair [69–71]. It is not clear whether these effects are specifically due to cadmium or were influenced by a simultaneous exposure to other substances such as lead.

Overall, there is no evidence of any influence of speciation on the type, severity, or duration of these effects.

4 OCCUPATIONAL HEALTH

Occupational exposure occurs mainly by inhalation in various industries that involve the production and recovery of cadmium metal, the production of cadmium oxide, the manufacture of

nickel-cadmium batteries, the production of pigments, alloys, and stabilizers and cadmium plating.

An additional exposure may occur by the oral route when workers eat with dirty hands or bite their fingernails at the workplace, for example. Limited dermal exposure may occur when cadmium compounds powder/dust are handled or when maintenance of the production machinery involved in the process is necessary. Tobacco smoking constitutes an additional intake of cadmium.

In the past, pyrometallurgical operations with cadmium have sometimes been associated with high concentrations (>1 mg m^{-3}) of cadmium oxide dust or fumes. Since the 1960s, considerable improvements in occupational hygiene have progressively been accomplished. As a result, present-day cadmium concentrations at the workplace are usually of the order of 10 μg m^{-3} or lower. In general, only airborne total cadmium concentrations are monitored in the working environment; factors that influence respiratory absorption, such as speciation of cadmium, are not taken into account, and the size distribution of the collected particles is rarely documented [2].

The current permissible limits (Threshold Limit Value-Time-Weighted Average) for cadmium in air, recommended by the American Conference of Governmental Industrial Hygienists, are currently set at 10 μg Cd m^{-3} (inhalable fraction) and 2 μg Cd m^{-3} (respirable fraction) [72]. These values are generic for all cadmium compounds and do not take speciation into account.

Acute poisonings and, in some cases, deaths have been reported among workers shortly after exposure to fumes of cadmium oxides, when cadmium metal or cadmium-containing materials were heated to high temperatures. At an early stage, the symptoms may be confused with those of "metal fume fever. However, these conditions are different, with cadmium-lung leading to delayed pulmonary edema and possibly death. Subjects who survive the acute cadmium poisoning may recover without damage, although some authors have reported delayed development of lung impairment. Cadmium concentrations in air were not reported in most case-reports. It has been estimated that an 8-hour exposure to 5 mg m^{-3} may be lethal and an 8-hour exposure of 1 mg m^{-3} is considered as immediately dangerous for life [2, 6].

Several authors concluded that long-term inhalation exposure to cadmium (most often CdO fumes and dust) leads to decreased lung function and emphysema [73–82]. Other studies, however, have not shown a cadmium-related increase in impaired respiratory function [78, 83, 84]. Possible explanations for these discrepancies are the use of different diagnostic criteria over time and the fact that earlier studies did not control for the effects of cigarette smoking. Additional respiratory symptoms reported in highly exposed workers are chronic rhinitis and impairment of the sense of smell. In a group of 73 heavily exposed workers (probably to CdO) in a plant producing nickel-cadmium batteries, 26% of the workers were diagnosed as suffering from hyposmia, 17.8% from paraosmia, and 1.4% from anosmia. Olfactory disorders were generally associated with hypertrophic changes of the nasal mucosa [85].

Clinical bone disease has been described in workers exposed to cadmium compounds (CdO dust and fumes), but the number of cases is limited. The incidence of bone disorders appears to have peaked 40 to 50 years ago when exposures were high and the dietary conditions may have been deficient in the countries with reported cases [86]. More recently, a cross-sectional study carried out in workers exposed to cadmium (compounds not specified) provided results compatible with a role of cadmium in the genesis of osteoporosis, as an inverse dose–effect relationship could be demonstrated between cadmium dose estimates and forearm bone mineral density [87].

The kidney is the main target organ after inhalation exposure to cadmium. No located data mentioned renal effects that would be specific for particular cadmium compounds [2, 5, 88, 89]. The first manifestation of cadmium nephrotoxicity in occupationally exposed subjects is usually a tubular dysfunction associated with an increased urinary excretion of low-molecular mass proteins. In some cases, an effect on the glomerulus may also be observed in cadmium-exposed workers,

as indicated by increased urinary excretion of high-molecular mass proteins, including albumin, immunoglobulins G, or transferrin. There are indications that the glomerular function of heavily exposed workers declines more rapidly than that of nonexposed subjects, but there is currently no evidence from mortality studies of a progression to end-stage renal disease [90–93]. An additional effect on the kidney seen in workers after high levels of exposure is an increased frequency of kidney stone formation [5, 94–98].

Studies performed on a limited number of occupationally exposed subjects are suggestive of an effect of cadmium on the peripheral and central nervous system, but these findings should be confirmed [99, 100].

Regarding genotoxic effects of cadmium compounds, examination of lymphocytes from workers occupationally exposed to both cadmium and lead in smelters have shown significant increases in chromosomal aberrations [101–103]. In men exposed primarily to cadmium oxide dust and fumes in a copper-cadmium alloy factory, only high-intensity, long-term exposure (>1000 $\mu g/m^3 \cdot y$) was associated with a significant increase in the frequency of chromosome-type aberrations [104–106].

Cadmium and its compounds have been classified as 'carcinogenic to humans (group 1)' by IARC in 1993. The observation of an increased number of lung cancers in a US cohort of cadmium-exposed workers and the finding of lung tumors in animals exposed by inhalation to various cadmium compounds (CdO fumes and dust, $CdCl_2$, CdS) played an important role in this assessment [1, 90, 107–110]. Initial studies conducted on workers indicated an elevation in prostate cancer among men employed at the production of batteries [111], alloys [112], and cadmium metal [113]. There is no solid subsequent evidence that cadmium acts as a prostate carcinogen following occupational exposure. With regard to lung cancer, results provided by the studies carried out in different types of occupational settings involving an exposure to cadmium compounds appear conflicting, and confounding by coexposure to other carcinogens and smoking can not be excluded. However, the weight of evidence collected in genotoxicity tests, animal experiments, and epidemiological studies leads to conclude that cadmium has to be considered at least as a suspected human carcinogen upon inhalation exposure.

No clear evidence indicates that inhaled cadmium had adverse effects on fertility or sex organs or on development of the offspring of women occupationally exposed to cadmium (generic).

Biomonitoring of exposure

In subjects occupationally exposed to cadmium compounds, biological monitoring may be used to characterize exposure. One advantage of biological monitoring in regard with exposure to cadmium, is that it evaluates the overall exposure, whatever the route of entry. Nonoccupational background exposure (smoking, diet, residence) will also be taken into account as the organism integrates the total external (environmental and occupational) exposure into one internal load [60].

At low exposure conditions (i.e., general environmental exposure or moderate occupational exposure), when the total amount of cadmium absorbed has not yet saturated all the available cadmium binding sites in the body (in particular in the kidney), the cadmium concentration in urine (Cd-U) mainly reflects the cadmium level in the body and in the kidney. There is a close relationship between the cadmium concentrations in urine and in kidneys. When integrated exposure has been so high as to cause a saturation of the binding sites, cadmium in urine may then be related partly to the body burden and partly to the recent exposure. When renal damage develops, a considerable increase of urinary cadmium excretion occurs.

Under occupational conditions, cadmium in blood may be considered as mainly a biomarker of recent exposure. However, the relative influence of the cadmium body burden may be more important or even dominant in subjects with previous exposure and subjects who have accumulated large amounts of cadmium [60].

Overall, in humans, there is no clear evidence of an influence of speciation on the type, severity, or duration of these effects, although one can

suspect that differences in absorption related to the chemical speciation may lead to different effect levels.

5 REFERENCES

1. IARC (International Agency for Research on Cancer), Cadmium and cadmium compounds, in *Beryllium, Cadmium, Mercury and Exposures in the Glass Manufacturing Industry*, Vol. 58, IARC, Lyon, 1993, pp. 119–237.
2. WHO (World Health Organisation), *Environmental Health Criteria 134: Cadmium*, IPCS, WHO, Geneva, 1992.
3. Morrow, H., The importance on recycling to life cycle analysis of nickel cadmium batteries, in *Proceedings of the eighth International Nickel Cadmium Battery Conference*, Prague, Czech Republic (1998), September 21–22 (1998); www.cadmium.org/env._emi.html (2005).
4. OECD (Organisation for Economic Cooperation and Development), *Risk Reductions Monograph No. 5: Cadmium*, Paris, 1994.
5. ATSDR (Agency for Toxic Substances and Disease Registry), *Cadmium (Update)*, Toxicological Profile, US Department of Health and Human Services, ATSDR, Atlanta, GA, 1999.
6. Friberg, L., Elinder, C. G., Kjellström, T. and Nordberg, G. F. (Eds.), *Cadmium and Health: A Toxicological and Epidemiological Appraisal*, *Volume II: Effects and Response*, CRC Press, Boca Raton, FL, 1986.
7. CEC, *Criteria (Dose/Effect Relationships) for Cadmium*, Commission of the European Communities, Pergamon Press, Oxford, 1978.
8. Bernard, A. and Lauwerys, R., *Toxicol. Lett.*, **46**, 293 (1989).
9. Iijima, M., *Nihon Univ. J. Med.*, **31**, 907 (1972).
10. Fox, M. R. S., *Fed. Proc.*, **42**, 1726 (1983).
11. McKenna, I. M. and Chaney, R. L., Cadmium transfer to humans from food crops grown in sites contaminated with cadmium and zinc, in *Proceedings of the Fourth International Conference Combined Effects of Environmental Factors*, Fechter, L. D. (Ed.), John Hopkins University School of Hygiene and Public Health, Baltimore, MD, 1991, pp. 65–70.
12. McKenna, I. M., Chaney, R. L., Tao, S. H., Leach, R. M. J. and Williams, F. M., *Environ. Res.*, **57**, 73 (1992).
13. Vahter, M., Berglund, M., Nermell, B. and Akesson, A., *Toxicol. Appl. Pharmacol.*, **136**, 332 (1996).
14. Groten, J. P., Sinkeldam, E. J., Luten, J. B. and van Bladeren, P. J., *Toxicol. Appl. Pharmacol.*, **111**, 504 (1991).
15. Groten, J. P., Luten, J. B. and van Bladeren, P. J., *Eur. J. Pharmacol.*, **228**, 23 (1992).
16. Gunshin, H., Mackenzie, B., Berger, U. V., Gunshin, Y., Romero, M. F., Boron, W. F., Nussberger, S., Gollan, J. L. and Hediger, M. A., *Nature*, **388**, 482 (1997).
17. Rolfs, A. and Hediger, M. A., *J. Physiol.*, **518**(Pt 1), 1 (1999).
18. Lind, Y., Wicklund-Glynn, A., Engman, J. and Jorhem, L., *Food Chem. Toxicol.*, **33**, 667 (1995).
19. Newton, D., Johnson, P., Lally, A. E., Pentreath, R. J. and Swift, D. J., *Hum. Toxicol.*, **3**, 23 (1984).
20. McLellan, J. S., Flanagan, P. R., Chamberlain, M. J. and Valberg, L. S., *J. Toxicol. Environ. Health*, **4**, 131 (1978).
21. Berglund, M., Akessson, A., Nermell, B. and Vahter, M., *Environ. Health Perspect.*, **102**, 1058 (1994).
22. Schilderman, P. A., Moonen, E. J., Kempkers, P. and Kleinjans, J. C., *Environ. Health Perspect.*, **105**, 234 (1997).
23. Foulkes, E. C., *Toxicology*, **37**, 117 (1985).
24. Squibb, K. S., Cousins, R. J., Silbon, B. L. and Levin, S., *Exp. Mol. Pathol.*, **25**, 163 (1976).
25. Engström, B. and Nordberg, G. F., *Acta Pharmacol. Toxicol.*, **45**, 315 (1979).
26. Morita, S., *Jpn. J. Pharmacol.*, **35**, 143 (1984).
27. Sugawara, N. and Sugawara, C., *Bull. Environ. Contam. Toxicol.*, **38**, 295 (1987).
28. Flaig, K. H., Schumann, K. and Elsenhans, B., *Toxicology*, **183**, 199 (2003).
29. McKenna, I. M. and Chaney, R. L., *Biol. Trace Elem. Res.*, **48**, 13 (1995).
30. Reeves, P. G. and Chaney, R. L., *Environ. Res. Sect.*, **85**, 215 (2001).
31. Sharma, R., Kjellström, T. and McKenzie, J., *Toxicology*, **29**, 163 (1983).
32. Nogawa, K., Honda, R., Kido, T., Tsuritani, I., Yamada, Y., Ishizaki, M. and Yamaya, H., *Environ. Res.*, **48**, 7 (1989).
33. Flanagan, P. R., McLellan, J. S., Haist, J., Cherian, G., Chamberlain, M. J. and Valberg, L. S., *Gastroenterology*, **74**, 841 (1978).
34. Park, J. D., Cherrington, N. J. and Klaassen, C. D., *Toxicol. Sci.*, **68**, 288 (2002).
35. Kostial, K., Kello, D., Jugo, S., Rabar, I. and Maljkovic, T., *Environ. Health Perspect.*, **25**, 81 (1978).
36. Engström, B. and Nordberg, G. F., *Toxicology*, **13**, 215 (1979).
37. Oberdörster, G., Pulmonary deposition, clearance and effects of inhaled soluble and insoluble cadmium compounds, in *Cadmium in the Human Environment: Toxicity and Carcinogenicity*, Nordberg, G. F., Herber R. F. M. and Alessio, L. (Eds.), IARC, Lyon, 1992, pp. 189–204.
38. Glaser, U., Klöppel, H. and Hochrainer, D., *Ecotoxicol. Environ. Saf.*, **11**, 261 (1986).
39. Rusch, G. M., O'Grodnick, J. S. and Rinehart, W. E., *Am. Ind. Hyg. Assoc. J.*, **47**, 754 (1986).
40. Task Group on Metal Accumulation, *Environ. Physiol. Biochem.*, **3**, 65 (1973).

41. Oberdörster, G. and Cox, C., Kinetics of inhaled $CdCl_2$, CdO, and CdS in rats and monkeys, in *Edited Proceedings of the Sixth International Cadmium Conference*, Hiscock, S. and Volpe, R. (Eds.), Cadmium Association/Cadmium Council, London/New York, 1989, pp. 147–154.
42. Grose, E. C., Richards, J. H., Jaskot, R. H., Ménache, M. G., Graham, J. A. and Dauterman, W. C., *J. Toxicol. Environ. Health*, **21**, 219 (1987).
43. Nordberg, G., Kjellström, T. and Nordberg, M., Kinetics and metabolism, cadmium and health: a toxicological and epidemiological appraisal, in *Vol. I: Exposure, Dose and Metabolism*, Friberg, L., Elinder, C. G., Kjellström, T. and Nordberg, G. F. (Eds.), CRC Press, Boca Raton, FL, 1985, pp. 103–178.
44. Krajnc, E. I., van Gestel, C. A. M., Mulder, H. C. M., de Vrijer, F. I., Sinkeldam, E. J., Vink, G. J., Canton, J. H., van Apeldoorn, M. E. and Janis, J. A., *Integrated Criteria Document Cadmium Effects*, RIVM Rijksinstituut voor Volksgezondheid en Milieuhygiene, No. 758476004, 1987.
45. Kjellström, T. and Nordberg, G. F., Kinetic model of cadmium metabolism, in *"Cadmium and Health: A Toxicological and Epidemiological Appraisal*, Friberg, L., Elinder, C. G., Kjellström, T. and Nordberg, G. F. (Eds.), CRC Press, Boca Raton, FL, 1985, pp. 179–199.
46. Lansdown, A. B. and Sampson, B., *Lab. Anim. Sci.*, **46**, 549 (1996).
47. Wester, R. C., Maibach, H. I., Sedik, L., Melendres, J., DiZio, S. and Wade, M., *Fundam. Appl. Toxicol.*, **19**, 1 (1992).
48. Kjellström, T., *Environ. Health Perspect.*, **28**, 169 (1979).
49. Elinder, C. G., Normal values for cadmium in human tissues, blood and urine in different countries, in *Cadmium and Health: A Toxicological and Epidemiological Appraisal. Exposure, Dose, and Metabolism*, Friberg, L., Elinder, C. G., Kjellström, T. and Nordberg, G. F. (Eds.), CRC Press, Boca Raton, FL, 1985, pp. 81–102.
50. Roels, H., Buchet, J. P., Truc, J., Croquet, F. and Lauwerys, R., *Am. J. Ind. Med.*, **3**, 53 (1982).
51. Hassler, E., *Exposure to Cadmium and Nickel in an Alkaline Battery Factory as Evaluated From Measurements in Air and Biological Material*, Department of Environmental Hygiene, Karolinska Institute, Stockholm, 1983.
52. Christoffersson, J. O., Welinder, H., Spang, G., Mattsson, S. and Skerfving, S., *Environ. Res.*, **42**, 489 (1987).
53. Leber, A. P. and Miya, T. S., *Toxicol. Appl. Pharmacol.*, **37**, 403 (1976).
54. Yoshikawa, H., *Ind. Health*, **11**, 113 (1973).
55. Jin, T., Nordberg, G. F. and Nordberg, M., *J. Appl. Toxicol.*, **6**, 397 (1986).
56. Waalkes, M. P. and Goering, P. L., *Chem. Res. Toxicol.*, **3**, 281 (1990).
57. Cherian, M. G., Goyer, R. A. and Valberg, L. S., *J. Toxicol. Environ. Health*, **4**, 861 (1978).
58. Cherian, M. G., *Bull. Environ. Contam. Toxicol.*, **30**, 33 (1983).
59. Maitani, T., Waalkes, M. P. and Klaassen, C. D., *Toxicol. Appl. Pharmacol.*, **74**, 237 (1984).
60. Lauwerys, R. and Hoet, P., Cadmium, *Industrial Chemical Exposure Guidelines for Biological Monitoring*, Lewis Publishers, Boca Raton, FL, 2001, pp. 54–69.
61. Gill, K. D., Pal, R. and Sandhir, R., *Med. Sci. Res.*, **17**, 921 (1989).
62. Petering, H. G., Choudhury, H. and Stemmer, K. L., *Environ. Health Perspect.*, **28**, 97 (1979).
63. Rème and Peres, *Arch. Mal. Prof. Med. Trav. Secur. Soc.*, **20**, 783 (1959).
64. Nordberg, G., Slorach, S. and Stenstrom, T., *Läkartidningen*, **70**, 601 (1973).
65. Baker, T. D. and Hafner, W. G., *Public Health Rep.*, **76**, 543 (1961).
66. Buckler, H. M., Smith, W. D. and Rees, W. D., *Br. Med. J.*, **292**, 1559 (1986).
67. Wisniewska-Knypl, J. M., Jablonska, J. and Myslak, Z., *Arch. Toxicol.*, **28**, 46 (1971).
68. Hellström, L., Elinder, C. G., Dahlberg, B., Lundberg, M., Järup, L. and Persson, B., *Am. J. Kidney Dis.*, **38**, 1001 (2001).
69. Bonithon-Kopp, C., Huel, G., Moreau, T. and Wendling, R., *Neurobehav. Toxicol. Teratol.*, **9**, 307 (1986).
70. Fréry, N., Nessmann, C., Girard, F., Lafond, J., Moreau, T., Blot, P., Lellouch, J. and Huel, G., *Toxicology*, **79**, 109 (1993).
71. Huel, G., Boudene, C. and Ibrahim, M. A., *Arch. Environ. Health*, **36**, 221 (1981).
72. ACGIH (American Conference of Governmental Industrial Hygienists), *Threshold Limit Values for Chemical Substances and Physical Agents & Biological Exposure Indices*, 2001.
73. L. Friberg, *Acta Med. Scand.*, **240**(Suppl.), 1 (1950).
74. Baader, E. W., *Ind. Med. Surg.*, **21**, 427 (1952).
75. Bonnell, J. A., *Br. J. Ind. Med.*, **12**, 181 (1955).
76. Smith, T. J., Petty, T. L., Reading, J. C. and Lakshminarayan, S., *Am. Rev. Respir. Dis.*, **114**, 161 (1976).
77. Kazantzis, G., *Br. J. Ind. Med.*, **13**, 30 (1956).
78. P. F. Gill, Respiratory function in a group of workers exposed to cadmium in Hobart, in *Proceedings of the First International Cadmium Conference*, Metal Bulletin Survey, San Francisco, CA, 1978, pp. 207–210.
79. Davison, A. G., Newman Taylor, A. J., Darbyshire, J., Chettle, D. R., Gutherie, C. and O'Malley, D., *Lancet*, **1**, 663 (1988).
80. Cortona, G., Apostoli, P., Toffoletto, F., Baldasseroni, A., Ghezzi, I., Goggi, E., Fornari, S. and Alessio, L., Occupational exposure to cadmium and lung function, in *Cadmium in the Human Environment: Toxicity and Carcinogencity*, Nordberg, G. F., Herber, R. F. M. and Alessio, L. (Eds.), IARC, Lyon, 1992, pp. 205–210.
81. Chan, O. Y., Poh, S. C., Lee, H. S., Tan, K. T. and Kwok, S. F., *Ann. Acad. Med. Singapore*, **17**, 283 (1988).

82. Sakurai, H., Omae, K., Toyama, T., Higashi, T. and Nakadate, T., *Scand. J. Work Environ. Health*, **8**(Suppl. 1), 122 (1982).
83. Edling, C., Elinder, C. G. and Randma, E., *Br. J. Ind. Med.*, **43**, 657 (1986).
84. Stanescu, D., Veriter, C., Frans, A., Goncette, L., Roels, H., Lauwerys, R. and Brasseur, L., *Scand. J. Respir. Dis.*, **58**, 289 (1977).
85. Rydzewski, B., Sulkowski, W. and Miarzynska, M., *Int. J. Occup. Med. Environ. Health*, **11**, 235 (1998).
86. Kjellström, T., Effects on bone, on vitamin D, and calcium metabolism, in *Cadmium and Health: a Toxicological and Epidemiological Appraisal*, *Volume II: Effects and Response*, Friberg, L., Elinder, C. G., Kjellström, T. and Nordberg, G. F. (Eds.), CRC Press, Boca Raton, FL, 1986, pp. 111–158.
87. Järup, L., Alfven, T., Persson, B., Toss, G. and Elinder, C. G., *Occup. Environ. Med.*, **545**, 435 (1998).
88. Staessen, J. and Lauwerys, R., *J. Hum. Hypertens.*, **7**, 195 (1993).
89. L. Järup, M. Berglund, C. G. Elinder, G. Nordberg and M. Vahter, *Scand. J. Work Environ. Health*, **24**, (1998).
90. Thun, M. J., Schnorr, T. M., Blair Smith, A., Halperin, W. and Lemen, R. A., *J. Natl. Cancer Inst.*, **74**, 325 (1985).
91. Armstrong, B. G. and Kazantzis, G., *Lancet*, **1**, 1425 (1983).
92. Kazantzis, G., Lam, T. H. and Sullivan, K. R., *Scand. J. Work Environ. Health*, **14**, 220 (1988).
93. Järup, L., Bellander, T., Hogstedt, C. and Spang, G., *Occup. Environ. Med.*, **55**, 755 (1998).
94. Falck, F. Y. J., Fine, L. J., Smith, R. G., Garvey, J., Schork, A., England, B., McClatchey, K. D. and Linton, J., *Br. J. Ind. Med.*, **40**, 305 (1983).
95. Thun, M. J., Osorio, A. M., Schober, S., Hannon, W. H., Lewis, B. and Halperin, W., *Br. J. Ind. Med.*, **46**, 689 (1989).
96. Kazantzis, G., *Contrib. Nephrol.*, **16**, 161 (1979).
97. Scott, R., Patterson, P. J., Burns, R., Ottoway, J. M., Hussain, F. E., Fell, G. S., Dumbuya, S. and Iqbal, M., *Urology*, **11**, 462 (1978).
98. Järup, L. and Elinder, C. G., *Br. J. Ind. Med.*, **50**, 598 (1993).
99. Viaene, M. K., Masschelein, R., Leenders, J., De Groof, M., Swerts, L. J. and Roels, H. A., *Occup. Environ. Med.*, **57**, 19 (2000).
100. Viaene, M. K., Roels, H. A., Leenders, J., De Groof, M., Swerts, L. J., Lison, D. and Masschelein, R., *Neurotoxicology*, **20**, 7 (1999).
101. Bauchinger, M., Schmid, E., Einbrodt, H. J. and Dresp, J., *Mutat. Res.*, **40**, 57 (1976).
102. Deknudt, G. and Léonard, A., *Environ. Physiol. Biochem.*, **5**, 319 (1975).
103. Deknudt, G., Léonard, A. and Ivanov, B., *Environ. Physiol. Biochem.*, **3**, 132 (1973).
104. Forni, A., Chromosomal effects of cadmium exposure in humans, in *Cadmium in the Human Environment: Toxicity and Carcinogenicity*, Nordberg, G. F., Herber, R. F. M. and Alessio, L. (Eds.), IARC, Lyon, 1992, pp. 377–383.
105. Forni, A., *Toxicol. Lett.*, **72**, 185 (1994).
106. Forni, A., Toffoletto, F., Ortisi, E. and Alessio, L., Occupational exposure to cadmium. cytogenetic findings in relation to exposure levels, in *Environmental Hygiene II*, Seemayer, N. H. and Hadnagy, W. (Eds.), Springer-Verlag, Berlin, Heidelberg, New York, 1990, pp. 161–164.
107. Stayner, L., Randall Smith, M. A., Thun, M. J., Schnorr, T. M. and Lemen, R. A., *Ann. Epidemiol.*, **2**, 177 (1992).
108. Stayner, L., Smith, R., Schnorr, T., Lemen, R. and Thun, M., *Ann. Epidemiol.*, **3**, 114 (1993).
109. Glaser, U., Hochrainer, D., Otto, F. J. and Oldiges, H., *Toxicol. Environ. Chem.*, **27**, 153 (1990).
110. Takenaka, S., Glaser, U., Oldiges, H. and Mohr, U., *Toxicol. Environ. Chem.*, **27**, 163 (1990).
111. Kipling, M. D. and Waterhouse, J. A. H., *Lancet*, **7**, 730 (1967).
112. Kjellström, T., Fribergand, L. and Rahnster, B., *Environ. Health Perspect.*, **28**, 199 (1979).
113. Lemen, R., Lee, J. S., Wagoner, J. K. and Blejer, H. P., *Ann. N. Y. Acad. Sci.*, **271**, 273 (1976).

2.6 Speciation of Chromium

2.6.1 Speciation of Chromium in Environment and Food

Detlef Metze*, Norbert Jakubowski and Dieter Klockow**

Institute for Analytical Sciences, Dortmund, Germany

**Present affiliation: North Rhine Westphalia State Environment Agency, Essen, Germany*
***Present affiliation: International Association of Environmental Analytical Chemistry, Allschwil, Switzerland*

1 INTRODUCTION

Chromium is a metallic element that occurs predominantly in its Cr(III) and Cr(VI) oxidation states. It is most commonly found in its trivalent form as chromite $Cr_2O_3 \times FeO$ (annual output of chromite worldwide in 1998: [1] 14.2 million t). This ore, which is mined, among other countries, mainly in South Africa (about 49% of the world's total), Zimbabwe (about 95% of chromium resources are geographically located in southern Africa), Kazakhstan, India, and Turkey, is the starting material for the production of metallic chromium, chromium alloys, and a variety of chromium compounds. They are mainly used in steel manufacturing (85% of chromite consumption), in production of ferrous and nonferrous alloys, in electroplating and tanning industries, and for the production of pigments. This extensive use in industrial processes is the dominant source of anthropogenic chromium emissions in liquid, solid and gaseous forms [2], which can have significant adverse biological and ecological effects. The production of 1 t of steel in an electric arc furnace, for instance, generates 10–15 kg of dust that can contain, besides some other toxic metals, up to 10% of hexavalent chromium. A part of this dust, consisting mainly of a mixture of metal oxides volatilized from the furnace and collected in the filtration system, is emitted to the atmosphere, whereas the material accumulated on the filters is usually deposited in landfill sites as hazardous waste. Here, the water

Handbook of Elemental Speciation II: Species in the Environment, Food, Medicine & Occupational Health
Edited by R. Cornelis, H. Crews, J. Caruso and K. G. Heumann
 ISBN: 0-470-85598-3 (HB)

soluble Cr(VI) can be washed out and eventually contaminate the groundwater. For estimation of the ecological and toxicological consequences of such a process, the knowledge on the kind and the amount of chromium species present is required. Cr(III) and Cr(VI) differ in charge and physicochemical properties and consequently in chemical and biochemical reactivity. Cr(III) is known as a trace element essential for proper functioning of lipid, glucose, and protein metabolism in mammalians [3], whereas Cr(VI) is much more a threat to biological systems because of its mutagenic and genotoxic effects. More details about the biological role of chromium, its essentiality, and its toxicity is given in the next chapter by P. Hoet.

Beside its toxicity, the mobility and bioavailability of a potentially hazardous substance needs to be investigated also with respect to possible environmental effects. Cr(VI) compounds, except some metal chromates like those of Pb, Ba, Sr, Ca, Ag, and Zn, are highly soluble, mobile, and bioavailable compared to the sparingly soluble Cr(III) compounds. It is therefore necessary to gain species selective information rather than results for the total chromium contents of environmental samples. Only a speciation approach will yield the data needed to evaluate distribution and transport processes, chemical transformations in water, soil, and atmosphere, and physiological and toxicological effects of chromium compounds.

During the past two decades, a growing number of papers pertaining to methods for chromium speciation and environmental occurrence of both species was published. Some remarkable reviews by Kotas and Stasicka [4] and by Marqués *et al*. [5, 6] summarize the zest of chromium speciation under an environmental point of view up to the year 1998, resp. 2000. A comprehensive review on chemistry and risk assessment of chromium in the environment was given by Kimbrough *et al*. [7].

2 CHROMIUM CHEMISTRY IN THE ENVIRONMENT

The different approaches used for chromium speciation can be better understood by looking at the chemistry of this element, which is very complex. Chromium exists in all possible oxidation states from −II up to +VI, but for environmental studies primarily Cr(III) and Cr(VI) are relevant. Cr(II), Cr(IV), and Cr(V) oxidation states may be produced as intermediates in the cellular metabolism, their lifetimes, however, are short. A stable and nontoxic compound that is not of environmental concern is CrO_2, which is produced on an industrial scale and is used as ferromagnetic material for audio- and videotapes.

Cr(VI) is predominantly produced by air oxidation of chromite in alkaline melts. The chromate formed readily dissolves in water as a salt with the anion CrO_4^{2-} or, depending on pH-value (<1) and concentration (>0.02 mol L^{-1}), as dichromate, $Cr_2O_7^{2-}$.

The equilibrium constants in Table 2.6.1.1 [8, 9] show the strong dependence of the relative fractions of the different species on the pH-value. At "ambient" pH-values, the predominant anion is $HCrO_4^-$. The dichromate anion is usually not found because it is formed at a pH-value below 1 and at concentrations above 0.02 mol L^{-1}, which might only be achieved in industrial landfills with chromate deposits. A simplified scheme of this behavior is given in Figure 2.6.1.1 [9].

Cr(VI) in acidic solution shows a very high positive redox potential [E] (equation 2.6.1.1), which denotes that it is strongly oxidizing and unstable in the presence of electron donors such as organic matter or reducing inorganic compounds, which are ubiquitous in soil, water, and airborne matter [10]. Under more basic conditions, the oxidation potential is noticeably lower, as indicated in equation (2.6.1.2).

$$\mathrm{E} = +1.35\mathrm{V} \quad HCrO_4^- + 7H^+ + 3\,e^- \rightleftarrows Cr^{3+} + 4H_2O \tag{2.6.1.1}$$

$$\mathrm{E} = -0.13\mathrm{V} \quad CrO_4^{2-} + 4H_2O + 3\,e^- \rightleftarrows Cr(OH)_3 + 5OH^- \tag{2.6.1.2}$$

Table 2.6.1.1. Equilibrium constants (ionic strength = 1).

$HCrO_4^- \rightleftarrows H^+ + CrO_4^{2-}$	$K = 1.8 \times 10^{-6}$
$H_2CrO_4 \rightleftarrows H^+ + HCrO_4^-$	$K = 5.0$
$2HCrO_4^- \rightleftarrows Cr_2O_7^{2-} + H_2O$	$K = 94$

Source: Date taken from Reference [8] and [9]

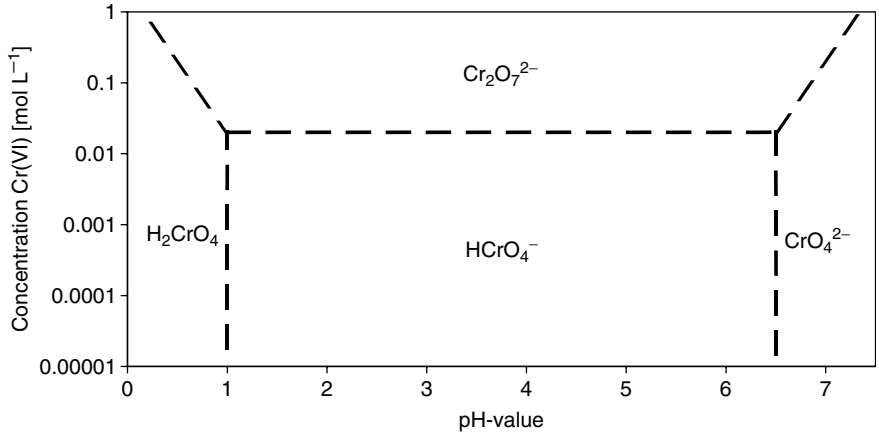

Figure 2.6.1.1. pH and concentration depending domains of Cr(VI)-species in aqueous solution (Data taken from Reference [9]).

Cr(III) is the most stable form in natural systems. As a "hard" Pearson acid, it can form a large variety of complexes with "hard" ligands like water and several inorganic and organic anions that contain oxygen or nitrogen as electron donor atoms [11]. Some of the hexacoordinated octahedral complexes are kinetically very stable and can prevent precipitation of Cr(III) at pH-values at which it would otherwise precipitate. The chemistry of Cr(III) shows similarities to that of Al(III): $Cr(OH)_3 \cdot aq$ is amphoteric but more basic than acidic. In aqueous solution and in the absence of complexing agents, other than H_2O or OH^-, Cr(III) exists as hexaaquochromium(3+) ion and its hydrolysis products [12]. $[Cr(H_2O)_6]^{3+}$ is a moderately strong acid with a $pK_a \sim 4$ as shown by equations (2.6.1.3–2.6.1.5).

$$Cr(H_2O)_6{}^{3+} + H_2O \rightleftarrows Cr(OH)(H_2O)_5{}^{2+} + H_3O^+ \quad (2.6.1.3)$$

$$Cr(OH)(H_2O)_5{}^{2+} + H_2O \rightleftarrows Cr(OH)_2(H_2O)_4{}^{+} + H_3O^+ \quad (2.6.1.4)$$

$$Cr(OH)_2(H_2O)_4{}^{+} + H_2O \rightleftarrows Cr(OH)_3\ aq + H_3O^+ \quad (2.6.1.5)$$

In environmental compartments, hexacoordinated Cr(III) complexes with single charged anions as ligands usually can carry charges from +3 to 0, that is, $[Cr(H_2O)_{6-n}X_n]^{(3-n)+}$, $n = 0$ to 3, which is important to consider when ion chromatography is used for separation of the different chromium species. The complexation of chromium with ligands other than OH^- increases its solubility when the ligands are discrete molecules or ions. In case the donor atoms belong to a macromolecular system like humic substances, the Cr(III) complexes can be more or less immobile. As has been shown by Marx and Heumann [13], Cr(III) and humic substances can form kinetically stable complexes, which is very important for the mobility of chromium in the environment. If humic substances are present and bound to soil or sediment, the mobility of Cr(III) will be very low because of the formation of stationary complexes. The presence of soluble humic substances, however, will increase the mobility of Cr(III) dramatically because of the formation of stable and soluble complexes.

Under certain conditions, Cr(III) in aqueous solution can be oxidized to Cr(VI), as can be taken from Table 2.6.1.2 [7].

Table 2.6.1.2 shows that the pH-value is essential for the interconversion of both oxidation states. High values of the redox potential [E] in waters correspond to strongly oxidizing conditions. Generally, there is an inverse relation between E and pH-value as to the redox behavior of chromium. That means that Cr(VI) is easily reduced at low pH and much more stable against reduction in alkaline

Table 2.6.1.2. Examples of Cr(III)/Cr(VI) redox reactions.

	E [V]
$2\ Cr^{3+} + 5\ H_2O + 3\ O_3 \rightleftarrows 2\ CrO_4^{2-} + 10\ H^+ + 3\ O_2$	0.87
$2\ Cr^{3+} + 2\ H_2O + 3\ H_2O_2 \rightleftarrows 2\ CrO_4^{2-} + 10\ H^+ + 3\ O_2$	0.58
$3\ MnO_2 + 2\ Cr(OH)_3 \rightleftarrows 3\ Mn^{2+} + 2\ CrO_4^{2-} + 2\ H_2O + 2\ OH^-$	1.33
$2\ Cr^{3+} + H_2O + 3\ PbO_2 \rightleftarrows Cr_2O_7^{2-} + 2\ H^+ + Pb^{2+}$	0.13
$HCrO_4^- + 3\ Fe^{2+} + 7\ H^+ \rightleftarrows Cr^{3+} + 3\ Fe^{3+} + 4\ H_2O$	0.56
$2\ HCrO_4^- + 3\ H_2S + 8\ H^+ \rightleftarrows 2\ Cr^{3+} + 8\ H_2O + 3\ S$	1.18
$2\ HCrO_4^- + 3\ HSO_3^+ + 5\ H^+ \rightleftarrows 2\ Cr^{3+} + 5\ H_2O + 3\ SO_4^{2-}$	2.12

Source: Data taken from Reference [7]

medium. Conversely, Cr(III) is very stable at low pH and is much more easily oxidized at strong alkaline conditions.

Another very important factor that affects the redox behavior of chromium is the concentration level of the oxidizing/reducing agents. Although several agents are capable of oxidizing Cr(III), only a few of them exist in high enough concentrations in the environment to oxidize Cr(III) to Cr(VI). In contrast, agents that reduce Cr(VI) are typically found at sufficiently high concentrations to play an important role, even if Cr(VI) reduction is thermodynamically less favored. The reduction of Cr(VI) by Fe(II), for instance, has a low redox potential of 0.56 V, but the concentrations of Fe(II) in the environment are high enough (e.g., in ambient aerosol in wintertime in municipal areas) to actually enforce this reduction [14]. Ozone, demonstrating the opposite, can react with Cr(III) to form chromate (redox potential of 0.87 V), but the concentration of ozone in most environmental media is rarely high enough to accomplish this oxidation [12].

Other important processes that influence the amounts of chromium species present in environmental compartments are precipitation and dissolution reactions. The water solubilities of both Cr(VI) and Cr(III) species vary over many orders of magnitude. Most Cr(VI) compounds are water soluble, and the solubilities are almost independent of the pH-value. Chromate, however, can also form sparingly soluble salts of a variety of divalent cations, such as Pb^{2+}, Ba^{2+}, Sr^{2+}, Zn^{2+}, and Cu^{2+}, which readily dissolve in acidic medium. Solubilities of some chromium compounds are given in Table 2.6.1.3 [7]. The chromates listed can be contaminants of the groundwater at industrial landfill sites.

Usually, the water soluble Cr(III) compounds do not occur naturally and are unstable in the environment. The principal reaction of Cr(III) in water is hydrolysis yielding different hydroxo species of varying solubility. In a pH range of approximately

Table 2.6.1.3. Solubilities of chromium(III)-hydroxide and a number of chromates.

	Solubility product constants L_S
$Cr(OH)_3\ (s) \rightleftarrows Cr^{3+} + 3\ OH^-$	1×10^{-30} [mol L^{-1}]^4
$CaCrO_4 \rightleftarrows CrO_4^{2-} + Ca^{2+}$	2.3×10^{-2} [mol L^{-1}]^2
$SrCrO_4 \rightleftarrows CrO_4^{2-} + Sr^{2+}$	3×10^{-5} [mol L^{-1}]^2
$BaCrO_4 \rightleftarrows CrO_4^{2-} + Ba^{2+}$	3×10^{-10} [mol L^{-1}]^2
$CuCrO_4 \rightleftarrows CrO_4^{2-} + Cu^{2+}$	3.6×10^{-8} [mol L^{-1}]^2
$PbCrO_4 \rightleftarrows CrO_4^{2-} + Pb^{2+}$	1.8×10^{-14} [mol L^{-1}]^2
$ZnCrO_4 \rightleftarrows CrO_4^{2-} + Zn^{2+}$	1.1×10^{-5} [mol L^{-1}]^2
$ZnCrO_4 \times 4\ Zn(OH)_2 \rightleftarrows CrO_4^{2-} + Zn^{2+} + 4\ Zn(OH)_2$	5×10^{-17} [mol L^{-1}]^2
$K_2CrO_4 \rightleftarrows CrO_4^{2-} + 2\ K^+$	0.23 [mol L^{-1}]^3
$Na_2CrO_4 \rightleftarrows CrO_4^{2-} + 2\ Na^+$	3.65 [mol L^{-1}]^3
$(NH_4)_2CrO_4 \rightleftarrows CrO_4^{2-} + 2\ NH_4^{2+}$	20 [mol L^{-1}]^3
$K_2Cr_2O_7 \rightleftarrows Cr_2O_7^{2-} + 2\ K^+$	4.9×10^{-3} [mol L^{-1}]^3
$Na_2Cr_2O_7 \rightleftarrows Cr_2O_7^{2-} + 2\ Na^+$	510 [mol L^{-1}]^3
$(NH_4)_2Cr_2O_7 \rightleftarrows Cr_2O_7^{2-} + 2\ NH_4^{2+}$	4 [mol L^{-1}]^3

Source: Data taken from Reference [7]

5 to 12 Cr(III) precipitates as $Cr(OH)_3$, and the formation of mixed hydroxides (e.g., (Cr, Fe)$(OH)_3$), which have even lower solubilities than $Cr(OH)_3$, can reduce the concentration of soluble Cr(III) to apparently zero. At a pH-value above 12, $Cr(OH)_3$ shows its amphoteric character and is transformed into the readily soluble tetrahydroxo complex $Cr(OH)_4^-$ (pK_a of 15.4) [12]. These strongly basic conditions are usually not found in the environment but can be a reason for chromium mobility in chemical landfill sites. The presence of organic complexing agents such as humic acids, tannins or polyhydroxyacids, can prevent Cr(III) species from precipitation under slightly acidic to basic conditions. This behavior is relevant for the mobility of chromium compounds and consequently for estimating chromium contamination of a specific environmental compartment.

Absorption and desorption reactions at mineral surfaces are important for understanding the fate and transport of chromium, as they affect its concentration in the environment. Sorption causes the removal of chromium from aqueous medium to the surface of a solid material. The sorption of Cr(III) and Cr(VI) from aqueous solution on bentonite, for example, was studied by Khan *et al.* [15] Chromate, for instance, can be sorbed to minerals that expose hydroxy groups on their surfaces [14]. This process can also be used for analytical purposes in connection with chromium speciation (e.g., Al_2O_3 filled chromatographic columns) (equation 2.6.1.6).

$$R\text{–}OH + H^+ + HCrO_4^- \rightleftarrows R\text{–}OH_2^+HCrO_4^- \quad (2.6.1.6)$$

Conversely, Cr(III) can sorb to partially negatively charged surfaces like silicates, and organic complexes of Cr(III) can sorb to organic matter [16]. Extent and kinetics of such processes depend highly on different variables like pH, surface area, temperature, or density of active sites. Therefore, generalized assumptions about sorption processes cannot be made.

3 SPECIATION PROCEDURES

As has been discussed in the previous chapter, speciation of chromium is most often reduced to the quantification of the two main oxidation states III and VI, following the requirements of governmental regulations that mainly cover only the quantification of the total amount of chromium or of Cr(VI). Therefore, in the following, we will discuss only those procedures and problems related to the main two species.

Speciation of chromium in environmental samples as an analytical process of identification and quantification involves five to six important steps (depending on the matrix), which have to be brought carefully into line with the respective analytical problem. These steps are typically sampling, sample storage, sample pretreatment (extraction, matrix separation, preconcentration), separation of species, detection, and calibration. Each one of these steps of the procedural chain can influence the accuracy of determination of both chromium species, and each one has to be optimized with respect to the others.

The most crucial steps are sampling, long-term storage, sample pretreatment, and species separation because during these operations species conversion has the highest probability to occur. As has been discussed in the previous chapter, conversion of the oxidation state could proceed in both directions, oxidation as well as reduction, but Cr(III) is unlikely to be oxidized to Cr(VI) under usually applied conditions of storage and sample pretreatment, at least in case of liquids. The oxidation of Cr(III) to Cr(VI) takes place only under drastic conditions, that is, heating and the presence of oxygen or an oxidizing agent such as Mn(IV) in a strongly alkaline medium. Therefore, for accurate quantification of both chromium species major emphasis has to be placed on preventing Cr(VI) from reduction during the whole analytical procedure.

3.1 Sampling and storage

Concerning the species conversion, the time needed for sampling and the lapse between sampling and analysis are becoming essential factors. This problem strongly changes with the matrix to be investigated. In the case of liquid samples,

such as natural water or sewage, the time of sampling is very short compared to storage/transport and analysis of the sample. The same applies to most solid matrices, such as soils or sediments. In the case of sampling airborne particulate matter, the conditions are different. Airborne particles are collected on filters, in impactors, or in impingers. Because of the very low concentration of chromium in this material (esp. Cr(VI)), large volumes of air have to be filtered, and therefore the sampling time has to be rather long (up to several days), which drastically increases the risk of species conversion. In general, sampling needs proper planning in order to obtain reliable results representative for the system under investigation. For instance, natural waters and sewages are in a persistent equilibrium with the sediments at the ground and with the atmosphere. Sampling may disturb this equilibrium and can lead to a significant change in the fractions of the species present. A means to avoid such changes is to collect a certain amount of the sediment as well, to permit the solution/dissolution equilibrium to exist for a longer time. Keeping the equilibrium between aqueous phase and atmosphere for a longer time is nearly impossible because of the limited volume of the closed vessels mostly used for sampling. Furthermore, if storage is necessary, it is important to keep the temperature as low as possible for two reasons. First, cooling resp. freezing the sample will slow down the reaction kinetics between chromium species and other redox partners present in the sample to a much lower level. Second, at lower temperatures the biological activity of microorganisms present in the sample decreases. In the case of samples heavily loaded with microorganisms (i.e., sewage), it might be appropriate to freeze the sample to stop practically any microbiological activity that could affect the species distribution. To minimize errors possibly caused by these problems, the sample should be analyzed immediately after collection.

3.2 Pretreatment

Sample pretreatment and analyte preconcentration are often necessary to remove the main portion of the interfering matrix, to bring the species into a separable and/or detectable form and to achieve the needed detection limit, and is often intended to prepare the species for separation, applying suitable chemical modification. Preconcentration and separation of the chromium species make use of obvious differences in their chemical behavior, that is, electrical charge, complexation properties, and solubilities. The difference in charge is utilized, for example, in ion chromatography to separate the negatively charged chromate anions from the positively charged Cr(III) complexes.

The mostly used means of pretreatment for chromium speciation consists in complex formation. Chromium, as has been discussed in the previous chapter, can form different complexes depending on its oxidation state. A frequently used method for detection of Cr(VI) is its selective reaction with diphenylcarbazide (DPC), first mentioned in 1900 [17], which results in a bright purple-colored Cr(III) complex that can be photometrically detected at 540 nm. This method is very robust and sensitive and tolerates many uncolored matrices. Another possibility is complex formation through reaction with different substituted dithiocarbamates, that is, ammonium pyrrolidine dithiocarbamate (APDC), dialkyl dithiocarbamates, and several alkylene bisdithiocarbamates (BDTCs). The chromium dithiocarbamate complexes are formed – in contrast to the DPC complex – with both species, Cr(VI) and Cr(III). It is therefore necessary to separate these complexes prior to detection. Several other complexes suitable for chromium speciation are described in the literature. They are formed with substituted quinolines and Cr(VI) and Cr(III), with ethylenedinitrilotetraacetic acid (EDTA) and some organic anions and Cr(III), and with a great number of other organic ligands and Cr(VI).

Oxidation/reduction procedures are another important means for pretreatment. Some authors describe the oxidation of Cr(III) to Cr(VI) in order to measure total chromium and to calculate the Cr(III) content as the difference between total chromium and Cr(VI). The method can be applied *vice versa* to calculate Cr(VI) as the difference.

3.3 Species separation

The next important step in the speciation procedure is the separation of the different species. Many different methods were described in the literature. Among them, liquid–liquid extraction was frequently applied. Both species can be separated, for instance, by using a liquid anion exchanger such as Amberlite LA-2, which extracts the chromate anion from the sample. Organic Cr(III) complexes, also those formed during sample pretreatment, can be extracted into an organic solvent, for example, 4-methyl-2-pentanone (MIBK or IBMK). Up to now, liquid–liquid extractions were carried out only as batch procedures, which makes them time consuming and sometimes difficult to handle. Because of the needed amount of solvent, its contamination with chromium is often the reason for a higher limit of detection.

The most commonly used method for chromium species separation is liquid chromatography in one or the other form. The major advantage is that separation and the subsequent detection can be directly coupled to each other. A large variety of column materials were used for chromium species separation, for example, activated or modified alumina, silica gel, sorbents based on cellulose, dextranes, and various other modified materials. Instead of treating all these solid phases in detail, we focus on the different types of chromatographic separation. The mainly used method for chromium species separation is ion chromatography. Cation-exchange material is capable of retaining positively charged Cr(III) ions, whereas anion-exchange material retains the negatively charged chromate anion. For this purpose, various strongly or weakly acidic cation-exchange resins and strongly or weakly basic anion-exchange resins were used. In some cases, ion-exchange chromatography was applied just for removing one species and to detect the other one. An elegant way to combine preconcentration with species separation is to retain the species of interest on the ion-exchange resin and to change the eluent afterward (either change of pH or change of ionic strength). Through the elution, the retained species is released from the column into a much smaller volume compared to the original sample, and accordingly the limit of detection can be increased dramatically. If a mixed bed ion-exchange resin is used and an adequate solvent employed (isocratic or gradient elution), both species can be retained and separated [18]. This chromatographic technique is mostly used with on-line detection, which means that preconcentration, separation, identification, and quantification of the different chromium species are carried out in a one-step analytical process. On-line detection offers several advantages because it noticeably reduces the time needed for the analysis and by this means reduces the danger of species conversion. Such modern hyphenated techniques that comprise on-line pretreatment, separation, and detection have become state of the art, especially for matrices with low chromium content and for routine analysis with a high sample throughput.

Another often-used chromatographic technique is ion pair chromatography. In this case, a reversed phase column material with a C_8 or C_{18} *n*-alkylated surface is used, which needs to be conditioned either with a tetra-*n*-butylammonium salt to retain anions or with an *n*-octylsulfonyl salt to retain cations. Such columns show reversed phase as well as ion-exchange properties and allow the separation of chromate and Cr(III) ions without any sample pretreatment. Additionally, the separation and detection of organic Cr(III) complexes, owing to interaction with the reversed phase material, is possible. In the ion-exchange mode, organic Cr(III) complexes will not be retained and arrive at the detector with the void volume. Reversed phase chromatography is also frequently recommended for separation of chromium species. Here, it is necessary to work with organic complexes of either one or both chromium species. Furthermore, capillary electrophoresis was applied to chromium species separation. This technique has the characteristic feature (which may be an advantage) that only a very small sample volume can be applied. An advantage is certainly the high separation efficiency; a serious disadvantage, however, is the sensitivity toward the composition of the sample matrix. If the sample contains higher concentrations of electrolytes or organic matter, the

separation will be seriously disturbed, if not impossible at all. Several fractionating techniques such as filtration, adsorption, precipitation, centrifugation, coprecipitation, and electrochemical procedures are described in the literature. These methods are often applied to a specific matrix or are used for samples that contain very high concentrations of chromium. These will not be discussed here – additional information is given elsewhere [4–6, 19].

3.4 Detection

Among the detection methods used for chromium speciation, spectrometric and photometric techniques are the most popular ones. The selection of the proper methodology is of course strongly related to the concentration of the species to be determined and the matrix in which they are present. Therefore, photometric techniques are most often applied to samples that contain higher chromium concentrations, for instance, to waste waters, whereas spectrometric techniques in combination with trace enrichment have been applied to matrices such as unspoiled groundwaters and environmental samples with a very low concentration of chromium, owing to their better sensitivity compared to the other methods.

The mainly used detectors for chromium speciation published during the last 20 years are ultraviolet visible (UV/VIS) photometry (more than 30% of published literature) and atomic absorption spectrometry (AAS) (more than 20% of published literature) [6]. The other detection methods like chemiluminescence or fluorescence (molecular spectrometry), diode laser atomic absorption spectrometry (DL-AAS), inductively coupled plasma atomic emission spectrometry (ICP-AES) or inductively coupled plasma mass spectrometry (ICP-MS), X-ray fluorescence spectrometry (XRF), neutron activation analysis (NAA), and various electrochemical methods are only used for special applications.

The most common way for chromium speciation is to determine the total amount of chromium and the amount of one of the species, the other one is then calculated by subtraction. The total amount of chromium can be determined either after acidic digestion or (mostly) after oxidation of all chromium to Cr(VI) followed by the measurement of the latter (either species selective or unselective). The reduction of Cr(VI) to Cr(III) is applied to a lesser extent. Some authors describe the quantification of both species (for example, with mixed bed ion-exchange chromatography) to determine the total content of chromium in a sample. In this case, the result of the quantification has to be carefully verified because only the soluble fractions of the chromium species can be determined, and the presence of different Cr(III) complexes can easily lead to false measurements and quantifications. By far the most frequently used method of detection and determination of the different chromium species in aqueous media is the reaction of Cr(VI) with DPC and the subsequent measurement with UV/VIS photometry. The overall content of chromium in the samples can be determined with the same method after oxidation of Cr(III) with alkaline hydrogen peroxide or sodium metaperiodate. This method is robust and only little susceptible to interferences. Nevertheless, the detection of the diphenylcarbazide-Cr(VI) complex can be interfered by the presence of high concentrations of Fe(III), Hg(II), Mo(VI), and V(V) ions, but these ions can be separated, if necessary, prior to detection, for example, by ion chromatography. Additionally, mathematical corrections can be applied to reduce the negative photometric effects of the interfering ions [20]. This method of Cr(VI) detection in aqueous media is up to now the most important method to quantify Cr(VI) and is documented by several national and international standards, for example, Environmental Protection Agency (EPA) methods 7196A [21], 7199 and 218.6 [22] in the United States, DIN 38405-24 [23] and DIN 19734 [24] in Germany, and ISO 11083 [25].

4 LIQUID MATRICES

Compared to solids, liquid samples are easier to analyze because sampling and sample preparation are straightforward operations and usually no

extraction procedure is required. Problems discussed in the literature are mostly related to native waters (ground- and surface waters), potable waters and waste waters [6]. The latter ones pertain to the group of most frequently investigated samples to clarify the question in which form chromium is released, transported and deposited in the environment. During the years 1983 up to spring 1999, more than 400 articles were published [6] that deal with chromium speciation in aqueous samples. This, on the one hand, shows the interest in chromium speciation in aqueous media and, on the other hand, points to the necessity of validating new speciation methods with liquid standards, which have to be easily accessible.

The sampling of liquids such as natural water or sewage requires only a very short time compared to the sampling of, for example, airborne particulate matter. Therefore, the possibility of species conversion during sample collection is negligible compared to the subsequent time consuming storage/transport and analysis steps. One approach to reduce species conversion during and after the sampling process is to couple the collection directly with a suitable preconcentration step. Sampling of river water directly on a micro chromatography column filled with aluminum oxide was described by Cox and McLeod [26]. After sampling, the column is inserted into a flow-injection system in order to carry out on-line elution and detection. This strategy, called "in-field sampling", has the advantage to preserve the species and to remove most of the matrix that can interfere with species detection and quantification. A risk of species transformation during sampling, however, still remains because of the increased concentration of the adsorbed chromium species and their reaction with redox partners present in the matrix.

In case only one species can be detected and quantified (e.g., via species selective complexation), oxidation or reduction may be applied to measure total chromium. This way was chosen by Mugo and Orians [27] for investigation of sea water. They prepared selectively a volatile complex of Cr(III) with 1,1,1-trifluoroacetone that was quantified with an electron capture detector after separation by gas chromatography. The overall chromium content was determined after reduction of Cr(VI), either keeping the acidified (pH = 2) sea water at room temperature for 24 h or adding sodium sulfite at a pH of 6. This method is carried out in a batch mode, and due to the larger sample volumes needed, the risk of contamination is significant. Such a disadvantage can be overcome by using an on-line system for separation and detection [28]. An exemplary article of Padarauskas *et al*. [29] should be mentioned. The authors describe an on-line preconcentration and determination of Cr(VI) in drinking water, surface water, and groundwater by high-performance liquid chromatography (HPLC) using precolumn complexation with DPC. The collected samples (up to 100 mL) are treated with an acidic DPC solution, and after the development of the purple color the complex is collected on a short concentrator column filled with reversed phase material. After the collection is accomplished, the liquid flow is switched to a water/acetonitrile mixture, for chromatography on a 100 mm-C_{18}-RP column and on-line detection with an UV/VIS detector. With skillful construction of the HPLC system, the whole process can be fully automated. The use of a concentrator column (which equals a solid phase extraction) increases the detection limit noticeably and eliminates a major part of the matrix that may disturb the detection. The reversed phase chromatography separates the chromium-DPC-complex from the rest of the matrix so that it leads to a sharp signal in the UV-detector. The authors reach a detection limit for Cr(VI) of 20 ng L^{-1}, which equals an absolute amount of 2 ng Cr(VI) in a 0.1 L sample. This example points out that hyphenation of preconcentration, chromatographic separation, and detection may significantly improve the selectivity and sensitivity of the determination of different chemical forms of chromium in liquid samples. Another example is given by Andrle *et al*. [30], who are able to detect both chromium species in galvanic waste waters. Except for sampling, the whole speciation process is performed on-line. The aqueous sample of about 15 mL is continuously mixed with a buffered ammonium pyrrolidine dithiocarbamate

(APDC) solution, and after passing a tube reactor to complete the reaction the resulting complexes of both chromium species are collected on an RP-SPE-column. From here, they are eluted with a 65% acetonitrile/water mixture, transferred onto a C_{18}-RP-HPLC column for separation and detected with ICP-MS, graphite furnace atomic absorption spectrometry (GFAAS) or UV-VIS photometry. The best results with respect to selectivity and sensitivity are achieved by coupling RP-HPLC with ICP-MS using a hydraulic high-pressure nebulizer (HHPN). Here, some oxygen has to be added to the sample gas to reduce the amount of molecular interferences (^{38}Ar-^{12}C-compounds). The authors chose the ^{50}Cr isotope for detection with respect to little interferences and a good signal/noise ratio. With this approach, the authors achieved a detection limit of 0.1 $\mu g L^{-1}$ (2 pg abs.) for Cr(VI) and 0.2 $\mu g L^{-1}$ (4 pg abs.) for Cr(III). Beside these very low detection limits, the ICP-MS detection offers the additional advantage of making possible multielement measurements. Since there exist many elements that can be complexed by APDC, this method has the potential for multielement speciation in a single-step analytical approach.

5 SOLID MATRICES

5.1 General remarks

Even nowadays, chromium speciation in solid material remains an analytical challenge because an extraction procedure has to be applied. The general approach described in the literature is extraction under acidic, neutral, or alkaline conditions. Each one of these is problematic, concerning recovery as well as species conversion. Because of some special features, the speciation of chromium in airborne particulate matter will be discussed in a separate chapter.

Sampling of solids requires about the same precautions as sampling of liquids. Care has to be taken that the sample keeps its original composition with respect to the chromium species, therefore freezing or freeze-drying is recommended. The subsequent step of species extraction is the most challenging part of speciation in solid matter because of the difficulties in achieving sufficiently high recoveries and in avoiding species conversion during this procedure. On the one hand, high recovery requires strongly acidic or alkaline conditions, but this increases the risk of species conversion. On the other hand, more moderate conditions of extraction prevent species conversion, but the dissolution of some chromium compounds (esp. Cr(III) complexes and some metal chromates) can be hindered. As can be taken from the chemical section, the use of acids for dissolution would lead to wrong results because of the high oxidation potential of chromate at low pH-values. At a pH above 6, the chromate is much more stable, but most of the Cr(III) compounds and some poorly soluble chromates such as $PbCrO_4$, $BaCrO_4$, or $ZnCrO_4$ will not be dissolved. Strongly alkaline conditions imply the risk of a possible oxidation of Cr(III) to Cr(VI) in the presence of oxidizing substances, for example, oxygen or Mn(IV) salts. The best compromise for extraction is a pH of 8 to 10, in which the major part of the sparingly soluble chromates can be dissolved. In case Cr(III) is present, masking by a complexing agent such as EDTA or TRIS will prevent Cr(III) (hydroxy- and aquo-complexes) from oxidation [31]. An interesting approach for species conserving extraction of Cr(VI) from solid matrices was published by Foy *et al.* [32] The authors used a supercritical fluid extraction (SFE) with carbon dioxide to extract selectively Cr(VI) from a solid soillike matrix and used lithium bis(trifluoroethyl)dithiocarbamate as chelating reagent. The dried chelate was then dissolved in methanol and quantified with ICP-AES. The authors received extraction recoveries of about 88% when using a National Institute of Standards and Technology (NIST) standard, but the usefulness of this method has to be proved in future with natural material. Another example for a gentle extraction method is given by Wang *et al.* [33] The use of ultrasonic extraction with an alkaline ammonium buffer is capable of extracting even sparingly soluble chromates such as $PbCrO_4$ with recoveries of more than 85%. In combination

with a strong anion-exchange solid phase extraction (SAE-SPE), which removes Cr(III) and the major part of the interfering matrix, the Cr(VI) is determined as Cr(III)-DPC-complex and quantified with UV/VIS-photometry. The authors received a detection limit of 80 ng Cr(VI) per sample. Their method is applicable for on-site monitoring of Cr(VI) in environmental and industrial hygiene samples. Several other examples of chromium speciation in solid matrices, for example, in soil, sediment, metal, ore, sludge, cement, leather, and so on, can be found in the review of Marqués *et al.* [5]

Considering the literature of the last decades, it is essential for a correct determination of Cr(VI) in solid material to use an alkaline buffer solution for extraction. In the presence of oxidizing compounds or if heat has to be applied to the sample during the extraction process, it is necessary to add a complexing agent to prevent oxidation of soluble Cr(III). Depending on the investigated material, it is appropriate to use a species selective determination of Cr(VI), that is, complex formation and unspecific (UV/VIS) or element specific (atomic absorption spectrometry (AAS), atomic emission spectrometry (AES), mass spectrometry (MS), etc.) detection. If chromatography is used for species separation, a critical alignment to the matrix has to be performed. Even if an element-specific detector is used, the determination of Cr(VI) can be seriously disturbed because of varying amounts of Cr(III) complexes.

Recently, Kingston *et al.* presented an important application of "speciated isotope dilution mass spectrometry" (SIDMS) for chromium speciation in water [34] and in solid samples [35]. This is to our knowledge the first approach to evaluate the species conversion that may occur during sampling, pretreatment, and separation. For this purpose, both species have to be accessible in different isotope-enriched forms, for example, Cr(III) as a ^{50}Cr-enriched standard and Cr(VI) as a ^{53}Cr-enriched standard, or *vice versa*. The sample is spiked with a known concentration of each isotope-enriched species that should equal the concentration present in the sample to achieve the highest accuracy during the isotope ratio measurement. After separation of the different species, for example, using ion-exchange chromatography, the isotope ratios in both chromium species are determined. With four isotope ratios (^{50}Cr(III)/^{52}Cr(III), ^{53}Cr(III)/^{52}Cr(III), ^{50}Cr(VI)/^{52}Cr(VI), ^{53}Cr(VI)/^{52}Cr(III)) a set of four equations can be solved to calculate the initial concentrations of Cr(III) and Cr(VI) as well as the degree of conversions between Cr(III) and Cr(VI) that have occurred after spiking. SIDMS as well as isotope dilution mass spectrometry (IDMS) can be applied to the development of standard reference materials for chromium speciation in the environment. The production and development of standards, which take into account possible matrix effects, is an urgent need, in particular, for solid matter. Only two matrix-adapted standards for chromium speciation were developed so far. One is freeze-dried matter in a lyophilized form (BCR-544) [36], which contains both chromium species in a concentration (approx. 25 $\mu g\,L^{-1}$) that can appear in natural/drinking water. In this form, the reference material can be stored for a long time without any species conversion. A simple dissolution in a carbon dioxide aerated sodium hydrogen carbonate buffer at a pH of 6.4 gives a ready-to-use reference standard. The other one is the only solid matrix adapted Cr(VI) reference standard. It consists of a glass fiber filter loaded with welding dust that contains about 100 μg Cr(VI) (BCR-545) [37].

5.2 Airborne particulate matter

Speciation of chromium in airborne particulate matter has received an increasing interest during the last decade [19] and is presently one of the most urgent analytical problems to be solved. In comparison to dust of some contaminated working places (e.g., welding shop [38] or stainless steel production), the concentration of Cr(VI) in airborne particulates is very low. Therefore, the sampling times have to be quite long as compared to the sampling times of other matrices, where the amount of collected matter is not time-dependent.

This particular requirement increases the risk of species conversion dramatically because Cr(VI) is in contact with the sampling substrate (filter, impinger solution, impactor membrane, etc.) for a long time, and possibly reducing material (e.g., Fe(II), organic matter) is accumulated likewise during collection or is in steady contact with the sampled material (for instance, sulfur dioxide).

For sampling of airborne particulate matter, different methods can be employed. The most frequently used technique is air filtration. Many filter materials were used for this purpose, for example, regenerated cellulose (RC), cellulose nitrate (CN), cellulose acetate (CA), glass fibers (GF), quartz fibers (QF), polycarbonate (PC), polyethersulfon (PES), nylon, polypropylene (PP), polyvinylchloride (PVC), polytetrafluoroethylene (PTFE) or polyvinylidenefluoride (PVDF), with pore diameters between 0.2 μm and up to 10 μm. Choosing the right material for chromium speciation is essential. The blank value and the stability of the different chromium species under sampling conditions have to be carefully investigated for each filter material before use. A very inert filter material, and one of the most expensive too, is PTFE. However, filters made of PTFE are a good choice in case they have to be coated with some aggressive chemicals. Neidhart *et al*. [39] coated PTFE filters with NaOH and PbO_2 to stabilize Cr(VI) in strongly alkaline medium and to suppress the reaction of sulfur dioxide with chromate because of oxidation of SO_2 by lead dioxide. Here, the use of PTFE filters is mandatory because most of the other filter materials would be destroyed under these conditions. This approach, however, is not useful for routine measurements. Only filters with a diameter of less than 50 mm can be used in this way, the handling of bigger filters coated with NaOH and PbO_2 is almost impossible without breaking up the coating. Therefore, the sample throughput is restricted to less than 7 m^3 in 24 h, which does not allow to achieve a limit of detection lower than approx. 2 ng m^{-3}. A significant extension of the sampling time would lead to Cr(VI) conversion for reasons already mentioned before. The typical half-life period of Cr(VI) in ambient particulate matter is about 13 h [40]. During the sampling process, it might decrease because of the accumulation of reducing particulate substances and the exposition to reducing trace gases. In Figure 2.6.1.2, the decrease of Cr(VI) on a loaded filter during collection of airborne particulate matter is shown as a function of sampling time. On a CN-filter loaded with 7.1 ng cm^{-2} Cr(VI) before sampling, airborne particulate matter is collected with a flow rate of 0.16 m^3 h^{-1} cm^{-2} in a municipal area. After 1 h, approx. 50% and after 6 h more than 80% of the Cr(VI) were reduced. In this case, speciation was carried out – after extraction of a part of the filter with a $NaHCO_3/CO_2$ buffer at pH 6.4 – with

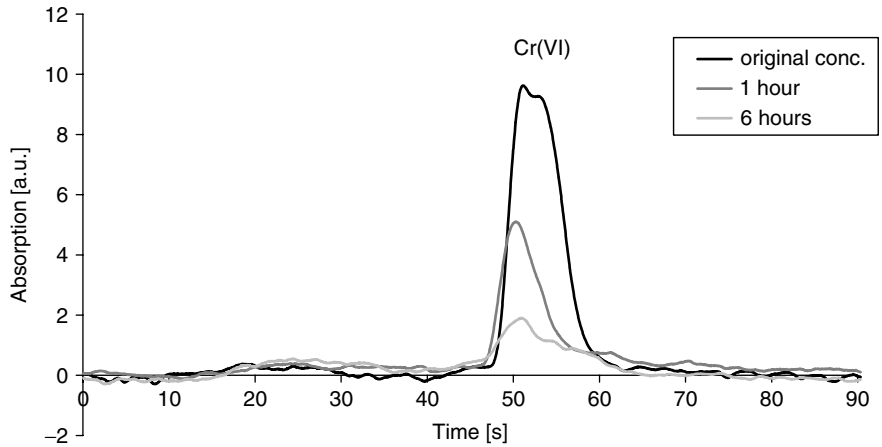

Figure 2.6.1.2. Reduction of Cr(VI) on a filter during sampling of airborne particulates.

ion pair chromatography coupled to DL-AAS [41] (diode laser atomic absorption spectrometry) for detection (conditions: see [42]).

Reducing gases may be (partially) removed with diffusion scrubbers (denuders or coated sieves) [39], assembled in front of the filter holder. A selective removal of reducing particles, however, is not possible. Even the size selective sampling of particles with an impactor does not help much since chromium containing particles can range in size from below 1 μm (incineration) over 5 to 50 μm (melts) up to 100 μm (Cr-plating). The mass median diameter of chromium containing particles in the environment is about 1.5 μm [43].

An example of metal speciation in airborne particulate matter is given in Figure 2.6.1.3. The aerosol was collected in an industrial urban area at wintertime. Here, a multielement chromatogram is shown after species separation with ion chromatography (Dionex, AS 7) with an Element 2 (Finnigan MAT) ICP-MS as detector. Figure 2.6.1.3 easily indicates the usefulness of ICP-MS as detector for metal speciation because of its multielement detection capability. Beside its high sensitivity for a variety of metal and nonmetal ions, the ICP-MS can give additional information of possible redox partners, for instance, Fe(II), present in the sample that can influence the presence of Cr(VI) in the environment.

Figure 2.6.1.3 shows the relative high amount of Fe(II), which is typically higher in winter than in summertime [44]. Rhodium and indium are used as internal standards, whereas Rh(III) indicates the void volume (no retention time on this column). In(III) is used for the internal calibration. In the case of a very difficult matrix, ion chromatography can be disturbed if, for example, a lot of different Cr(III) complexes are present in the sample, which could have nearly the same retention time as Cr(VI). If unknown samples have to be analyzed, a validation with a species selective detection method (e.g., complexation with DPC) is recommended.

An approach toward on-line monitoring of hexavalent chromium using filters for collection of airborne particulate matter was published recently by Samanta *et al.* [45] The authors describe a fully automated system for sampling, extraction, separation, and detection of aerosol Cr(VI). Particulate matter is collected on glass fiber filters (45-mm diameter) during 15 min (60 L throughput), therefore changes in species content should be very small. The system works with two different filters, one is collecting airborne particles, while the

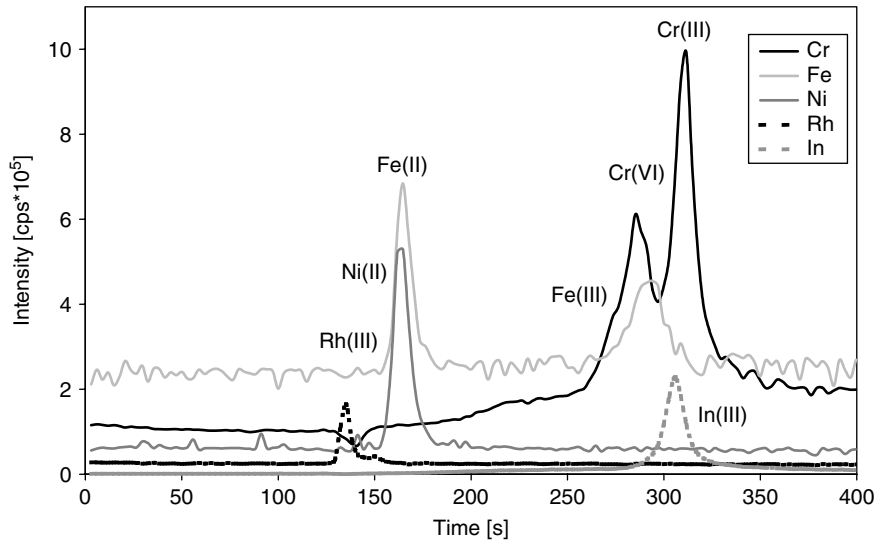

Figure 2.6.1.3. Multielement detection capability of ICP-MS.

second one is extracted and dried. By this means, monitoring of aerosol chromate with a good temporal resolution is possible. The loaded filter is extracted with 10 mmol L^{-1} NaOH (which is necessary for solubilization of lead chromate and other sparingly soluble chromates), the extract is neutralized in a suppressor system, and the chromate is collected on an anion-exchange preconcentration column. Then the chromate is eluted with an alkaline perchlorate solution and detected photometrically after reaction with DPC in a mixing coil. A detection limit of 5 ng m^{-3} Cr(VI) is reported for this system.

Another sampling device useful for chromium speciation is the traditional impinger. Compared to the filter sampling technique, the impinger is rather limited with respect to the gas flow rate (up to 10 m^3 per 24 h). Nevertheless, impingers offer some advantages, for instance, the dilution of the collected material during the sampling process through the sampling liquid, reducing the danger of unwanted side reactions of the chromium species. Furthermore, the species of interest can be stabilized immediately during sampling by a buffered medium. Cr(VI), for instance, can be stabilized by use of an alkaline buffer solution, which decreases the reactivity toward reducing substances. Cr(III), which is prone to oxidation in strongly alkaline medium because of oxidants such as oxygen and some highly oxidized metal ions, can be protected through complexation with EDTA or TRIS. The advantage of adjusting the impinger buffer solution to achieve maximum stability of the sampled species clearly outweighs the disadvantage of a lower flow rate. This is indicated in several papers that compare the collection of airborne particulate matter with filters and impingers. In nearly all cases, a higher Cr(VI) concentration was found when impinger sampling was applied [46].

6 FOOD

The speciation of chromium in food is only rarely performed during the last decades. Mainly soluble chromium has been detected and acid or high temperature digestions have been carried out to quantify the total amount of chromium (see [5]). It is not remarkable to find only very few references about determining Cr(VI) in food because of the reductive potential of organic matter. The lifetime of small concentrations of readily soluble chromates in food should be short (approx. minutes to hours). Sparingly soluble chromates such as $PbCrO_4$, in particular when higher concentrated, might be stable in food for a much longer time.

Chromium was first discovered as an essential trace element in 1955. The body of an average healthy individual contains only several milligrams. However, this small amount plays important roles in the enhancement of insulin's effectiveness, regulation of blood sugar levels, and the activation of various enzymes for energy production. These are some reasons why chromium picolinate, a trivalent form of chromium complexed with picolinic acid, is used as a nutritional supplement [47], but it is also promoted by manufacturers for weight loss, particularly for obese people who may be in danger of developing diabetes. Scientists have been studying the supplement's potential role in weight control, but so far the most carefully conducted studies have shown no benefits. Because chromium helps insulin to do its job, it seems reasonable that it might help people with Type 2 diabetes or those at high risk for developing it. Low levels of chromium are characteristic of diabetes, though there is no evidence that low chromium causes diabetes. Some studies have found that chromium picolinate supplementation in doses of 200 micrograms is beneficial, but others have not. The main reason for these inconsistent results is that even nowadays it is difficult to diagnose chromium deficiency by use of atomic spectroscopy and it is still an analytical challenge for speciation studies performed at molecular levels.

Concerning Cr(VI), there is one article given in the literature by Soares *et al*. [48], who performed a determination of Cr(VI) in animal feeds. The authors used an alkaline extraction with 0.01 M NaOH and, after centrifugation, determined the chromium content in the supernatant

liquid species unselective with electrothermal atomic absorption spectrometry (ET-AAS). This approach could lead to higher values for Cr(VI) than present in the sample. Due to the high pH-value of 12, some Cr(III) could be dissolved as $Cr(OH)_4^-$. Therefore, an additional species separation step or a species selective detection method is recommended.

7 CONCLUDING REMARKS

Despite the significant advances that have been made in metal speciation analysis techniques over the past 25 years, much remains to be done. Several new approaches for separation of chromium species using different pretreatments and various chromatographic techniques have been developed. During the last years, considerable efforts in the development of hyphenated techniques, that is to say coupling of high-performance separation techniques with element-selective or structure-selective detectors, have been made. The state of the art nowadays in chromium speciation is to perform the speciation process on-line, that includes sample pretreatment, species separation, determination and quantification, and sometimes even sampling in one continuous process. This approach can reduce the blank value of chromium due to usually smaller volumes of solvents necessary for pretreatment and species separation. In addition, on-line methods are much less time consuming compared to batch methods. It is now well established that flow methods provide the best alternative to obtain in-field preconcentration as well as removal of matrix at the same time, thus improving the sensitivity and selectivity of the detection methodologies. Moreover, the use of flow-injection methods provides an easy way to combine several chromatographic techniques with different detection methodologies. Very powerful separation techniques and extremely sensitive detection methods for chromium have been developed, such as capillary electrophoresis for separation or stripping voltammetry techniques for molecular detection. These techniques, however, are strongly interfered by the matrix and therefore are somewhat limited in use. The development of an efficient and selective matrix separation technique is a requirement to receive the low detection limits that are necessary for the determination of Cr(VI) in environmental matrices.

Another big problem that has to be solved in future is the realization of a sampling procedure of airborne particulate matter that keeps the species proportion. During the time-consuming sampling process, a lot of redox processes can take place that can change the ratio of Cr(III) to Cr(VI). Efforts have to be done to understand the fate of chromium in the environment and to develop a sampling technique that keeps chromium at its original oxidation state. The use of multielement detection techniques such as ICP-MS and ICP-AES offers the possibility of detecting several other possible redox partners of chromium, thus giving more information about chromium's fate in the specific matrix.

8 REFERENCES

1. *The Economics of Chromium*, 9th ed., Roskill Information Services Ltd. 27a, Leopold Road, London, UK, http://www.roskill.co.uk/chrome.html, 2000.
2. Nriagu, J. O., Production and uses of chromium, in *Chromium in the Natural and Human Environments*, Advances in Environmental Science and Technology Series, Vol. 20, Nriagu, J. O. and Nieboer, E. (Eds.), Wiley-Interscience, New York, 1988, p. 81.
3. Guthrie, B. E., The nutritional role of chromium, in *Biological and Environmental Aspects of Chromium*, Langård, S. (Ed.), Elsevier, Amsterdam, 1982, p. 117.
4. Kotas, J. and Stasicka, Z., *Environ. Pollut.*, **107**, 263 (2000).
5. Marqués, M. J., Salvador, A., Morales-Rubio, A. E. and de la Guardia, M., *Fresenius' J. Anal. Chem.*, **362**, 239 (1998).
6. Marqués, M. J., Salvador, A., Morales-Rubio, A. E. and de la Guardia, M., *Fresenius' J. Anal. Chem.*, **367**, 601 (2000).
7. Kimbrough, D. E., Cohen, Y., Winer, A. M., Creelman, L. and Mabuni, C., *Crit. Rev. Environ. Sci. Technol.*, **29**, 1 (1999).
8. Tandon, R. K., Crisp, P. T., Ellis, J. and Baker, R. S., *Talanta*, **31**, 227 (1984).
9. Shen-Yang, T. and Ke-An, L., *Talanta*, **33**, 775 (1986).
10. Stollenwerk, K. G. and Grove, D. B., *J. Environ. Qual.*, **14**, 396 (1985).
11. Saleh, F. Y., Parkerton, T. F., Lewis, R. V., Huang, J. H. and Dickson, K. L., *Sci. Total Environ.*, **86**, 25 (1989).

12. Rai, D., Sass, B. M. and Moore, D. A., *Inorg. Chem.*, **26**, 345 (1987).
13. Marx, G. and Heumann, K. G., *Fresenius' J. Anal. Chem.*, **364**, 489 (1999).
14. Rai, D., Eary, L. E. and Zachara, J. M., *Sci. Total Environ.*, **86**, 15 (1989).
15. Khan, S. A., Riaz-ur-Rehman, A. and Khan, M. A., *Waste Manage.*, **15**, 271 (1995).
16. Eary, L. E. and Rai, D., *Am. J. Sci.*, **289**, 180 (1989).
17. Cazeneuve, P., *Bull. Soc. Chim. Fr.*, **23**, 701 (1900).
18. Barnowski, C., Jakubowski, N., Stüwer, D. and Broekaert, J. A. C., *J. Anal. At. Spectrom.*, **12**, 1155 (1997).
19. Cleven, R. F. M. J. and de Boer, J. L. M., Characterization of the Cr(VI)/Cr(III) ratio in aerosols, in *Environmental Particles*, Environmental Analytical and Physical Chemistry Series, Vol. 1, Buffle, J. and van Leeuwen, H. P. (Eds.), Lewis Publishers, Boca Raton, FL, 1992, p. 145.
20. Llobat-Estelles, M., Mauri-Aucejo, A. R. and Lopez-Catalan, M. D., *Fresenius' J. Anal. Chem.*, **371**, 358 (2001).
21. Method 7196A, Chromium, Hexavalent (Colorimetric), 1992, Rev. 1, in United States Environmental Protection Agency, *Test Methods for Evaluating Solid Wastes, Physical/Chemical Methods*, SW-846, 3rd ed., Office of Solid Waste and Emergency Response, Washington, DC, 1998.
22. Method 7199, Determination of Hexavalent Chromium in Drinking Water, Groundwater and Industrial Wastewater Effluents by Ion Chromatography, 1996, Rev. 0, in United States Environmental Protection Agency, *Test Methods for Evaluating Solid Wastes, Physical/Chemical Methods*, SW-846, 3rd edition, Office of Solid Waste and Emergency Response, Washington, DC, 1998.
23. DIN 38405-24, Deutsche Einheitsverfahren zur Wasser-, Abwasser- und Schlammuntersuchung, Anionen (Gruppe D), Photometrische Bestimmung von Chrom(VI) mittels 1,5-Diphenylcarbazid (D 24), 1987.
24. DIN 19734, Bodenbeschaffenheit, Bestimmung von Chrom(VI) in phosphatgepufferter Lösung, 1999.
25. ISO 11083, *Water Quality, Determination of Cr(VI) – Spectrometric Method Using 1,5-diphenylcarbazide*, 1994.
26. Cox, A. G. and McLeod, C. W., *Microchim. Acta*, **109**, 161 (1992).
27. Mugo, R. K. and Orians, K. J., *Anal. Chim. Acta*, **271**, 1 (1993).
28. Das, A. K., de la Guardia, M. and Cervera, M. L., *Talanta*, **55**, 1 (2001).
29. Padarauskas, A. V., Judzentiene, A., Naujalis, E. and Paliulionyte, V., *J. Chromatogr., A*, **808**, 193 (1998).
30. Andrle, C. M., Jakubowski, N. and Broekaert, J. A. C., *Spectrochim. Acta B*, **52**, 189 (1997).
31. Pavel, J., Kliment, J., Stoerk, S. and Suter, O., *Fresenius' J. Anal. Chem.*, **321**, 587 (1985).
32. Foy, G. P. and Pacey, G. E., *Talanta*, **51**, 339 (2000).
33. Wang, J., Ashley, K., Marlow, D., England, E. C. and Carlton, G., *Anal. Chem.*, **71**, 1027 (1999).
34. Kingston, H. M., Huo, D., Lu, Y. and Chalk, S., *Spectrochim. Acta B*, **53**, 299 (1998).
35. Huo, D. and Kingston, H. M., *Anal. Chem.*, **72**, 5047 (2000).
36. Vercoutere, K., Cornelis, R., Dyg, S., Mees, L., Christensen, J. M., Byrialsen, K., Aaen, B. and Quevauviller, P., *Microchim. Acta*, **123**, 109 (1996).
37. Christensen, J. M., Byrialsen, K., Vercoutere, K., Cornelis, R. and Quevauviller, P., *Fresenius' J. Anal. Chem.*, **363**, 28 (1999).
38. Spini, G., Profumo, A., Riolo, C. and Beone, G. M., *Toxicol. Environ. Chem.*, **41**, 209 (1992).
39. Neidhart, B., Herwald, S., Müller, T. and Ruchti, B., Verfahren zur Speziesanalyse – spezifische Erfassung von sechswertigem Chrom im Schwebstaub, Umweltforschungsplan des Bundesministers für Umwelt, Naturschutz und Reaktorsicherheit, Luftreinhaltung, Forschungbericht 104 02 268, 1992.
40. Grohse, P. M., Gutknecht, W. F., Hodson, L. and Wilson, B. M., *The Fate of Hexavalent Chromium in the Atmosphere*, Research Triangle Institute, RTI/3798/00-01F, CARB Contract No. A6-096-32, Research Triangle Park, NC, 1988.
41. Koch, J., Zybin, A. and Niemax, K., *Appl. Phys. B*, **67**, 475 (1998).
42. Groll, H., Schaldach, G., Berndt, H. and Niemax, K., *Spectrochim. Acta B*, **50**, 1293 (1995).
43. Cawse, P. A., *A Survey of Atmospheric Trace Elements in the UK, 1972–1973*, Atomic Energy Research Establishment, Harwell, UK, 1974.
44. Barnowski, C., *Entwicklung und Untersuchung von Methoden zur Speziation von Chrom in Umgebungsaerosolen*, Ph.D. Dissertation, University of Dortmund, Germany, 2001.
45. Samanta, G., Boring, C. B. and Dasgupta, P. K., *Anal. Chem.*, **73**, 2034 (2001).
46. Zatka, V. J., *Am. Ind. Hyg. Assoc. J.*, **46**, 327 (1985).
47. Vincent, J. B., *Drugs Future*, **28**, 1079 (2003).
48. Soares, M. E., Bastos, M. L. and Ferreira, M. A., *J. Anal. At. Spectrom.*, **9**, 1269 (1994).

2.6.2 Speciation of Chromium in Occupational Exposure and Clinical Aspects

Perinne Hoet

Université catholique de Louvain, Brussels, Belgium

1 OCCUPATIONAL EXPOSURE

The toxicology of chromium does not reside in the elemental form. It varies greatly among a wide variety of very different chromium compounds. Oxidation state and solubility are particularly important factors in considering the toxicity of chromium with respect to its chemical speciation [1–8].

1.1 Main occupational exposures to chromium

Chromium is seldom used alone; as an additive it endows alloys or materials with new properties: strength, hardness, permanence, hygiene, color and resistance to temperature, wear and corrosion [7]. The metallurgical, refractory and chemical industries are the primary users of chromium. The metallurgical industries consumed 85% of primary chromium during the 1990s, compared to 78% in 1980. This increase is due to the high growth in demand for metallurgical products containing chromium, especially stainless steels. Demand from other markets has been static over the past decade, with 8% destined for chemicals and 7% for refractories and foundry sands [7].

In the metallurgical industry, chromium is used to produce stainless steels, alloy cast irons, nonferrous alloys and other miscellaneous materials. Ferrochromiums are the main intermediates used by the metallurgical industry. Chromium is used as an alloying and plating element on metal and plastic substrates for corrosion resistance in chromium-containing and stainless steels and in protective coatings for automotive and equipment accessories.

In the chemical industry, chromium is used primarily in pigments, metal finishing, leather

Handbook of Elemental Speciation II: Species in the Environment, Food, Medicine & Occupational Health
Edited by R. Cornelis, H. Crews, J. Caruso and K. G. Heumann
 ISBN: 0-470-85598-3 (HB)

tanning and wood preservatives. Chromium compounds offer two distinctive features that govern several main applications, namely, permanence and color stability. Natural materials such as leather, wood and timber are stabilized for durability and long service by chromium salts that also allow permanent fixing of other compounds (mordant behavior) such as colorful dyes, fungicides and insecticides. Leather tanning is the largest chemical use, and timber preservation with the well-known CCA (chromium-copper-arsenic) product has been the fastest growing in recent years. Chromium pigments that are used in paints, inks and plastic coloring are the second largest use. Feature colors are chrome green, chrome oxide green, chrome yellow and molybdenum yellow, while zinc and strontium chromates are used in corrosion-resistant priming paints [7]. Other uses are chromium electroplating, other surface coatings, catalysts, drilling muds, water treatment, textile dyes, inks, toners for copying machines, photography, process engraving, magnetic tapes, pyrotechnics and as catalysts. In the past, chromium was also used in cooling towers as a rust and corrosion inhibitor.

The high melting point of chromium ore has encouraged its use in refractory compositions for more than 100 years. In the refractory industry, chromium is a component in chrome and chrome-magnesite, magnesite-chrome bricks, and granular chrome-bearing and granular chromite, which are used as linings for high temperature industrial furnaces.

Occupational sources of chromium exposure are found in the following industries [1–7]:

With respect to Cr(VI) compounds, the most important exposures are:

- to sodium, potassium, calcium and ammonium chromates and dichromates during chromate production;
- to chromium trioxide (chromium oxide or chromic acid) during chromium plating. There are two types of chrome plating: the decorative plating in which a thin layer of chromium (0.5 to 1 μm: bright chromium platers) is deposited over another metal and the hard plating that produces a thicker coating (5 to 10 μm: hard chromium platers) much more resistant to corrosion than the decoratively plated material;
- to insoluble chromates of zinc and lead during pigment production and spray painting, chromate pigments are used in paints, metal primers, as colorants in rubber, paper and inks;
- to water-soluble alkaline chromates during steel smelting and welding. Cr(VI) compounds can be found in small amounts in highly oxidized fumes during the melting/smelting and pickling stages of the production process and during welding operations [3]. With most arc welding processes, such as Gas Metal Arc Welding (GMAW) also known as Metal Inert Gas (MIG); Flux-cored Arc Welding (FCAW); Shielded Metal Arc Welding (SMAW) also known as Manual Metal Arc (MMA); Submerged Arc Welding (SAW), a small fraction of the filler metal is vaporized-condensed (oxidized) or vaporized-(oxidized)-condensed, creating a fume consisting of small particles containing chromium that is mainly in the trivalent form. Cr(VI) is only present in small proportions. The fumes from SMAW (covered electrode) and FCAW processes contain the highest proportion of Cr(VI) compounds (K_2CrO_4, Na_2CrO_4, $NaK_3(CrO_4)_2$, K_2NaCrF_6), but with these two processes it is possible to employ very efficient fume extraction systems. Gas Tungsten Arc Welding (GTAW) also known as TIG Tungsten Inert Gas or WIG, Wolfram Inert Gas), GMAW and SAW processes do not generate signification amounts of Cr(VI) [9]. Chromium contained in scrap metal is metallic;
- to other chromates during cement production and use;
- to chromates in CCA (chromium(VI) trioxide – copper oxide – arsenic trioxide) timber preservatives. In wood, Cr(VI) is reduced to Cr(III) forming chromium arsenate. Wood used for joinery is well-dried and virtually all Cr(VI) is reduced to Cr(III) and no Cr(VI) was detected in any samples of the work environment in six joinery shops [10]. If wood

is improperly fixed, not as well dried as in joinery wood, exposure to Cr(VI) may occur. Dust from commercially available impregnated wood has been found to contain as much as 20% of total chromium as Cr(VI) [10].

Cr(III) compounds that are common in work place air include:

- chromite ore during chromate production;
- in the ferrochromium industry. Chromium in chromite ore exists entirely as Cr(III) and most is reduced to Cr(0) during the production of ferrochromium. However, oxides of Cr(VI) can be formed at high temperatures during the process because of oxidation of Cr(III); Hexavalent compounds are also found in small amounts in highly oxidized fumes from the melting/smelting process. Hence, during the production of ferrochromium, workers may be exposed to dust and fumes containing Cr(III) and Cr(VI) compounds;
- chromic oxide during pigment production and use;
- chromic sulfate during leather tanning;
- chromic oxide during the production of chromium-containing refractories, for example, the glass production industry, in cement, copper. During the use of chromium-containing refractories, the high temperatures involved and presence of alkalis may result in release of Cr(VI).

Cr(0):

- metallic chromium is an important and widely used alloying element in ferrous and nonferrous alloys. In alloys based on nickel, iron-nickel and cobalt chromium is primarily used to confer oxidation and corrosion resistance. In alloys of aluminum, titanium and copper, chromium is used to control microstructure. It markedly increases the hardness of steel and improves its resistance to corrosion. Stainless steel contains at least 12% and may contain up to 30% chromium. Chromium-containing tool steels contain 1–12% chromium. Chromium-containing steels are used in a wide variety of industrial and domestic applications: from engine and jet engine components to surgical implants. Occupational exposures to airborne dusts containing chromium metal may occur during production, welding, cutting and grinding of chromium alloys.
- Chromium powder is used in the production of welding electrodes and in chromium coatings.

Air limit values for workers exposed to chromium	
ACGIH [11]	
Cr(VI) water soluble compounds	50 $\mu g\,m^{-3}$ (TWA)
Cr(VI) insoluble compounds	10 $\mu g\,m^{-3}$ (TWA)
Cr(0), Cr(III)	500 $\mu g\,m^{-3}$ (TWA)
OSHA [12]	
Cr(VI)	100 $\mu g\,m^{-3}$ as CrO_3 (ceiling limit)
Cr(II), Cr(III)	500 $\mu g\,m^{-3}$ as Cr (TWA)
Cr(0), insoluble salts	1000 $\mu g\,m^{-3}$ as Cr (TWA)
NIOSH [13]	
Cr(VI)	1 $\mu g\,m^{-3}$ (TWA)
Cr(0), Cr(II), Cr(III)	500 $\mu g\,m^{-3}$ (TWA)

Note: TWA = time-weighted value

1.2 Biological monitoring: interpretation

Methods for the determination of chromium in biological and environmental samples are developing rapidly, and early results should be interpreted with caution. The determination of chromium species is currently a very sophisticated procedure, and few analytical data are available. The biological tissues appear to be the least adequately addressed of the matrices with respect to the chemical speciation of their chromium contents [8].

The five methods that have been used for determining low levels of chromium in biological samples are neutron activation analysis (NAA), mass spectrometry (MS), graphite spark atomic emission spectrometry (AES), graphite furnace atomic

absorption spectrometry (GFAAS), and inductively coupled plasma with mass spectrometry (ICP-MS). These methods measure chromium as Cr(total) and do not differentiate between Cr(III) and Cr(VI). Of these five methods, only the GFAAS is readily available in routine laboratories, and this method is capable of determining chromium levels in biological samples when an appropriate background correction method is used. However, in biological samples where chromium is generally present as Cr(III), the choice of a particular method is dictated by several factors such as the type of sample, its chromium level, and the scope of the analysis [1].

Numerous investigators report on biological chromium levels in workers exposed to various chromium compounds. Studies have been mainly performed on electroplaters and welders exposed to Cr(VI) but also in tannery workers exposed to Cr(III). Workers exposed mainly to Cr(VI) compounds have higher urinary Cr levels than those exposed primarily to Cr(III) compounds; hard chromeplaters have higher urinary chromium levels than bright chromeplaters; MMA stainless steel welders display higher levels than MIG or TIG stainless steel welders or mild steel welders [1–3, 14, 15].

Chromium in urine can be regarded as a marker of internal chromium exposure. However, on the basis of urinary chromium alone it is not possible to distinguish whether exposure to Cr(VI) or Cr(III) has occurred. It provides information on total chromium absorption: Cr(VI) and Cr(III) from occupational and environmental sources. Organic Cr(III) complexes taken as food supplements can be easily absorbed, and elevated urinary chromium levels can be misinterpreted if considered as specific biomarker of exposure to Cr(VI). Still, the determination of chromium in urine is often regarded as the most practical biological monitoring method for assessing exposure to water-soluble Cr(VI) compounds in occupationally exposed subjects. Both past and recent exposure influence the urinary chromium level, while the daily incremental increase in urine (postshift value minus preshift value) appears to be a better indicator of current exposure to water-soluble Cr(VI) compounds. Chromium accumulation is demonstrated by increasing preshift urinary chromium concentrations during the working week and slowly decreasing urinary chromium levels during periods of discontinued exposure [16].

The American Conference of Governmental Industrial Hygienists (ACGIH) has adopted as the biological exposure index for Cr(VI) water soluble fumes 10 μg total chromium/g creatinine as increase during a shift and 30 μg/g creatinine at the end of shift corresponding to a time-weighted-average exposure of 0.05 mg m^{-3} [11]. The Deutsche Forschungsgemeinschaft has estimated that exposure to chromium oxide concentrations of 0.03, 0.05, 0.08 and 0.1 mg m^{-3} leads to postshift urinary concentrations of 12, 20, 30 and 40 μg chromium L^{-1} [17].

Cr(VI) penetration into the erythrocytes can occur at any time in the three-month life span of the cells. Hence, chromium in red blood cells reflects internal exposure to Cr(VI) during the lifetime of the erythrocytes. According to the Deutsche Forschungsgemeinschaft [17], long-term exposures to airborne concentrations of chromium trioxide of 0.03, 0.05, 0.08 and 0.1 mg m^{-3} result in chromium concentrations of 0.9, 1.7, 2.5 and 3.5 μg/100 mL whole blood. It is suggested that exposure to highly soluble Cr(VI) compounds might be monitored by Cr determination in erythrocytes in parallel to the determination of Cr in urine. When low levels are found in erythrocytes with correspondingly higher urinary Cr levels, extracellular reduction of the Cr(VI) can be considered to have been sufficient for rapid detoxification and elimination of these compounds [18].

2 CLINICAL ASPECTS

2.1 Toxicokinetics

In mammals, differential kinetics of Cr(VI) and Cr(III) and reduction of Cr(VI) to Cr(III) are most important determinants of the disposition and toxicity of chromium. The bioavailability of chromium is a most important factor determining the toxicity of a specific chromium source. Absorption of

inorganic Cr(VI) compounds, by ingestion, inhalation or dermal contact is higher than that of inorganic Cr(III) compounds. Once absorbed, Cr(VI), which is unstable in the body, is reduced to Cr(V), Cr(IV) and ultimately to Cr(III) by many substances, including ascorbate and glutathione. Absorbed chromium is excreted primarily in urine mainly as Cr(III).

2.1.1 Absorption

2.1.1.1 Ingestion

The rate of chromium absorption after oral exposure is relatively low and depends on several factors such as the valence state, the water solubility and the chemical form of the compound, as well as the gastrointestinal pH.

Gastrointestinal absorption of inorganic Cr(VI), although limited, occurs with greater efficiency than absorption of inorganic Cr(III). Rates of chromium uptake from the gastrointestinal tract varies from practically null for highly insoluble inorganic Cr(III) compounds such as chromic oxide to 0.4–3.0% for inorganic Cr(III) compounds to approximately 2–10% for inorganic Cr(VI) as potassium chromate [1–4, 19–23].

Chromate is unstable in acid solution and tends to be rapidly reduced to the trivalent state.

Human and animal studies have demonstrated that, after intestinal administration, the absorption of Cr(III) (chromium chloride) is not significantly changed, while the absorption of Cr(VI) (^{51}Cr-labeled sodium chromate) is greatly increased. Moreover, incubation of Cr(VI) (sodium chromate) with gastric juices prior to intraduodenal or intrajejunal administration in humans and rats, respectively, virtually eliminated absorption of chromium. Samples of gastric juice from variously treated human subjects efficiently reduced Cr(VI) (as sodium dichromate). Hence, the absorption of (di)chromate is highly dependent on the degree of reduction of Cr(VI) to Cr(III) by the gastrointestinal tract. Reduction of Cr(VI) to Cr(III) by acidic fluids in the digestive tract, for example, by saliva and mainly gastric juice and sequestration by intestinal bacteria decrease intestinal absorption of Cr and probably account for the poor intestinal absorption of Cr(VI) [24, 25]. Fasting conditions may strongly influence the gastrointestinal pH, and hence Cr(VI) reduction and absorption rates. Many beverages or food components have reducing properties [26]. Some investigations show that nearly all the ingested Cr(VI) (potassium dichromate) is reduced to Cr(III) before entering the bloodstream [21, 22]. However, the absorption from the gastrointestinal tract is so fast, as reflected by the rapid apparition of chromium in the blood, that it is able to compete effectively with reduction in the stomach [27]. Alternatively, the rapid increase of chromium in blood, could be explained by the formation of well-absorbed Cr(III) organic complexes following the reduction of Cr(VI) in the gastrointestinal tract [20, 28].

Comparative ingestion of a single dose of potassium dichromate alone [Cr(VI)], potassium dichromate fully reduced to Cr(III) with orange juice (prior to ingestion) or chromium trichloride (Cr(III) resulted in a bioavailability of 6.9% for Cr(VI), 0.6% for Cr(VI) reduced by orange juice to Cr(III) and 0.13% for Cr(III), based on two-week urinary excretion. Hence, the reduction of Cr(VI) in orange juice leads to the formation of organic Cr(III) complexes that are more bioavailable than inorganic Cr(III) [21]. The absorption of Cr(III) is effectively dependent on its chemical form; while inorganic Cr(III) is poorly absorbed, organic Cr(III) appears to be more readily absorbed. The form of ligand linked to Cr(III) has a major influence on chromium's bioavailability. Organic complex forms of Cr(III) with ligands such as acetate, citrate, glycine, glutathione, nicotinate and picolinate are fairly well absorbed by comparison with inorganic salts. These complexes show different tissue distribution and access to biologically important storage depots than other chromium compounds [29]. The most popular form of chromium in dietary supplements, chromium picolinate, is remarkably stable; it remains intact for several hours in synthetic gastric juice and days to weeks under other physiologically relevant conditions and is much more absorbed than dietary Cr(III). The complex also appears to pass unhindered through the jejunum

and probably migrates to and is incorporated into cells in its original form [30].

Cr(VI) release from stainless steel during cooking is unlikely to occur to any significant level. Acidic food items leach more chromium from stainless steel than do neutral or basic food items. However, this acidity would rapidly reduce Cr(VI) to Cr(III), and it is unlikely that this leaching would result in actual absorption of Cr(VI) by the organism [31].

The ingestion of chromium-contaminated soil by children because of their mouthing behavior is a matter of concern. The geochemical and physical properties of soil influence the bioavailability of chromium. Animals orally administered chromium in soil excreted higher levels of chromium in both urine and feces compared to a group fed $CaCrO_4$ [32]. Utilizing simulated gastric conditions, the oral bioaccessibility of Cr(III) (as chromic chloride) and Cr(VI) (as sodium chromate) in soil was determined to range between 18 and 72%, depending on the temperature, the pH and the type of soil. Overall, it appears that Cr(III) is more readily extracted from soil than Cr(VI) by the synthetic gastric juice [33].

2.1.1.2 Inhalation

Numerous experimental and human studies indicate that several factors can influence the absorption of chromium following inhalation: the size of the particles or droplets, the oxidation state, the solubility of the chromium particles in the biological fluids, the activity of alveolar macrophages, the interaction of chromium with biomolecules following deposition in the lung [1–6]. In humans, absorption of inhaled chromium following occupational exposure has been demonstrated by detection of chromium in the serum, urine or/and hair of workers exposed to Cr(III) or Cr(VI).

Following inhalation exposure, chromium may be cleared from the lungs to the gastrointestinal tract by mucociliary clearance, absorbed into the systemic circulation or remain in the lung. While Cr(III) compounds, absorption and mucociliary clearance is estimated to be only 5–30%, about 53–85% of Cr(VI) compounds (particle size <5 μm) are cleared from the lungs by absorption into the bloodstream or by mucociliary clearance in the pharynx; the rest remaining in the lungs [1]. Intratracheal instillation of Cr(III) (as $CrCl_3$) in anesthetized rabbits resulted in limited absorption: in blood chromium was entirely confined to the plasma compartment and only trace amounts were deposited in liver and kidney. By contrast, after similar application of Cr(VI) (as Na_2CrO_4), the bulk of blood radioactivity was present in erythrocytes, and substantial deposition occurred in liver and kidneys [34]. This experiment illustrates the importance of chromium species in its bioavailability. Cr(III) compounds are poorly absorbed, but nevertheless increased urinary chromium concentrations have been observed in workers exposed to Cr(III), indicating that Cr(III) is absorbed at least to some extent.

Absorption of soluble Cr(VI) compounds is rapid compared to that of poorly soluble or insoluble Cr(VI) compounds. Following an initial phase of absorption, chromium remaining in the lungs is cleared more slowly. Hence, chromium accumulation in the lungs occurs after repeated inhalation of chromium compounds; this phenomenon being more pronounced for poorly soluble or insoluble compounds.

Within the respiratory tract, Cr(VI) is reduced to Cr(III) in the epithelial-lining fluid, pulmonary alveolar macrophages, bronchial tree and peripheral lung parenchyma cells. Ascorbate seems to play a main role in this process; reduction by glutathione is slower and results in a greater residence time of chromium in the lungs [35]. An enhanced chromium-reducing capacity of human pulmonary alveolar macrophages and peripheral lung parenchyma has been observed in smokers [36].

2.1.1.3 Dermal

Systemic toxicity has been observed in humans following dermal exposure to Cr(VI) compounds, mainly chromic acid, indicating a significant percutaneous absorption [37–41].

The systemic uptake of chromium in volunteers immersed below the shoulders during three

hours in water containing Cr(VI) at a concentration of 22 mg L^{-1} was calculated to be 1.5×10^{-4} $\mu g/cm^2$-hour [42].

In vitro, Cr(VI) (as potassium dichromate) was found to have a greater ability to penetrate the human skin than Cr(III) (as chromium chloride or chromium nitrate) and also a higher degree of accumulation in the skin. The uptake in the epidermis was more ten times higher than that of Cr(III) even when Cr(III) was applied at twofold higher concentrations [43].

Lower skin penetration of Cr(III) agrees with the observation that much smaller amounts of Cr(VI) than of Cr(III) are required to elicit a positive reaction in hypersensitive persons [44, 45].

Topical application of aqueous solution of Cr(VI) on the skin of rats generated the transient species, Cr(V). Partial removal of the stratum corneum increased the rates of formation of Cr(V) [46]. However, investigations indicated a limited reduction ability of the human skin *in vitro* [43].

2.1.2 Distribution and elimination

Once absorbed, the fate of chromium will depend on the oxidation state. At physiologic pH, Cr(VI) predominantly exists as the chromate ion $CrO_4^=$ with a structure similar to physiologic anions like $PO_4^=$ and $SO_4^=$ and readily penetrates cell membranes through the phosphate and sulfate anion-exchange carrier pathway. While Cr(III) compounds are unable to cross the cell membranes by the same pathway, soluble Cr(III) may enter cells via passive diffusion and phagocytosis, but only with very low efficiency [1–4]. It seems that Cr(III) can bind to the cell membrane because of the presence of cation-binding sites on it [47]. Insoluble lead chromates have been shown to adhere *in vitro* to the cell membrane and dissolve to release a high local concentration of chromate oxyanions that can enter the cell. Phagocytic uptake of these particles also occurs [48].

Once Cr(VI) has penetrated the cell, it is reduced to Cr(III). This reduction occurs probably in all tissues but has been mainly demonstrated in the kidneys and the liver. A wide variety of factors have been documented to reduce Cr(VI) *in vitro*; microsomal and mitochondrial enzymes as well as nonenzymatic reductants are involved (a.o. ascorbate, glutathione, cysteine, H_2O_2, cytochrome P450, glutathione reductase, NAD(P)H, DT diaphorase). Their respective role under physiological conditions is not yet clearly elucidated. Moreover, species differences observed in Cr(VI) metabolism suggest that observations in rodents cannot necessarily be extrapolated to humans. Ascorbate and glutathione seem to be the major reductants of Cr(VI) in cells. Cysteine also plays a role in the reduction process of Cr(VI), a role that appears to become more significant under conditions of occupational exposure to Cr(VI)-containing welding fumes [49–54]. The reduction inside the cell makes chromium essentially impermeable through the cell membrane.

Reduction of Cr(VI) to Cr(III) occurs in the plasma limiting the penetration of Cr(VI) into red blood cells. This reduction capacity is enhanced by a recent meal but may be overwhelmed at very high Cr(VI) concentrations [55]. The reductive capacity of plasma is lower than that of the red blood cells [55, 56]. The uptake of $^{51}Cr(VI)$ by RBCs in whole blood is characterized by two apparent half-times of about 23 seconds and 10 minutes *in vitro* [57]. Within the red blood cells, Cr(VI) undergoes rapid reduction to Cr(III) by hemoglobin, glutathione and other reductants [51, 55, 56]. The cellular reduction of Cr(VI) maintains its concentration within the cell at a low level, allowing continuing penetration of Cr(VI) into the cell. The rate of Cr(VI) uptake into red blood cells may not exceed the rate of intracellular reduction at these concentrations [55]. After a few hours, chromium is bound quantitatively intracellularly, and this intracellular chromium cannot be removed to the extracellular space even by addition of chelating agents as long as the cell membrane is intact. Unstable intermediates formed during the reduction, Cr(V) and Cr(IV), and Cr(III) bind to hemoglobin and other intracellular components such as glutathione and amino acids, resulting in increased total chromium levels that remain elevated in the red blood cells fraction of blood for

several weeks [20]. This explains why following Cr(VI) exposure, plasma and red blood cells chromium levels rise rapidly to a peak, and the red blood cells level remains consistently elevated for weeks, while plasma chromium level returns rapidly to background [20].

In the bloodstream, Cr(III) is mainly confined to the plasma compartment [57] and possesses a highly stable binding activity for the β-globulin fraction of serum proteins but also for other metal-transporting proteins such as transferrin. At higher concentrations, Cr(III) binds to serum albumin or α_1- or α_2-globulins [20].

Since the penetration of Cr(III) in the red blood cells is limited, the ratio of whole blood chromium to plasma chromium concentrations is significantly different following Cr(VI) and Cr(III) exposures. As only Cr(VI) appears to be able to penetrate the erythrocyte membrane significantly either because it exceeds the plasma reduction capacity or because it enters the erythrocytes before the reduction has occurred, monitoring of red blood cell-chromium may be a useful indicator of systemic uptake of Cr(VI), but not to trivalent.

Tissue levels are higher after exposure to Cr(VI) than to Cr(III). The highest concentrations are found in the lung, blood, liver, kidney, spleen, heart and bone tissues [1–4]. Autopsy studies indicate that chromium concentrations in the body are highest in kidney, liver, lung, aorta, heart, pancreas and spleen at birth and tend to decrease with age. In all tissues, except for the lungs, there was a rapid decline in chromium concentrations from birth to the age of 10 years, followed by a more gradual decrease until the age of 80 years. The levels in the lung first decline but increase again from mid life to old age. Following inhalation, high levels of chromium can be found in the lungs for extended periods since it is not completely cleared or absorbed. Insoluble chromium compounds that are not cleared may be retained for a considerable time.

After oral exposure to chromium compounds, especially those of Cr(III), chromium is recovered almost entirely in the feces because of the poor absorption rate. Absorbed chromium is mainly excreted via urine; minor routes include feces, milk, sweat, hair and nails [1–4]. The existence of a capacity-limited renal reabsorption process is suggested [1].

Following ingestion, the urinary excretion half-lives of chromium as Cr(III) chloride, potassium dichromate reduced with orange juice or potassium dichromate were approximately 10, 15 and 40 hours, respectively [20, 21]. In a case of acute oral potassium dichromate poisoning, urinary elimination proceeded according to an open one-compartment model with a half-life around 71 hours. Chromium elimination from serum followed an open two-compartment model, with average half-lives of 3.16 hours for phase one and 50 hours for the second phase [58]. In a man who was repeatedly given Cr(VI) in drinking water, a plasma elimination half-life of 36 hours was estimated [59].

A linear one-compartment kinetic model gave estimates of the half-times ranging from 15 to 41 hours for chromium in urine of welders and electroplaters mainly exposed via inhalation. Detailed kinetic studies in welders suggest the existence of three compartments showing elimination half-lives of approximately 7 h, 15–30 days and 3–5 years [1–4, 14, 15]. Observations in chromeplaters suggest that the excretion of chromium can be approximated to a two-compartment model; an initial rapid phase with an assumed half-life of 2–3 days being followed by a phase with a half-life of approximately one month [60]. A follow up of a former plasma cutter of stainless steel exposed to dust and fumes containing chromium during his work concluded to half-lives of more than three years in serum and about 10 years in urine. The study shows that exposure to airborne dust and fumes containing chromium may cause accumulation of chromium in the body (mainly in the lungs), and that when exposure ends, elimination of chromium is very slow [16].

There is indication that all chromium excreted in the urine is Cr(III) regardless of the nature of the exposure (Cr(III) or Cr(VI)), indicating the rapid reduction of Cr(VI) before excretion. [1, 27].

Figure 2.6.2.1 aims to summarize the main toxicokinetic aspects of chromium.

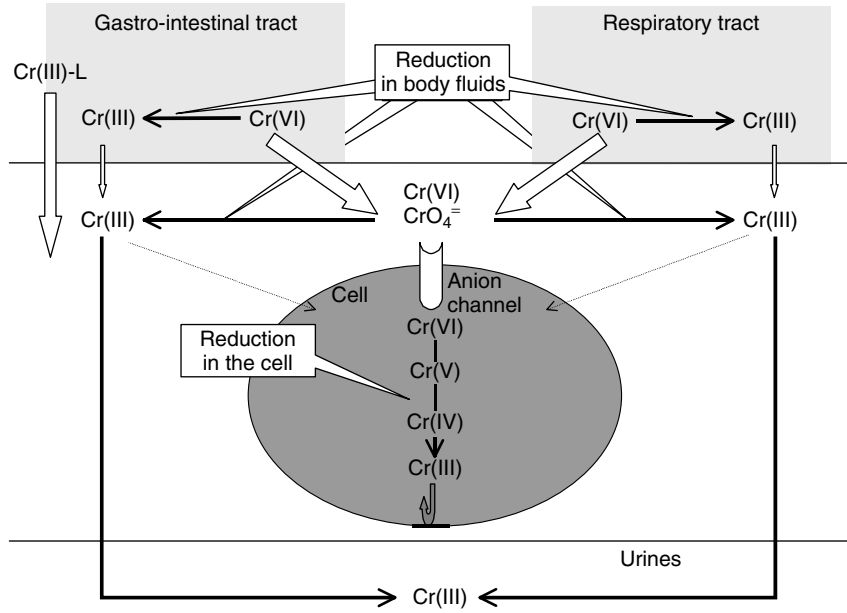

Figure 2.6.2.1. Summarizes the main characteristics of chromium toxicokinetics. Cr(VI) is readily reduced in the GI and respiratory tracts to Cr(III), which is much less bioavailable. This reduction also occurs in the plasma limiting the uptake of Cr(VI) by the cell. Organic Cr(III) complexes are more readily absorbed and able to cross the cell membranes. Cr(VI) penetrates the cell via the sulfate anion channel and is reduced to unstable intermediate, Cr(V), Cr(IV) and finally Cr(III), which bind to intracellular components. These complexes remain inside the cell for its life span. Cr(VI) is reduced to Cr(III) before urinary excretion. Cr(III)-L : Cr(III) bound to a ligand.

The values reported for chromium concentrations in the blood of nonoccupationally exposed human beings were considered to range from 0.2 to 70 $\mu g\,L^{-1}$ in serum and plasma and 5 to 54 $\mu g\,L^{-1}$ in red blood cells [1–4]. More recent studies indicate that chromium concentration in the plasma or serum of healthy subjects is of the order of 1 $\mu g\,L^{-1}$ or less [15, 61]. The reference values (arithmetic mean) reported in a review on trace element concentrations in biological specimens according to the TRACY protocol ranged from 0.5 to 1.5 $\mu g\,L^{-1}$ serum [62]. Highly variable values are reported for whole blood 0.7–28.0 $\mu g\,L^{-1}$ [61]. In red blood cells, values ranging from 3–7 $\mu g\,L^{-1}$ [63] to 20–36 $\mu g\,L^{-1}$ [61] are found.

Chromium in urine rarely exceeds 0.5 μg/g creatinine and is generally below 1 μg/g creatinine [1–4, 15]. Smokers display higher urinary chromium levels than nonsmokers do. Exercise, pregnancy, infection, physical trauma and other forms of stress, drinking beer, intake of mineral supplements and diabetic status all led to slightly elevated urinary chromium levels, while red blood cells chromium level were not affected by these factors [64]. A nearly fivefold increase in chromium excretion, associated with exercise-induced increases in glucose utilization, has been shown in volunteers 2 h after a strenuous 6-mile run [65].

2.2 Essentiality and toxicity of chromium

The biological reactivity of chromium depends on its valence state. Schematically, the metallic state (zero valence) is biologically inert, the trivalent state represents the essential element and the hexavalent chromium is considered to be the toxic form.

In humans and animals, Cr(III) is an essential nutrient; it plays a role in glucose, fat and

protein metabolism by facilitating interaction of insulin with its receptor site [66]. Till today, the essential form of the chromium carrying compound has never been unequivocally identified. It is suggested that the oligopeptide chromodulin binds chromic ions in response to an insulin-mediated chromic ion flux, and the metal-saturated oligopeptide can bind to an insulin-stimulated insulin receptor, activating the receptor's tyrosine kinase activity. The molecular agent responsible for transporting chromium from mobile pools to insulin-sensitive cells is probably the metal transport protein transferrin [30]. Increases in insulin levels should result in increased transport of transferrin, including the portion containing bound chromium, culminating in chromium transport from the blood to insulin-sensitive cells and ultimately chromodulin [30].

Suboptimal dietary intake of chromium is associated with increased risk factors linked with diabetes and cardiovascular diseases: elevated blood glucose, insulin, cholesterol and triglycerides, and decreased high-density lipoproteins. More severe signs of chromium deficiency (including nerve and brain disorders) that are reversed by supplemental chromium have been reported in patients on total parenteral nutrition without Cr(III) supplementation [66, 67]. Only Cr(III), and not Cr(VI), potentiates the action of insulin both *in vitro* and *in vivo*.

However, Cr(III) does not work physiologically as a free ion, but rather when linked with a suitable ligand [68]. The form of ligand is of primary influence in chromium's bioavailability, function and safety. In the past decades, some researchers have put forward the hypothesis of the occurrence of a chromium–nicotinic acid complex as the biologically active form of Cr(III) (glucose tolerance factor or GTF), a compound that could potentiate insulin function in regulating carbohydrate metabolism and reducing levels of low-density lipoprotein cholesterol (LDL) cholesterol [68]. The GTF factor has, however, never been identified, and its concept cannot be withheld anymore [30].

Niacin-bound chromium(III), or chromium polynicotinate, and chromium picolinate are used as micronutrients and dietary supplements. Trivalent chromium supplementation has been suggested as an attractive option for the management of type 2 diabetes and for glycemic control in persons at high risk of type 2 diabetes. It has been stated that serum glucose can be improved by chromium supplementation in both types 1 and 2 diabetes [69]. However, a recent systematic review and meta-analysis of randomized clinical trials concluded that no association between chromium and glucose or insulin concentrations among nondiabetic subjects could be shown, the data for persons with diabetes were assessed inconclusive [70].

Very rare cases of toxicity involving Cr(III) picolinate excessive ingestion have been reported [71–73].

The toxic mechanism of action differs for hexavalent versus trivalent chromium. Cr(VI) causes cellular damage via its role as a strong oxidizing agent, whereas Cr(III) can inhibit various enzyme systems or react with organic molecules [1–4]. Cr(VI) compounds were found to be 1000 times more cytotoxic to human cells than were the Cr(III) compounds at equimolar concentration [74, 75]. The difference in toxicity between Cr(VI) and Cr(III) compounds is believed to be due to the fact that Cr(VI) can penetrate biological membranes via nonspecific anion carriers more readily than Cr(III). However, it appears that Cr(III) compounds may cause toxicity at higher concentrations and/or depending on the ligands attached to it [76–78].

On the one hand, Cr(VI) and not Cr(III) penetrates the cell. On the other hand, Cr(III) and not Cr(VI) binds to DNA. Hence, although is Cr(VI) is considered to be the toxic form of chromium, there are strong indications that Cr(III) or the intermediates formed during the intracellular reduction of Cr(VI) contribute to the cytotoxicity, genotoxicity and carcinogenicity of Cr(VI) compounds. The intracellular reduction of Cr(VI) generates unstable, reactive Cr(V) and Cr(IV) intermediates as well as, in Fenton-like oxidative cycling, unstable reactive oxygen species (ROS) (superoxide anion, hydroxyl radicals and nitric oxide, thiyl radicals, ascorbate radical and carbon-based radicals) and finally Cr(III) that forms stable complexes with many biological ligands, including

DNA [77–85]. The toxicity of Cr(VI) is thought to result from either direct binding of these intermediates to cellular constituents and/or through the generation of free radicals (Figure 2.6.2.2 summarizes the main aspects involved in the toxicity of chromium). Chromium elicits numerous effects at the biochemical, the genomic and the cellular levels. *In vitro* and *in vivo* studies have demonstrated that Cr(VI) induces an oxidative stress leading to DNA damage and oxidative deterioration of lipids and proteins. A cascade of cellular events occurs following Cr(VI)-induced oxidative stress including increased lipid peroxidation, membrane damage with leakage of lactate dehydrogenase (LDH), modulation of intracellular oxidized states, activation of protein kinase C, apoptotic and necrotic cell death, and altered gene expression [86, 87]. A variety of DNA lesions are generated during the reduction of Cr(VI) to Cr(III), including DNA strand breaks, alkali–labile sites, DNA–protein and DNA–DNA crosslinks, Cr–DNA adducts and oxidative DNA damage, such as 8-oxodeoxyguanosine. The relative importance of the different chromium complexes and oxidative DNA damage in the toxicity of Cr(VI) is unknown [35].

Independent of any inherent ability to generate ROS, Cr(VI) might compromise the cell's antioxidant defenses, for example, by depleting ascorbate or glutathione or by inhibiting glutathione reductase [81].

Except at very high concentrations, most Cr(III)-containing compounds are relatively nontoxic, nonmutagenic and noncarcinogenic [54]. However, it is important to mention that the form of ligand is of primary importance in the bioavailability and potential toxicity of Cr(III). One should stress that release of chromium from chromium picolinate for use in cells requires reduction of the chromic center, a process that can lead potentially to the production of harmful hydroxyl radicals [30]. An *in vitro* study has demonstrated concentration-dependent effects of Cr(III) picolinate and niacin-bound Cr(III) on enhanced production of ROS including superoxide anion and hydroxyl radicals, and DNA. Although both Cr(III) supplements exhibited significantly much less oxidative stress and DNA damage compared with Cr(VI), Cr(III) picolinate exhibited higher production of noxious superoxide anion and increased DNA fragmentation compared with niacin-bound Cr(III) [87]. Cr(III) picolinate has been shown to be mutagenic *in vitro* at physiological relevant doses, whereas at the same dose Cr(III) chloride was not. Similarly, chromium picolinate caused significant cell death, while chromium nicotinate, nicotinic acid and chromium chloride did not cause

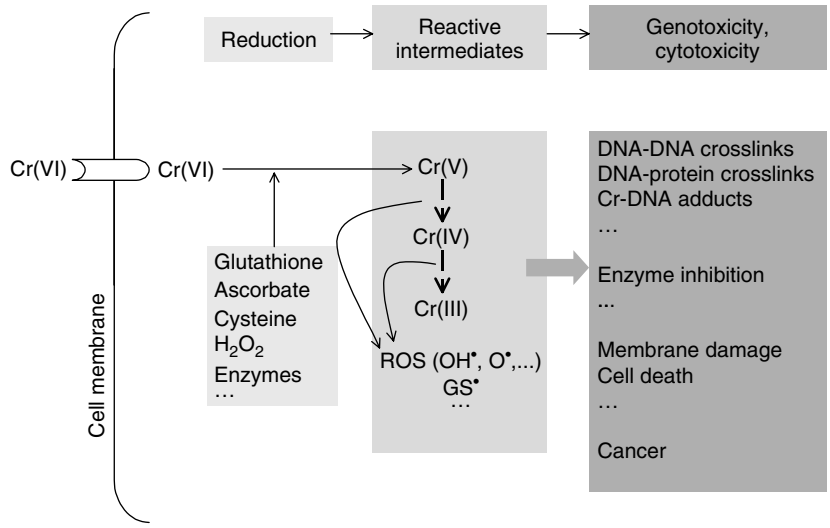

Figure 2.6.2.2. Summarizes the main aspects of chromium toxicity.

any cell death or toxicity. Hence, coordination of Cr(III) with picolinic acid might make chromium more genotoxic than other forms of Cr(III) [88].

If the reduction of Cr(VI) to Cr(III) inside of target cells is implicated in the toxicity of chromium compounds, this reduction in body fluids and nontarget cells results in detoxification and is a major mechanism of protection since the poor ability of Cr(III) to cross cell membranes [35]. When introduced by the oral route, Cr(VI) is efficiently detoxified upon reduction by saliva and gastric juice, and sequestration by intestinal bacteria. If some Cr(VI) is absorbed by the intestine, it is massively reduced in the blood of the portal system and then in the liver. It has been claimed that these mechanisms may explain the lack of genotoxicity, carcinogenicity and induction of other long-term health effects of Cr(VI) by the oral route [35]. Within the respiratory tract, chromium-reducing processes also lower the toxic potential of Cr(VI). Pulmonary macrophages phagocytose the Cr(VI) particles that are then reduced and sequestered. These macrophages can be expectorated or swallowed. Cr(VI) is also reduced in the epithelial-lining fluid; the lining layers of rat lungs provide an ascorbic acid-related capacity for protection of the cells against the toxic effects of chromates. Hence, it is suggested that lung cancer can only be induced when Cr(VI) doses overwhelm these defense mechanisms. The efficient uptake and reduction of Cr(VI) in red blood cells could explain its lack of carcinogenicity at a distance from the portal of entry into the body [35]. Cr(VI) compounds are easily reduced, but oxidation of trivalent to hexavalent chromium does not appear to occur in the organism.

2.3 Health effects

The overall toxicity, carcinogenicity and general hazards of chromium are highly related to chemical speciation, the hexavalent chromium compounds being more toxic than the trivalent compounds. Acute and/or long-term exposure to Cr(VI) is mainly associated with damage to the skin, the respiratory tract, the kidneys and an increased risk of lung cancer, the type of damage and the target organ being dependent on the route of exposure.

2.3.1 Acute exposure

Reported oral LD_{50} values in rats are in the range 13–80 mg of Cr(VI) per kg of body weight for soluble compounds; 250–3120 mg/kg bw for slightly soluble compounds. The oral LD_{50} for Cr(III) compounds range from 1900 to 3300 mg/kg bw. Hence, hexavalent compounds appear to be 10–100 times more toxic than the trivalent chromium compounds by the oral route. Acute inhalation LC_{50} values in rats for several soluble chromium(VI) compounds (sodium chromate, sodium dichromate, potassium dichromate, ammonium dichromate and chromium trioxide) ranged from about 30 to 140 mg chromium(VI)/m^3 [1–4]. In adult human subjects, the lethal oral dose is 50–70 mg soluble chromates/kg body weight [2].

Some Cr(VI) compounds, such as chromic acid, sodium and potassium chromates, are potent oxidizing agents, and are thus strong irritants of mucosal tissue. They may cause severe eye, skin, digestive tract and respiratory tract irritation with possible burns.

Fatal cases of accidental or intentional ingestion of Cr(VI) (potassium, sodium dichromate and ammonium dichromate) have been reported in the past and continue to be reported, but cases of acute occupational exposure to chromium are particularly rare. Caustic burns in the gastrointestinal tract resulting in thirst, vomiting and abdominal pain, severe hemorrhage, cardiovascular collapse due to severe hypovolemia, acute tubular necrosis (ATN) with oliguria/anuria, severe liver damage, coagulopathy, convulsions, coma and death are described [1–4]. About 1 g of potassium dichromate (VI) is considered a lethal dose. Persons who ingested 5 g or more experienced gastrointestinal bleeding, massive fluid loss and death within 12 hours after ingestion. When the ingested dose was 2 g or less, renal tubular necrosis or diffuse hepatic necrosis resulted, with acute renal failure before death in some cases. Typically, the kidney and liver effects develop 1 day to 4 days after

ingestion of a sublethal dose. Acute chromium poisonings are often fatal regardless of the therapy used [1]. A case of adult respiratory distress syndrome has also been reported following ingestion of potassium dichromate [89].

Intact or damaged skin contact with Cr(VI) compounds can result in severe systemic toxicity. In the past, external application of chromic acid for the treatment of warts and cauterization of hemorrhoids has given rise to many cases of poisoning with acute renal failure [5]. Antiscabies ointment containing Cr(VI) resulted in necrosis of skin at application sites, nausea, vomiting, shock, coma and death. Severe nephritis and death followed cauterization of an open wound with Cr(VI) oxide. An occupational fatality was described after an accident in which a worker was burned on the arms and trunk with hot potassium dichromate [1]. Chromium intoxication can occur from the cutaneous absorption of chromium following chromic acid burns that are as small as 1% of the total body surface area [40]. Fatal issues have been reported in cases with corrosions covering less than 10% of the body surface area [90].

Very little quantitative data are available concerning the acute toxicity produced by the inhalation of chromic acid and chromates.

The IDLH (Immediately Dangerous To Life Or Health Concentrations) established by the NIOSH [91] (30 mg m^{-3} as CrO_3, or expressed as its equivalent: 15 mg Cr(VI)/m^3) is based on the statements by ILO [92] that 'a man exposed for several days to concentrations of chromic acid mist of about 20–30 mg m^{-3} experienced cough, headache, dyspnea and substernal pain; the signs persisted for 2 weeks. Another man working on the same process was similarly but less severely affected'. No inhalation toxicity data were available on which to base an IDLH for Cr(III) compounds. Therefore, the revised IDLH for Cr(III) compounds was established at 25 mg Cr(III)/m^3 on the basis of acute oral toxicity data in animals. This may be a conservative value due to the lack of relevant acute toxicity data for workers exposed to concentrations above 25 mg Cr(III)/m^3.

2.3.2 Noncarcinogenic effects on the respiratory tract

The respiratory tract constitutes a major target following inhalation exposure. Occupational exposure to chromium compounds, which mainly occurs via inhalation, has been mainly studied in the chromate-production, chrome-plating and chrome-pigment, ferrochromium production, leather tanning and chrome alloy production industries.

2.3.2.1 Nasal and septal mucosa irritation

Nasal mucosa irritation and atrophy, nasal septum ulceration and perforation have been widely reported, in the past, in chromeplaters following exposures to Cr(VI) as chromic acid mist. Associated signs and symptoms include inflamed mucosa, rhinorrhea, nasal itching, soreness, sneezing, smeary and crusty septal mucosa and nose bleed. Initially, nasal septum ulceration may be painless but with continued exposure the narcotizing effect of chromates to underlying tissues may become painful and lead to permanent scarring [1–4]. Nasal ulcers and perforations have been associated with exposures to Cr(VI) concentrations of 0.09–9.1 $\mu g\, m^{-3}$ (average: 2.9 $\mu g\, m^{-3}$); almost all the workers employed longer than 1 year showed nasal tissue damage [93]. In another study, these lesions have been reported to occur in two-thirds of the subjects exposed to peak levels of 20 $\mu g\, m^{-3}$ or more near the baths; nasal irritation being a common complaint among subjects exposed to a daily average concentration exceeding 1 $\mu g\, m^{-3}$ of chromic acid (8 h-TWA: time weighted average exposure). It was concluded that short-term exposure to at least 20 $\mu g\, m^{-3}$ may cause septal ulceration and perforation [94]. On the basis of this study, the US Department of Health and Human Services used a lowest-observed-adverse-effect level (LOAEL) of 2 $\mu g\, m^{-3}$ to derive an inhalation minimal risk level (MRL) of 0.005 μg Cr(VI)/m^3 for intermediate-duration exposure to Cr(VI) as chromium trioxide mists and other dissolved Cr(VI) aerosols or mists [1]. This LOAEL was also used by the Environmental Protection

Agency (EPA) to derive the inhalation reference concentration (RfC) for upper respiratory effect of chromic acid mists and dissolved Cr(VI) aerosols at 0.008 $\mu g\,m^{-3}$ [4].

Such effects on the upper respiratory tract have also been reported in chromate-production workers [1–4, 95]. For example, a 43.5% incidence rate of nasal septal perforation has been reported among workers of a chromate-producing plant that manufactured sodium chromate and dichromate. At the time of the study, airborne chromate concentrations ranged from 10 to 2800 $\mu g\,m^{-3}$ [96]. Nasal septum perforation, assumed to be due to chronic exposure to low-level Cr(VI), has also been described in welders [97].

2.3.2.2 Changes in lung function

Effects on the lower respiratory tract including inflammatory changes and various disorders have been reported in workers exposed to chromium (VI) [1–4]. Changes in pulmonary function (slight, transient decreases in vital capacity (VC), forced vital capacity (FVC), forced expired volume in 1 second (FEV1), forced mid-expiratory flow during the workday) have been measured among electroplaters exposed to chromic acid [94, 98, 99]. These effects have been observed at Cr(VI) 8-h mean exposures exceeding 2 $\mu g\,m^{-3}$ and cigarette smoking was not a confounding variable [94]. This level was established as LOAEL to derive an inhalation MRL of 0.005 μg Cr(VI)/m^3 for intermediate-duration exposure to Cr(VI) as chromium trioxide mists and other dissolved Cr(VI) aerosols or mists [1].

In the ferrochromium and stainless steel production industry, exposure to dusts containing low concentrations of Cr(VI) or Cr(III), for an average duration of 18 years, did not lead to any respiratory changes detectable by lung function tests or radiography nor to any increase in symptoms of respiratory diseases [100].

2.3.2.3 Sensitization

Isolated cases of occupational asthma caused by Cr(VI) compounds have been reported in workers exposed to cement [101–103], in electroplaters [103–107] and in stainless steel welding [108–109].

In some reports, sensitization to Cr(VI) has been demonstrated by positive skin prick with $Cr_2(SO_4)_3$ [103, 105] and in a few studies, bronchial challenge tests with aerosolized solutions of $K_2Cr_2O_7$ have been performed to fully confirm the diagnostic [101, 102, 107]. Anaphylactoid reactions characterized by dermatitis, facial angioedema, bronchospasms accompanied by a tripling of plasma histamine levels and urticaria have been observed in chromium sensitive individuals exposed to chromium challenged with Cr(VI) as sodium chromate dichromate [110].

Cr(VI)-sensitized subjects may react following exposure by inhalation to Cr(III) compounds as shown by positive provocative test using $Cr_2(SO_4)_3$ chromium sulfate [103, 106]. A case of asthma has also been reported in a leather tanning worker mainly exposed to Cr(III), however, as already mentioned, these workers can also be exposed to small quantities of Cr(VI) [111].

Smoking of cigarettes contaminated with cement might be a significant factor in the causation or elicitation of asthma [101].

Most patients with chromium asthma reported in the literature presented a history of dermal involvement with either urticaria or allergic contact dermatitis, preceding the respiratory disease.

Cross reaction with nickel may exist [105, 112].

2.3.3 Effects on the skin

2.3.3.1 Irritating and ulcerating effects

Hexavalent chromium is a skin irritant and some compounds, such as, chromium trioxide, potassium (di)chromate and sodium (di)chromate are strong corrosive agents that can cause burns upon dermal contact. These burns can facilitate the absorption of the compound and lead to systemic toxicity [37–41].

Severe dermatitis and skin ulcers (‘chrome holes’, ‘chrome sores’) can result from direct contact with high concentrations of chromic acid, sodium or potassium chromate or dichromate.

These lesions have mainly been reported among chrome platers [1–4]. Common sites for these persistent ulcers include the nail root, knuckles and finger webs, backs of the hands and forearms. They also develop readily at the site of insect bites, sores or other injuries. The characteristic chrome sore begins as a papule, forming a 2–5-mm ulcer with raised hard edges. Ulcers can penetrate deep into soft tissue or become the site of secondary infection. The progression to ulceration is generally painless, the lesions heal slowly, can persist for months and lead to scars. There is no indication that these lesions lead to malignancy.

Trivalent compounds are not considered to produce such effects.

2.3.3.2 Sensitization

Chromium (VI) is one of the most common contact sensitizers in industrialized countries. Most occurrences of contact dermatitis result from occupational exposure. It is generally accepted that while chromium metal itself does not act as a hapten and is nonsensitizing, Cr(III) and Cr(VI) can both bind covalently to proteins and cause allergy.

Allergic contact dermatitis resulting from exposure to Cr(VI) has been demonstrated in numerous patch-testing studies of contact dermatitis patients during routine testing or in Cr(VI)-sensitized subjects, when challenged with potassium dichromate. Solubility and pH appear to be the primary determinants of the capacity of individual chromium compounds to elicit an allergic response [113, 114]. Equimolar challenge concentrations of several soluble chromates (potassium dichromate, potassium chromate, sodium dichromate, sodium chromate) induced similar skin responses [115].

Sensitization to trivalent compounds is much less frequent, but some subjects may react to high concentrations of these compounds. Guinea pigs sensitized with Cr(VI) react with Cr(III) and vice versa; this suggests that chromium hypersensitivity is not directed against chromium specific oxidation state [114]. In chromium-sensitive individuals, Cr(VI) elicit allergic receptions more frequently than Cr(III) compounds; however, patch-testing of Cr(VI)-sensitive subjects with Cr(III) compounds showed that high concentrations of Cr(III) can elicit a reception [116, 117]. The relatively lower skin-sensitizing potential of Cr(III) compounds is generally ascribed to their poorer degree of permeation through the skin [43, 118, 119].

Immunologically, trivalent chromium appears to form the hapten of concern in chromium sensitization. In contrast to Cr(VI), Cr(III) binds more strongly to proteins. Most likely, Cr(VI) readily penetrates the skin and the membrane of Langerhan's cells where it is transformed into Cr(III) that then binds to proteins and forms a hapten-carrier complex that acts as an antigen [114].

Occupational sources of chromium exposures associated with chromium sensitization include numerous materials and processes such as cement, tanning industry, chromium plating baths, chromium colors and dyes, wood preservatives, anticorrosive agents, welding fumes, lubricating oils and greases, cleaning materials, textiles and furs, printing, plant cleaners, automobile factory, glues, wood ash, foundry sand, match heads, boiler linings, making of television screens, magnetic tapes, tyre fitting, wood and paper industry, and even milk testing [113, 114, 120, 121].

Cement remains a major cause of allergic contact dermatitis [122–127]. This is due to the formation of Cr(VI) from Cr(III) present in the raw material from which cement is produced. Oxidation of Cr(III) to Cr(VI) occurs during cement processing in the kiln at temperatures between 1400 and 1500 °C [128]. Wet cement has a high pH so that it can alter the stratum corneum of the skin resulting in irritation, which in turn facilitates the penetration of Cr(VI) and the elicitation of allergic reactions. Occupational groups such as construction workers and bricklayers are therefore at risk of developing chromium allergy.

In some countries, ferrous sulfate is added to cement to reduce Cr(VI) to Cr(III), which in the alkaline cement water mixture precipitates as chromium hydroxide of very low water solubility. This results in a considerable reduction in the content of hexavalent chromium and a decrease in the

prevalence of chromium allergy among construction workers has been reported [128–131].

Workers within the tanning industry mainly exposed to trivalent chromium (chromium sulfate) may also develop chromium allergy. Leather often also contains trace amounts of leachable Cr(VI), which is formed by oxidation of Cr(III) during the tanning process [111, 132–135]. It has been estimated that, with traditional tanning methods, 4–9.5 kg of chromium (calculated as Cr_2O_3) per ton of skins are not chemically fixed (during processing if it is not carried out with a suitable high exhaustion tanning system (International Environmental Commission IUE, 1996). Chromium dermatitis is often due to exposure in the occupational environment, however, consumer products such as Cr(III)-tanned leather products are also an important source of chromium exposure. Small amounts of leachable hexavalent chromium were found in both chromium and vegetable tanned leathers. Thus, the risk of chromium dermatitis cannot be disregarded [132]. In a Danish study that assessed chromate-sensitive patients in an urban tertiary referral center with respect to primary cause of sensitization, in an area where the risk of chromate exposure from cement had been reduced, it was established that leather was the most frequent nonoccupational source of chromate sensitization [129].

Oral administration of chromium salts (potassium dichromate) may exacerbate dermatitis in sensitized patients. A case of systemic contact dermatitis ascribed to the ingestion of chromium picolinate has been reported [136].

Concern has been raised about the release, and biologic fate, of metal species from implant corrosion and wear. The issue of host hypersensitivity to these elements remains of concern. Cellular uptake of chromium was documented in red blood cells following corrosion of stainless-steel and cobalt-chromium surgical implants *in vivo*, in the red blood cells of patients undergoing total joint revisions and in fibroblasts subjected to products of fretting corrosion of stainless-steel and cobalt–chromium implants. These observations suggest that corrosion of implants can lead to the release of hexavalent chromium into the body [137]. A case of generalized eczematoid dermatitis apparently caused by allergy to chromium liberated from a metal dental plate has been reported [138]. Other isolated cases of allergic reactions attributed to dental and orthopedic implants have been described, but it is not always clear to determine whether chromium or other metals have caused the allergic reactions [139].

2.3.4 Effects on the kidneys

Cases of ATN and renal failure following massive ingestion of chromic acid, potassium or sodium dichromate are well described [1–4]. Systemic involvement following skin burns by chromic acid can also lead to renal failure. Moreover, some case studies suggest that chromium(III) picolinate might also cause nephrotoxicity when ingested in excess [71, 72].

In experimental studies, chromate selectively accumulates in the convoluted proximal tubule where necrosis occurs [140].

It has been suggested that kidney might be one of the targets of chromates upon chronic exposure conditions. Numerous biochemical markers of kidney damage have been studied in workers engaged in chromate and dichromate production, in chrome platers, in stainless steel welders, in workers employed in ferrochromium production, in boilermakers and in workers in an alloy steel plant: β-hexosaminidase, lysozyme, β_2-microglobulin, total proteins, albumin, protein 1, transferrin, retinol-binding protein (RBP), brush border protein antigen (BBPAg) or enzyme activities of alanine-aminopeptidase, LDH, *N*-acetyl-β-D-glucosaminidase (NAG), gammaglutamyl-transpeptidase (γGT), and β-galactosidase. These studies have yielded equivocal results. Signs of tubular dysfunction, with elevated urinary excretion levels of β_2-microglobulin, NAG, BBPAg or RBP, have been reported in chrome platers and chromates production workers but not in others [1–4].

No signs of kidney damage in tests of function of tubules or glomerules were found in stainless steel welders [1–4].

No renal impairment was found in workers with long-term low-level Cr(III) exposure

(mean airborne Cr(VI) concentration below detection limit) in ferro-alloy metallurgy [141]. Similarly, no increase in urinary β_2-microglobulin levels was found in tannery workers in comparison to referent control workers [142]. In boilermakers or in workers employed in an alloy steel plant exposed to Cr(0), no increase in urinary levels of chromium, and no differences in the levels of RBP, β_2-microglobulin, NAG or other indices of renal toxicity were found [143, 144].

2.3.5 Mutagenicity and carcinogenicity

In 1990, the IARC (International Agency for Research on Cancer) [6] assessed the carcinogenicity of chromium and chromium compounds and concluded as follows.

- There is sufficient evidence in humans for the carcinogenicity of Cr(VI) compounds as encountered in the chromate production, chromate pigment production and chromium plating industries.
- There is sufficient evidence in experimental animals for the carcinogenicity of calcium chromate, zinc chromates, strontium chromate and lead chromates.
- There is limited evidence in experimental animals for the carcinogenicity of chromium trioxide (chromic acid) and sodium dichromate.
- There is inadequate evidence in humans for the carcinogenicity of metallic chromium and of Cr(III) compounds.
- There is inadequate evidence in experimental animals for the carcinogenicity of metallic chromium, barium chromate and Cr(III) compounds.

The Working Group made the overall evaluation on Cr(VI) compounds on the basis of the combined results of epidemiological studies, carcinogenicity studies in experimental animals and several types of other relevant data that support the underlying concept that Cr(VI) ions generated at critical sites in the target cells are responsible for the carcinogenic action observed.

Final IARC evaluation			
	Degree of evidence for carcinogenicity		Overall evaluation
	Human	Animal	
Cr VI			1
Cr(VI) compounds as encountered in the chromate & chromate pigment production, chromate plating industries	Sufficient		
– Barium chromate		Inadequate	
– Calcium chromate		Sufficient	
– Chromium trioxide		Limited	
– Lead chromates		Sufficient	
– Sodium dichromate		Limited	
– Strontium chromate		Sufficient	
– Zinc chromate		Sufficient	
Cr III compounds	Inadequate	Inadequate	3
Metallic Cr	Inadequate	Inadequate	3
Welding fumes			2B
– Welding fumes and gases	Limited		
– Welding fumes		Inadequate	

Group 1: carcinogenic to humans
Group 2: 2A: probably carcinogenic to humans
2B: possibly carcinogenic to humans
Group 3: not classifiable as to its carcinogenicity to humans
Group 4: probably not carcinogenic to humans

The US Environmental Protection Agency (USEPA) has also classified chromium(VI) in Group A, which is a human carcinogen [145].

A huge literature covers the activity of chromium compounds on genetic and related effects in *in vitro* test systems.

In a recent review [35] on the genotoxicity and carcinogenicity of chromium compounds, it was concluded that (a) the lack of carcinogenicity of Cr(0) and Cr(III) compounds in experimental animals is well established (b) Cr(VI) can induce a variety of genetic and related effects *in vitro*, but only a minority of animal carcinogenicity data with Cr(VI) compounds were positive. As highlighted by the author, most positive studies used administration routes that do not mimic any human exposure and bypass physiological defense mechanisms; positive results were only obtained at implantation sites and at the highest dose tested. Exposure to Cr(VI) has been known for more than a century to be associated with induction of cancer in humans. However, carcinogenicity requires massive exposures, as is only encountered

in well-defined occupational settings, and is site specific, being specifically targeted to the lung and, in some cases, to the sinonasal cavity. The large majority of the results obtained with Cr(VI) compounds were positive as a function of Cr(VI) solubility and bioavailability to target cells. The activity was less frequently evident with Cr(VI) compounds having a low solubility, which often needed to be artificially solubilized, for example, with alkali, prior to challenge with target cells [35].

It should be noted, however, that recent *in vitro* investigations have reported a mutagenic activity of Cr(III) picolinate, while chromium nicotinate, nicotinic acid and Cr(III) chloride hexahydrate did not produce chromosome damage at equivalent nontoxic doses. Damage was inferred to be caused by the picolinate ligand because picolinic acid in the absence of chromium was clastogenic [88].

Epidemiological studies carried out in the chromate-production industry and in the chromate pigment production industry have consistently demonstrated an association with an increased risk of lung cancer. While some studies provide suggestive evidence of a causal relationship between chromium plating and lung cancer, others have reported inconclusive results, but they generally support the conclusion that Cr(VI) is carcinogenic. In ferrochromium workers (mainly exposed to Cr(III) but also to Cr(VI)) the overall results with regard to lung cancer were inconclusive. In leather tanning workers, where exposure is mainly to Cr(III), no excess risk of cancer is reported. Cases of sinonasal cancer were reported in epidemiological studies of primary chromate-production workers, of chromate pigment production workers and of chromium platers suggesting the possibility of an excess risk for these rare tumors [1–4, 6].

No clear relationship between exposure to welding fumes and occurrence of lung cancer has been demonstrated. In 1990, IARC [6] concluded that there is limited evidence in humans for the carcinogenicity of welding fumes and gases and inadequate evidence in experimental animals for the carcinogenicity of welding fumes. Welding fumes were classified as possibly carcinogenic to humans (Group 2B).

A meta-analysis conducted in 1997 calculated a 30 to 40% increase in the relative risk of lung cancer among welders when they are compared to the general population. The meta-analysis failed to demonstrate that stainless steel welders, although potentially exposed to nickel and hexavalent chromium, are at higher lung cancer risk than mild steel welders. Asbestos exposure and smoking are confounding factors [146]. The latest findings provide suggestive but not conclusive evidence of a modest lung cancer risk associated to mild-steel welding [147–149].

At present, the carcinogenicity of hexavalent chromium by the oral route of exposure cannot be determined because of a lack of sufficient epidemiological or toxicological data.

2.3.6 Reproductive and developmental effects

There is limited information on the reproductive and developmental effects of Cr(VI) in humans.

In 2001, The Health Council of the Netherlands [150], which evaluates the effects on the reproduction of substances at the workplace, considered that in men, fertility studies considering occupational exposure to Cr(VI) and its compounds had focused on welding. Some of these studies reported effects on semen quality in welders, whilst others reported no effects. Unfortunately, these studies generally lack information on exposure and confounding factors such as other exposures (a.o. other metals, heat and noise), age and smoking habits.

In view of the animal data, the committee's recommendations are as follows.

- For effects on fertility, the committee recommends classifying Cr(VI) and its compounds in category 3 (*substances that cause concern for human fertility*) and to label Cr(VI) with R62 (*possible risk for impaired fertility*)
- For developmental toxicity, the committee recommends classifying Cr(VI) and its compounds in category 2 (*substances which should be regarded as if they impair fertility in humans*) and to label Cr(VI) with R61 (*may cause harm to the unborn child*).

– For effects during lactation, the committee is of the opinion that because of a lack of appropriate data Cr(VI) and its compounds should not be labeled.

3 REFERENCES

1. ATSDR (Agency for Toxic Substances and Disease Registry), Toxicological Profile for Chromium, Update, U.S. Department of Health and Human Services, Public Health Service, Atlanta, GA, 2000.
2. WHO (World Health Organization), Environmental Health Criteria 61: Chromium, International Programme on Chemical Safety, Geneva, Switzerland, 1988.
3. Cross, J., Faux, S. P., Sadhra, S., Sorahan, T., Levy, L. S., Aw, T. C., Braithwaite, R., McRoy, C., Hamilton, L. and Calvert, I., Criteria Document for Hexavalent Chromium, Commissioned by International Chromium Development Association (ICDA), Paris, France, 1997.
4. EPA (Environmental Protection Agency), Toxicological Review of Hexavalent Chromium, U.S. Environmental Protection Agency, Washington, DC, 1998.
5. Browning, E., *Toxicity of Industrial Metals*, 2nd ed., Butterworths, London, 1969.
6. IARC (International Agency for Research on Cancer), Chromium and chromium compounds, *IARC Monographs on the Evaluation of Carcinogenic Risks to Humans and their Supplements*, Vol. 49, Chromium, Nickel and Welding, IARC, Lyon, France, 1990, pp. 49–256.
7. ICDA, International Chromium Development Association, http://www.chromium-asoc.com/index.html, (2003).
8. Katz, S. A. and Salem, H., *J. Appl. Toxicol.*, **13**, 217 (1993).
9. Cunat, P. J., *The Chromium File*, Issue No. 9, April 2002.
10. Nygren, O., Nilsson, C. A. and Lindahl, R., *Ann. Occup. Hyg.*, **36**, 509 (1992).
11. ACGIH (American Conference of Governmental Industrial Hygienists), TLVs and BEIs for Chemical Substances and Physical Agents, Cincinnati, OH, 2003.
12. OSHA (U.S. Department of Labor Occupational Safety & Health Administration) http://www.osha.gov/SLTC/pel/index.html, (2003).
13. NIOSH, *Pocket Guide to Chemical Hazards*, National Institute for Occupational Safety and Health, 2002.
14. Aitio, A., Jarvisalo, J., Kiilunen, M., Kalliomaki, P. L. and Kalliomaki, K., Chromium, in *Biological Monitoring of Toxic Metals*, *Rochester Series on Environmental Toxicity*, Clarkson, Th. W., Friberg, L., Nordberg, G. F. and Sager, P. R. (Eds.), Plenum Press, New York, 1988.
15. Lauwerys, R. and Hoet, P. *Industrial Chemical Exposure, Guidelines for Biological Monitoring*, 3rd ed., Lewis Publishers, Boca Raton, FL, 2001.
16. Petersen, R., Thomsen, J. F., Jorgensen, N. K. and Mikkelsen, S., *Occup. Environ. Med.*, **57**, 140 (2000).
17. DFG (Deutsche Forschungsgemeinschaft), List of MAK and BAT Values, Commission for the Investigation of Health Hazards of Chemical Compounds in the Work Area, Report No. 38, Wiley-VCH, Weinheim, 2002.
18. Miksche, L. W. and Lewalter, J., *Regul. Toxicol. Pharmacol.*, **26**, S94 (1997).
19. Finley, B. L., Scott, P. K., Norton, R. L., Gargas, M. L. and Paustenbach, D. J., *J. Toxicol. Environ. Health*, **48**, 479 (1996).
20. Kerger, B. D., Finley, B. L., Corbett, G. E., Dodge, D. G. and Paustenbach, D. J., *J. Toxicol. Environ. Health*, **50**, 67 (1997).
21. Kerger, B. D., Paustenbach, D. J., Corbett, G. E. and Finley, B. L., *Toxicol. Appl. Pharmacol.*, **141**, 145 (1996).
22. Kuykendall, J. R., Kerger, B. D., Jarvi, E. J., Corbett, G. E. and Paustenbach, D. J., *Carcinogenesis*, **17**, 1971 (1996).
23. Febel, H., Szegedi, B. and Huszar, S., *Acta Vet. Hung.*, **49**, 203 (2001).
24. De Flora, S., Badolati, G. S., Serra, D., Picciotto, A., Magnolia, M. R. and Savarino, V., *Mutat. Res.*, **192**, 169 (1987).
25. De Flora, S., Camoirano, A., Bagnasco, M., Bennicelli, C., Corbett, G. E. and Kerger, B. D., *Carcinogenesis*, **18**, 531 (1997).
26. Kerger, B. D., Richter, R. O., Chute, S. M., Dodge, D. G., Overman, S. K., Liang, J., Finley, B. L. and Paustenbach, D. J., *J. Expo. Anal. Environ. Epidemiol.*, **6**, 163 (1996).
27. O'Flaherty, E. J., Kerger, B. D., Hays, S. M. and Paustenbach, D. J., *Toxicol. Sci.*, **60**, 196 (2001).
28. Kerger, B. D., Finley, B. L., Corbett, G. E., Dodge, D. G. and Paustenbach, D. J., *J. Toxicol. Environ. Health*, **50**, 67 (1997).
29. Anderson, R. A., *Regul. Toxicol. Pharmacol.*, **26**, S35 (1997).
30. Vincent, J. B., *J. Nutr.*, **130**, 715 (2000).
31. Aitio, A., *The Chromium File*, Issue No. 1, September 1996.
32. Witmer, C. M., Harris, R. and Shupack, S. I., *Environ. Health Perspect.*, **92**, 105 (1991).
33. Skowronski, G. A., Seide, M. and Abdel-Rahman, M. S., *J. Toxicol. Environ. Health A*, **63**, 351 (2001).
34. Wiegand, H. J., Ottenwalder, H. and Bolt, H. M., *Toxicol. Lett.*, **22**, 273 (1984).
35. De Flora, S., *Carcinogenesis*, **21**, 533 (2000).
36. Balansky, R. M., D'Agostini, F., Izzotti, A. and De Flora, S., *Carcinogenesis*, **21**, 1677 (2000).
37. Harry, P., Mauras, Y., Chennebault, J. M., Allain, P. and Alquier, P., *Presse Med.*, **17**(13), 2520 (1984).

38. Wang, X. W., Davies, J. W., Zapata Sirvent, R. L. and Robinson, W. A., *Burns Incl. Therm. Inj.*, **11**, 181 (1985).
39. Terrill, P. J. and Gowar, J. P., *Br. J. Plast. Surg.*, **43**, 699 (1990).
40. Matey, P., Allison, K. P., Sheehan, T. M. and Gowar, J. P., *J. Burn Care Rehabil.*, **21**, 241 (2000).
41. Laitung, J. K. and Earley, M., *Burns Incl. Therm. Inj.*, **10**, 378 (1984).
42. Corbett, G. E., Finley, B. L., Paustenbach, D. J. and Kerger, B. D., *J. Expo. Anal. Environ. Epidemiol.*, **7**, 179 (1997).
43. Gammelgaard, B., Fullerton, A., Avnstorp, C. and Menne, T., *Contact Dermatitis*, **27**, 302 (1992).
44. Fregert, S. and Rorsman, H., *Acta Derm. Venereol.*, **46**, 144 (1966).
45. Bagdon, R. E. and Hazen, R. E., *Environ. Health Perspect.*, **92**, 111 (1991).
46. Liu, K. J., Mader, K., Shi, X. and Swartz, H. M., *Magn. Reson. Med.*, **38**, 524 (1997).
47. Levis, A. G. and Majone, F., *Br. J. Cancer*, **44**, 219 (1981).
48. Wise Sr, J. P., Stearns, D. M., Wetterhahn, K. E. and Patierno, S. R., *Carcinogenesis*, **15**, 2249 (1994).
49. Petrilli, F. L. and De Flora, S., *Sci. Total Environ.*, **71**, 357 (1988).
50. Quievryn, G., Goulart, M., Messer, J. and Zhitkovich, A., *Mol. Cell. Biochem.*, **222**, 107 (2001).
51. Debetto, P. and Luciani, S., *Sci. Total Environ.*, **71**, 365 (1988).
52. Myers, C. R. and Myers, J. M., *Carcinogenesis*, **19**, 1029 (1998).
53. Standeven, A. M. and Wetterhahn, K. E., *Carcinogenesis*, **13**, 1319 (1992).
54. De Flora, S., Serra, D., Camoirano, A. and Zanacchi, P., *Biol. Trace Elem. Res.*, **21**, 179 (1989).
55. Corbett, G. E., Dodge, D. G., O'Flaherty, E., Liang, J., Throop, L., Finley, B. L. and Kerger, B. D., *Environ. Res.*, **78**, 7 (1998).
56. Richelmi, P. and Baldi, C., *Int. J. Environ. Anal. Chem.*, **17**, 181 (1984).
57. Wiegand, H. J., Wiegand, H. J. and Bolt, H. M., *Arch. Toxicol.*, **57**, 31 (1985).
58. Kolacinski, Z., Kostrzewski, P., Kruszewska, S., Razniewska, G. and Mielczarska, J., *J. Toxicol. Clin. Toxicol.*, **37**, 785 (1993).
59. Paustenbach, D. J., Hays, S. M., Brien, B. A., Dodge, D. G. and Kerger, B. D., *J. Toxicol. Environ. Health*, **49**, 453 (1996).
60. Lindberg, E. and Vesterberg, O., *Am. J. Ind. Med.*, **16**, 485 (1989).
61. N. W. Tietz, *Clinical Guide to Laboratory Tests*, 3rd ed., Saunders Company, Philadelphia, PA, 1995.
62. Herber, R. F., *Int. Arch. Occup. Environ. Health*, **72**, 279 (1999).
63. Granadillo, V. A., Parra de Machado, L. and Romero, R. A., *Anal. Chem.*, **66**, 3624 (1994).
64. Bukowski, J. A., Goldstein, M. D. and Johnson, B. B., *Arch. Environ. Health*, **46**, 230 (1991).
65. Anderson, R. A., Polansky, M. M., Bryden, N. A., Roginski, E. E., Patterson, K. Y. and Reamer, D. C., *Diabetes*, **3**, 212 (1982).
66. Anderson, R. A., *Diabetes Metab.*, **26**, 22 (2000).
67. Wallach, S., *J. Am. Coll. Nutr.*, **4**, 107 (1985).
68. Mertz, W., *J. Nutr.*, **123**, 626 (1993).
69. Lamson, D. S. and Plaza, S. M., *Altern. Med. Rev.*, **7**, 218 (2002).
70. Althuis, M. D., Jordan, N. E., Ludington, E. A. and Wittes, J. T., *Am. J. Clin. Nutr.*, **76**, 148 (2002).
71. Cerulli, J., Grabe, D. W., Gauthier, I., Malone, M. and McGoldrick, M. D., *Ann. Pharmacother.*, **32**, 428 (1998).
72. Wasser, W. G., Feldman, N. S. and D'Agati, V. D., *Ann. Intern. Med.*, **126**, 410 (1997).
73. Martin, W. R. and Fuller, R. E., *Pharmacotherapy*, **18**, 860 (1998).
74. Biedermann, K. A. and Landolph, J. R., *Cancer Res.*, **50**, 7835 (1990).
75. von Burg, R. and Liu, D., *J. Appl. Toxicol.*, **13**, 225 (1993).
76. Barceloux, D. G., *J. Toxicol. Clin. Toxicol.*, **37**, 173 (1999).
77. Bagchi, D., Stohs, S. J., Downs, B. W., Bagchi, M. and Preuss, H. G., *Toxicology*, **180**, 5 (2002).
78. Stohs, S. J., Bagchi, D., Hassoun, E. A. and Bagchi, M., *J. Environ. Pathol. Toxicol. Oncol.*, **20**, 77 (2001).
79. Molyneux, M. J. and Davies, M. J., *Carcinogenesis*, **16**, 875 (1995).
80. Ding, M. and Shi, X., *Mol. Cell. Biochem.*, **235**, 293 (2002).
81. Standeven, A. M. and Wetterhahn, K. E., *Chem. Res. Toxicol.*, **4**, 616 (1991).
82. Liu, K. J. and Shi, X., *Mol. Cell. Biochem.*, **222**, 41 (2001).
83. Shi, X., Chiu, A., Chen, C. T., Halliwell, B., Castranova, V. and Vallyathan, V., *J. Toxicol. Environ. Health B Crit. Rev.*, **2**, 87 (1999).
84. Singh, J., Carlisle, D. L., Pritchard, D. E. and Patierno, S. R., *Oncol. Rep.*, **5**, 1307 (1998).
85. Sugden, K. D. and Stearns, D. M., *J. Environ. Pathol. Toxicol. Oncol.*, **19**, 215 (2000).
86. Pourahmad, J. and O'Brien, P. J., *Adv. Exp. Med. Biol.*, **500**, 203 (2001).
87. Bagchi, D., Bagchi, M. and Stohs, S. J., *Mol. Cell. Biochem.*, **222**, 149 (2001).
88. Stearns, D. M., Silveira, S. M., Wolf, K. K. and Luke, A. M., *Mutat. Res.*, **513**, 135 (2002).
89. Iserson, K. V., Banner, W., Froede, R. C. and Derrick, M. R., *J. Emerg. Med.*, **1**, 143 (1983).
90. Schiffl, H., Weidmann, P., Weiss, M. and Massry, S. G., *Miner. Electrolyte Metab.*, **7**, 28 (1982).
91. http://www.cdc.gov/niosh/idlh/intridl4.html, (2003).
92. ILO, Chromium, alloys, compounds. *Encyclopaedia of Occupational Health and Safety*, 2nd ed.,

International Labour Office, Geneva, Switzerland, 1991, pp. 295–297.
93. Cohen, S. R., Davis, D. M. and Kramkowski, R. S., *Cutis*, **13**, 558 (1974).
94. Lindberg, E. and Hedenstierna, G., *Arch. Environ. Health*, **38**, 367 (1983).
95. Gibb, H. J., Lees, P. S., Pinsky, P. F. and Rooney, B. C., *Am. J. Ind. Med.*, **38**, 127 (2000).
96. Machle, W. and Gregorius, F., *Public Health Rep.*, **63**, 1114 (1948).
97. Lee, C. R., Yoo, C. I., Lee, J. and Kang, S. K., *Ind. Health*, **40**, 286 (2002).
98. Bovet, P., Lob, M. and Grandjean, M., *Int. Arch. Occup. Environ. Health*, **40**, 25 (1977).
99. Kuo, H. W., Lai, J. S. and Lin, T. I., *Int. Arch. Occup. Environ. Health*, **70**, 272 (1997).
100. Huvinen, M., Uitti, J., Zitting, A., Roto, P., Virkola, K., Kuikka, P., Laippala, P. and Aitio, A., *Occup. Environ. Med.*, **53**, 741 (1996).
101. De Raeve, H., Vandecasteele, C., Demedts, M. and Nemery, B., *Am. J. Ind. Med.*, **34**, 169 (1998).
102. Leroyer, C., Dewitte, J. D., Bassanets, A., Boutoux, M., Daniel, C. and Clavier, J., *Respiration*, **65**, 403 (1998).
103. Park, H. S., Yu, H. J. and Jung, K. S., *Clin. Exp. Allergy*, **24**, 676 (1994).
104. Olaguibel, J. M. and Basomba, A., *Allergol. Immunopathol. (Madr.)*, **17**, 133 (1989).
105. Bright, P., Burge, P. S., O'Hickey, S. P., Gannon, P. F., Robertson, A. S. and Boran, A., *Thorax*, **52**, 28 (1997).
106. Novey, H. S., Habib, M. and Wells, I. D., *J. Allergy Clin. Immunol.*, **72**, 407 (1983).
107. Shirakawa, T. and Morimoto, K., *Arch. Environ. Health*, **51**, 221 (1996).
108. Dahl, R. and Mikkelsen, H. B., *Ugeskr. Laeger*, **144**, 801 (1982).
109. Keskinen, H., Kalliomaki, P. L. and Alanko, K., *Clin. Allergy*, **10**, 151 (1980).
110. Moller, D. R., Brooks, S. M., Berstein, D. I., Cassedy, K., Enrione, M. and Berstein, L., *J. Allergy Clin. Immunol.*, **7**, 451 (1986).
111. Lockman, L. E., *Can. Fam. Physician*, **48**, 1907 (2002).
112. Sastre, J., Fernandez-Nieto, M., Maranon, F., Fernandez-Caldas, E., Pelta, R. and Quirce, S. J., *Allergy Clin. Immunol.*, **108**, 650 (2002).
113. Fregert, S., *Br. J. Dermatol.*, **105**(Suppl. 21), 7 (1981).
114. Polak, L., Immunology of chromium, in *Chromium: Metabolism and Toxicity*, Burrows, D. (Ed.), CRC Press, Boca Raton, FL, 1983, pp. 51–136.
115. Samsoen, M., Stampf, J. L., Lelièvre, G. and Foussereau, J., *Derm. Beruf. Umwelt.*, **30**, 181 (1982).
116. Mali, J. W. H., van Knoten, W. J., Van Neer, F. C. J. and Spruit, D., *Acta Derm. Venereol.*, **44**, 44 (1966).
117. Fregert, S. and Rorsman, H., *Arch. Dermatol.*, **93**, 711 (1966).
118. Iyer, V. J., Banerjee, G., Govindram, C. B., Kamath, V., Shinde, S., Gaikwad, A., Jerajani, H. R., Raman, G. and Cherian, K. M., *Contact Dermatitis*, **47**, 357 (2002).
119. Nethercott, J., Paustenbach, D., Adams, R., Fowler, J., Marks, J., Morton, C., Taylor, J., Horowitz, S. and Finley, B., *Occup. Environ. Med.*, **51**, 371 (1994).
120. Peltonen, L. and Fraki, J., *Contact Dermatitis*, **9**, 190 (1983).
121. Kanerva, L., Jolanki, R., Estlander, T., Alanko, K. and Savela, A., *Am. J. Contact Dermatitis*, **11**, 155 (2000).
122. Halbert, A. R., Gebauer, K. A. and Wall, L. M., *Contact Dermatitis*, **27**, 214 (1992).
123. Guo, Y. L., Wang, B. J., Yeh, K. C., Wang, J. C., Kao, H. H., Wang, M. T., Shih, H. C. and Chen, C. J., *Contact Dermatitis*, **40**, 1 (1999).
124. Irvine, C., Pugh, C. E., Hansen, E. J. and Rycroft, R. J. G., *Occup. Med.*, **44**, 17 (1994).
125. Kaufman, J. D., Cohen, M. A., Sama, S. R., Shields, J. W. and Kalat, J., *Am. J. Public Health*, **88**, 1047 (1998).
126. Diepgen, T. L. and Coenraads, P. J., *Int. Arch. Occup. Environ. Health*, **72**, 496 (1999).
127. Andersen, K. E., Burrows, D. and White, I. R., Allergens from the Standard Series. Chromium, *Textbook of Contact Dermatitis*, 2nd ed., Rycroft, R. J. G., Mennè, T., Frosch, P. J. (Eds.), Springer-Verlag, Berlin, Germany, 1995, pp. 421–424.
128. Avnstorp, C., *Acta Derm. Venereol*, **179**(Suppl.), 1 (1992).
129. Zachariae, C. O., Agner, T. and Menne, T., *Contact Dermatitis*, **35**, 83 (1996).
130. Goh, C. L. and Gan, S. L., *Contact Dermatitis*, **34**, 51 (1996).
131. Johansen, J. D., Menne, T., Christophersen, J., Kaaber, K. and Veien, N., *Br. J. Dermatol.*, **142**, 490 (2000).
132. Nygren, O. and Wahlberg, J. E., *The Analyst*, **123**, 935 (1998).
133. Hansen, M. B., Rydin, S., Menne, T. and Duus, J., *Contact Dermatitis*, **47**, 127 (2002).
134. Estlander, T., Jolanki, R. and Kanerva, L., *Contact Dermatitis*, **43**, 114 (2000).
135. Kvitko, E., *Contact Dermatitis*, **45**, 256 (2001).
136. Fowler, J. F., Jr *Cutis*, **65**, 116 (2000).
137. Merritt, K. and Brown, S. A., *J. Biomed. Mater. Res.*, **29**, 627 (1995).
138. Hubler, W. R. Jr. and Hubler W. R. Sr., *Contact Dermatitis*, **9**, 377 (1983).
139. L. Kanerva, *The Chromium File*, International Chromium Development Association, Vol. 2, 1996.
140. Wedeen, R. P. and Qian, L. F., *Environ. Health Perspect.*, **92**, 71 (1991).
141. Foa, V., Riboldi, L., Patroni, M., Zocchetti, C., Sbrana, C. and Mutti, A., *Sci. Total. Environ.*, **71**, 389 (1988).
142. Saner, G., Yuzbasiyan, V. and Cigdem, S., *Br. J. Ind. Med.*, **41**, 263 (1984).
143. Triebig, G., Zschiesche, W. and Schaller, K. H., *J. Biochem. Toxicol.*, **1**, 29 (1987).
144. Verschoor, M. A., Bragt, P. C., Herber, R. F., Zielhuis, R. L. and Zwennis, C. M., *Int. Arch. Occup. Environ. Health*, **60**, 67 (1988).

145. USEPA Integrated Risk Information System (IRIS), US Environmental Protection Agency, Environmental Criteria and Assessment Office, June 1992, Cincinnati, OH, 1992.
146. Moulin, J. J., *Scand. J. Work Environ. Health*, **23**, 104 (1997).
147. Hansen, K. S., Lauritsen, J. M. and Skytthe, A., *Am. J. Ind. Med.*, **30**, 373 (1996).
148. Steenland, K., *Scand. J. Work Environ. Health*, **28**, 163 (2002).
149. Danielsen, T. E., Langard, S. and Andersen, A., *J. Occup. Environ. Med.*, **42**, 101 (2000).
150. Health Council of the Netherlands, Chromium VI and its Compounds, Evaluation of the Effects on Reproduction, Recommendation for Classification, Committee for Compounds Toxic to Reproduction. A Committee of the Health Council of the Netherlands to the Minister and State Secretary of Social Affairs and Employment, No. 2001/01OSH, The Hague, 25 January, 2001.

2.7 Speciation of Cobalt

Dominique Lison
Université catholique de Louvain, Brussels, Belgium

1 INTRODUCTION

The main oxidation states of cobalt are (II) and (III), the former being the most stable. Cobalt(I), (IV) and (V) compounds can be formed, but those are not well characterized. The most common simple and hydrated Co(II) salts include cobalt carbonate, cobalt chloride, cobalt hydroxide, cobalt nitrate, cobalt sulfide and cobalt sulfate. The most common Co(II) complexes include the hexacoordinated species with H_2O, NH_3 and dimethylsulfoxide as ligands (cationic complexes); the tetrahedral species with Cl^-, Br^-, I^-, SCN^-, $CH_3CO_2{}^-$ or OH^- (anionic complexes); and the tetrahedral complexes with pyridine, phosphine and arsine derivatives (neutral complexes). Cobalt(III) compounds mainly exist as complexes with ligands such as NH_3, CN^-, $NO_3{}^-$, ethylenedinitrilotetraacetic acid (EDTA), phtalocyanines and azo dyes. These electron-donor ligands stabilize Co(III) in solution, usually forming octahedral complexes. In the absence of such ligands, Co^{+++} is so unstable that, at acidic pH, it rapidly oxidizes water to molecular oxygen. In alkaline solutions containing ammonium hydroxide or cyanide, Co^{++} can be oxidized by air or hydrogen peroxide to form more stable Co(III) complexes. The ability of cobalt to form complex species and the interconversion between cobaltous and cobaltic compounds are important in many industrial applications, including their use as catalysts or paint dryers. As yet, their involvement in the biological mode of action of cobalt species, except for the reactions of vitamin B_{12}, is incompletely understood.

The most important Co(II) salts of carboxylic acids are formate, acetate, citrate, naphtenate,

Handbook of Elemental Speciation II: Species in the Environment, Food, Medicine & Occupational Health
Edited by R. Cornelis, H. Crews, J. Caruso and K. G. Heumann
 ISBN: 0-470-85598-3 (HB)

Table 2.7.1. The varying properties of cobalt compounds.

	CAS No.	Formulae	MW	Melting point (°C)	Density	Water solubility ($g \cdot L^{-1}$)	
Cobalt metal	7440-48-4	Co	58.93	1495	8.84	Insoluble	Hexagonal and cubic forms
Cobalt(II, III) oxide	1308-06-1	Co_3O_4	240.80	895	6.07	Insoluble (0.00084)	
Cobalt(II) oxide	1307-96-6	CoO	74.93	1795, 1935	6.45	Insoluble (0.000313)	
Cobalt(II) acetate (tetrahydrate)	71-48-7 (6147-53-1)	$Co(CH_3CO_2)_2$	177.03	–	–	Readily soluble	
Cobalt(II) carbonate	513-79-1	$CoCO_3$	118.94	Decomposes	4.13	Practically insoluble	
Cobalt(II) chloride (hexahydrate)	7646-79-9 (7791-13-1)	$CoCl_2$	129.84	Decomposes	3.36	Soluble (529 @ 20 °C)	
Cobalt(II) hydroxide	21041-93-0	$Co(OH)_2$	92.95	Decomposes	3.60	Very slightly soluble (0.0032)	
Cobalt(II) nitrate (hexahydrate)	10141-05-6 (10026-22-9)	$Co(NO_3)_2$	182.96	Decomposes (100)	2.49	Soluble	
Cobalt(II) sulfate (heptahydrate)	10124-43-3 ()	$Co(SO_4)$	154.99	Decomposes (735)	3.71	Soluble (362 @ 20 °C)	
Cobalt(II) sulfide	1317-42-6	CoS	90.99	>1100	5.45	Insoluble (0.0038 @ 18 °C)	α- and β-forms

linoleate, oleate, oxalate, resinate, stearate, succinate, sulfamate, 2-ethylhexanoate and cobalt carbonyl. A biologically important cobalt compound is vitamin B_{12} or cyanocobalamin, in which cobalt is complexed with four pyrrole nuclei joined in a ring called *corrin*, similar to porphyrins.

When heated, cobalt metal is oxidized to the mixed or cobaltocobaltic oxide, Co(II,III) oxide or Co_3O_4; above 900 °C, the cobaltous oxide Co(II) oxide or CoO is formed. The mixed Co(II, III) oxide has the spinel structure with Co(II) and Co(III) at tetrahedral and octahedral sites, respectively.

The main characteristics of the most common cobalt compounds are summarized in Table 2.7.1.

2 COBALT IN THE ENVIRONMENT

2.1 Natural and anthropogenic sources

Natural sources of cobalt in the environment are soil, dust, seawater, volcanic eruptions and forest fires. It is also released to the environment from burning coal and oil, from car, lorry and aeroplane exhausts, and from industrial processes that use the metal or its compounds.

Cobalt is the 33rd element on the earth crust with an average concentration of 10–20 $\mu g\,g^{-1}$, but much higher concentrations are found in ore deposits from which approximately 25,000 tons of cobalt metal are produced annually. The most important minerals from which cobalt is purified are cobaltite (CoAsS), smaltite ($CoAs_2$) and erythrite [$Co_3(AsO_4)_2$]. About 40% of the world cobalt mining is in Central Africa (Democratic Republic of Congo, Zambia) where it is extracted in association mainly with copper; other main locations include Australia, Canada, China, Russia, Morocco and New Caledonia [1]. Through the process of weathering, cobalt is leached from its parent earth crust material and enters the soil sediment system from which it is partially taken up by plants and animals and through the food chain to man. Elevated levels of cobalt in soil may also result from anthropogenic activities such as the application of cobalt-containing sludge or phosphate fertilizers, the disposal of cobalt-containing wastes and atmospheric deposition from activities such as mining, smelting, refining or combustion. Total cobalt is present in most soils in the range 0.1–50 $\mu g\,kg^{-1}$ and the cobalt available to plants between 0.1 and 2 $\mu g\,kg^{-1}$. The predominant cobalt species in soil is the Co(II) ion. Overall, in soil-plant systems, the behavior of cobalt follows that of the Fe-Mn system. Plant uptake of Co^{+2} is dependent on the fraction of the element adsorbed on Mn and organic complexes. Cobalt is required by the Rhizobium bacteria, which has a symbiotic association with legume roots and the free-living N-fixation bacteria Azobacter. Cobalt is probably an essential element for plants, as an enhanced supply results in increased yields for cereals. Lack of cobalt in the soil (less than 0.1 $\mu g\,kg^{-1}$, for example, in granitic soils, sandstones, sands, limestones) may result in a deficiency of vitamin B_{12} in ruminants (see below, [2]). Because of the rather low concentration of cobalt in many agricultural soils, the addition of cobalt compounds (simple salts or chelates) to fertilizers, lime and sewage sludge has been a common practice in most countries. The cobalt content of fertilizers (phosphate and nitrate types) is in the range 1–12 $\mu g\,kg^{-1}$. Toxic effects on plants are unlikely to occur below soil cobalt concentrations of 40 $\mu g\,kg^{-1}$. However, soil concentration is not the only parameter determining toxicity. Plant species greatly vary in their sensitivity to cobalt, and soil type and chemistry greatly influence cobalt toxicity. The most important soil properties is soil acidity; the more acidic the soil, the greater toxic potential for cobalt. Soils with high cobalt concentrations usually also have high arsenic and nickel concentrations that are generally more toxic to plants (and humans) than cobalt.

In environmental water, cobalt is naturally present in trace amounts as Co^{++} and as suspensions of the almost insoluble carbonate, hydroxide and sulfide compounds. An average concentration of 0.3 μg Co/L has been reported in seawater, cobalt ranking as the 44th element in abundance, but there is a large regional variability. Speciation methods have been developed using cathodic stripping voltammetry to determine the extent of cobalt complexation with ligands in seawater [3, 4]. A few

μg Co/L can be present in river water, lakes, spring water, ground or well water. Cobalt in river waters is present in the form of very stable complexes possibly associated with humic acids. Cobalt is also released into water from anthropogenic sources such as mining, discharge from industries and atmospheric deposition [2].

Natural and anthropogenic sources contribute almost equally to the emission of cobalt in the atmosphere. Natural sources of cobalt in the atmosphere are windblown continental dust, seawater sprays, volcanoes, forest fires and continental and marine biogenic emissions. The primary anthropogenic sources of cobalt in the atmosphere are the burning of fossil fuels and sewage sludge, phosphate fertilizers, mining and transformation of cobalt-containing ores and industries that produce or process cobalt. The natural background air concentration of cobalt is in the order of 1 pg m^{-3}, but concentrations up to 40 ng m^{-3} have been reported in urban areas [5]. The exact cobalt species present in the atmosphere are not well characterized.

3 COBALT IN FOOD

Cobalt enters the food chain via plants from water and soil. The cobalt status of plants may depend on a number of factors such as soil levels of available cobalt and other elements such as manganese and iron, the moisture content of the soil, the pH of the soil, the plant species, the plant organ and its stage of growth. The effect of cobalt on plants is not fully understood and may vary among different species. In general, plants do not require cobalt in their metabolism. The importance of cobalt in plants lies in its part in the food chain, in that it provides a source of the element to animals and particularly ruminants that synthesize vitamin B_{12}. Vegetables contain inorganic cobalt but little or no vitamin B_{12}. Green leafy vegetables and fresh cereals are the richest sources of cobalt (0.2–0.6 μg g^{-1} dry weight); dairy products, refined cereals and sugar contain the least cobalt (0.01–0.03 μg g^{-1} dry weight) [6].

Ruminants obtain the vitamin B_{12} necessary for their metabolism by absorbing rumen organisms that are able to synthesize the vitamin, other herbivores (horse, rabbit) synthesize vitamin B_{12} in their cecum. The presence of cobalt in their foodstuffs is therefore essential for the synthesis of vitamin B_{12} by the microorganisms and therefore for the survival of the animals and the downstream food chain. When the dried herbage contains more than 0.1 μg g^{-1}, the cobalt intake of the ruminant is generally sufficient to meet its need. Animal livers, kidney and muscles contain high concentrations of cobalt (0.15–0.25 μg g^{-1} dry weight, not exclusively in the form of vitamin B_{12}) [7].

Tobacco contains about <0.3–2.3 mg Co per kg dry weight and approximately 0.5% of the cobalt appears in the mainstream smoke. The exact speciation of cobalt in tobacco is not known. Very limited data are available on the exact species of cobalt present in food.

The contribution of drinking water and beverages to the dietary intake of cobalt is minimal.

Cobalt is the only essential oligoelement that needs to be supplied in a particular form, that is, vitamin B_{12}, to be physiologically active. Human dietary intake of cobalt is highly variable with reported values generally between 5 and 50 μg day^{-1} [8]. Most of the cobalt ingested by humans is inorganic, vitamin B_{12} representing only a small fraction. The main sources of vitamin B_{12} in food according to Leboulanger [9] are summarized in Table 2.7.2.

In a survey conducted during 1986–1988, foods were purchased at the retail level in Canada and prepared for consumption. Mean (range) levels of cobalt were 9.4 ng g^{-1} (<0.3–75.7) with the highest concentration in waffles (76 ng g^{-1}), corn cereal (74 ng g^{-1}) and potato chips (70 ng g^{-1}).

Table 2.7.2. Vitamin B_{12} content in food [9].

Food	Vitamin B_{12} (μg g^{-1})
Beef liver	0.40
Beef kidney	0.20
Pork heart	0.17
Herring	0.14
Mackerel	0.05
Cow milk	0.025
Beef meat	0.025
Cheese	0.01
Whole eggs	0.004

The estimated dietary intake was 11 μg per day [10]. However, in the United States, much higher values have been reported in a survey on the metal content in more than 230 foods collected in 1984 by the Food and Drug Administration; Co intakes were estimated at 493 to 1489 $\mu g\,day^{-1}$.

In the 1960s, cobalt sulfate has been added as a foam stabilizer (0.8–1.6 $\mu g\,mL^{-1}$) to several brands of beer in Belgium, USA and Canada in response to complaints of poor foaming qualities. This episode lead to outbreaks of cardiac disease among heavy beer consumers (up to 10 liters per day) of cobalt-fortified beer, and this practice was rapidly abandoned. Subsequently, it was found that the actual cause of poor foaming was detergent residue on beer glasses due to inadequate rinsing [11].

4 COBALT IN HEALTH AND DISEASE

As a constituent of vitamin B_{12}, cobalt is an essential element and, so far, another physiological role of cobalt has not been demonstrated in human nutrition. The human body (adult 70 kg) contains on an average 1.1 mg cobalt, 85% of which is in the form of vitamin B_{12}. The normal ranges of cobalt and vitamin B_{12} plasma concentrations are $<0.2\ ng\,mL^{-1}$ and 200 to 900 $pg\,mL^{-1}$, respectively [12]. The daily requirements of vitamin B_{12} are of about 1 μg (0.1–2.5 according to different authors), which corresponds to 0.0434 μg of cobalt per day (4.34% of vitamin B_{12} weight). Considering that only 50% of vitamin B_{12} is absorbed by the gastrointestinal tract, the recommended daily allowance of vitamin B_{12} is 2.4 μg (or 0.10 μg cobalt). Because 10–30% of older people may malabsorb food-bound vitamin B_{12}, in the United States it is recommended for individuals older than 50 to add a supplement of vitamin B_{12} to their diet (e.g. vitamin B_{12} fortified food) [13].

4.1 Metabolism of cobalt

A limited number of studies indicate that cobalt speciation influences the kinetics of absorption of the element by the oral and inhalation routes. Once absorbed, cobalt is mainly present in the organism as Co(II) ions (except for vitamin B_{12}), and distribution and excretion are less dependent on speciation.

4.1.1 Absorption

Quantitative data on the absorption of cobalt compounds and the influence of speciation are very limited.

The oral bioavailability of cobalt compounds varies with the solubility of the compound, the material ingested concomitantly, and incompletely characterized individual factors. In early experiments, Murdock (1959) cited in [14] showed that, following oral administration of Co(II) ions, the urinary excretion of the element was inversely proportional to the dose (0.25, 1.25, 5 or 10 mg Co per kg). The uptake of ionic cobalt from the gastrointestinal tract has been reported to occur from the proximal jejunum through a saturable process that limits the extent of uptake [14]. The intestinal absorption of ionic cobalt seems to involve mechanisms common with Fe(II), with a first step of mucous absorption followed by the transfer from the enterocytes. A competition for the digestive absorption of ionic iron and cobalt has been observed in rat. The respective gastrointestinal absorption rates of inorganic cobalt forms have, however, not been very well characterized. In the hamster, less than 0.5% of CoO is absorbed by the digestive route, whereas 9–45% of cobalt chloride is absorbed in humans by the same route [15]. In human volunteers, depletion of iron stores was associated with a significantly increased gastrointestinal absorption of the element administered as cobalt chloride [16]. In the rat, the gastrointestinal absorption of Co(II) ions administered as chloride was significantly reduced by complexation with low molecular weight compounds such as histidine, lysine, glycine, casein or EDTA. Administration of Co(II) ions with cow milk increased the gastrointestinal absorption up to 40%. The same study noted no difference in the gastrointestinal absorption rate between Co(II) and Co(III) chloride, but Co(II) complexed with glycine was absorbed in significantly greater amounts than

Co(III) complexes [17]. The digestive absorption of cobalt compounds is also influenced by nutritional factors such as the presence of albumin or lactose that increase the absorption of the element. Gastrointestinal absorption of radiolabeled cobalt citrate has been found to decrease rapidly from newborn to weaning and adult animals in both rats and guinea pigs [18]. The digestive absorption of vitamin B_{12} is dependent on the presence of several specific proteins (R-binder, intrinsic factor, receptor) (see below).

The deposition pattern of inhaled particles in the respiratory tract is related to particle density and size, the largest particles tending to deposit in the upper respiratory tract and the smallest particles (less than 2 μm) reaching the gas exchange regions. While approximately 30% of inhaled CoO is absorbed within 24 h in the hamster, considerably lower values have been reported in the rat [19]. The absorption of deposited cobalt particles is also dependent on the chemical species involved with soluble cobalt salts (e.g. cobalt(II) nitrate) being more readily absorbed than mixed oxides [20]. Studies in the rat have also shown that the respiratory absorption of cobalt metal particles is significantly increased in the presence of tungsten carbide particles [21]. In workers exposed to cobalt pigments in the pottery industry (mainly by inhalation), the absorption of the element estimated through the measurement of urinary cobalt concentration was significantly higher in workers exposed to soluble cobalt dye (cobalt-zinc-silicate) than in those using insoluble cobalt (cobalt aluminate) [22]. Significant differences in the absorption of cobalt have also been reported in workers exposed by inhalation to varying cobalt-containing particle species: cobalt metal alone or mixed with tungsten carbide in hard metals particles was rapidly excreted in urine and reflected recent airborne exposure, whereas no relation with recent exposure was found in workers exposed to cobalt oxides, suggesting lower or slower pulmonary absorption [23].

Limited information is available on dermal absorption of cobalt, and the influence of speciation is not documented. The absorption of Co(II) ions (radiolabeled $CoCl_2$ in acid) is less than 1% through intact skin in the guinea pig [24]. Significant dermal absorption of cobalt (as reflected by increased urinary excretion of the element) has been reported following prolonged skin contact with hard metal dust [25] or coolant solutions contaminated with cobalt-containing materials [26].

4.1.2 Distribution

In animals and in humans, cobalt does not accumulate in a specific organ [27]. In humans not specifically exposed to cobalt, the liver contains 10–20% of the body burden. There exists no indication of an accumulation of cobalt in the human body with age. Long-term oral exposure studies performed in the rat with $CoCl_2$ resulted in significantly increased levels of the element in all tissues (liver, kidney, muscle, brain, testes, myocardium and serum). Following inhalation, exposure of dogs to radiolabeled Co oxides, the highest levels of cobalt have been found in the lungs, kidney and liver. A toxicokinetic study in the rat has shown that, following a single subcutaneous administration of elemental cobalt or its protoporphyrin chelate, the elimination rate of the chelate was significantly slower than that of the element. Other studies that document the influence of speciation on the distribution of cobalt in the body have not been located.

In blood, cobalt is evenly distributed in plasma and cellular fractions; in nonoccupationally exposed people, the blood cobalt concentration is $<0.5\ \mu g\,L^{-1}$. Higher levels can occur in patients who consume multivitamin pills, with renal insufficiency or with orthopedic prostheses.

For the non-vitamin B_{12} fraction of cobalt in the organism, the form(s) in which it is distributed in the organism and specific ligands have not been characterized.

4.1.3 Excretion

In humans, whatever the exposure route, the excretion of cobalt is mainly through the urinary route (about 90% of inhaled cobalt) following a biphasic elimination pattern (fast phase of hours-days and

slow phase of months-years). In the absence of exposure, cobalt urinary concentrations are below 2 μg/g creatinine. Higher levels can be found in patients who take multivitamin medications or with surgical prosthesis. The form(s) of cobalt involved in the excretion of the element have not been characterized.

4.2 Physiological aspects

The most important biological activity of cobalt involves the vitamin B_{12} series of coenzymes that play a number of crucial roles in many biological functions. Cyanocobalamin (vitamin B_{12}) was isolated as a red crystalline compound in 1948. Its structure consists of a corrin ring system that provides four nitrogen donor atoms in a plane for bonding cobalt(III). In the isolated vitamin B_{12} crystals, a cyanide group is bound to the cobalt atom, but, as such, vitamin B_{12} has no biological activity. In the biochemically active forms, the cyanide is replaced by a methyl (methylcobalamin) or an adenosyl group (adenosylcobalamin). These structures constitute a way for nature to devise a labile organocobalt compound kept intact from external attack by the axial substituent on the corrin ring. As in most monogastric species, cobalamin cannot be synthesized in the human body and must be supplied in the diet. The only source of cobalamin is animal products: meat and dairy foods. Cobalamin is released from food during gastric digestion and forms a stable complex with a specific protein, gastric R-binder. On entering the duodenum, the cobalamin-R binder complex is digested and the released cobalamin binds to intrinsic factor, a 50 kDa protein secreted by parietal cells of the stomach epithelium. This complex is resistant to digestion and is specifically taken up in the distal ileon where it is released in the circulation bound to transcobalamin I, II or III and finally stored, mainly in the liver. A significant fraction of vitamin B_{12} (3–6 $\mu g\,day^{-1}$) is excreted in the bile and undergoes an entero-hepatic cycle.

Methylcobalamin is an essential cofactor in the conversion of homocysteine to methionine, a critical step in the biosynthesis of folate, purine and choline-containing compounds. Adenosylcobalamin is required for the physiological conversion of methylmalonyl coenzyme A to succinyl coenzyme A.

Except in true vegetarians, deficiency in cobalamin is almost always due to malabsorption resulting from a dysfunction at one of the several steps of its gastrointestinal absorption. The symptoms associated with cobalamin deficiency include hematologic (megaloblastic anemia), gastrointestinal and neurological (peripheral and central) manifestations. Apart from specific therapy related to the underlying disorder, the mainstay of treatment for cobalamin deficiency is replacement therapy. Because the defect is often related to malabsorption, replacement is generally administered parenterally in the form of cyanocobalamin (e.g. 100 μg per day for a week gradually decreased to achieve a total of 2000 μg during six weeks, followed by a maintenance therapy with 100 μg every month). While hematological and gastrointestinal manifestations ameliorate rapidly after treatment, neurological symptoms may not be fully corrected.

Numerous case-control and prospective studies have identified elevated plasma homocysteine as a strong independent risk factor for cerebrovascular, cardiovascular and peripheral vascular disease. The exact mechanism that explains the vascular toxicity of elevated homocysteine levels is unknown at present. Studies indicate that it is both atherogenic and thrombogenic. Many studies have noted strong inverse relationships between homocysteine levels and the status of both vitamin B_{12} and folate [28].

Metal ions such as zinc and iron, apparently more rarely cobalt, may play a variety of physiological roles in natural proteins including catalysis, electron transfer and stabilization. Several enzymes such as rat liver α-D-mannosidase are activated by Co^{++} ions, but it is not clear whether these ions are involved in these enzymes. Recent studies have shown that certain proteins contain cobalt in a form other than the corrin ring of vitamin B_{12} [29]. Eight non-corrin-cobalt containing enzymes have been characterized, including:

– methionine aminopeptidase: this metalloenzyme is ubiquitous in pro- and eucaryotic cells

and is involved in cell regulation, intracellular targeting and protein turnover through the cleavage of N-terminal methionine in newly synthesized polypeptides. It contains two Co^{++} ions per active subunit that catalyze hydrolysis.
- prolidase or proline dipeptidase is involved in the terminal degradation of cellular proteins. Its catalytic site contains two Co^{++} per unit.
- nitrile hydratase catalyses the hydration of nitriles to amides and is involved in the metabolism of toxic compounds in bacterial systems but also industrially for the large-scale production of acrylamide and nicotinamide from the corresponding nitriles. This enzyme is the first example of a non-corrin protein that contains one Co^{+++} ion in each active unit.
- glucose isomerase catalyses the reversible isomerization of D-glucose to D-fructose and is of outmost commercial importance for the industrial production of corn syrup. The actynomycetes enzyme requires the presence of one Co^{++} ion per four subunits. In the industrial processes that use this enzyme, reduction of the cobalt added to the culture medium is important because of the potential health risks associated with the consumption of cobalt in humans.
- methylmalonyl-CoA carboxyltransferase, lysine-2,3-aminomutase and bromoperoxidase are bacterial enzymes that also contain Co^{++} ions.
- aldehyde decarbonylase converts a fatty aldehyde to a hydrocarbon and CO; the enzyme isolated from green algae consists of one Co-porphyrin per subunit. Other cobalt-porphyrin containing proteins have been found in reducing bacteria and their prosthetic group appears to contain Co^{+++} ions.

Several cobalt transporters (COT1, NhlF, GRR1) have recently been characterized in yeast cells; their function is to concentrate Co^{++} ions from the extracellular milieu and to compartmentalize these ions in the cell mitochondria. Whether similar transporter proteins exist in mammalian and human cells and how they may affect cobalt metabolism and/or toxicity is not known [30].

Several genes such as heme oxygenase or erythropoietin are sensitive to hypoxia and respond in a similar manner to Co(II) ions *in vitro* (hypoxia mimetic effect of cobalt ions) [31]. Although the exact molecular mechanisms of this effect of Co(II) ions is not well characterized, it might contribute to explain the polycythemic effect of cobalt *in vivo* (see next section).

4.3 Toxicological aspects

As for other inorganics, it is unlikely that the toxic manifestations associated with excessive exposure to cobalt result from a single and specific mode of action. At least two types of cobalt species can elicit toxic manifestations through different mechanisms, that is, cobalt metal particles and cobalt ions.

In vitro at least some toxic effects are specifically caused by cobalt metal particles and cannot be explained by the presence of solubilized cobalt forms. Physicochemical studies have shown that cobalt metal, and not its (II) ionic species, is thermodynamically able to reduce oxygen in activated oxygen species (AOS); the kinetics of this process is, however, slow because of the poor oxygen-binding capacity at the surface of cobalt metal particles. In the presence of tungsten carbide particles, the oxidation of cobalt metal is catalyzed at the surface of these particles, reduction of dissolved oxygen in AOS is enhanced and soluble cobalt cations are produced in larger amounts [32].The increased capacity of hard metal particles to produce large quantities of AOS compared to cobalt metal alone provides an explanation for their inflammatory action in the lung (see parenchymal disease) and their mutagenic/carcinogenic potential (see below) and point to the necessity to consider these alloys as a specific toxic entity. In this system, soluble cobalt ions are also produced during the critical reaction, but they do not drive it. This mechanism is illustrated on Figure 2.7.1.

Cobalt ions can produce toxicity through several different mechanisms.

– There is evidence that Co(II) ions can inhibit the catalytic activity of certain enzymes such as

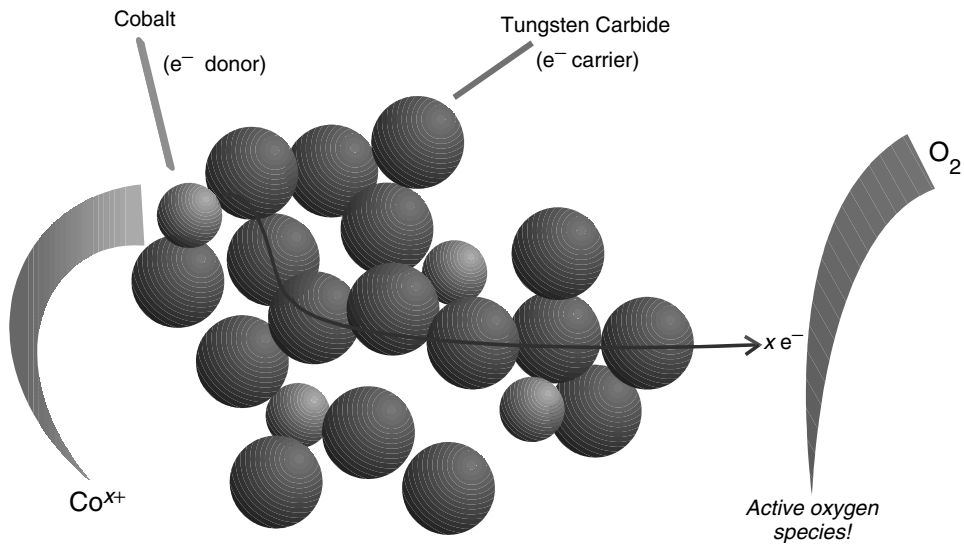

Figure 2.7.1. Physicochemical mechanism of the interaction between cobalt metal and tungsten carbide particles. (Adapted from Lison *et al. Chem. Res. Toxicol*., **8**, 600 (1995) with permission of American Chemical Society).

tyrosine iodinase, cytochrome P450 or peroxydase. This effect has also been demonstrated for deoxyribonucleic acid (DNA) repair enzymes (incision and polymerization steps), in which Co(II) ions interact with zinc finger domains in the protein [33].

– It has been demonstrated *in vitro* that, in the presence of H_2O_2, Co(II) ions are able to cause chemical damage in DNA bases from chromatin, probably through the production of hydroxyl radicals [34]. Such effects appear to be mediated by a Fenton system, also influenced by the concomitant presence of chelators (e.g. 1,10-phenanthroline) [35] and can be site-specifically formed, possibly through the binding of Co(II) ions in zinc fingerprint domains of DNA-binding proteins [36]. *In vivo*, intraperitoneal administration of Co(II) ions (3 and 6 mg Co per kg as cobalt acetate) in the rat produced oxidative DNA damage in renal, hepatic and pulmonary chromatin. The altered bases identified were typical products of hydroxyl radical attack on DNA, and some of them have been shown to be promutagenic [37]. It is probable, but not demonstrated, that this *in vivo* effect is dependent on the presence of endogenous levels of H_2O_2 in target tissues.

– Co(II) ions can act as hapten and bind to macromolecular components to produce immunogenic products that can account for allergic reactions.

– The irreversible chelation of lipoic acid by Co(II) ions under hypoxic conditions might represent a relevant mechanism for the pathogenesis of cobalt-induced cardiomyopathy in beer drinkers (Webb 1982 in [27]),

– Co(II) ions have been shown to alter calcium influx into cells, functioning as a calcium channel blocker [38], to alter the expression of glucose transporter proteins and modify glucose metabolism [39], but the clinical significance of these observations is not well documented.

When considering these possible modes of toxicity, it should, however, be kept in mind that, *in vivo*, the bioavailability of Co(II) ions is relatively limited because these cations precipitate in the presence of physiological concentrations of phosphates (solubility constant (Ksp): 2.5×10^{-35} at 25 °C) and nonspecifically bind to proteins such as albumin.

These mechanisms of action involving ionic cobalt forms are also relevant for metallic cobalt species (alone or associated with tungsten carbide

particles) because the toxic reaction that produces AOS leads in parallel to the oxidation of metallic cobalt and hence to the formation of ionic cobalt species.

In acute cyanide poisoning, the capacity of Co(II) ions to form stable complexes with CN^- cations is used to neutralize this toxicant. Several cobalt-containing complexes such as hydroxycobalamin or dicobaltic EDTA are proposed to treat cyanide poisoning [40].

Differences in the bioavailability of cobalt from different compounds are illustrated in the varying acute toxicity of these compounds (Table 2.7.3).

Occupational activities are the main source of potentially excessive exposure to various cobalt compounds, mainly by inhalation of particles and the respiratory tract is the main target organ (see below). Only a few toxic manifestations were in the past related to nonoccupational oral exposure to inorganic cobalt compounds. In man, no adverse effects of vitamin B_{12} have been reported from single oral doses as high as 100 mg and chronic administration of 1 mg weekly for up to five years.

Cobalt compounds exert a stimulating effect on erythropoiesis and have been used (mainly in the form of cobalt chloride) as a therapy for anemia (25–100 mg daily). A goitrogenic effect of cobalt compounds has been well documented in patients treated with cobalt chloride for hematological disorders [41]. Experimental studies have shown that Co(II) ions block the iodide uptake by follicular cells and the subsequent step of iodide organification (see above).

As mentioned above, outbreaks of cardiomyopathy were reported in Belgium, USA and Canada among heavy consumers of beer (up to 10 liters per day) to which cobalt sulfate had been added as a foam stabilizer (0.8–1.6 $\mu g\,mL^{-1}$) [11]. The classical cardiomyopathy syndrome associated with cobalt beer was characterized by left and then right heart failure accompanied by cardiomegaly, gallop rhythm, cyanosis, low cardiac output, pericardiac effusions and hypotension. Some of the patients regained normal cardiac status upon cessation of exposure. The serum cobalt concentration was reported as being 150 to 1500 $\mu g\,L^{-1}$ in one patient, but these values should be considered with caution since control values of 70 $\mu g\,L^{-1}$ were reported in the same study. Cobalt urinary excretion rates ranging from 34 to 533 $\mu g\,day^{-1}$ have also been found. The epidemiological evidence for a causal role of cobalt in the pathogenesis of this cardiomyopathy is convincing, but the exact mechanism remains unknown, although cardiac lesions have been produced in experimental animals treated with cobalt salts. Since the amount of metal ingested in the cobalt-beer drinkers was lower (up to 10 $mg\,day^{-1}$) compared with the doses used in anemia treatment, the influence of other factors has been considered. It has often been assumed that poor nutrition and ethanol had played a synergistic role in the development of the myocardium lesions. The development of a fatal cardiomyopathy in uremic patients treated with cobalt salts for anemia has also been described [42]. Interestingly, polycythemia has also been reported in heavy beer consumers [11].

Co(II) acetate and chloride were not found to be teratogenic in hamsters and rats, respectively. Cobalt chloride was found to be a potent teratogen for Xenopus laevis.

Cobalt-chromium alloys are used in prosthesis for human joint replacement (e.g. femoral head) and dental appliances because of their resistance to both wear and corrosion and their high fatigue strength. Cobalt and nickel released from orthopedic or dental prostheses may precipitate allergic reactions, with local effects and inflammation [43].

Adverse reactions in various organs such as the liver, kidney, testes and pancreas have been observed in animals treated with high doses of

Table 2.7.3. Acute oral toxicity of different cobalt compounds in the rat.

Compound	LD_{50} ($mg\,kg^{-1}$)	LD_{50} (mg Co/kg)
Cobalt metal	6171	6171
Cobalt(II) chloride	80	37
Cobalt(II) chloride hexahydrate	766	125
Cobalt(II) oxide	202	159
	1700 (gastric tubing)	1338
Cobalt sulfide	>5000	>5000

cobalt [19], but the relevance of these observations for human exposure conditions is uncertain.

5 OCCUPATIONAL HEALTH

The industrial uses of cobalt and its compounds are summarized in Table 2.7.4. The major uses are for the manufacture of alloys, hard metals and magnets. Because of the practical advantages of high melting point, strength and resistance to oxidation, cobalt metal is used for the production of a number of alloys. The CAS Registry lists approximately 5000 alloys of cobalt with other metals, of which cobalt is the base metal for about 2000. The main cobalt-based alloys are:

- the strong and corrosion-resistant *superalloys* that in addition to Co may contain Ni, Cr, Al, Y and small amounts of other metals,
- the *magnetic alloys* that also contain Pt, Sm and other rare earth minerals,
- the cobalt-containing high-strength steels,
- the electrodeposited Ni–Co alloys,
- the so-called hard metals or cemented carbides that are not genuine alloys but composite materials manufactured by a powder metallurgy process from tungsten carbide (about 90% in weight) and cobalt metal (up to 10%) particles. The hard metals possess extraordinary properties of hardness (close to that of diamond) and remarkably resist heat and wear. Unlike other metals, their hardness increases with temperature,
- alloys with special properties such as for surgical and dental implants (e.g. vitallium that associates chromium and cobalt).

Occupational exposure to cobalt occurs mainly by inhalation in various industries that involve the production and processing of the various cobalt-containing alloys and salts and/or the utilization of cobalt-containing tools for boring, drilling or polishing. The potential for exposure to cobalt is particularly significant during the production of cobalt powder, the production, processing and use of hard metals, the polishing of diamonds with cobalt-containing disks, and the use of cobalt compounds. Airborne concentrations up to a few mg m^{-3} have been measured at some workplaces [8]. It should be noted that, except in the production of cobalt powders, most activities usually involve not only exposure to cobalt compounds but also to other substances such as carbides, iron, diamond, and so on. As already mentioned, these other constituents may modulate the biological reactivity of cobalt.

Table 2.7.4. Industrial uses of cobalt compounds.

Uses	Cobalt compound(s)
Manufacture of alloys, hard metals and magnets	Co metal
Recycling	Co metal, oxides, salts
Surface treatment, galvanoplasty, coating	Co metal, sulfate, chloride
Rubber adherence on metals	Organic Co salts
Ink, paint and varnish dryers	Organic Co salts
Polymer reticulation process	Organic Co salts
Ceramics and earthenware (coloring)	Co sulfate
Glass industry	Co oxides, carbonate, hydroxide
Magnetic recording materials	Co oxides, sulfate, chloride
Rechargeable batteries (Li-ion, NiCd, Ni-metal hydride)	Co oxides, nitrate, hydroxide
Manufacture of thermistors, varistors	Co oxides, acetate, sulfate
Halogen lamps	Co metal
Catalyst	Co sponges, acetate
Medications (oligoelements)	Co sulfate, chloride, acetate
Animal feed (oligoelement)	Co sulfate, chloride, acetate, nitrate, carbonate
Fertilizers (adjuvant)	Co sulfate
Biocides	Co carbonate
Textile dyeing	Co chloride
Water treatment	Co sulfate

The importance of cobalt dissolution in cutting liquids used as coolants and working fluids aerosols for the processing of hard metals has also been emphasized [44].

In European countries, the current permissible exposure limit (time limit value-time weighted average (TLV-TWA)) is currently set between 100 and 20 μg cobalt per cubic meter, 20 $\mu g\,m^{-3}$ being recommended by the American Conference of Governmental Industrial Hygienists [45]. This value is generic for all cobalt compounds and does not differentiate according to speciation.

In the industry, the main target organ affected by excessive exposure to cobalt compounds is the respiratory tract with some significant variations according to the cobalt species involved. Other organs affected under occupational exposure circumstances are discussed in the next section.

5.1 Respiratory tract

Different types of reactions have been reported, which may involve the upper respiratory tract, the bronchial tree or the lung parenchyma (for a review see [46]) as follows.

5.1.1 Upper respiratory tract

Inflammation of the nasopharynx is frequent, and it is unclear whether this results from a nonspecific irritation by cobalt-containing particles or from an immunologically mediated reaction (allergic rhinitis). It is not known whether the occurrence and/or severity of these manifestations vary with the cobalt species involved.

5.1.2 Bronchial tree

The respiratory sensitizing potential of Co(II) ions is well documented. Exposure to cobalt salts, or cobalt metal in association with other metals, for example hard metal dusts and dusts released from diamond-polishing activities may cause typical bronchial asthma in a small proportion of workers (less than 5%). In some patients, a type I allergic reaction has been suspected because IgE antibodies against a complex of Co(II) with albumin could be identified. For the remaining patients, the mechanism of cobalt-induced asthmatic reaction remains to be elucidated (IgG-mediated, direct biochemical or irritant action). A specific inhalation challenge test with a cobalt salt, hard metal or cobalt metal powder may be positive. A positive lymphocyte transformation test with cobalt(II) ions has been described in hard metal asthma, suggesting a role for cellular immunity. Cross respiratory sensitization between nickel and cobalt compounds has also been reported. Overall, there is therefore strong evidence that all cobalt species that are significantly soluble in biological media can cause asthma, Co(II) ions are the most plausible causative agents of this bronchial reaction.

5.1.3 Parenchyma

The parenchymal reaction observed in some workers exposed to cobalt-containing dusts appears specific of some cobalt species [46]. Mainly workers exposed to hard metal dust are at risk for the development of interstitial pulmonary disorders grouped under the term ‘hard metal disease’. Histological changes have varied from intense desquamative alveolitis with giant multinucleated cells to end-stage nonspecific pulmonary fibrosis, these two conditions being probably the extremes of a continuous process. In the final stages, cardiorespiratory failure may lead to death. Individual susceptibility factors probably play an important role since only a small percentage of the exposed workers (probably less than 5%) develop the disease. A weak association of the disease with a specific human lymphocyte antigens (HLA) polymorphism (glutamate 69 in HLA-DP beta chain) has been reported [47].

Cases identical to hard metal disease have also been observed in workers from the diamond-polishing industry, a setting where tungsten carbide particles are absent. Fibrosis has also been described in dental technicians but besides cobalt, the latter workers are also exposed to several other known fibrogenic agents and the pathology of dental technician pneumoconiosis appears to

be different from that of hard metal lung. Only a few isolated and poorly documented cases of interstitial lung disease have been reported following exposure to cobalt alone. In a cross-sectional study conducted in a cobalt refinery in which workers are exposed to cobalt alone, no evidence of parenchymal effect was found despite the very high exposure levels recorded (up to more than 500 $\mu g\,m^{-3}$) [48].

Overall, clinical and epidemiological data indicate that this manifestation is rarely, if ever, induced by pure cobalt metal dust alone but requires the concomitant inhalation of other compounds such as tungsten carbide in the hard metal industry (hard metal disease). This view has been supported by several experimental studies *in vitro* and *in vivo* that demonstrated that cobalt metal and metallic carbides interact to produce a unique cellular or lung toxicity. The mechanism of this interaction has been discussed above. (Figure 2.7.1)

5.2 Skin

Soluble cobalt compounds may cause allergic dermatitis (eczema, urticaria mainly of the hands) and, as for the respiratory sensitization, cross reaction with nickel compounds seems frequent. Dissolution of cobalt in cutting fluids used during industrial operations represents an aggravating factor since appreciable amounts of the element can be solubilized in these fluids. The differentiation with an irritant reaction is difficult, and both types of response can coexist.

5.3 Cardiovascular system

Only rare cases implicating industrial exposure to cobalt compounds as a cause of clinical cardiomyopathy have been reported and it is uncertain whether occupational exposure was a real contributing factor. An excess of deaths from ischemic heart disease has been found among workers exposed to hard metal dusts for a minimum of 10 years [49].

5.4 Erythropoiesis

The possibility that polycythemia may result from industrial exposure to cobalt compounds has been raised, but it is difficult to differentiate between a direct effect of cobalt on the bone marrow and a response to arterial desaturation resulting from the lung disease caused by the inhalation of cobalt-containing particles. A trend towards reduced erythropoietic indices has been reported in workers exposed to cobalt metal powder [48].

5.5 Thyroid gland

In an industrial setting in which workers are exposed to cobalt compounds alone subclinical hypothyroid status or, inversely, increased concentrations of total and free serum T4 have been found [48].

5.6 Mutagenicity and carcinogenicity

In 1991, International Agency for Research on Cancer (IARC) concluded in an overall generic evaluation that cobalt and its compounds were possibly carcinogenic to humans (Group 2B). In the same evaluation, Co(II) compounds were reported to exhibit genotoxic properties.

Although many areas of uncertainty still remain, recent work indicates now that an assessment of the mutagenicity and carcinogenicity of cobalt, and its compounds requires a clear distinction between the different compounds of the element and needs to take into account the different mechanisms involved [50] (Figure 2.7.2).

With regard to Co(II) ions, further evidence is now available showing that they can affect DNA integrity either directly by the induction of DNA breaks [51] or indirectly through inhibition of specific repair systems [52]. In spite of their theoretically limited bioavailability in biological fluids, there is also evidence that Co(II) cations exert genotoxic as well as carcinogenic effects in animals. It seems therefore reasonable to consider that all soluble Co(II) salts (chloride, sulfate,

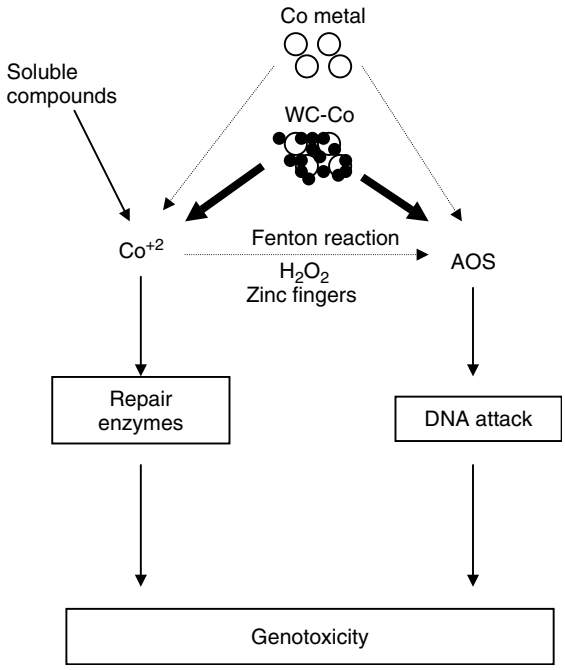

Figure 2.7.2. Mechanisms of genotoxicity of different cobalt species. (Reproduced by permission of British Medical Journal Publishing Group, D. Lison *et al.*, *Occup. Environ. Med.,* **58**, 619 (2001).)

acetate, etc.) share this carcinogenic potential. There is, however, no evidence of genotoxicity or carcinogenicity available in humans. In line with these conclusions, the specialized experts of the European Union have classified cobalt chloride and sulfate as C2 carcinogens (labeled R49).

As mentioned above, cobalt metal particles have biological activities that are not mediated by Co(II) ions and that, through the production of genotoxic AOS, can contribute to explain their mutagenic effects *in vitro* in human lymphocytes. Mortality studies in exposed workers did not, however, provide evidence of a carcinogenic potential for cobalt metal alone [53]. No significant increase of genotoxic effects was detected either in workers exposed to cobalt metal dust at a mean level corresponding to the current TLV-TWA (20 $\mu g\,m^{-3}$) [54].

When mixed with metallic carbide, cobalt metal has different genotoxic and carcinogenic properties and needs to be considered as a specific toxic entity (hard metal particles). There is evidence that hard metal particles exert a greater mutagenic activity than Co metal alone *in vitro*; and several epidemiological studies have shown that occupational exposure to hard metal particles was associated with an increased risk of lung cancer. This distinct biological activity of hard metal particles can be explained by the physicochemical mechanism of interaction between Co metal and WC particles described above. Whether Co(II) ions released from the interaction between WC-Co particles and oxygen contribute to the genotoxicity of these particles is not known.

5.7 Biomonitoring of exposure

In subjects occupationally exposed to cobalt compounds, the urinary excretion and the blood or serum concentration of the metal have been proposed as biological indicators of exposure. Most biological monitoring studies have been carried out in hard metal workers. Studying 10 groups of hard metal workers (airborne cobalt concentration: 28–367 $\mu g\,m^{-3}$), Ichikawa *et al.* (1985) found a good correlation between cobalt concentration in blood and cobalt in air on the basis of the mean values observed in the different groups [55]. In a survey that involved similar groups of workers (airborne cobalt concentration: 120–284 $\mu g\,m^{-3}$), Perdrix *et al.* (1983) have suggested that the difference between end- and beginning-of-shift urinary cobalt concentration reflected the day exposure [56]. The concentration in the Friday evening urine was indicative of the cumulative exposure during the week, and the level of cobalt in urine collected on Monday morning mainly reflected long-term exposure. In another group of hard metal workers exposed to cobalt airborne concentrations below 100 $\mu g\,m^{-3}$, it has been shown that there was an increase of urinary cobalt concentration as the workweek proceeded [57]. In a study in diamond polishers using cobalt-containing disks, the measurement of urine cobalt concentration, when considered on a workshop basis, was found to reflect the level of exposure to the metal (below 50 $\mu g\,m^{-3}$) [58]. Limited comparative data are available for other forms of

cobalt to which workers may be exposed. Their absorption rate is dependent on their solubility in biological media, which may also be influenced by the concomitant presence of other substances, and this is likely to affect the interpretation of biomarkers of exposure. The importance of the chemical nature of the exposure has been pointed out by Christensen *et al*. [22]. As already mentioned, these authors observed increased concentrations of cobalt in blood (0.2–24 $\mu g\,L^{-1}$) and urine (0.4–848 $\mu g\,L^{-1}$) of pottery plate painters who used a soluble cobalt pigment while only slightly increased values were measured in those using an insoluble cobalt pigment (0.05–0.6 and 0.05–7.7 $\mu g\,L^{-1}$ in blood and urine, respectively). The relationships between environmental and biological (blood and urine) parameters of exposure for different chemical forms of cobalt have been investigated in a cross-sectional study in workers exposed to cobalt metal, oxides and salts in a refinery or to a mixture of cobalt and tungsten carbide in a hard metal–producing plant [23]. The main conclusion of this study was that while biological monitoring of workers exposed to cobalt oxides revealed increased blood and urine levels comparatively with nonexposed subjects, these parameters poorly reflected the recent exposure level. In contrast, when exposure was to soluble cobalt compounds (metal, salts and hard metals), the measurement of urine and/or blood cobalt at the end of the workweek could be recommended for the monitoring of workers. It could be calculated that an 8-h exposure to 20 or 50 $\mu g\,m^{-3}$ of a soluble form of cobalt would lead to an average urinary concentration of 18.2 and 32.4 μg of cobalt per gram creatinine, respectively (postshift urine sample collected at the end of the workweek).

6 CONCLUSION

This short overview illustrates the fact that the health effects associated with occupational exposure to cobalt compounds cannot be limited to generic statements or classification. There is a need to make a distinction between the different compounds of the element and to take into account the varying pathomechanisms involved. Additional research efforts are needed to better integrate speciation in occupational medicine practices both in ambient measurements to refine the characterization of exposure and in biological measurements to focus on species of toxicological relevance (e.g. non vitamin B_{12} cobalt in blood). The medical surveillance of workers in the industries involving cobalt compounds should be adapted to the species involved (e.g. workers exposed to cobalt metal associated with tungsten carbide are at increased risk of developing lung parenchymal disease or cancer). The implementation of biological monitoring programmes to assess exposure of those workers should also integrate differences between cobalt compounds in their toxicokinetic behavior but also in the interpretation of data (e.g. the health significance of a urinary cobalt concentration of 20 $\mu g/g$ creatinine in a worker from the hard metal industry or from a ceramic manufacture is probably not equivalent).

7 REFERENCES

1. The Cobalt Development Institute, http://www.thecdi.com/, 2004.
2. Hamilton, E. I., *Sci. Total Environ.*, **150**, 7 (1994).
3. Ellwood, M. J. and van den Berg, C. M. G., *Mar. Chem.*, **75**, 33 (2001).
4. Saito, M. A. and Moffett, J. W., *Mar. Chem.*, **75**, 49 (2001).
5. Donaldson, J., Clarck, S. and Grimes, S., *Cobalt in Medicine*, *Agriculture and the Environment*. Cobalt Development Institute, 1986.
6. Pennington, J. A. T. and Jones, J. W., *J. Am. Diet Assoc.*, **87**, 1644 (1987).
7. Underwood, E. J., *Nutr. Rev.*, **33**, 65 (1975).
8. *IARC Monogr. Eval. Carcinog. Risks Hum.*, **52**, 1 (1991).
9. Leboulanger, J., Vitamine B_{12}, in *Les Vitamines, Biochimie, Mode d'action et Intérêt Thérapeutique*, Produits Roche Sa (Ed.), Editions SIF, 1977, pp. 153–162.
10. Dabeka, R. W. and McKenzie, A. D., *J. AOAC Int.*, **78**, 897 (1995).
11. Alexander, C. S., *Am. J. Med.*, **53**, 395 (1972).
12. Neve, J., *J. Pharm. Belg.*, **46**, 271 (1991).
13. Food and Nutrition Board, http://www4.nationalacademies.org/iom/iomhome.nsf/WFiles/webtablevitamins/$file/webtablevitamins.pdf, 2002.
14. Ayala-Fierro, F., Firriolo, J. M. and Carter, D. E., *J. Toxicol. Environ. Health A*, **56**, 571 (1999).
15. Christensen, J. M., Poulsen, O. M. and Thomsen, M., *Int. Arch. Occup. Environ. Health*, **65**, 233 (1993).

16. Sorbie, J., Olatunbosun, D., Corbett, W. E. and Valberg, L. S., *Can. Med. Assoc. J.*, **104**, 777 (1971).
17. Taylor, D., *Phys. Med. Biol.*, **6**, 445 (1962).
18. Naylor, G. P. and Harrison, J. D., *Hum. Exp. Toxicol.*, **14**, 949 (1995).
19. Elinder, C.-G. and Friberg, L., Cobalt, in *Handbook on the Toxicology of Metals*, Friberg, L., Nordberg, G. F. and Vouk, V. B. (Eds.), Elsevier Science Publishing, Amsterdam, 1986, pp. 211–232.
20. Kreyling, W. G., Ferron, G. A. and Haider, B., *Health Phys.*, **51**, 773 (1986).
21. Lasfargues, G., Lison, D., Maldague, P. and Lauwerys, R., *Toxicol. Appl. Pharmacol.*, **112**, 41 (1992).
22. Christensen, J. M. and Poulsen, O. M., *Sci. Total Environ.*, **150**, 95 (1994).
23. Lison, D., Buchet, J. P., Swennen, B., Molders, J. and Lauwerys, R., *Occup. Environ. Med.*, **51**, 447 (1994).
24. Inaba, J. and Suzuki-Yasumoto, M., *Health Phys.*, **37**, 592 (1979).
25. Scansetti, G., Botta, G. C., Spinelli, P., Reviglione, L. and Ponzetti, C., *Sci. Total Environ.*, **150**, 141 (1994).
26. Linnainmaa, M. and Kiilunen, M., *Int. Arch. Occup. Environ. Health*, **69**, 193 (1997).
27. Toxicological Profile for Cobalt – Draft for Public Comment (update), Agency for Toxic Substances and Disease Registry, 2001.
28. McKinley, M. C., *Proc. Nutr. Soc.*, **59**, 221 (2000).
29. Kobayashi, M. and Shimizu, S., *Eur. J. Biochem.*, **261**, 1 (1999).
30. Conklin, D. S., Culbertson, M. R. and Kung, C., *Mol. Gen. Genet.*, **244**, 303 (1994).
31. Minchenko, A. and Caro, J., *Mol. Cell. Biochem.*, **208**, 53 (2000).
32. Lison, D., Carbonnelle, P., Mollo, L., Lauwerys, R. and Fubini, B., *Chem. Res. Toxicol.*, **8**, 600 (1995).
33. Hartwig, A., *Toxicol. Lett.*, **102–103**, 235 (1998).
34. Nackerdien, Z., Kasprzak, K. S., Rao, G., Halliwell, B. and Dizdaroglu, M., *Cancer Res.*, **51**, 5837 (1991).
35. Mao, Y., Liu, K. J., Jiang, J. J. and Shi, X., *J. Toxicol. Environ. Health*, **47**, 61 (1996).
36. Sarkar, B., *Nutrition*, **11**, 646 (1995).
37. Kasprzak, K. S., Zastawny, T. H., North, S. L., Riggs, C. W., Diwan, B. A., Rice, J. M. and Dizdaroglu, M., *Chem. Res. Toxicol.*, **7**, 329 (1994).
38. Henquin, J. C. and Lambert, A. E., *Am. J. Physiol.*, **228**, 1669 (1975).
39. Ybarra, J., Behrooz, A., Gabriel, A., Koseoglu, M. H. and Ismail-Beigi, F., *Mol. Cell. Endocrinol.*, **133**, 151 (1997).
40. Beasley, D. M. and Glass, W. I., *Occup. Med. (Lond)*, **48**, 427 (1998).
41. Kriss, J., Carnes, W. and Ross, R., *JAMA*, **157**, 117 (1955).
42. Curtis, J. R., Goode, G. C., Herrington, J. and Urdaneta, L. E., *Clin. Nephrol.*, **5**, 61 (1976).
43. Hildebrand, H. F., Veron, C. and Martin, P., *Biomaterials*, **10**, 545 (1989).
44. Sjogren, I., Hillerdal, G., Andersson, A. and Zetterstrom, O., *Thorax*, **35**, 653 (1980).
45. ACGIH American Conference of Governmental Industrial Hygienists, *Threshold Limit Values and Biological Exposure Indices TLV® and BEI®*, 2000.
46. Lison, D., *Crit. Rev. Toxicol.*, **26**, 585 (1996).
47. Potolicchio, I., Mosconi, G., Forni, A., Nemery, B., Seghizzi, P. and Sorrentino, R., *Eur. J. Immunol.*, **27**, 2741 (1997).
48. Swennen, B., Buchet, J. P., Stanescu, D., Lison, D. and Lauwerys, R., *Br. J. Ind. Med.*, **50**, 835 (1993).
49. Hogstedt, C. and Alexandersson, R., *Scand. J. Work Environ. Health*, **13**, 177 (1987).
50. Lison, D., De Boeck, M., Verougstraete, V. and Kirsch-Volders, M., *Occup. Environ. Med.*, **58**, 619 (2001).
51. De Boeck, M., Lison, D. and Kirsch Volders, M., *Carcinogenesis*, **19**, 2021 (1998).
52. Kasten, U., Mullenders, L. H. and Hartwig, A., *Mutat. Res.*, **383**, 81 (1997).
53. Moulin, J. J., Wild, P., Mur, J. M., Fournier Betz, M. and Mercier Gallay, M., *Am. J. Ind. Med.*, **23**, 281 (1993).
54. De Boeck, M., Lardau, S., Buchet, J. P., Kirsch-Volders, M. and Lison, D., *Environ. Mol. Mutag.*, **36**, 151 (2000).
55. Ichikawa, Y., Kusaka, Y. and Goto, S., *Int. Arch. Occup. Environ. Health*, **55**, 269 (1985).
56. Perdrix, A., Pellet, F., Vincent, M., de Gaudemaris, R. and Mallion, J. M., *Toxicol. Eur. Res.*, **5**, 233 (1983).
57. Scansetti, G., Lamon, S., Talarico, S., Botta, G. C., Spinelli, P., Sulotto, F. and Fantoni, F., *Int. Arch. Occup. Environ. Health*, **57**, 19 (1985).
58. Nemery, B., Casier, P., Roosels, D., Lahaye, D. and Demedts, M., *Am. Rev. Respir. Dis.*, **145**, 610 (1992).

2.8 Speciation of Copper

2.8.1 Speciation of Copper in the Environment

J.F. Artiola
The University of Arizona, Tucson, Arizona, USA

1 INTRODUCTION

The use of Cu in the world is still rising, increasing from 13.7 M tons in 1993 to 16.3 M tons in 1997 [1].

There are numerous modern-day uses for Cu: electrical (conductors, printed circuits) remains the primary use of this metal, followed by corrosion resistance (water pipe), machinery parts, alloys (bronze and brass), chemicals (fungicides, algicides, pigments), ammunition, works of art (statues, domes). Copper is also known to be a necessary trace element (micronutrient) for plants and animals, including humans and has limited toxicity (except for invertebrates and microorganisms) when compared to other metals.

Copper is seldom found in its pure metallic state, and it must be mined. For all the benefits that the use of Cu metal continues to bring to human civilizations, its continued production has significant environmental impacts. For example, in ancient times the island of Cyprus was deforested several times over by the energy-intensive mining and smelting of Cu and generated millions of tons of slag [2]. Open-pit mining, common in the Western States of the United States, is used to extract vast quantities of low-grade Cu ore. This process continues to scar the surface of the earth, generates extensive piles of mine tailings that are difficult to manage, and can create offsite toxic metal contamination, see Section 3.

Handbook of Elemental Speciation II: Species in the Environment, Food, Medicine & Occupational Health
Edited by R. Cornelis, H. Crews, J. Caruso and K. G. Heumann
 ISBN: 0-470-85598-3 (HB)

The most stable oxidation state of Cu is Cu^{++}. When exposed to oxygen, Cu metal readily ionizes, losing its lone outer 4S e^- ($E^0 = 520$ mV, the second ionization potential is much lower (153 mV). This gives Cu a transition metal character that produces ions and complexes with characteristic colors (blue-green) [3].

2 NATURAL OCCURRENCE OF COPPER IN THE ENVIRONMENT

Copper is the 24th most abundant element in the lithosphere [4]. On average, the lithosphere contains about 70 mg kg^{-1} of Cu, making Cu relatively rare. However, geological processes have concentrated Cu in natural deposits that have been mined since ancient times. The origins and chemical composition of the most common Cu-bearing minerals are discussed in the following section. Copper is also ubiquitous in the weathered upper crust portion of the earth called the *soil environment* with an average concentration of 30 mg kg^{-1} and a range of 2–100 mg kg^{-1} [4]. The sources and forms of Cu in the soil, water, and air environments will be discussed in subsequent sections.

2.1 Geology and minerals

Most of the world's Cu is found and mined in the form of copper sulfides. However, pure Cu crystals and nuggets can be found in old lava flows and in veins. Copper sulfides are formed and deposited in the earth fracture zones located near large sources of magma [5]. Hot waters rich in dissolved sulfur and metals such as Cu may rise through the cooler fractured zones toward the earth surface. Upon cooling, metal-sulfides begin to precipitate, producing numerous types of minerals. Since the solubilities of minerals vary with temperature, copper sulfides are found in distinct zones, depending on the original temperature and pressure and the amounts of S, Cu and other metals present in solution. For example, Cu-S minerals may not form at temperatures above 813 °C. In sulfur-rich hydrothermal solutions the mineral covellite (CuS) will form at temperatures below 505 °C. Chalcocite (Cu_2S), a major Cu ore mineral, will start to form in Cu-rich solutions at 435 °C (cubic structure), but the hexagonal structured chalcocite will only form at temperatures below 103.5 °C. Other less common Cu-S minerals include anilite (Cu_7S_4) and djurleite ($Cu_{31}S_{16}$).

Copper is often found in combination with other metals that can also form multi-metal-sulfide minerals or simply as impurities, these metals include Fe, Sn, Pb, Se, As, Sb and Ag. Copper is most commonly found in combination with Fe, forming a complex (ternary) system Cu-Fe-S [6]. The three-phase relations (mineral stabilities) among these three elements have been extensively studied and suggest a complex set of temperature and elemental compositions and relations that can produce numerous Cu-S, Fe-S, and Cu-Fe-S minerals. For example, at 1000 °C, several sulfide mineral phases can coexist, including pyrite (FeS) (a dominant S mineral in hydrothermals), bornite (Cu_5FeS_4), and chalcocite. As the temperature of the system drops, other Cu and Fe minerals (besides the above mentioned) are formed, these include covellite (CuS), idaite (Cu_3FeS_4), and pyrrhotite ($Fe_{1-x}S$), where x varies from 0 to 0.2 [6]. Other multimetal-Cu sulfides include stromeyerite (AgCuS), stannite (Cu_5FeSnS_4), and bornite (Cu_5FeS_4), a common Cu ore often associated with higher temperature minerals such as chalcopyrite ($CuFeS_2$) and chalcocite.

More complex Cu-bearing sulfides are produced in the latter stages cooling of hydrothermal solutions when other metallic and semimetallic elements are added to the solutions. Some of other complex Cu-M-S minerals include tetrahedrite ($(Cu,Fe,Ag,Zn)_{12}Sb_4S_{13}$) commonly found in Cu mines, tennantite ($(Cu,AsFe,Zn)_{12}As_4S_{13}$) similar to tetrahedrite but denser and harder, enargite (Cu_3AsS_4), an important Cu ore found throughout the world, famatinite (Cu_3SbS_4), bournonite ($PbCuSbS_3$), a major ore for Pb and Cu, and seligmannite (Pb,Cu,AsS_3) with the same stoichiometry as bournonite (but As replaces Sb), but rarer and less dense [5].

After cooling and upon exposure to oxygen and water, copper sulfides begin to weather, oxidizing and releasing Cu (I and II) and sulfate ($SO_4^=$)

ions. Copper oxide (Cu_2O) forms in the upper parts of the copper sulfides veins where oxygen is limited but ultimately oxidizes to tenorite (CuO) when directly exposed to air. However, when exposed to air and in carbonate-rich environments, oxidized Cu(II) will readily react with carbonate ($CO_3^{=}$) and hydroxyl (OH^-) ions, producing the characteristic green Cu-carbonate-hydroxide mineral malachite ($Cu_2CO_3[OH]_2$) readily visible in exposed Cu sculptures, domes, and ornaments. This basic copper carbonate mineral is also commonly found in Cu mines together with the less abundant azurite ($Cu_2[CO_3]_2[OH]_2$). Copper cations can also react with aluminum (Al) and phosphate PO_4^{3-}) ions, producing turquoise ($CuAl_6[PO_4]_4[OH]_8{\cdot}4H_2O$), the popular blue-green gemstone.

2.2 Soil composition

The Cu minerals that govern the solubility of Cu in the soil environment are not known [4], but the Cu^{++} ion predominates. This cation can be adsorbed onto negatively charged soil minerals such as clays and strongly adsorbed on metal oxides, particularly Mn and Fe oxides [7]. Copper(II) is known to form very stable inner-sphere complexes with Fe and Al-hydroxyl surface groups. The sorbed Cu may eventually diffuse and irreversibly bind (chemisorp) into internal sorption sites of metal oxides [8]. The Cu ion is subject to cation-exchange reactions in the soil environment, mainly controlled by the presence of clay minerals and pH. Lindsay[4] estimated the soil-Cu<>$2H^+$ thermodynamic equilibrium constant (K°) to be $10^{2.80}$. Therefore, in a typical soil, if the pH is known, the activity of the Cu^{++} ion is given by the following relationship:

$$\text{Log } Cu^{++} = 2.8 - 2\text{pH} \qquad (2.8.1.1)$$

This makes the soil-Cu much less soluble than most of the other carbonates and oxides of Cu. For example, using equation (2.8.1.1), the log activity of soil-Cu at pH 7 is −11.2, whereas, if crystalline $CuCO_3$, azurite or malachite are present in the soil environment, the equilibrium activity of the Cu(II) ion may be about 6 orders of magnitude higher (∼−5.5). Sauve *et al.* [9] proposed an equation similar to equation (2.8.1.1), which includes total Cu and correlates free Cu with pH and total Cu in Cu-contaminated soils. Most of the known Cu minerals are unstable in the soil environment. However, under some conditions, Cu can form several relatively soluble sulfate, carbonate, hydroxide-based minerals such as chalcocyanite ($CuSO_4$), brochantite ($Cu_4[OH]_6SO_4$), and crystalline forms of copper carbonate ($CuCO_3$) and copper hydroxide ($Cu[OH]_2$). But it is unlikely that these minerals will form or be stable (long-lasting) soil environment because of their high solubilities [4].

Although Cu^{++} ion dominates the solid-solution chemistry of typical soils, it is possible to reduce this ion to Cu^+ when soil conditions favor it. The reduction of Cu^+ to elemental Cu^0 is unlikely in most soils since typically soil redox potentials are not lower than −400 mV and the redox potential of the Cu^+/Cu^0 couple is 525 mV. The redox reaction of Cu(II) to Cu(I) is:

$$Cu^{++} + e^- \rightleftarrows Cu^+ \qquad (2.8.1.2)$$

where $\log K^0 = 2.62$. Therefore, when the activities of these two species are equal, the log of soil redox potential (pe) will be equal to $\log K^0 = 2.62$ or +155 mV. Thus, under reducing (waterlogged-anaerobic) soil conditions, cuprous ferrite ($Cu_2Fe_2O_4$) may form and be stable. Under extremely reduced and acidic soil conditions ($pH + pe \leq 2.43$), reduced Fe minerals will become dominant and may lead to the formation of metallic Cu^0, which can coexist with cuprous ferrite and iron minerals like magnetite (Fe_2O_4). In sulfide-rich soil/sediment environments, the formation of copper sulfide minerals is possible. Chalcocite (stable), and even covellite (metastable) may form, and coexist with cuprous ferrite when the combined $pH + pe$ are ≤ 4.73 [4].

The chemistry of the soil solution is dominated by Cu^{++} ions, hydroxide, carbonate, and sulfate complexes. In organic soils, stable Cu chelates are readily formed with humic substances (fulvic and humic acids) and may dominate the solid-solution chemistry, see also Section 2.3. Soil Cu-organic matter chelates are known to significantly reduce Cu bioavailability and mobility in organic soils and

soils amended with organic wastes like biosolids (municipal sludge) and animal residues. This is due primarily to the formation of stable Cu-OM chelates using carbon and nitrogen groups like $-COO^-$, $-NH_2$, and other aliphatic and aromatic electron-rich groups found in organic matter structures. For example, insoluble peat and biosolids humic acids strongly chelate Cu^{++} ions by forming a square planar arrangement with two carboxylate and two aliphatic N ligands [10], thereby reducing the total soluble Cu in soil solutions. Alcacio *et al.* [11] showed that Cu forms four strong equatorial bonds with oxygen-containing groups from goethite and humate materials, and with two longer (axial) water groups, forming a distorted octahedral complex [10].

In the absence of significant amounts of natural organic matter (NOM) and in neutral to alkaline conditions, the $Cu(OH)_2$ species will predominate in solution. Normal soils usually contain significant amount of carbonates and sulfates. Therefore, $CuCO_3$ and $CuSO_4$, as well as Cu^{++} and $Cu[OH]_2$, species will dominate (>95%) the soil solution, depending on the pH and activities of these two counter anions. For example, in acidic soils with free sulfate ions ($\sim 10^{-2.4}$ M), the $CuSO_4/Cu^{++}$ may be near 1. Note that in a water solution, Cu^{++} is hydrated with four to six water molecules, for example, $Cu(H_2O)_4{}^{++}$, a favored complex. These complexes predominated at pH < 6 in the absence of any competing ligands. In alkaline soils with normally elevated CO_2 ($\sim 10^{-2.4}$ atm), the $CuCO_3/Cu(OH)_2$ may be near 1 [4]. In both cases, we assume that the Cu-organic complexes or chelates are negligible. Copper ions can also form complexes with N-based ligands like ammonia (NH_3), nitrate ($NO_3{}^-$), phosphates ($HPO_4{}^{2-}$, $H_2PO_4{}^-$), and chloride (Cl^-) ions (listed in order of importance) in soils solutions. But their contributions to the total Cu species in typical soils solutions are very small. Further discussion about the chemistry of Cu in water is presented in the next section.

2.3 Water composition

Copper is found in natural surface waters at an average concentration of 0.002 mg L^{-1}, ranging from 0.001 to $\sim$0.1 mg L^{-1}, Cu in seawater is at the upper end of the range [12, 13]. These Cu concentrations, while very low, are still much higher than those found in natural soil solutions (devoid of any known Cu minerals), which even in favorable acidic conditions (pH < 4) may be $< 1 \times 10^{-5}$ mg L^{-1} of Cu [4]. Much higher Cu concentrations can be found in some natural geothermal waters, waters exposed directly to copper rich ores and Cu mine tailings, some industrial wastewaters, and natural waters high in dissolved organic matter. As with soils, Cu(II) dominates the aquatic chemistry of this element, with few exceptions. Once released into the water environment, Cu^{++} ions will hydrolyze and form soluble Cu hydroxides that dominate at pH > 7. Since most natural waters, including seawater, contain carbonates, copper carbonates, in particular, $CuCO_3$, will predominate (>96%) at pH $\geq$ 8, followed by $Cu[OH]_2$ ($\sim$2%) [13]. Copper(II) also forms strong complexes with amines, particularly multidentate amines. While ammonia can form single and polyamine complexes with Cu, their formation is not likely because the typical concentration of ammonia in natural waters is less than 0.2 mg L^{-1} [12].

As previously indicated, waters exposed to most Cu minerals increase Cu in solution because many Cu minerals are very soluble in water or, like copper sulfide minerals, become unstable when exposed to oxygen, water, and microbial activity. For example, malachite will dissolve in acidic water (pH 4) and may raise the Cu concentration in water to >60 mg L^{-1} [13]. However, the overall solubilities and rates of dissolution of minerals depend on the size of the particles and their purity. Small and more pure particle minerals may dissolve faster and have a greater solubility than coarse, less pure particle (crystal) minerals. This is due to the molar surface effect that increases with surface area and mineral purity, thereby shifting (increasing) the solubility of minerals. For example, the solubility of CuO increases more than 3 orders of magnitude when its molar surface is increased 4 times [13]. This effect, while important in the recovery of Cu from ores, also has significant environmental implications in the management of Cu mine tailings (crushed and

extracted Cu minerals) that are high in pyrite and other potentially polluting metals like As, Pb, Cd, Zn, and Mo, see Section 4.2.

Copper(II) is perhaps the strongest-binding transition metal to many types of natural and synthetic chelating agents and ligands. It is ranked at the top of the Irwing–Williams order for complex stabilities due in part to its outer shell (sphere) asymmetry and polarizability [13], which makes this ion able to interact with most common anionic ligands. This property has important environmental significance since it affects the mobility and bioavailability of Cu in the soil and water environment. Synthetic chelates like EDTA (ethylenediaminetetraacetic acid) (Na salt form) react with Cu^{++} ion, forming a strong chelate with the general reaction in neutral to moderately basic conditions:

$$Cu^{++} + L^{4-} \rightleftarrows [CuL]^{2-}$$

where the log $K_{0.1} \cong 19$ and the ionic strength of the solution is 0.1 at 25 °C). The stability constant of Cu (and other transition metals) goes up significantly in moderately acidic conditions (pH 3 to 5) with the addition of a proton (H^+) into the chelate structure producing chelate species $[CuHL]^{1-}$ (log $K_{0.1} \cong 23$) [4]. Monodentate ligands like citric acid form more stable complexes with copper at neutral pH with Cu(II), as they are more affected by competing H^+ and OH^- ions [13]. Copper ions form an octahedral (distorted) structure with EDTA [3] and other synthetic multidentate chelates. However, as previously indicated, humic substances from different sources appear to chelate Cu in a square planar structure. Soluble forms of humic substances such as fulvates (from fulvic acid) may also prefer to form 4-dentate, preferably square planar or tetrahedral (distorted) chelates with Cu^{++} [13].

Copper(II), together with elements like Fe(II,III), Al(III), Ca(II) and other common metals, is found bound to organic matter that contain electron-rich groups. As previously indicated, Cu(II) forms very stable complexes and as such competes very well for many types of binding sites in natural insoluble and soluble organic matter. Studies have shown that most (>80%) of the Cu found in natural waters is bound to soluble humic substances [12]. However, the competing effects of Ca and Mg found in seawater limit Cu-OM complex formation to about 10% of the total. Copper-OM stability constants are relatively high but quite variable and difficult to measure, as they are affected by many environmental variables, type of OM, densities and type of functional groups, pH, ionic strength, and competing ions. Klaas *et al*. [14] reported an intrinsic stability constant (log K_i) for Cu-DOM of 6.8, at pH range of 3.5–4.5 in soluble OM extracted from acidic forest floor material.

The Cu(I) ion, much less common in the aquatic environment, may be formed when redox conditions are favorable, see Section 3.2. In general, this ion favors the formation of tetrahedral coordination structures with ligands like cyanide (CN^-). Copper(I) may be present in reduced sediments and waters but not in solution. In these systems, the likely presence of free metal–scavenging sulfide ions makes the formation of very insoluble Cu_2S (log $K_{sp} = -48$) likely.

2.4 Copper in air

Copper metal has a high boiling point, exceeding its melting point by more than 1300 °C. Thus, unlike other metals (Hg, As, Se, Cd, Zn, Pb), Cu will not be volatilized into the air during smelting. Also, there are no known volatile inorganic or organic compounds of Cu that can form or be released into the environment. However, mining and smelting activities, described below, can generate sporadic releases of Cu-containing dust (Cu minerals) into the air.

2.5 Copper in plants

Copper, as Cu^{++}, is an essential plant micronutrient involved in numerous biochemical functions. Copper is a constituent of the chloroplast protein plastocyanin and is involved in the electron transport system that links photosystems I and II. Additionally, Cu participates in plant protein and carbohydrate metabolism and nitrogen

(N_2) fixation. Copper is found in five oxidase-type enzymes involved in the reduction of molecular oxygen (O_2), in several low-molecular mass proteins, and aminoacid complexes [15]. Copper is also involved in the desaturation and hydroxylation of fatty acids [16].

Most plants have Cu concentrations in dry weight tissue that range from 5 to 30 mg kg^{-1} [17]. Some plant species can tolerate upto 200 mg kg^{-1} [15]. Plant toxicity usually shows in the form of chlorosis similar to Fe deficiency and may develop when plant tissue concentrations exceed 30 mg kg^{-1}. While free Cu ions are readily taken up by plant roots sometimes with toxic effects, leaf exposure to large Cu concentrations via the use of Cu fungicides like the Bordeaux mix (a hydrated lime-$CuSO_4$ suspension containing ~4% Cu^{++}), does not appear to be toxic to fruit-bearing plants like grape vines. When taken up in excess, Cu creates Fe micronutrient deficiency (with chlorotic symptoms) and may interact with the Mo micronutrient, limiting the enzymatic reduction of nitrate, an essential plant macronutrient [16].

Copper deficiencies in plants are rare since Cu plant requirements are very low and this element is ubiquitous in the soil environment. However, despite the presence of Cu in all soils, high soil organic content may limit Cu availability to plants and produce deficiencies, see also section 2.2. Conversely, sandy soils with low organic matter facilitate Cu translocation (leaching), which in turn can create Cu deficiencies in the root zone. When plants are Cu deficient, symptoms will include stunted growth, distortion of young leaves, and necrosis of the apical meristem (shoot top). See Benton Jones *et al.* [16] and Bennett [18] for more detailed descriptions of Cu plant toxicity and deficiency symptoms.

Copper plant deficiencies can be corrected with Cu (as Cu^{++} or Cu^{+}) that may be applied to soils in the form of soluble inorganic complexes (sulfates, oxides, chlorides) or as organically bound Cu-polyflavonoid and NaCu-EDTA and NaCu-HEDTA chelates [17]. Note that the Cu^{+} ion is unstable in typical agricultural soils and will quickly oxidize to Cu^{++}.

3 ANTHROPOGENIC SOURCES AND RELEASES OF COPPER

3.1 Mining

New copper sources come from mining operations active in many countries and on all the continents. Chile is the largest producer of Cu in the world, followed by the USA and Canada [19], which when combined produce about 40% of the world's Cu. Copper is also mined in many countries of Africa, Asia, Europe, and Australia.

Traditional Cu mining was done using tunnels (underground mining) to follow the rich veins of Cu while leaving low-grade Cu minerals undisturbed. Although underground Cu mining continues, many of the world's Cu-rich vein-deposits are exhausted. Modern Cu mining makes use of open pit excavations to facilitate the removal of vast quantities of low-grade (<1% Cu) ores. Open-pit mining is common in the South-Western States of the United States and Mexico.

Although ancient civilizations began to mine the rare pure copper metal, soon they would discover that smelting was necessary to recover Cu metal from more abundant oxidized forms of Cu (sulfides, oxides, carbonates – see Section 2.1) minerals. This energy-intensive technique is still used but is preceded by a Cu extraction-concentration step. Sulfuric acid leaching is the most common method of Cu extraction and concentration of Cu ores. This process is optimized by crushing the ore materials prior to leaching. Copper oxide–containing minerals (tenorite, malachite) are relatively easy to leach with acid since Cu^{++} and Cu^{+} oxides are readily (hours) dissolved with a strong acid and complexed by $SO_4^{=}$ ions. On the other hand, this acid leaching process requires much longer periods of time (months to years) when applied to much less soluble copper sulfide minerals like cuprite and chalcolite [20]. Chemical and microbial oxidation of sulfides to sulfates is required prior to the release of Cu ions from the ore. Sulfuric acid Cu leaching can be done in vats, heaps, or dumps that ultimately generate enormous quantities of inert (sterile, plant nutrient limited, structureless) materials called *mine tailings* (often

stocked-piled in terraces) that are very difficult to revegetate. Copper mine tailings and spoils are often associated with acid mine releases because of the progressive oxidation of pyritic minerals present in these wastes. When exposed to air and water, pyrite (FeS_2) commonly found with copper sulfides is oxidized (catalyzed by autotrophic bacteria), releasing acid into water. The copious acid production from pyrite oxidation is due to the oxidation of S^{2-} and Fe^{++} with the following overall reaction [13].

$$FeS_2 + 14Fe^{3+} + 8H_2O \rightleftarrows 15Fe^{++} + 2SO_4^{=} + 16H^+$$

Acid mine drainage also contributes to the release of residual Cu and other potentially toxic metals like As, Cd, and Pb, from minerals commonly associated with Cu ores and found in mine spoils and tailings, into waterways. In arid and semiarid environments, wind and water erosion of unprotected Cu mine tailing can release significant amounts of metal-bearing dust particles and sediments into the air and surface water. Copper mine smelting activities can also release Cu into the air, especially during the handling of Cu concentrates. However, more worrisome are the ancillary emissions of volatile and toxic metals like As and Pb emitted from copper smelter stacks during the smelting of Cu. Other metals that can be emitted during Cu smelting include Sb, Be, Cd, Cr, Co, Mn, Ni, and Se [21]. The large emissions of sulfur dioxide (related to acid rain) and carbon dioxide (related to global warming) gases, associated with Cu mining and smelting, should also be of concern. Despite the economic and environmental costs associated with Cu production, discussed previously, Cu is mined throughout the world, making Cu metal prices very competitive (~$2/kg).

3.2 Industrial

Copper is not very toxic to animals and humans but can be toxic to some fish, many invertebrates and microbes, particularly fungi, algae, and bacteria. Copper releases into the environment must be reported to State and/or Federal authorities under the Community Right-to-Know Act of 1986 in the United States [22]. The Cu^{++} ion bacterial fungal, algal, and insect repellent actions are well known and exploited by humans. There are numerous inorganic salts and some organic chelates of Cu sold commercially (carbonates, sulfates, chlorides, oxides, hydroxides, phosphates, oxalates, naphthenate, quinolinolate, and Cu-metals mixtures) sold as fungicides, algicides, bactericides, seed disinfectants, and wood preservatives [23]. However, most Cu-containing salts are exempt from food residue regulations (although these chemicals are poisonous because of the relatively low toxicity of Cu to humans and its ubiquity in the soil and water environment). In combination with Cr and As, Cu forms two powerful wood-preserving chemical mixtures, copper arsenate and chromated copper arsenate (CCA). However, the use of CCA is being restricted by the US Environmental Protection Agency (EPA) for the treatment of wood that comes in direct contact with humans because of its high toxicity associated with the presence of toxic arsenate and chromate anions.

Other forms of controlled release of Cu into the environment include the land application and land filling of municipal (biosolids) and industrial wastes. Applications of Cu-based fungicides, biosolids, phosphate fertilizers, lime, and manures to agricultural soils continue to raise the Cu concentrations above the natural level of 30 mg kg^{-1} in soils. Current Federal regulations limit cumulative Cu additions to agricultural soils up to 1500 kg of Cu ha^{-1} in agricultural fields from repeated applications of biosolids [24]. Industrial wastes that contain copper may not be disposed on land and are usually recycled or neutralized, solidified, and buried in permitted landfills. Industrial waste waters, containing Cu and other metals, discharged into open water ways must comply National Pollution Discharge Regulations (NPDES) that are protective of sensitive aquatic species environments, as determined by the USEPA National Ambient Water Quality Criteria (AWQC). Current chronic

and acute water quality criteria protective of fish and invertebrates for Cu vary between ~5 and ~30 $\mu g\,L^{-1}$, depending on the water hardness. Other water quality parameters such as pH and alkalinity may also play a significant role in Cu bioavailability and therefore toxicity to aquatic organisms in arid environments [25]. Copper(II) used in marine paints to control algae and barnacles and ship worm (teredo) can also be released into the aquatic environment. Copper salts are used as algicide and parasiticide at concentrations above AWQC (as free Cu^{++}) ranging from 30 to 1000 $\mu g\,L^{-1}$ in pools, ponds, and in aquaculture where Cu-sensitive fish and invertebrates are not present. These sources of Cu eventually find their way into the open environment soil and water environments impacted by sewage works (reclaimed waters and biosolids).

4 CHARACTERIZATION AND MEASUREMENT OF COPPER SPECIES

There are numerous methods to measure copper concentrations in minerals, soils, sediments, and water. The most popular methods require the dissolution or extraction (partial or total) of Cu species into a liquid that is subsequently analyzed. Ancient civilizations learned to recognize and roughly estimate copper metal and copper ore purity by the surface colors and density changes. Alchemists and modern chemists made and still make use of the clever separation techniques and the unique color properties of Cu coupled with advanced colorimetric, electrometric, X-ray, and atomic particle probes and separation techniques to precisely measure ultra-trace amounts of total Cu and Cu species in environmental samples [26, 27].

4.1 Sample preparation methods

The analysis of Cu requires some form of sample preparation and/or preservation. Solid samples in any form usually require drying and grinding and even encapsulation prior to analysis. This physical homogenization is required for all techniques, specifically modern methods like X-ray fluorescence. Typically, with a view on total copper determinations, tissue samples may be digested 'ashed' or oven dried at 60 °C for 48 h or more and ground to a 500 μ or less size. Soil and sediments may be oven dried at 105 °C and ground to 10–100 μ size. However, each method has its specific requirements that if ignored can lead to serious bias in the results. For example, most modern liquid spectrometric techniques, like atomic absorption spectrometry (AAS) and inductively coupled plasma optical emission spectroscopy (ICP-OES), require that all Cu species be in acid solution, preferably undissociated or weakly associated with nitrate or sulfate ions. Modern acid digestion favors the use of wet ashing over dry ashing (furnace at 450–550 °C) methods using one or more acids and oxidizing agents like nitric, sulfuric acids, and hydrogen peroxide with closed vessels and microwaves to control sample heating and minimize Cu contamination from ambient sources. These acid treatment methods are acceptable for the pretreatment of plant and animals tissues prior to total Cu analysis. The USEPA Methods 3050B Methods (see also other 3000 series methods) recommend wet ashing of soil and sediment samples using a combination of peroxide-nitric-hydrochloric acids that solubilizes most but not all of the Cu-bearing soil minerals. Total Cu in minerals like Cu ores require their complete dissolution, which can only be accomplished with fusion methods like the sodium carbonate (Na_2CO_3), and with wet ashing acids such as (aqua regia) that include hydrofluoric acid (HF) [28]. The wet digestion of samples that contain highly refractory organic fractions may also be accomplished adding (in addition to the previous acids) perchloric acid ($HClO_4$). However, this oxidizing agent is very reactive and explosive when heated and forms unstable compounds, therefore, its use is discouraged.

Bioavailable Cu is an important measurement in agricultural soils. All forms of water-soluble Cu are not available to plants, microbes and aquatic organisms for uptake. In soils, some solid forms of Cu may be bioavailable providing that root exudates are able to complex or chelate and

therefore facilitate the dissolution and transport of Cu into the root. Solutions containing synthetic chelates have been developed to mimic the ability of plants to uptake Cu from soils. Widely used soil tests for Cu (and other metal micronutrients) plant availability index include the DTPA (diethylenetriaminepentaacetic acid), the DTPA-TEA (diethylenetriaminepentaacetic acid-triethanolamine), and the DTPA-ammonium bicarbonate (NH_4HCO_3) extracting solutions [29]. Following soil-extractant equilibration and filtration, the Cu-DTPA-TEA chelates containing extracts (liquids) are subsequently analyzed using modern spectrophotometric methods. There are numerous other extraction methods designed to selectively extract different metal fractions from solids (soils, sediments). For example, electrolyte solutions may be used to extract cation exchangeable Cu species from soil particles, weak acid solutions may be used to dissolved metal carbonates and amorphous metals oxides that may contain sorbed Cu. Finally, solid particles may also be separated by size to identify the different fractions of Cu in minerals (clay, Fe oxides, Mn oxides, carbonates, etc.) and organic carbon fractions using particle sedimentation and micro sieving techniques [30].

In general, liquid water samples must be filtered and preserved with acid ($pH \leq 2$) and/or kept cool (4 °C) prior to analysis for total Cu or Cu speciation. The USEPA [31] and Clesceri *et al*. [27] provide sample collection, preservation, and storage guidelines and analytical methods for the analysis of Cu in drinking water and wastewater samples.

4.2 Detection techniques for Cu in liquid samples

Volume 1 describes in great detail the various modern elemental detection techniques used in an analytical laboratory [26]. Whereas gravimetric methods are no longer practical or used, there are still a few colorimetric methods accepted for the routine analysis of Cu in drinking water and waste water samples. These are neocuproine and bathocuproine methods [27] and the Callan colorimetric method based on diethyldithiocarbamate [28].

Today, atomic absorption spectrometry is widely used, as is inductively coupled plasma optical emission spectroscopy (ICP-OES) for the routine analysis of Cu in water, wastewaters, acid-digested materials (plant tissue, soil, sediments), and soil–water extracts. The preferred atomic light emission line of Cu is at 324.7 nm, with an alternate one but less sensitive at 219.96 nm (see Method 3120B in Standard Methods [27]). The reported estimated detection limit for this technique is 6 $\mu g\,L^{-1}$. But this value may vary as much as an order of magnitude, depending on matrix chemical interferences. Sample and standard matrix matching for unusual samples and optimized instrument operating conditions for Cu analysis are recommended.

Inductively coupled plasma mass spectrometry (ICP-MS) is the newest and most sensitive method for the analysis of Cu. Despite its high capital costs and need for a skilled technician, this method of analysis is fast becoming routine in many commercial and research laboratories. This technique has an extraordinary sensitivity and allows isotopic analysis. For example, the naturally occurring Cu isotopes ^{63}Cu and ^{65}Cu (69.2% and 30.8% abundant, respectively) may be detected together or separately at 0.003 $\mu g\,L^{-1}$. No practical detection limits are reported for Cu using ICP-MS (Method 3215) in Standard Methods [27], probably because molecular ion interferences are common in ICP-MS. The measurement of Cu may be interfered with by $ArNa^+$ ions (Mass = 63) formed in the Ar plasma in samples with high Na concentrations. Like other low level (ultra-trace) analysis methods, this technique is particularly prone to false positives if sufficient care is not taken to control common Cu reagent-vessel contamination.

Electrochemical methods are not routinely used for analysis of metals in water, due in part to their complexity, and the development of much faster, equally or more sensitive spectrometric methods like GF-AAS, ICP-OES, and ICP-MS. However, some electro-chemical methods like anodic and cathodic stripping voltammetry are used routinely for the Cu detection and characterization of trace quantities Cu species in aquatic environments.

Rump and Krist [28] describe a polarographic method that measures the half-wave potential of Cu^{++} in a complexing solution of 1 M NH_3/NH_4Cl with a range of 0.02–0.5 mg L^{-1} Cu^{++}. Modern direct current and normal and differential pulse polarographic methods have been used for trace Cu analysis in research laboratories to assist in the speciation of Cu-organic matter complexes [29]. Anodic and cathodic stripping voltammetry is widely used for the trace measurement of labile Cu^{++} and Cu complexes in environmental samples in research laboratories [29, 30]. A major advantage of these techniques is the preconcentration (stripping) of metal species prior to analysis, increasing its sensitivity to Cu (species) and other metals orders of magnitude. For example, in recent years several studies have measured the distributions, the temporal and spatial distributions of free and organic matter–bound Cu species in aquatic river and coastal environments using these two techniques [32–35]. However, these highly sensitive methods must be used carefully since the proportions of free, labile, and complexed Cu species may shift during the stripping step. Copper ion-selective electrodes can also be used to measure only free Cu^{++} activities in water samples, as the presence of inorganic and organic Cu complexes will not be sensed by the ion-selective membrane. The sensitivity and linear response of any membrane and mercury drop-based sensors may be compromised by the adsorption of reactive organic matter, O_2 and high concentrations of common ions such as Cl^- [30], and require careful evaluation of these data [36, 37].

Hyphenated analytical techniques can also be used for the speciation of Cu and other trace metals in waters. Itoh *et al*. [38] reports the use of liquid chromatography [39] ion exclusion, UV spectroscopy, and ICP-MS, as well as ultrafiltration (as a concentration step) to isotopic ratios of $^{65}Cu/^{63}Cu$ in natural waters.

4.3 Detection techniques for Cu in solid samples

The most common techniques for total copper determinations are X-Ray fluorescence spectroscopy (XRFS) and X-Ray Diffraction (XRD). Both are nondestructive methods that are well suited for the major element analysis and mineral identification in soils, sediments, and geologic samples requiring minimal sample preparation. A survey of methods for the detection of species in solid samples can also be read in Volume 1 of this Handbook [40]. A specialized use of this technique includes the study of Cu(II,I)-Cl complexes formed at high temperatures in hot brines from hydrothermal systems [41]. Neutron Activation Analysis is a technique applicable to multielemental analysis including Cu in solid samples, such as soils, sediments and tissues. This is a very sensitive but very expensive technique requiring highly trained technicians and specialized equipment that is typically only available at facilities with research nuclear reactors. X-ray Photoelectron Spectroscopy and X-ray Absorption Fine structure spectroscopy (EXAFS), and derivative X-ray absorption near edge structure (XANES) are three new highly specialized research analytical tools for the study of the surface and structure of minerals. Details about the principles of these techniques are given in [40, 42]. These and other related techniques are capable of detecting and mapping Cu species and Cu complexes in mineral surfaces and solids [29, 43]. The previously mentioned studies by Alcacio *et al*. [11] on the Cu(II) bonding characteristics with goethite (α-FeOOH) and humate materials using EXAFS and XANES demonstrate the formation of multiple types of Cu-solid bonds. These usually include inner-sphere complexation of Cu(II) at goethite sites, and complexes with phenolic and carboxylic groups from humates (see Figure 2.8.1.1.)

5 IMPACT AND FATE OF COPPER IN THE ENVIRONMENT

Copper is found in all environments naturally and as the result of anthropogenic activities. Its impact and fate are derived from its sources, uses, and chemical forms previously discussed. Since Cu is not very toxic to humans, its effect on the environment has not been studied as extensively as

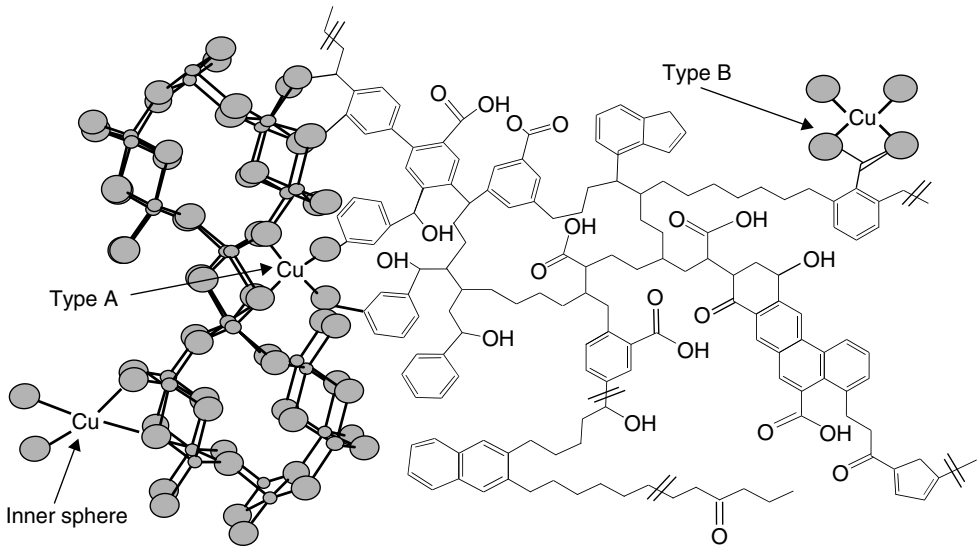

Figure 2.8.1.1. Possible bonding configurations of Cu(II) on goethite-humate soil materials: Cu-O bonds with (H_2O, OH^-) and (–COOH) functional groups forming three types of complexes: inner sphere, and ternary type A (Cu bonded to goethite and humate) and type B (Cu bonded to humate only). Note that the axial water molecules are not included. (Reprinted from *Geochim. Cosmochim. Acta*, 65, Alcacio, T.E., Hesterberg, D., Chou, J.W., Martin, J.D., Beauchemin, S. and Sayers, D.E., 1355–1366 (2001) by permission of Elsevier.)

that of much more toxic metals like As, Se, Hg and Pb. Most of the Cu mined in the world is concentrated in buildings, cars, and modern appliances in the form of Cu metal that does not pose a direct threat to humans and animals. Copper metal must oxidize before it becomes mobile in the environment, becomes toxic and/or bioaccumulate. But pure metal oxidizes (corrodes) very slowly, forming a relatively insoluble layer of copper carbonates and oxides at the Cu metal/air interface that effectively stops further Cu corrosion (passivated surface). In previous sections, we noted that many Cu minerals are fairly soluble and can release Cu ions in the soil and water environments. Also, a small portion of all the Cu mined annually in the world is used to for the production of soluble and potentially toxic Cu(II) and Cu(I) chemicals that are widely utilized in food production, paints and dyes and are eventually disposed of in the open environment. Increasing production and land application of biosolids and animal wastes will continue to increase Cu content in the soil environment. Copper released into the environment, as Cu^{++} and much less prevalent Cu^{+}, can accumulate in the upper layers of the soil and aquatic sediments since it forms stable complexes with naturally occurring organic matter (humates) and carbonates. Numerous Cu-based water-soluble chemicals are used extensively for multiple forms of biological control in industrial and home water storage systems. (See Section 3.2). In freshwater environments, free Cu(II) is very toxic to some fish, invertebrates, and microorganisms at very low $\mu g\, L^{-1}$ concentrations. Copper is typically less bioavailable at pH above 7, likely due to the formation of carbonates and oxides complexes. (See Section 2.3). Copper(II) ions are also very reactive toward inorganic soil minerals like Mn and Fe oxides and clays, forming heterogeneous complexes, soil metal oxide and OM-Fe-oxide systems, reducing their mobility and bioavailability considerably. On the other hand, Cu may be very mobile in aquatic environments because of its ability to form stable complexes with naturally occurring soluble inorganic (carbonates) and organic (fulvic acids) molecules in particular. However, these Cu-OM complexes are much less toxic to aquatic organisms that free Cu^{++}. (See Sections 2.2 and

2.3.) Copper does not form volatile species at low temperature, but may be found in air particulates, in inorganic and organic forms similar to those described in Sections 2 and 3.

6 SUMMARY

Copper as Cu(II) is found in all living tissue, many minerals, and all soils and water sources. Its discovery and use in the metal form set in motion the beginnings of human civilizations. The unique chemical and physical properties of this element (particularly in its metal state) have made it indispensable for the continued growth and evolution of modern society. Copper-mining activities continue to sustain increasing demand and diverse uses driven by population growth. In minute quantities, copper(II) is a life-sustaining element with a relatively low toxicity and with unique physical and chemical properties that make it difficult to replace. However, some fish and many invertebrates and microorganisms can be adversely affected by very low concentrations of free Cu^{++} in natural water systems. Although Cu is a ubiquitous metal found in soils and sediments throughout the world, we should be mindful of the environmental impacts associated with the increasing amounts of Cu and related toxic metals that we are releasing into our soil and particularly in our water systems.

7 REFERENCES

1. Copper Development Association, *Global Copper & Copper Consumption Table 1997*, http://marketdata.copper.org/graphs/cucon.htm, 2003.
2. Constantinou, G., *Ancient Copper Mining in Cyprus*, From "Cyprus, Copper and the Sea" by A. Marangou, Seville 1992, http://www.pio.gov.cy/features/history/copper mining.htm, 2003.
3. Cotton, F. A. and Wilkinson, G., *Advanced Inorganic Chemistry*, 5th ed., John Wiley & Sons, New York, 1988.
4. Lindsay, W. L., *Chemical Equilibria in Soils*, John Wiley & Sons, New York, 1979.
5. Sorrell, C. A. and Sandstrom, G. F., *Rocks and Minerals*, Golden Press, New York, 1973.
6. Barnes, H. L., *Geochemistry of Hydrothermal Ore Deposits*, 3rd ed., John Wiley & Sons, New York, 1997.
7. Dixon, J. B. and Weed, S. B., *Minerals in Soil Environments*, 2nd ed., Soil Science Society of America, Madison, WI, 1989.
8. Jenne, E. A., *Adsorption of Metals by Geomedia*, Academic Press, New York, 1998.
9. Sauve, S., McBride, M., Norvell, W. A. and Hendershot, W., *Water, Air Soil Pollut.*, **100**, 133 (1997).
10. MacCarthy, P., Clapp, C. E., Malcolm, R. L. and Bloom, P. R., *Humic Substances in soil and Crop Sciences: Selected Readings*, American Society of Agronomy, Soil Science Society of America, Madison, WI, 1990.
11. Alcacio, T. E., Hesterberg, D., Chou, J. W., Martin, J. D., Beauchemin, S. and Sayers, D. E., *Geochim. Cosmochim. Acta*, **65**, 1355 (2001).
12. Dojlido, J. R. and Best, G. A., *Chemistry of Water and Water Pollution*, Ellis Horwood, New York, 1993.
13. Stumm, W. and Morgan, J. J., *Aquatic Chemistry*, 3rd ed., John Wiley & Sons, New York (1996).
14. Klaas, G. J., Nierop, G. J., Jansen, B., Vrugt, J. A. and Vestraten, J. M., *Chemosphere*, **49**, 1191 (2002).
15. Howell, J. McC. and Gawthorne, J. M., *Copper in Animals and Man*, Vol. I, CRC Press, Boca Raton, FL, 1987.
16. Benton Jones, J. Jr., Wolf, B. and Mills, H. A., *Plant Analysis Handbook*, Micro – Macro Publishing, Athens, GA, 1991.
17. Pais, I. and Benton Jones, J. Jr., *The Handbook of Trace Elements*, St. Lucie Press, Boca Raton, FL, 1997.
18. Bennett, W. F., *Nutrient Deficiencies & Toxicities in Crop Plants*, ASP Press, St. Paul, MN, 1993.
19. Lugaski, T., *Copper: The Red Metal*, Geology Project Homepage, Copyright University of Nevada, Reno. http://www.unr.edu/sb204/geology/copper2.html, 1996.
20. Eltringham, T., *Technology Changes Forge the Future of Copper Mining*, http://innovations.copper.org/bp/technology-changes.html., 2003.
21. USEPA, *National Emission Standards for Hazardous Air Pollutants for Source Categories: National Emission Standards for Primary Copper Smelters*, 1998.
22. USEPA, *Copper Metal: Toxic Chemical Release Reporting: Community Right-to-Know*, 1996.
23. Meister, R. T. (Ed.), *Farm Chemicals Handbook 1996*, Meister Publishing Company, Hopewell Junction, New York, 1996.
24. USEPA, *Code of Federal Regulations 40, Part 503*, 1999.
25. ENSER, *Extant Criteria Evaluation Study-Draft Report*, Pima County Wastewater Management Department, Tucson, AZ, ENSR Corporation, Fort Collins, CO Document Number 5426-022-610, http://www.co.pima.az.us/wwm/wqrp/index.html, 2002.
26. Cornelis, R., Caruso, J., Crews, H. and Heumann, K. (Eds.), *Handbook of Elemental Speciation, Techniques and Methodology*, John Wiley & Sons, Chichester, West Sussex, UK, 2003.
27. Clesceri, L. S., Greenberg, A. E. and Eaton, A. D., *Standard Methods for the Examination of Water*

and Wastewater, 20th ed., American Public Health Association, Washington, DC, 1998.
28. Rump, H. H. and Krist, H., *Laboratory Manual for the Examination of Water, Wastewater and Soil*, VHC Publishers, New York, 1988.
29. Sparks, D. L., Page, A. L., Helmke, P. A., Loeppert, R. H., Soltanpour, P. N., Tabatapai, M. A., Johnston, C. T. and Summer, M. E., *Methods of Soil Analysis, Part 3 Chemical Methods*, Number 5 in the SSSA Book Series, SSSA Inc, ASA Inc, Madison, WI, 1996.
30. Batley, G. E., *Trace Element Speciation: Analytical Methods and Problems*, CRC Press, Boca Raton, FL, 1989.
31. USEPA, *Methods and Guidance for Analysis of Water*, EPA-821 C 97 001, Unites States Environmental Protection Agency, Office of Water, Washington, DC, 1997.
32. Moffett, J. W., *Oceanogr. Res. Pap.*, **42**, 1273 (1995).
33. Skrabal, S. A., Donat, J. R. and Burdige, D. J., *Geochim. Cosmochim. Acta*, **64**, 1843 (2000).
34. Muller, F. L., *Estuarine Coastal Shelf Sci.*, **46**, 419 (1998).
35. Rozan, T. F. and Benoit, G., *Geochim. Cosmochim. Acta*, **63**, 3311 (1999).
36. Gerringa, L. J. A., Herman, P. M. J. and Poortvliet, T. C. W., *Mar. Chem.*, **48**, 131 (1995).
37. Voelker, B. M. and Kogut, M. B., *Mar. Chem.*, **74**, 303 (2001).
38. Itoh, A., Iwata, K. and Haraguchi, H., *Anal. Sci.*, **16**, 1011 (2000).
39. Ackley, K. L. and Caruso, J. A., 4.1. Liquid chromatography, in *Handbook of Elemental Speciation, Techniques and Methodology*, Cornelis, R., Caruso, J., Crews, H. and Heumann, K. (Eds), John Wiley & Sons, Chichester, West Sussex, UK, 2003, pp. 147–162.
40. Welter, E., 6.2. Direct speciation of solids: X-ray absorption fine structure spectroscopy for species analysis in solid samples, in *Handbook of Elemental Speciation, Techniques and Methodology*, Cornelis, R., Caruso, J., Crews, H. and Heumann, K. (Eds), John Wiley & Sons, Chichester, West Sussex, UK, 2003, pp. 526–546.
41. Mavrogenes, J. A., Berry, A. J., Newville, M. and Sutton, S. R., *Am. Mineral.*, **87**, 1360 (2002).
42. Ortner, H. M., 6.1. Characterization of individual aerosol particles with special reference to speciation techniques, in *Handbook of Elemental Speciation, Techniques and Methodology*, Cornelis, R., Caruso, J., Crews, H. and Heumann, K. (Eds), John Wiley & Sons, Chichester, West Sussex, UK, 2003, pp. 505–525.
43. Clapp, C. E., Hayes, M. H. B., Senesi, N., Bloom, P. R. and Jardine, P. M., *Humic Substances and Chemical Contaminants*, Soils Science Society of America, Madison, WI, 2001.

2.8.2 Speciation of Copper in Clinical and Occupational Aspects

Donatus Nohr and Hans-Konrad Biesalski
University of Hohenheim, Stuttgart, Germany

1 PREFACE

A major part of this chapter is based on the outcome of the 15th Consensus talk at the University at Hohenheim, Stuttgart, Germany, in March 1999, during which experts from clinical and basic sciences discussed some urgent questions concerning the role of copper in physiology, nutrition and disease [1].

2 PHYSIOLOGICAL FUNCTIONS OF COPPER

For decades, copper (Cu) has been looked upon as an essential nutrient for animals and humans. The continuing efforts in analytical and molecular cell biology clarify more and more its major functions in the immune system, the skeletal apparatus, the formation of blood and blood vessels and also the nervous system. The body of an adult human contains about 80 to 100 mg of Cu and, in comparison, 4 g of iron (Fe). The mean concentration in body fluids is 10 μM, with 70 μM in the cerebrospinal fluid (CSF) and 250 μM in the synaptic cleft [1]. Cu is an essential part of the reactive centers of a number of enzymes, which need either Cu alone or Cu and other metal ions as cofactors, for example, Cu/Zn-superoxide dismutase (Cu/Zn-SOD), ceruloplasmine, cytochromoxidase (COX), tyrosinase, or lysineoxidase. In addition, Cu-dependent transcription factors play a major role in gene expression. Those enzymes that use Cu as a major part of their catalytic centers are oxidoreductases with a wide field of physiological functions in cellular respiration, defense of free radicals, synthesis of melanin ('color' of the skin produced by melanocytes), formation of connective tissue, and iron metabolism.

Handbook of Elemental Speciation II: Species in the Environment, Food, Medicine & Occupational Health
Edited by R. Cornelis, H. Crews, J. Caruso and K. G. Heumann
 ISBN: 0-470-85598-3 (HB)

One of the most extensively investigated enzymes is Cu/Zn-SOD, which is located in the cytoplasm, catalyzing the dismutation of superoxide anions from cellular respiration. During this process, Cu in the active center is reduced by the substrate O_2^-, thus forming O_2 and H_2O_2. Cu is not replaceable during such a process. Genetic mutations of the superoxidedismutase (SOD) with different enzymatic activities result in an enhanced amount of apoptosis and can be seen, for example, in amyotrophic lateral sclerosis (ALS), a defect of mainly spinal motoneurons.

The metabolisms of Cu and Fe are combined by ceruloplasmin and its ferroxidase activity. A malfunction of the protein due to genetic mutation leads to a deficiency in Cu [2], and consecutively of Fe, or, on the other hand, to a surplus of Fe, for example, in some areas of the brain, leading to neurodegeneration [3]. A deficiency in ceruloplasmine and a respective decrease in its ferroxidase activity leads to a smaller amount of Fe(II) bound to transferrin than Fe(III).

Ceruloplasmine, besides its function as a Cu transporter, is regarded as an antioxidant (see Section 3), as it prevents reactions that are dependent on Fe(II) [4]. In contrast, Cu ions that are bound to albumin or free amino acids are still able to take part in the Fenton reaction, thus producing hydroxyl radicals in concert with reactive oxygen species (ROS) [5]. Interestingly, the coupling of Cu to viruses, DNA, carbohydrates, enzymes or other proteins, for example, amyloid, can lead to local damage through the formation of radicals [6, 7], hence indicating that the toxicity of ROS *in vivo* is possibly dependent on catalytic metal ions.

Besides its role in the catalytic centers of Cu enzymes, there is growing evidence for the participation of Cu in the gene expression of several proteins via transcriptional factors, at least in yeast [8].

The function of Cu in the process of oxidative stress will be described in the following section.

3 THE ROLE OF COPPER IN OXIDATIVE STRESS

Copper overload favors the development of oxidative stress. Cu deficiency has also been proposed as a possible cause of oxidative stress, although this has not been established with any certainty. There are, however, individual results to support this suggestion.

In situations of oxidative stress, newly formed oxygen radicals cannot be adequately detoxified by antioxidants, and excess free radicals cause cellular damage. Hydroxyl radicals are formed mainly *in vivo* by reaction with H_2O_2, in accordance with the following equation.

$$M^{n+} + H_2O_2 \longrightarrow M^{(n+1)+} + {}^{\bullet}OH + OH^- \qquad (2.8.2.1)$$

Although the metal ion M^{n+} can represent Ti(III), Fe(II), Cu(I) and Co(II), as well as ions in chromium, manganese, vanadium and nickel complexes, only Fe(II) and Cu(I) seem to be capable of catalyzing the Fenton reaction *in vivo* [9, 10]. The rate for this second-order reaction is as low as $10^2 \times M^{-1}\,s^{-1}$. If one considers that the reaction partners H_2O_2, Fe(II) and Cu(I) are present at a concentration of about 1 μM under physiological conditions and the assumed reaction rates for Fe(II) and Cu(I) can be compared. If a liver cell volume of 10^{-12} L is assumed with a second-order reaction constant of $k = 76 \times M^{-1}\,s^{-1}$, about 46 $^{\bullet}OH$ radicals are formed per cell per second [11] when Fe(II) is used as the catalyst, as follows.

$$N = 7.6 \times 10^{-11} \times 10^{-12} \times 6.023 \times 10^{23} \qquad (2.8.2.2)$$

In contrast, the turnover rate with Cu(I) as a catalyst is $4.7 \times 10^3\,M^{-1}\,s^{-1}$. This is orders of magnitude greater than with Fe(II) as a catalyst and results in the production of 2840 $^{\bullet}OH$ radicals per cell per second. It must be considered here that Cu(III) may be produced in addition to, or instead of, radicals.

Cu(I) and Cu(III) can be produced by reaction with superoxide anions:

$$Cu(II) + O_2^- \longrightarrow Cu(I) + O_2 \qquad (2.8.2.3)$$

$$Cu(II) + O_2^- + 2H \longrightarrow Cu(III) + H_2O_2 \qquad (2.8.2.4)$$

However, it is not clear whether *in vivo* metal ions undergo reactions with superoxide anions and hence can produce oxidative stress.

Cu deficiency is also reported to produce oxidative stress, as studied in different model systems. Under the prerequisite that the activities of antioxidative enzymes and the extent of oxidative modification of erythrocyte proteins are reliable indicators for oxidative stress, rats were fed a Cu-deficient diet. Interestingly, while the hepatic Cu concentrations *per se* decreased by about 80% during Cu-deficient feeding, the Cu content in nuclei of hepatocytes did not change [12]. The transcription rates of the enzymes Cu/Zn-SOD, glutathione peroxidase and glycerine aldehyde-3-phosphate-dehydrogenase remained unaltered, whereas those of Mn-SOD and of beta-actin increased and the transcription rate of catalase decreased in Cu deficiency [12]. The activity of cytoplasmic Cu/Zn-SOD in erythrocytes also decreased, while the amount of carbonylated subunits of spectrin, an erythrocyte membrane protein [13], increased significantly. These examples show that experimentally induced Cu deficiency in rats influences the activity of hepatic antioxidative enzymes differentially. The activity of Cu/Zn-SOD is reduced, although the rate of transcription remains unchanged. Thus, presumably, the ratio of apo-enzyme to enzyme will increase in situations of inadequate Cu supply. This finding is in further support for the importance of Cu/Zn-SOD as an indicator for Cu deficiency.

4 FOOD SOURCES, INCLUDING POTABLE WATER

Copper can be ingested either via different kinds of food, the drinking water from normal plumbing or (in a very few specific situations) inhaled via respiration, with the latter being a negligible amount under normal conditions. The Cu content of some selected food examples is listed in Table 2.8.2.1. For drinking water, there is a given maximum contamination level goal (MCLG) of 1.3 $mg\,L^{-1}$ given by the US Environmental Protection Agency. In Germany and in the EU, the maximum level in water is set at 3 $mg\,L^{-1}$ after 12 h stagnation; the latter because the content of water from plumbing varies over a wide range,

Table 2.8.2.1. Copper content of various foods.

Food	Copper concentration ($\mu g\,g^{-1}$ wet weight)	Food	Copper concentration ($\mu g\,g^{-1}$ wet weight)
Meats			
Fish	0.61	Hamburger	0.95
Turkey	0.71	Steak	1.20
Chicken	0.34	Pork Liver	141.14
Dairy			
Egg	0.8	Cheddar cheese	0.44
Bread			
Whole wheat	1.07		
Shellfish			
Scallops	0.27	Mussels	4.75
Clams	6.08	Lobster	36.60
Shrimp	1.75		
Chocolate			
Syrup	43.36	Milk	0.33
Candy bar	1.18		
Vegetables			
Peas	2.38	Soy beans	109
Fruits			
Apple sauce (bottle)	0.30	Raisins	1.68
Avocado	1.68		
Nuts			
Walnuts	6.51	Peanut butter	8.53
Mushrooms			
Dry/canned	2.12–2.30		
Miscellaneous			
Tofu	0.28	Spaghetti sauce	1.13
Tofu patties	1.67	Soy chicken	0.28
Red beans and rice	1.31	Soy beef	1.01
Beverages			
	$mg{\cdot}L^{-1}$[a]		$mg{\cdot}L^{-1}$
Drinking water	1.3		
Coca Cola (bottle)	0.001	Sprite (bottle)	0.004
Coca Cola (can)	0.004	Sprite (can)	0.001

[a] Maximum contamination level goal (MCLG; see Section 4).
Source: Adapted from http://www.wilsonsdisease.org/copper.html.

as it depends on the kind of water (pH, salts, etc.) and even more on the water pipes and plumbing fixtures from which Cu can be dissolved. In general, the levels in running water drop to about 10% of the level of stagnating water (see http://www.umweltministerium.bayern.de/service/umwberat/kupfer_w.htm; http://books.nap.edu/books/0309069394/html/1.html)

5 UPTAKE, BIOAVAILABILITY AND HOMEOSTASIS

The uptake of Cu from food takes place mainly in the duodenum and proximal parts of the jejunum, with the resorptional amount being comparable throughout these regions of the intestine. In addition, the *per se* possible uptake by the stomach (which is in contrast to other metals) reaches only marginal amounts because of the largely incompletely digested nutrients at this location, and thus can be almost neglected. About 20–70% of nutritional Cu is resorbed, reaching a maximum of 50% in adults and up to 77% in sucklings. The overall resorption is degressive and can be strongly influenced by other metals and/or complexing agents.

The bioavailability depends on size, solubility and stability of the Cu complexes in the intestinal lumen and also on the various kinds of ligands. Resorption can take place either by an active, saturable transport mechanism or via diffusion [14]. A major candidate protein for active uptake is hCtr1, which shows high homology to the yeasts Ctr1 and Ctr3 (for details, see Pena *et al*. [15]). In rat offspring, diffusion is the main transport system, together with water cotransport (solvent drag), with this being reduced if sodium is missing or intestinal sodium transport is inhibited [16]. The offspring's resorption seems unsaturable [17] and has a greater capacity than that of adults [18]. The concentration of metallothionein (Cu sequestrator) is lower than in adults and seems not to be responsible for the enhanced resorption, whereas in adult rats intestinal metallothionein seems to limit the resorption under permanent enhanced Cu-exposition [19]. Human studies using isotopes showed a decreasing Cu uptake under rising Cu levels – a rise from 0.8 mg to 7.5 mg day^{-1} resulted in an essentially doubled resorption and the retention in the organism dropped to about 12%, while normally a maximum of 65% can be achieved [20]. These results indicate a homeostatically regulated Cu resorption with a target value of 0.8–1.0 mg Cu/day. Very little is still known about the human intestinal Cu transportation mechanisms and their regulation, whereas for Cu transfer from erythrocytes to the blood an involvement of the MNK-ATPase has been identified. However, this P-type ATPase should also be involved in human Cu transfer from enterocytes to the portal circulation.

The bioavailability strongly depends on interactions with other nutrients, which can be very heterogeneous. For example, in newborn breast-fed sucklings a bioavailability of Cu of 75–77% has been reported, which was reduced to 23% in such babies fed with fortified formulated food based on cow's milk [21, 22]. It was concluded that 75% of the Cu is bound to soluble proteins in breast milk (K19), whereas in cow's milk it is bound to insoluble casein [18], which is only incompletely cleaved in the incompletely developed digestive system. Therefore, a well-pronounced difference in the Cu uptake in breast-fed babies, when compared to bottle-fed babies, has to be pointed out.

A low pH in the stomach supports peptic digestion in the latter and as such principally enhances the available Cu amounts; however, the resorption here remains low. In the intestine, a neutral to higher pH decreases the bioavailability by the formation of Cu hydroxides or other Cu bonds, with a low dissociation constant. Phytates seem to have a lower impact on the bioavailability of Cu than on that of other divalent cations such as Fe or Zn [23], although dephytation has an indirect influence on the Cu bioavailability, as under these conditions less Fe or Zn are bound and thus can decrease Cu resorption [24]. As a consequence, Zn is used as a therapeutic in Wilsons disease (*vide infra*).

When compared to sodium, polymers of glucose enhance Cu resorption with water (solvent drag), while fructose decreases resorption, probably via a reduction in the energy metabolism [25]. Amino

acids and peptides have opposing effects, depending on their concentration. Low amounts support, whereas high amounts limit Cu resorption. Organic acids such as citrate, lactate or malate support the resorption, whereas it is decreased by ascorbic acid via the reduction of Cu(II) to Cu(I) [26].

Maintaining an appropriate Cu homeostasis depends on a critical orchestration between Cu uptake and its distribution within a cell on one side and removal and/or detoxification on the other side. Cu is taken up from the nutrients by the high-affinity Cu transporter hCtr1 on the luminal membranes of intestinal enterocytes. Intracellularly, Cu is then distributed by small cytoplasmic chaperones (hCOX17, HAH1 and copper chaperone for superoxide dismutase CCS) to specific cellular compartments for the incorporation of Cu into Cu-requiring proteins. These targets are the mitochondria (hCOX17), secretory compartment (HAH1) and Cu/Zn-SOD (CCS). Intensive and numerous studies on Menkes disease (*vide infra*) could show that a membrane-bound P-type ATPase Menkes protein (P-type ATPase) (MNK) is responsible for the efflux of Cu from intestinal cells to the portal blood (see K27). In the plasma, Cu is bound to albumin and histidine and deposited in the liver. Here again, hCtr1 plays a major role in the uptake of Cu into the liver cells. In the cell, the localization of MNK is concentration-dependent: in the presence of low concentrations, MNK is localized at the trans-Golgi network (TGN) for delivering Cu to the secretory pathway. High concentrations translocate the MNK to the plasma membrane to support the efflux of Cu and to avoid high, toxic levels. As Ag(I) also stimulates the translocation of MNK, the reduced form of copper (Cu(I)) seems to be responsible. The translocation process is energy-dependent and reversible, and the MNK protein and mRNA levels remain constant, for example, no production of additional protein or mRNA takes place. In the liver (and the brain), the Wilson disease protein (WND) P-type ATPase is required for biliary excretion of Cu and for the incorporation of Cu into ceruloplasmin – this is localized to the TGN. Ceruloplasmin, in addition to albumin and histidine, is the predominant Cu-containing protein in the serum. The latter is a glycosylated multi Cu ferroxidase that is mainly synthesized in the liver and carries more than 95% of total-serum Cu. In the presence of elevated Cu concentrations, WND moves from the TGN to an incompletely characterized cytoplasmic vesicular compartment [27], possibly on its way to the canalicular plasma membrane of the hepatocyte for excretion of Cu into the biliary ducts – a main pathway for Cu excretion. In addition, an ATP-independent, but GSH-dependent, transport of Cu to bile has been discussed [28]. There is only a very low and negligible amount of Cu reabsorption after biliary excretion.

It is not yet fully understood how the transport proteins relinquish Cu from the serum to the target tissues; however, it seems possible that Cu is transferred over to the hCtr1 Cu transporter at the respective cell membrane, either directly or indirectly [15].

6 RECOMMENDED UPTAKE

6.1 Children and adults

The German Society for Nutrition (DGE) recommends an intake of 1.0–1.5 mg Cu/day for adolescents and adults. The corresponding recommendation of the Scientific Committee on Food of the European Commission is 1.1 mg Cu/day for adults [29]. The DGE assessment was based on dietary balance studies, from which intakes of 75 μg Cu/kg in infancy, 50 μg kg^{-1} in older infants, 40 μg Cu/kg in children aged seven to ten years of age, and finally 20 μg Cu/kg in adults were derived [30–32]. In addition to the recommended dietary Cu intake, which is required to maintain normal plasma levels, the World Health Organization (WHO) has set an upper safe level for Cu in food (12 mg day^{-1} for male and 10 mg day^{-1} for female adults on the basis of 180 μg kg^{-1} body weight and day) that should not be exceeded [32].

Data on Cu concentrations in plasma show that a Cu intake, according to current DGE recommendations, was not sufficient in all cases investigated to keep plasma Cu concentrations in the normal range for children, adolescents and the elderly (0.8–1.2 mg L^{-1}) [33, 34]. Correspondingly, the

mean Cu intake in various European countries was below the recommended minimum intake of 1.2 mg Cu/day in adult males in about 10% of the subjects under investigation and below the minimum normal population intake in about 25% [32, 35]. In spite of these findings, according to the WHO, Cu deficiency is relatively rare in humans under normal physiological conditions. Clinical signs of deficiency are only observed under exceptional circumstances [36], for example, in children with 'cow's milk anemia', during rehabilitation after malnutrition or when formula milks are inadequately fortified with Cu, in adults with protein–energy malnutrition, in enteropathies and during total parenteral nutrition as a consequence of inadequate Cu supplementation of infusion solutions [35].

A daily dietary intake of 1–2 mg Cu/day seems necessary to provide for Cu-dependent metabolic processes in adults. This corresponds to the most recent lower limit of the 'acceptable range of oral intake' (AROI) for adults of 20 μg Cu/kg/day [35]. Because of the increased metabolic requirement, the corresponding value for infants is 50 μg Cu/kg/day (= 0.2–0.3 mg Cu/day). On the other hand, the WHO stated that the upper limit of the AROI for adults is not known; this is probably of the order of several, but not many, mg per day per adult. There is no statement regarding the upper limit of the AROI in infants or as to whether the 'upper limit of the AROI' is a threshold for adverse Cu effects or rather a maximum for a physiologically desirable Cu intake [35].

6.2 Physiologically desirable copper concentrations in drinking water for bottle-fed babies

The Cu content in 75 different commercial milk formulae from 10 manufacturers varies between 400 and 700 $\mu g\,L^{-1}$ (mean: ca. 500 $\mu g\,L^{-1}$), when the milk was rehydrated with Cu-free drinking water [37]. The corresponding Cu intake of bottle-fed babies is up to 75 $\mu g\,kg^{-1}\,day^{-1}$, which is 1.5 times the minimum intake recommended by the WHO [35]. Additional Cu intake from water is therefore not needed from a physiological point of view. The upper limit of the excretory capacity in infants is estimated to be 50 μg Cu/kg/day [38]. Taking this value, and assuming 50% absorption for Cu in the gastrointestinal (GI) tract, no more than 0.17 mg Cu/L in milk is needed to satisfy physiological requirements. However, the preliminary WHO drinking water standard (2 mg Cu/L) [39] is more than 10 times higher. This value derives from data obtained on the acute GI side effects of Cu, which were regarded as not being very conclusive. Because of this situation, it was reported that exposure to milk that contains 2 mg Cu/L (as approved by the WHO), and possibly also to lower Cu concentrations, might be hazardous for infants regarding the development of liver cirrhosis [40]. On the other hand, a single case of liver cirrhosis was proven to be associated with the public water supply, although millions of German homes are equipped with copper plumbing [41]. However, the scarcity of positive observations still does not rule out completely that Cu in drinking water may increase the hazard for hepatic damage in infants [42].

6.3 Copper deficiency

A deficiency of Cu might be due to increased requirements. Cu-deficiency states in children with massive diarrhea in developing countries [43, 44], especially in association with growth 'spurts' after protein-energy malnutrition, seem to be the most common cause of Cu deficiency. The loss of Cu in children with diarrhea was twice that in controls. Consequently, plasma levels of Cu were reduced by a half. In addition, concomitant administration of zinc, fructose or various chelators increase the demand and appear to cause Cu deficiency more frequently than inadequate dietary Cu supply [45]. In nephrotic syndrome and in patients with severe burns, excessive loss of Cu may occur and the Cu requirement is increased. Other conditions of this type are short bowel syndrome, cystic fibrosis, celiac disease, tropical and nontropical sprue, intestinal fistulas and following gastrectomy and ileo-jejunal bypass operations [46].

During the second half of pregnancy, the fetus acquires about 50 μg Cu/kg/day. Correspondingly,

pregnant women reduce biliary Cu excretion by hormonal adjustment [47], whereas serum Cu concentration increases by a factor of about 2 until the final trimester [45]. Therefore, Cu deficiency in pregnancy is rare. Premature babies have an increased risk of Cu deficiency. *In utero*, the fetus stores Cu predominantly during the final trimester. A mature infant has acquired Cu stores of ca. 15–17 mg Cu during pregnancy, 2.5–9.0 mg of which are found in the liver. These reserves prevent Cu deficiency in the first 47 months after full-term birth [48]. If delivery becomes due before the 34th week of pregnancy, plasma Cu concentrations are decreased correspondingly [49]. Cu mobilization from hepatic stores depends on liver maturation [50].

Because of rapid growth, premature babies have an increased Cu requirement as their digestive capacity and intestinal Cu absorption are not yet fully matured. Therefore, about a third of very low-birth-weight infants fed with normal infant formulae have a suboptimal Cu status at the age of 6 to 12 months [46]. The American Academy of Paediatrics has recommended the feeding of infant formulae with a Cu content of 900 μg Cu/L to premature babies to compensate for these deficits. This recommendation seems to be justified because these children absorb no more than ca. 15% of the Cu supplied with bottled milk due to its high casein content, whereas they absorb about 60% from breast milk.

Cu deficiency can also be due to inadequate intake (see Schumann *et al*. [1]). Malabsorption in the context of chronic enteropathies may result in hypocupremia. Several case reports have described Cu-deficiency states in association with celiac disease. Total parenteral nutrition without adequate Cu supplementation can lead to overt Cu deficiency, not only during rapid growth but also in adults. Accordingly, the American Medical Association has recommended the guarantee of supplying 0.5–1.5 mg Cu/day during total parenteral nutrition. Cu deficiency was compensated by the administration of 1 mg Cu/day over a period of two weeks, followed by 0.5 mg Cu/day in adults and 0.2 mg Cu/day in children to maintain this status.

6.4 Copper overload

6.4.1 Acute toxicity

Copper is relatively nontoxic for man after acute oral intake, with the lowest acutely fatal dose in man being about 10 g. Acute intoxications have primarily been observed after accidental or suicidal ingestion, and because of inhalation of dusts and/or fumes with high Cu concentrations, for example, at specific work places. Milligram amounts of soluble Cu salts can be ingested with fruit juices that have been stored in Cu containers or with water from Cu plumbing, although the water has to be standing in the plumbing for several hours, even days. Such an intake may cause vomiting and diarrhea. In severe cases, the intake of soluble Cu compounds in high gram quantities leads to hemolysis, liver and kidney damage, coma and also to death. Inhalation of Cu fumes irritates the upper airways and may lead to malaise, stomach pain and diarrhea.

6.4.2 Chronic toxicity

Chronic Cu intoxication from contaminated food is rare and mainly affects the GI tract and the liver. In patients with Wilson's disease, hemolysis, neurological symptoms and renal damage are also observed. Some examples include the following. A family in Vermont (in the United States) experienced recurrent GI irritation as a result of Cu-contaminated water (2.8–7.8 mg Cu/L). Excess Cu concentrations are also found in infant milk stored in Cu containers or resuspended in Cu-contaminated water. A 26-year-old man, who had taken 30 mg Cu/day as Cu gluconate tablets for two years and then 60 mg Cu for a further year, developed cirrhosis of the liver and acute liver failure (see Schumann *et al*. [1]).

Cu toxicity is linked to its unique electron configuration. Thus, Cu(I) ions can easily be polarized and bind predominantly to ligands rich in nitrogen and sulfur. Cu(II) ions tend to form complexes with ligands containing nitrogen and sulfur. Therefore, Cu is comparably reactive in biological matrices and can form strong bonds with a

wide variety of structures that are rich in electrons. The replacement of other essential metals in enzymes by Cu, or through Cu binding to macromolecules, may have deleterious effects on their function and structure. This can result, for example, in enzyme inhibition and alterations of DNA and membrane structures [51]. In addition, Cu can be involved in redox reactions. Cu ions are able to catalyze the formation of hydroxyl radicals via the Fenton reaction [52], and these redox reactions can increase cytoplasmatic calcium concentrations and cause ATP depletion and excess oxidation of thiols, DNA and membranes, which may finally lead to a loss of cellular integrity [53].

Although the overall Cu content of the body is a major prerequisite, the subcellular distribution and binding behavior is of crucial importance for Cu toxicity. Klein and coworkers have reported that Cu transfer from the cytoplasm into lysosomes appears to be essential for the development of Cu-induced liver damage [54]. Chaperones mediate intracellular Cu distribution to the sites of functional or toxic action. The low-molecular-mass protein metallothionein is crucial for intracellular Cu storage and detoxification. Thus, Cu administration induces metallothionein synthesis *in vivo*, while high metallothionein concentrations reduce Cu toxicity. Metallothionein is also assumed to have a direct antioxidant effect by reacting readily with hydroxyl radicals. Correspondingly, mouse cells that cannot synthesize metallothionein have proved to be particularly sensitive to oxidative stress [55] (see also Schumann *et al*. [1] and Pena *et al*. [15]).

6.4.3 Idiopathic copper toxicosis

Idiopathic copper toxicosis (ICT), Indian childhood cirrhosis, non-Indian childhood cirrhosis and Tyrolian childhood cirrhosis are probably identical disorders in which excess hepatic copper causes cirrhosis. All of these appear to be caused by ingesting high amounts of copper, either from drinking water, Cu cooking utensils or bottle-fed milk.

The idea that Cu concentrations between 0.2 and 2.0 mg L^{-1} may be harmful to the health of bottle-fed babies seems unlikely on the basis of plausible pharmacokinetic considerations [56]: Assuming that the liver of a one-year-old child suffering from ICT weighs 900 g (normal wt = 300–400 g) and has the average pathological content of ca. 400 μg Cu/g wet weight, the total liver Cu content would be 360 mg Cu. Up to 9 mg of Cu are acquired by the liver during pregnancy and are likely to be excreted or redistributed during the first year of life. If the child is assumed to consume over a year 1 L of formula milk that contains 3 mg Cu/L – which is a high estimate and if absorption amounted to 50%, then the total Cu absorption corresponds to 550 mg Cu. Thus, the liver would store over 70% of the absorbed Cu quantity without providing for Cu excretion. However, a healthy child excretes ca. 30 μg Cu/kg/day, corresponding to 100 to 200 μg day^{-1}, which corresponds to at least 50 mg during the first year of life [38].

During the perinatal period, the liver contains 50 to 60% of the body Cu content at most. From the sixth month on, this fraction decreases to 10–20%, unless a genetic disorder of Cu metabolism was present. By taking these figures, the daily absorption of 1.5 mg Cu/day from the diet would correspond to a hepatic Cu content of 60–70 mg Cu at the end of the first year of life. This corresponds to a Cu concentration of about 200 μg g^{-1} wet weight in a normal weight liver (300–400 g) and to just 70 μg g^{-1} wet weight in an enlarged liver of 900 g. However, hepatic Cu concentrations determined in ICT children are 20–30 times higher than that! Assuming an intake of 3 mg Cu/day with reconstituted milk, such high hepatic Cu concentrations can accumulate only if biliary Cu excretion were far below the normal rate (30 μg kg^{-1} day^{-1}) and if much less than 80% of the body Cu content were distributed to other organs after the sixth month of life, that is, when Cu metabolism were markedly disturbed.

Interestingly, in more recent times a still unknown genetic defect (an autosomal recessive disorder) could well be responsible for ICT.

Table 2.8.2.2. Copper content of major body organs, including blood [87].

Tissue/organ	Copper concentration ($\mu g\,g^{-1}$)	Total (%)
Skeleton	4.1	40.4
Muscle	0.9	23.3
Liver	6.2	8.8
Brain	5.2	7.8
Blood	1.1	5.5
Skin	0.8	3.4
Kidney	12.7	2.8
Fat	0.2	2.7
GI tract	1.9	2.5
Others[a]	–	2.8

[a] For example, plasma, CSF, salivary excretions and other body fluids.
Source: Adapted from Linder, 1991.

7 DETERMINATION OF COPPER STATUS

The copper content of major body organs, including blood, is given in Table 2.8.2.2. De- and repletion studies in several mammalian species (dogs, pigs, cattle, sheep, rats, etc.) showed decreases in serum/plasma Cu concentrations, in the hepatic Cu content, in plasma ceruloplasmin concentrations, in the SOD activity in liver or erythrocytes or in the activity of cytochrome-C-oxidase in the liver and duodenal mucosa during Cu-deficient feeding [57]. A decreasing dietary Cu intake is reflected in a lowered hepatic Cu content, and reduced SOD activity. When the dietary Cu-supply increases there is an even better correlation as to the increase in hepatic Cu. The degree of correlation between dietary and hepatic Cu is, however, a parameter that is highly dependent on the mammalian species [57].

Depletion and repletion studies in healthy volunteers help assess the value of the different diagnostic parameters. As a first example, the concentration of Cu and ceruloplasmin in the plasma remained unaltered, when these were 'challenged' by a daily supply of 0.57 mg of Cu for 105 days. The SOD activities in erythrocytes and the cytochrome-C-oxidase activity in the platelets, however, were decreased. Administration of 2 mg of Cu for 35 days increased the activity of cytochrome-C-oxidase and glutathione peroxidase [58]. Second, the plasma concentrations of Cu and ceruloplasmin decreased following a dietary challenge with an amount of 0.38 mg of Cu for 42 days. A 24 days repletion with 2.5 mg Cu/day leads to an insignificant increase in these parameters [59]. Third, after dietary Cu depletion (0.79 mg Cu/day for 24 h) and subsequent Cu repletion (7.53 mg Cu/day for 42 and 24 day), no changes in plasma Cu and ceruloplasmin concentrations, or in the erythrocyte's SOD activity were observed [60]. Finally, after reduced Cu intake for 77 days (1.03 mg day^{-1} 2850 kcal, with 20% fructose), the plasma concentrations of Cu and ceruloplasmin were unchanged, while the erythrocyte's SOD activity decreased and increased again after repletion (3 mg Cu/day for 21 days) [61]. The serum Cu concentration is homeostatically regulated. This parameter shows circadian changes with a peak in the morning, is higher in women than in men and increases with age. Oestrogen intake, pregnancy, infections, inflammation and stress increased the plasma Cu concentrations, while corticosteroids and corticotrophin administration decreased these levels. Ceruloplasmin in the plasma is regarded as an acute phase protein [62]. The latter is influenced in analogy to plasma Cu concentrations. The activity of Cu/Zn-SOD in erythrocytes, in contrast, is not affected by such influences. This is reduced in Cu depletion and increases again on repletion and, therefore, appears as a useful marker of Cu status. However, because of the limited sensitivity of all of these parameters, no optimal method is available to assess marginal Cu deficiency.

A promising new parameter for the determination of excess Cu intake is an elevated serum diamine oxidase (DAO) activity [63, 64] suggested for determining free plasma Cu concentrations directly, instead of calculating it from other parameters. A suitable method was developed by Gutteridge for other purposes [65]. The Cu-specific parameter measured colorimetrically in this case is the extent of oxygen radical formation during Cu-dependent DNA oxidation.

8 CLINICAL ASPECTS

8.1 Copper and neurodegenerative disorders

Neurodegenerative diseases appear to be directly related to Cu metabolism*. Menkes syndrome and

* For additional, older literature sources, see Schumann *et al.* [1].

Wilson's disease are inherited disorders with a functional disturbance of two membrane-located ATPases for the transport of Cu ions. In Wilson's disease, Cu excretion via the bile ducts is disturbed. Consequently, Cu accumulates predominantly in the liver. In Menkes syndrome, on the other hand, Cu-dependent enzymes, such as cytochrome-C-oxidase and lysyloxidase, are not adequately supplied with Cu.

In Menkes syndrome, clinical and pathological features are already present at birth, implying that Cu-dependent enzymes are already of importance in the prenatal phases of central nervous system (CNS) growth and development. Myelination disorders of nerve cells, diffuse atrophy of the brain, focal disintegration of the grey matter with destruction of axons in the white matter and extensive necrosis of Purkinje cells in the cerebellum are observed in Menkes syndrome. These are sequels of inadequate Cu supply to Cu-containing enzymes and lead to mental retardation of the patients.

Hepatic Cu deposits in Wilson's disease lead to damage of the liver. In adolescents and young adults, an increased number of neurological deficits also show up. Enhanced Cu deposition in the basal ganglia leads to gliosis and to neurological deficits with symptoms of Parkinson's disease. These occur along with changes in personality, depression and schizophrenia. In any case, whether Cu plays a direct role or acts via other (molecular) mechanisms of these events is still unclear. Interestingly, in one case investigated, the transplantation of a liver in Wilson's disease dramatically improved the neurological symptoms [66].

Amyotrophic lateral sclerosis (ALS) is a neurodegenerative disease with a sporadic and an inherited form. A loss of motor neurones in the spinal cord and in the brain causes progressive muscular weakness. Observations in siblings have shown that mutations in Cu/Zn-superoxide dismutase (SOD1) may be responsible for the disease [67]. Animal experiments showed that this disease is not due to decreased enzyme activity. The mutant SOD1 enzyme can also act as a peroxidase as a result of a change in protein conformation. In the presence of Cu, the peroxidase activity increases free radical activity, which can be demonstrated by indirect methods in transgenic animals and in patients [55, 68]. As cofactor for the mutant SOD-1 molecules, Cu is likely to be directly responsible for the toxic effects. The radicals seem to oxidize and aggregate proteins. These changes may retard axonal transport and damage the neurofilaments of motor neurones [69].

Alzheimer's disease is regarded as being the most common type of dementia. Its particular characteristic is a deposition of amyloid-Aβ-proteins (a plaque) [70]. Oxidative stress seems to be involved in Alzheimer pathogenesis. Thus, an increase in oxidation of proteins and DNA is seen in those brain regions that show amyloid deposits first [71]. Cu ions can stimulate the aggregation of synthetic Aβ-protein *in vitro*, and the concentration is increased six- to eight-fold in the characteristic protein deposits in affected patients [72, 73]. This fits in with the finding that amyloid-Aβ deposits can be redissolved in the presence of Zn- or Cu-specific chelators in the brain of Alzheimer patients at post mortem [74]. A probable source for the Cu that concentrates in the deposits is the amyloid precursor protein (APP). This contains a Cu-binding domain from which amyloid-Aβ is naturally formed by proteolytic activity.

There is growing evidence for the hypothesis that APP is involved in the transport of Cu into the cell, it binds Cu and can reduce Cu(II) to Cu(I). The protein is transported from the cell to the axonal and dendritic plasma membrane and could thus transport Cu(I) along this way. Cu(I) bound to this protein is rapidly oxidized by ROS, whereby APP is split in to several fragments, some of which contain the entire Aβ domain and are regarded as neurotoxic derivatives of APP within the cell [75]. By virtue of their Cu-binding domains, APP-Cu complexes themselves can cause oxidative stress in neurons *in vitro* [76]. In mice that do not produce any APP, Cu concentrations in the liver and cerebral cortex are increased by 80 and 40%, respectively [76]. Furthermore, additional Cu in the medium also affects the physiological processing of APP, presumably by regulation of APP transport via a conformational change in the protein. Thus, an involvement of Cu in Alzheimer pathogenesis is conceivable.

Prion diseases generally occur as sporadic, dominantly inherited or infective diseases [77]. Creutzfeldt–Jacob disease (CJD) in man, for example, is characterized by a rapidly progressing dementia and cerebellar ataxia. Spongiform changes are found in the tissue with gliosis of the astrocytes. In the course of pathogenesis, the cellular prion protein PrP^{C} is transformed into an infectious prion protein PrP^{Sc} and aggregates in the form of amyloid-like plaques in affected brains.

There are reasons to believe that cellular PrP is involved in CNS Cu homeostasis. The Cu chelating agent cuprizone induces similar neurological alterations in mice as were observed seen in prion diseases. In contrast to APP-deficient mice (see above), the brain cells of mice in which the PrP gene is turned off are more sensitive to Cu salts. They show a reduced SOD1 activity and a lower Cu content in the cell membranes [78]. Since Cu ions stimulate PrP uptake into cells, it is assumed that PrP might be involved in cellular uptake.

Cu binds to the N-terminus of PrP [79] and changes the conformation of the protein into a β-folding structure. *In vitro*, Cu binding causes the prion protein (PrP) to regain its infective potential and its resistance to proteolytic destruction. PrP^{Sc} molecules are found in the affected tissues as protein–metal ion complexes that contain Zn and Cu. Obviously, Cu binding causes conformational changes in PrP^{Sc}, which could also explain the diversity of prion strains [80].

The physiological significance of Cu binding to PrP is not yet elucidated. However, on the basis of the findings described above one can assume that PrP co-regulates cellular Cu homeostasis. It is involved in cellular Cu uptake and subsequently, as a Cu chaperone, it delivers Cu to corresponding target proteins.

8.2 Copper and coronary heart disease

Disturbed Cu uptake has been proposed as a risk factor for coronary heart disease (CHD). HMG-CoA-reductase is a key enzyme in endogenous cholesterol synthesis, and its activity is increased in Cu deficiency. In parallel, the sensitivity of very low density lipoproteins (VLDL) and low density lipoproteins (LDL) to oxidation increases in Cu deficiency [81]. LDL oxidation is a significant pathogenetic factor in the development of arteriosclerosis, and hence of CHD. An increase in total cholesterol, LDL-cholesterol and a decrease in HDL-cholesterol were observed in Cu deficiency. The effect of Cu depletion in animal vessels and the changes found in patients with CHD show apparent similarities (elastin destruction, fibrosis, intramural hemorrhages, increase in mucopolysaccharides, necrosis and the proliferation of smooth muscle cells) [82]. The Yi People Study [83] found an inverse correlation between serum Cu and the risk of CHD, whereas other epidemiological studies found a positive correlation.

Macroangiopathy in Cu-deficient animals is primarily attributable to a decreased activity of lysyloxidase. This Cu-dependent enzyme crosslinks collagen and elastin, and a decreased activity enzyme impairs the integrity of the arterial wall. In addition, secreted protein, acidic, rich in cysteine (SPARC), an extracellular matrix protein with Cu-dependent angiogenetic properties, may also contribute to vascular problems [84]. Cu deficiency might also impair the effect on the elasticity of the arterial wall via a reduction in NO-induced vasodilatation. This effect is supposed to be mediated via increased NO degradation by superoxide anions as a consequence of decreased SOD activity in Cu deficiency.

8.3 Copper deficiency and skeletal malformations

Several animal tests with various C-deficient mammalian species resulted in poorly developed, light brittle bones, malformed leg bones, thinning of trabecula and cortex of long bones, so indicating an impairment of osteogenesis. Besides low levels of amineoxidase, COX and lysiloxidase, a low ratio of soluble-to-insoluble collagen as well as the number of crosslinks in the collagenous matrices have been described [85].

8.4 Copper deficiency and the lung

Lung abnormalities are a frequent consequence of perinatal Cu deficiency. In neonatal rabbits,

offspring from deficient dams were characterized by low concentrations of Cu and lysiloxidase activity and a high amount of poorly crosslinked elastin and collagen; in addition, low concentrations of surfactant phospholipids were found. In mice, an administered Cu solution led to morphological changes, as well as to enhanced numbers of immune cells [86].

9 REFERENCES

1. Schumann, K., Classen, H. G. and Dieter, H. H. *et al*., *Eur. J. Clin. Nutr.*, **56**, 469 (2002).
2. Wang, X., Manganaro, F. and Schipper, H. M., *J. Neurochem.*, **64**, 1868 (1995).
3. Gitlin, J. D., *Pediatr. Res.*, **44**, 271 (1998).
4. Gutteridge, J. M., *Med. Lab. Sci.*, **37**, 267 (1980).
5. Brigelius, R., Spottl, R. and Bors, W. *et al*., *FEBS Lett.*, **47**, 72 (1974).
6. Multhaup, G., Ruppert, T. and Schlicksupp, A. *et al*., *Biochemistry*, **37**, 7224 (1998).
7. Quinlan, G. J. and Gutteridge, J. M., *Free Radical Res. Commun.*, **5**, 149 (1988).
8. Yonkovich, J., McKenndry, R., Shi, X. and Zhu, Z., *J. Biol. Chem.*, **277**, 23981 (2002).
9. Gutteridge, J. M., *Ann. N. Y. Acad. Sci.*, **738**, 201 (1994).
10. Wiedau-Pazos, M., Goto, J. J. and Rabizadeh, S. *et al*., *Science*, **271**, 515 (1996).
11. Halliwell, B. and Gutteridge, J. M., *Methods Enzymol.*, **186**, 1 (1990).
12. Lai, C. C., Huang, W. H., Klevay, L. M., Gunning, W. T. and Chiu, T. H. III, *Free Radical Biol. Med.*, **21**, 233 (1996).
13. Sukalski, K. A., LaBerge, T. P. and Johnson, W. T., *Free Radical Biol. Med.*, **22**, 835 (1997).
14. Crampton, R. F., Matthews, D. M. and Poisner, R., *J. Physiol.*, **178**, 111 (1965).
15. Pena, M. M., Lee, J. and Thiele, D. J., *J. Nutr.*, **129**, 1251 (1999).
16. Wapnir, R. A., *Proc. Soc. Exp. Biol. Med.*, **196**, 410 (1991).
17. Varada, K. R., Harper, R. G. and Wapnir, R. A., *Biochem. Med. Metab. Biol.*, **50**, 277 (1993).
18. Lonnerdal, B., Bell, J. G. and Keen, C. L., *Am. J. Clin. Nutr.*, **42**, 836 (1985).
19. Hall, A. C., Young, B. W. and Bremner, I., *J. Inorg. Biochem.*, **11**, 57 (1979).
20. Turnlund, J. R., *Crit. Rev. Food Sci. Nutr.*, **30**, 387 (1991).
21. Dorner, K., Dziadzka, S., Hohn, A., Sievers, E., Oldigs, H.D., Schulzlell, G. and Schaub, J., *Br. J. Nutr.*, **61**, 559 (1989).
22. Lonnerdal, B., *Am. J. Clin. Nutr.*, **67**, 1046S (1998).
23. Turnlund, J. R., King, J. C., Gong, B., Keyes, W. R. and Michel, M. C., *Am. J. Clin. Nutr.*, **42**, 18 (1985).
24. Morris, E. R., Ellis, R., Steele, P. and Moser, P. B., *Nutr. Res.*, **8**, 445 (1988).
25. Wapnir, R. A. and Devas, G., *Am. J. Clin. Nutr.*, **61**, 105 (1995).
26. Van Campen, D. and Gross, E., *J. Nutr.*, **95**, 617 (1968).
27. Hung, I. H., Suzuki, M., Yamaguchi, Y., Yuan, D. S., Klausner, R. D. and Gitlin, J. D. *J. Biol. Chem.*, **272**, 21461 (1997).
28. Dijkstra, M., Vonk, R. J. and Kuipers, F., *J. Hepatol.*, **24**(Suppl. 1), 109 (1996).
29. Scientific Committee on Food, *Nührstoff und Energiezufuhr in der Europäischen Gemeinschaft*, Luxemburg, Belgium, 1994.
30. Deutsche Gesellschaft für Ernährung, *Empfehlungen für die Nährstoffzufuhr*, Umschau Verlag, Frankfurt, 1991.
31. National Research Council, *Recommended Dietary Allowances*, Washington, DC, 1989.
32. WHO, *Trace Elements in Human Nutrition and Health*, Geneva, Switzerland, 1996.
33. Konig, J. S. and Elmadfa, I., *Ann. Nutr. Metab.*, **44**, 129 (2000).
34. Elmadfa, I., Burger, P., Derndorfer, E., Kiefer, I. and Kunze, M., *Österreichischer Ernährungsbericht 1998*. Wien, Austria, 1999.
35. WHO, Copper. *Environmental Health Criteria*, Geneva, Switzerland, 1998.
36. Underwood, E. J., *J. Hum. Nutr.*, **35**, 37 (1981).
37. Blasco, N., Galindo, A. and Perez, M., *Estimated Daily Intakes and Concentrations of Essential Trace Elements in Infant Formulas*, Abstract on behalf of TEMA 10, Evian, France, 1999.
38. Aggett, P. J., *Eur. J. Med. Res.*, **4**, 214 (1999).
39. WHO, *Guidelines for Drinking Water Quality*, Geneva, Switzerland, 1993.
40. Hadorn, H. B., *Eur. J. Med. Res.*, **4**, 212 (1999).
41. Vergara, J. D., Zietz, B. and Dunkelberg, H., *Bundesgesundheitsblatt*, **43**, 272 (2000).
42. Dieter, H. H., Schimmelpfennig, W., Meyer, E. and Tabert, M., *Eur. J. Med. Res.*, **4**, 233 (1999).
43. Castillo-Duran, C., Vial, P. and Uauy, R., *Am. J. Clin. Nutr.*, **51**, 1088 (1990).
44. Sachdev, H. P., Mittal, N. K. and Yadav, H. S., *J. Pediatr. Gastroenterol. Nutr.*, **8**, 212 (1989).
45. Keen, C. L., Uriu-Hare, J. Y., Hawk, S. N., Jankowski, M. A., Daston, G. P., Kwik-Uribe, C. L. and Rucker, R. B., *Am. J. Clin. Nutr.*, **67**, 1003S (1998).
46. Beshgetoor, D. and Hambidge, M., *Am. J. Clin. Nutr.*, **67**, 1017S (1998).
47. McArdle, H. J. and Ashworth, C. J., *Br. Med. Bull.*, **55**, 499 (1999).
48. Cordano, A., *Am. J. Clin. Nutr.*, **67**, 1012S (1998).
49. Sann, L., Rigal, D., Galy, G., Bienvenu, F. and Bourgeois, J., *Pediatr. Res.*, **14**, 1040 (1980).
50. Mason, R., Bakka, A., Samarawickrama, G. P. and Webb, M., *Br. J. Nutr.*, **45**, 375 (1981).

51. Alt, E. R., Sternlieb, I. and Goldfischer, S., *Int. Rev. Exp. Pathol.*, **31**, 165 (1990).
52. Goldstein, S. and Czapski, G., *J. Free Radical Biol. Med.*, **2**, 3 (1986).
53. Bremner, I., *Am. J. Clin. Nutr.*, **67**, 1069S (1998).
54. Klein, D., Lichtmannegger, J., Heinzmann, U., Muller-Hocker, J., Michaelsen, S. and Summer, K. H., *Eur. J. Clin. Invest.*, **28**, 302 (1998).
55. Liu, R., Althaus, J. S., Ellerbrock, B. R., Becker, D. A. and Gurney, M. E., *Ann. Neurol.*, **44**, 763 (1998).
56. Tanner, M. S., *Adv. Exp. Med. Biol.*, **448**, 127 (1999).
57. Baker, D. H. and Ammermann, C. B., in *Bioavailability of Nutrients for Animals*, Baker, D. H., Ammermann, C. B. and Lewis, A. J. (Eds.), Academic Press, San Diego, CA, 1995, pp. 127–156.
58. Milne, D. B. and Nielsen, F. H., *Am. J. Clin. Nutr.*, **63**, 358 (1996).
59. Kelley, D. S., Daudu, P. A., Taylor, P. C., Mackey, B. E. and Turnlund, J. R., *Am. J. Clin. Nutr.*, **62**, 412 (1995).
60. Turnlund, J. R., Keen, C. L. and Smith, R. G., *Am. J. Clin. Nutr.*, **51**, 658 (1990).
61. Reiser, S., Smith, J. C. Jr., Mertz, W., Holbrook, J. T., Scholfield, D. J., Powell, A. S., Canfield, W. K. and Canary, J. J., *Am. J. Clin. Nutr.*, **42**, 242–251 (1985).
62. Milne, D. B., *Clin. Chem.*, **40**, 1479–1484 (1994).
63. Kehoe, C. A., Faughnan, M. S., Gilmore, W. S., Coulter, J. S., Howard, A. N. and Strain, J. J. *J. Nutr.*, **130**, 30 (2000).
64. Evans, P. J., Bomford, A. and Halliwell, B. Non-coeruloplasmin copper in human serum, does it exist, *5th Meeting of the European Copper Research Group*, Kinsale, Ireland, 1998.
65. Gutteridge, J. M., *Biochem. J.*, **218**, 983 (1984).
66. Stracciari, A., Tempestini, A., Borghi, A. and Guarino, M., *Arch. Neurol.*, **57**, 384 (2000).
67. Deng, H. X., Hentati, A., Tainer, J. A., Iqbal, Z., Cayabyab, A., Hung, W. Y., Getzoff, E. D., Hu, P., Herzfeldt, B., Roos, R. P., Warner, C., Deng, G., Soriano, E., Smyth, C., Parge, H. E., Ahmed, A., Roses, A. D., Hallewell, R. A., Pericakvance, M. A. and Siddique, T., *Science*, **261**, 1047 (1993).
68. Ferrante, R. J., Browne, S. E., Shinobu, L. A., Bowling, A. C., Baik, M. J., MacGarvey, U., Kowall, N. W., Brown, R. H. and Beal, M. F., *J. Neurochem.*, **69**, 2064 (1997).
69. Williamson, T. L. and Cleveland, D. W., *Nat. Neurosci.*, **2**, 50 (1999).
70. Selkoe, D. J., *Trends Cell Biol.*, **8**, 447 (1998).
71. Markesbery, W. R. and Carney, J. M., *Brain Pathol.*, **9**, 133 (1999).
72. Atwood, C. S., Moir, R. D., Huang, X., Scarpa, R. C., Bacarra, N. M. E., Romano, D. M., Hartshorn, M. K., Tanzi, R. E. and Bush, A. I., *J. Biol. Chem.*, **273**, 12817 (1998).
73. Lovell, M. A., Robertson, J. D., Teesdale, W. J., Campbell, J. L. and Markesbery, W. R., *J. Neurol. Sci.*, **158**, 47 (1998).
74. Cherny, R. A., Legg, J. T., McLean, C. A., Fairlie, D. P., Huang, X. D., Atwood, C. S., Beyreuther, K., Tanzi, R. E., Masters, C. L. and Bush, A. I., *J. Biol. Chem.*, **274**, 23223 (1999).
75. Simons, M., Ikonen, E., Tienari, P. J., Cidarregui, A., Monning, U., Beyreuther, K. and Dotti, C. G., *J. Neurosci. Res.*, **41**, 121 (1995).
76. White, A. R., Reyes, R., Mercer, J. F., Camakaris, J., Zheng, H., Bush, A. I., Multhaup, G., Beyreuther, K., Masters, C. L. and Cappai, R., *Brain Res.*, **842**, 439 (1999).
77. Aguzzi, A. and Brandner, S., *Lancet*, **354**(Suppl. 1), SI22 (1999).
78. Brown, D. R., *Biochem. Soc. Trans.*, **30**, 742 (2002).
79. Hornshaw, M. P., McDermott, J. R., Candy, J. M. and Lakey, J. H., *Biochem. Biophys. Res. Commun.*, **214**, 993 (1995).
80. Wadsworth, J. D., Jackson, G. S., Hill, A. F. and Collinge, J., *Curr. Opin. Genet. Dev.*, **9**, 338 (1999).
81. Rayssiguier, Y., Gueux, E., Bussiere, L. and Mazur, A., *J. Nutr.*, **123**, 1343 (1993).
82. Klevay, L. M., *J. Trace Elem. Electrolytes Health Dis.*, **7**, 63 (1993).
83. He, J. A., Tell, G. S., Tang, Y. C., Mo, P. S. and He, G. Q., *J. Am. Coll. Nutr.*, **11**, 74 (1992).
84. Lane, T. F., Iruela-Arispe, M. L., Johnson, R. S. and Sage, E. H., *J. Cell Biol.*, **125**, 929 (1994).
85. Rucker, R. B., Kosonen, T., Clegg, M. S., Mitchell, A. E., Rucker, B. R., Uriu-Hare, J. Y. and Keen, C. L., *Am. J. Clin. Nutr.*, **67**, 996S (1998).
86. Prieditis, H. and Adamson, I. Y., *Exp. Lung Res.*, **28**, 563 (2002).
87. Linder, M. C., *Biochemistry of Copper*, Plenum Press, New York, 1991.

2.9 Speciation of Iron

2.9.1 Speciation of Iron in the Environment

Peter Hoffmann

Darmstadt Technical University, Darmstadt, Germany

1 INTRODUCTION

The aim of this contribution is to give a review of experimental methods for speciation of iron and to specify in detail the reactions of iron in atmospheric samples. Obviously, all the methods and procedures mentioned and reviewed in this chapter can also be used in other fields, for example, environmental science, materials' science, chemistry, or medical science. Therefore, it is necessary to discuss the behavior of iron in the aqueous phase and in solids separately. Speciation is defined as the determination of the chemical forms of traces of an element. The determination of species of iron in an aqueous phase is focused on the separation and detection of the oxidation states Fe^{2+} and Fe^{3+}. Additionally, the knowledge of ligands is of high importance. The speciation of iron in solids is concentrated on the determination of electron energy levels, on accompanying elements and their stoichiometric relation to iron, and on the structure of iron containing compounds.

Handbook of Elemental Speciation II: Species in the Environment, Food, Medicine & Occupational Health
Edited by R. Cornelis, H. Crews, J. Caruso and K. G. Heumann
 ISBN: 0-470-85598-3 (HB)

Consequently, various experimental methods may be applied to get information about the species of iron, and the choice of the method used is a function of the question, which has to be answered.

Iron is fourth in the abundance of the elements (after O, Si, Al) and second in abundance of the metals on the earth's crust. The most important oxidation states in the chemistry of iron are +2 and +3. The major iron ores are hematite (Fe_2O_3), magnetite (Fe_3O_4), limonite (FeO(OH)), and siderite ($FeCO_3$) [1].

Iron plays an outstanding role in chemical reactions, for example, in geological processes, in environmental and atmospheric chemistry, and in biochemistry. As an example, a paper of A. J. Ghio *et al*. may be mentioned [2]. The reasons for the important role of iron are due to the following three properties [3, 4].

1. The two common oxidation states (Fe^{2+} and Fe^{3+}) can easily change from one to the other. The position of the redox equilibrium is a strong function of pH, temperature, and of additional components in a solution. The standard potential is $E^\circ = +0.77$ V at 25 °C. Therefore, Fe^{3+} can act as an oxidant and Fe^{2+} as a reducing agent.
2. The solubilities of compounds of these two oxidation states may be very different. For example, salts of Fe^{2+} show high solubility in aqueous solutions, whereas salts of Fe^{3+} undergo stepwise hydrolysis at pH > 1 [5]. At pH > 2, condensed and colloidal species are formed, leading finally to the precipitation of Fe^{3+}-oxide-hydrates, which are only very slightly soluble. The solubility products of these compounds, given in the literature, have to be handled with care, if the exact composition is not defined.
3. Both oxidation states of Fe form a great variety of chemical complexes. In pure, aqueous solutions, aquo-hydroxo-complexes are present. At very low pH values, octahedral hexaquo-complexes are dominant and are transformed at increasing pH in various steps into hydroxo complexes and hydroxides. In the case of Fe^{3+}, redbrownish $Fe_2O_3 \cdot nH_2O$ is precipitated as final product. In the presence of complexing components, slightly soluble complexes are formed, for example, sulfato, carbonato, cyano, amino and oxalato complexes.

As an example, in groundwater Fe is preferably present in the soluble divalent state in the form of $Fe(HCO_3)_2$. By accessing oxygen, Fe is oxidized to the trivalent state and forms colloidal and precipitating oxide-hydrates.

Iron is introduced into the atmosphere in particulate form. The compounds identified by Mößbauer spectrometry and by electron probe analysis with X-ray detection are magnetite, hematite, goethite, and Fe^{2+}- and Fe^{3+}-silicates. Their particle number, mass, or volume ratio is a function of the character of the sources and of the history of the air mass examined. The chemical reactions at the surface of the particulate matter with gaseous or aqueous compounds have not been examined in detail up to now. The fraction of iron in the aqueous samples is usually determined by ion chromatography or by electrochemical methods. After filtration and/or ultrafiltration, this fraction consists of molecular dispersed species, colloidal forms, and particles with a distinct size distribution [6]. After ultrafiltration, between 10 and 20% of the total iron content in an original sample are found in the aqueous phase. The fraction of Fe^{2+} in the molecular dispersed form is about 65% at daytime and about 50% at nighttime due to sunlight reduction. At pH 3, the complexes identified in the molecular dispersed form are $[Fe(H_2O)_6]^{2+}$ and $FeSO_4$ for Fe(II), and $[Fe(OH)(H_2O)_5]^{2+}$, $[Fe(OH)_2(H_2O)_4]^{+}$, $[Fe(C_2O_4)_3]^{3-}$, $[Fe(C_2O_4)_2(H_2O)_2]^{-}$, and $[Fe(C_2O_4)(H_2O)_4]^{+}$ for Fe(III). The fractions of these species differ with pH, redox potential, and the concentrations of the various compounds.

2 SPECIATION OF IRON IN THE AQUEOUS PHASE

2.1 General remarks

Quantitative determination of traces or ultra-traces of total iron in aqueous samples (e.g. from the

Table 2.9.1.1. Quantification of Fe(II) and Fe(III) traces.

Method	LOD ($\mu g\,L^{-1}$)	Remarks	Reference
Flow injection analysis, chemiluminescence, reduction of Fe(III) by L-ascorbic acid, enrichment on cationic exchanger	0.012	Fe(III)-det. by calculation differences	[12]
Photometry, di-2-pyridylketone-benzoyl-hydrazone	0.1	Interference by other transition metals	[13, 14]
Reduction of cacotheline by Fe(II), photochemical reduction of Fe(III)	600 (Fe(II))	–	[15]
	800 (Fe(III))		
Photometry of Fe(II)-ferrozine, Fe(III) masking by ethylenedinitrilotetraacetic acid (EDTA)	900	–	[16–20]
Photometry of Fe(II)-1,10-phenanthroline, Fe(III) masking by fluoride	–	–	[21]
Various methods (photometry, chemiluminescence, fluorescence, voltammetry, potentiometry), review	–	Shift of the redox equilibrium by complexing agents possible	[22]
Ion chromatography, conductometric detection	5	–	[23]
Acidic cation exchanger, eluent: ethylenediamine, tartaric, oxalic and citric acid, post column derivatization with 4-(2-pyridylazo)resorcin (PAR) and ZnEDTA	<100	–	[24, 25]
Ion chromatography, eluent: pyridine-2,6-dicarboxylic acid, photometry by PAR derivatization	–	Separation of Fe(II) and Mn(II) not adequate	[26]
Ion chromatography on Nucleosil10SA, eluent: lactic acid, reduction of Fe(III) with L-ascorbic acid, derivatization of Fe(II) by ferrozin	2 (Fe(II))	–	[27–30]
	5 (Fe(III))	–	

atmosphere) was performed by means of various methods: for example, graphite furnace atomic absorption spectrometry (GFAAS) and proton induced X-ray emission (PIXE) [7], total reflection X-ray fluorescence (TXRF), and inductively coupled plasma mass spectrometry (ICP-MS) [8, 9].

Photometrical methods are well known for the distinction between Fe(II) and Fe(III). Fe(II) forms colored chelates with ligands of ferroin structure. The most often used compounds are those with 1.10-phenanthroline, 2.2′-dipyridyl, and 2.2′.2″-tripyriyl [10]. The phenolic OH-group is selective for Fe(III). From this large group, only sulfosalicylic acid, 7-iodine-8-hydroxychinoline-5-sulfonic acid (ferron), and pyrocatechine-3.5-disulfonic acid (tiron) are of practical importance. Additionally, thiocyanate has to be mentioned. Unfortunately, other metal ions interfere with the analytical identification. A new, simple, selective, and sensitive spectrophotometric procedure for on-site quantification of total and ferric iron was described [11]. It is based on the color reaction of Fe(III) with SCN^- ions in the presence of cationic surfactants with subsequent extraction of the complex with N-octylacetamide into toluene or chloroform. The detection limit was determined to be 5 μg Fe/L. Co(II), Cu(II), Zn(II), Mo(VI), W(VI), and Tl(III) interfere at concentrations $>5\ mg\,L^{-1}$ and Ti(III), Cd(II), and Hg(II) at concentrations above 10 $mg\,L^{-1}$ in the determination of 100 μg Fe/L.

For the separate determination of Fe(II)- and Fe(III)-species at trace levels in the low $nmol\,L^{-1}$ range, only a few references are given. The methods are summarized in Table 2.9.1.1 and comprise specific analytical procedures for Fe(II) or Fe(III), respectively, and chromatographic separations with various detection methods.

2.2 Calculations

The distribution of species can be calculated from stability and equilibrium constants and from the concentrations of the components. It should be pointed out that reliable results are only obtained for

simple chemical systems. However, the results of the calculations allow an assessment of the trends in the reaction steps. The dominating species of Fe(II) in neutral and acidic solutions in the absence of complexing agents is the Fe(II)-hexaquo-complex $[Fe(H_2O)_6]^{2+}$, whereas Fe(III) exists only in acidic solutions as the hexaquo-complex, which at increasing pH is subsequently transformed to mono- and the dihydroxo-complexes as $[Fe(H_2O)_5(OH)]^{2+}$ and $[Fe(H_2O)_4(OH)_2]^{+}$ [31]. At Fe(III) concentrations $>10^{-3}$ mol L^{-1} dimer and further polymer condensation products are observed: for example, $[(H_2O)_4Fe(OH)_2Fe(H_2O)_4]^{4+}$ [32]. With further increasing pH, neutral polynuclear hydroxo complexes and anionic complexes, such as the tetrahydroxoferrate(III)-ion, are formed. The mechanism of the precipitation and the aging of the precipitate are described at different conditions [33]. For the calculation of the species distribution, the equations (2.9.1.1–2.9.1.3) were used with equilibrium constants, which are mean values of reference data [34].

$$[Fe(H_2O)_6]^{3+} \Leftrightarrow [Fe(H_2O)_5(OH)]^{2+} + H^+ \qquad K_1 = 1.39 \times 10^{-3}\ \text{mol L}^{-1} \qquad (2.9.1.1)$$

$$[Fe(H_2O)_5(OH)]^{2+} \Leftrightarrow [Fe(H_2O)_4(OH)_2]^{+} + H^+ \qquad K_2 = 3.12 \times 10^{-4}\ \text{mol L}^{-1} \qquad (2.9.1.2)$$

$$[Fe]_T = [Fe(H_2O)_6]^{3+} + [Fe(H_2O)_5(OH)]^{2+} + [Fe(H_2O)_4(OH)_2]^{+} \qquad (2.9.1.3)$$

A complex distribution results (Figure 2.9.1.1) by plotting the concentration of Fe(III) species relative to the total Fe(III) as function of pH.

In the presence of oxalate ions in an aqueous Fe(III)-solution (10^{-7}–5×10^{-5} mol L^{-1} in atmospheric aqueous samples) Fe(III)-oxalate complexes are formed instead of Fe(III)-hydroxo complexes [35]. The fractions of the hydroxo- and of the oxalato complexes are functions of the Fe(III)/oxalate concentration ratio, the pH value, the complex formation constants, and of the dissociation constants of the oxalic acid. The equations (2.9.1.4–2.9.1.8) were used for construction of Figure 2.9.1.2, taking data from the literature [36, 37].

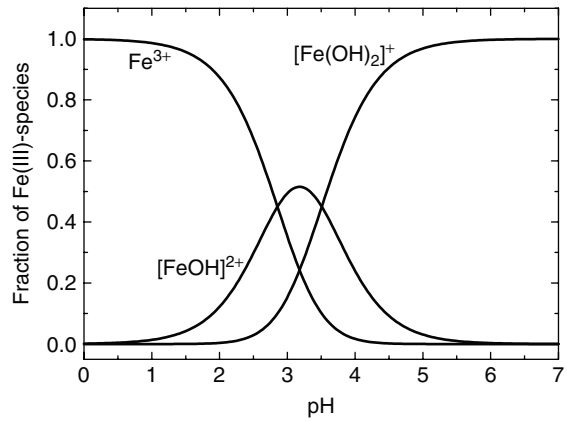

Figure 2.9.1.1. Calculated species distribution of Fe(III) in water as function of the pH value; 25 °C; ionic strength: 0.2 mol L^{-1}.

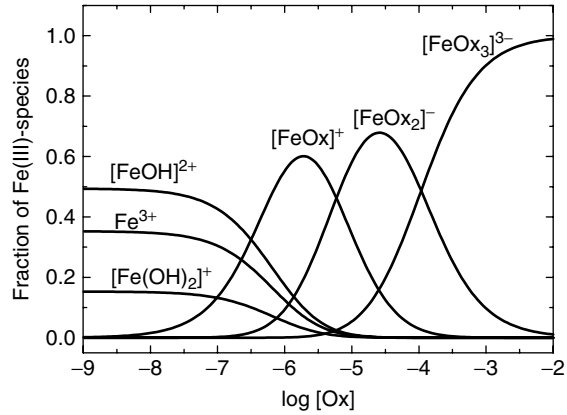

Figure 2.9.1.2. Calculated complex distribution in the system Fe(III)/water/oxalate at pH 3; 25 °C.

$$[Fe(H_2O)_6]^{3+} + C_2O_4^{2-} \Leftrightarrow [Fe(H_2O)_4C_2O_4]^{+} + 2H_2O \quad K_3 = 3.39 \times 10^{7}\ \text{L mol}^{-1} \qquad (2.9.1.4)$$

$$[Fe(H_2O)_4C_2O_4]^{+} + C_2O_4^{2-} \Leftrightarrow [Fe(H_2O)_2(C_2O_4)_2]^{+} + 2H_2O \qquad K_4 = 1.29 \times 10^{6}\ \text{L mol}^{-1} \qquad (2.9.1.5)$$

$$[Fe(H_2O)_2(C_2O_4)_2]^{+} + C_2O_4^{2-} \Leftrightarrow [Fe(C_2O_4)_3]^{+} + 2H_2O \quad K_5 = 7.08 \times 10^{4}\ \text{L mol}^{-1} \qquad (2.9.1.6)$$

$$C_2O_4H_2 \Leftrightarrow C_2O_4H^- + H^+ \qquad K_6 = 10.96\ \text{mol L}^{-1} \qquad (2.9.1.7)$$

$$C_2O_4H^- \Leftrightarrow C_2O_4^{2-} + H^+$$

$$K_7 = 6.61 \times 10^3 \text{ mol L}^{-1} \quad (2.9.1.8)$$

This complex distribution changes drastically with pH value. With increasing pH, the dominance of the tris-oxalato-complex (as the most stable species) increases. The complex distribution shown in Figure 2.9.1.2 is a simplified picture of the reality as the existence of hydroxo-oxalato- and of bisoxalato-complexes and the formation of oligomer and polymer compounds (their fraction increases with the iron concentration) is neglected.

The situation in surface, ground, and drinking water is much more complicated. In these systems, iron was found to exist as carbonate, hydrocarbonate, sulfato, and humic complexes.

2.3 Experimental

2.3.1 General remarks

The results of calculations and of additional experimental examinations show an identical complex distribution of Fe in pure aqueous (atmospheric) solutions [38]. Additionally, the formation of a monosulfito-complex $[Fe(SO_3)(H_2O)_5]^+$ is possible [39]. The so-called Pourbaix diagram (redox potential vs pH) of iron for pure aqueous solutions is helpful for the validation of the thermodynamic stability of individual oxidation states and species; however, it is only valid for systems without any complexing agents [40]. Nowadays, it is known that remarkable concentrations of organic acids are present in atmospheric aqueous samples: for example, formic acid (2–20 μmol L^{-1}), acidic acid (1–19 μmol L^{-1}), oxalic acid (0.1–7 μmol L^{-1}), glyoxylic acid (0.1–5 μmol L^{-1}), and pyruvic acid (0.1–4 μmol L^{-1}) [41]. Taking into account the very high complex formation constant of oxalate with Fe(III), nearly all aspects of the chemistry of iron in the atmosphere are influenced by this ligand: increase of the solubility of Fe(III), photolysis of Fe(III)-oxalato-complexes, shifting of the redox equilibrium, and so on.

For differentiation of Fe(II) and Fe(III) in aqueous solutions, principally two ways are possible. Specific complexing agents can be added, such as *o*-phenanthroline for Fe(II) and thiocyanate for the colorimetric or spectrophotometric determination of Fe(III), or Fe(II) and Fe(III) can be separated in a chromatographic procedure followed by non-specific detection and quantification. A selection of the methods is given in Table 2.9.1.1.

2.3.2 Ion chromatography

Ion chromatography is the most suitable way to determine Fe(II) and Fe(III) in one run. This method is described very often and improved by Sinner to a high sensitivity [27]. 400 μL were injected through a 100 μL-sampling coil. A glass-lined-tubing-column (to prevent Fe contamination and shifting of the Fe(II)/Fe(III) equilibrium), filled with Nucleosil100-10SA (Macherey-Nagel) – a cation exchanger with sulfonic functional groups – was used. After the separation column, as reagent Spectroquant Iron (Merck, Art. No. 14761) was post column on-line added. Iron was detected as the highly absorbing violet-colored Fe(II)-ferrozine complex ($\varepsilon = 27{,}570$ L mol^{-1} cm^{-1}). Beside the ferrozine (3-(2-pyridyl)-5,6-bis(4-phenylsulfonic acid)-1,2,4-tri-azine sodium salt), the reagent contains thioglycolic acid acting as a reducing agent for Fe(III) and as a pH-buffer. The obvious advantage of this reagent is the easy way of application without any danger of contamination, lowering the detection limits attainable with this method. For a complete and rapid reduction of Fe(III), L-ascorbic acid was supplied to the reagent as additional reducing agent. Moreover, to further improve the separation of Fe(II) and Fe(III), the eluent's composition was somewhat modified [42]. An optimal separation and detection of Fe(II) and Fe(III) was achieved using an eluent that contained 135 mmol L^{-1} lactic acid and 10 mmol L^{-1} calcium chloride (to prevent adsorption of Fe at system walls), adjusted to pH 2.7 with ammonia. The reagent contained a mixture of 2.5% L-ascorbic acid and 2.4% Spectroquant Iron in water, adjusted to pH 4.3 with ammonia. Limits of determination of 1 μg L^{-1} for Fe(II) and 2.2 μg L^{-1} for Fe(III) were

achieved using a 100-μL sample loop. These low limits of determination could only be realized by using reagents with extremely low blank values of the ubiquitous element iron. The uncertainty of the results ($\pm\sigma$) was determined to be 6% (threefold measurement) for concentrations between 10 and 100 $\mu g\,L^{-1}$.

Some results are summarized in Table 2.9.1.2. As can be seen from the data, only between 10 and 20% of the total Fe was found in the aqueous phase. This fraction consists of molecular dispersed species, colloidal forms, and of suspended matter with very low particle size. As was proposed by the Pourbaix diagram (constructed from electrochemical measurements), the dissolved fraction of Fe(II) in rain, snow, and fog samples is about 50% at nighttime, whereas it is increased to about 65% at daytime by sunlight radiation reduction. However, in cloud samples the fraction of Fe(II) is in the region of 10–30%. The identified complexes are $[Fe(H_2O)_6]^{2+}$ and $FeSO_4$ for Fe(II), and $[Fe(OH)(H_2O)_5]^{2+}$, $[Fe(OH)_2(H_2O)_4]^{+}$, $[Fe(C_2O_4)_3]^{3-}$, $[Fe(C_2O_4)_2(H_2O)_2]^{-}$, and $[Fe(C_2O_4)(H_2O)_4]^{+}$ for Fe(III). The concentration of Fe in aqueous atmospheric samples is much higher (about four orders of magnitude) in comparison with the concentration that would result from the low solubility of Fe(III) compounds and the relatively slightly soluble Fe(II) compounds. The total concentration of iron in aqueous atmospheric samples is a result of the high solubility of Fe(II)- and Fe(III)-sulfates, the complexation of Fe(III) with organic ligands, mainly oxalate, the photochemical reduction of Fe(III) producing an increasing dissolved fraction of Fe(II), and the colloidal and particulate fraction.

Table 2.9.1.2. Iron in aqueous atmospheric samples.

Site	Total [$\mu mol\,L^{-1}$]	Content of the aqueous phase [$\mu mol\,L^{-1}$]
Urban	5–500	1–100
Rural	0.1–20	0.1–2
Maritime	0.1–2	0.02–0.2
Antarctic	0.01–0.04	–

2.3.3 Electrochemistry

The electrochemical methods for elemental speciation are described in detail in Volume 1 of this issue [43]. In polarographic and voltammetric methods, the limiting diffusion current is a measure of the concentration of an ion in solution, whereas the halfwave potential is a measure of the decomposition potential, which itself is a measure of the chemical environment of this ion (identical to the complexation state of the ion) [44]. Therefore, such procedures can be used for speciation of elements, for example, for distinguishing Fe(II) and Fe(III), too [45]. The different concentration ranges for Fe(II) ($>5\ \mu g\,L^{-1}$) and for Fe(III) ($>20\ ng\,L^{-1}$) are the disadvantage of the method. These electrochemical methods are applied in environmental and food analysis and characterization in a very broad manner [46]. Very low detection limits were obtained by an absorptive stripping voltammetry yielding a value of about 7 $ng\,L^{-1}$ with a reproducibility of $3 \times \sigma = \pm 2.5\ ng\,L^{-1}$. Unfortunately, this low value can only be reached for the total iron content.

Therefore, a new method was proposed [47]. The concentration of reactive iron was determined without pretreatment of the seawater sample. The reactive iron concentration is defined by the iron that is bound within a period of 3 min by 20 μM 1-nitroso-2-naphthol (NN) added to seawater of pH 8. This fraction includes all inorganic iron (II and III) and part of the organically complexed iron. The total (inorganic and organic) concentration of iron in seawater was determined after UV-digestion (3 h) at pH 2. 10 mL of seawater was pipetted into the cell and 20 μL NN (final concentration 20 μM), 100 μL *N*-2-hydroxylethylpiperazine-*N*′-3-propanesulfonic acid (HEPPS) (final concentration 0.01 M) and 1 mL BrO_3^- (final concentration 40 mM) were added. The analyses were quantified by two standard additions.

The concentration of reactive Fe(II) was calculated from the difference between the concentration of the combined reactive iron and the reactive Fe(III). The concentrations of dissolved reactive Fe(III) in seawater was determined to be $1.7 \pm 0.1\ nmol\,L^{-1}$ ($\approx 100 \pm 6\ ng\,L^{-1}$), whereas

the values for reactive Fe(II) did not reach the limits of detection.

3 SPECIATION OF IRON IN SOLID SAMPLES

3.1 General remarks

Quantitative nondestructive determination of elements and especially of Fe in solid samples can be performed mainly by neutron activation and by X-ray fluorescence (XRF) analyses [48]. For speciation of Fe in solid samples, special methods have to be used. Some of them are described in the following paragraphs.

3.2 Mößbauer spectrometry

The method consists in the resonance absorption of definite γ-rays emitted from certain isotopes by identical isotopes in the ground state. Mainly, relatively small differences in energy are measured. These differences are produced by the influence of different electron levels that themselves are initiated by various chemical bonding. About 100 γ-transitions at about 40 elements can be used for Mößbauer spectrometry. But only some of them are of enhanced significance. The most important element accessible to Mößbauer spectrometry is iron. The reasons are mainly the 14.4 keV transition in the isotope ^{57}Fe on the one hand and the abundance of iron and of its compounds in nature on the other hand [49, 50].

The experiments described in this paper were performed at a constant-acceleration type Mößbauer spectrometer, operating in the timescale mode, and a 25 mCi ^{57}Co/Rh source was used [51]. The isomer shifts reported are relative to α-Fe at room temperature. Spectra of the samples (thickness of about 5–10 mg Fe/cm^2) were collected at 293 and 8 K by means of a He continuous flow cryostat. The Mößbauer spectra were analyzed with the computer program MOSFUN [52]. The lower limit of detection for iron is 0.1 mg ^{57}Fe in conventional Mößbauer spectrometry identical to about 5 mg of total Fe. Taking 10 weight-% of iron in an aerosol sample, a minimum of 50 mg aerosol are needed for an identification of Fe compounds. The Mößbauer spectra of an original aerosol sample taken at 293 and 8 K are shown in Figure 2.9.1.3. The 293-K spectrum (Figure 2.9.1.3, top) is dominated by two resonance lines in its central part, components of sextet lines show up in its outer parts covering about 25% of the whole spectral area. These magnetically split components are analyzed, as indicated in the figure by the stick diagrams, to consist of three different species, one being definitely hematite (α-Fe_2O_3); the second one is most probably magnetite (Fe_3O_4), but because of its small fraction in the sample and the poor statistical quality of the spectrum, a reliable identification is not possible. A third sextet component can only be tentatively attributed to poorly crystalline goethite (α-FeOOH) and/or hematite. The pronounced Fe^{3+} doublets may partly arise from the presence of very small goethite microcrystals exhibiting superparamagnetic (spm) behavior [53]. In order to analyze the nature of these doublet components, Mößbauer data at 8 K were collected (Figure 2.9.1.3, bottom). In contrast to the 293-K spectrum, this spectrum exhibits quite a number of sextets, the portion of the quadrupole doublets being very small. This strongly indicates that the main fraction of the doublet in the 293-K spectrum originates in spm microcrystals of goethite and/or hematite, in which Fe is partially substituted by nonmagnetic ions such as Al^{3+} [53]. This is in agreement with the data of Flynn [33] and Spokes *et al*. [54] given for hydrolysis products of Fe(III) forming at first small spheres of 2–4-nm diameter, observed by electron microscopy of precipitates and of transformation of lepidocrocite to goethite,

Table 2.9.1.3. Assignment of relative area (RA) fractions of the Fe species in an aerosol sample as determined by Mößbauer spectrometry.

Assignment				RA (%)
A: Fe_3O_4	Magnetite			9.8
B: α-Fe_2O_3	Hematite			7.5
C: α-FeOOH	Goethite			60.8
D: Fe^{2+}	Silicate			9.4
E: Fe^{3+}	Silicate I			6.8
F: Fe^{3+}	Silicate	+	SPM goethite	5.7

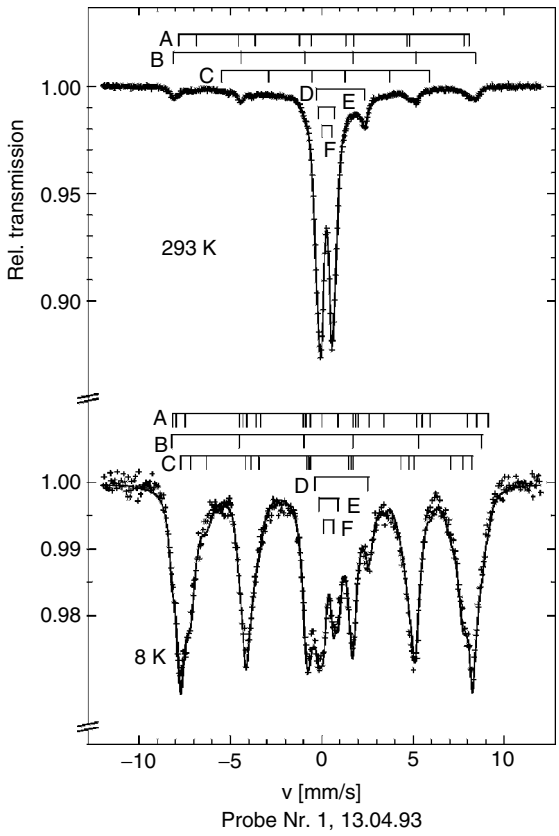

Figure 2.9.1.3. 293 K (top) and 8 K (bottom) Mößbauer spectra of an aerosol sample; the decomposition into the spectral components is indicated by the stick bars, where A stands for magnetite, B for hematite, C for goethite, D for Fe^{2+}, E and F for Fe^{3+} compounds. (Reprinted from *J. Aerosol Sci.*, **27**, Hoffmann, P., Dedik, A. N., Ensling, J., Weinbruch, S., Weber, S., Sinner, T., Gütlich, P. and Ortner, H. M., Speciation of Iron in Atmospheric Samples, 325, (1996), with permission from Elsevier Science.)

respectively [33, 54]. The results are summarized in Table 2.9.1.3.

In order to corroborate the presence of magnetite in the sample, a wet magnetic separation into magnetic and nonmagnetic material was performed. Both fractions were contaminated mutually, however, the essential result of this experiment is the definite presence of magnetite and of hematite.

Much smaller samples or the surface-near region of samples can be analyzed by a Mößbauer spectrometer using an orange type magnetic spectrometer (special design for high resolution) for the detection of electrons [55]. As an example, the fractions of Fe^{2+} and Fe^{3+} in a 1-μg sample with about 0.5 μg total iron could be determined with an uncertainty of about 10–20% relative.

3.3 Electron probes

3.3.1 Electron micro probe analysis

Individual aerosol particles can be characterized by electron micro probe analysis (EMPA) by measuring secondary electrons (SE), back scattered electrons (BSE), and X-rays as well [56]. The qualitative chemical composition and the correlation of elements will usually be determined with element distribution maps. For this purpose, a small fraction of the aerosol sample was spread out on a carbon substrate. The counting time was 0.5 s per pixel (about 9 h total measuring time). A total of 16 elements (4 per WDX-detector) could be investigated. The SE image and the Fe distribution map are displayed in Figure 2.9.1.4.

The observed size distribution does not represent the pristine grain size of the atmospheric aerosol particles. Large particles with diameters exceeding about 10 μm are agglomerations of smaller grains with diameters up to a few μm. The iron-containing particles are mostly too small (<500 nm) to be clearly resolved as individual grains with the used electron microprobe working with a W-hairpin electron source. In most cases, Fe-containing agglomerations predominantly consist of silicates, as indicated by the presence of the elements O, Al, and Si. Within these agglomerations, Fe occurs mostly in form of oxides. The images in Figure 2.9.1.4 show very clearly that most of the atmospheric aerosol particles are mixed from two or more components. A semiquantitative procedure for an automatic evaluation of the element distribution maps was developed [57]. The EMPA method leads to a speciation statement by elemental correlations, by the morphology of the particles and by the stability of a particle in the electron beam.

An additional method is described that allows the determination of Fe^{2+}/Fe^{3+} ratios with the

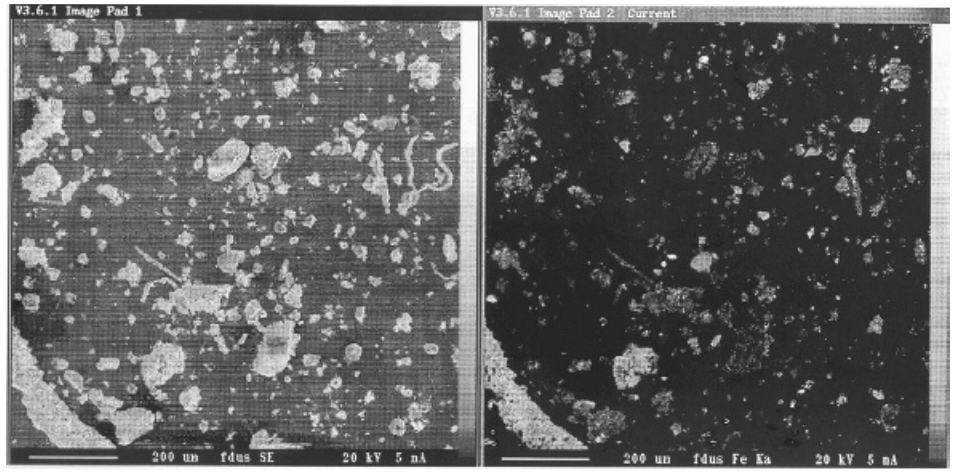

(a) (b)

Figure 2.9.1.4. EMPA-images of the partition of particles (secondary electrons, (a) and of the element iron (K_α-line, (b) in the same sample aliquot. (Reprinted from *J. Aerosol Sci.*, **27**, Hoffmann, P., Dedik, A. N., Ensling, J., Weinbruch, S., Weber, S., Sinner, T., Gütlich, P. and Ortner, H. M., Speciation of Iron in Atmospheric Samples, 325, (1996), with permission from Elsevier Science.)

electron microprobe by analyzing the FeL_α and $FeL_ß$ X-ray emission spectra [58]. Improved results are obtained by evaluation of the high-energy part of the L_α peak and the low-energy part of the $L_ß$ peak. The sensitivity achieved with this 'flank method' is about 3 to 4 times higher in comparison with the conventional peak shift method or peak intensity ratio method.

3.3.2 High resolution scanning electron microscopy

Individual particles can more precisely be characterized by high resolution scanning electron microscopy (HRSEM), as the lateral resolution is much better in comparison to EMPA. At optimal conditions, particles with a diameter of about 10 nm can be analyzed. This excellent property is reached by using a field emission gun. X-ray analysis is carried out with an energy-dispersive Si(Li) detector (ultrathin window) allowing simultaneous detection of elements with $Z \geq 5$ (boron). In two papers, grain size, morphology, electron impact stability, and chemical composition of many thousands of particles were used for speciation. The particles are classified into 10 groups, one of them is the metal oxides/hydroxides. This group consists of compounds from Al, Ti, Mn, Fe, Cu, Ni, Zn, or Pb, but the most abundant element is Fe [59, 60]. Almost all Fe-rich particles are oxides or hydroxides and occur as spheres (fly ash) with diameters between 0.1 and 3 μm (Figure 2.9.1.5). The volume size distribution of the metal oxides/hydroxides is shown in Figure 2.9.1.6 exhibiting maxima at 0.3–0.4 μm and at 1–3 μm. From these values, the average complex refractive index was determined to be $m = 2.5 - 0.05i$, where the real part represents the scattering and the imaginary part represents the absorption of sunlight. These values can be explained by the crystal structure and by the color of these Fe-containing particles. The dominant influence of the iron oxide/hydroxide amounts on the variation of the real part of the refractive index of atmospheric aerosol samples is rarely discussed in the literature [61]. However, Fe is also one of the most abundant elements in alumosilicates.

3.3.3 Transmission electron microscopy

The transmission electron microscope is normally used to record electron micrographs at high

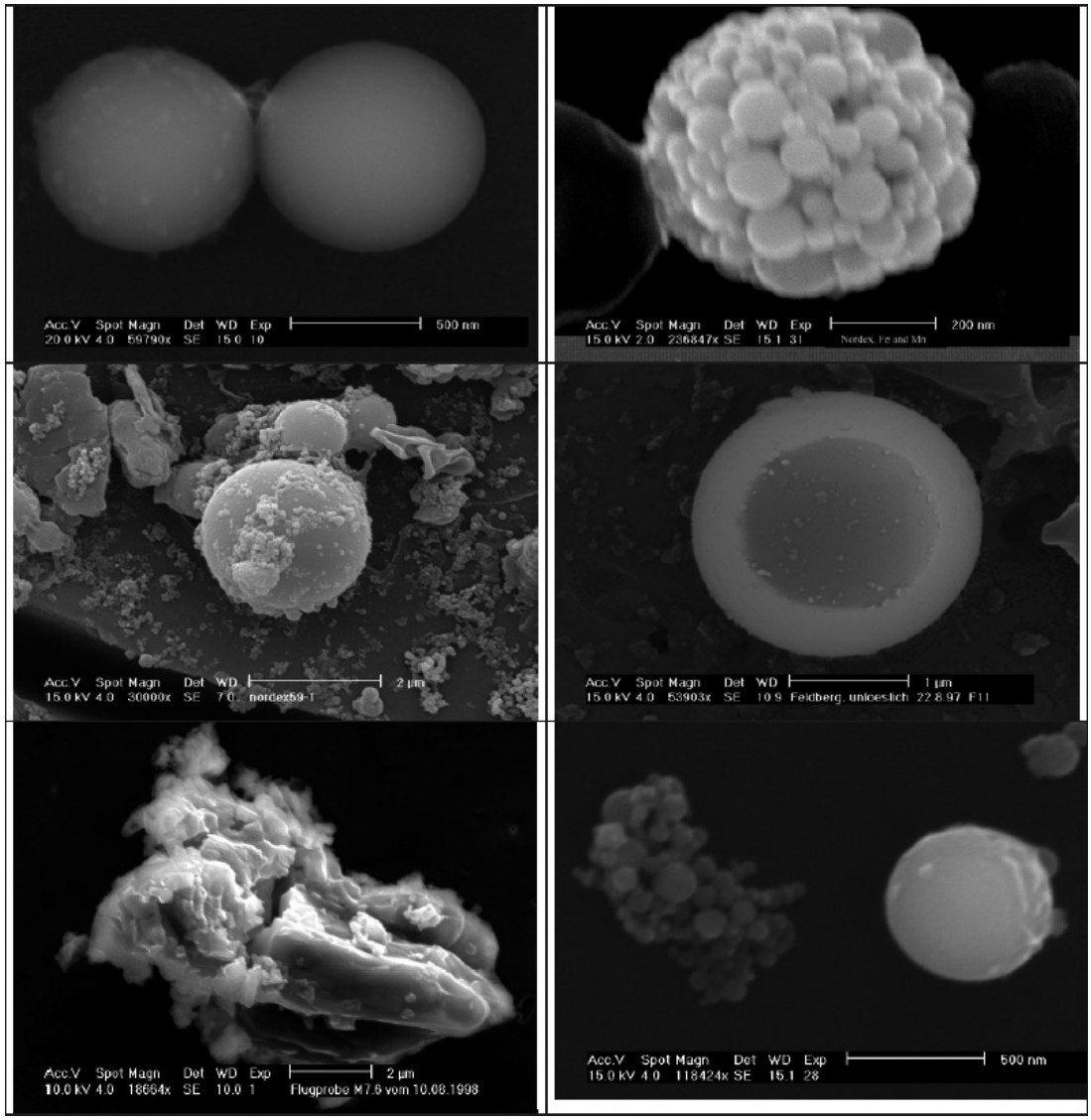

Figure 2.9.1.5. Selection of Fe-containing particles.

resolution from samples prepared as thin foils (less than about 0.15 µm thick for silicate minerals) [56]. This measure is identical to the diameter of small aerosol particles or to the thickness of particles' edges. The electron beam passing through the sample is capable of exciting characteristic X-rays within the sample for element identification. Chemical information is, therefore, normally obtained with a spatial resolution of less than about 20 nm. The elemental composition is determined down to boron.

The samples were positioned on transmission electron microscopy (TEM) carriers or collected with an impactor directly on Formvar® carrier foils and then carbon coated. In a first step, the elemental composition of each individual particle was measured by energy-dispersive detection (EDX). All Fe-containing particles were

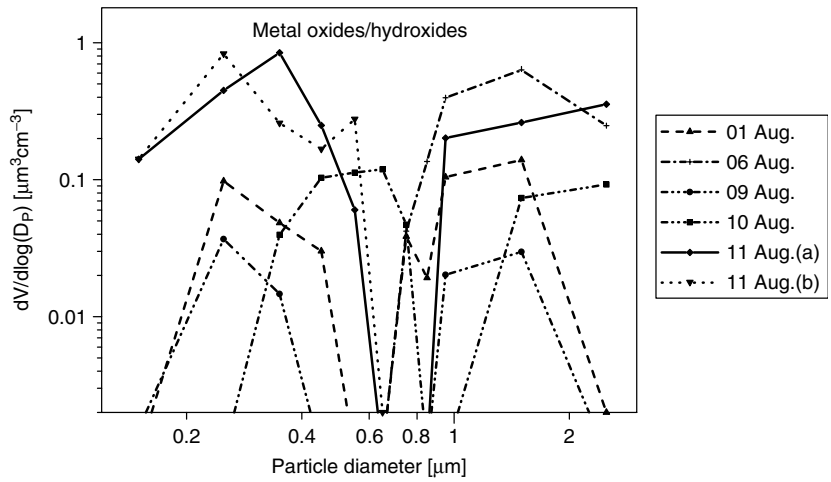

Figure 2.9.1.6. Volume distribution of iron oxides/hydroxides for different sampling days in 1998 [60]. (Reproduced from Ebert, M., Weinbruch, S., Rausch, A., Gorzawski, G., Helas, G., Hoffmann, P. and Wex, H., The complex refractive index of aerosols during LACE 98 as derived from the analysis of individual particles, *J. Geophys. Res. Atmos.* 107(D21) 8121 (2002), by permission of The American Geographical Union.)

subsequently characterized by electron diffraction. The advantage of this method is that both elemental composition and structural informations are obtained. The diffraction images were assigned using the ICSD data library and the evaluation program PIEP [62]. The TEM measurements allow only the characterization of a small number of particles. The identification of the crystalline components is not easy due to the complex (internal mixture!) composition of the particles and the presence of agglomerates from different sources. First, all particles that contain Fe above the limit of detection were identified and, second, the crystal structure of some 30 particles was determined by electron diffraction. A reflection pattern obtained for hematite is given in Figure 2.9.1.7.

The main components identified are hematite (α-Fe_2O_3), magnetite (Fe_3O_4) (cannot be distinguished from maghemite (γ-Fe_2O_3) by selected area electron diffraction), goethite (FeOOH), pyroxene ($(Mg,Ca,Fe)_2[Si_2O_6]$), biotite ($K(Mg,Fe^{2+})_3[(OH)_2(Al,Fe^{3+})Si_3O_{10}]$), chlorite ($(Mg,Fe)_3[(OH)_2(Al,Si)_4O_{10}]$), alloys (Fe-Co-Ni-Zn, Fe-Co-V, Fe-Co-Si), and wuestite ($Fe_{1-x}O$). Additionally, many other components (e.g. gypsum, feldspar, graphite, mica) contain considerable amounts of Fe.

Additional information and quantitative determination of iron oxidation states can be derived from electron energy loss spectroscopy (EELS), or from $FeL_{2,3}$- or $FeM_{2,3}$-edge electron energy loss near-edge structure spectroscopy (ELNES) [63, 64]. Small particles are suspended using ethanol onto a standard holey TEM grid. Using this equipment, a continuous correlation between the integral intensity ratio $I(L_3)/I(L_2)$ and the Fe(III) concentration $Fe^{3+}/\Sigma Fe$ from 0 to 1.0 was obtained. The same method using the M-lines has several advantages: since the $FeM_{2,3}$ edges have high intensities, beam-sensitive material can be analyzed at short measuring times and low current densities.

3.4 X-ray diffraction

Identification of oxidation states or of compounds may also be possible by determination of the structure of crystalline material. This method is touched in this chapter only very shortly as it is not specific for Fe-containing compounds. However, goethite, akaganeite, ferrihydrite, ferroxyhyte, and hematite were identified by their hexagonal structures, whereas lepidocrocite, maghemite, and magnetite crystallize in a cubic structure. The distinction between compounds of the same structure can

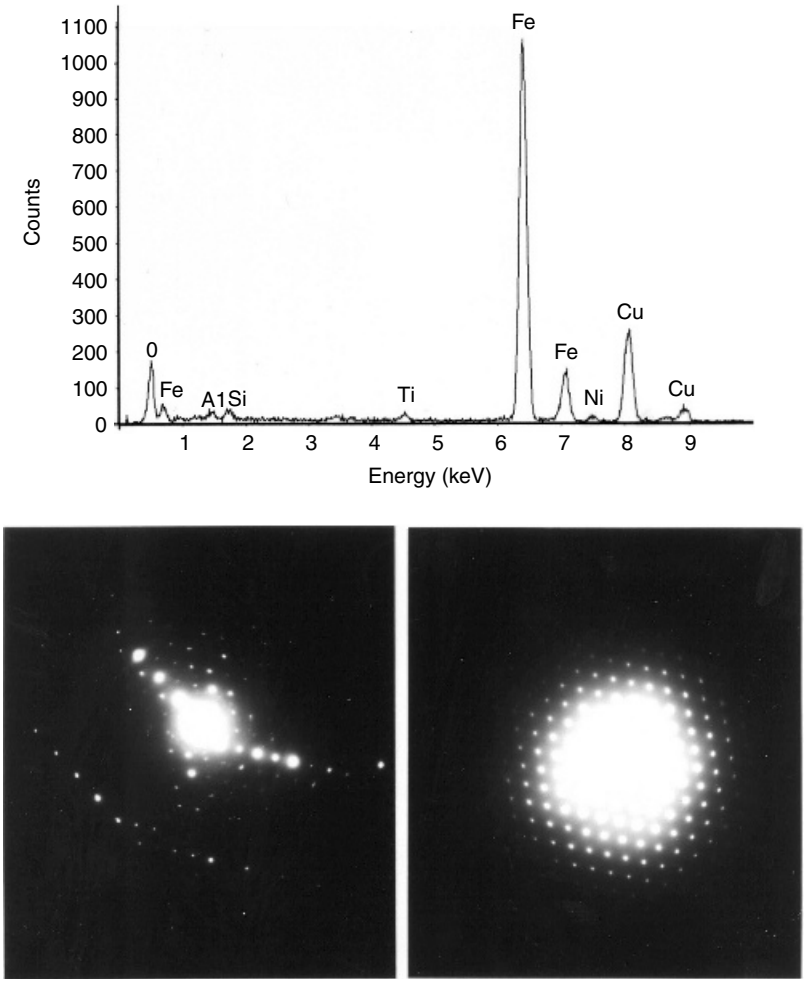

Figure 2.9.1.7. X-ray spectrum and electron diffraction images from transmission electron microscope for hematite (α-Fe_2O_3) exhibiting the interplanar spacing (left) and the size of the elementary cell/lattice constant (right).

be obtained by determination of lattice constants and by crystal angles [65].

3.5 X-ray photoelectron spectroscopy

X-ray photoelectric spectroscopy, also known as *electron spectroscopy for chemical analysis* (ESCA), is a highly specialized surface analytical technique. Samples are excited with a very intense beam of low-energy X-rays. The photoelectric effect causes electrons to be ejected from outer orbitals. These electrons have a characteristic energy, equivalent to the energy of the incident photon less the ionization energy of the appropriate electron orbital. From the data, it is possible to determine the binding energy that varies from compound to compound and is a function of both oxidation state and coordination number of that element. The depth of sample analyzed comprises the first 5 to 10 nm of surface layer.

Core line X-ray photoelectron spectra are reported for the iron compounds α-Fe_2O_3, γ-Fe_2O_3, α-FeOOH, $NiFe_2O_4$, $CoFe_2O_4$, Fe_3O_4, and FeO [66]. The powder specimens were mounted by smearing them onto a grooved copper flat.

The spectra are of particular value in characterizing surface films that contain corrosion products. For the oxides and hydroxides FeOOH, FeO and Fe_3O_4, the observed chemical shift is sufficiently large to permit these species to be uniquely distinguished from other iron oxides. In Fe_3O_4, both Fe(II) and Fe(III) oxidation states are observed and their relative concentrations can be determined using spectral line fitting procedures. The oxides α-Fe_2O_3, γ-Fe_2O_3, $NiFe_2O_4$, and $CoFe_2O_4$ have almost identical core binding energies, but the multiplet splitting patterns observed in their Fe(2p) core levels are sufficiently different to permit their use for characterization.

3.6 Extended X-ray absorption fine structure spectroscopy

An absorption of X-rays takes place if an electron of the absorbing atom is raised above the Fermi level. A photoelectron is generated, which interacts with neighbor atoms. The product absorption coefficient μ times the path length x is plotted versus the energy of the incident radiation over an energy region extending about 1 keV above the K absorption edge. In this energy range, oscillations are observed, which arise from interfering effects due to the scattering of the outgoing electron with nearby atoms. From analysis of the absorption spectrum for a given atom, one can assess the types, numbers, and distances of atoms surrounding the absorber. Extended X-ray absorption fine structure spectroscopy (EXAFS) is primarily sensitive to short range order in that it probes out to about 0.6 nm in the immediate environment around each absorbing species. Synchrotron radiation is used in EXAFS measurements because it provides an intense, monoenergetic beam of variable energy. Details of this method are to be found in the 1st volume of this issue [67].

This method is used, as an example, for the characterization of iron oxide films produced by sputtering. The formed iron oxide phase was found to depend on the substrate and the sputtering voltage. During the sputtering, the α-Fe_2O_3 was reduced forming a mixture of Fe_2O_3 and Fe_3O_4 [68]. The incorporation of transition metals into hematite may limit the aqueous concentration and bioavailability of important nutrients and toxic metals [69]. In this paper, the mechanism of Ni^{2+} and Mn^{3+}

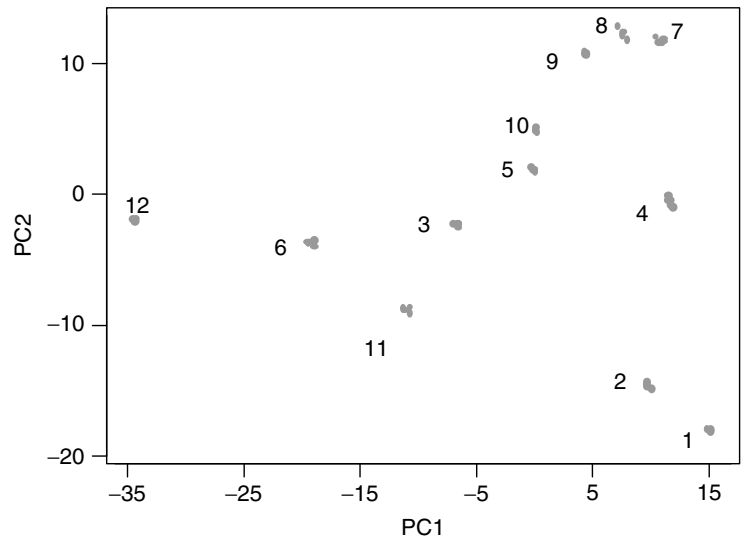

Figure 2.9.1.8. PCA-scoreplot of 12 Fe compounds (1 = $C_{12}H_{22}O_{11}Fe$, 2 = $C_{12}H_{22}O_{14}Fe(II)2H_2O$, 3 = $C_6H_5Fe(III)O7H_2O$, 4 = $(NH_4)_2Fe(SO_4)_26H_2O$, 5 = $FeSO_47H_2O$, 6 = $C_4H_2O_4Fe(II)$, 7 = $K_4[Fe(CN)_6]3H_2O$, 8 = $K_3[Fe(CN)_6]$, 9 = $FeCl_36H_2O$, 10 = $Fe_2(SO_4)_3$, 11 = FeS, 12 = Fe_{met}).

uptake into synthetic hematite and the replacing of Fe^{3+} was studied.

3.7 Chemometrical evaluation of X-ray fluorescence spectra

Energy- or wavelength-dispersive X-ray fluorescence are usually used for the identification and quantification of elements. For that purpose, the fluorescence lines of the elements are evaluated. Additionally, the Compton- (inelastic/incoherent) and Rayleigh- (elastic/coherent) scattering signals give information about the electron density and with that of the mean atomic number of all the elements in the sample. Consequently, the evaluation of this part of the spectrum leads to the possibility of identification of chemical compounds. This evaluation cannot be performed by hand but has to be run by computer-aided multivariate statistical methods [68]. In the cited case, the principal component analysis (PCA) was derived from the variance/covariance (correlation) matrix and the singular value decomposition (SVD) algorithm. Identifying at first the cluster 'Fe' by evaluation of the FeK_{α}/K_{β}-lines region, a distinction of 12 Fe-containing compounds was possible (Figure 2.9.1.8). The first two principal components are significant and cover 96.9% of the variance [69]. As the scattering of X-rays is also a function of other physical and technical parameters, the following properties have to taken into account: particle size of the sample, position of the sample, thickness of the sample container, and stability of the measuring device. In contrast, the bulk density of the sample does not influence the result [70–72].

4 SPECIATION OF IRON AT SOLID–LIQUID INTERFACES

4.1 General remarks

The chemical forms of Fe play an important role in the interaction between liquids (water, effluents) and solids (soils, sediments). Poorly crystallized Fe oxides and oxy hydroxides are widely distributed in soils, sediments, rivers, and seawater, where they are able to bind cations, for example, Cd(II), Hg(II), Pb(II). In the liquid parts of the systems, the Fe species mentioned are present as particulates (not the molecular or finely dispersed (colloids) fraction). They have been recognized to be important in the geochemical cycles of trace metals. Their high sorption capacity is due to the great density of structural and chemical defects and their large surface areas. The number of binding sites, to which trace cations are attached, diminishes as the stoichiometry increases [73]. The mineralogy, reactivity (towards sulfide), and the bacterial Fe liberation in pore water were explored in subaqueous sediments [74]. The mobility, biodisponibility, and toxicity of metals as Cd, Hg, Pb are largely controlled by chemical reactions that take place at the hydrous oxide/water interface [75].

4.2 Sequential extraction

For characterization of soils or sediments, individual and sequential extraction procedures are applied. For examination of the 'reducible fraction' (containing Fe- and Mn-oxide-hydrates), hydroxylamine hydrochloride or sodium dithionite are used [76, 77]. However, these methods were criticized for several reasons: for example, overlapping of the fractions, changes of the sample at each extraction step, irreproducible, or incomparable results. Therefore, the European Commission (Community Bureau of Reference) organized round robins in this field [78, 79]. The results of chemical extraction for speciation were, additionally, compared with those of electro-ultrafiltration procedures [80] and of the method of progressive acidification [81]. A combination of various leaching (extraction) agents (HCl, dithionite, HF/H_2SO_4, acetic Cr(II)) was applied to sediments and more than 80% of total iron were extracted. Subsequent determination of Fe species led to the distinction between specific mineral fractions that are available for Fe reduction and fractions formed as products of Fe diagenesis [82]. Direct, nondestructive methods for speciation, for

example, electron spin resonance, infrared spectroscopy, X-ray diffraction (XRD), nuclear magnetic resonance, and Mößbauer-spectroscopy, are in most cases not sensitive enough for the characterization of elemental traces [83].

The examination of two contrasting, Fe-poor and Fe-rich, marine sediments showed that oxide minerals are the most important Fe phases in early diagenetic pyrite formation [74]. However, lepidocrocite and ferrihydrite are more reactive toward sulfide than goethite and hematite. Relatively high concentrations of Fe oxides in the solids correspond to high concentrations of dissolved Fe and nearly to the absence of dissolved sulfide from sediment pore water. There is evidence for distinct microenvironments, where either sulfide reacts with Fe oxides, locally precipitating Fe sulfide minerals, or Fe is reduced, solubilized by microorganisms and migrating freely into solution.

For marine sediments, the results of a combination of extractions to give the Fe(II)/Fe(III)-ratio were compared with Mößbauer-spectroscopy and showed agreement within 10% [82]. The chosen extractants give the possibility to distinguish iron oxyhydroxides from iron oxides. Mößbauer-spectroscopy indicates the occurrence of siderite in the presence of free sulfide and pyrite. Down to a depth of about 14 m, the concentration of total Fe was found to be nearly constant, whereas the fraction of Fe(III) decreases from 100% to about 40%. On the basis of these data, Fe is of no importance as a potential electron acceptor for anoxic sulfide oxidation. Fe(III) does not show any distinctive variation at 10 m, where sulfide oxidation is indicated by pore water data.

4.3 Iron speciation in soils and sediments

The results of the characterization of Fe-containing sediments mentioned above may be explained by determination of the structures of Fe oxides and hydroxides [73]. This was realized by EXAFS, a method that is sensitive to the nature of interpolyhedral linkages depending on metal to nearest metal distances [67]. Using this method, it was possible to confirm that lepidocrocite form chains linked by edges, whereas goethite and akaganeite form chains linked by corners, and hematite forms chains linked by faces.

Likewise, the structural forms of hydrous Fe oxides can be studied after sorption of ions, such as Cr^{3+}, SeO_3^{2-}, Pb^{2+}, and UO_2^{2+} [75]. Cations (except Cr^{3+}) share edges and anions two corners with $Fe(O,OH)_6$ octahedra. The distances between these two surface sites are quite identical so that steric factors cannot account for the difference of sorption processes between cations and anions. The high reactivity of hydrous Fe (and Mn) oxides results from the fact that hydroxyl groups of the two active sites form an ideal template for bridging metals.

A summary of sorption and desorption mechanisms at the soil mineral/water interface highlights the question of the rates of these processes [84]. The examinations are mainly performed by EXAFS. The number of adsorption sites determines the quantity of plant nutrients, metals, radionuclides, pesticides, and other organic compounds that are retained on soil surfaces. Therefore, adsorption is one of the primary processes that affect transport of nutrients and contaminations in soils. Adsorption can be a physical (e.g. van der Waals) and/or a chemical (e.g. condensation) process. Furthermore, ion exchange reactions play an important role in the interaction of liquids and solids. Sorption of Co^{2+}, Cd^{2+}, and Pb^{2+} on hydrous ferric oxide (HFO) was studied as a function of oxide aging and metal-oxide residence time [85].

In a very new contribution, the competitive adsorption of arsenate and silicate on natural hydrous oxides is examined in thermal water scales [86]. The samples were found by XRF to consist on average of 74 wt.% $CaCO_3$, 22 wt.% $Fe(OH)_3$, 3.7 wt.% SiO_2, 0.1 wt.% MnO_2, and 0.5 wt.% As. By XRD, no crystalline goethite, akaganeite, or ferrihydrite could be detected. By EXAFS, two As–Fe bond lengths of 0.283 ± 0.002 Å and 0.326 ± 0.002 Å were determined. The first radial distribution function (RDF) represents the Fe–O bond with four (O,OH) ligands at 0.1984 nm and two elongated (O,OH) distances at 0.226 nm. These data are consistent with the

formation of $Fe^{III}(O,OH)_6$ octahedra. The second RDF represents Fe–Fe bonds at 0.303 ± 0.002 nm and at 0.345 ± 0.002 nm, respectively, the shorter one being characteristic for edge-sharing and the longer one for corner-sharing $Fe^{III}(O,OH)_6$ octahedra. This result compares well with goethite but not with that of lepidocrocite or akaganeite reference samples. EXAFS shows an X-ray amorphous HFO with competing arsenate and silicate for inner sphere bidentate binuclear ^2C complexation sites. Adsorption efficiency of HFO for arsenate is not weakened to the same extent because it forms additionally bidentate mononuclear ^1E surface complexes, for which silicate does not compete.

5 SUMMARY

Iron species are complex and have very interesting properties. The relatively easy change of the oxidation state at environmental conditions, the formation of various labile or stabile chemical complexes, together with a drastic change in solubility (in inorganic and organic media), require in most cases that iron speciation be done as well in solutions as in the solid state.

Identification of species in solutions is mainly based on the chemical properties of the species: for example, spectrophotometry of complexes at optimal absorbance, calculations using equilibrium constants, ion chromatography, electrochemistry, or a combination of these.

A very special method for the speciation of iron in the solid state is Mößbauer spectrometry. Other methods based on physical procedures, not specific for iron only, are, for example, electron probes, diffraction methods, X-ray photoelectron spectroscopy (XPS) and extended X-ray absorption spectrometry. Combinations of all these methods are needed for solving questions concerning the study of mechanisms occurring at the solid–liquid interface (boundary layers).

6 ACKNOWLEDGMENTS

I would like to thank my colleagues F. Deutsch, M. Ebert, H. Hofmann, T. Sinner, and S. Weber for the excellent results they have produced during the preparation of their PhD thesis. Furthermore, I wish to thank M. Heck for the substantial help in preparing the manuscript. M. Kersten is gratefully acknowledged for the help in preparing Section 4.3. Last but not least, I want to thank K. H. Lieser for his valuable discussions.

7 REFERENCES

1. Cotton, F. A. and Wilkinson, G., *Advanced Inorganic Chemistry*, 5th ed., John Wiley & Sons, New York, Chichester, Brisbane, Toronto, Singapore, 1988, p. 711ff.
2. Ghio, A. J., Pritchard, R. J., Lehmann, J. R., Winsett, D. W. and Hatch, C. E., *J. Toxicol. Environ. Health*, **49**, 11 (1996).
3. Holleman, A. F. and Wiberg, E., *Lehrbuch der Anorganischen Chemie*, 91-100 Auflage, Walter de Gruyter, Berlin, New York, p. 1134ff, (1985)
4. Riedel, E., *Anorganische Chemie, 2. Auflage*, Walter de Gruyter, Berlin, New York, 1990, p. 744ff.
5. Lieser, K. H., *Angew. Chem.*, **81**, 206 (1969).
6. Lieser, K. H., *GIT Fachz. Lab.*, **36**, 293 (1992).
7. Hansson, H. C., Ekholm, A. K. P. and Ross, H. B., *Environ. Sci. Technol.*, **22**, 527 (1988).
8. Hoffmann, P., Karandashev, V. K., Sinner, T. and Ortner, H. M., *Fresenius' J. Anal. Chem.*, **357**, 1142 (1997).
9. Stössel, R. P. and Prange, A., *Anal. Chem.*, **57**, 2880 (1985).
10. Fadrus, H. and Maly, J., *Anal. Chim. Acta*, **77**, 315 (1975).
11. Patel, K. S., Shukla, A., Goswami, A., Chandavanshi, S. K. and Hoffmann, P., *Fresenius' J. Anal. Chem.*, **369**, 530 (2001).
12. Elrod, V. A., Johnson, K. S. and Coale, K. H., *Anal. Chem.*, **63**, 893 (1991).
13. Suárez Iha, M. E. V., Pehkonen, S. O. and Hoffmann, M. R., *Environ. Sci. Technol.*, **28**, 2080 (1994).
14. Pehkonen, S. O., Erel, Y. and Hoffmann, M. R., *Environ. Sci. Technol.*, **26**, 1731 (1992).
15. Krishna Murty, N., Pulla Rao, Y. and Rama Rao, K., *Acta Cienc. Indica*, **3**, 15 (1977).
16. Behra, P. and Sigg, L., *Nature*, **344**, 419 (1990).
17. Erel, Y., Pehkonen, S. O. and Hoffmann, M. R., *J. Geophys. Res.*, **98**, 18423 (1993).
18. Pehkonen, S. O., Erel, Y., Siefert, R. L., Klewicki, K., Hoffmann, M. R. and Morgan, J. J., *Isr. J. Earth Sci.*, **43**, 279 (1994).
19. Sedlak, D. L., Hoigné, J., David, M. M., Colvile, R. N., Seyffer, E., Acker, K., Wieprecht, W., Lind, J. A. and Fuzzi, S., *Atmos. Environ.*, **31**, 2515 (1997).
20. Voelker, B. M. and Sedlak, D. L., *Mar. Chem.*, **50**, 93 (1995).

21. Sedlak, D. L. and Hoigné, J., *Atmos. Environ.*, **27A**, 2173 (1993).
22. Pehkonen, S. O., *Analyst*, **120**, 2655 (1995).
23. Frahne, D., Läubli, M. and Zimmermann, G., *GIT Fachz. Lab.*, **12**, 1167 (1987).
24. Yan, D. and Schwedt, G., *Fresenius' Z. Anal. Chem.*, **320**, 325 (1985).
25. Yan, D. and Schwedt, G., *Fresenius' Z. Anal. Chem.*, **327**, 503 (1987).
26. Kanai, Y., *Analyst*, **115**, 809 (1990).
27. Sinner, T., *Mikroanalytische Charakterisierung Atmosphärischer Proben mit Besonderer Berücksichtigung der Verschiedenen Oxidationsstufen des Eisens*, Ph.D. thesis, TH Darmstadt, 1994.
28. Sinner, T., Hoffmann, P., Knapp, C. P. and Ortner, H. M., *Fresenius' J. Anal. Chem.*, **349**, 334 (1994).
29. Sinner, T., Hoffmann, P. and Ortner, H. M., *Beitr. Phys. Atmos.*, **67**, 353 (1994).
30. Schwanz, M., *Bestimmung der Chemischen Form von Eisen in Wolkenwasser, Nebelwasser und Aerosolen*. Ph.D. thesis, University Leipzig, 1997.
31. Brandt, C. and van Eldik, R., *Chem. Rev.*, **95**, 119 (1995).
32. Benkelberg, H. J. and Warneck, P., *J. Phys. Chem.*, **99**, 5214 (1995).
33. Flynn, C. M. Jr., *Chem. Rev.*, **84**, 31 (1984).
34. Betterton, E. A., *J. Atmos. Chem.*, **17**, 307 (1993).
35. Sedlak, D. L. and Hoigné, J., *Atmos. Environ.*, **27**, 2173 (1993).
36. Deneux, M., Meilleur, R. and Benoit, R. L., *Can. J. Chem.*, **46**, 1383 (1968).
37. Smith, R. M. and Martell, A. E., *Critical Stability Constants*, Plenum, New York, 1976.
38. Hofmann, H., Hoffmann, P. and Lieser, K. H., *Fresenius' J. Anal. Chem.*, **340**, 591 (1991).
39. Weschler, C. J., Mandich, M. L. and Graedel, T. E., *J. Geophys. Res.*, **91**, 5189 (1986).
40. Pourbaix, M., *Atlas d'équilibres électrochimiques*, Gauthier-Villars, Paris, 1963.
41. Beck, J., Andreae, M. O. and Helas, G., *FELDEX95 – Bericht Cap Cloud Experiment*, 1996, p. 73.
42. Deutsch, F., Hoffmann, P. and Ortner, H. M., *J. Atmos. Chem.*, **40**, 87 (2001).
43. Town, R. M., Emons, H. and Buffle, J., Speciation analysis by electrochemical methods, in *Handbook of Elemental Speciation: Techniques and Methodology*, Cornelis, R., Crews, H., Caruso, J. and Heumann, K. (Eds.), John Wiley & Sons, 2003, p. 427, Chapter 5.9.
44. Nürnberg, H. W., *Differentielle Pulspolarographie, Pulsvoltammetrie und Pulsinvers-voltammetrie. Analytiker-Taschenbuch*, Bd. 2, 1981, p. 211ff.
45. Emons, H., *Voltammetrische Analytik Anorganischer Stoffe. Analytiker-Taschenbuch*, Vol. 13, Springer-Verlag, 1995, p. 132.
46. Brainina, K. Z., Malakhova, N. A. and Stojko, N. Y., *Fresenius' J. Anal. Chem.*, **368**, 307 (2000).
47. Aldrich, A. P. and van den Berg, C. M. G., *Electroanalysis*, **10**, 369 (1998).
48. Hoffmann, P. and Lieser, K. H., *Sci. Total Environ.*, **64**, 1 (1987).
49. Naumer, H. and Heller, W. (Eds.), *Untersuchungsmethoden in der Chemie – Einführung in die Moderne Analytik*, Georg Thieme Verlag, Stuttgart, New York, 1986.
50. Gütlich, P., Link, R. and Trautwein, A., *Mößbauer Spectroscopy and Transition Metal Chemistry*, Springer-Verlag, Berlin, Heidelberg, New York, 1978.
51. Hoffmann, P., Dedik, A. N., Ensling, J., Weinbruch, S., Weber, S., Sinner, T., Gütlich, P. and Ortner, H. M., *J. Aerosol Sci.*, **27**, 325 (1996).
52. Müller, W. E., *Mößbauer Effect Data J.*, **4**, 89 (1981).
53. Bronger, A., Ensling, J., Gütlich, P. and Spiering, H., *Clays Clay Miner.*, **31**, 269 (1983).
54. Spokes, L. J., Jickells, T. D. and Lim, B., *Geochim. Cosmochim. Acta*, **58**, 3281 (1994).
55. Stahl, B. and Kankeleit, E., *Nucl. Instrum. Methods Phys. Res., Sect. B*, **122**, 149 (1997).
56. Ortner, H. M., Characterization of individual aerosol particles with special reference to speciation techniques, in *Handbook of Elemental Speciation: Techniques and Methodology*, Cornelis, R., Crews, H., Caruso, J. and Heumann, K. (Eds.), John Wiley & Sons, 2003, pp. 506–525, Chapter 6.1.
57. Weinbruch, S., Wentzel, M., Kluckner, M., Hoffmann, P. and Ortner, H. M., *Mikrochim. Acta*, **125**, 137 (1997).
58. Höfer, H. E., Brey, G. P., Schulz-Dobrick, B. and Oberhänsli, R., *Eur. J. Miner.*, **6**, 407 (1994).
59. Ebert, M., Weinbruch, S., Hoffmann, P. and Ortner, H. M., *J. Aerosol Sci.*, **31**, 613 (2000).
60. Ebert, M., Weinbruch, S., Rausch, A., Gorzawski, G., Helas, G., Hoffmann, P. and Wex. H., *J. Geophys. Res.-Atmos.* **107**(D21) 8121 (2002)
61. Sokolik, I. N. and Toon, O. B., *J. Geophys. Res.*, **104**, 9423 (1999).
62. Miehe, G., *Gitterkonstanten- und Phasenbestimmung mit Elektronenbeugungsbildern Unbekannter Relativer Orientierung, 3*. Jahrestagung der Deutschen Gesellschaft für Kristallographie, Oldenbourg Verlag, München, 1995, p. 51.
63. van Aken, P. A., Liebscher, B. and Styrsa, V. J., *Phys. Chem. Miner.*, **25**, 323 (1998).
64. van Aken, P. A., Styrsa, V. J., Liebscher, B., Woodland, A. B. and Redhammer, G. J., *Phys. Chem. Miner.*, **26**, 584 (1999).
65. Jasmund, K. and Lagaly, G., *Tonminerale und Tone*, Steinkopff Verlag, Darmstadt, 1993, pp. 71–77.
66. McIntyre, N. S. and Zetaruk, D. G., *Anal. Chem.*, **49**, 1521 (1977).
67. Welter, E., Direct speciation of solids: X-ray absorption fine structure spectroscopy for species analysis in solid samples, in *Handbook of Elemental Speciation: Techniques and Methodology*, Cornelis, R., Crews, H., Caruso, J. and Heumann, K. (Eds.), John Wiley & Sons, 2003, pp. 526–546, Chapter 6.2.

68. Stenberg, T., Vuoristo, P., Keränen, J., Mäntylä, T., Büchler, M., Virtanen, S., Schmuki, P. and Böhni, H., *Thin Solid Films*, **312**, 46 (1998).
69. Balwant Singh, Sherman, D. M., Gilkes, R. J., Wells, M. and Mosselmans, J. F. W., *Clays Clay Miner.* **48**, 521 (2000)
70. Henrich, A., Hoffmann, P., Ortner, H. M., Greve, T. and Itzel, H., *Fresenius' J. Anal. Chem.*, **368**, 130 (2000).
71. Keßler, T., *Multivariat-statistische Auswertung von energiedispersiven Röntgenfluoreszenzspektren zur Identifizierung von Substanzen*. Ph.D. thesis, Darmstadt Technical University, 2001.
72. Keßler, T., Hoffmann, P., Greve, T. and Ortner, H. M., *X-Ray Spectrom.*, **31**, 383 (2002).
73. Manceau, A. and Combes, J. M., *Phys. Chem. Miner.*, **15**, 283 (1988).
74. Canfield, D. E., *Geochim. Cosmochim. Acta*, **53**, 619 (1989).
75. Manceau, A., Charlet, L., Boisset, M. C., Didier, B. and Spadini, L., *Appl. Clay Sci.*, **7**, 201 (1992).
76. Tessier, A., Campbell, P. G. C. and Bisson, M., *Anal. Chem.*, **51**, 844–851 (1979).
77. Förstner, U., Ahlf, W., Calmano, W., Kersten, M. and Schoer, J., in *Metal Speciation in the Environment*, NATO ASI Series G23, Broekaert, J. A. C., Gücer, S. and Adams, F. (Eds.), Springer-Verlag, Berlin, 1990, pp. 1–41.
78. Ure, A. M., Quevauviller, P., Muntau, H. and Griepink, B., *Int. J. Environ. Anal. Chem.*, **S51**, 135 (1993)
79. Eadem Report EUR 14763 EN, Commission of the European Communities, Community Bureau of Reference, Bruxelles, 1993, p. 85.
80. Murthy, A. S. P. and Schoen, H. G., *Plant Soil*, **102**, 207 (1987).
81. Rudd, T., Lake, L., Mehrotra, I., Sterritt, R. M., Kirk, P. W. W., Campbell, J. A. and Lester, J. N., *Sci. Total Environ.* **74**, 149 (1988)
82. Haese, R. R., Wallmann, K., Dahmke, A., Kretzmann, U., Müller, P. J. and Schulz, H. D., *Geochim. Cosmochim. Acta*, **61**, 63 (1997).
83. Alloway, B. J. (Ed.), *Schwermetalle in Böden*, Springer-Verlag, Berlin, 1999, pp. 99–110.
84. Scheidegger, A. M. and Sparks, D. L., *Soil Sci.*, **161**, 813 (1996).
85. Ainsworth, C. C., Pilou, J. L., Gassman, P. L. and Van Der Sluys, W. G., *Soil Sci. Soc. Am. J.* **58**, 1615 (1994).
86. Tommaseo, C. E. and Kersten, M., University Mainz, Germany, private communication.

2.9.2 Iron Speciation in Biomedicine

Thomas Walczyk
Swiss Federal Institute of Technology (ETH), Zurich, Switzerland

1 IRON IN THE HUMAN BODY

The adult human body contains 3–5 g iron, which is distributed among different physiological compartments [1]. Most iron (∼3 g) is bound for oxygen storage and transported as hemoglobin in red blood cells and as myoglobin in muscle tissue (∼200 mg). The dominant iron species in the liver, spleen, and bone marrow are ferritin and hemosiderin. Iron amounts bound to these storage proteins are highly variable and depend on iron status of the individual (0–1000 mg). About 400 mg are bound in nonheme enzymes, mostly iron–sulfur proteins, and about 10 mg iron in cytochromes and other heme proteins. The remainder (∼10 mg) circulates in plasma and extravascular fluids in the form of transferrins, proteins that are used for iron transport between compartments. Because of its vital role for normal physiological body function and the limited supply via dietary sources, the body is highly conservative in preserving functional iron and storage iron. Less than 0.003% of total body iron is lost per day mainly via intestinal bleedings, gastrointestinal juices, and desquamation of mucosal

Handbook of Elemental Speciation II: Species in the Environment, Food, Medicine & Occupational Health
Edited by R. Cornelis, H. Crews, J. Caruso and K. G. Heumann
 ISBN: 0-470-85598-3 (HB)

cells. Because of menstrual blood losses, mean iron losses that need to be replaced are higher in women (1.5 $mg\,d^{-1}$) when compared to men (1.0 $mg\,d^{-1}$) [2, 3].

If iron supply of the body is not sufficient to balance iron losses, hemoglobin concentration in blood is maintained by using storage iron and, in parallel, by upregulating intestinal iron absorption [4]. When iron stores are empty and iron supply is still insufficient, hemoglobin concentration in blood cannot be maintained and iron-deficiency anemia develops. Cutoff levels defined by the World Health Organization (WHO) for anemia range from 110 $g\,L^{-1}$ hemoglobin in blood for pregnant women and children 6 months to 5 years of age to 120 $g\,L^{-1}$ for nonpregnant women to 130 $g\,L^{-1}$ for men [5]. Cutoff levels vary with race, altitude, and smoking habits. Iron-deficiency anemia is associated with retarded mental and psychomotor development in childhood, an increased morbidity and mortality of mother and child around childbirth, a decrease in work performance, and a decreased resistance to infection [6]. It is estimated that 30% of the world population are affected by anemia, from which 600–700 million suffer from iron-deficiency anemia [7]. This makes iron deficiency, besides vitamin A and iodine deficiency, one of the main micronutrient-related public health issues on a global scale.

Iron overload may develop, on the opposite side, if regulatory mechanisms at the absorptive stage fail to downregulate iron absorption permanently despite full iron stores. Patients with inherited disorders such as hemochromatosis and thalassemia are most at risk to accumulate iron continuously. Hereditary hemochromatosis is the most common genetic disorder in populations of European ancestry. Most patients with clinical features of hemochromatosis are homozygous for a C282Y mutation of the HFE gene. Estimates of gene frequency range from 5 to 10% with a homozygote frequency of 2 to 5% in Caucasian populations [8]. Clinical manifestations include skin pigmentation, hepatomegaly, diabetes, joint pains and, frequently, endocrine and cardiac manifestations [9]. Thalassemia syndromes are among the most common single-gene disorders in regions with past or present exposure to *malaria falciparum*. In thalassemia major (Cooley anemia) as the most extreme form, patients accumulate iron in the body while showing all clinical signs of anemia due to ineffective hemoglobin synthesis. Clinical expressions, besides anemia, include hepatosplenomegaly, skeletal abnormalities, and cardiac manifestations. Without frequent blood donations and intensive iron chelating therapy, few thalassemia major patients survive beyond the age of 20 [10].

Because each iron species in the body has its distinct physiological function, iron speciation is essential not only to assess iron status but also to distinguish between anemias and disorders of iron metabolism. It also plays a vital role in the diagnosis of a number of organ diseases such as colon cancer and hepatic disorders. Numerous iron species with a known physiological role in the human body have been identified and characterized, not considering the large number of subspecies that often exist for iron species such as hemoglobin [11]. Most body iron is present in the form of hemoproteins in which the iron is located in the center of a porphyrin ring system, the heme subunit. Ferrous iron is incorporated into protoporphyrin by the enzyme ferrochelatase located on the matrix face of the inner mitochondrial membrane to form heme that is subsequently incorporated into the different proteins [12]. Hemoproteins fulfill three distinct functions. They can act as (a) oxygen carriers (hemoglobin and myoglobin), (b) as oxygen activators (oxidases, peroxidases, oxygenases, and oxidoreductases) and (c) as electron transporters (cytochromes). Remaining body iron is bound in nonheme enzymes and nonheme proteins that are essential for iron transport (transferrins) and iron storage (ferritin, hemosiderin). By these proteins, free ionized iron can be immobilized to preserve cells from oxidative damage.

To cover even the most prominent iron species in sufficient detail is clearly beyond this overview. Instead, this overview will be limited to those iron species that are quantified routinely in biomedical research and clinical chemistry to determine iron status and to identify disorders of iron metabolism. Techniques developed for iron speciation in this

Table 2.9.2.1. Hematological indices for differential diagnosis of anemia and iron metabolism disorders [13–15]. Normal ranges are given for adults of Caucasian descent in units as used in clinical practice (⇔ = normal, ⇓ = decreased, ⇑ = increased relative to normal range).

	Hemoglobin	Serum ferritin	Serum iron	Total iron-binding capacity	Transferrin saturation	Free erythrocyte protoporphyrin	Serum transferrin receptor
Unit	$g\,dL^{-1}$	$\mu g\,L^{-1}$	$\mu g\,dL^{-1}$	$\mu g\,dL^{-1}$	%	μmol/mol heme	$mg\,L^{-1}$
Normal range	13.0–18.0 (m) 12.0–16.0 (w)	15–300 (m) 15–120 (w)	40–175	250–410	20–55	<80	2.8–8.5
Iron deficiency	⇔	⇓	⇓	⇑	⇓	⇑	⇑
Iron-deficiency anemia	⇓	⇓	⇓	⇑	⇓	⇑	⇑
Anemia of chronic disease	⇓	⇑	⇓	⇓	⇔ to ⇓	⇑	⇔
Sideroblastic anemia	⇓	⇑	⇑	⇔ to ⇓	⇑	⇓⇔⇑	⇔ to ⇑
Thalassemia major	⇓	⇑	⇑	⇔ to ⇓	⇑	⇔ to ⇓	⇑
Hemochromatosis	⇑	⇑	⇑	⇓	⇑	⇔	⇔ to ⇓

context have been designed to the needs in clinical practice and research, that is, high sample throughput at an accuracy and precision that is sufficient to identify pathological conditions in the individual. In Table 2.9.2.1, the most common hematological parameters for iron status assessment and their normal ranges are given [13]. From these, hemoglobin, ferritin, and transferrin are discussed in more detail as the dominant iron species of clinical interest and the most routinely determined iron species in biomedical research.

2 HEMOGLOBIN ANALYSIS

Iron speciation in clinical practice is dominated by hemoglobin analysis owing to the key role of hemoglobin in oxygen transport to and CO_2 from the body's tissues. Hemoglobin is a tetramer of four globin polypeptide chains. In each of the globin chains, one heme is bound via a noncovalent binding to histidine, that is, one hemoglobin molecule can bind four molecules of oxygen. Iron in hemoglobin is present in its ferrous form, protected by the globin chain from oxidation to methemoglobin, which has no oxygen-binding capacity. Oxygen binding to iron involves a change in the globin confirmation and in iron electronic state, that is, from high spin (desoxyhemoglobin) to low spin (oxyhemoglobin). Hemoglobin analysis is performed in blood primarily as an iron status parameter to identify disorders of iron metabolism, to detect occult intestinal bleedings in stool, and to identify pathological iron losses in urine.

2.1 Hemoglobin in blood

2.1.1 Cyanmethemoglobin method

Total hemoglobin concentration in blood is determined in routine clinical practice by spectrophotometry. Stadie proposed as early as 1920 to determine total hemoglobin in blood as its cyano-derivative [16]. Present methods are based on King and Gilchrist [17] and Betke und Savelsberg [18] and date back to the early work of Drabkin and Austin in the 1930s [19]. Hemoglobin in circulating blood is a mixture of hemoglobin, oxyhemoglobin, carboxyhemoglobin, and minor amounts of other species of this pigment. In order to consider all hemoglobin forms, species are transformed into cyanmethemoglobin, a stable hemoglobin derivative. Hemoglobin is determined in capillary or venous blood. Venipuncture specimens have to be collected in tubes that contain anticoagulants such as oxalate, citrate, ethylenediaminetetraacetic acid (EDTA), or heparin. Blood is oxidized in solution at alkaline pH with potassium ferricyanide to ferric iron to form methemoglobin, which reacts subsequently with potassium cyanide to form cyanmethemoglobin. The used reagent mixture is known as *Drabkin's solution*. Cyanmethemoglobin concentration in the prepared sample is determined spectrophotometrically at 540 nm using external calibration techniques. In 1966, the International Committee on Standardization approved the proposal that clinical laboratories should adopt the cyanmethemoglobin

method exclusively for hemoglobin quantification in blood [20]. The method is now standardized and the use of quality control material is common practice [21]. The same principles can be used to quantify methemoglobin (Met–Hb) in blood. Oxidation of ferrous iron in hemoglobin to ferric iron in methemoglobin results in a loss of oxygen-binding capacity. Methemoglobin in blood is formed upon exposition to toxic substances such as nitrites (pickle salt) or nitrous gases but can be also due to an inherited disorder (methemoglobinopathy M) or an enzyme defect (diaphorase deficiency). Methemoglobin has a maximum absorbance band at 630 nm. The addition of cyanide causes the band to disappear, and the change in absorbance is proportional to the concentration of methemoglobin [22].

Hemoglobin quantifications by the cyanmethemoglobin technique are often performed using automated hematology analyzers. Coulter counters allow differential blood analysis including blood cell counts and blood cell size measurements by measuring change in electrical resistance as cells in solution flow through a narrow aperture across which a direct current is maintained [23]. Other techniques in automated differential blood analysis include light scattering, fluorescence spectroscopy, absorption spectroscopy, and conductivity measurements [24]. From the hemoglobin concentration in whole blood and the red blood cell count, the mean corpuscular hemoglobin (MCH) can be calculated, that is, the average amount of hemoglobin in the individual red blood cell. Mean corpuscular hemoglobin concentration (MCHC) as the average concentration of hemoglobin in each individual red blood cell is obtained from hemoglobin concentration in whole blood and hematocrit. Both are common red blood cell indices in hematology for identifying disorders of iron metabolism and red blood cell formation.

2.1.2 Hemoglobin typing

Hemoglobin in healthy individuals consists of three species. In adults, most hemoglobin (>95%) is hemoglobin A (HbA) in which two α chains and two β chains form the tetramer ($\alpha_2\beta_2$). The two others are HbA_2 in which the β chains are replaced by δ chains ($\alpha_2\delta_2$) and hemoglobin HbF or fetal hemoglobin (<1%) with two γ chains replacing the β chains. Hemoglobin diseases or abnormalities can be either a defect in the rate of synthesis (thalassemias) or in the synthesis of abnormal hemoglobin (hemoglobinopathies). The number of identified Hb variants has exceeded the 700 mark to date [25], with sickle cell anemia being the most prominent hemoglobinopathy. It results from a single-gene defect causing substitution of valine for glutamic acid in position 6 of the β chain of adult hemoglobin (HbS). This point mutation exerts its effect by causing precipitation and polymerization of the deoxygenated HbS with resulting sickling of the red cells. Permanently deformed red cells are removed from the circulation well before the usual 120-day life span of a healthy red cell, contributing to a chronic hemolytic anemia. Thalassemic disorders are a group of genetic disorders that cause a decreased rate of synthesis or absence of either one or two globin chains [26]. Defects in hemoglobin synthesis result in an ineffective red blood cell formation and maturation. Clinical manifestations are most severe in homozygotes and include anemia of variable severity that can be even fatal [10].

Screening for hemoglobinopathies and thalassemias is performed in risk populations either by DNA analysis or by hemoglobin speciation [27, 28]. Hemoglobin typing is most widely employed and allows judging the severity of the disease by the ratio of the different hemoglobin species or globin chains in blood. Traditionally, electrophoresis has been the method of choice for identification and quantification of Hb variants [29–31]. Cellulose acetate electrophoresis is capable of separating common hemoglobin variants at pH 8.6, while acidic citrate agar electrophoresis at pH 6.2 allows to positively identify a number of variants, including HbS, that cannot be separated from other species under alkaline conditions. Hemoglobin species are quantified by scanning densitometry after staining. Electrophoretic methods, still widely used, are declining, given their difficulty to automation and inaccurate quantification of minor Hb species. Difficulties

have only been partly overcome by using polyacrylamide or agarose gels and isoelectric focusing (IEF) techniques that offer a higher resolution power [32]. The need for better separation of hemoglobin species and automation of the analysis has been the impetus to make use of high performance liquid chromatography (HPLC) for hemoglobin typing [33, 34]. Blood of normal subjects, fetal blood from fetoscopy, or cord blood from newborns are collected in EDTA containing tubes and lysed. Blood lysates are centrifuged and the supernatant is separated using a cation-exchange column [35] or a reversed-phase column [36] followed by spectrophotometric or fluorometric detection of the separated hemoglobin species. Hemoglobin typing by HPLC is commonly performed using fully automated systems at analysis times of less than 10 min. [37]. A more recent development is the use of capillary isoelectric focusing (CIEF) and spectrophotometric detection [38, 39] that can be considered competitive with HPLC regarding the accuracy, precision, and sample throughput that can be achieved [40].

2.1.3 Glycated hemoglobin

Glycation of hemoglobin is used routinely as a long-term measure of plasma glucose levels in diabetes mellitus and hypoglycemia. Glucose combines with hemoglobin continuously via a nonenzymatic reaction. HbA_{1c} accounts for 80% of glycated hemoglobin (gHb) and is formed by glycation of the N-terminal valine of the β-chain within the hemoglobin tetramer. The remaining species (HbA_{1a}, HbA_{1b} etc.) have glucose, glucose-6-phosphate, fructose-1,6-diphosphate, or pyruvic acid bound to 1 of 44 additional sites occurring at the lysine residues or at the N-terminus of the α-chain [41]. Glycation is nearly irreversible during the life span of red blood cells (about 120 days). This permits using HbA_{1c} levels to assess mean plasma glucose levels over 6–12 weeks, smoothing out day-to-day variations in serum glucose levels. Since its first detection of gHb in the 1960s, HbA_{1c} became the 'gold standard' in diabetes control with recommended checks at least twice a year in patients [42].

A number of automated methods are in use to determine the amount ratio of HbA_{1c} to total HbA in blood including ion exchange chromatography, affinity chromatography, electrophoresis, and immunoassays [43, 44]. The gHb analysis is dominated by ion exchange chromatography and affinity chromatography using spectrophotometric detection. Techniques for separation of hemoglobin species by cation-exchange chromatography were developed in the 1970s by Trivelli *et al.* [45]. Glycation of the N-terminus of the β-chain reduces the net positive charge of hemoglobin. HbA_{1c} binds less firmly to the negatively charged resin and elutes quicker from the column than nonglycated HbA. By introducing microcolumns [46] or HPLC [47], ion exchange techniques became available for routine analysis. Boronate affinity chromatography (BAC) allows for separation of gHb, including HbA_{1c}, by reversible binding of the *cis*-diol groups of gHbs to m-aminophenylboronic, being cross-linked to agarose or glass beads. Addition of sorbitol dissociates the complex and elutes gHb, which can be quantified spectrophotometrically or by quenching of hemoglobin fluorescence with an added fluorophore [41].

Although all commercially available methods are able to detect HbA_{1c}, they vary in their ability to separate HbA_{1c} from other gHbs and HbA from other hemoglobin variants. This gives rise either to falsely low or falsely high HbA_{1c}/HbA ratios that affect data interpretation [44]. Because interferences are method/analyzer specific, HbA_{1c} cutoff values for healthy, nondiabetic individuals vary between 4 and 6% HbA_{1c} relative to total HbA, dependent on the technique. Because available techniques for HbA_{1c} analysis are numerous and cutoff values are method/analyzer specific, data cannot be interpreted and compared independently from the used technique [48].

Despite the widespread use of HbA_{1c} for glycemic control and a strong interest from the international community, no standardized protocols for analysis are available to date for improving data comparability [49–51]. Recent activities of the International Federation of Clinical Chemistry and Laboratory Medicine (IFCC) can be

considered a major progress in this context. A reference method for HbA_{1c} analysis based on electrospray ionization mass spectrometry (ESI-MS) has been developed and validated [52]. In a first step, hemoglobin is cleaved enzymatically into peptides by endoproteinase Glu-C, and in a second step the glycated and nonglycated N-terminal hexapeptides of the β-chain are separated and quantified by HPLC and ESI-MS. Alternatively, a two-dimensional approach using HPLC and capillary electrophoresis can be used.

2.2 Hemoglobin in stool

Fecal iron losses account for 0.6 mg Fe per day compared to total iron losses of 1.0 mg Fe per day in men and 1.5 mg Fe per day in women, including menstrual blood losses [1]. Iron in stool comes from bile, desquamated mucosal cells, and blood with most iron coming from intestinal bleedings [53]. Intestinal blood losses can be higher in trained athletes [54] and when taking therapeutic agents that affect the intestinal mucosa such as aspirin [55]. Pathological iron losses in developed regions are mostly associated with bleeding ulcers or tumors [56] and with intestinal parasites, predominantly hookworm infestation, in developing countries [57].

In stool samples, hemoglobin iron from blood has to be differentiated from unabsorbed dietary iron, which represents about 90% of total iron in fecal material. The most commonly used approach is the qualitative guaiac-test (Hemoccult®, Fecatwin®) [58]. A fresh stool sample is applied on a blotting paper impregnated with guaiac, a natural resin, and dried. The test is based on the oxidation of α-guaiaconic acid to blue furoguaiacin by hydrogenperoxide in the presence of oxidized heme (hematin). When hydrogen peroxide is added, hematin exhibits peroxidase activity in an enzymelike manner and catalyzes guaiac oxidation. Being relatively insensitive, blood losses have to be pathologically high for a positive reaction. However, interferences may result both in false-positive and false-negative reactions, and the test does not allow quantification of blood losses.

Quantitative hemoglobin analysis in stool is performed by fluorescence spectroscopy based on the HemoQuant technique developed by Schwartz *et al*. [59, 60]. Nonfluorescent heme can be transformed into fluorescing protoporphyrin by removing iron from the heme molecule. This is achieved by incubating the stool sample with hot oxalic acid in the presence of ferrous sulfate as a reducing agent. Porphyrins are extracted using a mixture of ethyl acetate and acetic acid. To remove co-extracted coproporphyrins, that is, hemoglobin precursors/degradation products in fecal material, porphyrins are back-extracted into n-butanol-containing potassium acetate and potassium hydroxide. Hemoglobin porphyrin is finally separated from fluorescing phaeophytins, chlorophyll degradation products, by extraction into a mixture of phosphoric acid and acetic acid. Fluorescence in the aqueous phase is usually measured at an excitation wavelength of 402 nm and an emission wavelength of 653 nm. Cyanmethemoglobin standards are processed in parallel to the samples in an identical manner for external calibration. For quantitative screening for intestinal blood losses, a number of immunochemical test have also been developed and are in use [61–64]. Basic principles of immunochemical testing are described for ferritin analysis in Section 4.

2.3 Hemoglobin in urine

Urinary excretion of free hemoglobin or intact red blood cells can be considered a pathological condition in general. Conclusively, techniques are required only for qualitative and semiquantitative analysis. Free hemoglobin may indicate severe hemolysis or can result from severe burns (hemoglobinuria). Urinary tract bleedings, for example, due to urinary tract infection, result in the excretion of intact red blood cells (hematuria). Muscle injuries may cause urinary myoglobin excretion. Routine screening for free hemoglobin and red blood cells is performed by use of test strips for simultaneous screening of a number of urinary indices such as bilirubin, urobilirubin, ketones, ascorbic acid, glucose, protein, pH, and

leukocytes. Test strips are commercially available from a number of manufacturers. The test strip is immersed in a fresh sample of morning urine for about 1 sec. After removal from the specimen, color development within 1 to 2 minutes allows semiquantitative estimates. For hemoglobin and red blood cells, the test is based on the peroxidase-like activity of hemoglobin, which catalyzes the reaction of cumene hydroperoxide and 3,3′,5,5′-tetra-methyl-benzidine as the chromogen on the test field. Red blood cells react as diffuse patches on the field while hemoglobin and myoglobin produce a uniform color that ranges from orange through green. The test is very sensitive and allows to visualize down to 5–10 red blood cells per μL urine.

3 TRANSFERRIN

Serum transferrin is a β-globulin that is synthesized mainly in the liver and consists of a single polypeptide chain of 679 amino acids. The adult human body contains 7–15 mg transferrin, equally distributed between serum and interstitial space. Transferrin and the closely related proteins lactoferrin and melanotransferrin are the main iron transport proteins of the body. Per transferrin molecule, two Fe(III) atoms can be bound. Transferrin binding prevents precipitation of Fe(III) at physiological pH and, therefore, allows for transport of iron from mucosal cells to body tissues and body's storage areas such as the liver and bone marrow. However, most transferrin molecules in serum are present as apotransferrin, that is, they have no iron bound to them. Besides iron transport, they serve as scavengers of free ionized iron in the organism to preserve cells from oxidative damage [65, 66].

Since serum iron principally reflects the amount of iron bound to transferrin, determination of transferrin concentration and saturation in serum can provide information about the maximal iron-binding capacity, and hence iron status, in an individual. Higher transferrin values are found in infancy and during pregnancy. Elevated levels are also seen in iron deficiency, as the liver synthesizes more protein in an attempt to sequester iron more efficiently from a diminishing pool. Serum transferrin concentrations are usually diminished in inflammation, malignancy, chronic liver disease, infection, and nephrotic diseases [67].

With transferrin being the predominant iron-binding protein in plasma, serum transferrin levels are correlated with the total iron-binding capacity (TIBC) of the serum. Current methodologies date back to the early work of Ramsey [68], and a number of different techniques have been developed and modified over the past 40 years. However, there is still no single recognized, internationally accepted method for the determination of TIBC as well as serum iron, although attempts have been made in the past to harmonize techniques [69–71]. Most techniques for TIBC measurement consist of saturating all transferrin sites by addition of an excess amount of iron, removal of unbound iron with solid magnesium carbonate or an ion exchange resin and, finally, quantification of transferrin-bound iron in the sample [13]. Iron is determined using the same techniques as commonly used for serum iron analysis by liberating iron from transferrin and protein precipitation at acidic pH (<4.5). Liberated ferric iron is reduced to ferrous iron, commonly by addition of ascorbic acid, and is quantified spectrophotometrically after reaction with a suitable chromagen.

Many chromagens have been used in the past, including thiocyanate *o*-phenanthroline, bathophenanthroline and TPTZ (tripyridyl-triazine) for serum iron and TIBC analysis. In 1971, Persijn *et al.* [72] presented a method using the chromagen FerroZine® (pyridyl-diphenyl-triazine-disulfonate), described by Stookey [73]. This method did not require protein precipitation/separation and was more sensitive than previous methods. Today, FerroZine® is the most commonly used chromagen for serum iron and TIBC analysis. By making protein precipitation/separation superfluous, automated sample analysis for routine screening purposes becomes possible. To the serum sample, a known amount of ferrous iron is added together with an alkaline buffer (pH 8). The ferrous iron binds with transferrin at unsaturated iron-binding sites. The additional unbound ferrous

iron forms a violet complex with FerroZine®, which can be quantified spectrophotometrically at 560 nm. The difference between the amount of ferrous iron added and the unbound iron measured is reported as the unsaturated iron-binding capacity (UIBC). The TIBC is equal to the serum iron concentration plus the UIBC. Percent iron saturation of transferrin is obtained by dividing serum iron as an approximate measure of transferrin bound iron in blood through TIBC as the maximum iron amount that can be complexed. When compared to serum iron, transferrin saturation is less susceptible to diurnal variation. Variations in serum iron concentration are strong with normal values mid-morning, low values in mid-afternoon, and very low values near midnight [74].

For more than two decades, measurement of transferrin saturation became the standard method for assessment of iron status. Direct assessment of iron stores via liver biopsies, bone marrow smears, or quantitative phlebotomy is too invasive to be useful for routine screening purposes. Although other hematological indices for iron status evaluation became available over the past two decades, serum iron and TIBC measurements still have their place in hematology, in particular, for hemochromatosis screening. In iron deficiency, serum iron concentration falls but TIBC rises. In iron overload, the reverse applies. However, concerns have been raised about the accuracy of the techniques in use [75]. Both suffer from methodological limitations that have been summarized comprehensively by Bothwell *et al.* [74]. Separation of excess iron not bound to transferrin during the assay is often incomplete and may result in an overestimate of TIBC when using adsorbent methods. For direct assays not requiring protein precipitation, serum proteins may jeopardize spectrophotometric iron analysis. An alternative approach is to measure transferrin directly by immunological assay. Nephelometric, turbidimetric, and radial immunodiffusion techniques are now widely used in hematological laboratories employing autoanalyzers. Data obtained by chemical and immunological techniques do correlate [76]; however, different immunochemical assays for transferrin were reported to show significant variability [77, 78].

4 FERRITIN

4.1 Characteristics

At the physiological pH of 7, the Fe(III) ion concentration in aqueous solution is minimal. However, intracellular concentration of Fe(III) is several orders of magnitude higher than simple aqueous solutions would permit. Iron can cause oxidative damage to cells, so the ability to store and release iron in a controlled fashion is essential. This is accomplished by ferritins, iron-storage proteins that can be found in iron-dependent organisms ranging from bacteria to man [79]. The ferritin molecule is a spherical protein shell synthesized with a molecular weight of approximately 480 kDa that consists of 24 subunits folded into ellipsoids. Each subunit is an individual peptide chain that joins to its neighboring subunits through noncovalent binding. Subunits combine to form a hollow sphere with approximately 8 nm in diameter and with walls that are approximately 1-nm thick. Heavy (H) and light (L) subunits exist that combine in different proportions and give rise to isoferritins having characteristic isoelectric points and specific tissue distributions [80].

Up to 4500 iron atoms can be stored inside of this protein coat as a hydrous ferric oxide-phosphate mineral, similar in structure to the mineral ferrihydrite [81]. Among the important structural features of ferritin is the presence of channels that occur in the protein wall at the intersection of the subunits. Iron is taken up as Fe(II) through these channels, oxidized to Fe(III) at the surface, and channeled into the core [82]. Release mechanisms involve enzymatic reduction by ferritinreductase and subsequent oxidation to Fe(III) by the enzyme ferrioxidase I to allow for transferrin binding of the iron released.

Good correlations have been found between serum ferritin concentrations and storage iron mobilized by phlebotomy as well as stainable iron and nonheme iron and ferritin concentrations in the bone marrow. The close correlation between total iron stores and serum ferritin concentrations in normal individuals has been confirmed directly [83, 84] and is the key to use serum ferritin concentration as an iron status indicator.

The normal range for serum ferritin concentrations in healthy adults is 15–300 $\mu g\,L^{-1}$, depending on iron stores. Mean serum ferritin concentrations are lower in children than in adults and are higher in men than women from puberty to middle age [85]. Serum ferritin concentrations below 15 $\mu g\,L^{-1}$ are a reliable indicator of iron deficiency in adults and, if hemoglobin concentrations are also below normal, of iron-deficiency anemia. However, serum ferritin concentrations within or above the normal range do not necessarily indicate adequate iron stores or iron overload, respectively. Serum ferritin concentrations are compromised by inflammatory processes and liver disease that both result in an increased ferritin release into the serum. Accompanying measures such as C-reactive protein as an inflammation biomarker are required to confirm the absence of confounding factors [13]. Despite these limitations, serum ferritin has established itself as the key marker of iron status together with hemoglobin concentration in clinical practice. This became possible by the development of a number of immunochemical techniques that allow quantifying ferritin in serum and plasma samples reliably without sophisticated sample preparation techniques and specialized equipment. Because immunochemical techniques have not been discussed in Volume 1, a short overview of the underlying principles and techniques will be given here. For a more detailed description, the reader is referred to available textbooks [86–88].

4.2 Principles of immunochemical analysis

Immunoassays are widely employed to quantify biologically active compounds in body fluids. Immunoreactions can be used for element speciation as they are usually highly specific to a defined organic ligand that is often characteristic for an element species of distinct physiological function. Immunoassays are based on the immunochemical reaction between the analyte, acting as the antigen, and added antibody that binds to the antigen selectively. To obtain antibodies for a specific analyte antigen, the analyte is injected into an animal species to which it is foreign, such as rabbit, goat, or rat. Once the organism recognizes the antigen, specific antibody to this antigen is produced that can be recovered from the animal's serum. The obtained 'polyclonal' antibody is a heterogeneous mixture of antibody molecules produced by a variety of constantly evolving B-lymphocytes. More specific 'monoclonal' antibodies can be obtained *in vitro* in a second step from cell lines of individual, immortalized B-lymphocytes.

In immunoassays, the analyte is quantified either by using a limited amount of tagged standard analyte that competes for the limited binding sites on the antibody (competitive assays) or by adding tagged antibody in excess that binds effectively all analyte in the sample (noncompetitive assay). The tag may be a radioactive tracer (radioactive immunoassay, RIA; immunoradiometric assay, IRMA), an enzyme (enzyme immunoassay, EIA; enzyme linked immunosorbent assay, ELISA), or a fluorophore (fluorescence immunoassay, FIA). Luminescence immunoassays (LIA) are more recent developments that utilize luminescent compounds for antibody tagging. FIA and LIA follow basically EIA or ELISA concepts and are, therefore, not discussed here.

4.2.1 Radioimmunoassays

The first analytical application of immunoassays dates back to the early 1960s in which Solomon Berson and Rosalyn Yalow demonstrated the ability to selectively measure small quantities of insulin by radioimmunoassay (RIA) [89]. In recognition of the importance of immunoassays in clinical practice, Yalow was awarded the Nobel prize in physiology in 1977, following Berson's death. RIA is the most basic immunochemical approach for quantitative analysis. To a mixture of antibody solution (antiserum) and radiolabeled standard antigen, the serum sample to be analyzed is added. The standard antigen can be labeled radioactively either with ^{131}I or ^{125}I if it is a polypeptide by iodination of the tyrosine phenyl ring. If the antigen is a vitamin, drug, or steroid hormone, ^{3}H and ^{14}C labeled compounds can be used. Upon incubation of the mixture, both

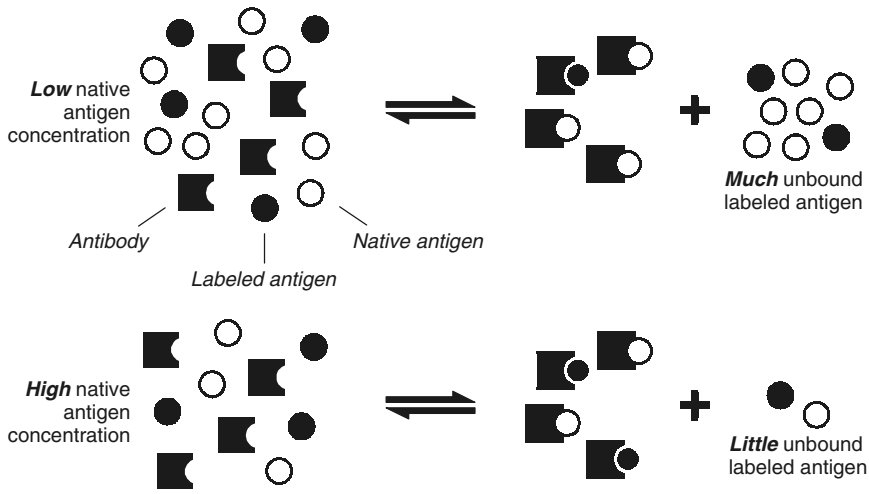

Figure 2.9.2.1. Principle of competitive immunoassays. Antibody and labeled antigen are added to the sample that contains the native antigen. Labeled antigen and analyte antigen are present in excess and compete for the limiting binding sites of the antibody. After separation of the antibody–antigen complex from free antigen, the amount of remaining labeled antigen in the sample depends on the amount ratio of analyte antigen and labeled antigen added at the beginning.

the radiolabeled antigen and the analyte antigen from the sample compete for complexation by the antibody. The amount ratio of labeled and analyte antigen in the complex or in solution is finally defined by the amount of analyte antigen in the sample. The more analyte antigen is in the sample, the less labeled antigen can bind to the antibody (see Figure 2.9.2.1).

To determine the percent bound radioactive tag, various techniques are used to separate the bound antigen from the free antigen after incubation. This includes precipitation of the complex by denaturation at high salt concentrations ($(NH_4)_2SO_4$, Na_2SO_4) or using organic solvents (e.g. acetone, ethanol). The complex is usually separated by centrifugation to determine the radioactivity in either phase. Other techniques involve the addition of a second antibody to precipitate the primary antigen-antibody complex (double-antibody technique), electrophoresis, or absorption of unbound antigen on dextran-coated charcoal. Separation of free and bound antigen in RIA has been facilitated significantly by the solid-phase antibody approach. Here, the antibody is bound to the inside wall of the reaction tube or to insoluble particles (glass beads, carbohydrate polymers) that precipitate easily. Solid-phase methods are used currently in most automated RIA systems.

Calibration curves for RIA are prepared using antigen standards of known concentration by plotting either the percent bound labeled antigen or the ratio of percent bound to free as a function of the unlabeled antigen concentration. Obtained calibration curves are nonlinear, in general. The amount of bound antigen is not directly proportional to the antigen concentration in the sample, as both the labeled and unlabeled antigen compete for the limited antibody binding sites. The sensitivity and range of an assay is largely determined by the initial dilution of the antibody. To obtain a very high sensitivity, it is advisable to use a dilution of antiserum so that the added antibody will bind about 50% of the labeled standard antigen in the absence of analyte antigen. A wider range of antigen concentrations can be covered by using a more concentrated antiserum instead.

4.2.2 Immunoradiometric assay

To improve the sensitivity and specificity of competitive RIA, the noncompetitive *immunoradiometric assay* (IRMA) has been developed. In

IRMA, the antibody is bound to a solid phase, usually the inner walls of the test tubes itself. When the sample containing the analyte antigen is added and allowed to incubate, it binds firmly to the antibody. Because the antibody is present in excess, virtually all analyte antigen is bound to the antibody. A second antibody is then added to the test tube, likewise in excess. This antibody is radioactively labeled with either ^{123}I or ^{125}I and is commonly sensitive to a different part of the analyte molecule than the antibody attached to the walls of the test tube. Because the analyte is finally bound to both antibodies, IRMAs are sometimes referred to as 'sandwich immunoassays' (see Figure 2.9.2.2).

The sandwich structure in IRMA is responsible for the higher selectivity of IRMA when compared to RIA. The analyte has to bind to two different antibodies that are selective for two different parts of the analyte molecule. Since the entire sandwich complex is finally attached to the walls of the test tube, unbound radiolabeled antibody can be simply decanted and completely removed by washing the test tube. Thus, the amount of radioactive label remaining in the test tube corresponds directly to the amount of analyte antigen in the sample. The difference between competitive RIA and noncompetitive IRMA becomes obvious from the calibration curves. Because all analyte antigen is bound to isotopically tagged antibody, a nearly linear calibration curve is obtained for IRMA when the counting rate is plotted against analyte concentration.

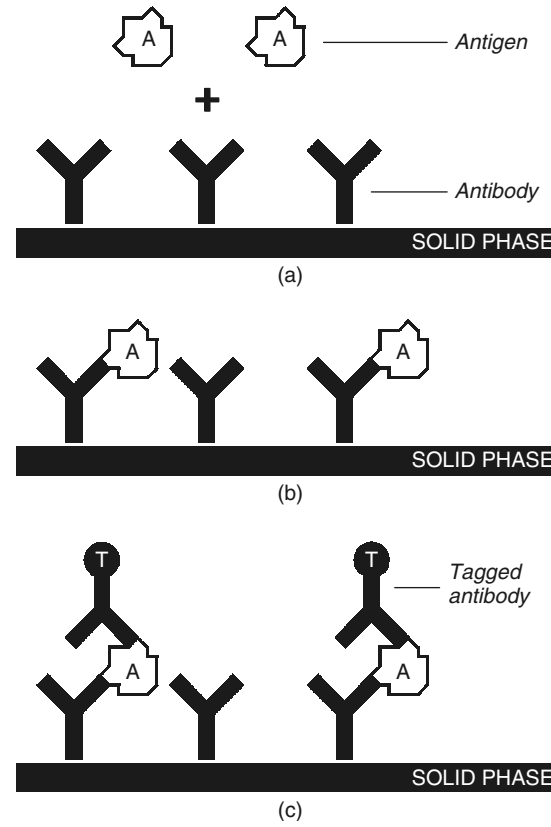

Figure 2.9.2.2. Principle of solid-phase sandwich immunoassays. Antibody is covalently attached to the surface of a support material (inner surface of a test tube or beads) (Figure 2.9.2.2a). The sample containing the analyte antigen is added. After incubation, the antigen binds to the antibody (Figure 2.9.2.2b). Binding is noncompetitive, as the antibody is present in excess. A second, labeled antibody is added, which is sensitive to another part of the analyte antigen (Figure 2.9.2.2c). Unbound labeled antigen is removed by decanting or by washing the test tube. The amount of remaining labeled antigen is proportional to the amount of analyte antigen in the sample.

4.2.3 Enzyme immunoassay

RIA and IRMA are well established in biomedical research and clinical chemistry, but there are some drawbacks that have to be considered: (1) Handling of radioisotopes requires dedicated laboratories and radiometric equipment. (2) Radioactive emission of the label may destruct progressively the antigen to which it is bound to and may adversely affect the assay. (3) RIA and IRMA are time-consuming because samples have to be incubated and free antigen has to be separated from the antigen–antibody complex.

To overcome these limitations, enzyme immunoassays EIAs have been developed. Instead of using radioactive tags, the sample containing the analyte antigen is added to a mixture of antibody and standard antigen that is bound to an enzyme. Both enzyme bound standard antigen and analyte antigen from the sample compete for the limited binding sites of the antibody. Because the antibody is a large molecule, binding blocks the active site of the enzyme and reduces enzyme activity (see Figure 2.9.2.3). This change in enzyme activity

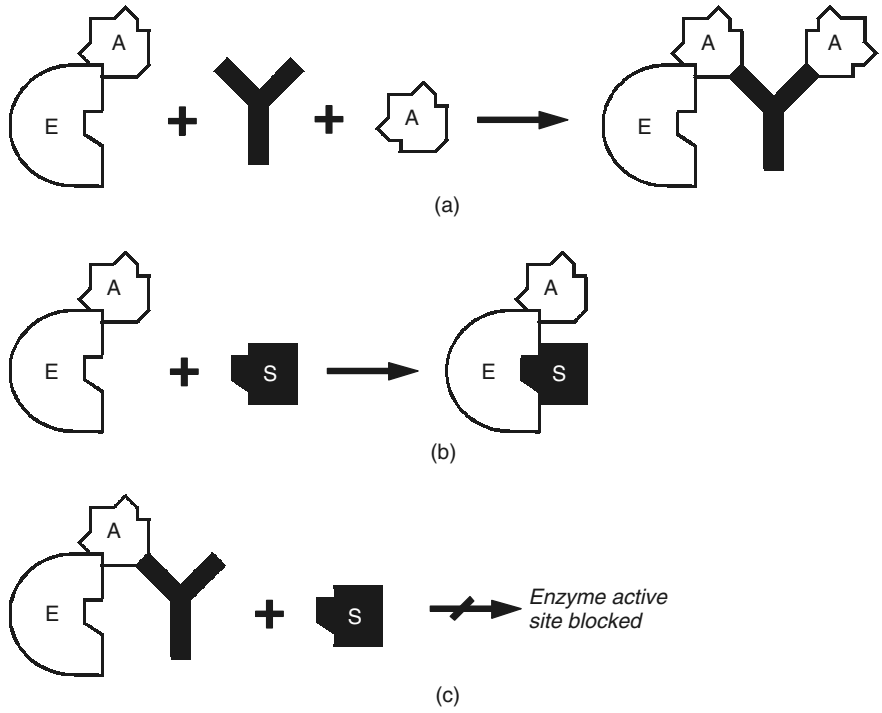

Figure 2.9.2.3. Principles of enzymatic immunoassays. The sample containing the analyte antigen (A) is added to a mixture of antibody (Y) and standard antigen that is bound to an enzyme (E-A). Both analyte antigen (A) and enzyme-linked antigene (E-A) compete for the limited binding sites of the antibody (Figure 2.9.2.3a). Free enzyme-linked antigene (E-A) shows enzyme activity upon addition of a substrate (S), see Figure 2.9.2.3b. In the enzyme–antigen–antibody complex (E-A-Y), the enzyme active site is blocked and no reaction occurs (Figure 2.9.2.3c).

can be measured and allows quantification of the analyte antigen in the sample. The more analyte antigen is in the sample, the less enzyme tagged antigen is bound by the antibody and the higher is the measured enzyme activity.

Theoretically, any enzyme system can be used as a label in enzymatic immunoassays. For practical reasons, however, horseradish peroxidase, alkaline phosphatase, and ß-D-galactosidase are the dominating enzymes in commercially available diagnostic tests and for research applications. Using a suitable chromogenic substrate for the respective enzyme, changes in enzyme activity can be measured spectrophotometrically. Compared to RIA and IRMA principles, EIAs do not require a preliminary separation of bound and free fractions. This approach is referred to as a *homogeneous assay*, indicating that separation does not take place during the analysis. Because EIA is based on the competition between enzyme tagged standard antigen and analyte antigen from the sample for binding to the antibody, calibration graphs are not linear, similar to RIA assays.

4.2.4 Enzyme-linked immunosorbent assay

In parallel to the development of EIA techniques, other immunochemical methods have been explored to overcome the limitations of using radioactive markers. Of these techniques, enzyme-linked immunosorbent assay (ELISA) can be considered the most successful approach. As in EIA, the standard antigen is labeled with an enzyme instead of a radioisotope and changes in enzymatic activity are used for quantitative analysis. Unlike EIA, ELISA belongs together with RIA and IRMA to the heterogeneous immunochemical methods.

Free and unbound fractions have to be separated during the analytical process. However, separation in ELISA is facilitated by the use of solid-phase systems. The antibody is covalently bound to the wall of the reaction container, and separation of the fractions can be achieved by simply washing the container with a buffer or water.

ELISA techniques are based on three major methods: (1) competitive assay, (2) indirect assay, and (3) double-antibody sandwich assay. Competitive assays are similar to RIA and involve the competition of the analyte antigen in the sample and added enzyme-tagged standard antigen for the limited binding sites of the antibody. After washing away any material not bound to antibodies, a suitable enzyme substrate is added as a chromogen. Following a time period of incubation, the reaction is stopped and the enzyme activity is determined via the change in absorbance. Contrary to EIA as the alternative enzymatic technique, the enzyme remains active after binding. The antigen attached to the enzyme in the standard is used only for antibody binding and does not block the active site of the enzyme. Because of the competitive nature of the assay, calibrations curves are not linear and show an inverse relationship between analyte concentration in the sample and enzyme activity. The less analyte is in the sample, the less analyte antigen competes with the added enzyme labeled antigen for antibody binding. Accordingly, the enzyme activity is higher because proportionally more enzyme is bound finally to the antibody.

Indirect ELISA and double-antibody sandwich ELISA are both noncompetitive, that is, all analyte in the sample is bound during the assay. As for IRMA, calibration graphs are linear and show an increase in enzyme activity with an increasing analyte concentration in the sample. Indirect ELISA is used for quantitative and qualitative analysis of immunoglobulins or large protein molecules. The assay is considered indirect, as the analyte in the sample acts as the antibody and binds to the antigen immobilized on the surface of the reaction container. For quantification, an enzyme-labeled antibody is added in excess, being sensitive to the antigen bound analyte molecule. Once the excess of labeled antibody is washed away, enzyme substrate is added, and the analyte concentration can be determined spectrophotometrically using a calibration graph based on standards that are processed in parallel.

Sandwich ELISA bears a strong resemblance to IRMA methodology. Antibody specific to the analyte antigen is immobilized on the surface of the reaction container. The sample or standard is added, and analyte antigen is bound by the antibody. Since the antibody is present in excess, all the analyte antigen should attach. After washing to remove extraneous material, a second antibody is added, which is labeled with an enzyme. The tagged antibody is sensitive to a different part of the analyte molecule than the solid-phase bound antibody and attaches to the analyte antigen to form an antibody–antigen–second antibody complex. After excess antibody has been washed away, chromogenic substrate is added to determine enzyme activity that is proportional to the concentration of the analyte.

One of the main advantages of ELISA is its versatility. It can be used both for the analysis of large and small molecules, unlike homogeneous EIA, which is restricted to compounds of low molecular weight and limited by a narrower concentration range of analysis. ELISA techniques do not require radioactive tags by which the limitations regarding handling, storage, and stability of RIA and IRMA assays can be overcome. ELISA techniques are certainly less economical than other approaches. However, costs for enzyme and antibody are balanced by the ease of analysis and standardization as well as sample throughput as decisive factors for routine applications.

4.2.5 Turbidimetric and nephelometric immunoassays

Quantitative analysis using enzymatic- and radioimmunoassays requires either tagging of the antibody or the antigen for monitoring antigen–antibody complex formation. In nephelometric and turbidimetric assays, complex formation is measured directly on the basis of particle formation. When a solution of antigen and a solution

of antibody are combined, the result is a cloudy suspension. The degree of cloudiness can be used as a measure of the amount of antigen–antibody complex being formed. In turbidimetric assays, the reduction in transparency can be measured by placing the sample directly in the line of a light beam, for example, of a conventional UV–VIS spectrophotometer. In nephelometric assays, the generated immune complexes are quantified by measuring the side-scattered light. The fundamental optical design of a nephelometer equals that of a fluorometer, that is, the detector is placed off axis to the incident light beam. Compared to conventional fluorometers, dedicated nephelometers use a laser light source (400–500 nm) and forward angle detection. By setting off the detector at an angle greater than 90° from the light source and sample, sensitivity can be increased.

Turbidity and light scattering of the suspension can be used as a measure of analyte concentration. Both measures increase with the number and size of antibody–antigen particles in suspension. Quantifications can be based either on the endpoint of the immunochemical reaction or kinetic measurements. When using endpoint techniques, measurement time and experimental conditions have to be standardized carefully. Furthermore, there is no linear correlation between light scattering and analyte concentration in endpoint techniques. At excess amounts of antibody, any added antigen is complexed immediately and light scattering increases. Turbidity reaches its peak when antigen and antibody are present in similar amounts. Any further increase in antigen concentration, however, decreases turbidity. With the antigen being present in excess, each antigen binds to only one antibody. The resulting particles are smaller and scatter the light less. Accordingly, the same turbidity may reflect two entirely different situations. This ambiguity can be overcome by measuring how rapidly the signal intensity changes with time. The rate of formation of the antigen–antibody complex and, thus, the rate of light scattering, increases with antigen concentration, irrespective of the antibody–antigen amount ratio in the sample. Rate nephelometry has generally been shown to be more sensitive than the corresponding endpoint techniques.

Turbidimetric and nephelometric assays require the formation of insoluble antigen–antibody complexes. If analyte molecules are too small to form an insoluble complex with the antibody, modifications are required. In nephelometric inhibition assays, the antibody is added together with so called developer antigen. This molecule is composed of a large protein to which hapten molecules are attached that can react with the antibody. Native antigen in the sample and developer antigen having the same hapten in common compete for the limiting binding sites of the antibody. While the native antigen–antibody complex stays in solution, the developer antigen–antibody complex forms a suspension. The less native antigen in the sample, the more precipitate is formed and the higher the amount of turbidity in the reaction mixture. The use of particle-enhanced immunoassays is another common approach. Small particles (0.1–0.2 μm), such as latex beads or colloidal gold, are coated with antibody, antigen, or haptens. If the corresponding antigen or antibody is present in the sample, particles agglutinate when mixed with the sample and turbidity increases. Agglutination techniques can be used both in direct nephelometric assays and nephelometric inhibition immunoassays.

4.3 Ferritin analysis by immunochemical techniques

Over the past two decades, ferritin analysis in serum or plasma has become a standard tool for assessing iron stores both in biomedical research and clinical practice. The demand of clinical laboratories for a highly sensitive technique that allows processing of large sample numbers in parallel has made immunoassays the approach of choice for ferritin analysis. Numerous immunochemical methods have been developed in the past using IRMA, ELISA, nephelometric, and chemiluminescence techniques. Ferritin analysis is nowadays performed nearly exclusively by using commercially available test kits. Assays come together with all reagents, standards, and quality control material needed to perform the analysis. Ferritin

antibodies used in the assays come from rabbits, goats, or mice injected with purified human ferritin from liver or spleen. Depending on the assay, antibodies can be monoclonal or polyclonal. For ferritin analysis, irrespective of the used assay, venous blood (5 mL) is collected and plasma or serum is being separated. Samples can be stored refrigerated up to 24 hours before analysis. If more time will elapse before analysis is performed (up to 4 months), the serum specimen should be frozen. For the actual analysis, 10–30 μL of plasma or serum are taken and analyzed either manually or using fully automated systems. High sample throughput is certainly one of the big advantages of immunochemical analysis. Because of the high specificity of the antibodies, sample processing is reduced to a number of simple pipetting steps with intermediate incubation of the sample to allow for antigen–antibody binding.

4.3.1 Ferritin analysis by ELISA techniques

ELISA assays are usually carried out in microtiter plates. Standard plates are made from polystyrene and contain a series of small wells (8×12 wells, ca. 300 μL working volume per well) to which sample and reagents are added. Special plate-scanning devices (microplate-readers) are available for parallel spectrophotometric readout. The wavelength for readout in these devices is usually set by insertion of suitable bandwidth filters in the pathway of the light beam and not by using prism or grid monochromators. Commercial ELISA test kits for ferritin are based on the double-antibody sandwich approach. Microtiter plates are supplied precoated with ferritin antibody by the manufacturer. Well coating in ELISA is mostly achieved by passive absorption of the antibody at the polystyrene surface of the wells. For covalent binding of biomolecules to the well's surface, polystyrene plates with a chemically modified surface (e.g. by nitration) are also available. Packing density of the monolayer at the well's surface is in the order of 100–500 $\mathrm{ng\,cm^{-2}}$. Coated microtiter plates can be stored, dependent on the product, refrigerated in physiological buffer with added preservatives (e.g. sodium azide) or dried with a desiccant for a couple of weeks up to several months. Required reagents are ready to use and have to be stored refrigerated.

After the wells and reagents have reached room temperature, samples and standards are pipetted into the wells. For calibration, 4–6 standards that contain ferritin in serum matrix are used, which correspond to the range of ferritin concentrations in human serum (0–300 $\mu\mathrm{g\,L^{-1}}$). To the samples/standards, a defined volume (100–200 μL, assay dependent) of conjugated antihuman ferritin in buffered solution is pipetted. This antibody is sensitive to a different site of the ferritin molecule than the antibody attached to the surface of the well and is conjugated with a suitable enzyme. To allow for complete binding of ferritin to both antibodies, the microplate is shaken on a clinical rotator table for 2 hours at room temperature. To remove excess conjugated antibody, solutions are removed and wells are washed several times by pipetting, shaking, and decanting with water or buffer solution. After the final wash, the tops of the wells are tapped on top on absorbent material for about 30 seconds to drain. Complete removal of conjugated antibody from the wells is essential as the amount of conjugated enzyme immobilized in the antibody–antigen complex defines the analytical signal. A defined volume of substrate solution (100–200 μL, assay dependent) is added, and the microplate is incubated for a standardized time interval at room temperature for the enzymatic reaction to take place (15–30 min, assay dependent). If necessary, the enzymatic reaction is stopped, for example, by acidifying the solution. For spectrophotometric readout, a suitable chromogen is added to transform the product of the enzymatic reaction into a colored compound.

While commercial ELISA test kits are very similar in the principle steps, they differ in the enzyme/substrate/chromogen system used. Common systems include a combination of alkaline phosphatase as the conjugated enzyme, disodium phenylphospate as the substrate and potassium ferricyanide as the chromogen with spectrophotometric readout at 500 nm (Spectro Ferritin, Ramco Laboratories Inc., Stafford, TX). Another

suitable conjugated enzyme for ferritin assays is horseradish peroxidase. Hydrogenperoxide is added as the substrate and 3,3′,5,5′-tetra-methylbenzidine as the chromogen. Addition of HCl or H_2SO_4 stops the enzymatic reaction and produces a bright yellow color that is read at 450 nm (Ferritin ELISA, IBL, Hamburg, Germany; Micro-ELISA ferritin, KMI Diagnostics, Minneapolis, Minnesota). Background absorbance of samples and standards is determined at a different wavelength. Standard containing only serum matrix is processed in parallel to the samples as a blank to correct for nonspecific binding of the antibodies. On the basis of the standards, a calibration line is set up by plotting the corrected absorbance against the nominal ferritin concentration in the standards. Ferritin concentrations in the serum samples are determined by external calibration.

4.3.2 Ferritin analysis by IRMA techniques

Despite the practical disadvantages of using radiotracers and the availability of ELISA techniques, IRMA assays are still in use for ferritin analysis. Historically, IRMA techniques laid the foundations to use ferritin as a measure of iron status. It was only after the development of a sensitive IRMA technique in the early 1970s that ferritin was detected in the serum of normal subjects [90]. Principles and methods of IRMA assays closely resemble those for ferritin analysis by ELISA. Both techniques use a solid-phase double-antibody sandwich approach. Sample ferritin is immobilized by an antibody attached to the solid phase of a test tube and is quantified via binding to a second antibody that is tagged. The main difference between both techniques lies in how the amount of tagged antibody is quantified in the formed sandwich complex. By using ^{125}I labeled antiferritin antibody, antibody binding can be determined directly via the remaining activity in the test tube using a scintillation counter. Within a usual assay, about 2 kBq ^{125}I are being added to each test tube.

As for ELISA techniques, IRMA assays for ferritin are normally performed using commercially available test kits. Test tubes precoated with antibody and solutions that contain isotopically labeled ferritin are available from various suppliers (FER-CTRIA, CIS Bio International, Gif-sur Yvette, France; IRMA-mat® Ferritin, Byk-Sangtec Diagnostica, Dietzenbach, Germany). Quantification is performed by external calibration using the supplied standards that are processed in parallel to the samples. Analytical performances of commercial IRMA and ELISA assays for ferritin are comparable. Coefficients of variation for intra-assay and inter-assay variability, respectively, are in the order of 3–8% dependent on the assay and ferritin concentration in the sample. Detection limits for ferritin in serum samples are in the order of 1 $\mu g\,L^{-1}$ for the different assays. However, at comparable analytical performance, IRMA assays are significantly cheaper than ELISA assays that partly balance the disadvantages of IRMA assays, specifically the lower shelf life and the need for dedicated radiochemistry facilities.

4.3.3 Ferritin analysis by immunoturbidimetric techniques

Homogeneous immunoassays based on light-scattering measurement are well established now, and techniques have been developed for ferritin analysis recently [91–93]. Methods are based on microparticle agglutination technology using latex particles (<500-nm diameter) that are coated with antiferritin antibody. Coated particles aggregate once they have bound to sample ferritin, thereby forming larger particles that scatter the light. Turbidimetric assays for ferritin are usually performed using autoanalyzers. All reagents (sample, buffer, and microparticle suspension) are combined in one mixture, and incubation time is short, usually below 10 min. Quantifications are performed by external calibration and turbidimetric read out at a wavelength of 550 nm. Analytical performance of turbidimetric assays is comparable to the other immunochemical techniques, but sensitivity is inferior, that is, detection limits are in the order of 5–10 $\mu g\,L^{-1}$, which makes turbidimetric techniques less suitable for measuring iron status in individuals with low or emptied iron stores.

4.3.4 Ferritin analysis by chemiluminescence immunoassays

A more recent development is the use of chemiluminescence tags for routine immunochemical ferritin analysis. Ferritin is quantified in these systems, similar to ELISA techniques, by a solid-phase double-antibody sandwich approach. Ferritin is immobilized by biotinylated antiferritin antibodies that are bound to streptavidin-coated magnetic particles or plastic beads as the solid phase. The second antibody is labeled with acridiniumester as the chemiluminescent tag and added in excess to ensure that all immobilized ferritin can bind to tagged antibody. After washing away unbound antibody, the amount of acridiniumester in the sandwich complex is directly proportional to the ferritin amount present. Addition of hydrogenperoxide triggers the decomposition of the ester under light emission, which is measured. The more ferritin is in the sample, the more acridiniumester is present and the higher is the light emission. When using an indirect assay, the second antibody in the sandwich complex is tagged with an enzyme instead and a chemiluminescent substrate is used.

Ferritin analysis by chemiluminescence immunoassay is mostly performed using fully automated systems. Use of magnetic particles and plastic beads for binding the ferritin–antibody sandwich complex facilitates automated separation of the sandwich complex from excess antibody. Commercially available lab automates for chemiluminescence immunoassays are multipurpose instruments, that is, they can be used for quantitative analysis of a large number of biomolecules of diagnostic value provided the suitable assay is available. For human serum ferritin, assays became available recently (IMMULITE® Ferritin, Diagnostics Products Corp., Los Angeles, CA; ACS Ferritin Assay, Bayer Diagnostics, Leverkusen, Germany). Sample throughput for chemiluminescence autoanalyzers is high, usually in the order of 100–200 samples per hour. Intra-assay variability, inter-assay variability, and detection limits for automated ferritin analysis are comparable with other immunochemical techniques.

5 IRON SPECIATION – FIT TO PURPOSE

Any analytical technique can be evaluated on the basis of basic parameters such as accuracy, precision, sensitivity, sample throughput, and the infrastructure and analytical skills required. However, none of these parameters can be looked at independently from the analytical question to be answered. In one case, highest accuracy and precision in the analysis is the precondition to generate meaningful data and no commitments can be made to reduce time demands and costs. In another case, data of moderate accuracy and precision are sufficient for the purpose of the analysis and sample throughput and costs become decisive factors. When developing or installing a technique, it has to be known what level of accuracy and precision is required and what the limits of the chosen technique are when interpreting results.

Iron speciation in biomedical samples is commonly hampered by factors that are well beyond the well quantifiable performance of an analytical instrument or technique. Human physiology is complex, and iron species concentrations in tissues, body fluids, or excreta can vary significantly during the day and between days. Serum iron levels show marked diurnal variation with the morning values being approximately 30% higher than later in the day. Day-to-day variations for ferritin concentration in venous blood are of similar order. Hemoglobin concentrations are less variable and are stable within $\pm 3\%$ between days [13, 94]. In addition, variations between subjects limit data interpretation, at least in the individual. Normal ranges for a measure are commonly derived from population-based studies by analyzing the distribution of the data obtained. Ranges are defined using the 95% confidence interval for the measure in apparently healthy subjects or by identifying the threshold in a population from which there is statistical evidence that a pathological condition may develop. However, it remains largely an open question if normal ranges and cutoff values as determined in a population group truly reflect the situation in the individual.

Keeping these limitations in mind, there are two possible basic approaches for iron speciation. Iron speciation in clinical samples is mostly related to iron containing biomolecules, specifically proteins or peptides. In direct speciation analysis, the biomolecule of interest is separated from other element species, for example, using a chromatographic technique. In a second step, the element content of the isolate is determined by an element-sensitive detector or a technique such as inductively coupled plasma mass spectrometry (ICP-MS), often on-line. In the alternative, indirect approach, it is the metal containing biomolecule itself that is quantified either directly or after separation. If the biomolecule binds specifically to the element of interest, this information can be used as a proxy for element speciation. Both strategies differ obviously in analytical performance. The first approach is more accurate. The second approach is usually less time-demanding and more cost-effective.

A large number of techniques used for iron speciation in biomedicine belong to the second category, such as immunoassays. Assays are highly sensitive and specific, sample throughput is high, and they do not require expensive equipment unless automation is envisaged. By using immunoassays, however, element speciation is shifted from quantifying the fraction of an element in a sample that is bound to a biomolecule to the quantification of an organic ligand that may, or may not, be saturated with the respective element. Ferritin immunoassays are sensitive to the hollow sphere of the protein irrespective of whether the sphere has been filled up with iron to its maximum capacity or not. Data quality is further compromised when assays employing polyclonal antibodies are used. Each batch of raised antibodies is unique and differs in specificity, which limits data comparability between different assays. For ferritin, cutoff levels vary between 12 and 15 $\mu g\,L^{-1}$ between different assays according to the manufacturers. Users are encouraged furthermore to establish their own normal ranges and cutoff values.

The different aspects combined are an obstacle to systematic validation of immunoassays. Often, no classical analytical reference technique is available to which the assay can be validated. In such a case, it is common practice to validate newly developed assays against established immunoassays [95, 96]. To improve relative accuracy and, thus, data comparability, assays are calibrated using a reference material, if available, and quality control materials are processed in parallel with each batch of samples. For ferritin analysis, as an example, data comparability has been improved significantly by the availability of a reference material of lyophilized recombinant human ferritin, which is distributed by the World Health Organization (WHO) within their International Biological Reference Preparations Program. Since 1996, the third preparation of this reference material is in use (3^{rd} International Standard, 94/572).

Despite obvious limitations in accuracy, immunoassays for ferritin became indispensable tools in biomedicine. Techniques are designed to the needs and it is highly unlikely that they will be replaced in routine applications in the near future by direct techniques for element speciation. Sample throughput cannot be surpassed by classical techniques, and undisputable limits in absolute accuracy are largely balanced by significant biological variations and by performing relative measurements, that is, data are compared with normal ranges and cutoff levels as determined using the same technique. Limits are further diminished when using a multiparameter approach to assess iron status. Serum or plasma ferritin concentrations are usually evaluated in combination with hemoglobin concentration and at least one additional hematological parameter such as zinc protoporphyrine or transferrin receptor.

6 CRITICAL NOTE

Techniques used for iron speciation in biomedicine and clinical chemistry are optimized in sample throughput, sensitivity, and precision for routine applications. However, this does not necessarily imply that they are fit to the purpose of the analysis, as to give an unambiguous answer to the analytical question. Development of analytical tests in biomedicine is often driven by the sometimes urgent demand for a reliable diagnostic test or a clinical parameter to assess the risk

of an individual of developing a particular disease. Because of its potential value in diagnosis or therapy, techniques are developed and applied quickly, often without proper validation. If proven successful, hybrid techniques and alternative methods are developed, which are validated against the original technique, irrespective of its accuracy. Limits in data quality are recognized only after years of routine application. To improve data comparability, reference materials are produced and, finally, a reference technique is identified or developed, which can be used to validate the numerous techniques that are used in parallel.

For HbA_{1c} analysis, as an example, this process took more than 30 years. Standardization attempts culminated finally in the formation of a working group within the IFCC. A reference technique based on peptide separation by HPLC and quantification by ESI-MS has been approved in 2002, which will be the basis for validation and future uniform standardization of HbA_{1c} routine assays [52]. It has to be noted in this context that the 'fit-to-purpose' concept involves two components. One part is to define what commitments regarding the accuracy and precision are acceptable to answer the analytical question. The other part is to carefully evaluate the limits in accuracy and precision before and not after the technique has been applied and conclusions been drawn from the data.

7 REFERENCES

1. Yip, R. and Dallman, P. R., Iron, in *Present Knowledge in Nutrition*, 7th ed., Ziegler, E. E. and Filer, L. J. (Eds.), ILSI Press, Washington, DC, 1996, pp. 277–292.
2. Green, R., Charlton, R. W., Seftel, H., Bothwell, T. H., Mayet, F., Adams, E. B., Finch, C. A. and Layrisse, M., *Am. J. Med.*, **45**, 336 (1968).
3. Hallberg, L., Hogdahl, A. M., Nilsson, L. and Rybo, R., *Acta Obstetr. Gynecol. Scand.*, **45**, 320 (1966).
4. Andrews, N. C., *N. Engl. J. Med.*, **341**, 1986 (1999).
5. World Health Organization/United Nations University/UNICEF, *Iron Deficiency Anemia, Assessment, Prevention and Control: A Guide for Programme Managers*, WHO, Geneva, 2001.
6. Beard, J. L., *J. Nutr.*, **351**, 568S (2001).
7. DeMaeyer, E. and Adiels-Tegma, M., *World Health Stat. Q.*, **38**, 302 (1985).
8. Leggett, B. E., Halliday, J. W., Brown, N. N., Bryant, S. and Powell, L. W., *Br. J. Haematol.*, **74**, 525 (1990).
9. Powell, L. W., Jazwinska, E. and Halliday, J. W., Primary iron overload, in *Iron Metabolism in Health and Disease*, Brock, J. H., Halliday, J. W., Pippard, M. J. and Powell, L. W. (Eds.), WB Saunders, London, 1994, pp. 227–270.
10. Pippard, M. J., Secondary iron overload, in *Iron Metabolism in Health and Disease*, Brock, J. H., Halliday, J. W., Pippard, M. J. and Powell, L. W. (Eds.), WB Saunders, London, 1994, pp. 272–300.
11. Messerschmidt, A., Huber, R., Poulos, T. and Weighardt, K. (Eds.), *Handbook of Metalloproteins*, Vol. 1 and 2, Wiley, Chichester, 2001.
12. Jones, M. S. and Jones, O. T. G., *Biochem. J.*, **113**, 507 (1969).
13. Worwood, M., *Clin. Chim. Acta*, **259**, 3 (1997).
14. Wallach, J., *Interpretation of Diagnostic Tests*, 7th ed., Lippincott Williams & Wilkins Publishers, 2000.
15. LaBounty, A., Anemia of abnormal iron metabolism, in *Clinical Hematology*, Lotspecih-Steininger, C. A., Stiene-Martin, E. A. and Koepke, J. A. (Eds.), JB Lippincott Company, Philadelphia, PA, 1992, pp. 172–184.
16. Stadie, W. C., *J. Biol. Chem*, **41**, 237 (1920).
17. King, E. J. and Gilchrist, M., *Lancet*, **242**, 201 (1947).
18. Betke, K. and Savelsberg, W., *Biochem. Z.*, **320**, 431 (1950).
19. Drabkin, D. L. and Austin, J. H., *J. Biol. Chem.*, **98**, 719 (1932).
20. Eilers, R. J., *Am. J. Clin. Pathol.*, **47**, 212 (1967).
21. International Committee for Standardization in Haematology, Expert Panel on Haemoglobinometry, *Clin. Lab. Haematol.*, **9**, 73 (1987).
22. Evelyn, E. R. and Malloy, H. T., *J. Biol. Chem.*, **126**, 655 (1938).
23. Coulter, W. H., *Proc. Natl. Elect. Conf.*, **12**, 1034 (1956).
24. Ryan, D. H., Automated analysis of blood cells, in *Hematology – Basic Principles and Practice*, 3rd ed., Hoffman, R., Benz, E. J., Shattil, S. J., Furie, B., Cohen, H. J., Silberstein, L. E. and McGlave, P. (Eds.), Churchill Livingstone, Pennsylvania, PA, 2000, pp. 2469–2481.
25. International Hemoglobin Information Center, *Hemoglobin*, **20**, 215 (1996).
26. Fairbanks, V. F., Thalassemias and related disorders, in *Hemoglobinopathies and Thalassemias*, Fairbanks, V. F. (Ed.), Brian C. Decker, New York, 1980, pp. 18–27.
27. Lubin, B. H., Witkowska, H. E. and Kleman, K., *Clin. Biochem.*, **24**, 820 (1991).
28. Clarke, G. M. and Higgins, T. N., *Clin. Chem.*, **46**, 1284 (2000).
29. Schneider, R. G., *CRC Crit. Rev. Clin. Lab. Sci.*, **9**, 243 (1978).
30. Basset, P., Braconnier, F. and Rosa, J., *J. Chromatogr.*, **227**, 267 (1982).
31. Alter, B. P., Coupal, E. and Forget, B. F., *Hemoglobin*, **5**, 357 (1981).

32. Valkonen, K. H., Gianazza, E. and Righetti, P. G., *Clin. Chim. Acta.*, **107**, 223 (1980).
33. Shelton, J. B., Shelton, J. R. and Schroeder, W. A., *Hemoglobin*, **3**, 353 (1979).
34. Congote, L. F., *Blood*, **57**, 353 (1981).
35. Riou, J., Godart, C., Hurtrel, D., Mathis, M., Bimet, C., Bardakdjian-Michau, J., Prehu, C., Wajcman, H. and Galacteros, F., *Clin. Chem.*, **43**, 34 (1997).
36. Leone, L., Monteleone, M., Gabutti, V. and Amione, C., *J. Chromatogr.*, **321**, 407 (1985).
37. Papadea, C. and Cate, J. C., *Clin. Chem.*, **42**, 57 (1996).
38. Hempe, J. M. and Graver, R. D., *Clin. Chem.*, **40**, 2288 (1994).
39. Cotton, F., Lin, C., Fotaine, B., Gulbis, B., Janssens, J. and Vertongen, F., *Clin. Chem.*, **45**, 237 (1999).
40. Mario, N., Baudin, B., Aussel, C. and Giboudeau, J., *Clin. Chem.*, **43**, 2137 (1997).
41. Sacks, D. B., Carbohydrates, in *Tietz Textbook of Clinical Chemistry*, 3rd ed., Burtis, C. A. and Ashwood, E. R. (Eds.), WB Saunders, Philadelphia, PA, 1999, pp. 790–796.
42. American Diabetes Association, *Diabetes Care*, **17**, 616 (1994).
43. Hallwachs-Baumann, G., Katzensteiner, S., Schnedl, W., Pürstner, P., Pieber, T. and Wilders-Truschnig, M., *Clin. Chem.*, **43**, 511 (1997).
44. Bry, L., Chen, P. C. and Sacks, D. B., *Clin. Chem.*, **47**, 153 (2001).
45. Trivelli, L. A., Ranney, H. M. and Lai, H. T., *N. Engl. J. Med.*, **248**, 353 (1971).
46. Abraham, E. C., Huiff, T. A. and Cope, J. D., *Diabetes*, **27**, 931 (1978).
47. Gruber, C. A. and Koets, M. D., *Clin. Chem.*, **25**, 1970 (1979).
48. Kullberg, C. E., Bergstrom, A., Dinesen, B., Larsson, L., Little, R. R. and Goldstein, D. E. and Arnqvist H. J., *Diabetic Care*, **19**, 726 (1996).
49. Scott, A., Casson, I. F. and Higgins, G. J., *Diabet. Med.*, **18**, 274 (2001).
50. Little, R. R., Wiedmeyer, H. M., England, J. D., Wilke, A. L., Rohlfing, C. L., Wians, F. H., Jacobson J. M., Zellmer V. and Goldstein D. E., *Clin. Chem.*, **38**, 2472 (1992).
51. Bruns, D. E., *Clin. Chem.*, **38**, 2363 (1992).
52. Jeppson, J. O., Kobold, U., Barr, J., Finke, A., Hölzel, W., Hoshino, T., Miedema, K., Mosca, A., Mauri, P., Paroni, R., Thienpont, L., Unemoto, M. and Weykamp, C., *Clin. Chem. Lab. Med.*, **40**, 78 (2002).
53. Green, R., Charlton, R., Seftel, H., Bothwell, T., Mayet, F., Adams, B., Finch, C. and Layrisse, M., *Am. J. Med.*, **45**, 336 (1968).
54. Newhouse, I. J. and Clement, D. B., *Sports Med.*, **5**, 337 (1988).
55. Fleming, J. L., Ahlquist, D. A., McGill, D. B., Zinsmeister, A. R., Ellefson, R. D. and Schwartz, S., *Mayo Clin. Proc.*, **62**, 159 (1987).
56. Rockey, D. C. and Cello, J. P., *N. Engl. J. Med.*, **329**, 1691 (1993).
57. Layrisse, M. and Roche, M., *Am. J. Hyg.*, **79**, 279 (1964).
58. Greegor, D. H., *Cancer*, **28**, 131 (1971).
59. Schwartz, S., Dahl, J., Ellefson, M. and Ahlquist, D., *Clin. Chem.*, **29**, 2061 (1983).
60. Ahlquist, D. A., McGill, D. B., Schwartz, S., Taylor, W. F., Ellefson, M. and Owen, R. A., *Ann. Intern. Med.*, **101**, 297 (1984).
61. Heinrich, H. C., Kamal, R. and Leberecht, P., *Klin. Wochenschr.*, **61**, 765 (1983).
62. Turunen, M. J., Liewendahl, K., Thomas, W. M. and Hardcastle, J. D., *Br. J. Cancer*, **49**, 141 (1984).
63. Barrows, G. H., Burton, R. M., Jarrett, D. D., Russell, G. G., Alford, M. D. and Songster, C. L., *Am. J. Clin. Pathol.*, **69**, 342 (1978).
64. Adams, E. C. and Layman, K. M., *Ann. Clin. Lab. Sci.*, **4**, 343 (1978).
65. de Jong, G., van Dijk, J. P. and van Eijk, H. G., *Clin. Chim. Acta*, **190**, 1 (1990).
66. Aisen, P. and Listowsky, I., *Annu. Rev. Biochem.*, **49**, 357 (1980).
67. Baker, E. and Morgan, E. H., Iron transport, in *Iron Metabolism in Health and Disease*, Brock, J. H., Halliday, J. W., Pippard, M. J. and Powell, L. W. (Eds.), WB Saunders, London, 1994, pp. 62–94.
68. Ramsey, W. N. M., *Clin. Chim. Acta*, **2**, 221 (1957).
69. International Committee for Standardisation in Haematology (Iron Panel), *Br. J. Haematol.*, **38**, 281 (1978).
70. International Committee for Standardisation in Haematology (Iron Panel), *Br. J. Haematol.*, **38**, 291 (1978).
71. International Committee for Standardisation in Haematology (Iron Panel), *Br. J. Haematol.*, **75**, 615 (1990).
72. Persijn, J. P., van der Slik, W. and Riethorst, A., *Clin. Chim. Acta*, **35**, 91 (1971).
73. Stookey, L. L., *Anal. Chem.*, **42**, 779 (1970).
74. Bothwell, T. H., Charlton, R. W., Cook, J. D. and Finch, C. A., *Iron Metabolism in Man*, Blackwell Scientific Publications, Oxford, 1979.
75. Tietz, N. W. and Rinker, A. D., *Clin. Chem.*, **40**, 1347 (1994).
76. Huebers, H. A., Eng, M. J., Josephson, B. M., Ekpoom, N., Rettmer, R. L., Labbe, R. F., Pootrakul, P. and Finch, C. A., *Clin. Chem.*, **33**, 273 (1987).
77. Bandi, Z. L., Schoen, I. and Bee, D. E., *Clin. Chem.*, **31**, 1601 (1985).
78. Gottschalk, R., Wigand, R. and Dietrich, C. F., *Clin. Chim. Acta*, **293**, 127 (2000).
79. Theil, E. C., *Annu. Rev. Biochem.*, **56**, 289 (1987).
80. Worwood, M., *Blood Rev.*, **4**, 259 (1990).
81. Harrison, P. M., Ford, G. C., Rice, D. W., Smith, J. M. A., Treffry, A. and White, J. L., *Biochem. Soc. Trans.*, **15**, 744 (1987).
82. Bakker, G. R. and Boyer, R. F., *J. Biol. Chem.*, **261**, 13182 (1986).
83. Walters, G., Miller, F. M. and Worwood, M., *J. Clin. Pathol.*, **26**, 770 (1973).

84. Skikne, B. S., Flowers, C. H. and Cook, J., *Blood*, **75**, 1870 (1990).
85. The British Nutrition Foundation Task Force, *Iron Nutritional and Physiological Significance*. Chapman & Hall, London, 1995.
86. Calbreath, D. F., *Clinical Chemistry – A Fundamental Textbook*, WB Saunders, Philadelphia, PA, 1992.
87. Crowther, J. R., *The ELISA Guidebook*, Humana Press, Totowa, NJ, 2001.
88. Gosling, J. P., *Immunoassays – A Practical Approach*, Oxford University Press, Oxford, 2000.
89. Berson, S. A. and Yalow, R. S., *Trans. N. Y. Acad. Sci.*, **24**, 487 (1962).
90. Addison, G. M., Beamish, M. R., Jacobs, A., Hales, C. N., Hodgkins M. and Llewelli P., *J. Clin. Pathol.*, **25**, 326 (1972).
91. Bernard, A. and Lauwerys, R., *J. Immunol. Methods*, **71**, 141 (1984).
92. Simo, J. M., Joven, J., Civille, X. and Sans, T., *Clin. Chem.*, **40**, 625 (1994).
93. Borque, L., Rus, A., Bellod, L. and Seco, S. L., *Clin. Chem. Lab. Med.*, **37**, 899 (1999).
94. Borel, M. J., Smith, S. M., Derr, J. and Beard, J. L., *Am. J. Clin. Nutr.*, **54**, 729 (1991).
95. Zemelka, S. and Biesalski, H. K., *J. Immunoassay Immunochem.*, **22**, 371 (2001).
96. Hamwi, A., Endler, G., Rubi, K., Wagner, O. and Endler, A. T., *Clin. Chem. Lab. Med.*, **40**, 365 (2002).

2.10 Speciation of Lead

2.10.1 Environmental Speciation of Lead

Stephen J. Hill
University of Plymouth, Plymouth, UK

1 INTRODUCTION

During the 1970s and early 1980s, there was increasing concern about the adverse effects of lead on health. Over the same period, the increasing availability of analytical techniques such as those coupling various forms of atomic spectrometry with both gas chromatography (GC) and liquid chromatography (LC) provided for the first time unequivocal qualitative and quantitative information on the level of lead and its speciation in the environment. Thus, it was realized that inorganic lead species, such as those found in the formulation of older types of house paints, were not the only source of toxic lead in environmental samples since anthropogenic alkyllead compounds such as tetraalkyllead species used as antiknock additives in petrol were ubiquitous in the environment being identified in waters, sediments, soils, fish and vegetation. Vehicular emissions of tetraalkyllead (R_4Pb) are broken down in the atmosphere by the reaction with hydroxyl radicals and sunlight to form stable vapor phase trialkyllead (R_3Pb^+) and dialkyllead (R_2Pb^{2+}), which are then scavenged from the atmosphere by rainfall [1]. The decomposition productions are more stable than R_4Pb in water and may be deposited in road drainage and surface waters [2]. Around this time, there were also reports that organolead compounds could be derived from natural processes [3]. Although early reports of natural biomethylation were fairly circumstantial and the predicted amounts reported likely to be produced were not significant when compared to anthropogenic emissions [4], more recent studies have identified a range of natural sources of methylated lead. With the reduction in anthropogenic emissions, the biomethylation of lead, although a slow process, may well become more significant in terms of natural levels.

2 NATURAL LEAD SPECIES IN THE ENVIRONMENT

Inorganic lead rarely exists in its elemental state but is found in the environment in various complexes [5]. In water, these include simple inorganic species such as $Pb(OH)_2$, $Pb(OH)_3^-$

Handbook of Elemental Speciation II: Species in the Environment, Food, Medicine & Occupational Health
Edited by R. Cornelis, H. Crews, J. Caruso and K. G. Heumann
 ISBN: 0-470-85598-3 (HB)

and polymeric lead ions such as $Pb_2(OH)_3^+$ and $Pb_4(OH)_4^{4+}$. Insoluble compounds such as PbO, $PbCO_3$ and $PbSO_4$ may also be present. However, most studies refer to the inorganic species simply as the Pb^{2+} ion.

The separation of the inorganic compounds referred to above is not normally classified as chemical speciation but selective extraction procedures to differentiate between such forms do exist. One such example in the recent literature is the quantitative determination of the forms of Pb in different size fractions of stream sediment samples from a historic mining area in Scotland [6]. In this study, comparison of X-ray powder diffraction analysis with determination of Pb by atomic absorption spectrometry (AAS) showed that a large proportion of the Pb present in the stream sediments was in the form of cerussite ($PbCO_3$). However, this study (and others) has also demonstrated that the quantitative analysis of specific size fractions may have inherent limitations. In this specific example, the cerussite tends to be concentrated in the silt fraction yet the lead was also adsorbed to clay minerals, organic matter and/or amorphous Fe and Mn oxides. The binding of lead to the organic fractions in soil has also been studied, for example, gel electrophoresis has been used with laser ablation inductively coupled plasma mass spectrometry LA-ICP-MS to measure the binding of Pb to various molecular size functions of humic and fulvic acid [7]. The great majority of studies investigating the environmental chemistry of lead have, of course, not focused on characterizing the inorganic lead by selective extraction but have focused on the true speciation of lead in the sample, including the identification and quantification of a range of organolead species. The major organolead species most likely to be found in the environment are listed in Table 2.10.1.1. In addition, a number of other species such as monoalkyllead (RPb^{3+}) have tentatively been identified in laboratory studies although no evidence exists to date of their presence in the environment.

The results of several studies have shown that lead can be methylated in aqueous sediments from which it is released in the vapor phase to potentially sustain enhanced concentrations in the biosphere over long periods [8, 9]. Early studies used a range of bacteria and fungi [10, 11] in controlled modeling experiments to investigate the methylation process, but more specific experiments with selected marine phytoplankton and macroalgae have also been performed [12, 13]. In one example, both mixed and pure cultures of marine bacteria of polar origin were used to evaluate the production of trimethyllead. The release rate of the methyllead was found to vary with the type of macroalgae used, for example, *Laminaria saccharina* was found to produce methylated compounds from a range of metals, including trimethyllead, whilst *Fucus distichus* and *Desmarestia aculeate* were more specific and whilst methylating other metals did not show evidence of lead methylation [14]. The releasing rates for trimethyllead was found to be up to 110 pg of trimethyllead per gram of wet alga and incubation times of 1–5 days.

Table 2.10.1.1. Organolead compounds encountered in environmental samples.

R_4Pb	Me_4Pb
	Me_3EtPb
	Me_2Et_2Pb
	$Me\ Et_3Pb$
	Et_4Pb
R_3Pb^+	Me_3Pb^+
	Me_2EtPb^+
	$MeEt_2Pb^+$
	Et_3Pb^+
R_2Pb^{2+}	Me_2Pb^{2+}
	$MeEtPb^{2+}$
	Et_2Pb^{2+}

3 ANTHROPOGENIC LEAD SPECIES

Tetraalkylleads have been added to petrol since 1923 to improve the octane ratings for fuels used in high-compression internal combustion engines. Although this use far exceeds other applications, there are also commercial applications that may result in the release of organoleads into the environment. These include their use in the manufacture of fungicides, marine antifouling paints, lubricant additives, as catalysts in the production of polyurethane foams, stabilizers for polyvinylchloride (PVC), in flame retardants and rodent repellants. Although some of these applications are now little used, and indeed the use of tetraalkyllead

in petrol has been phased out in many countries, there are still substantial environmental concerns that reflect the scale of past usage. As indicated above, the alkyllead species R_3Pb^+ and R_2Pb^{2+} are persistent intermediates of the environmental decomposition of R_4Pb. Monoalkyllead (RPb^{3+}), which has also been postulated, and intermediates in the decomposition of organic lead to Pb^{2+} are far more unstable and decompose readily to Pb^{2+} [15]. The rate of decomposition of organolead species is accelerated by solar radiation [16], although compounds that contain methyl groups are more stable to photochemical decomposition than those with ethyl groups, and the degradation reactions may be influenced by other species found in environmental media. The harmful effects of organolead compounds are considered to be much larger than those of inorganic lead [4, 17]. The toxicity of alkyllead species diminishes in the order $R_4Pb \rightarrow R_3Pb^+ \rightarrow R_2Pb^{2+} \rightarrow Pb^{2+}$, where R is a methyl- or ethyl-group. However, the ionic forms are more persistent in the environment. The degradation products of tetraalkyllead compounds are unique indicators of automotive environmental pollution by lead. Thus, the introduction of ultrasensitive analytical procedures has facilitated a range of environmental studies, such as those of organoleads in ancient Greenland snow [18] and high alpine sites [19], which provide archives of northern hemisphere pollution. These studies indicate the global range of petrol related pollution, not only with respect to Pb^{2+} and the more toxic organometallic compounds [18]. The data obtained from snow and ice core samples collected in the Mont Blanc area [19] revealed no organolead deposition prior to 1962. The levels were then found to increase up to the late 1980s but then declined significantly during the 1990s, reflecting the usage of organolead additives to petrol in Europe over this period. The levels found ranged from 0.1 to 3 pg g^{-1} for dimethyllead; 0.08 to 3.4 pg g^{-1} for trimethyllead; 0.01 to 0.57 pg g^{-1} for diethyllead; and 0.01 to 0.13 pg g^{-1} for triethyllead.

The marine environment has also been studied, again demonstrating the ubiquitous nature of lead pollution. In one such study of the total and organic lead distribution in rainwater, seawater, sediment and marine organisms from the Eastern Adriatic Court [20], mussels were found to accumulate total and organic lead more efficiently than fish, indicating an absence of biomagnification of lead compounds in the marine food chain. In the same study, rainwater was found to contain the highest levels of both total and organic lead, with seawater levels lower by factors of 150 and 15, respectively. Thus, the percentage of organic lead in seawater is higher than rainwater. However, in contrast to total lead, organolead compounds were not found to accumulate in sediment ($0.001 \pm 0.0002\%$).

4 ANALYTICAL METHODS FOR LEAD SPECIATION

The analytical methods currently used for lead speciation have been reviewed in detail elsewhere [21]. The most widely used approaches and some examples of the application of these techniques for environmental studies are presented in Table 2.10.1.2. In nearly all cases, the methods employ a sequence of analytical steps, including extraction, derivation, separation and detection.

To date, the most popular approach to lead speciation studies has been the coupling of GC with an element-specific detector. Originally, flame atomic absorption detectors were used, usually employing some form of device to retain the atoms and hence improve detection limits [22]. More recently, atomic emission detectors [34], inductively coupled plasma-mass spectrometry (ICP-MS) [51, 52] and mass spectrometry (MS) [53] have been used. The use of MS for the detection of organoleads following separation by GC has increased in recent years although the application of electron impact ionization MS in the single-ion monitoring mode was reported as far back as 1981 [54]. In many cases, derivatization of the lead species is achieved using either butylation or propylation, employing a range of chemistries, although ethylation has also been used. A popular approach to facilitate preconcentration of the lead species is to use an on-line cryogenic trap [55].

The development of cryogenic trapping systems has continued with particular application to air

Table 2.10.1.2. Overview of techniques available for lead speciation.

Techniques	Application	Notes	References
Hydride generation-ETAAS	Differentiation between inorganic and organic lead species	Speciation limited	16
GC AAS	Petrol, rainwater, air, water, atmospheric aerosols, street dust	–	22–28
Ethylation/GC-QF AAS	*In situ* analysis from aqueous solutions	Ethylation converts Pb^{2+} and ethyllead ions to Et_4Pb. Therefore only suitable for methylated species	29
Butylation/GC-QF AAS		Good recoveries reported for R_3Pb^+ but R_2Pb^{2+} recovery varies. Some peaks poorly resolved	26, 30–32
Propylation/GC-QF AAS	Various environmental samples	Results in R_4Pb compounds that are more volatile than butylated species. Good GC resolution	33
GC-MIP-AES	Alpine snow, tapwater, peat	*In situ* butylation	19, 34
GC-ICP-MS	Air monitoring	System can include use of cryogenic trap	24, 25
Pentylation/GC-MS	Snow	Derivatization with a Grignard reagent followed by extraction into hexane as diethyldithiocarbamate complexes	35
HPLC-AAS	Petrol, waste oils	Not suitable for low-level studies	36, 37
HPLC-ID-ICP-MS	Rainwater	TML isotopically enriched in the 206 isotope used to enhance accuracy	38
HPLC-AES	Petrol, contaminated soils	Recent applications have used on-line hydride generation	39–41
HPLC-ICP-MS	Reference materials, rainwater	Isotope dilution studies possible	42–44
ASV	Seawater, sediments, fish, bird tissue	–	20, 45–48
GC-MS	Aqueous systems, road dust	Ethylation, extraction and preconcentration may be carried out in a single step	49, 50

monitoring. Recent work has recorded tetraalkyllead species in air samples at around 15.5 $ng\,m^{-3}$ using a silanized glass wool system at $-175\,^{\circ}C$ followed by GC-ICP-MS [51]. A similar study [52] again using GC-ICP-MS but with a homemade heated transfer line was able to achieve method detection limits of less than 10 fg for organolead species in airborne particular matter. Local air surveys recorded levels of 1.6–3.8 $pg\,m^{-3}$ and 5.5–23.5 $pg\,m^{-3}$ for dimethyllead and diethyllead, respectively.

LC has also been employed, usually in conjunction with ICP-MS detection. Modified sample introduction systems have been reported employing, for example, the use of a direct injection nebulizer (DIN) [42] or direct injection high efficiency nebulizer (DIHEN) [44]. In the first of these examples, a fused silica capillary was modified by coating the surface with a cation exchange active organic molecule. In the second example, the nebulizer was unmodified and used in conjunction with both reverse-phase and ion-pairing columns. No plasma instability or carbon deposition on the nebulizer tip was found when using organic modifiers (up to 20%) in the mobile phase.

Hydride generation has been used in conjunction with HPLC-ICP-MS to obtain better detection limits than with conventional pneumatic nebulization systems. Recent applications include the determination of alkylleads in soil samples from an old industrial production site [41] and urban particulate matter [43].

Other approaches to coupling GC and LC separation systems to element-specific detectors include the application of ICP-time-of-flight MS for the analysis of environmental waters [56], the use of GC-microwave–induced plasma atomic emission spectrometry (AES) for the determination of organoleads in tap water and peat [34], and isotope dilution analysis using TML chloride isotopically enriched in the stable 206 isotope to enhance accuracy [38]. The speciation of lead in environmental samples has also been studied by using preconcentration resins. One of the more recent approaches involves the sorption of species onto a C-60 fullerene column as diethyldithiocarbamate complexes that were subsequently eluted with hexane or isobutyl methyl ketone. In essence, the inorganic Pb was precipitated as $PbCrO_4$, which was redissolved in acid. TEL and TML were complexed with NaDDC and then adsorbed onto the C_{60} fullerene column and desorbed sequentially with hexane and isobutyl methyl ketone (IBMK). Speciation was then achieved using gas chromatography-mass spectrometry (GC-MS) following derivatization [57, 58]. This approach offered detection limits of $1–4\ ng\,L^{-1}$. The same workers have also modified this method to include a chelating group attached to the fullerene core for use with inorganic lead [16].

An alternative approach to using chromatography coupled to an element-specific detector is the use of voltammetry. Such methods facilitate the determination of the 'labile' fraction in addition to total metal levels, ligand concentration and related conditional stability constants. One of the more popular applications of differential pulse anodic stripping voltammetry (DP-ASV) has been seawater analysis [45], although rainwater, surface waters, estuarine waters, sediments and marine organisms have also been investigated [20, 46]. An intercomparison of the determination of alkyllead compounds in both water and mussels using both gas chromatography-atomic absorption spectrometry (GC-AAS) and DP-ASV has been made [32]. This study also critically evaluated sample preparation techniques for each approach and reported that digestion of the mussel tissue with tetramethylammonium hydroxide should be performed at room temperature to avoid the decomposition of some alkylleads; that tetraalkyllead and ionic organolead compounds should be extracted and determined separately; and for extraction into hexane and reextraction into aqueous solution, a double extraction should be used. Cleaning of extracts through a silica column was also recommended prior to GC-AAS measurement. These specific recommendations reinforce the importance of appropriate sample preparation for all speciation analyses.

Finally, the speciation of lead in environmental samples has been the subject of a number of collaborative projects. The complexity of the methods used to determine alkyllead compounds has prompted a project within the framework of the Measurement and Testing Programme (formerly the BCR) of the Commission of the European Communities. The aim of the project was to first carry out a feasibility study to investigate the stability of alkyllead compounds in solution [35] and then to use the outcome of this work to produce a number of certified reference materials (CRMs). The results from the first phase indicated that dialkyllead and triethyllead compounds were not sufficiently stable to be kept in water and that the only compound that could be stored without significant degradation was trimethyllead [35]. This led to the certification campaign of trimethyllead in artificial rainwater and urban dust in the mid-1990s. Full details of this exercise may be found elsewhere [21], however, the results obtained for the determination of TML in rainwater by 10 laboratories in the latter stages of evaluation are shown in Figure 2.10.1.1. The technical discussions that followed the early rounds of the certification exercise accepted the results following both technical and statistical evaluation. Variations were noted relating to both the calibrants used and the conditions for the Grignard reactions, which adversely affected the precision in some cases. Although the quality of the measurements was not in doubt, concerns over the stability of the reference material and the requirement for very careful storage did not encourage the production of the reference material. However, the results shown in Figure 2.10.1.1 demonstrate the quality of the data that may be obtained using a range

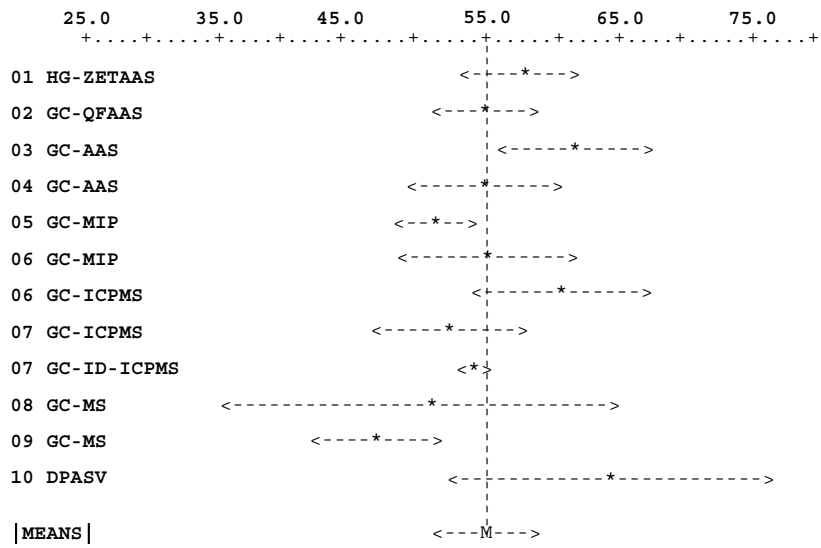

Figure 2.10.1.1. Trimethyllead in rainwater. Bar graph for laboratory mean and 95% confidence interval. The results correspond to the trimethyllead content as mass fractions of Me_3Pb^+ (ng kg^{-1} as TML); the mean of laboratory means obtained was (55.2 ± 3.5) ng kg^{-1} as TML. (Reproduced with permission from Quevauviller, P., *Method Performance Studies for Speciation Analysis,* The Royal Society of Chemistry, 1998.)

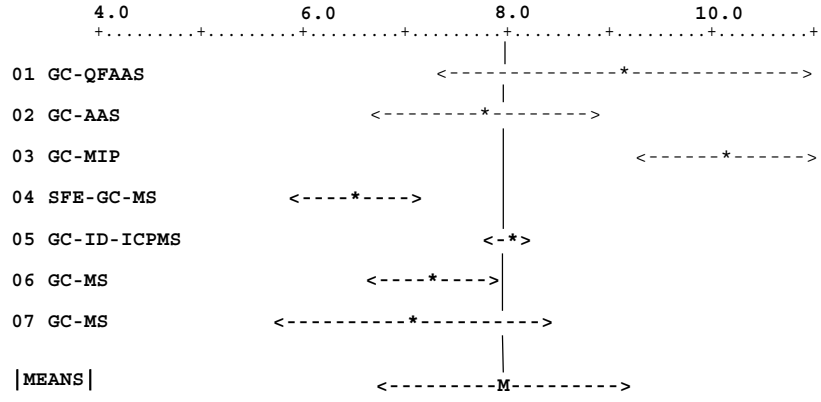

Figure 2.10.1.2. Trimethyllead in urban dust in μg kg^{-1} as TML. (Reproduced with permission from Quevauviller, P., *Method Performance Studies for Speciation Analysis,* The Royal Society of Chemistry, 1998.)

of techniques. The preparation of the candidate reference material for trimethyllead in urban dust was more successful. The results obtained from a number of laboratories for trimethyllead in candidate reference urban road using various techniques are shown in Figure 2.10.1.2. This study resulted in the production of a CRM 605 – trimethyllead in urban dust, with a certified value for TML of 7.9 ± 1.2 μg kg^{-1}.

5 CONCLUSIONS

The speciation of lead in the environment has been extensively studied (Table 2.10.1.3) and sensitive

Table 2.10.1.3. Concentration of alkyllead compounds reported in selected environmental studies.

	Range	Reference
Rainwater	9–65 ng L^{-1}	20
	10–96 ng L^{-1}	59
Seawater	0.2–6.0 ng L^{-1}	20
	<0.5–12.5 ng L^{-1}	59, 60
River water	<0.5–7.5 ng L^{-1}	60
Lake water	0.4–2.4 ng L^{-1}	60
Drinking water	0.5–10 ng L^{-1}	59
Urban waste water	7.5–27.5 ng L^{-1}	60
Snow/ice	0.1–3.0 pg g^{-1} DML	19, 61
	0.8–3.4 pg g^{-1} TML	
	0.1–5.7 pg g^{-1} DEL	
	0.1–0.13 pg g^{-1} TEL	
	15–800 fg g^{-1}	
Sediments	0.001%	20
Fish	20–80 ng g^{-1}	20
Mussels	6.0–18.2 ng g^{-1}	20
	0.2–43.6 ng g^{-1} TAL	62
	0.1–9.2 ng g^{-1} DAL	62
Air	15.5 ng m^{-3}	63

yet species-specific techniques are now available. A species-specific reference material does now exist, but only for a single species and matrix. Thus, as with many speciation studies, there is a need for more reference materials to help validate techniques for environmental analysis. The relatively recent introduction of commercial GC-ICP-MS instruments may serve to stimulate more studies in this area, and further research efforts are required to fully elucidate both the environmental chemistry of lead and to provide reliable methodology for the ongoing monitoring of natural and anthropogenic sources. It is clear that the legacy from the widespread and global use of organoleads in petrol will be with us for some time to come.

6 REFERENCES

1. Harrison, R. M., Radojevic, M. and Wilson, S. T., *Sci. Total Environ.*, **21**, 260 (1986).
2. Harrison, R. M., Radojevic, M. and Wilson, S. T., *Sci. Total Environ.*, **50**, 129 (1986).
3. Harrison, R. M. and Laxen, D. P. H., *Nature,* **275**, 738 (1978).
4. Van Cleuvenbergen, R. J. C. and Adams, F. C., in *Handbook of Environmental Chemistry*, Hutzinger, O. (Ed.), Springer, 1990.
5. Hill, S. J., in *Hazardous Metals in the Environment*, Stoeppler, M. (Ed.), Elsevier, 1992.
6. Ahnstrom, Z. S. and Parker, D. R., *Soil Sci. Soc. Am. J.*, **63**, 1650 (1999).
7. Evans, R. D. and Villeneuve, J. Y., *J. Anal. At. Spectrom.*, **15**, 157 (2000).
8. Wong, P. T. S., Chau, Y. K. and Luxon, P. L., *Nature*, **253**, 263 (1975).
9. Schmidt, U. and Huber, F., *Nature*, **259**, 157 (1976).
10. Berman, M., Chase, T. and Bartha, R., *Appl. Environ. Microbiol.* **56**, 298 (1990).
11. Yanni, S., Berdicevsky, I. and Duck, L., *Appl. Environ. Microbiol.*, **57**, 245 (1991).
12. Walton, A. P., Ebdon, L. and Millward, G. E., *Appl. Organomet. Chem.*, **2**, 87 (1988).
13. Harrison, R. M. and Allen, A. G., *Appl. Organomet. Chem.*, **3**, 49 (1989).
14. Pongratz, R. and Heumann, K. G., *Chemosphere*, **39**, 89 (1999).
15. Shapiro, H. and Frey, F. W., *The Organic Compounds of Lead*, Wiley-Interscience, New York, 1968.
16. Baena, J. R., Gallego, M. and Valcarcel, M., *Anal. Chem.,* **74**, 1519 (2002).
17. Grandjean, P. and Grandjean, E. C. (Eds.), *Biological Effects of Organolead Compounds*, CRC Press, Boca Raton, FL, 1984.
18. Lobinski, R., Szpunlobinska, J. and Adams, F. C., *Analusis,* **22**, 4 (1994).
19. Heisterkamp, M., Van de Velde, K., Ferrari, C., Boutron, C. F. and Adams, F. C., *Environ. Sci. Technol.,* **33**, 4416 (1999).
20. Mikac, N., Branica, M. and Harrison, R. M., *Chem. Spec. Bioavail.,* **13**, 8 (2001).
21. Quevauviller, P., *Method Performance Studies for Speciation Analysis*, The Royal Society of Chemistry, 1998.
22. Ebdon, L., Ward, R. W. and Leathard, D. A., *Analyst,* **107**, 129 (1982).
23. Chau, Y. K., Wong, P. T. S. and Goulden, P. D., *Anal. Chim. Acta,* **85**, 421 (1976).
24. Radziuk, B., Thomassen, Y., Butler, L. R. P., Van Loon, J. C. and Chau, Y. K., *Anal. Chim. Acta,* **108**, 31 (1979).
25. Kolb, B., Kremmer, G., Schleser, F. H. and Wiedeking, E., *Z. Anal. Chem.*, **221**, 166 (1966).
26. Harrison, R. M. and Radojević, M., *Environ. Technol. Lett.,* **6**, 129 (1985).
27. de Mora, S. J., Hewitt, C. N. and Harrison, R. M., *Anal. Proc.,* **21**, 415 (1984).
28. Alonso, J. I. G. and Encinar, J. R., 4.2. Gas chromatography and other gas based methods, in *Handbook of Elemental Speciation: Techniques and Methodology*, Cornelis, R., Caruso, J., Crews, H. and Heumann, K. (Eds.), Wiley, 2003, pp. 163–200.
29. Rapsomanikis, S., Donard, O. F. X. and Weber, J. H., *Anal. Chem.,* **58**, 35 (1986).
30. Chakraborti, D., De Jonghe, W. R. A., Van Mol, W. E., Van Cleuvenbergen, R. J. A. and Adams, F. C., *Anal. Chem.,* **56**, 2692 (1984).
31. Chau, Y. K., Wong, P. T. S. and Kramar, O., *Anal. Chim. Acta,* **146**, 211 (1983).

32. Mikac, N., Wang, Y. and Harrison, R. M., *Anal. Chim. Acta,* **326**, 57 (1996).
33. Radojević, M., Allen, A., Rapsomanikis, S. and Harrison, R. M., *Anal. Chem.,* **58**, 658 (1986).
34. Heisterkamp, M. and Adams, F. C., *Fresenius' J. Anal. Chem.,* **362**, 489 (1998).
35. Heisterkamp, M., DeSmaele, T., Candelone, J. P., Moens, L., Dams, R. and Adams, F. C., *Anal. At. Spectrom.,* **12**, 1077 (1997).
36. Botre, C., Cacace, F. and Cozzani, R., *Anal. Lett.,* **9**, 825 (1976).
37. Messman, J. D. and Rains, T. C., *Anal. Chem.,* **53**, 1632 (1981).
38. Ebdon, L., Hill, S. J. and Rivas, C., *Spectrochim. Acta B At. Spectrosc.,* **53**, 289 (1998).
39. Sommer, D. and Ohls, K., *Fresenius' Z. Anal. Chem.,* **295**, 337 (1979).
40. Ibrahim, M., Gilbert, T. W. and Caruso, J-A., *J. Chromatogr. Sci.,* **22**, 111 (1984).
41. Elfering, H., Andersson, J. T. and Poll, K. G., *Analyst,* **123**, 669 (1998).
42. Garcia-Sanchez, R., Feldhaus, R., Bettmer, J. and Ebdon, L., *J. Anal. At. Spectrom.,* **16**, 7 (2001).
43. Yang, H. J. and Jiang, S. J., *J. Anal. At. Spectrom.,* **10**, 963 (1995).
44. Acon, B. W., McLean, J. A. and Montaser, A., *Anal. At. Spectrom.,* **16**, 6 (2001).
45. Capodaglio, G., Scarponi, G., Toscano, G., Barbante, C. and Cescon, P., *Fresenius' J. Anal. Chem.,* **351**, 386 (1995).
46. Lindim, C., Mota, A. M. and Goncalves, M. L. S., *Water Res.,* **34**, 10 (2000).
47. Bernie, S. E. and Hodges, D. J., *Environ. Technol. Lett.,* **2**, 443 (1981).
48. Bull, K. R., Every, W. J., Freestone, P., Hall, J. R. and Osborne, D., *Environ. Pollut.,* **31A**, 239 (1983).
49. Teeling, H. and Cypionka, H., *Appl. Microbiol. Biotechnol.,* **48**, 275 (1997).
50. Zufiaurre, R., Pons, B. and Nerin, C., *Chromatography A,* **779**, 299 (1997).
51. Pecheyran, C., Lalere, B. and Donard, O. F. X., *Environ. Sci. Technol.*, **34**, 27 (2000).
52. Leal-Granadillo, I. A., Alonso, J. I. G. and Sanz-Medel, A., *Anal. Chim. Acta*, **423**, 21 (2000).
53. Van Cleuvenbergen, R. J. C., Dirkx, W. M. R., Quevauviller, Ph. and Adams, F. C., *Int. J. Environ. Anal. Chem.,* **47**, 21 (1992).
54. Neilson, T., Egsgaard, H., Larsen, E. and Schroll, G., *Anal. Chim. Acta,* **124**, 1 (1981).
55. De Jonghe, W. R. A., Chakraborti, D. and Adams, F. C., *Anal. Chem.,* **52**, 1974 (1980).
56. Heisterkamp, M. and Adams, F. C., *Fresenius' J. Anal. Chem.,* **370**, 597 (2001).
57. Baena, J. R., Gallego, M. and Valcarcel, M., *Spectrochim. Acta B*, **54**, 1869 (1999).
58. Baena, J. R., Cardenas, S., Gallego, M. and Valcarcel, M., *Anal. Chem.,* **72**, 1510 (2000).
59. Mikac, N., Branica, M. and Harrison, R. M., *Chem. Spec. Bioavail.*, **4**, 109 (1992).
60. Sadiki, A. I. and Williams, D. T., *Chemosphere,* **32**, 1983 (1996).
61. Lobinski, R., Boutron, C. F., Candelone, J. P., Hong, S. R., Szpunlobinska, J. and Adams, F. C., *Environ. Sci. Technol.,* **28**, 1459 (1994).
62. Mikac, N., Branica, M., Wong, Y. and Harrison, R. M., *Environ. Sci. Technol.,* **30**, 499 (1996).
63. Mikac, N. and Branica, M., *Sci. Total Environ.,* **154**, 39 (1994).

2.10.2 Speciation of Lead in Food and Wine

Helen M. Crews
Central Science Laboratory, Sand Hutton, UK

1 INTRODUCTION

The major source of Pb for nonoccupationally exposed adults is food and drink [1]. Children may be additionally exposed via Pb in dust and soils, and these matrices may actually be the primary source of exposure for some infants [2]. The element can be present in foodstuffs either because of uptake from the environment or, more likely, because of adventitious contamination. Drinking water has been contaminated particularly in areas where the water is extremely soft and Pb plumbing or Pb-lined storage tanks were used. Wine and port wines can contribute to dietary intake. Wine vintage and color were considered the most significant contributing factors (older vintages tended to be more contaminated with lead than younger vintages, and red wines tended to contain more lead than white wines), but a relatively recent study has shown the presence of brass tubes and faucets in wineries to be the main contamination source with significant reductions in Pb content of wine achieved by changing enological procedures [3].

Lead is the 'oldest' recognized toxic metal [4] and has been recognized for centuries as a cumulative general metabolic poison in high doses, giving rise to acute symptoms such as tiredness, abdominal discomfort, irritability and anemia. This ubiquitous element can be detected in all environmental media with the majority of Pb in the last century arising from automobile and industrial emissions, and from the use of Pb-containing solder and paints [1, 4, 5].

The reader is referred to Chapters 2.10.1 and 2.10.3 in this text for more detailed information about environmental speciation of Pb and its clinical toxicity. However, the lack of ambiguity concerning the toxicity of Pb at elevated levels has resulted in strenuous efforts to decrease exposure. In the United Kingdom, limits for Pb were set very early on in the history of food legislation [6] with review and amendments as scientific and technological knowledge advanced [7].

More recently, Pb exposure has also been of concern because of possible detrimental effects on intelligence [1, 8, 9]. In the United Kingdom, food, air (mainly Pb dust originating from petrol) and drinking water were the major sources for Pb. Although the health effects of long-term, low-level exposure to Pb are less clear than those found with acute high-level intake, the emphasis remains on reduction of exposure. Thus, Pb exposure from

Handbook of Elemental Speciation II: Species in the Environment, Food, Medicine & Occupational Health
Edited by R. Cornelis, H. Crews, J. Caruso and K. G. Heumann
 ISBN: 0-470-85598-3 (HB)

all three sources has been reduced. Mean exposures for the UK population declined from an estimated 0.12 mg per day in 1980 to 0.026 mg per day in 1997. The dietary exposures for mean and 97.5th percentile adult consumers were 0.024 and 0.043 mg per day, respectively, in 1997, with UK figures being similar to those reported internationally, for example, for the United States of America, Canada, The Netherlands, New Zealand, France and Spain [8].

2 IMPACT OF SPECIATION

For Pb in food, drinking water and wines, the reduction of the number of sources of contamination has been a major factor in reducing risk. The increase in international trade in food and raw materials is one factor that drives international regulation of trace elements; real or perceived food safety problems are another factor of which industrial or environmental contamination is one. On 5 April 2002, European Commission (EC) Regulation No. 466/2001, which set maximum limits (MLs) for some contaminants (Pb, Cd, Hg, nitrate and mycotoxins) in foods, came into force. These revised MLs are extremely similar to those set for total Pb in foods in the recent Codex Draft Standard for Lead in Foods (the Codex Alimentarius Commission was set up in 1961 by the FAO and WHO) [8]. In their publication, Berg and Licht [10] cite international rather than national MLs and fixed lower rather than higher MLs as being important trends in food regulation. In this context, they also note that for the future, speciation of contaminants will be important rather than just the total element concentration.

Data on speciation and subsequent bioavailability of an element could contribute significantly to the risk assessment of the threat that it poses from dietary intake. Duffus [11] elegantly exemplified the need for well-informed risk assessment and management when considering exposure legislation. Citing a report [12] that assessed the risk and health hazard of exposure to metals from Alaskan ores, in which Pb bioavailability had been found to be lower than that for other ores, Duffus reports that this information concerning the relatively low bioavailability explained the lower adverse health risk (as demonstrated by the low blood Pb levels found) from environmental Pb in this area than would otherwise have been predicted on the basis of environmental monitoring (high Pb in soils) and the use of default assumptions about Pb bioavailability. Similarly, Oomen *et al.* [13] comment that in a recent Dutch risk assessment of contaminated soils, oral bioavailability of a contaminant from soil was assumed to be the same as in the matrix used for toxicity studies that are typically liquid or food. However, the authors pointed out that studies using test animals demonstrated that absorption and toxicity for Pb ingested with soil was lower than for Pb ingested with food or aqueous solution (assuming of course that bioavailability in test animals is a reasonable measure of the behavior in humans).

What is surprising about Pb is that relatively little work has been undertaken with regard to the chemical form of Pb in foodstuffs and its subsequent bioavailability. As stated earlier, the lack of ambiguity as regards high-level Pb toxicity has meant, correctly, that efforts have been directed at reducing exposure. Studies of Pb behavior and toxicity, *in vitro* and *in vivo*, primarily deal with the Pb^{2+} cation. The most common treatment for acute and chronic Pb intoxication (usually due to occupational or environmental exposure) is chelation therapy, whereby the success of chelating agent depends essentially on its ability to compete with the *in vivo* binding site for possession of the toxic metal ion [14].

Ironically, both the reduction in maximum permitted levels for Pb is food and wine, and improved monitoring and analytical techniques have given rise to some work that has investigated what the likely chemical species are and how bioavailable they might be. For, although adventitious contamination of wine and foodstuffs by Pb has been drastically reduced, the ubiquitous nature of this element means there will always be the possibility of low levels in some foods. Information on the speciation and bioavailability will inform the assessment of risk posed by the ingestion of Pb from these sources.

3 WINE

Historically, the contamination of wine by Pb is associated with the fall of Rome. A popular method of wine 'improvement' was to take low-grade wine that contained fruit acids and evaporate it to obtain a sweetening grape syrup called *sapa*. The subsequent contamination of the wine by the dissolution of Pb from the lining of the vessels (up to 15–30 mg Pb/L) may have resulted in chronic Pb poisoning (saturnism) due to Pb intake from wine exceeding 500 μg per day. This disastrous combination can be explained by the behavior of Pb in aqueous solution. With a redox potential of $E(Pb^{2+}/Pb) = -0.13$ V versus a normal hydrogen electrode, Pb is not a noble metal. However, at pH 7 the potential $2H^+/H_2$ is -0.42 V so that Pb is not attacked by oxygen-free water. The insoluble basic Pb carbonates and sulfates at the surface of the metal form a protective layer [4].

In more recent times, it has been accepted that the trace element content of wines and their possible contamination may reflect several factors, including soil type, wine-processing equipment, agricultural and vinification processes [15]. Medina *et al*. [16] have looked at the influence of atmospheric pollution on the Pb content of some French wines using inductively coupled plasma-mass spectrometry (ICP-MS) and Pb isotope ratio measurements. They were able to demonstrate that during the last century the Pb content reflected the contribution from industrial sources and gasoline. They also noted that the isotopic signature was specific to the continental origin of the wines. In a later publication [17], this group investigated the accuracy and precision of the measurement of Pb isotope ratios in wine using different mass analyzers. Quadrupole, time-of-flight and multicollector ICP-MS were studied, and whilst the accuracy was generally good, the precision at that time (2001) was not considered sufficient to permit the use of Pb isotope ratios as a means of determining geographic origin.

Kaufmann [3] concluded that brass tubes and faucets in wineries were the main contamination source, with significant reductions in Pb content of wine achieved by changing enological procedures. A very recent, detailed study by Almeida and Vasconcelos [18] looked at the entire Portuguese wine-making process from vineyard (including atmospheric aerosols) through to the wine itself as produced in both a modern and a traditional winery. Quadrupole ICP-MS measurement of Pb isotope ratios at the different production stages permitted an assessment of the likely origin of the Pb contamination. The authors concluded that the major sources of Pb were the different containers and devices used during the vinification process. Drastic reduction in Pb content might be made by strict control of the alloys used, for example, in welded materials and small fittings like taps. Soil and atmosphere contributed only about 25–30% of the Pb for concentrations of 17.2 and 13.1 μg Pb/L for fortified (traditional process) and table (modern process) red wines, respectively.

Szpunar *et al*. [19] found that the Pb present in wines was associated with macromolecular complexes, especially polysaccharides. Using results from size exclusion chromatography (SEC) with ICP-MS, they thought that the Pb was mainly complexed by the dimer of a pectic polysaccharide, Rhamnogalacturonan II, which has a high number of negatively charged glycosyl residues. Azenha and Vasconcelos [20] used *in vitro* simulated gastrointestinal digestion, anodic stripping voltammetry and reverse-phase high-performance chromatography with UV and electrothermal atomic absorption spectroscopy detection to study the speciation and bioavailability of Pb in port wine. Their results indicated the presence of a majority of species with low molecular mass and/or high ionic character as well as some other Pb-containing moieties with high molecular and/or apolar character. The former findings were considered compatible with the results from Szpunar *et al*. [19] The Pb speciation remained unaltered after simulated gastric digestion with the Pb present as a soluble form, which was considered potentially bioavailable [20]. However, treatment with simulated intestinal juice reduced solubility and it was postulated that tannins in wine would have this effect. Vasconcelos's group concluded from other work [21] with electrochemical studies of Pb complexation in red wines that the Pb was tightly

bound and possibly associated with polyphenols such as tannins as well as polysaccharides.

Finally, Pb poisoning from wine still occurs, albeit rarely. Mangas *et al*. [22] reported the case of a 66-year-old man who suffered symptoms of severe Pb poisoning for two years before diagnosis. The poisoning was the result of drinking home-made red wine that had been prepared from grape crushings and juice stored, prior to bottling, for one week in a corroded enamel bathtub. The high Pb concentration of the wine was consistent with solubilization of metal from the glaze and highlights the importance of using food grade materials for the preparation of beverages and food.

4 FOOD

Szpunar *et al*. [23] have also investigated the speciation of metal-carbohydrate complexes in fruits and vegetables. For Pb (as well as Be, Sr, Ce and B), a carbohydrate – high molar mass, polysaccharide fraction of greater than 50 kDa – was identified in the solid water-insoluble fraction of the analyzed samples. Enzymatic digestion of apple and carrot samples was used to release these species into the aqueous phase with separation by SEC and parallel refractometric and ICP-MS detection. The carbohydrate was identified as the dimer of Rhamnogalacturonan II, a pectic polysaccharide present in plant cell walls, which has also been associated with Pb species in wine [19].

Three closely related papers by Mounicou *et al*. [24–26] have reported to concentration, speciation and bioavailability of Pb and Cd from cocoa powder and related products (beans, liquor, butter). Children are a key market for cocoa and chocolate, and therefore the bioavailability of these two elements is of interest.

Fifteen extraction procedures were assessed [24, 26], which targeted water-soluble compounds, polypeptide and polysaccharide complexes as well as compounds soluble under simulated gastrointestinal conditions. Separation and detection was by SEC-ICP-MS. Poor extraction recoveries were observed for all extractants, and cocoa powder appeared to demonstrate an enormous capacity for binding both Pb and Cd. The total Pb was below legal limits, and it was concluded that only 10–20% of this could be released in realistic biological conditions. An *in vitro* simulated gastrointestinal digestion indicated that Pb bioavailability did not exceed 5–10%, regardless of the geographical origin of the cocoa [25, 26]. Addition of phytase and cellulase did release further Cd but in contrast, virtually no Pb could be released from the residue remaining after gastrointestinal treatment. A significant proportion of Pb was removed by the shelling process, and most of the remaining Pb was bound and made insoluble by fermentation and roasting processes.

5 CONCLUSIONS

Lead speciation in foodstuffs remains poorly understood. Advances in measurement techniques permit a limited degree of qualitative assessment of the chemical form in complex food matrices. Treatment for Pb poisoning is primarily based on chelation therapy to 'mop up' Pb^{2+} but does not successfully remove Pb from bone and brain tissue. Thus, quite rightly, tremendous progress has been made in recognizing and reducing the concentration of Pb in food, drinking water and wine, but the way in which remaining Pb species from food behave following human ingestion warrants further study if we are to understand the impact of long-term low-level exposure to this ubiquitous element. The key to understanding the risk posed by Pb is to have reliable information relating to realistic exposure levels, the chemical form present in the matrices studied, the interactions with other species and components of the diet and the hazard presented by the combined set of circumstances under which exposure occurs.

6 REFERENCES

1. Environmental Health Criteria 165, *Inorganic Lead*, World Health Organization, Geneva, 1995.
2. Oomen, A. G., Tolls, J., Sips, A. J. A. M. and van den Hoop, M. A. G. T., *Arch. Environ. Contam. Toxicol.*, **44**, 107 (2003).

3. Kaufmann, A., *Food Addit. Contam.*, **15**, 437 (1998).
4. Kaim, W. and Schwederski, B., *Bioinorganic Chemistry: Inorganic Elements in the Chemistry of Life*, John Wiley & Sons, Chichester, UK, 1999, pp. 332–335.
5. Ebdon, L., Hill, S. J. and Rivas, C., *Spectrochim. Acta B*, **53**, 289 (1998).
6. The Public Health (Preservatives etc in Food) Regulations 125, S, R & O, 1925/775, HMSO, UK, 1925.
7. Council of Europe, *Lead, Cadmium and Mercury in Food: Assessment of Dietary Intakes and Summary of Heavy Metal Limits of Foodstuffs*, Council of Europe Press, HMSO, UK, 1994.
8. Ysart, G., Miller, P., Croasdale, M., Crews, H., Robb, P., Baxter, M., de L'Argy, C. and Harrison, N., *Food Addit. Contam.*, **17**, 775 (2000).
9. Pocock, S. J., Smith, M. and Baghurst, P., *Br. Med. J.*, **309**, 1189 (1994).
10. Berg, T. and Licht, D., *Food Addit. Contam.*, **19**, 916 (2002).
11. Duffus, J. H., Risk assessment and trace element speciation, in *Trace Element Speciation for Environment, Food and Health*, Ebdon, L., Pitts., L., Cornelis, R., Crews, H., Donard, OFX and Quevauviller, Ph (Eds), Royal Society of Chemistry, Cambridge, UK, 2001.
12. Middaugh, J. P., Li, C. and Jenkerson, S. A., Health hazard and risk assessment from exposure to heavy metal ore in Skagway, AK (Final report), Alaska Department of Health and Social Services, Anchorage, 1989, in *Reproductive and Developmental Toxicology*, in Korach, K. S. (Ed.), Marcel Dekker, New York, 1993, p. 449.
13. Oomen, A. G., Tolls, J., Sips, A. J. A. M. and Groten, J. P., *Arch. Environ. Contam. Toxicol.*, **44**, 116 (2003).
14. Jones, M. M., Chemistry of chelation: chelating agent antagonists for toxic metals, in *Handbook of Experimental Pharmacology*, *Toxicology of Metals, Biochemical Aspects*, Vol. 115, Goyer, R. A. and Cherian, M. G. (Eds), Springer-Verlag, Berlin, Heidelberg, 1995.
15. Salvo, F., La Pera, I., Di Bella, G., Nicotina, M. and Dugo, G., *J. Agric. Food Chem.*, **51** 1090–1094 (2003).
16. Medina, B., Augagneur, S., Barbaste, M., Grouset, F. E. and Buat-Meard, P., *Food Addit. Contam.*, **17**, 435 (2000).
17. Barbaste, M., Halicz, L., Galy, A., Medina, B., Emteborg, H., Adams, F. C. and Lobinski, R., *Talanta*, **54**, 307 (2001).
18. Almeida, R. and Vasconcelos, M. T. S. D., *J. Agric. Food Chem.*, **51**, 3012 (2003).
19. Szpunar, J., Pellerin, P., Markarov, A., Doco, T., Williams, P., Medina, B. and Lobinski, R., *J. Anal. At. Spectrom.*, **13**, 749–754 (1998).
20. Azenha, M. A. G. O. and Vasconcelos, M. T. S. D., *J. Agric. Food Chem.*, **48**, 5740 (2000).
21. Vasconcelos, M. T., Azenha, M. and de Freitas, V., *Analyst*, **125**, 743 (2000).
22. Mangas, S., Visvanathan, R. and van Alpen, M., *Environ. Health Perspect.*, **109**, 433 (2001).
23. Szpunar, J., Pellerin, P., Markarov, A., Doco, T., Williams, P. and Lobinski, R., *J. Anal. At. Spectrom.*, **14**, 639 (1999).
24. Mounicou, S., Szpunar, J., Lobinksi, R., Andrey, D. and Blake, C. J., *J. Anal. At. Spectrom.*, **17**, 880 (2002).
25. Mounicou, S., Szpunar, J., Andrey, D., Blake, C. and Lobinksi, R., *Analyst*, **127**, 1638 (2002).
26. Mounicou, S., Szpunar, J., Andrey, D., Blake, C. and Lobinksi, R., *Food Addit. Contam.*, **20**, 343 (2003).

2.10.3 Speciation of Lead in Occupational Exposure and Clinical Health Aspects

Perinne Hoet

Université catholique de Louvain, Brussels, Belgium

1 OCCUPATIONAL EXPOSURE

1.1 Introduction

Lead in the environment may derive from either natural or anthropogenic sources. The major natural sources of lead are volcanic emissions, geochemical weathering, and emissions from sea spray. Lead occurs naturally in four isotopic forms of mass numbers 204, 206, 207, and 208. The isotopic abundance, and so the atomic weight, varies in lead from different locations. The average atomic weight is 207.22. Although lead has four electrons in its valence shell, only two ionize readily. The usual valence state in inorganic lead compounds is therefore +2 rather than +4. It is widely distributed all over the world in the form of its sulfide, the ore galena (PbS). Ores of secondary importance are cerussite ($PbCO_3$) and anglesite ($PbSO_4$) [1–4].

Lead has a unique combination of physical and chemical properties that have made it extremely useful. These properties are high density, high opacity to γ- and X-ray energies, low sound conductance, low melting point (about 327 °C), high boiling point (>1700 °C), relatively poor conduction of electricity, high resistance to corrosion and acid, and chemical stability in air, water, and soil. Lead is a very soft and malleable metal, easily melted, cast, rolled and extruded. In the form of metal, either pure or alloyed with other metals, or as chemical compounds, lead has had and still has many and varied uses [1–5].

Handbook of Elemental Speciation II: Species in the Environment, Food, Medicine & Occupational Health
Edited by R. Cornelis, H. Crews, J. Caruso and K. G. Heumann
 ISBN: 0-470-85598-3 (HB)

It has been among the first metals to be extensively utilized by humanity: it is believed that it was used as early as 5000 B.C. Lead-rich glazes have been found on pottery in ancient Egypt. Prior to the time of the Roman Empire, the principal goal of lead extraction appears to have been the obtaining of silver, as the two metals frequently occur together. However, following the beginning of this era, lead was used, as a material in its own right, for a host of miscellaneous uses. It became a key component in cosmetics (face powders, rouges, mascara); the pigment in many paints; a spermicide for informal birth control; the ideal 'cold' metal for use in the manufacture of chastity belts; a wine preservative perfect for stopping fermentation or disguising inferior vintages; the malleable and inexpensive ingredient in pewter cups, plates, pitchers, pots and pans; the component of lead coins as well as counterfeit silver and gold coins. Lead's most enduring use probably has been as pipes for the transportation of water, an application that has extended from Egyptian and Roman times to the present day. The word 'plumbing' comes from 'plumbum', the Latin word for lead.

The use of lead declined after the collapse of the Roman Empire, but in the Middle Ages in Europe, lead began to be used again for many applications. At the dawn of the third millenary, lead is still wildly used: for example, in batteries, cable sheathing, medical equipment (protective shielding for radioactive material, electronic ceramic parts of ultrasound machines, intravenous pumps, monitors, etc.), paints and pigments, ceramic glazes, metal rolled and extruded products (such as sheet lead, solder, some brass and bronze products, and pipes), military equipment (jet turbine engine blades, military tracking systems), ammunition and lead fishing weights, crystal glass, alloys, gasoline additives. These last decades, some of these applications, such as for water piping, as an antiknock agent in gasoline, a solder in food cans, in house paints and in pesticides, have recently been phased out, or at least greatly reduced, in view of the potential for risks to health [3, 6]. However, nonoccupational exposure to lead still occurs, for example,

1. by eating foods or drinking water contaminated by lead via the environment (lead-contaminated dust falling onto food), dissolution from glazed pottery or ceramic dishes, lead-crystal glassware, or lead-soldered containers;
2. by spending time in areas contaminated by flaking leaded paints;
3. by having hobbies such as indoor firing or in which lead may be used such as in sculpturing (lead solder) and staining glass;
4. by using folk remedies or cosmetics that contain lead.

The improvement in working conditions and health surveillance programs has decreased the level of exposure in many work settings. Nevertheless, relatively high exposures are still present in less controlled work settings in industrialized countries. Moreover, concerns about the possible effects of long-lasting exposure to low lead level have been raised.

1.2 Main lead compounds

The following are the main lead compounds [5, 7, 8].

Lead metal: Pb

Lead has a bright silvery luster when its surface is freshly cut. In contact to air, it quickly becomes covered by a dull, bluish-gray layer; a rapid reaction between metallic lead and O_2 to form lead oxide that then reacts with CO_2, forming a protective film of lead carbonate. When placed in sulfuric acid, lead is protected by a similar layer of $PbSO_4$ that adheres strongly. For these reasons, lead is often used to sheathed cables for burial, to protect roofs from the atmosphere, and as tanks and pipes for sulfuric acid. Lead is considered to be insoluble in water. In leaded pipes, soft water, containing nitrates, ammonium salts, and CO_2 in solution, dissolves appreciable amounts of lead. The presence of carbonates from limestone or chalk prevents this process by the formation of a coating of lead carbonate on the interior of pipes, which protects the water from further

contamination with lead [9]. Lead is fairly soluble in nitric acid and to some extent in organic acids such as acetic and food acids but is little affected by sulfuric or hydrochloric acids at room temperature. The large interval between the melting point of lead and its boiling point allows processes in liquid state over a wide temperature range.

Lead monoxide (litharge or massicot or lead oxide yellow or plumbous oxide; PbO) is a reddish-yellow (yellow above 489 °C) crystalline powder formed by heating lead in air. At 300–450 °C, it converts slowly into Pb_3O_4 but at higher temperature reverts to PbO. It is poorly soluble in water but highly soluble in acetic acid and diluted nitric acid. *Lead dioxide* (lead peroxide or lead brown; PbO_2) is a dark-brown powder that evolves oxygen when heated first, forming Pb_3O_4 and, at high temperature, PbO. Insoluble in water, it is soluble in hydrochloric acid and oxalic acid. *Lead tetroxide* (red lead or minium or Paris red or Saturn red; Pb_3O_4) is a bright red to orange-red, heavy crystalline powder formed by oxidation of lead metal or lead monoxide. It is almost insoluble in water but soluble in acetic acid and in diluted nitric acid. When heated at ~500 °C, it decomposes with release of O_2 and emission of lead fumes.

Lead acetate (sugar of lead or Goulard's powder; $Pb(CH_3COO)_2$) occurs as trihydrate ($Pb(CH_3COO)_2 \cdot 3H_2O$), colorless crystals, or white granules or powder highly water-soluble but very slightly soluble in alcohol. It is made by dissolving PbO with acetic acid. Called sugar of lead because of its sweet taste, it has been used to sweeten sour wine. This is also the reason many wine producers processed their wines in lead vessels. *Lead subacetate* (basic lead acetate) is obtained by dissolving PbO with lead hydroxide in aqueous solution of lead acetate. *Basic lead carbonate* (ceruse; $2PbCO_3 \cdot Pb(OH)_2$) is a mixture of lead carbonate and lead hydroxide; it is a heavy, white powder, insoluble in water and soluble in acids. It is one of the oldest paint pigments that have been used for over 2000 years as a white pigment. *Lead chromate* (chrome yellow or King's yellow or Paris yellow; $PbCrO_4$) is a crystalline yellow or orange-yellow powder prepared by the reaction of lead acetate and potassium bichromate. It is one of the most water-insoluble salts and is also insoluble in acetic acid but soluble in diluted nitric acid. *Lead sulfate* ($PbSO_4$) occurs as the mineral anglesite (and lanakite). Anglesite crystals are usually white or yellow but can also be colorless, gray, and green. Lead sulfate is poorly soluble in water and is formed by roasting galena to a high temperature and driving off some of the sulfur. *Lead arsenate* ($AsHO_4Pb$) is a white heavy powder or crystal insoluble in water but soluble in nitric acid and caustic alkalies. At ~280 °C, it loses H_2O and is converted into pyro-arsenate. It has been used extensively as an agricultural insecticide in fruit orchards until the advent of synthetic organochlorine in the 1950s.

Organic lead compounds The most important organolead compounds are the tetra-alkyl compounds: *tetraethyl lead* ($Pb(C_2H_5)_4$) (TEL) and *tetramethyl lead* ($Pb(CH_3)_4$) (TML). TEL is a highly volatile and lipid soluble liquid with a boiling point at about 200 °C. TML is also highly volatile and lipid soluble.

In the United States, the domestic use pattern for lead in 1990 was as follows: lead-acid storage batteries, used for motor vehicles, motive power, and emergency backup power, accounted for 80% of total lead consumption; ammunition, bearing metals, brass and bronze, cable covering, extruded products, sheet lead, and solder represented 12.4%; the remaining 7.6% was used for ceramics, type metal, ballast or weights, tubes or containers, oxides, and gasoline additives [1].

1.3 Main occupational exposures

The main occupational activities that may present lead hazards for workers involve exposure to metallic lead or inorganic lead compounds and are the following [1–4, 8, 9].

- *Lead and nonferrous smelting and casting*: While primary smelting involves the extraction of the metal from lead-containing minerals, the secondary lead-smelting plants recycle lead from scrap metal or batteries. Lead is obtained

from its most common ore, galena or lead sulfide, by roasting the ore to remove the sulfur and to obtain lead oxide that is then reacted with coke in a furnace. The resulting 'lead bullion' contains many impurities such as silver and gold as well as antimony, arsenic, copper, tin and zinc. These impurities are then removed by various refining steps to obtain pure lead. Recycling accounts for about 70% of usage. Smelting is associated with considerable exposure. The risk comes partly from the lead fumes generated at the high temperatures required and partly from the lead oxide dust spread around the workplace. Operations involving molten lead, at temperature $>500\,^{\circ}C$, generate lead fumes and particles of small size range. Studies have shown that 95% of the particles emitted from secondary lead-smelting operations are less than 5 μm in diameter. The chemical forms most often detected are lead sulfide (PbS), lead sulfate (PbSO4), and elemental lead [10]. Another form emitted from mining operations and smelters is lead oxide-lead sulfate (PbO$\times$PbSO4) [1]. The spillage of molten waste products results in dusty floors. Lead sheets are mainly used in the building industry to prevent water penetrating and for roofing and cladding as well as in lining of chemical treatment baths, acid plants, and storage tanks and vessels. It also has sound insulating properties. Lead pipes have not been used in new domestic water supplies for about 30 years, but they are still used for carriage of corrosive chemicals at chemical plants.

- *Lead-acid battery manufacturing*: Schematically, lead is cast into grids, and a paste of lead oxides is pressed into the grids. Lead dioxide is pasted on to the battery grids and is the active material in the electrochemical reaction. Lead–antimony alloys are also used. Hence, at all stages in battery manufacture, that is, pasting, forming, assembling, welding of battery connectors, except for final assembly and finishing, workers can be exposed to high air lead concentrations, particularly lead oxide dust.
- *Welding, soldering activities*: Welding and soldering lead creates lead vapor, which is easily inhaled. Soft solders are largely lead–tin alloys with or without antimony, while fusible alloys are various combinations of lead, tin, bismuth, cadmium and other low melting point metals. Varying the tin content varies both the melting temperature and the melting characteristics. Lead-rich solders that contain very little tin are used for applications such as soldering parts of car radiators in which the temperatures reached require that the solder has a higher melting point so that the joint strength is maintained. Lead alloy solder is used in electrical or electronic assemblies: transistors, relays, and other components in the printed circuit boards used in all computers and advanced electronic equipment. When metals containing lead or lead-containing coating are heated in the process of welding or cutting, copious quantities of lead in the respirable size may be emitted [4].

  Many occupational activities may involve lead melting, welding, or soldering, for example,
  - ammunition manufacturing (melting lead and molding bullets);
  - production of lead weights for fishing as well as for other weighting applications, for example, curtain weights, wheel balance weights, weights for analytical instruments;
  - assembling of cars, automobile repair, automobile radiators repair;
  - plumbing activities in older building;
  - stained-glass windows manufacturing.
- *Lead-glazed pottery, crystal glass, and ceramicware making*: Crystal glass is one of the most attractive forms in which lead is used. Lead oxide (PbO) is used in producing fine 'crystal glass' and 'flint glass' of a high index of refraction for achromatic lenses. The term 'semicrystal' indicates a lead content in the region of 14–24% as lead oxide, the term 'Full Lead Crystal' indicates a 24% lead content. The very finest quality crystal will have up to 36–70% lead content. It adds clarity, density and brilliance to the glass. Lead is also used in optical glasses (e.g. telescopes, binoculars), ophthalmic glass (e.g. spectacles), electrical glass (e.g. lamp tubing), and radiation protection glasses (e.g. for windows for radiation remote handling boxes, TV tubes). High-purity lead

oxide is used to make precision glasses needed for lasers, low-dose X-ray machines, fiber-optic probes, medical camera systems, and low-light military equipment such as night vision scopes and goggles.

Lead is used in a wide range of glaze formulations for items such as tableware (earthenware and china), wall and floor tiles, porcelain, and some sanitary equipment. The lead compounds used are largely litharge, red lead, and lead silicates. The properties offered by lead compounds are lower melting points and wider softening ranges, low surface tension, good electrical properties and a hard-wearing and impervious finish. Lead compounds are also used in the formulation of enamels used on metals and glasses. Another application for lead compounds, such as the lead zirconate/lead titanate, is piezoelectric ceramics used in the electronics industry: spark generators, sensors, electrical filters, sound generators, and so on.

- *Pigments and paints production and use*: The use of white lead (ceruse) in interior paints has been largely discontinued since 1930–1940 but lead continues to be used in pigments. Chrome red, orange chrome yellow, and lemon chrome yellow are some of the pigments obtained from lead chromate. Lead chromate is used extensively as the yellow pigment in road marking. Lead sulfates are used as white pigments. Lead acetate is used in hair dyes but also as dryer in paints, pigments inks, and varnishes. Lead monoxide produces iridescent colors on brass and bronze. It is also the traditional pigment for rust-inhibiting priming paints applied directly to iron and steel. Calcium plumbate-based paints are particularly effective on galvanized steel, avoiding the need for etch primers. Hence, occupational activities with particularly high potential lead exposures include construction, renovation or demolition work involving welding, cutting, brazing, blasting, and so on, on leaded paint surfaces. Burning metallic lead or lead-coated materials can result in the generation of high concentrations of lead fumes. Workers engaged in the demolition of ships, bridges, railways and various other iron and steel – structures often covered by several layers of leaded paint – are at risk of occupational exposure to extremely high air lead levels as they cut, weld, or burn through the painted metal. Sanding and scraping lead-based paint from such lead-painted metal constructions or from walls in old houses also create airborne lead dust, which is easily inhaled and/or ingested.
- *Radiation (X-rays, γ-rays), vibration, and sound shielding production*: The shielding of containers for radioactive materials is usually metallic lead. Radioactive materials in laboratories and hospitals are usually handled by remote control from a position of safety behind a wall of lead bricks, and X-ray machines are normally installed in rooms lined with sheet lead. Lead compounds are a constituent of the glass used in shielding partitions to permit safe viewing. Lead powder can be incorporated into plastic and rubber sheeting as a material for protective clothing. This material is used to make radiation protective clothing and aprons for the medical, scientific, and nuclear industries. Lead is used in radiation protection glasses (e.g. for windows' computers, TV, which emit γ-rays and X-rays). Lead–antimony alloys are used in radiation shielding both for lining the walls of X-ray rooms and for bricks to house radioactive sources in the nuclear industry. Lead shields are also very effective as sound and vibration absorbers.
- *Plastics and rubber products industry*: Lead compounds (tri-, tetrabasic lead sulfate, basic lead carbonate, lead stearates) are used in the manufacture of polyvinyl chloride to extend the temperature range at which they can be processed without degradation (thermal stabilizer). Dibasic lead phosphite has the additional property of protecting the article from degradation by ultraviolet light. Additionally, normal and dibasic lead stearates are incorporated as lubricants. All these lead compounds are pigmenting white powders and thus cannot be used when clear or translucent articles are required. The potential hazard of the use of such lead compounds is

mainly the dust that is generated when they are milled and mixed with the polyvinyl chloride and the plasticizer.

- *Other more or less common occupational exposures entailing lead exposure are*:
  - firearms instructors who spend most of their time in poorly ventilated indoor ranges are exposed to lead fumes and dust generated by the firing of a gun;
  - jewelry and decorative wares;
  - cable sheathing;
  - textile industry: lead acetate, nitrate and dioxide are used as mordant in textile printing and dyeing;
  - explosive industry: lead nitrate and azide are used in the manufacture of some explosives.
- The overall market of organic lead (TEL, TML) has declined considerably, as its primary use as chief antiknock compound added to gasoline is now banned in many countries because of its significant contribution to air pollution. Some developing countries still use it. Workers involved in the manufacture of both tetraethyl and TML are exposed to both inorganic and alkyl lead. A major potential hazard in the manufacture of these lead compounds appears to be from skin absorption.

According to the Occupational Health and Safety [11] (Lead) Regulations 2000, 'lead-risk job' means a job in which the blood lead level of the employee is reasonably likely to rise above

1. 300 $\mu g\,L^{-1}$; or
2. 100 $\mu g\,L^{-1}$ for female employees of reproductive capacity;

2 CLINICAL: HEALTH ASPECTS

2.1 Toxicokinetics

2.1.1 Absorption

The bioavailability and hence the toxicity of lead are dependent on the route of exposure, dose, chemical structure, solubility, particle size, matrix incorporation, and other physiological and physicochemical factors. Lead and lead compounds enter the body mainly through ingestion and inhalation [1–4].

2.1.1.1 Ingestion

Gastrointestinal absorption of lead involves uptakes from food and beverages, ingestion of nonfood material mainly in children because of their hand-to-mouth behavior, and swallowing of lead particles that travel up the mucociliary system in the upper respiratory tract. Ingestion may occur through eating, smoking, or nail-biting with lead-contaminated hands. In occupational settings with poor hygienic standards, and where workers eat and smoke cigarettes in a lead-contaminated workplace, this route of exposure may become of main importance. Airborne dusts settle out of the air onto food, water, the worker's clothing and other objects, and may be subsequently transferred to the mouth. A hand-to-mouth behavior or 'pica' (the habit of eating nonfood objects; e.g. toys, hands) is normal in preschool children, but in a lead-contaminated environment, they are at greater risk, and this behavior may pose sometimes serious threats [1, 2, 4].

Absorption of lead from the gastrointestinal tract is influenced by several factors such as the physiological state of the individual (e.g. age, fasting, pH of stomach, nutritional status, diet) and the physicochemical nature of the ingested material (e.g. particle size, solubility in biological media, species). In adults, it is generally considered that about 10% of the lead is absorbed when ingested with food while under fasting conditions absorption rates ranging from 40–70% are reported. In infants and young children, gastrointestinal absorption of lead appears to be higher than in adults and may account for 40–50% of the ingested dose.

The gastrointestinal bioavailability of lead is dependent on its *species*: the rate of gastrointestinal absorption of lead nitrate, lead sulfide, and lead cysteine in adults was 16–53% compared to the 40–70% of lead chloride. Beverages stored in lead-crystal glass can accumulate high concentrations of readily bioavailable lead. A study on

volunteers indicated that, on average, 70% of the ingested dose of lead was absorbed [12]. Studies on rats showed that bioavailability was highest for lead carbonate followed by lead tallate and acetate, intermediate for lead oxide, followed by lead sulfide, naphthenate, and octoate and lowest for lead chromate [13, 14]. A key factor in regard with lead bioavailability appears to be its *solubility* at the *pH of the fluid*. The higher absorption of lead carbonate (poorly water-soluble compound) by comparison to lead acetate (a more water-soluble compound) possibly reflects its greater solubility in gastric juice. Lead sulfide was shown to be relatively insoluble in water and saliva, but 800 times more soluble in simulated gastric juice [15]. *In vitro* studies showed that at pH 1.3, simulating a gastric fluid, PbS solubility was 0.94% while at pH 7.2 simulating duodenal alkalinity, 99.82% lead precipitated [16]. Lead in soil dust or mining waste has a low water solubility [13, 17, 18]; however, a higher degree of solubilization is observed at a pH about 1 [19–22].

Absorption is also influenced by the *size* of the ingested particles: large particles (e.g. paint chips) are poorly absorbed, whereas fine dust particles licked from the fingers or other objects may contribute to an increased lead load. An absorption rate of 17% was estimated for lead in paint chips in children aged 2–3 years [1, 2]. An inverse relationship was found between particle size and Pb absorption; this relationship being most marked in the 0–100 μm range. A marked enhancement of absorption was observed for Pb from dried paint films containing lead chromate and lead octoate when particle size was reduced from 500 to 1000 μm to less than 50 μm [23]. The solubility of lead sulfide in gastric juice *in vitro* was shown to be much greater for particles of 30 μm diameter than of 100 μm [15].

Gastrointestinal absorption of lead is influenced by the *nutritional status* and several *dietary factors* [24–26].

The presence of calcium and phosphate in a meal reduces the gastrointestinal absorption of lead. An inverse relationship has been observed between dietary *calcium* intake and blood lead concentration in children [1]. It seems that milk alone may not be an effective source of calcium for this purpose; possibly because other dietary constituents of milk such as lactose and fat may enhance lead absorption. The effect of a meal on the rate of lead absorption is probably largely due to its content of calcium and phosphate salts [27, 28]. It has been shown that the uptake of lead from the gastrointestinal tract declines progressively as the amount of minerals ($CaCO_3$ and NaH_2PO_4) taken simultaneously increases. Taken alone at amounts present in an average meal, calcium and phosphorus reduced lead uptake by a factor of 1.3 and 1.2, respectively. Both together caused an effect that was more than additive and reduced the uptake by a factor 6 [27]. Complexation with calcium (and phosphate) in the gastrointestinal tract and competition for a common transport protein have been proposed as possible mechanisms for this interaction. Actually, the mechanisms by which dietary calcium reduces gastrointestinal lead absorption involve complex interactions among lead, dietary calcium, intestinal calcium-binding proteins, and vitamin D, specifically 1,25-dihydroxyvitamin D [29]. During pregnancy and lactation, there is an increased need for calcium, and at the same time lead absorption is increased.

Gastrointestinal absorption of lead occurs primarily in the duodenum. The exact mechanisms of absorption are unknown and may involve active transport and/or diffusion through intestinal epithelial cells or between cells, and ionized lead (Pb^{++}) and/or inorganic or organic complexes of lead [1]. A metal-ion transporter (DMT) 1 for divalent metal transporter or (DCT) 1 for divalent cation transporter has been recently identified in the rat. DMT 1 has an unusually broad substrate range that includes Fe^{++}, Zn^{++}, Mn^{++}, Co^{++}, Cd^{++}, Cu^{++}, Ni^{++}, and Pb^{++} with as consequence the possibility of interplay among all these elements. DMT 1 mediates active transport that is proton-coupled, depends on the cell membrane potential, and seems ubiquitously expressed, most notably in the proximal duodenum [30]. Expression of this protein in the proximal duodenum, the site of metal transport, has been shown to be dramatically increased by

dietary iron deficiency [31]. Furthermore, an association between iron deficiency and elevated Pb-B is observed, and it is suggested that iron deficiency can result in increased lead absorption [2, 32, 33]. Data are, however, not very clear. On the one hand, a weak positive correlation between iron levels in food and lead absorption (administered as lead sulfate) has been reported [33]. On the other hand, the body lead retention in human volunteers was found not to be related to the capacity to absorb iron or to the size of body iron stores, nor was it affected by the simultaneous ingestion of a 10-fold molar excess of iron [34].

Other dietary components bind lead particles and increase their elimination; a.o. organic acid such as sodium citrates in agrumes, ascorbic acid, lipids, lactose, phytates found in leafy green vegetables [28]. On the contrary, deficiency in vitamin B1 and fibers are reported to enhance gastrointestinal lead absorption [35].

The primary importance of the diet can be illustrated by the following experiment. The bioavailability of lead was studied in rats fed various baby foods, cow's milk, bread, liver, and standard rat diet. Highest absorption values ranging from 17 to 20% were obtained in animals fed cow's milk and fruit foods. Rats on other 'human' diets absorbed between 3 and 8% of the dose. While animals fed on a typical rat diet showed a lead gastrointestinal absorption below 1%, those on a 'human' diet showed absorption values similar to those in humans. This might indicate that the bioavailability of lead is primarily dependent on dietary habits [36].

Some data are consistent with a saturable transport process across the gastrointestinal tract [1, 2].

2.1.1.2 Inhalation

Inhalation is another common route of exposure to lead in both the general and the working environments [1–4]. The movement of lead from ambient air to the bloodstream is a two-part process: deposition of a fraction of inhaled air lead in the respiratory tract and absorption of the deposited fraction [4]. When particles are inhaled, depending on the *particle size*, lead is deposited in the upper and/or lower respiratory tracts. Only lead particles smaller than 1 μm in diameter and lead fumes reach the lower respiratory tract. Almost all lead in ambient air is bound to fine particles of less than 1 μm diameter, although some may be solubilized in acid aerosol droplets. The size of these particles varies with the source and with the age of the particle from the time of emission [2, 4]. Traffic-generated lead aerosols are mostly of the submicron size; they can penetrate deeply into the lungs after inhalation. Lead fumes and vapors, such as those generated in operations where metals are cut or heated, are of very small size and are respirable [2]. Lead inhalation is a particular hazard to workers in many lead industries, including mining, smelting, metal repair, or foundry work, demolition, and renovation activities that generate fumes and dusts. Activities involving the sanding, scraping, burning, welding, cutting, casting of lead, or lead-painted objects can generate respirable lead fumes and lead particles [2, 4].

In adults, the deposition rate of particulate airborne lead is around 30–50%, depending on factors such as particle size and ventilation rates. It appears that the chemical form of the lead compound inhaled is not a major determinant of the extent of alveolar absorption of lead. It is considered that regardless of chemical form, over 90% of lead deposited in the lungs is absorbed because the rate of lead uptake is mainly governed by the length of time lead is retained in the lungs [4]. However, workers exposed to aerosols of lead silicate-containing crystal particles showed lower lead blood levels than workers exposed to similar atmospheric lead levels in plants manufacturing lead-acid batteries, for instance. This was assumed to be due to the lower bioavailability of this lead species [37]. Larger particles are mainly deposited in the upper respiratory tract, cleared by mucociliary transport, swallowed, and eventually absorbed in the gastrointestinal tract at different rates based largely on speciation.

When PbS dust is heated by welding, then relatively more soluble PbO particles with smaller size are generated. The smaller PbO particles reach

the alveoli to a much greater extent than the larger PbS particles and are more readily absorbed [4].

Case reports of lead intoxication after gasoline sniffing indicate lung absorption of TML [38–40]. In workers exposed to tetralkyllead, absorption was evident as shown by elevated urinary lead [41, 42]. In volunteers, at least 30% of the inhaled dose was found to be absorbed via the lungs [1]. Deposition of TEL in lung was also shown to depend on particle size, varying from 40% for fresh, highly diluted aerosols to 14% for mature, aggregated aerosols, at a breathing rate of 15 breaths per minute. Uptake from the lung was rapid ($T\ 1/2 = 6.6$ h) and virtually complete with little, if any, ciliary clearance [43].

2.1.1.3 Dermal

Dermal absorption of inorganic lead through unabraded human skin is considered to be minimal [1, 2]. There is some indication of limited percutaneous absorption of compounds such as finely powdered lead metal, lead nitrate, or acetate solution [44–48].

Organolead compound such as tetrabutyllead, tetraethyl lead, tetramethyllead, or lead naphthenate are, on the opposite, quickly absorbed via the skin [1, 48].

2.1.2 Distribution

The distribution of lead appears to occur in a similar manner regardless of the route of absorption, implying a common transport system [1, 2]. Lead can cross the cell membrane in various ways, which are not yet entirely understood. Lead transport through the erythrocyte membrane is mediated by the anion exchanger in one direction and by the Ca-ATPase pump in the other. In other tissues, lead permeates the cell membrane through voltage-dependent or other types of calcium channels [1].

Lead is not distributed homogeneously throughout the body. Several pharmacokinetic models have been proposed to characterize the different compartments and their interactions [1, 49–55]. Three main compartments, comprising each several pools, can be defined: blood, soft tissues, and bones.

The blood compartment, with a half-life of about 35 days, includes the red cells Pb pool, the protein-bound lead in plasma and the free diffusible lead in plasma. Under steady state conditions, over 98% of lead present in blood is found in erythrocytes. Hemoglobin is generally regarded as the principal lead-binding protein in erythrocytes. However, a stronger affinity of lead for another protein of 240 kDa and identified as aminolevulinic acid dehydratase (ALA-D) has been found. Two other proteins have also been identified: a 45-kDa protein (possibly pyrimidine-5-nucleotidase) and a $<$10-kDa protein [56].

The plasma pool appears to be more related than the erythrocyte pool to the diffusibility of lead outside the blood stream and to membrane permeability. Because of its greater bioavailability, the plasma fraction is considered to directly influence the lead concentrations in other compartments. The percentage ratio for lead in plasma to lead in whole blood has been proposed as a 'bioavailability index', and this index was shown to be at least two times higher for stearate workers than for workers exposed to inorganic Pb compounds. These data suggest that the different chemical properties of Pb stearate may result in different distributional patterns of the metal in different blood components [57, 58]. Serum Pb was found to correlate more strongly with bone lead (both tibia and calcaneum) than did whole blood Pb. The ratio of serum lead to whole blood Pb varies from 0.8 to 2.5% and shows a positive correlation with tibia, and even a stronger relation with calcaneus (trabecular) lead [59].

The second compartment, mainly composed of soft tissues with different turnover, has an average biological half-life of about 40 days. The highest lead levels in soft tissues were found in liver, followed in order of concentration by kidney, lung, and brain, among both exposed workers and controls [60]. In accidents involving exposure to tetraethyl lead, highest lead levels were observed in liver, kidney, brain, followed by pancreas, muscle, and heart [61]. Higher concentrations of lead are

found in the brain following exposure to tetra-alkyl lead than following exposure to inorganic lead compounds, reflecting the affinity of organic lead compounds for the lipid-rich tissue of the human CNS [62].

The third compartment, the skeleton, is the major reservoir of lead; it contains about 95% of total body Pb in adults. It seems that children do not possess the same capacity as adults to retain lead in bone, as only about 75% of their body burden is stored in their skeleton [63]. The bone compartment seems to have at least two, probably three, kinetically distinct lead pools: trabecular (spongy) and cortical (compact) bones. The half-life in the first pool is probably less than 10 years, while the half-life in the second one is more than ten or even 15 years. Bone is considered as a major storage site for Pb but not as an inert storage site; it constitutes an endogenous source of exposure to lead. Not all the lead in bone is equally exchangeable with blood. The inability of chelation to remove appreciable proportions of lead bone indicates that some is unavailable for exchange. Once lead has penetrated the crystal surface of bone, it becomes firmly buried and must await osteoclatic turnover to be released [64]. Bone lead storage is a two-way process of active influx and efflux that follows the general physiology of bone mineral (Ca^{++}) metabolism [65, 66]. The release of lead from the skeleton was calculated to contribute to 40–70% of the lead in the blood in workers exposed to inorganic lead [67]. Mobilization of lead from bone can occur in physiological or pathological situations entailing an increased bone turn over or demineralization [65] such as in pregnancy and lactation, senile or idiopathic osteoporosis [68, 69], bone fracture or immobilization [70, 71], bone cancer [72], hyperthyroidism [73–76], and chemotherapy [77, 78]. This mobilization can greatly affect the blood lead concentration and cause adverse effects, including to the fetus. Lead mobilized from skeletal stores at an accelerated rate during pregnancy contributes significantly to blood lead levels during pregnancy. Increases in Pb-B of approximately 20% during pregnancy, mainly the second half, have been detected even in subjects with low blood lead levels. The skeletal contribution to blood lead level showed a mean increase of 31% (from 9 to 65%) [79]. Transplacental transfer of lead is well documented. The mechanism for lead transport is not well defined but might be a matter of simple diffusion. There is no placental-fetal barrier to lead transport: the lead concentration in cord blood is 85–90% that of maternal blood [80–83].

Inorganic lead is not biotransformed in the body, but Pb^{++} form complexes with protein and nonprotein ligands. It was demonstrated that in a totally asymptomatic patient with a Pb-B at 1800 $\mu g\,L^{-1}$, most of the erythrocyte lead was associated with a metallothionein-like protein. It was suggested that this protein acted to sequester lead into a nonbioavailable form, hence protecting the body from lead toxicity as in another patient with clinical signs of intoxication and a Pb-B level 1610 $\mu g\,L^{-1}$, the protein only contained about 20% of the total lead, with significant amounts bound to high molecular weight proteins, including Hb [84]. Actually, the intracellular bioavailability of lead in major target organs such as the kidney and brain appears to be largely determined by complexation with a group of low molecular weight proteins [85].

Alkyllead compounds undergo a dealkylation mediated by cytochrome P-450. Dealkylation of tetraethyl and TML leads to the formation of triethyl and trimethyl metabolites and inorganic lead [1]. Further degradation to dialkyl lead compounds also occurs in the liver and the predominant metabolite excreted after exposure to TEL is diethyl lead.

The higher toxicity of TEL by comparison with TML appears to be related to the rate at which each is dealkylated *in vivo*; TML is dealkylated more rapidly than is TEL in rats. Dialkyl lead compounds do not appear to be of toxicological significance [62]. Organic lead is also partly degraded *in vivo* to inorganic lead [62].

2.1.3 Excretion

Unabsorbed lead is eliminated in the feces; inhaled lead that has been swallowed after clearance by

the mucociliary process and not absorbed in the gastrointestinal tract is also eliminated in the feces. Absorbed lead that is not retained is mainly excreted through urine (about 75%) and feces via biliary excretion (about 15–20%). It is also excreted in sweat, nails, and hairs [1, 2].

The main aspects of lead toxicokinetics are summarized in Figure 2.10.3.1.

2.2 Mechanisms of action

Lead can affect virtually every organ or system in the body through mechanisms that involve fundamental biochemical processes. These mechanisms are mainly based on (a) the similarity of ionized lead (Pb^{++}) and essential divalent elements such as Ca^{++} and Zn^{++} and hence, its ability to inhibit or mimic their action, and (b) the ability of Pb^{++} to interact with proteins. These two phenomena often overlap. Many effects of lead are thought to be mediated through metal ion-protein interactions in a variety of cellular targets (e.g. lead–calcium interaction: ion channels, calmodulin, protein kinase C (PKC), etc.; lead–zinc interaction: delta aminolevulinic acid (ALA), metallothionein (MT), zinc finger proteins, etc.) [1, 2, 4, 85–89].

Lead–metal interactions can occur in two different ways, direct and indirect. In the direct mechanism, lead binds at a site normally occupied by another metal, and produces either a positive (stimulatory) or negative (inhibitory) effect. Lead can also displace a metal (e.g. calcium) from a binding site, increasing the free concentration of this metal that can in turn produce an effect at a second site [86].

The interaction of lead with proteins may represent a fundamental mechanism underlying lead toxicity. Pb^{++} binds with the greatest affinity to sulfhydryl groups but also interacts with a diverse array of nucleophilic ligands, including amine, phosphate, and carboxyl groups. Lead binding to enzymatic proteins can inhibit the activity of the enzyme and alter the processing of other chemicals. Lead binding to membranes or transport proteins can inhibit or alter ion transport across the membrane or within a cell [89].

In its binding with sulfhydryl groups, lead may interfere with the activity of zinc metalloenzymes, as zinc binds to a sulfhydryl group at the active site. Zinc metallo-enzymes affected by lead include delta-aminolevulinate dehydratase and ferrochelatase involved in the synthesis of heme and MT that acts as a cytoplasmic store for zinc [86].

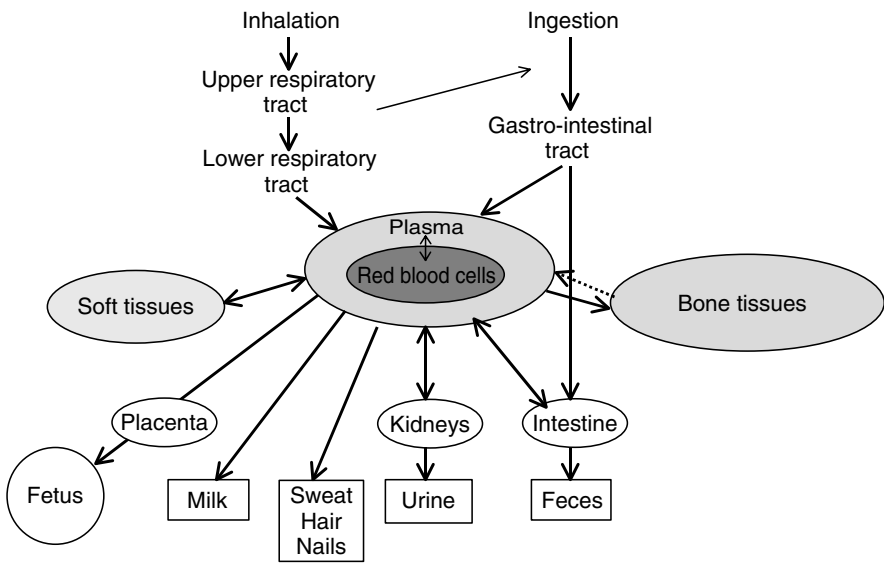

Figure 2.10.3.1. Main aspects of lead toxicokinetics.

In heavy alcohol drinkers, not only are lead levels increased in the blood but also the inhibition of ALA-D is enhanced. Hence, people who consume excess alcohol may be at increased risk of adverse effects from lead [90–92]. Heme is the prosthetic group of many hemoproteins that participate in many biological processes, including transport and storage of oxygen (hemoglobin and myoglobin, respectively), electron transport (b and c cytochromes), breakdown of hydrogen peroxide (peroxidases and catalases), and hydrocarbon oxidation (cytochrome P450). Hence, the potential impact of a reduction in the body pool of heme synthesis by lead is not limited to the hematopoietic system and the reduction in hemoglobin concentration in blood. Moreover, ALA, which blood concentration increases, can cross the blood brain barrier. This molecule resembles the structure of the inhibitory neurotransmitter GABA (gamma-aminobutyric acid), and the excitatory neurotransmitter L-glutamic acid leading to possible interplay between these molecules [93].

The main aspects of the toxic action of lead on heme synthesis are represented in Figure 2.10.3.2.

The binding of Pb^{++} to nonenzyme proteins with high affinity may influence the bioavailability, the intracellular transfert, and the transport of lead [89]. On the one hand, binding to Pb bound protein (PbBPs) and MT may result in an attenuation of Pb toxicity: PbBPs and MT appear to regulate Pb^{++} inhibition of ALA-D via a mechanism that involves Pb chelation and Zn donation. On the other hand, binding may increase Pb toxicity by a mechanism that facilitates the translocation of lead into mitochondria and thus results in ALA-S and ferrochelatase inhibition. These Pb-protein complexes appear to translocate Pb into the cell nucleus where it may influence gene expression [85, 89].

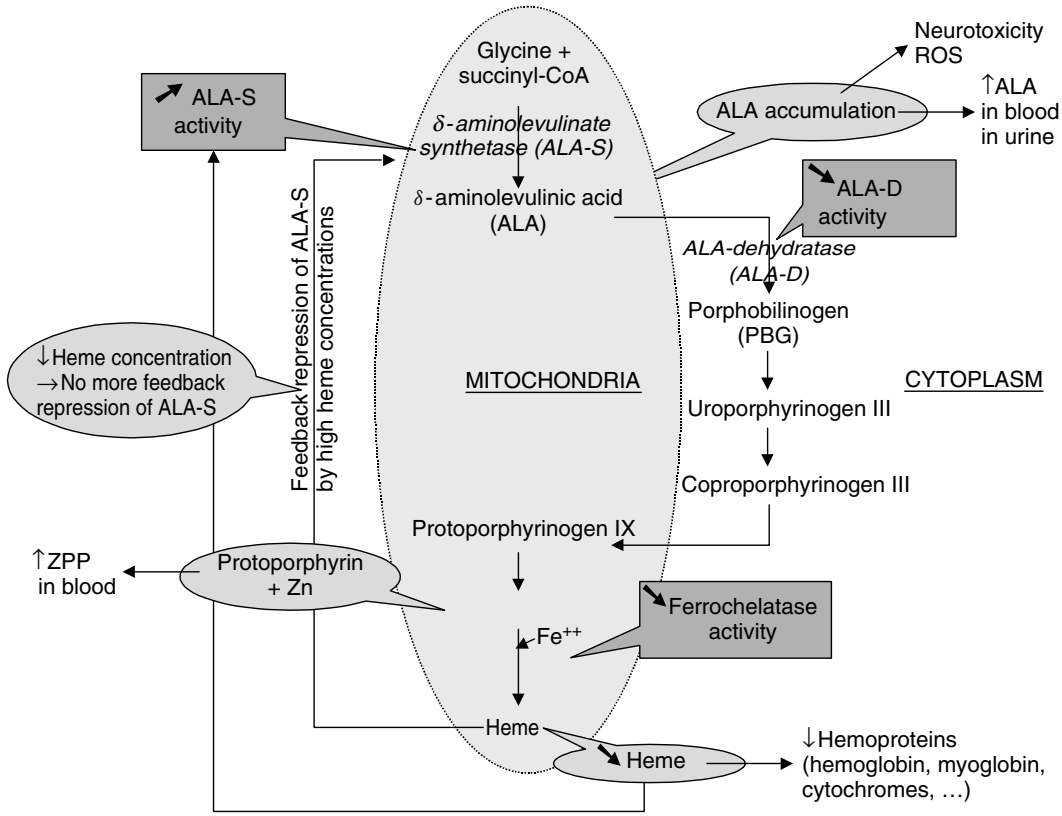

Figure 2.10.3.2. Main aspects of the toxic action of lead on heme synthesis.

Pb^{++} has been found to interfere with cellular calcium metabolism occupying the calcium-binding sites on numerous calcium-dependent proteins; for example, the calmodulin and the protein kinase C (PKC) [89]. Calmodulin, a major intracellular receptor for calcium, is a protein that acts as a sensor of free calcium concentration in the synaptic terminal and as a mediator of neurotransmitter release. PKC, a virtually ubiquitous protein, is of crucial importance in numerous physiological functions and plays a central role in signal transduction, cell growth, and differentiation [88, 94].

Several lines of evidence also suggest the involvement of an oxidative stress in some aspects of the cellular toxicity of lead by disrupting the delicate prooxidant–antioxidant balance that exists within cells [95, 96]. Some data indicate that lead exposure might cause generation of reactive oxygen species (ROS) and alteration of antioxidant defense systems in animals and workers [97–101]. When formation of reactive oxygen intermediates exceeds the scavenging capacity of the antioxidant defense mechanisms, free radicals accumulate and increase the likelihood of oxidative damage to critical macromolecules, such as enzymes, proteins, DNA, and membrane lipids. This oxidative stress could be caused by a direct participation of Pb^{++} in free radical mediated reaction or to an accumulation of delta ALA that has been shown to enhance ROS and lipoperoxidation. Biotransformation of trialkyllead compounds may also lead to the formation of free radicals that can induce lipid peroxidation [102].

2.3 Biomonitoring of exposure and effect

Biomonitoring of exposure and effect [1, 2, 4, 103] can be done in the following ways.

2.3.1 Biomarkers of exposure

Lead in blood (Pb-B)

The measurement of lead in whole blood is the most widely used biomarker to assess the absorbed dose of inorganic lead. However, one must keep in mind that organic lead exposure can affect blood lead levels, probably after dealkylation to inorganic lead [104].

Since the half-life of lead in blood is about 35 days, Pb-B mainly reflects relatively recent exposure. In view of the cycling of lead between blood, bone, and soft tissues, lead in blood is also influenced by lead stored in tissues that reenters the blood during tissue mobilization. When bone mobilization is accelerated, or when a lead worker is removed from exposure to lead, a greater fraction of Pb-B will be derived from tissue stores. It is important to keep in mind that the relationship between lead exposure and Pb-B concentrations is curvilinear; the increase in Pb-B concentration is less at high exposure than at low exposure levels.

Plasma lead concentrations may better reflect the 'metabolic active' fraction of lead in blood and defines the relationship between Pb-B and tissue or organ accumulation (and effect). However, in view of the difficulty of accurately measuring very low concentrations of lead, the determination of lead in plasma has up to now not been recommended for the routine monitoring of lead exposure. This could change with inductively coupled mass spectrometry (ICP-MS), which has a high analytical sensitivity and can achieve a much lower limit of detection than atomic absorption spectrometry (AAS) methods. It is suggested that the considerable variation reported between symptoms and signs and Pb-B might be caused by differences between people in the distribution of lead between erythrocytes and plasma [105].

In many countries, the progressive removal of organolead from gasoline and other preventive measures (such as removal of lead from soldered cans) has been associated with a progressive decline of blood lead levels of the general population. In nonoccupationally exposed adults, blood lead levels rarely exceed 100–150 $\mu g\,L^{-1}$. For instance, the US National Health and Nutrition Examination Surveys (NHANES) concluded that the mean blood lead level of persons aged 1 to 74 years dropped 78% (from 128 to 28 $\mu g\,L^{-1}$) during the period between 1976 and 1991 [106].

According to the U.S. Center for Disease Control and Prevention [107], the goal of all

activities preventing lead poisoning should be to reduce children's blood lead levels below 100 $\mu g\,L^{-1}$.

For occupationally exposed subjects, the American Conference of Governmental Industrial Hygienists (ACGIH) [108] proposes 300 $\mu g\,L^{-1}$ as Biological Exposure Index but makes clear that women of childbearing potential, whose blood Pb exceeds 100 $\mu g\,L^{-1}$ are at risk of delivering a child with a blood Pb >100 $\mu g\,L^{-1}$. The Deutsche Forschungsgemeinschaft [109] recommends 400 $\mu g\,L^{-1}$ as Biological Tolerance Value for male workers and 300 $\mu g\,L^{-1}$ for women under 45 years. According to the Occupational Health and Safety (Lead) Regulations 2000 [11], an employer must immediately remove an employee from a lead-risk job if Pb-B is above

1. 500 $\mu g\,L^{-1}$ – for females not of reproductive capacity and males;
2. 200 $\mu g\,L^{-1}$ – for females of reproductive capacity;
3. 150 $\mu g\,L^{-1}$ – for females who are pregnant or breast feeding;

The employer must ensure that the employee does not return to a lead-risk job until the Pb-B is less than

1. 400 $\mu g\,L^{-1}$ – for females not of reproductive capacity and all males;
2. 100 $\mu g\,L^{-1}$ – for females of reproductive capacity.

Lead in urine

Although urinary lead level is used occasionally as a screening test to measure current exposure, its use as a biomarker of environmental lead exposure appears to be of limited value in view of the relatively low and variable level of lead excreted in the urine [1, 2, 4, 103]. Although on a group basis there exists a satisfactory correlation between lead in blood and lead in urine, in the same individual lead in urine fluctuates with time more than lead in blood. Moreover, in occupationally exposed workers there is a risk of external contamination.

Urinary levels of lead after administration of a chelating agent ($CaNa_2$-EDTA, DMSA (dimercaptosuccinic acid)) is considered to reflect the mobilizable pool of lead from soft tissues and blood, as well as subcompartments of bone. The EDTA-chelatable lead is reported to be a better estimate of the cumulative lead dose while DMSA-chelatable lead is more described as an estimate of bioavailable stores [110, 111]. However, DMSA-chelatable lead appeared to be directly associated with tibial lead in workers exposed to organic and inorganic lead compounds [112]. Interestingly, DMSA-chelatable lead was found to be the best predictor of lead-related symptoms (particularly, CNS, peripheral nervous systems (PNS)) than were the other lead biomarkers in lead workers [111].

Urinary diethyllead has been proposed as a qualitative marker of exposure to tetraethyl lead [113, 114].

Lead in tooth

Teeth can be useful tissues for assessing long-term lead accumulation from prenatal exposures to the time of shedding of the tooth. The accumulation of lead in teeth has been used as a measure of environmental exposure of children to lead in several epidemiological studies. However, the method of sampling and analysis, the tooth type, the sample (circumpulpar dentine, dentine or whole tooth), and resorption and tooth age at exfoliation influence the results.

Lead in bone

The human skeleton begins to accumulate lead during fetal development and continues to about age 60 [87]. Skeletal lead (finger, tibia, patella, calcaneus) can be measured by bone biopsy and more interestingly by noninvasive X-ray fluorescence (L-shell XRF (L-XRF) and K-shell XRF (K-XRF)). This technique is not applicable in routine at present but constitutes a powerful analytical methodology for evaluating bone lead levels as a measure of time-integrated (i.e. cumulative) lead dose in epidemiological studies of the effects of chronic lead exposure [115–117].

Lead in hair

Hair lead has been proposed as a noninvasive indicator of exposure to lead. However, hair color, texture, treatment, location on the body and growth phase can influence the metal analysis of hair. Moreover, it is almost impossible to avoid external contamination, and it is extremely difficult to differentiate between externally and internally deposited lead. To date, no validated methods are available for cleaning. Methods that are sufficiently vigorous to remove superficial lead also remove lead from the hair shaft [2].

The most common methods currently used for the analysis of lead in biological samples are flame AAS, graphite furnace atomic absorption spectrometry (GFAAS), anode stripping voltammetry (ASV), inductively coupled plasma-atomic emission spectroscopy (ICP/AES). Spectrophotometric methods were commonly used in the past; however, they are not as sensitive or reliable as the newer methods. Other specialized methods for lead analysis are ICP/MS, X-ray fluorescence spectroscopy (XRFS), differential pulse ASV, and isotope dilution mass spectrometry (IDMS). The most reliable method for the determination of lead at low concentrations is IDMS, but because of the technical expertise required and high cost of the equipment, this method is not commonly used [1, 2].

2.3.2 *Biomarkers of effect*

Zinc protoporphyrin (blood)

The accumulation of protoporphyrin in erythrocytes results from the action of lead in the bone marrow, and the average life span of the erythrocytes is about 120 days. This explains the time lag in the increase of erythrocyte protoporphyrin as compared to the rise of lead in blood. Zinc protoporphyrin (ZPP) requires more time than the blood lead to reach significantly elevated levels; the return to normal after discontinuing lead exposure is also slower. Under steady-state conditions, there is a relationship between the concentration of lead in blood and the erythrocyte protoporphyrin content. ZPP starts to increase significantly at blood lead levels of about 350 $\mu g\,L^{-1}$ in males and 250 $\mu g\,L^{-1}$ in females. The ZPP test is simple, fast, not expensive to perform, and no contamination is possible.

An increase in ZPP is not specific to lead intoxication, slight iron deficiency, or iron metabolism disturbances being the first cause of ZPP increase. Some hereditary hemoglobin disorders (thalassemia) also cause an elevated ZPP.

ALA-D – delta aminolevulinic acid dehydratase activity (blood)

Aminolevulinic acid dehydratase (ALA-D) activity measurement in erythrocytes is a particularly sensitive indicator of recent exposure to lead. There is no large time lag between exposure and decreased activity. A potential lead threshold was identified between 32 and 48 $\mu g\,L^{-1}$, above which ALA-D may be inhibited by lead [118]. This extreme sensitivity renders the test of little value in routine clinical practice. Moreover, the inhibition of the enzyme may be so extensive at Pb-B $>300\ \mu g\,L^{-1}$ that it could not distinguish between moderate and severe exposure [119].

ALA-U – delta aminolevulinic acid (urine)

Delta-aminolevulinic acid, the intermediate that accumulates because of ALA-D inhibition, is largely used for biological monitoring of exposure to lead. An increase in urinary excretion of ALA can be detected when Pb-B levels exceed 350 $\mu g\,L^{-1}$ in adults and 250–750 $\mu g\,L^{-1}$ in children, and is not considered as a very sensitive measure of lead exposure. There seems to be considerable interindividual variation of excretion at the same level of lead absorption. Urinary ALA level is also raised in patients with porphyrias.

2.4 Health effects

Toxic effects [1, 2, 4] of lead are described from more than 2000 years [6, 120]. Hippocrates, around 370 BC described severe attack of abdominal pain without knowing the etiology. In 200 BC, the Greek poet and philosopher Nicander already

described the palsy but was not yet able to attribute it to lead exposure. Numerous epidemics of lead poisoning are reported in the old literature. The ancients regarded lead as the father of all metals, but the deity they associated with the substance was Saturn, the 'ghoulish titan who devoured his own young'. The word 'saturnine' applies to an individual whose temperament has become uniformly gloomy, cynical, and taciturn as the results of lead intoxication. The high lead concentration in food and wine causing sterility, infertility, and stillbirths among the aristocracy is postulated to have contributed to the downfall of the Roman Empire. The high lead content in wine or cider, due to the addition of lead bars to enhance taste and prevent spoilage, has also been involved in the occurrence of the 'Coliques du Poitou' and the 'Devonshire colic' in the seventeenth and eighteenth centuries. In the late 1920s, an epidemic of chronic nephritis has been described in lead-poisoned children in Queensland, Australia. Whiskey made 'in the light of the moon' (moonshine whiskey) during prohibition in the United States (1920–1933) has also been a source of widespread lead intoxication among individuals who consumed this beverage.

Lead exposure can result in a wide range of effects depending on the level and duration of exposure. Effects at the biochemical, subclinical, and clinical levels can occur over a broad range of doses and range from inhibition of enzymes to acute intoxication [2]. A greater ingestion ('pica') and a greater absorption rate cause relatively greater exposure and body burden in children during sensitive periods of development. Moreover, it appears that children are generally more sensitive to the toxicological effects of lead at a given internal exposure level. The lowest-observed-effect levels for various end points (e.g. neurobehavioral perturbation, encephalopathy, slowed nervous conduction velocity, reduced hemoglobin, elevated erythrocytes porphyrins (EP)) are lower in children than in adults [4].

The main target organs/systems of lead toxicity are the hematopoietic system, the nervous system, the kidney, and the reproductive system.

2.4.1 Hematopoietic system

Lead affects the hematopoietic system by interfering with hemoglobin production and by diminishing red blood cell survival. A prominent feature of lead poisoning is its interference with the production of heme by inhibiting several steps in its biosynthesis, but it also affects the synthesis of the globin moiety of hemoglobin. The hemolytic component of lead-induced anemia is assumed to be due to increased cell fragility and altered osmotic resistance.

Anemia occurs only with chronic high levels of exposure leading to blood lead levels of 700 $\mu g\,L^{-1}$ in children and 800 $\mu g\,L^{-1}$ in adults. It is moderate, normochromic or mildly hypochromic, normocytic, sideroblastic, and mildly hypersideremic. In children, the hypochromic, microcytic anemia associated to iron deficiency is exacerbated by the effect of lead, and vice versa. It is associated with reticulocytosis, owing to shortened cell survival and with the variable presence of basophilic stippling attributed to the accumulation of pyrimidine nucleotides. As heme synthesis is impaired, iron also accumulates during cell maturation, and iron-laden mitochondria can be seen in normoblasts in bone marrow explaining the finding of ringed sideroblasts.

The threshold Pb-B level for a decrease in hemoglobin has been estimated to 500 $\mu g\,L^{-1}$ for occupationally exposed adults and approximately 400 $\mu g\,L^{-1}$ for children [2, 4].

The following table summarizes the lowest-observed-effect levels in regard to heme synthesis and hematological effects.

Heme synthesis and hematological effects

Parameters	Lowest observed effect level Pb-B ($\mu g\,L^{-1}$)	
	Children	Adults
ALA-D inhibition	<100	100
EP elevation	150–200	Female: 150–200 Male: 250–300
Increased ALA urine levels	400	350–400
Reduced Hb production	400	500
Frank anemia	700	800

Note: Pb-B = blood lead concentration, ALA-D = aminolevulinic acid dehydratase, ALA = aminolevulinic acid, Hb = hemoglobin, EP = erythrocyte protoporphyrin.

2.4.2 Nervous system

Both the central and peripheral nervous system are important targets of lead.

2.4.2.1 Central nervous system

The central nervous system (CNS) is probably the most sensitive target of lead. From subtle effects on intellectual functioning, deficits in memory, attention, and concentration, psychomotor performance intelligence to severe encephalopathy, a broad range of CNS effects is associated with lead exposure depending on the level of intoxication.

Severe lead encephalopathy associated with hallucinations and in most serious cases delirium, convulsions, paralysis, coma, and death is currently rarely seen in adults and occurs at markedly elevated blood lead levels. Acute lead toxicity to the nervous system is characterized by edema or swelling of the brain due to altered permeability of capillary endothelial cells. Cerebral edema, associated with arterial hypertension and purpuric hemorrhagic extravations, is the principal gross neuropathological finding of persons dying of inorganic lead encephalopathy [62].

Early clinical features of lead toxicity are nonspecific and subjective. Symptoms including headache, dizziness, poor attention, insomnia, asthenia, lethargy, irritability, dullness, loss of memory, anxiety, depression, general malaise are described at Pb-B levels ranging from approximately 400–1200 $\mu g\,L^{-1}$ following short- or long-term; occupational or nonoccupational exposure in adults.

Central nervous system symptoms are found in lead-exposed adults when there is a history of several years of exposure to lead at Pb-B levels that may not have exceeded 700 $\mu g\,L^{-1}$ and a Pb-B level at the time of clinical assessment of at least 400 $\mu g\,L^{-1}$ [1, 2].

Impairment of psychological, cognitive, and neurobehavioral functions has been found after long-term lead exposure of workers. Current Pb-B levels in these workers were between 40 and 800 $\mu g\,L^{-1}$. However, some measures of cumulative exposure might be better predictors of impaired performance in workers with current levels $<400\ \mu g\,L^{-1}$ [1]. Meta-analytical reviews on neurobehavioral effects in lead exposed workers analyzed 24 selected publications covering exposure conditions with blood lead concentration $<700\ \mu g\,L^{-1}$. These results provide evidence for subtle deficits being associated with average blood lead levels between 370 and 520 $\mu g\,L^{-1}$ [121].

Neuroelectrophysiological tests appear to be sensitive indicators of the CNS effects of lead. Reductions in latencies of sensory evoked potentials, and auditory event-related potentials have been found in workers with average Pb-B levels of approximately 400 $\mu g\,L^{-1}$ [2].

Of particular concern are the possible neurotoxic effects on the developing child. The higher vulnerability of children to the neurotoxic effects of lead is well documented.

With acute lead exposure resulting in a Pb-B level in excess of 800 $\mu g\,L^{-1}$, severe encephalopathy and/or coma may occur. While a childhood episode of acute encephalopathy is associated with significant brain damage and persistent cognitive deficits of chronic encephalopathy, available evidence is not sufficient to determine whether chronic low-level lead-associated deficits are irreversible [2, 107]. Long-term exposure to low lead levels has been shown to cause subtle effects on the CNS that manifest as deficits in intelligence, impaired neurobehavioral functioning, and poorer school performance. The blood lead threshold level associated with such disorders remains debated and according to the WHO [2], below the Pb-B range of 100–150 $\mu g\,L^{-1}$, the effects of confounding variables and limits in the precision in analytical and psychometric measurements increase the uncertainty attached to any estimate of effect. However, there is some evidence of an association below this range. In 1991, the Centers for Disease Control and Prevention [107] revised downward to 100 $\mu g\,L^{-1}$ the 1985 intervention level of 250 $\mu g\,L^{-1}$ on the basis of new data indicating the possibility of some adverse health effects at blood lead levels at least as low as 100 $\mu g\,L^{-1}$ of whole blood. However, some very recent data are suggestive of intellectual impairment in children with Pb-B lower than this threshold [122].

The trialkyl metabolites, trimethyl, and triethyl lead are potent neurotoxicants. The clinical syndrome caused by organic lead exposure in humans is different from inorganic lead poisoning because of its prominent CNS presentations rather than peripheral neuropathy and milder CNS effects. The clinical picture includes marked irritability, insomnia, disturbing dreams, hallucinations, anorexia, nausea, vomiting, tremor, hyperreflexia, muscular contractions, bradycardia, arterial hypertension, and hypothermia. Most severe cases present episodes of complete disorientation, mania, ataxia, hallucinations, exaggerated muscular activity, and violent convulsive seizures, which may terminate in coma and death. Muscle, hepatic, and renal damage may occur. A rapid onset of symptoms after exposure indicates a poor prognosis. Constipation, abdominal colic, pallor, and peripheral neuropathy typical of inorganic lead poisoning are not so common following exposure to organic lead.

Symptoms of mild acute organic lead poisoning have been reported at blood lead levels as low as 510 $\mu g\,L^{-1}$ [62]. When the onset of symptoms is delayed for many days recovery is usually complete, but some neurological sequelae have been reported. Prolonged deliberate sniffing of gasoline has resulted in encephalopathy and death [123].

2.4.2.2 Peripheral nervous system

In the peripheral nervous system, inorganic lead can cause primary segmental demyelination and secondary axonal degeneration [62].

The old literature reports that prolonged exposure to very high lead levels can produce weakness and paralysis that typically occur without sensory effects. This weakness first occurring most commonly in the fingers and wrist extensors caused in extreme cases 'the wrist drop'. The upper limb involvement was generally more prominent than that of the lower extremity and the dominant side can be more severely affected. Weakness in the legs and ankle extensor muscles' palsy leading to foot drop have also been reported. Actually, several combinations in the simultaneous distribution of palsy in different occupations according to the nature of the muscular effort entailed have been described [124, 125]. While these features have become particularly rare, subclinical neuropathy can develop insidiously during chronic exposure and reflect the accumulation of lead in the body. Electrophysiological studies on lead-exposed workers have yielded somewhat mixed results, with some showing a decrease in nerve conduction velocity at low Pb-B levels and a few showing no effect or occasionally even an increase in nerve conduction velocity (NCV) associated with lead exposure. The reduction in human peripheral nerve conduction velocity may occur in adults at Pb-B levels $<700\ \mu g\,L^{-1}$ and possibly at level as low as 300 $\mu g\,L^{-1}$ [1, 2, 62, 125, 126]. There is suggestive evidence indicating that the changes in NVC associated with lead exposure are reversible after cessation of exposure [1, 2, 62].

2.4.3 Cardiovascular system

The possible relationship between Pb-B concentration and blood pressure has been examined in occupationally exposed cohorts [127–129], in several large-scale general population studies including the British Regional Heart Study (BRHS) [130, 131], the US NHANES II and III (National Health and Nutrition Examination Survey) [132–138], and epidemiological studies in Wales [139], England [140], Denmark [141, 142], Canada [143], and Belgium [144].

The results of both occupational and general population studies do not provide conclusive evidence that lead exposure, as assessed by Pb-B levels, is associated with hypertension. There is some evidence of very weak associations between Pb-B concentration and systolic or diastolic blood pressure. However, there is doubt about whether these statistical associations are really due to an effect of lead exposure or are an artifact due to confounding factors (e.g. age, body weight, alcohol consumption, cigarette smoking) [1, 2, 145, 146].

There is suggestive evidence that low-blood lead levels have a small but demonstrable association with pregnancy hypertension and toxemia [147, 148].

2.4.4 The kidneys

Acute lead exposure is known to cause reversible proximal renal tubular damage characterized by aminoaciduria, phosphaturia and glycosuria: the Fanconi syndrome.

A characteristic histopathological finding during the early phase is the formation of nuclear inclusion bodies that are dense spherical eosinophilic bodies composed of a lead-protein complex. It is suggested that individual differences in susceptibility to lead poisoning may lie in genetic variability of the lead-binding proteins [149, 150].

Chronic exposure to high lead levels can progress to a nephropathy manifested by progressive interstitial fibrosis, dilatation of tubules and atrophy or hyperplasia of the tubular epithelial cells, and reduction in glomerular filtration rate resulting in decreased kidney function and possible renal failure. These effects appear to be irreversible. Nuclear inclusion bodies become less common, as renal tubular atrophy and interstitial fibrosis increase in severity. Proximal tubular dysfunction is usually not demonstrable in chronic phase of nephropathy, but interstitial fibrosis is usually associated with asymptomatic renal azotemia and reduced glomerular filtration rate [1, 2, 149].

Many studies have documented an association between chronic occupational exposure to lead and impairment of renal function. Measurements of parameters in serum (blood urea nitrogen, creatinine, urea, uric acid, ß2-microglobulin, retinol-binding protein) and urinary excretion of a panel of low and high molecular weight proteins, brush border proteins and enzymes have been used to evaluate renal tubular and glomerular function in occupationally or nonoccupationally lead-exposed subjects. These studies provide evidence for an increased risk of nephropathy in workers with a Pb-B level of over 600–700 $\mu g\,L^{-1}$ [1, 2, 4, 151, 152]. Most studies in the general population attempting to relate renal function impairment to Pb-B concentration have not demonstrated an effect with Pb-B levels below 400 $\mu g\,L^{-1}$. Actually, the level of Pb exposure causing early adverse renal effects remains uncertain. Some very sensitive parameters have been reported to be disturbed at low level of exposure, but the health significance and the predictive value of these nonspecific renal changes are not always known. Moreover, the Pb-B levels measured at the time of renal function testing may not fully reflect the history that contributed to the development of chronic nephropathy in lead workers [1].

An acceleration of age-related impairment of renal function in association with long-term low-level lead exposure has been suggested [153]. Whether such small changes in renal function will result in clinically significant health problems is uncertain.

Epidemics of gout have been ascribed to lead intoxication in the Romans. Gout is suspected of being a potential complication of lead nephropathy. Studies have reported enhanced reabsorption and reduced excretion of uric acid, explaining the high incidence of gout. Altered purine metabolism or increased nucleoprotein metabolism is also implicated [149, 154, 155].

2.4.5 Reproductive system

While it is generally accepted that lead adversely affects the reproductive process in both men and women, the evidence is mostly qualitative and dose-effect relationships have not been established [2]. The mechanisms underlying these effects are not clear but factors ranging from indirect effects on maternal nutrition or hormonal status before and during pregnancy to more direct gametogenic effects that could affect parental fertility in both sexes are suggested [1].

The lead-induced effects on reproductive function are less clearly defined in humans than in animals. Male reproductive effects from occupational exposure to lead include asthenospermia, hypospermia, teratospermia, and hypogonadism [1, 2, 4]. Decreased concentrations of circulating testosterone probably associated with hypothalamic-pituitary-gonadal axis and LH secretion dysfunction can be seen at Pb-B $> 600\ \mu g\,L^{-1}$. There is substantial evidence that a long-standing exposure to lead entailing Pb-B levels $> 400\ \mu g\,L^{-1}$ can cause a sperm decreased production leading to a risk of lowered fertility. Teratospermia has been noted at mean

blood lead levels of 530 $\mu g\,L^{-1}$ and hypospermia and asthenospermia at 410 $\mu g\,L^{-1}$ [11]. No direct effect on sperm production or on sexual hormones levels has been observed at Pb-B $<400\ \mu g\,L^{-1}$, but a transient LH increase has been observed [156].

Developmental effects that have been observed in humans following exposure to low levels of lead include reduced birth weight, reduced gestational age and neurobehavioral deficits or delays. Studies on the risk of spontaneous abortion and reduced birth weight associated with maternal Pb-B levels below 300 $\mu g\,L^{-1}$ have yielded mixed results [2]. An association between the risk of spontaneous abortion and Pb-B in the range of 100–250 $\mu g\,L^{-1}$ has been observed; whether this is causal remained to be determined [157]. Exposure-related perturbations have been shown in the length of gestation and some indices of fetal growth and maturation, significantly greater risks being associated with Pb-B levels of 150 $\mu g\,L^{-1}$ or more [2]. There is no apparent maternal–fetal barrier to lead, and the developing nervous system of the fetus is particularly vulnerable to lead toxicity. The blood brain barrier is not mature and does not provide any barrier to lead entry into the brain. Up to 2 years of age, children with umbilical cord blood lead levels $>100\ \mu g\,L^{-1}$ achieve significant lower scores on tests of cognitive development than do children with lower prenatal exposures [158].

No evidence of an association with major congenital malformations has been found [1, 2, 156].

2.4.6 Cancer

In 1987, the IARC [159] classified lead and inorganic lead compounds as 'possibly carcinogenic to humans (Group 2B)' on the basis of sufficient animal data and insufficient human data. On the basis of inadequate evidence from two epidemiological human studies as well as animal studies, organolead compounds were considered as not classifiable as to their carcinogenicity to humans (Group 3) [159].

In 1995, the WHO concluded that the evidence for the carcinogenicity of lead and inorganic lead compounds in humans was inadequate [2].

In 2004, the IARC [160] reevaluated the potential carcinogenic hazards to humans from exposure to inorganic and organic lead compounds and reached the following overall evaluations: inorganic lead compounds are *probably carcinogenic to humans (Group 2A)*; organic lead compounds are *not classifiable as to their carcinogenicity to humans (Group 3)*. To evaluate the epidemiological evidence of possible cancer hazards from exposure to lead and lead compounds, the Working Group considered six occupational cohort studies of high-exposed workers to be particularly informative. These concerned battery workers in the United States and the United Kingdom, and primary smelter workers in Italy, Sweden and the United States. The conclusions are the following:

Lung cancer – One of the six cohort studies showed a statistically significant twofold excess of lung cancer among smelter workers, but this excess may well have been caused by exposure to arsenic.

Stomach cancer – Five of the six cohort studies were judged to be informative for stomach cancer. In four of these five studies, there was a fairly consistent 30–50% excess of stomach cancer compared with external reference populations. It is possible that ethnicity, dietary habits, prevalence of *Helicobacter pylori* infections or socioeconomic status played a role in the stomach cancer excesses.

Kidney cancer – Five of the six cohort studies reported findings for kidney cancer. In one study, there was a statistically significant twofold excess of kidney cancer, based on comparison with an external reference population. All five studies were based on small numbers of deaths.

Brain cancer – Four of the six cohort studies reported findings for tumors of the brain and nervous system, but there was no consistent pattern in these studies. In addition, in a separate cohort of workers, a nested case–control study did show a statistically significant, positive dose–response relationship between blood lead concentrations and the risk for glioma; this cohort had lower exposures to lead than the other occupational cohorts. All studies were based on small numbers of deaths.

On the basis of these data, the Working Group concluded that there is *limited evidence* for the carcinogenicity to humans of exposure to inorganic lead compounds. The available epidemiological data on occupational exposure to organic lead compounds were considered to provide *inadequate evidence* for carcinogenicity to humans'.

Lead can certainly be considered as an established animal carcinogen [1, 2, 4, 159, 160].

Lead is weakly mutagenic but exerts pronounced indirect genotoxic effects and increases the mutagenicity of other mutagens. These indirect genotoxic effects are observed at low, nontoxic concentrations, possibly via interference with DNA repair processes [161]. Recent data indicate that lead can substitute for zinc and calcium in several proteins with important roles in cell growth, differentiation, as well as cell-cycle control and DNA repair. Lead is also a strong mitogen (a substance that causes cells to begin division and hence their proliferation) and may generate ROS and cause oxidative damage to DNA [1, 2].

2.4.7 Other effects

Gastrointestinal complaints are frequent in subjects with increased lead absorption, and the severity of symptoms span a broad range. Colics in adults typically occur at Pb-B levels of 1000–2000 $\mu g\,L^{-1}$, but symptoms have been noted at levels as low as 400–600 $\mu g\,L^{-1}$ [1, 2, 4]. The lowest-observed-adverse-effect level for lead colics in children was assessed in the range of 600–1000 $\mu g\,L^{-1}$ [4].

At moderate Pb-B levels, symptoms include epigastric discomfort, dyspepsia, nausea, decreased appetite, and weight loss. At higher Pb-B levels, painful abdominal cramps known as *lead colic* typically associated with constipation of several days and increased blood pressure can occur.

Arthralgia and myalgia are also frequent symptoms of lead poisoning, prompting the experienced lead worker to seek medical attention.

Thyroid function has been examined in lead workers [162–166] and in lead-exposed children [167]. It appears that thyroid dysfunction can be found at Pb-B levels >600–700 $\mu g\,L^{-1}$ [156].

Relatively poor attention has been given to the potential effects of lead on bone. Bone homeostasis depends on a complex interaction of its various components, that is, minerals, cells and the extracellular matrix composed of collagenous and noncollagenous proteins [2]. Potential effects of lead on bone have been summarized [87]. It seems that lead intoxication directly and indirectly alters many aspects of bone cell function. Lead is associated with changes in the circulating levels of hormones, particularly 1,25-dihydroxyvitamin D3, which modulate bone cell function. The 1,25-dihydroxyvitamin D3-stimulated synthesis of osteocalcin, a calcium-binding protein synthesized by osteoblastic bone cells, is inhibited by low levels of lead. Impaired osteocalcin production may inhibit new bone formation, as well as the functional coupling of osteoblasts and osteoclasts. Lead may impair the ability of cells to synthesize or secrete other components of the bone matrix, such as collagen or bone sialoproteins (osteopontin). Finally, lead may directly effect or substitute for calcium in the active sites of the calcium messenger system, resulting in loss of physiological regulation.

3 REFERENCES

1. ATSDR (Agency for Toxic Substances and Disease Registry), *Toxicological Profile for Lead, Update*, U.S. Department of Health and Human Services, Public Health Service, Atlanta, GA, 1999.
2. WHO (World Health Organization), *Environmental Health Criteria 165: Inorganic Lead*, International Programme on Chemical Safety, Geneva, 1995.
3. Thornton, I., Rautiu, R. and Brush, S., *LEAD: The Facts*, LDAI – Lead Development Association International, Ian Allan Printing, Hersham, Surrey KT12 4RG, UK, 2001.
4. EPA, *Air Quality Criteria for Lead (EPA-600/8-83/028aF)* U.S. Environmental Protection Agency, Research Triangle Park, NC, 1986.
5. *The Merck Index*, 13th ed., Merck & Co, Whitehouse Station, NJ, 2001.
6. http://www.epa.gov/history/topics/perspect/lead.htm, 2004.
7. *The Columbia Encyclopedia*, 6th ed., Columbia University Press, 2002.
8. Smith, http://minerals.er.usgs.gov/minerals/pubs/commodity/lead/Smith_1998, 2004.

9. Browning, E., *Toxicity of Industrial Metals*, 2nd ed., Butterworths, London, 1969.
10. Corrin, M. L. and Natusch, D. F. S., Physical and chemical characteristics of environmental lead, in *Lead in the Environment*, Boggess, W. R. and Wixson, B. G. (Eds.), NSF/RA-770214, National Science Foundation, Washington DC, 1977, pp. 7–31.
11. OSHA, *Occupational Health and Safety (Lead) Regulations 2000*, U.S. Department of Labor Occupational Safety & Health Administration, S.R. No. 62/2000, 29 June 2000.
12. Graziano, J. H., Blum, C. B., Lolacono, N. J., Slavkovich, V., Manton, W. I., Pond, S. and Moore, M. R., *Environ. Health Perspect.*, **104**, 176 (1996).
13. Dieter, M. P., Matthews, H. B., Jeffcoat, R. A. and Mosema, R. F., *J. Toxicol. Environ. Health*, **39**, 79 (1993).
14. Barltrop, D. and Meek, F., *Postgrad. Med. J.*, **51**, 805 (1975).
15. Healy, M. A., Harrison, P. G., Aslam, M., Davis, S. S. and Wilson, C. G., *J. Clin. Hosp. Pharm.*, **7**, 169 (1982).
16. Roy, B. R., *Am. Ind. Hyg. Assoc. J.*, **38**, 327 (1977).
17. Freeman, G. B., Dill, J. A., Johnson, J. D., Kurtz, P. J., Parham, F. and Matthews, H. B., *Fundam. Appl. Toxicol.*, **33**, 109 (1996).
18. Polak, J., O'Flaherty, E. J., Freeman, G. B., Johnson, J. D., Liao, S. C. and Bergstrom, P. D., *Fundam. Appl. Toxicol.*, **29**, 63 (1996).
19. Duggan, M. J. and Williams, S., *Sci. Total Environ.*, **7**, 91 (1977).
20. Harrison, R. M., *Sci. Total Environ.*, **11**, 89 (1979).
21. Day, J. P., Fergusson, J. E. and Chee, T. M., *Bull. Environ. Contam. Toxicol.*, **23**, 497 (1979).
22. Gulson, B. L., Davis, J. J., Mizon, K. J., Korsch, M. J., Law, A. J. and Howarth, D., *Arch. Environ. Health*, **49**, 326 (1994).
23. Barltrop, D. and Meek, F., *Arch. Environ. Health*, **34**, 280 (1979).
24. Ragan, H. A., *Sci. Total Environ.*, **28**, 317 (1983).
25. Goyer, R. A., *Annu. Rev. Nutr.*, **17**, 37 (1997).
26. Mahaffey, K. R., *Environ. Health Perspect.*, **103**(Suppl. 6), 191 (1995).
27. Blake, K. C. and Mann, M., *Environ. Res.*, **30**, 188 (1983).
28. James, H. M., Hilburn, M. E. and Blair, J. A., *Hum. Toxicol.*, **4**, 401 (1985).
29. Fullmer, C. S., *Environ. Res.*, **72**, 45 (1997).
30. Gunshin, H., Mackenzie, B., Berger, U. V., Gunshin, Y., Romero, M. F., Boron, W. F., Nussberger, S., Gollan, J. L. and Hediger, M. A., *Nature*, **388**, 482 (1997).
31. Canonne-Hergaux, F., Gruenheid, S., Ponka, P. and Gros, P., *Blood*, **93**, 4406 (1999).
32. Hammad, T. A., Sexton, M. and Langenberg, P., *Ann. Epidemiol.*, **6**, 30 (1996).
33. Watson, W. S., Morrison, J., Bethel, M. I. F., Baldwin, N. M., Lyon, D. T. B., Dobson, H., Moore, M. R. and Hume, R., *Am. J. Clin. Nutr.*, **44**, 248 (1986).
34. Flanagan, P. R., Chamberlain, M. J. and Valberg, L. S., *Am. J. Clin. Nutr.*, **36**, 823 (1982).
35. Ito, Y., Niiya, Y., Otani, M., Sarai, S. and Shima, S., *Toxicol. Lett.*, **37**, 105 (1987).
36. Kostial, K. and Kello, D., *Bull. Environ. Contam. Toxicol.*, **21**, 312 (1979).
37. Pierre, F., Vallayer, C., Baruthio, F., Peltier, A., Pale, S., Rouyer, J., Goutet, P., Aubrege, B., Lecossois, C., Guillemin, C., Elcabache, J. M., Verelle, B. and Fabries, J. F., *Int. Arch. Occup. Environ. Health*, **75**, 217 (2002).
38. Gething, J., *Br. J. Ind. Med.*, **32**, 329 (1975).
39. Robinson, R. O., *JAMA*, **240**, 1373 (1978).
40. Burns, C. B. and Currie, B., *Aust. N. Z. J. Med.*, **25**, 197 (1995).
41. Duydu, Y. and Vural, N., *Biol. Trace Elem. Res.*, **63**, 185 (1998).
42. Cope, R. F., Pancamo, B. P., Rinehart, W. E. and Ter Haar, G. L., *Am. Ind. Hyg. Assoc. J.*, **40**, 372 (1979).
43. Wells, A. C., Venn, J. B. and Heard, M. J., *Inhaled Part.*, **4**(Pt 1), 175 (1975).
44. Rastogi, S. C. and Clausen, J., *Toxicology*, **6**, 371 (1976).
45. Lilley, S. G., Florence, T. M. and Stauber, J. L., *Sci. Total Environ.*, **76**, 267 (1988).
46. Sun, C. C., Wong, T. T., Hwang, Y. H., Chao, K. Y., Jee, S. H. and Wang, J. D., *AIHA J.*, **63**, 641 (2002).
47. Stauber, J. L., Florence, T. M., Gulson, B. L. and Dale, L. S., *Sci. Total Environ.*, **145**, 55 (1994).
48. Bress, W. C. and Bidanset, J. H., *Vet. Hum. Toxicol.*, **33**, 212 (1991).
49. Marcus, A. H., *Environ. Res.*, **36**, 441 (1985).
50. Marcus, A. H., *Environ. Res.*, **36**, 459 (1985).
51. Marcus, A. H., *Environ. Res.*, **36**, 473 (1985).
52. Rabinowitz, M. B., Wetherill, G. W. and Kopple, J. D., *J. Clin. Invest.*, **58**, 260 (1976).
53. Pounds, J. G. and Leggett, R. W., *Environ. Health Perspect.*, **106**(Suppl. 6), 1505 (1998).
54. O'Flaherty, E. J., *Environ. Health Perspect.*, **106**(Suppl. 6), 1495 (1998).
55. Leggett, R. W., *Environ. Health Perspect.*, **101**, 598 (1993).
56. Bergdahl, I. A., Sheveleva, M., Schutz, A., Artamonova, V. G. and Skerfving, S., *Toxicol. Sci.*, **46**, 247 (1998).
57. Cavalleri, A. and Minoia, C., *J. Work Environ. Health*, **13**, 218 (1987).
58. Ong, C. N., Chua, L. H. and Teramoto, K., *J. Appl. Toxicol.*, **10**, 65 (1990).
59. Cake, K. M., Bowins, R. J., Vaillancourt, C., Gordon, C. L., McNutt, R. H., Laporte, R., Webber, C. E. and Chettle, D. R., *Am. J. Ind. Med.*, **29**, 440 (1996).
60. Gerhardsson, L., Englyst, V., Lundstrom, N. G., Nordberg, G., Sandberg, S. and Steinvall, F., *J. Trace Elem. Med. Biol.*, **9**, 136 (1995).
61. Bolanowska, W., Piotrowski, J. and Garczynski, H., *Arch. Toxicol.*, **22**, 278 (1968).

62. R. G. Feldman, *Occupational and Environmental Neurotoxicology*, Lippincott-Raven, Philadelphia, PA, 1999, pp. 30–68.
63. Barry, P. S., *Br. J. Ind. Med.*, **32**, 119 (1975).
64. Rabinowitz, M. B., *Environ. Health Perspect.*, **91**, 33 (1991).
65. Silbergeld, E. K., *Environ. Health Perspect.*, **91**, 63 (1991).
66. Nordberg, G. F., Mahaffey, K. R. and Fowler, B. A., *Environ. Health Perspect.*, **91**, 3 (1991).
67. Smith, D. R., Osterloh, J. D. and Flegal, A. R., *Environ. Health Perspect.*, **104**, 60 (1996).
68. Berlin, K., Gerhardsson, L., Borjesson, J., Lindh, E., Lundstrom, N., Schutz, A., Skerfving, S. and Edling, C., *Scand. J. Work Environ. Health*, **21**, 296 (1995).
69. Silbergeld, E. K., Schwartz, J. and Mahaffey, K., *Environ. Res.*, **47**, 79 (1988).
70. Markowitz, M. E. and Weinberger, H. L., *Pediatrics*, **86**, 455 (1990).
71. McQuirter, J. L., Rothenberg, S. J., Dinkins, G. A., Manalo, M., Kondrashov, V. and Todd, A. C., *J. Trauma*, **50**, 892 (2001).
72. Brown, A. and Tompsett, S. L., *Br. Med. J.*, **2**, 764 (1945).
73. Goldman, R. H., White, R., Kales, S. N. and Hu, H., *Am. J. Ind. Med.*, **25**, 417 (1994).
74. Osterloh, J. D. and Clark, O. H., *Environ. Res.*, **62**, 1 (1993).
75. Klein, M., Barbe, F., Pascal, V., Weryha, G. and Leclere, J., *Eur. J. Endocrinol.*, **138**, 185 (1998).
76. Cagin, C. R., Diloy-Puray, M. and Westerman, M. P., *Ann. Intern. Med.*, **89**, 509 (1978).
77. El-Sharkawi, A. M., Morgan, W. D., Cobbold, S., Jaib, M. B., Evans, C. J., Somervaille, L. J., Chettle, D. R. and Scott, M. C., *Lancet*, **2**, 249 (1986).
78. Beaney, R., Buxton, E. J., El-Sharkawi, A. M., Todd, A. C., Braithwaite, R. A., Somervaille, L. J., Chettle, D. R., Scott, M. C., Jones, S. J. and Hainsworth, I. R., *Br. J. Cancer*, **61**, 169 (1990).
79. Gulson, B. L., Mahaffey, K. R., Jameson, C. W., Mizon, K. J., Korsch, M. J., Cameron, M. A. and Eisman, J. A., *J. Lab. Clin. Med.*, **131**, 324 (1998).
80. Goyer, R. A., *Environ. Health Perspect.*, **89**, 101 (1990).
81. Moore, M. R., Goldberg, A., Pocock, S. J., Meredith, A., Stewart, I. M., MacAnespie, H., Lees, R. and Low, A., *Scott. Med. J.*, **27**, 113 (1982).
82. Ong, C. N., Phoon, W. O., Law, H. Y., Tye, C. Y. and Lim, H. H., *Arch. Dis. Child*, **60**, 756 (1985).
83. Nashashibi, N., Cardamakis, E., Bolbos, G. and Tzingounis, V., *Gynecol. Obstet. Invest.*, **48**, 158 (1999).
84. Church, H. J., Day, J. P., Braithwaite, R. A. and Brown, S. S., *Neurotoxicology*, **14**, 359 (1993).
85. Fowler, B. A., *Environ. Health Perspect.*, **106**(Suppl. 6), 1585 (1998).
86. Simons, T. J., Lead, in *Mineral and Metal Neurotoxicology*, Yasui, M., Strong, M. J., Ota, K. and Verity, M. A. (Eds.), CRC Press, Boca Raton, FL, 1997, pp. 243–252.
87. Pounds, J. G., Long, G. J. and Rosen, J. F., *Environ. Health Perspect.*, **91**, 17 (1991).
88. Goldstein, G. W., *Neurotoxicology*, **14**, 97 (1993).
89. Goering, P. L., *Neurotoxicology*, **14**, 45 (1993).
90. Bortoli, A., Fazzin, G., Marin, V., Trabuio, G. and Zotti, S., *Arch. Environ. Health*, **41**, 251 (1986).
91. Lopez, C. M., Vallejo, N. E., Pineiro, A. E., Uicich, R., Damin, C. F., Sarchi, M. I., Villaamil Lepori, E. C. and Roses, O. E., *Pharmacol. Res.*, **45**, 47 (2002).
92. Candela, S., Piccinini, R., Viappiani, F. and Lari, U., *Med. Lav.*, **82**, 533 (1991).
93. Silbergeld, E. K., Hruska, R. E., Bradley, D., Lamon, J. M. and Frykholm, B. C., *Environ. Res.*, **29**, 459 (1982).
94. Bressler, J. P., Kim, K. A., Chakraborti, T. and Goldstein, G., *Neurochem. Res.*, **24**, 595 (1999).
95. Adonaylo, V. N. and Oteiza, P. I., *Toxicology*, **132**, 19 (1999).
96. Hsu, P. C. and Guo, Y. L., *Toxicology*, **180**, 33 (2002).
97. Ito, Y., Niiya, Y., Kurita, H., Shima, S. and Sarai, S., *Int. Arch. Occup. Environ. Health*, **56**, 119 (1985).
98. Solliway, B. M., Schaffer, A., Pratt, H. and Yannai, S., *Pharmacol. Toxicol.*, **78**, 18 (1996).
99. Monteiro, H. P., Abdalla, D. S., Arcuri, A. S. and Bechara, E. J., *Clin. Chem.*, **31**, 1673 (1985).
100. Costa, C. A., Trivelato, G. C., Pinto, A. M. and Bechara, E. J., *Clin. Chem.*, **43**, 1196 (1997).
101. Sandhir, R. and Gill, K. D., *Biol. Trace Elem. Res.*, **48**, 91 (1995).
102. Ramstoeck, E. R., Hoekstra, W. G. and Ganther, H. E., *Toxicol. Appl. Pharmacol.*, **54**, 251 (1980).
103. R. Lauwerys, and P. Hoet, *Industrial Chemical Exposure, Guidelines for Biological Monitoring*, 3rd ed., Lewis Publishers, Boca Raton, FL, 2001.
104. McGrail, M. P., Stewart, W. and Schwartz, B. S., *J. Occup. Environ. Med.*, **37**, 1224 (1995).
105. Schutz, A., Bergdahl, I. A., Ekholm, A. and Skerfving, S., *Occup. Environ. Med.*, **53**, 736 (1996).
106. Pirkle, J. L., Brody, D. J., Gunter, E. W., Kramer, R. A., Paschal, D. C., Flegal, K. M. and Matte, T. D., *JAMA*, **272**, 284 (1994).
107. CDC, Center for Disease Control and Prevention, *Preventing Lead Poisoning in Young Children*, A Statement by the CDC, U.S. Department of Health and Human Services, Public Health Service, October 1991, http://www.cdc.gov/nceh/lead/lead.htm.
108. ACGIH (American Conference of Governmental Industrial Hygienists), *TLVs and BEIs for Chemical Substances and Physical Agents*, Cincinnati, OH, 2003.
109. DFG (Deutsche Forschungsgemeinschaft), *List of MAK and BAT Values*, Commission for the Investigation of Health Hazards of Chemical Compounds in the work Area, Report No. 38, Wiley-VCH, Weinheim, 2002.

110. Cory-Slechta, D. A., *J. Pharmacol. Exp. Ther.*, **246**, 84 (1988).
111. Lee, B. K., Ahn, K. D., Lee, S. S., Lee, G. S., Kim, Y. B. and Schwartz, B. S., *Int. Arch. Occup. Environ. Health*, **73**, 298 (2000).
112. Schwartz, B. S. and Stewart, W. F., *Arch. Environ. Health*, **55**, 85 (2000).
113. Turlakiewicz, Z. and Chmielnicka, J., *Br. J. Ind. Med.*, **42**, 682 (1985).
114. Zhang, W., Zhang, G. G., He, H. Z. and Bolt, H. M., *Int. Arch. Occup. Environ. Health*, **65**, 395 (1994).
115. Todd, A. C. and Chettle, D. R., *Environ. Health Perspect.*, **102**, 172 (1994).
116. Chettle, D. R., Scott, M. C. and Somervaille, L. J., *Environ. Health Perspect.*, **91**, 49 (1991).
117. Hu, H., Rabinowitz, M. and Smith, D., *Environ. Health Perspect.*, **106**, 1 (1998).
118. Campagna, D., Huel, G., Girard, F., Sahuquillo, J. and Blot, P., *Toxicology*, **134**, 143 (1999).
119. Graziano, J. H., *Clin. Chem.*, **40** (7 Pt 2), 1387 (1994).
120. Hernberg, S., *Am. J. Ind. Med.*, **38**, 244 (2000).
121. Seeber, A., Meyer-Baron, M. and Schaper, M., *Arch. Toxicol.*, **76**, 137 (2002).
122. Canfield, R., Kreher, D., Cornwell, C. and Henderson, C., *Neuropsychol. Dev. Cogn. Sect. C Child Neuropsychol.*, **9**, 35 (2003).
123. WHO (World Health Organization), *Environmental Health Criteria 3: Lead*, International Programme on Chemical Safety, Geneva, 1977.
124. Ehle, A. L., *Neurotoxicology*, **7**, 203 (1986).
125. Beritic, T., *Crit. Rev. Toxicol.*, **12**, 149 (1984).
126. Buchthal, F. and Behse, F., *Br. J. Ind. Med.*, **36**, 135 (1979).
127. Moreau, T., Orssaud, G., Juguet, B. and Busquet, G., *Rev. Epidemiol. Sante Publ.*, **30**, 395 (1982).
128. Orssaud, G., Claude, J. R., Moreau, T., Lellouch, J., Juguet, B. and Festy, B., *Br. Med. J. (Clin. Res. Ed.)*, **290**, 244 (1985).
129. Parkinson, D. K., Hodgson, M. J., Bromet, E. J., Dew, M. A. and Connell, M. M., *Br. J. Ind. Med.*, **44**, 744 (1987).
130. Pocock, S. J., Shaper, A. G., Ashby, D., Delves, T. and Whitehead, T. P., *Br. Med. J. (Clin. Res. Ed.)*, **289**, 872 (1984).
131. Pocock, S. J., Shaper, A. G., Ashby, D., Delves, H. T. and Clayton, B. E., *Environ. Health Perspect.*, **78**, 23 (1988).
132. Harlan, W. R., Landis, J. R., Schmouder, R. L., Goldstein, N. G. and Harlan, L. C., *JAMA*, **253**, 530 (1985).
133. Harlan, W. R., *Environ. Health Perspect.*, **78**, 9 (1988).
134. Pirkle, J. L., Schwartz, J., Landis, J. R. and Harlan, W. R., *Am. J. Epidemiol.*, **121**, 246 (1985).
135. Landis, J. R. and Flegal, K. M., *Environ. Health Perspect.*, **78**, 35 (1988).
136. Schwartz, J., *Environ. Health Perspect.*, **78**, 15 (1988).
137. Gartside, P. S., *Environ. Health Perspect.*, **78**, 31 (1988).
138. Den Hond, E., Nawrot, T. and Staessen, J. A., *J. Hum. Hypertens.*, **16**, 563 (2002).
139. Elwood, P. C., Davey-Smith, G., Oldham, P. D. and Toothill, C., *Environ. Health Perspect.*, **78**, 119 (1988).
140. Bost, L., Primatesta, P., Dong, W. and Poulter, N., *J. Hum. Hypertens.*, **13**, 123 (1999).
141. Grandjean, P., Hollnagel, H., Hedegaard, L., Christensen, J. M. and Larsen, S., *Am. J. Epidemiol.*, **129**(4), 732 (1989).
142. Moller, L. and Kristensen, T. S., *Am. J. Epidemiol.*, **136**, 1091 (1992).
143. Neri, L. C., Hewitt, D. and Orser, B., *Environ. Health Perspect.*, **78**, 123 (1988).
144. Staessen, J. A., Buchet, J. P., Ginucchio, G., Lauwerys, R. R., Lijnen, P., Roels, H. and Fagard, R., *J. Cardiovasc. Risk*, **3**, 26 (1996).
145. Staessen, J. A., Bulpitt, C. J., Fagard, R., Lauwerys, R. R., Roels, H., Thijs, L. and Amery, A., *J. Cardiovasc. Risk*, **1**, 87 (1994).
146. Nawrot, T. S., Thijs, L., Den Hond, E. M., Roels, H. A. and Staessen, J. A., *J. Hum. Hypertens.*, **16**, 123 (2002).
147. Rabinowitz, M., Bellinger, D., Leviton, A., Needleman, H. and Schoenbaum, S., *Hypertension*, **10**, 447 (1987).
148. Sowers, M., Jannausch, M., Scholl, T., Li, W., Kemp, F. W. and Bogden, J. D., *Arch. Environ. Health*, **57**, 489 (2002).
149. Goyer, R. A., *Toxicol. Lett.*, **46**, 153 (1989).
150. Goyer, R. A., *Environ. Health Perspect.*, **100**, 177 (1993).
151. Loghman-Adham, M., *Environ. Health Perspect.*, **105**, 928 (1997).
152. Roels, H. A., Hoet, P. and Lison, D., *Ren. Fail.*, **21**, 251 (1999).
153. Kim, R., Rotnitsky, A., Sparrow, D., Weiss, S., Wager, C. and Hu, H., *JAMA*, **275**, 1177 (1996).
154. Emmerson, B. T., Mirosch, W. and Douglas, J. B., *Aust. N. Z. J. Med.*, **1**, 353 (1971).
155. Batuman, V., *Am. J. Med. Sci.*, **305**, 241 (1993).
156. INSERM, (Institut National de la Santé et de la recherche Médicale), *Expertise Collective, Plomb dans l'Environnement*, Quels risques pour la santé? Paris, 1999.
157. Hertz-Picciotto, I., *Am. J. Ind. Med.*, **38**, 300 (2000).
158. Bellinger, D., Leviton, A. and Sloman, J., *Environ. Health Perspect.*, **89**, 5 (1990).
159. IARC (International Agency for Research on Cancer), *Overall Evaluations of Carcinogenicity: An Updating of IARC Monographs*, Vols. 1 to 42, Geneva, 1987.
160. http://www-cie.iarc.fr/monoeval/allmonos.html, 2004.
161. Hartwig, A., *Environ. Health Perspect.*, **102**(Suppl. 3), 45 (1994).
162. Robins, J. M., Cullen, M. R., Connors, B. B. and Kayne, R. D., *Arch. Intern. Med.*, **143**, 220 (1983).

163. Refowitz, R. M., *J. Occup. Med.*, **26**, 579 (1984).
164. Tuppurainen, M., Wagar, G., Kurppa, K., Sakari, W., Wambugu, A., Froseth, B., Alho, J. and Nykyri, E., *Scand. J. Work Environ. Health*, **14**, 175 (1988).
165. Schumacher, C., Brodkin, C. A., Alexander, B., Cullen, M., Rainey, P. M., van Netten, C., Faustman, E. and Checkoway, H., *Int. Arch. Occup. Environ. Health*, **71**, 453 (1998).
166. Gennart, J. P., Bernard, A. and Lauwerys, R. R., *Int. Arch. Occup. Environ. Health*, **64**, 49 (1992).
167. Siegel, M., Forsyth, B., Siegel, L. and Cullen, M. R., *Environ. Res.*, **49**, 190 (1989).

2.11 Speciation of Manganese

Rita Cornelis

Laboratory for Analytical Chemistry, Ghent University, Ghent, Belgium

1 INTRODUCTION

Manganese is present throughout the world. It is eleventh in the order of abundance of the elements in the earth's lithosphere, ahead of such common elements as sulfur, carbon, copper, lead, zinc, and nickel [1]. It is estimated to comprise about 0.1% of the earth's crust. Manganese has the oxidation states 0, +1, +2, +3, +4, +5, +6, and +7. The most stable is +2. Manganese dioxide is the predominant tetravalent compound, and permanganate is the prevailing heptavalent one.

2 SPECIATION OF MANGANESE IN THE ENVIRONMENT

2.1 Water

In aqueous media, the common features are that Mn^{2+} is stable in acidic solutions and MnO_2 in alkaline solutions in the presence of oxygen [2].

The number of publications on speciation or fractionation of manganese species in natural waters is very limited. The work on manganese speciation in Magele creek, a tropical river in Northern Australia [3], is to be classified as fractionation of manganese [4]. The water is characterized by low pH, high temperature and extremely low ionic strength. Low concentrations (about 2–5 $\mu g\,L^{-1}$) of soluble Mn (i.e. filtration size $<0.02\ \mu m$) are typically found in these waters during the wet season, the main natural sources apparently being rainwater and groundwater. An additional source of soluble Mn has been identified, possibly being seepage from a mine retention pond. Rather surprisingly, the concentration of colloidal Mn (0.4–0.02 μm) was almost three times higher than that of soluble Mn and was correlated with it. The primary process controlling the concentration of soluble Mn in this system appears to be rapid adsorption of soluble Mn to existing colloidal matter, followed by slower transfer of part of this surface-bound Mn to the interior of the colloid. Colloidal Mn is postulated to have a particularly long lifetime in this system because the removal process (aggregation to form particulate Mn) would be slow because of the extremely

Handbook of Elemental Speciation II: Species in the Environment, Food, Medicine & Occupational Health
Edited by R. Cornelis, H. Crews, J. Caruso and K. G. Heumann
 ISBN-10 0-470-85598-3 (HB)

low concentrations of Ca and Mg ions during the wet season. A mixing experiment, undertaken to provide information on the possible fate of Mn in a mine retention pond, should this wastewater be discharged to the creek, clearly showed that Mn would be rapidly removed from the water column via colloidal and particulate forms. The precise mechanism was discovered to be rather complex. It depended on the amount and characteristics of the colloidal and particulate matter present at the time of discharge, the changes in the Ca and Mg concentrations (which would influence the rate of aggregation) and the amount of turbulence in the creek.

Similarly, the work described as speciation of dissolved and particulate manganese in the Seine river estuary is to be classified as fractionation in as far as it covers dissolved and particulate manganese [5]. Taking into consideration the composition of the solution as well as the values of the stability constants of the complexes, dissolved manganese has been calculated using an equilibrium speciation program. Sequential extraction procedures (Tessier's scheme) have been applied to assess the manganese distribution in solid samples (sediment, suspended matter). The operational nature inherent to these procedures has been partly eliminated by determining the physicochemical form of Mn by electron spin resonance, made possible by the paramagnetic properties of manganese. The latter measurements may be classified as speciation analysis. This study showed that the behavior of manganese in the Seine estuary is strongly influenced: (i) in solid samples, by the presence of calcium carbonate that stabilizes the Mn(II) form; (ii) in solution, by the increase in salinity and in calcium, magnesium and suspended matter concentrations, through the formation of complexes and by diffusion from sediments to water.

A study about microorganisms and manganese-cycling in a seasonally stratified freshwater dam describes investigations into the role that biotic and abiotic mechanisms play in the manganese redox cycle in a freshwater dam over a 12-month period [6]. Enzymatic control of manganese oxidation was taking place with a temperature optimum of approx. 30 °C. Manganese oxidation was only significant above about 19 °C. The temperature and season play vital roles in determining the extent to which abiotic and microbial mechanisms contribute to manganese oxidation. Results showed that microbial catalysis is overwhelmingly responsible for manganese oxidation in the lower epilimnion (the layer of water that overlies the thermally stratified lower part of the lake) from November to May. Significant abiotic catalysis (up to 25%) can occur in late summer/autumn when the water temperature is greatest. In winter, biological control could not occur because of the lower temperature of the water column. The measurement of 'x' in MnOx showed that higher manganese oxidation states were expected when the manganese oxidation rate was at a maximum and therefore when microbial activity was greatest. Direct microbial reduction of MnOx in the water column was of much less significance. However, indirect reduction may have taken place through the reaction of MnOx with sulfide.

2.2 Air

Speciation of manganese compounds in urban air is important in relation to emissions of, for example, foundries, manganese industries and car exhausts, especially in those countries where methylcyclopentadienyl manganese tricarbonyl (MMT) is used as a fuel additive.

An interesting study using X-ray absorption near edge structure (XANES) spectroscopy speciated Mn-containing auto-exhaust particulates of automobile engines running on MMT-treated gasoline [7]. A series of Mn compounds was also measured to model and aid quantification of the unknown species in the particulates. The results showed that the average Mn valence in these particulates is similar to 2,2 and that MnO, Mn_3O_4, $MnSO_4$. H_2O and an Mn phosphate are the predominant phases present. The amount of each component varies depending on engine history and test cycle. The XANES analysis was found to corroborate the data obtained by K-edge X-ray absorption fine structure (XAFS), according to which the Mn species in these particulates were similarly

consisting of Mn_3O_4, $MnSO_4 \cdot H_2O$, and a divalent manganese phosphate [8].

3 SPECIATION OF MANGANESE IN FOOD

Manganese concentration in foodstuffs varies widely. The highest concentrations can be found in foods of plant origin, such as wheat, rice, and tea leaves (between 10 and 100 $mg\,kg^{-1}$). Dairy products, fruit and meat contain less than 1 $mg\,kg^{-1}$.

There are few studies about the speciation of manganese in foodstuffs. Worth mentioning is the attempt to speciate manganese using enzymes, a method that so far should be categorized as fractionation [9]. The protein, pectin, and lipid-splitting enzymes pepsin, pectinase, papain, bromelain, and lipase were used in stepwise extraction procedures. Milk powder, wheat germ, oat flakes, lentils, rice and rye flour, with Mn contents between 0.1 and 12 mg/100 g, were examined. The use of enzymes in the extraction procedures indicated distinct differences in the solubility. This method was considered a suitable precursor to a biochemical, that is, enzymological, method for manganese-speciation analysis of foodstuffs.

4 SPECIATION OF MANGANESE IN LIVING SYSTEMS

The importance of manganese in living systems remains poorly explored. Manganese compounds share with certain other elements the property of being essential for life, but certain manganese species and large doses are toxic. Manganese biochemistry largely results from its association with enzymes and proteins (at least 18), in which it has predominantly the valences (II) and (III). Generally, Mn(II) does not form metalloproteins but exchangeable metal complexes with proteins [2].

Speciation of manganese in body fluids and tissues is a very difficult task for two reasons. Firstly, the total concentration is low, typically 0.5 $\mu g\,L^{-1}$ in serum. Secondly, the risk of contamination with exogenous manganese is very high because of the omnipresence of this element in air (dust) and on surfaces and utensils [10]. It is absolutely mandatory that the balance be made between, on the one hand, the total element concentration in the matrix and, on the other hand, the sum of the measured manganese concentrations of the various species or fractions. The latter should not exceed the former.

Recently, some attempts were made to fractionate manganese in human milk, using size exclusion chromatography (SEC) combined with strong anion exchange (SAX) chromatography and inductively coupled plasma mass spectrometry detection [11]. In a first step, the milk was centrifuged and Mn measured in the different fractions by inductively coupled plasma-atomic emission spectrometry (ICP-AES). It turned out that the Mn concentrations were approximately 3 $\mu g\,L^{-1}$ in whole human milk, 2.85 $\mu g\,L^{-1}$ in the defatted fraction, 0.25 $\mu g\,L^{-1}$ in the pellet fraction and 2.6 $\mu g\,L^{-1}$ in the low molecular mass (LMM) supernatant fraction. The defatted fraction was investigated further by on-line coupling of SEC to inductively coupled plasma-mass spectrometry (ICP-MS). The columns had either a separation range between 10 and 150 kDa or 100 and 2000 Da. It was shown that manganese was predominantly present in the LMM fraction at mass 300 Da. Analysis of the respective SEC-fractions by SAX-ICP-MS revealed the existence of inorganic manganese species and an Mn-citrate complex. Some further Mn compounds of low concentration were seen but could not be assigned to specific standard compounds.

5 SPECIATION OF MANGANESE IN OCCUPATIONAL AND NONOCCUPATIONAL HEALTH ISSUES

The oxidation state of manganese is thought to be an important aspect of its toxicity. Human health risks have been documented upon exposure to organic manganese-containing pesticides, such as manganese ethyl-bis-dithiocarbamate [12], inorganic manganese dust [13] and also MMT

used as an antiknock fuel additive in the United States and Canada [14]. Neurotoxicity is a major concern in case of exposure to such manganese compounds. They are known to accumulate in the brain [15] where they cause important disruptions in cell function [16]. Once inside the cells, manganese accumulates within mitochondria [17]. The oxidation state of manganese and its binding to transferrin (to which it binds only in the trivalent state) likely represent key determinants in its differential distribution, accumulation and secretion. It is thought that Mn(III) is the primary means by which manganese mediates cellular damage.

Some very interesting basic knowledge has been obtained from the application of sophisticated analytical techniques, such as XANES spectroscopy. Using this tool, Gunter *et al*. [18] were able to provide information on the oxidation state of metal ions within a biological sample and also on the complexes in which they are found. This technique is being applied in an ongoing study of manganese in brain mitochondria and neuron-like cells. The results will be of great use to toxicologists in understanding the action-mechanism of manganese ions. Evidence is found that both Mn(II) and Mn(III) may be present in brain mitochondria. Since it is known that manganese superoxide dismutase (MnSOD) is present in these mitochondria and that MnSOD requires manganese to take both the +2 and +3 oxidation states in order to function, it was postulated that part of the XANES spectra is due to MnSOD [18].

6 CONCLUSION

Although speciation of manganese is an extremely difficult undertaking because of the very low concentrations at which the species are present, research in that area is expanding steadily. Progress is going hand in hand with the development of new and more refined analytical and bioanalytical techniques. The results contribute to a better understanding of the essentiality and the neurotoxicity of manganese species in the human body.

7 REFERENCES

1. Cooper, M. D. and Winter, P. K., Manganese in Treatise on Analytical Chemistry, Part II, in *Analytical Chemistry of the Elements*, Vol. 7, Kolthoff, I. M., Elving, P. J., Sandell, E. B. (Eds.), Interscience Publishers, John Wiley & Sons, New York, London, 1961, pp. 425–502.
2. Fraústo da Silva, J. J. R. and Williams, R. J. P., *The Biological Chemistry of the Elements: The Inorganic Chemistry of Life*, Clarendon Press, Oxford, 1991, pp. 370–399.
3. Hart, B. T., Noller, B. N., Legras, C. and Currey, N., *Aust. J. Mar. Freshw.*, **43**, 421 (1992).
4. Templeton, D. M., Ariese, F., Cornelis, R., Danielsson, L. -G., Muntau, H., van Leeuwen, H. P. and Lobinski, R., *Pure Appl. Chem.*, **72**, 1453 (2000).
5. Ouddane, B., Martin, E., Boughriet, A., Fischer, J. C. and Wartel, M., *Mar. Chem.*, **58**, 189 (1997).
6. Johnson, D., Chiswell, B. and Ohalloran, K., *Water Res.*, **29**, 2739 (1995).
7. Ressler, T., Wong, J. and Roos, J., *J. Synchrotron Radiat.*, **6**, 656 Part 3 (1999).
8. Ressler, T., Wong, J., Roos, J. and Smith, I. L., *Environ. Sci. Technol.*, **34**, 950 (2000).
9. Schwedt, G. and Neumann, K. D., *Z. Lebensm. Unters. Forsch.*, **194**, 152 (1992).
10. Versieck, J., Barbier, F., Cornelis, R. and Hoste, J., *Talanta*, **29**, 973 (1982).
11. Michalke, M. and Schramel, P., *J. Anal. At. Spectrom.*, **19**, 121 (2004).
12. Ferraz, H. B., Bertolucci, P. H. F., Pereira, J. S., Lim, J. G. C. and Andrade, L. A. F., *Neurology*, **38**, 550 (1988).
13. Roels, H., Lauwerys, R., Buchet, J. P., Genet, P., Sarhan, M. J., Hanotiau, I., de Fays, M., Bernard, A. and Stanescu, D., *Am. J. Ind. Med.*, **11**, 307 (1987).
14. Dobson, A. W., Erikson, K. M. and Aschner, M., *Ann. N. Y. Acad. Sci.*, **1012**, 115 (2004).
15. Newland, M. C., Ceckler, T. L., Kordower, J. H. and Weiss, B., *Exp. Neurol.*, **106**, 251 (1989).
16. Barbeau, A., *Neurotoxicology*, **5**, 13 (1984).
17. Liccione, J. J. and Maines, M. D., *J. Pharmacol. Exp. Ther.*, **247**, 156 (1988).
18. Gunter, K. K., Miller, L. M., Aschner, M., Eliseev, R., Depuis, D., Gavin, C. E. and Gunter, T. E., *Neurotoxicology*, **23**, 127 (2002).

2.12 Speciation of Mercury: Environment, Food, Clinical, and Occupational Health

Milena Horvat and Darija Gibičar

Jožef Stefan Institute, Ljubljana, Slovenia

1 INTRODUCTION

Mercury is widely considered to be among the highest priority environmental pollutants of continuing concern on the global scale. Although there is a continuous problem of occupational exposure to inorganic Hg, predominantly elemental Hg, possible effects on broader segments of the population due to widespread dispersal of Hg in the environment has become the major concern in recent years. Mercury is among the most highly bioconcentrated trace metals in the human food chain, and many national and international agencies and organizations have targeted mercury for possible emission control. Mercury toxicity depends on its chemical form, among which alkylmercury compounds are the most toxic.

The biogeochemistry of mercury has received considerable attention because of the toxicity of methylmercury compounds (MeHg), the accumulation of Hg in biota, and its biomagnification in aquatic food chains. Concerns about Hg are based on its effects both on ecosystems and human

Handbook of Elemental Speciation II: Species in the Environment, Food, Medicine & Occupational Health
Edited by R. Cornelis, H. Crews, J. Caruso and K. G. Heumann
 ISBN: 0-470-85598-3 (HB)

health. The principal pathway for human exposure is the consumption of contaminated fish, through dental amalgams and in specific cases through occupational exposure. Numerous recent studies have concluded that the majority, if not all, of the Hg that is bioaccumulated through the food chain as MeHg. Therefore, knowledge of the concentration, transport, transformation, and dynamics of MeHg in aquatic ecosystems is needed to predict its potential impact on humans, as well as on aquatic life.

Many of the environmental aspects of mercury and its compounds have been reviewed [1, 2]. Most comprehensive reviews of current understanding of mercury are summarized in the United States of America Environmental Protection Agency's (EPA) Mercury Report to Congress that is available on the internet (http://www.epa.gov/tnn/uatw/112nmerc/mercury.html), UNEP's (United Nations Environmental Programme) Global Mercury Assessment Report (http://www.chem.unep.ch) and the report from the European Commission on Ambient Air Pollution by Mercury (Hg) also available on internet (http://europa.eu.int/comm/environment/air/background.htm#mercury) [3].

This chapter is organized in such a manner that principal information on mercury distribution in the environment is given with emphasis on mercury speciation. In order to understand the importance of mercury speciation in food medicine and occupational health, basic information is also provided on mercury toxicity, human exposure pathways, and biomonitoring. The second part of the manuscript describes analytical protocols for mercury speciation in various samples in the environment (air, water, soil, sediments) and biological samples.

2 PHYSICAL AND CHEMICAL PROPERTIES OF MERCURY SPECIES

2.1 Metallic mercury

Elemental Mercury (Hg^0) is usually referred to as *mercury vapor* when present in the atmosphere or as metallic mercury in liquid form. Hg^0 is of considerable toxicological as well as of environmental importance because it has a relatively high vapor pressure (14 $mg\,m^{-3}$ at 20 °C, 31 $mg\,m^{-3}$ at 30 °C) and a certain water solubility (~0.060 $g\,L^{-1}$ at room temperature). Because of its high lipophilicity, elemental mercury dissolves readily in fatty compartments. Of equal significance is the fact that the vapor exists in a monatomic state.

2.2 Inorganic ions of mercury

Many salts of divalent mercury (Hg^{2+}) are readily soluble in water, such as mercury sublimate ($HgCl_2$: 62 $g\,L^{-1}$ at 20 °C), and, by this, highly toxic. In contrast, the water solubility of HgS (cinnabar) is extremely low (~0.000010 $g\,L^{-1}$), and, correspondingly, HgS is much less toxic than $HgCl_2$ [4]. The extreme high affinity of Hg^{2+} to sulfhydryl groups of amino acids as cysteine and methionine in enzymes explains its high toxicity. However, the affinity to SeH-groups is even greater, which may explain the protective role of selenium from a mercury intoxication [5].

Monovalent mercury is found only in dimeric salts such as Hg_2Cl_2 (calomel), which is sparingly soluble in water and, again correspondingly, much less toxic than $HgCl_2$ (sublimate).

2.3 Organic mercury compounds

Divalent organic mercury compounds all have a linear structure, only the ligands can be bound differently. In R–Hg–R with R as an organic ligand directly bound to carbon, a covalent binding is found, whereas in the case that one of the ligands is different (R = X = halogen) the Hg-X binding is highly ionic. For all practical purposes, organic mercury compounds are limited to the alkylmercurials monomethyl-Hg, monoethyl-Hg and dimethyl-Hg, to the alkoxymercury compounds and to the arylmercurials (phenylmercury). Organic mercury cations ($R–Hg^+$) form salts with inorganic and organic acids (e.g. chlorides and acetates) and react readily with biologically important ligands, notably sulfhydryl

groups. Organic mercurials also pass easily across biological membranes, perhaps since the halides (e.g. CH_3HgCl) and dialkylmercury are lipid-soluble. The major difference among these various organomercury compounds is that the stability of carbon–mercury bonds *in vivo* varies considerably. Thus, alkylmercury compounds are much more resistant to biodegradation than either arylmercury or alkoxymercury compounds.

Monomethylmercury compounds are of greatest concern, as these highly toxic compounds are formed biotically by microorganisms in sediment and algae in sea water [6] and/or abiotically [7–9]. Once it is formed, MeHg is bioaccumulated and biomagnified in the aquatic food chains, thus resulting in exposure levels among fish-eating populations, often at levels exceeding what is regarded as a safe level. The term 'methylmercury' is used throughout this text to represent monomethylmercury compounds. In many cases, the complete identity of these compounds is not known except for the monomethylmercury cation, CH_3Hg^+, which is associated either with a simple anion, like chloride, or a large charged molecule (e.g. a protein).

A specific source of exposure is the use of thiomersal for preservation of vaccines and immunoglobulins (usually 25–50 μg of mercury per injection) [10, 11]. Its metabolite, ethylmercury, behaves toxicologically much like methylmercury but is less stable. Because of the possible health significance to infants of this bolus injection, the use of thiomersal is being phased out.

3 MERCURY IN THE ENVIRONMENT

Mercury can exist in a large number of different physical and chemical forms with a wide range of properties. Conversion between these different forms provides the basis for mercury's complex distribution pattern, for local and global cycles and for its biological enrichment and effects (Figure 2.12.1).

The most important chemical forms are elemental mercury (Hg^0), divalent inorganic mercury (Hg^{2+}), methylmercury (CH_3Hg^+), and dimethylmercury ($(CH_3)_2Hg$).

Organomercury compounds may enter the environment from both anthropogenic sources and

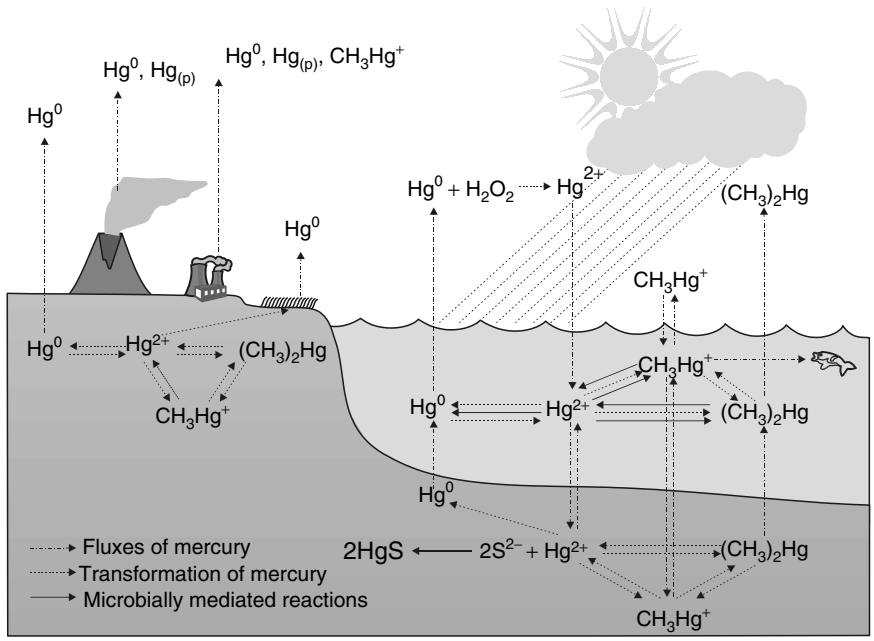

Figure 2.12.1. Mercury cycle in the biosphere.

from production by natural *in situ* biogenic alteration of inorganic or other organomercury compounds. Environmental problems that arise from the use of commercial products are generally localized. Phenylmercury compounds are still used in exterior paints and as slimicides in the pulp and paper industry. However, most governments have now banned their use for other purposes. In some countries, organic mercury compounds are still used in agriculture (mainly phenylmercury, methoxymethylmercury, and small quantities of ethylmercury compounds). In general, however, production and usage of organomercurials is declining [1].

Once methylmercury is formed, it enters the food chain by rapid diffusion and firm binding to proteins in aquatic biota and attains its highest concentrations in the tissues of fish at the top of the aquatic food chain because of biomagnification through the trophic levels, therefore fish predators, for example, shark, seal, showing even higher levels. The main factors that affect the levels of methylmercury in fish are the diet and trophic level of the species, the age of the fish, microbial activity and mercury concentration in the upper layer of the sediment, dissolved organic carbon (DOC) content, salinity, pH, and redox potential. Extensive investigations have recently been conducted in Scandinavia and North America where it was discovered that the long-range transport of Hg^0 and the potential role of acidification (through acid rain) have become major factors concerning future exposure of humans to methylmercury. As a result, methylmercury has exceeded regulatory safety limits in fish (0.5–1.0 $mg\,kg^{-1}$, fresh weight) in large numbers of remote lakes. Because of long-range transport and deposition, high mercury concentrations were observed in communities in remote Northern environments that depend heavily on mercury-contaminated local diets (fish, birds, marine mammals) [12].

Concentrations of mercury in biological and environmental samples are relatively low except in mercury-contaminated and industrial areas. For clarity, only a very brief description is given below.

3.1 Air

The major form of mercury in air is elemental mercury vapor (Hg^0) [3]. Typical concentrations of mercury and its compounds in ambient air may range between 1 and 4 $ng\,m^{-3}$ for elemental mercury, from 1 to 50 $pg\,m^{-3}$ for reactive gaseous mercury (water-soluble gaseous mercury species) and total particulate mercury, whereas MeHg has been found in the range between 1 and 20 $pg\,m^{-3}$. Volatile mercury(II) compounds represent a large part of the total gaseous mercury in stack gases from coal burning power plants. Even though Hg^0 and dimethylmercury are the most volatile forms of mercury, dimethylmercury has rarely been detected in the atmosphere. An interesting negative correlation between Me_2Hg and ozone concentrations was found in a north–south profile of the marine atmosphere of the Atlantic Ocean [13].

Its presence was detected in gases from landfill waste sites [14] and in geothermal gases and waters [15]. It is interesting to note that although significant quantities of dimethylmercury may be emitted to the atmosphere, the lifetime of this species is short, owing to photochemical and/or chemical degradation. Reliable data on mercury species in air are still very limited, and further analytical developments are needed.

3.2 Water

Concentrations of total mercury in water samples are very low (at the $ng\,L^{-1}$ level or below), so that accurate analysis is still a major problem. The theoretical approach *via* stability calculations can be of great help in making rough estimates of the predominant mercury species under various conditions. Mercury compounds occurring in natural waters are most often defined by their ability to be reduced to elemental mercury (see part (a) of this manuscript). In lake waters, methylmercury species account for 1–30% of total mercury. Most of the methylmercury is probably associated with DOC. Limited data are available on the formation constants between the

methylmercury cation and DOC [16]. Thiol groups (–RSH) have been shown, however, to have a higher capability to bind methylmercury in comparison with ligands containing oxygen and nitrogen donor atoms and the inorganic ions (CN^-, Cl^-, OH^-). Methyl mercury compounds in surface runoff waters, soil pore waters, and ground waters are similar to the species in lake waters and are generally quite strongly associated with DOC. Dimethylmercury has rarely been reported in surface waters except in the deep ocean [17–20] and during some seasons in the slurry of salt marshes [21]. Mercury in seawater exists mainly in the form of Hg^{2+} complexed with Cl^- ions. Methylmercury concentrations in seawater are generally lower than in lake waters. Dissolved gaseous mercury vapor is also present in ocean waters [22]. The presence of organomercury species, including dimethylmercury, was also detected in geothermal gases and waters [15], as well as in surface seawater samples [6].

3.3 Sediments and soils

Mercury in these two compartments of the environment is mainly associated with humic matter. Following methylation, methylmercury does not usually build up in sediments to more than about 1.5% of the total mercury present. This appears to be an approximate equilibrium level between formation and removal. Methylation-demethylation reactions are assumed to be widespread in the environment, and each ecosystem attains its own steady state with respect to the individual species of mercury. Dimethylmercury is considered to be unstable in sediments but is assumed to be stabilized by a conjunction of factors, such as high sulfide levels, salinity, anoxic conditions, and constant inputs of methane into the media [21]. It is also important to note that sampling of sediment samples from anoxic/suboxic bottoms must be conducted with extreme care, as, otherwise, changes of environmental conditions (temperature, redox potential) during sampling may significantly influence the concentrations of mercury species and their portioning.

3.4 Biota

The highest levels found in fresh and marine organisms are found at the highest trophic levels, where mercury levels can exceed the 'black list limit' of 0.5 $mg\,kg^{-1}$ [22]. The percentage of methylmercury to total mercury in fish muscle varies from 80 to 100%, but in other organs its concentration is smaller (in liver and kidney, up to 20%). In other aquatic organisms, the percentage of methylmercury is more variable, depending on water depth, location, and the type of organism. Relatively high mercury and methylmercury concentrations have been reported for fish-eating marine birds. Birds feeding on wild vegetation generally have much lower mercury in their bodies. There have recently been many studies performed on terrestrial ecosystems (particularly in Canada, Sweden, and the United States). Mercury also passes from vegetation into the food chains of fauna [23].

4 MERCURY IN FOOD, MEDICINE, AND OCCUPATIONAL HEALTH

From the toxicological point of view, mercury is one of the most toxic, nonessential chemical elements. The most important species of mercury to which living organisms are exposed can be classified into three broad categories having different toxicokinetic properties with regard to absorption, body distribution, accumulation, and toxic hazards. The most important, from a toxicological point of view, are the metallic form, also called the *elemental form*, the divalent inorganic forms, and organic mercury compounds. In a similar way, these species differ greatly in their relevance to the cycle of mercury in the environment, as mentioned above.

4.1 Toxic effects

A summary of the toxic effects of mercury in humans is given in Table 2.12.1. Kidney is the target tissue for retention of Hg in populations exposed to inorganic Hg compounds or Hg vapor.

Table 2.12.1. Summary of toxic properties of different forms of mercury in humans.

Form	Exposure	Effects	Biological indication	Disposition and mechanism of action
Hg^0	*Occupational:*	*Severe exposure:*	*Hg in urine:* chronic exposure, indication of Hg levels in kidney	Inhaled Hg^0 is absorbed in the lung and enters the blood stream, high lipid solubility allows it to cross the blood/brain and placenta barriers easily, dissolved Hg^0 is oxidized in red cells, brain, liver, lung and other tissues where it may inhibit the activity of some enzymes that contain – SH groups, denaturate proteins, damage cell membranes. At high concentrations it causes cell death and destruction of tissue. Mechanism of damage to the CNS is still not well understood.
	Chlor-alkali industry, production of thermometers, thermostats and fluorescent bulbs, mercury mining, dentistry	Tremor, gingivitis, erethism, loss of memory, emotional and psychological disturbance, damage to kidneys	*Hg in blood:* indicator of short-term exposure	
	Nonoccupational:	*Lower exposure:*	*Exhaled air:* short-term exposure	
	Dental amalgam fillings	Cognitive deficits, mild proteinuria, insomnia, loss of appetite, immunological disturbances. Damages are reversible.	No good indicators for brain	$T_{1/2}$: 1–2 months.
Hg(I)	Removed from medical use. Rare in use.	Acrodynia, pink disease. Damage is reversible.	–	Inhibition of enzymes, its action is poorly understood.
Hg(II)	Antiseptic, leather industry, production of batteries, fungicides, use in bleaching soaps and creams	Chronic toxicity: neurological disorders similar to the effects of Hg^0. Repeated exposure to low doses effects the immune systems. Acute exposure may cause irreversible damage of kidney and indirectly cardiovascular collapse.	Urine	Similar to Hg^0, except direct passage through the above-mentioned biological barriers is more difficult.
				$T_{1/2}$: 1–2 months.
Alkoxyalkyl or aryl compounds	Industry	Similar to inorganic mercury	Urine	Similar to intoxications with inorganic mercury compounds because these organomercurials are relatively unstable and are broken down to form mercuric mercury.

Table 2.12.1. (*continued*)

Form	Exposure	Effects	Biological indication	Disposition and mechanism of action
MeHg	Fungicide, slimicide, food – mainly fish and other marine products	Immediate damage of neuronal cells and delayed symptoms of sensory disturbance, constriction of visual field, deafness, motor aberrations, mental disorders, cramps, paralysis.	Blood and hair	MeHg is distributed in all tissues including brain. Prenatal damage occurs in all parts of the brain while in adults the damage is local. Inhibition of protein synthesis, it affects cell division and abnormal neuronal migration. It causes the destruction of microtubules in neuronal and astrocystic cells. MeHg damage to the CNS is still unexplained. $T_{1/2}$: 70 days. Damage is irreversible.

Brain is a target organ for exposure to organic Hg and mercury vapor, which both pass blood–brain and placental barriers. MeHg is more toxic because of the irreversibility of its effects on the central nervous system. Organomercury compounds are more readily absorbed in the gastrointestinal tract than inorganic ones, and subsequently are excreted preferentially in feces rather than in urine, which is a dominant route for excretion of inorganic Hg.

Most understanding of mercury toxicity is based principally on the results of experimental animal studies, while most evidence of clinical signs, symptoms, and neuropathology of MeHg toxicity in humans has been obtained from studies of the epidemics in Iraq and Japan [22, 24] and of populations that eat mercury-contaminated fish, as well as cases of occupational exposure.

The methylated forms of Hg are of most concern for human health. MeHg is a potent toxin that causes impairment of the central nervous system and developmental toxicity in humans. MeHg readily crosses the walls of the gastrointestinal tract because of its fast transport through biological membranes, thus accumulating in the envelopes of nerve cells and causing neurological damage. MeHg bound to proteins in tissue is relatively stable and only slowly degraded and excreted from the body. As a result, MeHg is accumulated by organisms through their lifetime, and the concentrations of MeHg are further magnified through the trophic interactions of the food web. Fish can therefore contain levels that are magnified by a factor of 10^7 above the mercury concentration in water [2].

It is generally accepted and well known that the major risks to human health arise from the neurotoxic effects of mercury. The assessment of genotoxicity and carcinogenicity of mercury compounds is difficult to interpret because of the complexity and variability observed in numerous studies [25]. Although different chemical forms of Hg tended to produce qualitatively comparable genetic effects, MeHg derivatives and other ionizable organomercury compounds were in short-term tests more active than either nonionizable mercury compounds (DMHg) or inorganic salts (mercuric chloride). The results of cytogenetic monitoring in peripheral blood lymphocytes of humans exposed to elemental Hg or Hg compounds from accidental, occupational, and alimentary sources were either negative or uncertain. Both genotoxic and nongenotoxic mechanisms may contribute to the renal carcinogenicity of Hg, demonstrated in male rodents treated with MeHg [26].

However, recent studies suggest [27] that other effects may also be present when accompanied by

other risk factors such as poor diet comprised of saturated animal fats and low antioxidant intake (e.g. poor in selenium). It is known that unsaturated lipids are subject to peroxidative degradation, a process that plays a key role in the development of the arteriosclerosis process. Mercury can reduce the antioxidative capacity of selenium superoxide dismutase, catalase activity and glutathione peroxidase activity, and can promote free radical stress and lipid peroxidation. A correlation between increased accumulation of MeHg and the incidence of mortality from ischemic heart disease was found in the inhabitants of eastern Finland, whose nutrition is primarily comprised of fish, meat, and saturated animal fat with a low selenium intake [27]. The preliminary, unpublished data of an international study conducted by IARC [28], which also included 1589 workers in mercury mines, show, among other things, a relation between long-term work in European mercury mines with exposure to elemental mercury (Hg^0) vapor and increased mortality due to ischemic heart disease. This result is specific only for workers in the mercury Mine of Idrija, Slovenia, and not for workers from the mercury mines and mills of Spain and Italy. It is assumed that the differences in mortality due to ischemic cardiac disease in mines and mills are due to differences in nutrition in particular countries. It could also be a consequence of higher exposure to elemental Hg in the Mercury mine (where it occurs naturally as native mercury as well as cinnabar), leading to depletion of catalase and lowered antioxidative capacity.

4.2 Sources and patterns of exposure to mercury and its compounds

There is a considerable variation of mercury levels in those media that are the sources of human exposure, and, consequently, in their contribution to the toxicity risk. Main mercury absorption routes in humans are through respiratory and dietary routes. Nonoccupational groups are primarily exposed through the diet and dental amalgam.

4.2.1 Ambient air

The concentrations in rural areas are normally very low (below 2.5 $ng\,m^{-3}$) [29]. The values in urban areas are usually higher and vary between 5 and 15 $ng\,m^{-3}$ [24] and in some contaminated places even higher [30]. The reference concentrations (RfC) recommended by the US EPA amounts to 0.3 $\mu g\,m^{-3}$ [31], which means that in general mercury concentrations in air do not represent a considerable intake of Hg for humans. The WHO has estimated the daily intake of each form of Hg on the assumption that 75% of Hg is in elemental Hg form, 5% as inorganic Hg, and 20% of MeHg. By assuming a daily ventilation of 20 m^3, and the amount absorbed across the pulmonary membranes (80% of elemental Hg, 50% of inorganic Hg, and 80% of MeHg), daily intakes were calculated and given in Table 2.12.2

4.2.2 Dental amalgam

Dental mercury fillings are reported to release Hg vapor into the oral cavity [32]. The resulting concentrations in intraoral air can substantially exceed

Table 2.12.2. Estimated average daily intakes and retention in (μg per day) of different mercury forms in the general population not occupationally exposed [24].

Exposure	Elemental Hg vapor	Inorganic Hg compounds	Methylmercury
Air	0.03 (0.024)[a]	0.002 (0.001)	0.008 (0.0069)
Dental amalgams	3.8–21 (3–17)	0	0
Food			
– Fish	0	0.60 (0.042)	2.4 (2.3)[b]
– Nonfish	0	3.6 (0.25)	0
Drinking water	0	0.050 (0.0035)	0
Total	3.9–21 (3–1–17)	4.3 (0.3)	2.41 (2.31)

The data in parenthesis represent retained Hg in the body of an adult.
[a] If the concentration is assumed to be 15 $ng\,m^{-3}$ in an urban area, the figure would be 0.3 (0.24) μg/day.
[b] 100 g of fish per week with the Hg concentration of 0.2 $mg\,kg^{-1}$.

those found in the ambient atmosphere, especially after a period of chewing. It is estimated that average daily amounts of Hg entering the pulmonary system ranges from 3 to 17 μg of Hg [24, 33], but there is variability among populations, and intakes in the order of 100 μg per day may occur.

4.2.3 Water

Concentration of mercury in drinking water is normally very low (below 1 ng L^{-1}). Values of up to 25 ng L^{-1} are reported [24]. On the basis of the assumption that an adult consumes about 2 L of water per day, the daily intake of Hg from drinking water is insignificant. The WHO guidelines and many national legislation set the values of 1000 ng L^{-1} [34].

4.2.4 Soil

The average mercury concentration in surface soil is reported to be from 20 to 625 μg kg^{-1} [35]. Higher concentrations are reported in soils from urban locations and close to sources of Hg pollution (smelting, mining, coal burning facilities, chlor-alkali industry, etc.). In Europe, very little knowledge is available for volatilization of Hg from soil and consequently on the direct exposure of humans to Hg in soils.

4.2.5 Diet

Daily intake and retention of mercury from food is difficult to estimate accurately. In most food stuff, Hg concentration is below 20 μg kg^{-1}. Mercury is known to bioconcentrate in aquatic organisms and it is biomagnified in aquatic food webs. For example, the concentration of Hg in small fish at the low food web level (such as anchovies) is below 0.085 mg kg^{-1}, while in sward fish, shark, and tuna values above 1.2 mg kg^{-1} are frequently reported [24]. In Scandinavian predatory freshwater fish (perch and pike), average levels are about 0.5 mg kg^{-1}.

The use of fish meal as feed for poultry and other animals used for human consumption may result in increased levels of Hg. In Germany, poultry contains 0.03–0.04 mg kg^{-1}. Cattle are able to demethylate Hg in the rumen, and therefore, beef and milk contain very low concentrations of Hg.

The main problem to accurately estimate daily intakes of various Hg forms from diet is that national survey programs mainly report total Hg concentrations, and the percentage of Hg as MeHg is not known. In some national surveys, the percentage of Hg originating from fish is provided. It is assumed that in this foodstuff the percentage of Hg as MeHg is from 60 to 90%. Therefore, fish and fish products represent the major source of methylmercury.

The joint Food and Agriculture Organization and World Health Organization (FAO/WHO) Expert Committee on Food Additives [24, 36] provisionally recommended that total Hg intake should not exceed 5 μg kg^{-1} of body weight per week, with no more than 3.3 μg kg^{-1} per week as MeHg. Of 26 nations reviewed [37], none showed mean dietary intakes approaching these values.

Consumption of contaminated fish is the primary route of exposure to MeHg for humans and wildlife. Public health regulations in the United States of America prohibit consumption of fish with tissue mercury concentrations of >1 mg kg^{-1} fresh weight, while some other countries regulate at the 0.5 mg kg^{-1} level.

In 1997, the US EPA set a new guideline for methylmercury in the diet of 0.1 microgram of mercury per kilogram of body weight per day (0.1 μg kg^{-1} day^{-1}). This is 4.7 times as strict as the World Health Organization's (WHO) standard of 0.47 μg kg^{-1} day^{-1}. The average concentration of Hg in fresh and marine fish is about 0.2 mg kg^{-1}. In practical terms, this means that an average person who weighs 60 kg can only consume about 30 g of fish per day [38]. This recommendation is based on epidemiological studies conducted in Iraq after the MeHg epidemic. The value for a reference dose is currently under review, before being officially adopted. Two large epidemiological studies in the Seychelles [39] and the Faroe Islands [40] that were designed to evaluate childhood development and neurotoxicity in relation to fetal exposures to MeHg will provide

more information for further refinement of reference dose values. The provisional tolerated daily intake (PTWI) set by the Welfare Ministry of Japan is 0.17 mg of methylmercury (0.4 μg per kg body weight per day) [41]. In Europe, the recommended limits for mercury vary. In Scandinavian countries, Hg in fish should not exceed 0.5 mg Hg kg^{-1}. The Swedish Food and Health Administration is at present evaluating the relevance of a new limit at 0.3 mg Hg kg^{-1}, while Japan has already adopted a 0.3 mg kg^{-1} guideline [42]. In Sweden, pregnant women are advised not to eat perch and pike at all during pregnancy.

4.3 Biomonitoring of mercury exposure in humans

This chapter deals with biological samples that are used to assess mercury exposure in humans. The selection of biological media depends on mercury compounds, exposure pattern (e.g. chronic, acute), and time of sampling after exposure.

4.3.1 Elemental and inorganic mercury

In case of exposure to elemental mercury, blood and urinary mercury are commonly used to assess occupational exposure. Elemental Hg^0 in exhaled air and urine has also been used to assess the level of recent exposure to elemental Hg. One should note that inhaled vapor of Hg is oxidized to Hg(II), and both species are present (elemental and divalent Hg). The elemental Hg is highly mobile, readily crosses the placenta, cell membranes, and the blood–brain barrier. The Hg(II) ions are much less mobile, crossing the above barriers at a much slower rate.

At low levels of elemental Hg exposure, individual differences in total Hg in blood could be explained by current exposure to Hg because of the number of amalgam fillings, fish consumption, and other possible exposure routes (e.g. living environment in Hg mining area). At low-level elemental Hg exposure, blood Hg poorly represents information on current and past Hg^0 exposure. A separation of whole blood into its plasma and erythrocyte fractions permits better discrimination between exposure to Hg^0 and methylmercury. Such discrimination will, of course, be more correct using speciation of mercury in blood.

The concentration of Hg in urine is a good indicator of a long-term integrated exposure, while total Hg in blood is a good indicator of recent exposure [43, 44].

An attempt has been made to use the exhaled air as a possible bioindicator of exposure to elemental Hg [45, 46]. A portion of absorbed Hg is excreted via the lungs. At a lower level of exposure, the usefulness of this biomarker is limited because of numerous confounding factors, such as Hg released from amalgam filling, drinking of alcohol, and so on. The kinetics of uptake and release in blood and urine are fairly rapid, while Hg levels in target organs may change far more slowly [32]. Mercury levels in blood and urine may not reflect the accumulation of Hg in the brain, while urinary Hg mainly reflects kidney Hg [32]. As the elemental Hg vapor is readily oxidized to inorganic Hg after absorption, similar biomarkers (blood and urine) could be used to assess exposure to inorganic Hg.

4.3.2 Methylmercury

In case of exposure to methylmercury, two bioindicators are normally used: blood and hair samples. In the *blood*, MeHg accumulates mainly in the red blood cells, therefore Hg in red blood cells is frequently used as an index to MeHg exposure. Exposure to elemental Hg will lead to increased values of Hg in plasma, therefore through the analysis of total Hg in these samples it is possible to differentiate between exposure to elemental Hg and MeHg. However, it is recommended to measure total Hg and MeHg in order to take into account possible co-exposure to elemental/inorganic Hg. This is not difficult, as a number of methods have been developed in recent years to facilitate accurate analysis of total and MeHg in biological materials.

Scalp hair has widely been used as a good indicator of exposure to MeHg in the diet. MeHg is incorporated into the hair follicle in

proportion to its content in blood. The hair-to-blood ratio in humans has been estimated as approximately 250 : 1, expressed as μg/g hair to mg Hg/L blood. Once MeHg is incorporated into hair, MeHg is stable, and therefore provides a longitudinal history of blood MeHg. However, because of possible co-exposure to elemental Hg or possible external contamination of hair samples with inorganic Hg, it is recommended that both total Hg and MeHg are measured, in cases when high levels of Hg are found. Concentrations of MeHg in body and/or pubic hair were as well proven to be good indicators of MeHg burden [47].

It is well understood that pregnant women and their fetus are the most critical population group as to exposure to MeHg through food consumption. Some recent studies carried out in Faroe islands [40] indicated the usefulness of umbilical cord blood as good exposure indicator during pregnancy. There is a good correlation between MeHg in maternal and *umbilical cord blood*, with higher values found in cord blood, indicating efficient transport of MeHg through the placental barrier to the fetus. At more elevated levels of MeHg in maternal blood (about 7 ng mL^{-1}), the umbilical: maternal blood ratio is about 3. The usefulness of *placenta* as an indicator of exposure is still not clear, although most studies show very good correlation between MeHg in blood, hair, and placenta. The percentage of Hg and MeHg in placenta is much lower than in blood samples, most probably reflecting removal of inorganic Hg before it can be transferred to the fetus [47].

The poisoning nature of mercury is well acknowledged [24, 48]. But less known are the effects of mercury on humans as a consequence of long-term exposure to low concentrations. In many cases, the use of biomarkers, such as Hg concentrations in blood and urine, are not sufficient to assess the internal doses and potential effects on the central nervous system, kidney, the immune system, and other possible effects. Therefore, better scientific understanding of risks to human health, especially to those citizens living close to potentially dangerous sites, is needed. Therefore, other biomarkers than mercury measurements alone should be used. An example is N-acetyl-glucose-aminidase (NAG) and other low molecular mass proteins in urine that seem to reflect effects at low-level exposure to Hg^0. There is a need for continuous research, and, for example, markers of oxidative damage should be tested.

5 ANALYTICAL METHODS

During recent years, new analytical techniques, which have become available, have been used in environmental studies, and the understanding of mercury chemistry in natural systems has improved significantly [2, 49, 50].

5.1 Determination of total mercury

Earlier methods used for the determination of total mercury in biological samples were mainly colorimetric, using dithizone as the complexing agent. However, during the past decades cold vapor atomic absorption and atomic fluorescence have become widely used because of their simplicity, sensitivity, and relatively low price. Briefly, the mercury vapor, produced by the reduction of ionic mercury in solution with proper reductants (sodium borohydride or tin(II) chloride), is swept out by an inert carrier gas and introduced into an optical beam where the mercury atoms are detected. Since the cold vapor techniques are based on the determination of total Hg^{2+}, all mercury species in a sample have to be converted to Hg^{2+}. This can be achieved by proper acid digestion techniques [51]. Neutron activation analysis (NAA), either in the instrumental and radiochemical mode, is still used where nuclear reactors are available. Inductively coupled plasma mass spectrometry (ICP-MS) has become a valuable tool, in particular, in mercury speciation. The emphasis in this chapter is on speciation methods, as methods for total mercury have been extensively reviewed elsewhere [2, 52].

Numerous analytical protocols have been developed and optimized by instrument producers worldwide. For example, solid sampling cold vapor (CV) atomic absorption spectrometry (AAS) has been increasingly used for the determination

of total Hg in solid and liquid samples [53]. CV AAS procedure is also frequently based on flow injection analysis [54].

5.2 Mercury speciation

In general, methods are classified according to the isolation technique and the detection system [2, 55]. Most methods for the isolation/separation of organomercury compounds have been based on solvent extraction, differential reduction, difference calculations between 'total' and 'ionic' mercury, derivatization, or with paper- and thin layer chromatography (TLC). The most common approaches to organomercury separation and detection are schematically presented in Figure 2.12.2.

5.2.1 Sample collection and pretreatment

The various sampling procedures must be appropriate to the sample type and methylmercury concentration. Organic mercury is present at much lower concentrations than total mercury, except in fish, seafood and hair. Therefore, apart from the methylmercury specific-separation and detection techniques, careful handling of samples prior to analysis is necessary. A general difference between total and organomercury analyses is that the contamination of samples by organomercurials prior to analysis is much less probable. They are not usually present at detectable levels in laboratory environments.

Cleaning procedures: Rigorous cleaning procedures must be used for all laboratory ware and other equipment that come into contact with samples. Reagents that are used for the analyses of total and organomercury species must be of suitable quality (preanalyzed and shown to contribute minimally to blanks). The best materials for sample storage and sample processing are Pyrex and silica (quartz) glass and Teflon (polytetrafluoroethylene (PTFE) or fluorinated ethylene propylene (FEP)). Plastics such as polypropylene are not recommended since these materials can contribute to either contamination or losses of mercury. There are several cleaning procedures that

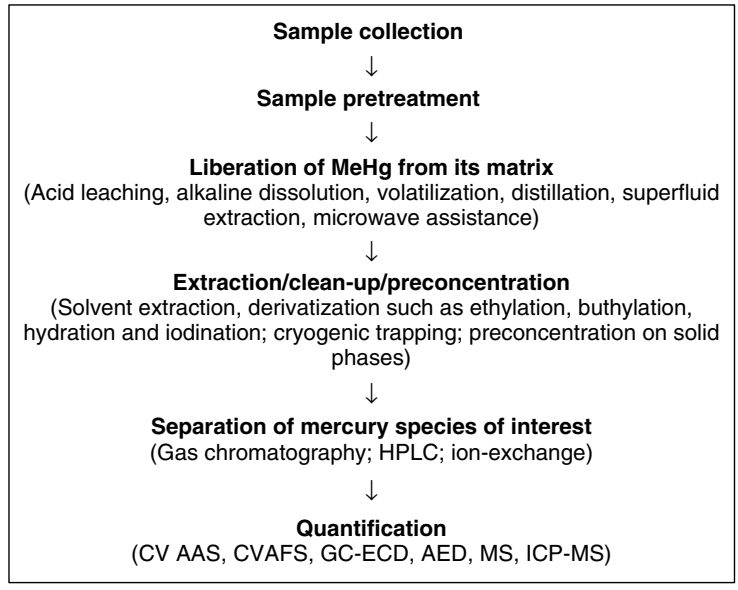

Figure 2.12.2. Steps for determination of organomercury compounds CV AAS – cold vapor atomic absorption spectrometry, CV AFS – cold vapor atomic fluorescence spectrometry, GC-ECD – gas chromatography-electron capture detector, AED – atomic emission detector, ICP-MS – inductively coupled mass spectrometry, HPLC – high performance liquid chromatography.

are recommended [1]: aqua regia treatment followed by soaking in dilute (~5–10%) nitric acid for a week [2], soaking in a hot oxidizing mixture of $KMnO_4$ and $K_2S_2O_8$, followed by $NH_2O{\cdot}HCl$ rinsing and soaking for a week in 5 M HNO_3 [3]; soaking in a 1 : 1 mixture of concentrated chromic and nitric acids for a few days [4]; soaking in BrCl (mixture of HCl and $KBrO_3$); and [5] for Teflon, cleaning in hot concentrated HNO_3 for 48 h, followed by soaking in dilute HNO_3 (50%) (which is repeated twice). After such treatments, laboratory ware is usually rinsed with mercury-free deionized water or double distilled water and stored in a mercury-free place, preferably sealed in mercury-free plastic bags. Some authors recommend storage in dilute (1%) hydrochloric acid until use. Laboratory ware that is used for methylmercury analyses should be prepared with extreme caution. It has been shown that final soaking (after using one of the above-mentioned cleaning procedures) of laboratory ware, particularly Teflon, in hot (70 °C) 1% HCl removes any oxidizing compounds (e.g. chlorine), which may subsequently destroy methylmercury in solution.

Air: Most techniques employ sampling of large volumes of air through one or more media (solid or liquid sorbents), which trap the mercury species of interest. Therefore, one of the important parameters in obtaining accurate final results is the determination of the sample volume collected under standard conditions (of temperature and pressure). Contamination also represents an important source of error for low-level mercury determination. Usually, a high degree of accuracy is achieved when sampling ambient (indoor and outdoor) air. The presence of excessive amounts of water vapor and CO_2 (e.g. in fuel or combustion gases) may necessitate a correction to the flow meter readings.

The first operational step is the removal of particulate matter, which is usually separated by glass fiber filters, Teflon, or a plug of glass or quartz-wool. If selective adsorption methods (see Section 5.2.2) are used, the first step is usually to separate mercury(II) compounds. Various adsorption materials have been used in the past. One of the most common is Chromosorb W, treated by HCl alone or coated with a polar stationary phase (e.g. OV-1 or SE-30). In recent years, methods for reactive gaseous mercury(II) compounds were validated and are based on mist chamber techniques, tubular and annular denuders. Following the trapping of mercury(II) species, a second trap is then used to collect methylmercury compounds. Chromosorb W, treated with NaOH, has been employed. The use of impingers with aqueous solutions and/or high-flow refluxing mist chambers has recently been optimized for the direct preconcentration of extremely low concentrations of methylmercury in ambient air [56]. Methylmercury (and dimethylmercury if present) can also be trapped using Tenax or Carbotrap and cryogenic trapping followed by one of the mercury-specific instrumental techniques. Hg^0 is retained or captured on the final trap, usually consisting of a silver- or gold-coated adsorbent. In most cases, the total gaseous mercury fraction in air is determined directly by noble metal amalgamation, or by other methods described in the previous section on inorganic mercury determination.

Water: Collection and handling of aqueous samples for low-level determination of mercury must address factors such as whether the sample is representative of the system sampled, possible interconversion processes, contamination, as well as preservation and storage of the sample before analysis. The measurement (sampling and analysis) protocol must be even more carefully designed if speciation of mercury forms in aqueous samples is intended. There have been remarkable improvements in sampling and analytical techniques, which over the past 15 years have resulted in a dramatic increase in the reliability of data for mercury levels in water samples. The stability of mercury in solution is affected by many factors. These include (a) the concentration of mercury and its compounds (e.g. particularly at low levels of concentration, the relative change in the value is easily affected by transformation processes, contamination and adsorption) (b) the type of water sample, (c) the type of containers used, (d) the cleaning and pretreatment of the containers, and (e) the preservative added.

Contamination-free sampling devices (e.g. Teflon-coated Go–Flo samplers) are commonly used. Alternatively, the water can be pumped through Teflon tubing using a peristaltic pump. Collection of surface waters is usually performed by hand, using arm-long plastic gloves. Samples are taken upwind of a rubber raft or a fiber glass boat. Automatic samplers, with in-line filtration, can collect precipitation samples if desired. Teflon wide-mouth jars have been favored for sampling waters with low mercury concentrations. Containers and other sampling equipment, which come into contact with water samples, should be made of borosilicate glass, Teflon, or silica glass. These materials have been found to be free from mercury contamination and therefore suitable for work at low, ambient levels. However, Teflon showed the best performance regarding both contamination and loss-free storage of aqueous samples. The most volatile mercury forms potentially present in water are Hg^0 and dimethylmercury. They should be removed from the samples immediately after the sampling step by aeration (purging) with collection on Carbotrap or other suitable adsorption media for subsequent analysis in the laboratory.

Measurement of dissolved mercury compounds requires removal of particulate materials from the sample by either filtration or centrifugation. Various types of filters can be employed: 0.45 μm membrane filters (precipitation, sea water), disposable polystyrene units (Nalgene) with nitrocellulose membrane filters, and pretreated glass fiber filters.

In order to store samples prior to analysis, samples should be preserved, generally by acidification. However, acidification is subject to two limitations: (a) suspended matter has to be removed prior to acidification, and (b) dimethylmercury and Hg^0 have to be removed prior to acidification, otherwise conversion of these species into ionic mercury compounds may occur [17, 51, 57]. In general, samples for speciation of gaseous mercury species in water are processed immediately after sampling. However, if water samples do have to be stored for longer periods, adding preservatives may stabilize the mercury present. For the analyses of organomercurials, preservation with oxidative reagents (as advised for total mercury analyses) should be avoided, since organomercurials are converted into inorganic mercury. Stabilization by HNO_3 results in decreased methylmercury, while Hg(II) remains stable in the presence of this acid. HCl was found the most appropriate acid for storing aqueous methylmercury solutions. Sulfuric acid can also be used for preservation of methylmercury solutions in distilled water, although it is not suitable for natural water samples. Inorganic complexing agents, such as Cl^-, I^-, CN^-, Br^-, and organic complexes (L-cystein), have also been proved to stabilize organomercury compounds in solution. Some authors claim that for methylmercury determinations, storage of samples without preservatives but at low temperatures (or even deep-frozen) is better than adding acid.

Biological samples: Relatively little is known about the effects of storage on the stability of methylmercury in biological samples. Significant external contamination of samples with methylmercury is unlikely to occur; however, extreme precautions are necessary to avoid contamination by inorganic mercury.

Blood and hair samples are often analyzed in order to estimate exposure of humans to mercury and its compounds. Blood is a suspension of cellular components in a protein-containing medium in a ratio of approximately 43 : 57. It should be taken by venipuncture. It is compulsory to collect the blood without addition of any preservative, neither of any anticoagulant, and this is for two reasons. First, because the preservative may contain a mercury compound or be contaminated with mercury impurities. Second, because any preservative and/or anticoagulant is liable to break up the original mercury species. Most anticoagulants are either polyanions (e.g. heparin) or metal chelators (e.g. Ethylenedinitrilotetraacetic acid (EDTA), citrate) and therefore have a high affinity for metal species. As a rule, neither heparinized samples nor EDTA, citrate, or any other anticoagulant doped samples will be used. Add to this that when blood is collected with an anticoagulant, it separates into plasma and red blood cells that are different from

serum and packed cells. Serum contains no fibrinogen. Packed cells not only consist of red blood cells but also include all other cellular material.

As speciation of the mercury species is the aim of the analysis, it is inconceivable to analyze total blood because of the very different nature of its constituents (serum and packed cells).

After the blood has been sampled without anticoagulant, it will clot spontaneously and separate into serum and packed cells. The process lasts 15–30 min at room temperature. It is then submitted to centrifugation, which should be completed within 1 h. This separation should be done as soon as possible to avoid hemolysis of blood. Hemolyzed samples cannot be considered for analysis, more so not for speciation analysis. The distribution of the different trace element species between serum and cells may vary several orders of magnitudes. Concentrations in the two phases are controlled by different mechanisms. The determination of trace element species in whole blood is, therefore, far less informative than the analysis in serum and packed cells separately.

Serum and packed cells may be deep-frozen only once, as repeatedly frozen and thawed samples showed a remarkable decrease in methylmercury concentrations [58]. There is also some evidence that methylmercury may be destroyed during lyophilization of blood samples [58, 59].

Analysis of human hair offers several advantages over analysis of blood samples: for example, ease of sampling and sample storage, the concentration of methylmercury is approximately 250 times higher than in blood, and analysis of different longitudinal sections of hair can give information on the history of the exposure to methylmercury ingested through food. Adhering dust and grease should be removed by one of the following solvents: hexane, alcohol, acetone, water, diethylether, or detergents. IAEA and WHO [60] recommend the use of only water and acetone. Long-term storage of human hair samples has shown that methylmercury is stable for a period of a few years if stored dry and in darkness at room temperature.

Biological samples are preferably analyzed fresh or after lyophilization. Deep-freezing of fresh samples, especially with long storage, should be avoided since it has been noticed that in some organisms methylmercury may decompose with repeated freezing and unfreezing (particularly in bivalves) [58]. Methylmercury and total mercury in lyophilized biological samples, such as biological certified reference materials (CRMs), are stable for years. The CRMs are, however, sterilized either by autoclaving or by γ-irradiation. This important step prevents bacteriological activity, which may otherwise lead to methylation/demethylation processes. In general, very little is known on the effects of sterilization on the stability of methylmercury compounds. More studies are needed to investigate the stability of organomercury compounds in biological samples, particularly under various sample preparation and long-term storage conditions.

Sediment and soil: Sediment and soil samples should also be prepared with caution since the percentage of methylmercury in these samples is very low (e.g. $<2\%$ of total mercury) and improper handling and storage may lead to inaccurate results. These samples should be analyzed fresh or, if long-term storage is unavoidable, samples should be kept in the dark at low temperatures or freeze-dried. Drying at elevated temperatures (in the oven) results in high losses of total and methylmercury. Moreover, changes of pH, redox potential, moisture, and so on, may significantly influence the stability of methylmercury in sediments. Because of changes during sampling, conversion of mercury species may occur (methylation, demethylation, reduction), particularly in case of sediments taken from the oxygen-depleted bottom of water bodies [61]. These samples should better be analyzed fresh or, if long-term storage is unavoidable, samples should be kept in the dark at low temperature, at an inert atmosphere, and deep-frozen.

Calibration standards: There have been a few studies performed concerning the stability of organomercurials in standard solutions [62]. A decrease of methylmercury in aqueous solutions can be caused by adsorption onto the container walls or decomposition to Hg(II), Hg^0,

or $(CH_3)_2Hg$. Losses of methylmercury chloride due to volatilization is unlikely to occur [Kd (gas–liquid distribution coefficient: C_{gas}/C_{H_2O}) is 1.07×10^{-5} at 20 °C]. The stability is strongly dependent on the concentration, the container materials, and the storage temperature. An aqueous methylmercury concentration of 10 $\mu g\,L^{-1}$, stored in Pyrex glass (precleaned with $HNO_{3)}$ at low temperature (e.g. in a refrigerator), is stable for approximately one month. If Teflon containers are used, the solution is stable for several months if stored in the dark at room temperature. Some authors recommend storage of methylmercury solutions in 0.2–0.5% HCl. Methylmercury standard solutions in organic solvents stored in Pyrex glass bottles (for gas chromatography (GC) analyses) are even more stable than water solutions. Recently, the European Institute produced new CRM for calibration of $Me^{202}Hg$ for Reference Materials and Measurements [63].

Calibration standards may also be prepared in the gas phase. Elemental mercury vapor is often used for calibration of detectors for elemental or total mercury determination employing preconcentration by amalgamation. Volatile organomercury compounds could also be prepared in the gas phase. This is of importance for the optimization of methodologies for organomercury speciation in air. An aliquot of vapor is removed from a temperature-stabilized vessel using a gas tight syringe. The concentration can be calculated from data on the partial pressure of the individual compound and the gas-law equation. Calibration standards for inorganic mercury can also be ordered from major producers of CRM.

5.2.2 Separation and detection systems

During the last 20 years, hundreds of papers that deal with determination of organomercury compounds in environmental samples have been published. Most of them are based on solvent extraction and detection by GC electron capture detector (ECD), the method originally developed by Westöö [64]. In recent years, however, significant improvements of analytical methods in terms of specificity and sensitivity have been developed. This has allowed the determination of mercury speciation in all environmental compartments. Only a brief overview of methods is given, which have been reported in review articles [65, 66]. Instead, particular emphasis has been placed on more recent analytical developments and future needs.

Air: The concentration of total mercury in air can be determined with high precision and accuracy [52]. There are still, however, analytical problems in separating and analyzing all the specific mercury compounds that can be present in air. Since concentrations of organomercurials are so low, a preconcentration step has to be employed. Schroeder [52, 67] has reviewed atmospheric mercury determinations. In general, two approaches are possible for measurements of mercury compounds in air [1]: selective adsorption methods (usually coupled with nonselective detectors), in which the separation is operationally defined and a true species identification is not obtained (therefore it is not clear whether the species determined are the actual mercury compounds present in the atmosphere), and [2] gas chromatographic methods that allow identification of various organic species by their unique retention times and specific mercury detection system. The most readily determined forms are Hg^0 and dimethylmercury, as these are the most volatile and nonpolar species. Water vapor does not disturb their speciation and analysis. More problematic is the separation of methylmercury and mercury(II) compounds, where water vapor affects both the isolation and measurement steps. From the publications cited in the review article of Schroeder, it is evident that in studies where selective adsorption methods are used, a maximum of four mercury species (Hg^0, Hg(II), monomethyl mercury, and dimethylmercury) are reported. In studies where GC separations are used, only Hg^0, monomethyl and dimethylmercury are reported, although total mercury is usually determined separately. The main difference between these approaches is the identification of Hg(II) compounds. Many authors have addressed the effect of moisture on the performance of the above-mentioned adsorption techniques, although the problem has not, as yet, been

solved completely. There is a large risk of the $Hg^0 + O_3$ reaction in sampling bubblers or traps, which may result in very high Hg(II) values.

Improvements have been made recently for the preconcentration of gaseous methylmercury in air by preconcentration in mist chambers and subsequent determination by aqueous-phase ethylation, precollection on Carbotrap columns and separation by GC and detection by cold vapor atomic fluorescence spectrometry (CV AFS) [56]. In order to understand the behavior and fate of mercury compounds in the atmosphere and their role in environmental mercury cycling, there is an urgent need for further development of analytical methods to identify mercury species in the atmosphere by compound-specific analytical methods (as opposed to operationally defined protocols).

Water: Only a few analytical techniques have so far been developed for the reliable determination of organomercury species in water samples. In many studies, mercury compounds in aquatic environments are speciated according to their ability to be reduced to the elemental state. Dimethylmercury and Hg^0 (the most volatile mercury compounds) can be isolated by aeration and adsorption on a suitable adsorbent (dimethylmercury on Carbotrap or Tenax and Hg^0 on gold trap) or by cryotrapping, or separation by noble metal amalgamation (for Hg^0), immediately after sampling. Alternatively, they can be directly analyzed by separation on GC columns and detected by one or more suitable mercury detectors. Samples should not be acidified prior to such separations since dimethylmercury and Hg^0 are transformed into methylmercury and Hg(II), respectively. For specific organomercury compound determinations, a preseparation and preconcentration method, followed by a very sensitive detection system, is necessary. In a typical extraction method, CH_3HgX (X is a halide ion) is extracted into an organic solvent (benzene or toluene) after acidification. This is followed by derivatization to a water-soluble adduct of methylmercury-cysteine, which is extracted into a water phase. After acidification, CH_3HgX is back-extracted into a small amount of organic solvent. An aliquot is then injected onto a gas–liquid chromatography (GLC) column and detected by an ECD or any other suitably sensitive detector (such as a plasma emission detector). Packed or capillary columns can be used. More precise descriptions of the chromatographic conditions are given below. There are quite a few modifications to this extraction procedure, and these have been reviewed by Craig [66]. For example, the methylmercury-cysteine compound may be transferred into dithizone chloroform solution and quantified by AAS. Inorganic and organic mercury species can be preconcentrated on dithiocarbamate or sulfhydryl cotton-fiber adsorbent that is then extracted as described above. The common drawbacks of most of these extraction procedures are the large sample requirements, low extraction yields, and nonspecific separation of dimethylmercury, if present.

There are also methods for determination of 'total' organomercury compounds. Inorganic and organic mercury are preconcentrated on a dithiocarbamate resin and are subsequently eluted with thiourea. Separation of organic and inorganic mercury is achieved by differential reduction and detection by CV AAS [68]. Inorganic and organic mercury can also be separated using anion-exchange resins [69]. Organic mercury is then decomposed (by UV irradiation) and measured by CV AAS. It has, however, been shown that the levels obtained by this method do not necessarily correspond to methylmercury (owing to the lack of specificity of the protocol).

Another method based on aqueous-phase ethylation, room temperature precollection, and separation by GLC with CV AFS detection has been described [70]. Modifications of this method are frequently used in laboratories involved in studies of the biogeochemical cycle of mercury.

Ethylated mercury species are volatile and can therefore be purged from solution at room temperature and then collected on adsorbent materials such as Carbotrap or Tenax. After thermal release, individual mercury compounds are separated by cryogenic or isothermal GC. As the species are eluted, they are thermally decomposed (pyrolized) at 900 °C and measured as Hg^0 using a CV AFS detector, which achieves very low detection limits ($<10^{-12}$ g). A CV AAS detector can also be used

but its detection limit is much higher, 167 pg [57]. In recent years, ICP-MS is more and more frequently used, as it offers numerous advantages over AAS and AFS detectors. Instead of ethylation, propylation was recently shown to be an even more suitable derivatization procedure, being free from interferences caused by halide ions [71]. Hydration was also proven to be a useful derivatization method, in particular, when coupled with preconcentration by cryotrapping [72].

In any case, the critical part of this procedure is the preparation of samples prior to derivatization. Methylmercury compounds must be removed from bound sites to facilitate the ethylation reaction. Interfering compounds (such as sulfides) must also be removed. Two approaches have been used so far. The first is based on extraction of methylmercury compounds into methylene chloride and then back-extraction into water by solvent evaporation [70]. The second is based on water vapor distillation. Distillation has advantages since it quantitatively releases methylmercury from sulfur and organic-rich water samples [73].

The analysis of different mercury compounds at environmental concentrations should be developed further. Reliable data can be obtained for monomethyl mercury compounds and dimethylmercury. There is, however, a need to identify biogeochemically important mercury fractions, which are currently measured by operationally defined rather than direct ('analytically rigorous') protocols.

Other environmental samples: The basis of most present methods was introduced by Japanese and Scandinavian workers [64, 74]. It involves the extraction of organomercury chloride from acidified homogeneous samples into benzene (however, the use of toluene is strongly recommended, for health and safety reasons). Organomercury compounds are then back-extracted into an aqueous cysteine solution. The aqueous solution is then acidified, and organomercury compounds are reextracted with benzene or toluene. This double partitioning enables removal of many interferences (e.g. benzene-soluble thiols). Finally, methylmercury is analyzed by GC with electron capture detection. Several modifications have been made to this protocol for the separation and identification of organic mercury in biological and other samples. For example, in the initial step the addition of copper(II) ions (or mercury(II)) enhances the removal of mercury bound to sulfur. Copper(II) was found superior to mercury(II) since it avoided the problem of decomposition of dimethylmercury, if present. The method has also been modified in terms of the quantity of chemicals used. A semimicro scale method developed by Uthe and coworkers [75] has been widely applied. However, inorganic mercury cannot be determined by this procedure unless a reagent is added to form, for example, alkyl and aryl derivatives, which can then be extracted and determined by GLC [76]. In general, solvent extraction procedures are time consuming, corrections for the recovery of the procedure vary from sample to sample, and with some sample types (e.g. those rich in lipids) phases are difficult to separate because of the presence of persistent emulsions, particularly during the separation of the aqueous cysteine phase. To overcome these problems, methylmercury can be adsorbed on cysteine paper (instead of into cysteine solution) during the cleanup stage. Using additional preseparations prior to extraction (such as volatilization of methylmercury in a microdiffusion cell [77] and distillation [78]) may also facilitate separation of phases during extraction.

When speciation is required with insoluble samples (such as sediments and soils), it is difficult to estimate recovery. In such samples, spiked methylmercury is not equivalent to the methylmercury originally present. By comparing various isolation techniques for methylmercury compounds in sediment samples and soils [73, 78], it has been shown that conventional methods based on acid leaching of organomercury compounds prior to extraction of methylmercury compounds into an organic solvent are inadequate in most cases to release methylmercury from sediment samples. Improved recoveries have been achieved by extraction of methylmercury by nitric acid at elevated temperature or assisted by microwave energy [79]. It is important to mention that some protocols may lead to artifact methylmercury production,

especially in procedures where methylmercury is isolated at higher temperatures. The quality of the results should therefore be regularly checked by the use of appropriate reference materials, if available, or by comparison of the results from different laboratories and/or the use of different analytical approaches.

It is important to mention that by the use of ICP-MS and isotope dilution analysis (IDA), problems associated with incomplete recoveries of organomercury species are overcome. The key stage in the IDA procedure is the equilibration of the isotopically modified spike and the MeHg, in which case the spike material acts as the ideal internal standard. So far, such a protocol has been successfully applied to numerous environmental and biological samples [7, 63, 80–82].

Chromatographic conditions: Apart from the above-mentioned problems associated with the extraction of organomercurials, problems also exist in the chromatography of organomercurial halides. Many investigators have recommended that columns packed with 5% diethylene glycol succinate-polystyrene (DEGS-PS) on 100–120 mesh Supelcoport be used. Some other polar stationary phases have also been employed, for example, PEGS, Carbowax 20 M, Durapak, Carbowax 400, PDEAS, HIEFF-2AP, and so on. In order to prevent ion-exchange and adsorption processes on the column (which cause undesirable effects such as tailing, changing of the retention time, and decrease of peak areas/heights), passivation of the packing material is needed with Hg(II) chloride in benzene [83]. Although the more inert nature of capillary columns would be expected to minimize such effects, improved chromatographic performance over packed columns cannot be readily achieved. Some workers still prefer to use packed columns since the analytical protocols using capillary columns require additional research to optimize performance. The following capillary columns have so far been reported to give good results: OV-17 WCOT, Beijing Chemical Industry Works; Superox 20 M FSOT, and OV 275.

Several workers have chosen to derivatize the mercury species to their corresponding nonpolar, alkylated analoges such as butyl derivatives, which can then be separated on nonpolar packed [57, 70] or capillary columns [84].

Detectors: Various detectors can be used in combination with GLC for the determination of mercury species. The ECD is a very sensitive detector with an absolute detection limit of approximately a few picograms. It does not, however, measure mercury directly, but responds to the halide ion attached to the CH_3Hg^+ ion. The identification of small methylmercury peaks can sometimes be subject to a positive systematic error owing to coeluting contaminants. The use of a plasma atomic emission detector (AED), a mass spectrometric detector, CV AAS, CV AFS, or ICP-MS can avoid such problems, since mercury is measured directly. Miniaturized automated speciation analyzers have recently been developed for the determination of organomercury compounds, based on microwave-induced plasma emission detector [85].

In recent times, ICP-MS has been more and more frequently used as a powerful tool for mercury speciation. Introducing mercury in the form of gaseous species into dry plasma greatly reduces memory effects, achieving absolute detection limits of less than 100 pg of Hg. On the basis of the principle of isotope dilution, ICP-MS is characterized as a very precise and accurate analytical method. Moreover, IDA, which has recently been applied to inorganic mass spectrometry (MS) is regarded as a definitive analytical technique, as the precision and accuracy obtained are unsurpassed by alternative analytical techniques. Equally important, multiple stable tracer experiments allow studies of the fate of Hg species in the environment and in biological systems. This concept allows the investigation of multiple transformation processes simultaneously. The simplified principle is presented in Figure 2.12.3. The isotope pattern of ambient Hg is presented in Figure 2.12.3(a) and the composition of a typical isotope-enriched solution ($^{199}Hg^{2+}$) in Figure 2.12.3(b). Adding such a solution to the sample will change the isotope pattern of inorganic mercury in the sediment. Figure 2.12.3 also shows a GC-ICP-MS chromatogram of a sediment extract

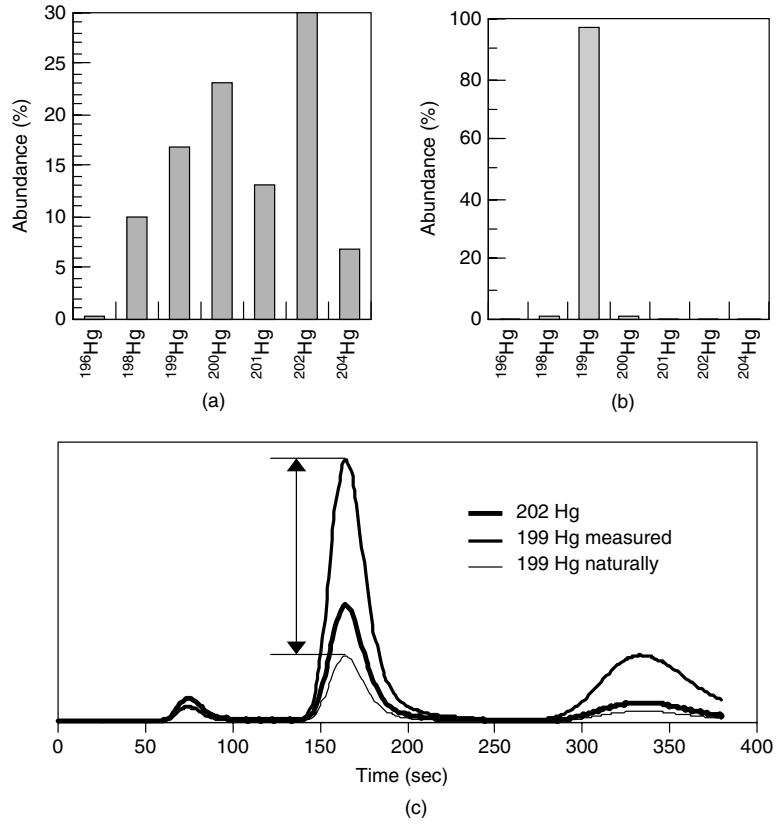

Figure 2.12.3. (a) Hg isotope abundance in nature and (b) ^{199}Hg tracer solution (c) GC-ICP/MS chromatogram of a sediment extract after incubation with ^{199}Hg(II) showing the relative increase in the $CH_3^{199}Hg^+$ signal. (Reprinted with permission from [86]. Copyright (2003) American Chemical Society.)

from a methylation assay. The concentration of $CH_3^{199}Hg^+$ is enriched in the sample relative to the fraction of $CH_3^{199}Hg^+$ in the original sample and the magnitude of the relative changes related to the amount of $^{199}Hg^{2+}$ methylated [86].

Derivatization methods: Many methods use the formation of volatile organomercury derivatives (through ethylation, propylation, butylation, hydration, and iodination) in order to separate them from the bulk of the sample by simple room-temperature aeration. The same ethylation method as described for water samples has also been applied to biological and sediment samples [70]. An aliquot of alkaline-digested sample or a distilled sample is subjected to ethylation by sodium tetraethyl borate. Methylmercury is transformed into methylethylmercury, and mercury(II) is transformed into diethylmercury. The two species can be determined simultaneously, although precision and accuracy for the determination of Hg(II) is problematic with some matrices [87]. In case EtHg is to be determined in samples, propylation is the method of choice [88]. Volatile ethylated mercury compounds, as well as elemental and dimethylmercury, are removed from solution by aeration and are then trapped on an adsorbent (Carbotrap or Tenax). Mercury compounds are separated on a GC column and pyrolized to elemental Hg^0 at elevated temperatures (typically between 600 and 900 °C) for subsequent mercury determination by CV AFS or CV AAS, while for ICP-MS no thermal conversion is necessary prior to detection. As mentioned previously, CV AFS and ICP-MS may achieve very low detection

limits, particularly if methylmercury is preseparated by distillation (6 pg L^{-1} for water and 1 pg g^{-1} for biota and sediment samples) [73]. Instead of sodium tetraethyl borate, sodium borohydride may also be used to form volatile methylmercury hydride, which is then quantified by GC in line with a Fourier transform infrared spectrophotometer [89]. The CH_3I formed in a headspace vial may also be introduced onto a GC column and detected by microwave-induced plasma atomic emission spectrometry (MIP-AES) or AFS detectors [90]. Propylation and hydration has also been applied with great success as described above [71, 72].

Differential reduction: There are also a few methods that are based on differential reduction. In the method developed by Magos [91], the inorganic mercury in an alkaline-digested sample is selectively reduced by stannous chloride, while organomercury compounds are reduced to elemental mercury by a stannous chloride–cadmium chloride combination. CV AAS can measure released elemental mercury. The method has been successfully applied for biological samples in toxicological, epidemiological, and clinical studies. CV AAS has also been used for detection of organomercury compounds after preseparation of organomercury by (a) anion exchange [69], (b) volatilization and trapping on cysteine paper [77], and (c) water vapor distillation [78]. Organomercury compounds must be destroyed by either UV irradiation or acid digestion prior to detection by CV AAS. In most biological samples, the organomercury concentrations usually correspond to methylmercury. In some environmental samples such as sediment, soil, and water samples, the concentrations of organic mercury (particularly if separated by anion exchange) have been found to be much higher than those of methylmercury compounds. This is probably due to presence of some other organic mercury compounds, which have not, as yet, been identified.

Fractionation of mercury in soils and sediments: The biogeochemical and especially the ecotoxicological significance of Hg input is determined by its specific binding form and coupled reactivity rather than by its accumulation rate in the solid material [92]. Consequently, these are the parameters that have to be determined in order to assess the potential for Hg transformation processes (such as methylation, reduction, demethylation) and to improve data for environmental risk assessment. Hg pyrolysis followed by AAS detection was developed to distinguish among cinnabar bound Hg, metallic Hg, and matrix bound Hg [93, 94]. Alternative approaches used for mercury fractionation are based on sequential extractions and leaching to provide information on solubility and reactivity of Hg [93]. Sequential extraction schemes developed by Bloom *et al.* [95] consist of six steps, including water-soluble, 'human stomach acid' soluble, organo-chelated, elemental Hg, mercuric sulfide, and residual fraction. An additional step was incorporated into this scheme in order to provide information on volatilization potential of mercury present in soil [96]. It is important to note that these schemes are based on the analytical protocols and that slight changes may result in different relative distribution of mercury fractions.

Recently, X-ray absorption spectroscopy (XAS), in particular, extended X-ray absorption fine structure (EXAFS) spectroscopy, has been applied for mercury speciation in mercury-bearing mine wastes [97, 98].

Miscellaneous methods: The first practical method for differentiating between organic and inorganic mercury was a colorimetric method developed by Gage [99]. Organomercury compounds were extracted into an organic solvent and determined spectrophotometrically as dithizone complexes. The method basically suffers from low sensitivity. Simple extraction procedures have also been successfully used followed by AAS (Figure 2.12.1). High performance liquid chromatography (HPLC) has proven of use with reductive amperometric electrochemical detection, ultraviolet detection, inductively coupled plasma emission spectrometric detection, or AAS detection. NAA has been used for methylmercury determinations in fish, blood, and hair samples after suitable preseparation procedures. Graphite furnace AAS has also been used for the final determination of methylmercury in toluene

extracts to which dithizone was added. An anodic stripping voltammetry technique has been developed for determination of methylmercury. However, the method has never been used for environmental samples. Methylmercury has also been extracted into dichloromethane (CH_2Cl_2). This was then evaporated down to 0.1 mL and subjected to GC with an atmospheric pressure active nitrogen detector. The results of many diverse papers published on analytical techniques are summarized by Craig [66].

Recently, an enzymatic method for specific detection of organomercurials in bacterial cultures has been developed. It is based on the specific conversion of methylmercury (no other methylmetallo groups are enzymatically converted) to methane by organomercurial lyase. Ethyl and phenylmercury can also be detected [100].

5.2.3 Determination of other organomercurials

Among organomercury species currently of interest, ethylmercury (EtHg) is a compound that requires further attention as it is still used in Thiomersal for the preservation of vaccines. It is important to analyze ethylmercury in vaccines, in wastewater from waste treatment plants in industries using ethylmercury, as well as biological samples in order to understand ethylmercury uptake, distribution, excretion, and effects. In principle, methods developed for methylmercury can also be used for ethylmercury, except in protocols using derivatization by ethylation. In such cases, propylation is recommended.

Only a few investigations concerning the determination of other organomercurials used in agricultural and for other purposes (cited in Table 2.12.1) have been reported. Methoxyethyl- and ethoxyethylmercury have been examined by thin layer chromatography (TLC) and gas–liquid chromatography (GLC). It would appear that the only method that can separate and measure many of the compounds simultaneously is HPLC with UV detection [101, 102]. It offers several advantages. The separation of the compounds is performed at ambient temperatures, hence thermal decomposition does not occur. It offers the possibility to separate less volatile or nonvolatile species such as mersalylic acid or the aromatic organomercurials, which usually present a problem for GLC. It is, however, very important to isolate these compounds from the environmental samples quantitatively. Methyl- and ethylmercury can easily be isolated from soils by extraction from acidified samples. Several extraction agents have been tested in order to release organomercurials from soils. Methyl- and phenylmercury can be extracted by potassium iodide–ascorbic acid and oxalic acid with satisfactory yields, whereas ethylmercury is only partly extracted. No suitable extraction techniques have been found for methoxyethyl- and ethoxyethylmercury in soils (due to decomposition of these compounds under acidic conditions).

6 REFERENCES

1. UNEP/IOMC, *Global Mercury Assessment*, UNEP Chemicals, Geneva, 2002.
2. Drasch, G., Horvat, M. and Stoeppler, M., Mercury, in *Elements and their Compounds in the Environment*, 2nd ed., Merian, E., Anke, M., Ihnat, M. and Stoeppler, M. (Eds.), Wiley-VCH Verlag GmBH & Co. KgaA, Weinheim, 2004, pp. 931–1005.
3. Pirrone, N., Ahrens, R., Barregård, L., Boffetta, P., Borowiak, A., Ehrlich, H. C., Fernandez, R., Grandjean, P., Hansen, J. C., Horvat, M., Munthe, J., Pacyna, J. M., Petersen, G., Steinnes, E. and Wichmann-Fiebig, M. (2001): EU Ambient Air Pollution by Mercury (Hg) – Position Paper on Mercury. Office for Official Publications of the European Communities, Brussels, ISBN 92-894-2053-7. (available: http://europa.eu.int/comm/environment/air/background.htm#mercury, (2005).
4. Simon, M. and Wuhl-Couturier, G., Mercury, in *Ullmann's Encyclopedia of Industrial Chemistry*, 6th Completely Revised Edition, Bohnet, F. (Ed.), Wiley-VCH, Weinheim, 2002.
5. Yoneda, S. and Suzuki, K. T., *Biochem. Biophys. Res. Commun.*, **231**, 7 (1997).
6. Pongratz, R. and Heumann, K., *Chemosphere*, **39**, 89 (1999).
7. Falter, R., *Chemosphere*, **39**, 1051 (1999).
8. Ose, Y., Sato, T. and Ishikawa, T., *Sci. Total Environ.*, **25**, 133 (1982).
9. Ose, Y., Sato, T. and Ishikawa, T., *Sci. Total Environ.*, **32**, 147 (1984).
10. Knezevic, I., Griffiths, E., Reigel, F. and Dobbelaer, R., *Vaccine*, **22**, 1836 (2004).
11. Pichichero, M. E., Cernichiari, E., Lopreiato, J. and Treanor, J., *Lancet*, **360**, 1737 (2002).

12. Wagemann, R., Trebacz, E., Biola, G. and Lockhart, W. L., *Sci. Total Environ.*, **218**, 19 (1998).
13. Heumann, K. C., Biomethylation in the Southern ocean and its contribution to the geochemical cycle of trace elements in Antarctica, in *Environmental Contamination in Antarctica*, Caroli, S., Cescon, P. and Walton, D. W. H. (Eds.), Elsevier, Amsterdam, 2001, p. 213.
14. Lindberg, S. E., Wallschlager, D., Prestbo, E. M., Bloom, N. S., Price, J. and Reinhart, D., *Atmos. Environ.*, **35**, 4011 (2001).
15. Hirner, A. V., Feldmann, J., Krupp, E., Grumping, R., Guguel, R. and Cullen, W. R., *Org. Geochem.*, **29**, 1765 (1998).
16. Martell, A. E., Smith, R. M. and Motekaitis, R. J., *NIST Critically Selected Stability Constants of Metal Complexes Data Base*, NIST Std. Ref. Database, No. 46, Department of Commerce, Gaithersburg, MD, 1998.
17. Horvat, M., Kotnik, J., Logar, M., Fajon, V., Zvonaric, T. and Pirrone, N., *Atmos. Environ.*, **37**, 93 (2003).
18. Cossa, D., Martin, J. -M. and Sanjuan, J., *Mar. Pollut. Bull.*, **28**, 281 (1994).
19. Cossa, D., Martin, J. -M., Takayanagi, K. and Sanjuan, J., *Deep Sea Res. Part II*, **44**, 721 (1997).
20. Vandal, G. M., Mason, R. P., McKnight, D. and Fitzgerald, W., *Sci. Total Environ.*, **213**, 229 (1998).
21. Weber, J., Evans, R., Jones, S. H. and Hines, M. E., *Chemosphere*, **36**, 1669 (1998).
22. IPCS/WHO, Environmental health criteria 101, *Methylmercury*, WHO, Geneva, 1990.
23. Gnamuš, A., Byrne, A. R. and Horvat, M., *Environ. Sci. Technol.*, **34**, 3337 (2000).
24. IPCS/WHO, Environmental health criteria 118, *Inorganic Mercury*, WHO, Geneva, 1991.
25. De Flora, S., Bennicelli, C. and Bagnasco, M., *Mutat. Res.*, **317**, 57 (1994).
26. Boffetta, P., Merler, E. and Vainio, H., *Scand. J. Work Environ. Health*, **19**, 1 (1993).
27. Salonen, J. T., Seppanen, K., Nyyssonen, K., Korpela, H., Kauhanen, J., Kantola, M., Tuomilehto, J., Esterbauer, H., Tatzber, F. and Salonen, R., *Circulation*, **91**, 645 (1995).
28. Boffetta, P., Garcia-Gomez, M., Pompe-Kirn, V., Zaridze, D., Bellander, T., Bulbulyan, M., Caballero, J. D., Ceccarelli, F., Colin, D., Dizdarevic, T., Espanol, S., Kobal, A., Petrova, N., Sallsten, G. and Merler, E., *Cancer Causes Control*, **9**, 591 (1998).
29. EMEP, *Monitoring and Modelling of Lead, Cadmium and Mercury Transboundary Transport in the Atmosphere of Europe* in Joint Report of EMEP Centers: MSC-E and CCC, EMEP Report 3/99, 1999.
30. Dizdarevič, T., *Mater. Geoenviron.*, **48**, 56 (2001).
31. IRIS, Mercury, Elemental, CASRN 7439-97-6. Available on World Wide Web: http://www.epa.gov/iris/subst/0370.htm, 1995.
32. Clarkson, T. W., Hursh, J. B., Sager, P. R. and Syversen, T. L. M., Mercury, in *Biological Monitoring of Biological Metals*, Clarkson, T. W., Friberg, L., Nordberg, G. F. and Sager, P. R. (Eds.), Plenum Press, New York, 1988, pp. 199–246.
33. Barregård, L., Sällsten, G. and Järvholm, B., *Occup. Environ. Med.*, **52**, 124 (1995).
34. WHO/FAO, *Toxicological Evaluation of Certain Food Additives and Contaminants*, WHO Technical Report Series No. 837, 1993.
35. Reimann, C. and de Caritat, P., *Chemical Elements in the Environment*, Facts sheets for the geochemist and environmental scientist, Springer, 1998.
36. FAO/WHO, Expert Committee on Food Additives, *Evaluation of Certain Food Additives and Contaminants*, WHO Technical Report Series No. 631, Geneva, 1978.
37. Parr, R. M., Crawley, H., Abdulla, M., Iyengar, G. V. and Kumpulainen, J., *Human Dietary Intakes of Trace Elements*. A global literature survey mainly for the period 1970–1991, Report Nutritional and Health Related Environmental Studies (NAHRES), IAEA, Vienna, 1992.
38. Mahafey, R. K., Rice, G. E. and Schoeny, R., *Mercury Study Report to Congress Volume IV: Characterisation of Human Health and Wildlife. Risk from Mercury Exposure in the United States*, EPA -452/R-97-009, Washington, DC, 1997.
39. Myers, G. J., Davidson, W., Cox, C., Shamlaye, C. F., Tanner, M. A., Marsh, D. O., Cernichiari, E., Lapman, L. W., Berlin, M. and Clarkson, T. W., *Neurotoxicology*, **16**, 711 (1995).
40. Grandjean, P., Weihe, P., White, R. F., Deves, F., Araki, S., Yokoyama, K., Murata, K., Sorensen, N., Dahl, R. and Jorgensen, P. J., *Neurotoxicol. Teratol.*, **19**, 477 (1997).
41. Nakagawa, R., Yumita, Y. and Hiromoto, M., *Chemosphere*, **35**, 2909 (1997).
42. Dickman, M. D. and Leung, K. M., *Chemosphere*, **37**, 991 (1998).
43. Gompertz, D., *J. Soc. Occup. Med.*, **32**, 141 (1982).
44. Barregård, L., *Scand. J. Work Environ. Health*, **19**, 45 (1993).
45. Sallsten, G. and Nolkrantz, K., *Analyst*, **123**, 665 (1998).
46. Sällsten, G., Kreku, S. and Unosson, H. A., *J. Toxicol. Environ. Health*, **60**, 89 (2000).
47. Horvat, M., Stegnar, P., Byrne, A. R., Dermelj, M. and Branica, Z., A study of trace elements in human placenta, blood, and hair from the Yugoslav Central Adriatic, in *Trace Element Analytical Chemistry in Medicine and Biology*, Proc. 5th Int. Workshop, Bratter, P. and Schramel, P. (Eds.), Walter de Gruyter, Berlin, New York, 1988, pp. 243–250.
48. Ishihara, N. and Urushiyama, K., *Occup. Environ. Med.*, **51**, 660 (1994).
49. Lindqvist, O., Johansson, K., Aastrup, M., Andersson, A., Bringmark, L., Hovsenius, L., Hakanson, L.,

Iverfeldt, A., Meili, M. and Timm, B., *Mercury in the Swedish Environment – Recent Research on Causes, Consequences and Corrective Methods*, Kluwer Academic Publishers, Dordrecht, 1991. Reprinted from *Water, Air, Soil Pollut.* **55**(1–2) (1991).
50. Morita, M., Yoshinaga, J. and Edmonds, J. S., *Pure Appl. Chem.*, **70**, 1585 (1998).
51. Horvat, M., in *Global and Regional Mercury Cycles: Sources, Fluxes and Mass Balances*, Baeyens, R., Ebinghaus, W. and Vasiliev, O. (Eds.), Kluwer Academic Publishers, Netherlands, 1996, pp. 1–31.
52. Schroeder, W. H., Mercury: inorganic (and total) determination, *Encyclopedia of Analytical Science*, Academic Press, 1995, pp. 3050–3059.
53. Roos-Barraclough, F., Givelet, N., Martinez-Cortizas, A., Goodsite, M. E., Biester, H. and Shotyk, W., *Sci. Total Environ.*, **292**, 129 (2002).
54. Murphy, J., Jones, P. and Hill, S. J., *Spectrochim. Acta B*, **51**, 1867 (1996).
55. Sanchez Uria, J. E. and Sanz-Medel, A., *Talanta*, **47**, 509 (1998).
56. Lee, Y. H., Wangberg, I. and Munthe, J., *Sci. Total Environ.*, **304**, 107 (2003).
57. Rapsomanikis, S. and Craig, P. J., *Anal. Chim. Acta*, **248**, 563 (1991).
58. Horvat, M. and Byrne, A. R., *Analyst*, **117**, 665 (1992).
59. LaFleur, P. D., *Anal. Chem.*, **45**, 1534 (1973).
60. UNEP/WHO/IAEA, The determination of methylmercury, total mercury and total selenium in human hair, *Reference Methods for Marine Pollution Studies No. 46*, UNEP, 1987.
61. Horvat, M., Logar, M., Ogrinc, N., Fajon, V., Lojen, S., Akagi, H., Ando, T., Tomiyasu, T. and Matsuyama, A., *Mater. Geoenviron.*, **51**, 1939 (2004).
62. Lansens, P., Meuleman, C. and Baeyens, W., *Anal. Chim. Acta*, **229**, 281 (1990).
63. Snell, J. P., Quetel, C. R., Lambertsson, L. and Qvarnstrom, J., *Mater. Geoenviron.*, **51**, 2026 (2004).
64. Westöö, G., *Acta Chem. Scand.*, **20**, 2131 (1966).
65. Rodriguez-Vazquez, J. A., *Talanta*, **25**, 299 (1978).
66. Craig, P. J., *Organometallic Compounds in the Environment – Principles and Reactions*, Longman Group, UK, 1986.
67. Schroeder, W. H., *Environ. Sci. Technol.*, **16**, 394 (1982).
68. Minagawa, K., Takizawa, Y. and Kifune, I., *Anal. Chim. Acta*, **115**, 103 (1979).
69. May, K., Stoeppler, M. and Reisinger, K., *Toxicol. Environ. Chem.*, **13**, 154 (1987).
70. Bloom, N. S., *Can. J. Fish. Aquat. Sci.*, **46**, 1131 (1989).
71. Demuth, N. and Heumann, K. G., *Anal. Chem.*, **73**, 4020 (2001).
72. Tseng, C. M., de Diego, A., Pinaly, H., Amouroux, D. and Donard, O. F. X., *J Anal. At. Spectrosc.*, **13**, 755 (1998).
73. Horvat, M., Liang, L. and Bloom, N. S., *Anal. Chim. Acta*, **281**, 135 (1993).
74. Sumino, K., *Kobe J. Med. Sci.*, **14**, 131 (1968).
75. Uthe, J. F., Solomon, J. and Grift, B. A., *J. Assoc. Off. Anal. Chem.*, **55**, 583. (1972).
76. Zarnegar, P. and Mushak, P., *Anal. Chim. Acta*, **69**, 389 (1974).
77. Zelenko, V. and Kosta, L., *Talanta*, **20**, 115 (1973).
78. Horvat, M., May, K., Stoeppler, M. and Byrne, A. R., *Appl. Organomet. Chem.*, **2**, 515 (1988).
79. Liang, L., Horvat, M., Feng, X., Shang, L., Li, H. and Pang, P., *Appl. Organomet. Chem.*, **18**, 264 (2004).
80. Clought, R., Belt, S. T., Evans, E. H., Fairman, B. and Catterick, T., *Anal. Chim. Acta*, **500**, 155 (2003).
81. Snell, J., Steward, I., Sturgeon, R. and Frech, W., *J. Anal. At. Spectrom.*, **15**, 1540 (2000).
82. Hintelmann, H., *Chemosphere*, **39**, 1093 (1999).
83. O'Reilly, J. E., *J. Chromatogr.*, **238**, 433 (1982).
84. Bulska, E., Emteborg, H., Baxter, D. C. and Frech, W., *Analyst*, **117**, 657 (1992).
85. Slaets, S. and Adams, F. C., *Anal. Chim. Acta*, **414**, 141 (2000).
86. Hintelmann, H. and Ogrinc, N., Determination of stable mercury isotopes by ICP-MS and their application in environmental studies, in *Biogeochemistry of environmentally important trace elements*, Y. Cai and Braids, O. C. (Eds.), ACS Symposium Series 835, American Chemical Society, 2003, pp. 321–338.
87. Liang, L., Bloom, N. and Horvat, M., *Clin. Chem.*, **40**, 602 (1994).
88. Logar, M., Horvat, M., Horvat, N., Benedik, M., Marn-Pirnat, A., Ponikvar, R. and Osredkar, J., *Mater. Geoenviron.*, **51**, 1976 (2004).
89. Fillipelli, M., Baldi, F., Brinckman, F. E. and Olson, G. J., *Environ. Sci. Technol.*, **25**, 1457 (1992).
90. Lansens, P., Meuleman, C., Laino, C. C. and Baeyens, W., *Appl. Organomet. Chem.*, **7**, 45 (1993).
91. Magos, L., *Analyst*, **96**, 847 (1971).
92. Quevauviller, P., Donard, O. F. X., Wasserman, J. C., Martin, F. M. and Schneider, J., *Appl. Organomet. Chem.*, **6**, 221 (1992).
93. Biester, H., Gosar, M. and Müller, G., *J. Geochem. Explor.*, **65**, 195 (1999).
94. Biester, H., Gosar, M. and Covelli, S., *Environ. Sci. Technol.*, **34**, 3330 (2000).
95. Bloom, N. S., Preus, E., Katon, J. and Hiltner, M., *Anal. Chim. Acta*, **479**, 233 (2003).
96. Kocman, D., Horvat, M. and Kotnik, J., *J. Environ. Monitor.*, **6**, 696 (2004).
97. Kim, C. S., Brown, G. E. and Rytuba, J. J. Jr., *Sci. Total Environ.*, **261**, 157 (2000).
98. Kim, C. S., Rytuba, J. J. and Brown Jr., G. E., *Appl. Geochem.*, **19**, 379 (2004).
99. Gage, J. C., *Analyst*, **86**, 457 (1961).
100. Baldi, F. and Fillipelli, M., *Environ. Sci. Technol.*, **25**, 302 (1991).
101. Holak, W., *J. Liq. Chromatogr.*, **8**, 563 (1985).
102. Hempel, M., Hintelmann, H. and Wilken, R. D., *Analyst*, **117**, 669 (1992).

2.13 Speciation of Molybdenum

Rita Cornelis

Laboratory for Analytical Chemistry, Ghent University, Ghent, Belgium

1 INTRODUCTION

As a transition element in group VI B of the periodic table, molybdenum exhibits various oxidation states, +6 being the highest and most common. Molybdenum in the +5, +4, +3 and +2 state is known, although the lower states are progressively unstable and tend to revert to molybdenum(VI) [1]. Molybdenum forms the basis of a big array of valuable materials. It is a very important agent in alloys (ferrous and nonferrous) and the core ingredient of important chemicals (pigments, lubricants, photochemicals, catalysts). Molybdenum is considered an essential element for plants and animals. It is used in agriculture to prevent molybdenum deficiency in crops.

The scope of this chapter is limited to describing the occurrence of molybdenum species in the environment (rain water, estuarine water, river water, air, sediments and sludges) excluding geological formations, and to summarizing the existing knowledge about molybdenum species in food and living systems.

Although the work in these different areas has been described as speciation analysis, in nearly all cases it concerns fractionation analysis as per the IUPAC definitions of both concepts. Fractionation indicates the process of classifying an analyte or a group of analytes from a certain sample according to physical (e.g. size, solubility) or chemical (e.g. bonding reactivity) properties [2].

2 SPECIATION OF MOLYBDENUM IN THE ENVIRONMENT

2.1 Water

Molybdenum is a characteristic element associated with airborne particulates originating from oil combustion. These airborne particulates may be transported into surface waters by the rainout and washout effects of rainfall, because comparable concentrations (0.1 $\mu g\,L^{-1}$ levels) of molybdenum were found in rain, river and lake water samples [3].

Handbook of Elemental Speciation II: Species in the Environment, Food, Medicine & Occupational Health
Edited by R. Cornelis, H. Crews, J. Caruso and K. G. Heumann
 ISBN: 0-470-85598-3 (HB)

2.1.1 Rainwater

A method for fractionation of molybdenum, defined as physicochemical speciation, in rainwater has been described by Kawakubo *et al*. [3]. The molybdenum was fractionated in natural and synthetic rainwater samples by filtration and ultrafiltration to distinguish labile (free or weakly complexed) from nonlabile Mo with different particle sizes and molecular masses.

The concentration of labile molybdenum was evaluated by direct catalytic determination. The total concentration of molybdenum was determined after acid decomposition of the sample and allowed the calculation of the nonlabile concentration.

Molybdenum species in the rainfall samples were found in a fraction with molecular masses $<10^3$ Da and characterized as labile forms, that is, simple molybdate ions. The nonlabile molybdenum existed predominantly in the initial fresh rainwater, associated with particulate matter (0.45 μm in particle size).

Iron and humic substances were also analyzed to determine their influence on the fractionation of Mo. Iron occurs as polyhydroxo Fe(III) complexes, to which molybdenum compounds coprecipitate as nonlabile molybdenum. Nevertheless, in the initial rainfall sample, a small part of labile molybdenum is probably absorbed or complexed with particulate matter, on the surface of humic iron aggregates.

2.1.2 River water

Kawakubo *et al*. [4] also studied different fractions of molybdenum in river water along the same lines as they did for rain water. They used an analytical scheme based on size fractionation by filtration and ultrafiltration and the catalytic spectrophotometric determination of the reactive (or labile) molybdenum concentration. The total concentration of molybdenum was determined after acid decomposition and this allowed calculating the unreactive molybdenum. About 50% of the molybdenum in natural river water samples was found to be reactive in the molecular mass fraction $<10^3$ and was estimated from the chemical equilibria of molybdate ions to be MoO_4^{2-}. The residual part of molybdenum was found in the colloidal and particle fractions (molecular mass greater than or equal to 10^4), and was characterized as reactive molybdenum adsorbed or complexed on humic iron aggregates. Silicate contributed to the formation of reactive molybdenum in the colloidal fraction in the presence of humic acid.

Interesting descriptions of the association between molybdenum and humic acids can also be found in Section 2.26 of this Handbook 'Metal complexes of humic substances' [5].

2.1.3 Estuaries

Vandenberg [6] studied the estuarine chemistry of several metals and anion-forming elements, including molybdenum. Voltammetric measurements of the chemical speciation of molybdenum in estuarine waters indicated the unexpected presence of a nonlabile species for this element.

2.2 Sediments

Molybdenum is studied in aquatic environments because it is an element that is redox-sensitive and can behave differently in oxic and anoxic conditions. The study of this element may provide insight into processes that occur during sediment diagenesis and mobility [7].

Here again, research on molybdenum species is confined to fractionation studies. The well-known three-stage sequential extraction procedure, proposed by the Commission of the European Communities, Bureau of Reference Materials (BCR), has been applied to a freshwater sediment collected from River Clyde (UK) by Davidson *et al*. [7]. Total molybdenum amounted to 0.56 $\mu g\,g^{-1}$ sediment dry weight. The Mo concentrations in the three consecutive extraction steps (1. acetic acid, 2. hydroxylammonium chloride, 3. hydrogen peroxide) were below the limit of detection, described as $<0.002–0.003\ \mu g\,g^{-1}$ sediment dry weight. The main share of the Mo was in the residue at 0.51 $\mu g\,g^{-1}$ sediment dry weight.

As concentrations as high as 200 $\mu g\,Mo\,L^{-1}$ in water have been reported in areas near mining sites, it is fitting to have a model to predict molybdenum absorption by soils. Goldberg *et al*. [8] applied a chemical surface model to describe Mo adsorption on 36 samples from 27 soil series selected for variation in soil properties. A general regression model was developed for predicting soil Mo surface complexation constants from four independently measured soil chemical characteristics: cation exchange capacity, organic carbon content, inorganic carbon content and iron oxide content. The constant capacitance model was well able to predict Mo adsorption on all 36 soil samples. Incorporation of these regression prediction equations into chemical speciation-transport models will allow simulation of soil solution Mo concentrations under diverse environmental and agricultural management conditions without requiring soil specific adsorption data and subsequent parameter optimization.

2.3 Air

The concentrations of molybdenum in urban air range from 0.01 to 0.03 $\mu g\,m^{-3}$, whereas in nonurban areas they vary between 0.001 and 0.0032 $\mu g\,m^{-3}$ [9]. Molybdenum is a characteristic element associated with airborne particulates originating from oil combustion. Molybdate is probably the chemical form of Mo in the aerosols.

A very interesting development in the quest for molybdenum species in air was the identification of volatile organic molybdenum-based compounds in landfill gases, compost heaps and forest air [10–12]. These belong to the group of volatile metal compounds of biogenic origin as described by J. Feldmann in Section 2.25 of this Handbook [13]. The presence of molybdenum hexacarbonyl ($Mo(CO)_6$) was confirmed in all cases.

3 SPECIATION OF MOLYBDENUM IN FOOD

The essentiality of molybdenum for plant growth and the functional role played by this element in several bacterial-, plant- and animal enzymes have long been recognized. The biochemistry, the nutritional aspects, the dietary source of molybdenum and the pathologic states can be read in a review by Rajagopalan [14].

Besides the quest for the Mo-containing enzymes, research has been published about the chemical form of molybdenum in seeds and the effect of technological processing, cooking and maturity stage on the species.

Fractionation of molybdenum species in seeds of peas and lentils has been performed by size-exclusion chromatography-inductively coupled plasma mass spectrometry [15]. Molybdenum elution profiles of pea and lentil were completely different. In lentil extract, the main Mo peak appeared in the high molecular mass (HMM) region (approx. 200 kDa) and the other one in the low molecular mass (LMM) region (<2 kDa), whereas in pea extract (similarly as in white bean and soybean flour), practically all Mo is eluted in a single peak in the LMM region.

The same group, using the same techniques, studied the effect of cooking on molybdenum species in peas. It revealed changes in solubility and changes in the proportions of individual element species fractions, occurring as a result of soaking and boiling of peas [16]. Compared to other element species, LMM species of molybdenum were relatively stable against thermal treatment, although boiling increased the proportions of ionic species and labile complexes.

Koplík *et al*. studied the effect of technological processing and of the maturity stage of seeds on the content and speciation of molybdenum and various other elements in peas [17]. Changes in speciation that occurred as a result of blanching and boiling of green peas were also investigated. Element speciation in green peas was compared with that of mature peas. No notable differences between fresh and blanched green peas were found. During boiling of peas, most of the elements were partly leached into water. LMM species of molybdenum were more stable against thermal treatment than those of other elements. The mature pea accumulated higher concentrations of elements than did the green pea.

4 SPECIATION OF MOLYBDENUM IN LIVING SYSTEMS

As stated previously, molybdenum is an essential element. Its biological function can be traced to its role as a prosthetic group in a number of enzymes that catalyze oxidation–reduction reactions and contain, in addition to molybdenum, other prosthetic groups. Mo is a requisite for the activities of a number of enzymes. Three molybdenum enzymes are known to be present in animal tissue: xanthine dehydrogenase/oxidase, aldehyde oxidase and sulfite oxidase [18]. Molybdenum is probably absorbed into living systems as the molybdate anion (MoO_4^{2-}) [19].

An agricultural problem may arise when there is an excess of Mo in soil since it causes copper deficiency in animals grazing on such lands. It would appear that the difficulty arises from the metabolism of anaerobic bacteria in the rumen of these animals. One of the reactions of Mo on entering the anaerobic first digestive system of the ruminant is the conversion of the molybdate into thiomolybdate by the bacteria of the stomach. Unfortunately, MoS_4^{2-} is a very good scavenging precipitation reagent for Cu and so the Cu content of the diet becomes critically low. Then the animals suffer from weakened connective tissue since Cu enzymes are required to cross-link collagen external to the animal cells [20].

The measurement of molybdenum, and all the more so that of individual molybdenum species in biological fluids and tissues, is a very difficult undertaking because of the very low levels at which it is present. In human blood serum, for instance, the total Mo concentration amounts to only about 0.6 $\mu g\,L^{-1}$ [21].

To the author's knowledge, no attempts have yet been made to speciate molybdenum in human body fluids or tissues.

The speciation of various elements, among which molybdenum, in salmon egg cell cytoplasm has been reported, using a surfactant-mediated high performance liquid chromatography (HPLC)/inductively coupled plasma-mass spectrometry (ICP-MS) hyphenated system [22]. ICP-MS was used as an element-selective detector. Molybdenum in egg cell cytoplasm was present as molybdate.

5 CONCLUSION

Research results in the area of speciation and fractionation of molybdenum in environmental and biological materials are very few. This may be explained by the great analytical difficulties to handle the very low concentrations at which Mo-species do occur.

6 REFERENCES

1. Parker, G. A., *Analytical Chemistry of Molybdenum*, Springer-Verlag, Berlin, Heidelberg, New York, Tokyo, 1983.
2. Templeton, D. M., Ariese, F., Cornelis, R., Danielsson, L.-G., Muntau, H., van Leeuwen, H. P. and Lobinski, R., *Pure Appl. Chem.*, **72**, 1453 (2000).
3. Kawakubo, S., Hashi, S. and Iwatsuki, M., *Water Res.*, **35**, 2489 (2001).
4. Kawakubo, S., Ichikawa, S. and Iwatsuki, M., *Anal. Sci.*, **18**, 651 (2002).
5. Heumann, K. G., Metal complexes of humic substances, section 2.26., in *Handbook of Elemental Speciation: Species in the Environment, Food, Medicine and Occupational Health*, Cornelis, R., Caruso, J., Crews, H. and Heumann, K. (Eds.), John Wiley & Sons, UK, 621 2005.
6. Vandenberg, C. M. G., *Estuaries*, **16**, 512 (1993).
7. Davidson, C. M., Thomas, R. P., McVey, S. E., Perala, R., Littlejohn, D. and Ure, A. M., *Anal. Chim. Acta*, **291**, 277 (1994).
8. Goldberg, S., Lesch, S. M. and Suarez, D. L., *Soil Sci. Soc. Am. J.*, **66**, 1836 (2002).
9. Schroeder, H. A., *Arch. Environ. Health*, **21**, 173 (1970).
10. Feldmann, J. and Cullen, W. R., *Environ. Sci. Technol.*, **31**, 2125 (1997).
11. Feldmann, J., *J. Environ. Monitor.*, **1**, 33 (1999).
12. Maillefer, S., Lehr, C. R. and Cullen, W. R., *Appl. Organomet. Chem.*, **17**, 154 (2003).
13. Feldmann, J., Volatile metal compounds of biogenic origin, section 2.25, in *Handbook of Elemental Speciation: Species in the Environment, Food, Medicine and Occupational Health*, Cornelis, R., Caruso, J., Crews, H. and Heumann, K. (Eds.), John Wiley & Sons, UK, 598 2005.
14. Rajagopalan, K. V., *Annu. Rev. Nutr.*, **8**, 401 (1988).
15. Koplík, R., Borková, M., Mestek, O., Komínková, J. and Suchánek, M., *J. Chromatogr. B-Anal. Technol. Biomed. Life Sci.*, **775**, 179 (2002).

16. Koplík, R., Mestek, O., Komínková, J., Borková, M. and Suchánek, M., *Food Chem.*, **85**, 31 (2004).
17. Koplík, R., Komínková, J., Borková, M., Mestek, O., Kvasnicka, F. and Suchánek, M., *Food Chem.*, **87**, 423 (2004).
18. Rajagopalan, K. V., *Nutr. Rev.*, **45**, 321 (1987).
19. Bizot Swedo, K. and Enemark, J. H., *J. Chem. Educ.*, **56**, 70 (1979).
20. Fraústo da Silva, J. J. R. and Williams, R. J. P., *The Biological Chemistry of the Elements: The Inorganic Chemistry of Life*, Clarendon Press, Oxford, 1991, pp. 411–427.
21. Versieck, J. and Cornelis, R., *Anal. Chim. Acta*, **116**, 217 (1980).
22. Matsuura, H., Hasegawa, T., Nagata, H., Takatani, K., Asano, M., Itoh, A. and Haraguchi, H., *Anal. Sci.*, **19**, 117 (2003).

2.14 Speciation of Nickel

Dirk Schaumlöffel

Centre National de la Recherche Scientifique, Pau, France

1 INTRODUCTION

The element nickel is found at low levels – 0.0099% – in the earth's crust and exists mainly in the form of sulfide, oxide and silicate minerals [1]. Natural geochemical activity and weathering has resulted in the ubiquitous occurrence of nickel in the natural environment at a modest level. Depending on geological factors, nickel levels in unpolluted soils vary between 5 and 500 $\mu g\,g^{-1}$; open ocean water contains between 0.2 and 0.7 $\mu g\,L^{-1}$ Ni. Nickel has been shown to be an essential element for several animals and plants [2]; it is also assumed to be essential for humans, but confirmatory studies have turned out to be difficult.

The manifold applications of nickel in industrial society have led to increased concentrations of nickel in rural and urban environments. Today nickel is used, for example, in alloys (stainless steel), electroplating, foundries, catalysts, welding rods and coinage, and can be found in electronic equipment, construction materials, aerospace equipment and consumer goods such as batteries, paints and ceramics (Figure 2.14.1) [3].

Anthropogenic sources, which emit nickel into the ambient air or into aquatic systems, are industrial processes such as (i) mining, milling, melting and refining, (ii) steel and nickel alloy manufacturing, (iii) combustion of heavy residual oil, coal and sewage sludge, (iv) nickel chemical and battery manufacturing, electroplating and catalyst production.

Nickel-bearing particles present in the atmosphere as a result of geological and industrial activities are deposited to soils and surface water. From the environment, nickel finds its way into plants, animals and humans. The major routes of nickel intake for humans are dietary ingestion and inhalation, where the intake by food is the

Handbook of Elemental Speciation II: Species in the Environment, Food, Medicine & Occupational Health
Edited by R. Cornelis, H. Crews, J. Caruso and K. G. Heumann
 ISBN: 0-470-85598-3 (HB)

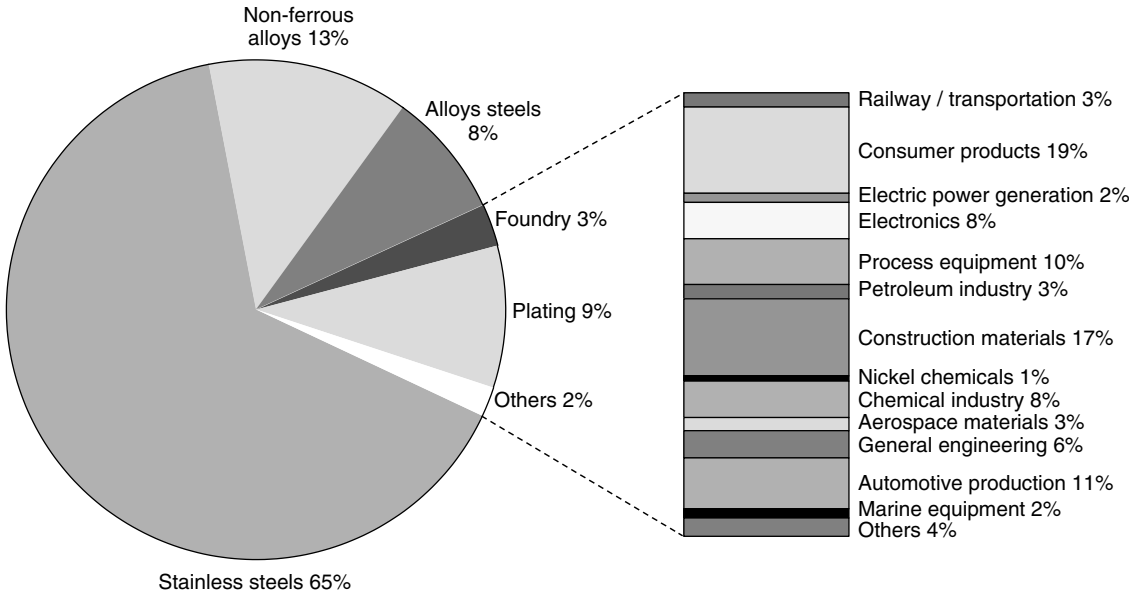

Figure 2.14.1. Approximate proportional worldwide nickel consumption in different nickel-using industry sectors. The nickel consumption in the non-steel and non-alloy production (foundry, plating, others) is again split in different industry sectors [3]. (Reproduced by permission of The Nickel Institute.)

main one. The average dietary intake is approximately 0.2–0.3 mg nickel/day, and, in comparison, an average urban resident would inhale only 0.0004–0.0008 mg nickel/day [4]. Other sources of exposure include dermal contact with nickel-containing items (e.g. jewelry and coins). Tobacco smoke can contribute to an uptake of up to 0.023 mg nickel/day (Table 2.14.1) [5]. The human organism absorbs nickel, which can be found in various organs and in the blood. Unabsorbed nickel is excreted mainly in urine but also via feces. The effect of nickel on human health, especially regarding carcinogenesis and allergic contact dermatitis (ACD), is the subject of a huge number of clinical studies.

Table 2.14.1. Levels of daily intake by humans from different types/sources of exposure [5].

Type/route of exposure	Daily nickel intake/mg	Absorption/mg
Foodstuffs	<0.3	0.045 (<15%)
Drinking water	<0.02	0.003 (<15%)
Ambient air (urban resident)	<0.0008	0.0004 (50%)
Ambient air (smoker)	<0.023	0.012 (50%)

Source: Reproduced from Reference [5] by permission of the World Health Organization, Regional Office for Europe

Special attention is paid to individuals who are occupationally exposed to nickel, for example, workers engaged in the nickel-producing or using industries. Their total nickel intake is likely to be higher than that of the general population, and their main sources of exposure are inhalation and, to a lesser extent, skin contact.

All processes regarding nickel emission, distribution and transformation in the environment, bioavailability of nickel to plants, animals and humans, biochemical processes of nickel in organisms and occupational nickel exposure are strongly dependent on the physical and chemical form (species) of nickel. This chapter describes the environmental, food, clinical and occupational health aspects of nickel speciation.

2 NICKEL SPECIATION IN THE ENVIRONMENT

The fate of nickel species in the environment depends on their sources, the physical processes that control mobility and transportation, chemical processes and biological processes that move

nickel species across membranes and influence distribution and metabolism within an organism. All of these processes are complex and interrelated [6].

2.1 Air

Besides emissions from natural sources (estimated to be $8.5–160 \times 10^6$ kg/year [4]), such as volcanic activities or geological processes, industrial processes are another source of airborne nickel species in the environment (estimated to 42.85×10^6 kg/year [4]). The primary anthropogenic source categories are:

- combustion and incineration sources (e.g. heavy residual oil and coal or municipal waste)
- high temperature metallurgical operations (e.g. steel and nickel alloy production)
- primary production operations (mining, milling, smelting and refining)
- chemical and catalyst sources (e.g. electroplating and catalyst production).

Because of the large number of nickel-releasing sources, the nickel concentration in ambient air may show considerable variation. In a remote area (Canadian Arctic), levels of $0.38–0.62\ ng\,m^{-3}$ were recorded [7], as compared to $124\ ng\,m^{-3}$ in the vicinity of a nickel smelter [8]. Concentrations of $18–42\ ng\,m^{-3}$ were recorded in eight US cities [9]. Ranges of $10–50\ ng\,m^{-3}$ and $9–60\ ng\,m^{-3}$ have been reported in European cities. Higher values ($110–180\ ng\,m^{-3}$) have been reported from heavily industrialized areas [10].

The conventional approach for classifying airborne nickel species is operationally defined by the analytical procedure applied [11–13]. Airborne particulate matter is sampled on a filter and then submitted to a four-stage extraction procedure resulting in four fractions: soluble, sulfidic, metallic and oxidic nickel (Figure 2.14.2). In brief, the soluble fraction is leached by ammonium citrate solution ($0.1\ mol\,L^{-1}$, pH 4.4) for 90 min at room temperature, the sulfidic fraction with ammonium citrate ($0.067\ mol\,L^{-1}$) – hydrogen peroxide (10% (m/m)) for 60 min at room temperature, the metallic fraction with bromine in anhydrous methanol (2% (v/v)) and finally the oxidic fraction by hot plate digestion in concentrated nitric–perchloric acids [14]. These nickel fractions are often also called 'species' without a clear definition of the nickel compounds present. Usually, the total nickel content of each fraction is determined without a further chemical characterization of the fraction. More information about health-relevant aerosol size fractions (e.g. inhalable, thoracic, and respirable) can be gained by sampling on filters in cascade impactors (Figure 2.14.3) [14, 15]. Other approaches aim for a more precise characterization of the airborne nickel species classes. An investigation of the sulfidic nickel phase after sequential extraction of fly ash from a power plant emission by carbon paste electrode voltammetry shows that $NiSO_4$ is predominant besides sulfidic nickel (NiS and NiS_2) and that nickel subsulfide (Ni_2S_3) is absent in these

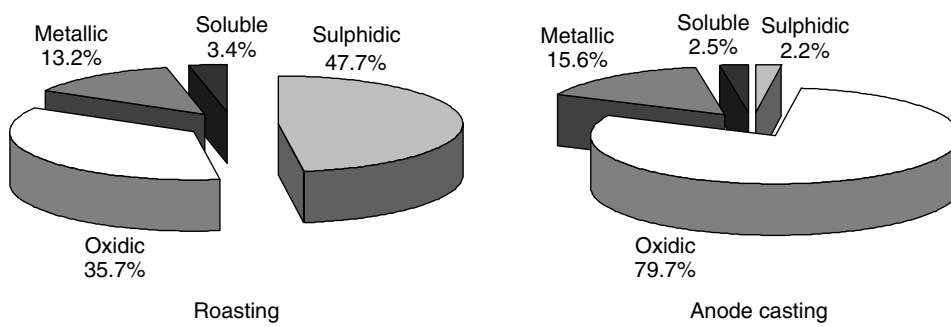

Figure 2.14.2. Proportional distribution of airborne oxidic, sulfidic, metallic and water soluble nickel species in the workroom air in a nickel refinery at two different stages of the roasting process. (Reproduced from Reference [14] by permission of The Royal Society of Chemistry.)

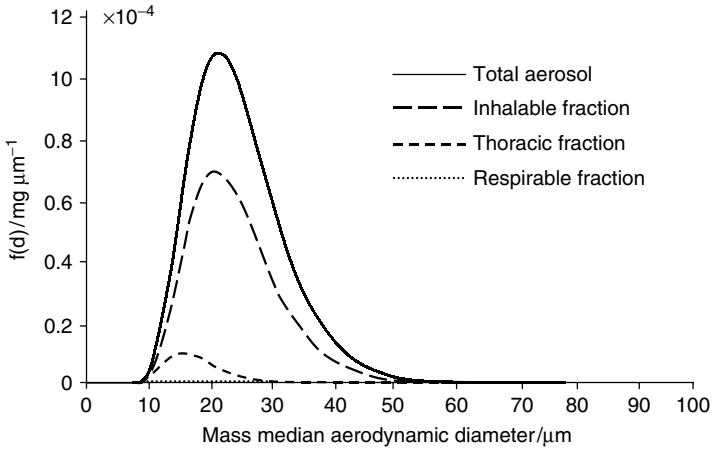

Figure 2.14.3. Particle-size distributions curves for total airborne nickel, the inhalable fraction, the thoracic fraction and the respirable fraction in the workroom air of a nickel refinery. (Reproduced from Reference [14] by permission of The Royal Society of Chemistry.)

ash samples [16]. In another study, X-ray absorption fine structure spectroscopy (XAFS) was applied to determine the nickel speciation in fly ash. More than 95% of the total nickel was found to be present as $NiSO_4 \cdot xH_2O$ and a Ni-bearing spinel, $NiFe_2O_4$ [17].

In summary, the following compounds usually can be found in the four fractions after sequential extraction of nickel-containing particulate matter (the exact composition of a fraction varies from sample to sample, depending on the industrial process, and can contain compounds not listed here):

- *soluble nickel* – $NiSO_4 \cdot 6H_2O$ and $NiCl_2 \cdot 6H_2O$
- *sulfidic nickel* – NiS, NiS_2 and Ni_2S_3
- *metallic nickel* – elemental nickel and nickel alloys
- *oxidic nickel* – NiO, Ni_2O_3, $Ni(OH)_2$, $NiCO_3$, $Ni_3(CO_3)(OH)_4$, and complex nickel oxides including spinels

Recent investigations of individual aerosol particles from working areas in a nickel refinery revealed that there was an absence of well-defined phases and simple stoichiometries in the fractions. This indicates that pure substances such as nickel subsulfide (Ni_2S_3) or specific oxides appeared not to occur [18].

The major nickel species in ambient air is nickel sulfate. This soluble form is estimated to comprise 60–100% [19], or 15–93% (average 54%) [20] of the nickel components emitted by fly ash from oil-fired utility boilers. The corresponding value for nickel sulfate emission arising from coal combustion is 20–80%. The insoluble (oxidic) fraction of fly ash emitted from both oil and coal combustion exists as nickel oxides and complex nickel oxides (ferrites, aluminates, vanadates).

In the view of environmental monitoring and ecological risk assessment of air emissions, a distinction between soluble and insoluble nickel species is important. For example, refractory high temperature nickel oxide (NiO) emitted from a nickel smelter stack and deposited into water or soil will be unreactive even at a very low pH of the receiving medium. Such NiO would sink into sediment or remain unchanged in soil for several years. Nickel from this species, NiO, will not be available for biological uptake. Even if taken into a terrestrial organism intestinal tract, the NiO would not release Ni^{2+} ions to be absorbed into the organism because of the insolubility of the NiO even in high concentration acids. On the other hand, $NiSO_4 \cdot 6H_2O$, emitted from the same smelter stack and falling into the same aqueous or terrestrial area, would initially be

highly solubilized in the lake water and in the soil pore water.

2.2 Water

Sources of nickel in ambient waters include physical and chemical degradation of rocks and soils, deposition of atmospheric nickel-containing particulate matter and discharges from industrial processes. In unpolluted water supplies, nickel concentrations range from 1 to 50 μg Ni/L [21]. In aquatic systems, such as ambient or drinking water, nickel is usually present as the nickel cation (Ni^{2+}), together with other anions such as hydroxyl (OH^-), sulfate (SO_4^{2-}), chloride (Cl^-), carbonate (CO_3^{2-}), or nitrate (NO_3^-). For an ecotoxicological assessment, the hydrated Ni^{2+} cation is regarded as the most important bioavailable nickel species because it is able to be transported through or interact with external membranes of a biological organism. In the natural aquatic environment, there usually exists a complex mixture of compounds that are able to bind Ni^{2+} in complexes, precipitate it into insoluble compounds or adsorb it strongly to the surfaces of particulate matter. The most important physicochemical parameters that control the fate of Ni^{2+} ions in the environment are pH, redox potential, temperature, ionic strength, Ca^{2+} content, complexing and precipitating organic and inorganic ligands, other cations that compete for binding sites, solid organic and inorganic matter and cation exchange capacity [6].

Speciation studies of nickel in natural aquatic environments such as rivers, lakes and estuaries are dealing in a first step with the distinction of dissolved from particulate nickel [22]. A further characterization of the dissolved nickel fraction distinguishes between free Ni^{2+} cations and nickel complexes of different stability, for example, classified as labile, slowly labile and stable complexes [23]. An important group of complexing agents in natural waters is called the *dissolved organic matter* (DOM), defined analytically as the concentration of dissolved organic carbon (DOC) [24]. This is, of course, a sum parameter, but a clear characterization of the composition, stoichiometry and structure of the DOM is often not possible. Competitive ligand equilibration studies with synthetic ligands may be used to elucidate the composition of Ni-DOM complexes [25] or to predict the release of Ni^{2+} from Ni-DOM [26]. Thus, similar complex stabilities as in Ni-fulvic acid and Ni-nitriloacetic acid were found for one dissociation step of Ni-DOM in a river surface water sample [25].

Since speciation of nickel in water is a dynamic process, theoretical models can serve in kinetic speciation studies to predict the adsorption of nickel to particles, the Ni-DOM complexation, and the concentration of free Ni^{2+} cations [24, 27]. In addition to experimental results, model calculations indicate that the toxicity, bioavailability and transport of nickel in freshwater environments are largely dictated by the concentration of DOM, and also by the nickel species entering the watercourse [24].

Waste water and biosludge are particular aquatic environments, and the nickel speciation can differ from that found in river or lake water. For example, the very stable Ni-EDTA complex was found in municipal waste water in California [28], and the speciation analysis of biosludge indicated the occurrence of nickel phosphate ($Ni_3(PO_4)_2 \cdot 8H_2O$) [29]. Furthermore, in fermentation gases from a municipal sewage treatment plant, the metalloorganic species nickel tetracarbonyl, $Ni(CO)_4$, could also be found on the sub-$\mu g\, m^{-3}$ level [30].

2.3 Soil

Nickel speciation in soils and pore water (soil solution) is dependent on many parameters, such as the sources and mineralogy of particulates depositing onto the soil, the age of the soil, historical land uses, the presence of naturally occurring humic acid complexing ligands and the presence of silica and hydrous oxides of iron and manganese.

Significant amounts of nickel, for example, can be strongly bound to the surfaces of hydrous oxides and silica, rendering it not bioavailable. This binding is very dependent on pH, as shown

in Figure 2.14.4. At low pH, oxides of manganese adsorb nickel. As the pH increases, oxides of iron become important and are seen, with oxides of manganese, to be strong adsorbers at a neutral pH of 7. Silica is a weaker binder. This diagram shows that the presence of these oxides can dramatically alter the concentration of the divalent nickel ion [31]. Figure 2.14.5 demonstrates the calculation of this effect for a site-specific example. For the specific soil composition at the site, the calculations show that Ni^{2+} is an important species at pH 5, but nickel bound to iron oxides increases dramatically from pH 5 to 6 to become the most abundant species, followed at pH 6 to 7 by nickel being increasingly bound to manganese oxides [31].

In an approach operationally defined by a sequential extraction procedure, nickel species in soils can be distinguished as water soluble, exchangeable and complexed/adsorbed species [32]. In soil solutions, nickel species are classified as free Ni^{2+} cations and organic as well as inorganic complexes. In solutions from urban soils, over 40% of the nickel was found to be $NiCO_3$ when the pH exceeds pH 8.1 [33]. The complexation with DOM is an especially important parameter to describe the solubility and mobility of nickel in soil and soil solution. The concentration of free Ni^{2+} ions in the soil solution can be predicted by model calculations, where the solid–solution partitioning of nickel is a function of nickel binding to soil organic matter, DOM, clay and iron hydroxides. As a result, the solubility of nickel depends mainly on the nickel loading over soil sorbents, pH, and the concentration of inorganic ligands and DOM in the soil solution [34].

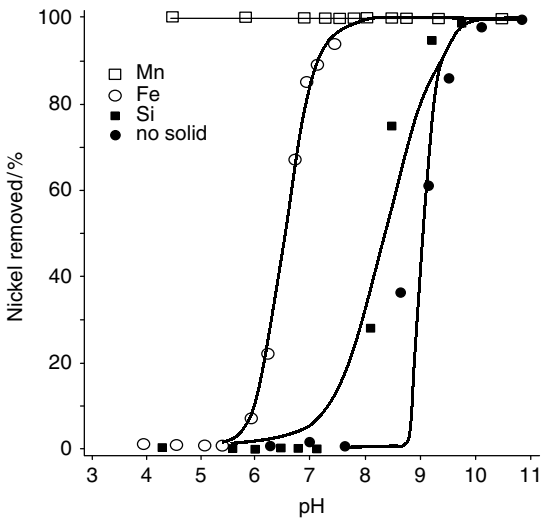

Figure 2.14.4. Sorption of nickel on hydrous oxides of iron, manganese or silica as a function of the solution pH. (Reproduced with permission from Reference [31]. Copyright (1979) American Chemical Society.)

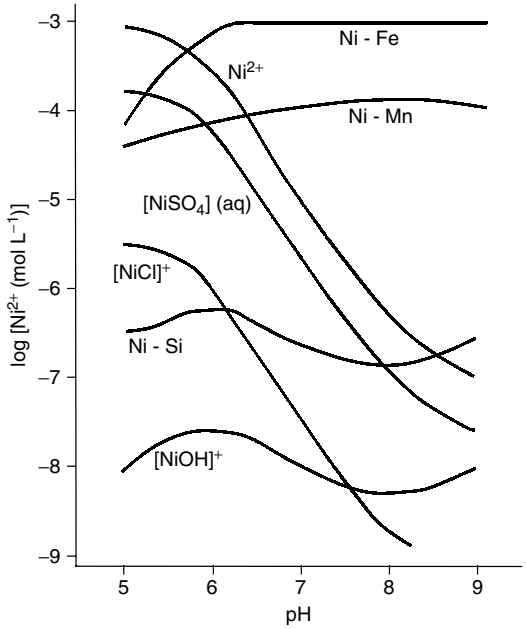

Figure 2.14.5. Effect of the pH on the distribution of nickel between adsorption sites, complexes and the free Ni^{2+} cation. (Reproduced with permission from Reference [31]. Copyright (1979) American Chemical Society.)

2.4 Biota

From the air, water or terrestrial environment, nickel can enter biological systems in order to form new species in a living organism. Possible ligands for nickel in biological systems are, for example, carboxylic acids, amino acids, peptides, proteins, adenosine triphosphate and deoxyribonucleic acid (DNA).

Plants are able to take up metals directly from the soil. The soil–plant interface, especially in the direct environment of the plant roots (rhizosphere), is of particular interest to study the

metal uptake of plants. In this context, the discovery of metal hyperaccumulating properties in certain plants spurred research on using them for the cleanup of metal contamination in soil [35]. The term 'hyperaccumulator' refers to a plant with a highly abnormal level of metal accumulation, for example, a plant with a concentration exceeding 0.1% nickel (dry mass). The success of using plants to extract metals from contaminated soils requires a better understanding of the mechanisms of metal uptake, translocation and accumulation by plants [36]. The efficiency of metal phytoextraction is a function of plant species, metal availability to plant roots, metal uptake by roots, metal translocation from roots to shoots and plant tolerance to toxic metals [36, 37]. The prerequisite for the understanding of these mechanisms is the identification of molecules involved, notably bioligands and metal complexes synthesized by a plant to be used for metal transport and suitable for bioaccumulation.

In the rhizosphere of the nickel-hyperaccumulator *Thlaspi goensingense Halacsy*, an enhanced nickel solubility was found to be driven by the formation of Ni-organic complexes, whereas the organic ligands were probably exuded by the plant [38]. Remarkably, little is known of the molecular forms of metals occurring in hyperaccumulating plants. The notable few exceptions include the subcellular localization of nickel in the vacuole of *T. goensingense* complexed by citrate and histidine [39], the correlation of free nickel and histidine levels in *Alyssum lesbiacum*, suggesting that a Ni-histidine complex is responsible for the xylem transport [40], and the demonstration of citrate as one of the ligands binding nickel in the latex of *Sebertia acuminata* [41]. Recent studies identified a nickel complex with nicotianamine in *Thlaspi caerulescens* [42] as well as in *S. acuminata* [43]. As an example for nickel speciation analysis in plants, Figure 2.14.6 shows the size exclusion chromatography (SEC) separation of nickel complexes in the extract of the latex from the hyperaccumulating plant *S. acuminata* with subsequent mass spectrometric identification of the major peak.

Apart from hyperaccumulation plants, there are only a few nickel speciation studies in biota in the context of environmental aspects. For example, nickel speciation was investigated amongst many other metals in the mussel *Mytilus edulis*, revealing that in the cytosol nickel is bound to large molecules in the size range of 6–7 and 200–2000 kDa [44].

3 NICKEL SPECIATION IN FOOD

The main route of nickel intake for nonoccupationally exposed humans is dietary ingestion of food and drinking water (Table 2.14.1). In most food products, the nickel content is less than 0.5 mg kg^{-1} fresh weight. Cacao products and nuts may, however, contain as much as 10 and 3 mg kg^{-1}, respectively [45]. Several studies are dealing with nickel contamination of food products by cooking utensils and packing materials. Stainless steel pans and pots show only a small release of nickel to the cooking food even when the most aggressive (acidic) foods are prepared [46–48]. The values for nickel uptake were negligible under human health considerations so that the European Commission concluded in their report that nickel-sensitized persons who suffer from allergy gain no advantage by avoiding uncorroded stainless steel utensils [49]. Another study demonstrated that coffee machines also did not release nickel in quantities of any significance while on the contrary 10 out of 26 commercial available electric kettles released more than 50 $\mu g\,L^{-1}$ nickel to water [50]. An earlier study shows higher nickel concentrations in canned vegetables, sugars and preserves, bread and cereals in comparison to other food groups, suggesting a contribution from food processing equipment, and possibly, food cans [51]. Diet studies indicate a total average oral nickel intake of 0.2–0.3 mg/day [4], with an absorption rate of less than 15% from the gastrointestinal tract [52]. The quantity of nickel absorbed depends on the nickel bioavailability and thus on the nickel species and nickel content in the food, wherein the Ni^{2+} cation is considered as the most bioavailable species.

Although dietary intake is the most important route for nickel exposure, information on nickel

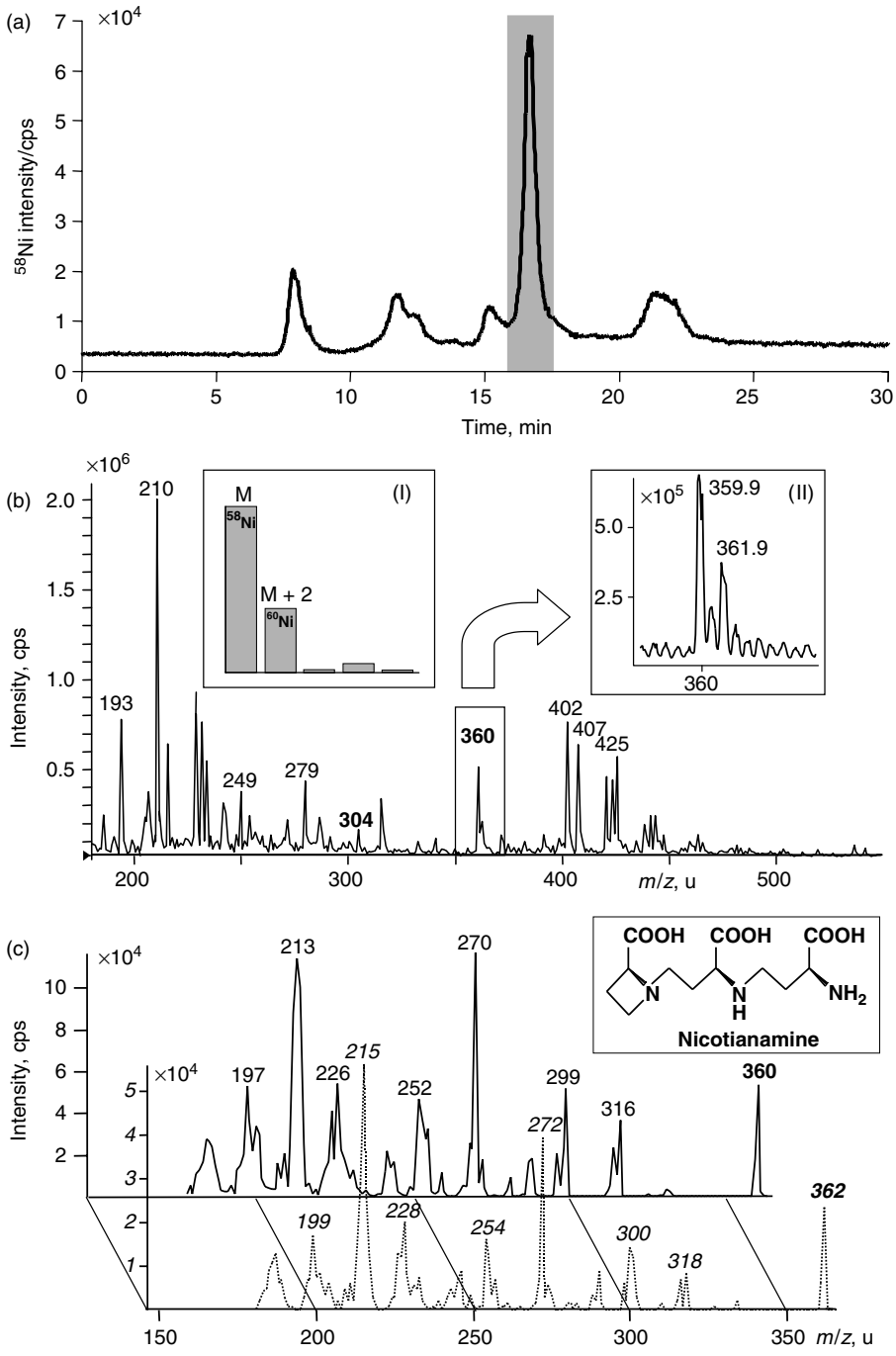

Figure 2.14.6. Nickel speciation analysis in the hyperaccumulating plant *Sebertia acuminata* [43]. (a) SEC high performance liquid chromatography (HPLC) – inductively coupled plasma mass spectrometry (ICP MS) chromatogram of the latex extract, elution with 5 mM ammonium acetate buffer (pH 6.8) from the Superdex peptide HR (30 cm×10 mm) column; (b) ESI MS spectrum of the fractions corresponding to the major peak (shaded area) in Figure 2.14.6(a), inset (I): theoretical nickel isotopic pattern, inset (II): observed nickel isotopic pattern; (c) electrospray tandem mass spectrometry (ESI MS/MS) spectrum of the m/z 360 and 362 ions leads to the identification of a nickel complex with nicotianamine, inset: structure of the ligand. (Reproduced from [43] by permission of The Royal Society of Chemistry.)

speciation in foodstuffs is rather scarce. The very few speciation studies concern mainly tea, soybeans and human milk. Nickel in black tea leaves was classified as a highly extractable element that is present as complexes with large organic molecules [53]. Organic nickel complexes in Kenyan and Indian black teas as well as Chinese green tea were found primarily associated with the flavanoid components [54]. However, the main part of nickel in tea infusions appears to be present in the cationic form as Ni^{2+}, besides large organic nickel complexes in the size range of 4–6 kDa [55]. In soybean flour, 66% of the total nickel was extractable and was present mainly as complexes of 2–3 kDa size [56]. Also, in human milk, nickel was found to be associated with high molecular mass biomolecules, probably caseins, lactotransferrin, serum albumin or immunoglobulins [57]. The edible biopolymer arabinogalactan, extracted from the leaves of the Brazilian plant *Pereskia aculeata* and proposed as a food additive, was found to be a ligand for nickel. The molecule has a tridimensional web structure, where Ni^{2+} is complexed by galacturonic groups [58].

4 CLINICAL AND OCCUPATIONAL HEALTH ASPECTS OF NICKEL SPECIATION

There are indications that nickel is an essential trace element in several animal and plant species [2], and nickel also appears to be essential for humans, although no data are available concerning nickel deficiency. Besides this, nickel compounds show toxic effects to organisms [59]. Little is known about risk groups in the general population. Occupationally exposed people have higher exposures to nickel than other groups within the population because nickel concentrations in workroom air, particularly in the nickel-refining industry (crushing, roasting, smelting and electrolysis), may be significantly increased compared to those in ambient air. Therefore, the majority of clinical studies concerns respiratory (lung and nasal) cancer risks for occupationally exposed persons. Nickel ACD by occupational and nonoccupational nickel contact is also studied. The latter has reportedly sensitized about 5–15% of females and about 0.5–1% of males in Europe for nickel ACD, primarily through nickel-plated clothing fasteners and jewelry in pierced ears [60, 61].

4.1 Occupational exposures to nickel

The main route of nickel intake for occupationally exposed humans, unlike the general population, is inhalation of airborne nickel at the workplace and, to a lesser extent, dermal absorption by skin contact. Occupational exposures occur in different industrial sectors of the nickel-producing (mining, milling, smelting and refining) and the nickel-using industry (stainless and alloy steel production, nickel alloy production, welding and hot cutting, nickel plating, production and blending of chemicals, manufacturing of nickel catalysts, manufacturing of Ni/Cd batteries, and other uses including coinage, pigments and powders). As an example, Figure 2.14.7 shows historical exposures in a nickel refinery in Norway in the period between 1910 and 1994 [62]. Time trends for the average concentrations of total nickel in air in selected departments as well as the dominating nickel species class are presented, adapting the classification of airborne nickel into soluble, sulfidic, metallic and oxidic nickel species (Figure 2.14.2). Although the average total nickel concentration decreased from more than 5 $mg\,m^{-3}$ in 1910 to 30–730 $\mu g\,m^{-3}$ in 1994 at the workplace, the latter values are still more than three orders of magnitude higher than in ambient air.

4.2 Absorption, distribution, metabolism and elimination of nickel species in organisms

Because of the focus of clinical studies on occupational health aspects, the intake of airborne nickel species by inhalation and their absorption by the respiratory tract is mainly studied applying a physical and chemical classification into inhalable,

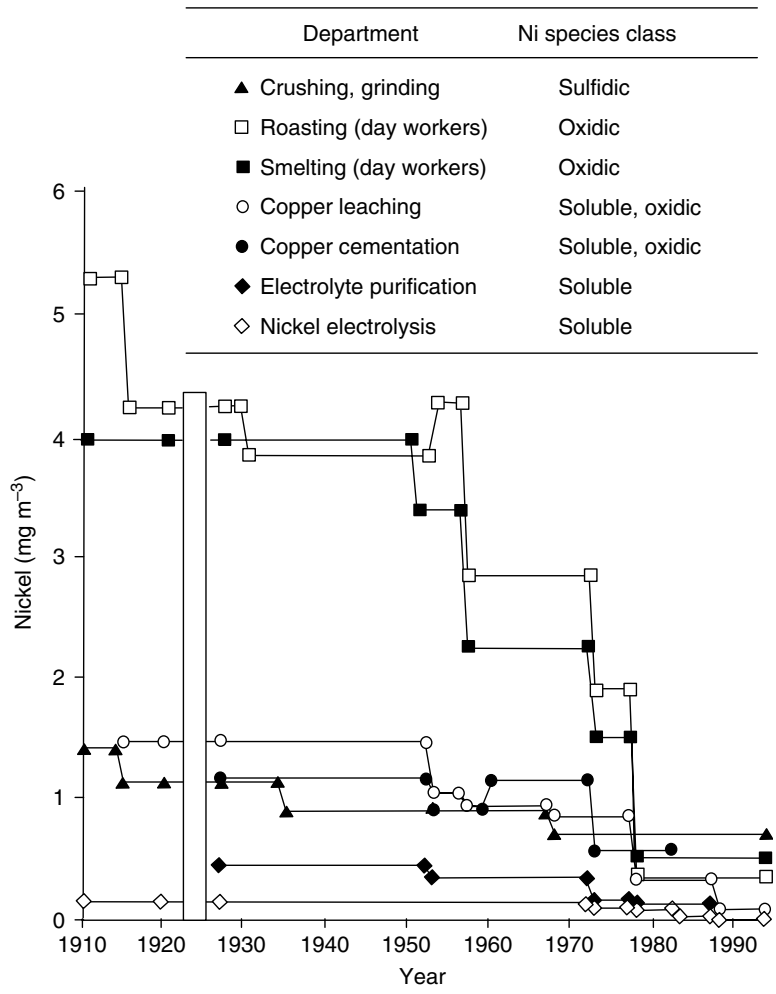

Figure 2.14.7. Historical exposures in a nickel refinery in Norway. Time trends for the average total nickel concentration in selected departments and the dominant nickel species class. Between 1921 and 1926, the refinery was closed because of economical problems. (Reproduced from Reference [62] by permission of the Scandinavian Journal of Work Environment and Health.)

thoracic and respirable particle-size fractions as well as soluble, sulfidic, metallic and oxidic nickel species (Figures 2.14.2 and 2.14.3).

Deposition, absorption and retention of nickel particles in the respiratory tract follow the general principles of lung dynamics. Hence, factors such as the aerodynamic size of a particle and ventilation rate will largely dictate the deposition of nickel particles into the nasopharyngeal, tracheobronchial or pulmonary (alveolar) regions of the respiratory tract. Not all particles are inhalable. Humans inhale only about half of the particles with aerodynamic diameters $>30\ \mu m$, and it is believed that this efficiency may decline rapidly for particles with aerodynamic diameters between 100 and 200 μm (Figure 2.14.3). Of the particles inhaled, only a small portion with aerodynamic diameters larger than 10 μm are deposited in the lower regions of the lung, with deposition in this region predominantly limited to particles $<4\ \mu m$ [63]. Factors such as the amount deposited and particle solubility, surface area, and size will influence the behavior of particles once deposited in the respiratory tract and will probably

account for differences in retention and clearance via absorption or through mechanical means (such as mucociliary clearance).

Soluble nickel compounds are removed rapidly from the lung. It was demonstrated, for example [64], that only 0.1% of the dose was found in the lungs 21 days after tracheal instillation of nickel chloride in rats. Menzel *et al*. [65] demonstrated a saturable clearance mechanism of soluble nickel compounds from rat lungs.

Oxidic nickel remains in the lungs following exposure. In golden hamsters exposed to artificial nickel oxide aerosols, 20% of inhaled nickel oxide remained after the initial elimination, and 45% of this was still present after 45 days [66]. Continuous inhalation (for six weeks) of nickel oxide (NiO) at a concentration of 50 $\mu g\,m^{-3}$ gave rise to comparable figures [67]. Wehner *et al*. [68] exposed Syrian hamsters to nickel-enriched fly ash aerosols. Nickel leaching from the nickel-enriched fly ash did not seem to occur to any extent.

Sulfidic nickel takes an intermediate position. In mice, about 10% of an intratracheally administered dose of nickel subsulfide (Ni_2S_3) was retained 35 days after the exposure [69].

During intimate and prolonged contact with the skin, metallic nickel and nickel salts can be solubilized by sweat, leading to the formation of nickel ions. Ni^{2+} has been shown to penetrate the skin fastest at sweat ducts and hair follicles where it binds to keratin and accumulates in the epidermis. However, the surface area of these ducts and follicles is small; hence, dermal absorption by penetration through the skin is primarily determined by the rate at which nickel is able to diffuse through the horny layer of the epidermis [70]. Nickel penetration of skin is enhanced by many factors including sweat, solvents, detergents and occlusion, such as wearing gloves [60, 71, 72].

After absorption, the nickel is distributed in the body by the blood. The main carrier protein of nickel in serum is albumin, but nickel can also be bound to α-2 macroglobulin and histidine [73]. Reference values for nickel concentrations in serum and urine from healthy persons without occupational exposure to nickel compounds have recently been compiled [73, 74]. Values for serum/plasma are in the range 0.14–0.65 $\mu g\,L^{-1}$; values of around 0.2 $\mu g\,L^{-1}$ seem to be the most reliable. Corresponding values for urine are 0.9–4.1 $\mu g\,L^{-1}$, with values of 1–2 $\mu g\,L^{-1}$ the most reliable. For whole blood, values of 0.34–1.4 $\mu g\,L^{-1}$ are given.

On average, the body of adult humans contains about 0.5 mg nickel per 70 kg. The highest concentrations of nickel are found in the lung and in the thyroid and adrenal glands (about 20–25 $\mu g\,kg^{-1}$ wet weight). Most other organs (e.g. kidney, liver, brain) contain about 8–10 $\mu g\,kg^{-1}$ wet weight [75].

Nickel may undergo redox metabolism generating the trivalent form and thus forming reactive oxygen species. The intracellular release of nickel ion following phagocytosis of particles of oxidic and/or sulfidic nickel is an important metabolic pathway. Minute particles containing nickel have been found close to the nuclear membrane. Nickel ions may also enter the cell directly, although possible transport mechanisms are unclear.

Absorbed nickel is predominantly extracted by the kidneys and eliminated in the urine [76]. Excretion via sweat, secretion via saliva and deposition in hair has been reported [77]. However, urinary excretion is the main clearance route. The biological half-time of nickel depends on the nickel species tested. For soluble compounds, the half-time of plasma nickel is 11–39 hours in humans; for particulate compounds, half-times of 30–54 hours have been recorded [78]. A urinary elimination half-time of 17–48 hours has been reported for the absorbed dose following experimental oral exposure in humans [52]. Nickel particles in nasal tissue and lungs can have a half-time of 3.5 years [79], while nickel was found in respiratory tissue of nickel refinery workers even more than 20 years after exposure. These particles were identified as trevorite, an insoluble, spinel-type mineral, which is probably biologically inert [80].

4.3 Toxicological and carcinogenic effects of nickel species

The critical organ following exposure by inhalation is the respiratory tract. After short-term high-dose inhalation exposure, all types of nickel species induce lung irritation, chemical pneumonia, emphysema and varying degrees of hyperplasia of pulmonary cells and fibrosis (pneumoconiosis) [45, 81]. Increased mortality from nonmalignant respiratory disease has been reported in nickel refinery workers with more than 5 years of exposure, and pneumoconiosis has been reported following 12–20 years of exposure. No details on nickel compounds or exposure levels was given, but nickel oxide (Ni_2O_3) was found to be fibrogenic when instilled intratracheally [4]. The respiratory tract is also a target organ for allergic manifestations of exposure to inorganic nickel species. Allergic asthma has been reported among workers in the plating industry following exposure to nickel sulfate.

Nickel ACD has been documented both in nickel workers and in the general population after prolonged, rather than short-term, skin contact with metallic nickel or soluble nickel salts, resulting in inflammation of areas of the skin in sensitized individuals. However, the significance of nickel as a cause of occupationally induced skin reaction is decreasing. In contrast, there is evidence that nickel is increasingly a major allergen in the general population, especially in women. It was first observed in individuals who had skin contact with clothing items having nickel-coated buckles, zippers and clasps. About 0.5–1% of males and 5–15% of females show a positive skin reaction to patch testing with nickel sulfate. Ear-piercing considerably increases the risk of nickel sensitization [60, 61]. Ni^{2+} ions by themselves are not regarded as antigenic, but nickel complexes with histidines or proteins, which are bound to Langerhans' cells. These cells located in the basal layer of the epidermis actively participate in cutaneous immune regulation and surveillance and are responsible for antigen processing. This can elicit an allergic reaction in sensitized individuals, resulting in tissue inflammation and other allergic reactions in an attempt to rid the body of the foreign entity.

Inhalation studies on experimental animals are most relevant for the assessment of potential human cancer risk from exposure to airborne nickel species. Ottolenghi *et al*. [82] described a significant increase in the number of lung tumors in rats following inhalation exposure to nickel subsulfide for about two years. Nickel sulfate hexahydrate, green nickel oxide and nickel subsulfide have been tested in two-year inhalation studies in mice and rats under the United States National Toxicology Program [83–85]. No tumorigenic activity was found with any of the compounds in mice or with nickel sulfate in rats. Increases in lung adenomas and carcinomas were found in rats for both nickel oxide and nickel subsulfide. The increase was related to the exposure dose but not to the retained dose, and nickel subsulfide was the most potent tumorigen, while nickel was retained in the lung to a considerably higher degree after oxide exposure. Both the oxide and the subsulfide also caused an increase in adrenal pheochromocytomas in rats.

Studies linking nickel uptake from the environment and cancer incidence in the general population are not available. The most complete historical analysis of epidemiological data (before 1990) from occupationally exposed individuals was carried out by the International Committee on Nickel Carcinogenesis in Man (ICNCM) [86]. Ten groups of workers (cohorts) from a variety of occupations were analyzed. The total number of workers involved was about 80,000, located in the US, Canada, England, Wales, Norway, Finland and New Caledonia. Nickel refinery workers exposed by inhalation to various nickel compounds in the past are at a significantly higher risk for cancer of the lungs and the nasal cavity than the nonoccupationally exposed population [45, 86]. In the ICNCM report, the most broad historical dataset could be obtained from the Clydach refinery, Wales, which covers a period from 1907 to 1984: a high relative risk of nasal and lung cancer has been associated with inhalation exposure in the calcining, roasting and leaching departments before 1920. Much of the risk was related to work at the linear calciner where nickel exposure levels were 10–100 $mg\,m^{-3}$ with a composition of about 60%

oxidic, 20% sulfidic, 20% metallic and 3% soluble nickel. Even if the exposure to soluble nickel compounds is low compared to the particulate form, analysis indicates that exposure to soluble forms together with the oxidic or sulfidic forms increases the risk. A recent more precise characterization of historical nickel refinery dust samples from the Clydach refinery revealed the presence of nickel arsenide, Ni_5As_2 (orcelite), in dust samples obtained in 1920 [87, 88]. In 1923, the refining process was changed, eliminating the nickel arsenide in the dust. The substantial decrease of respiratory cancers between 1925 and 1930 and recent toxicological studies on mouse embryo cells support the hypothesis that nickel arsenide in the refinery dust samples before 1923 contributed to its carcinogenicity [89]. The main conclusion of the ICNCM report is that more than one nickel species gives rise to lung and nasal cancer. Although much of the respiratory cancer risk seen among the nickel refinery workers could be attributed to exposure to a mixture of oxidic and sulfidic nickel at very high concentrations (>10 mg Ni/m^3), exposure to large concentrations of oxidic nickel in the absence of sulfidic nickel was also associated with increased lung and nasal cancer risks. There was also evidence that exposure to soluble nickel species increased the risk of these cancers and that it may enhance risks associated with exposure to less soluble forms of nickel [86]. The carcinogenicity assessment of soluble nickel species has turned out to be difficult and is still under critical discussion [90]. There was no evidence that metallic nickel was associated with increased lung and nasal cancer risks. Laryngeal cancer, kidney cancer and cancer of the prostate or bone in nickel workers have also been reported by this study, but the epidemiological evidence does not indicate a relationship to nickel exposure or to any other occupational origin [86].

Exposures in the refining sector should not be confused with those in mining, where the predominant mineral from sulfidic ores is pentlandite [$(Ni,Fe)_9S_8$]. Pentlandite is very different from the sulfidic nickel species found in refining (NiS, NiS_2 and Ni_2S_3) and has not been shown to be carcinogenic in rodents intratracheally instilled with the mineral over their lifetimes [91]. There is no statistical evidence that the lung cancer seen in miners is nickel-related [86].

Further research was made to elucidate the molecular mechanism of nickel carcinogenesis and to explain why inhaled soluble nickel species are less carcinogen than insoluble sulfidic and oxidic species. The reason for this lies in the cellular uptake mechanism. The soluble nickel particles dissolve in the mucus covering the airways, and the resulting ionic or complexed Ni^{2+} is promptly removed by the ciliary transport mechanism. In contrast, the insoluble particles can be ingested by either macrophages or epithelial cells (phagocytosis) [92]. Once inside the cell, these particles are then slowly dissolved, providing a continuous source of Ni^{2+} ions [93]. The cell nucleus is regarded as the site of nickel attack because, as a potential mutagen, nickel can cause chromosome damage and on a molecular basis, nickel is found to induce DNA damage by binding of Ni^{2+} ions to DNA and nuclear proteins [94]. Because of the weak binding of Ni^{2+} to DNA [95], histones, a group of highly abundant nuclear proteins, were recently proposed as primary targets for the binding of Ni^{2+} ions [96].

Nickel forms a limited range of organic compounds and, excluding those synthesized purely for research and academic purposes, nickel tetracarbonyl is the only one that needs to be considered. The respiratory tract is the main target of concern following exposure to nickel carbonyl. Unlike other nickel species, however, acute toxicity is of paramount importance in controlling risks associated with exposure to nickel tetracarbonyl. The severe toxic effects by inhalation have been recognized for many years. The clinical course of nickel tetracarbonyl poisoning involves two stages. The initial stages are characterized by headache, chest pain, weakness, dizziness, nausea, irritability and a metallic taste in the mouth [97, 98]. There is then generally a remission lasting 8–24 hours followed by a second phase characterized by a chemical pneumonitis but with evidence, in severe cases, of cerebral poisoning. Common clinical signs in severe cases include tachypnoea, cyanosis, tachycardia and hyperemia of the throat [99]. The

Table 2.14.2. Current threshold limit values for nickel species classes in the workplace air given by governmental authorities (8-h time-weighted average, unless otherwise noted) [100].

Country	Threshold limit values for standards (mg Ni/m^3)		
	Metallic nickel and insoluble nickel species	Soluble nickel species	Nickel tetracarbonyl
European Union	Metallic Ni: 1.0[a] Oxidic Ni: 0.5[a] Sulfidic Ni: 0.1[a]	0.1	0.24
Austria	0.5	0.05	0.05 (mL m^{-3})
Belgium	1.0	0.1	0.12
Denmark	Metallic Ni: 0.05 NiO, $NiCO_3$: 0.1 Insoluble Ni: 1.0	0.01	0.1
Finland	Metallic Ni: 1.0 NiO, $NiCO_3$: 0.1	0.1	0.007
France	1.0	0.1	0.12
Germany	0.5[b]	0.05	0.24 (15 min)
Greece	Not available	Not available	Not available
Ireland	1.0	0.1	0.12
Italy	1.0	0.1	0.12
Luxembourg	1.0	0.1	0.12
Netherlands	Metallic Ni: 1.0 NiO, $NiCO_3$: 0.1	0.1	0.12
Portugal	1.0	0.1	0.12
Spain	1.0	0.1	0.12
Sweden	Metallic Ni: 0.5 NiO, $NiCO_3$: 0.1 Ni_2S_3: 0.01	0.1	0.01
United Kingdom	0.5	0.1	0.24 (15 min)
Australia	1.0	0.1	0.12
Canada	1.0	0.1	0.35[c]
USA	1.0	1.0	0.007

[a] Recommended.
[b] Potential change to 0.05 mg Ni/m^3.
[c] Potential change in Ontario to 0.12 mg Ni/m^3.
(The values are believed to be accurate at the time of publication but should not be taken as authoritative.)
Source: Reproduced from Reference [100] by permission of The Nickel Institute.

second stage reaches its greatest severity in about four days, but convalescence is often protracted. Evidence of chronic effects at levels of exposure below those that produce symptomatic acute toxicity is difficult to find.

4.4 Exposure limits for nickel species in workplace surveillance

One of the main results of the ICNCM report was that respiratory cancers in occupationally exposed individuals could be observed in the past for high nickel concentrations in the workplace air, namely, >10 mg m^{-3} for sulfidic and oxidic nickel and >1 mg Ni/m^3 for soluble species [86]. Although the mechanism of nickel carcinogenesis is not fully elucidated yet and precise health risks, if any, of exposures to low levels of nickel are uncertain, governmental authorities have given maximum exposure levels designed to adequately protect the worker. Table 2.14.2 summarizes the current threshold limits for nickel species classes in the workplace air established in the European Union Member States, Australia, Canada and the United States.

5 CONCLUSIONS

When reviewing the literature on the fate of nickel species from their sources (natural or anthropogenic) to the environment and to humans, the

majority of the studies concern nickel speciation in air, in particular, workplace air in the nickel-producing and using industry, with respect to health effects of nickel species to occupationally exposed people. In the frame of these studies, a generally accepted classification of nickel species is the distinction between soluble, sulfidic, metallic, and oxidic species without further chemical characterization of the nickel compound within these fractions. This classification has turned out to be useful to investigate health effects of nickel, namely, ACD and respiratory tract cancer, to occupationally exposed workers in the nickel industry. Since an extensive historical study from the International Committee on Nickel Carcinogenesis in Man revealed that high relative risk of nasal and lung cancer for workers has been associated with inhalation of nickel compounds at the workplace, the classification into four species categories entered governmental regulations of exposure levels in the industrial countries.

6 REFERENCES

1. Greenwood, N. and Earnshow, A., Nickel, palladium und platin, *Chemie der Elemente*, VCH, Weinheim, Basel, Cambridge, 1990, pp. 1464–1503.
2. Brown, P. H., Welch, R. M. and Cary, E. E., *Plant Physiol.*, **85**, 801 (1987).
3. Nickel Institute, Health Guide: Safe Use of Nickel in the Workplace, 2nd edition, 1997.
4. International Programme on Chemical Safety, *Environmental Health Criteria 108, Nickel*, WHO, Geneva, 1991.
5. *Air Quality Guidelines for Europe 2000*, Full Background Material to WHO Regional Publications, European Series. No. 91 [CD-ROM], WHO Regional Office for Europe, Copenhagen, 2001, Chapter 6.10 (Nickel), Table 1.
6. Nieboer, E., Fletcher, G. G. and Thomassen, Y., *J. Environ. Monitor.*, **1**, 1 (1999).
7. Hoff, R. M. and Barrie, L. A., *Water Sci. Technol.*, **18**, 97 (1986).
8. Chan, W. H. and Lusis, M. A., *Adv. Environ. Sci. Technol.*, **17**, 113 (1986).
9. Saltzman, B. E., Cholak, J., Schafer, L. J., Yeager, D. W., Meiners, B. G. and Svetlik, J., *Environ. Sci. Technol.*, **19**, 328 (1985).
10. Bennett, B. J., Environmental nickel pathways to man, in *Nickel in the Human Environment*, Sunderman, F. W. (Eds.), International Agency for Research on Cancer, Lyon, 1994, pp. 487–495.
11. Fuichtjohann, L., Jakubowski, N., Gladtke, D., Klocko, D. and Broekaert, J. A., *J. Environ. Monitor.*, **3**, 681 (2001).
12. Bolt, H. M., Noldes, C. and Blaszkewicz, M., *Int. Arch. Occup. Environ. Health*, **73**, 156 (2000).
13. Zatka, V. J., Warner, J. S. and Maskery, D., *Environ. Sci. Technol.*, **26**, 138 (1992).
14. Thomassen, Y., Nieboer, E., Ellingsen, D., Hetland, S., Norseth, T., Odland, J. O., Romanova, N., Chernova, S. and Tchachtchine, V. P., *J. Environ. Monitor.*, **1**, 15 (1999).
15. Kerr, S. M., Vincent, J. H. and Ramachandran, G., *Ann. Occup. Hyg.*, **45**, 555 (2001).
16. Liu, A. and Wong, J. L., *J. Hazard. Mater.*, **74**, 25 (2000).
17. Galbreath, K. C., Toman, D. L., Zygarlicke, C. J., Huggins, F. E., Huffman, G. P. and Wong, J. L., *J. Air Waste Manage. Assoc.*, **50**, 1876 (2000).
18. Hoflich, B. L. W., Wentzel, M., Ortner, H. M., Weinbruch, S., Skogstad, A., Hetland, S., Thomassen, Y., Chaschin, V. P. and Nieboer, E., *J. Environ. Monitor.*, **2**, 213 (2000).
19. Henry, W. M. and Knapp, K. T., *Environ. Sci. Technol.*, **14**, 450 (1980).
20. Dietz, R. N. and Wieser, R. F., *Sulfate Formation in Oil-Fired Power Plant Plumes*, Report No. EA-3231, Brookhaven National Laboratory, Upton, NY, 1983.
21. Stoeppler, M., Analysis of nickel in biological materials and natural waters, in *Nickel in the Environment*, Nriagu, J. O. (Ed.), John Wiley & Sons, New York, 1980, pp. 661–821.
22. Turner, A., Nimmo, M. and Thuresson, K. A., *Mar. Chem.*, **63**, 105 (1998).
23. Banerjee, D. K. and Pani, B., *Environ. Sci. Res.*, **55**, 23 (1998).
24. Martino, M., Turner, A. and Millward, G. E., *Environ. Sci. Technol.*, **37**, 2383 (2003).
25. Lam, M. T., Murimboh, J. and Chakrabarti, C. L., Kinetic speciation of nickel complexes in aqueous environmental samples by competitive ligand equilibration/adsorptive cathodic stripping voltammetry (CLE/AdCSV), Presented at *EnviroAnalysis, Proceedings of the Biennial International Conference on Chemical Measurement and Monitoring of the Environment*, Ottawa, ON, Canada, May 11–14, 1998, pp. 589–594.
26. Mandal, R., Hassan, N. M., Murimboh, J., Chakrabarti, C. L., Back, M. H., Rahayu, U. and Lean, D. R. S., *Environ. Sci. Technol.*, **36**, 1477 (2002).
27. Christensen, J. B. and Christensen, T. H., *Water Res.*, **34**, 3743 (2000).
28. Bedsworth, W. W. and Sedlak, D. L., *Environ. Sci. Technol.*, **33**, 926 (1999).
29. Pumpel, T., Macaskie Lynne, E., Finlay John, A., Diels, L. and Tsezos, M., *Biometals*, **16**, 567 (2003).
30. Feldmann, J., *J. Environ. Monitor.*, **1**, 33 (1999).

31. Theis, T. L. and Richter, R. O., *Environ. Sci. Technol.*, **13**, 219 (1979).
32. Barbafieri, M., *Int. J. Phytorem.*, **2**, 105 (2000).
33. Ge, Y., Murray, P. and Hendershot, W. H., *Environ. Pollut.*, **107**, 137 (2000).
34. Weng, L., Temminghoff, E. J. M., Lofts, S., Tipping, E. and Van Riemsdijk, W. H., *Environ. Sci. Technol.*, **36**, 4804 (2002).
35. Ensley, B. D., Rationale for the Use of Phytoremediation, in *Phytoremediation of Toxic Metals. Using Plants to Clean Up the Environment*, Raskin, I. and Ensley, B. D. (Eds.), John Wiley & Sons, New York, 2000.
36. Blaylock, M. J. and Huang, J. W., Phytoextraction of metals, in *Phytoremediation of Toxic Metals. Using Plants to Clean Up the Environment*, Raskin, I. and Ensley, B. D. (Eds.), John Wiley & Sons, New York, 2000.
37. Saxena, P. K., KrishnaRaj, S., Dan, T., Perras, M. R. and Vettakkorumakankav, N. N., Phytoremediation of metal contaminated and polluted soils, in *Heavy Metal Stress in Plants*, Prasad, M. N. V. and Hagemayer, J. (Eds.), Springer, Berlin, 1999, pp. 305–329.
38. Wenzel, W. W., Bunkowski, M., Puschenreiter, M. and Horak, O., *Environ. Pollut.*, **123**, 131 (2003).
39. Krämer, U., Pickering, I. J., Prince, R. C., Raskin, I. and Salt, D. E., *Plant Physiol.*, **122**, 1343 (2000).
40. Krämer, U., Cotter-Howells, J. D., Charnock, J. M., Baker, A. J. M. and Smith, J. A. C., *Nature*, **379**, 635 (1996).
41. Sagner, S., Kneer, R., Wanner, G., Cosson, J. P., Deus-Neumann, B. and Zenk, M. H., *Phytochemistry*, **47**, 339 (1998).
42. Vacchina, V., Mari, S., Czernic, P., Marques, L., Pianelli, K., Schaumlöffel, D., Lebrun, M. and Lobinski, R., *Anal. Chem.*, **75**, 2740 (2003).
43. Schaumlöffel, D., Ouerdane, L., Bouyssiere, B. and Lobinski, R., *J. Anal. At. Spectrom.*, **18**, 120 (2003).
44. Ferrarello, C. N., Fernandez de la Campa, M. R., Sariego Muniz, C. and Sanz-Medel, A., *Analyst*, **125**, 2223 (2000).
45. Nickel and nickel compounds, in *Chromium, Nickel and Welding*, Vol. 49, International Agency for Research on Cancer, Lyon, 1990, pp. 257–445, IARC Monographs on the Evaluation of Carcinogenic Risks to Humans.
46. Flint, G. N. and Worn, D. K., Hygiene and other health and safety aspects of stainless steel in food-handling and processing plant, Presented at *Innovation Stainless Steel, European Stainless Steel Conference*, Florence, Italy, Oct. 11–14, 1993, Associazione Italiana di Metallurgia, Milan, Italy, 1993, pp. 43–47.
47. Accominotti, M., Bost, M., Haudrechy, P., Mantout, B., Cunat, P. J., Comet, F., Mouterde, C., Plantard, F., Chambon, P. and Vallon, J. J., *Contact Dermatitis*, **38**, 305 (1998).
48. Ruckert, J., Isecke, B. and Zietelman, C., *Mater. Corros.*, **53**, 579 (2002).
49. Baroux, B. and Haudrechy, P., *Assessment of the Stainless Steels Compatibility in Food and Health Applications Regarding to their Passivation Ability*, EUR 18922, European Commission, 1999, pp. 125–134.
50. Berg, T., Petersen, A., Pedersen, G. A., Petersen, J. and Madsen, C., *Food Addit. Contam.*, **17**, 189 (2000).
51. Smart, G. A. and Sherlock, J. C., *Food Addit. Contam.*, **4**, 61 (1987).
52. Sunderman, F. W., Hopfer, S. M., Swenney, K. R., Marcus, A. H. and Creason, B. M., *Proc. Soc. Exp. Biol. Med.*, **191**, 5 (1989).
53. Matsuura, H., Hokura, A., Katsuki, F., Itoh, A. and Haraguchi, H., *Anal. Sci.*, **17**, 391 (2001).
54. Cairns, W. R. L., Hill, S. J. and Ebdon, L., *Microchem. J.*, **54**, 88 (1996).
55. Odegard, K. E. and Lund, W., *J. Anal. At. Spectrom.*, **12**, 403 (1997).
56. Fingerova, H. and Koplik, R., *Fresenius' J. Anal. Chem.*, **363**, 545 (1999).
57. Coni, E., Alimonti, A., Bocca, A., La Torre, F., Menghetti, E., Miraglia, E. and Caroli, S., *Trace Elem. Electrolytes*, **13**, 26 (1996).
58. Merce, A. L., Landaluze, J. S., Mangrich, A. S., Szpoganicz, B. and Sierakowski, M. R., *Bioresour. Technol.*, **76**, 29 (2001).
59. Denkhaus, E. and Salnikow, K., *Crit. Rev. Oncol. Hematol.*, **42**, 35 (2002).
60. Fischer, T., Occupational nickel dermatitis, in *Nickel and the Skin: Immunology and Toxicology*, Maibach, H. I. and Menne, T. (Eds.), CRC Press, Boca Raton, FL, 1989, pp. 117–132.
61. Nielsen, N. H. and Menne, T., *Contact Dermatitis*, **29**, 16 (1993).
62. Grimsrud, T. K., Berge, S. R., Resmann, F., Norseth, T. and Andersen, A., *Scand. J. Work Environ. Health*, **26**, 338 (2000).
63. Vincent, J. H., *Aerosol Sampling: Science and Practice*, John Wiley & Sons, Chichester, 1989.
64. Carvalho, S. M. and Ziemer, P. L., *Arch. Environ. Contam. Toxicol.*, **11**, 245 (1982).
65. Menzel, D. B., Deal, D. L., Tayyeb, M. I., Wolpert, R. L., Boger, J. R., Shoaf, C. R., Sandy, J., Wilkinson, K. and Francovitch, R. J. III, *Toxicol. Lett.*, **38**, 33 (1987).
66. Wehner, A. P. and Craig, D. K., *Am. Ind. Hyg. Assoc. J.*, **33**, 146 (1972).
67. Oberdörster, G. and Hochrainer, D., Effect of continuous nickel oxide exposure on lung clearance, in *Nickel Toxicology*, Brown, S. S. and Sunderman, F. W. (Eds.), Academic Press, London, 1980, pp. 125–128.
68. Wehner, A. P., Dagle, G. E. and Milliman, E. M., *Environ. Res.*, **26**, 195 (1981).
69. Valentine, R. and Fisher, G. L., *Environ. Res.*, **34**, 328 (1984).
70. Grandjean, P., Nielson, G. D. and Anderson, O., Human nickel exposure and chemobiokinetics, in *Nickel and the Skin: Immunology and Toxicology*, Maibach, H. I. and

Menne, T. (Eds.), CRC Press, Boca Raton, FL, 1989, pp. 9–34.
71. Malten, K. E., *Contact Dermatitis*, **7**, 238 (1981).
72. Wilkinson, D. S. and Wilkinson, J. D., Nickel allergy and hand eczema, in *Nickel and the Skin: Immunology and Toxicology*, Maibach, H. I. and Menne, T. (Eds.), CRC Press, Boca Raton, FL, 1989, pp. 133–164.
73. Sunderman, F. W., *Scand. J. Work Environ. Health*, **19**, 34 (1993).
74. Templeton, D. M., Sunderman, F. W. and Herber, R. F. M. Jr., *Sci. Total Environ.*, **148**, 243 (1994).
75. Rezuke, W. N., Knight, J. A. and Sunderman, F. W., *Ann. J. Ind. Med.*, **11**, 419 (1987).
76. Christensen, O. B. and Lagesson, V., *Ann. Clin. Lab. Sci.*, **11**, 119 (1981).
77. Christensen, O. B., Moller, H., Andrasko, L. and Lagesson, V., *Contact Dermatitis*, **5**, 312 (1979).
78. Sunderman, F. W., Aitio, A., Morgan, L. O. and Norseth, T., *Toxicol. Ind. Health*, **2**, 17 (1986).
79. Nieboer, E. and Fletcher, G. G., in *Handbook of Metal-Ligand Interactions in Biological Fluids. Bioinorganic Medicine*, Vol. 1, Berthon, G. (Ed.), Marcel Dekker, New York, 1995, pp. 412–417.
80. Andersen, I. and Svenes, K., *J. Environ. Monitor.*, **5**, 202 (2003).
81. Schäfer, S. G., Forth, W. and Schürmann, K., Metalle, in *Lehrbuch der Toxikologie*, Marquardt, H. and Schäfer, G. (Eds.), BI Wissenschaftsverlag, Mannheim, Leipzig, Wien, Zürich, 1994, pp. 504–549.
82. Ottolenghi, A. D., Haseman, J. K., Payne, W. W., Falk, H. L. and MacFarland, H. N., *J. Natl. Cancer Inst.*, **54**, 1165 (1974).
83. National Toxicology Program, *NTP Technical Report on the Toxicology and Carcinogenesis Studies of Nickel Sulfate Hexahydrate in F344/N Rats and B6C3F1 Mice: Inhalation Studies* (NTP TR 454), NIH Publication No. 94–3370, National Institutes of Health, Research Triangle Park, NC, 1994.
84. National Toxicology Program, *NTP Technical Report on the Toxicology and Carcinogenesis Studies of Nickel Oxide in F344/N Rats and B6C3F1 Mice: Inhalation Studies* (NTP TR 551), NIH Publication No. 94–3363, National Institutes of Health, Research Triangle Park, NC, 1994.
85. National Toxicology Program, *NTP Technical Report on the Toxicology and Carcinogenesis Studies of Nickel Subsulfide in F344/N Rats and B6C3F1 Mice: Inhalation Studies* (NTP TR 453), NIH Publication No. 94–3369, National Institutes of Health, Research Triangle Park, NC, 1994.
86. International Committee on Nickel Carcinogenesis in Man, *Scand. J. Work Environ. Health*, **16**, 1 (1990).
87. Draper, M. H., Duffus, J. H., John, P., Metcalfe, L., Morgan, L., Park, M. V. and Weitzner, M. I., *Exp. Toxicol. Pathol.*, **46**, 111 (1994).
88. Draper, M. H., Duffus, J. H., John, P., Metcalfe, L., Morgan, L., Park, M. V. and Weitzner, M. I., *Sci. Total Environ.*, **148**, 263 (1994).
89. Clemens, F. and Landolph, J. R., *Toxicol. Sci.*, **73**, 114 (2003).
90. Oller, A. R., *Environ. Health Perspect.*, **110**, 841 (2002).
91. Muhle, H., Bellmann., B., Takenaka, S., Fuhst, R., Mohr, U. and Pott, F., Chronic effects of intratracheally instilled nickel containing particles in hamsters, in *Nickel and Human Health: Current Perspectives*, Nieboer, E. and Nriagu, J. O. (Eds.), John Wiley & Sons, New York, 1992, pp. 467–480.
92. Evans, R. M., Davies, P. J. A. and Costa, M., *Cancer Res.*, **42**, 2729 (1982).
93. Kasprzak, K. S. and Sunderman, F. W., *Res. Commun. Chem. Pathol. Pharmacol.*, **16**, 95 (1977).
94. Shen, H. M. and Zhang, Q. F., *Environ. Health Perspect.*, **102**, 275 (1994).
95. Lee, J. E., Ciccarelli, R. B. and Wetterhahn, J., *Biochemistry*, **21**, 771 (1982).
96. Bal, W., Kozlowski, H. and Kasprzak, K. S., *J. Inorg. Biochem.*, **79**, 213 (2000).
97. Vuopala, U., Huthi, E., Takkunen, J. and Huikko, M., *Ann. Clin. Res.*, **2**, 214 (1970).
98. Sunderman, F. W. and Kinkaid, J. F., *J. Am. Med. Assoc.*, **155**, 889 (1954).
99. Shi, Z., *Br. J. Ind. Med.*, **43**, 422 (1986).
100. Nickel Development Institute, *Status Report No. 5: Occupational Exposure Limits for Nickel and Nickel Compounds*, 1998, http://www.nidi.org/index.cfm/ci_id/226/la_id/1.htm.

2.15 Speciation of Platinum, Palladium, Gold and Rhodium

2.15.1 Importance of Platinum Group Elements and Gold Speciation in the Environment and Medicine

Sebastien Rauch and Gregory M. Morrison
Chalmers University of Technology, Göteborg, Sweden

1 INTRODUCTION

Platinum group elements (PGEs) and gold are amongst the scarcest metals in the Earth's crust [1], and their environmental relevance has not previously been a major concern, although the use of three of the PGEs (platinum, palladium and rhodium) in automobile catalysts and their release into the environment during vehicle operation has recently been the subject of extensive research [2]. This research has primarily focused on the determination of total metal concentration, which has been important for the assessment of environmental pathways. Only a few speciation studies have been performed, owing to low concentrations and analytical difficulties. Speciation of PGEs and gold has found wider application in studying the use of Pt and Au for cancer and arthritis treatment, respectively. Speciation plays a key role in the therapeutic properties of drugs, and speciation investigations are made possible by the higher concentrations in the samples.

2 ANALYTICAL CONSIDERATIONS

The determination of PGEs and gold in a sample is greatly affected by analyte concentration and matrix composition. While industrial and medical samples generally present relatively high concentrations, PGE concentrations remain low in most

Handbook of Elemental Speciation II: Species in the Environment, Food, Medicine & Occupational Health
Edited by R. Cornelis, H. Crews, J. Caruso and K. G. Heumann
 ISBN: 0-470-85598-3 (HB)

Table 2.15.1.1. PGE concentrations in environmental samples.

Sample	Concentration			Unit	Note	Reference
	Pt	Pd	Rh			
Earth crust	0.4	0.4	0.06	$ng\,g^{-1}$		[1]
Urban air	14.1	4.9	2.9	$pg\,m^{-3}$	PM10, mean	[3]
Particles	5.4	1.5	1.6		PM2.5, mean	
Road sediments	213	56	74	$ng\,g^{-1}$	<63 μm	[4]
Urban river sediments	53.9	38.7	9.4	$ng\,g^{-1}$	Mean	[4]
Roadside grass	10.6	–	1.54	$ng\,g^{-1}$	–	[5]
Asellus Aquaticus	38.0	155.4	17.9	$ng\,g^{-1}$	Mean	[6]
Human urine	1.02	9.5	11.7	$ng\,L^{-1}$	Median, unexposed	[7]

PM2.5: aerosol-fine particles, 2.5–10 μm aerodynamic size
PM10: aerosol-coarse particles, 10 μm cut

environmental compartments (Table 2.15.1.1), and their determination requires sensitive analytical techniques.

Sensitive and selective electrochemical methods have been developed for the determination of trace Pt and Rh with detection limits in the lower $ng\,L^{-1}$ or even $pg\,L^{-1}$ range [8]. The most common electrochemical approach is based on the catalytic properties of PGEs, with cathodic stripping after preconcentration of a Pt or Rh formazone complex at the surface of a hanging mercury drop electrode. However, catalytic cathodic stripping voltammetry (CSV) suffers from severe interference from organic matter, and it is necessary to perform a complete oxidation before the analysis. Voltammetry has been used to determine the electrochemically available fraction of an analyte, sometimes equated as the bioavailable or toxic fraction, but the oxidation step does not allow this distinction here. Moreover, CSV does not allow the determination of environmentally relevant Pd concentrations. In contrast to PGE determination by CSV, the determination of Au has been performed in the anodic stripping mode with a detection limit of about $5\,\mu g\,L^{-1}$ [9].

Inductively coupled plasma-mass spectrometry (ICP-MS) has been applied to the determination of PGE and gold concentrations in environmental samples with detection limits in the sub-$ng\,L^{-1}$ range. However, the determination of PGEs and gold suffers from spectral interference from elements present in the sample matrix [4]. Interference-free determination of Pt and Au can be achieved through the use of a sector field mass spectrometer (SFMS) with a sufficiently high resolution [4] or dry plasma conditions resulting from, for example, membrane desolvation [10], but the determination of Rh and especially Pd presents greater difficulty, as not all interferences can be resolved and analysis requires matrix separation or mathematical correction.

Mass spectrometric techniques are finding increasing use for Pt and Au speciation owing to the capability for on-line determination of species obtained by chromatographic or electrophoretic separation. The coupling of separation techniques with ICP-MS has been used when lower detection limits are required and has been applied to environmental [11] and medical [12–14] studies. On-line separation of interferents has been achieved by ion chromatography (IC) [15], and the coupling of a separation technique with ICP-MS for speciation analysis might therefore allow the simultaneous removal of interferences. However, while the inductively coupled plasma (ICP) is a very efficient source of ions to the mass spectrometer (MS), it results in the loss of structural information, and species generally have to be identified on the basis of retention time. Electrospray ionization (ESI) provides a less efficient, softer ionization, and it has therefore been used to identify Pt species, either directly [16] or after separation by liquid chromatography (LC) [17] or capillary electrophoresis (CE) [18], in medical applications for which higher concentrations are expected. Other techniques that have been used in medical studies include matrix-assisted laser desorption ionization-mass spectrometry (MALDI-MS), nuclear magnetic resonance (NMR) and X-ray crystallography.

3 PLATINUM GROUP ELEMENTS IN THE ENVIRONMENT

3.1 Automobile exhaust catalysts and vehicle emissions

Automobile exhaust catalysts are devices fitted to a vehicle's exhaust to catalytically remove harmful pollutants using Pt, Pd and Rh as main active components for the oxidation of carbon monoxide and hydrocarbons, and the reduction of nitrogen oxides. Modern catalysts usually consist of a honeycomb cordierite or metallic support coated with an aluminum oxide (γ-Al_2O_3) layer onto which PGEs are deposited together with base metal oxide additives. While catalysts efficiently remove pollutants from vehicle exhaust, several phenomena are known to affect catalyst performance, including thermal deactivation, chemical poisoning and mechanical deterioration. The loss of PGEs from the catalyst during operation is usually not considered a major deactivation process and has therefore not been widely studied, although a number of studies have been performed because of environmental concern [2, 19].

Emission rates from automobile catalysts are believed to be in the ng km^{-1} range and depend on catalyst type and composition, age of the catalyst, speed, driving conditions and temperature [19]. Studies of PGE emission have usually dealt with the determination of emission rates rather than the emission mechanism, and the forms in which PGEs are emitted is still unclear. X-ray photoelectron spectroscopy analysis of automobile exhaust particles revealed the occurrence of metallic platinum Pt(0) attached onto aluminum oxide together with a small amount of Pt(IV) [20]. However, a significant soluble fraction has also been measured in automobile exhaust, suggesting the occurrence of soluble Pt species on the catalyst surface as a result of catalyst manufacture or the transformation into soluble species by reaction with fuel additives [19].

A further understanding of PGE emissions has also been achieved through the analysis of the catalyst surface by scanning electron microscopy (SEM) [21] or laser-based techniques [22]. SEM was used to study catalyst deactivation and physical and chemical transformations, and revealed a change in the morphology of precious metal particles. [21] But SEM is hampered by several difficulties such as relatively high detection limits, interference and the presence of a coating on the surface of aged catalyst. Spatially resolved analysis of a gasoline catalyst was performed by (laser ablation) LA-ICP-MS and shows a decrease in PGE concentration at the front end of the catalyst and indicates mechanical abrasion as the emission mechanism. The loss of PGEs was more even along channels of the diesel catalyst and indicates a different emission mechanism, possibly through both mechanical abrasion and reactions with fuel contaminants, including sulfur [22].

3.2 Platinum group elements in the environment

It is now clear that PGEs are emitted from automobile catalysts [19] and that their concentrations are increasing in the urban and roadside environment [2], raising concern for the environment and human health. Understanding of PGE pathways has primarily been provided through the determination of total concentration in samples as diverse as automobile exhaust particles [19] and freshwater macroinvertebrates (Table 2.15.1.1) [6].

Once emitted from the catalysts, PGEs spread into the environment. While increasing PGE concentrations have recently been reported in arctic snow [23], the highest occurrence remains in the urban or roadside environment. PGEs are found in airborne particles where they occur at the pg m^{-3} air level [3]. Particles deposit on the road surface or roadside soil with decreasing concentration at increasing distance from the road. An increase in PGE concentrations in road sediments has been found since the introduction of automobile catalysts [24]. During rain events, the accumulated PGEs can be further transported to rivers or water bodies where they accumulate in sediments, while concentrations in water remain low [24].

PGEs are mostly emitted in a metallic form with a relatively low soluble fraction and should not

be directly available for living organisms. PGEs were therefore believed to be relatively inert, but this belief is changing and there is a growing concern about potential ecological and health risks. PGE bioaccumulation has been reported for the freshwater invertebrate *Asellus aquaticus*, indicating that these metals occur in a bioavailable form in the aquatic environment. Palladium had a higher accumulation rate compared with Pt and Rh and might therefore present a higher risk [6]. Higher Pd concentrations were also found in the urine of nonoccupationally exposed persons [7].

Effluents of hospitals applying Pt-based cancer treatment are another source of Pt into the environment. The emission is due to the urinary excretion of administered drugs, and therefore the emitted species are expected to differ from species released from automobile catalysts [25].

3.3 Analytical procedures to understand the fate of PGEs in the environment

The determination of the chemical form in which PGEs occur is important in the assessment of the risks posed by these metals. The uptake of Pt by the freshwater isopod *A. aquaticus* is dependent on chemical speciation [26], while sensitization by Pt salts in humans is directly related to both Pt concentration and the salt itself [27]. In addition, environmental mechanisms, for example, Pt behavior in soil [12] or uptake by plants [28], can be further understood through speciation analysis. Different analytical procedures have been developed with the aim of providing a better understanding of the transformation of Pt in the environment (Table 2.15.1.2).

Determination of the chemical forms of an element has been performed after their separation using chromatographic and electrophoretic techniques. Different detection techniques have been applied to determine the obtained species, depending on the separation technique and the concentration to be determined. While UV detection can be used for high concentration samples, ICP-MS and CSV have been employed for the speciation of Pt in environmental samples, ICP-MS presenting the advantage of on-line detection [12]. The study of Pt transformation in soil exposed to tunnel dust has been performed by speciation analysis of the soluble Pt fraction using LC, with a reversed-phase column, and CE coupled to ICP-MS [12], and it has been shown that Pt is subject to complex transformations, with progressive oxidation as Pt is released from the surface of the particles by complexing agents. Organic complexes may be formed, possibly with sulfur containing humic acids [12], and therefore Pt is relatively immobile in soil but can be dissolved by a strong complexing agent such as ethylene diamine tetra-acetic (EDTA) [31].

Plants use complexones for metal uptake, and therefore Pt could be taken up from soil. Several studies have investigated the form of Pt in grass, and a number of analytical techniques have been used for this purpose. Low and high molecular mass species were separated by ultrafiltration, and it was found that Pt is mainly present in the molecular mass fraction below 10 kDa [30].

Table 2.15.1.2. PGE speciation in environmental samples.

Sample	Instrumental	Investigation	Reference
Automobile exhaust	X-ray photoelectron spectroscopy	Automobile exhaust particles (Pt(0))	[20]
Soil extracts	HPLC-ICP-MS and CE-ICP-MS	PGE transformations in soil	[12]
Plants	Gel chromatography and isotachophoresis with voltammetric detection	High molecular mass species (>10 kDa)	[29]
Plants	Gel chromatography, isotachophoresis and LC with UV, voltammetric and PAD detection	Low molecular mass species (<10 kDa)	[30]
Plants	SEC-ICP-MS	Low molecular mass species (<10 kDa)	[28]
Aqueous samples and urine	HPLC-ICP-MS	Degradation products of cisplatin	[25]

Pt species were further separated through a combination of gel chromatography and preparative isotachophoresis, with determination by adsorptive voltammetry and UV detection. Five fractions below 10 kDa could be distinguished on the basis of retention time and further separated by LC with UV and pulse amperometric detection (PAD). It was concluded that low molecular mass Pt species are carbohydrates, possibly small oligosaccharides [31]. The coupling of size exclusion chromatography (SEC) to ICP-MS has also been used for the investigation of the speciation of Pt in plants [28]. Five fractions could be separated, and the multielement capability of the ICP-MS provided information relevant to their identification as nonmetabolized inorganic Pt and organic molecules including phytochelatins and precursors of macromolecules such as polygalacturonic acids [28]. Further separation of the high molecular mass fraction was performed by the gel chromatography-isotachophoresis combination with determination of the species by adsorptive voltammetry [29]. While seven species were observed between 10 and >1000 kDa for grass that was exposed to Pt, only one Pt species with a molecular mass of 180–195 kDa was found for native grass.

While speciation investigations have been performed for extracts and biological materials, speciation in solid environmental samples such as sediments is difficult because samples usually have to be analyzed in a liquid form and dissolution requires strong acids, which might change the chemical form in which metals occur. The study of metal association with solid materials has been performed by the sequential extraction of individual geochemical fractions and associated metals. Platinum was found to have a significant exchangeable fraction in road dust [32]. However, doubts have emerged about sequential extraction schemes owing to their operationally defined character, and it seems likely that sequential extraction does not provide the true phase associations or speciation. Further investigation of PGE association with road dust was performed by LA-ICP-MS [33]. Multielement analysis of road dust particles indicates that PGEs mostly occur in Ce-containing particles in road dust. Cerium is a major component of catalyst washcoat and it is therefore believed that PGEs mostly occur in catalyst washcoat particles on the road surface [33].

While the environmental pathways of Pt are starting to be understood, there are still many questions to be answered for the full assessment of PGE contamination. Firstly, the true environmental levels of Pd and Rh are to be established. Environmental transformations of PGE and bioaccumulation mechanisms should be further studied, especially for Pd. Finally, the source of PGEs in remote environments, for example, Greenland, should be further investigated. These questions can only be answered through further development of analytical techniques. Sensitive, interference-free analysis is required for the establishment of environmental PGE levels, as well as for speciation purposes.

Emission of Pt in hospital effluents is a further source of Pt into the environment, and the degradation of cisplatin has been studied by HPLC-ICP-MS with the application of isotope dilution for quantification [25]. Monoaquacisplatin was found in diluted urine from a patient treated with cisplatin, and it was estimated that 75% of the excreted Pt enters sewage treatment as monoaquacisplatin. The study also reveals that cisplatin is transformed into monoaquacisplatin and diaquacisplatin in chloride-containing solutions, while an unidentified species was also found in chloride-free solution [25].

4 PLATINUM AND GOLD IN MEDICINE

Platinum and gold compounds have important clinical applications, owing to their therapeutic properties against cancer and rheumatoid arthritis, respectively. While Pt- and Au-based drugs are already in use, their mechanisms of action are still not fully understood and side effects and low efficiency have still to be overcome. The *in vivo* transformations of these drugs are known to play an important role in the results of the therapy, and therefore a number of studies have investigated the speciation of Pt and Au in clinical samples.

4.1 Platinum-based drugs in cancer treatment

Since the discovery of the therapeutic properties of Pt against cancer, intensive medical studies have been carried out to develop new drugs and better understand their mechanisms of action. Cisplatin (*cis*-diamine-dichloroplatinum(II)) is the most widely used drug in cancer therapy, and its success in the treatment of testicular cancer has provided hope that most cancers could be treated with Pt-based drugs. Therefore, a number of drugs such as carboplatin, oxaliplatin, lobaplatin and nedaplatin have been developed. These drugs have received approval for their use, either worldwide or locally. A further drug, JM216, is currently undergoing clinical trials [34]. Figure 2.15.1.1 provides the structure of aforementioned drugs.

The activity of a Pt-based drug depends on the chemical species in which Pt is administrated, and therefore a number of drugs have been tested. Platinum should be administrated as *cis*-$[PtX_2(Am_2)_2]$ or *cis*-$[PtX_2Y_2(Am)_2]$, where X is an anion of medium binding strength (Cl in the case of cisplatin) and Am is an inert amine with at least one NH group. Figure 2.15.1.2 shows the sequence of events in cisplatin binding to deoxyribonucleic acid (DNA). The drug forms hydrated complexes in biological fluids, with X leaving the molecule. These hydrated species react with DNA to form mostly intrastrand, but also interstrand, cross-linkages through binding to guanosine, thereby inhibiting cell reproduction. However, Pt-based drugs exhibit side effects, including cytotoxicity. Monohydrated complexes exhibit a higher cytotoxicity than other hydrates. In addition, the drugs react with thiol compounds such as L-methionine in body fluids, resulting in increased nephrotoxicity [34].

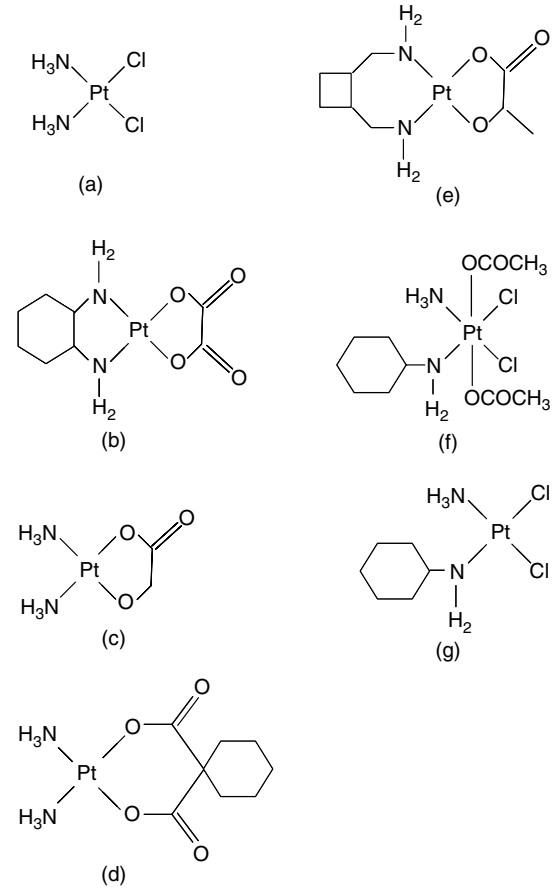

Figure 2.15.1.1. Structure of Pt-based drugs. (a) Cisplatin, (b) oxaliplatin, (c) nedaplatin, (d) carboplatin, (e) lobaplatin, (f) JM-216, (g) JM-118.

The form in which Pt is administered and the transformation of the drug into metabolites plays an important role in the treatment and therefore, several Pt-based drugs, as well as their reaction products, have been tested under defined conditions. Medical studies were supported by

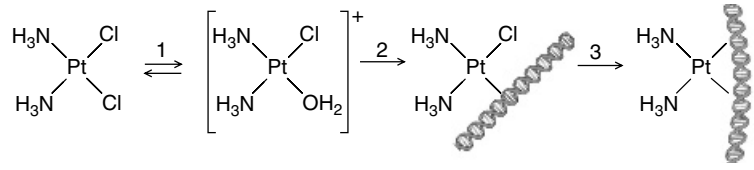

Figure 2.15.1.2. Sequence of events in cisplatin binding to DNA. (1) aquation (monoaquated form), (2) formation of monoadduct, (3) formation of bis-adduct.

analytical techniques, which focused on the determination of total concentrations and Pt species in biological samples [34, 35].

Total Pt concentrations were determined in blood, serum, plasma, urine, tissue and cells by atomic absorption spectrometry, voltammetry, neutron activation analysis, ICP-atomic emission spectroscopy and ICP-MS [35]. Elevated Pt concentrations have been reported in the urine of patients treated with Pt-based drugs, even 16 years after the drug has been administrated [36]. High Pt concentrations have been reported in the liver and kidney of patients, where it is stored through binding to metallothioneins and only a small fraction of the drug actually reaches its target [37].

While total Pt concentrations are relevant to pharmacokinetic studies, speciation has been important in understanding the mechanisms of action of Pt drugs. Speciation studies have mostly been performed through the separation of Pt compounds by electrophoretic and chromatographic techniques followed by spectrophotometric, electrochemical or mass spectrometric detection. A number of studies have aimed at determining the reaction products of Pt-based drugs, and research has mainly focused on the binding of Pt to proteins in blood and the formation of adducts with DNA (Table 2.15.1.3).

Blood proteins play a major role in the transport and metabolism of the drugs administered. Once bound to proteins, Pt is transported to the kidneys and excreted unless it can be released from the protein after transport. The binding of Pt-based drugs with proteins has been investigated through ultrafiltration. Different drugs were found to bind to proteins with different molecular masses. While cisplatin binds to large proteins, DBP (*cis*-diamine{bis(phosphonatomethyl)amino(2-)-O^1,N^1} platinum(II)) was found to bind to smaller proteins or remain unbound [37]. Increased precision for molecular mass separation was obtained by electrophoretic and chromatographic techniques. The reaction of Pt and Ru drugs with serum proteins was investigated by SEC with ICP-MS detection. Albumin and transferrin having similar molecular masses, their separation could not be achieved by SEC alone but could be achieved by a preliminary separation using an ion-exchange column. After three hours, a large fraction of the incubated cisplatin was still unbound, showing a slow kinetic behavior. After 24 h, most of the cisplatin was bound at a molecular mass of 60 kDa, while most of the DBP remains unchanged [13]. LC was coupled to ICP-MS and ESI-MS for the investigation of Pt complexes formed from the interaction of JM216 with human plasma. While direct coupling of high performance liquid chromatography (HPLC) with ICP-MS is possible under optimized chromatographic conditions, a desolvation unit enabled the use of HPLC solvents [38]. The occurrence of the JM118 metabolite was determined on the basis of retention time, and further evidence was obtained from the identification of JM118 by ESI-MS [17].

In a study, which aimed to investigate the target of cisplatin in whole cell systems, gel

Table 2.15.1.3. Speciation of platinum in pharmaceutical and medical samples.

Investigation	Instrumental	Drug	Reference
Binding to blood proteins	Ultrafiltration and ICP-MS analysis	Cisplatin, DBP	[37]
Binding to serum proteins	SEC-ICP-MS	Cisplatin, DBP	[13]
Metabolites in plasma	LC-ICP-MS	JM216	[38]
Metabolites in plasma	LC-ESI-MS	JM216	[17]
Cell target	Gel chromatography and LA-ICP-MS	Cisplatin	[39]
Interaction with monophosphates and oligonucleotides	CE-DAD (UV) and MALDI-MS	Pt complexes	[40]
Binding to 5′-GMP	IC-ESI-MS	Pt complexes	[41]
Binding to 5′-GMP	IC-ICP-SFMS	Cisplatin	[12]
Binding to 5′-GMP	CE-ESI-MS	Cisplatin, carboplatin	[18]
Binding to DNA	Crystallography, NMR and molecular models	Pt drugs	[42]

electrophoresis was used in combination with direct LA-ICP-MS of the electrophoresis plate. The protein to which Pt binds was identified as outer membrane protein A, a protein that traverses the cell membrane allowing the penetration of small solutes and that is involved in maintaining the shape of cells [39].

A number of studies have focused on the mechanism through which Pt complexes bind to DNA through the reaction of Pt complexes with guanosine 5′-monophosphate (5′-GMP). CE with a diode array detector (DAD) was used to separate reaction products, and the identification of the Pt species was based on electrophoretic mobility and UV absorption spectra. This has permitted studies of the interaction of Pt-based drugs with monophosphates and oligonucleotides [40]. The major reaction products of platinum(II) complexes were identified by MALDI-MS, showing the importance of bis-adduct formation during the incubation of Pt complexes in a 5′-GMP containing buffer solution [40]. Further evidence for the formation of bis-adducts was obtained by an IC coupled to ICP-SFMS. The use of a sufficient mass resolution ($m/\Delta m = 4500$) enabled not only the determination of platinum but also the determination of phosphorus, which is hampered by severe interferences. This technique was used to investigate the reaction of cisplatin with 5′-guanosine monophosphate (5′-GMP) through the determination of the platinum-to-phosphorus ratio in reaction products [12] and confirmed the importance of the bis-adduct *cis*-$[Pt(NH_3)_2(GMP)_2]^{2-}$. ESI-MS allowed the identification of adducts of 5′-GMP with platinum(II) complexes after separation by ion-exchange LC. In addition to mono and bis-adducts, other molecules could be monitored, including structures with two Pt centers [41]. In another study, the reaction products of cisplatin and carboplatin with mononucleotides was investigated by CE with ESI-MS detection, and the formation of Pt adducts could be monitored [18]. Detailed information on the interaction of drugs with DNA has also been obtained by crystallography, NMR and molecular models. Hydrated forms of Pt drugs were found to bind to guanine in interstrand or intrastrand bis-adducts, resulting in the bending of the DNA chains, which is believed to interfere with DNA repair and removal of Pt from its binding sites [42].

In recent years, a number of studies have provided a detailed understanding of the metabolism and mechanism of action of Pt drugs. Transformations of the drugs in body fluids and interaction with DNA have been the main focus of this research. The metabolism of drugs was shown to depend on the chemical form in which Pt is administered. Binding to proteins also plays a key role, both in blood and at the cell membrane. Once a drug metabolite enters the cell, it binds to DNA, thereby inhibiting its replication and preventing the proliferation of cancerous cells.

4.2 Gold in antiarthritis treatment

While the main medical application of gold is in dental restoration, gold-containing drugs have also been used for many years in the treatment of rheumatoid arthritis or chrysotherapy. The main drugs that are currently in use include myocrysin (aurothiomalate), solganol (aurothioglucose), sanocrysin (aurothiosulfate), allocrysin (aurothiopropanol sulfonate) and auranofin (triethylphosphinegold(I) tetraacetylthioglucose), which is a second-generation drug (Figure 2.15.1.3).

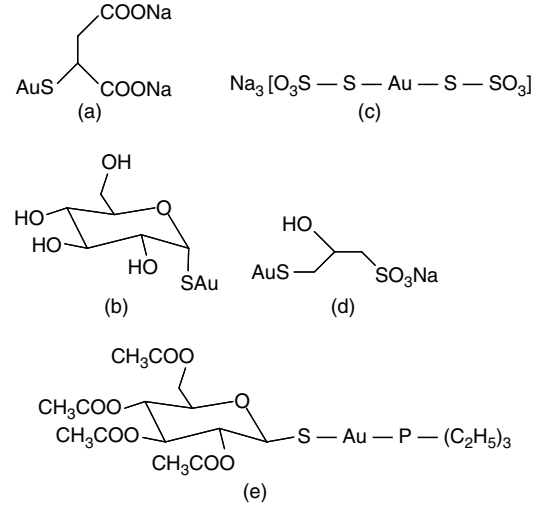

Figure 2.15.1.3. Structure of gold drugs. (a) Myocrysin, (b) solganol, (c) sanocrysin, (d) allocrysin and (e) auranofin.

The drugs are not effective for all patients treated and exert severe side effects. The determination of gold concentrations in biological fluids has demonstrated that the efficiency of drugs cannot be predicted solely from the knowledge of total concentrations [43]. Therefore, a number of studies have focused on the determination of the mechanisms of gold-based drugs through speciation analysis (Table 2.15.1.4).

The speciation of gold in the urine and blood of patients treated with auranofin, myocrysin or solganol has been performed by reversed-phase, ion pairing chromatography with ICP-MS detection and the drug metabolite dicyanogold(I) could be found in the urine and blood of some patients [14, 44]. The distribution of gold in blood and its speciation in the presence of red cells has been performed by flow injection-ICP-MS and LC-ICP-MS with ion pairing, reversed-phase and size-exclusion columns. The uptake of gold into red blood cells differs with patients. A significant amount of the gold in red cells was found to be associated with a high molecular mass protein (330 kDa). Low molecular species include dicyanogold(I), which enters the cells rapidly, possibly through the sulfhydryl channel with a loss of the cyanide group. Once in the cell, gold can recombine with other species. Goldgluthione may also occur in red cells [48]. The formation of dicyanogold(I) has also been investigated by ^{13}C NMR using ^{13}C-enriched cyanide. This study showed the formation of the intermediate complex $[Au(Stm)(CN)]^-$ [45].

^{13}C NMR studies have demonstrated that gold binds strongly to thiols with low pK_a values. Therefore, the blood protein albumin plays a major role as a gold transport site for gold transport in patients treated with antiarthritic drugs through binding to Cys34 [46]. ^{31}P NMR has also been used in the study of gold phosphine drugs, showing the release of PEt_3 [45]. In a recent study, the interaction of the antiarthritic complex $[AuPEt_3]^+$ with the protein cyclophilin-3 (cyp-3) has been investigated through LC-ESI-MS and X-ray crystallography. Gold was found to be associated with cyclophilin, with a molar ratio of 3.5:1 (Au:cyp-3). The interaction involves chloride displacement and $[AuPEt_3]^+$ binding to the protein followed by PET_3 displacement. Histidine imidazole rings in the protein were found to be the target site for $[AuPEt_3]^+$ through binding to a nitrogen atom. Histidine is an active site of the protein, which may be inhibited by gold [47].

While the mechanisms of action of gold-based drugs have not been clearly established, these studies have provided a better understanding of the metabolism of the drugs. It is believed that antiarthritic drugs act as prodrugs, providing gold to inflammation sites [48]. The drugs rapidly react with sulfur containing molecules, such as albumin and glutathione, although binding to nitrogen has also been observed [48]. Binding to albumin plays a key role in the transport of gold, which is dispersed in the blood to practically every tissue with a fraction excreted in urine. Although it is used in the treatment of rheumatoid arthritis, only a small amount is found in articular structures [49]. Metabolism of gold drugs also involves cyanide, a natural

Table 2.15.1.4. Speciation of gold in pharmaceutical and medical samples.

Investigation	Instrumental	Drug	Reference
Metabolites in blood and urine	LC-ICP-MS	Auranofin, solganol, myocrysin	[44]
Metabolites in urine	LC-ICP-MS	Auranofin, myocrysin	[14]
Red blood cells	LC-ICP-MS and SEC-ICP-MS	Myocrysin	[43]
Formation of dicyanogold	^{13}C NMR after interaction with ^{13}C-enriched cyanide	Myocrysin	[45]
Binding to blood albumin	^{13}C NMR and ^{31}P NMR	$[AuPEt_3]^+$	[46]
Interaction with cyclophilin-3	LC-ESI-MS and X-ray crystallography	$[AuPEt_3]^+$	[47]

metabolite of thiocyanate in the body, through the formation of dicyanogold(I), which is known to inhibit the oxidative bursting of cells present in the synovial fluid of patients with rheumatoid arthritis [47]. Therapeutic mechanisms at articular structures may involve scavenging of reactive oxygen species by the generation of gold(III) from gold(I), denaturation of proteins that enhance inflammation by gold(III) and interference with enzymes involved in antigen processing [49].

While gold speciation has been determined through techniques as diverse as LC-ICP-MS, NMR and X-ray crystallography, there is clearly a need for further speciation studies. Such studies would aid the development of gold-based drugs with increased efficiency and lower side effects.

5 REFERENCES

1. Wedepohl, K. H., *Geochim. Cosmochim. Acta*, **59**, 1217 (1995).
2. Alt, F. and Zereini, F. (Eds), *Anthropogenic Platinum Group Elements and their Impact on Man and the Environment*, Springer-Verlag, Berlin, 2000.
3. Rauch, S., Lu, M. and Morrison, G. M., *Environ. Sci. Technol.*, **35**, 595 (2001).
4. Rauch, S., Motelica-Heino, M., Morrison, G. M. and Donard, O. F. X., *J. Anal. At. Spectrom.*, **15**, 329 (2000).
5. Helmers, E. and Mergel, N., *Fresenius' J. Anal. Chem.*, **362**, 522 (1998).
6. Moldovan, M., Rauch, S., Morrison, G. M., Gomez, M. M. and Palacios, M. A., *Water Res.*, **35**, 4176 (2001).
7. Krachler, M., Alimonti, A., Petrucci, F., Irgolic, K. J., Forastiere, F. and Caroli, S., *Anal. Chim. Acta*, **363**, 1 (1998).
8. León, C., Emons, H., Ostapczuk, P. and Hoppstock, K., *Anal. Chim. Acta*, **356**, 99 (1997).
9. Lintern, M., Mann, A. and Longman, D., *Anal. Chim. Acta*, **209**, 193 (1988).
10. Koellensperger, G., Hann, S. and Stingeder, G., *J. Anal. At. Spectrom.*, **15**, 1553 (2000).
11. Lustig, S., Michalke, B., Beck, W. and Schramel, P., *Fresenius' J. Anal. Chem.*, **360**, 18 (1998).
12. Hann, S., Zenker, A., Galanski, M., Bereuter, T. L., Stingeder, G. and Keppler, B. K., *Fresenius' J. Anal. Chem.*, **370**, 581 (2001).
13. Szpunar, J., Makarov, A., Pieper, T., Keppler, B. K. and Lobinski, R., *Anal. Chim. Acta*, **387**, 135 (1999).
14. Zhao, Z., Jones, W. B., Tepperman, K., Dorsey, J. G. and Elder, R. C., *J. Pharm. Biomed. Anal.*, **10**, 279 (1992).
15. Hann, S., Kollensperger, G., Kanitsar, K. and Stingeder, G., *J. Anal. At. Spectrom.*, **16**, 1057 (2001).
16. Poon, G. K., Bisset, G. M. F. and Mistry, P., *J. Am. Chem. Soc. Mass Spectrom.*, **4**, 588 (1993).
17. Poon, G. K., Raynaud, F. I., Mistry, P., Odell, D. E., Barnard, C. F. J. and Murrer, B. A., *J. Chromatogr., A*, **712**, 61 (1995).
18. Warnke, U., Gysler, J., Hofte, B., Tjaden, U. R., Van der Greef, J., Kloft, C., Schunack, W. and Jaehde, U., *Electrophoresis*, **22**, 97 (2001).
19. Moldovan, M., Palacios, M. A., Gómez, M. M., Morrison, G. M., Rauch, S., McLeod, C., Ma, R., Caroli, S., Bocca, B., Schramel, P., Zischka, M., Pettersson, C. and Wass, U., *Sci. Total Environ.*, **296**, 199 (2002).
20. Schölg, R., Indlekofer, G. and Oelhafen, P., *Angew. Chem.*, **99**, 312 (1987).
21. Stenbom, B., Smedler, G., Nilsson, P. H., Lundgren, S. and Wirmark, G., *Thermal Deactivation of a Three-way Catalyst: Changes in Structural and Performance Properties*, Society of Automotive Engineers, Technical Paper Series No. 900273, 1990.
22. Moldovan, M., Rauch, S., Morrison, G. M., Gomez, M. M. and Palacios, M. A., *Surf. Interface Anal.*, **35**, 354 (2003).
23. Barbante, C., Veysseyre, A., Ferrari, C., Van de Velde, K., Morel, C., Capodaglio, G., Cescon, P., Scarponi, G. and Boutron, C., *Environ. Sci. Technol.*, **35**, 835 (2001).
24. Rauch, S., Morrison, G. M., Motelica-Heino, M. and Donard, O. F. X., Evaluation of speciation, transport and ecological risks of palladium, platinum and rhodium in urban stormwater systems, *Proceedings of the 8th International Conference on Urban Storm Drainage*, Vol. 1, Sydney, Australia; The Institution of Engineers, Sydney, Australia, 1999, pp. 202–209.
25. Hann, S., Koellensperger, G., Stefánka, Z., Stingeder, G., Fürhacker, M., Buchberger, W. and Mader, R. M., *J. Anal. At. Spectrom.*, **18**, 1391 (2003).
26. Rauch, S. and Morrison, G. M., *Sci. Total Environ.*, **235**, 261 (1999).
27. Linnett, P. J. and Hughes, E. G., *Occup. Environ. Med.*, **56**, 191 (1999).
28. Klueppel, D., Jakubowski, N., Messerschmidt, J., Stuewer, D. and Klockow, D., *J. Anal. At. Spectrom.*, **13**, 255 (1998).
29. Messerschmidt, J., Alt, F. and Tolg, G., *Electrophoresis*, **16**, 800 (1995).
30. Alt, F., Messerschmidt, J. and Weber, G., *Anal. Chim. Acta*, **359**, 65 (1998).
31. Lustig, S., Zang, S., Michalke, B., Schramel, P. and Beck, W., *Sci. Total Environ.*, **188**, 195 (1996).
32. Wei, C. and Morrison, G. M., *Anal. Chim. Acta*, **284**, 587 (1994).
33. Rauch, S., Morrison, G. M., Motelica-Heino, M., Donard, O. F. X. and Muris, M., *Environ. Sci. Technol.*, **34**, 3119 (2000).
34. Barefoot, R. R., *J. Chromatogr., B*, **751**, 205 (2001).
35. Barefoot, R. R. and Van Loon, J. C., *Anal. Chim. Acta*, **334**, 5 (1996).

36. Gerl, A. and Schierl, R., *Acta Oncol.*, **39**, 519 (2000).
37. Einhäuser, T. J., Galanski, M. and Keppler, B. K., *J. Anal. At. Spectrom.*, **11**, 747 (1996).
38. Cairns, W. R. L., Ebdon, L. and Hill, S. J., *Fresenius' J. Anal. Chem.*, **355**, 202 (1996).
39. Allardyce, C. S., Dyson, P. J., Abou-Shakra, F. R., Birtwistle, H. and Coffey, J., *Chem. Commun.*, (24), 2708 (2001).
40. Zenker, A., Galanski, M., Bereuter, T. L., Keppler, B. K. and Lindner, W., *J. Biol. Inorg. Chem.*, **5**, 498 (2000).
41. Zollner, P., Zenker, A., Galanski, M., Keppler, B. K. and Lindner, W., *J. Mass Spectrom.*, **36**, 742 (2001).
42. Hambley, T. W., *J. Chem. Soc., Dalton Trans.*, 2711 (2001).
43. Zhang, Y. F., Hess, E. V., Pryhuber, K. G., Dorsey, J. G., Tepperman, K. and Elder, R. C., *Inorg. Chim. Acta*, **229**, 271 (1995).
44. Elder, R. C., Zhao, Z., Zhang, Y. F., Dorsey, J. G., Hess, E. V. and Tepperman, K., *J. Rheumatol.*, **20**, 268 (1993).
45. Graham, G. G., Bales, J. R., Grootveld, M. C. and Sadler, P. J., *J. Inorg. Biochem.*, **25**, 163 (1985).
46. Isab, A. A. and Sadler, P. J., *J. Chem. Soc., Dalton Trans.*, 135 (1982).
47. Zou, J., Taylor, P., Dornan, J., Robinson, S. P., Walkinshaw, M. D. and Sadler, P. J., *Angew. Chem., Int. Ed.*, **39**, 2931 (2000).
48. Berners-Price, S. J. and Sadler, P. J., *Coord. Chem. Rev.*, **151**, 1 (1996).
49. Merchant, B., *Biologicals*, **26**, 49 (1998).

2.15.2 Speciation of Platinum Group Elements and Gold in Occupational Exposure

Olle Nygren

National Institute for Working Life, NIWL North – Work and the Physical Environment, Umeå, Sweden

1 INTRODUCTION

This chapter deals with the platinum group elements (PGEs) and gold (Au) from an occupational hygiene perspective. PGEs and Au all exhibit unique properties that have given these elements a significant anthropogenic use. They will consequently occur in various work environments and may cause undesired and possibly hazardous occupational exposure to various groups of workers.

PGEs all belong to groups 8–10 in the periodic system and are divided into two subgroups, 'light' and 'heavy' PGEs. In the light PGE subgroup, ruthenium (Ru), rhodium (Rh) and palladium (Pd) are found, and in the heavy PGE subgroup osmium (Os), iridium (Ir) and platinum (Pt) are found. Gold (Au) belongs to group 11 in the periodic system.

Gold (Au) and the PGEs are elements with relatively inert properties in their elemental state. They are widely distributed but rare in the earth crust, for example, Pt that has the highest abundance is only about 10^{-7}% [1–2].

Of the PGEs, primarily Rh, Pd, and Pt have, together with Au, gained significant anthropogenic use [1]. There are three major categories of sources for occupational exposure: mining, refining and processing. These elements can therefore be expected to be present in various work environments, and undesired exposure to these elements may, consequently, occur.

A number of criteria that serve as a basis for environmental and occupational standards have been produced during the last 15-year period [2–6]. There is, however, very limited information on speciation methods used for the assessment of occupational exposure to PGEs and Au.

Handbook of Elemental Speciation II: Species in the Environment, Food, Medicine & Occupational Health
Edited by R. Cornelis, H. Crews, J. Caruso and K. G. Heumann
 ISBN: 0-470-85598-3 (HB)

2 ANALYTICAL METHODS FOR THE ELEMENTS

2.1 Platinum

Occupational exposure to platinum has primarily been regarded as an aerosol exposure. Traditional aerosol sampling, personal or static, has been employed followed by Pt determination using graphite furnace atomic absorption spectrometry (GFAAS) [3], inductively coupled plasma atomic emission spectrometry (ICP-AES) [7], flame atomic absorption spectrometry (FAAS) [8]. During later years, inductively coupled plasma mass spectrometry (ICP-MS), an analytical technique with a low detection limit, has been employed for the Pt determination of aerosol samples from workplace atmospheres [3, 4]. Adsorptive cathodic stripping voltammetry (ACSV) has also been employed for determination for the same purpose [9].

For the determination of Pt in biological samples, a variety of methods have been applied [2, 10]. Most of these methods, however, lack in sensitivity for analysis of Pt in samples from exposed workers. More sensitive analytical techniques have been introduced during the past 10 years. ACSV [9, 11, 12] and ICP-MS [13–15] are the most widely accepted techniques for determination of Pt in blood and urine samples from exposed workers.

2.2 PGEs

The analytical methods used for studies of Pd and Rh are primarily atomic absorption spectrometry (AAS) and ICP-AES [16–18], ICP-MS [19], X-Ray fluorescence (XRF) [20], high performance liquid chromatography (HPLC) with ultraviolet (UV) detection [21], and neutron activation analysis (NAA) [22–24]. Pd cannot be analyzed by ACSV. Rh can be determined simultaneously with Pt using ACSV [11].

2.3 Gold

Today, the predominant analytical method used for studies of Au in biological materials is ICP-MS [21, 25]. Other methods used are NAA [22–24] and XRF [20].

3 PLATINUM

3.1 Anthropogenic use

Pt in alloys with Pd and Rh is widely used in the oil industry for upgrading petrol octane rate as well as in the chemical industry, for example, for production of nitric acid [2, 26, 27]. Pt-impregnated porous ceramics are used for exhaust gas control [27]. The resistance of Pt to various types of corrosion and to temperature is another important property. Pt is therefore often alloyed with other PGEs or base metals and used as contacts in electrical circuits and for other applications in electronic products and electrochemical industrial processes [2]. Some Pt alloys are used in dentistry, surgical tools and in implants. Well-known is the widespread use of Pt in jewelry [4, 26].

Pt salts play an important role in the manufacturing of catalysts. They also find applications in photography. Hexachloroplatinic(IV) acid is one of the most important precursors for the production of catalysts and other Pt compounds and products [2, 4]. Platinum electrodeposition can be achieved from a number of platinum salts. Recycling of products is a secondary source for Pt in the work environment.

The use of Pt has increased during the past 25 years because of the introduction of catalytic converters in automobile exhaust systems [4]. Whereas today this is the dominating field of application, in the past the major share of Pt was used as catalyst in the chemical and petrochemical industries. In Sweden, the largest amount of Pt is still used in the petrochemical industry [28].

Some specific amine complexes with platinum are the active component in anticancer drugs as described in the previous chapter by Rauch *et al.*

3.2 Occupational exposure measurements

In mining operations, Pt is usually found in the insoluble form as metal or in very insoluble

mineral compounds [29]. In case of occupational exposure, other sources are of great concern, for example, dust and exhausts.

In a Pt production operation, especially in the final steps of the refining, the major occupational exposure is to soluble Pt salts where chloroplatinic acids, complexes and salts (e.g. ammonium and sodium hexa- and tetrachloroplatinate) dominate [2, 30]. Soluble Pt salts are highly sensitizing and have been reported to cause respiratory allergic problems and skin reactions [2]. Asthma, rhinoconjunctivitis and contact urticaria are examples of symptoms among workers in noble metal refineries and catalyst production [31, 32]. A variety of other symptoms have been described, for example, lacrimation, sneezing, coughing, tightness of the chest, wheezing, shortness of breath, angioedema and eczematous skin lesions [2]. Usually, sensitization develops within 12 months but can occur within 10 days or be delayed up to 25 years. The sensitivity is considered to be allergic and not toxic or irritant because there is a period of exposure without symptoms, only a fraction of all those exposed becoming sensitized. Affected subjects are sensitive to extremely small amounts of the Pt salt [33].

Specific exposure to hexachloroplatinic(IV) acid may occur during production of automotive exhaust catalysts [2, 29, 34, 35]. Exposure to Pt salts and hexachloroplatinic(IV) acid has also been monitored during manufacturing of emission control systems and catalysts for fertilizers as well as during plating and photography and in laboratory work [2, 33, 36–40].

Urinary excretion of Pt from Pt industry workers and students exposed to powdered Pt compounds showed that occupational exposure does occur, but as individuals with dental gold fillings also have slightly higher Pt excretion, the monitoring is not unequivocally traceable to the occupational exposure. Use of protective masks significantly reduces the exposure [41, 42]. Urinary Pt has been determined in samples from dental technicians and road construction workers. The results showed significantly higher Pt values in the dental technicians. The road construction workers had similar values as a control group of urban residents [43]. Outside contractors specialized in handling catalysts (e.g. loading, unloading and sieving) have been shown to be exposed above the current OEL (Occupational Exposure Limit) in many cases [17]. Lindell [2] presents a summary of workplace air concentrations of Pt in various work environments (Table 7, p. 11). The reported concentrations vary significantly among different reports and industrial processes.

In South Africa, sensitization to Pt in refinery workers was investigated. The skin prick test and the radioallergosorbent test were developed to detect sensitivity to Pt. Among 306 workers, 38 tested positive. The total immunoglobulin E (IgE) level was raised in 63% of the workers showing a positive Pt salt skin prick test compared with only 16% in the negative skin prick test group [44]. In the platinum industry in the United Kingdom, respiratory sensitization among workers has been reported despite the fact that the 8-h time weighted average (TWA) value never exceeded the OEL. Short-term high exposure levels were suggested as a plausible cause, but measurements at three sites did not show significant high exposure levels during short-term worst-case situations [13]. The effect of transferring workers with occupational asthma after exposure to Pt salts to low exposure areas has also been investigated [45]. Pt refinery workers who also are smokers have about an eight times higher risk to be sensitized to Pt salts than nonsmokers [46].

Besides reports of occupational exposure during production of automotive catalytic converters [13, 38], there are only a few reports on occupational exposure to Pt from exhaust emissions or handling catalytic converters during maintenance or recycling [13]. Merget *et al*. [32] and Rosner *et al*. [47] have, however, made some risk evaluations of the exposure to PGEs emitted from automotive catalytic converters. Their calculations point out a no-effect level (NOEL) of 1.5 $\mathrm{ng\,m^{-3}}$. The level of Pt in urban ambient air is significantly lower [42]. Therefore, it is considered unlikely that the exposure of workers in environments with dense traffic exceeds the suggested NOEL.

The use of Cisplatin and other Pt-containing anticancer drugs is increasing, and occupational

exposure can be expected among medical staff. There are a number of general studies on occupational exposure to anticancer drugs [48, 49]. These and similar studies do not distinguish among different anticancer drugs. Specific studies on occupational exposure to Pt-containing drugs are not equally common. Airborne exposure has been studied in Sweden [9], while measurable urinary excretion has been reported in several studies [50–52]. Measurable blood levels have also been reported [9, 51]. The presence of elevated Pt levels in samples from medical workers indicates that exposure to Pt anticancer drugs does occur. These reports have caused concern among medical staff in many countries [53], and various technical equipment (e.g. closed drug preparation and administration systems) and ventilation devices (e.g. biological safety cabinets) have been designed and implemented to reduce possible exposure. These measures are aimed at decreasing the exposure to all anticancer drugs, including Cisplatin and similar drugs, but their efficiency may have been evaluated using other drugs as markers [54–56]. Methods to test possible spill and leakage from drug preparation systems have been developed [55, 57]. The effectiveness of various protective gloves has been investigated for a number of anticancer drugs including Cisplatin [58, 59], and the recommendation is to change gloves every 30 min or when visible spill occur. Various handling regulations and guidelines, as well as practical measures and advice, to improve working routines and drug handling and administration procedures have also been developed to decrease possible exposure [60–62]. There have, however, been problems to introduce such protective measures because of apprehension among staff to use extensive protective clothing. The reason claimed is that it could impair the contact with the patients [63]. There has also been concern that some anticancer drugs may be vaporized and that airborne exposure to gaseous compounds may occur [64]. Cisplatin and similar compound have, however, a low vapor pressure and are not expected to be present in vapor phase in the workplace atmosphere. Another source of exposure to Cisplatin and other drugs could be contamination of the drug vials during the manufacturing process. Contaminated drug vials have also been found [65, 66].

Although there are several studies on Pt background levels in the general population and on occupational exposure in various work environments, there is still a need for research to distinguish between different exposure sources, for example, inorganic Pt salts and organic Pt complexes used in anticancer drugs. These Pt compounds have different health effects, and methods for speciation would improve the assessment of occupational exposure to the various Pt compounds.

4 PALLADIUM AND RHODIUM

4.1 Anthropogenic use

Pd and Rh are primarily used because of their catalytic properties and their chemical resistance. They are utilized alone or more frequently in combination with Pt, in alloys with Pt or in combination with other base metals [1, 2]. Some examples can be found in their application for production of sulfuric acid [26, 27], for catalytic increase of the petrol octane rate [26, 27] and for exhaust-gas control [27]. Over the years, Pd has been the cheapest PGE and has therefore been used for budget price Pt-like jewelry [1] and recently as replacement of Pt in catalytic converters [32]. Pd in alloys with Au is also used in dentistry [1]. The lower price of Pd and comparable properties also makes Pd a useful substitute for Au. Pd alloys with nickel and silver are used in the electronic industry. Plating with Pd can be made using several low-temperature processes, which are suitable for electronic products [67]. Electrolytic plating with Rh is used in the electronic industry for applications requiring hard, durable layers with low conductivity or layers with high reflectivity, for example, headlight reflectors and technical mirrors. Rh is also used in alloy with Pt in bimetallic thermal sensors [1].

4.2 Occupational exposure measurements

In contrast to the situation for Pt, only a limited number of studies on Pd and Rh can be

found in the literature. Studies of Pd and Rh exposure in the occupational environment and for biological control of exposed workers are lacking almost completely.

Pt appears to be the PGE with the strongest respiratory sensitizing property [68]. Pd can cause skin contacts dermatitis, which is in direct contrast to Pt. This cannot, however, be extrapolated to the respiratory sensitizing potential of Pd and its salts. Immediate-type of sensitization to Pd only occurred in workers already sensitized to Pt and there were only limited cross-reactions between both elements [32]. In South Africa, sensitizing of Pt refinery workers was investigated. Skin prick and radioallergosorbent tests were made to detect sensitivity to Pd and Rh. Among 306 workers tested, none showed isolated positive response to Pd or Rh. Among workers testing positive to Pt, a few also showed a positive response for Pd and Rh [44].

The National Institute for Occupational Safety and Health (NIOSH) has made an evaluation concerning dermatitis and hoarseness among workers in screener stacker areas. A significant health hazard existed, since 20 workers out of 36 had work-related dermatitis [16]. There is also a significant diversity of the immune response between Pt and Pd salts [69].

Only a few reports on Pd urinary levels in exposed workers have been found. Philippeit *et al*. [21] analyzed spot urine samples from 10 subjects occupationally exposed to Pd and found levels in the range $<10–2538\ \mathrm{ng\,L^{-1}}$, while unexposed subjects were in the range $<10–28\ \mathrm{ng\,L^{-1}}$ ($n = 44$). In another study, urine samples from workers in a catalyst recycling facility were determined for Pd and Au. The Pd level found was in the range $200–1000\ \mathrm{ng\,L^{-1}}$ ($n = 7$), while five nonexposed subjects were below the detection limit $<2.5\ \mathrm{ng\,L^{-1}}$ [20]. In a third study, urine samples from 12 exposed subjects were in the range $<80–3400\ \mathrm{ng\,L^{-1}}$ [18]. Urinary Pd has also been determined in samples from dental technicians and road construction workers. The result showed significantly higher Pd values in the dental technicians as compared to a control group of urban residents. The road construction workers showed a tendency to have higher Pd values as compared to the control group [43]. No studies of Rh in urine from exposed workers or of airborne Pd or Rh levels in workplace atmospheres have been found.

The lack of reports regarding occupational exposure to Pd and Rh clearly demonstrates the need for further research on this issue. Increasing use of Pd in automotive catalytic converters will continuously increase the use and emission of Pd, which, in due time, will increase the number of occupationally exposed groups. The significantly different health effects of Pd compared to other PGEs, that is, that elemental Pd can cause contact dermatitis, is another motive for additional research. Development of methods to monitor skin exposure would be valuable tools for the assessment of occupational exposure. Additionally, methods for PGE speciation analysis could be of paramount importance to reveal different exposure routes.

5 GOLD

5.1 Anthropogenic use

Au in jewelry is normally alloyed with other metals to obtain increased hardness, copper being most commonly used, followed by nickel, silver and Pd. To give an example, Pd is alloyed with Au to produce ‘white gold’ [1]. Esthetic plating of, for example, porcelain and glass is made by thermal decomposition of a gold compound. Gilding of wood, leather and plaster is made using gold foil. The inertness to oxidation has made Au a useful metal to plate onto contacts and other components in the electronic industry [1]. Au plating can be done both electrolytically and electrodeless for electronic applications. For some purposes, a cyanide-free plating bath can be used and this is a promising new plating technique [70]. A large amount of gold is also utilized in dentistry mostly alloyed with copper, but also with silver, nickel and PGEs [1].

In medicine, Au compounds have gained significant importance since the 1920s for the treatment of primarily progressive polyarticular rheumatoid

arthritis. The predominant compounds used are aurothiomalate, aurothioglucose and aurothiosulfate. Au therapy is also recommended for juvenile rheumatoid arthritis, psoriatic arthritis or ankylosing spondilitis [71]. Clinical properties and analytical considerations of Au drugs, besides occupational exposure, are discussed elsewhere in this book.

5.2 Occupational exposure measurement

The largest production fields of gold today are situated in developing countries in the southern half of Africa and in remote areas in South America, Australia and Canada. The work environment and refining facilities are very poor in many of these mining areas. Occupational exposure to hazardous compounds is common. Exposure to Au is not the most important issue. During refining, Au is amalgamated with mercury followed by cyanide leaching [1]. Exposure to mercury and cyanide among gold refinery workers is well known [72–76]. Tuberculosis and silicosis are other frequent occupational diseases among gold miners in developing countries [77].

There are, however, only very few reports on occupational exposure to Au. In Italy studies on goldsmith workers have been carried out. Hair from goldsmiths were analyzed for a number of metals. In one of the studies, goldsmiths from three different areas in Italy were investigated and the results showed increased levels of Au as well as silver, copper and indium in the goldsmiths' hair as compared to unexposed controls [25]. In the other study, an investigation was carried out on goldsmiths in the Rome area, and the results showed only increased Au level in the goldsmiths' hair [78]. In gold casting processes, occupational exposure to silver has been reported [79, 80]. Art pottery can be another source for occupational exposure to Au, among many other elements. In British Columbia a study was carried out in 50 sites. The results showed that the airborne levels of Au were well below the OEL at all sites [81]. Urinary Au has also been determined in samples from dental technicians and road construction workers. The result showed significantly higher Au values in the dental technicians as compared to a control group of urban residents. The road construction workers showed a tendency to have higher Au values as compared to the control group [43]. Individuals with many dental gold fillings will have an increased urinary Au level [82], which may affect occupational assessment. A health evaluation report from NIOSH describes a case where three workers got retinal detachment after welding noble metal alloys. It was concluded that there was no relation between the disease and exposure to Au or Pt [83].

Occupational exposure to drugs has so far been focused primarily on anticancer drugs and to some extent on antibiotics. No reports of occupational exposure to gold drugs have been found. Gold drugs are, however, known to induce autoimmunity in treated patients as well as renal lesions. A number of symptoms can occur, such as skin eruptions, proteinuria, leukopenia and trombocytopenia [71]. Hazardous exposure among medical staff can therefore not be excluded.

In gold mining and refining, it appears that there are other chemicals that dominate hazardous exposure. Attempts to find alternative leaching procedures to exclude hazardous cyanide leaching are in progress [84, 85]. Continuous research is needed to document the effects of these new leaching procedures. There is also evidently a need for further research on exposure to gold drugs and possible auto-immunological effects in exposed workers. Speciation methods would be useful tools to assess and distinguish occupational exposure to Au drugs from that of other Au sources, for example, dental fillings.

6 REFERENCES

1. Hägg, G., *Allmän och Oorganisk Kemi*, Almqvist & Wiksell, Stockholm, 1963, p. 422 (In Swedish).
2. Lindell, B., *Arbete & Hälsa*, Vol. 4, Arbetslivsinstitutet, Solna, 1997.
3. HSE, *Platinum Metal & Soluble Platinum Salts. Criteria for an Occupational Exposure Limit*, Health and Safety Executive, Sudbury, 1996.
4. IPCS, *Environmental Health Criteria No. 125, Platinum*, World Health Organization, Geneva, 1991.

5. Jakubowski, M., *Podstawy i Metody Oceny Srodowiska Pracy*, **18**, 153 (2002).
6. Sakurai, H., *J. Occup. Health*, **42**, 213 (2000).
7. NIOSH, Method 7300. Elements by ICP, *NIOSH Manual of Analytical Methods*, 4th ed., US Department of Health and Human Services, Washington, DC, 1996.
8. OSHA, Method ID 121. Metal and metalloid particulates in workplace atmospheres, *OSHA Analytical Methods Manual*, 2nd ed., US Department of Labor, Occupational Safety and Health Administration, Salt Lake City, Utah, 1991.
9. Nygren, O. and Lundgren, C., *Int. Arch. Occup. Environ. Health*, **70**, 209 (1997).
10. Nygren, O., Vaughan, G. T., Florence, M. T., Morrison, G. M. P., Warner, I. M. and Dale, L. S., *Anal. Chem.*, **62**, 1637 (1990).
11. León, C., Emons, H., Ostapczuk, P. and Hoppstock, K., *Anal. Chim. Acta*, **356**, 99 (1997).
12. Messerschmidt, J., Alt, F., Tölg, G., Angerer, J. and Schaller, K. H., *Fresenius' J. Anal. Chem.*, **343**, 391 (1992).
13. Maynard, A. D., Northage, C., Hemingway, M. and Bradley, S. D., *Ann. Occup. Hyg.*, **41**, 77 (1997).
14. Schramel, P., Wendler, I. and Angerer, J., *Int. Arch. Occup. Environ. Health*, **69**, 219 (1997).
15. Webster, P. J., Ng, K., Snitch, P., Jones, S. L., Amos, N. and Harnett, P. R., *J. Oncol. Pharm. Pract.*, **1**, 41 (1995).
16. Bernhard, B. P. and Hanley, K. W., *Health Hazard Evaluation*, Report HETA 91–0510177, AVX Corporation, Myrtle Beach, South Carolina. Gov. Rep. Announce Index 92-19. Abstr. No: 254203, NTIS Order No: PB92-193994, 1992.
17. Hery, M., Gerber, M., Hecht, G., Hubert, G., Elcabache, J. M. and Honnert, B., *Cahiers de Notes Documentaires*, **149**, 479 (1992).
18. Schuster, M., Schwarzer, M. and Risse, G., in *Emissionen von Platinametallen – Analytik, Umwelt und Gesundheitsrelevanz*, Zereini, F. and Alt, F. (Eds), Springer-Verlag, Berlin, 1999.
19. Rauch, S., Motelica-Heino, M., Morrison, G. M. and Donard, O. F. X., *J. Anal. At. Spectrom.*, **15**, 329 (2000).
20. Messerschmidt, J., von Bohlen, A., Alt, F. and Klockenkämper, R., *Analyst*, **125**, 397 (2000).
21. Philippeit, G. and Angerer, J., *J. Chromatogr., B*, **760**, 237 (2001).
22. Nicolaou, G., Pietra, R., Sabbioni, E., Mosconi, G., Cassina, G. and Seghizzi, P., *J. Trace Elem. Electrolytes Health Dis.*, **1**, 73 (1987).
23. Sabbioni, E., Pietra, R., Mousty, F., Colombo, F. and Scansetti, G., *J. Radioanal. Nucl. Chem.*, **110**, 595 (1987).
24. Tomza, U., Janicki, T. and Kossman, S., *Radiochem. Radioanal. Lett.*, **58**, 209 (1983).
25. Caroli, S., Senofonte, O., Violante, N., D'Ilio, S., Caimi, S., Chiodo, F. and Menditto, A., *Microchem. J.*, **59**, 32 (1998).
26. Beliles, R. P., Platinum group metals: platinum, Pt; palladium, Pd; iridium, Ir; osmium, Os; rhodium, Rh; ruthenium, Ru, in *Patty's Industrial Hygiene and Toxicology*, 4th ed., Clayton, G. D. and Clayton, F. E. (Eds.), John Wiley & Sons, New York, 1994.
27. NAS, *Platinum Group Metals*, EPA-600/1-77-040, National Research Council, NTIS PB-600/1-77-040, Washington, DC, 1977.
28. SCB website, http://www.scb.se, Statistics Sweden, Stockholm, 2002.
29. Johnson, N. P., Tillery, J. B. and Prevost, R. J., *Environ. Health Perspect.*, **10**, 151 (1975).
30. Baker, D. B., Gann, P. H., Brooks, S. M., Gallager, J. and Bernstein, I. L., *Am. J. Ind. Med.*, **18**, 653 (1990).
31. Merget, R., Occupational platinum salt allergy. Diagnosis, prognosis, prevention and therapy, in *Anthropogenic Platinum-Group Element Emissions*, Zereini, F. and Alt, F. (Eds.), Springer-Verlag, Berlin, 2000.
32. Merget, R. and Rosner, G., *Sci. Total Environ.*, **270**, 165 (2001).
33. Parkes, W. R. *Occupational Lung Disorders*, 2nd ed., Butterworths, London, 1982.
34. Bernstein, I. L. and Brooks, S. M., Metals, in *Asthma in the Workplace*, Bernstein, I. L., Chan-Yeung, M., Malo, J. L. and Bernstein, D. I. (Eds.), Marcel Dekker, New York, 1993.
35. Parrot, J. L., Herbert, R., Saindelle, A. and Ruff, F., *Arch. Environ. Health*, **19**, 685 (1969).
36. Baumgärtner, M. E. and Raub, C. J., *Platinum Metal Rev.*, **32**, 188 (1988).
37. Granlund, M., *Hexaklorplatinasyra och rodiumklorid vid tillverkning av katalysatorer*, Report from National Institute of Occupational Health, Umeå, 1991 (In Swedish).
38. Mastromatteo, E., *Encyclop. Occup. Health Saf.*, **2**, 1723 (1983).
39. Skinner, P. E., *Platinum Metal Rev.*, **33**, 102 (1989).
40. Woolf, A. D. and Ebert, T. H., *Clin. Toxicol.*, **29**, 467 (1991).
41. Schierl, R., Biomonitoring of platinum in urine in occupational medicine, in *Emission von Platinmetallen*, Zereini, F. and Alt, F. (Eds), Springer-Verlag, Berlin, 1999.
42. Schierl, R., *Microchem. J.*, **67**, 245 (2000).
43. Begerow, J., Sensen, U., Wiesmuller, G. A. and Dunemann, L., *Zentalbl. Hyg. Umweltmed.*, **202**, 411 (1999).
44. Murdoch, R. D., Pepys, J. and Hughes, E. G., *Br. J. Ind. Med.*, **43**, 37 (1986).
45. Merget, R., Schulte, A., Gebler, A., Breitstadt, R., Kulzer, R., Berndt, E.-D., Baur, X. and Schultze-Werninghaus, G., *Int. Arch. Occup. Environ. Health*, **72**, 33 (1999).
46. Calverley, A. E., Rees, D., Dowdeswell, R. J., Linnett, P. J. and Kielkowski, D., *Occup. Environ. Med.*, **52**, 661 (1995).
47. Rosner, G., Artelt, S., Mangelsdorf, I. and Merget, R., *Umweltmedizin in Forschung und Praxis*, **3**, 365 (1998).
48. Baker, E. S. and Connor, T. H., *Am. J. Health Syst. Pharm.*, **53**, 2713 (1996).

49. Bos, R. P. and Sessink, P. J. M., *Rev. Environ. Health*, **12**, 43 (1997).
50. Ensslin, A. S., Pethran, A., Schierl, R. and Fruhmann, G., *Int. Arch. Occup. Environ. Health*, **65**, 339 (1994).
51. Schaller, K. H., Angerer, J., Alt, F., Messerschmidt, J. and Weber, A., *Proc. SPIE-Int. Soc. Opt. Eng.* (International Conference on Monitoring of Toxic Chemicals and Biomarkers, 1992), **1716**, 498 (1993).
52. Venitt, S., Crofton-Sleigh, C., Hunt, J., Speechley, V. and Briggs, K., *Lancet*, **1**, 74 (1984).
53. Zellmer, W. A., *Am. J. Hosp. Pharm.*, **41**, 665 (1984).
54. Nygren, O., Gustavsson, B., Strom, L., Eriksson, R., Jarneborn, L. and Friberg, A., *J. Environ. Monitor.*, **4**, 739 (2002).
55. Sessink, P. J. M., Wittenhorst, B. C. J., Anzion, R. B. M. and Rob, R. P., *Arch. Environ. Health*, **52**, 240 (1997).
56. Sessink, P. J. M., Rolf, M.-A. E. and Rydèn, N. S., *Hosp. Pharm.*, **34**, 1311 (1999).
57. Nygren, O., Gustavsson, B. and Eriksson, R., *Int. Arch. Occup. Environ. Hyg.*, 2004, submitted.
58. Connor, T. H., *Am. J. Health Syst. Pharm.*, **56**, 2450 (1999).
59. Connor, T. H. and Xiang, Q., *J. Oncol. Pharm. Pract.*, **6**, 109 (2000).
60. Harrison, R. B., *Am. J. Hosp. Pharm.*, **38**, 1686 (1981).
61. Nygren, O., Cytotoxic drugs, in *ICOH Occupational Health in Medical Care*, Hasselhorn, H., Tomingas, A. and Lagerkvist, M. (Eds.), Elsevier, Amsterdam, 1999.
62. Valanis, B., Wollmer, W. M., Labuhn, K., Glass, A. and Corelle, C., *J. Occup. Med.*, **34**, 149 (1992).
63. Barhamond, B. A., *Cancer Nurs.*, **9**, 138 (1986).
64. Kiffmeyer, T. K., Kube, C., Opiolka, S., Schmidt, K. G., Schoppe, G. and Sessink, P. J. M., *Pharm. J.*, **268**, 331 (2002).
65. Kiffmeyer, Th. K., Ing, K. G. and Schoppe, G., *J. Oncol. Pharm. Pract.*, **6**, 13 (2000).
66. Nygren, O., Gustavsson, B., Ström, L. and Friberg, A., *Ann. Occup. Hyg.*, **46**, 555 (2002).
67. Abys, J. A., *Plating Surf. Finish.*, **87**, 57 (2000).
68. D'Amato, G., Cocco, G., Liccardi, G., Natale, M. R. and D'Urso, B., *Riforma Med.*, **95**, 79 (1980).
69. Biagini, R. E., Bernstein, I. L., Gallagher, J. S., Moorman, W. J., Brooks, S. and Gann, P. H., *J. Allergy Clin. Immunol.*, **76**, 794 (1985).
70. Okinaka, Y. and Hoshino, M., *Gold Bull.*, **31**, 3 (1998).
71. Bigazzi, P. E., *Environ. Health Prespect.*, **107**(Suppl. 5), 753 (1999).
72. Drake, P. L., Rojas, M., Reh, C. M., Mueller, C. A. and Jenkins, F. M., *Int. Arch. Occup. Environ. Health*, **74**, 206 (2001).
73. Jones, H., Robinson, T., Whitely, M. and Vernon, B., *Publ. Aust. Mining Metall.*, **2**, 101 (1990).
74. Ogola, J. S., Mitullah, W. V. and Omulo, M. A., *Environ. Geochem. Health*, **24**, 141 (2002).
75. Prokhorenkov, V. I. and Kolpakov, F. I., *Gig. Tr. Prof. Zabol.*, **12**, 44 (1978).
76. van Straaten, P., *Sci. Total Environ.*, **259**, 45 (2000).
77. Steen, T. W., Gyi, K. M., White, N. W., Gabosianelwe, T., Ludick, S., Mazonde, G. N., Mabongo, N., Ncube, M. and Monare, N., el al *Occup. Environ. Med.*, **54**, 19 (1997).
78. D'Ilio, S., Violante, N., Senofonte, O. and Caroli, S., *Microchem. J.*, **67**, 343 (2000).
79. Minoia, C., Oppezzo, M. C., Pozzoli, L., Catenacci, G. and Capodaglio, E., *G. Ital. Med. Lav.*, **7**, 65 (1985).
80. Minoia, C., Catenacci, G. and Oppezzo, M. C., Biological monitoring of silver exposure in gold casting process. *Occup. Environ. Chem. Hazards*, in *Proc Int Symp Biochem Cell Indices Hum Toxic Occup Environ Med*, Foa, V. (Ed.), Horwood, Chichester, 1987, pp. 349–354.
81. Hirtle, B., Teschke, K., Van Netten, C. and Brauer, M., *Am. Ind. Hyg. Assoc. J.*, **59**, 706 (1998).
82. Philippeit, G., Schramel, P. and Angerer, J., *Umweltmed. Forshung Praxis*, **5**, 167 (2000).
83. Watanabe, A. S., Moss, C. E., Leffingwell, S. S., Tharr, D. *Health Hazard Evaluation*, Report No. TA-80-023-865, Gov Rep Announce Index 83 (1983), 54. National Institute for Occupational Safety and Health, Cincinnati, OH, 1981.
84. Aylmore, M. G. and Muir, D. M., *Miner. Eng.*, **14**, 135 (2001).
85. Ritchie, I. M., Nicol, M. J. and Staunton, W. P., in *Proceedings of the Cyanide: Social, Industrial and Economic Aspects*, Young, C. A., Twidwell, L. G. and Anderson, C. G. (Eds), Minerals, Metals & Material Society, Warrendale, PA, 2001, pp. 427–440.

2.16 Speciation of Selenium

Peter C. Uden
University of Massachusetts, Amherst, Massachusetts, USA

1 INTRODUCTION

Selenium (Se) and its compounds are essential for animals and humans, but its physiological nature is ambivalent. It can cause disease by deficiency, but it is toxic at levels less than an order of magnitude above those required for health. Se is present in the environment and in biomaterials in inorganic and organic forms, and the need for analytical speciation is clear because the bioavailability and toxicity of an element depend on its binding form.

The discussion of selenium speciation has been divided for convenience into the focus areas of environmental selenium, nutrition and food aspects, and medical and biological speciation. However, there is much overlap and interaction among these fields, and coverage of chemical and analytical speciation is treated where it is most appropriate in the development of the discussion and should be cross-referenced by the reader.

2 SELENIUM IN THE ENVIRONMENT

There are no substantive deposits of elemental selenium, and it cannot economically be recovered from the earth directly. It usually occurs in the sulfide ores such as pyrite. Soils in the neighborhood of volcanoes tend to have enriched amounts

Handbook of Elemental Speciation II: Species in the Environment, Food, Medicine & Occupational Health
Edited by R. Cornelis, H. Crews, J. Caruso and K. G. Heumann
 ISBN: 0-470-85598-3 (HB)

of selenium. Selenium is strongly enriched in some coal deposits, being present as organoselenium compounds, chelated species, or as the adsorbed element. Selenium compounds are released to the air during the combustion of coal and petroleum fuels and during the smelting and refining of other metals. From 1987 to 1993, according to the Toxics Release Inventory, selenium releases to land and water in the United States of America totaled over 1 million lbs., of which about 99% were to the land. These releases were primarily from copper-smelting industries. An overview of selenium in agriculture and the environment, edited by Jacobs, contains extensive information on its geochemistry and occurrence, seleniferous environments, solubility, speciation and transformation of selenium in soils, bioaccumulation, and so on [1].

Selenate (SeO_4^{2-}) is thermodynamically stable in alkaline and well-oxidized environments. Selenates are very soluble and less strongly adsorbed than selenite (SeO_3^{2-}); they are easily leached from soils, transported to ground waters, and most readily taken up by plants [2]. Selenite occurs in mildly oxidizing neutral pH environments, salts being less soluble than selenates. It is strongly adsorbed by particles and may be reduced chemically or biochemically to elemental Se^0. Selenides (Se^{2-}) and selenium-enriched sulfides exist in reducing acidic environments but are very insoluble, resistant to oxidation, and unavailable to plant and animals. Selenium pollution of waters, sediments, and soils results from industrial activities. Oil refineries release significant amounts into coastal waters, and electric utilities produce contaminated aqueous discharges from the storage of coal, coal ash, landfill, and so on [3].

The toxicity of selenium depends on whether it is in the biologically active oxidized forms SeO_3^{2-} or SeO_4^{2-}. In alkaline soils and oxidizing conditions, selenium may be oxidized sufficiently to maintain the availability of biologically active forms and cause plant uptake of the metal to be increased. In acidic or neutral soils, it tends to remain relatively insoluble and the amount of biologically available selenium should steadily decrease. Comprehensive treatment of environmental selenium is available in the texts authored by Frankenberger *et al*. [4, 5].

It is known that selenium accumulates in living tissues. For example, the selenium content of human blood is about 200 $ng\,mL^{-1}$. This value is about 1000 times greater than the selenium found in surface waters. It is clear that the human body does accumulate or concentrate selenium with respect to the environmental levels of selenium. Selenium has been found in marine fish meal at levels of about 2 $\mu g\,g^{-1}$. This amount is around 50,000 times greater than the selenium found in seawater.

Selenium dioxide is the primary source of problems from industrial exposures since the dioxide forms selenious acid with water or sweat, and the acid is an irritant. Selenium compounds released during coal or petroleum combustion may be a significant source of exposure.

Biogeochemical cycling of selenium in aquatic systems involves geological erosion and anthropogenic influences to contribute to Se in seawater, mainly as selenite, Se(IV), and selenate, Se(VI), at levels below 1 $ng\,mL^{-1}$. It is considered to be incorporated as organoselenium compounds sequentially through phytoplankton and zooplankton, lower and higher vertebrates or can be recycled through microorganisms to Se(IV) and (VI), and also to Se(−II) as HSe^- and colloidal elemental Se(0) [2]. Such pathways are also postulated to involve biomethylation. The chemical and biochemical transformations involved require analytical identification and quantification of selenium species at the highest sensitivity possible. Natural selenium levels in soils vary widely from below 100 $ng\,g^{-1}$ to 10 $\mu g\,g^{-1}$ or above. Selenium volatilization contributes an estimated 6×10^6 kg Se per year to the atmosphere [3], being affected by selenium speciation, soil texture, soil water content, soil organic matter, and carbon source, temperature, and trace metals. Dimethyl selenide (DMSe) and dimethyl diselenide (DMDSe) have been proposed as primary Se carrier species [6]. The concentrations of Se in most plants and agricultural crops are below 1 $mg\,kg^{-1}$ dry mass, but plants belonging to the families *compositae, leguminosae, cruciferae*, and

allium, when grown in selenium-rich soils, may accumulate Se to concentrations of several thousands of mg kg^{-1} dry mass [7]. Hyperaccumulating plants such as *Brassica juncea* can also be used to remove selenium from contaminated soils by phytoremediation [8]. Bacterial remediation is also under current investigation, *Bacillus subtilis* being a substantive Se bioaccumulator [9].

D'Ulivo [10] lists different types of selenium species identified in the environment (Table 2.16.1), ranging from simple inorganic forms and methylated species to selenoamino acids, selenoenzymes, and selenium nucleic acids. Typical concentrations of selenium in solid phase samples of differing origin, such as sediments, soil, coal, plants, algae, and fish, range from ng g^{-1} to μg g^{-1} with levels to mg g^{-1} in highly seleniferous substrates.

Pyrzynska has reviewed the determination of selenium species in environmental samples [11]. Concentrations of selenite and selenate in environmental seawater, groundwater, and freshwater samples have been reported to range from sub-ng L^{-1} in pristine conditions to hundreds of ng L^{-1} in contaminated sources; organoselenium levels have been found with similar ranges. The selenium content of surface water is greatly influenced by pH, being high in acidic (pH < 3.0) and in alkaline waters (pH > 7.5). Traces of selenium ranging from 0.001 to 10 ng L^{-1} are found in drinking water. Concentrations of volatile organoselenium compounds such as DMSe and DMDSe in air samples have been reported at ng m^{-3} levels.

The provision of speciation information is needed for the following fields of environmental importance. The elucidation of biogeochemical transformations of selenium compounds, the identification of natural and anthropogenic compounds with beneficial or detrimental effects, improvement in species-defined environmental remediation, and increasing knowledge about suitable methods to prevent or decrease toxicoses in plants, animals, and humans.

The evaluation of selenium's ecotoxicity is complicated since Se exists in many chemical forms, each of which has a different bioavailability and ecotoxic potential. Insoluble forms, such as elemental Se, pose little threat because of their low bioavailability, but highly cytotoxic selenium species, such as selenocysteine, catalyze formation of free radicals and may be harmful at very low concentration [12]. Other species, such as selenomethionine, may present an ecotoxic threat, not by being directly cytotoxic [13]. The ecotoxicity of the Se pool changes, as it is bioaccumulated, metabolized, and transferred through the food chain [14, 15]. Living organisms are able to metabolize Se to different chemical species than those to which they were exposed, particularly organoselenium compounds. Organisms at higher trophic levels, such as birds, obtain most of their Se from eating lower trophic level organisms, so the chemical forms of Se to which they are primarily exposed may vary. The key to a mechanistic biochemical understanding of Se ecotoxicity lies in a more complete knowledge of the processes of biotransformation and accumulation of Se in the food chain [16, 17]. Thus, to evaluate Se ecotoxicity in a given ecosystem, the Se species present in different compartments of that ecosystem must be determined.

Table 2.16.1. Some selenium compounds in environmental and biological systems.

Inorganic species
Se^0 (element), selenide – Se(-II), selenate – SeO_4^{2-}, selenite – SeO_3^{2}
Simple organic and methylated species
Methylselenol (MeSeH), dimethylselenide (Me_2Se), dimethyldiselenide (Me_2Se_2)
Trimethylselenonium cation (Me_3Se^+), dimethylselenone (Me_2SeO_2),
Dimethylselenoxide (Me_2SeO), methylseleninic acid anion ($MeSe(O)O^-$)
Dimethylselenosulfide (MeSSeMe), selenourea ($Se{=}C(NH_2)_2$)
Amino acids and low molecular mass species
Selenomethionine, selenocysteine, selenocystine, Se-methylselenocysteine, selenocysteic acid,
Se-methylselenomethionine, selenomethionine selenoxide, selenocholine, selenobetaine
Other compounds
Selenoproteins, selenoenzymes, Se-metal metallothionines

2.1 Selenium phytoremediation

The removal of high concentrations of selenium from soils and waters is complicated, expensive

by conventional methods, and may produce large quantities of polluted sludges. Phytoremediation provides a viable environmental alternative [18]. Some plants with extensive root systems can scavenge large volumes of soil or water, removing selenium as Se anions. Thereafter, conversion may occur to volatile selenium species such as DMSe, which is 600 times less toxic than selenate, whence it is removed from the ecosystem (phytovolatilization) [19]. Rhizosphere microorganisms may also volatilize selenium species directly.

Evaluating the benefits and risks of Se phytoremediation requires the thorough speciation of Se forms in different compartments of the ecosystem. Depending on the species, organoselenium compounds may pose (1) an ecotoxic risk or (2) facilitate safe removal of Se through Se phytovolatilization. When plants are treated with organic forms of Se, such as SeMet, they produce substantially more volatile Se than if treated with inorganic forms [20]. Recent studies carried out by gas chromatography (GC) as sample introduction and inductively coupled plasma mass spectrometry (ICP-MS) detection have shown that Indian mustard treated with Se-methionine produced much higher concentrations of DMSe than those treated with Se(IV), Se(VI), or selenocyanate. This methodology also provided enough sensitivity to observe traces of DMDSe [21]. Thus, although free selenomethionine might be more toxic than selenate/selenite, it would be removed at a much faster rate from the ecosystem through plant or microbial volatilization.

2.2 Regulatory issues

Determination of the chemical forms of Se is highly important from a regulatory point of view, because Se is directly linked to devastation of wildlife. Regulators have difficulty in developing adequate regulatory policy with respect to Se, and levels in the environment are regulated on the basis of measurements of total Se, thus the total maximum daily load of Se entering grassland marshes and salt sloughs in California has been set at $2\ \mu g\,kg^{-1}$. This limit was recommended by the US Fish and Wildlife Service, whose work demonstrated that Se concentrations of $2.3–2.5\ \mu g\,kg^{-1}$ in the tissue of aquatic birds was correlated with impaired egg hatching and increased susceptibility to disease [22]. However, this regulation does not consider the chemical form of Se. In this example, the same concentration of Se present in different chemical forms in the water could lead to both different concentrations and different forms of Se in the birds' tissues, leading to varied toxic effects. Because of the different toxicities of the various Se forms, measurements of total Se in one component of the ecosystem do not accurately represent Se risk. In order to develop a better regulatory policy, the ability to speciate Se within different compartments of a Se-contaminated ecosystem is needed.

2.3 The importance of selenium speciation

The myriad of selenium species present in environmental and biological materials presents a great analytical challenge. Biologically, in contrast to metal-protein complexes, selenium is not bound by coordination but forms covalent C–Se and Se–S bonds. Species can be divided into two categories: enzyme products and gene products, although this distinction is not always complete. The former arises from enzymatic reactions such as reduction, methylation [23], and reactions leading to selenoamino acid synthesis. Selenium is incorporated into gene products, according to the UGA codon that encodes for the selenocysteinyl residue [24]. To elucidate the complexities of selenium chemistry, the determination of *total element*, although essential to determine element mass balance, provides insufficient information and must be accompanied by *speciation* of selenium compounds, as related to a mammalian biochemical cycle such as is shown above [25].

Selenomethionine can be incorporated into general body proteins in place of methionine because it readily acylates Met-tRNA. Alternatively, it can be converted through a transsulfuration mechanism to selenocysteine, which is in turn degraded to hydrogen selenide by the enzyme selenocysteine

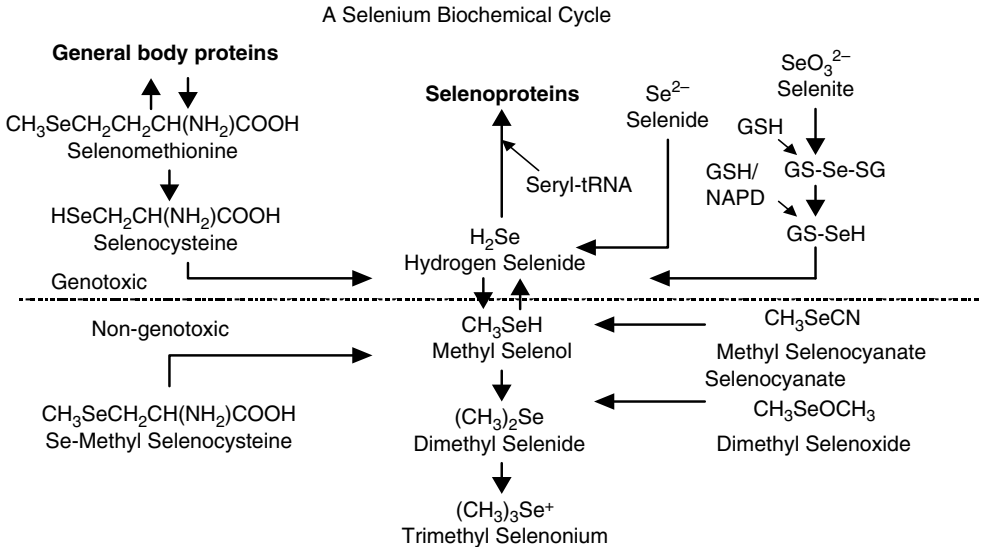

lyase. In contrast, selenite is metabolized to hydrogen selenide via selenodiglutathione. Hydrogen selenide is generally regarded as a precursor for supplying selenium in an active form to be inserted during the synthesis of selenoproteins such as glutathione peroxidase (GPX). The further metabolism of hydrogen selenide involves sequential methylation by S-adenosylmethionine to methylselenol, dimethylselenide, and trimethylselenonium ion [26].

Speciation of Se forms, especially organic Se, is needed, and some advances have been made in speciating Se in different compartments of certain ecosystems. These speciation analyses have been achieved using fractionation techniques [27] and by X-ray absorption spectroscopy (XAS) [28, 29]. Se has been speciated into selenate, selenite, elemental Se, and 'organic Se'. However, very little research has been done in speciating organic forms of Se present in environmental samples, where 'organic forms' include bio-forms such as amino acids and Se analogs of *S*-metabolites. Up to now, the composition and relative toxicities of the organic Se forms constitute an unknown 'black box', and a complete and precise description of the composition of organic Se pools in environmental samples (such as sediment, plant tissue, insects, etc.) has yet to be determined. In fact, many Se compounds in plant tissues have still to be identified [30]. Very few studies have even attempted a minimal speciation of organic Se in environmental samples and generally consider the toxicity of the pool to be equal to that of SeMet, a debatable assumption. Those few have either made a general speciation, combining all selenoamino acids [31], or have focused on only selenocysteine and selenomethionine [32]. Selenoamino acids comprise not just the protein amino acids, SeCys and SeMet, but also nonprotein amino acids such as Se-methylselenocysteine, for which there are no data on their toxicity [32]. Even SeCys and SeMet are thought to induce toxic effects through different mechanisms and to different extents [12]. As discussed above, the ecotoxicity of Se to wildlife depends not only on the level of exposure to total Se but also more specifically on the Se species within the food chain to which organisms are exposed.

3 FOODS AND NUTRITION

Much of the variation in the Se content of both animal- and vegetable-based foodstuffs is due to geographical differences in the amounts and availability of soil Se as transferred to the food chain. Selenium-deficiency diseases are recognized in parts of China and elsewhere, but soils rich

in Se (e.g. in excess of 5 mg kg^{-1}) are found in parts of the US (northern Great Plains, parts of the Southwest and California) and other regions. The Se present in most plant-derived foods, notably as selenomethionine (SeMet) and selenocysteine (SeCys) derivatives, tends to have reasonably good bioavailability. However, the Se in animal-derived foods has a wider range of bioavailability from low to moderate [33, 34] to high for beef, as assessed by its ability to increase liver concentrations and GPX activity [35].

Selenium was first recognized as being nutritionally significant in the late 1950s, when it was found to partially replace vitamin E in the diets of experimental animals [36]. It was not until the early 1970s that a discrete metabolic function was found for Se as an essential component of the enzyme GPX [37] that participates in the antioxidant protection of cells by reducing hydroperoxides. Several Se enzymes are now recognized, at least 5 GPX isoforms, three-iodothyronine 5′-deiodinases (DIs), three thioredoxin reductases (TRs), and selenophosphate synthetase [38]; and at least four other proteins are recognized as specifically incorporating Se, although their metabolic functions remain unclear. Plasma selenoprotein-P (SeP) [39], muscle selenoprotein W [40], and selenoproteins occur in prostate and placenta [38, 41]. Each of these proteins has been shown to contain Se in a highly specific form, selenocysteine (SeCys). The nutritional essentiality of Se appears to be due to formation of the active selenol group of such SeCys-proteins, antioxidant protection by the GPXs, energy metabolism affected by the DIs and redox regulation of transcriptional factors, and gene expression by the TRs.

Desirable Se dietary levels are in a relatively narrow range of consumption: food containing less than 0.1 mg kg^{-1} will result in deficiency, whereas levels above 1 mg kg^{-1} will lead to toxicity. While severe Se deficiency is recognized as being a risk factor for Keshan-type cardiomyopathy and Kaschin–Beck chondrodystrophy [33], there is evidence that less severe Se deficiency may predispose to goiter and myxedematous cretinism [42], as SeCys-containing deiodinases are essential for the metabolic production of thyroid hormone. The finding that Se deficiency in low-vitamin-E hosts can increase the virulence of RNA viruses [43] suggests that low Se status may increase risks to such RNA-viral diseases as measles, influenza, hepatitis, and AIDS. Se has also attracted attention for its apparent ability to ameliorate the toxicity of metals such as mercury and cadmium [44]. Recent interest in Se has focused on its role in the maintenance of low risk to cancer, relevant speciation studies being covered later [45].

Increasing attention has been paid to the speciation of Se in common foods. Plants metabolize inorganic Se anions, selenite, and selenate to generate selenoaminoacids such as selenomethionine, selenocysteine, selenocystathionine, and methylselenocysteine. Gluten hydrolysate of high-Se wheat comprised half of selenium as selenomethionine [46] as did soybean lectin [47] and soybean whey [48]. The *allium* family whose sulfur chemistry is well-defined exhibit parallel selenium chemistry, and high-selenium garlic has found promise in mammary cancer prevention [49]. Animal tissues contain selenocysteine as a constituent of selenoproteins. Beef is the single greatest dietary source of Se for North Americans; concentrations varying with Se content of soil and forage and may potentially be a means of supplying extra dietary Se. The Se content of beef from a moderately seleniferous area averaged 0.7 μg Se/g and thus a 100-g serving would supply more than the recommended daily nutritional requirement of Se [50]. An ion-exchange HPLC-IC-PMS study of Se speciation in cooked cod (total Se 1.52 μg Se/g) showed ca 12% of Se as selenite, but the remainder consisted of unidentified organoselenium species [51]. Since animal Se deficiencies are typically treated by dietary supplementation with sulfur-containing amino acids and because *Allium* and *Brassica* spp. are rich sources of such amino acids, the presence of related selenoamino acids in both natural and Se-enriched plants is predictable. Se speciation for garlic (*Allium Sativum*) and broccoli (*Brassica oleracea botrytis*) [52] employing ethylchloroformate derivatization and Se-specific detection

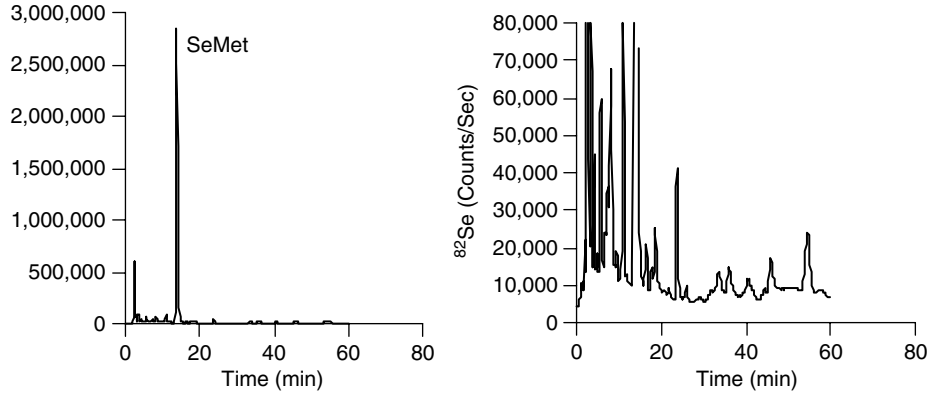

Figure 2.16.1. Se-specific HPLC-ICP-MS chromatograms of enzymatic hydrolysis products of 1250 mg kg^{-1} Se-enriched yeast using 0.1% HFBA ion-pairing agent (right scale expanded).

by GC with atomic emission detection showed Se-methylselenocysteine predominated with some selenocysteine present [53].

At present, no Se-enriched food or nutritional supplements have been fully characterized with respect to Se compounds. This is of great importance since, with no standard of product identity, many different materials may be designated 'Se-enriched' although they contain unknown amounts of different forms of Se that differ in both biopotency and/or anticarcinogenic potential. A widely available selenium supplement is 'selenized yeast', which has been employed in a number of human nutritional clinical trials [54]. There is evidence that the pattern of Se compounds in different Se-enriched products varies substantially. Only those made with active yeasts cultured for at least some fermentation contain selenomethionine, γ-glutamyl Se-methyl selenocysteine and Se-adenosylselenohomocysteine and perhaps other compounds with methyl-Se bonds such as Se-methylselenocysteine, and methylselenides $[CH_3]SeR$, arguably the most directly anticarcinogenic of the known Se-metabolites. As with any speciation analysis of natural materials, the target species must be extracted without modification of their chemical forms or disturbance of the equilibrium between the various species present. Extensive studies of sample preparation and separation approaches have shown that speciation results depend critically on the sample preparation procedure used [55]. Different yeast preparations have been found to contain organically bound Se in a range from 0 to 97% of total Se, with some showing only a few Se species and others containing more than 20 different selenium compounds [56, 57]. Figure 2.16.1 shows Se-specific HPLC-ICP-MS chromatograms of enzymatic hydrolysis products of 1250 mg kg^{-1} Se yeast using 0.1% heptafluorobutanoic acid (HFBA) ion-pairing agent (right scale expanded).

Reliable speciation analysis also mandates evaluation of the stability of target species. Stability studies performed on lyophilized oysters gave important information to ensure adequate transport and storage conditions without loss in total selenium and selenium species concentrations [58]. Total Se, trimethylselenonium, and selenomethionine were stable in freeze-dried samples for at least one year at 20 °C in polyethylene or Pyrex containers. Other recent speciation studies on selenized yeast are discussed later [59–66].

4 BIOLOGY AND MEDICINE

The essential metabolic need for selenium has as its basis formation of the active selenol group (–SeH) center of GPX, thioredoxin reductase, and of other selenoenzymes [67, 68]. Cancer chemoprevention is associated with inorganic selenium

salts, selenoaminoacids, and other organoselenium compounds. Monomethylated forms of selenium such as methylselenol (CH_3SeH) are thought to be important chemopreventive selenium metabolites [26]. Many epidemiological studies have pointed to an inverse association of Se status and risk to at least some cancers [45, 69]. Most animal studies have shown that supranutritional levels of various Se compounds can reduce the yields of tumors caused by chemical or viral carcinogens [45, 69–71]. Of the more than 200 relevant studies, most showed reduction in tumor incidence, with half reporting reductions of at least 50% and few found Se ineffective. Supplemental Se has been found to promote cellular phenomena thought to be anticarcinogenic, to support cellular redox regulation via GPXs and TRs, to enhance immune functions, to increase carcinogen metabolism, to promote apoptotic responses [72], and to inhibit angiogenesis (blood-vessel formation) in mammary cancer [73].

Clinical intervention trials in the United States of America [54, 73, 74] and China have shown lower cancer risks among subjects taking Se supplements compared to controls. In a multicenter, double-blind, randomized, placebo-controlled study performed in eastern United States, a total of 1312 older Americans with histories of basal or squamous cell carcinomas of the skin were randomized to dietary supplement of Se-enriched yeast (200 μg Se/day) or placebo [54]. After over six years of follow-up, Se-treatment did not affect risk to recurrent skin cancers in this high-risk cohort, but subjects taking supplemental Se had lower incidences of total cancer, specifically cancers of the lung colon-rectum and prostate and overall cancer mortality. That these reductions were seen after relatively short periods of Se supplementation and that fewer prostate cancer cases occurred in each year of the trial [74] suggests that Se is effective in the latter stages of carcinogenesis.

Evidence suggests that antitumorigenic activities can be supported by metabolites of forms of the element that naturally occur in foods: the Se-amino acids, SeMet and SeCys, and methylated Se-compounds such as Se-methyl-SeCys. With varying efficiencies, these species can be converted to a number of Se-metabolites, including methylselenol (CH_3SeH), which appears to be a key antitumorigenic metabolite [75, 76]. These findings make the consideration of 'Se status' important in the maintenance of overall health. In so doing, they raise questions about the parameters by which Se status should be defined, and the values of those parameters that should be taken as appropriate for the maintenance of good health. If robust analytical methods can be devised to determine CH_3SeH and/or other critical Se-metabolites in accessible tissues, these would be valuable for monitoring the antitumorigenic efficacy of Se.

5 METHODS FOR SELENIUM SPECIATION

5.1 HPLC-techniques

For practical purposes, an instrumental method must be specific to a particular selenium species or the species must be separated in time or space prior to arriving at a selenium-specific detector. The first group of techniques includes, in particular, radioimmunological assays (RIA) for selenoproteins, which offer very low detection limits but require the proteins to be isolated in amounts sufficient for antibody production [77]. The second approach, using hyphenated techniques, is based on the coupling of an electrophoretic or chromatographic separation technique with an atomic spectrometric or other selenium-specific measurement [25]. This coupling may be off-line, for example, sodium dodecyl sulfate polyacrylamide gel electrophoresis (SDS-PAGE) with laser ablation dynamic reaction cell ICP-MS (LA-DRC-ICP-MS), or on-line, for example, HPLC-ICP-MS. Selenite or selenate anions, selenomethionine, and other selenoamino acids have often been used as model compounds in experimental development.

Selenium chemistry sometimes parallels sulfur chemistry, thus presenting considerable analytical challenges since selenium species are often present at 3 orders of magnitude below sulfur. There are, however, some major differences between their chemistries, particularly in redox behavior. Ionic, zwitterionic, and neutral selenium species

Table 2.16.2. Inorganic and organoselenium analytical target compounds.

Selenous acid, selenite	SeO_3^{2-}
Selenic acid, selenate	SeO_4^{2-}
Selenocyanate	$SeCN^-$
Methylseleninic acid anion	$MeSe(O)O^-$
Methylselenenic acid anion	$MeSeO^-$
Dimethylselenide	Me_2Se
Dimethyldiselenide	Me_2Se_2
Methylselenol	MeSeH
Trimethylselenonium cation	Me_3Se^+
Selenocysteine	$H_3N^+–CH(COO^-)–CH_2–SeH$
Selenocystine	$H_3N^+–CH(COO^-)–CH_2–Se–Se–CH_2–CH(COO^-)–NH_3^+$
Selenomethionine	$H_3N^+–CH(COO^-)–CH_2–CH_2–Se–Me$
Se-methylselenocysteine	$H_3N^+–CH(COO^-)–CH_2–Se–Me$
γ-glutamyl-Se-methylselenocysteine	$H_3N^+–CH(COO^-)–CH_2–CH_2–CO–NH–CH(COO^-)–CH_2–Se–Me$
Selenocystathionine	$H_3N^+–CH(COO^-)–CH_2–CH_2–Se–CH_2–CH(COO^-)–NH_3^+$
Selenohomocysteine	$H_3N^+–CH(COO^-)–CH_2–CH_2–SeH$
Se-adenosylselenohomocysteine	$NH_2CH(COOH)CH_2CH_2SeCH_2C_4H_5O_3C_5N_4–NH_2$

are all present in biological systems, but low-level determinations are very difficult. Table 2.16.2 shows some of the small selenium compounds that are of biological and clinical interest [78]. In the living body, Se is not coordinated but forms covalent C–Se bonds; major species in living organisms are listed in Table 2.16.3 [79]. Selenoproteins contain selenium in the form of selenocysteinyl residues; proteins that contain selenomethionyl residues are not formally classified as selenoproteins.

Analytical techniques for the determination of selenium species, including selenoproteins, have been reviewed [25, 78–80]. Many methods have only been applied to the commercially available standards, however, rather than address a specific biochemical problem.

Table 2.16.3. Selenium species in living organisms.

Selenium in proteins	
Selenoproteins	Selenocysteinyl residues (genetically encoded)
Se-containing proteins	Selenomethionyl residues
Nonprotein selenium species	
Inorganic selenium	Selenite (SeO_3^{2-}), selenate (SeO_4^{2-})
Methylated selenium	Monomethylselenol, dimethylselenide, trimethylselenonium ions
Selenoamino acids	Selenocystine, selenomethionine, Se-methylselenolcysteine, selenoglutathione (polypeptide)

The complexity of analyte matrixes and the typically low level of selenium compounds present even in enriched samples makes speciation a challenging task. The combination of separation processes with selenium-specific detection is a powerful approach. To function as an element specific detector, high sensitivity is mandatory, and mass spectrometry with an atmospheric pressure ionization source, such as the ICP, has been successful for high performance liquid chromatography (HPLC) detection [81, 82]. However, determination of selenium by ICP-MS has problems of moderate ionization efficiency and isobaric interferences that can be partially overcome with high-resolution mass spectrometers or dynamic reaction cell (DRC)/collision cell technology. Significant isotopic overlap from $^{40}Ar_2^+$ on the most abundant isotope ^{80}Se (49.6%) often necessitates monitoring the less abundant isotopes ^{82}Se (8.6%) or ^{77}Se (7.6%). However interelement isobaric interferences are less pronounced in HPLC-ICP-MS than when it is used for the determination of total selenium. The coupling of HPLC with ICP-MS is straightforward, but in reversed-phase HPLC, if the concentration of organic modifier exceeds 5%, a cooled spray chamber, auxiliary oxygen gas, and platinum sampler and skimmer cones are mandatory.

A typical material with a high concentration of selenium is selenium-enriched yeast with a selenium content of 1200 mg kg^{-1}. If a 250-mg sample is taken and dissolved in 5 mL of solution,

and target compounds are present at 10% of the total concentration, then prior to separation, the concentration of selenium in solution is 6 mg L^{-1}. If the separation procedure produces a dilution of 100, the concentration of material after separation is of the order of 60 μg L^{-1}. This aspect of analytical speciation, namely the low concentrations of the target species, represents a clear challenge; another comes from the need that sample pretreatment must not change the chemical forms of the target species, or must change them in a known and controllable fashion.

HPLC-ICP-MS for selenium speciation has been applied for size exclusion, ion exchange (cation and anion), and ion-interaction reversed phase. Size exclusion, also used in combination with affinity chromatography, has been mainly used for the determination of selenoproteins and studies of interactions of selenium with proteins in the body [83–86]. Ion-exchange and reversed-phase HPLC have often been reported for the separation of Se(IV), Se(VI), selenomethionine, and other selenoamino acids. Jakubowski *et al*. considered HPLC-ICP-MS interface factors in determining selenocystine, selenocystamine, selenomethionine, and selenoethionine in natural samples. They used a double-focusing magnetic sector field mass spectrometer to resolve isotopic interferences and obtained detection limits to 2 ng L^{-1} for selenocystine, speciating Se in herring gull eggs at these limits [87, 88].

5.1.1 HPLC modes for selenium speciation

Four HPLC modes have been employed for selenium speciation, reversed phase, paired ion reversed phase, ion exchange, and exclusion. Paired ion and ion exchange have been most widely adopted. Olivas *et al*. used a polymer-based reversed-phase column to separate selenocystine, selenomethionine, and trimethylselenonium cation, obtaining detection limits of ca 1 μg L^{-1} for each species, but chromatographic resolution was poor [89]. Anion exchange was used for speciation of *in vitro* gastrointestinal extracts of cooked cod by ICP-MS [51], but the degree of separation was strongly dependent on the pH of the mobile phase [82, 90, 91].

Pedersen and Larsen used a polymer-based strong anion-exchange column to resolve selenite, selenate, selenomethionine, and selenocystine at pH 8.5. They added 3% methanol to the mobile phase that enhanced the ICP-MS signal to give ca 1 μg L^{-1} detection limits for 100-μl injections [82]. Gammelgaard *et al*. determined selenite in human urine after selenomethionine supplementation, by anion-exchange chromatography on a Dionex AS11-HC column with 25 mM NaOH in 2% methanol mobile phase and ICP-MS detection. The concentration found ranged from 0.4 to 7.1 μg L^{-1}, while the total Se concentration was from 12.4 to 97.6 μg L^{-1} [92, 93]. It was clear that selenite did not contribute substantially to the total selenium concentration, and important selenium constituents of urine still remained unknown. Johansson *et al*. demonstrated assisted on-line species conversion hydride generation atomic absorption spectrometry (AAS) for quantitative selenium speciation analysis of selenate, selenite, selenomethionine, and selenocystine in the certified reference material (CRM) 402 and biological samples [94]. Emteborg *et al*. [91, 95] quantified selenium species in CRM by anion exchange with interfaced direction injection nebulization – inductively coupled plasma atomic emission spectrometry (ICP-AES) and graphite furnace AAS. An important advance in ICP-MS technique involved detection as ^{80}Se by a DRC MS method. Sloth and Larsen showed that the argon-dimer and other mass interferences at m/z 74, 76, 78 and 80 were reduced by as much as 5 orders of magnitude with methane as reactive cell gas [96]. Larsen *et al*. achieved the most comprehensive ion exchange separation of selenium species yet reported [97]; cations were separated on a cation-exchange column at pH 3 with a gradient of pyridinium formate, anions on an anion-exchange column at pH 8.5 with a TRIS salicylate mobile phase. Selenomethionine-Se-oxide was observed at a high level in selenized yeast and dimethylselenonium propionate (DMSeP) in an algal extract.

Many organoselenium compounds especially selenoamino acids are insufficiently hydrophobic to be retained and separated on C_8 and C_{18} reversed-phase stationary phases with salt-free

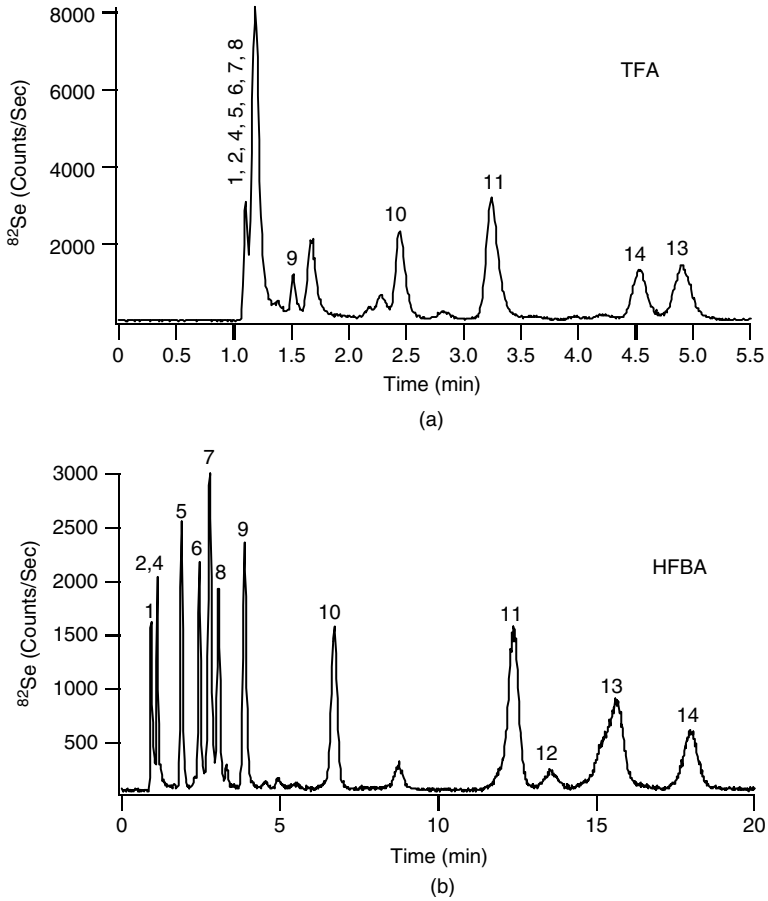

Figure 2.16.2. Se-specific HPLC-ICP-MS chromatograms using 0.1% TFA ion-pairing agent (a) and 0.1% HFBA ion-pairing agent (b) 1, selenous acid (selenite); 2, selenic acid (selenate); 4, methylseleninic acid (methylseleninate); 5, selenolanthionine; 6, trimethyl selenonium cation; 7, selenocystine; 8, selenocystathionine; 9, Se-methylselenocysteine; 10, Se-2-propylylselenocysteine; 11, selenomethionine; 12, unknown; 13, γ-glutamyl-Se-methylselenocysteine; 14, Se-allylselenocysteine. (Reprinted from *J. Chromatogr.,* 866, M. Kotrebai, J. F. Tyson, E. Block, P. C. Uden, "High-performance liquid chromatography of selenium compounds utilizing perfluorinated carboxylic acid ion-pairing agents and ICPMS and electrospray MS detection", 51–63, copyright (2000), with permission from Elsevier.)

aqueous mobile phases, but retention and separation is increased by using ion-pairing reagents such as trifluoroacetic acid (TFA) [81, 98] or octane sulfonic acid [59]. Perfluorinated carboxylic acids ion-pairing reagents afford better resolution and are advantageous for characterizing samples that contain many different classes of organoselenium compounds [56, 99–101]. TFA is a good general-purpose system but compromises between resolution and retention time. However, HFBA provides considerable resolution enhancement and allows separation of many additional organoselenium species including the *cis*-trans isomers of Se-1-propenyl-DL-selenocysteine; eight inorganic and organoselenium species coeluting within an early eluted band with TFA were fully separated with HFBA (Figure 2.16.2) [101]. The method also can determine the presence of selenoxides and organoanions. pH control in the region of 2.0–2.5 enable cations such as trimethylselenonium and protonated selenoamino acids and selenoxides to be effectively paired. Anionic species show some retention as protonated forms retained by reversed-phase partition. McSheehy *et al.* used

semi-preparative scale reversed-phase columns for two-dimensional HPLC to isolate fractions of selenized yeast extracts for on-line and off-line investigations by ICP-MS [102]. Montes-Bayon *et al.* speciated wild type and genetically modified selenium accumulating *B. juncea* with HPLC-ICP-MS and ES-MS detection and found notable differences, a high preponderance of Se-methylselenocysteine being found in the modified sample (Figure 2.16.3) [60]. Zheng *et al.* demonstrated a mixed ion pair technique in which butanesulfonate and tetramethylammonium hydroxide were used simultaneously; selenite, selenate, selenocystine, selenourea, selenomethionine, selenoethionine, selenocystamine, and trimethylselenonium were resolved [103].

5.1.2 Detection of biomacromolecular selenium species by HPLC-ICP-MS

Lobinski *et al.* have summarized applications of HPLC with selenium-specific detection for the analysis of biological samples with respect to column type, mobile phase and detection modes including between others ICP-MS, ES MS/MS and GFAAS [78]. Although separation of biomacromolecular selenium species by size-exclusion chromatography (SEC) is mainly based on the molecular mass of the analytes, adsorption and ion-exchange effects can play an important role. Resolution of small compounds of similar molecular mass may be achieved in addition to the possibility of the detection of selenoproteins [104]. SEC-ICP-MS has enabled speciation of a number of metals bound to various macromolecular ligands [105, 106] but has had limited success for selenoproteins, the large dilution factor for Se limiting sensitivity in attempts to speciate GPX [83]. SEC-HPLC was the first procedure to measure SeP in human plasma, but it lacks the resolution and sensitivity for separation of the major Se-proteins; a human serum sample yielded three signals, but none coeluted with the GPX activity [83]. Speciation of human breast milk whey gave four Se signals corresponding to apparent molecular weights of 15, 60, 1500 and >2000 kDa [107]. A combination of affinity chromatography with SEC-ICP-MS separated three major Se-containing proteins (albumin, GPX and SeP) in human plasma [86].

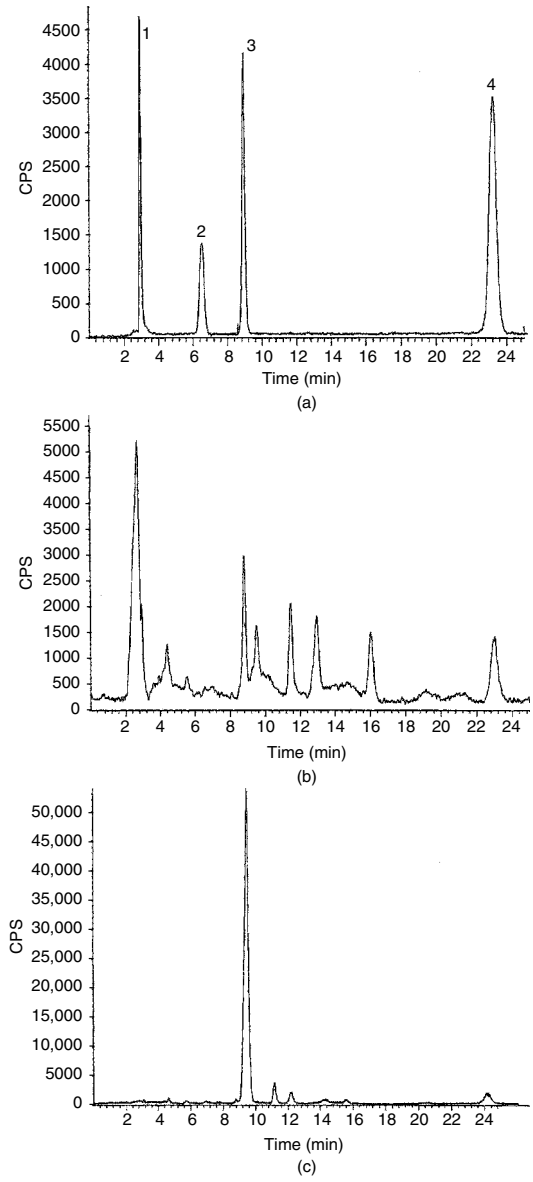

Figure 2.16.3. Se-specific HPLC-ICP-MS chromatograms using 0.1% HFBA ion-pairing agent of selenium species in Se-accumulating *Brassica juncea*; (a) – standards (50 ng mL^{-1}), 1, inorganic Se; 2, selenocystine; 3, Se-methylselenocysteine; 4, selenomethionine. (b) – Wild type *B. juncea* grown in presence of sodium selenite. (c) – Genetically modified *B. juncea* grown in presence of sodium selenite. (Reproduced from Reference [60] by permission of The Royal Society of Chemistry.)

Suzuki *et al*. used HPLC-ICP-MS with ^{82}Se to study speciation of both endogenous and enriched selenium species [108, 109]. Selenium incorporation into cyanobacterial metallothionein induced under metal stress was studied using SEC-ICP-MS, two pathways being indicated [110]. Selenite and selenate metabolism in rats was investigated [111] and exchange of endogenous and dietary selenium examined in brain, liver, and kidney [112].

5.1.3 Chiral speciation of selenium species by HPLC-ICP-MS

The presence of asymmetric carbons in selenomethionine and other α-selenoamino acids and related compounds produces different chiral enantiomers with distinct physiological activities. HPLC enantiomer separation is possible with a range of chiral stationary phases. Mendez *et al*. speciated D and L-selenomethionine isomers with a α-cyclodextrin stationary phase [113]. They examined yeast and parenteral solutions [114] and also employed a teicoplanin-based chiral phase [61]. Sanz-Medel and Blanco-Gonzalez [115] compared hybrid chiral methodologies based on GC, HPLC and capillary electrophoresis, coupled with ICP-MS. Sutton *et al*. [116] speciated enantiomers of D, L-selenocystine, D, L-selenomethionine and D, L-selenoethionine using a chiral crown ether stationary phase and examined a range of commercial dietary supplements with ICP-MS detection. Ponce de Leon *et al*. applied the same method to separate nine selenoamino acids. Selenium-enriched onion, garlic and yeast were analyzed and some of the selenoamino acid enantiomers were identified [117]. Montes-Bayon *et al*. used 1-fluoro-2, 4-dinitrophenyl-5-L alanine amide to derivatize enantiomers of selenoamides for enhanced resolution [118].

5.2 Gas chromatography

5.2.1 GC microwave plasma atomic-emission detection of selenium

GC interfaced with atomic plasma emission spectroscopic detection (GC-AED) is an established tool for specific element detection of volatilizable species [119, 120] and has been used to detect and determine many volatile organoselenium compounds present in or produced by plants. Headspace-GC-AED was used to detect selenium compounds in members of the *Allium* family such as garlic, elephant garlic, onion, and broccoli (*Brassica*) [53]. A common structure is R-S_x(Se_y)-R′, where the R and R′ are methyl or allyl groups and x or y may be 1–3. Natural abundance of organoselenium compounds in human breath after ingestion of garlic were identified using Tenax trap/cryogenic-GC-AED [121]. Calle-Guntinas *et al*. reported absolute detection limits of 10 pg for dimethylselenide with the same instrument [122].

Free selenoamino acids, selenocysteine, Se-methyl selenocysteine, and selenomethionine in normal and selenium-enriched plants have been determined by GC-AED of ethylated derivatives [53]. Calle-Guntinas *et al*. compared AED, flame photometry and GC-MS detection for selective determination of selenomethionine in wheat samples [123].

Selenomethionine is the predominant selenium moiety in plants, whereas selenocysteine is probably formed from glycine and selenite in mammalian tissues. Analytical approaches are typically based on degradation of the original matrix to these and other aminoacids followed by their determination [100]. For this purpose, GC with element-selective or mass spectrometric detection provides a valuable alternative to HPLC because of improved sensitivity. Selenoaminoacids have been derivatized with isopropylchloroformate and bis (*p*-methoxyphenyl) selenoxide [124], and with ethyl chloroformate [53, 125]. Figure 2.16.4 shows comparative selenium-specific GC-AED chromatograms for ethylated extracted enzymatic yeast hydrolyzates of archived selenized yeast employed in the ‘Clark trial’ [74], a reference fresh selenized yeast and reference selenomethionine. Selenomethionine forms volatile methylselenocyanide with CNBr [126].

5.2.2 GC with ICP-MS detection

Mendez *et al*. resolved selenomethionine enantiomers by capillary GC as trifluoroacetyl-O-isopropyl

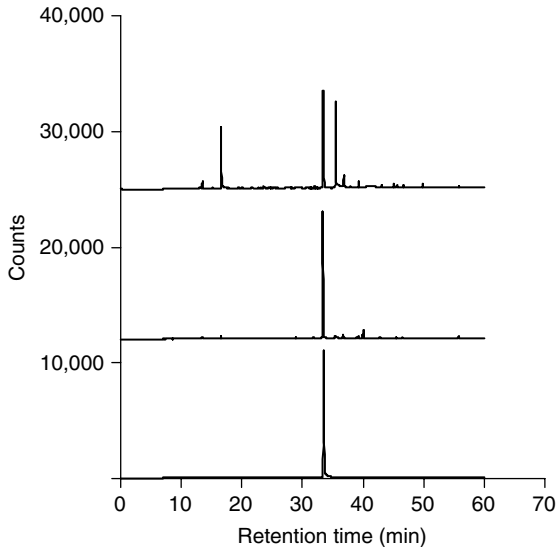

Figure 2.16.4. Se-specific GC-AED chromatograms (Se 196 nm) of ethylated enzymatic hydrolyzates of archived (Clark trial [71]) 200-μg Se tablets (top), reference 200-μg Se tablets (center), and selenomethionine (bottom). Peak at ca 36 minutes also contains sulfur.

derivatives with a 1-valine-tert-butylamide modified chiral stationary phase [114]. Detection limits below 250 pg were obtained for each isomer with ICP-MS. Bayon *et al.* used a glow discharge (rf-GD) mass spectral ion source as a sample introductory technique for selenoamino acids, detection limits of 100 pg being seen for derivatized selenomethionine [127]. Vonderheide *et al.* used solid phase microextraction (SPME) as a sample preparation strategy followed by isopropylchloroformate derivatization for GC-ICP-MS obtaining sub-ppb detection limits [128].

5.3 Capillary zone electrophoresis with ICP-MS detection

Capillary zone electrophoresis (CZE) is an effective technique for the definitive verification of the chromatographic purity of the target compound because of the large number of theoretical plates obtainable. The advantages of CZE, such as the possibility of analyzing for relatively labile species because of the absence of chromatographic packing, must be considered given the need for ultrasensitive detection, such as high resolution ICP-MS because of the small sample amount injected. A commercial interface for CZE-ICP-MS is available that optimizes electrophoretic and nebulizer flows and has minimal dilution and sample consumption [129].

The potential of CZE-ICP-MS has been particularly realized by Michalke *et al.* in the identification and determination of selenoglutathione in human milk and differentiation of methionine, selenomethionine, cystamine, and selenocystamine in milk [130–134]. Se(IV), Se(VI), selenate-carrying glutathione (GSSeSG), selenomethionine, selenocystine, and selenocystamine were speciated at the 10–50 μg Se/L level. Mounicou *et al.* utilized a two-dimensional separation approach for selenized yeast speciation, based on size exclusion followed by CZE-ICP-MS, coupling to the ICP via a self-aspirating total consumption nebulizer [135] (Figure 2.16.5). Detection limits of low molecular mass selenium species were in the range 7–18 $\mu g\,L^{-1}$, but problems were encountered with recovery of high molecular mass Se species from the CZE capillary.

5.4 Identification of selenium species

HPLC-ICP-MS, GC-AED and CZE-ICP MS offer sufficient sensitivity and selenium selectivity for the speciation of selenium compounds in many samples but do not give structural identification of known, unknown or unpredicted compounds. This lack becomes more important as more efficient separations are achieved. Chromatographic identification may be based on migration time through a chromatographic support, but authentic standards of selenium compounds are often not available for retention-based identification, except for simple compounds. The major approaches to analyte authentication involve preparation of additional synthetic standards or isolation of purified selenium compounds from sample matrixes for further characterization, for example, by electrospray (ES-MS) [51, 56, 62, 63, 100, 101] or matrix-assisted laser desorption ionization (MALDI-MS) [136].

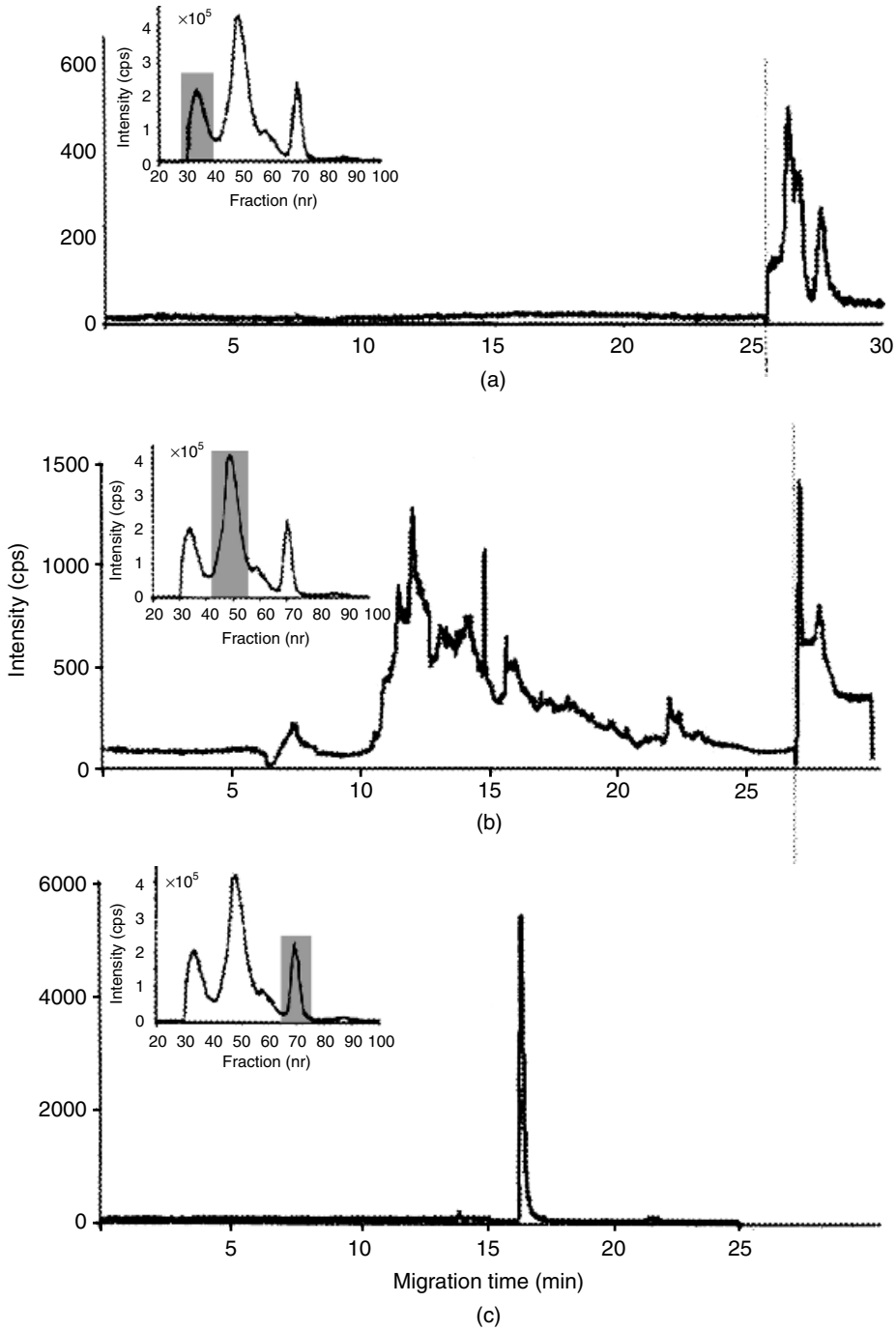

Figure 2.16.5. Analysis of a selenized yeast extract by SEC-CZE-ICP-MS. The SEC-ICP-MS chromatograms (^{80}Se, off-line detection) are shown as insets. Panels (a), (b), and (c) show CZE-ICP-MS electropherograms of the SEC fractions shaded in the insets. The dotted line marks the end of an electropherogram after which pressure (5 psi) was applied to remove the rest of the sample from the capillary. (Reproduced from Reference [135] by permission of The Royal Society of Chemistry.)

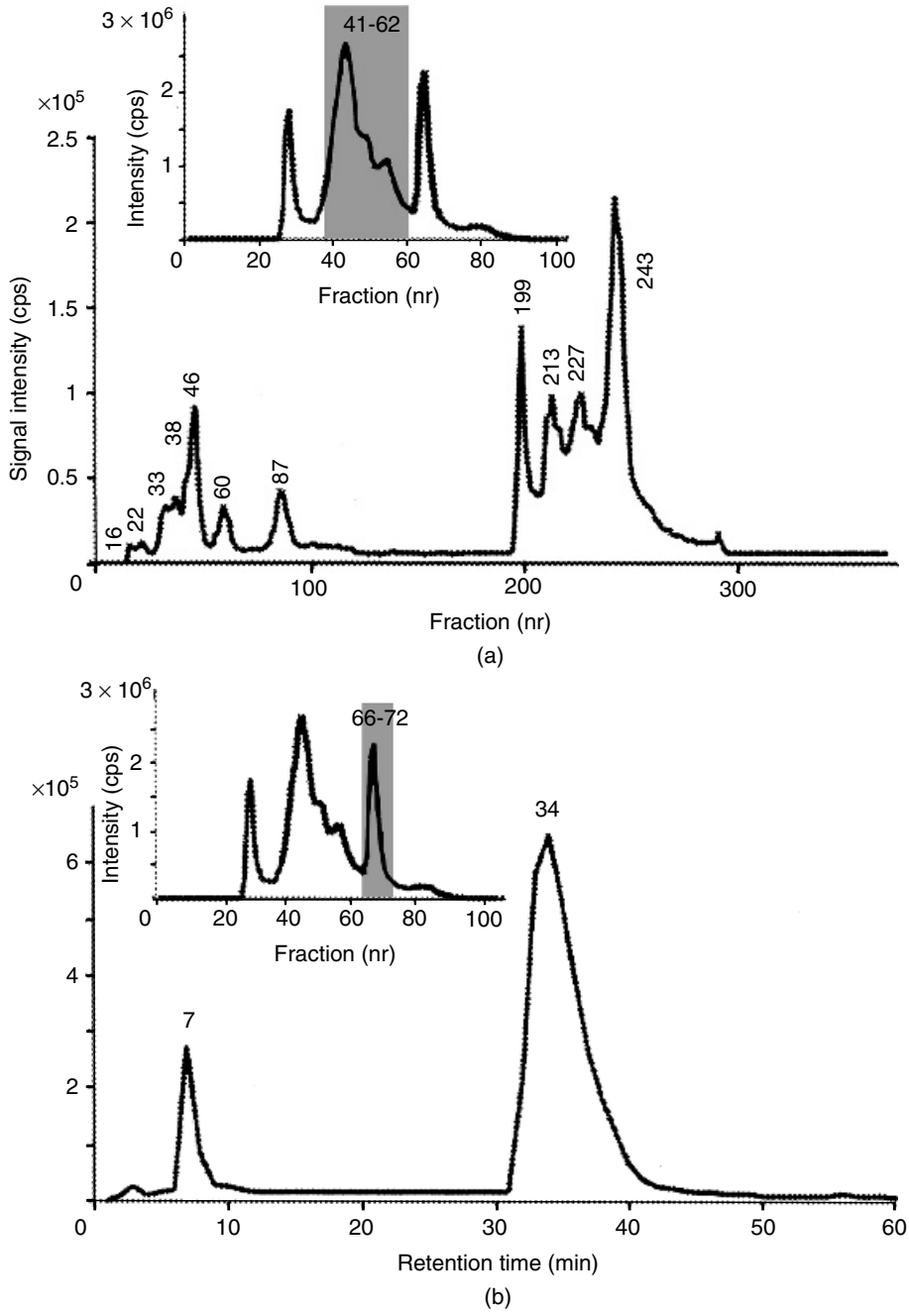

Figure 2.16.6. Preparative anion-exchange chromatograms of the selenium-containing fractions isolated by size-exclusion chromatography. (a) Medium-molecular mass fraction; (b) low molecular mass fraction. The fractions concerned are shaded in the SEC-ICP-MS chromatogram shown in the inset. (Reproduced from Reference [139] by permission of The Royal Society of Chemistry.)

The identification of selenium species by matching retention (migration) times with those of authentic standards demands the assurance that the resolution of the chromatographic technique produces at a given retention time a signal corresponding to this compound only, and that peak shapes are not distorted by sample overload or unacceptable adsorption. Also, peaks obtained by selenium selective detection may shift because of interactions with sample components. Thus, hyphenated molecular characterization by mass spectrometry or NMR spectroscopy provides valuable confirmatory data for chromatographic speciation of standards and identifications of unknowns.

Fan *et al.* synthesized Se-methylselenomethionine, Se-methylselenocysteine and DMSeP and employed a combination of 2-D multinuclear NMR, electrospray MS, and GC-MS methods to identify Se compounds in synthetic preparations [63]. GC-MS is sensitive but restricted to volatilizable species; for the nonvolatilizable metabolites, there is often a discrepancy between the sensitivity of HPLC-MS techniques and that needed for speciation in real samples. For real-world samples, purification and preconcentration of Se species is usually needed.

Electrospray MS that allows a ± 1 Da determination of molecular mass is an invaluable tool for the identification and a prerequisite for further characterization of compounds in speciation analysis. Higher-resolution techniques such as ESI – triple quadrupole MS, ESI-MALDI-TOF, and ESI-QTOF provide higher precision and exact mass determination. ESI MS has been applied mostly to commercial standards [51, 136] or synthetic preparations of Se-methylselenomethionine, Se-methylselenocysteine, and DMSeP (precursors of volatile alkylselenides) [62]. Pneumatically assisted ESI MS was used to identify Se-adenosylhomocysteine in an extract of selenized yeast [137]. Kotrebai *et al.* synthesized a number of selenoamino acids and tried with some success to match their retention times with signals produced by extracts of yeast supplements and garlic and plant extracts [99–101]. McSheehy *et al.* speciated selenium in garlic by parallel ICP-MS and electrospray tandem MS [138]. Subsequently, they speciated yeast extracts by three-dimensional SEC-CZE-ICP-MS [139] (Figure 2.16.6). Ogra *et al.* identified a novel selenium metabolite in rat urine, the selenosugar diasteriomer Se-methyl-N-acetylhexosamine by this method [64]. It should be emphasized that when authentic standards are not available, the use of tandem MS is vital to confirm selenium speciation indicated by means of hyphenated selenium-specific detection. Encinar *et al.* identified water soluble and triptic digests of yeast selenoproteins by HPLC-ICP-MS followed by MALDI-TOF and Q-TOF mass spectrometry [65, 66].

6 CONCLUSION AND ANTICIPATED DEVELOPMENTS IN SELENIUM SPECIATION

The development of procedures for the speciation of environmentally and biologically important organoselenium compounds such as selenoaminoacids and selenoproteins remains challenging. While much has been achieved in terms of the detection of many selenium species in complex matrices, the very low analyte levels frequently make the identification of the species present problematic. The prerequisite is wider use of techniques that give direct access to structural information such as NMR and high-resolution mass spectrometry. The marginal sensitivity and vulnerability to matrix interferences sometimes experienced with these techniques can be overcome by the classical approach of the concentration, purification, and isolation of the seleno species detected. Specific chemical derivative transformation of analyte compounds is a powerful approach that, nevertheless, requires careful control if speciation is not to be disrupted. More substantial work is needed to eliminate remaining barriers to a molecular-level understanding of Se clinical chemistry, ecotoxicology, and nutrition eliminated.

7 REFERENCES

1. Jacobs, L. W. (Ed.), *Selenium in Agriculture and the Environment*, Soil Science Society of America, Madison, WI, 1989.

2. Cooke, T. D. and Bruland, K. W., *Environ. Sci. Technol.*, **21**, 1205 (1987).
3. Nriagu, J. O. and Pacyna, J. M., *Nature (London)*, **333**, 134 (1988).
4. Frankenberger Jr., W. T. and Benson, S. (Eds.), *Selenium in the Environment*, Marcel Dekker, New York, 1994.
5. Frankenberger Jr., W. T. and Engberg, R. A. (Eds.), *Environmental Chemistry of Selenium*, eds. Marcel Dekker, New York, 1998.
6. Wang, B. and Burau, R. G., *Environ. Sci. Technol.*, **29**, 1504 (1995).
7. Banuelos, G. S. and Meek, D. W., *J. Plant Nutr.*, **12**, 1255 (1989).
8. Banuelos, G. S., Meek, D. W. and Hoffman, G. J., *Plant Soil*, **127**, 201 (1990).
9. Garbiso, C., Ishii, T., Leighton, T. and Buchanan, B. B., *Chem. Geol.*, **132**, 199 (1996).
10. D'Ulivo, A., *Analyst*, **122**, 117R (1997).
11. Pyrzynska, K., *Microchim. Acta*, **140**, 55 (2002).
12. Spallholz, J. E., *Biomed. Environ. Sci.*, **10**, 260 (1997).
13. Fan, T. W., The, S. J., Hinton, D. E. and Higashi, R. M., *Aquat. Toxicol.*, **57**, 65 (2002).
14. Skorupa, J. and Ohlendorf, H. M., Contaminants in drainage water and avian risk thresholds, in *The Economy and Management of Water and Drainage in Agriculture*, Dinar, A. and Zilberman, D. (Eds.), Kluwer Academic Publishers, Norwell, MA, 1991.
15. Maier, K. J. and Knight, W., *Rev. Environ. Contam. Toxicol.*, **134**, 31 (1994).
16. U.S. EPA, *Report on the Peer Consultation Workshop on Selenium Aquatic Toxicity and Bioaccumulation*, EPA-822-R-98-007, Office of Water, EPA, Washington, DC, 1998.
17. Fan, T. W. and Higashi, R., Microphyte-mediated selenium biogeochemistry and its role in *in situ* selenium bioremediation, in *Phytoremediation of Contaminated Soil and Water*, Terry, N. and Banuelos, G. (Eds.), Lewis Publishers, New York, 2000, pp. 283–302.
18. Zayed, A., Pilon-Smits, E., deSouza, M., Lin, Z.-Q. and Terry, N., Remediation of selenium-polluted soils and waters by phytovolatilization, in *Phytoremediation of Contaminated Soil and Water*, Terry, N. and Banuelos, G. (Eds.), Lewis Publishers, New York, 2000, pp. 61–83.
19. Wilber, C. G., *Clin. Toxicol.*, **17**, 171 (1980).
20. Zayed, A., Lytle, C. M. and Terry, N., *Planta*, **206**, 284 (1998).
21. Meija, J., Montes-Bayon, M., LeDuc, D. L., Terry, N. and Caruso, J. A., *Anal. Chem.*, **74**, 5837 (2002).
22. California Regional Water Quality Control Board, Central Valley Region, Fourth Edition of the *Water Quality Control Plan (Basin Plan) for the Sacramento River and San Joaquin River Basins*, 1998.
23. Chasteen, T. G. and Bentley, R., *Chem. Rev.*, **103**, 1 (2003).
24. Kryukov, G. V., Castellano, S., Novoselov, S. V., Lobanov, A. V., Zehtab, O., Guigo, R. and Gladyshev, V. N., *Science*, **300**, 1439 (2003).
25. Uden, P. C., *Anal. Bioanal. Chem.*, **373**, 422 (2002).
26. Ganther, H. E. and Lawrence, J. R., *Tetrahedron*, **53**, 12229 (1997).
27. Gao, S., Tanji, K. K., Peters, D. W. and Herbel, M. J., *J. Environ. Qual.*, **29**, 1275 (2000).
28. Pickering, I. J., Brown, G. E. and Tokunaga, T. K. Jr., *Environ. Sci. Technol.*, **29**, 2456 (1995).
29. Lee, A., Lin, Z. Q., Pickering, I. J. and Terry, N., *Planta*, **213**, 977 (2001).
30. Montes-Bayón, M., Yanes, E. G., Ponce de León, C. A., Jayasimhulu, K., Stalcup, A., Shann, J. and Caruso, J. A., *Anal. Chem.*, **74**, 107 (2002).
31. Zhang, Y. and Frankenberger, W. T. Jr., *Sci. Total Environ.*, **269**, 39 (2001).
32. Guo, X. and Wu, L., *Ecotoxicol. Environ. Saf.*, **39**, 207 (1998).
33. Combs, G. F. and Combs, S., Selenium in human nutrition and health, *The Role of Selenium in Nutrition*, Academic Press, New York, 1986, pp. 327–400.
34. Combs, G. F., *Br. J. Nutr.*, **85**, 517 (2001).
35. Shi, B. and Spallholz, J., *Br. J. Nutr.*, **72**, 873 (1994).
36. Schwartz, K. and Foltz, C. M., *J. Am. Chem. Soc.*, **79**, 3292 (1957).
37. Rotruck, J. T., Ganther, H. E., Swanson, A. B., Hafeman, D. G. and Hoekstra, W. G., *Science*, **179**, 588 (1972).
38. Allan, C. B., Lacourciere, G. M. and Stadtman, T. C., *Annu. Rev. Nutr.*, **19**, 1 (1999).
39. Hill, K. E., Xia, Y., McKesson, B., Boeglion, M. E. and Burk, M. F., *J. Nutr.*, **126**, 138 (1996).
40. Vendeland, S. C., Beilstein, M. A., Yeh, Y., Ream, W. and Whanger, P. D., *Proc. Natl. Acad. Sci. U.S.A.*, **92**, 8749 (1995).
41. Gladyshev, V. N., Jeang, K. T., Wooton, J. C. and Hatfield, D. L., *J. Biol. Chem.*, **273**, 8910 (1998).
42. Thilly, C. H., Swennan, B., Bourdoux, P., Ntambue, K., Moreno-Reryes, R., Gillies, J. and Vanderpas, J. B., *Am. J. Clin. Nutr.*, **57**, 267S (1993).
43. Beck, M. A., *Biomed. Environ. Sci.*, **10**, 307 (1997).
44. Sasakura, C. and Suzuki, K. T., *J. Inorg. Biochem.*, **71**, 159 (1998).
45. Combs, G. F. and Gray, W. P., *Pharmacol. Ther.*, **79**, 179 (1998).
46. Olson, O. E., Novacek, E. J., Whitehead, E. I. and Palmer, I. S., *Phytochemistry*, **9**, 1181 (1970).
47. Sathe, S. K., Mason, A. C., Rodibayge, R. and Weaver, M., *J. Agric. Food Chem.*, **40**, 2084 (1992).
48. Wang, Z. J., Xie, S. M. and Peng, A. J., *J. Agric. Food Chem.*, **44**, 2754 (1996).
49. Ip, C., Lisk, D. J. and Stowesan, G. S., *Nutr. Cancer*, **17**, 279 (1992).
50. Hintze, K. J., Lardy, G. P., Marchello, M. J. and Finley, J. W., *J. Agric. Food Chem.*, **49**, 1062 (2001).

51. Crews, H. M., Clarke, P. A., Lewis, J., Owen, L. M., Strutt, P. R. and Izquierdo, A., *J. Anal. At. Spectrom.*, **11**, 1177 (1996).
52. Finley, J. W., Ip, C., Lisk, D. J., Davis, C. D., Hintze, K. J. and Whanger, P. D., *J. Agric. Food Chem.*, **49**, 2679 (2001).
53. Cai, X.-J., Block, E., Uden, P. C., Zhang, X., Quimby, B. D. and Sullivan, J. J., *J. Agric. Food Chem.*, **43**, 1754 (1995).
54. Clark, L. C., Combs, G. F., Turnbull, B. W., Slate, E. H., Chalker, D. K., Chow, J., Davis, L. S., Glover, R. A., Graham, G. F., Gross, E. G., Krongrad, A., Lesher, J. L., Park, H. K., Sanders, B. B., Smith, C. L. and Taylor, J. R., *JAMA*, **276**, 1957 (1996).
55. Casiot, C., Szpunar, J., Lobinski, R. and Potin-Gautier, M., *J. Anal. At. Spectrom.*, **14**, 546 (1999).
56. Kotrebai, M., Birringer, M., Tyson, J. F., Block, E. and Uden, P. C., *Analyst*, **125**, 71 (2000).
57. Sutton, K. L., Ponce de Leon, C. A., Ackley, K. L., Sutton, R. M. C., Stalcup, A. M. and Caruso, J. A., *Analyst*, **125**, 281 (2000).
58. Moreno, P., Quijano, M. A., Gutierrez, A. M., Perez-Conde, M. C. and Camara, C., *Anal. Bioanal. Chem.*, **374**, 466 (2002).
59. Kajander, E. O., Pajula, R. L., Harvima, R. J. and Elorata, T. O., *Anal. Biochem.*, **179**, 396 (1989).
60. Montes-Bayon, M., LeDuc, D. L., Terry, N. and Caruso, J. A., *J. Anal. At. Spectrom.*, **17**, 872 (2002).
61. Mendez, S. P., Gonzalez, E. B. and Sanz Medel, A., *J. Anal. At. Spectrom.*, **15**, 1109 (2000).
62. Casiot, C., Vacchina, V., Chassaigue, H., Szpunar, J., Potin-Gautier, M. and Lobinski, R., *Anal. Commun.*, **36**, 77 (1999).
63. Fan, T. M., Lane, A. N., Martens, D. and Higashi, R. M., *Analyst*, **123**, 875 (1998).
64. Ogra, Y., Ishiwata, K., Takayama, H., Aimi, N. and Suzuki, T., *J. Chromatogr., B*, **767**, 301 (2002).
65. Encinar, J. R., Ruzik, R., Buchmann, W., Toratjada, J., Lobinski, R. and Szpunar, J., *Analyst*, **128**, 220 (2003).
66. Encinar, J. R., Ouerdane, L., Buchmann, W., Toratjada, J., Lobinski, R. and Szpunar, J., *Anal. Chem.*, **75**, 3765 (2003).
67. Ganther, H. E., *Carcinogenesis*, **20**, 1657 (1999).
68. Levander, O., *Annu. Rev. Nutr.*, **7**, 227 (1987).
69. Combs, G. F. and Clark, L. C., Selenium and cancer, in *Nutritional Oncology*, Heber, D., Blackburn, G. L. and Go, V. L. W. (Eds.), Academic Press, New York, 1999, pp. 215–222.
70. Combs, G. F., Selenium, in *Nutrition and Cancer Prevention*, Moon, T. and Micozzi, M. (Eds.), Marcel Dekker, New York, 1989, pp. 389–420.
71. El-Bayoumy, K., The role of selenium in cancer prevention, in *Practice of Oncology*, 4th ed., DeVita, V. T., Hellman, S. and Rosenberg, S. S. (Eds.), Lippincott, Philadelphia, PA, 1991, pp. 1–15.
72. Lu, J., Jiang, C. M., Kaeck, M., Ganther, H., Ip, C. and Thompson, H., *Carcinogenesis*, **16**, 513 (1995).
73. Jiang, C. M., Jiang, W., Ganther, H. and Lu, J., *Mol. Carcinog.*, **26**, 213 (1999).
74. Clark, L. C., Dalkin, B., Krongrad, A., Combs, G. F., Turnbull, B. W., Slate, E. H., Witherington, R., Herlog, J. H., Janosko, E., Carpenter, D., Borosso, C., Falk, C. and Rounder, J., *Br. J. Urol.*, **81**, 730 (1998).
75. Ip, C., *J. Nutr.*, **128**, 1845 (1998).
76. Ip, C. and Ganther, H., *Cancer Res.*, **50**, 1206 (1990).
77. Moschos, M. P., Huang, W., Srikumar, T. S., Akesson, B. and Lindberg, S., *Analyst*, **120**, 833 (1995).
78. Lobinski, R., Edmonds, J. S., Suzuki, K. T. and Uden, P. C., *Pure Appl. Chem.*, **72**, 447 (2000).
79. Pyrzynska, K., *Analyst*, **121**, 7R (1996).
80. Behne, D., Hammel, C., Pfeifer, H., Rothlein, D., Gessner, H. and Kyriakopoulos, A., *Analyst*, **123**, 871 (1998).
81. Bird, S. M., Ge, H., Uden, P. C., Tyson, J. F., Block, E. and Denoyer, E. J., *Chromatography*, **789**, 349 (1997).
82. Pedersen, G. A. and Larsen, E. H., *Fresenius' J. Anal. Chem.*, **358**, 591 (1997).
83. Koyama, H., Kasanuma, Y., Kim, C., Ejima, A., Watanabe, C., Nakatsuka, H. and Satoh, H., *Tohuku J. Exp. Med.*, **178**, 17 (1996).
84. Harrison, I., Littlejohn, D. and Fell, G. S., *Analyst*, **121**, 189 (1996).
85. Plecko, T., Nordmann, S., Rukgauer, M. and KruseJarres, J. D., *Fresenius' J. Anal. Chem.*, **363**, 517 (1999).
86. Koyama, H., Omura, K., Ejima, A., Kasanuma, Y. and Watanabe, C., *Anal. Biochem.*, **267**, 84 (1999).
87. Feldman, I., Jakubowski, N., Stuewer, D. and Thomas, C., *J. Anal. At. Spectrom.*, **15**, 371 (2000).
88. Jakubowski, N., Stuewer, D., Klockow, D., Thomas, C. and Emons, H. J., *J. Anal. At. Spectrom.*, **16**, 135 (2001).
89. Olivas, R., Donard, O. X. F., Gilon, N. and Potin-Gautier, M., *J. Anal. At. Spectrom.*, **11**, 1171 (1996).
90. Zheng, J., Goessler, W. and Kosmus, W., *Trace Elem. Electrolytes*, **15**, 70 (1998).
91. Emteborg, H., Bordin, G. and Rodriguez, A. R., *Analyst*, **123**, 245 (1998).
92. Gammelgaard, B. and Jons, O., *J. Anal. At. Spectrom.*, **15**, 499 (2000).
93. Gammelgaard, B., Jessen, K. D., Kristensen, F. H. and Jons, O., *Anal. Chim. Acta*, **404**, 47 (2000).
94. Johansson, M., Bordin, G. and Rodriguez, A. R., *Analyst*, **125**, 273 (2000).
95. Emteborg, H., Bordin, G. and Rodriguez, A. R., *Analyst*, **123**, 893 (1998).
96. Sloth, J. J. and Larsen, E. H., *J. Anal. At. Spectrom.*, **15**, 669 (2000).
97. Larsen, E. H., Hansen, M., Fan, T. and Vahl, M., *J. Anal. At. Spectrom.*, **16**, 1403 (2001).
98. Casiot, C., Szpunar, J., Lobinski, R. and Potin Gautier, M., *J. Anal. At. Spectrom.*, **14**, 645 (1999).
99. Kotrebai, M., Birringer, M., Tyson, J. F., Block, E. and Uden, P. C., *Anal. Commun.*, **36**, 249 (1999).
100. Kotrebai, M., Bird, S. M., Tyson, J. F., Block, E. and Uden, P. C., *Spectrochim. Acta, Part B*, **54**, 1573 (1999).

101. Kotrebai, M., Tyson, J. F., Block, E. and Uden, P. C., *J. Chromatogr., A*, **866**, 51 (2000).
102. McSheehy, S., Pohl, P., Szpunar, J., Potin-Gautier, M. and Lobinski, R., *J. Anal. At. Spectrom.*, **16**, 68 (2001).
103. Zheng, Z., Ohata, M., Furata, N. and Kosmus, W., *J. Chromatogr., A*, **874**, 55 (2000).
104. Behne, D., Hammel, C., Pfeifer, H., Rothlein, D., Gessner, H. and Kyriakopoulos, A., *Analyst*, **123**, 871 (1998).
105. Makarov, A. and Szpunar, J., *Analusis*, **26**, M44 (1998).
106. Szpunar, J. and Lobinski, R., *Pure Appl. Chem.*, **71**, 899 (1999).
107. Negretti de Braetter, V. E., Recknagel, S. and Gawlik, D., *Fresenius' J. Anal. Chem.*, **353**, 137 (1995).
108. Suzuki, K. T., Itoh, M. and Ohmichi, M., *J. Chromatogr., B*, **666**, 13 (1995).
109. Suzuki, K. T. and Itoh, M., *J. Chromatogr., B*, **692**, 15 (1997).
110. Takatera, K., Osaki, N., Yamaguchi, H. and Watanabe, T., *Anal. Sci.*, **10**, 567 (1994).
111. Kobayashi, Y., Ogra, Y. and Suzuki, K. T., *J. Chromatogr., B*, **760**, 73 (2001).
112. Shiobara, Y., Ogra, Y. and Suzuki, K. T., *Life Sci.*, **67**, 3041 (2000).
113. Mendez, S. P., Gonzalez, E. B., Fernandez Sanchez, M. L. and Sanz Medel, A., *J. Anal. At. Spectrom.*, **13**, 893 (1998).
114. Mendez, S. P., Bayon, M. M., Gonzalez, E. B. and Sanz Medel, A., *J. Anal. At. Spectrom.*, **14**, 1333 (1999).
115. Sanz Medel, A. and Blanco-Gonzalez, E., *J. Anal. At. Spectrom.*, **16**, 957 (2001).
116. Sutton, K. L., Ponce de Leon, C. A., Ackley, K. L., Sutton, R. M. C., Stalycup, A. M. and Caruso, J. A., *Analyst*, **125**, 281 (2000).
117. Ponce de Leon, C. A., Sutton, K. A., Caruso, J. A. and Uden, P. C., *J. Anal. At. Spectrom.*, **15**, 1103 (2000).
118. Montes-Bayon, M., B'Hymer, C., Ponce de Leon, C. A. and Caruso, J. A., *J. Anal. Ab. Spectrum.*, **16**, 945 (2001).
119. Quimby, B. D., Uden, P. C. and Barnes, R. M., *Anal. Chem.*, **50**, 2112 (1978).
120. Uden, P. C., *Element-Specific Chromatographic Detection by Atomic Emission Spectroscopy*, American Chemical Society Symposium Series No. 479, American Chemical Society, Washington, DC, 1992.
121. Cai, X. J., Block, E., Uden, P. C., Sullivan, J. J. and Quimby, B. D., *J. Agric. Food Chem.*, **43**, 1751 (1995).
122. de la Calle-Guntinas, M. B., Lobinski, R. and Adams, F., *J. Anal. At. Spectrom.*, **10**, 111 (1995).
123. de la Calle-Guntinas, M. B., Brunori, C., Scerbo, R., Chiavarini, S., Quevauviller, P., Adams, F. and Morabito, R., *J. Anal. At. Spectrom.*, **12**, 1041 (1997).
124. Kataoka, H., Miyanaga, Y. and Makita, M., *J. Chromatogr., A*, **659**, 481 (1994).
125. Yasumoto, K., Suzuki, T. and Yoshida, M., *J. Agric. Food Chem.*, **36**, 463 (1988).
126. Onyang, Z., Wu, J. and Xie, L. Q., *Anal. Biochem.*, **178**, 77 (1989).
127. Bayon, M. M., B'Hymer, C., Ponce de Leon, C. A. and Caruso, J. A., *J. Anal. At. Spectrom.*, **16**, 492 (2001).
128. Vonderheide, A. P., Bayon, M. M. and Caruso, J. A., *Analyst*, **127**, 49 (2002).
129. Application note for CE-100, Cetac, Omaha, NE, USA.
130. Michalke, B., *Fresenius' J. Anal. Chem.*, **351**, 670 (1995).
131. Michalke, B., *J. Chromatogr., A*, **716**, 323 (1995).
132. Michalke, B., *Fresenius' J. Anal. Chem.*, **354**, 557 (1996).
133. Michalke, B. and Schramel, P., *J. Chromatogr., A*, **807**, 71 (1998).
134. Schramel, O., Michalke, B. and Kettrup, A., *J. Chromatogr., A*, **819**, 231 (1998).
135. Mounicou, S., McSheehy, S., Szpunar, J., Potin-Gautier, M. and Lobinski, R., *J. Anal. At. Spectrom.*, **17**, 15 (2002).
136. Sathe, S. K., Mason, A. C., Rodibaugh, R. and Weaver, C. M., *J. Agric. Food Chem.*, **40**, 2084 (1992).
137. Quijano, M. A., Guiterrez, M., Perez-Conde, C. and Camara, C., *J. Anal At. Spectrom.*, **11**, 407 (1996).
138. McSheehy, S., Yang, W., Pannier, F., Szpunar, J., Lobinski, R., Auger, J. and Potin-Gautier, M., *Anal. Chim. Acta*, **421**, 147 (2000).
139. McSheehy, S., Pannier, F., Szpunar, J., Potin-Gautier, M. and Lobinski, R., *Analyst*, **127**, 223 (2002).

2.17 Speciation of Silicon

Alfred V. Hirner and Daniela Flaßbeck
University of Duisburg-Essen, Essen, Germany

1 ENVIRONMENT

1.1 Introduction

Following oxygen (abundance 50.5%), silicon is the second most abundant element of the earth's crust. More than 99% of the silicon in the earth resides in the mantle, silica ranges from 35 to 85% in igneous rocks. Mean elemental abundance is 27.5% in the crust and approx. 32% in soils; about 10^{16} g of silica are involved in the global geochemical cycle [1]. Si is mostly inert and only slightly soluble.

Because of its high affinity to oxygen, silicon is present in nature only as salts of silicic acids. Silicon dioxide SiO_2 (silica) as the simplest solid compound of both elements is of great chemical, geological and economic importance. Silicates (e.g. feldspar, talc, mica, garnet, amphiboles, pyroxenes) that constitute significant crystalline building blocks of the geosphere are structurally based on SiO_4^- tetrahedron units derived from H_4SiO_4; when the latter separate water in an exothermic reaction, amorphous polymeric silicic acids are formed. As an important member of the group of main elements in abiotic natural samples, geologists and geochemists use a wide variety of gravimetric and instrumental techniques for analyzing total silicon, especially for differentiating acid (>65% SiO_2) from intermediate (52–65% SiO_2) and basic rocks (<52% SiO_2).

While biogenic natural materials also contain silicon in the form of silica, silicic acid and silicates from trace level up to main component concentrations (e.g. skeletons) naturally occurring organosilicon species have not been found yet.

Anthropogenically produced silicones typically contain Si–O–Si bonds (siloxanes). They have had a significant impact as specialty materials for consumer and industrial products since their commercial introduction in 1943. More than 80% of the commercial products are based on the polymer system of the polydimethylsiloxanes (PDMS) described by the formula $Me_3SiO(SiMe_2O)_nSiMe_3$. Because of the organic substituents in silicones – usually methyl, but among others, also H, alkyl, aryl, trifluoropropyl, amino-, epoxy-, polyether-, mercaptoalkyl groups – PDMS contain Si–C bonds and thus resemble elementorganic compounds.

Handbook of Elemental Speciation II: Species in the Environment, Food, Medicine & Occupational Health
Edited by R. Cornelis, H. Crews, J. Caruso and K. G. Heumann
 ISBN: 0-470-85598-3 (HB)

PDMS are characterized by molecular weights >600 u and are nonvolatile liquids insoluble in water, and thus partitioning onto solids (e.g. sediments, sewage sludge). Down-the-drain use of PDMS is estimated to be 14 million kg/year (data from US silicone industry) with a yearly increase of approximately 7% from 1991 to 1995; recycling is not yet realized. About 89,000 metric tons of PDMS-based elastomers were produced or imported in the United States in 1993, representing about 50% of all organosilicon products and 69% of all those becoming either landfilled or incinerated [2].

PDMS tend to be stable and inert in the presence of heat, chemicals and UV radiation. Their low surface tension and physical properties are relatively insensitive to temperature change over a range of −50 to +150 °C; near 200 °C, formaldehyde will evolve. PDMS can be modified to formulate a wide range of products with tailored hydrophobicity and durability [2]. Therefore, silicones find application in many diverse markets, such as aerospace, automotive, construction, electrical, electronics, medical materials, performance chemicals and coatings, personal care, household care, healthcare, food, paper and textiles. Silicones have broad utility in textile processing and finishing, antifoams for fabric and carpet dyeing and coatings. They are used as softeners, wetting agents and water repellents and in sewing operations.

Treated as biologically inert and toxicologically not relevant, highly polymeric silicones are used in medical equipment, and for implantation. Of special importance are silicone breast implants (SBIs) consisting of an elastomer shell that contains dimethyl and vinylmethyl siloxane gel copolymer networks [3].

PDMS fluids comprise the vast majority of organosilicon releases to wastewater [2]. Because of their physical properties, PDMS are effectively removed from the aqueous phase by adsorption onto sludge during sewage treatment. The ultimate fate of PDMS will therefore depend on the sludge disposal route. Incineration results in complete degradation of the siloxane polymer to carbon dioxide, water, and SiO_2. Sludge-associated PDMS incorporated into soil during soil amendment will be expected to undergo soil-catalyzed degradation und ultimately get converted to silica, water and carbon dioxide. Similar soil-catalyzed degradation will also be expected to occur if sludge-borne PDMS is landfilled.

Low PDMS levels detected in fish tissue confirm the conclusion that PDMS is unlikely to bioaccumulate [4]. While PDMS fluids have a high *n*-octanol/water partition coefficient, suggesting the ability to partition preferentially into cells and organisms, the high molecular weight of PDMS (>10 cs viscosity) prevents the fluid from bioaccumulating. The dominant pathway of PDMS dispersal in the environment is through sludge amendment of soil. PDMS not removed during wastewater treatment will be introduced into the aquatic environment as a component of suspended solids, which will settle onto bottom sediments. Summarized, 25–30% of the down-the-drain PDMS directly flows to land application, 70–75% enters wastewater treatment [2]. Of the latter, 97% is sorbed to sludge, 3% are discharged to surface waters and will eventually end up in sediments, where slow hydrolysis will happen.

In contrast to the high molecular PDMS, volatile methylsiloxanes (VMS) are siloxanes with relatively low molecular weight (<600 u) and high vapor pressure [2]. A representative VMS is octamethylcyclotetrasiloxane (OMCTS) or D4. VMS find application in PDMS manufacturing, antiperspirant/deodorants and hair and skin care products (cosmetic and pharmaceutical industry). Thirteen percent or about 20,000 metric tons of VMS is used in personal care applications, of which 92% (mainly as $(Me_2SiO)_{4-5}$) partitions to the air [2]. An emerging application for oligomeric methylsiloxanes is their use as solvents to replace ozone-forming VOCs and ozone-depleting chlorinated and fluorinated carbons (CFCs).

D4 has relatively high vapor pressure (1.33 hPa) and low water solubility (74 and 33 $\mu g\,L^{-1}$ in fresh and saltwater, resp.) [5]. VMS molecules could be small enough to pass through biological membranes [2]. D4 in aquatic organisms is concentrated by a factor of 12,400 compared to the water, will readily volatilize from

water and would equilibrate to a half-life ranging from 3 hours to 6 days in rivers and streams [6]. Gas-phase VMS compounds can be removed from the troposphere by wet and dry deposition; tropospheric lifetimes are sufficiently long for transport over regional and longer distances (>1000 km).

Organosilanols are monomeric organosilicon compounds with at least one hydroxyl group. Silanols have high aqueous solubilities and low values of the Henry constant, indicating lower volatilization rates compared to siloxanes [2]. The octanol-water partition coefficients for linear and cyclic siloxanes are higher than those of silanols, which also correlates with higher bioconcentration factors.

The monomeric methylsilanols $Me_xSi(OH)_{4-x}$ ($x = 1-3$) are the fundamental building blocks of the silicone industry [2]. They are also the predominant transient intermediates in the environmental degradation of silicones. Silanols are generally unstable and tend to condense in acidic or alkaline environments to produce organosiloxanes. $Me_2Si(OH)_2$ can only be kept in a stable state over a long period under special, acid- and base-free conditions. The tendency of silanols to self-condense is reversed in dilute aqueous solutions. The condensation is a reversible reaction, which produces water and is driven in reverse by excess water if an appropriate catalyst is present.

In the environment, PDMS hydrolysis is a source of silanols: PDMS will hydrolyze in dry soil to $Me_2Si(OH)_2$ and its low oligomer diols, and to a much lesser extent, Me_3SiOH (from end-groups) and $MeSi(OH)_3$ (from any branching) [2]. Thus, most silanols generated in the environment will consist of $Me_2Si(OH)_2$ and its low oligomer diols. Dimethylsilanediol and methylsilanetriol are very water-soluble organosilicon compounds that are not easily extracted from water partitioning between water and ethyl acetate. The water solubility of the methylsilanols, combined with their low to moderate vapor pressures, indicates that they will be found in both aqueous and atmospheric compartments of the environment.

1.2 Analytical methods

Total silicon contents of solid/liquid environmental samples can be determined by many analytical techniques, like atomic absorption spectrometry and atomic emission spectrometry (AAS and AES, resp.) after complete sample digestion (esp. by hydrofluoric acid (HF) for silicates) or like activation and X-ray techniques in case of solid samples. Essentially, the same instrumental methods are applied in total silicon determination of biological samples, and will be described in more detail in Section 3.1. Probably the best option for accurate quantification of silicon contents in environmental materials is the application of isotope-dilution high-resolution mass spectrometry (ID-HR-ICP-MS) [7, 8].

A few reviews are available concerning the analytical chemistry of silicones [2, 9, 10]. To obtain species-specific informations, highly specific and sensitive analyses for silicones are usually performed by gas chromatography (GC)/mass spectrometry (MS) of the organic extract; an additional derivatization step to transform the analyte into more mobile or soluble species may be necessary. Figure 2.17.1 shows a typical gas chromatogram of selected cyclosiloxanes D3 to D6.

PDMS extraction from soil, sediment, sludge and water is performed by Soxhlet and ultrasonic extraction with diethyl ether, chloroform, petroleum ether, hexane, cyclohexane, dichloromethane, acetone, tetrahydrofurane (THF), methylisobutylketone (MIBK), acetonitrile or water (to remove polar degradation products like silanols) or mixtures of these solvents.

Low detection limits for organosilicon compounds can be received by size exclusion chromatography (SEC) coupled with ICP/AES. Capillary supercritical fluid chromatography (SFC) for separation of a series of organosiloxanes with ICP detection and desorption chemical ionization mass spectrometry (DCI-MS) for determining the molecular weight of PDMS oligomers were used. Protonated molecular ions of the oligomeric species are produced without fragmentation, thus enabling the determination of molecular mass up to several thousand Daltons. Time-of-flight secondary

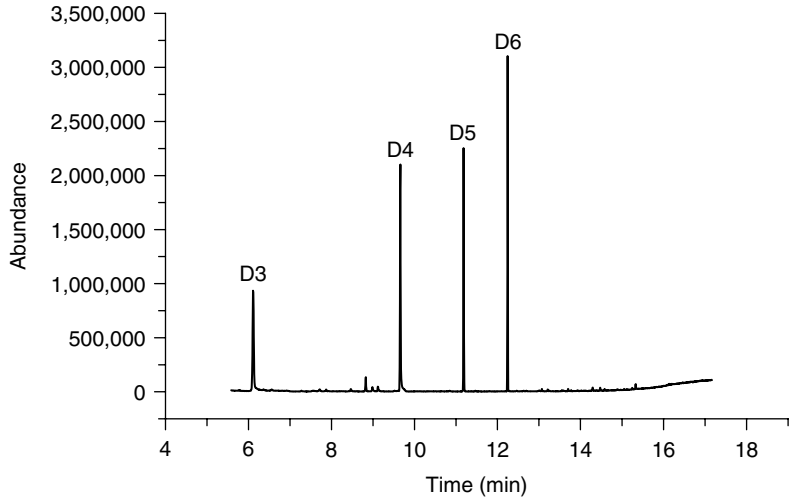

Figure 2.17.1. Chromatogram of selected cyclosiloxanes as measured by GC/MS.

ion mass spectrometry (TOF-SIMS) was applicable up to 10,000 u. SFC with ion mobility detection to separate and detect a series of 70 PDMS oligomers was described [11].

Methods have been developed for the sampling, extraction and detection of VMS in biogas and for the analysis of silanols in environmental samples [2]. In a method similar to techniques for volatile metal(loid) species, VMS gases are trapped at $-80\,^{\circ}C$ (acetone/liquid nitrogen mixture) and analyzed by low temperature gas chromatography (LTGC)/inductive coupled plasma with atomic emission spectrometry (ICP-AES) [12]. Another group determined siloxanes in landfill and sewage gases by GC separation and simultaneous detection by MS and AES [13]. Also a combination of high performance liquid chromatography (HPLC) for separation and inductively coupled plasma-atomic emission spectroscopy for detection was reported [14]. As the silanol trimethyl silanol (TMSOL) has hydrophilic as well as volatile properties, this compound can be analyzed by HPLC/ICP-AES as well as by LTGC/ICP-AES; the results of both methods were comparable, but the latter showed significant lower detection limits [12, 15]. Other analysis techniques for silicones are Pyrolysis-GC/MS, ^{29}Si nuclear magnetic resonance (NMR) and gradient polymer elution chromatography (GPEC).

1.3 PDMS, VMS and organosilanols

Concentrations ranges for silicones (PDMS and VMS) found in gaseous, liquid and solid environmental samples are compiled in Table 2.17.1. Although usually within the lower $mg\,kg^{-1}$-range, PDMS concentrations in marine sediments range up to 126 $mg\,kg^{-1}$ [16–19]. Significant levels of PDMS in surface waters were only detected in the proximity of heavily industrialized areas. However, concentrations of trace organics in the surface microlayer can be greater by a factor of 10 or more than concentrations in the bulk water, leading to measurable concentrations of PDMS in surface microlayer samples.

Up to 10 $\mu g\,m^{-3}$ D3 and 20 $\mu g\,m^{-3}$ D4 were determined in the industrial area of Guangzhou (China) [23]; similar maximal concentrations were found for D4 and D5 in indoor air. While one part of VMS is volatilized directly during application (e.g. in deodorants or perfumes), the other one is emitted from sewage waters into the atmosphere. The concentration of D4 in surface waters should be low ($<1\ \mu g\,L^{-1}$) and transient. With a half-life of 16 days, D4 and other VMS would not be expected to build up in the atmosphere but instead undergo constant degradation via the hydroxyl radical mechanism.

Table 2.17.1. VMS contents of environmental gases and PDMS in water and solids.

Silicone class	Phase	Scenario	Concentrations	Reference
VMS	Gases	Waste gases	<0.1 to 66 $mg\,m^{-3}$	[12, 20]
		Sewage gases	<0.1 to 73 $mg\,m^{-3}$	[20, 21]
		Diffuse sources	17 to 4000 $\mu g\,m^{-3}$	[22]
		Air (industrial area)	Up to 30 $\mu g\,m^{-3}$	[23]
PDMS	Water	Effluent WWTP	Up to 13 $\mu g\,L^{-1}$	[16, 17]
		Bays (Japan)	Up to 2.5 $\mu g\,L^{-1}$	[19]
	Solids	Sewage sludge US	284 to 1593 $mg\,kg^{-1}$	[16]
		Sewage sludge Germany	65 to 701 $mg\,kg^{-1}$	[18]
		Marine sediments	Up to 126 $mg\,kg^{-1}$	[16]
		Contaminated sediments	Up to 309 $mg\,kg^{-1}$	[24]
		Sediments Potomac	Up to 96 $mg\,kg^{-1}$	[25]
		Sediments Chesapeake	Up to 36 $mg\,kg^{-1}$	[17, 26]
		Sediments NY Bight	Up to 50 $mg\,kg^{-1}$	

During the combustion of landfill gas, siloxanes are converted into microcrystalline silicon dioxide, which contributes to the abrasion of the surfaces within the combustion chamber. Given a daily gas production rate of 30,000–40,000 m^3 at each of the sewage plants sampled, several hundred grams of siloxanes per day are combusted, causing severe problems in regard to the lifetime of the gas engines and revealing the necessity of gas pretreatment with effective siloxane elimination. Effective relevant processes for the removal of siloxanes are chemical degradation by acid-catalyzed rapture of Si–O bonds at elevated temperatures, and adsorption onto activated charcoal or silica beds [27, 28].

There is strong evidence for PDMS degradation occurring under strictly anaerobic conditions: TMSOL was determined in waste deposit gases in the $mg\,m^{-3}$-range, and in leachates in the $\mu g\,L^{-1}$-range together with dimethyl silanediol (DMSD) in the $mg\,L^{-1}$-range [12, 15]. This is in accordance with the PDMS structure consisting of *n* intermediate D blocks (which are degraded to DMSD) and two end capping M blocks (which are degraded to TMSOL) in the proportion of several thousands to one.

Within aerobic environments, it is well known that PDMS will degrade in some agricultural soils predominantly by hydrolyzation through random scission of its Si–O–Si backbone [29]. PDMS degradation mechanisms also involve biological degradation by bacteria and/or fungi, which takes place after an initial abiotic reaction initiating depolymerization [2]. Simultaneous with the formation of water desorbable products, a decrease in molecular mass of extracted material was observed. DMSD was identified as the major PDMS degradation product [30].

Organosilicon materials can be found in the Grey List of marine wastes by the London Treaty of 1972; it was recognized that these substances are persistent, and thus may accumulate in the environment. In Germany, PDMS and VMS are classified as water pollution class (Wassergefährdungsklasse WGK) 1 (slightly hazardous to water), in the Netherlands organic silicon compounds are listed in class C9 as hazardous waste in 'The Hazardous Waste Designation Decree'.

2 FOOD

There is an estimation that man assimilates 9–14 mg of silicon daily. Although silicon is an essential element for animals like chicken and rat, it could not been demonstrated yet that this element is also essential to man. However, it is known that Si has beneficial effects on several human disorders.

Significant amounts of inorganic silicon are incorporated in foods such as vegetables, grain, rice and dairy products and in beverages such as beer. Also a variety of sources of silicones (VMS and PDMS) exist within personal

surroundings (e.g. body care products), and from environmental sources [31]. At least part of this silicon and silicone is thought to be transported in the blood and excreted via urination. Urine silicon levels were reported to exceed blood serum levels by 20 to 100 fold ranging from 2 to 52 $mg\,L^{-1}$; the authors interpreted these differences to reflect different dietary (particularly vegetable) intakes of silicon [32, 33]. However, there is experimental evidence that a silicon-rich diet is not able to provide enough available silicon to result in a statistically significant increase in urinary silicon excretion or serum elemental content; concerning the latter silicon serum content was $102 \pm 13\ \mu g\,L^{-1}$ in the blank period compared to $119 \pm 41\ \mu g\,L^{-1}$ in the Si supplemented period [34]. It cannot be ruled out, however, that the dietary Si was excreted absorbed to feces.

Additional to 13 physiologically essential nutrients, there exist nonessential elements enhancing plant growth under certain agroclimatic conditions. These so-called functional nutrients may be regarded as agronomically essential to sustainable crop production, for example, as is Si for rice and sugarcane crops, especially when grown on organic soils. Sugarcane is known to absorb more Si than any other mineral nutrient, accumulating approx. 380 $kg\,ha^{-1}$ of Si in a 12-month-old crop [35]. Inside the plant, the absorbed monosilicic acid $Si(OH)_4$ is condensing into a hard polymerized SiO_2 (plant opal) on epidermal surfaces, thus creating an effective barrier against both infections and water loss [36]. Consequently, fertilization of rice in the Everglades Agriculture Area by Si resulted in higher yields and less disease [37]. The 'critical' level for Si in soil solution (point below which response to Si fertilizer is expected) was found in the Florida case to be 19 $mg\,L^{-1}$ [38]. Generally increasing weathering of soils with alternating wetting/drying cycles will lead to increasing desilication (SiO_2 formation). However, not the total Si but only its soluble fraction taken up by plants is of interest. The latter is conventionally received by soil extraction by 0.5 $mol\,L^{-1}$ acetic acid or by 0.5 N ammonium acetate at pH 4.0 [39].

3 BIOLOGICAL MATERIALS

3.1 Analytical methods

During the last few years, several element-specific methods for the investigation of silicon in biological substances were developed [9, 40, 41]. While the classical molybdenum blue colorimetric method may still be useful for the analysis of simple aqueous solutions, trace silicon analysis of complex matrices requires powerful modern instrumental analytical techniques combined with specific sample pretreatment procedures.

Several techniques are used for the determination of the total silicon content of a sample: electrothermal atomic absorption spectrometry (ETAAS) also called graphite furnace atomic absorption spectrometry (GFAAS) and inductively coupled plasma-atomic emission spectrometry (ICP-AES) are the most frequently used techniques in laboratories for the determination of traces of the element silicon in biological samples; flame atomic absorption spectrometry (FAAS) obviously lacks sensitivity. For microscopic silicon analysis, usually the X-rays produced in SEM (scanning electron microscopy) are quantified by EDXA (energy-dispersive X-ray analysis) or electron-probe X-ray spectrometry (EPXRS). Photon activation analysis (PAA) with high energy photons has also been used for the analysis of Si. The element was also measured by instrumental and radiochemical neutron activation analysis through irradiation in a nuclear activation analysis through irradiation in a nuclear reactor with thermal or fast neutrons. Radiochemical separation techniques were developed to enable utilization of the $^{29}Si(n,p)^{29}Al$ reaction for the determination of silicon down to the $\mu g\,g^{-1}$ level.

With exception of X-ray and activation techniques on solid samples, the other mentioned instrumental methods require total sample digestion before analysis. The latter may pose problems because of the low solubility of most silicon compounds in acid media and the volatility of silicon tetrafluoride (generated by silicate digestion by HF) as well as many silicones. A nonoxidative alkaline sample digestion procedure

using tetramethylammonium hydroxide and a high pressure microwave digestion system combined with ICP-AES analysis of the received solutions yielded reliable results for 100-mg solid biological samples [43]. In an interlaboratory study, it was demonstrated that silicon determination in biological matrices (serum, urine, water, beer and spinach) can properly be performed by the spectrometric methods mentioned above [44]; remaining problems were found to be associated with difficulties in sample digestion. Consequently, it could be shown that silicates may be substantial components in biological samples (e.g. spinach, bovine muscle) and can only be dissolved by applying HF [7]. The same authors demonstrated that inductively coupled plasma – high-resolution isotope dilution mass spectrometry (ICP-HRIDMS) in combination with microwave-assisted sample digestion with HNO_3/HF may be the best available method for trace silicon quantification even avoiding sample pretreatment problems (e.g. loss of volatile SF_4).

Silicon species have been measured in biological tissues by GC with flame ionization detection (FID), infrared spectroscopy (IR), and NMR spectrometry. GC and GC/MS are appropriate for the molecular identification and structure determination of silicones and for the sensitive determination of trace amounts of these species in biological materials. Separation (using high-resolution capillary columns) together with identification on the basis of retention times and quantification of silicones by GC, usually with an FID, is a common procedure. GC/MS is the most sensitive and selective technique for the quantification of specific silicone species. The characterization of silicones is possible through a combination of the structural information given by EI (electron impact) fragmentation patterns and the molecular mass information provided by the chemical ionization (CI) method. Silanols must be derivatized before introduction into the GC column.

Several studies have focused on the extraction of low molecular mass silicones from biological matrices with use of different chromatographic equipment like HPLC, GC/AES, and GC/MS [45–48]. A sensitive method for detection and quantification of D4 to D6 in plasma and blood using GC/MS with detection limits of 1 pg has been developed [49]. There were no blank values found when running hexane extracts; extraction efficiency was 80–90%.

^{29}Si NMR has become widespread in recent times and is the technique of choice for structural differentiation, because of its ability to distinguish between different silicone species and the specificity of its response [10]. Although NMR is usually not used in trace analysis because of its lower sensitivity compared with other techniques, a combination of *in vivo* ^{1}H NMR localized spectroscopy and *in vitro* ^{29}Si NMR spectroscopy was developed to investigate the migration and chemical modification of silicones in animal models and humans [3].

Silicones can be very easily identified by their IR spectra because of the high specificity of the spectral patterns of organic groups attached to silicon. UV spectrometry is not a very good tool for identifying silicones because of their lack of absorption of UV radiation, except for aromatic substituents. Raman spectrometry and attenuated total reflectance (ATR) IR spectrometry are very attractive techniques for the characterization of biological materials: for example, a laser Raman probe was used to detect silicones in the lymph node [50], and by FTIR-ATR detection protein adsorption on silanized surfaces [51], especially *in vivo* adsorption of blood components on silicone rubber [52] and silicone membranes [53] was investigated.

Raman and FT-IR microscopy have been used to identify silicone in capsular tissue and in regional lymph nodes of women with implants [54, 55]. A limitation of IR and Raman spectroscopy is that these methods do not give quantitative information.

Generally accidental contamination by omnipresent silicone compounds can occur during all steps of the analytical procedure: silicon-containing dust in the laboratory atmosphere, stopcock grease, lubricants in syringes, pump fluids, fluids for glassware treatment, silicone rubber for different tubing, sealing, septa or O-ring elements and self-adhering labels are only some of the potential sources of silicones in laboratories. In gas chromatographic analysis, for

example, leakage of chromatographic columns at temperatures above 200 °C takes place. Further, it is essential to avoid contamination during sampling procedures. When collecting biological samples, some commonly used items such as talc-powdered gloves or silicone-lubricated syringes should be absolutely avoided. It is important to control the purity of available reagents, solvents, and standards and to use 'silicone-decontaminated' plasticware; sample preparation should be done under Class 10 or 100 (clean room) laboratory conditions or in cabinets under laminar air flow.

3.2 PDMS, VMS and organosilanols

Because silicones are widely used as inert and persistent materials in medicine, it is very important to know about possible interactions between these compounds and biological systems, that is, to investigate the bioactivity of PDMS and VMS. Especially in connection with the question on safety of SBIs, this topic is still the subject of tremendous current controversies among scientists [9] and will be summarized in this section.

As described for environmental systems, the siloxane bond can be hydrolyzed by exposure to water, creating two silanol groups. This reaction is highly reversible, and accelerated greatly in both directions by the presence of acid or base catalysts, and also occurs within normal physiological ranges (37 °C and mixed aqueous environment). Thus, methylsilanes undergo hydroxylation *in vivo* [25]; ingested siloxanes and silanes are broken down to silanols in the highly acidic environment of the stomach. Therefore, originally liposoluble silicone compounds could be excreted as water-soluble silanols via the kidneys. The hydroxylation reactions could be simple chemical reactions rather than enzyme-promoted processes. The only *in vivo* reaction at silicon so far reported that may be enzyme catalyzed is the direct transfer of methyl groups from silicon without prior oxidation.

Consequently, various diols ($MeSi(OH)_3$, $Me_2Si(OH)_2$, $MeSi(OH)_2$-*O*-$SiMe_2OH$, $HOMe_2Si$-*O*-$SiMe_2OH$, H-$(OSiMe_2)_3$-OH) were found as urinary metabolites in rats by HPLC radiochromatogram after THF extraction [47].

Numerous animal experiments were performed to examine the hypothesis that silicone oils (PDMS) migrate to distant sites along tissue planes [56], are associated with fibrinogen [57], and are carried by macrophages to regional lymph nodes [58]. Polysiloxanes were injected in rats and were found together with partially hydrolyzed polysiloxanes and silica in lymph nodes [59]. Following subcutaneous administration of 1 mL of dimethylpolysiloxane into mice, accumulations of silicone-containing cells in the regional lymph nodes and formation of generalized foci of fat atrophy appeared as early as two weeks postinjection [60]. Mice were injected with either breast implantate distillate composed primarily of D3 to D7 or a PDMS oil [45]. Subsequently, low molecular mass silicones were found in brain, heart, kidney, liver, lymph nodes and other organs. While highest levels of cyclosiloxanes were found in the mesenteric lymph nodes, ovaries and uterus, linear siloxanes were highest in the brain, lungs and mesenteric lymph nodes. The observation that linear siloxanes accumulate preferentially in brain can only be explained on the base that these species are passing the blood–brain barrier.

In several studies, no differences between the blood silicon concentrations of women with SBIs and controls were found [41]. Low molecular mass silicone in plasma and blood of women who are or were exposed to silicone gel-filled implants and controls were measured [49]. However, D3-D6 were not detectable in plasma and blood of controls and even in some patients' plasma and blood. In contrast, D3 and D4 could be found in most of the plasma and blood samples of women with silicone implants and even in blood of women who had undergone reimplantation up to 5 years ago unambiguously: D3 varied between 6 and 12 $\mu g\,L^{-1}$ (plasma) and 20 and 28 $\mu g\,L^{-1}$ (blood), whereas the concentration range of D4 was 14–50 $\mu g\,L^{-1}$ (plasma) and 79–92 $\mu g\,L^{-1}$ (blood). Therefore, because of the various sources of Si in blood, silicon levels cannot be assumed to be a proxy measurement for silicone: Generally, concentrations from 2 $\mu g\,L^{-1}$ up to 5 $mg\,L^{-1}$ of total Si in blood are reported, indicating variations due to different dietary and environmental influences; there

does not exist a 'normal' level. Even in the most severe cases observed yet with SBI patients, the silicone contribution to total blood silicon does not exceed 30%.

Another potential for human exposure to cyclic siloxanes is by the respiratory route (antiperspirants, hair spray). Low levels (about 1 $\mu g\,g^{-1}$) of D4, a material commonly found in personal care products, were detected in indoor air samples. The respiratory intake und uptake of D4 has been measured [48]: After 1 h exposure to 122 $\mu g\,L^{-1}$ D4, the mean D4 intake of the volunteers was 137 ± 25 mg, exhibiting D4 plasma concentrations of $79 \pm 5\ \mu g\,L^{-1}$. The major routes for excretion were urine and expired air, the latter process being characterized by a half-time of 5 1/2 h. No immunotoxic or proinflammatory effects of respiratory exposure of the volunteers to D4 were found on the base of a panel of immune tests to screen for immunotoxicity and for an adjuvant effect [61].

In contrast to blood, silicon contents of capsule and breast tissues seem to be higher in women with SBIs compared to control persons (Table 2.17.2). However, there are also examples that there generally does not exist this relationship [62] arguing for the necessity of silicone species analysis [8]. For example, siloxanes were found in muscle tissue of a woman with SBIs, although the silicon content of this tissue was lower than the controls, in which no siloxanes could be detected [8].

4 PERSONAL AND OCCUPATIONAL HEALTH

It is well known for long that crystalline silica is fibrinogenic and cancerogenic, has been associated with severe inflammatory reactions, and is known to cause lung and kidney problems (e.g. lung fibrosis and Balkan nephropathy) [32, 64]. Inflammatory reactions are also known in respect to amorphous silica whose submicroscopic spherical particles with diameters between 7 and 22 nm tend to form aggregates.

There may exist certain cases in which silicon and its species may directly and indirectly be involved in human health problems [65]: patients with chronic renal failure show elevated Si levels in blood and tissue components, women with

Table 2.17.2. Silicon content in breast tissue and capsular tissue of control group and patients with silicone gel breast implants.

	Si concentration ($\mu g\,g^{-1}$)						
Tissue	Control group			Patients with implants			Reference
Capsular				370	–	14,000	[63]
Breast	0.5	–	6.8				
Capsular[a]	0.235					25,047[b]	[31]
						13,388[c]	
Capsular				33	–	58,800[d]	[62]
				410	–	45,532[e]	
Breast	4.0	–	446.0	7	–	2995[d]	
				5	–	30,333[e]	
Capsular				37	–	88,703[d]	[40]
				3235	–	65,396[f]	
				1762	–	15,238[e]	
Breast	0.025	–	0.742				
Capsular				73	–	85[d]	[8]
Breast	11	–	33				

[a] Extractable silicon content in tissue.
[b] Implantation of silicone gel-filled implants before 1986.
[c] Implantation of silicone gel-filled implants after 1986.
[d] Intact silicone gel-filled implants.
[e] Ruptured silicone gel-filled implants.
[f] Silicone bleed.

leaking SBIs, and Alzheimer patients with aluminosilicates in the brain.

Generally, there may exist four possible pathways that lead to potential health problems caused by silicones in organisms:

1. degradation to inorganic silica
2. synergistic processes with other biochemical components
3. presence of additives (e.g. UV stabilizers, softeners, flame retardants, biostabilizers)
4. toxicity of silicones.

While (3) does not need any further comments, toxicological aspects of inorganic silicon as discussed above may apply whenever a degradation (pathway (1)) is occurring *in vivo* as proposed by several authors expressing the opinion that silicone can be broken down *in vivo* to inorganic silica [3]. Also because of the presence of fumed silica in the implant elastomer, immunology/toxicology of silica may also be considered when discussing the safety of SBIs.

In respect to pathway (2), it has been argued that dimethylsilicones are not themselves immunogenic but, when emulsified with immunogenic proteins, lead to higher immune responses; that is, silicones behave as adjuvants similar to mineral oils. D4 can induce denaturation and conformational changes in fibrinogen and fibronectin and it can be expected that protein molecules that have undergone denaturation or conformational change induced by D4 may act as antigens and stimulate the immune system to generate antibodies, ultimately resulting in autoimmune disease [66]. Silicone compounds may also possess the potential for creating antigen–antibody binding sites by providing a major electronegative static charge. Moreover, hydrogen bonding (through side groups of silicones) and hydrophobic interactions will also be important in antigen–antibody binding. Finally yet importantly, bioactivity of D4 could be demonstrated in enabling certain bacteria to methylate inorganic bismuth [67].

The most straightforward explanation for silicone-associated health problems would be pathway (4). Unfortunately, some of the physicochemical properties of the organosilicon materials that are particularly advantageous for commercial purposes, do cause major difficulties when trying to test their toxicity and ecotoxicity by conventional methods [2]. Thus, although the toxicology and immunology of silicones has been extensively reviewed [3, 25, 68, 69], many aspects of this field are still controversial, and divergent interpretations exist. With a few exceptions like the biocides silatranes (rodenticide) and mival (herbicide), it is stated that silicones generally show very low toxicity, and no indications of carcinogenicity or mutagenicity [25]. While PDMS is considered to be biologically inactive, D4 was found to have an adjuvant effect ascribed to its inflammatory properties [3]. There is some early evidence that certain low molecular mass siloxanes are toxic to cells in tissue cultures: Low molecular mass siloxanes produce lethal effects on B-lymphocyte derived target cells *in vitro* and permeabilize the plasma membranes at lower sublethal concentrations [3]. Silicone gel distillate containing D3 to D6 was found to be lethal, and all the mice injected with 35 $g\,kg^{-1}$ died within 5–8 days; mice developed inflammatory lesions of the lung and liver as well as liver cell necrosis [70]. D4 alone showed an LD_{50} of 6–7 $g\,kg^{-1}$, being about as toxic as carbon tetrachloride or trichloroethylene. Since long, it has been speculated that certain low molecular mass silicones like cyclosiloxanes may have potent biological activities that mimic estrogens [71]; pharmacologically active silicone, considered at one time for use as an oral estrogen, consists of a 2,6-*cis*-biphenyl-substituted D4.

The symptoms women with breast implants experienced ranged in severity from minor aching joints to debilitating pain and chronic fatigue [72]. Other symptoms include hair loss, stomach irritability, rashes, fevers, and allergic reactions to certain foods and chemicals found in, for example, perfumes and household cleansers. The existence of a relationship between implants and disease has remained the subject of both public and scientific debate (e.g. see literature cited by Zimmermann [72]). By January 1992, so many implant recipients had reported experiencing implant-related complications and health effects to the Food and Drug Administration (FDA) that the FDA restricted the use of silicone gel–filled

devices. Silicone elastomers *in vivo* may provoke an inflammatory response, fibrosis and (in the long term) calcification, and generate immune reactions, specifically various types of connective tissue disease; considerable controversy exists as to the nature and magnitude of these effects. The question of the safety of breast implants and their possible adverse effects on health is the subject of numerous discussions: At the one side, it is stated that breast implants are 'safe' [73], at the other side support groups and information networks for breast implant recipients have created home pages in the internet including bibliographies listing the latest scientific and epidemiological studies on the risks associated with these devices. While there is still unresolved dispute concerning increased or reduced breast cancer risk among women with implants, excesses of cervical and vulvar cancers were observed compared to the general population [74].

Summarizing, there is still concern about the safety of silicones triggered by case reports of autoimmune disease in women with breast implants, and controlled epidemiological studies have not been univocally evaluated yet.

There exist usual applied Industrial Hygiene Guidelines limiting D4 in workplace air to $5-10\ \mu g\,g^{-1}$ based on an 8-h working day. D4 in blood caused by leaking implants, however, may significantly exceed this inhalation standard [9] when taking into account D4 blood concentrations [49] and published inhalation dose/blood concentration partition ratios [48].

Recently, the European Union argued for additional research demand, until firm decisions concerning the safety of SBIs can be made (European Parliament Report A5-0186/2001).

5 REFERENCES

1. Wedepohl, K. H. (Ed.), *Handbook of Geochemistry, Vol. II-2*, Springer-Verlag, Berlin, 1973.
2. Hutzinger, O. (Ed.), *Organosilicon Materials*, Springer-Verlag, Berlin, 1997.
3. Potter, M. and Rose, N. R. (Eds.), *Immunology of Silicones*, Springer-Verlag, Berlin, 1996.
4. Annelin, R. B. and Frye, C. L., *Sci. Total Environ.*, **83**, 1 (1989).
5. Hobson, J. and Silberhorn, E., *Environ. Toxicol. Chem.*, **14**, 1667 (1995).
6. Fackler, P., Dionne, E., Hartley, D. and Hamelink, J., *Environ. Toxicol. Chem.*, **14**, 1649 (1995).
7. Klemens, P. and Heumann, K. G., *Fresenius' J. Anal. Chem.*, **371**, 758 (2001).
8. Flassbeck, D., Pfleiderer, B., Klemens, P., Heumann, K. G., Eltze, E. and Hirner, A. V., *Anal. Bioanal. Chem.*, **375**, 356 (2003).
9. Hirner, A. V., Flassbeck, D. and Grümping, R., Organosilicon compounds in the environment, in *Organometallic Compounds in the Environment*, 2nd ed., Craig, P. J. (Ed.), John Wiley & Sons, New York, 2003.
10. Smith, A. L., *The Analytical Chemistry of Silicones*, John Wiley & Sons, New York, 1991.
11. Morrissey, M. A., Siems, W. F. and Hill, H. H. Jr., *J. Chromatogr.*, **505**, 215 (1990).
12. Grümping, R., Mikolajczak, D. and Hirner, A. V., *Fresenius' J. Anal. Chem.*, **361**, 133 (1998).
13. Schweigkofler, M. and Niessner, R., *Environ. Sci. Technol.*, **33**, 3680 (1999).
14. Dorn, S. B. and Skelly-Frame, E. M., *Analyst*, **119**, 1687 (1994).
15. Grümping, R. and Hirner, A. V., *Fresenius' J. Anal. Chem.*, **363**, 347 (1999).
16. Fendinger, N. J., McAvoy, D. C., Eckhoff, W. S. and Price, B. B., *Environ. Sci. Technol.*, **31**, 1555 (1997).
17. Pellenbarg, R. E., *Environ. Sci. Technol.*, **13**, 565 (1979).
18. Siebert, F., *Verteilung von Siliconen in der Umwelt*, Unpublished Ph.D. Dissertation, University of Heidelberg, 1988.
19. Watanabe, N., Nagase, H. and Ose, Y., *Sci. Total Environ.*, **73**, 1 (1988).
20. Ahrendt, G. and Kohl, E. G., Spurenstoffe im Deponiegas, in *Trierer Berichte zur Abfallwirtschaft*, Vol. 9, Rettenberger, G. (Ed.), Economica Verlag, Bonn, 1996, pp. 9–20.
21. Martin, P., Ellersdorfer, E. and Zeman, A., *Korrespondenz Abwasser*, **43**, 1574 (1996).
22. Schröder, H. F., *Biochemisch schwer abbaubare organische Stoffe in Abwässern und Oberflächenwässern*, Unpublished Habilitation Thesis, Technische Hochschule Aachen, 1997.
23. Wang, X. M., Lee, S. C., Sheng, G. Y., Chan, L. Y., Fu, J. M., Li, X. D., Min, Y. S. and Chan, C. Y., *Appl. Geochem.*, **16**, 1447 (2001).
24. Powell, D. E., Annelin, R. B. and Gallavan, R. H., *Environ. Sci. Technol.*, **33**, 3706 (1999).
25. Jarvie, A. W. P., Environmental aspects of organosilicon chemistry and use, in *Organometallic Compounds in the Environment – Principles and Reactions*, Craig, P. J. (Ed.), Longman Group, Harlow, 1986, pp. 229–253.
26. Pellenbarg, R. E., *Mar. Pollut. Bull.*, **13**, 427 (1982).
27. Huppmann, R., Lohoff, H. W. and Schröder, H. F., *Fresenius' J. Anal. Chem.*, **354**, 66 (1996).
28. Schweigkofler, M. and Niessner, R., *J. Hazard. Mater.*, **B83**, 183 (2001).

29. Xu, S., *Environ. Sci. Technol.*, **32**, 3162 (1998).
30. Lehmann, R. G., Varaprath, S. and Frye, C. L., *Environ. Toxicol. Chem.*, **13**, 1753 (1994).
31. Lugowski, S. L., Smith, D. C., Bonek, H., Lugowski, J. Z., Peters, W. and Semple, J., *J. Trace Elem. Med. Biol.*, **14**, 31 (2000).
32. Roberts, N. B. and Williams, P., *Clin. Chem.*, **36**, 1460 (1990).
33. Belliveau, J. F., Griffiths, W. C., Wright, G. C. and Tucci, J. R., *Ann. Clin. Lab. Sci.*, **21**, 328 (1991).
34. Van Dyck, K., Van Cauwenbergh, R., Robberecht, H. and Deelstra, H., *Fresenius' J. Anal. Chem.*, **363**, 541 (1999).
35. Savant, N. K., Korndörfer, G. H., Datnoff, L. E. and Snyder, G. H., *J. Plant Nutr.*, **22**, 1853 (1999).
36. Yoshida, S., Ohnishi, Y. and Kitagishi, K., *Soil Sci. Plant Nutr.*, **8**, 107 (1962).
37. Savant, N. K., Snyder, G. H. and Datnoff, L. E., *Adv. Agron.*, **58**, 151 (1997).
38. Korndörfer, G. H., Snyder, G. H., Ulloa, M., Powell, G. and Datnoff, L. E., *J. Plant Nutr.*, **24**, 1071 (2001).
39. Korndörfer, G. H., Datnoff, L. E. and Correa, G. F., *J. Plant Nutr.*, **22**, 93 (1999).
40. Peters, W., Smith, D., Lugowski, S., McHugh, A. and Baines, C., *Ann. Plast. Surg.*, **34**, 343, (1995).
41. Jackson, L. W., Dennis, G. J. and Centeno, J. A., Analytical determination of blood silicon in patients with silicone breast implants, in *Metal Ions in Biology and Medicine*, Vol. 5, Collery, Ph., Braetter P., Negretti de Braetter, V. N., Khassanova, L. and Etienne, J. C. (Eds.), John Libbey Eurotext, Paris, 1998, pp. 33–38.
42. Kucera, J. and Randa, Z., *Fresenius' J. Anal. Chem.*, **370**, 241 (2001).
43. Hauptkorn, S., Pavel, J. and Seltner, H., *Fresenius' J. Anal. Chem.*, **370**, 246 (2001).
44. Van Dyck, K., Robberecht, H., Van Cauwenbergh, R., Deelstra, H., Arnaud, J., Willemyns, L., Benijts, F., Centeno, J. A., Taylor, H., Soares, M. E., Bastos, M. L., Ferreira, M. A., D'Haese, P. C., Lamberts, L. V., Hoenig, M., Knapp, G., Lugowski, S. J., Moens, L., Riondato, J., Van Grieken, R., Claes, M., Verheyen, R., Clement, L. and Uytterhoeven, M., *J. Anal. At. Spectrom.*, **15**, 735 (2000).
45. Kala, S. V., Lykissa, E. D., Neely, M. W. and Lieberman, M. W., *Am. J. Pathol.*, **152**, 645 (1998).
46. Kala, S. V., Lykissa, E. D. and Lebovitz, R. M., *Anal. Chem.*, **69**, 1267 (1997).
47. Varaprath, S., Salyers, K. L., Plotzke, K. P. and Nanavati, S., *Anal. Biochem.*, **256**, 14 (1998).
48. Utell, M. J., Gelein, R., Yu, C. P., Kenaga, C., Geigel, E., Torres, A., Chalupa, D. and Gibb, F. R., *Toxicol. Sci.*, **44**, 206 (1998).
49. Flassbeck, D., Pfleiderer, B., Grümping, R. and Hirner, A. V., *Anal. Chem.*, **73**, 606 (2001).
50. Abraham, J. L. and Etz, E. S., *Science*, **206**, 716 (1979).
51. Deng, X. M., Castillo, E. J. and Anderson, J. M., *Biomaterials*, **7**, 247 (1986).
52. Seifert, L. M. and Greer, R. T., *J. Biomed. Mater. Res.*, **19**, 1043 (1985).
53. Kennedy, J. H., Ishida, H., Staikoff, L. S. and Lewis, C. W., *Biomater. Med. Dev. Art. Org.*, **6**, 215 (1978).
54. Kidder, L. H., Kalasinsky, V. F., Luke, J. L., Levin, I. W. and Lewis, E. N., *Nat. Med. (NY)*, **3**, 235 (1997).
55. Ali, S. R., Johnson, F. B., Luke, J. L. and Kalasinsky, V. F., *Cell. Mol. Biol.*, **44**, 75 (1998).
56. Raso, D. S. and Greene, W. B., *Ultrastruct. Pathol.*, **21**, 263 (1997).
57. Whitlock, P. W., DeAnglis, A. P., Ackley, K. L., Clarson, S. J. and Retzinger, G. S., *Exp. Mol. Pathol.*, **72**, 161 (2002).
58. Hardt, N. S., Emery, J. A., Steinbach, B. G., Latorre, G. and Caffee, H., *Int. J. Occup. Med. Toxicol.*, **4**, 127 (1995).
59. Pfleiderer, B., Moore, A., Tokareva, E., Ackerman, J. L. and Garrido, L., *Biomaterials*, **20**, 561 (1999).
60. Ben-Hur, N., Ballantyne, D. L., Rees, T. D. and Seidman, I., *Plast. Reconstr. Surg.*, **39**, 423 (1967).
61. Looney, R. J., Frampton, M. W., Byam, J., Kenaga, C., Speers, D. M., Cox, C., Mast, R. W., Klykken, P. C., Morrow, P. E. and Utell, M. J., *Toxicol. Sci.*, **44**, 214 (1998).
62. Schnur, P. L., Weinzweig, J., Harris, J. B., Moyer, T. P., Petty, P. M., Nixon, D. and McConnell, J. P., *Plast. Reconstr. Surg.*, **98**, 798 (1996).
63. Evans, G. R. D., Netscher, D. T., Schustermann, M. A., Kroll, S. S., Robb, G. L., Reece, G. P. and Miller, M. J., *Plast. Reconstr. Surg.*, **97**, 1207 (1996).
64. Hokosawa, S. and Yoshida, O., *Int. Urol. Nephrol.*, **22**, 373 (1990).
65. Hornung, M. and Krivan, V., *J. Anal. At. Spectrom.*, **12**, 1123 (1997).
66. Sun, L., Alexander, H., Lattarulo, N., Blumenthal, N. C., Ricci, J. L. and Chen, G., *Biomaterials*, **18**, 1593 (1997).
67. Wickenheiser, E. B., Michalke, K., Hirner, A. V., Hensel, R. and Flassbeck, D., The biological methylation of bismuth; evidence for the involvement of polydimethylsiloxanes in the biologically-mediated methylation of metals, in *Metal Ions in Biology and Medicine*, Vol. 6, Centeno, J. A., Collery, Ph., Vernet, G., Finkelman, R. B., Gibb, H. and Etienne, J. C. (Eds.), John Libby Eurotext, Paris, 2000, pp. 120–122.
68. Marcus, D. M., *Arthritis Rheum.*, **39**, 1619 (1996).
69. Kossovsky, N., *Appl. Organomet. Chem.*, **11**, 353 (1997).
70. Lieberman, M. W., Lykissa, E. D., Barrios, R., Ou, C. N., Kala, G. and Kala, S. V., *Environ. Health Perspect.*, **107**, 161 (1999).
71. Hayden, J. F. and Barlow, S. A., *Toxicol. Appl. Pharmacol.*, **21**, 68 (1972).
72. Zimmermann, S. N., *Silicone Survivors*, Temple University Press, Philadelphia, PA, 1998.
73. Angell, M., *Science on Trial: The Clash of Medical Evidence and the Law in the Breast Implant Case*, WW Norton, New York, 1996.
74. Brinton, L. A., Lubin, J. H., Burich, M. C., Colton, T., Brown, S. L. and Hoover, R. N., *Ann. Epidemiol.*, **11**, 248 (2001).

2.18 Speciation of Sulfur

Norbert Jakubowski
Institute for Analytical Sciences, Dortmund, Germany

Nikos Mihalopoulos
Environmental Chemical Processes Laboratory, University of Crete, Heraklion, Greece

Sabine Mann
AnalytikSupport, Niederkassel, Germany

Wolf D. Lehmann
Central Spectroscopy, German Cancer Research Center, Heidelberg, Germany

1 INTRODUCTION

Sulfur is a nonmetallic element that exists in several liquid, solid, and gaseous allotropic forms [1]. It is the 15th most abundant element on the earth since sulfur is present in the earth's crust at a mixing ratio of about 400–500 mg kg^{-1} and in the atmosphere at a total mixing ratio of less than

Handbook of Elemental Speciation II: Species in the Environment, Food, Medicine & Occupational Health
Edited by R. Cornelis, H. Crews, J. Caruso and K. G. Heumann
 ISBN: 0-470-85598-3 (HB)

1 μmol mol^{-1}. Sulfur is found in nature both in the elemental form and as a constituent of inorganic and organic compounds. It is found in meteorites, volcanoes, hot springs, and as galena, gypsum, Epsom salts, and barite.

The key resources for the commercial recovering of sulfur are salt domes along the Gulf Coast of the USA, Mexico, Iraq, and Sicily and sediment rocks (as a volcanic sublimate) in the southwest of Poland for elemental sulfur, natural gas, and crude oil for H_2S, metal sulfides, especially pyrite FeS_2 ("fool's gold"), and sulfates, mainly gypsum, $CaSO_4x2H_2O$.

The elemental sulfur found in nature is extracted by the Frasch process, where underground deposits of sulfur are forced to the surface using superheated water and steam (160–170 °C, 16 atmospheres for melting the sulfur) and compressed air (25 atmospheres). By this energy-intensive process, a purity of 99.5% can be reached.

Hydrogen sulfide, H_2S, is an important impurity in natural gas that can be removed by an absorption and regeneration process to concentrate the H_2S, followed by a catalytic oxidation (Claus process) using porous catalysts such as Al_2O_3 or Fe_2O_3 ("recovered sulfur"). Over the years, the Claus process has been improved and a modified process can yield 98% recovery.

$$8H_2S + 4O_2 \longrightarrow S_8 + 8H_2O \qquad (2.18.1)$$

FeS_2 and other metal sulfides are oxidized by roasting, and the formed gaseous SO_2 is often used directly for the production of sulfuric acid, H_2SO_4.

More than 80% of the sulfur produced is used for the production of H_2SO_4. Sulfuric acid is an oxidizing and dehydrating agent and utilized for the manufacturing of HCl and HNO_3. It is used for the manufacturing of fertilizers and polyamides, and it is the most important electrolyte in batteries ('battery acid'). Sulfur is a component of matches and black gunpowder (a mixture of potassium nitrate, KNO_3, carbon, and sulfur). It is used in the vulcanization of natural rubber, as a fungicide and as a fumigant. Sulfur compounds like sulfur dioxide, SO_2, are used in the bleaching of dried fruits and for paper products, as a disinfectant, an insecticide, and a refrigerant. Other important compounds include sodium bisulfite, $NaHSO_3$, which is used in paper manufacture. Carbon disulfide, H_2S, sulfur trioxide, SO_3, thionyl chloride, and $SOCl_2$ are used as reagents in chemistry, and numerous sulfate compounds are applied in dermatology and cosmetics. Carbon disulfide, CS_2, is an important solvent in the laboratory and in the industry. It is poisonous and is easily absorbed by inhalation and through skin [2].

Sulfur reacts with all the halogens upon heating and forms a variety of different compounds in different oxidation states, whereas the most important compound for technical use is sulfur hexafluoride, SF_6, which is used as an insulating gas for high voltage lines and circuit breakers. The anthropogenic sources of SF_6 emissions are from leaking and destroying of this equipment and also arise from the primary production of magnesium and the casting of magnesium parts. Sulfur hexafluoride is extremely stable and long lasting, with an estimated atmospheric lifetime of 3200 years. It is not flammable and is nontoxic. But as the global warming potential of SF_6 has been calculated to be 23,900 times greater than that of CO_2 over a 100-year time horizon [3], monitoring of SF_6 emissions into the atmosphere is of great interest.

Another compound of sulfur, sodium dodecylsulfate (SDS), an ester of sulfuric acid, is important in various applications. It is used as a surfactant in washing powder for delicate fabrics, because it can cover particles as well as macromolecules with negatively charged micelles. This effect is used in gel electrophoresis, for instance, in the well known polyacrylamide gel electrophoresis (PAGE), to add additional charges, proportional to the molecular mass, to a macromolecule, so that the mobility of the biomolecule becomes proportional to the weight. By this principle, weight calibration by marker molecules is easily possible.

Sulfur is one of the major elements essential to life on this planet since numerous functionally important cellular components contain sulfur. It is a minor constituent of skeletal minerals, body fluids, and fats. Sulfur is a component of coenzymes (Coenzyme A), vitamins (Thiamine) and of the essential amino acids methionine

(Met), $H_3CS(CH_2)_2CH(NH_2)CO_2H$, and cysteine (Cys), $HSCH_2CH(NH_2)CO_2H$, which are either synthesized (in case of plants and microorganisms) or procured with the food supply (in case of animals). Although both Cys and Met occur with less than average abundance in proteins, they are present in the vast majority of proteins. Together, they exhibit an amino acid abundance of about 3–4% in eukaryotic proteomes. A derived amino acid found in many proteins is cystine $[-SCH_2CH(NH_2)CO_2H]_2$. It is formed by the oxidation of two cysteine thiol side chains to form a disulfide covalent bond. Within proteins, disulfide links of cystine formed from cysteines have an important role in stabilizing the folded conformation of proteins.

Concerning its biological activity, selenium shows a similar behavior, but for more details please see Section 2.16 from P.C. Uden 'Speciation of Selenium' in this handbook.

Many sulfur-containing substances are important pharmaceutical products and are frequently used as antibiotics (penicillin, sulfonamides) or in chemotherapy (busulfan).

From an historical point of view, the most important drug that has ever been developed is penicillin, which belongs to the group of the β-lactame antibiotics (see Figure 2.18.1) and inhibits the peptide glycan synthesis of the bacteria cell wall.

The second group of sulfur-containing antibiotics consists of the sulfonamides, synthetic organic sulfur compounds containing the radical $-SO_2NH_2$ (the amide of sulfonic acid). They act as antimicrobial agents by inhibiting bacterial growth and activity. The protection principle is based on the inhibition of folic acid synthesis. They are used in the prevention and treatment of bacterial infections, diabetes mellitus, edema, hypertension, and gout. Today, sulfonamides are mainly used in combination with other antibiotics [4].

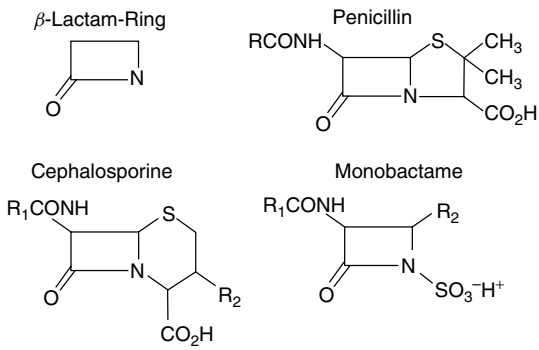

Figure 2.18.1. Group of the β-lactame antibiotics.

N-acetyl cysteine (NAC; $C_5H_9NO_3S$) is an altered form of the amino acid cysteine [5], which is commonly found in food and synthesized by the body. NAC helps break down mucus and prevents recurrences in people with chronic bronchitis. NAC may also protect lung tissue through its antioxidant activity.

So far, the useful aspects of sulfur compounds had been briefly summarized, but there is also another side of the medal. Elemental sulfur is relatively harmless for humans but is very toxic to many fungi and bacteria. Hydrogen sulfide can be metabolized in very small concentrations, but in higher concentrations can cause death by respiratory paralysis (maximum allowable concentration (MAC) [H_2S]: 15 mg m^{-3}). Sulfur dioxide, SO_2, a colorless gas, is toxic, highly soluble, and consequently absorbed in the moist passages of the upper respiratory system. Depending on the levels and the exposure period, SO_2 can be the origin of several health effects ranging from increased cardiovascular morbidity to increased airway resistance. Exposure to SO_2 levels in the order of 3 mg m^{-3} leads to constriction of the airways in the respiratory tract. At lower levels (down to 0.7 mg m^{-3}), SO_2 causes significant bronchial constriction in asthmatics (MAC [SO_2]: 5 mg m^{-3}). More details of the toxicology, recommended maximum levels, and possible health effects are given by Seinfeld and Pandis [6] in reports of the World Health Organization (WHO) [7].

Historically, SO_2 and particulate matter derived from the combustion of fossil fuels have been the main components of air pollution in many parts of the world. The most serious problems have been experienced in large urban areas where coal has been used in poorly controlled combustion systems for domestic heating and/or industrial installations. Especially, cities in cold climates where electric power generation and domestic heating are major sources of emissions are affected. The most typical

example was the famous "London smog" and the December 1952 incident leading to a significant number (about 4000) of deaths. Since that time, a lot of efforts have been made to reduce the anthropogenic emission of SO_2 by desulfurization of waste gases.

In Western Europe and North America, concentrations of sulfur dioxide in urban areas have declined in recent years because of regulations and control of emissions. Many highly industrialized countries have already established national monitoring networks, so that SO_2 meanwhile belongs to one of the most measured species and is often measured simultaneously with CO_2 and NO_X.

Annual mean concentrations in industrial areas are now mainly in the range 20–60 $\mu g\,m^{-3}$, with daily means seldom above 125 $\mu g\,m^{-3}$. However, in large cities where coal is still widely used for domestic heating or cooking or where there are poorly controlled industrial sources, concentrations may be 5–10 times higher than the latter value.

Sulfuric acid is a strong acid that is formed from the reaction of sulfur trioxide gas (SO_3) with water. Sulfuric acid is strongly hygroscopic. The formation of very small particles of sulfuric acid occurs by nucleation. Many vapors are able to condense on the surface of existing very fine nuclei and lead to the growth of composite particles. Sulfuric acid vapor, unlike many other vapors, exhibits the property of being able to condense and produce nuclei *de novo*. Oxidation of sulfur dioxide, especially at the surface of particles in the presence of metallic catalysts, leads to the formation of sulfurous and sulfuric acids. Neutralization, by ammonia, leads to the production of bisulfates and sulfates.

SO_2 via its oxidation to H_2SO_4 can also affect several atmospheric properties by reducing the visibility, increasing fog formation and precipitation, and finally by reducing solar radiation [6]. SO_2 and consequently H_2SO_4 are among the major constituents of the acid rain. They are transported by air streams to areas with low local anthropogenic emission. Therefore, both compounds have been suspected to play a key role in the rapid forest decline observed in some areas of Central Europe in the 1980s and 1990s.

To summarize, the industrial importance and the great extent of sulfur compounds used as fertilizers, pesticides, insecticides, and drugs compels the analysis of sulfur-containing species in the environment as well as in foodstuff, for instance, in plants (fruits, grain), in meat, or in beverages such as in wine. On the one hand, as the physiological and toxicological effects of sulfur compounds highly differ, it is necessary to gain species-selective information about manmade sulfur pollution. On the other hand, sulfur compounds are present in the environment naturally, and also here speciation analysis is needed to trace back the source of origin as well as to understand the processes involved.

2 CHEMISTRY

The most stable allotropic form of elemental sulfur is the yellow orthorhombic α-modification, which consists of S_8 molecules. Sulfur occurs in five oxidation states varying from (-2) (sulfides) to $(+6)$ (sulfate). Compounds at the highest oxidation state are relatively stable. On the other hand, compounds with oxidation states of $(-2, -1,$ 0 and $+4)$ are quite reactive, especially under atmospheric conditions, leading to formation of S at oxidation state of $(+6)$. Water solubility of sulfur compounds increases with oxidation state; reduced sulfur species occur mainly in the gas phase, whereas the S $(+6)$ compounds often tend to be found in particles or droplets [8].

Sulfur does not react with water under normal conditions but is soluble in carbon disulfide. It reacts with oxygen to form the gaseous sulfur dioxide, SO_2.

$$S_8(s) + 8O_2(g) \longrightarrow 8SO_2(g) \qquad (2.18.2)$$

SO_2 is also produced whenever metal sulfides are oxidized. By further oxidation, SO_3 is formed, which is used for the production of sulfuric acid, H_2SO_4.

$$2SO_2 + O_2 \longrightarrow 2SO_3 \qquad (2.18.3a)$$

$$SO_3 + H_2O \longrightarrow H_2SO_4 \qquad (2.18.3b)$$

$$SO_3 + H_2SO_4 \longrightarrow H_2S_2O_7 \qquad (2.18.3c)$$

In the troposphere, similar reactions for the oxidation of SO_2 to H_2SO_4 via SO_3 take place,

whereas the oxidizing process depends on the concentration of free radicals (NO, OH) and oxidants (H_2O_2, O_3, NO), on temperature and humidity conditions (stationary temperature inversions), and time of day (photolytic oxidation).

$$SO_2 + 2O_2 \longrightarrow SO_3 + O_3$$

("photo smog" conditions, with NO) (2.18.4a)

$$SO_2 + O_3 \longrightarrow SO_3 + O_2$$

("lack" of NO, OH radical as catalyst) (2.18.4b)

$$SO_2^{(\text{dissolved})} + 2H_2O \longrightarrow HSO_{3^-} + H_3O^+$$

(reaction with water droplets, rain, or fog) (2.18.5a)

$$HSO_3^- + H_2O_2 \longrightarrow SO_4^{2-} + H_3O^+ \quad (2.18.5b)$$

$$SO_2 + H_2O + 1/2O_2 \longrightarrow H_2SO_4$$

(catalytic reaction at sooty particles) (2.18.6)

As already mentioned, manmade SO_2 can also cause severe health effects in the respiratory tract of human beings. Absorption of sulfur dioxide mainly takes place in the mucous membranes of the nose and upper respiratory tract, which is a result of its solubility in aqueous media: 1 volume of water dissolves 45 volumes of sulfur dioxide at 15 °C. Absorption is concentration-dependent, with 85% absorption in the nose at 4–6 $\mu g\,m^{-3}$ and about 99% at 46 $\mu g\,m^{-3}$. Amdur pointed out that at common ambient concentrations of sulfur dioxide [9], absorption in the upper airways may be inefficient. Increased flow rates reduce the percentage of inspired sulfur dioxide absorbed in the nose and upper airways, and thus promote delivery to the smaller airways. Ammonia is found in the mouth (a product of bacterial metabolism) and may play a role in neutralizing acid aerosols. Sulfite and bisulfite are thought to be the major ions formed on absorption of sulfur dioxide. The key reactions are:

$$SO_2 + H_2O \longrightarrow H_2SO_3 \quad (2.18.7)$$

$$H_2SO_3 + H_2O \longrightarrow HSO_3^- + H_3O^+ \quad (2.18.8)$$

$$HSO_3^- + H_2O \longrightarrow SO_3^{2-} + H_3O^+ \quad (2.18.9)$$

The pK_a values of equations (2.18.8) and (2.18.9) are 1.86 and 7.2, respectively. The pH of the surface fluid in the respiratory tract is 6.5–7.5, and thus appreciable amounts of both the bisulfite and the sulfite will be present. Absorbed bisulfite is converted to sulfate by molybdenum-dependent sulfite oxidase. The highest concentrations of this enzyme occur in the liver and kidney, while lower levels are found in the lung, too.

Sulfur forms a variety of oxides and oxygen-containing acids in nearly all oxidation states. Among the oxides, SO_2 and SO_3 are the most important and most stable ones. Most of the acids exist only in aqueous solution or in form of their salts. Thiosulfates ($S_2O_3^{2-}$), sulfites (SO_3^{2-}), disulfites ($S_2O_5^{2-}$), and dithionites ($S_2O_4^{2-}$) are important reducing agents for many applications. There are several oxidation-reduction-equilibrations among the acids and salts, most of which depend on the pH-value.

Four stable isotopes (32, 33, 34, and 36) exist for sulfur. Their abundance is 95, 0.76, 4.22, and 0.014%, respectively, leading to an average atomic weight of 32.064. In biological and geochemical processes, slight changes of the isotope ratios are observed. This fractionation of sulfur isotopes can be caused, for instance, by exchange reactions between sulfates and sulfides, kinetic isotopic effects in the bacterial reduction of sulfate, or during precipitation of sulfates in seawater. Sulfur isotope ratios show variations due to matrix, location, and origin.

3 SULFUR SPECIES IN THE ENVIRONMENT

In the environment, in the course of biological utilization sulfur participates in a complex chain of oxidation-reduction reactions, whereby the element is circulated through the various biosphere reservoirs of organic and inorganic sulfur compounds. Table 2.18.1 summarizes the active reservoirs of sulfur near the earth's surface.

Lithosphere, sedimentary rocks, and seawater are the most important reservoirs of sulfur in the environment. The atmosphere balance, although among the smallest reservoirs of S balance,

Table 2.18.1. Active reservoirs of sulfur near the surface of the earth ([9] and [10]).

Reservoir	Mass (10^{12} gS)
Atmosphere	1.6–3.2
Seawater	1.3×10^9
Ocean sediments	3×10^8
Lithosphere	2×10^{10}
Marine biota	30
Soils and land biota	3×10^5
Lakes and rivers	300
Total	2.2×10^{10}

plays an important role in both the tropospheric and stratospheric balance of atmospheric gases. Investigations of the atmospheric sulfur cycle have been a subject of intense scientific interest for many years.

Table 2.18.2 compiles an overview of the most important sulfur compounds in the environment. Sulfur is emitted into the atmosphere both in gaseous and particulate forms from various sources. A summary of the most important sources and species emitted is given in Table 2.18.3. Estimates of manmade sulfur emissions to the atmosphere fall into a relatively narrow range of 73–80 Tg (S) a^{-1} [11, 12]. In contrast, the characteristics of the natural biogeochemical sulfur cycle in the atmosphere-biosphere-ocean system are much less well known because of 1) the difficulty of accurately determining the various biogenic sulfur species; 2) the technical problems of measuring emission fluxes from natural sources; and 3) the inadequate geographical coverage of existing data.

As can be seen from Table 2.18.3, the total flux of sulfur compounds into the atmosphere, including anthropogenic sources, is varying from 140 to 450 Tg (S) a^{-1}. The most uncertain flux is the emission of particulate sulfate as sea spray. Without this uncertain source, the flux of sulfur compounds into the atmosphere would be in the range of 100–120 Tg (S) a^{-1}.

In industrialized regions such as the United States and most parts of Europe, anthropogenic sulfur emissions (mainly comprised of SO_2) exceed natural emissions almost by 1 order of magnitude. On a global scale, biogenic emissions become important with contributions to the sulfur budget of 15–20% and 50–60% in the northern and

Table 2.18.2. Identified atmospheric sulfur compounds ([8], [10], and [12]).

Name	Formula	Chemical structure	Oxidation state	Usual atmospheric state
Hydrogen sulfide	H_2S		−2	Gas
Dimethyl sulfide	CH_3SCH_3	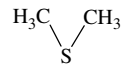	−2	Gas
Carbon disulfide	CS_2	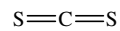	−2	Gas
Carbonyl sulfide	COS	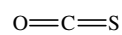	−2	Gas
Methyl mercaptan	CH_3SH	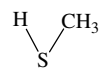	−2	Gas
Dimethyl disulfide	CH_3SSCH_3	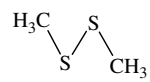	−1	Gas
Dimethyl sulfoxide	CH_3SOCH_3	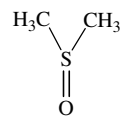	0	Gas

(*continued overleaf*)

Table 2.18.2. (*continued*)

Name	Formula	Chemical structure	Oxidation state	Usual atmospheric state
Sulfur dioxide	SO_2	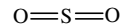	4	Gas
Sulfuric acid	H_2SO_4	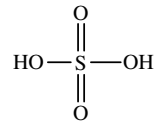	6	Gas aqueous/aerosol
Methane sulfonic acid	CH_3SO_3H	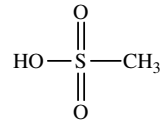	6	Gas aqueous/aerosol
Methane sulfinic acid	CH_3SO_2H	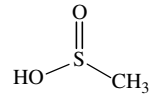	6	Gas aqueous/aerosol
Dimethyl sulfone	$CH_3SO_2CH_3$	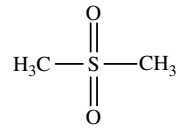	6	Gas
Monomethyl sulfate	CH_3SO_4H	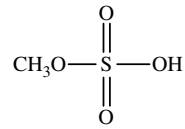	6	Gas
Dimethyl sulfate	$(CH_3O)_2SO_2$	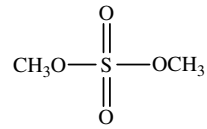	6	Gas
Hydroxymethane sulfonic acid	$HOCH_2SO_3H$	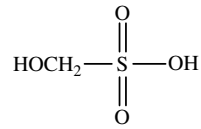	6	Aqueous
Bis-hydroxymethyl sulfone	$(CH_2OH)_2SO_2$	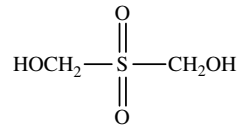	6	Aqueous/aerosol

southern hemispheres, respectively. Dimethyl sulfide (DMS: CH_3SCH_3) constitutes approximately 50% of the biogenic emissions. Thus, atmospheric sulfur compounds can have a significant environmental impact both locally and globally [8, 10, 12].

3.1 Transformation of sulfur compounds in the environment

3.1.1 Biochemical transformations

A simplified, conceptual overview of the global biogeochemical cycle of sulfur is shown in

Table 2.18.3. Estimates of sulfur emissions (Tg (S) a^{-1}) ([12] and [11]).

Compound source	H_2S	DMS	CS_2	COS	SO_2	Sulfate
Oceans	<0.5	15–25	0.3	0.17	–	40–320 (Sea spray)
Coastal wetlands	0.006–1.0	0.003–0.7	0.06	0.0006–0.12	–	–
Soils and plants	0.17–0.53	0.05–0.2	0.6–0.8	0.01–0.03	–	2–4 (Dust)
Biomass burning	–	–	–	0.01	2.8	–
Volcanoes	0.5–1.5			0.01	7–8	2–4
Total	0.7–3.5	15–26	0.1–1.3	0.2–0.3	10–11	4–8
Total natural sulfur emissions (without sea salt sulfate and dust)						25–40
Anthropogenic sulfur emissions						73–80
Total global sulfur emissions (without sea salt sulfate)						98–120

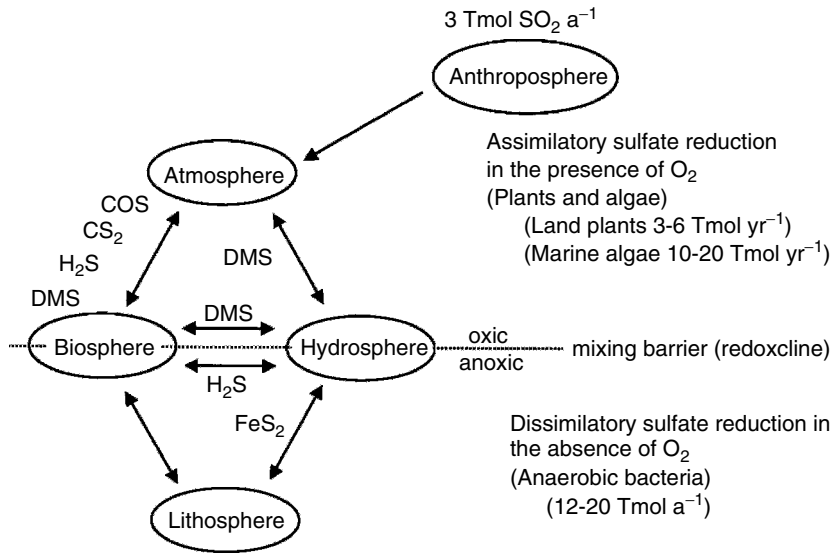

Figure 2.18.2. Interactions in the global biogeochemical sulfur cycle. (Reproduced with permission from Andreae, M. O. and Jaeschke, W., Exchange of sulphur between biosphere and atmosphere, over temperate and tropical regions, Scope 48, in *Sulphur Cycling on the Continents: Wetlands, Terrestrial Ecosystems and Associated Water Bodies*, Howarth, R. W., Stewart, J. W. B. and Ivanov, M. V. (Eds.), copyright SCOPE, 1992, John Wiley & Sons Ltd., Chichester, UK 376 [11].)

Figure 2.18.2. The global environment is subdivided into four compartments: atmosphere, biosphere, hydrosphere, and lithosphere, the latter including sediments and rocks of the earth's crust. Two types of biochemical pathways of sulfate reduction are important in the global cycles: dissimilatory and assimilatory sulfate reduction. The influence of these two pathways on sulfur cycling between biosphere and atmosphere is shown in Figure 2.18.3.

Dissimilatory reduction of sulfate is a strictly anaerobic process that takes place only in anoxic environments (such as stratified, anoxic water basins and in sediments of wetlands, lakes, and coastal marine ecosystems). Sulfate-reducing bacteria use a variety of sulfur compounds for their respiratory metabolism. In these cases, sulfate instead of molecular oxygen [11] acts as terminal electron acceptor. Globally, dissimilatory sulfate reduction is the major pathway for the production of H_2S.

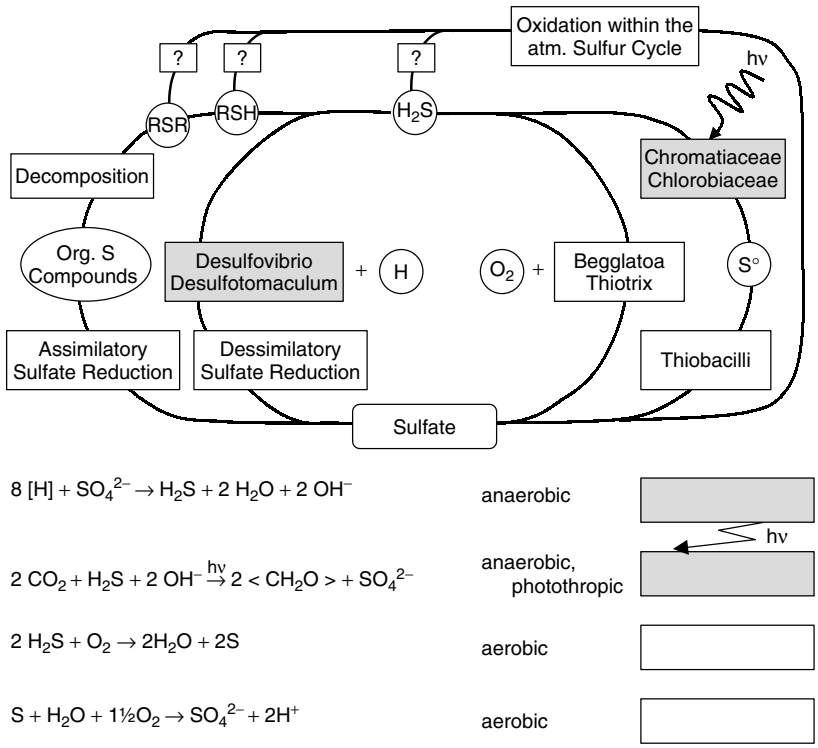

Figure 2.18.3. Scheme of the microbiological cycle of sulfur and its possible influence on the atmosphere. (Reproduced with permission from Andreae, M. O. and Jaeschke, W., Exchange of sulphur between biosphere and atmosphere, over temperate and tropical regions, Scope 48, in *Sulphur Cycling on the Continents: Wetlands, Terrestrial Ecosystems and Associated Water Bodies*, Howarth, R. W., Stewart, J. W. B. and Ivanov, M. V. (Eds.), Copyright SCOPE, 1992, John Wiley & Sons Ltd., Chichester, UK 376 [11].)

In contrast to animals, which are dependent on organo-sulfur compounds in their food to supply their sulfur requirement, other biota (bacteria, cyanobacteria, fungi, eukaryotic algae, and vascular plants) can obtain sulfur from assimilatory sulfate reduction in order to synthesize organo-sulfur compounds [13]. Sulfate is assimilated from the environment, reduced inside the cell, and fixed into sulfur-containing amino acids and other organic compounds. The process is ubiquitous in both oxidic and anoxic environments. Most of the reduced sulfur is fixed by the intracellular assimilation process, and only a minor fraction of the reduced sulfur is released as volatile compounds as long as the organisms are alive. However, when organisms die, microbial degradation liberates reduced sulfur compounds to the atmosphere. A compilation of the most prominent biochemical precursors of volatile sulfides produced in soils by microbial degradation of organic matter under aerobic and anaerobic conditions is given in Table 2.18.4.

Table 2.18.4. Biochemical origin of volatile sulfides produced in soils by the microbial degradation of organic matter under aerobic and anaerobic conditions ([14]).

Compound	Precursor
H_2S	Proteins, polypeptides, cystine, cysteine, glutathione
CH_3SH	Methionine, methionine sulfoxide, methionine sulfone, *S*-methyl cysteine
CH_3SCH_3	Methionine, methionine sulfoxide, methionine sulfone, *S*-methyl cysteine, homocysteine
CH_3SSCH_3	Methionine, methionine sulfoxide, methionine sulfone, *S*-methyl cysteine
CS_2	Cysteine, cystine, homocysteine, lanthionine, djenkolic acid
COS	Lanthionine, djenkolic acid

Source: Warneck, P., *Chemistry of the Natural Atmosphere*, Academic Press, San Diego, CA, New York, 1988, p. 499.

Table 2.18.5(a,b). Summary of the most relevant gas/aqueous-phase reactions of the most abundant S species in the atmosphere.

(a)

Gas phase reaction	Products	k (298 K) (cm^3 $molecule^{-1}$ s^{-1})	Reference
$CH_3SCH_3 + OH \rightarrow$ (Abstraction channel)	SO_2, MSA	4.8×10^{-12}	Atkinson *et al*. [15]
$CH_3SCH_3 + OH \rightarrow$ (Addition channel)	DMSO	1.7×10^{-12}	Atkinson *et al*. [15]
$CH_3SCH_3 + NO_3 \rightarrow$	SO_2, MSA, HNO_3	1.1×10^{-12}	Atkinson *et al*. [15]
$CH_3SCH_3 + Cl \rightarrow$	SO_2, MSA, HCl	$3.3 \pm 0.5 \times 10^{-10}$	Stickel *et al*. [16]
$CH_3SCH_3 + BrO \rightarrow$	DMSO	4.40×10^{-12}	Ingham *et al*. [17]
$CH_3SOCH_3 + OH \rightarrow$	MSIA	$(8.7 \pm 1.6) \times 10^{-11}$	Urbanski *et al*. [18]
$CH_3SO_2H + OH \rightarrow$	SO_2	$(1 \pm 0.2) \times 10^{-10}$	Kukui *et al*. [19]
$SO_2 + OH$ (multiple steps) $\rightarrow$	H_2SO_4	8.9×10^{-13}	Berresheim *et al*. and references therein [12]
$CS_2 + OH + M \rightarrow$ $M = (N_2$ and/or $O_2)$	$SO_2 + COS + CO$	1.2×10^{-12}	Berresheim *et al*. and references therein [12]
$H_2S + OH + M \rightarrow$ $M = (N_2$ and/or $O_2)$	$SH + H_2O$	4.8×10^{-12}	Berresheim *et al*. and references therein [12]
$COS + hv \rightarrow$	$CO + S$		
$S + O_2 \rightarrow$	$SO + O$	2.1×10^{-12}	Berresheim *et al*. and references therein [12]
$SO + O \rightarrow$	$SO_2 + O$	6.7×10^{-17}	

(b)

Liquid-phase reaction	Products	k (M^{-1} s^{-1}) at 295 ± 2 K	Reference
$OH + DMS \rightarrow$	DMSO, MS^-	1.9×10^{10}	Bonifacic *et al*., 1975 [20]
$O_3 + DMS \rightarrow$	DMSO	$6.1–8.6 \times 10^8$	Lee and Zhou [21] Gershenzon *et al*. [22]
$OH + DMSO \rightarrow$	MSI^-	$4.5–5.4 \times 10^9$	Milne *et al*. [23] Bardouki *et al*. [24]
$OH + MSI^- \rightarrow$	MS^-	1.2×10^{10}	Bardouki *et al*. [24]
$S(IV) + O_3$	SO_4^{2-}	$5 \times 10^4–10^8$	(pH dependent) Seinfeld and Pandis [8]
$S(IV) + H_2O_2$	SO_4^{2-}	$0.7–5 \times 10^5$	(pH dependent) Seinfeld and Pandis [8]

3.1.2 Chemical transformations (gaseous/aqueous-phase reactions) in the atmosphere

Tables 2.18.5(a,b) list the most important reactions of DMS, sulfur dioxide (SO_2), dimethyl sulfoxide (DMSO), methanesulfinic acid (MSIA), and methanesulfonic acid (MSA) reported for the gas/aqueous phase.

3.1.2.1 Gas phase

In the remote marine atmosphere, DMS is the most important gaseous sulfur species. It can react with several radicals (OH, NO_3, BrO and Cl), leading to a variety of products. Indeed, reaction of DMS with OH radicals will lead to SO_2 and DMSO formation, reaction with Cl and NO_3 will lead to SO_2, and reaction with BrO will mainly produce DMSO. Reaction of DMS with OH and eventually BrO dominates during daytime, whereas reaction with NO_3 radicals occurs during nighttime. The relative importance of these pathways is most likely a function of latitude, altitude, and season of the year [12].

DMSO is considered to be an important intermediate in the atmospheric oxidation of DMS. DMSO reacts an order of magnitude faster than DMS with OH. Kukui *et al*. [19] report that the

reaction of OH with DMSO forms predominantly MSIA and a rate coefficient of $(1 \pm 0.2) \times 10^{-10}$ cm^3 molecule^{-1} s^{-1} was determined for OH and MSIA at room temperature, leading mainly to SO_2 formation.

For carbon disulfide (CS_2), the dominant sink is the reaction with OH radicals. Carbonyl sulfide (COS), CO, and SO_2 have been observed as products with yields of 0.83, 0.165 and 1.15%, respectively. The above reaction generates about 30% of total COS in the atmosphere (Berresheim *et al.* [12] and references therein).

COS is the S compound with longest lifetime in the atmosphere (see Berresheim *et al.* [12] and references therein). Consequently, it mixes into the stratosphere, where the dominant loss processes are photolysis and reaction with atomic oxygen, leading to sulfate formation. Thus, COS is the main source of stratospheric sulfate during volcanically quiescent periods.

Hydrogen sulfide (H_2S) in the atmosphere reacts mainly with OH radicals, leading to SO_2 formation that consequently participates either in homogeneous (gas phase) or in heterogeneous (fog, cloud droplets and on surface of aerosols) reactions, or both. The gas phase oxidation of SO_2 by OH radicals involves four elementary steps and leads to H_2SO_4 formation.

3.1.2.2 Aqueous phase

In aqueous solution, DMS reacts very rapidly with OH radicals via a complex reaction forming mainly DMSO with a diffusion-limited second-order rate constant of 1.9×10^{10} M^{-1} s^{-1} [20].

A very rapid reaction of $6.1 - 8.6 \times 10^8$ M^{-1} s^{-1} (more than 10^6 times faster compared to the gas phase) was also reported for DMS and O_3 by Lee and Zhou [21] and Gershenzon *et al.* [22], respectively. Contrary to the gas phase, this reaction will lead to DMSO formation with 100% yield.

The mechanism of aqueous-phase oxidation of SO_2 has been extensively reviewed by several authors (see, for instance, Martin *et al.* [25]). For SO_2, a major heterogeneous removal pathway may be absorption on aerosols or hydrometeors followed by oxidation of SO_2 by O_3, H_2O_2, and/or metal-catalyzed oxidation by oxygen, which is pH dependent. Model calculations suggest that about 80–90% of SO_2 transformation to sulfate in the atmosphere takes place in the aqueous phase [26].

DMSO, MS^-, and MSI^- are highly water soluble. Multiphase reactions are expected to play an important role in determining the fate of these compounds in the atmosphere.

Bardouki *et al.* [24] studied the kinetics and product distribution of the reaction of DMSO and MSI^- with OH radicals in the aqueous phase. They found that DMSO reacts very fast ($k = 4.5 \times 10^9$ M^{-1} s^{-1}) with OH radicals. MSI^- has been identified as the main intermediate product, while MS^- and sulfate were the final products owing to the very fast reaction of MSI^- with OH radicals ($k = 1.2 \times 10^{10}$ M^{-1} s^{-1}).

MS^- can further react with OH radicals, leading to SO_4^{2-} production. However, as cited by Milne *et al.* [23], this reaction is almost 2 orders of magnitude slower compared to that of DMSO with OH radicals (4.7×10^9 M^{-1} s^{-1}).

Considering the rate constants of DMSO, MSI^-, and MS^- and the concentrations of the various reactants in the liquid phase (reported in Table 2.18.5(b)), it is clear that reactions of OH radicals with DMSO, MSI^-, and MS^- are the most important reactions that control the levels of these compounds in the liquid phase.

3.2 Analytical techniques for sulfur compounds

A variety of organic and inorganic S compounds occur in soil–plant–water systems. Although the sulfate ion is predominant, other inorganic S species and organic compounds can exist in significant levels. The variability ranges from accumulation of thiosulfate in mine tailing effluents [27] to accumulation of sulfides and organic S compounds in estuaries (like DMS, DMSO, COS, CS_2; see, for instance, *Watts* [28] and references therein). For convenience, the methods used will be discussed according to the type of samples analyzed.

3.2.1 Sulfur in soils

S compounds occur in soils both in inorganic and organic forms. Inorganic sulfate is present in soils as water-soluble salts, adsorbed onto soil colloids, or may occur as insoluble forms. Organic S is the dominant form of S in most soils. A detailed review of the analytical techniques for S determination in soils and plants can be found in the paper of Tabatabai [29]. In this work, only a short overview will be given.

3.2.1.1 Total sulfur

Wet chemical methods: The available methods for accurate determination of total S in soils involve two steps: (i) conversion of the various S compounds to one form, either by oxidation to sulfate (dry or wet procedure) or by reduction to sulfide (conversion to sulfate is more common than conversion to sulfide); and (ii) determination of the sulfate or sulfide produced [29].

Various techniques have been employed to oxidize soil S to sulfate. One of the most widely accepted procedures is fusion with Na_2CO_3 and an oxidizing agent. The procedure recommended by the Association of Official Agricultural Chemists (AOAC) 1955 requires fusion of the sample with Na_2CO_3 and Na_2O_2. This method is probably the best for all types of soils but tedious and operator-sensitive.

Several methods are available for determination of the oxidized S. Most of the oxidation procedures described lead to sulfate, which can be determined gravimetrically as $BaSO_4$ (AOAC, 1955), turbidimetrically [30], colorimetrically after its reduction to H_2S [31] or by use of ion chromatography (IC). IC is a simple, highly sensitive, and accurate method for determination of SO_4^{2-} with the lowest detection limit among the above-mentioned techniques (lower than 1 ng mL^{-1}). Ion chromatographs feature high-speed separation and continuous monitoring, which yield instantaneous readout of analytical data. One of the advantages of the IC method is that in addition to sulfate, several other anions can be determined simultaneously in about 10 min.

However, methods involving conversion of soil S to SO_2 and determination of the SO_2 evolved are also available [32, 33]. An ion chromatographic method was also developed for determination of total S in soils [34]. It involves ignition of a mixture of soil and $NaHCO_3$ containing Ag_2O at 550 °C for 3 h. The residue thus obtained is dissolved in 1 M HOAc, diluted with deionized water, filtered, and analyzed for SO_4^{2-} by an ion chromatograph.

Automated instrumental methods: Several instrumental methods are available for the determination of total S in soils. An example is the LECO S analyzer (LECO Corp., St Joseph, Mich.). The sample is mixed with combustion accelerators in a ceramic boat and combusted in a resistance furnace at 1371 °C in an O_2 atmosphere. The SO_2 thus produced is passed through an infrared (IR) cell, which continuously detects total S as SO_2. David *et al.* [35] used this analyzer for determination of total S in soils and sediments and showed that the results obtained by this instrument agreed with those by current methods used for determination of total S in such materials. Sample analysis lasts <3 min and the instrument provides a direct readout of total S values.

3.2.1.2 Inorganic sulfur

The inorganic S fraction in soils may occur as sulfate and compounds of lower oxidation state such as sulfide, polysulfide, sulfite, thiosulfate, and elemental S. Accurate determination of the reduced forms of inorganic S in soils is difficult, partly because of the ease with which they can be oxidized when exposed to the air, but mainly because of the limitations of current analytical methods. There is no procedure entirely satisfactory for determination of sulfide in soils.

A polarographic method for determination of the reduced S species in marine pore waters has been proposed by Luther *et al.* [36]. They have demonstrated that, with polarographic techniques, it is possible to measure thiosulfate, sulfide, bisulfide, and polysulfide ions using a mercury

electrode. Tetrathionate and other polythionates can be measured by this technique.

Inorganic sulfate may occur in soils as water-soluble salts, may be absorbed by soil colloids, or may occur as insoluble forms, depending on several soil properties [37]. Because of the effect of seasonal conditions on mineralization of organic S, leaching of soluble sulfate, and sulfate uptake by plants, it is very common to observe a considerable seasonable fluctuation in the amounts of water-soluble sulfate in surface soils. Other factors that may affect the concentration of water-soluble sulfate in soils are application of fertilizer materials and the sulfate content of rain and irrigation waters [38].

An approach involving displacement of the adsorbed sulfate in soils by shaking with an appropriate solution can be used to estimate the amount of adsorbed sulfate in soils. Several reagents have been proposed for extraction of soluble sulfate plus a fraction of the adsorbed sulfates, like $NaHCO_3$ [39], $CaCO_3$ suspensions [40], neutral 1 mol L^{-1} NH_4OAc [41], acid NH_4OAc [42], and Morgan's solution [43]. The adsorbed sulfate may also be displaced by solutions containing anions of greater coordinating ability according to the following order [44]:

$$\text{Hydroxyl} > \text{Phosphate} > \text{Sulfate} = \text{Acetate} > \text{Nitrate} = \text{Chloride}$$

Sulfate can be extracted by one of the methods described in 3.2.1.1.

3.2.1.3 Organic sulfur

Although the chemical nature of organic S in soils has been under investigation for the past decades, still little is known about the organic S compounds present in soils, but three broad groups of S compounds have been recognized:

1. Organic S that is reduced to H_2S by HI. This S is not bound directly to C and is believed to be largely in the form of ester sulfates (e.g. phenolic sulfates).
2. Organic S that is reduced to inorganic sulfide by Raney Ni and that seems to consist almost entirely of S in the form of amino acid (e.g. Cys and Met).
3. Organic S that is not reduced by either HI or Raney Ni. This fraction is assumed to consist of S bound directly to C but not recoverable by current methods used for estimation of C-bonded S (fraction 2).

Unfortunately, no satisfactory direct method is available for the determination of the total organic S or the organic S fraction reducible by HI. These fractions, however, can be determined indirectly. The total organic S can be determined in a soil residue after extraction of inorganic S or by the difference involving subtraction of the inorganic S fraction from total S. The organic S reducible by HI or Raney Ni can be estimated by subtracting the extractable inorganic S fraction from the fraction of S reducible by HI and by subtracting inorganic reduced S compounds from the fraction of S reducible by Raney Ni [45].

3.2.2 Sulfur in plants

Sulfur as an essential plant nutrient occurs in a variety of different forms in many plant compounds. Sulfur metabolism in plants and the role and requirements of S in plant nutrition have been reviewed by Thompson *et al*. [46] and Duke and Reisenauer [47]. Although S in plants can be found as organic and inorganic compounds, in most plant materials more than 90% of the total sulfur consists of Met and Cys [48].

3.2.2.1 Total sulfur

To estimate the total S in plant materials, it is necessary to convert all S into one form that can be determined accurately. This can be accomplished by one of several dry ashing or wet digestion procedures. Determination of S in the ashed or digested material is then performed by a suitable analytical technique. A characteristic example is

the technique developed by Tabatabai *et al*. [34] (see Section 3.2.1.1).

Guthrie and Lowe [49] evaluated the Fisher Model 475 sulfur analyzer for the determination of total S in plant materials. In this method, the sample was weighed into a ceramic combustion boat and covered with V_2O_5 powder, which acts as a flux to moderate sample combustion. The sample and boat were placed into a high temperature (1350 °C) resistance type tube furnace, in which all forms of S were converted to SO_2 in an oxygen atmosphere at reduced pressure and can be analyzed by IR spectroscopy. The time required for each analysis depends on the sample size and S concentration, but was generally between 3 and 4 min.

3.2.2.2 Inorganic sulfur

The various extractants used for obtaining sulfate and extractable S from plant tissue are summarized by Beaton *et al*. [50]. Among the extractants most frequently used are dilute HC1, direct treatment with the Johnson and Nishita [31] reducing mixture, water, ethanol, and trichloroacetic acid. A number of other extractants including acetic acid, ammonium acetate plus acetic acid, sodium acetate plus acetic acid, sodium hydroxide, water plus magnesium carbonate, refluxing with water plus magnesium oxide and cadmium chloride or cadmium hydroxide, acetone and ninhydrin have also been used to remove sulfate and extractable S from plant tissue. Sulfate was also extracted with electrodialysis and determined using one of the techniques already described in Section 3.2.1.1.

3.2.3 Sulfur in waters

Sulfur enters natural waters from various sources. The weathering of rocks and soil directly exposed to surface waters is usually the largest natural source. Atmospheric fallout can introduce relatively large quantities of S compounds into the natural-water systems. Other anthropogenic inputs, including the discharge of various treated and untreated waters to the receiving waters or the contamination of the aquatic systems through mining operations, can introduce large quantities of S compounds into natural waters. Degradation products of plant and animal tissues also contribute organic and inorganic S compounds to receiving waters. Other sources of S in natural waters are the S-containing fertilizers added to agricultural lands. The organic and inorganic S in natural waters is subject to complex abiotic and biological interactions [51].

Most of the S in natural waters occurs as SO_4^{2-}. Reduced organic S species (like DMS, its precursor dimethylsulfoniopropionate (DMSP), and its oxidation products DMSO, COS, CS_2, mercaptans, etc.) are also present in natural waters.

Sulfate, being a stable highly oxidized and soluble form of S, is the form in which the element is generally present in natural surface and ground waters. Sulfates in water are generally bound to alkali and alkaline earth metals and are readily soluble. Their concentration in natural waters, precipitation, and wastewaters will vary depending on the source and on the type of terrain to which they have been exposed. High concentrations may be found in some well waters and surface waters in arid regions where sulfate minerals abound.

Sulfur can also exist in natural waters under various forms. DMSx species (DMS, its precursor DMSP, and its oxidation product DMSO), CS_2 and COS are among the most common organic forms of S in natural waters (especially seawater). DMS is produced by some marine phytoplankton species, and once released in the atmosphere can have – through its oxidation products – direct and indirect effects on the climate [52, 53]. DMS is produced in seawater by the cleavage of β-DMSP that is associated in most of the cases with bacteria [53, 54]. Yield of the DMS production from DMSP cleavage is highly variable and reported to vary between 12 and 66% [54]. DMSP is produced by some classes of marine phytoplankton and is dependent on taxonomic groups (Liss *et al*. [55] and references therein). Ventilation to the atmosphere as well as bacterial consumption, photodegradation, and downward mixing has been identified as the major sinks for DMS in seawater. Even though DMSO has been firmly identified

as a major DMS oxidation product in seawater from photodegradation and/or microbial and anaerobic processes, its biotic production in oxic waters remains unclear. Production and fate of DMSO in seawater is an important issue since DMSO can in turn act as a source of DMS from bacteria reduction. Besides DMS, seawater has also been identified as a significant source of various sulfur compounds (S compounds) and especially COS and carbon disulfide (CS_2) (Watts [28] and references therein).

DMS, COS, and CS_2 in natural waters are measured after extraction, which can be conducted under helium flow. Sulfur species are preconcentrated on a support immersed in liquid nitrogen (e.g. Tenax, Teflon, or gold wool). After trapping, the sulfur gases are introduced in a packed column (e.g. Chromosil 310 or 330) by heating the trap. The analysis is made using a gas chromatograph (GC) equipped with a sulfur chemiluminescence detector or flame photometric detector (FPD). The detection limit is in the order of 0.1 ng or below for all compounds of interest [56, 57].

For DMSP analysis, the samples are conditioned by addition of 1 mL of NaOH (10 M) in 60-mL glass vials. Thus, DMSP is hydrolyzed to DMS, which is subsequently analyzed using the technique described above [58].

For DMSO, the samples are conditioned with 1 mL HCl (fuming acid) in 60 mL plastic vials following the recommendation made by Andreae [56]. A technique based on an *in situ* reduction of DMSO to DMS using sodium borohydride ($NaBH_4$) can be used to determine DMSO in seawater. Produced DMS was subsequently preconcentrated using the previously described purge-and-cryotrap technique and GC-FPD analysis. More details about the analysis of DMSO are reported by Sciare and Mihalopoulos [57]. Presence of DMS in the sample as well as the quantitative reduction of DMSP by $NaBH_4$ in the samples should be taken into account by analyzing an aliquot for DMS+DMSP after alkaline hydrolysis as described above. DMSO corresponds to the difference of the measured DMS (after the reduction by $NaBH_4$) minus (DMS+DMSP).

3.2.4 Sulfur in the atmosphere

As already discussed at the beginning of this Section (Table 2.18.3), S is emitted into the atmosphere both in gaseous and particulate forms from various sources.

3.2.4.1 Sulfur species in particulate form

Sulfate and methanesulfonate are the main S species existing in the atmosphere in particulate form. Their collection is performed using filters (preferably inert filters like Teflon). After collection, the filters are extracted by Milli-Q water, and the extracts are analyzed using ion chromatography.

Nonsoluble (for instance, some metal-) sulfides are more difficult to analyze. Some of these metal sulfides can have carcinogenic properties and therefore are of analytical interest. They can be set free during metal production and can even be transported over long distances by particulate matter. A speciation procedure for sulfidic nickel in particulate matter has been described by Füchtjohann *et al*. [59]. The procedure is based on sequential extraction of aerosols collected close to a metallurgical plant and detection by graphite furnace (GF-AAS) and inductively coupled plasma mass spectrometry (ICP-MS). The sulfidic fraction never exceeded 10% of total Ni in the vicinity of the plant for steel production.

3.2.4.2 Sulfur species in gaseous form

DMS, SO_2, DMSO, COS, and CS_2 are the main S species in the atmosphere. For DMS, COS, and CS_2, the most widely used technique includes preconcentration of the gaseous S species on an inert substrate usually kept at a low temperature (down to $-187\,^{\circ}C$). After preconcentration, the

trap is heated and the sulfur species are analyzed as in the natural-water samples by a GC.

Bandy and his coworkers [60] developed a chromatographic technique coupled with mass spectrometry (GC/MS) with isotopically labeled S species (DMS, CS_2, COS, SO_2) used as internal standards. The sampling resolution ranged from 4 to 6 min, and the overall system had limits of detection (LOD) of about 1 pmol mol^{-1}. The system has been successfully applied in several occasions for airborne measurements.

The first measurements of DMSO in the gas phase were reported by Harvey and Lang [61] using preconcentration of DMSO on Tenax GC, followed by extraction with methanol, solvent evaporation, and subsequently analysis by gas chromatography (GC) using a Hall electrolytic conductivity detector. Berresheim *et al*. [62] reported a new technique without sample preconcentration for measuring DMSO in ambient air at the sub-pmol mol^{-1} level with a sampling time of about 60 s. This sensitive and precise technique is based on atmospheric pressure chemical ionization mass spectrometry (CIMS). Its major drawback is the need for a mass spectrometer in the field, which is not always feasible and is certainly quite expensive. Sciare and Mihalopoulos [57] presented a new technique for sampling and analyzing of atmospheric DMSO, based on the nebulization/reflux principle that has been proven very effective in quantitatively scrubbing water-soluble trace gases, such as DMSO, into aqueous media [63]. Air is drawn through a Teflon filter (porosity of 0.5 μm) to remove aerosol particles and create a mist with the water present in the nozzles that capture the DMSO existing in the atmosphere. The water droplets that contain DMSO are collected on the membrane and the wall of the chamber and coalesced into larger droplets falling back to the collector. DMSO analysis was performed by reduction of DMSO to DMS using sodium borohydride ($NaBH_4$) as described by Andreae [56]. This method has also been adapted and successfully improved for nanomolar aqueous DMSO determinations [58]. By using the above-mentioned flow rate and a classic FPD detector with detection limits of about 1 ng (DMS), atmospheric concentrations of DMSO down to 0.35 pmol mol^{-1} can be achieved for sampling times of 1 h.

3.2.4.2.1 Sulfur dioxide For SO_2 (especially for trace level determination), various techniques have been developed for sampling and analysis. They can be separated in three categories: 1) Wet chemical techniques, 2) GC-based techniques and 3) automatic techniques. A description of these techniques as well as the results of an intercomparison exercise among these techniques can be found at Stecher *et al*. [64].

The wet chemical techniques include nebulization/reflux principle, denuders, and Na_2CO_3-impregnated filters. All the above techniques are coupled with IC. After collection, the filters and denuders are extracted with water and the extract is analyzed for SO_2 using IC [65–67]. Aqueous chemiluminescence and high-performance liquid chromatography (HPLC) coupled with a fluorescence detector are two other widely used wet chemical techniques. At the aqueous chemiluminescence technique, air is passed through a filter impregnated with a solution of tetrachloromercurate(II) as absorbent. SO_2 forms a stable complex that is treated with an acidic cerium(IV) solution, and the occurring chemiluminescence is detected by a photomultiplier [68]. At the HPLC technique, SO_2 was analyzed by equilibrating the gaseous sample with aqueous SO_2, sulfite, and bisulfite, then converting the aqueous S(IV) to an isoindole derivative. The derivative was separated by reversed phase HPLC and detected via fluorescence [69]. The GC technique includes a cryogenic preconcentration as in the case of gaseous DMS and subsequently analysis using an FPD detector or GC/MS [60]. A modified pulsed fluorescence detector developed by Thermo Environmental Instruments (TECO 43s) is able to detect as little as 30 pmol mol^{-1} SO_2 in a 25-min sampling interval and can be used for continuous measurements of low-level SO_2 even in the remote troposphere [70].

3.2.4.2.2 Hydrogen sulfide For H_2S, a filter impregnated technique has been reported by Saltzman and Cooper [71], using a method similar to

that of Natusch *et al*. [72]. Air is drawn through a nitrate silver impregnated filter. Sulfide is recovered from the silver nitrate filters and analyzed by the fluorescence quenching of dilute fluorescein mercuric acetate added to the sample.

3.2.4.2.3 Atmospheric sulfuric acid and methanesulfonic acid H_2SO_4 and MSA in the gas phase are measured using CIMS on the basis of methods previously developed by Eisele and coworkers [73, 74]. At 5 min signal integration, the overall 2-sigma precisions and detection limits for both the H_2SO_4 and MSA measurements were 21% and 3×10^4 molecules cm^{-3} (5 min signal integration).

4 SPECIATION OF SULFUR IN ANALYTICAL BIOCHEMISTRY

The revolutionary improvements of mass spectrometric protein analysis in the last decades have been driven by the introduction and refinement of matrix assisted laser desorption/ionization mass spectrometry (MALDI-MS) and electrospray ionization mass spectrometry (ESI-MS) in combination with improvements in tandem MS technologies. This progress has been further fueled by bioinformatic methods that create direct links between MS raw data and biopolymer databases, which dramatically speed up the otherwise extremely time-consuming conversion of MS data into biologically meaningful results. In spite of the outstanding success of the organic mass spectrometric techniques in the molecular characterization of proteins and protein-derived peptides, a number of important analytical goals in proteomics are difficult to assess by the established MS methodologies. Quantification is one of these issues, which requires costly derivatization procedures [75] or metabolic stable-isotope labeling [76, 77] when performed by MALDI-MS or ESI-MS.

As an alternative, atomic spectroscopy has direct access to protein analysis via the determination of sulfur, which is present in the proteinogenic amino acids cysteine and methionine. As already mentioned, although both Cys and Met occur with less than average abundance in proteins, they are present in the vast majority of proteins. Together, they exhibit an amino acid abundance of about 3–4% in eukaryotic proteomes, which means that statistically all peptides/proteins with a length of at least 30 residues contain sulfur. Therefore, sulfur determination can be considered as a generic tool for the detection and quantification of proteins.

For speciation of heteroelements, in particular, of metals present in bio-macro-molecules more and more atomic spectroscopy is applied for detection in combination with high-resolution separation techniques [78]. Techniques for interfacing chromatography with atomic absorption spectroscopy (AAS), atomic fluorescence spectroscopy (AFS), inductively coupled plasma atomic emission spectrometry (ICP-AES), and ICP-MS look promising for many heteroelements [79, 80], but for sulfur speciation mainly ICP-MS is applied because of its high sensitivity, although detection of this element is hampered by spectral interferences. Instrumental approaches are most often used to overcome this limitation, for instance, by application of sector field mass spectrometers operated in a high mass resolution mode or alternatively by application of collision and reaction cell instruments operated with chemical or physical discrimination of the O_2 interference or by oxidation of sulfur for a shift in the mass range.

Thus, sulfur detection via ICP-MS, which is an established technique for quantitative trace element determination, can be applied directly to most proteins in their native, underivatized form. Finally, four stable isotopes of sulfur exist, so that sulfur can be detected with a certain flexibility including the application of stable-isotope dilution assays (see below).

In recent years, on-line coupling of ICP-MS to essential liquid chromatographic or electrophoretic techniques has been realized, so that complex samples of biological origin can be analyzed. With regard to all these technically favorable items, sulfur determinations by ICP-MS in proteomics can be identified as an emerging topic. The potential of this approach is highlighted in the following by a concise review of the recent applications in this field.

4.1 Metallothioneins

Metallothioneins are small cysteine-rich proteins (20 Cys residues) of about 6 kDa size optimized for binding of divalent cations such as Zn^{2+}, Cd^{2+}, or Cu^{2+}, which have widespread functions in homeostasis of both essential and toxic metals. For instance, upon Cd^{2+} stress, metallothionein expression is strongly upregulated with a concomitant increase in Cd-metallothionein complexes to reduce the levels of free Cd to physiological levels. In a study of Cd^{2+} stress-induced changes of the yeast proteome, it was observed that metallothionein induction is part of a dramatic shift of the cellular sulfur metabolism: Cd^{2+} stress effects that the biosynthetic sulfur flux is directed mainly to the synthesis of metallothioneins and glutathione, whereas the remaining proteome is depleted in sulfur [81]. As a mechanism for sulfur-depletion of the proteome without dramatic functional impairment, the expression of sulfur-poor enzyme-isoforms has been recognized.

Metal-loaded metallothioneins were analyzed in various studies by ICP-MS with respect to their metal content, but obviously sulfur is also a target element in metallothionein analysis. Thus, monitoring of sulfur in addition to the selected metals provides an extra evidence for their presence as metallothionein-bound species. Capillary electrophoresis (CE) [82–84] or anion-exchange chromatography [85] are the techniques frequently employed as separation techniques in these studies. In general, metallothionein analysis is a chromatographically demanding task, since natural metallothioneins are complex mixtures of several iso- and subisoforms with a potential of additional metal-microheterogeneity at their up to seven metal-binding sites.

A reverse isotope dilution principle was applied in combination with CE-ICP-MS for metallothionein quantification: The sheath liquid supplied to the CE-ICP interface was spiked with isotopically enriched metals and isotopically enriched sulfur (^{32}S or ^{33}S). Continuous isotope ratio monitoring was then performed with ICP-MS, which enabled the detection of a variety of metallothionein species, since their elution (with natural isotopic abundances) introduced changes in the isotope ratios [83, 84]. In this way, both the amounts and the degree of saturation of individual metallothioneins with specified metals were accessible, following their prior separation by chromatography. Quadrupole ICP-MS with a reaction cell was recently introduced for sulfur determination [86] including metallothionein analysis [87].

4.2 Other metalloproteins/ metallopeptides

The characterization of metalloproteins other than metallothioneins by inclusion of sulfur determinations is just emerging. In a set of metalloproteins that contain either Fe or Mn the stoichiometric, sulfur-to-metal ratio was successfully determined to characterize their metal content. Hann *et al*. [88] have investigated the sulfur-to-metal content in 5 commercially available proteins (myoglobin, hemoglobin, cytochrom c, arginase, and Mn superoxide dismutase) and two in-house produced proteins after heterologous expression in a host organism. In a DTPA-peptide nucleic acid-peptide construct (DTPA: diethylene triamine pentaacetic acid) loaded with Gd, the sulfur-to-gadolinium ratio was measured to determine its gadolinium saturation by Krüger *et al*. [89].

4.3 Peptides/proteins

In general, sulfur-containing proteinogenic amino acids (Cys, Met), nonproteinogenic amino acids (e.g. taurine, homocysteine, cystathionine), or peptides (e.g. glutathione) have functional importance in key cellular processes, for example, in controlling the redox status, so that new analytical techniques with selectivity for sulfur-containing peptides are highly welcome. Here, the quantitative determination of sulfur by ICP-MS may develop into an established method for this purpose. A few pioneering studies pushing this development have been published recently. For instance, the coupling of GC to high-resolution ICP-MS has been used for quantification of homoserine in human serum by

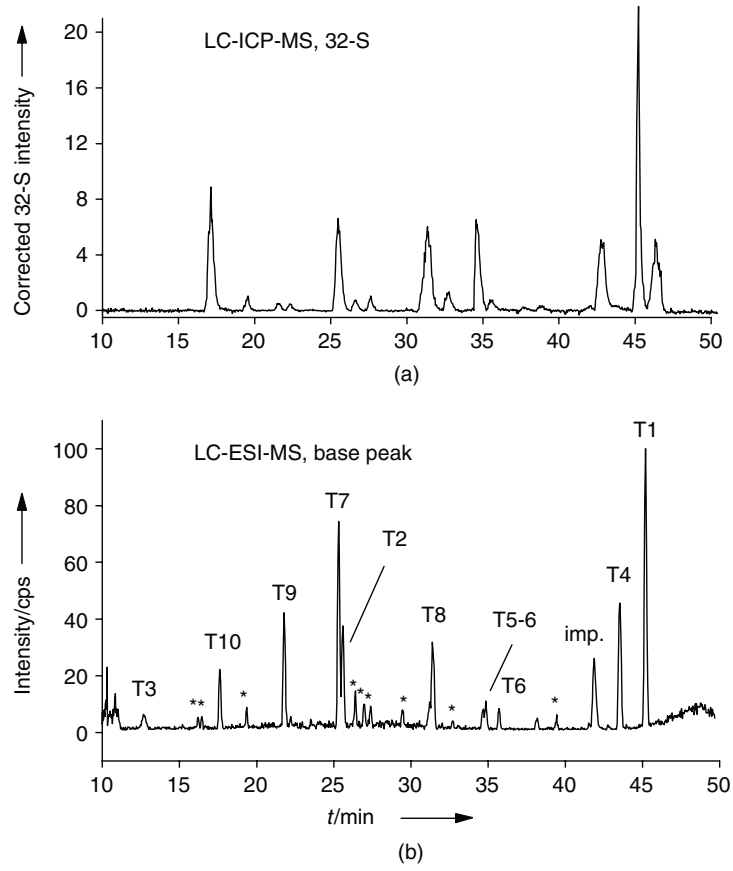

Figure 2.18.4. Tryptic digest of a mixture of the two recombinant proteins cheA-H and cheA-C (ratio 10 : 1); (a) μLC-ICP-MS of this digest with ^{32}S detection; (b) μLC-ESI-MS of the same digest displayed as base peak chromatogram. Tryptic fragments of cheA-C are marked with an asterisk, the T symbols annotate those of cheA-H. For documentation of the peptide sequences, see Table 2.18.6. (Reproduced from Reference [92] by permission of Wiley VCH.)

monitoring of ^{32}S [90]. As an alternative approach, CE coupled to quadrupole ICP-MS equipped with a reaction cell demonstrated the quantification of homocystine in urine [91]. In the latter study, sulfur was determined as $^{32}S^{16}O^{+}$.

As an example for a quantitative analysis of a small protein by determination of sulfur, the insulin concentration in a drug formulation has been quantified correctly by isocratic capillary LC-HR-ICP-MS [92]. In the same study, it was demonstrated that a tryptic digest of a recombinant chemotaxis protein could also be characterized by monitoring of ^{32}S. Since the recombinant chemotaxis proteins investigated contained a relatively large number of Met residues, sulfur determination provided a very informative insight into the quantitative composition of this digest, as demonstrated in Figure 2.18.4(a). This figure also shows the total ion chromatogram of an identical μLC-ESI-MS run (Figure 2.18.4(b)) performed on the same sample for identification of the tryptic peptides.

As expected for a roughly complete digest, almost all tryptic fragments of the main component (cheA-H protein) with one sulfur-containing amino acid showed signals of comparable intensity. The only tryptic fragment with two Met residues (T1) was found to show a signal of higher (roughly twofold) intensity. These quantitative data and the sequences of the tryptic peptides are listed in Table 2.18.6.

Table 2.18.6. Sequences and ICP-MS signal integrals of the analyzed tryptic peptides of the proteins cheA-H and cheA-C. The molar ratio of the proteins (cheA-H/cheA-C of 10 : 1) is reflected in the ICP-integrals of the corresponding peptides. Sulfur-containing amino acids are printed in bold ([92]).

Retention time min	Sequence	Protein	ICP-signal (integrated)
17.1	GETPSA**M**R	cheA-H; T10	3.17
19.5	**M**GGHVEIQSK	cheA-C; T26	0.29
21.6	?		0.18
22.4	GVG**M**DVVK	cheA-C; T23	0.16
25.5	DI**M**QEQLDAYK	cheA-H; T7	2.67
26.6	DLQESV**M**SIR	cheA-C; T7	0.26
27.6	SSELDPVNHGDLITS**M**GQLQR	cheA-C; T5	0.29
31.3	QSQEPDAASFDYI**C**QALR	cheA-H; T8	3.23
32.7	NSVGNLILSAEHQGGNI**C**IEVTDDGAGLNR	cheA-C; T19	0.57
34.6	RGE**M**QLNTDIINLFLETK	cheA-H; T5-6	2.42
35.5	GE**M**QLNTDIINLFLETK	cheA-H; T6	0.33
37.7	?		0.08
38.8	VDQLINLVGELVITQS**M**LAQR	cheA-C; T4	0.13
42.8	GGAGTFGFSVLQETTHL**M**ENLLDEAR	cheA-H; T4	2.81
45.2	**M**DISSFYQTFFDEADELLAD**M**EQHLLVLQPEAPDAER	cheA-H; T1	5.31/2
46.4	?		2.61

Source: Reproduced from Reference [92] by permission of Wiley VCH.

The quantitative evaluation in Table 2.18.6 also shows that the signal intensities of the tryptic peptides of the minor protein component (cheA-C) in the investigated mixture reflect the composition of the original protein mixture, which was about 10 : 1 for the ratio of cheA-H to cheA-C. A set of quantitative LC-ICP and LC-ESI-MS data generated from one sample as demonstrated in Figure 2.18.4 can form the basis for an evaluation of the compound-specific ionization efficiency of a molecular ionization technique. The ICP-response, in this case for sulfur, provides the analyte concentration to which the molecular ion intensities, in this case the sum of the differently charged peptide ions, can be normalized. In this way, it could be demonstrated that the ESI-ionization efficiency of tryptic peptides increases in proportion to the liquid chromatography (LC) retention time and is decreased by the presence of an additional basic residue [92].

Quantification of various intact proteins has also been demonstrated, and a careful investigation of different standards revealed that inorganic standards such as sulfate are well suited for this purpose [93], which resulted in a simple and robust quantification procedure. Determination of the degree of phosphorylation of a phosphoprotein has also been demonstrated by LC-ICP-MS. For this purpose, normalization of the HR-ICP-MS signal of phosphorus of β-casein was normalized by the simultaneously determined signal of sulfur. The ratio of these signals allowed the direct calculation of the degree of phosphorylation, which was found to be close to the expected value of this reference protein [94]. Finally, the degree of phosphorylation was also determined on the proteomic level by monitoring the signals of $^{31}P^{16}O^{+}$ and $^{32}S^{16}O^{+}$ in total protein extracts of cultured malignant cells and of human malignant tissue by use of a reaction cell instrument [95]. The samples from malignant cells were found to display an increased global degree of phosphorylation compared to controls, which is in agreement with expectations from biochemical knowledge, which predicts an increased degree of protein phosphorylation for cells in mitosis compared to resting cells.

4.4 Summary and outlook

Direct analyses of sulfur in peptides and proteins by different techniques of chromatography-ICP-MS or electrophoresis-ICP-MS demonstrate the great potential of this innovative approach in peptide and protein analysis. Current applications range from basic biochemical investigations

to those with evident potential in clinical studies. As a further field of interest for ICP-MS analyses of sulfur, cellular sulfur metabolism, including protein redox chemistry, can be identified.

5 SPECIATION OF SULFUR IN FOOD

5.1 Naturally occurring sulfur species in food

Many sulfur species are naturally occurring in food, for instance, amino acids such as cystine, cysteine and methionine are present in monomeric or protein-bound form. The sulfur chemistry in food cannot be reviewed here in all its complexity, but some aspects shall be dealt with using selected examples.

The first example is derived from the very popular beverage wine. Mineral substances are present in wine as anions or cations in a concentration range from 10 to 1000 $\mu g\,mL^{-1}$. Among these, the elements N, P, S, C, and Cl are present as anions like nitrate, phosphate, sulfite, sulfate, carbonate, and chloride. They are present in the form of more or less soluble salts. Naturally, wine contains only low concentrations of sulfates mainly K_2SO_4 ranging between 100 and 400 $mg\,L^{-1}$. Concentrations can gradually increase during aging because of the addition of sulfiting agents, which will be discussed later in more detail.

In the production of white wines, SO_2 is often added to inhibit microbiological spoilage. High concentrations of copper and free SO_2 in bottled wine may lead to "copper casse" in white wines. "Copper casse" (browning) consists of a turbidity that gradually precipitates to form a brownish-red deposit. These deposits contain colloidal CuS and copper metal, as well as proteins. Bentonite treatment is a simple method for protecting wines from copper casse by eliminating proteins. Copper casse is specific to white wines. They are not as well protected from oxidation phenomena as red wines, in which phenols have a certain redox buffer capacity. Furthermore, the colloidal cupric derivative contains proteins, while red wines have low free protein content because of combination reactions with phenols.

SO_2 can also initiate the formation of various sulfur-containing organic compounds in wine among which volatile sulfur compounds (VSCs) can cause severe problems during vinification and storage. Nearly 100 different VSCs have been reported in wines, which is a low number in comparison to more than 700 detected in food [96]. They can add to the character and complexity, while many of them can significantly detract wine quality because of their bad olfactory sensation or their palate components. Specifically, they can influence the perception of the wine volume and body and bring about a bitter taste.

The process of VSCs generation in wine is very complex and not well understood in detail. It is not possible to discuss the various VSCs in wine comprehensively but some key players should be mentioned. The most important sulfur species contributing to a bad odor of rotten eggs is H_2S (sensory threshold of 1 $\mu g\,m^{-3}$). It is also the key compound involved in the generation of other VSCs in wine. All sulfur compounds with a higher oxidation state such as SO_2, SO_3^{2-}, SO_4^{2-}, S_6, sulfur-containing amino acids, and sulfur-containing pesticides are possible sources for H_2S formation. It is mainly generated under reducing conditions in the yeast cells during fermentation by assistance of an enzyme and readily penetrates cell walls. During a regular fermentation, the generated CO_2 is often sufficient to remove the main fraction of H_2S from the wine. Nevertheless, it can react relatively quickly with the alcohol produced during the fermentation process leading to thioalcohols, for instance, ethyl mercaptan (EtSH). EtSH contributes to the sensation with a taste of burnt rubber, and methyl mercaptan (MeSH) causes odors described as rotten or cooked cabbage and both have a sensory threshold of about 1 $\mu g\,m^{-3}$, too. By reaction with oxygen, mono- and disulfides are synthesized. They contribute to a much milder sensory character than the previously mentioned ones. DMS has the odor of canned corn, cooked cabbage, or vegetables, and is one of the most abundant VSC. It increases with bottle age and can severely contribute to the bottle bouquet. It can affect wine quality positively or negatively, depending on the concentration and the

balance with other wine odors. Optimum levels contribute to complexity and roundness, while excessive concentrations detract. Another oxidized sulfide, diethyl sulfide, can also be present but at much lower concentrations causing a rubberlike character. Other disulfides are also present but most often below the sensory threshold.

In general, sulfur-containing volatiles, especially thiols, belong to the most important flavor compounds in foods and, in particular, fruits [97]. Because of their volatility, GC is the most important means for separation. For element detection, chemiluminescent nitrogen, sulfur selective and mass-specific detection is most often applied. In this research area also, the sensory evaluation by GC in combination with olfactometry plays an important role.

For very complex samples such as foodstuffs, multidimensional techniques are applied, which involve the use of two GC columns with dissimilar phases and time switching to increase the chromatographic resolution [98]. Recent research concentrates on new matrix separation and preconcentration techniques by using of solid-phase micro extraction, for instance, by application of stir-bars or by extraction of volatile compounds from the head-space [99].

Many of the VSCs can develop pleasant flavors at very low concentrations, and this is the reason why they are of industrial interest as food additives as well as starting products for the scent industry. Therefore, enzyme-catalyzed transformation processes of sulfur-containing flavor precursors have recently been studied in detail by application of GC-Flame Ionisation Detection, LC- and Gas Chromatography Mass Spectrometry (GC-MS), Nuclear Magnetic Resonance (NMR) and Fourier–Transform Infrared Radiation (FT-IR) [100].

Another peculiarity of the VSCs (well known since the early 1960s) is the finding that different enantiomers of chiral odorants can have significant differences in their odors. A comprehensive overview is given by Brenna *et al.* [101]. From an analytical point of view, in this case it is not sufficient any more to determine only the sulfur species as such, but also their enantiomeric form. This can be achieved by application of adequate derivatization techniques in combination with GC separations or by the application of special cyclodextrin phases for GC columns. Problems that may arise from overlapping peaks may be overcome by multidimensional GC that, for instance, consists of two columns, an achiral precolumn, and a chiral main column [102].

5.2 Sulfur-containing food additives

Elemental sulfur as well as a number of sulfur-containing compounds is allowed to be added to food samples. The most important are the sulfiting agents (E220–224, E226–228), which are widely used in food and beverages to inhibit microbiological spoilage, enzymatic and nonenzymatic browning reactions and oxidative deterioration. They can suppress the uptake of vitamin B1 (thiamine). The most important food additive is sulfur dioxide (E220). It is mainly applied for production of white wines, dried fruits, and products made from potatoes. Depending on the concentration, sulfiting compounds can cause health problems, and some of the side effects are nausea and headache, for instance, if single doses of more than 250 $mg\,L^{-1}$ SO_2 (4 mmol sulfite) are incorporated. For asthmatics, sulfite can cause bronchoconstrictions, the so-called sulfite-asthma. Because of these reasons, the maximum daily allowance has been set to 0.7 mg SO_2 per kg body weight [103], which can be reached easily by consumption of dessert wines with a typically high SO_2 concentration.

Because of these adverse effects, regulations restrict SO_2 levels in foods and beverages. For instance, for wine the following limits have been implemented: 160 $mg\,L^{-1}$ SO_2 for red wine, 210 $mg\,L^{-1}$ SO_2 for white and rosé wine, and 300–400 $mg\,L^{-1}$ for dessert wine (more than 5 $g\,L^{-1}$ of sugar).

Various methods for determination of sulfur dioxide exist, among which the Ripper method is one of the oldest, but although more than 100 years old, it is still in use. This method uses iodine to titrate the free or total SO_2 in a sample. The

procedure is simple and is still applied with some minor modifications. In this procedure, free sulfur dioxide is determined directly, while total sulfur dioxide is determined after release of bound sulfur dioxide by sodium hydroxide. The analysis for free and total SO_2 is dependent upon the redox reaction:

$$H_2SO_3 + I_2 \longrightarrow H_2SO_4 + 2HI$$

The end point of this reaction is measured by complexation with added starch (blue black end point). The Ripper procedure for free and total SO_2 suffers from several limitations: 1) volatilization and loss of SO_2 during titration; 2) reduction of the iodine titrant by compounds other than sulfite; and 3) difficulty of end point detection in colored analytes such as red wines, where this method is most inaccurate.

Another traditionally often applied method to measure sulfite in foods and beverages is the acid distillation in the Monier-Williams method [104, 105]. The acid distillation is used to release sulfite as sulfur dioxide into a stream of nitrogen followed by trapping of SO_2 in alkaline hydrogen peroxide that converts sulfite into sulfate. This method is laborious and time consuming and therefore recently an alternative method has been developed, which is based on separation by ion-exchange chromatography and conductivity detection [106]. Coelution problems of sulfate with other organic acids such as tartaric acid were avoided by using a special anion-exchange column (ICSep AN 300B from Transgenomic, Omaha, USA) with a bicarbonate mobile phase. The ED40 electrochemical detector from Dionex following a regenerating suppressor column (ASRS Ultra, Dionex) was used for detection. Depending on the sample, coelution of analytes can occur, which complicates determination of sulfite. In this case, sulfate is determined first and then sulfite is oxidized by H_2O_2 and the increase of the sulfate peak then is a measure for the sulfite present in the sample. The limit of detection of this assay in wine is 50 $\mu mol\,L^{-1}$ (3.2 $mg\,L^{-1}$) SO_2, which is quite sufficient to control permitted values.

A different sulfur-containing food additive is the noncaloric artificial sweetener acesulfame k, the potassium salt of 6-methyl-1, 2, 3-oxathiazine-4(3H)-one-2,3-dioxide, which was formulated first by German chemists in the late 1960s. It is 200 times sweeter than sugar, and unlike aspartame, the most well-known artificial sweetener, retaining its sweetness even after heating, making it suited for cooking and baking. It is proposed for use as a tabletop sweetener, and for use in soft drinks, fruit preparations, desserts, breakfast cereals, and bakery products. In many countries, application of artificial sweeteners must be declared and therefore the control of corresponding products is required. Because of the fact that most saccharides and acesulfame k contain ionizable functional groups, it can be separated easily from other food additives by ion-exchange chromatography. Ultra violet (UV) detection at 254 nm can be applied. An elegant method to separate and detect acesulfame k among other food additives such as food colors, sweeteners, and preservatives in carbonated soft drinks is described by Frazer *et al.* [107]. The mentioned food additives had been separated by use of capillary zone electrophoresis (CZE) with a short (48.5 cm × 50 μm ID) fused silica column in less than 10 min. For detection, a UV-visible range diode array detector was applied in the wavelength region from 190 to 600 nm. The identity of the various compounds detected could be verified by matching the migration time with those of the standard compounds. In case of the short column, the resolution was not sufficient in all samples to separate benzoic acid completely from saccharin. Increasing the capillary length solved this problem but increased the migration time of the last eluting components. Therefore, alternatively micellar electrokinetic chromatography (MEKC) was applied by using SDS to produce the surfactant micelles. Such an approach looks promising because now neutral components can also be separated with CZE. By this approach, a complete separation was achieved in less than 15 min for all compounds investigated.

5.3 Residues in foodstuff

The food industry is becoming increasingly industrialized, and foods are distributed on a global

Table 2.18.7. Sulfur-containing pesticides.

Compound	Formula	Compound	Formula
Azinphos-methyl	$C_{10}H_{12}N_3O_3\ PS_2$	Fensulfothion	$C_{11}H_{17}O_4\ PS_2$
Chlorphyrifos	$C_9H_{11}Cl_3NO_3\ PS$	Malathion	$C_{10}H_{19}O_6\ PS_2$
Chlorphyrifos-methyl	$C_7H_7Cl_3O_3\ PS$	Prothiofos	$C_{11}H_{15}Cl_2O_2\ PS_2$
Coumaphos	$C_{14}H_{16}ClO_5\ PS$	Phorate	$C_7H_{17}O_2\ PS_3$
Demeton	$C_8H_{19}O_3\ PS_2$	Sulprofos	$C_{12}H_{19}O_2\ PS_3$
Diazinon	$C_{12}H_{21}N_2O_3\ PS$	Terbufos	$C_9H_{21}O_2\ PS_3$
Disulfoton	$C_8H_{19}O_2\ PS_3$	Tokuthion	$C_{11}H_{15}Cl_2O_2\ PS_2$
Ethoprop	$C_8H_{19}O_2\ PS_2$	Trichloronate	$C_{10}H_{12}Cl_3O_2\ PS$
Fenthion	$C_{10}H_{15}O_3\ PS_2$	–	–

scale. The differences in climate and differences in production prices due to lower income in developing countries favor the import of food to countries with higher economic standards. Intensive farming and monocultures in developing countries facilitate the proliferation of illnesses in man, animals, and crops.

Thus, the application of pesticides in agriculture and antibiotics during meat production is increasing, and their residues can be found in the whole food chain of animals and man. Therefore, the assessment of food quality and its control is increasingly becoming a major concern of the consumers in many industrialized countries. A comprehensive discussion would by far exceed this overview, but some selected examples shall be given here for sulfur-containing pesticides and antibiotics.

5.3.1 Pesticides

The increased use of pesticides in agriculture is a growing problem, and especially insecticides are widely used in the cultivation of fruits and vegetables. Unfortunately, many pesticides are neurotoxic with severe adverse effects on humans. This is the reason why for many of these compounds national and international regulations with strict maximum limits exist. For instance, the European Union (EU) has set a very low limit for pesticides in infant food, which must not exceed 10 $\mu g\,kg^{-1}$ for any given pesticide. The Maximum Residue Limits (MRL) have been set to be near the determination threshold that is typically achieved for pesticides with traditional analytical methods. In the year 2000, certain pesticides were included in the EU Water Framework Directive for the protection of EU drinking water resources.

Moreover, because of the recent commercial agreements for the import of vegetables from developing countries, pesticide control is becoming even more important.

A list of sulfur-containing pesticides is compiled in Table 2.18.7. GC and HPLC are most often applied for separation of pesticides and are combined with different methods for detection, among which molecular mass spectrometry with different ionization sources is the preferred method because of the high sensitivity, and molecule-selective detection needed for identification [108–111].

Since almost all pesticides contain heteroelements, element-selective detectors such as the nitrogen-phosphorus flame photometric, electron capture and atomic spectroscopy detectors are becoming a low-cost alternative in combination with GC separations [108, 112–117]. Among detectors based on atomic spectroscopy, ICP-MS looks promising because of its high sensitivity. Additionally convincing is the substance–independent detection, which can be used for quantification by use of chromatographic internal standards, so that this detector is well suited for screening purposes and determination of sum parameters.

Concerning GC-ICP-MS, it is not possible to measure sulfur at low concentrations with a quadrupole mass analyzer directly. Therefore, Pröfrock *et al.* [118] have applied a collision and reaction cell instrument using helium as a buffer gas to overcome the polyatomic interferences from $^{16}O_2$ and $^{14}N^{18}O$ at mass 32. Helium is not

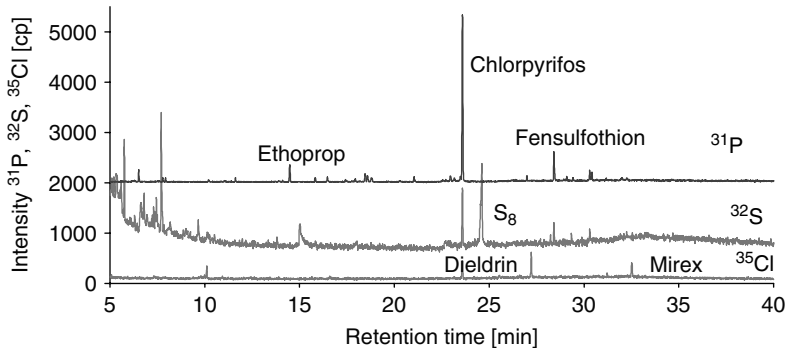

Figure 2.18.5. Element-specific detection of pesticides in tomato extract. Chromatograms for P, S, and Cl are shown. (Reproduced from Pröfrock, D., Leonhard, P., Wilbur, S. and Prange, A., *J. Anal. At. Spectrom.*, **19**, 623 (2004) by permission of The Royal Society of Chemistry [118].)

reacting with these molecules, but in the buffer gas polyatomic species with their larger cross sections are much faster thermalized so that they can be discriminated from the sulfur isotope only by energy filtering. The authors had used compromise instrumental conditions for multielement analysis so that they could additionally detect pesticides containing P, Cl, Br, and I. LOD's (International Union of Pure and Applied Chemistry – IUPAC guidelines) in the range of 0.02–4 $\mu g\,L^{-1}$ have been calculated using a pesticide mixture and 1-μL injections.

An example is given in Figure 2.18.5, where the chromatograms of a GC separation and element-specific detection by ICP-MS for pesticides in a tomato extract are shown for the isotopes of ^{31}P, ^{32}S, and ^{35}Cl. The peaks identified in the chromatograms could be assigned to ethoprop ($C_8H_{19}O_2\,PS_2$), chlorphyrifos ($C_9H_{11}Cl_3NO_3\,PS$), dieldrin ($C_{12}H_8Cl_6O$), fensulfothion ($C_{11}H_{17}O_4\,PS_2$), mirex ($C_{10}Cl_{12}$), and elemental sulfur (S_8). For instance, by this approach chlorpyrifos in the tomato extract can be quantified to 33.79, 31.39, and 32.02 $\mu g\,L^{-1}$ using ^{31}P, ^{32}S, and ^{35}Cl detection. This value fits well with 31 $\mu g\,L^{-1}$ determined by GC-MS. Identification and quantification were possible by application of external standards.

The advantage of this approach is that ICP-MS can be used here as a screening detector because many pesticides can be quantified directly by use of the heteroelements only and this can become more important in future because of the following reason. Concerning pesticides, at present data are missing to estimate the actual exposure of consumers, which is required for a more accurate risk assessment. Little is known about the metabolization chain of pesticides in the environment, in plants, animals, and human beings. Here, speciation of sulfur-, phosphorus- and halogen-containing pesticides, their degradation products, and their metabolites are becoming a new challenge for analytical chemistry, in particular, for organic as well as for inorganic mass spectrometry.

5.3.2 Sulfonamides

Another group of residues found in food samples are the sulfur-containing antibiotics (see introduction) and, in particular, the sulfonamides. They are widely used in veterinary practice to treat bacterial infections in livestock and poultry and in farmed fish. Sulfonamide residues are of concern because of their potential carcinogenic character. Additionally, these drugs can create antibiotic-resistant strains of bacteria [119, 120]. The residues have already been detected in meat, milk, and fish flesh [121–124]. For foodstuff, regulatory limits exist, for instance, in the EU and in Canada that are as low as 100 $\mu g\,kg^{-1}$ in edible animal tissue and 10 $\mu g\,kg^{-1}$ in milk [125].

A multiresidue determination of 21 sulfonamide antibiotics in milk has been developed by

Volmer [126]. After clean up of the samples by removal of proteins and lipids, the sulfonamides had been extracted in methanol. After evaporation to dryness, the residue had been dissolved in water, and 25-μL aliquots have been injected on a short reversed-phase column coupled to a triple quadrupole mass analyzer with electrospray ionization. Separation was achieved in less than 6 min with detection limits at low ng g^{-1} and pg g^{-1} levels depending on the substance.

Sulfonamides have also been detected in various kinds of animal meat and its by-products by application of LC with UV, fluorescence and electrochemical detection and mass spectrometry [127–134]. GC-MS methods by use of adequate derivatization techniques were also developed for this purpose [135–137].

Of course, in case of meat samples the most crucial step is the multistep sample preparation, which can consist of several extraction, preconcentration, and reextraction steps. An extraction procedure for CE separation and detection with a photodiode array detector has been described recently by Fuh and Chu [138]. The procedure, which consists of more than 20 single sample preparation steps, starts with a total amount of 5-g homogenized meat, which is extracted by acetonitrile. For enrichment of the sulfonamides and separation from matrix compounds, two different solid-phase extraction (SPE) cartridges were applied for sample cleanup. After washing of the SPE cartridges with organic solvents, the washing solution is evaporated to dryness and redissolved in acetonitrile/water containing the internal standard. After centrifugation and filtering, the sample is injected into the capillary. Complete separation of 8 sulfonamides in less than 30 min has been achieved with detection limits in the range of 5–10 $\mu g\,kg^{-1}$.

The Canadian Food Inspection Agency method for sulfonamides in meat tissue consists of an extraction procedure in ethyl acetate, partitioning with glycine buffer, followed by a pH-adjusted back extraction into methylene chloride [139]. The extract is evaporated, reconstituted, then separated by thin layer chromatography (TLC), derivatized, and finally quantified by densitometry. Again, such a procedure is laborious and time consuming, and because of the complexity it is also a permanent source of errors. A very easy and fast method has been recently described by Hindle [140]. After homogenization, the samples were extracted in acidified methanol, centrifuged, and a portion of the extract is diluted (ratio 1 : 4) with water. After filtering, the sample is filled into an autosampler vial and then is automatically analyzed by HPLC mass spectrometry with chemical ionization. All compounds investigated are eluting in less than 5 minutes with detection limits in the range of 10–25 $ng\,g^{-1}$, thus below the required value.

5.4 Sulfur isotope ratios

Many animal epidemics such as the recent chicken virus, Bovine Spongiform Encephalopathy (BSE), foot and mouth disease, and also contaminated fodder, for example, with the herbicide nitrofen in Germany in 2002, have led to additional national and international regulations on trade. These force traders to trace back their products to their origin. The general principles and requirements of food law, which cover food safety, have been laid down in the new EU regulation 178/2002. Most often, the authenticity and the provenance is documented only by bookkeeping methods, for instance, in case of beef by a registration system of cows. An efficient control was not possible in the past because of a lack of analytical methods for this purpose.

For the control of the authenticity of food in most cases, it is not required to determine the exact geographical origin, but to confirm or reject the hallmark of products. Among various parameters suited for the authenticity control, the isotopic composition of food looks most promising because it is a natural property for some elements and it can easily be related to the origin. It can therefore serve as a kind of natural 'fingerprinting'. Organisms more or less reflect the isotopic composition of the environment in which they have been grown, and this holds true, in particular, for the isotopes of sulfur, carbon, oxygen, and nitrogen, so that these elements can become important for authenticity control of meat [141–143].

Recently, Boner and Förstel have used stable-isotope variations as a tool to trace the authenticity of beef [144]. For this purpose, usually the patterns of D/H and $^{18}O/^{16}O$ can be applied, which vary in ground and rainwater all over the world and this pattern is stored in the tissue water. Boner and Förstel have complemented this pattern by the measurement of $^{15}N/^{14}N$ and $^{34}S/^{32}S$ isotope ratios. The latter elements are part of the biosphere, they have stable isotopes, and they are present in soils and show different isotope ratios depending on geological composition, cultivation, and atmospheric deposition. As farming is mainly dependent on locally produced fodder, this ratio therefore should be reflected in the beef as well. They could show that by using the isotopes of hydrogen and oxygen, it was possible to trace back the meat to the main geographical region, for instance, discriminating beef from Argentina and Germany. Because the seasonal variations of D/H and $^{18}O/^{16}O$ ratios alone are not always sufficient for the differentiation, the $^{15}N/^{14}N$ and $^{34}S/^{32}S$ ratios have been added as a complement because these stable isotopes are more related to local geographical variations. Investigation of the sulfur isotope ratios of the raw protein show enrichment relative to an isotope standard with a median value given in the well-known delta-notation of about 5‰ for Germany, 8.5‰ for Argentina, and 15.2‰ for Chile. A standard deviation of 0.3‰ has been achieved so far in routine measurements. Investigating local farmers, it was surprising to see that even over a period of 18 months this individual isotope signature was constant and could even be related to single farmers. Further research is needed to establish and extend data bases as well as to see if meat from conventional beef production can be differentiated from organic farming by use of isotope ratios only.

In summary, the control of food quality and authenticity will become an important challenge of analytical chemistry in the future.

6 CONCLUSION

Sulfur speciation in complex samples from environmental, medical, biochemical, and nutritional applications is still a challenge for analytical chemistry. For species in a gaseous and liquid medium, we still have a number of different analytical methods at hand, including sample preparation and detection. The challenge starts with sample preparation and species extraction from soft and hard materials, for instance, from tissues or from particulate matter or even from soils. Here, we have to develop new strategies to extract, to conserve, to enrich, and to separate the species of interest. Multidimensional separation techniques, combined with various kinds of atomic and molecular spectrometric detection methods, are efficient in determining binding partners, oxidation and redox states, molecular mass, the enantiomeric or structural form. Many problems on a global, local, as well as on a molecular scale remain unsolved, and new analytical tools need to be developed for speciation of sulfur in the different compartments. Most of the methods applied so far measure static and/or integrated signals in time and space for certain species. A difficult analytical challenge is popping up as we have to embark on dynamic systems as occurring in living organisms and their global environment.

7 REFERENCES

1. Schmidt, M., *Angew. Chem., Int. Ed. Engl.*, **12**, 445 (1973).
2. Reinhardt, F., Drexler, H., Bickel, A., Claus, D., Ulm, K., Angerer, J., Lehnert, G. and Neundörfer, B., *Int. Arch. Occup. Environ. Health*, **70**, 249 (1997).
3. Webster, M. D., Babiker, M., Mayer, M., Reilly, J. M., Harnisch, J., Hyman, R., Sarofim, M. C. and Wang, C., *Atmos. Environ.*, **36**, 3659 (2002).
4. Khazaei, A., Sadeghian, S. F., Hesami, S. and Manesh, A. A., *Asian J. Chem.*, **14**, 173 (2002).
5. McEvoy, G. K., *AHFS Drug Information*, American Society of Hospital Pharmacists Inc, Bethesda, MD, 1992.
6. Seinfeld, J., *Atmospheric Chemistry and Physics of Air Pollution*, John Wiley & Sons, New York, 1986.
7. *Air Quality Guidelines*, 2nd ed., WHO Regional office for Europe, Copenhagen, 2000.
8. Seinfeld, J. and Pandis, S., *Atmospheric Chemistry and Physics: From Air Pollution to Climate Changes*, John Wiley & Sons, London, 1997, p. 1326.
9. Amdur, M. O., Air pollutants, in *Casarett and Doull's Toxicology: The Basis Science of Poisons*, 3rd ed.,

Klaassen, C. D., Amdur, M. O. and Doull, J. (Eds.), Macmillan Publishing, London, New York, Toronto, 1986, p. 801.
10. Charlson, R. J., Andreson, T. L. and MucDuff, R. E., The sulphur cycle, in *Global Biogeochemical Cycles*, Butcher, S. S., Charlson, R. J., Oriana, G. H. and Wolfe, G. V. (Eds.), Academic Press, New York, 1992, p. 285.
11. Andreae, M. O. and Jaeschke, W., Exchange of sulphur between biosphere and atmosphere, over temperate and tropical regions, Scope 48, in *Sulphur Cycling on the Continents: Wetlands, Terrestrial Ecosystems and Associated Water Bodies*, Howarth, R. W., Stewart, J. W. B. and Ivanov, M. V. (Eds.), John Wiley & Sons, Chichester, 1992, p. 376.
12. Berresheim, H., Wine, P. H. and Davis, D. D., Sulfur in the atmosphere, in *Composition, Chemistry and Climate of the Atmosphere*, Singh, H. B. (Ed.), van Nostrand Reinhold, New York, 1995, p. 527.
13. Anderson, J. W., Assimilation of inorganic sulfate into cysteine, in *The Biochemistry of Plants*, Vol. 5, Stumpf, P. K. and Conn, E. E. (Eds.), Academic Press, New York, 1980, p. 203.
14. Warneck, P., *Chemistry of the Natural Atmosphere*, Academic Press, San Diego, CA, New York, 1988, p. 499.
15. Atkinson, R., Baulch, D. L., Cox, R. A., Hampson, R. F. Jr., Kerr, J. A., Rossi, M. J. and Troe, J., *J. Phys. Chem. Ref. Data*, **26**, 1329 (1997).
16. Stickel, R. E., Nicovich, J. M., Wang, S., Zhao, Z. and Wine, P. H., *J. Phys. Chem.*, **96**, 9875 (1992).
17. Ingham, T., Bauer, D., Sander, R., Crutzen, P. J. and Crowley, J. N., *J. Phys. Chem. A.*, **103**, 7199 (1999).
18. Urbanski, S. P., Stickel, R. E. and Wine, P. H., *J. Phys. Chem.*, **102**, 10522 (1998).
19. Kukui, A., Borissenko, D., Lavedret, G. and Le Bras, G., *J. Phys. Chem. A*, **107**, 5732 (2003).
20. Bonifacic, M., Moeckel, H., Bahnemann, D. and Asmus, K. D., *J. Chem. Soc. Perkin Trans.*, **2**, 675 (1975).
21. Lee, Y. N. and Zhou, X., *J. Geophys. Res.*, **99**, 3597 (1994).
22. Gershenzon, M., Davidovits, P., Jayne, J. T., Kolb, C. E. and Worsnop, D. R., *J. Phys. Chem. A*, **105**, 7031 (2001).
23. Milne, P. J., Zika, R. G. and Saltzman, E. S., *ACS Symposium Series*, American Chemical Society, 1989, Chapter 33, p. 518.
24. Bardouki, H., Barcellos da Rosa, M., Mihalopoulos, N., Palm, U. and Zetzsch, C., *Atmos. Environ.*, **36**, 4627 (2002).
25. Martin, L. R., Kinetic studies of sulfite oxidation in aqueous solution, in *SO_2, NO and NO_2 Oxidation Mechanisms: Atmospheric Considerations*, Calvert, J. G. (Ed.), Butterworths, Boston, MA, 1984, p. 63.
26. Lelieveld, J. and Heintzenberg, J., *Science*, **258**, 117 (1992).
27. Wolkoff, A. W. and Larose, R. H., *Anal. Chem.*, **47**, 1003 (1975).
28. Watts, S. F., *Atmos. Environ.*, **34**, 761 (2000).
29. Tabatabai, M. A., Methods of measurement of sulphur in soils, plant materials and waters, Scope 48, in *Sulphur Cycling on the Continents: Wetlands, Terrestrial Ecosystems and Associated Water Bodies*, Howarth, R. W., Stewart, J. W. B. and Ivanov, M. V. (Eds.), Wiley, London, 1992, p. 376.
30. Steinbergs, A., *Analyst (London)*, **80**, 457 (1955).
31. Johnson, C. M. and Nishita, H., *Anal. Chem.*, **24**, 736 (1952).
32. Bloomfield, C., *Analyst (London)*, **87**, 586 (1962).
33. Jenkinson, D. S., *Analyst (London)*, **93**, 535 (1968).
34. Tabatabai, M. A., Basta, N. T. and Pirela, H. J., *Commun. Soil Sci. Plant Anal.*, **19**, 1701 (1988).
35. David, M. B., Mitchell, M. J., Aldcorn, D. and Harrison, R. B., *Soil Biol. Biochem.*, **21**, 119 (1989).
36. Luther, G. W. III, Giblin, E. A. and Varsolona, R., *Limnol. Oceanogr.*, **30**, 727 (1985).
37. Tabatabai, M. A., *J. Air Pollut. Control Assoc.*, **37**, 34 (1987).
38. Olson, R. A. and Rhem, G. W., Sulfur in precipitation and irrigation waters and its effect on soil and plants, in *Sulfur in Agriculture*, Monograph No. 27, Tabatabai, M. A. (Ed.), American Society Agronomy, Madison, WI, 1986, p. 279.
39. Kilmer, V. J. and Nearpass, D. C., *Soil Sci. Soc. Am. Proc.*, **24**, 337 (1960).
40. Williams, C. H. and Steinbergs, A., *Plant Soil*, **17**, 279 (1962).
41. McClung, A. C., DeFreitas, L. M. and Lott, W. L., *Soil Sci. Soc. Am. Proc.*, **23**, 221 (1959).
42. Stanford, J. O. and Lancaster, J. D., *Soil Sci. Soc. Am. Proc.*, **26**, 63 (1962).
43. Chesnin, L. and Yien, C. H., *Soil Sci. Soc. Am. Proc.*, **15**, 149 (1950).
44. Bingham, F. T., Sims, R. J. and Page, A. L., *Soil Sci. Soc. Am. Proc.*, **29**, 670 (1965).
45. Neptune, A. M. L., Tabatabai, M. A. and Hanaway, J. J., *Soil Sci. Soc. Am. Proc.*, **39**, 51 (1975).
46. Thompson, J. F., Smith, I. K. and Madison, J. T., Sulfur metabolism in plants, in *Sulfur in Agriculture*, Monograph No. 27, Tabatabai, M. A. (Ed.), American Society Agronomy, Madison, WI, 1986, p. 57.
47. Duke, S. H. and Reisenauer, H. M., Role and requirements of sulfur in plant nutrition, in *Sulfur in Agriculture*, Monograph No. 27, Tabatabai, M. A. (Ed.), American Society Agronomy, Madison, WI, 1986, p. 123.
48. Allaway, W. H. and Thompson, J. F., *Soil Sci.*, **101**, 240 (1966).
49. Guthrie, T. F. and Lowe, L. E., *Can. J. For. Res.*, **14**, 470 (1983).
50. Beaton, J. D., Burns, G. R. and Platou, J. Jr., *Determination of Sulfur in Soils and Plant Material*, Technical Bulletin No. 14, The Sulfur Institute, Washington, DC, 1968.
51. Stumm, W. and Morgan, J. J., *Aquatic Chemistry*, Wiley-Interscience, New York, 1970.

52. Andreae, M. O., The ocean as a source of atmospheric sulfur compounds, in *The Role of Air-Sea Exchange in Geochemical Cycling*, Buat-Ménard, P. (Ed.), Reidel, Dordrecht, NL, 1986, p. 331.
53. Charlson, R. J., Lovelock, J. E., Andreae, M. O. and Warren, S. G., *Nature*, **326**, 655 (1987).
54. Kiene, R. P., *Mar. Chem.*, **54**, 69 (1996).
55. Liss, P. S., Hatton, A. D., Malin, G., Nightingale, P. D. and Turner, S. M., *Philos. Trans. R. Soc. London.*, **352**, 159 (1997).
56. Andreae, M. O., *Limnol. Oceanogr.*, **25**, 1054 (1980).
57. Sciare, J. and Mihalopoulos, N., *Atmos. Environ.*, **34**, 151 (2000).
58. Simo, R., Grimalt, J. O. and Albaiges, J., *Anal. Chem.*, **68**, 1493 (2001).
59. Füchtjohann, L., Jakubowski, N., Gladtke, D., Klockow, D. and Broekaert, J. A. C., *J. Environ. Mon.*, **3**, 681 (2003).
60. Bandy, A. R., Thornton, D. C. and Driedger, A. R. III, *J. Geophys. Res.*, **98**, 23423 (1993).
61. Harvey, G. and Lang, R. F., *Geophys. Res. Lett.*, **13**, 49 (1986).
62. Berresheim, H., Tanner, D. J. and Eisele, F. L., *Anal. Chem.*, **65**, 84 (1993).
63. Cofer, W. R. and Edahl, R. A., *Atmos. Environ.*, **20**, 979 (1986).
64. Stecher, H., Luther, G. W., MacTaggart, D. L., Farwell, S. O., Crosley, D. R., Dorko, W. D., Goldan, P. D., Beltz, N., Krischke, U., Luke, W. T., Thornton, D. C., Talbot, R. W., Lefer, B. L., Scheuer, E. M., Benner, R. I., Wu, J., Saltzman, E. S., Gallagher, M. S. and Ferek, R. J., *J. Geophys. Res.*, **102**, 16219 (1997).
65. Ferek, R. J., Hegg, D. A., Herring, J. A. and Hobbs, P. V., *J. Geophys. Res.*, **96**, 22373 (1991).
66. Talbot, R. W., Scheuer, E. M., Lefer, B. L. and Luke, W. T., *J. Geophys. Res.*, **102**, 273 (1997).
67. Benner, R. I., Wu, J. and Knicks, D. K. Jr., *J. Geophys. Res.*, **102**, 287 (1997).
68. Jaeschke, W., Beltz, N., Haunold, W. and Krischke, U., *J. Geophys. Res.*, **102**, 279 (1997).
69. Gallagher, M. S., King, D. B., Whung, P.-Y. and Saltzman, E. S., *J. Geophys. Res.*, **102**, 16247 (1997).
70. Luke, W. T., *J. Geophys. Res.*, **102**, 255 (1997).
71. Saltzman, E. S. and Cooper, D. J., *J. Atmos. Chem.*, **7**, 191 (1988).
72. Natusch, D. F. S., Klonis, H. B., Axelrod, H. D., Teck, R. J. and Lodge, J. P. Jr., *Anal. Chem.*, **44**, 2067 (1972).
73. Tanner, D. J., Jefferson, A. and Eisele, F. L., *J. Geophys. Res.*, **102**, 6415 (1997).
74. Eisele, F. L. and Tanner, D. J., *J. Geophys. Res.*, **98**, 9001 (1993).
75. Gygi, S. P., Rist, B., Gerber, S. A., Turecek, F., Gelb, M. H. and Aebersold, R., *Nat. Biotechnol.*, **17**, 994 (1999).
76. Krijgsveld, J., Ketting, R. F., Mahmoudi, T., Johansen, J., Artal-Sanz, M., Verrijzer, C. P., Plasterk, R. H. and Heck, A. J., *Nat. Biotechnol.*, **21**, 927 (2003).
77. Ong, S. E., Foster, L. J. and Mann, M., *Methods*, **29**, 124 (2003).
78. Szpunar, J., *Analyst*, **125**, 963 (2000).
79. Zhang, X. and Zhang, C., Atomic absorption and atomic emission spectrometry, in *Handbook of Speciation – Techniques and Methodology*, Cornelis, R., Caruso, J., Crews, H. and Heumann, K. (Eds.), Wiley, West Sussex, 2003, p. 241.
80. Vanhaecke, F. and Köllensperger, G., Detection by ICP-mass spectrometry, Section 5.3 in *Handbook of Elemental Speciation – Techniques and Methodology*, Cornelis, R., Caruso, J., Crews, H. and Heumann, K. (Eds.), Wiley, West Sussex, 2003, pp. 281–312.
81. Fauchon, M., Lagniel, G., Aude, J.-C., Lombardia, L., Soularue, P., Petat, C., Marguerie, G., Sentenac, A., Werner, M. and Labarre, J., *Mol. Cell*, **9**, 713 (2002).
82. Prange, A., Schaumlöffel, D., Brätter, P., Richarz, A. N. and Wolf, C., *Fresenius' J. Anal. Chem.*, **371**, 764 (2001).
83. Schaumlöffel, D., Prange, A., Marx, G., Heumann, K. G. and Brätter, P., *Anal. Bioanal. Chem.*, **372**, 155 (2002).
84. Wang, Z. and Prange, A., *Anal. Chem.*, **74**, 626 (2002).
85. Rodriguez-Cea, A., Dela Campa, M. D. F., Gonzalez, E. B., Fernandez, B. A. and Sanz-Medel, A., *J. Anal. At. Spectrom.*, **18**, 1357 (2003).
86. Bandura, D. R., Baranov, I. and Tanner, S. D., *Anal. Chem.*, **74**, 1497 (2002).
87. Pröfrock, D., Leonhard, P. and Prange, A., *Anal. Bioanal. Chem.*, **377**, 132 (2003).
88. Hann, S., Koellensperger, G., Binger, C., Furtmüller, P. G. and Stingeder, G., *J. Anal. At. Spectrom.*, **19**, 74 (2004).
89. Krüger, R., Braun, K., Pipkorn, R. and Lehmann, W. D., *J. Anal. At. Spectrom.*, **19**, 852 (2004).
90. Yeh, C. F., Jiang, S. H. and His, T. S., *Anal. Chim. Acta*, **502**, 57 (2004).
91. St. Remy, R. R., Montes-Bayon, M. and Sanz-Medel, A., *Anal. Bioanal. Chem.*, **377**, 299 (2003).
92. Wind, M., Wegener, A., Eisenmenger, A., Kellner, R. and Lehmann, W. D., *Angew. Chem., Int. Ed. Engl.*, **42**, 3425 (2003).
93. Svantesson, E., Pettersson, J. and Markides, K. E., *J. Anal. At. Spectrom.*, **17**, 491 (2002).
94. Wind, M., Wesch, H. and Lehmann, W. D., *Anal. Chem.*, **73**, 3006 (2001).
95. Bandura, D. R., Ornatsky, O. and Liao, L., *J. Anal. At. Spectrom.*, **19**, 96 (2004).
96. Blank, I., Sensory relevance of volatile organic sulfur compounds in food, in *Heteroatomic Aroma Compounds*, ACS Symposium Series 826, Reineccius, G. A. and Reineccius, T. A. (Eds.), Oxford University Press, 2002, p. 25.

97. Engel, K. H., The importance of sulfur-containing compounds to fruit flavors, in *Flavor Chemistry: Thirty Years Progress*, Teranishi, R., Wick, E. L. and Hornstein, I. (Eds.), Kluwer Academic/Plenum Publishers, New York, 1999, p. 265.
98. MacNamara, K., Leardi, R. and Hoffmann, A., *LC-GC North Am.*, **22**, 166 (2004).
99. David, F., Tienpont, B. and Sandra, P., *LC-GC North Am.*, **21**, 108 (2003).
100. Wakabayashi, H., *Enzyme-Catalyzed Transformation of Sulfur-Containing Flavor Precursors*, PhD Thesis, Technical University of Munich, 2004.
101. Brenna, E., Fuganti, C. and Sierra, S., *Tetrahedron: Asymmetry*, **14**, 1 (2003).
102. Werkhoff, P., Brennecke, S. and Bretschneider, W., *Chem. Mikrobiol. Technol. Lebensm.*, **13**, 129 (1991).
103. Joint FAO/WHO Expert Committee on Food Additives, *Toxicological Evaluation of Certain Food Additives with a Review of General Principles and Specifications*, FAO nutrition Meeting Report Series, No. 53. WHO Technical Report Series, No. 539, 1974.
104. Monier-Williams, G. W., *Determination of Sulphur Dioxide in Foods*, Public Health and Medical Subjects Report No. 43, Ministers of Health, London, 1927.
105. AOAC, Official Method 990.28, Sulfides in Food (Optimized Monier-Williams Method), *J. AOAC Int.*, **70**, 572 (1987).
106. Edmont, L. M., Magee, E. A. and Cummings, J. H., *LC+GC Eur.*, February 88 (2003).
107. Frazer, R. A., Inns, E. I., Dossi, N., Ames, J. M. and Nursten, H. E., *J. Chromatogr., A*, **876**, 213 (2000).
108. Pablos-Espada, M. C., Arrebola-Liebanas, F. J., Garrido-Frenich, A. and Martinez-Vidal, J. L., *Int. J. Environ. Anal. Chem.*, **75**, 165 (1999).
109. Vreeken, R. J., Vandongen, W. D., Ghijsen, R. T. and Brinkman, U. A. T., *Int. J. Environ. Anal. Chem.*, **54**, 119 (1994).
110. Bell, A. J., Despeyroux, D., Murrell, J. and Watts, P., *Int. J. Mass Spectrom.*, **165**, 533 (1997).
111. Cook, J., Engel, M., Wylie, P. and Quimby, B., *J. AOAC Int.*, **82**, 313 (1999).
112. Lartiges, S. B. and Garrigues, P., *Analusis*, **23**, 418 (1995).
113. Torres, C. M., Pico, Y. and Manes, J., *Chromatographia*, **41**, 685 (1995).
114. Mukherjee, I. and Gopal, M., *J. Chromatogr., A*, **754**, 33 (1996).
115. Rinkema, F. D., Louter, A. J. H. and Brinkman, U. A. T., *J. Chromatogr., A*, **678**, 289 (1994).
116. Linkerhagner, M. and Stan, H. J., *Z. Lebensm.-Unters.-Forsch.*, **198**, 473 (1994).
117. Hankemeier, T., Louter, A. J. H., Rinkema, F. D. and Brinkman, U. A. T., *Chromatographia*, **40**, 119 (1995).
118. Pröfrock, D., Leonhard, P., Wilbur, S. and Prange, A., *J. Anal. At. Spectrom.*, **19**, 623 (2004).
119. Littlefield, N. A., Sheldon, W. G., Allen, R. and Gaylor, D. W., *Food Chem. Toxicol.*, **28**, 157 (1990).
120. Neu, H. C., *Science*, **257**, 1064 (1992).
121. Bevill, R. F., Sharma, R. M., Meachum, S. H., Wozniak, S. C., Bourne, D. W. and Dittert, L. W., *Am. J. Vet. Res.*, **38**, 973 (1977).
122. Dixon-Holland, D. E. and Katz, S. E., *J. Assoc. Off. Anal. Chem.*, **72**, 447 (1989).
123. Larocque, L., Garignan, C. and Sved, S., *J. Assoc. Off. Anal. Chem.*, **73**, 365 (1990).
124. Pleasance, S., Blay, P., Quilliam, M. A. and O'Hara, G., *J. Chromatogr.*, **558**, 155 (1991).
125. *Council regulation (EEC) No. 2377/90*, Off. J. Europ. Comm., No. L 224/1, 1990.
126. Volmer, D. A., *Rapid Commun. Mass Spectrom.*, **10**, 1615 (1996).
127. Ikai, Y., Oka, H., Kawamura, N., Hayakawa, J., Yamada, M., Harada, K., Suzuki, M. and Nakazawa, H., *J. Chromatogr.*, **541**, 393 (1991).
128. Balizs, G., Benesch-Grike, L., Borner, S. and Hewitt, S. A., *J. Chromatogr., B*, **661**, 75 (1994).
129. Agarwal, V. K., *J. Chromatogr.*, **624**, 411 (1992).
130. Stoev, G. and Michailova, A. I., *J. Chromatogr., A*, **871**, 37 (2000).
131. Hartig, C., Storm, T. and Jekel, M., *J. Chromatogr., A*, **854**, 163 (1999).
132. Combs, M. T., Ashra-Khorassani, M. and Tayor, L. T., *J. Pharm. Biomed. Anal.*, **25**, 301 (1999).
133. Ito, Y., Oka, H., Ikai, Y., Matsumoto, H., Miyazaki, Y. and Nagase, H., *J. Chromatogr., A*, **898**, 95 (2000).
134. Fuh, M. S. and Chan, S. A., *Talanta*, **55**, 1127 (2001).
135. Takatsuki, K. and Kikuchi, T., *J. Assoc. Off. Anal. Chem.*, **73**, 886 (1990).
136. Carignan, G. and Carrier, K., *J. Assoc. Off. Anal. Chem.*, **74**, 479 (1991).
137. Tarbin, J. A., Clarke, P. and Shearer, G., *J. Chromatogr., B*, **729**, 127 (1999).
138. Fuh, M.-R. S. and Chu, S.-Y., *Anal. Chim. Acta*, **499**, 215 (2004).
139. *TLC-Densiometric Procedure for Sulfonamide Residues in Animal Tissue*, SUL-SP08, Canadian Food Inspection Agency, Saskatoon, 2001/04.
140. Hindle, R., *A Validated Atmospheric Pressure Chemical Ionisation Method for Analyzing Sulfonamides in Pork Muscle*, Agilent Technologies, Application Note 5989-0182EN, 2004.
141. Krouse, H. R., *Geochim. Cosmochim. Acta*, **48**, 187 (1984).
142. DeNiro, M. J. and Epstein, S., *Science*, **15**, 261 (1977).
143. Steele, K. W. and Daniel, R. M., *J. Agric. Sci.*, **90**, 7 (1978).
144. Boner, M. and Förstel, H., *Anal. Bioanal. Chem.*, **378**, 310 (2004).

2.19 Speciation of Thallium

Klaus Günther and Bernd Kastenholz

Institute for Chemistry and Dynamics of the Geosphere, Institute III: Phytosphere, Research Center Juelich, Germany

1 ENVIRONMENT

Thallium is a trace element that occurs in small amounts in sulfur-containing ores and potassium minerals. The anthropogenic environmental occurrence of this element is caused by ore smelting, handling and processing of waste products from the metallurgic industry, resulting in thallium emissions [1]. Vegetation damages have been observed and researched around a cement plant using thallium-containing pyrite smelting residues [2]. Ecotoxicological importance of this element is derived from its high acute toxicity on living organisms [1].

1.1 Analytical procedures

There is an urgent need for reliable analytical methods to determine thallium in environmental matrices [3, 4]. In this context, growing interest is paid to the determination of the oxidation states of thallium, Tl(I) and Tl(III), and the respective thallium organyls that occur in nature [5].

In recent times, many studies deal with the determination of total thallium amounts in the different environmental matrices such as water [6, 7], snow [8], soil [9, 10], sediment [9, 11–13] and cement [11, 14]. For this purpose, different analytical techniques, for example, isotope dilution inductively coupled plasma mass spectrometry (ICP-MS) [6, 9], atomic absorption spectrometry [10, 14], laser-induced atomic fluorescence spectrometry [8, 12, 13], spectrophotometry [7] and differential pulse anodic stripping voltammetry [11] were applied.

Handbook of Elemental Speciation II: Species in the Environment, Food, Medicine & Occupational Health
Edited by R. Cornelis, H. Crews, J. Caruso and K. G. Heumann
 ISBN: 0-470-85598-3 (HB)

1.2 Aquatic environment and model systems

With respect to speciation analysis of thallium in environmental samples, Guenther and Umland developed a combination of extraction and secondary ion mass spectrometry (SIMS) for the selective determination of dimethylthallium (Me_2Tl^+) in aqueous solutions [15]. Positive thermal ionization isotope dilution mass spectrometry (PTI-IDMS) was applied to the determination of dimethylthallium ions in environmental matrices [16].

The sample treatment procedure for the determination of this compound in ocean water by PTI-IDMS is shown in the schematic Figure 2.19.1. As a result, in different surface water samples of the Atlantic Ocean and in one depth profile down to 4000 m, Me_2Tl^+ concentrations in the range of 0.6–3.0 ng L^{-1} were determined [16]. The organothallium compound was found in about 20% of all samples analyzed. From its occurrence in the remote areas of the South Atlantic, from positive correlation with the bioactivity in the corresponding ocean water and from the fact that Me_2Tl^+ is not known as an anthropogenic substance, it follows that a biogenic origin must be assumed [16].

The same method was also used in another study of Schedlbauer and Heumann to investigate the biomethylation of thallium by bacteria isolated from a sewage sludge and present in a sewage sludge by adding Tl(I) nitrate to these systems [17]. Both trials were carried out under

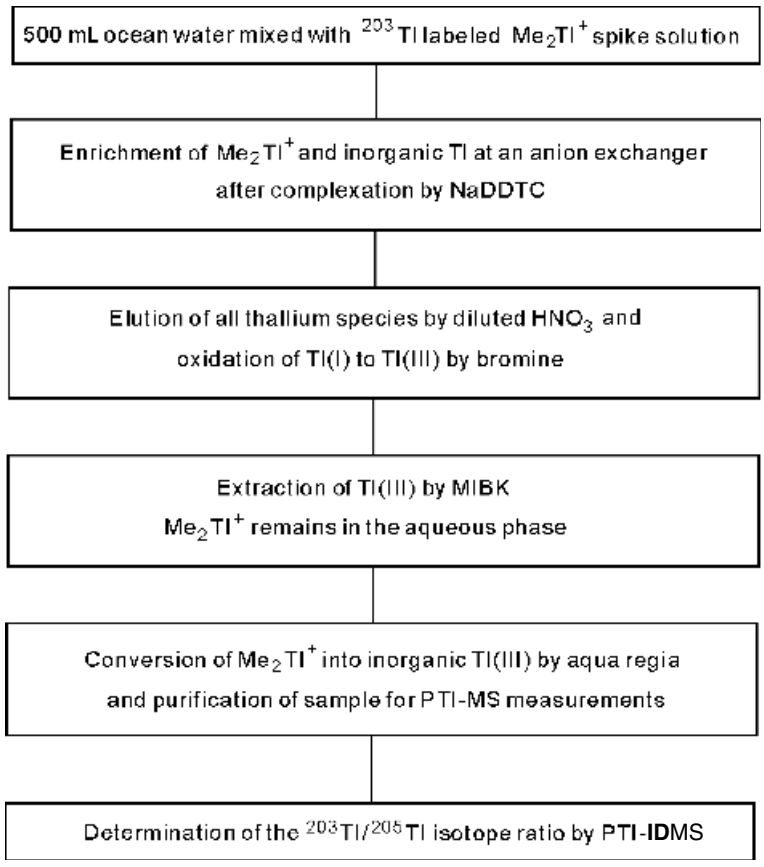

Figure 2.19.1. Schematic figure of sample treatment procedure for the determination of Me_2Tl^+ species in ocean water by PTI-IDMS. (NaDDTC = sodium diethyldithiocarbamate; MIBK = methyl isobutyl ketone.) (Reprinted with the permission from Reference [16]. Copyright (1999) American Chemical Society.)

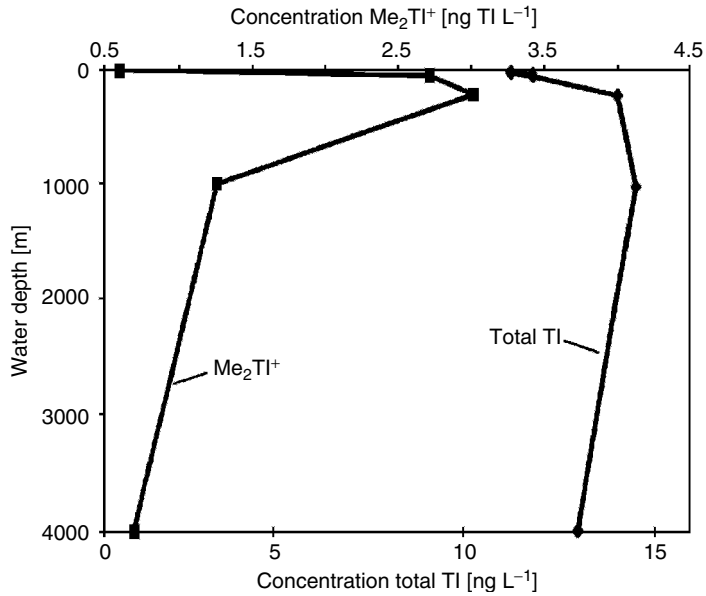

Figure 2.19.2. Depth concentration profile of dimethylthallium and total thallium at 50°43′S, 09°32′E in the South Atlantic. (Reproduced from *Appl. Organomet. Chem.*, **14**, 330, Schedlbauer, O. F. and Heumann, K. G. 2000 with permission [17]. © John Wiley & Sons Limited.)

aerobic conditions. In these cases, no significant production of dimethylthallium was observed. Under anaerobic conditions, however, significant amounts of this species were detected in a freshwater lake sediment by adding Tl(I) nitrate [17].

Analyzing a seawater sample from a single depth profile down to 4000 m as shown in Figure 2.19.2, a maximum of the dimethylthallium concentration was found between 40 and 200 m. This result correlates well with the known depth for a normally high bioactivity in the water column of the ocean. Significant Me_2Tl^+ contents were also analyzed at depths of 1000 m and 4000 m. In Figure 2.19.2, it is also demonstrated that the Me_2Tl^+ concentration profile did not fit the corresponding profile for total thallium, which did not vary much with depth [17].

Lin and Nriagu used thermodynamic data for modeling the speciation of thallium in natural waters [18, 19]. An ion exchange separation technique followed by analysis with atomic absorption spectroscopy (AAS) was used to study the chemical forms and distribution of thallium in lake water. The dominant thallium form found in water samples analyzed was the oxidized Tl(III), which comprised $68 \pm 6\%$ of the total dissolved thallium, contrary to thermodynamic prediction that Tl(I) is favored in natural waters. A significant proportion of Tl(III) may be in colloidal form. No definite horizontal or vertical pattern was found in the distribution of total dissolved thallium in the water columns of the Great Lakes in North America [20–22].

A Chelex-100 resin separation technique as followed by analysis with graphite furnace AAS was evaluated for the study of thallium speciation in river waters [23]. The detection limit for the method was 1.0 ng L^{-1} for both Tl(I) and Tl(III). Water samples from selected stations in the polluted Huron River and Raisin River in Michigan were passed through a Chelex-100 resin column. Average dissolved thallium concentrations of the river water samples were found in the range of about 20–30 ng L^{-1} [23]. The dominant thallium form found in these rivers was oxidized Tl(III), and the proportion of Tl(III) to the total dissolved thallium ranged from 43% to 73% and averaged of 66% in water samples analyzed. A significant proportion of Tl(III) may also be in colloidal form [23].

1.3 Thallium in solutions

A procedure that allows detection and speciation of thallium in flowing solutions has been developed [24]. Thallous ions (Tl^+) are determined using oxidative detection at a platinum electrode in an acid solution. In the presence of thallic ions (Tl^{3+}), irradiation of the solution with ultraviolet (UV) light induces the reduction of Tl(III) to Tl(I) that is subsequently detected as in the previous case. Discrimination between Tl(I) and Tl(III) can be easily accomplished by carrying out detection with and without photolysis [24].

Complexation chemistry of thallium was studied with regard to the effects of various buffering agents and pH conditions investigated by flame atomic absorption spectrometry (FAAS) to optimize complexation of Tl^{3+} with 8-hydroxyquinoline, immobilized on controlled-pore glass beads in a 5-cm column. As thallium normally exists as Tl^+ in solution, an oxidation method was developed to convert the ions to Tl^{3+}, which is more efficiently complexed by 8-hydroxyquinoline. Concentrations of Tl^+ and Tl^{3+} in the same matrix can be derived by using the described procedure, allowing speciation of inorganic thallium [25].

An electrochemical method was developed for thallium speciation and analysis, on the basis of the determination of Tl(I) while masking Tl(III) with ethylene diamine tetra-acetic acid (EDTA) followed by chemical reduction of Tl(III) to Tl(I) with hydroxylamine hydrochloride [26].

In aqueous media, thallium(I) can be determined by measuring its fluorescence as $TlCl_3^{2-}$. Thallium(III) is also determined after the rapid reduction of this ion by hydrazine into thallium(I). A flow injection method for the speciation of TI(I) and TI(III) with spectrofluorimetric detection has been developed in [27].

1.4 Soil and soil solutions

A rapid and simple method is developed for the determination of the total and mobile thallium content in soils [28]. Ammonium acetate or potassium chloride are proposed as extractants of mobile thallium from the soils. After soil pretreatment, the extract is subjected to anion-exchange separation and preconcentration of thallium [28]. By this procedure, the plant available thallium in these matrices is detected by flame AAS, assuming that thallium is present as Tl^+ because of the reducing substances in its environment. The limit of detection of the method is 0.04 $\mu g\, g^{-1}$. The mobile percentage of total thallium in the analyzed soil samples was 6% [28].

A simple flow injection spectrofluorimetric method allows speciation and fluorimetric detection of thallium in flowing solutions. It was applied to determine thallium in soils and other matrices. The determination of Tl(III) is based on the rapid reduction of this ion by thiourea with the concomitant formation of fluorescent Tl(I). Tl(I) in the respective solutions is determined by measuring its fluorescence in an acidic medium [29].

1.5 Sediments

In river sediments, the speciation of thallium was carried out by consecutive leaching techniques followed by graphite furnace atomic absorption spectrometry (GFAAS) measurements [30]. As a result of the leaching sequence, Tl is found largely in the nitric-acid leachable and the oxalate-leachable fractions. In the alternative sequence, it is evenly distributed among alkali-mobile and acid-mobile fractions. Soluble thallium in tap water was completely adsorbed by added sediments after overnight contact. In subsequent sequential leaching, it was found highly exchangeable at pH 7 against ammonium chloride or ammonium acetate [30].

A Tl-polluted river sediment was studied with respect to the mobility of thallium under different conditions [31]. Thereby, it was found out that the complexing agents NTA (nitrilotriacetic acid) and HEDP (1-hydroxyethane-1,1-diphosphonic acid) had no influence on the mobilization behavior of this element. The resistance of thallium against the influence of these chemicals could indicate that the metal is exclusively available as Tl(I) that forms less stable complexes contrary to the trivalent oxidation state of this element [31].

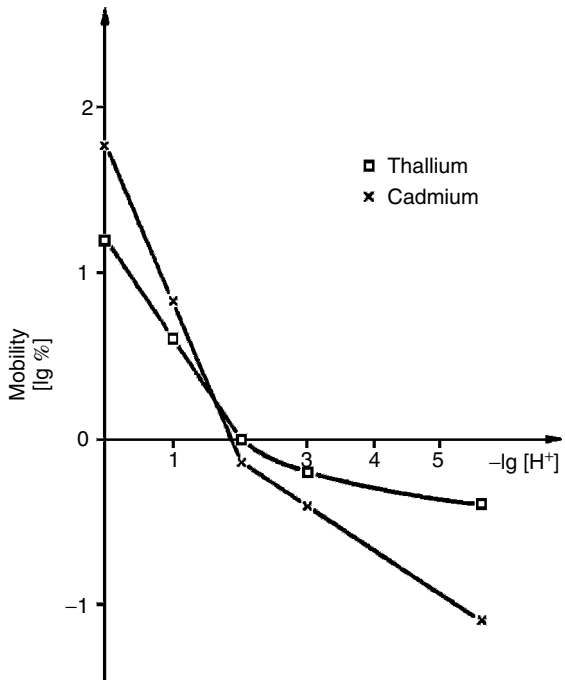

Figure 2.19.3. Mobilized percentages of thallium and cadmium from a Tl-polluted river sediment in the absence of complexing agents and 14 hours of agitation time (double logarithmic application) using atomic absorption spectrometry as detection method. (Reproduced from Reference [31] by permission of Springer-Verlag GmbH & Co KG.)

Another trial dealt with a possible remobilization of Tl in a polluted sediment by lowering the pH value. The element is released in significant amounts beyond pH 2 as shown in Figure 2.19.3. Conclusively, thallium is strongly bound to the sediment matrix. This result means that a danger for the ecosphere in the investigated part of this river by this metal can nearly be excluded [31].

2 FOOD

Thallium is a rare, toxic element. Thallium(I) salts are readily absorbed from the mucous membranes of the mouth, the gastrointestinal tract and from the skin. It is toxic to the gastrointestinal tract. Therefore, it is very important to determine sources of thallium in food and to investigate dietary intakes of this element [32].

2.1 Thallium concentrations in foodstuffs

Table 2.19.1 presents information on thallium in vegetables, meat and salt. In studies of the Sixties, Seventies and Eighties, it is indicated that most fresh foods should contain no more than 0.1 mg kg^{-1} Tl and that most concentrations should be <0.05 mg kg^{-1}. There is a wide range of reported thallium concentrations in food plants, namely 0.005–0.125 mg kg^{-1} [32]. Higher concentrations occur in some wild mushrooms, but this is unlikely to have much significance for the diet. The dietary intake of thallium in the United Kingdom is estimated to be about 0.005 mg per day. It is considered that *Brassicae* are likely to be the main source of dietary exposure to thallium in food produced on contaminated land [32].

2.2 Thallium uptake by plants

Thallium is reported to be widely distributed in the vegetable kingdom [39] and is rapidly taken up by the plant root [32]. In this context, the thallium-transfer from soils to plants was investigated with respect to the correlation between the chemical form and the plant uptake of this element [40]. From observations made near a source of emissions of thallium to the atmosphere, it was concluded that deposition from the atmosphere leads to an accumulation of the element in soil from whence it is transferred to food crops, fodder crops and pastures [32].

For example, the Tl uptake from different soils treated with cement furnace dust was investigated for green rape, bush beans and Weidel grass [41]. The investigations were carried out with regard to the plant availability of Tl and the question of contamination of agricultural products with this toxic element [41]. As a result, green rape accumulated higher amounts of the element than the other plants. Generally, a positive linear proportion between the available thallium amounts of the investigated soils and the Tl uptake, respectively, Tl contents of the plants examined was observed [41].

Table 2.19.1. Thallium in foods [32].

Food	Thallium concentrations mg kg^{-1} fresh weight	Number of samples	Reference
Potatoes	0.02	3	AERE, Report [33]
	<0.02–0.02		Hislop *et al.* [33]
Lettuce (inner leaves)	0.005	9	AERE, Report [33]
	0.003–0.12		Hislop *et al.* [33]
Lettuce	0.02	n.s.	Geilmann *et al.* [34]
Red cabbage	0.04	n.s.	Geilmann *et al.* [34]
Green cabbage	0.125	n.s.	Geilmann *et al.* [34]
Leek	0.075	n.s.	Geilmann *et al.* [34]
Endive	0.08	n.s.	Geilmann *et al.* [34]
Beet leaf	0.025–0.030	n.s.	Geilmann *et al.* [34]
KCl, technical	0.3	n.s.	Geilmann *et al.* [34]
Table salt	All 0.02	4	Toots and Parker [35]
Sodium-free salt substitutes	0.02; 0.035; 0.42	3	Toots and Parker [35]
Low sodium salt substitute	0.045	1	Toots and Parker [35]
Pig muscle	<0.07	22	Konermann *et al.* [36]
Pig kidney	<0.07	22	Konermann *et al.* [36]
Pig liver	<0.07	22	Konermann *et al.* [36]
Sheep muscle	0.05–0.06	3	Hapke *et al.* [37]
Sheep kidney	0.05–0.06	3	Hapke *et al.* [37]
Sheep liver	<0.05	3	Hapke *et al.* [37]
Wild mushrooms	0.007–1.2	1107	Seeger and Gross [38]
	85% of samples contained <0.25 mg kg^{-1} on a dry weight basis		

Note: n.s. = not specified.
Source: Reproduced from Reference [32] by permission of Taylor & Francis Ltd., http://www.tandf.co.uk/journals.

In another study, the uptake of thallium by vegetables was investigated with respect to its significance for the human health, phytoremediation and phytomining [42]. For that purpose, 11 common vegetables and a thallium-hyperaccumulator plant as shown in Figure 2.19.4 were grown in pot trials that contained 0.7 and 3.7 mg kg^{-1} thallium added to a silt loam soil. Maximum thallium levels ranged from nearly 400 mg kg^{-1} (dry mass) in *Iberis* down to just over 1 mg kg^{-1} in green bean [42]. The four vegetables with the highest thallium levels were watercress, radish, turnip and green cabbage. At a thallium concentration of 0.7 mg kg^{-1} in the soil, only green bean, tomato, onion, pea and lettuce would be safe for human consumption. At 3.7 mg kg^{-1} thallium, only green bean and tomato could be eaten [42].

2.3 Rape

As a model plant for *Brassicae*, native rape (*Brassica napus*) was investigated with regard to the thallium and cadmium-binding forms in these fodder plants [43]. The leaves from unpolluted rape of two different growth stages were homogenized in buffer at 5 °C and centrifuged. In average, the resulted supernatant (cytoplasmic fraction) contained 37% of the whole cadmium and 84% of the total thallium [43]. Gel filtration of the cytoplasmic samples revealed high and low molecular mass cadmium species, but one thallium species (M = 3800 Da). No free ionic species have been detected. The determination of Tl was done with electrothermal atomic absorption spectrometry (ET-AAS) [43].

In the chromatogram shown in Figure 2.19.5, thallium is eluted as one peak in the low molecular mass range of a Sephadex G-75 column. The maximum Tl concentration corresponds with a relatively high UV absorption at 280 nm. Further gel chromatographic investigations of the cytosols confirmed that there is only one thallium species in native rape [43]. Probably, the cytosolic thallium binding factor is a 3800 Da peptide containing no sulfurous amino acids [44].

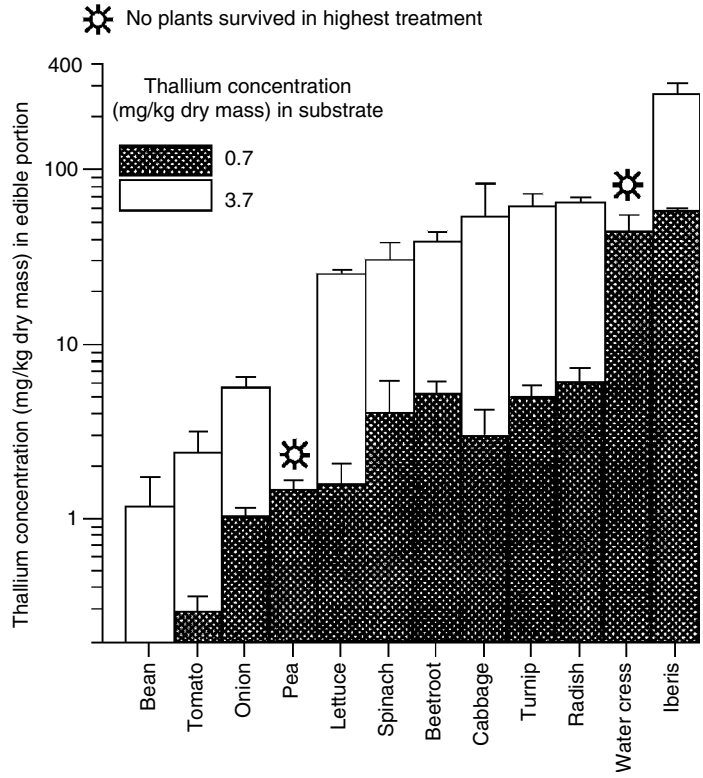

Figure 2.19.4. Thallium concentrations in vegetables and in the thallium-hyperaccumulator *Iberis intermedia* when grown in loam with added thallium. Tl in the digested vegetation and soil samples was measured by the use of FAAS or GFAAS. (Reprinted from Reference [42], pp. 1205 by courtesy of Marcel Dekker Inc.)

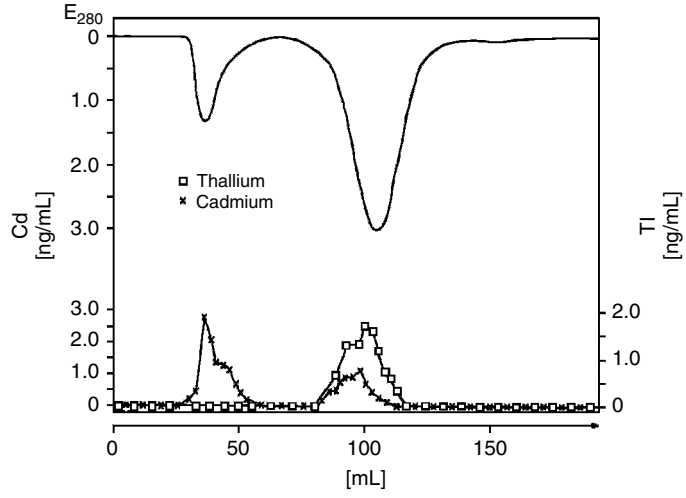

Figure 2.19.5. Gel permeation chromatogram that shows the UV absorption profile ($\lambda = 280$ nm) of native rape cytosol separated on a Sephadex G-75 column. Metal concentrations were determined by ET-AAS. (Reproduced from Reference [43] by permission of Springer-Verlag GmbH & Co KG.)

By a combination of gel filtration on Sephadex gels, homogenization in buffer and subsequent ultracentrifugation, the bonding states of thallium and cadmium were also studied in leaves of thallium-treated rape [44]. The separated cytosols contained about 70% of the total thallium and 50% of the total cadmium. Determinations of metals were performed by electrothermal and flame AAS. The thallium-treated plants contained about 23 mg thallium/kg referring to wet weight. Almost all of the cytoplasmic thallium was found as uncomplexed ionic species [44]. Moreover, no dimethylthallium compounds have been detected by means of secondary-ion mass spectrometry after extraction. Additionally, analysis for Tl^{3+} was negative. Conclusively, in contaminated rape the predominant portion of thallium exists as free Tl^{+} – ions [44]. This is an important result because the toxicity of thallium probably stems in part from the way in which the thallous ion, Tl^{+} ionic radius 1.44 Å, is able to mimic the behavior of the potassium ion, K^{+} ionic radius 1.33 Å [32].

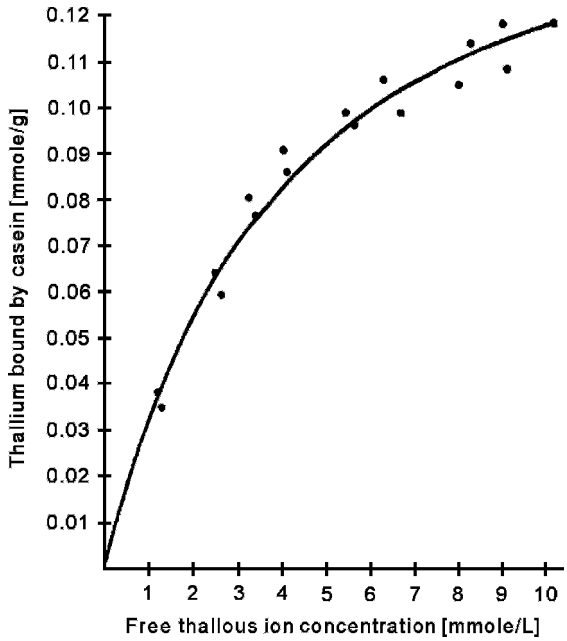

Figure 2.19.6. Thallium binding by casein in buffer pH 7 after equilibrium dialysis. Experimental results and fitted curve. (Reproduced from Reference [45] by permission of ADSA.)

2.4 Milk

To analyze the effect of milk protein on thallous ion, the binding of this species by whole casein was studied by the equilibrium dialysis method at pH 7 [45]. The sample preparation consisted of several analytical steps, including acid precipitation of fat-free whole casein being dispersed in buffer. The suspension was treated with cation-exchange resin (Amberlite) to exchange Ca^{2+}, Mg^{2+}, and Na^{+} for K^{+}, which is considered not to be bound by the casein. After filtration, dialysis, concentration and lyophilization of the protein suspension dispersions of casein (~4%) were prepared in different standard TlCl solutions [45].

Equilibrated dialysis tubings were completely filled with 50 mL each of different standard TlCl solutions. They were then suspended in glass tubes that contained 25 mL each of the corresponding casein dispersion. The tubes were placed in a shaker and agitated until equilibrium was achieved. The TlCl solutions and casein dispersions were then separated and analyzed for protein, thallous ion and chloride concentrations. Results of the dialysis equilibrium study are illustrated in Figure 2.19.6. Herein, the relationship between the free and bound thallium is represented. It is evident from the results received that casein does bind thallous ion [45].

In human breast milk, ^{201}Tl was measured with respect to radiation safety considerations for infants whose mothers are administered radioactive materials [46]. Aliquots from milk samples were counted in a sodium iodide well counter and compared to a ^{201}Tl standard that was prepared from a dilution of a ^{201}Tl source measured in a dose calibrator. It could be shown that ^{201}Tl is secreted through human milk, and it was recommended that nursing be delayed 24–48 hours following the administration of 111 MBq (3 mCi) of ^{201}Tl [46].

2.5 Other foodstuffs

In the literature, it is generally accepted that thallium accumulates in the edible parts of animals. As example, thallium was analyzed in muscle,

kidney and liver of sheep and pig [32]. Thallium amounts were also determined in other foodstuffs, such as lake trout [47], contaminated candies [48] and wines [49]. It is well known that the yeast *Saccharomyces cerevisiae* is inhibited by thallium in its growth. The intoxication with this element is explained by an accumulation of the thallous ion in the mitochondria of these organisms. The uptake of Tl^+ into the yeast cell follows the potassium transport systems, which seem to possess a higher affinity to thallium compared to potassium [38].

As chronic poisoning by thallium appears to be a phenomenon associated with growing environmental pollution [47] and, although rare, thallium poisoning still occurs [48], in future more foodstuffs have to be investigated with regard to the available Tl binding forms in these matrices to assess the toxicological effects and resorption properties of thallium in organisms.

3 CLINICAL

Thallium is a cumulative poison of high toxicity, and is without taste, smell or other warning attributes. Because of the properties of this element, thallium compounds (e.g. Tl_2SO_4) are used for the control of rodents under restricted conditions. In human beings, poisoning from toxicologic exposure to thallium happened in case of homicide, suicide and inadvertence [50]. In a later study, it is shown that thallium occurs as regular trace element of the human and the animal body. Its occurrence in hair can be demonstrated easily [34].

3.1 Human matrices

A spectrographical method to determine and to define the natural thallium content of the human body as compared to Tl-intoxicated organisms was developed, and physiological amounts of this element in biological material could be registered. Thallium is greatly enriched through extraction with diethylammonium diethyl dithiocarbamate (D-DDC), resulting in a high sensitivity [51]. Tl concentrations in different organs of the human body were analyzed by mass spectrometry using an internal standard of a ^{203}Tl-enriched mixture of Tl isotopes at the beginning of the digestion process of the different matrices. None of the organs examined was free of Tl. The highest amounts of the element with ranges from 4.8 to 15.8 ng g^{-1} were found in hair, and the lowest concentrations were present in fat, fat-containing tissues, fluids and blood [52].

3.2 Cases of intoxications

Chronic Tl intoxication in case of criminal poisoning was treated by the administration of potassium-iron(III) hexacyanoferrate(II) (*Berlin Blue*), combined with forced diuresis [53]. Human thallium toxicity generally has been described and reviewed [54–57] by several authors and also the chelation treatment of the intoxication by Tl and other metals [58, 59]. The reported estimated half-life of thallium in humans is highly variable [54].

It is a well-known fact that thallium ions are able to pass through the placenta [32]. In this context, special regard has to be paid to the treatment of an intoxication by Tl during the time of pregnancy and lactation [60]. The fetus of a woman was aborted after this woman had been detoxified by a differential procedure consisting of heme dialysis, forced diuresis and local antidot therapy with *Berlin Blue*. At the time of abortion, the thallium concentrations of the fetal organs were up to 12-fold higher as compared to the Tl contents of the mother's blood [60]. The concentrations of this element in breast milk from another woman who attempted suicide were several times higher compared to the Tl content of her blood. Thus, the poison was transferred to the suckling infant [60].

3.3 Measurement methods

Total amounts of Tl were analyzed in different biological samples [61] with special regard to urine [62–68], saliva [63], feces [63], tissues [69] and blood [67]. These matrices were analyzed for Tl by different analytical methods such as atomic absorption spectrophotometry [61–64], spectrophotometry [68, 69], coulometry [67] and differential

pulse anodic stripping voltammetry [64–66]. A few studies deal with the speciation analysis of thallium in clinical matrices.

3.4 Biofluids

In this context and in favor of the research of new thallium sequestering agents, the thallium interactions in biological fluids were examined with regard to the investigation of dimethylthallium complex equilibria with some typical amino acids [70]. Thereby, formation constants for dimethylthallium complexes with L-cysteine (Cys), DL-penicillamine (Pen), *N*-acetyl-L-cysteine (Acy), *N*-acetyl-DL-penicillamine (Ape) and glycine (Gly) were determined under physiological conditions using glass electrode potentiometry. The authors concluded that the coordination of dimethylthallium by the carboxylate anion was insignificant [70].

Using the same method to the investigation of thallium(I) complex equilibria with sulfur-containing amino acids, the formation constants for Tl(I) complexes of L-cysteine and other amino acids in aqueous solutions were determined [71]. This procedure is necessary because the metabolic action and fate of thallium(I) is not clear. Nevertheless, there are experimental evidences that suggest that there are similarities between the ionic transport of thallium(I) and potassium through cell membranes, although intracellular thallium(I) seems to be less rapidly released than potassium. The biological effects of thallium(I) have also been thought to be due to its interference with the metabolism of sulfur-containing compounds. Thus, clearly a greater understanding of thallium(I) binding by these compounds would give an insight of the toxicity mechanisms of this metal [71].

As an example Figure 2.19.7 gives the formation curves of the thallium(I)-L-cysteine system showing the species distribution as a function of pH. In this system, the $Tl(Cys)^-$ complex is continuously increasing from about pH 8 to a maximum pH value of 11, while the percentage of Tl^+ ions steadily decreases from about pH 7 to 11. At pH 9, both ionic Tl species are evenly distributed with nearly 50% each in this system. Consequently,

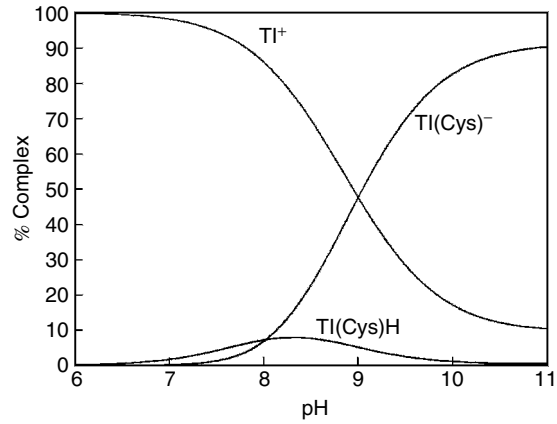

Figure 2.19.7. Thallium species distribution as a function of pH in the aqueous thallium(I)-L-cysteine system. (Reprinted from *J. Inorg. Biochem.*, **35**, Garcia Bugarin, M., Sergio Casas, J., Sordo, J. and Filella, M., 95, Thallium(I) interactions in biological-fluids – a potentiometric investigation of thallium(I) complex equilibria with some sulfur-containing amino-acids, copyright (1989) with permission of Elsevier [71].)

having pH values >9, the metal-ligand is the dominant complex, while the protonated metal-ligand, which is formed in the pH range 6.0 to 10.5 with a maximum near 8, always accounts for less than 10% of the total metal [71].

Dimethylthallium complex equilibria with further compounds, for example, 2-thiobarbiturate [72], 2-thioorotate [73] and glutathionate [74] in the presence of hydrogen ions in aqueous solutions were also investigated by means of potentiometric techniques by Garcia-Tasende, Garcia Bugarin and Filella.

3.5 Serum

By using a combination of gel permeation chromatography and ICP-MS, it was shown that thallium and alkali metals occurring in bovine serum are not bound to proteins or to other molecules [75]. It was revealed that these metals are present primarily as free ions as shown in Figure 2.19.8. A double focusing mass analyzer provides very high sensitivity, low background and sufficient spectral resolution to separate the atomic ions of interest from most polyatomic ions at the same nominal m/z value. The chromatogram reveals that Tl^+ elutes at long

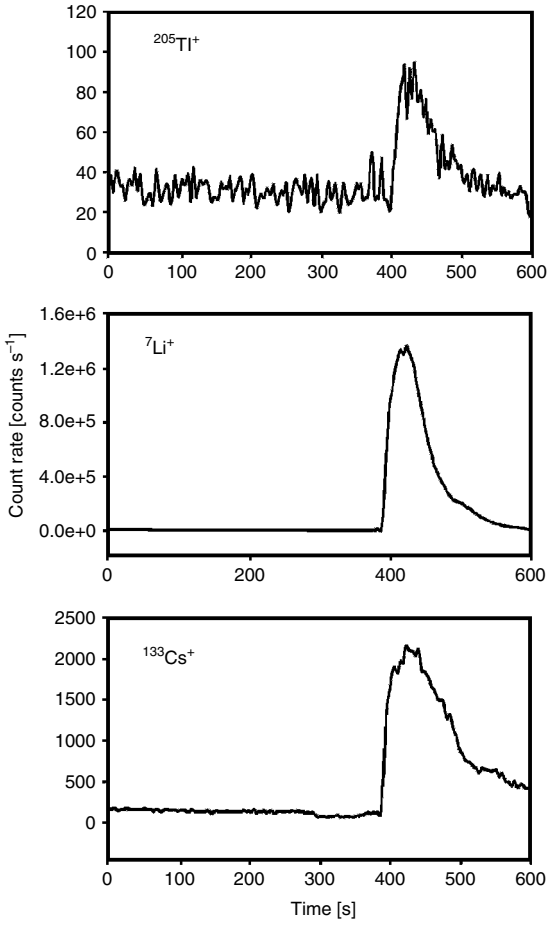

Figure 2.19.8. Chromatograms for Tl, Li and Cs in bovine serum (*NIST* 1598). Results were received after separation by gel permeation chromatography on-line coupled with ICP-MS. (Reproduced from Reference [75] by permission of Springer-Verlag GmbH & Co KG.)

retention times, like the alkali metals Li^+ and Cs^+, which themselves coelute with Na^+ and K^+ [75]. This is an important result because if the concentration of uncomplexed thallium(I) ions becomes too high, then Tl^+ interferes with the biological functions of K^+ [75].

4 OCCUPATIONAL HEALTH

Thallium and its compounds can enter the organism of persons working with them through the respiratory organs (aerosols), through the gastrointestinal tract and through the skin. The toxicity of thallium is approximately the same in all routes of intake [76]. The latter two routes of intake predominate in cases of nonoccupational poisoning. Industrial thallium poisoning can either be acute or chronic, but in all cases it is characterized by a long duration and severity of its course [76].

Both acute and chronic studies show that the highest concentration of Tl(I) is found in the kidney. In humans and animals poisoned with thallium(I), the metal is widely distributed in the body. With chronicity, the centers of concentration shift to include the central nervous system and hair [71]. As example, examination of hair from a glass factory worker revealed that the thallium content of the hair, as determined by an ICP-MS method, was 20 ng g^{-1} [77].

4.1 Epidemiological studies

A cohort study involving a population of workers exposed to Tl and a control group was performed to determine whether there were any clinical effects attributed to this toxic metal. The conclusion was that there was no statistically significant difference [78]. In another study, urinary thallium was measured by ET-AAS in a group of nonexposed individuals and in two groups of workers employed in industrial plants [79]. In the first group, the urinary Tl mean value was 0.22 μg L^{-1}. Significantly higher values with mean urinary Tl concentrations of 0.38 and 0.33 μg Tl/L, respectively, were found in urine samples from two groups of workers with suspected industrial exposure [79].

Flameless AAS was used to analyze thallium in samples of 'spontaneous' urine of over 100 male employees from all areas of production in three cement factories [80]. In part, the group of persons investigated revealed excretions of thallium slightly or moderately above the normal level with ranges from <0.3 to 6.3 μg Tl/g creatinine. As the upper normal limit of thallium excretion, a value of 1.1 μg Tl/g creatinine was computed [80]. In no case, however, did the case history data or the findings of the physical examination of a worker reveal any indication of the symptoms characteristic

Table 2.19.2. Disposition and renal intracellular distribution of different thallium species [81].

		Tl^+	Tl^{3+}	Dimethyl-Tl
		Thallium content (% dose)		
Tissue distribution	Kidneys	6.80 ± 1.00	6.10 ± 0.8	0.56 ± 0.16
	Liver	3.80 ± 0.25	2.90 ± 0.3	0.12 ± 0.02
	Testes	3.70 ± 0.32	3.90 ± 0.51	0.07 ± 0.004
	Salivary glands	1.21 ± 0.22	1.32 ± 0.07	0.02 ± 0.006
	Heart	0.65 ± 0.14	0.51 ± 0.19	0.06 ± 0.002
	Brain	0.57 ± 0.02	0.75 ± 0.09	0.02 ± 0.003
		Thallium content (% of total kidney homogenate)		
Intracellular distribution	Nuclei	26.1 ± 2.6	26.5 ± 3.9	23.2 ± 3.5
	Mitochondria	9.7 ± 2.1	10.8 ± 2.8	10.6 ± 1.5
	Lysosomes	14.6 ± 2.4	18.5 ± 3.2	15.6 ± 2.9
	Microsomes	9.0 ± 2.4	8.1 ± 2.2	8.4 ± 2.1
	Cytosol	40.6 ± 3.3	36.1 ± 4.4	42.2 ± 5.3

Rats sacrificed 16 hours after oral administration of 3.15 mg Tl/rat as ^{201}thallium-labeled inorganic Tl(I) or Tl(III) ions, or dimethylthallium. $n = 5$ experiments.
Source: Reproduced from Reference [81] by permission of the European Commission.

of thallium poisoning. The concentration of T1 in urine is used as an indicator for exposure in line with the norm set as 'biological work material tolerance (BAM value)' [80], to give just this example.

From the results obtained, it *cannot* be concluded that thallium in urine is associated to creatinine. However, it would be interesting to examine which thallium binding factors are present in urine from workers employed in cement factories or other industrial areas to get information on the metabolic fate of thallium in the human organism.

4.2 Metabolic behavior

As a first step to understand the metabolism and to elucidate the forms of thallium in organisms, the metabolic pattern of the different Tl species occurring in the environment (Tl^+, Tl^{3+}, organothallium) was examined in the rat following the administration of Tl doses ranging from acute toxic doses to minute amounts. After preparation of the different forms of ^{201}Tl-labeled thallium compounds, the animals were treated with these substances by intraperitoneal or oral route. At various time intervals after treatment, the rats were sacrificed, and subsequently, the organs were homogenized in buffer, and subcellular fractions were obtained by differential centrifugation [81].

In Table 2.19.2, the disposition and renal intracellular distribution of different thallium species are shown. The percentage distributions of inorganic Tl^+ compared to Tl^{3+} species among the different rat organs are very similar. In contrast to this result, the percentage of dimethylthallium is very low in the respective tissues. Consequently, the distribution of Tl among the organs of the rat is dependent on the Tl-species. The intracellular distribution of Tl^+, Tl^{3+} and dimethylthallium in rat kidney showed a rather similar thallium distribution pattern among the investigated cell organelles of this organ with respect to all administered thallium compounds [81]. As also shown in Table 2.19.2, inorganic Tl^+ or Tl^{3+} ions are accumulated in endocrine glands (testes). In a later study, it was found out that Tl accumulated in testicles leads to reduced sperm motility [1].

The metabolic fate of different inorganic and organic species of thallium in the rat was investigated by Sabbioni, Goetz, Marafante, Gregotti and Manzo [82], while the distribution and excretion of thallium after oral and intraperitoneal administration of thallous mallonate and thallous sulfate in hamsters was revealed by Aoyama [83]. There are evidences that Tl ions could be transported from the colon into the intestinal lumen by carrier proteins [60].

Since toxic effects on the eye and epilation are symptoms of occupational and nonoccupational

thallium intoxication, the binding of the element in animal eyes and tissues was investigated by using $^{201}Tl^{+}$ autoradiography [84]. The results are consistent with the concept that a binding of thallium occurs to the free carboxyl groups of the eye melanin and that the structure of the polymer has a marked influence on the affinity. Thus, toxic effects in these cases may be related to the thallium melanin binding [84].

4.3 Outlook

First of all the results demonstrate the importance and the needs for more Tl speciation studies in matrices from animals and human beings, in order to obtain fundamental data for the treatment of subjects who suffer from chronic or acute Tl intoxication. On the basis of this knowledge, new detoxicating medicaments could be developed. These should consist of chemical molecules with a high affinity and specificity to toxic thallium species in the different organs or tissues.

Focusing our view on some human tragedies due to Tl intoxications in the past century [85], we hope that the reader will no longer be able to echo the words of Mr. Venables in Agatha Christie's 'The Pale Horse' (Christie, 1961); 'Thallium... I don't think I've ever heard of it' [86].

5 REFERENCES

1. Kemper, F. H. and Bertram, H. P., Thallium, in *Metals and Their Compounds in the Environment: Occurrence, Analysis and Biological Relevance*, Merian, E., (Ed.), VCH, Weinheim, 1991, Chapter II.29, pp. 1227–1241.
2. Prinz, B., Krause, G. H. M. and Stratmann, H., *Staub Reinhalt. Luft*, **39**, 457 (1979).
3. Waidmann, E., Hilpert, K. and Stoeppler, M., *Fresenius' J. Anal. Chem.*, **338**, 572 (1990).
4. Waidmann, E., Stoeppler, M. and Heininger, P., *Analyst*, **117**, 295 (1992).
5. Sager, M., Trace analysis of thallium, in *Analytical Chemistry in Practice*, Hulpke, H., Hartkamp, H. and Toelg, G., (Eds.), Georg Thieme Verlag, Stuttgart, New York, 1986, pp. 1–103.
6. Wei, M.-T. and Jiang, S.-J., *J. Anal. At. Spectrom.*, **14**, 1177 (1999).
7. Chandrawanshi, S., Sharma, M. and Patel, K. S., *Fresenius' J. Anal. Chem.*, **351**, 305 (1995).
8. Cheam, V., Lawson, G., Lechner, J., Desrosiers, R. and Nriagu, J., *Fresenius' J. Anal. Chem.*, **355**, 332 (1996).
9. Mestek, O., Koplik, R., Fingerova, H. and Suchanek, M., *J. Anal. At. Spectrom.*, **15**, 403 (2000).
10. Asami, T., Mizui, C., Shimada, T. and Kubota, M., *Fresenius' J. Anal. Chem.*, **356**, 348 (1996).
11. Allus, M. A. and Brereton, R. G., *Analyst*, **117**, 1075 (1992).
12. Cheam, V., Lechner, J. and Desrosiers, R., *Fresenius' J. Anal. Chem.*, **360**, 81 (1998).
13. Zhou, J. X., Hou, X., Yang, K. X. and Michel, R. G., *J. Anal. At. Spectrom.*, **13**, 41 (1998).
14. Lopez-Garcia, I., Navarro, E., Vinas, P. and Hernandez-Cordoba, M., *Fresenius' J. Anal. Chem.*, **357**, 642 (1997).
15. Guenther, K. and Umland, F., *Fresenius' Z. Anal. Chem.*, **333**, 6 (1989).
16. Schedlbauer, O. F. and Heumann, K. G., *Anal. Chem.*, **71**, 5459 (1999).
17. Schedlbauer, O. F. and Heumann, K. G., *Appl. Organomet. Chem.*, **14**, 330 (2000).
18. Lin, T.-S. and Nriagu, J. O., Speciation of thallium in natural waters, in *Thallium in the Environment*, Nriagu, J. O., (Ed.), John Wiley & Sons, Chichester, 1998, Chapter 3, pp. 31–43.
19. Lin, T.-S. and Nriagu, J. O., *J. Air Waste Manage. Assoc.*, **48**, 151 (1998).
20. Lin, T.-S. and Nriagu, J., *Environ. Sci. Technol.*, **33**, 3394 (1999).
21. Cheam, V., *Environ. Sci. Technol.*, **34**, 2367 (2000).
22. Lin, T.-S. and Nriagu, J., *Environ. Sci. Technol.*, **34**, 2369 (2000).
23. Lin, T.-S. and Nriagu, J. O., *Anal. Chim. Acta*, **395**, 301 (1999).
24. Barisci, J. N. and Wallace, G. G., *Electroanalysis*, **4**, 139 (1992).
25. Mohammad, B., Ure, A. M. and Littlejohn, D., *Mikrochim. Acta*, **113**, 325 (1994).
26. Cai, Q. and Khoo, S. B., *Electroanalysis*, **7**, 379 (1995).
27. Ensafi, A. A. and Rezaei, B., *Microchem. J.*, **60**, 75 (1998).
28. Tsakovski, S., Ivanova, E. and Havezov, I., *Talanta*, **41**, 721 (1994).
29. Perez-Ruiz, T., Martinez-Lozano, C., Tomas, V. and Casajus, R., *Analyst*, **121**, 813 (1996).
30. Sager, M., *Mikrochim. Acta*, **106**, 241 (1992).
31. Guenther, K., Henze, W. and Umland, F., *Fresenius' Z. Anal. Chem.*, **327**, 301 (1987).
32. Sherlock, J. C. and Smart, G. A., *Food Addit. Contam.*, **3**, 363 (1986).
33. Hislop, J. S., Collier, T. R., Pickford, C. J. and Norvell, W. E. *Atomic Energy Research Establishment, Harwell*, Report number AERE G 2383, 1982.
34. Geilmann, W., Beyermann, K., Neeb, K.-H. and Neeb, R., *Biochem. Z.*, **333**, 62 (1960).
35. Toots, H. and Parker, R. B., *Environ. Res.*, **14**, 327 (1977).

36. Konermann, H., Crossmann, G. and Hoppenbrock, K. H., *Tierarztl. Umsch.*, **37**, 8 (1982).
37. Hapke, H. J., Barke, E. and Spikermann, A., *Dtsch. Tierarztl. Wochenschr.*, **87**, 376 (1980).
38. Seeger, R. and Gross, M., *Z. Lebensm.-Unters.-Forsch.*, **173**, 9 (1981).
39. Horn, E. E., Ward, J. C., Munch, J. C. and Garlough, F. E., *Circular U. S. Dep. Agric.*, **409**, 1 (1936).
40. Lehn, H. and Schoer, J., *Plant Soil*, **97**, 253 (1987).
41. Makridis, H. and Amberger, A., *Landwirtsch. Forsch.*, **42**, 324 (1989).
42. LaCoste, C., Robinson, B. and Brooks, R., *J. Plant Nutr.*, **24**, 1205 (2001).
43. Guenther, K. and Umland, F., *Fresenius' Z. Anal. Chem.*, **331**, 302 (1988).
44. Guenther, K. and Umland, F., *J. Inorg. Biochem.*, **36**, 63 (1989).
45. Sundararajan, N. R. and Whitney, R. Mc. L., *J. Dairy Sci.*, **52**, 1445 (1969).
46. Murphy, P. H., Beasley, C. W., Moore, W. H. and Stabin, M. G., *Health Phys.*, **56**, 539 (1989).
47. Lin, T.-S., Nriagu, J. and Wang, X.-Q., *Bull. Environ. Contam. Toxicol.*, **67**, 921 (2001).
48. Meggs, W. J., Hoffman, R. S., Shih, R. D., Weisman, R. S. and Goldfrank, L. R., *J. Toxicol. Clin. Toxicol.*, **32**, 723 (1994).
49. Eschnauer, H., Gemmer-Colos, V. and Neeb, R., *Z. Lebensm.-Unters.-Forsch.*, **178**, 453 (1984).
50. Munch, J. C. and Olden, G., *J. Am. Med. Assoc.*, **102**, 1929 (1934).
51. Goenechea, S. and Sellier, K., *Dtsch. Z. Gesamte Gerichtl. Med.*, **60**, 135 (1967).
52. Weinig, E. and Zink, P., *Arch. Toxikol.*, **22**, 255 (1967).
53. Trenkwalder, P., Bencze, K. and Lydtin, H., *Dtsch. Med. Wschr.*, **109**, 1561 (1984).
54. Repetto, G., del Peso, A. and Repetto, M., Human thallium toxicity, in *Thallium in the Environment*, Nriagu, J. O., (Ed.), John Wiley & Sons, 1998, Chapter 9, pp. 167–199.
55. Galvan-Arzate, S. and Santamaria, A., *Toxicol. Lett.*, **99**, 1 (1998).
56. Leonard, A. and Gerber, G. B., *Mutat. Res.*, **387**, 47 (1997).
57. Mulkey, J. P. and Oehme, F. W., *Vet. Human Toxicol.*, **35**, 445 (1993).
58. Andersen, O., *Chem. Rev.*, **99**, 2683 (1999).
59. Hoffman, R. S., Stringer, J. A., Feinberg, R. S. and Goldfrank, L. R., *J. Toxicol. Clin Toxicol.*, **37**, 833 (1999).
60. Graben, N., Kloeppel, H.-A., Heidemann, H. and Weiler, G., *Med. Welt*, **31**, 1391 (1980).
61. Rios, C. and Galvan-Arzate, S., Analysis of thallium in biological samples, in *Thallium in the Environment*, Nriagu, J. O., (Ed.), John Wiley & Sons, 1998, Chapter 8, pp. 155–166.
62. Dolgner, R., Brockhaus, A., Ewers, U., Wiegand, H., Majewski, F. and Soddemann, H., *Int. Arch. Occup. Environ. Health*, **52**, 79 (1983).
63. Richelmi, P., Bono, F., Guardia, L., Ferrini, B. and Manzo, L., *Arch. Toxicol.*, **43**, 321 (1980).
64. Bessems, G. J. H., Westerhuis, L. W. and Baadenhuijsen, H., *Ann. Clin. Biochem.*, **20**, 321 (1983).
65. Franke, J. P., Coenegracht, P. M. J. and de Zeeuw, R. A., *Arch. Toxicol.*, **34**, 137 (1975).
66. Curtis, A. R., *J. AOAC Int.*, **57**, 1366 (1974).
67. Christian, G. D. and Purdy, W. C., *Am. J. Clin. Pathol.*, **46**, 185 (1966).
68. Ariel, M. and Bach, D., *Analyst*, **88**, 30 (1963).
69. Tewari, S. N., Harpalani, S. P. and Tripathi, S. S., *Mikrochim. Acta*, **I**, 13 (1975).
70. Garcia Bugarin, M., Esther Garcia, M., Berthon, G., Sergio Casas, J. and Sordo, J., *Polyhedron*, **7**, 2487 (1988).
71. Garcia Bugarin, M., Sergio Casas, J., Sordo, J. and Filella, M., *J. Inorg. Biochem.*, **35**, 95 (1989).
72. Garcia-Tasende, M. S., Garcia Bugarin, M. and Filella, M., *Polyhedron*, **10**, 517 (1991).
73. Garcia-Tasende, M. S., Garcia Bugarin, M. and Filella, M., *J. Coord. Chem.*, **25**, 63 (1992).
74. Garcia Bugarin, M. and Filella, M., *J. Inorg. Biochem.*, **73**, 17 (1999).
75. Wang, J., Houk, R. S., Dreessen, D. and Wiederin, D. R., *J. Biol. Inorg. Chem.*, **4**, 546 (1999).
76. Shabalina, L. P. and Spiridonova, V. S., *J. Hyg. Epidemiol. Microbiol. Immunol.*, **23**, 247 (1979).
77. Hirata, M., Taoda, K., Ono-Ogasawara, M., Takaya, M. and Hisanaga, N., *Ind. Health*, **36**, 300 (1998).
78. Marcus, R. L., *J. Soc. Occup. Med.*, **35**, 4 (1985).
79. Apostoli, P., Maranelli, G., Minoia, C., Massola, A., Baldi, C. and Marchiori, L., *Sci. Total Environ.*, **71**, 513 (1988).
80. Schaller, K.-H., Manke, G., Raithel, H. J., Buehlmeyer, G., Schmidt, M. and Valentin, H., *Int. Arch. Occup. Environ. Health*, **47**, 223 (1980).
81. Sabbioni, E., Marafante, E., Rade, J., Di Nucci, A., Gregotti, C. and Manzo, L., Metabolic patterns of low and toxic doses of thallium in the rat, in *Mechanisms of Toxicity and Hazard Evaluation*, Holmstedt, B., Lauwerys, R., Mercier, M. and Roberfroid, M., (Eds.), Elsevier, North-Holland, 1980, pp. 559–564.
82. Sabbioni, E., Goetz, L., Marafante, E., Gregotti, C. and Manzo, L., *Sci. Total Environ.*, **15**, 123 (1980).
83. Aoyama, H., *Bull. Environ. Contam. Toxicol.*, **42**, 456 (1989).
84. Tjaelve, H., Nilsson, M. and Larsson, B., *Acta Pharmacol. Toxicol.*, **51**, 147 (1982).
85. Hoffman, R. S., *J. Toxicol. Clin. Toxicol.*, **38**, 767 (2000).
86. Douglas, K. T., Bunni, M. A. and Baindur, S. R., *Int. J. Biochem.*, **22**, 429 (1990).

2.20 Speciation of Tin

Erwin Rosenberg
Vienna University of Technology, Vienna, Austria

1 INTRODUCTION

The metal tin (chemical symbol: Sn, atomic number: 50, atomic mass: 118.69) is the 24th most abundant element in the earth's crust, with an average concentration of 2.2 mg kg^{-1} [1]. It is known since the Bronze Age to mankind, and it has mainly been used in the form of its alloys. Tin is an element of group 14 of the periodic table – the same as carbon – which thus partially explains the affinity of this element to carbon and the relative stability of the tin–carbon bond. About 200×10^3 tons of tin are produced per year worldwide [2]. The major ore used for tin production is cassiterite (tinstone) with the remarkably high specific gravity of about 7. The concentrate can therefore be obtained through ore dressing by gravity separation. From the concentrate, the crude tin is reduced with coke or anthracite by reverberating furnaces, electric furnaces or smelting furnaces. The crude tin normally contains small amounts of Cu, Pb, Sb, Bi, Fe, As and others. To produce the pure metal, tin is refined by electrolysis with hexafluorosilicate (H_2SiF_6) as electrolyte.

Tin occurs in the valence states 2 and 4, where the divalent form is always positive. The valence

Handbook of Elemental Speciation II: Species in the Environment, Food, Medicine & Occupational Health
Edited by R. Cornelis, H. Crews, J. Caruso and K. G. Heumann
 ISBN: 0-470-85598-3 (HB)

state 4, however, has amphoteric properties and appears as +4 or −4, depending on the reaction partner. Two allotropic modifications of tin are known, that is, the α- and β-forms. The normally occurring modification of tin is the β-form (= white tin), which is transformed into the α-form (= grey tin) at temperatures below 13.2 °C. The impurities normally present in tin inhibit the transformation from white to grey tin. Tin is inert to water and air, and even to oxygen at normal temperatures. Only at higher temperatures, tin reacts with oxygen to form tin oxide. Tin reacts with chlorine, bromine and iodine to form the respective stannic halides at room temperature and with fluorine at elevated temperatures. Tin also reacts vigorously at elevated temperatures with sulfur, selenium or tellurium. The amphoteric nature of tin becomes evident as it reacts with both, strong acids and strong bases. Metallic tin is attacked by hydrogen halides and readily dissolved by hot alkaline solutions to form alkaline stannite and hydrogen.

More interesting than the inorganic chemistry of tin is its organic chemistry that has attracted major interest since 1945. This was about one century after the first preparation of organotin compounds (OTCs) by Sir Edward Frankland in 1849 [3] and by Löwig in 1852 [4]. However, for about 100 years, the OTCs remained a 'laboratory curiosity' without any known practical application. This changed in the 1940s, when the plastics industry discovered the stabilizing effect of certain OTCs for polyvinyl chloride (PVC). While PVC becomes brittle and loses its color under the influence of heat and light, the addition of OTCs can significantly reduce these effects [5]. The use of mono- and dialkylsubstituted OTCs for PVC stabilization still accounts for about 70% of the world production and usage of OTCs.

However, other important industrial applications of OTCs have evolved over the past more than five decades. A research group at the Institute of Organic Chemistry at the TNO, Utrecht (The Netherlands) discovered the biocidal properties of notably the trisubstituted OTCs in the mid-1950s [6]. This paved the way for their use as toxic ingredient in timber preservatives some years later, and much later for their use in fungicides, miticides, molluscicides, rodent repellents, wood preservatives and antifouling paints. In the latter, the active components are mostly tributyl-, triphenyl- and tricyclohexyltin (TCyT). It is estimated that about 20% of the total annual production of organotins is used for this purpose [7].

The world production of OTCs was ca 50 $t\,a^{-1}$ in 1950, 35,000 $t\,a^{-1}$ in 1981, and was, before the International Marine Organisation's ban on the use of OTCs in 2003, estimated at 40,000 $t\,a^{-1}$. As the tin content of these materials is ca 25%, the production of OTCs represented thus approximately 7–10% of the usage of Sn metal [8].

In the main producing and consuming areas – the United States, Western Europe and Japan – 76% of the OTCs are used as stabilizers for PVC, 10% as antifouling biocides, 8% as agricultural biocides and 5% as catalysts for the production of polyurethanes and silicones. In less industrialized countries, the pattern of use is more biased towards agricultural applications [9].

The widespread use of OTCs has led to their entrance into various ecosystems. Because of the high toxicity at already very low concentration levels, tributyltin (TBT) has received the greatest attention. However, other OTCs, such as triphenyltin (TPhT), are also highly toxic, and their occurrence and transformation in the environment has consequently been investigated. Although the threat to the environment posed by OTCs has been recognized and legislative restrictions have been made particularly for their use as antifouling paints for ship hulls, environmental pollution due to these compounds will persist to represent a significant problem for the coming years.

2 CHEMICAL AND PHYSICAL PROPERTIES OF ORGANOTIN COMPOUNDS OTCS

Organometallic compounds of tin are characterized by covalent Sn–C bonds that are established to one or more alkyl or aryl substituents. Organometallic compounds of the tetravalent tin are of the general formula R_nSnX_{4-n} with $n = 1 \ldots 4$, where R may

be an alkyl or aryl group (for example, methyl, ethyl, butyl or phenyl) and X represents an anionic species, for example, chloride, hydroxide or acetate. Very few divalent OTCs also exist but have no practical importance.

Under the influence of light, atmospheric oxygen or certain microorganisms, OTCs are degraded in a relatively short time, with the hydrocarbon groups being split off to eventually leave behind nontoxic inorganic products after a stepwise degradation. Although both the tin–carbon bond (average dissociation energy 209 kJ mol^{-1}) and the tin–oxygen bond (average dissociation energy 318 kJ mol^{-1}) are reactive, they are sufficiently stable for general handling purposes.

The symmetrical tetraalkyltin compounds have a very slight odor. They are colorless, form monomolecular solutions, are fairly stable towards water and air and can be distilled without decomposition at $<200\,^{\circ}$C. This implies that thermal decomposition is no significant route of degradation in the environment. The higher homologues are waxy substances.

The symmetrical tetraaryltin compounds are stable towards air and water and are also colorless. They melt at temperatures above $150\,^{\circ}$C.

The organotin hydrides, with the exception of some aryltin hydrides, which are solid at room temperature, are colorless, nonassociated liquids that are rapidly attacked by oxygen and therefore can only be prepared and stored under inert gas. They are important reducing agents.

The organotin fluorides, the diorganotin dihalides and the aromatic organotin monohalides are solids at room temperature, whereas the aliphatic organotin monohalides and trihalides are liquids.

The tin–carbon bond is readily cleaved by strong acids, halogens and other electrophilic agents. Tin establishes preferentially covalent bonds to other elements, with these bonds possessing a strong ionic character. Tin is usually the electropositive partner in these compounds. The triorganotin hydroxides act more like inorganic bases than as alcohols because of the amphoteric character of tin. The bis(triorganotin) compounds, $(R_3Sn)_2O$, are thus strong bases and react with both inorganic and organic acids, forming salt-like compounds that, however, are not conducting and insoluble in water. Tin does not form double bonds with oxygen, and diorganotin oxides, R_2SnO, are polymers of usually high degree of polymerization via intermolecular tin–oxygen bonds.

It is evident that the number of organic substituents and particularly their nature has a significant effect on the physicochemical properties of OTCs, and particularly their solubility. Generally speaking, the water solubility decreases with the degree of substitution and the length of the substituent chain (if aliphatic). However, experimental solubility data are strongly varying as a result of different experimental conditions (Table 2.20.1).

3 TOXICITY OF OTCS

While the inorganic forms of tin are generally considered nontoxic, its organic derivatives exhibit a complex pattern of toxicity. The biological effects of the organotin species are mostly depending on the number and kind of organic moieties bound to the tin atom. The toxicity of the anion in the case of ionic OTCs is of subordinate importance, except when the anionic group is toxic itself. In that case, the biological effects of cation and anion are cumulative.

In general, the toxicity is largest for the trisubstituted compounds of any R_nSnX_{4-n} series. However, even among the different trisubstituted compounds, there are remarkable differences as to the profile and extent of their toxicity, depending on the chain length of the alkyl substituent (Table 2.20.2). The most toxic compound for mammals is triethyltin acetate (Et_3SnOAc) with an oral LD_{50} of 4 mg kg^{-1} for rats. The increase in chain length of the alkyl moiety is accompanied by a stronger decrease of its biocidal activity, making long-chain species such as the octyltin compounds essentially nontoxic for mammals. Thus, octyltin compounds may be considered as relatively safe stabilizers for PVC materials used for food packaging (Table 2.20.3).

In contrast to mammals, TBT exhibits a high toxicity towards aquatic life. Acute poisoning of sensitive aquatic organisms, such as algae, zooplankton, mollusks and fish larvae have been

Table 2.20.1. Physical properties of selected OTCs (compiled from [10, 11 and 12]).

	Melting point [°C]	Boling point [°C]	Density [g cm^{-3}]	Solubility [mg dm^{-3}]	CAS-No.
Bu_4Sn	−97	145 (1.3 kPa)	1.057		1461-25-2
Bu_3SnCl	−16	172 (3.3 kPa)	1.21	50[a]	1461-22-9
Bu_3SnF	248–242	>350	1.25	6	1983-10-4
Bu_3SnOAc	86–87		1.27	65	56-36-0
$(Bu_3Sn)_2O$	−45	493–513 (1.3 kPa) 180 (267 Pa)	1.17	18	56-35-9
$(Bu_3Sn)_2S$	<RT[c]			1	4808-30-4
Bu_2SnCl_2	39–41	135 (1.3 kPa)	1.36	50; 5–17[b]	683-18-1
$BuSnCl_3$	−63	93 (1.3 kPa)	1.693	4–50[a]; 92[b]	1118-46-3
n-Pr_4Sn	<RT	222	1.1065		2176-98-9
iso-Pr_4Sn	<RT	112–114 (2.4 kPa)	1.124		2949-42-0
n-Pr_3SnCl	−23.5	123 (1.7 kPa)	1.2678	50	2279-76-7
$(n\text{-}Pr_3Sn)_2O$				50	
iso-Pr_3SnCl				25	
Et_4Sn	−112	181	1.187		597-64-8
Et_3SnOH				35,000	
Et_3SnOAc				7500	
Et_3SnCl	<RT	206	1.429		994-31-0
Et_2SnCl_2	84	220			866-55-7
Me_4Sn	−54	74–75	1.291		594-27-4
Me_3SnCl	37–39	154			1066-45-1
Me_3SnOH	118	Begins to sublime at 80°C			56-24-6
Me_2SnCl_2	106–108	188–190		20,000	753-73-1
$MeSnCl_3$	48–51	171			993-16-8
Ph_4Sn	224–227	>420	1.49		595-90-4
Ph_3SnCl	106	249 (1.8 kPa)		1	639-58-7
$PhSnF_3$	>281			1.2	379-52-2
Ph_2SnCl_2	42	333–337 (dec)[d]		50	1135-99-5
$PhSnCl_3$	<RT		1.84	5.2	1124-19-2

[a] In seawater.
[b] In distilled water.
[c] RT: room temperature.
[d] dec: decomposes.

Table 2.20.2. Toxicity pattern of trisubstituted OTCs [13].

Organotin compound	Target species
CH_3 (methyl)	Insects
C_2H_5 (ethyl)	Mammals
C_3H_7 (propyl)	Gram-negative bacteria
C_4H_9 (butyl)	Gram-positive bacteria, fish, algae, mussels, mollusks, fungi
C_6H_5 (phenyl)	Fungi, mollusks, fish
C_6H_{11} (cyclohexyl)	Mites, fish

demonstrated to occur even at low ng L^{-1} concentrations [15]. For short-term exposures, lethal doses are in the range of 0.04–0.16 µg L^{-1}, depending on the individual species [16]. Although the highest toxicity of butyltin compounds is exhibited by TBT, the less toxic derivatives dibutyltin (DBT) and monobutyltin (MBT) have also to be considered. DBT and MBT may not only result from the photochemical or microbial degradation of TBT but also be introduced into the aqueous environment, for example, from the leaching of PVC tubing [17]. As mono- and disubstituted butyltin compounds are significantly more water soluble than their trisubstituted analogue, this may lead to potentially higher concentrations in freshwater and groundwater.

3.1 Effects on animals

3.1.1 Effects on microorganisms

As a result of its toxicity to microorganisms, TBT has been used commercially as a bactericide and algicide. Depending on the species,

Table 2.20.3. Toxicity of various mono- to tetrasubstituted OTCs to different animal species [14].

	Medium lethal dose		
Trivial name of compound	LD_{50} [mg kg^{-1}]	Form of administration	Species
Monosubstituted			
Butylstannoic acid	>6000		Mouse
Butyltin trichloride	1400		Mouse
	2140		Rat
Octyltin trichloride	4600		Mouse
Disubstituted			
Dibutyltin di(butyl maleate)	120	Oral	Rat
Dibutyltin dichloride	100	Oral	Rat (male)
	182	Oral	Rat (male)
	112	Oral	Rat (female)
	35	Oral	Mouse
	190	Oral	Guinea pig
	150	Oral	Rat
Dibutyltin dilaurate	243	Oral	Rat
	45	Oral	Rat
Dibutyltin oxide	520	Oral	Rat (male)
	39.9	i.p.[a]	Rat (female)
	24	Oral	Mouse
Dioctyltin acetate	2030	Oral	Rat
Dioctyltin dichloride	5500–8500	Oral	Rat (male)
Dioctyltin dilaurate	6450	Oral	Rat (male)
	800	i.p.[a]	Rat (female)
Dioctyltin maleate	4500	Oral	Rat (male)
Dioctyltin			
Dioctyltin oxide	2500	Oral	Rat (male)
Trisubstituted			
Triethyltin acetate	4	Oral	Rat (female)
Triethyltin chloride	5	i.p[a]	Rat (female)
Triethyltin sulfate	5.7	i.p[a]	Rat (male)
	5.3	i.p[a]	Guinea pig
Tributyltin acetate	46	Oral	White mouse
	99	Oral	Rat
	133	Oral	Rat (male)
Tributyltin benzoate	108	Oral	White mouse
	132	Oral	Rat
Tributyltin chloride	117	Oral	White mouse
	129	Oral	Rat
Bis-tributyl oxide	112–132	Oral	Rat (male)
	180	Oral	Rat
	234	Oral	Rat
	194	Oral, aq. solution	Rat (male)
	148	Oral, oil solution	Rat (male)
	11.7	Dermal	Albino rabbit
	10	Oral	White mouse
Trihexyltin acetate	1000	Oral	Rat
Trioctyltin chloride	10,000	Oral	Rat (male)
Triphenyltin acetate	21	Oral	Guinea pig
	24	Oral	Guinea pig
	136	Oral	Rat
	81	Oral	Mouse (male)
	7.9	i.p[a]	Mouse (male)
	136	Oral	Rat (male)
	491	Oral	Rat (female)

(*continued overleaf*)

Table 2.20.3. (*continued*)

Medium lethal dose			
Trivial name of compound	LD_{50} [mg kg^{-1}]	Form of administration	Species
	450	Dermal	Rat (male)
	8.5	i.p[a]	Rat (female)
	11.9	i.p[a]	Rat (female)
	13.2	i.p[a]	Rat (male)
	21	Oral	Guinea pig (male)
	3.7	i.p[a]	Guinea pig (male)
	5.3	i.p[a]	Guinea pig (male)
	30–50	Oral	Rabbit (male)
Triphenyltin chloride	80	Oral	Rat (male)
	135	Oral	Rat (female)
Triphenyltin hydroxide	245	Oral	Mouse (male)
	209	Oral	Mouse (female)
	240	Oral	Rat (male)
	360	Oral	Rat (female)
	27.1	Oral	Guinea pig (male)
	31.1	Oral	Guinea pig (female)
	171	Oral	Rat (male)
	268	Oral	Rat (female)
Tricyclohexyltin hydroxide	710[b]	Oral	Mouse-peromyscus
	1070[b]	Oral	Mouse-Swiss white
	540	Oral	Rat
	13	i.p[a]	Rat
	780	Oral	Guinea pig
	9	i.p[a]	Guinea pig
	500–1000	Oral	Rabbit
	>126	i.p[a]	Rabbit
	150[b]	Oral	Sheep
	14	i.v[c]	Dog
	6	i.v[c]	Cat
Tetrasubstituted			
Tetraethyltin	40		Mouse
	9–15		Rat
	40		Guinea pig
	7		Rabbit
Tetrabutyltin	6000		Rat

[a] Intraperitoneal.
[b] Approximate lethal dose.
[c] Intravenous.

the concentrations that produce toxic effects may vary considerably. TBT is more toxic to Gram-positive bacteria with minimal inhibitory concentrations (MIC) (between 0.2 and 0.8 mg L^{-1}) than to Gram-negative bacteria (MIC: 3 mg L^{-1}). The TBT acetate MIC for fungi is 0.5–1 mg L^{-1} and the TBTO (bis(tri-*n*-butyloxide)) MIC for the green alga *Chlorella pyrenoidosa* is 0.5 mg L^{-1}. At a TBTO concentration of 3 μg L^{-1}, the primary productivity of a natural community of freshwater algae was reduced by 50%. Recently established no-observed-effect level (NOEL) values for two species of algae are 18 and 32 μg L^{-1}. The toxicity to marine microorganisms varies between species and between studies to a similar

Table 2.20.4. Growth inhibition of marine fouling organisms by organotins [19].

Organism	Growth inhibiting concentrations in water [μg L^{-1}]	
	TBTO	TBT fluoride
Barnacles	0.1	0.1
Enteromorpha sp.	0.02	0.01
Chlamydomas sp.	0.005	0.001
Lobsters	0.02	0.005

extent (Table 2.20.4); NOEL values are difficult to assign but lie below 0.1 $\mu g\,L^{-1}$ for most species. Algicidal concentrations range from $<1.5\ \mu g\,L^{-1}$ to $>1000\ \mu g\,L^{-1}$, depending on the species [18].

3.1.2 Effects on aquatic organisms

Effects on marine and estuarine organisms

The lethal and sublethal effects of TBT to marine and estuarine organisms are summarized in Figure 2.20.1. In many locations, concentrations have been found that exceed those at which acute effects are observed, particularly near yachting harbors.

TBT is highly toxic to marine mollusks and has been shown experimentally to exert various and severe effects, ranging from shell deformations of growing oysters, impaired gonadal development and gender of adult oysters, settlement, growth and high mortality of larval oysters and other bivalves, and to cause imposex (the development of male characteristics) in female gastropods. The NOEL for the most sensitive oyster species (*Crassostrea gigas*) has been reported to be about 20 $ng\,L^{-1}$. TBT causes deformation of the shell of adult oysters in a dose-related manner above the experimental NOEL for TBT concentrations of 2 $ng\,L^{-1}$.

The shell thickening was found to be due to the appearance of chambers in the oyster shell and interlamellar gel formation in these cavities [20]. TBT is known to inhibit oxidative phosphorylation and it has been suggested that this forms the basis of its action on the shell. It is also known to complex amino acids. The effect on calcification derives from inadequate calcium addition to the organic matrix (a process dependent on ATP) and incorrect deposition of this matrix.

In addition to shell malformation, also poor growth and reduction in tissue was attributed to high organotin concentrations along the east coast of England where the Pacific oyster has been reintroduced [21]. The types of shell abnormality exhibited by oysters in France were very similar to those observed in oysters from the east coast of England, which had been attributed to sediment. In 1982, it was decided to reassess the causes of poor oyster shell growth in Britain. Levels of TBT were measured in the estuaries of the Rivers Crouch and Blackwater, on the east coast of England, and were found regularly to exceed 0.2 $\mu g\,L^{-1}$, a level shown by the French studies to be harmful to the oyster [21].

The NOEL for the development of imposex in female dogwhelks is below 1.5 $ng\,L^{-1}$. Larval forms are generally more sensitive than adults; in the case of oysters this difference is particularly marked.

The phenomenon of imposex has been detected in a study by Smith who sampled mud snails (*Nassarius obsoletus*) from four locations along the coastside in Westport and Fairfield, Connecticut,

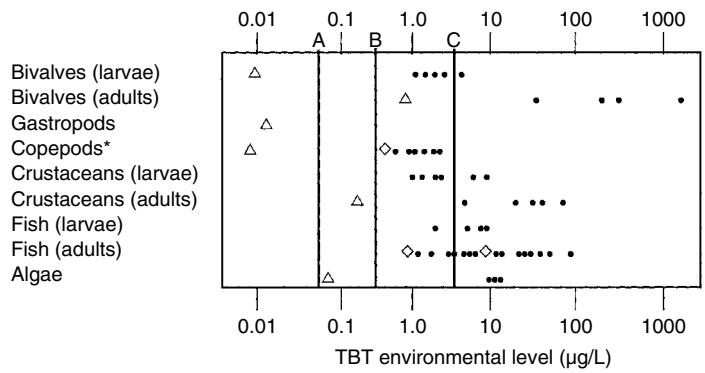

Figure 2.20.1. Toxicity of TBT to marine organisms [18] ● LC_{50} following exposure for 96 h or less; ◊ LC_{50} following exposure for more than 96 h; △ the lowest concentration causing a sublethal effect; *copepods are displayed separately because of their greater sensitivity than other crustaceans; A = highest measured concentration in the open sea; B = highest measured concentration in open estuary; C = highest measured concentration in marinas.

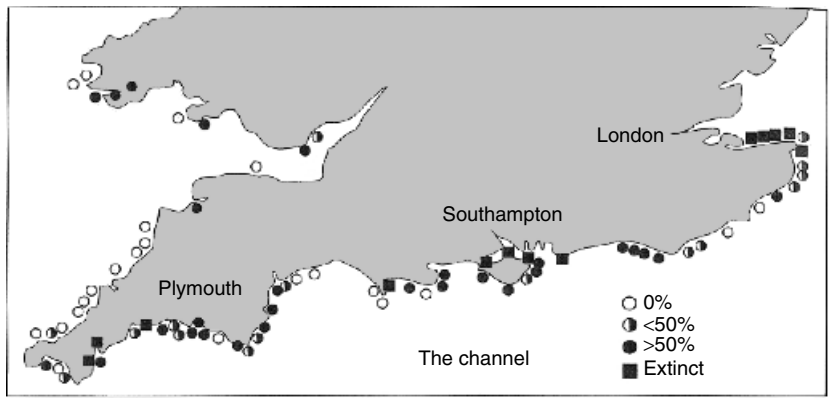

Figure 2.20.2. Occurrence of imposex in the dogwhelk, *Nucella lapillus*. The fraction of female gastropods with male sexual organs correlates with the degree of pollution of the water. In highly TBT-contaminated harbors, the dogwhelk is completely absent (after Bryan *et al.* [23]).

United States, in the years 1972 and 1976 [22]. In two of the areas, adjacent to yacht harbors, 95–100% of snails had some degree of imposex. An analysis of chemicals present in water from the areas exhibiting a high degree of imposex was then carried out and snails were exposed to some of the contaminants individually, that is, marina disinfectants, detergents, copper antifouling paints, leaded gasoline, combustion emissions and TBT-based antifouling paints. Only the tin-containing antifouling paints increased the level of penis expression in female snails, thus giving evidence to the correlation between TBT exposure and imposex.

In a survey of the dogwhelk *Nucella lapillus* around the southwest of England, Bryan *et al.* [23] found imposex to be widespread. The south coast of England was the most severely affected (Figure 2.20.2). Populations showing the highest incidence and highest intensity of imposex were close to areas of boating or shipping activity. The degree of imposex had increased markedly between 1969 and 1985 in Plymouth Sound (an area on the south coast with large numbers of small boats and ships), coinciding with the introduction and increasing use of TBT-containing antifouling paints in the area. Imposex correlated with TBT concentrations of seawater and residues of organotins in the dogwhelks (Figure 2.20.3).

One of the effects of imposex on the female dogwhelk is the blocking of the pallial oviduct,

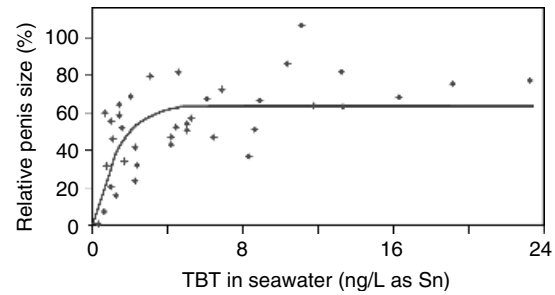

Figure 2.20.3. Relationship between TBT concentrations in seawater and tissues of the dogwhelk and degree of imposex (expressed as relative penis size) in the females from southwest England sampled in the years 1984–1986. (Redrawn after [24]).

preventing the release of egg capsules and thus rendering the female sterile. A high incidence of females carrying aborted capsules was found in declining populations close to sources of TBT. The buildup of aborted capsules seemed, eventually, to be lethal to the female, as there were fewer females than expected in affected areas [23]. It was stated that imposex in the dogwhelk was seen in seawater with TBT concentrations of less than 1 ng Sn/L. Reproductive failure was reported to have led to population declines, almost to the point of extinction, in areas of heavy TBT contamination. As adults are irreversibly affected by imposex, recolonization is unlikely until the TBT levels in seawater fall to significantly lower than around

1 ng Sn/L, a concentration at which the juveniles are not sterilized before they reach sexual maturity.

While it was stated that TBT may not be solely responsible for imposex in the dogwhelk, there is indisputable evidence for TBT levels being related to the occurrence of imposex. There is a significant relationship between imposex and the body burden of organotin (Figure 2.20.4, [24, 25]).

Copepods are more sensitive than other crustacean groups to the acute lethal effects of TBT, LC_{50} values for exposure periods up to 96 h ranging from 0.6 to 2.2 $\mu g\,L^{-1}$. These values are comparable to those of the more sensitive larvae of other crustacean groups. TBT reduces reproductive performance, neonate survival and juvenile growth rate in crustaceans. The NOEL for reproduction in the shrimp *Acanthomysis sculpta* has been estimated at 0.09 $\mu g\,L^{-1}$. The toxicity of TBT to marine fish is highly variable, 96-h LC_{50} values ranging between 1.5 and 36 $\mu g\,L^{-1}$. Larval stages are more sensitive than adults (Figure 2.20.1). There are indications that marine fish avoid TBTO concentrations of 1 $\mu g\,L^{-1}$ or more [18].

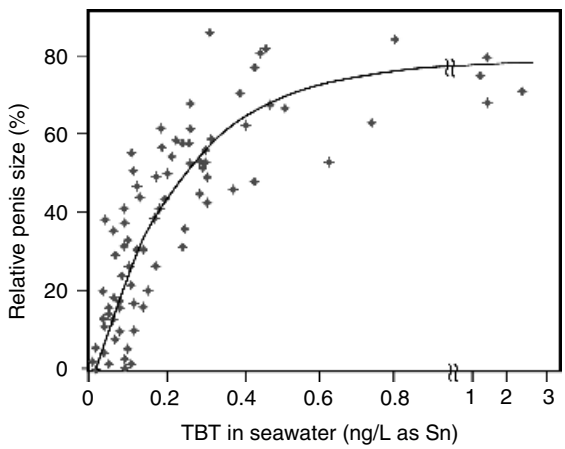

Figure 2.20.4. Relationship between TBT concentration in tissue (whole body) of dogwhelks sampled between 1984 and 1986 around southwest England and the degree of imposex in females, expressed as the relative penis size (redrawn after [24]).

Effects on freshwater organisms

Figure 2.20.5 summarizes the lethal and sublethal effects of TBT to the measured concentrations in freshwater. Notably in the vicinity of marinas, concentrations exceeding those producing sublethal effects have been found.

Data on freshwater invertebrate species are limited, and exist only for three species other than target organisms. Different salts of TBT yield 48-h LC_{50} values for *Daphnia* of 2.3–70 $\mu g\,L^{-1}$ and for *Tubifex* of 5.5–33 $\mu g\,L^{-1}$. The reversal of normal response to light has been taken as measure for the NOEL for *Daphnia*, which has been estimated to be 0.5 $\mu g\,L^{-1}$. For the Asiatic clam, a 24-h LC_{50} value of 2100 $\mu g\,L^{-1}$ has been reported, while for target snail adults in schistosomiasis control the corresponding values are 30–400 $\mu g\,L^{-1}$.

TBT has been shown to be toxic to schistosome larvae in the aquatic stages, with an LC_{50} (for

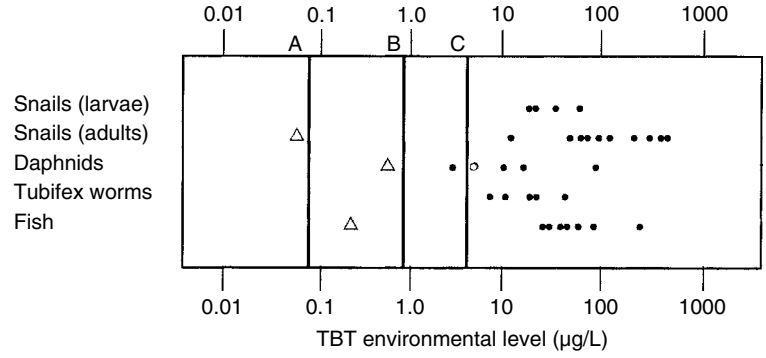

Figure 2.20.5. Toxicity of TBT to freshwater organisms [18]: ● LC_{50} following exposure for 96 h or less; ○ LC_{50} following exposure for more than 96 h; △ the lowest concentration causing a sublethal effect; A = highest measured concentration upstream from marina; B = highest measured concentration downstream from marina; C = highest measured concentration in marinas.

TBT fluoride) estimated at 16.8 $\mu g\,L^{-1}$ for a 1 h-exposure. The sensitivity of snails to TBT decreases with age, while eggs are more resistant than both young and adults organisms. TBTO application significantly affects egg laying already at a TBTO concentration of 0.001 $\mu g\,L^{-1}$. In contrast to this, the acute toxicity of TBT to freshwater fish in LC_{50} tests up to 168 h ranges from 13 to 240 $\mu g\,L^{-1}$. No effect on survival was found when eggs and larvae of the frog *Rana temporaria* were exposed to TBT concentrations in the range of 3 to 30 $\mu g\,L^{-1}$, above which very significant mortality was observed [18].

3.1.3 Effects on terrestrial organisms

The use of TBT as a wood preservative is the main factor for the exposure of terrestrial organisms. The toxicity of TBTO to bees housed in hives made from TBT-treated wood has been demonstrated. TBT compounds are also toxic to insects exposed topically or via feeding on treated wood. The acute toxicity of TBT to wild mice is moderate, with estimated dietary LC_{50} values ranging from 37 to 240 $mg\,kg^{-1}$ per day, based on the consumption of treated seeds used in repellency tests [18].

3.1.4 Toxicity to laboratory mammals

Acute toxicity

The toxicity of TBT to laboratory mammals is moderate to high, with acute oral LD_{50} values ranging from 94 to 234 $mg\,kg^{-1}$ body weight for the rat and from 44 to 230 $mg\,kg^{-1}$ body weight for the mouse and values for the acute toxicity to the guinea pig and the rabbit in the same range (Table 2.20.3). The anion of the TBT salt may be held responsible for this variation. OTCs exhibit greater toxicity when administered parentally, as opposed to orally, which probably reflects their only partial absorption from the gut. Other effects of acute exposure may include alterations in blood lipid levels, the endocrine system, liver and spleen and transient deficits in brain development.

The acute toxicity via the dermal route is low, the LD_{50} being $>9000\ mg\,kg^{-1}$ body weight for the rabbit. Inhalation through the nose leads to an LD_{50} (4 h) of 77 $mg\,m^{-3}$ (or 65 $mg\,m^{-3}$ when only the inhalable fraction is considered) for the rat. TBT vapor/air mixtures do not exhibit any observable toxic effect, even at saturation. In contrast to this, TBT is very hazardous as an inhaled aerosol, producing lung irritation and edema. TBT is severely irritating to the skin and an extreme irritant to the eye. TBTO is not a skin sensitizer [18].

Short-term toxicity

The effect of TBT has most extensively been studied in the rat (to which all data presented in this section refers, unless otherwise indicated). A dietary intake of 320 $mg\,kg^{-1}$ food (approximately 25 $mg\,kg^{-1}$ body weight) led to high mortality rates when the exposure time exceeded 4 weeks. At the level of 100 $mg\,kg^{-1}$ diet (corresponding to 10 $mg\,kg^{-1}$ body weight) or with a daily administration of 12 $mg\,kg^{-1}$ body weight by gavage, no deaths were noted. However, rats that were exposed during early postnatal life to 3 $mg\,kg^{-1}$ body weight showed an increased mortality. Typical symptoms at lethal doses were loss of appetite, weakness and emaciation.

It is important to point out the differences in exposure to TBTO aerosol (which at 2.8 $mg\,m^{-3}$ led to high mortality, respiratory distress, inflammatory reaction within the respiratory tract and histopathological changes of lymphatic organs) or to a saturated atmosphere of TBT in the gas phase (vapor concentration 0.16 $mg\,m^{-3}$), which produced no observable effects.

A characteristic toxic effect of TBTO is the suppression of the immune system. Because of the action of TBT on the thymus, the cell-mediated function is impaired. The exact mechanism of action is unknown, but may involve the metabolic conversion to dibutyltin compounds. Nonspecific resistance is also affected.

General effects on the immune system (e.g. on the weight and morphology of lymphoid tissues) have been reported in several different studies with TBTO using rats and dogs, but not mice, at exceedingly high dose levels (effects in mice have been seen with TBT chloride

at 150 mg kg^{-1}). Only the rat exhibits general effects on the immune system without other obvious signs of toxicity and is clearly the most sensitive species. The NOEL in short-term rat studies was 5 mg kg^{-1} diet (corresponding to 0.6 mg kg^{-1} body weight). TBTO was also shown to compromise specific immune function in rat *in vivo* host resistance studies.

With present knowledge, the effects on host resistance are probably most relevant in assessing the potential hazard to man, but there is insufficient experience in these test systems to fully assess their significance. It would be prudent to base assessment of the potential hazard to humans on data from the most sensitive species.

Long-term toxicity

TBT has been demonstrated in a long-term study in rats to exhibit only a marginal effect on general toxicological parameters (of limited toxicological importance) at a level of 5 mg kg^{-1} diet (0.25 mg kg^{-1} body weight).

Genotoxicity

The genotoxicity of TBT has been investigated in several studies. So far, however, there is no convincing evidence that TBTO has any mutagenic potential.

Reproductive toxicity

The potential embryotoxicity of TBTO was evaluated for three mammalian species (mouse, rat and rabbit) after oral dosing of the mother. Although malformations were observed in rat and mouse fetuses, these occurred only at dosages already toxic to the mothers and they are thus not considered to prove the teratogenic effects of TBTO at doses below those producing maternal toxicity. The lowest NOEL, with regard to embryotoxicity and fetotoxicity for all three species, was 1.0 mg kg^{-1} body weight.

Carcinogenicity

The carcinogenicity study performed with rats and mice did not show any significantly increased tumor incidence rate at 0.5 mg kg^{-1} diet and can thus be considered as having no biological significance since there was no dose-response relationship.

3.2 Effects on humans

Local effects

Comparatively little is known on the effects of OTCs in humans.

Local effects are known, for example, the direct exposure of workers to dibutyl- and tributylin compounds produced skin irritation 1–8 h after contact. Experimental application to the skin of volunteers showed that some compounds (e.g. dibutyltin dichloride and TBT chloride) produced this effect, whereas others such as dibutyltin maleate and tetrabutyltin did not. Di- and tributylin compounds caused eye irritation after brief contact. A 20% solution of TPhT acetate produced irritation of the skin and the mucous membranes of the upper respiratory tract, whereas TCyT hydroxide was reported not to cause skin irritation at a concentration of 0.01 mg kg^{-1} body weight [14].

Systemic effects

Occupational exposure to TPhT acetate has also lead to the observation of systemic effects. The effects reported to have followed both dermal and inhalation exposure include general malaise, nausea, gastric pain, dryness of the mouth, vision disturbance and shortness of breath. Hepatomegaly and elevated levels of liver transaminase activity have been found in some cases. Recovery has generally been complete but liver damage has been known to persist for up to two years.

The hazard associated with the use of OTCs was unmasked by an episode of intoxication in France in 1954, involving over 200 cases, 100 of which were fatal [26]. The cause was the ingestion of an oral preparation of a medication used for the treatment of staphylococcal skin infections ('Stalinon') containing diethyltin diiodide at 15 mg/capsule. It was suggested, however, that the highly toxic triethyltin iodide was present as impurity. A few other cases of occupational exposure have been reported, including two casualties [10].

Table 2.20.5. Toxicity of OTCs in early phases of fish development [30].

Fish species		Toxicity	Compound	Concentration [$\mu g\,L^{-1}$]
Rainbow trout:	Juvenile	Acute (LC_{50}, 96 h)	TBT	3.5
		Chronic (immune system)	TBT	0.6
		Chronic (immune system)	TPhT	1.0
	Larvae	Chronic (LC_{100}, 12 d)	TBT	1.8
		Chronic (110 d)	TBT	0.2
Minnow: (*Phoxinus*)	Larvae	Acute (LC_{100}, 8 d)	TBT	3.5
		Histological malformations	TBT	0.7
		Histological malformations	TPhT	1.8
Fathead minnow:	Larvae	Chronic, growth (LOEC)	TBT	0.3
(*Pimephales promelas*)		Chronic, growth (30 d)	TPhT	0.2
		Acute (LD_{50}, 96 h)	TPhT	7.1

Currently, no production or use of ethyltin compounds exists on an industrial scale as a result of its high toxicity to humans. Predominant symptoms and signs included severe headache, nausea and vomiting, visual and psychological disturbances and sometimes loss of consciousness. At autopsies and decompressive surgery, cerebral edema of the white matter was found. In many cases, symptoms lasted for at least four years.

3.3 Mechanism of action

Although it is generally accepted that mollusks are very sensitive to low concentrations of TBT, only limited information concerning the mechanism of action of the OTCs is available. Increases in testosterone levels or imbalance in the androgens/estrogens ratio have been described for several gastropod species after exposure to TBT, and these findings have been associated with the phenomenon of imposex, the imposition of male characteristics (penis and vas deferens) in females of some gastropod species [27]. Imposex was first reported in the Eastern United States in the mud snail *Ilyanassa obsoleta* [28] and soon afterwards in many other species worldwide. The inhibition of the P450-aromatase responsible for the conversion of androgens to estrogens has been proposed as the causal mechanism [29]. Despite this, information on the interaction of OTCs with the molluskan cytochrome P450 system is practically unavailable. This system has a key function in the metabolization of xenobiotic compounds but also in the conversion of cholesterol into a variety of hormones. Inhibition or stimulation of cytochrome P450 isozymes may therefore result in changes in hormone production or metabolization.

TPhT also exhibits serious toxicity to aquatic life. It was found that toxic effects were already observed at levels of 1 $\mu g\,L^{-1}$ for rainbow trout (Table 2.20.5). A comparison of the LD_{50} values of different OTCs in rats is given in Table 2.20.6.

Both tributyl- and TPhT have been recognized as causing malformations of oyster shells [20]. In addition to the endocrine disrupting effect of TBT, retardation of the growth of mussels [32] and immunological dysfunction [33] have been reported. DBT and TBT are also said to cause immune suppression in rodents. There is no evidence for carcinogenic effects or teratogenic effects of OTCs for mammals [34].

Table 2.20.6. Acute oral toxicity of several OTCs to rats [31].

Organotin compound	LD_{50} [$mg\,kg^{-1}$]
Et_3SnOAc	4
Me_3SnOAc	9
Me_3SnCl	13
Me_3SnOH	540
Me_2SnCl_2	74
$MeSnCl_3$	1370
Ph_3SnOH	125
Hex_3SnOAc	1000
$(Bu_3Sn)_2O$	150–234
Bu_3SnOAc	380
$BuSnCl_3$	100
$BuSnCl_3$	2140
Bu_4Sn	>4000
Oct_4Sn	50,000

4 PRODUCTION OF OTCs

The first organotin compound was prepared more than 150 years ago by Frankland in 1849 and described as a side note in a paper devoted largely to the reaction that occurred when ethyl iodide and zinc were heated together in a sealed tube [35]. Frankland observed that a reaction occurred also with a number of other metals, including tin:

$$2EtI + Sn \rightarrow Et_2SnI_2 \qquad (2.20.1)$$

This paper is often held to mark the first systematic study in organometallic chemistry. Frankland subsequently showed that the crystals that he had produced were diethyltin diiodide. In independent work, Löwig established that ethyl iodide reacted with a tin/sodium alloy to give what is now recognized to be oligomeric diethyltin [4]. Diethyltin readily reacted with air to give diethyltin oxide and with halogens to give diethyltin dihalides. As an alternative to this so-called direct method, an indirect route was devised by Buckton in 1859 [36], who obtained tetraethyltin by treating tin tetrachloride with Frankland's diethylzinc:

$$2EtI + 2Zn \rightarrow 2EtZnI \rightarrow Et_2Zn + ZnI_2 \qquad (2.20.2)$$

$$2Et_2Zn + SnCl_4 \rightarrow Et_4Sn + 2ZnCl_2 \qquad (2.20.3)$$

The direct route was found incidentally by Letts and Collie [37] who were attempting to prepare diethylzinc according to Frankland's route (equation 2.20.2), but isolated tetraethyltin formed from tin instead present as an impurity in the zinc. They were subsequently able to show that tetraethyltin could be prepared by heating ethyl iodide with a mixture of zinc and tin powder:

$$4EtI + 2Zn/Sn \rightarrow Et_4Sn + 2ZnI_2 \qquad (2.20.4)$$

The indirect route was improved by Frankland who showed that the tin(IV) tetrachloride could be replaced by tin(II) dichloride, which is easier to handle and reacts in a more controllable fashion:

$$2Et_2Zn + SnCl_2 \rightarrow Et_4Sn + 2ZnCl_2 \qquad (2.20.5)$$

The early literature on OTCs made exclusive use of the two above-mentioned (direct and indirect) routes of synthesis. In 1900, Grignard published his synthesis of organomagnesium halides in ether solution. As these reagents were much less sensitive to air than Frankland's solvent-free organozinc compounds, they rapidly replaced and extended the scope of the zinc reagents as a source of nucleophilic alkyl and aryl groups. In 1903, the preparation was described of a number of simple and mixed tetraalkylstannanes, and of tetraphenyltin, from Grignard reagents and tin tetrachloride or alkyltin halides [38]. Very soon, reactions of this type became the standard route of synthesis for alkyl- and aryltin compounds. Tin assumed a major role in the great increase of activity in organometallic chemistry that began in about 1949, and which was stimulated by the discovery of a variety of applications.

There exist four principal routes according to which OTCs can be produced on an industrial scale (Figure 2.20.6). These are:

1. the reaction of tin tetrachloride with a Grignard reagent,

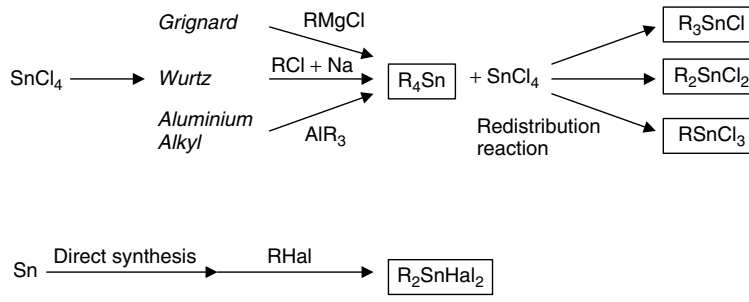

Figure 2.20.6. Industrial manufacture routes to OTCs (adapted from [10]).

2. the reaction of tin tetrachloride with an alkyl- or arylhalide and elemental sodium ('Wurtz reaction'),
3. the reaction of tin tetrachloride with an aluminumalkyl compound (transmetallation or metathesis),
4. or the direct synthesis from tin metal with an alkyl halide.

The first three routes of formation involve two steps, the first being the reaction of $SnCl_4$ with a suitable reagent to form the respective tetraalkyltin compound, R_4Sn. In the second reaction step, the less substituted compounds are produced as the result of a redistribution reaction between $SnCl_4$ and R_4Sn. These organotin chlorides are the starting point for the production of various other OTCs. For the direct reaction route, which involves the reaction between tin and alkyl halides, iodides are needed to achieve a reasonable reaction rate. Because of the high costs of organoiodine compounds, the process is therefore only viable industrially when the iodine can be recovered.

While the Grignard process was already used very early for the commercial production of OTCs (in the late 1940s by the Metal & Thermit Corporation in Rathway, NJ, USA) [39], it is, despite giving high yields, economically not feasible, since it requires the usage of large amounts of solvents. The same holds true for the Wurtz synthesis, which in addition to the large solvent volumes also requires the use of metallic Na. Both from the economic and from the technical point of view (since the synthesis is accompanied by side reactions), the process is thus not feasible. The currently most important way of synthesis of the OTCs is their production by the alkyl aluminum route. This process was introduced at the Schering AG company in Bergkamen, Germany, in the early 1960s. It is particularly advantageous because of the fact that it can be run continuously and does not require any solvent. Direct synthetic routes starting from alkyliodides or the less reactive alkylbromides were developed in Japan in the 1950s. They are still in use for the direct synthesis of methyltin compounds in the United States [40].

5 APPLICATIONS OF OTCS

The remarkable variety in the physical, chemical and biological properties of OTCs has lead to a great number of industrial applications of the individual compounds (Table 2.20.7). The most important ones will be discussed in the following.

5.1 PVC stabilizers

More than two-thirds of the annual production of OTCs are used in the plastics industry as additives for thermal and light stabilization, and as catalyst in the production of polyurethane foams and silicones. The first reported use of OTCs as PVC stabilizers dates back to 1940 [5]. Since then, the use of OTCs for the stabilization of PVC has continuously increased. PVC is still the second important synthetic polymer after polyethylene. The annual production was estimated at ca 25 million tons in 2000 [41]. Even if the relative amount of OTCs added to the PVC is only in the low and subpercent range, this accounts for about 3.5% of the world's total tin consumption. OTCs are more effective stabilizers than the previously and alternatively used organolead compounds, metal soaps and organic compounds. They prevent the decomposition of PVC that may occur at elevated temperatures (above ca 180 °C) or upon extended exposure to light by loss of HCl. Mixtures of mono- and dialkyltin salts are used and commercial tin heat stabilizers typically vary the ratio, depending on the performance and property requirements of the final product [42]. The two main types of tin heat stabilizers for PVC are:

1. thio acid half esters such as thioglycolates often known as thiotins or mercaptides.
2. dicarboxylic half esters, often referred to as *maleates* or *carboxylates*.

PVC tin stabilizers are always based on methyl, butyl or octyl groups (Table 2.20.8). The former are not generally used in Europe but are commonly incorporated in a range of compounds, including potable water pipe formulations in the United States.

Table 2.20.7. Principal industrial uses of OTCs.

Application	Function	Principal compound used
PVC stabilization	Stabilization against effects of heat and light	R_2SnX_2 (R = Me, Bu, Oc, 2-butoxy-carbonylethyl; X_2 = diisooctylthioglycolate, maleate)
Polyurethane foams RTV silicones[a]	Homogeneous catalysis	Bu_2SnX_2 (X = acetate, octoate, laurate)
Esterification	Homogeneous catalysis	Butanestannoic acid Bu_2SnAc_2 Bu_2SnO
Glass treatment	Precursor for tin(IV) oxide films on glass	$MeSnCl_3$ Me_2SnCl_2 $BuSnCl_3$
Poultry management	Dewormer	Bu_2SnX_2 (X = laurate)
Wood preservation	Fungicide	$(Bu_3Sn)_2O$ Bu_3SnX (X = naphthenate, phosphate)
Agricultural chemicals	Fungicide Insecticide Miticide Antifeedant	Ph_3SnX (X = acetate, hydroxide) Cy_3SnOH
Antifouling paints	Biocide	Ph_3SnX (X = chloride, fluoride) Bu_3SnX (X = chloride, fluoride) $(Bu_3Sn)_2O$ Tributyltin acrylate polymers
Materials protection (e.g. for stone, leather, paper)	Fungicide Algicide Bactericide	$(Bu_3Sn)_2O$ Tributyltin benzoate
Moth proofing of textiles	Insecticide Antifeedant	Ph_3SnX (X = chloride, hydroxide)
Disinfection	Bacteriostat	Tributyltin benzoate

[a]RTV: room-temperature vulcanizing

Table 2.20.8. Common OTCs used as PVC stabilizers [2].

Stabilizers	Formula	R
Dialkyltin diisooctylthioglycolate	$R_2Sn(SCH_2COO\text{–}i\text{–}Oct)_2$	Me, n-Bu, n-Oct
Dialkyltin maleate	$[\text{–}Sn(R_2)\text{–}OOCH{=}CHCOO\text{–}]_n$	Me, n-Bu, n-Oct
Dialkyltin maleate ester	$R_2Sn(OOCCH{=}CHCOOR')_2$[a]	Bu, Oct[a]
Dialkyltin dilaurate	$R_2Sn(OOCC_{11}H_{23})_2$	n-Bu, n-Oct
Dibutyltin mercaptopropionate	n-$Bu_2SnSCH_2CH_2C{=}O$ └──────O┘	
Diestertin diisooctylthioglycolate	$(n\text{-}BuOOCCH_2CH_2)_2Sn(SCH_2COO\text{-}i\text{-}Oct)_2$	

[a]R′ = Me, n-Bu, n-Oct.

Both butyl- and octyl tin stabilizers are found in an extensive range of applications in Europe. When good outdoor weathering performance or low odor are especially required, it is common to use maleates or carboxylates, while for all other applications the thiotins are commonly used. Both butyl- and octyl tins provide very good heat stability and color control, combined with the option of manufacturing crystal clear products. A considerable number of octyl tin stabilizers also have obtained approval from official bodies for food contact applications. PVC compounds

incorporating tin heat stabilizers are used in a diverse range of applications such as sheets, bottles, profiles, injection moulded fittings, credit cards, blister packs, food containers and display trays.

Mechanism of action: Various mechanisms have been proposed for the stabilization of PVC by OTCs [43]. It was found that the OTCs of type R_2SnY_2 retard the unzipping reaction of the PVC because the Y component of the organotin compound is substituted to labile chlorine atoms of the PVC resin. As PVC decomposition is occurring through dehydrohalogenation, the substitution of labile Cl atoms by the Y group of the organotin stabilizer prevents this reaction from taking place. This reaction is shown schematically in Figure 2.20.7.

Since organotin-stabilized PVC finds numerous applications for packaging materials, foils and piping for potable water, the leaching of OTCs is of special concern.

The transfer of OTCs from packaging material to food is a still largely uninvestigated area. There are some studies indicating that food and, in particular, acidic fruit juices will take up significant amounts of stabilizer from packaging materials [44], however, no systematic study has been done on a large scale (Table 2.20.9). On the other hand, it is remarkable that organotin stabilizers will not degrade completely when the food is processed even at elevated temperatures [45].

Organotin use in toys, consumer products and food contact applications: Depending on the application and regional government regulations where the material is produced, there are a variety of regulations that apply to the use of tin stabilizer compounds in toys, consumer products and food contact applications [47]. In Europe, the use of tin stabilizers in PVC toys is regulated by the European Union (EU) Toy Directives (88/378/EEC), which establish the permitted levels of materials allowable in PVC toys. The responsibility for

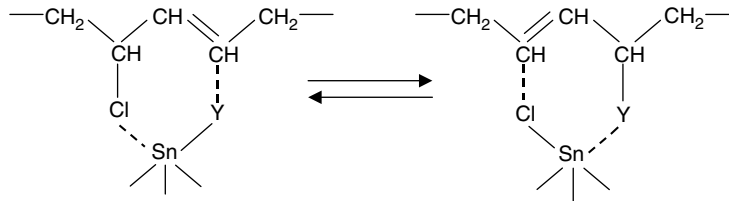

Figure 2.20.7. Mechanism of the stabilization of PVC against dehydrochlorination by OTCs of the general formula R_3SnY [2].

Table 2.20.9. Total and organotin concentrations in foodstuffs after storage for 2 months in PVC bottles at 30 °C [46].

Food product	Tin content at beginning of experiment ($mg\,kg^{-1}$)	Tin content after aging in PVC bottle ($mg\,kg^{-1}$)	Tin extracted from bottle ($mg\,kg^{-1}$)	Organotin stabilizer extracted from PVC bottle ($mg\,kg^{-1}$)
Mineral water	0.076	0.088	0.01	0.063
Tomato juice	0.03	0.03	0	0
Peanut oil	0.05	0.06	0.01	0.063
Vegetable oil	0.08	0.09	0.01	0.063
Apple juice	0	0.02	0.02	0.126
Cherry soda	0	0.07	0.07	0.443
Beer	0	0.01	0.01	0.063
Milk[a]	0.02	0.04	0.02	0.126
Red wine	0	0	0	0
Blended whisky	0.01	0.02	0.01	0.063

[a]Milk sample in PVC bottle aged for 2 weeks at 65 °C.

enforcement lies with the EU Commissioner for Industrial Affairs. EU Directive 92/59 and the Scientific Committee for Food (SCF) establish migration limits for tin stabilizers in toy and food contact applications on the basis of the tolerable daily intake (TDI) value. The TDI represents the chemical dose that is unlikely to cause harm to human health if ingested on a regular (i.e. daily) basis (see Table 2.20.10 for TDI values for some of the common organotins associated with stabilizers). In the United States, octyl-, methyl- and dodecyltin compounds satisfy the requirements of the Food and Drug Administration (FDA) for use as stabilizers for certain indirect food contact applications (21 CFR 178.2650) such as packaging. Several European countries have also approved them for food packaging applications (Directive 90/128/EEC).

Drinking water: Organotin stabilizers, specifically octyl- and methyl tin products, have extensive national approvals for food contact applications. In the case of potable water pipes, tin stabilizers are approved in all European countries and in the United States [49]. However, in Europe their usage in water pipes has been largely confined to France and Belgium, while it is the dominant stabilizer type used for this application in the United States where the regulatory authorities have concluded that the use of tin stabilizer is safe since there is no leaching of stabilizer to the water once the initial surface layer of stabilizer has been washed off by flushing. This was shown in a study where water passing through a tube length of 46 m of PVC piping led to a concentration of 35 mg Sn/m^3 in the water for the first usage, while this value dropped to a constant release rate of 1 mg Sn/m^3 water in subsequent use [50]. The leaching rates will certainly depend on the alkyl chain length of the organotin stabilizer and on the properties of the leachant (e.g. pH value).

Several studies have been performed and published by Health Canada documenting the measured concentrations of butyltins to which people could be exposed through their drinking water. In both PVC and chlorinated PVC (CPVC) pipe, levels of MBT and dibutyltin in potable water have been noted in the parts per trillion (ng L^{-1}) range after only a few liters of water have passed through the pipe, washing away any butyltin compounds from the surface of the pipe. One study [51] involved 45 municipalities and found butyltins at only six of these with a maximum concentration of 44 ng L^{-1}. The values at most municipalities were below detectable levels (i.e. <0.5 ng L^{-1}).

Table 2.20.10. TDI values of common organotins.

Chemical	TDI[1] ($\mu g\,kg^{-1}$)	Unit	Source/comment
Mono-methyltin tris-(isooctyl mercaptoacetate (IOMA))[2]	3	BW/day	[a]
Dimethyltin-S′-bis-(IOMA)[2]	3	BW/day	[a]
Mono-*n*-octyltin-tris-(2-EHMA)[3]	20	BW/day	[a]
Di-*n*-octyltin-bis-(2-EHMA)[3]	0.6	BW/day	[b], TDI is the same for all di-*n*-octyltin species[4]
Dibutyltin	5	BW/day	[c]
Di-*n*-octyltin	0.6	BW/day	[b], TDI is the same for all di-*n*-octyltin species[4]
Mono-*n*-octyltin tris(alkyl(C10-C16)MA)	20	BW/day	[a]
Mono-*n*-octyltin tris-(IOMA)[2]	20	BW/day	[a]

Note: IOMA = isooctyl mercaptoacetate; EHMA = ethylhexylmercaptoacetate; MA = mercaptoacetate; BW = body weight.
[1] Tolerable daily intake.
[2] Isooctylmercaptoacetate.
[3] 2-ethylhexylmercaptoacetate.
[4] Listed di-*n*-octyltin species in Commission of the European Communities (CEC) – Synoptic Document Nr. 7 are: di-*n*-octyltin bis-(IOMA), −1, 4-butanediol-bis-(MA), -dilaurate, -dimaleate, -ethyleneglycol-bis-(MA), -(MA), -benzoate-2-ethylhexyl-MA, -bis(*n*-alkyl(C10-C16)MA), bis-(7-ethylhexyl maleate), -bis-(2-ethylhexyl-MA), -bis-(ethyl-maleate), -bis-(isooctyl-maleate).
[a] Commission of the European Communities (CEC) – Synoptic Document Nr. 7 – Draft of Provisional List of Monomers and Additives Used in the Manufacture of Plastics and Coatings Intended to Come into Contact with Foodstuffs.
[b] Commission of the European Communities (CEC) – Scientific Committee for Food (SCF), 1994.
[c] K.H. Summer, K. Dominik, and H. Greim (1996). Ecological and toxicological aspects of mono- and disubstituted methyl-, butyl-, octyl-, and dodecyltin compounds [48].

In another study [52], organotins were measured in the distribution (tap) water of five of these municipalities, with butyltins being positively detected at only 1 of 22 homes sampled. The level of butyltins in water from freshly purchased CPVC pipe were found to drop very rapidly after a small amount of water washed the surface. By the time a few liters of water had passed through the pipe, the level of butyltin in the water had already fallen into the parts per trillion range. In a more comprehensive study [53], Canadian drinking water distributed through recently installed PVC pipe was monitored and only a few positive detections of butyltins (dibutyltin maximum of 53 $ng\,L^{-1}$, MBT maximum of 28.5 $ng\,L^{-1}$) were found although in most cases the concentrations were not detectable. The trace levels of butyltins measured ($<0.5\ ngL^{-1}$ to 53 $ng\,L^{-1}$) are well within the range deemed safe for drinking water. Using the predicted tolerable daily intake (pTDI) value for dibutyltin of 5 $\mu g\,kg^{-1}$ (as tin) [48], an adult who weighs 60 kg and who consumes two liters of drinking water per day could safely ingest water with a butyltin concentration of 150 $\mu g\,L^{-1}$ (as tin). This 'safe' concentration is over 2000 times greater than the highest dibutyltin concentration that was measured (53 $ng\,L^{-1}$ as tin) in drinking water from PVC piping. Furthermore, actual concentrations over the long-term (used pipes) can be expected to be lower, due to rinsing away of the initial organotins on the pipe surface. Thus, although organotins have been detected in water at extremely low levels, they are well below levels of concern for any effects on health [50].

Improvements in organotin compound usage for PVC stabilization: Continued product development has led to an increased efficiency of stabilizer products over the years, allowing for improved overall performance of the PVC (such as color of the finished product, outdoor weatherability and durability and extrusion output rates) and use at lower concentrations in PVC. The first-generation tin mercaptide stabilizers were dialkyltin long-chain mercaptans having an average tin content of 18%. Used at an application level of 2–3%, the tin content of the PVC was in the range of 3000–5400 $mg\,kg^{-1}$. Second-generation products were mixed mono/dialkyltin long-chain mercaptans. Although the tin content increased to about 22%, these products were often used in diluted form to aid in their handling while reducing losses. These second-generation stabilizers were more efficient and only had to be utilized at a level of about 1–2%, with the resulting tin content of the PVC decreasing to 2200–4400 $mg\,kg^{-1}$. A third generation of stabilizers has recently been introduced, which are all monoalkyltin, short chain and/or functionalized mercaptans or sulfides. These increased efficiency stabilizers, available in diluted versions, contain around 24% tin, are used at 0.25 to 0.75% levels and result in tin content of the PVC of about 900 to 1800 $mg\,kg^{-1}$. There are even high-performance products available, which have an increased tin content, but can be used in highly diluted form at 0.04 to 0.08% levels, and result in PVC with only 172 to 344 $mg\,kg^{-1}$ tin content.

Consideration OT compound release in the life-cycle of PVC: Considering the large quantities of PVC still produced and used, the European Commission, in 1999, launched a comprehensive study program to assess the impact of PVC wastes on the environment. Five studies were commissioned dealing with landfill, recycling (chemical and mechanical), incineration and economic evaluation of PVC waste management. As a result, a 'Green Paper' that was then drafted in July 2000 identified and analyzed a number of issues regarding PVC and its impact on the environment [54]. However, no issues or unresolved questions on tin stabilizers were raised in this paper, while the two main issues brought up in the paper were the use of additives such as phthalate softeners and metal stabilizers (lead and cadmium were singled out). Although disagreeing with the views presented in this Green Paper, the PVC industry, represented by several European associations, signed a voluntary commitment on the sustainable development of PVC, which addresses the reduction of the use of cadmium stabilizers, conducting risk assessments on lead-based stabilizers, the mechanical recycling

of certain post consumer wastes, and the development of further recycling technologies [55].

Landfill studies: The decomposition of PVC continues to be investigated to determine whether groundwater could potentially be affected from plastic deposited in landfills. Because of the leaching and biodegradation processes that take place there, landfills can present a 'worst case' for environmental studies on PVC behavior. The findings have indicated that, even under aggressive soil conditions, PVC leaching results in a negligible amount of organotins in landfill leachate [49, 56]. A three-year study recently completed at universities in Germany and Sweden, in consultation with the Swedish EPA, concluded that PVC is resistant to breakdown under landfill conditions [57]. Any release of tin stabilizers from PVC is subject to biological or abiotic dealkylation processes such that the mono and dialkyltin species from the tin stabilizers are successively transformed to inorganic tin. Naturally occurring methylation of tin by bacteria can also be a confounding factor [58] affecting background levels and analytical results obtained. Landfills, under current technical regulations, are considered an appropriate disposal option for PVC. When the predicted no-effect concentrations (PNEC), derived from aquatic toxicity studies are compared to the predicted environmental concentrations (PEC) of the various PVC additives, including tin stabilizers, indications are that they do not contribute significantly to any toxicity of leachate from the landfill [57]. Although negligible loss of stabilizers may occur, organotin in PVC in landfill sites does not appear to constitute a risk to the environment.

5.2 Antifouling coatings

The growth of aquatic organisms (mainly macroalgae, sponges, mollusks and barnacles) on the ship hull creates a surface roughness that significantly increases friction of the marine vessel and therefore energy consumption. It was estimated by Champ and Seligman [59] that already a 10 μm increase of the surface roughness of the ship hull will cause an increase of fuel consumption in the range of 0.3–1% with the corresponding increase in running costs. For this reason, a great variety of antifouling paints have been in use since the 1960s, particularly based on Cu_2O [19]. The useful lifetime of these coatings, however, typically does not exceed one year (Figure 2.20.9), which makes frequent repainting necessary, and consequently means a financial loss to the shipping company when the ship has to stay in the dry dock. The introduction of TBT in the early 1970s responded to this problem by offering effective protection of the ship hulls for significantly longer than one year, and in the case of the so-called copolymer or self-polishing paints for up to five years. This is why these paints have very soon come into widespread use. In the United States, the annual use of TBT in antifouling paints was estimated to be 450 tons in 1987 [60].

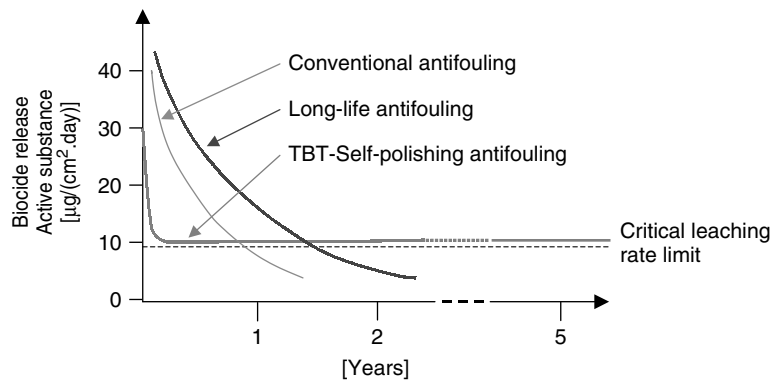

Figure 2.20.8. Comparison of release of active substance versus time for various biocides used for antifouling paints [61].

An antifouling paint consists of a film-forming material with the active, biocidal ingredient and the pigment(s). Its function is to release controlled amounts of the biocide from the paint layer into the water layer surrounding the ship hull so that a thin zone of water with a high TBT concentration is shielding the boat. The toxic concentration of biocide prevents the marine organisms such as barnacles, tubeworms or seaweeds from settling on the ship hull. Antifouling paints can be classified into the following two principal categories:

Free-association antifouling paints – Free-association paints are physical mixtures of the paint and the biocidal compound that is released into the environment by diffusion from the paint film (Figure 2.20.9). As the biocide concentration in the outer regions of the antifouling paint is eventually depleted, the release of active compound decreases exponentially with time (Figure 2.20.8). The initial very high release of biocidal compound and the relatively short effective lifetime of this type of antifouling paint, associated with a difficult-to-control release rate during this period (since microcracks or clogging of the surface of the coating may arbitrarily increase or decrease the biocide release rate), have led to the phasing out of this type of antifouling paint in most countries.

Self-polishing antifouling paints – In this type of antifouling paints, the biocidal compound is chemically bound to the paint matrix that typically contains a polymer binder. The TBT-binder, in most cases a copolymer of TBT methacrylate and methyl methacrylate, hydrolyzes in seawater at a constant linear rate, thus releasing TBT (Figure 2.20.10). The binder becomes water soluble as soon as the bound

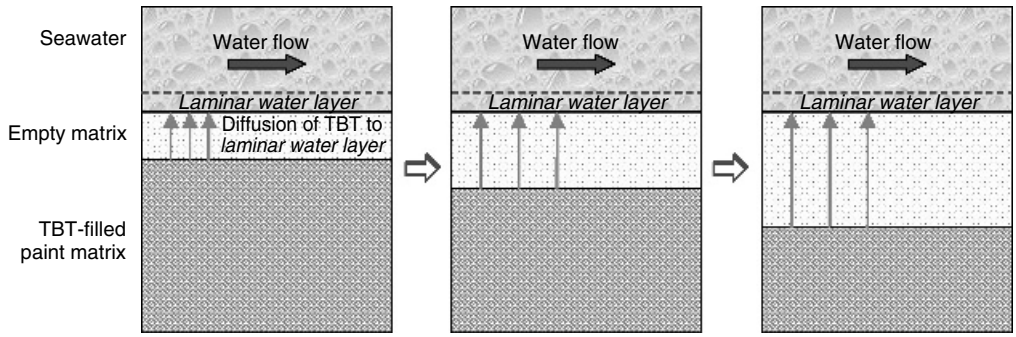

Figure 2.20.9. Crosscut of a conventional antifouling paint film: representation of the biocide release (redrawn after [61]).

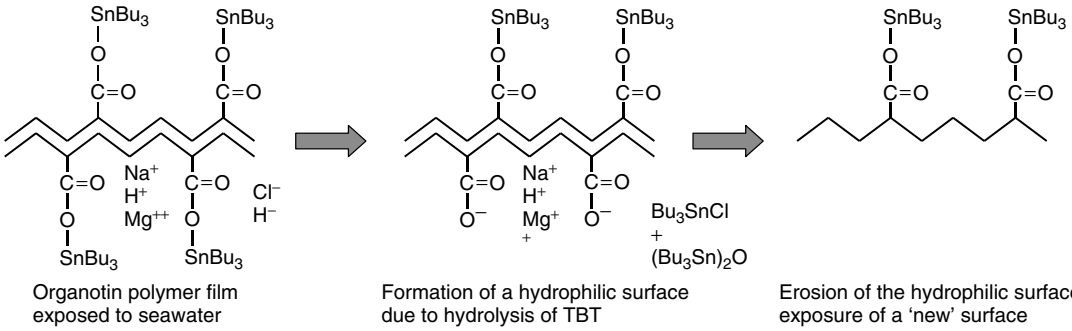

Figure 2.20.10. Mechanism of action of self-polishing TBT-based copolymers to prevent fouling: while the bioactive TBT is chemically fixed to the polymer backbone, a controlled and slow reaction with the seawater takes place at the paint surface and guarantees a constant but very low TBT release. This is the fundamental requirement for self-polishing properties, which could not be achieved by other techniques so far (after [61]).

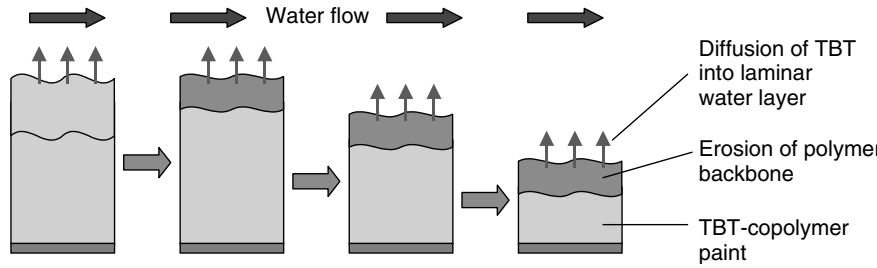

Figure 2.20.11. Cross-section of a self-polishing TBT-copolymer paint system, which illustrates the effect of continuous release of the active component while the polymer backbone is continuously eroded back to the hull. At the same time, smoothing of the surface occurs as a result of preferential removal of exposed areas of the paint layer (after [62]).

TBT has hydrolyzed. The seawater movement against the ship's hull polishes off the hydrolyzed remainder of the binder. By exposing a fresh surface, the entire process is started again. In addition to the antifouling action of the TBT-copolymer paints, their self-polishing effect that smoothens the exposed surface is also highly beneficial: smoothing is the result of different polishing rates for peaks and valleys, because the turbulence created by the flow of water is higher on elevated features of the surface, leading to their preferential removal (Figure 2.20.11).

Not only for environmental but also for economic reasons (since TBT is a comparatively expensive biocide), TBT-containing self-polishing paints are designed to reach a constant low TBT leach rate of 1.6 μg Sn/(cm^2·day), which is considered just above the effective concentration and roughly half of the limit of 4 μg Sn/(cm^2·day) set by the US Congress in the Organotin Antifouling Paint Control Act of 1988 [63]. The initial release rate may, however, be as high as 6 μg Sn/(cm^2·day) and is reduced within a few weeks to the desired constant value [64]. As an example, a commercial sea vessel can release during a three-day-stay in a harbor about 200 g TBT into the water when having reached the constant leach rate, or a value even three times higher when freshly painted. This results in increased concentrations of TBT of up to 600 ng Sn/L in harbor waters [64]. The hot spots of TBT pollution are consequently the harbors for big commercial vessels where there are shipbuilding, repairing and repainting activities. While the concentrations of TBT in harbor waters have significantly been reduced with the ban of the use of TBT-containing antifouling paints in Europe, Canada, the United States and Japan in 1990 [65], this is not the case for harbor sediments (Table 2.20.11). Sediments may be considered as sinks for TBT, although also a remobilization (e.g. through resuspension) is likely. The high TBT concentrations in sediments thus represent an environmental burden that is particularly of concern in the disposal of dredged material from harbor and channel refurbishing activities.

The fate of OTCs in the water column is determined by adsorption to particles and their subsequent sedimentation, biological degradation and accumulation in nontarget marine organisms. Studies in harbors indicate that TBT is enriched in particles, sediments and biota by a factor of 1000–10,000 in comparison to the concentration in water (Figure 2.20.12). Biodegradation of OTCs

Table 2.20.11. Trends in the observed organotin concentrations after the ban of TBT-containing antifouling paints for small vessels in 1990. The data refers to investigations from Poole harbour (UK) and illustrates the relatively slow degradation of TBT in anaerobic sediments in comparison to the faster decrease of TBT levels in the water [65].

Year	n^a	TBT concentration in the water [as ng Sn/L]	TBT concentration in the sediment [as μg Sn/g]
1985–89	24	44.4	0.160
1988–90	29	16.5	0.141
1990–92	39	6.9	0.101

[a] Number of samples investigated.

Table 2.20.12. Stability of OTCs in different matrices and under different conditions reported in the literature.

Organotin compound(s)	Matrix	Half-life	Conditions of degradation	Reference
TBT	Clean water	9 days 19 days	Dark treatment Light treatment	[66]
TBT	Water	3 months	Photolysis	[67]
TBT	Marine water	>89 days	Photolysis	[68]
TBT	Marine water	1 week	Biological/chemical	[69]
TBT	Seawater	Weeks–months		[70]
TBT	Freshwater, seawater	6 days–several weeks	Biotic	[64, 71]
TBT	Surface waters	3–10 days	Biotic	[72]
TBT	Harbor estuarine water	4–14 days	–	[73]
TPhT acetate	Soil	140 days	–	[74]
TBT	Sediments	1–5 years	–	[75]
TBT	Aerobic sediments	>5.5 months	–	[76]
TBT	Anaerobic sediments	2–10 years	–	[64, 71]
TBT	Sediment	2.1 years	–	[77]
DBT	–	1.9 years	–	–
MBT	–	1.1 years	–	–
TBT	Sediment	2.5 years	Biological/chemical	[69]
TBT	Sediment	About 2.5 years	–	[78]
TBT	Sediment	About 8.7 years	–	[79]
TBT	Bivalve *Venerupis decussata*	4–17 years	–	[80]

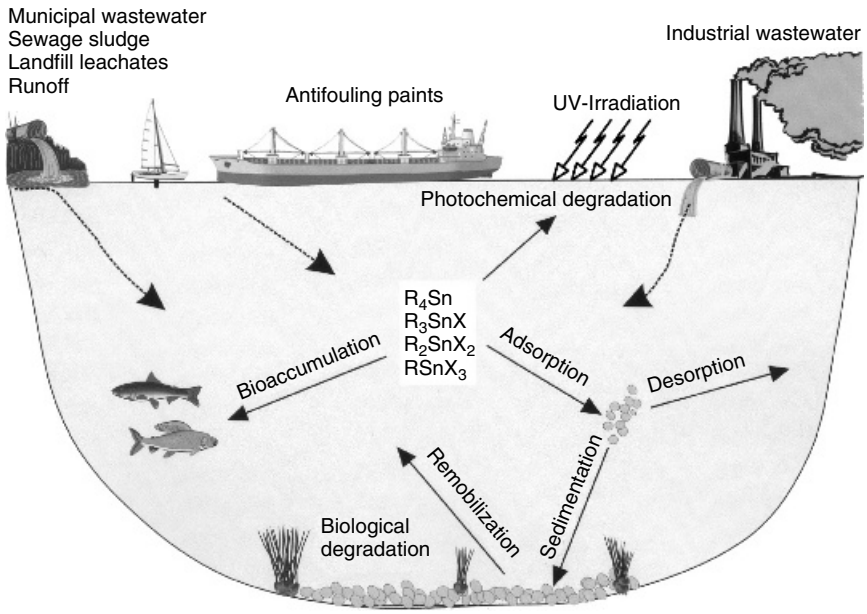

Figure 2.20.12. Distribution and fate of organotin compounds in the aqueous environment (from [11]).

typically takes 1–3 weeks under optimum conditions. Under the anoxic conditions normally encountered in sediments, however, hardly any degradation is observed (Figure 2.20.13 and Table 2.20.12).

5.3 Agricultural use

While in the evaluation of possible harmful effects to the environment most attention was hitherto paid to the use of OTCs as antifouling paints, their use

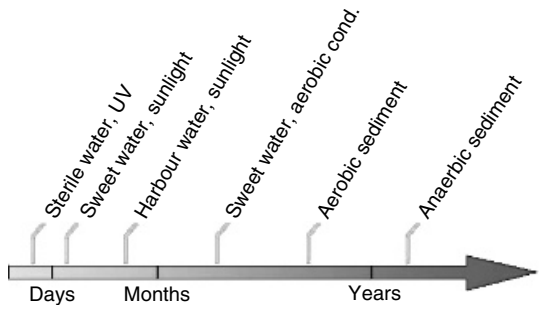

Figure 2.20.13. Stability of TBT under different conditions, expressed as their half life (from [81]).

as pesticides in agriculture also contributes to the contamination of freshwater and soils. The environmental impact of the agricultural and pesticidal use of OTCs may be, despite their considerably lower amounts of usage, still significant as it represents a direct input into the soil and the water. The fungicidal effect of OTCs was used since the early 1960s when TPhT (= fentin) was used as hydroxide or as acetate to control fungal diseases of sugar beets, celery, carrots, onions and rice and also for peanuts, pecans, coffee and cocoa [59]. TCyT has been introduced in 1968 as an acaricide for the control of mites on apples, pears and citrus fruits. The short chain length linear trialkyltin compounds (e.g. butyltin) are highly phytotoxic and thus cannot be applied as agricultural biocides. Also, trimethyltin derivatives such as $(CH_3)_3SnSn(CH_3)_3$ cannot be applied in agriculture despite their high insecticidal activity because of their high mammalian toxicity [82].

No current figures are available for the worldwide usage of OTCs in agriculture. In the Netherlands, however, about 300 tons of OTCs are assumed to be used in agriculture per year [83], of which 96% is TPhT, 3% FBTO (fenbutatin oxide, hexakis-(2-methyl-2-phenylpropyl)-distannoxane) and 1% TCyT. They are typically sold as formulations under the trade names 'Brestan' and 'Brestan 60', which contain ca 50% TPhT acetate and TPhT hydroxide, respectively. These nonsystemic fungicides excel by their good sticking properties, rain fastness and a good persistence on the plant surface. In contrast to this, the World Health Organisation (WHO) has classified TPhT compounds as 'safe agricultural chemicals' because of their rapid degradation under the influence of light and air. Furthermore, organotin residues were supposed to be easily removed by washing, peeling or cooking before consumption. Although it was experimentally found that cooking is not an efficient way of eliminating OTCs from food [45], it can still be concluded that the risk of taking up significant amounts of OTCs through the food is very low.

Various routes are assumed for the input of OTCs used as pesticides into the agricultural environment. After application by spraying, they are either volatilized from the plant leaves [84] or are adsorbed to soil particles. Very little is known about the persistence and fate of these compounds in soils. In a laboratory study, Huang *et al.* [85] found that OTCs degraded slowly in soils with half-lives of 0.5–15 years. The degradation rates in soils generally decreased in the order mono- $\geq$ di- $>$ trisubstituted compounds. Stepwise dealkylation was observed in all cases of dialkylated OTCs, but only in some cases of triorganotin compounds.

5.4 Timber treatment

In order to protect wood against the attack of insects, fungi and bacteria, it is treated with preservers. From the early 1960s, OTCs were marketed as wood preservers. Typical formulations contained 1–3 wt% of TBT oxide, TBT naphthenate or TBT phosphate in an organic solvent as active ingredient [7]. The wood was treated by dipping, spraying, brushing or double vacuum impregnation in specially designed impregnation chambers, which was the most effective treatment and was mostly used in the timber industry. Although TBT leaching from wood treated in this way is negligible, OT-based wood protection agents are phased out because of their high toxicity. Their role is eventually taken over by formulations containing synthetic pyrethroids [7].

6 ENVIRONMENTAL FATE OF OTCS

The industrial use of OTCs has lead to their introduction into the environment. In addition to

the known sources of mainly butyltin and phenyltin emission, there are, however, also indications that OTCs occur in municipal and industrial wastewater and consequently also in sewage sludge and landfill leachates. A discussion of the processes leading to the distribution and transformation of OTCs is thus following.

6.1 Degradation

Tetrasubstituted OTCs are undergoing stepwise degradation according to the following scheme, eventually leading to the Sn^{4+}:

$$R_4Sn \rightarrow R_3SnX \rightarrow R_2SnX_2 \rightarrow RSnX_3 \rightarrow SnX_4$$

where X is a monovalent anionic group. The three mechanisms mainly responsible for the removal of the organic groups are (a) exposure to ultraviolet irradiation, (b) biological degradation and (c) chemical degradation.

Photolysis by UV radiation (exposure to sunlight) is the fastest degradation mechanism in aqueous solution: since the mean bond energy of a Sn–C bond is in the range of 220 kJ mol^{-1} [86], this bond can be cleaved by irradiation of UV radiation that has an energy of approximately 300 kJ mol^{-1} at a wavelength of 290 nm. However, when considering this degradation mechanism, it has to be kept in mind that UV radiation is strongly absorbed by water. Thus, photodegradation may not be the most important degradation route in greater depths of water or in sediments or soils. Among the different organotin species, TPhT and TCyT species are more rapidly decomposed by UV irradiation in comparison with TBT.

The biodegradation of fungicidal OTCs was first demonstrated in 1973 [74]. The stepwise degradation of TPhT acetate was only observed in nonsterile soils containing some bacteria, such as *Pseudomonas putida C* and *Pseudomonas aeruginosa* or *Alcaligenes faecalis* under certain conditions. In aquatic systems, biodegradation of OT compounds occurs as a result of the activity of various microalgae and bacteria of which only a small fraction has been identified up to now. Biodegradation of OTCs, however, is limited by the high toxicity of these compounds to which only few microorganisms are resistant and other conditions like sunlight, temperature and availability of nutrients [87].

Chemical degradation of OTCs is possible by both nucleophilic and electrophilic attack to the Sn–C bond, for example, by mineral acids or carboxylic acids, or by alkali metals. However, at environmental pH values and temperatures, these processes are not relevant.

The time scales reported for the half-lives of OT compounds differ greatly because of the different experimental conditions chosen by the authors for their studies (Figure 2.20.13). Moreover, they may be only indicative for actual circumstances since they were mostly determined in laboratory experiments. Table 2.20.12 gives an overview of values reported in the literature.

6.2 Bioaccumulation

One of the reasons for the great concern caused by OTCs in the aquatic environment is their lipophilic character, leading to a strong enrichment by aquatic invertebrates. An additional motivation is that the mostly concerned mollusks (bivalves) and crustaceans (decapods) also represent important seafood commodities. The magnitude of organotin compound accumulation depends on the following three factors: (a) lipophility/hydrophobicity of the OTC, expressed as octanol/water partition coefficient K_{ow}, (b) conditions of the aqueous phase (pH value, presence of humic acids or other complexing agents) and (c) ability of the organism to eliminate the accumulated organotin species. As a consequence of particularly the factors (a) and (c), respectively, organotin compound concentrations of up to 5 $\mu g\, g^{-1}$ have been observed in marine bivalves [88]. In contrast to this, the concentrations typically observed in fish and crustaceans are significantly lower since they possess efficient elimination mechanisms for organotins (Figure 2.20.12) [89]. The accumulation of TBT by higher trophic organisms takes places either direct from solution

or in combination with uptake by their diet. As a result, marine mammals and birds have recently been shown to also accumulate high levels of butyltins in their tissue and organs [90–92].

6.3 Adsorption

In the discussion of environmental distribution of OTC, adsorption plays a major role. Soils and sediments may serve as adsorbents for these compounds, as hydrophobic compounds tend to adsorb on particulate organic and inorganic matter. The triorganotin cation can be classified as 'hard' cation and at neutral pH strongly interacts with the permanently negative charged surfaces of clays and with the deprotonated surface hydroxyl groups [30, 93]. Laboratory studies indicate that the interaction of OTCs and minerals, however, not only are of pure ionic character but also have a lipophilic contribution in addition to the ion-exchange mechanism. This is evidenced, for example, by the higher adsorption capacity of clay minerals for MBT in comparison to the cation exchange capacity of this material [94]. Also, the decrease in the strength of interaction of butyltins and hydrated iron oxide in the order MBT > TBT > DBT indicates that there is a superposition of different mechanisms [95] and suggests that MBT is most likely to adsorb on the solid matter, whereas DBT preferentially will stay in solution. The TBT has an intermediate affinity and will be found both adsorbed to particulate matter and in the water column. Fent [30] cited data from investigations in sea water and lake water according to which 95–99% of the total TBT was present in the dissolved phase. Also for freshwaters, TBT seems to be largely present in the operationally defined dissolved phase [71]. In wastewater with high amounts of suspended solids, TBT was mainly associated with particulate matter (88%, [30]). The adsorption is not only dependent on suspended matter content but also increases at lower pH and with higher salt concentrations in the water [64]. It was further shown that the sorption of OTCs to particulate organic matter is a fast and reversible process [96]. Therefore, any resuspension of contaminated sediment will lead to enhanced organotin concentrations in the surrounding water phase. This may be relevant particularly for the transport and distribution of coastal zones with periodically changing properties such as the Wadden Sea. Furthermore, the material is potentially bioavailable to filtrators and benthic organisms. Adsorption can therefore not be considered a sink for OTCs.

6.4 Biomethylation

In addition to the anthropogenic sources of organotin compound emission, methyltin compounds may also be produced by biomethylation. Biomethylation may occur under the action of several biotic and also abiotic methylation agents. Of the three mainly occurring biological methylating agents – S-adenosylmethionine, methylcobalamin and N-methyltetrahydrofolate – only methylcobalamin, CH_3B_{12}, the methyl coenzyme of vitamin B_{12}, has been described to methylate tin. In methylcobalamin, the methyl group is transferred as a carbanion (CH_3^-) while the receiving atom must be electrophilic [97]. Inorganic Sn(IV) can thus be converted to different methyltin species. Although methylcobalamin appears to be the sole natural carbanion-donator, in the natural environment the carbanion may also be transferred from other organometallic species that may be present, for example, $(CH_3)_3Pb^+$. Regardless of the methylating agent, only one methyl group is transferred to the metal(loid) at one time, although further methyl groups may be transferred to the same receiving atom. Reactivity of organotin intermediates towards further methylation seems to decrease as the number of organic groups increases [98].

Also methyl iodide that is produced by certain marine algae and seaweeds can methylate inorganic tin(II) salts in the aqueous phase to produce monomethyltin species, while tin(IV) has not been reported to react [99]. It should be mentioned, though, that the chemical form of tin added in laboratory experiments is probably not

the one that underwent biomethylation. Tin(II) would exist within a cell most probably as a complex. What chemical form a tin(IV) compound might take in a biological system can only be speculated. In aqueous solution and at environmental pH values, tin(IV) is most likely existing as hydrated $Sn(OH)_4$. This species is, upon absorption into cells, likely to form complexes through esterification of the hydroxyl groups and/or bonding to oxygen or nitrogen atoms. In anoxic sediments, and probably also within cells, tin(IV) may well undergo reduction to tin(II) prior to further reaction, particularly with enzymatic assistance [100].

Because of the usage of TBT, the question whether biomethylation of the butyltin species occurs is of interest. Laboratory studies with TBT chloride in seawater-sediment mixtures and methanol as methyl source indicated the formation of methyltributyltin and methyltin compounds [101]. Mixed methylbutyltin compounds have also been reported in the environment, with methyltributyltin being the most abundant [102].

Tetramethyltin was one component found in the volatile emissions from the anaerobic digestion of sewage sludge [103].

7 OCCURRENCE AND DISTRIBUTION OF OTCS IN THE ENVIRONMENT

Because of the widespread use of OTCs, they have entered various ecosystems and environmental matrices and can be detected therein in relevant concentrations with the atmosphere being the only exception (Figure 2.20.14).

7.1 Organotins in the marine systems

The direct input of OTCs, and particularly TBT, has raised questions about its occurrence and distribution in the marine ecosystems. Essential to the understanding of the behavior of OTCs in coastal waters is the knowledge of hydrodynamic and biogeochemical conditions, which govern their distribution and transformation (Figure 2.20.15). Because of the hydrophobic nature of triorganotin compounds, they are mostly associated with particulate matter in the aquatic environment. As a consequence, TBT would hardly remain truly dissolved but would rather either accumulate on particulate matter or at the surface microlayer at the

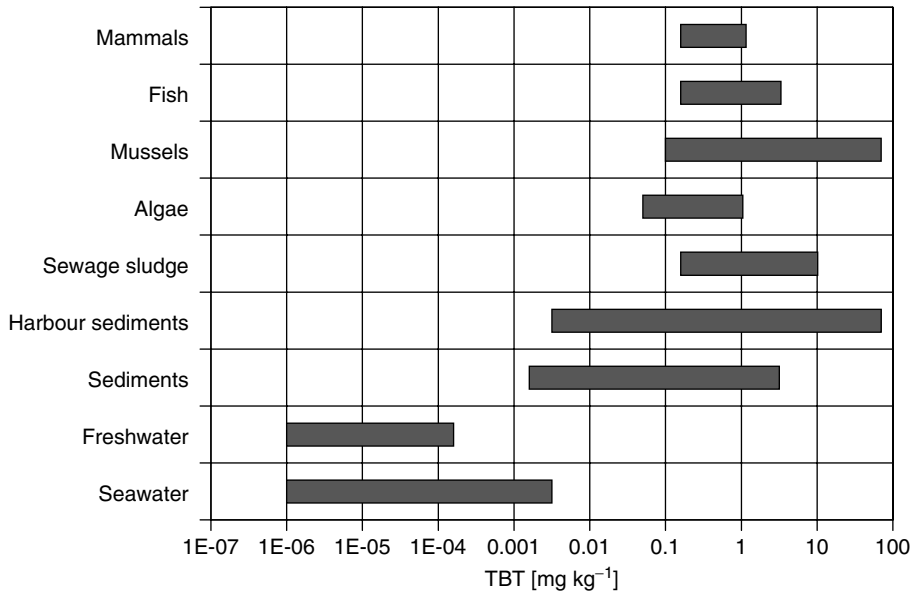

Figure 2.20.14. Ranges of TBT concentrations in various environmental samples (given as mg TBT kg^{-1}) [104].

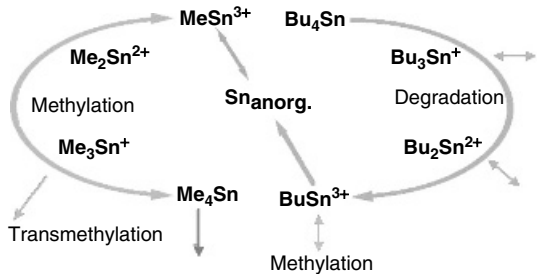

Figure 2.20.15. Transformation pathways of OTCs in the environment [81].

air-water interface. In the latter case, degradation of triorganotin compounds, following a stepwise dealkylation to inorganic tin under the action of UV light may occur rapidly. In the former case, however, organotins are bound to sediments, which leads to a long-term storage of the contaminant. OTCs adsorption to suspended particles can, however, be reversible under certain conditions [105].

Recent new findings have indicated that volatilization of tinorganic compounds may be an important mechanism of remobilization of OTCs entrapped in sediments [106]. Several volatile species of tin were detected, with the mixed butylmethyl species of the form $Bu_nMe_{4-n}Sn$ (with $n = 0-3$) being the most abundant, which are believed to contribute to the continuous volatilization and release of organotin species from the sediments. The calculated flux rates for the transfer from sediment to water were 50–470 nmol/(m^2·year) under the assumption of low turbulent mixing (as, for example, in the case of Arcachon harbour), or 80–790 nmol/(m^2·year) in the case of higher turbulent mixing such as expected in the Scheldt estuary [107]. The underlying assumption for the sediment to water exchange is that all volatile tin species are produced by chemical or biological mechanisms in the bulk sediment and they are passively released into the pore waters. In a similar way, the water to air fluxes were estimated in the range of 20–510 nmol/(m^2·year) for a turbulent estuary such as that of the Gironde or the Scheldt, and about 90 nmol/(m^2·year) for a less perturbed system such as the Arcachon bay.

The implication of these findings and model calculations is significant, as they point out that the remobilization of OTCs from the sediments to the water column and the subsequent volatilization may be a significant factor for the removal of OTCs from the sediments (and at the same time a significant input to the atmosphere). Whatever the magnitude of this process may be, it forces us to reconsider our picture of sediments acting as the final sink for OTCs in the environment.

7.2 Organotins in freshwater environments

Little is known on the occurrence and fate of OTCs in freshwater ecosystems. It is assumed that they will follow the same trends as in marine

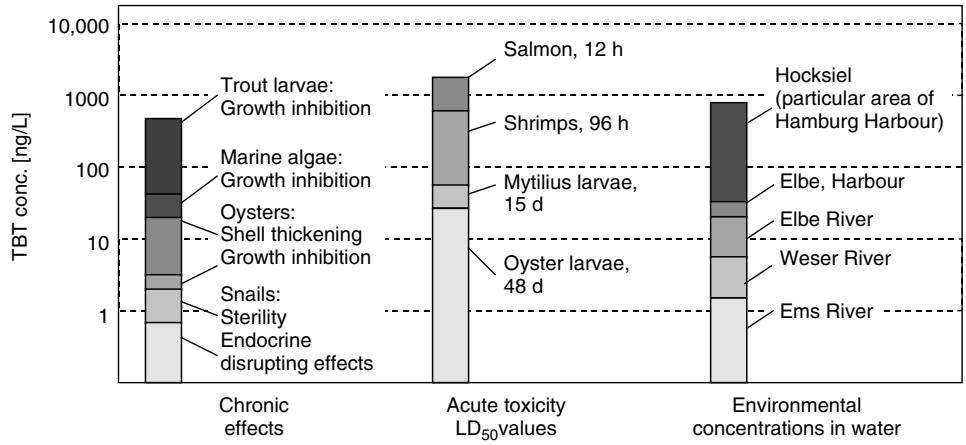

Figure 2.20.16. Chronic effects and LD_{50} values for TBT and concentrations met in the environment [81].

environments (Figure 2.20.16). A major difference, however, is the fact that freshwaters typically contain high levels of humic substances to which OTCs preferentially bind. This will not only affect the amount in truly dissolved form but also the recovery and performance of the analytical method. The adsorption of OTCs to humic substances is strongly depending on the physicochemical properties of the system, and particularly its pH value [108]. This is also reflected by the largely differing half-life times given for TBT under different conditions (Figure 2.20.13 and Table 2.20.12).

Even less data are available on the other organotin species, notably phenyl- and cyclohexyltins, which appear in surface waters mainly because of their use in agriculture, either from the spraying process directly or in the runoff water from organotin-treated plantations. The lack of comprehensive data may be due to both their lower stability as compared to the butyltins and the greater difficulty of their analytical determination.

Attention must also be given to the input of OTCs from wastewater and sewage sludge and from leachates from landfills. Selected organotin species could, for example, be detected in the wastewater treatment plant (WWTP) of Zürich, Switzerland [109]. This indicated that municipal wastewater and sewage sludge contain considerable amounts of particularly the butyltin species (Table 2.20.13). Mono- and dibutyltin not only occur as degradation products of TBT but also enter the WWTP directly, for which the leaching from PVC materials is held responsible. OTCs are eliminated from the water column in the WWTP mainly by adsorption to suspended matter and sedimentation of the sludge. It was demonstrated that elimination rates of around 90% can be reached in a WWTP, reducing the initial concentration of organotins to the low ng L^{-1} level [109].

Table 2.20.13. Concentration of butyltin compounds in municipal wastewater [as ng Sn/L] and sewage sludge [as μg Sn/kg dry weight].

	MBT	DBT	TBT
Zürich (Switzerland)[a]	245	523	157
Goslar Ost (Germany)[b]	<10	60	15
Bomlitz (Germany)[b]	35	40	15
Hildesheim (Germany, 1994)[b]	135	215	140
Hildesheim (Germany, 1996)[b]	136	269	83
Harsfeld (Germany)[b]	64	78	12
Sarnia (Canada)[c]	16–31	11–61	5–175
Toronto (Canada)[c]	440	210–305	245–277

Source: data taken from: [a] Fent and Müller [109], [b] Kuballa *et al.* [110], [c] Chau *et al.* [111]

7.3 Organotins in sediments

It is beyond the possibilities of this chapter to discuss the variability of organotin compound levels that are found throughout the world, since these depend too strongly on the actual location of sampling (e.g. open sea, bay, yachting or commercial harbor). The data published in the literature indicate similar average concentrations or concentration ranges, and, where decrease of organotin concentrations is found, also comparable trends with respect to the location. The trends that are seen in consistent data sets are that the TBT concentrations should decrease in the following order:

$$\text{commercial and fishing harbors} > \text{leisure harbors} \gg \text{open bays}$$

The validity of the data, however, strongly depends on the consideration of basic geochemical parameters, such as grain size or organic carbon content, and would ideally require the normalization to a conservative biogeochemical parameter (e.g. the fraction <2 μm and aluminum or scandium content). These aspects are of particular importance if data of different origin are to be compared. It is known that TBT shows a strong size-dependence of its association to particulate matter, resulting in a bimodal behavior [112]. While TBT is associated to the fine part of the sediment in a similar way as trace metals, it is also associated with the coarse fraction of sediments (>300 μm), which is particularly rich in organic matter.

A further point of consideration is that the concentration profile of OTCs in sediments shows

a characteristic distribution in many cases, with a maximum concentration typically 10–15 cm from the top of the core. The observation that surface concentrations are always lower than those in the buried sediments may be interpreted in two ways: First, it may be taken as a proof of the decrease of TBT input in the water of marinas, which was clearly seen in France and the UK (see Table 2.20.11), although not in the Dutch coastal regions. Second, it may point to the possibility of remobilization of OTCs from sediments that would be most pronounced for the top layers of sediment, as described above.

7.4 Organotins in soils

Various formulations of TPhT are used as fungicide in agriculture, which accounts for its direct input into soils. Depending on the carbon content of the soils, the half-life of fentin acetate may vary from 47 to 70 days in soils with 1% organic carbon and between 115 and 140 days in soils with 2% organic carbon [113]. The low vapor pressure and the comparatively low aqueous solubility together with its high affinity for the soil matrix result in a high persistence in soils, with only 4% of the applied TPhT having leached from the soil column within one year [113]. Still, the spraying of crops with organotin-based pesticides may lead through a contamination of freshwaters due to the runoff. Elevated concentrations of TPhT have been found in waterways close to fields where TPhT-containing fungicides have been applied. In the Netherlands, the input of TPhT into freshwaters due to agricultural activities is estimated at 2.6 tons per year [114].

Another important input of organotins into soils is the common practice of spreading activated sludges over cultivated fields. In view of the anticipated high concentrations of organotins in sewage sludge, this may lead to significant contamination of land by OTCs and must therefore be critically reevaluated. The same concern applies to the deposition of dredged harbor sediments along the coastline of the Netherlands, Belgium and Germany [115].

7.5 Organotins in organisms

Since the discovery of the detrimental effects of even low organotin concentrations in marine organisms, their levels have regularly been monitored in numerous studies worldwide. While the concentrations of OTCs in aquatic invertebrates is well documented, relatively little data exists on the accumulation of OTCs in higher trophic vertebrate predators, which may ingest these pollutants via the food chain, and related effects.

OTCs have been found in the tissues of cetaceans from the North West Pacific region, and Japan, in bottlenose dolphins from Italian and US coastal waters, in Stellar sea lions from Japan, Ganges River dolphins from India, Harbour Porpoise from the Black Sea and sea otters from California coastal waters [11]. Although these examples have only exemplary character, they indicate, nevertheless, the higher degree of butyltin accumulation in comparison with exponents of the species from offshore areas.

Not only aquatic life is affected by organotin compound pollution: birds that are at a higher level of the trophic food chain generally show high levels of xenobiotics and can thus be considered as bioindicators for monitoring environmental pollution. From the comparison of organotin levels in wild birds and their foodstuffs, the enrichment of organotins due to ingestion may be derived. On the basis of the whole body concentration of butyltins in some cormorans in Japan in comparison to the organotin body burden in the fish they ingested, the biomagnification factor was estimated to be in the range of 1.1–4.1. This gives reason to assume that a widespread contamination of OTCs is also present in the higher members of the food chain.

The lower MBT/TBT and DBT/TBT ratios that are typically found in marine mammals in comparison to birds suggests that mammalian degradation and excretion of TBT is less efficient than in birds.

7.6 Organotins in humans

Despite the fact that humans should, as being at the top of the food web, also be affected

by contamination with OTCs, accumulation of OTCs in human tissue is not well documented. Generally, two routes of exposure have to be taken into account: the ingestion of contaminated foodstuff, and indirect exposure from household items containing OTCs. For the former pathway, the contamination of seafood by OTCs has to be taken into account. Seafood consumption is considered to pose a health risk if the amount of organotins taken up with food exceeds the maximum TDI. On the basis of the TDI of 0.25 μg/(kg bodyweight × day) for TBT [116], the maximum TDI for TBT is 15 μg per day for a person with an average body weight of 60 kg. The tolerable average residue level (TARL) is defined as the level in seafood that is tolerable for the average consumer with an average weight of 60 kg. This value can be calculated according to [117]:

$$\text{TARL} = (\text{TDI} \times 60\ \text{kg bodyweight})/(\text{average daily seafood consumption})$$

On the basis of this model calculation, it was concluded that TARLs in seafood are exceeded in one or more samples in nine of the 22 countries for which data were available, that is, Canada, France, Italy, Japan, Korea, Poland, Taiwan, Thailand and the United States. Also in Italy, the average TBT residue level in seafood exceeded the TARL with a factor of 2.5, while in Japan the average TBT residue level in seafood almost equaled the TARL for this country [117].

In one of the few studies reporting organotin levels in humans, Kannan *et al*. investigated the blood of 32 American nationals of different origin and age [118]. The mean concentrations detected were 8 ng mL^{-1} MBT (present in 53% of the samples), 5 ng mL^{-1} DBT (81%) and 8 ng mL^{-1} TBT (71%), while the levels ranged from concentrations below the limit of determination up to 101 ng mL^{-1} of total butyltins in blood. The authors assume that the residues are due to exposures of humans to OTCs as stabilizers or as biocides in household articles. The toxicological relevance of the observed contamination levels is unknown. Both the validity of the statistical evaluation, as well as that of the conclusions drawn by these authors from their above mentioned data and that presented on the elevated levels of butyltin residues in tissues from the Polish coast of the Baltic sea, [119] has, however, been questioned by another group [120].

A similar human monitoring study was recently conducted with blood samples from the Environmental Specimen Bank/Human Specimen Bank in Germany. Only low levels of OTCs were detected [121]. The investigation comprised blood samples from student collectives from two German cities. From the 30 samples analyzed, only one sample showed a concentration above the limit of determination for DBT (1.6 ng mL^{-1}, with the limit of determination at 0.4 ng mL^{-1} blood). In 5 samples, MBT levels were found above the limit of determination (0.3 ng mL^{-1} blood) with a range of 0.7–1.4 ng mL^{-1} blood. The concentrations of the other OTCs were below the limits of determination of each species (TBT $<0.3\ \text{ng mL}^{-1}$; TPhT $<0.4\ \text{ng mL}^{-1}$; DPhT $<0.3\ \text{ng mL}^{-1}$; MPhT $<1\ \text{ng mL}^{-1}$).

8 ANALYTICAL METHODS FOR OTCS

Although methods that are not based on chromatographic separation but on selective extraction have been developed for the discrimination of organotins ('toxic tin') from inorganic ('nontoxic') tin in a sample [122–124], most of the methods in use today for the speciation analysis of OTCs are based on the use of hyphenated techniques, that is, the combination of a suitable separation technique with a molecule- or element-specific detector [125]. The requirements to be met by an analytical technique for the determination of organotins in environmental samples are quite stringent, requiring detection limits in the ng L^{-1} level for water samples and at the ng g^{-1} level for sediments and biota. At the same time, selectivity must be high enough to avoid interferences by the matrix, and simultaneous determination of all relevant organotin species must be possible.

This calls for procedures that typically comprise the following steps: (a) extraction and/or

enrichment form the matrix, (b) derivatization of ionic organotin species in the case of gas chromatographic separation, (c) cleanup (if required), (d) chromatographic separation and (e) selective detection [126].

Gas chromatography (GC), coupled with element-specific detection methods, is the most widely used technique for the determination of OTCs and provides the separation of many species with very good resolution [127]. In the early years of organotin compound speciation analysis, GC was coupled to AAS (GC-AAS) as element-specific detector [128], however, because of the fact that there never was a commercial GC-AAS system, the use of this technique was restricted to few laboratories. At about the same time, GC with atomic emission detection (GC/AED) became commercially available in the form of a microwave-induced plasma-atomic emission detector (GC-MIP-AED) that gave a great impetus to the speciation analysis of organotin and other organometallic compounds [129]. Alternatively, optical emission detection with an inductively coupled plasma (ICP) as emission source has been used, although with little improvement in detection limits but at significantly higher instrumental expenditure [130]. The use of glow-discharge plasmas as excitation source for elemental speciation may represent here a viable, although currently underestimated possibility [131]. The flame photometric detector (FPD) is also very well suited for the detection of OTCs. Although tin is difficult to thermally excite in flames, instrumental improvements and modifications allowed the sensitive and selective detection of OTCs based on the red molecular fluorescence of the Sn–H species at 609.5 nm [132]. The recent introduction of the pulsed flame photometric detector (P-FPD) even improved sensitivity and selectivity for OTCs [133]. It shall be pointed out that OTCs can also be detected with common gas chromatography-mass spectrometry (GC-MS) systems with a sensitivity comparable to gas chromatography-atomic emission detection (GC-AED) [83] (Figure 2.20.17). The use of GC-ICP-MS is increasingly propagated for the analysis of OTCs [134]. The very high investment and operation costs of this technique justify its use only where its superior sensitivity to all other common techniques is essential (Figure 2.20.18). ICP mass spectrometric detection also offers quantitation based on isotope-dilution mass spectrometry (IDMS), which is a unique asset for both highly accurate and precise speciation measurements [135]. In addition, GC-ICP-MS in combination with isotopically labeled standards can be used to study the species-specific decomposition processes of OTCs observed with various sample preparation techniques [136].

Common to all GC-based techniques is the fact that the ionic OTCs are not volatile and can only be separated via the gas phase after conversion to more volatile derivatives. Three techniques are particularly useful for this aim, namely, (a) hybridization, (b) Grignard derivatization and (c) alkylation with sodium tetraalkylborates. For the former approach, sodium tetraborohydride ($NaBH_4$) is used for *in situ* hydride formation [139]. However, only for methyl- and butyltin compounds acceptable recovery rates are obtained. The higher-boiling phenyltin compounds either do not react completely or are prone to thermal decomposition during GC analysis [140]. Grignard alkylation was for a long time the most common approach for the derivatization of ionic OTCs. Grignard reagents were available with different alkyl chain lengths and enabled the formation of different derivatives. However, since the Grignard reagent is sensitive towards water, a solvent exchange step had to be performed after the initial extraction of OTCs from the matrix that was tedious and time consuming [141]. As a consequence, direct aqueous phase derivatization with tetraalkylborate reagents was immediately adopted as soon as the $NaBEt_4$ reagent became widely available. In contrast to the Grignard reagent, the $NaBEt_4$ is sufficiently stable in water to be used for derivatization. As this reagent does not require a solvent exchange and the aqueous extracts resulting from the extraction of the sample can be directly used for derivatization, this method has become very popular [139]. The derivatized OTCs are extracted with a small volume of apolar solvent (hexane or isooctane), eventually cleaned up

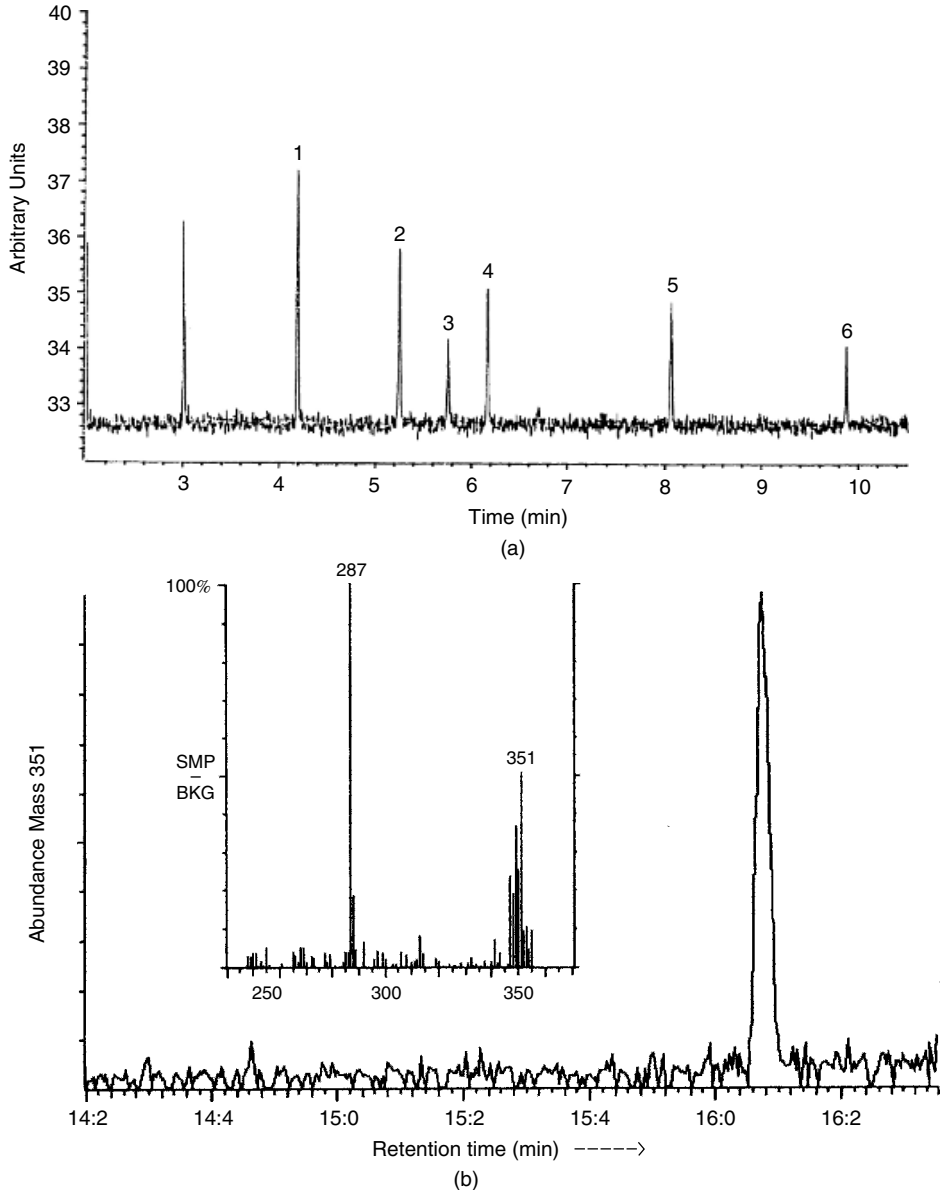

Figure 2.20.17. Examples of gas chromatographic speciation analysis of OTCs. (a) GC-AED chromatogram of a seawater sample, spiked with 4 pg (as Sn) of each organotin compound: 1, MBT; 2, DBT; 3, MPhT; 4, TBT; 5, DPhT; 6, TPhT [137], and (b) GC-MS extracted ion chromatogram at mass 351 of a wet-only rainwater sample from location Nieuwekerk a/d Ijssel containing 8 ng TPhT (as Sn) L^{-1}. The insert shows the background-corrected mass spectrum of TPhT that can be identified from the characteristic signal cluster at m/z 351. [138].

if needed, and are ready for analysis by GC. Recently, the propyl analogue of this reagent ($NaBPr_4$) has been introduced and was successfully used in organotin speciation [134]. While the analytical performance of the method with this reagent is comparable to $NaBEt_4$, its use is essential when organotin and organolead species are to be analyzed simultaneously in order to preserve the

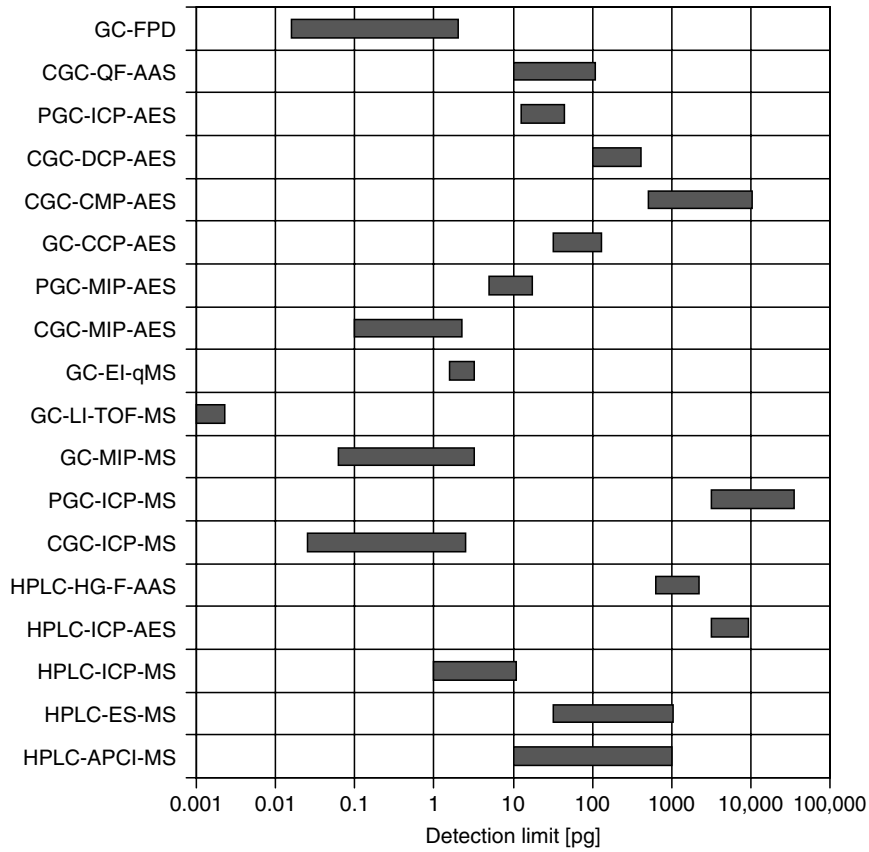

Figure 2.20.18. Absolute limits of detection for organotin species obtained by the most widely used coupled techniques. Abbreviations: capillary gas chromatography (CGC); packed-column gas chromatography (PGC); quartz furnace (QF); flame atomic absorption spectrometry (F-AAS); inductively coupled plasma (ICP); atomic emission spectrometry (AES); direct-current plasma (DCP); capacitively coupled microwave plasma (CMP); capacitively coupled plasma (CCP); microwave-induced plasma (MIP); electron-impact ionization (EI); quadrupole mass spectrometry (qMS); laser-induced time of flight (LI-TOF); hydride generation (HG). (Data taken from [125].)

species information of the methyl- and ethyllead species potentially present [142].

In contrast to GC-based methods, liquid chromatography (LC), and particularly high-performance LC (high-performance liquid chromatography (HPLC) offers the advantage of avoiding the time-consuming step of derivatization and minimizes the sample handling steps, which makes the procedure less prone to contamination or loss of analyte. By avoiding derivatization, the possibility of rearrangements and loss of analyte integrity is avoided. The liquid chromatographic methods can be classified into the following three main categories [143, 144].

(a) Cation-exchange chromatography, (b) reversed phase chromatography, and (c) normal phase chromatography. The detectors employed range between nonelement specific ones (UV absorption detectors, differential pulse voltammetric detection systems or reversed pulse amperometric detectors) and element-specific ones, such as atomic absorption (graphite furnace or flame), laser-enhanced ionization, laser excited atomic fluorescence, fluorescence, ICP-AES or ICP-MS. Different approaches have been employed for the coupling of the chromatographic systems to the detector in order to improve the sensitivity of the overall system (such as hydride

generation (HG)) or to make both parts compatible (by blending oxygen into the nebulizer gas in ICP-MS to avoid the deposition of carbon on the surface of the cones). While the separation efficiency of LC is generally poorer than that of GC, the advantages of its use are still convincing, particularly with the use of the highly sensitive ICP-MS detector. In recent years, HPLC-MS with atmospheric pressure ionization (electrospray or atmospheric pressure chemical ionization (APCI)) has also been described for the analysis of OTCs (Figure 2.20.19) [145, 146]. The advantage of mass spectrometric detection with soft ionization is the preservation of structural integrity of the analytes that may help elucidating the identity of analytes in case of doubt [147].

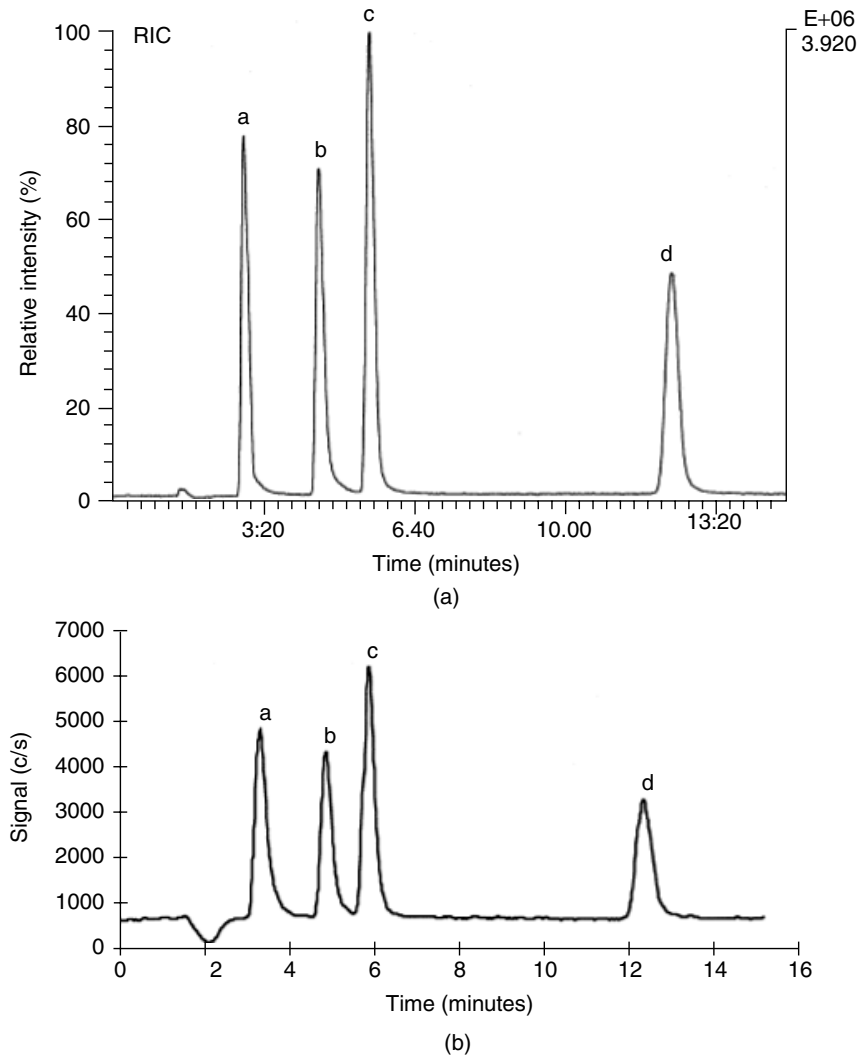

Figure 2.20.19. (a) Liquid chromatography-mass spectrometry (LC-MS) chromatogram for organotin standards using positive-ion APCI. Peak assignment: a, DPhT; b, DBT; c, TPhT; d, TBT. Concentration 50 $\mu g\,mL^{-1}$ as chlorides. (b) LC-ICP-MS chromatogram for organotin standards. a, DPhT; b, DBT; c, TPhT; d, TBT. Concentration 10 $ng\,mL^{-1}$ as chlorides. (c) Positive-ion APCI mass spectrum for diphenyltin. (d) Positive-ion APCI mass spectrum for dibutyltin [148].

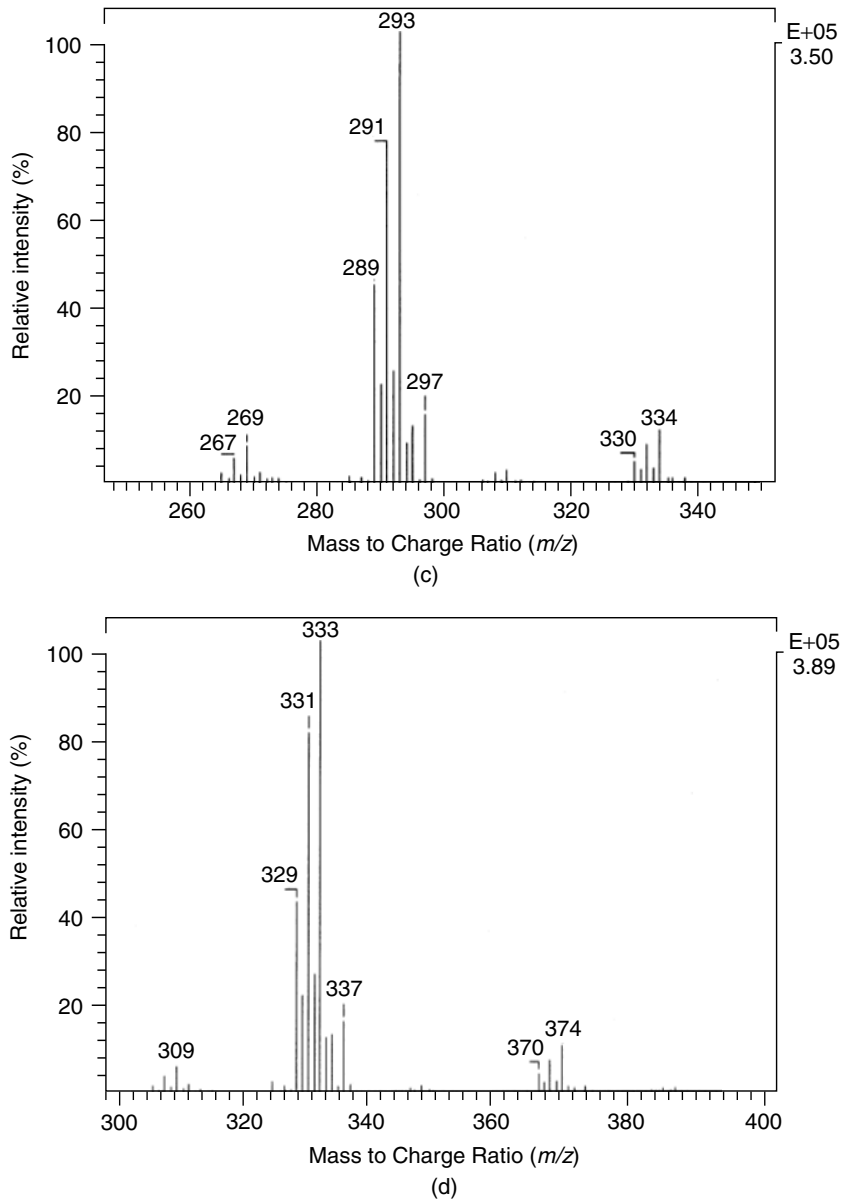

Figure 2.20.19. (*continued*)

Prior to chromatographic analysis, there is normally an extraction step to isolate and preconcentrate the analytes from the matrix. Typically, this is done by acid leaching for sediments, leaves and other biotic samples with the aid of a complexing agent, for example, tropolone or different diethyl carbamates. Alternatively, fish or tissue samples may be digested in tetramethyl hydroxide, followed by direct aqueous phase derivatization. Sample preparation strategies have been reviewed comprehensively [149] and have also been subject to a technical report of the IUPAC Commission on Microchemical Techniques and Trace Analysis [150]. More detailed discussion of technical

aspects of organotin compound analysis can be found in recent papers on the comparison of extraction methods [151], derivatization methods [152], and their application to sediment and mussel tissue [153].

Quality related issues are of even greater concern in speciation analysis than in inorganic analysis because of the various sources of uncertainty and the great difficulties to control the analytical process. The reasons for this lie, among others, in the complex analytical procedure, in the potential decomposition of analytes or formation of artifacts during the sample preparation, in the limited availability of high purity calibrants, and of (certified) reference materials (CRMs). For this reason, great efforts have been undertaken by the BCR (Community Bureau of Reference of the European Union) and by other organizations such as the Canadian Research Council (NRCC), the US National Institute of Standards and Technology (NIST) and the Japanese National Institute of Environmental Studies (NIES) to provide reference materials (RMs) and CRMs for organometallic species in various matrices. These matrix CRMs are usually characterized by interlaboratory studies using different analytical techniques [154]. They were developed with the intention of validating the analytical procedures and to ensure that they do not include sources of systematic error. An overview of most available reference materials for the determination of the most important organotin compounds is given in Table 2.20.14.

9 LEGISLATIVE SITUATION

The impact of TBT on marine organisms put pressure on many governments to restrict its use [155]. France was the first country to ban the application of TBT-based antifouling paints on vessels less than 25 m long in 1982. England followed in 1987, and similar restrictions were

Table 2.20.14. (Certified) reference materials for organotin species.

(Certified) reference material	Matrix	Certified values (as cation) with associated uncertainty (Ass. Unc.)
PACS-2	Marine harbor sediment	MBT[a]: 0.45 $\mu g\,g^{-1}$, Ass. Unc.: 0.05 $\mu g\,g^{-1}$ DBT[a]: 1.09 $\mu g\,g^{-1}$, Ass. Unc.: 0.15 $\mu g\,g^{-1}$ TBT[a]: 0.98 $\mu g\,g^{-1}$, Ass. Unc.: 0.13 $\mu g\,g^{-1}$
RM 424	Harbor sediment	TBT[b]: 20 ± 5 $ng\,g^{-1}$
CRM 462	Coastal sediment	DBT: 68 $ng\,g^{-1}$, Ass. Unc.: 12 $ng\,g^{-1}$ TBT: 54 $ng\,g^{-1}$, Ass. Unc.: 15 $ng\,g^{-1}$
CRM 477	Mussel tissue	MBT: 1.50 $\mu g\,g^{-1}$, Ass. Unc.: 0.28 $\mu g\,g^{-1}$ DBT: 1.54 $\mu g\,g^{-1}$, Ass. Unc.: 0.12 $\mu g\,g^{-1}$ TBT: 2.20 $\mu g\,g^{-1}$, Ass. Unc.: 0.19 $\mu g\,g^{-1}$
CRM 646	Freshwater sediment	MBT: 0.61 $\mu g\,g^{-1}$, Ass. Unc.: 0.12 $\mu g\,g^{-1}$ DBT: 0.77 $\mu g\,g^{-1}$, Ass. Unc.: 0.09 $\mu g\,g^{-1}$ TBT: 0.48 $\mu g\,g^{-1}$; Ass. Unc.: 0.08 $\mu g\,g^{-1}$ MPhT: 0.069 $\mu g\,g^{-1}$, Ass. Unc.: 0.18 $\mu g\,g^{-1}$ DPhT: 0.036 $\mu g\,g^{-1}$, Ass. Unc.: 0.008 $\mu g\,g^{-1}$ TPhT: 0.029 $\mu g\,g^{-1}$; Ass. Unc.: 0.011 $\mu g\,g^{-1}$
NIES 11	Fish tissue	TBT[a]: 1.3 ± 0.1 $\mu g\,g^{-1}$ (TPhT[ab]: 6.3 $\mu g\,g^{-1}$)
NIES 12	Marine sediment	TBT[a]: 0.044 ± 0.004 $mg\,kg^{-1}$ DBT[a]: 0.056 ± 0.006 $mg\,kg^{-1}$ MBT[a] 0.058 ± 0.013 $mg\,kg^{-1}$
NIST 1941b	Marine sediment	MBT: 0.08 $\mu g\,g^{-1}$, Ass. Unc.: 38% DBT: 0.27 $\mu g\,g^{-1}$, Ass. Unc.: 19% TBT: 0.17 $\mu g\,g^{-1}$, Ass. Unc.: 24% (Values withdrawn in the revision of the certificate of analysis from August 2004)

[a] As elemental Sn.
[b] Indicative value.

adopted in other European countries, Australia and North America [156]. A US federal law was introduced in early 1989, banning the use of organotin paints on small boats and limiting the release rate of OTCs from antifouling paints for commercial vessels to equal or less than 4 $\mu g/(cm^2 \cdot day)$ [63].

Continuing this line, the International Maritime Organisation's (IMO) Marine Environment Protection Committee (MEPC) passed a resolution in November 1990 on the 'Measures to control potential adverse impacts associated with the use of TBT compounds in antifouling paints' [157]. The three main issues of the resolution were 1) the elimination of usage of TBT-containing antifouling paints on nonaluminum vessels of less than 25 m length, 2) the elimination of usage of paints having an average release rate greater than 4 $\mu g/(cm^2 \cdot day)$, and 3) the development of alternative systems.

Such regulations apparently were effective in reducing TBT contamination: Measurements carried out by the US Navy and other monitoring programmes reported a decrease of organotin concentrations in water to below the US EPA-proposed water quality criteria level of 10 $ng\,L^{-1}$ [158], although not to the same degree for sediments [65], and mollusk tissues [159] (Table 2.20.15). Moreover, decreasing levels of imposex and recovery of gastropod populations were recorded [156]. Along the Italian coast, *Stramonita haemastoma* recovered at sites from where it almost disappeared prior to 1998 [155].

These reports have, however, particularly in the recent years, not remained uncontradicted: the results of a study on the status of imposex in *Nucella lapillus* along the Portuguese coast revealed that TBT contamination has even increased along the Portuguese coast over the five-year period since the ban in 1993. The degree of imposex had increased more near small harbors than near ports served by commercial vessels [160, 161]. A related study on imposex occurrence frequency in the muricid *Bolinus brandaris* sampled at the Northwest Mediterranean Spanish coast arrives to a similar conclusion as concerns the persistence of contamination by TBT [162].

In November 1999, a further resolution was approved by the MEPC of the IMO, proposing a total ban of organotins in antifouling paints. On this basis, the MEPC was initiating legislation that should enforce (1) a ban on the application of TBT-based antifouling paints by 1 January 2003, and (2) that the last date for having TBT-based antifouling paint on a vessel is 1 January 2008. Moreover, the development and use of environmentally safe alternatives to TBT-containing antifouling paints is to be promoted [158].

The restriction on the use of TBT is leading to a renewed use of old-fashioned copper-based paints and/or to the use of new paints incorporating high booster levels of copper. Copper (and other metals) may also pose problems to the environment [163], and the possible impact linked to a renewed use of copper-based paints was hypothesized by several authors (e.g. [156]). It was found that the copper content of oysters increased at Arcachon Bay following the ban on TBT-based anti-foulants on small vessels [164].

Besides the increasing use of copper-based antifouling paints, several alternatives to TBT have been developed. The effects of new biocides as antifouling agents, however, are poorly known, and concerns have been expressed about

Table 2.20.15. Typical concentrations of OTCs in various environmental compartments after the ban of organotin-containing antifouling paints in Switzerland (data taken from [30]).

	Unit	MBT	DBT	TBT	TPhT
Harbor waters	$[ng\,L^{-1}]$	2–10	1–100	1–320	1–5
Harbor sediments	$[\mu g\,kg^{-1}$ dry weight]	150	200	100–9800	120–170
Communal waste water	$[ng\,L^{-1}]$	140–560	130–1030	60–220	–
Waste water treatment plant effluent	$[ng\,L^{-1}]$	9	6	2–10	–
Sewage sludge	$[\mu g\,kg^{-1}$ dry weight]	0.1–3.1	0.4–13.4	0.3–10.3	0.5
Zebra mussel	$[\mu g\,g^{-1}$ dry weight]	0.2–1.0	0.5–2.4	2.8–9.3	0.6–3.9

their putative impact on nontarget organisms. It was found, for instance, that low concentrations of the algicide Irgarol 1051 were sufficient to change the structure of periphyton communities off the west coast of Sweden [165]. Other 'booster biocides', which in fact are agrochemicals must be incorporated in copper-containing antifouling paints since copper is not effective against diatoms and algae. These biocides, such as diuron and 'Sea nine 211', have been found in coastal environments in concentrations of up to several hundred ng L^{-1} [19]. The search for more suitable replacements for TBT as active ingredient in antifouling paints must thus continue, as also its current substitutes could not be successfully designed as to maximize their efficiency while minimizing the side effects to nontarget organisms.

10 REFERENCES

1. Bowen, H. J. M., *Environmental Chemistry of the Elements*, Academic Press, New York, 1979.
2. Omae, I., *Applications of Organometallic Compounds*, John Wiley & Sons, Chichester, 1999.
3. Frankland, E., *Ann. Chem. Pharm.*, **71**, 171, 212 (1849).
4. Löwig, C., *Liebigs Ann. Chem.*, **84**, 308 (1852).
5. Yngve, V., US Patent 2219463 (1940); *Chem. Abstr.*, **35**, 1145 (1941).
6. van der Kerk, G. J. M. and Luitjen, J. G. A., *J. Appl. Chem.*, **4**, 314 (1954).
7. Bennett, R. F., in *Tributyltin: A Case Study of an Environmental Contaminant, Cambridge Environmental Chemistry Series*, De Mora, S. J. (Ed.), Cambridge University Press, Cambridge, MA, 1996, pp. 21–61.
8. Donard, O. F. X. and Pinel, R., in *Environmental Analysis Using Chromatography Interfaced with Atomic Spectrometry*, Harrison, R. M. and Rapsomanikis, S. (Eds.), Wiley, New York, 1989, pp. 189–257.
9. Fent, K., in *Organotin – Environmental Fate and Effects*, Champ, M. A. and Seligman, P. F. (Eds.), Chapman & Hall, London, 1996, pp. 1–25.
10. Blunden, S. J. and Evans, C. J., Organotin compounds, in *The Handbook of Environmental Chemistry*, Vol. 3, Part E, Anthropogenic Compounds, Hutzinger, O. (Ed.), Springer, Berlin, 1990, pp. 1–44.
11. Hoch, M., *Appl. Geochem.*, **16**, 719 (2001).
12. Alfa Aesar product catalogue, available on the World Wide Web at: http://www.alfa.com, (2004).
13. Evans, C. J. and Smith, P. J., *J. Oil Col. Chem. Assoc.*, **58**, 160 (1975).
14. UNEP/WHO, *Environmental Health Criteria 15, Tin and Organotin Compounds*, World Health Organization, Geneva, 1980.
15. Gibbs, P. E. and Bryan, G. W., in *Organotin – Environmental Fate and Effects*, Champ, M. A. and Seligman, P. F. (Eds.), Chapman & Hall, London, 1996, pp. 259–281.
16. World Health Organization, *Tributyltin Compounds*, United Nations Environment Programme-World Health Organization, Environmental Health Criteria 116, World Health Organization, Geneva, 1990.
17. Sadiki, A. I., Williams, D. T., Carrier, R. and Thomas, B., *Chemosphere*, **32**, 2389 (1996).
18. UNEP/Intern. Labour Organisation/WHO, *Environmental Health Criteria 116: Tributyltin Compounds*, World Health Organization, Geneva, 1990.
19. Omae, I., *Appl. Organomet. Chem.*, **17**, 81 (2003).
20. Alzieu, C., Sanjuan, J., Deltreil, J. P. and Borel, M., *Mar. Pollut. Bull.*, **17**, 494 (1986).
21. Thain, J. E. and Waldock, M. J., *Water Sci. Technol.*, **18**, 193 (1986).
22. Smith, B. S., *J. Appl. Toxicol.*, **1**, 22 (1981).
23. Bryan, G. W., Gibbs, P. E., Hummerstone, L. G. and Burt, G. R., *J. Mar. Biol. Assoc. U. K.*, **66**, 611 (1986).
24. Gibbs, P. E., Bryan, G. W., Pascoe, P. L. and Burt, G. R., *J. Mar. Biol. Assoc. U. K.*, **67**, 507 (1987).
25. Ten Hallers-Tjabbes, C. C., Kemp, J. F. and Boon, J. P., *Mar. Pollut. Bull.*, **28**, 311 (1994).
26. Nicklin, S. and Robson, M. W., *Appl. Organomet. Chem.*, **3**, 487 (1988).
27. Spooner, N., Gibbs, P. E., Bryan, G. W. and Goad, L. J., *Mar. Environ. Res.*, **32**, 37 (1991).
28. Smith, P. J., *Proc. Malac. Soc. (London)*, **39**, 377 (1971).
29. Oehlmann, J. and Bettin, C., *Molluscan Reprod.*, **6**, 157 (1996).
30. Fent, K., *Crit. Rev. Toxicol.*, **26**, 1 (1996).
31. Bulten, E. J. and Meinema, H. A., Tin, in *Metals and their Compounds in the Environment*, Merian, E. (Ed.), VCH, Weinheim, 1991, pp. 1245–1259.
32. Salazar, M. H. and Salazar, S. M., *Mar. Environ. Res.*, **32**, 131 (1991).
33. Suzuki, S., Matsuda, R. and Saito, Y., *J. Agric. Food Chem.*, **40**, 1437 (1992).
34. Zuckerman, J. J., Reisdorf, R. P., Ellis, H. V. and Wilkinson, R. R., in *Organometals and Organometalloid Occurrence and Fate in the Environment, ACS Symposium Series 82*, Brinckman, F. E. and Bellama, J. M. (Eds.), American Chemical Society, Washington, DC, 1978, pp. 388–422.
35. Frankland, E., *J. Chem. Soc.*, **2**, 263 (1849).
36. Buckton, G. B., *Phil. Trans.*, **149**, 417 (1859).
37. Letts, E. A. and Collie, J. N., *Phil. Mag.*, **22**, 41 (1886).
38. Pope, W. J. and Peachey, S. J., *Proc. Chem. Soc.*, **19**, 290 (1903).
39. Bennett, R. F., *Ind. Chem. Bull.*, **2**, 171 (1983).

40. Bennett, R. F., Industrial manufacture and application of tributyltin compounds, in *Tributyltin: A Case Study of an Environmental Contaminant*, Cambridge Environmental Chemistry Series, De Mora, S. J. (Ed.), Cambridge University Press, Cambridge, MA, 1993, pp. 21–61.
41. European Council of Vinyl Manufacturers (ECVM), Brussels, *Voluntary commitment of the PVC industry* (March 2000), joint declaration of the ECVM, ESPA, ECPI and EuPC. Available online at: http://www.evc-int.com/she/Downloads/VoluntaryCommitmentDoc.pdf, (2005).
42. http://www.products.arkemagroup.com/pdf/additives/TinStabilizers_A HistoryOfSafeUse.pdf (2005).
43. Frye, A. H., Host, R. W. and Palioagis, M. A., *J. Polym. Sci., Part A*, **2**, 1765, 1785, 1801 (1964).
44. Forsyth, D. S., Weber, D. and Barlow, L., *Appl. Organomet. Chem.*, **6**, 579 (1992).
45. Takahashi, S., Mukai, H., Tanabe, S., Sakayama, K., Miyazaki, T. and Masuno, H., *Environ. Pollut.*, **106**, 213 (1999).
46. Carr, H. G., *Soc. Plast. Eng.*, **25**, 72 (1969).
47. Batt, J. M., *Tin Stabilizers, A History of Safe Use*, Available on the World Wide Web: http://www.atofinachemicals.com/additives/literature/TinStabilizers_AHistoryOfSafeUse.pdf.
48. Summer, K. H., Klein, D. and Greim, H., *Ecological and Toxicological Aspects of Mono- and Disubstituted Methyl-, Butyl-, Octyl-, and Dodecyltin Compounds*, Organotin Environmental Programme Association (ORTEPA), 1996.
49. European Council of Vinyl Manufacturers (EVCM), '*ECVM Background Paper: PVC and Stabilizers*, December 7, 1997.
50. Wu, W., Roberts, R. S., Chung, Y. C., Ernst, W. R. and Havlicek, S. C., *Arch. Environ. Contam. Toxicol.*, **18**, 839 (1989).
51. Sadiki, A. and Williams, D., *Chemosphere*, **32**, 1983 (1996).
52. Sadiki, A., Williams, D., Carrier, R. and Thomas, B., *Chemosphere*, **32**, 2389 (1996).
53. Sadiki, A. and Williams, D., *Chemosphere*, **38**, 1541 (1999).
54. EU Commission Green Paper, *Environmental Issues of PVC*, published 26 July 2000 in Brussels, COM 2000, 469 final.
55. European PVC Industry Voluntary Commitment, *Sustainable Development – The Voluntary Commitment of the PVC Industry*, March, 2000.
56. Ejlertsson, J., Fredricksson, A., Hörsing, M., Svensson, B. H. and Mersiowsky, I., ORTEPA landfill study 1999: long term behaviour of PVC-products and fate of organotin stabilizers under landfill conditions, Presented at *ORTEPA World Meeting*, Cagliari, Italy, Oct. 2000.
57. Mersiowsky, I., *Long-Term Behaviour of PVC Products and Their Additives Under Landfill Conditions – Integrative Review and Evaluation of the Research Programme*, TUHH Technologie GmbH (Tu Tech) Integrated Management, 2001. Available on the World Wide Web: http://home.t-online.de/home/ivo.mersiowsky/pvc.htm, accessed 2005.
58. Feldmann, J., Hirner, A. V. and Cullen, W. R., Volatilization of organotin compounds in the environment, *Proceedings of the Workshop on Organotin Compounds in the Canadian Aquatic Environment, Sidney*, National Water Research Institute, Department of the Environment Canada Centre for Inland Waters, British Columbia, February 19–20, 1996, Contribution 96–153.
59. Champ, M. A. and Seligman, P. F., An introduction to organotin compounds and their use in antifouling coatings, in *Organotin – Environmental Fate and Effects*, Champ, M. A. and Seligman, P. F. (Eds.), Chapman & Hall, London, 1996, pp. 1–25.
60. Champ, M. A. and Bleil, D. F., *Research Needs Concerning Organotin Compounds Used in Antifouling Paints in Coastal Environments*, Science Applications International Corporation US Department of Commerce, National Oceanic and Atmospheric Administration, Rockville, MD, 1988.
61. Haak, P. W., The present status of TBT-copolymer antifouling paints, *Proceedings of the International One-Day Symposium on Anti-Fouling Paints for Ocean-Going Vessels*, Organotin Environmental Program Association (ORTEP), The Hague, 21st February, 1996, pp. 9–16.
62. Anderson, C. D. and Dalley, R., Use of the organotins in antifouling painting, *Proceedings of IEEE Oceans '86 Organotin Symposium*, Marine Technology Society, Washington, DC, 1986, pp. 1108–1113.
63. US Congress, *The Organotin Antifouling Paint Control Act of 1988*, (33 USC 2401). Public Law 1988, pp. 100–333.
64. Batley, G. E., The distribution and fate of tributyltin in the marine environment, in *Tributyltin: A Case Study of an Environmental Contaminant*, De Mora, S. J. (Ed.), Cambridge University Press, Cambridge, MA, 1996, pp. 139–165.
65. Langston, W. J. and Pope, N. D., *Mar. Pollut. Bull.*, **31**, 32 (1995).
66. Seligman, P. F., Valkirs, A. O. and Lee, R. F., *Environ. Sci. Technol.*, **20**, 1229 (1986).
67. Maguire, R. J., Tkacz, R. J., Chau, Y. K., Bengert, G. A. and Wong, P. T. S., *Chemosphere*, **15**, 253 (1986).
68. Wuertz, S., Miller, C. E., Pfister, R. M. and Cooney, J. J., *Appl. Environ. Microbiol.*, **57**, 2783 (1991).
69. Atireklap, S. K., Tanabe, S. and Sanguansin, J., *Mar. Pollut. Bull.*, **34**, 894 (1997).
70. Jacobsen, A. H. and Willingham, G. L., *Sci. Total Environ.*, **258**, 103 (2000).
71. Maguire, R. J., The occurrence, fate and toxicity of tributyltin and its degradation products in fresh water environments, in *Tributyltin: Case Study of an Environmental Contaminant*, Mora, S. J. (Ed.),

Cambridge University Press, Cambridge, MA, 1996, pp. 94–138.
72. Lee, R. F., Valkirs, A. O. and Seligman, P. F., *Environ. Sci. Technol.*, **23**, 1515 (1989).
73. Huggett, R. J., Unger, M. A., Seligman, P. F. and Valkirs, A. O., *Environ. Sci. Technol.*, **26**, 233 (1992).
74. Barnes, R. D., Bull, A. T. and Poller, R. C., *Pestic. Sci.*, **4**, 305 (1973).
75. Waldock, M. J., Thain, J. E., Smith, D. and Milton, S., The degradation of TBT in estuarine sediments, *Proceedings of the 3rd International Organotin Symposium*, Monaco, 1990, pp. 46–49.
76. Watanabe, N., Sakai, S. and Takatsuki, H., *Chemosphere*, **31**, 2809 (1995).
77. Sarradin, P. M., Lapaquellerie, Y., Astruc, A., Latouche, C. and Astruc, M., *Sci. Total Environ.*, **170**, 59 (1995).
78. De Mora, S. J., Stewart, C. and Phillips, D., *Mar. Pollut. Bulletin*, **30**, 50 (1995).
79. Stewart, C. and Thompson, J. A., *J. Environ. Technol.*, **18**, 1195 (1997).
80. Gómez-Ariza, J. L., Giráldez, I. and Morales, E., *Environ. Pollut.*, **108**, 279 (2000).
81. Homepage of GALAB Laboratories GbR, Geesthacht, Germany, http://www.galab.de, accessed 2005
82. Blunden, S. J. and Chapman, A., Organotin compounds in the environment, in *Organometallic Compounds in the Environment*, Craig, P. J. (Ed.), Longman, London, 1986, pp. 111–159.
83. Stäb, J. A., Cofino, W. P., van Hattum, B. and Brinkman, U. A. Th., *Fresenius' J. Anal. Chem.*, **347**, 247 (1993).
84. Stäb, J. A., Cofino, W. P., van Hattum, B. and Brinkman, U. A. Th., *Anal. Chim. Acta*, **286**, 335 (1994).
85. Huang, J.-H. and Matzner, E., *J. Plant Nutr. Soil Sci.*, **167**, 33 (2004).
86. Craig, P. J., Eng, G. and Jenkins, R. O., Occurrence and pathways of organometallic compounds in the environment – general considerations, in *Organometallic Compounds in the Environment*, 2nd ed., Craig, P. J. (Ed.), John Wiley & Sons, 2003, pp. 1–55.
87. Dubey, S. K. and Roy, U., *Appl. Organomet. Chem.*, **17**, 3 (2003).
88. Laughlin, R. B., Bioaccumulation of TBT by aquatic organisms, in *Organotin – Environmental Fate and Effects*, Champ, M. A. and Seligman, P. F. (Eds.), Chapman & Hall, London, 1996, pp. 331–357.
89. Belfroid, A. C., Purperhart, M. and Ariese, F., *Mar. Pollut. Bull.*, **40**, 226 (2000).
90. Iwata, H., Tanabe, S., Mizuno, T. and Tatsukawa, R., *Environ. Sci. Technol.*, **29**, 2959 (1995).
91. Kannan, K., Senthilkumar, K., Logannathan, B. G., Takahashi, S., Odell, D. K. and Tanabe, S., *Environ. Sci. Technol.*, **31**, 296 (1997).
92. Kannan, K., Senthilkumar, K., Elliot, J. E., Feyk, L. A. and Giesy, J. P., *Arch. Environ. Contam. Toxicol.*, **35**, 64 (1998).
93. Weidenhaupt, A., Arnold, C., Müller, S. R., Haderlein, S. B. and Schwarzenbach, R. P., *Environ. Sci. Technol.*, **31**, 2603 (1997).
94. Hermosin, M. C., Martin, P. and Cornejo, J., *Environ. Sci. Technol.*, **27**, 2606 (1993).
95. Randall, L. and Weber, J. H., *Environ. Sci. Technol.*, **57**, 191 (1986).
96. Berg, M., Arnold, C. G., Müller, S. R., Mühlemnann, J. and Schwarzenbach, R. P., *Environ. Sci. Technol.*, **35**, 3151 (2001).
97. Craig, P. J. and Rapsomanikis, S., *Inorg. Chim. Acta*, **107**, 39 (1985).
98. Ashby, J. and Craig, P. J., *Sci. Total Environ.*, **100**, 337 (1991).
99. Chau, Y. K., Wong, P. T. S., Kramar, O. and Bengert, C. A., Methylation of tin in the aquatic environment, in *Heavy Metals in the Environment*, Proceedings of the 3rd International Conference (Amsterdam), Ernst, W. H. O. (Ed.), CEP Consultants, Edinburgh, 1981, pp. 641–644.
100. Thayer, J. S., *Appl. Organomet. Chem.*, **16**, 677 (2002).
101. Vella, A. J. and Adam, J. P. T., *Appl. Organomet. Chem.*, **15**, 901 (2001).
102. Eggleton, J. and Thomas, K. V., *Environ. Intern.*, **30**, 973 (2004).
103. Michalke, K., Wickenheiser, E. B., Mehring, M., Hirner, A. V. and Hensel, R., *Appl. Environ. Microbiol.*, **66**, 2791 (2000).
104. Weidenhaupt, A., Arnold, C., Müller, S. R., Haderlein, S. B. and Schwarzenbach, R. P., *Environ. Sci. Technol.*, **31**, 2603 (1997).
105. Unger, M. A., MacIntyre, W. G. and Huggett, R. J., *Environ. Toxicol. Chem.*, **7**, 907 (1988).
106. Eggleton, J. and Thomas, K. V., *Environ. Intern.*, **30**, 973 (2004).
107. Donard, O. F. X., Lespes, G., Amouroux, D. and Morabito, R., Organotin compounds in the environment: still a critical issue, in *Trace Element Speciation for Environment, Food, Health*, Ebdon, L., Pitts, L., Cornelis, R., Crews, H., Donard, O. F. X. and Quevauviller, Ph. (Eds.), Royal Society of Chemistry, Cambridge, MA, 2001, pp. 142–175.
108. Fent, K. and Looser, P. W., *Water Res.*, **29**, 1631 (1995).
109. Fent, K. and Müller, M. D., *Environ. Sci. Technol.*, **25**, 489 (1991).
110. Kuballa, J., Jantzen, E. and Steffen, D., *Wasser Boden*, **50**, 30 (1998).
111. Chau, Y. K., Zhang, S. and Maguire, R. J., *Sci. Total Environ.*, **121**, 271 (1992).
112. Quevauviller, P., Donard, O. F. X. and Etcheber, H., *Environ. Pollut.*, **84**, 89 (1994).
113. Loch, J. P. G., Greve, P. A. and van den Berg, S., *Water, Air, Soil Pollut.*, **53**, 119 (1990).
114. Kortland, E. and Stronkhorst, J., *An Issue of Substance: TBT in Marine Antifouling Paints*, National Institute for Coastal and Marine Management/RIKZ, Amsterdam, NY, 1998.

115. Stronkhorst, J., TBT contamination and toxicity of sediments: a persistent problem, *The Present Status of TBT-Copolymer Antifouling Paints*, ORTEP, The Hague, Proceedings of the International Symposium on Antifouling Paints for Ocean-Going Vessels, February 21, 1996, pp. 47–59.
116. WHO, *Concise International Chemical Assessment Document*, IPCS-Report No. 14, Tributyltin oxide, World Health Organization, Geneva, 1999.
117. Belfroid, A. C., Purperhart, M. and Ariese, F., *Mar. Pollut. Bull.*, **40**, 226 (2000).
118. Kannan, K., Senthilkumar, K. and Giesy, J. P., *Environ. Sci. Technol.*, **33**, 1776 (1999).
119. Kannan, K. and Falandysz, J., *Mar. Pollut. Bull.*, **34**, 203 (1997).
120. Robinson, S., Volosin, J., Keithley, J. and Cardwell, R., *Mar. Pollut. Bull.*, **38**, 57 (1999).
121. Rüdel, H. and Steinhanses, J., *Organotin Compounds in Biota Samples From the Environmental Specimen Bank – Supplementary Measurements*, Report of Fraunhofer IME for the Umweltbundesamt Berlin (in German), 2001.
122. Lobinski, R. and Marczenko, Z., *Spectrochemical Trace Analysis for Metals and Metalloids*, Elsevier, Amsterdam, NY, 1996.
123. Camel, V., *Spectrochim. Acta, Part B*, **58**, 1177 (2003).
124. Krishan Puri, B., Muñoz-Olivas, R. and Cámara, C., *Spectrochim. Acta, Part B*, **59**, 209 (2004).
125. Lobinski, R., *Appl. Spectrosc.*, **51**, 260A (1997).
126. Bouyssiere, B., Szpunar, J., Poitin-Gautier, M. and Lobinski, R., Sample preparation techniques for elemental speciation studies, in *Handbook of Elemental Speciation, Techniques and Methodology*, Cornelis, R., Caruso, J., Crews, H. and Heumann, K. (Eds.), John Wiley & Sons, Chichester, 2003, pp. 95–118.
127. Garcia Alonso, J. I. and Ruiz Encinar, J., Gas chromatography and other gas based methods, in *Handbook of Elemental Speciation, Techniques and Methodology*, Cornelis, R., Caruso, J., Crews, H. and Heumann, K. (Eds.), John Wiley & Sons, Chichester, 2003, pp. 163–200.
128. Dirkx, W., Lobinski, R., Ceulemans, M. and Adams, F., *Sci. Total Environ.*, **136**, 279 (1993).
129. Lobinski, R., Dirkx, W. M. R., Ceulemans, M. and Adams, F. C., *Anal. Chem.*, **64**, 159 (1992).
130. Minganti, V., Capelli, R. and De Pellegrini, R., *Fresenius' J. Anal. Chem.*, **351**, 471 (1995).
131. Marcus, K., Glow discharge plasmas as tunable sources for elemental analysis, in *Handbook of Elemental Speciation, Techniques and Methodology*, Cornelis, R., Caruso, J., Crews, H. and Heumann, K. (Eds.), John Wiley & Sons, Chichester, 2003, pp. 334–355.
132. Carlier-Pinasseau, C., Lespes, G. and Astruc, M., *Talanta*, **44**, 1163 (1997).
133. Aguerre, S., Lespes, G., Desauziers, V. and Potin-Gautier, M., *J. Anal. At. Spectrom.*, **16**, 263 (2001).
134. De Smaele, T., Moens, L., Dams, R., Sandra, P., Van der Eycken, J. and Vandyck, J., *J. Chromatogr., A*, **793**, 99 (1998).
135. Centineo, G., Rodriguez-Gonzalez, P., Gonzalez, E. B., Garcia Alonso, J. I. and Sanz-Medel, A., *J. Mass Spectrom.*, **39**, 485 (2004).
136. Encinar, J. R., Rodriguez Gonzalez, P., Garcia Alonso, J. I. and Sanz-Medel, A., *Anal. Chem.*, **74**, 270 (2002).
137. Girousi, S., Rosenberg, E., Voulgaropoulos, A. and Grasserbauer, M., *Fresenius' J. Anal. Chem.*, **358**, 828 (1997).
138. Stäb, J. A., *Organotin Compounds in the Aquatic Environment*, Ph.D. thesis, Free University Amsterdam, The Netherlands, 1995.
139. Cai, Y., Rapsomanikis, S. and Andreae, M. O., *Anal. Chim. Acta*, **274**, 243 (1993).
140. Ritsema, R., Martin, F. M. and Quevauviller, P., in *Quality Assurance for Environmental Analysis*, Quevauviller, P., Maier, E. A. and Griepink, B. (Eds.), Elsevier, Amsterdam, NY, 1995, Chapter 19.
141. Tolosa, I., Bayona, J. M., Albaiges, J., Alencastro, L. F. and Tarradellas, J., *Fresenius' J. Anal. Chem.*, **339**, 646 (1991).
142. Schubert, P., Rosenberg, E. and Grasserbauer, M., *Fresenius' J. Anal. Chem.*, **366**, 356 (2000).
143. Harrington, C. F., Eigendorf, G. K. and Cullen, W. R., *Appl. Organomet. Chem.*, **10**, 339 (1996).
144. Ebdon, L., Hill, S. J. and Rivas, C., *Trends Anal. Chem.*, **17**, 277 (1998).
145. Rosenberg, E., Kmetov, V. and Grasserbauer, M., *Fresenius' J. Anal. Chem.*, **366**, 400 (2000).
146. Wu, J., Mester, Z. and Pawliszyn, J., *J. Anal. At. Spectrom.*, **16**, 159 (2001).
147. Wahlen, R. and Catterick, T., *J. Chromatogr., A*, **783**, 221 (2003).
148. White, S., Catterick, T., Fairman, B. and Webb, K., *J. Chromatogr., A*, **794**, 211 (1998).
149. Abalos, M., Bayona, J.-M., Compañó, R., Granados, M., Leal, C. and Prat, M.-D., *J. Chromatogr., A*, **788**, 1 (1997).
150. Leroy, M. J. F., Quevauviller, P., Donard, O. F. X. and Astruc, M., *Pure Appl. Chem.*, **70**, 2051 (1998).
151. Pellegrino, C., Massanisso, P. and Morabito, R., *Trends Anal. Chem.*, **19**, 97 (2000).
152. Morabito, R., Massanisso, P. and Quevauviller, P., *Trends Anal. Chem.*, **19**, 113 (2000).
153. Quevauviller, P., Astruc, M., Morabito, R., Ariese, F. and Ebdon, L., *Trends Anal. Chem.*, **19**, 180 (2000).
154. Quevauviller, P., Reference materials, in *Handbook of Elemental Speciation, Techniques and Methodology*, Cornelis, R., Caruso, J., Crews, H. and Heumann, K. (Eds.), John Wiley & Sons, Chichester, 2003, pp. 563–590.
155. Terlizzi, A., Fraschetti, S., Gianguzza, P., Faimali, M. and Boero, F., *Aquat. Conserv. Mar. Freshw. Ecosyst.*, **11**, 311 (2001).
156. Evans, S. M., *Mar. Pollut. Bull.*, **38**, 629 (1999).

157. European Chemical Industry Council (CEFIC), *TBT Copolymer Anti-Fouling Paints. The Facts*, 1992.
158. Champ, M. A., *Sci. Total Environ.*, **258**, 21 (2000).
159. Dowson, P. H., Bubb, J. M. and Lester, J. N., *Mar. Pollut. Bull.*, **26**, 487 (1993).
160. Santos, M. M., Ten Hallers-Tjabbes, C. C., Santos, A. M. and Vieira, N., *J. Sea Res.*, **48**, 217 (2002).
161. Barroso, C. M. and Moreira, M. H., *Mar. Pollut. Bull.*, **44**, 480 (2002).
162. Morcillo, Y. and Porte, C., *Trends Anal. Chem.*, **17**, 109 (1998).
163. Young, D. R., Alexander, G. V. and McDermott-Ehrlich, D., *Mar. Pollut. Bull.*, **10**, 50 (1979).
164. Claisse, D. and Alzieu, C., *Mar. Pollut. Bull.*, **26**, 395 (1993).
165. Dahl, B. and Blanck, H., *Mar. Pollut. Bull.*, **32**, 342 (1996).

2.21 Speciation of Vanadium

Koen De Cremer
Ghent University, Ghent, Belgium

1 INTRODUCTION

In contrast to other trace elements such as selenium, arsenic or chromium, vanadium is an element that is much less studied for speciation purposes. An indication for this is the few papers published on vanadium as compared to more common elements (Se, Zn, As, Fe, Cu). The data collected from the Web of Science database using 'speciation' and 'name of the element' as search words (1972–January 2002) are given in Figure 2.21.1. The interest for the element vanadium is, however, increasing considering the number of researchers (180) that participated at the Third International Symposium on Chemistry and Biological Chemistry of Vanadium, November 2001, Osaka, Japan. During the conference, it was obvious that much more speciation is needed in vanadium research and, more specifically, in the area of clinical (diabetes, cancer), environmental (ascidians, enzymes in seaweeds) and catalytic applications of vanadium.

Vanadium was first discovered in 1802 by Andres Manuel del Rio but his claim to the

Handbook of Elemental Speciation II: Species in the Environment, Food, Medicine & Occupational Health
Edited by R. Cornelis, H. Crews, J. Caruso and K. G. Heumann
 ISBN: 0-470-85598-3 (HB)

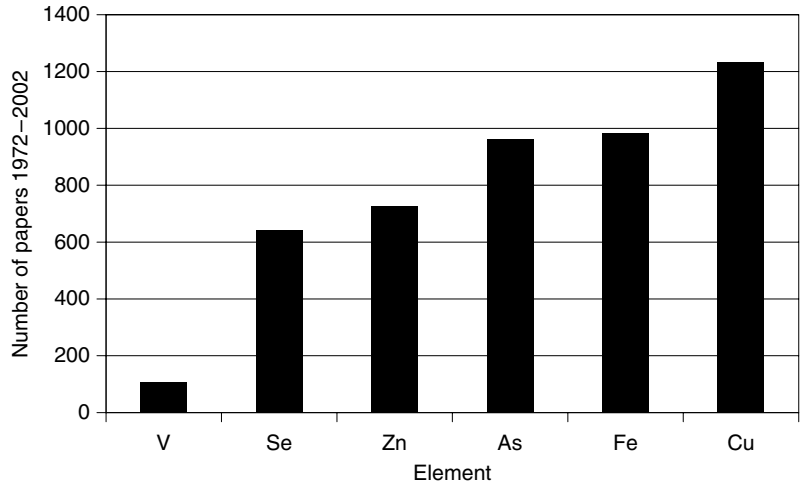

Figure 2.21.1. Number of papers relating to vanadium speciation in comparison to other elements as found on the Web of Science database using 'speciation' and 'name of the element' as search words (1972–January 2002).

discovery was lost in a shipwreck. In 1831, Nils Gabriel Sefstrom rediscovered the element in collaboration with Jons Jacob Berzelius. It was named 'vanadium' after the Norse goddess of beauty, Vanadis, because of the striking colors that vanadium derivatives and solutions possess [1].

Vanadium is widely distributed in soil and it is the 21st most abundant element in the earth's crust (100 $\mu g\, g^{-1}$). It is more abundant than, for example, iron, copper, zinc and molybdenum. However, there is yet no convincing evidence that it is an essential element for man. In chickens and rats, deficiency of vanadium led to retarded growth, impairment of reproduction, and disturbance of lipid metabolism and inhibition of Na^+/K^+-ATP-ase activity in kidney, brain and heart. All these symptoms indicate that vanadium is supposed to be essential for these animals, but this is still not proven for humans. In some other organisms (mushrooms, ascidians and fan worm), vanadium is being accumulated in specific cells [1]. Speciation of vanadium is needed because the two most occurring oxidation states of vanadium in biological systems, vanadyl(IV) and vanadate(V), have different nutritional and toxic properties, vanadate(V) being the most toxic form.

Vanadium is produced as a by-product in the extraction of other elements such as iron, phosphorus and uranium. Metallurgical applications account for about 85–95% of the worldwide vanadium consumption. Addition of small quantities (<0.2%) of vanadium to steel improves the shock and wear resistance. Because of its catalytic properties, vanadium is being widely used as a catalyst in the synthesis and production of organic compounds (e.g. production of sulfuric acid). Minor applications of vanadium include its use as a pigment and as a therapeutic agent (antiseptic) at the beginning of the twentieth century in France [1].

Interest in vanadium was stimulated by the discovery in 1977 of the ability of vanadium to inhibit the activity of ATP-ases [2]. Numerous studies on the inhibiting and stimulating effects of vanadium on phosphate enzymes were published. These studies also pointed to the similar behavior of the elements phosphate and vanadium in a biological environment. A next milestone was the discovery in 1980 of the insulin-mimetic properties of vanadium [3]. Interest of researchers from different fields was attracted and the hormonal effects of vanadium were investigated. This led in 1995 to the first clinical trials with a vanadium compound as a drug against diabetes instead of insulin [4–7]. A major obstacle hampering the breakthrough of vanadium compounds as an antidiabetic drug is the possible toxicity for the

patients arising from long-time, chronic vanadium administration [8]. The scientific debate about this continues [9, 10]. Nowadays, numerous organic vanadium compounds are tested to solve this problem [7, 11–14].

In the mid-eighties, the first vanadium-containing enzymes were discovered. In 1984, Vilter found a vanadium-bromoperoxidase in marine algae, and shortly thereafter, Robson discovered a vanadium-nitrogenase in a nitrogen-fixating bacteria [15, 16]. These new facts motivated the search to prove the essentiality of vanadium in humans.

Around the nineties, antitumor properties were suggested for vanadium [17, 18]. Similar to the well-known cisplatin compound, vanadium compounds were suggested to possess characteristics that prevent the formation of cancer. In contradiction, other reports were published in which carcinogenic effects were attributed to vanadium. Under the auspices of the IARC (International Agency for Research on Cancer, Lyon), an investigation on the carcinogenic effects of vanadium pentoxide after inhalation has been initiated. The results, however, are not yet published [19].

It should be clear from the previous paragraphs that a lot of work still needs to be done about the speciation of vanadium, for example, in the clinical field, where speciation can come in handy to help assess the toxicity of the different vanadium compounds that are tested as antidiabetic drugs.

2 SPECIFIC PROBLEMS RELATED TO VANADIUM SPECIATION

Before starting speciation studies on vanadium, one should be aware of some specific pitfalls encountered with vanadium. The most important are listed below.

2.1 Interconversion between different vanadium forms in solution

Vanadium can occur in different oxidation states starting from -2 to $+5$, although the forms naturally found in the environment are restricted to $+3$, $+4$ and $+5$ [20]. All the forms will air-oxidize to vanadium(V) although the rates vary with the initial oxidation state [21]. In humans and animals, only the oxidation states $+4$ and $+5$ are common. Biological studies are complicated by the complex aqueous chemistry of vanadyl(IV) and vanadate(V) [22, 23]. Vanadium(IV) is a cation (VO^{2+}) that will oligomerize or polymerize under physiological conditions at concentrations above 10^{-6} M and generate complexes in the presence of phosphates, sulfates, thiols and carboxylic acids. In addition, it oxidizes to vanadate(V) in the presence of oxygen at neutral or basic conditions. Also, vanadium(IV) complexed to a ligand can readily be oxidized. For example, the half-time for the oxidation of a vanadium(IV)-albumin or a vanadium(IV)-transferrin complex in solution is 6.5 ± 1.4 min and 8.1 ± 1.3 min, respectively [24]. For ideal results, research on vanadyl(IV) complexes should be carried out under nitrogen atmosphere. Vanadate(V), on the other hand, is more stable as free vanadate ($H_2VO_4^-$ or HVO_4^{2-}) in the presence of oxygen. In an acidic environment ($pH \leq 3$), vanadate(V) exists as a cation (VO^{2+}) and under strong basic conditions it prevails as an anion (VO_4^{3-}) [22, 23]. Vanadium(V) is readily reduced by various organic molecules (e.g. glutathione and NADH) and it oligomerizes at concentrations above 10^{-4} M [22, 23].

2.2 Interaction of vanadium(IV) and vanadium(V) with buffers and additives

Because most biological systems are sensitive to pH, researchers will control this pH during an experiment with the use of a buffer. However, vanadium shows a high affinity for elements such as oxygen, nitrogen, phosphorus and sulfur, which are present in most of the common buffers [1, 22, 25]. Previous experiments have clearly shown that vanadyl(IV) and vanadate(V) interact with many buffers and additives [22, 26, 27]. Ignoring these facts will lead to erroneous results or artifacts. Both vanadyl(IV) and vanadate(V) do not interact strongly with HEPES buffer ([4-(2-hydroxyethyl)-1-piperazineethanesulfonic acid]), and HEPES is

therefore the buffer of choice for biological and clinical speciation (except for studying redox behavior) [22, 26]. Tris buffer (tris(hydroxymethyl)aminomethane) slightly interacts with vanadate(V) but strongly with vanadyl(IV). In case HEPES buffer is not compatible with an investigated enzyme system for vanadate(V) interactions, Tris can be applied when used in moderate concentration (20 mM) [26]. Despite complex formation, imidazole is recommended as buffer in assays where the redox behavior of vanadium is studied and the reduction of vanadium must be kept to a minimum [26].

Other buffers that can be used for vanadate(V) include *N*-ethylmorpholine, Bis-Tris propane (1,3-bis[[tris(hydroxymethyl)methyl]amino]propane), EPPS (*N*-(2-hydroxyethyl)piperazine-*N*′-3-propanesulfonic acid), barbitol, TAPS (3-[[tris(hydroxymethyl)-methyl]amino]propanesulfonic acid), MES (2-[*N*-morpholino]ethanesulfonic acid), PIPES (piperazine-*N*,*N*′-bis[ethanesulfonic acid]) and acetate, even though some of these buffers form complexes with vanadate at high concentrations [22, 26]. Buffers that cannot be used for vanadate(V) include phosphate buffer, DIPSO (3-[*N*-[tris(hydroxymethyl)methyl]amino]-2-hydroxy-propanesulfonic acid), TAPSO (3-[*N*-tris(hydroxymethyl)methylamino]-2-hydroxy-propanesulfonic acid), triethanolamine, Bicine (*N*,*N*-bis[2-hydroxyethyl]glycine) and Tricine (*N*-[tris(hydroxymethyl)methyl]glycine) [22, 26]. Also for DTT (dithiothreitol), caution is needed [27]. Additives for vanadium(V) that should be avoided are citrate, glycine, glycylglycine and EDTA (ethylenediaminetetraacetic acid) [26].

In case of vanadyl(IV), some differences are seen. Barbitol and HEPES complex vanadyl(IV) the least, while Tris interacts fairly strongly. TAPS and Tricine also interact, whereas DIPSO (3-*N*-[tris(hydroxymethyl)methyl]amino-2-hydroxy-propanesulfonic acid) and glycineglycine interact most strongly [26]. In general, the vanadyl(IV) cation forms more stable complexes with buffers than vanadate(V). One of the exceptions is the vanadate(V)-Tricine complex that is eight times more stable than the vanadyl(IV)-Tricine complex [26].

In conclusion, when the use of a buffer or additive is needed, it is advised to test if complexes may be formed between vanadium and the chemicals. NMR (nuclear magnetic resonance) spectroscopy is a widely used tool for this purpose [28].

2.3 Interaction of vanadium with column stationary phases in chromatography

Another major problem with vanadium is encountered when using HPLC (high performance liquid chromatography) for vanadium speciation. Vanadium seems to be adsorbed by several different column stationary phases to a great extent [29]. This kind of problem was first recognized for biological studies by Sabbioni *et al*. [30] and Chasteen *et al*. [31]. They found a very low recovery for their vanadium compounds in serum after elution over a Sephadex G (Amersham Pharmacia Biotech, Sweden) gel filtration column. The more dialyzable the vanadium, the more vanadium was adsorbed to the column. They suggested that, because of this affinity of vanadium for the column matrix, several species originally present in the sample would remain undetected or would be destroyed. The behavior of vanadium on different column stationary phases was investigated using a [^{48}V] vanadate tracer. It was found that an agarose matrix or an acrylamide-bisacrylamide matrix showed the best characteristics for vanadium, while silica-based, dextran and polystyrene-divinylbenzene matrices adsorbed vanadium to a different extent [29]. It is therefore very important to be aware of the importance of choosing an adequate column stationary phase to avoid loss of vanadium complexes and subsequently valuable information.

2.4 Low stability of vanadium complexes

In comparison with other elements such as arsenic and selenium, which most of the time are covalently bound in their different species, vanadium can be hydrogen-bonded to a protein, as in, for example,

Table 2.21.1. Formation constants $K[M^{-1}]$ of selected vanadyl(IV) and vanadate(V) complexes (1 : 1) with biogenic or related ligands.

Vanadyl(IV) $[VO^{2+}]$		Vanadate(V) $[HVO_4^{2-}]$	
Ligand	K^a	Ligand	K^a
Phosphate	$10^{4.3}$	Oxalate	13
Triphosphate	$10^{9.87}$	Lactate	0.54
AMP	$10^{5.1}$	Salicylate	1.7
ATP	$10^{5.9}/10^{6.7}$	Glycol	0.34
Creatine phosphate	$10^{3.6}$	Mannose	24
Glutamic acid	$10^{3.4}$	Ribose	230
Serine	$10^{5.7}$	AMP	$5.4–19.6^b$
Alanine	$10^{6.9}$	Uridine	130
H-Gly-Gly-Gly-OH	$10^{4.6}$	Inosine	685
Ascorbic acid	$10^{3.3}$	Picolinate	200
Citric acid	$10^{4.0}$	H-Gly-His-OH	113
Glutathione	501	H-Gly-Asp-OH	49
Serum albumin	$10^{3.1}$	H-Gly-His-Lys-OH	11
Serum transferrin	$6.10^{3.1}$	Glutathione	$10^{4.2}$
		Glutathione disulfide	$10^{3.26}$
		H-Gly-Gly-Gly-OH	200
		Ribonuclease T_1	145
		Acid phosphatase	$10^{4.8}$
		Serum albumin	$600–10^{3.3}$
		Serum transferrin	$10^{6.5}$

[a] Data for 1 : 1 complexes. Complexes of a different composition are in many cases also observed.
[b] Dependent on pH (8.0–6.5).
Source: Reproduced from Reference [66] by permission of Wiley-VCH.

$H_2VO_4^-$/ribonuclease-T_1 or bound covalently to functional groups (O, N, and S functions) of amino acid side chains of the protein matrix [32]. Apart from these kinds of bindings, vanadium species may also be associated to a protein through salt bridges, including alkali metal (Na^+, K^+) contact ion-pair interaction, either exclusively or together with covalent linkages and/or hydrogen bonding [32]. Among the different biological vanadium complexes, the vanadium(V)-transferrin complex is one of the stronger ones (stability constant $K = 10^{6.5}\ M^{-1}$, Table 2.21.1). In comparison with other metal-transferrin complexes, however, the vanadium-transferrin binding is rather weak [Al^{3+}, Ga^{3+} and Fe^{3+} bind to transferrin with a stability constant of $10^{12.9}$, $10^{20.3}$ and $10^{22.7}\ M^{-1}$, respectively] [33–35]. Bearing these facts in mind, it is important to choose mild separation techniques in order to avoid artifacts in the resulting chromatograms. Therefore, the stability of the vanadium-transferrin complex was tested under different conditions that are commonly encountered during chromatographic runs [36]. The goal of these experiments was to outline the limits of the pH, salt molarity and acetonitrile concentration that could be used during chromatography without altering the vanadium-transferrin complex. During these experiments, several parameters were varied: (1) the pH ranging from 1 to 13; (2) NaCl concentration from 0 to 2 M; (3) the acetonitrile concentration from 0 to 25% and (4) the type of buffer salt (Na-acetate, NaBr, NaI, LiCl, $CaCl_2$ and NH_4Cl instead of NaCl). All these experiments were carried out by ultrafiltration. The resulting figures are depicted in Part I of this series (Chapter 3.2, sampling and storage of clinical samples). Out of these figures, it is clear that the vanadium-transferrin binding is only stable (1) over a limited pH-range (7–9); (2) below 0.5 M NaCl; (3) below 15% acetonitrile in the buffer and (4) that Na-acetate and LiCl have little effect on the binding, but that $CaCl_2$ and NH_4Cl disrupt the binding, even at low concentrations. These results indicate that care should be taken when using salt gradients (e.g. in anion-exchange chromatography or hydrophobic interaction chromatography) or

acetonitrile gradients (e.g. in reversed phase chromatography). Therefore, gel filtration chromatography is preferably used because of its mild character (low salt concentration, no organic additives). Unfortunately, this technique has also a limited resolution for protein peaks, so other (more aggressive) chromatographic techniques, like anion-exchange chromatography, are needed, but one should remember its limitations.

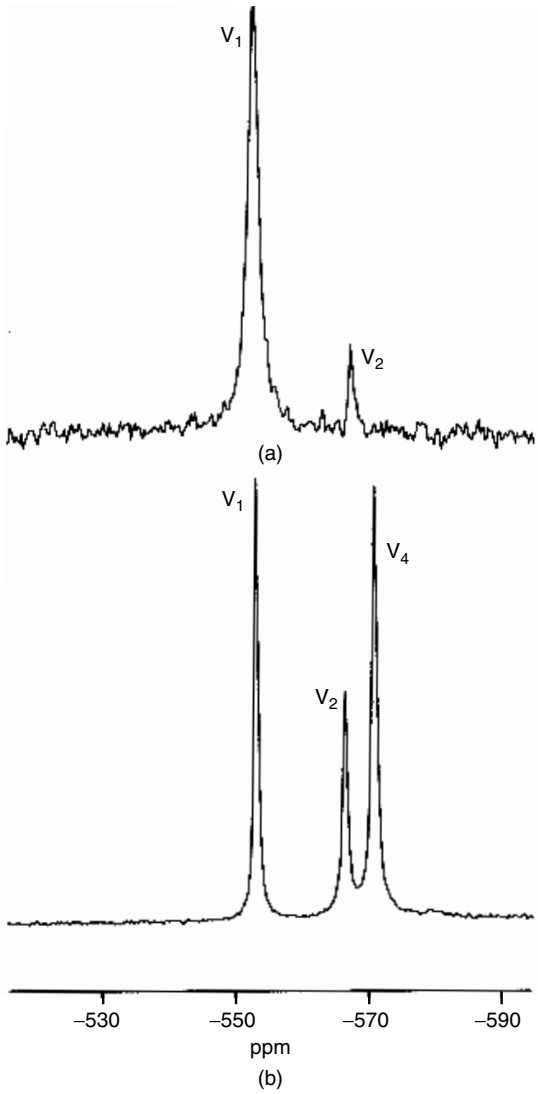

Figure 2.21.2. ^{51}V NMR spectra at 78.9 MHz of ammonium metavanadate. (a) 0.1 mM at pH 7; (b) 2.5 mM at pH 7. V_1: monomeric vanadate, V_2: dimeric vanadate, V_4: tetrameric vanadate. (Reproduced from Reference [20] by permission of John Wiley & Sons.)

2.5 Some remarks about stock solutions of vanadium

Regarding the oligomerization of vanadate at *high* concentrations and its interaction with some buffers, as previously described, it is tedious to prepare vanadium stock solutions [26]. A stock solution of 25 mM vanadate will contain a mixture of labile oxovanadates in a composition dependent on pH, temperature and ionic strength. It is recommended not to add buffer or other additives to a stock solution because these interactions can interfere (delay) with the formation of a new equilibrium. When adding an aliquot of the stock solution to an assay solution, a new equilibrium will be established within milliseconds (pH > 6.5). In case of adding acid to a concentrated stock solution to lower the pH, orange vanadate decamer will be formed at a pH < 6.5. Although this decamer is thermodynamically unstable at neutral or basic pH, the slow hydrolysis of this oligomer at pH > 7 allows it to persist for up to two days [20]. Therefore, it is better to remake the solution or to wait some days to reach equilibrium. Because of the rapid exchange rates between the vanadate anion and the vanadate esters, in the absence of the decamer, it is impossible to isolate each species for examination. As a consequence, a mixture of species will take part in the conducted experiments. A suitable technique to determine the population of the vanadium species involved in an assay is NMR (Figure 2.21.2) [26, 37].

3 DETECTION OF VANADIUM

Detection of vanadium can be accomplished by different techniques such as, for example, inductively coupled plasma mass spectrometry (ICP-MS), graphite furnace-atomic absorption spectrometry (GF-AAS), neutron activation analysis (NAA), NMR, electron paramagnetic resonance (EPR) or by using a radiotracer. The most commonly used techniques are described in Volume 1.

These paragraphs will give specific details concerning vanadium.

3.1 Use of a ^{48}V radiotracer

The ^{48}V-tracer decays ($t_{1/2}$: 15.97 d) by electron capture and β^+ while emitting main γ-energies of 511, 983 and 1312 keV [38]. Detection consists of a simple measurement of the radioactivity by means of a NaI(Tl) or Ge(Li) detector without requiring tedious sample preparation and calibration as is necessary in atomic absorption spectrometry (AAS), ICP-MS, and so on. [39]. Additionally, this procedure avoids the hazard of contamination of the trace element from other (nonradioactive) sources because only the radioactive tracer is measured. Radiotracers are most useful (1) during the exploratory phase of method development, especially for chromatographic and electrophoretic techniques (no sample preparation for the numerous collected fractions) and (2) for *in vivo* and *in vitro* studies about mobility, storage, retention, metabolism and toxicity of trace elements [40]. In the latter case, screening of the (very low) concentration in different tissues is fairly easy.

Disadvantages of this technique include the necessity of a nuclear facility (not all the tracers are commercially available), equipped laboratories licensed to work with radioactivity and the limited time frame (for short living tracers, <5 days) in which the tracer is sufficiently radioactive.

3.2 NAA, ICP-MS, AAS

In NAA, the stable ^{51}V isotope is irradiated with neutrons to produce the radioactive ^{52}V isotope ($t_{1/2}$: 3.74 m, E_γ: 1434 keV). Although the method of radiochemical NAA is very reliable, the use of this method is very limited because of the very short half-life of ^{52}V [41].

Another detection method is ICP-MS (inductively coupled plasma-mass spectrometry). In speciation research, this is one of the most common detection techniques because of its low detection limits, on-line coupling possibility and multielement capabilities. The sample is ionized in hot plasma (>6000 K) and the elements are detected in a mass spectrometer. The ^{51}V isotope is mainly interfered by the $^{35}Cl^{16}O^+$ and $^{37}Cl^{14}N^+$ adducts [42]. These interferences can be overcome by using a high resolution ICP-MS, cryogenic desolvation or a DRC-cell (dynamic reaction cell) [43].

In case of AAS, vanadium is atomized in a flame (flame atomic absorption spectrometry (FAAS)) or in a graphite furnace (GF-AAS) and its absorption is measured using a wavelength of 318.5 nm. FAAS is applicable only to samples that contain vanadium at least in the $\mu g\,mL^{-1}$ range [44]. Because vanadium forms refractory V_2O_5 the temperature of an air-acetylene flame is insufficient to dissociate V_2O_5 into atoms. A nitrous-acetylene mixture instead dissolves this problem. The addition of an ionization buffer to the sample and standards, for example, KCl, is recommended. GF-AAS also suffers from the formation of refractory vanadium carbides with the graphite tube as well with organic matrix residues. High ashing (1100–1800 °C) and atomization (2400–2900 °C) temperatures are needed and matrix effects are expected [45]. GF-AAS is more sensitive than FAAS by about 3 orders of magnitude (low $ng\,mL^{-1}$ range). The use of a Zeeman effect background correction is recommended. In spite of the high sensitivity of GF-AAS, the very low concentrations in serum and urine of the general population cannot be determined directly. A wet mineralization and a subsequent preconcentration of vanadium are needed [44]. On-line coupling using GF-AAS is not possible.

3.3 NMR spectroscopy

NMR spectroscopy gives, in contradiction to previous described methods, information about the nature of the immediate environment of the nuclei being studied [46]. The sample is placed in a magnetic field, and energy is applied through electromagnetic waves. Resonance occurs when the frequency of the incoming radiation matches the

frequency of the examined nucleus [46]. NMR has great utility because the different nuclei in a molecule have resonance at different frequencies (shift) depending on their direct environment. From these shifts (δ), various types of donor sets (ligands) for vanadium can be established [28]. As mentioned previously, NMR is used to study the complex mixtures of mono- and oligovanadates. Because each vanadate species gives resolved resonances in the ^{51}V NMR spectrum, the species distribution can be calculated from the integrated ^{51}V NMR signals [26, 28, 47]. Since the d^0 configuration of the vanadium(V) oxidation state, vanadate(V) is diamagnetic and therefore not suitable for techniques such as EPR.

3.4 EPR spectroscopy

EPR is, like NMR, able to give information about the direct environment of a nucleus. The main difference with NMR is that EPR, in vanadium research, is mainly used to probe the vanadyl(IV) form, which is paramagnetic (d^1) opposite to the diamagnetic vanadate(V) form [28, 47]. In EPR, transitions of unpaired electrons between the magnetic energy levels are examined, while in NMR the nucleus itself is probed. Different forms of EPR, such as ENDOR (electron nuclear double resonance) and ESEEM (electron spin echo envelope modulation), exist. Each of these techniques can provide additional information [47].

4 SPECIATION OF VANADIUM

4.1 Speciation in the environment

4.1.1 In soils and sediments

The average crustal abundance of vanadium is estimated to be 100 $\mu g\,g^{-1}$ [1]. About 80 different minerals containing vanadium have been found. Four major categories can be distinct: (1) sulfides; (2) sulfosalts of lead, copper, zinc and manganese; (3) silicates and (4) oxides. Elevated levels of vanadium have been reported in iron ores (600–4100 $\mu g\,g^{-1}$), rock phosphate (10–1000 $\mu g\,g^{-1}$) and superphosphate (50–2000 $\mu g\,g^{-1}$) [1]. Vanadium exists in oxidation states 3–5 in its main minerals. The higher the oxidation state, the more soluble they are. Vanadium(V) minerals are easily leached from soils into water [20]. Fossil fuels are also enriched in vanadium. Vanadium concentrations in crude oil range from 3 $\mu g\,g^{-1}$ (Qatar) to 257 $\mu g\,g^{-1}$ (Venezuela) [1]. The oxidation state is almost exclusively vanadyl(IV). The VO^{2+} ion exists in oil either as porphyrin (up to 50%) or non-porphyrin complexes [20]. Non-porphyrin complexes include all molecular mass ranges [48]. Recently, it has been shown that contamination of drinking water by vanadium released from crude oils is small and that the metal in the aqueous phase is primarily in a complexed form, which reduces concerns about its toxicity [49]. Both vanadyl(IV) and vanadate(V) have the potential to bind to humic acid. For vanadate(V), the binding constants with different humic acid models varied from 10^7 to 10^{13} M^{-1} for one ligand complexes (ML) and from 10^4 to 10^{10} M^{-1} for two-ligand complexes (ML_2) [50].

Operationally defined (according to the reagents or procedures used for their isolation) speciation for some sediments was done using the three-stage sequential extraction procedure proposed by the Commission of European Communities Bureau of Reference (BCR) [51, 52]. Vanadium was mainly (80%) found in the residual phase. Small amounts were present in the reducible and oxidizable phases. The latter may indicate an association with organic matter [51]. This partition can vary according to the sampling site [53]. Speciation in soil was done by the same procedure [54] or by a five-step procedure [55]. Generally, vanadium is depleted in streams draining 'average acid sulfate soil' but is substantially increased in severely acidic streams in basins with particularly acidic soil [56]. A review about vanadium accumulation in carbonaceous rocks is also published [57].

4.1.2 In the atmosphere

Combustion of fossil fuels and wastes represent the major sources of vanadium in the atmosphere.

Estimated worldwide emissions of vanadium from natural sources range from 1 to 54 tons per year, while the worldwide industrial emissions of vanadium amounted to 71.000 tons in 1995 [58]. Because vanadium is a nonvolatile metal, most of the airborne vanadium chemistry involves particulate forms of vanadium in the air [59]. Vanadium originating from the burning of fossil fuels is emitted as oxides with oxidation states ranging from 2 to 5 (VO, V_2O_3, VO_2 and V_2O_5) [20]. The mass median diameter of vanadium particles was approximately 1 μm, with a range of 0.4–5.0 μm [60, 61]. Because of more efficient control of the oil-fired power plants, these diameters decreased to 0.22–0.4 μm [62]. A preliminary investigation, using HPLC coupled to ICP-MS, showed that vanadium in coal fly ash existed both as vanadate(V) and vanadyl(IV) [63].

4.1.3 In water

In most natural environments, low vanadium concentrations are found, typically in the order of a few $\mu g\,L^{-1}$ [64]. Near Mount Fuji (Japan), rather high (24.5–81.5 $\mu g\,L^{-1}$) vanadium concentrations are present in spring water [65]. This water is commercially available in plastic bottles with a concentration of 59 $\mu g\,L^{-1}$ ('Vanadium water', Aqua International Inc). In the Pacific Ocean, the concentration is only 1.6 $\mu g\,L^{-1}$ [66]. In case higher than micromolar concentrations of vanadium are present in a sample, oligomeric species of vanadium come into play. As mentioned previously, vanadyl(IV) is only stable in acidic solution below pH 2 [20, 23, 67].

In order to clarify the species of vanadium in natural waters, an accurate and rapid fractional analytical method for determining vanadium species is needed. Many separation and preconcentration techniques have been proposed, including chelation and extraction, precipitation and the use of ion-exchange resins [64, 68]. Many of these methodologies are performed in batch, thus requiring large sample volumes in order to reach low detection limits. Consequently, contamination risks are higher, and their use in routine analysis is limited [64]. Some papers have studied HPLC of vanadium species using EDTA [69–71] or 4-(2-pyridylazo)resorcinol (PAR) [72]. The main weakness of this technique is the physical and chemical weakness of the HPLC columns [73]. Separation on chelating resins containing the iminodiacetate group (e.g. Chelex 100) consists of adsorbing both vanadyl(IV) and vanadate(V) at a pH of about 4.5, and stripping of vanadate(V) at basic condition (pH 10) and subsequently vanadyl(IV) at acidic condition (pH 0.8) [74]. A chelating silica gel with ethylenediamine or ethylenediaminetriacetate allows to elute both vanadyl(IV) and vanadate(V) at acidic conditions (6 M HCl) [75]. The disadvantage of this latter method is that this gel can only be used under acidic conditions [73]. In a recent report, a newly developed chelating resin (acetylacetone and 8-quinolinol immobilized on partially fluorinated silicon alkoxide glass columns) with catalytic detection for vanadium was used [73]. Two major advantages of this automated technique include (1) a low detection limit (21 pM) and (2) vanadyl(IV) and vanadate(V) can be measured at the same sensitivity. This resin can be used both under acidic and basic conditions. A technique more suited for routine analysis is flow-injection analysis (FIA). FIA approaches to measure vanadyl(IV) and vanadate(V) species simultaneously without separation and/or concentration have been reported [76, 77]. Recently, FIA with preconcentration and coupled to ICP-OES (inductively coupled plasma-optical emission spectrometry) has been proposed for the speciation of vanadyl(IV) and vanadate(V) in natural waters [64].

Vanadium can be found in different oxidation states and forms (soluble, insoluble and organic complex forms) in natural waters. In seawater, vanadium exists mainly in soluble forms, whereas in river water, some of the vanadium is present in insoluble or colloidal forms and is therefore filtered with the particulate matter [75]. In sufficiently aerated waters, the most commonly found oxidation states are vanadyl(IV) and vanadate(V) [64]. It has been predicted that the vanadate(V) state is thermodynamically predominant in an oxygen-rich environment [78, 79]. These oxidation states change in aqueous solution [80]. It appears that the redox equilibration between

vanadyl(IV) and vanadate(V) is not particularly stable in natural waters and is closely related to the presence of matrix elements such as iron(III) and organic substances [80]. As a consequence, several researchers found that both vanadyl(IV) and vanadate(V) were present in natural waters, although other workers tend to report only vanadate(V) [75]. For example, vanadyl(IV) and vanadate(V) were both found in rain water, but only vanadate(V) was measured in samples from seawater or lake water [73]. Redox experiments showed that added vanadyl(IV) is gently oxidized to vanadate(V) in lake and seawater with half-lives of respectively 15 and 7 min. These results indicate that vanadium could not exist as vanadyl(IV) in neutral and/or basic natural waters [73]. The same researchers state that natural water samples should be analyzed immediately after sampling without acidification, to determine vanadyl(IV) and vanadate(V) accurately. Therefore, *in situ* measurements are suggested to be indispensable for a precise determination of vanadyl(IV) and vanadate(V) species [73].

4.1.4 In ascidians

Ascidians, known as *tunicates* or *sea squirts*, are marine organisms and are an evolutionary link between Invertebrata and Vertebrata. They possess a notochord, a dorsal nerve cord, and pharyngeal gill slits. More than 2500 species are distributed from polar waters to the tropics [81]. In 1911, Martin Henze discovered high levels of vanadium in the blood cells of an ascidian [82]. The highest vanadium concentration (350 mM) was found in the blood cells of the *Ascidia gemmata*. This concentration corresponds to 10^7 times the vanadium concentration in seawater. The physiological role of vanadium in these organisms, however, remains to be elucidated [81, 83]. Tissues different from blood cells contained less vanadium. For many years, the morula blood cells were thought to be the vanadium-containing cells (vanadocytes), but at the beginning of the nineties it was confirmed that the signet ring blood cells were the true vanadocytes [84]. By using noninvasive physical methods such as NMR and electron spin resonance (ESR), it was shown that the vanadium ions in ascidian blood cells were predominantly in the vanadium(III) oxidation state, and a small amount in the vanadium(IV) oxidation state. The ratio of vanadium(III) to vanadium(IV) is 97.6 : 2.4 [85]. In association with vanadium, a considerable amount of sulfate has always been found in ascidian blood cells, suggesting that sulfate might be involved in the biological function and/or accumulation and reduction of vanadium. The content ratio of sulfate to vanadium is approximately 1.5, as would be predicted if sulfate ions were present as the counter ions of vanadium(III). Evidence of coordination of sulfate to vanadium(III) in *A. gemmata* was obtained by vanadium K-edge absorption spectroscopy, which proved that at least 90% of the vanadium(III) exists as a mixture of $[V(H_2O)_6]^{3+}$ and $[V(SO_4)(H_2O)_{4-5}]^{+}$ ions [86, 87]. The presence of 10% vanadium(III) chelated by organic substances can yet not be ruled out. Some controversy around the intracellular pH of the vanadocytes prevailed. Most reports indicate a very acidic pH (pH < 2), while others find a more neutral pH [81]. A reason for this disagreement may be that some measurements were made with entire populations of blood cells and not with the subpopulation of vanadocytes specifically [81]. It is now generally accepted that the pH inside vanadocytes of *A. gemmata* is acidic.

In the signet ring blood cells, a vanadium-associated protein was isolated, composed of 12.5 and 15 kDa peptides [88]. Three enzymes (β-phosphogluconate dehydrogenase, glucose-6-phosphate dehydrogenase and glycogen phosphorylase, all of which are involved in the pentose phosphate pathway) have been localized in the vanadocytes [89, 90]. It is suggested that the pentose phosphate pathway functions exclusively in vanadocytes and that this pathway may conjugate the reduction of vanadate(V) to vanadyl(IV) in the vanadocytes of ascidians.

Recently, three unprecedented chelated forms of vanadium(III) were observed in the blood cells of *Phallusia nigra* using K-edge X-ray absorption spectroscopy [83]. In the *P. nigra*, previous observations indicated that 75% of the

vanadium occurred as chelated vanadium(III) and 25% as vanadyl(IV), in contradiction to *A. gemmata*. A significant part of the V(III) fraction was most likely to be bound to molecules other than water or sulfate. The three unprecedented forms of vanadium(III) could be represented by the model ligand environments V(acetylacetonate), K_3V(catecholate) and the 7-coordinate N_2O_5 complex Na[V(edta)(H_2O)] [83]. The same author concludes that large differences in blood cell vanadium storage and allocation exist, calling for caution when generalizing results from one biological species to the other.

4.1.5 In Pseudopotamilla occelata

In 1993, it was discovered that the branchial crown of the fan worm *Pseudopotamilla occelata* possessed a very high level of vanadium (5.5 ± 1.8 mg g^{-1} dry weight) [91, 92]. Using K-edge spectra obtained by X-ray absorption near-edge structure analysis (XANES), it was shown that most vanadium exists as vanadium(III) [92]. However, the presence of vanadium as a vanadyl(IV) ion being a minor component of *P. occelata* could not be ruled out. Furthermore, it is suggested that vanadium in the *P. occelata* exists in a chemical form similar to that in ascidians, that is, as an aqua complex of vanadium(III) in sulfuric acid media [92]. The same antigens were found in the *P. occelata* as in ascidians, pointing to the same vanadium-associated proteins and to a possible similar mechanism for the accumulation of vanadium in both species [93]. During the last years, very few papers were published on this subject. As for the ascidians, no clear physiological role can yet be attributed to vanadium in the *P. occelata*.

4.1.6 In Amanita muscaria

The mushroom *Amanita muscaria* accumulates vanadium in high concentrations (36–250 mg kg^{-1} dry weight) [94, 95]. The stem and the root of the mushroom show a higher accumulation than the hat. Vanadium occurs in this mushroom as amavadin, a naturally occurring vanadium compound that is yet not found in other organisms. Amavadin was the first natural vanadium compound for which the structure has been completely elucidated. Its biological function is still unknown. Amavadin is a blue-colored complex with a molecular mass of 420 ± 20 Da. Vanadium occurs in this complex as vanadium(IV). Opposite to previous vanadium(IV) complexes, no double bonding with oxygen (as in VO^{2+}) is present, meaning that vanadium(IV) occurs here as a 'bare' metal ion [96].

4.2 In food

Vanadium is present in most food products, although most of the time in low concentrations (see Table 2.21.2) [97, 98]. Relatively high concentrations (>40 ng g^{-1}) are found in shellfish, mushrooms, parsley, dill seed, black pepper and some prepared foods. Cereals, liver and fish possess lower amounts (5–40 ng g^{-1}), whereas beverages, fats and oils, fresh fruit and fresh vegetables usually contain less than 5 ng g^{-1}, and often less than 1 ng g^{-1} [99]. Consequently, reported daily intakes of humans for vanadium are low, ranging from 5 to 30 μg/day. This corresponds to the estimated daily requirement of about 10 μg. Nutritional supplements, containing vanadyl sulfate, are believed to increase muscle mass and are commercially available. However, research has shown that vanadyl sulfate does not appear to be effective in increasing lean body mass [100].

Absorption of vanadium can occur via the respiratory, gastrointestinal or dermal routes. Vanadate(V) is absorbed three to five times more effectively than vanadyl(IV). In air, water and soil vanadium is mainly present as vanadate(V). In tissues, it may be stored, either totally or in part, as the vanadyl(IV) form. This reduced form would probably be oxidized to vanadate(V) once these tissues are ingested as food. Thus, it appears that vanadate(V) is the primary form of vanadium that is absorbed, regardless of the exposure route [101]. However, it is also suggested that most ingested vanadium is transformed in the acidic milieu of the stomach to vanadyl(IV) and remains in this form

Table 2.21.2. Vanadium concentration in food (ng g^{-1} wet weight).

Food	[V]	Food	[V]
Vegetables		***Fruits***	
Garlic	0.62	Apple	0.3
Onion	0.64	Pear	0.2
Brussel sprouts	0.5	Banana	<0.2
Cauliflower	0.85	Orange	0.95
Peas (frozen)	<0.4	Cherry	0.4
Leek	0.3 (heart); 3.0 (green leaf)	Apricot	0.2
Lettuce	1.0 (heart); 2.7 (green leaf)	Peach	0.15
Carrot	2.3, 2.4	Hazelnut	3.7
Cabbage	0.27		
Spinach	35		
	840, 533 freeze dried	***Beverages***	
Potato	1.2, 1.9	White wine	13 (Riesling)
Tomato	0.33	Red wine	3.5 (teran)
Radish	0.59		32 (merlot)
Mushrooms, wild	50–2000 dry weight	Beer	8.4
Parsley, ground	1800 dry weight	Coca Cola	1.5
		Tea, liquid	0.3
		Leaf, dry	150
Cereals		Cocoa powder	610
Oats	3		
Barley	1.6		
Maize	0.7	***Oils and fats***	
Rice Macedonia	30	Cooking oil, corn	<3
Italy	12	Pumpkin seed oil	<0.2
Flour	15, 40	Pork fat	<0.2
Bread	13, 10		

Source: Reprinted from *Sci. Total Environ.*, **10**, Byrne, A. R. and Kosta, L., 17–30, Copyright (1978), with permission from Elsevier Science.

as it passes into the duodenum [99]. Therefore, the effect of other dietary components on the form of vanadium in the stomach and the speed at which it is transformed into vanadyl(IV) probably affect the percentage of absorbed ingested vanadium. Most studies indicate that the absorption of ingested vanadium in higher animals is much lower than 10%, and probably is normally near 1–3% [99]. Inhalation through the lungs is reported to be more effective [102, 103]. Dermal absorption is to be considered of minor importance [102].

Although the total vanadium content was determined in different kinds of food and new detection methods are being developed [104, 105], speciation reports of vanadium in foods are scarce. Subcellular distribution and translocation of vanadium with growth was investigated in soybean and cucumber [106]. Approximately 10% of the vanadium was fixed in the mitochondrial fraction of the supernatant. The vanadium was predominantly accumulated in the root. The accumulation, distribution and form of vanadium in the tissues and organelles of mussels and goldfishes were also studied [107]. Vanadium was found in increased concentrations in all mussel tissues. The vanadium present in the cytosol of the gills was associated with low molecular mass components, whereas in the mantle and hepatopancreas also high molecular mass vanadium components were present. In the goldfish, the intestine showed the highest concentration (0.05% of the dose after 4 days exposure). In the cytosol of the fish intestine, vanadium was found associated with low molecular mass compounds. Accumulation, assimilation, tissue distribution and elimination of ^{48}V tracer were also investigated in benthic fish [108]. Tissue distribution indicated that vanadium accumulated from water penetrated little into internal tissues, muscle or liver, and is preferentially fixed in tissues in direct contact with the water. Vanadium accumulated directly from the water is rapidly lost (biological half-life 19 d). Therefore, assimilation

of vanadium through the food chain is low: only 2–3% of the ingested vanadium is retained in tissues of fish.

Regarding the few papers on food speciation, it should be clear that a lot of work still has to be done in this field.

4.3 Clinical speciation

4.3.1 Essentiality and toxicity

As mentioned earlier, vanadium is not yet unequivocally considered as an essential trace element for humans, although a lot of indications exist [20, 109–111]. Vanadium is defined as a nutritionally beneficial element. This means that too low an intake eventually has detrimental consequences, which implies that a certain intake is desirable [109]. If vanadium should be essential for humans, its requirement is most likely very small. Vanadium deficiency has not been identified in humans, although the normal diets only supply <30 μg vanadium daily. A daily dietary intake of 10 μg is therefore considered to meet any postulated requirement. Reports indicate that an intake of over 10 mg daily can result in toxicity [109]. Apparently, humans are more tolerant to high vanadium intakes than experimental animals such as rats. A safe daily intake for vanadium is suggested to be less than 1 mg/day and might be 100 μg or less/day [109].

The degree of toxicity depends on the route of administration, valence and chemical form and is also to some extent species dependent (Table 2.21.3) [112–114]. In general, the toxicity of vanadium is high by injection, low by the oral route and intermediate by the respiratory tract. Pentavalent vanadate(V) is considered to be more toxic than tetravalent vanadyl(IV) [115]. Toxic effects in humans and animals do not occur frequently under natural conditions. Toxicity usually occurs only as a result of industrial exposure to high amounts of airborne vanadium. This will be discussed in the next paragraph that deals with occupational health. In the future, however, toxicity by the oral route may increase because of recently marketed nutritional vanadium supplements or because of vanadium-based drugs. Biological detoxification mechanisms in the body for vanadium includes reduction of vanadate(V) to vanadyl(IV) by, for example, glutathione or ascorbic acid, accumulation in the bone, and incorporation into serum albumin, transferrin or ferritin. Chemical detoxification using chelating agents (EDTA, Tiron, Desferrioxamine B, ascorbic acid) has been shown to be very effective. Ascorbic acid appears to be the most convenient [115]. As it has been suggested that elevated tissue levels of vanadium might be of etiological importance in manic-depressive illness, clinical therapies using ascorbic acid and EDTA have been shown to be effective in treating both mania and depressives. However, the results did not support the suggestion that vanadium metabolism could be of etiological significance in mania [116–120].

In contradiction to food, a lot of reports are dealing with speciation of vanadium in the clinical field. The interaction with ATP-ases, the insulin-mimetic activity and the anticarcinogenic properties of vanadium attracted a lot of researchers from different disciplines such as chemistry, biology, biochemistry, medicine, and so on. Nevertheless, the exact mechanisms of the different biological actions of vanadium remain undisclosed. The inhibitory, stimulatory, regulatory, toxicological and pharmacological effects of vanadate are probably attributable to the similarity between vanadate and phosphate [66]. However, vanadate differs from phosphate in several ways; (1) monovanadate exists as a diprotonated molecule ($H_2VO_4^-$) at physiological pH while phosphate is monoprotonated (HPO_4^{2-}); (2) vanadate(V) is easily reduced

Table 2.21.3. Survey of LD_{50} doses of vanadium compounds and strychnine.

Compound	Animal	Intake route	LD_{50} (mmol kg^{-1})
$NaVO_3$	Mice	Intraperitoneal	0.29[a]
$NaVO_3$	Rats	Intraperitoneal	0.15[b]
$NaVO_3$	Rats	Oral	0.8[b]
$VOSO_4$	Rats	Intraperitoneal	0.3[b]
$VOSO_4$	Rats	Oral	1.8[b]
Strychnine	Rats	Oral	0.048[c]

[a] Ref. 112.
[b] Ref. 111.
[c] Ref. 113.

Table 2.21.4. Vanadium concentrations in human fluids and organs on fresh weight basis.

Fluid/organ	[V] (ng g^{-1} or mL^{-1})	Fluid/organ	[V] (ng g^{-1} or mL^{-1})
Amniotic fluid	12	Placenta (dry weight)	4.8–8.3
Bile	1.0	Red blood cells	0.026
Blood	0.058	Serum	0.031–0.071
Bone	3.5	Teeth	3.6
Brain	0.75	Thyroid	3.1
Bronchus	60	Trachea	38
Fat, subcutaneous	0.72	Urine	0.24
Fingernails	80–150	Muscle	0.54
Hair (scalp)	29–40	Lung	30
Heart	1.1	Kidney	3.0
Liver	7.0		

Source: Reprinted from Reference [99], pp. 543–574 by courtesy of Marcel Dekker Inc.

under physiological conditions with formation of vanadium(III) and vanadyl(IV) cationic species; (3) vanadate forms oligomers at concentrations above 0.1 mM; (4) vanadium, as a transition metal, shows a more flexible coordination sphere than phosphate because of the available *d*-orbitals. Therefore, vanadium can also have coordination numbers 5, 6, 7 and 8, while biological active phosphate only carries coordination numbers 4 or 5 [66, 121].

4.3.2 In blood

Many reports are dealing with the distribution and accumulation of vanadium in the body [122–126]. Very low concentrations of vanadium are found in blood and tissues (Table 2.21.4) [99]. Elevated concentrations were found in manic-depressive patients and in hemodialysis patients [116–120, 127–129]. In case of hemodialysis patients, this increase is not induced by the dialysis procedure [129]. In blood, >90% of the vanadium is present in serum and only 10% in blood cells [99]. In serum, both vanadyl(IV) and vanadate(V) are present as a result of the oxygen tension [99]. Ascorbate, catecholamines and cysteine reduce vanadate(V) to vanadyl(IV). Vanadyl(IV) is transported in serum by transferrin and albumin, whereas vanadate(V) is thought to be transported by transferrin only [24, 30, 99]. Low molecular mass species should account only for 3% of the vanadium present in plasma [24]. More recent calculations have shown that the distribution of vanadium over the possible ligands depends on the total vanadium concentration [130, 131]. With a concentration of 10 μM vanadium in serum, all the vanadyl(IV) is bound to transferrin, and the binding to low molecular mass components is negligible. At a concentration of 100 μM, ~70% of the vanadyl is bound to transferrin, while the rest is distributed among the low molecular complexes with citrate as primary binder. These calculations refer to the thermodynamic equilibrium state and do not take into account the kinetic aspects of biodistribution. Therefore, the authors state that it is very likely that the binding of vanadyl(IV) to the high molecular mass proteins is significantly slower than to the low molecular mass bioligands, which means a more mobile fraction of bound metal ions. The amount of vanadyl(IV) bound in this fraction is certainly high immediately after absorption. This agrees well with recent experimental results (Figure 2.21.3) [132]. Using chromatography, apart from binding to transferrin and albumin, no complexed low molecular mass species of vanadium were detected but a significant amount of readily exchangeable vanadium [132]. This 'dialyzable' form of vanadium, next to a low molecular mass complex, was also observed previously [30]. The amount of this readily exchangeable form depends on the time elapsed after intraperitoneal injection [30]. No binding to immunoglobulines (IgG) is observed in serum [7, 30, 132].

Vanadate(V) enters the erythrocytes via the same anion transport system used by phosphate [133]. Inside erythrocytes, vanadate(V) is

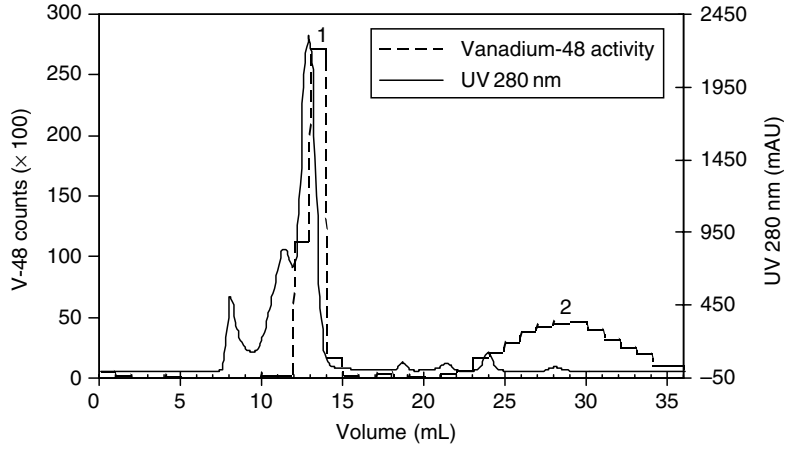

Figure 2.21.3. Elution of 1 : 1 diluted rat serum in 20 mM HEPES + 0.15 M NaCl, pH 7.5 on Superose 12 HR 10/30 column: (1) protein-bound vanadium, (2) readily exchangeable vanadium. (Reproduced from *J. Biol. Inorg. Chem.*, Fractionation of vanadium complexes in serum, packed cells and tissues of Wistar rats by means of gel filtration and anion-exchange chromatography, De Cremer, K., Van Hulle, M., Chéry, C. C., Cornelis, R., Strijckmans, K., Dams, R., Lameire, N. and Vanholder, R., **7**, 884, figure numbers (1, 3b, 4d), 2002, by permission of Springer Verlag GmbH & Co KG.)

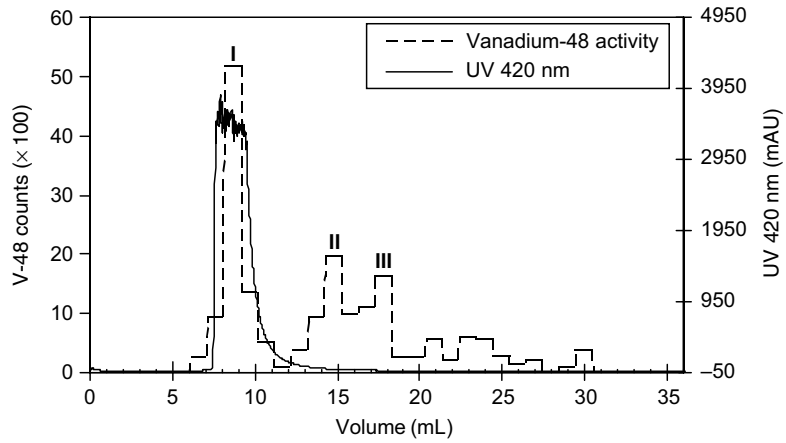

Figure 2.21.4. Elution of rat erythrocytes in 20 mM HEPES + 0.15 M NaCl, pH 7.5 on Superdex Peptide 10/30 column: (I) hemoglobin-bound vanadium, (II) vanadium complex (>2 kDa), (III) vanadium complex ~1 kDa. (Reproduced from *J. Biol. Inorg. Chem.*, Fractionation of vanadium complexes in serum, packed cells and tissues of Wistar rats by means of gel filtration and anion-exchange chromatography, De Cremer, K., Van Hulle, M., Chéry, C. C., Cornelis, R., Strijckmans, K., Dams, R., Lameire, N. and Vanholder, R., **7**, 884, figure numbers (1, 3b, 4d), 2002, by permission of Springer Verlag GmbH & Co KG.)

thought to be slowly converted to vanadyl(IV) by glutathione and to bind quantitatively to hemoglobin [99, 133, 134]. Recently, however, some doubts have been expressed about this mechanism [135]. In the homogenate of erythrocytes, three major vanadium peaks were found. One large peak coeluted with hemoglobin and two smaller peaks eluted in the low molecular mass range (Figure 2.21.4). No peak of readily exchangeable vanadium was detected (not shown) [132]. Speciation of vanadium in serum and erythrocytes is a very hot topic at the time of writing because of its potential use in the treatment of diabetes. No correlation, however, was found between the insulin-mimetic effects of vanadium and the *total* vanadium concentration in blood [7]. Therefore, it is

important to identify a vanadium pool in the body that correlates well with these effects. Speciation is an excellent tool for this purpose. Modeling of the different vanadium compartments in the body with their corresponding connections and half-times has previously been assayed [122, 125]. It was found that the residence time is low for blood (5–7 min) and high for bone (11–31 d). Other tissues show intermediate values. In blood, this residence time depends on the chemical form of the injected vanadium [11]. Using a new technique (BCM-ESR, blood circulation monitoring-electron spin resonance), it is possible to measure *in vivo* paramagnetic species [*in casu* vanadyl(IV)] [11, 12, 136]. From these results, it is clear that the vanadyl(IV) form is stable at physiological conditions and that the concentration of vanadyl(IV) in blood rapidly decreases after intake. This decrease, however, is due to transport and absorption of vanadyl(IV) to peripheral tissues and not to oxidation processes [12, 136].

4.3.3 In tissues

Through the blood circulation, vanadium is transported to the different tissues. Vanadium is supposed to enter the cells through anion-transporters as vanadate(V) (as phosphate analogue) and transferrin bound vanadium could be passed off to tissues via the transferrin receptor system [66, 101]. In adipocytes, vanadate(V) is incorporated after reduction by extra cellular reducing agents [137]. Vanadium can be reduced to vanadyl(IV) by glutathione, catechols, cysteine, NADH, NADPH and ascorbic acid once it is inside the cells [66, 101, 133]. However, the intracellular form of vanadate may depend on the ratio of the whole pool of reductants to the cell oxidants. In rats treated with $VOSO_4$, about 90% of the intracellular vanadium is present in the vanadyl(IV) form in nearly all organs [138]. Target tissues for vanadium in decreasing order include bone>kidney>liver>spleen>stomach>blood>lung>brain [12, 115, 123, 132]. Especially tissues rich in transferrin and ferritin are favored by vanadium, which points to a similar behavior as iron [31, 115, 133]. The high amounts in kidney and liver can be explained by their role in the excretion mechanism. Part of the retention of vanadium in bone is thought to occur because vanadate can substitute for phosphate in the hydroxyapatite crystal [115].

By oral or intratracheal intake, higher amounts are respectively found in the stomach and intestines and lungs [123, 124]. Further on, tissue distribution seems to be independent from the intake route or injected oxidation state [123, 133]. However, important differences were found in the metabolism of rats treated with vanadium as thiovanadate anionic species in comparison with other compounds [139]. The differences refer to the uptake of vanadium in the kidney, its intracellular distribution in the liver and the distribution between the molecular components in the kidney cytosol. This difference was ascribed to the nature of the ligand of the anionic VS_4^{3-} (V). Also in later reports, a different distribution due to different ligands is seen [12, 136]. As a consequence, a lot of energy is put in designing new ligands for vanadium as a way to enhance its insulin-mimetic actions and to lower its toxicity.

Inside tissues, vanadium is distributed over different cell organelles (nuclei, mitochondria, lysosomes, microsomes) and the remaining cytosol. The major amount (30–40%) is always present in the nuclei fraction, followed by mitochondria and cytosol [30, 123, 133]. Small amounts are found in microsomes and lysosomes. This distribution was shown to be variable with respect to time [30]. Experiments concerning the identification of vanadium components in the liver nuclei after administration of tetravanadate ions show that 70% of nuclear vanadium was associated with bulk chromatin components, while 30% was fixed by the nuclear membranes [139].

In tissue cytosol, vanadium can be further speciated by use of chromatographic techniques. It was suggested that over 90% of intracellular vanadium is complexed to phosphates, with lesser amounts bound to ferritin and, although rather weakly, to glutathione and ascorbate [140]. In *in vivo* experiments, however, vanadium was found to bind to high molecular mass proteins such as ferritin

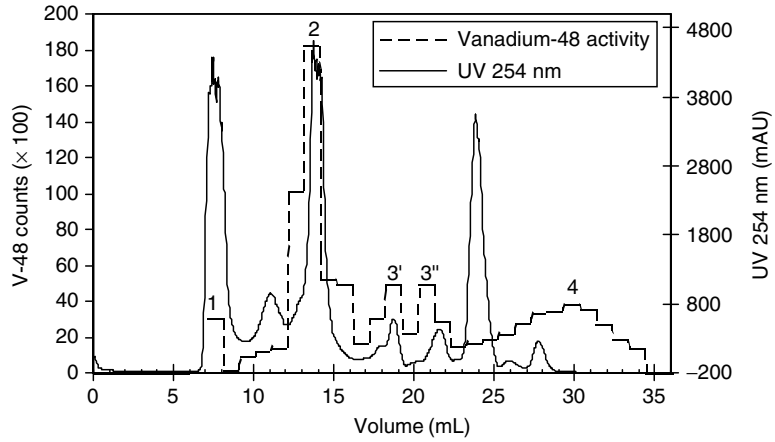

Figure 2.21.5. Elution of rat lung homogenate in 20 mM HEPES + 0.15 M NaCl, pH 7.5 on Superose 12 HR 10/30 column. (1) ferritin fraction (>300 kDa); (2) transferrin and hemoglobin fraction; (3′) and (3″) low molecular complexed vanadium; (4) readily exchangeable vanadium. (Reproduced from *J. Biol. Inorg. Chem.*, Fractionation of vanadium complexes in serum, packed cells and tissues of Wistar rats by means of gel filtration and anion-exchange chromatography, De Cremer, K., Van Hulle, M., Chéry, C. C., Cornelis, R., Strijckmans, K., Dams, R., Lameire, N. and Vanholder, R., **7**, 884, figure numbers (1, 3b, 4d), 2002, by permission of Springer Verlag GmbH & Co KG.)

and transferrin, and to nonidentified low molecular mass complexes (Figure 2.21.5) [30, 123, 132]. In most tissues, a readily exchangeable vanadium pool was also present [132]. As a function of time, the high molecular mass complexes become more important [123]. In lung, additional vanadium complexes are seen in the chromatogram, not present in any other tissue [132].

Future work will imply the identification of the different vanadium pools in the tissue homogenates, for example, by using ESI-MS-MS (electro spray ionization-mass spectrometry), especially in tissues related to diabetes and (subsequent) kidney insufficiency.

4.3.4 In urine

In the general population, mean concentrations in urine average about 0.1–0.2 μg V/L and possess usually <1 μg V/g creatinine [111]. The high vanadium levels in the kidney immediately after injection accounts for the diuretic and natriuretic effect of vanadate(V). The reversal of this effect with time can be due to the reduction to vanadyl(IV) and/or to the excretion of vanadium in urine [133]. The kidney reaches a maximum loading about at 2 h after injection. This time, however, depends on the structure of the compound [133, 136]. After 24 h, circa 30% of the injected dose (as $VOSO_4$) was found in urine [30, 136]. For organic complexes such as bis(picolinato)oxovanadium(IV) (VO-PA) or bis(6-methylpicolinato)oxovanadium(IV) (VO-MPA), the recovery respectively amounts to 53% and 61% [136]. The more effective excretion of VO-MPA in urine compared to VO-PA and $VOSO_4$ is in good agreement with its lower toxicity [136]. After oral intake, very low concentrations are found in urine and excretion mainly occurs through the feces [124].

Using gel filtration chromatography, vanadium is found to be excreted in urine (24 h) in four fractions of different molecular mass, one of which may be transferrin. The ratio between the peaks changed considerably with a strong decrease of the low molecular mass peaks at 24–48 h postinjection. At 72 h, the elution profiles showed that vanadium was mainly eluted as one peak in the high molecular mass region of the chromatogram [30]. Addition of a pH 7.0, 0.05 M vanadate(V) solution to urine immediately results in the appearance of low molecular mass vanadyl(IV) complexes. Reduction therefore seems to readily occur in this fluid. Thus, it is likely that

the vanadium excreted via the kidney is present as VO^{2+} [133]. This is supported by recent ESR measurements [136].

Recently, a low molecular vanadium complex, vanadium(IV)-diascorbate (MM: 403), was identified in human urine of salt-loaded (30 g NaCl/day) healthy subjects using gel filtration and reversed phase chromatography [141, 142].

In a study using gel filtration chromatography (Superose 12 and Superdex Peptide) to fractionate vanadium complexes in urine of rats as a function of time (1–96 h), maximal excretion (V/mL urine) of vanadium was found 3 h after intraperitoneal injection [143]. Vanadium in urine existed both as high (protein bound) and low molecular mass species and the partition about these forms depends on the time elapsed after injection (Figure 2.21.6(a–c)). The chromatograms of the Superose 12 and Superdex Peptide column of urine collected after 1 h showed respectively four (one high and three low molecular mass species) and five (one high and four low molecular mass) vanadium species. Three hours after injection, a different high molecular mass species showed up, while the first high and some low molecular mass species disappeared. After 8 h, vanadium occurred as one high (slightly different from the high molecular complex after 3 h) and one low molecular mass complex. However, after 48 h the pattern had changed again and urine was largely excreted as one low molecular mass species, presumably one of the species that also occurred 1 h after injection, but that was not present in the period 6–24 h. The identity of the different vanadium species is to be established in the future by means of ESI-MS-MS.

4.4 Occupational health

Occupational exposure mainly occurs through inhalation in metallurgical industries (discharges from furnaces roasting vanadium slag, vanadium pentoxide smelting furnaces, etc.) and more pronounced during boiler-cleaning operations (because of the high vanadium content of fuel-oil) [111]. Vanadium levels near metallurgical industries average about 1 $\mu g\,m^{-3}$. During boiler-cleaning operations, concentrations of 50–100 mg V/m^3 are frequent with concentrations ranging up to 500 mg V/m^3. Regulations and recommendations for exposure to vanadium have been outlined (Table 2.21.5) [111]. Several reports are dealing with this industrial exposure [144–151]. Acute adverse effects include irritative effects of the upper airways, nose and eyes, mucous membrane coughs, bronchial wheezing, nasal hemorrhage, conjunctivitis, rhinitis and green tongue that cleared within several days of cessation of exposure. Bronchitis and pneumonitis may occur after prolonged exposure, but chronic respiratory dysfunction has not been reported in clinical studies of workers exposed to vanadium compounds [111, 144, 149]. The FEV_1 (forced expiratory volume in 1 s) decreased in boilermakers after 4 weeks exposure to low levels of vanadium, however, no direct correlation between the vanadium concentration and the change in FEV_1 was seen [151]. No symptoms or signs of illness have been detected in the workers during or after exposure (levels $> 100 \times$ TLV), so that in this case occurrence of acute vanadium intoxication could be excluded [146].

The urinary elimination rate of vanadium has been found to be dependent on the amount absorbed. In all cases, however, after a rapid initial clearance of the vanadium, subsequent elimination was rather slow, with a half-life between 12 and 20 h [146, 148, 152]. On the basis of the elimination curves, a long-term vanadium accumulation into the organism seems also to be possible during continuous low-level exposure [145, 146].

Urinary vanadium excretion has proved to be a good indicator of vanadium absorption in exposed subjects, while the blood vanadium concentration does not seem to be as sensitive as urinary excretion [146]. S-O-S (start-of-shift) urine is preferred to the E-O-S (end-of-shift) urine for across shift biological monitoring of vanadium exposure [148]. It was proved that exposure to vanadium has no effect on cystine levels in fingernails or in hair [144, 152]. The determination in hair and fingernails yielded the highest sensitivity for detecting occupational exposure, because values up to 4 orders of magnitude higher were found in the exposed workers than in the controls [152]. However, because of possible external contamination, common to hair and fingernail samples, different values are found depending on

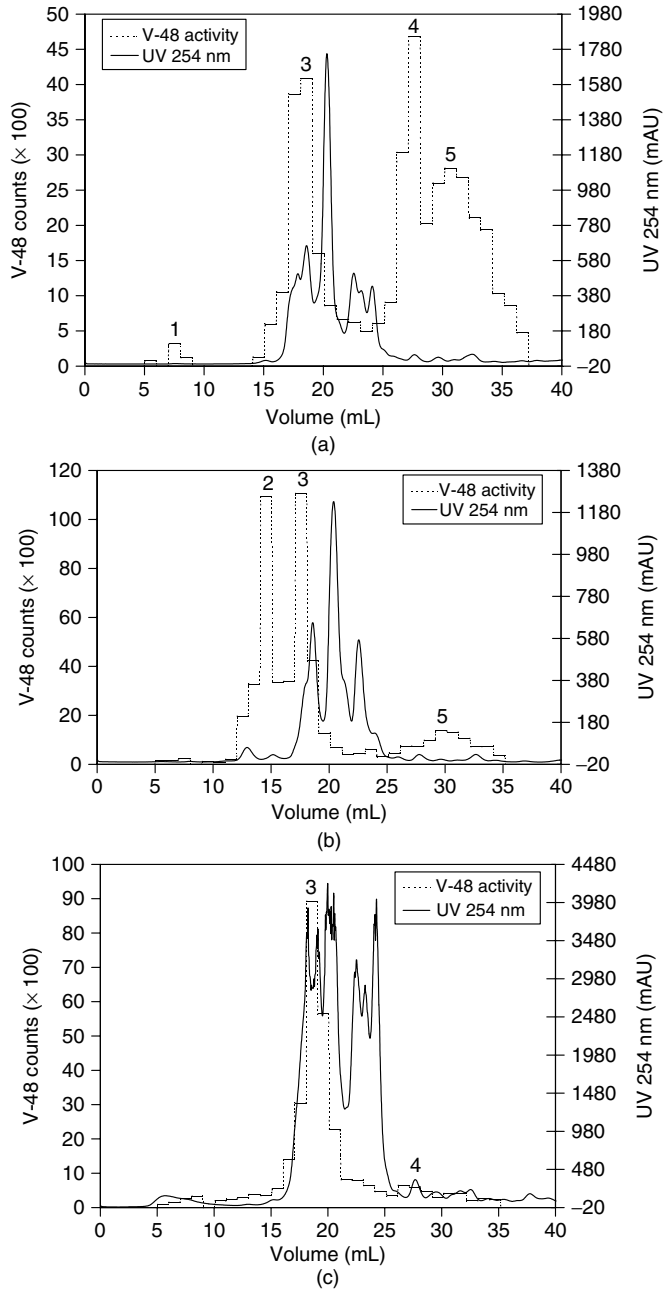

Figure 2.21.6. Elution of vanadium species in urine of Wistar rats on Superose 12 HR 10/30 column (20 mM HEPES buffer + 0.15 M NaCl, pH 7.5) (a) 1 h; (b) 8 h; and (c) 96 h after intraperitoneal injection with [^{48}V] vanadium tracer. (1): >300 kDa; (2): 7–80 kDa; (3) and (4): ~1 kDa; (5): readily exchangeable vanadium. (Reprinted from Fractionation of vanadium in urine of Wistar rats as a function of time after intraperitoneal injection, *J. Inorg. Biochem*, **90,** De Cremer, K., Cornelis, R., Strijckmans, K., Dams, R., Lameire, N. and Vanholder, R., 71, Copyright (2002), with permission from Elsevier.)

Table 2.21.5. Regulations and recommendations for exposure to vanadium.

Agency	Description	Value
OSHA	PEL-ceiling (transitional)	
	Vanadium pentoxide (respirable dust)	0.5 $mg\,m^{-3}$
	Vanadium pentoxide (fume)	0.1 $mg\,m^{-3}$
OSHA	PEL-TWA (8 h)	
	Vanadium pentoxide (respirable dust)	0.05 $mg\,m^{-3}$
	Vanadium pentoxide (fume)	0.05 $mg\,m^{-3}$
ACGIH	TLV-TWA	
	Ferrovanadium dust	1.0 $mg\,m^{-3}$
	BEI	
	50 $\mu g\,g^{-1}$ creatinine (end-of-shift at end of workweek urine sample)	
NIOSH	IDLH	
	Vanadium pentoxide (dust/fume)	70 $mg\,m^{-3}$
WHO	Air quality guideline as 24 hour TWA	1 $\mu g\,m^{-3}$
US EPA	Oral reference dose-vanadium pentoxide	9 $\mu g\,kg\,d^{-1}$

Note: OSHA = Occupational Safety and Health Administration.
ACGIH = American Conference of Governmental and Industrial Hygienists.
NIOSH = National Institute for Occupational Safety and Health.
WHO = World Health Organization.
EPA = Environmental Protection Agency.
PEL = Permissible exposure limit.
TWA = Time weighted average.
TLV = Threshold limit values.
BEI = Biological exposure index.
IDLH = Immediately dangerous to life or health concentrations.
Source: Reprinted from Reference [111], p. 265 by courtesy of Marcel Dekker Inc.

the cleaning method, which hampers the interpretation of these results. For these reasons, blood and urinary vanadium levels should be considered the most reliable indicators of occupational exposure. These tests exhibit up to 1 order of magnitude lower in sensitivity, but the interpretation of these tests appears to be straightforward. Both tests (blood and urine) should be considered as having a complementary role: urinary vanadium appears to be the best indicator of very recent exposure, and blood vanadium levels may be regarded as the most suitable indicator of long-term body burden [152]. The concentrations of vanadium in blood, serum and urine of occupationally exposed persons should then be compared with normal vanadium concentrations in blood and serum (0.02–0.08 $ng\,mL^{-1}$) and urine (0.2–0.4 $ng\,mL^{-1}$) [152].

5 CONCLUSION

Since the late seventies, interest in vanadium has been growing because of its significant occurrence in several organisms (e.g. ascidians) and to its biochemical actions, for example, in relation to diabetes and cancer. Research on vanadium, however, is hampered by its complex chemistry and instability of the vanadium complexes. Therefore, some precautions have to be taken, and interpretation of the results should be done carefully. Especially for vanadium, one must bear in mind that 'what you observe is what you isolate, which is not necessarily what was in the animal (or in the analyzed matrix)'. From previous paragraphs, it is clear that future speciation work on vanadium will comprise the identification of the different vanadium ligands and their respective oxidation state and, in addition, their possible useful role in treating, for example, diabetes.

6 REFERENCES

1. Nriagu, J. O., History, occurrence, and uses of vanadium, in *Vanadium in the Environment: Chemistry and Biochemistry, Part I*, Nriagu, J. O. (Ed.), John Wiley & Sons, New York, 1998, Chapter 1, pp. 1–24.

2. Cantley, L. C., Josephson, L., Warner, R., Yanagisawa, M., Lechene, C. and Guidotti, G., *J. Biol. Chem.*, **252**, 7421 (1977).
3. Shechter, Y. and Karlish, S. J. D., *Nature*, **286**, 556 (1980).
4. Cohen, N., Halberstam, M., Schlimovich, P., Chang, C. J., Shamoon, H. and Rossetti, L., *J Clin. Invest.*, **95**, 2501 (1995).
5. Goldfine, A. B., Simonson, D. C., Folli, F., Patti, M. E. and Kahn, C. R., *Mol. Cell. Biochem.*, **153**, 217 (1995).
6. Goldfine, A. B., Patti, M. E., Zuberi, L., Goldstein, B. J., Leblanc, R., Landaker, E. J., Jiang, Z. Y., Willsky, G. R. and Kahn, C. R., *Metabolism*, **49**, 400 (2000).
7. Willsky, G. R., Goldfine, A. B., Kostyniak, P. J., McNeill, J. H., Yang, L. Q., Khan, H. R. and Crans, D. C., *J. Inorg. Biochem.*, **85**, 33 (2001).
8. Srivastava, A. K., *Mol. Cell. Biochem.*, **206**, 177 (2000).
9. Domingo, J. L., *Mol. Cell. Biochem.*, **203**, 185 (2000).
10. McNeill, J. H., *Mol. Cell. Biochem.*, **208**, 167 (2000).
11. Sakurai, H., Sano, H., Takino, T. and Yasui, H., *J. Inorg. Biochem.*, **80**, 99 (2000).
12. Takino, T., Yasui, H., Yoshitake, A., Hamajima, Y., Matsushita, R., Takada, J. and Sakurai, H., *J. Biol. Inorg. Chem.*, **6**, 133 (2001).
13. Reul, B. A., Amin, S. S., Buchet, J. P., Ongemba, L. N., Crans, D. C. and Brichard, S. M., *Br. J. Pharmacol.*, **126**, 467 (1999).
14. Yao, J., Battell, M. L. and McNeill, J. H., *Can. J. Physiol. Pharmacol.*, **75**, 83 (1997).
15. Vilter, H., *Phytochemistry*, **23**, 1387 (1984).
16. Robson, R. L., Eady, R. R., Richardson, T. H., Miller, R. W., Hawkins, M. and Postgate, J. R., *Nature*, **322**, 388 (1986).
17. Köpf-Maier, P., *Naturwissenschaften*, **74**, 374 (1987).
18. Bishayee, A. and Chatterjee, M., *Br. J. Cancer*, **71**, 1214 (1997).
19. IARC, International Agency for Research on Cancer, 150 Cours Albert Thomas, F-69372 Lyon cedex 08, France, http://www.iarc.fr
20. Crans, D. C., Amin, S. S. and Keramidas, A. D., Chemistry of relevance to vanadium in the environment, in *Vanadium in the Environment: Chemistry and Biochemistry, Part I*, Nriagu, J. O. (Ed.), John Wiley & Sons, New York, 1998, Chapter 4, pp. 73–96.
21. Rubinson, K. A., *Proc. R. Soc. Lond.*, **B 212**, 65 (1981).
22. Crans, D. C., Bunch, R. L. and Theisen, L. A., *J. Am. Chem. Soc.*, **111**, 7597 (1989).
23. Willsky, G. R., Vanadium in the biosphere, in *Vanadium in Biological Systems, Physiology and Biochemistry*, Chasteen, N. D. (Ed.), Kluwer Academic Publishers, Dordrecht, Chapter 1, 1990, pp. 1–24.
24. Chasteen, N. D., Grady, J. K. and Holloway, C. E., *Inorg. Chem.*, **25**, 2754 (1986).
25. Chasteen, N. D., Vanadium-protein interactions, in *Metal Ions in Biological Systems, Vanadium and its Role in Life*, Vol. 31, Sigel, H. and Sigel, A. (Eds.), Marcel Dekker, New York, 1995, Chapter 7, pp. 231–248.
26. Crans, D. C., *Comments Inorg. Chem.*, **16**, 1 (1994).
27. Paul, P. C. and Tracey, A. S., *J. Biol. Inorg. Chem.*, **2**, 644 (1997).
28. Micera, G. and Sanna, D., Spectroscopic methods for the characterization of vanadium complexes, in *Vanadium in the Environment: Chemistry and Biochemistry, Part I*, Nriagu, J. O. (Ed.), John Wiley & Sons, New York, 1998, Chapter 7, pp. 131–166.
29. De Cremer, K., Cornelis, R., Strijckmans, K., Dams, R., Lameire, N. and Vanholder, R., *J. Chromatogr., B*, **757**, 21 (2001).
30. Sabbioni, E. and Marafante, E., *Bioinorg. Chem.*, **9**, 389 (1978).
31. Chasteen, N. D., Lord, E. M., Thompson, H. J. and Grady, J. K., *Biochim. Biophys. Acta*, **884**, 84 (1986).
32. Rehder, D. and Jantzen, S., Structure, function, and models of biogenic vanadium compounds, in *Vanadium in the Environment: Chemistry and Biochemistry, Part I*, Nriagu, J. O. (Ed.), John Wiley & Sons, New York, 1998, Chapter 11, pp. 251–284.
33. Martin, R. B., Savory, J., Brown, S., Bertholf, R. L. and Wills, M. R., *Clin. Chem.*, **33**, 405 (1987).
34. Harris, W. R. and Carrano, C. J., *J. Inorg. Biochem.*, **22**, 201 (1984).
35. Harris, W. R. and Pecoraro, V. L., *Biochemistry*, **22**, 292 (1983).
36. De Cremer, K., De Kimpe, J. and Cornelis, R., *Fresenius' J. Anal. Chem.*, **363**, 519 (1999).
37. Crans, D. C., Willging, E. M. and Butler, S. R., *J. Am. Chem. Soc.*, **112**, 427 (1990).
38. Gallorini, M., Biratarri, C., Bonardi, M., Magon, L. and Sabbioni, E., *J. Radioanal. Nucl. Chem.*, **160**, 549 (1992).
39. Cornelis, R., *Analyst*, **117**, 583 (1992).
40. Cornelis, R., *J. Radioanal. Nucl. Chem.*, **244**, 255 (2000).
41. Cornelis, R., Versieck, J., Mees, L., Hoste, J. and Barbier, F., *J. Radioanal. Nucl. Chem.*, **55**, 35 (1980).
42. Vanhoe, H., Goossens, J., Moens, L. and Dams, R., *J. Anal. At. Spectrom.*, **9**, 177 (1994).
43. Latino, J., Neubauer, K. and Wolf, R. E., *At. Spectrosc.*, **22**, 306 (2001).
44. Seiler, H. G., Analytical procedures for the determination of vanadium in biological materials, in *Metal Ions in Biological Systems, Vanadium and its Role in Life*, Vol. 31, Sigel, H. and Sigel, A. (Eds.), Marcel Dekker, New York, 1995, Chapter 20, pp. 671–688.
45. Tsalev, D., *Atomic Absorption Spectrometry in Occupational and Environmental Health Practice*, Vol. II, CRC Press, Boca Raton, 1984.
46. Pavia, D. L., Lampman, G. M. and Kriz, G. S., *Introduction to spectroscopy*, Saunders College Publishing, Fort Worth, 1996.
47. Garner, C. D., Collision, D. and Mabbs, F. M., Methods for the spectroscopic characterization of vanadium centers in biological and related chemical systems, in *Metal Ions in Biological Systems, Vanadium and its Role*

in Life, Vol. 31, Sigel, H. and Sigel, A. (Eds.), Marcel Dekker, New York, 1995, Chapter 19, pp. 618–670.
48. Fish, R. H. and Komlenic, J. J., *Anal. Chem.*, **56**, 510 (1984).
49. Cantu, R., Stencel, J. R., Czernuszewicz, R. S., Jaffe, P. R. and Lash, T. D., *Environ. Sci. Technol.*, **34**, 192 (2000).
50. Merce, A. L. R., Spir, I. H. Z., Salmon, M. J. O., Gianonni, R. A. and Mangrich, A. S., *J. Braz. Chem. Soc.*, **10**, 463 (1999).
51. Davidson, C. M., Thomas, R. P., McVey, S. E., Perala, R., Littlejohn, D. and Ure, A. M., *Anal. Chim. Acta*, **291**, 277 (1994).
52. Ure, A. M., Quevauviller, P., Muntau, H. and Griepink, B. EUR. Improvements in the determination of extractable contents of trace metals in soil and sediment prior to certification. EN. Report No. 14763, Commission of the European Communities, Brussels, 1993.
53. Belazi, A. U., Davidson, C. M., Keating, G. E., Littlejohn, D. and McCartney, M., *J. Anal. At. Spectrom.*, **10**, 233 (1995).
54. Davidson, C. M., Duncan, A. L., Littlejohn, D., Ure, A. M. and Garden, L. M., *Anal. Chim. Acta*, **363**, 45 (1998).
55. Ovari, M., Csukas, M. and Zaray, G., *Fresenius' J. Anal. Chem.*, **370**, 768 (2001).
56. Astrom, M., *J. Geochem. Explor.*, **73**, 181 (2001).
57. Breit, G. N. and Wanty, R. B., *Chem. Geol.*, **91**, 83 (1991).
58. Nriagu, J. O. and Pirrone, N., Emission of vanadium into the atmosphere, in *Vanadium in the Environment: Chemistry and Biochemistry, Part I*, Nriagu, J. O. (Ed.), John Wiley & Sons, New York, 1998, Chapter 2, pp. 25–36.
59. Keeler, G. J. and Pirrone, N., *Water Sci. Technol.*, **33**, 259 (1996).
60. Duce, R. A. and Hoffman, G. L., *Atmos. Environ.*, **10**, 986 (1976).
61. Mamane, Y. and Pirrone, N., Vanadium in the atmosphere, in *Vanadium in the Environment: Chemistry and Biochemistry, Part I*, Nriagu, J. O. (Ed.), John Wiley & Sons, New York, 1998, Chapter 3, pp. 37–72.
62. Divita, F., Ondov, J. M. and Suarez, A. E., *Aerosol Sci. Technol.*, **25**, 256 (1996).
63. Wang, J. S., Tomlinson, M. J. and Caruso, J. A., *J. Anal. At. Spectrom.*, **10**, 601 (1995).
64. Wuilloud, R. G., Wuilloud, J. C., Olsina, R. A. and Martinez, L. D., *Analyst*, **126**, 715 (2001).
65. Hamada, T., High vanadium content in Mt. Fuji groundwater and its relevance to the ancient biosphere, in *Vanadium in the Environment: Chemistry and Biochemistry, Part I*, Nriagu, J. O. (Ed.), John Wiley & Sons, New York, 1998, Chapter 5, pp. 97–124.
66. Rehder, D., *Angew. Chem., Int. Ed. Engl.*, **30**, 148 (1991).
67. Patel, B., Haswell, S. J. and Grzeskowiak, R., *J. Anal. At. Spectrom.*, **4**, 195 (1989).
68. Taylor, M. J. C. and van Staden, J. F., *Analyst*, **119**, 1263 (1994).
69. Komarova, T. V., Obrezkov, O. N. and Shpigun, O. A., *Anal. Chim. Acta*, **254**, 61 (1991).
70. Jen, J. F. and Yang, S. M., *Anal. Chim. Acta*, **289**, 97 (1994).
71. Jen, J. F., Wu, M. H. and Yang, T. C., *Anal. Chim. Acta*, **339**, 251 (1997).
72. Tsai, S. J. J. and Hsu, S. J., *Analyst*, **119**, 403 (1994).
73. Okamura, K., Sugiyama, M., Obata, H., Maruo, M., Nakayama, E. and Karatani, H., *Anal. Chim. Acta*, **443**, 143 (2001).
74. Soldi, T., Pesavento, M. and Alberti, G., *Anal. Chim. Acta*, **323**, 27 (1996).
75. Hirayama, K., Kageyama, S. and Unohara, N., *Analyst*, **117**, 13 (1992).
76. Teshima, N., Itabashi, H. and Kawashima, T., *Chem. Lett.*, **11**, 2227 (1992).
77. Taylor, M. J. C. and van Staden, J. F., *Anal. Chim. Acta*, **307**, 1 (1995).
78. Sadiq, M., *Mar. Chem.*, **23**, 87 (1988).
79. Wehrli, B. and Stumm, W., *Geochim. Cosmochim. Acta*, **53**, 69 (1989).
80. Cole, P. C., Eckert, J. M. and Williams, K. L., *Anal. Chim. Acta*, **153**, 61 (1983).
81. Michibata, H. and Kanamori, K., Selective accumulation of vanadium by ascidians from sea water, in *Vanadium in the Environment: Chemistry and Biochemistry, Part I*, Nriagu, J. O. (Ed.), John Wiley & Sons, New York, 1998, Chapter 10, pp. 217–250.
82. Henze, M., *Hoppe-Seyler's Z. Physiol. Chem.*, **72**, 494 (1911).
83. Frank, P., Robinson, W. E., Kustin, K. and Hodgson, K. O., *J. Inorg. Biochem.*, **86**, 635 (2001).
84. Michibata, H., Iwata, Y. and Hirata, J., *J. Exp. Zool.*, **257**, 306 (1991).
85. Hirata, J. and Michibata, H., *J. Exp. Zool.*, **257**, 160 (1991).
86. Tullius, T. D., Gillum, W. O., Carlson, R. M. K. and Hodgson, K. O., *J. Am. Chem. Soc.*, **102**, 5670 (1980).
87. Frank, P., Kustin, K., Robinson, W. E., Linebaugh, L. and Hodgson, K. O., *Inorg. Chem.*, **34**, 5942 (1995).
88. Kanda, T., Nose, Y., Wuchiyama, J., Uyama, T., Moriyama, Y. and Michibata, H., *Zool. Sci.*, **14**, 37 (1997).
89. Uyama, T., Kinoshita, T., Takahashi, H., Satoh, N., Kanamori, K. and Michibata, H., *J. Biochem.*, **124**, 377 (1998).
90. Ueki, T., Uyama, T., Yamamoto, K., Kanamori, K. and Michibata, H., *Biochim. Biophys. Acta Gene Struct. Expr.*, **1494**, 83 (2000).
91. Ishii, T., Nakai, I., Numako, C., Okoshi, K. and Otake, T., *Naturwissenschaften*, **80**, 268 (1993).
92. Ishii, T., Characterization of vanadium in the fan worm, *Pseudopotamilla occelata*, in *Vanadium in the Environment: Chemistry and Biochemistry, Part I*, Nriagu, J. O. (Ed.), John Wiley & Sons, New York, 1998, Chapter 9, pp. 199–216.

93. Uyama, T., Nose, Y., Wuchiyama, J., Moriyama, Y. and Michibata, H., *Zoolog. Sci.*, **14**, 43 (1997).
94. Bayer, E. and Kneifel, H., *Z. Naturforsch., B*, **27**, 207 (1972).
95. Garner, C. D., Armstrong, E. M., Berry, R. E., Beddoes, R. L., Collison, D., Cooney, J. J. A., Ertok, S. N. and Helliwell, M., *J. Inorg. Biochem.*, **80**, 17 (2000).
96. Bayer, E., Amavadin, the vanadium compound of Amanitae, in *Metal Ions in Biological Systems, Vanadium and its Role in Life*, Vol. 31, Sigel, H. and Sigel, A. (Eds.), Marcel Dekker, New York, 1995, Chapter 12, pp. 407–422.
97. Byrne, A. R. and Kosta, L., *Sci. Total Environ.*, **10**, 17 (1978).
98. Byrne, A. R. and Kosta, L., *Sci. Total Environ.*, **13**, 87 (1979).
99. Nielsen, F. H., Vanadium in mammalian physiology and nutrition, in *Metal Ions in Biological Systems, Vanadium and its Role in Life*, Vol. 31, Sigel, H. and Sigel, A. (Eds.), Marcel Dekker, New York, 1995, Chapter 16, pp. 543–574.
100. Clarkson, P. M. and Rawson, E. S., *Crit. Rev. Food Sci.*, **39**, 317 (1999).
101. Kustin, K. and Robinson, W. E., Vanadium transport in animal systems, in *Metal Ions in Biological Systems, Vanadium and its Role in Life*, Vol. 31, Sigel, H. and Sigel, A. (Eds.), Marcel Dekker, New York, 1995, Chapter 15, pp. 511–542.
102. Lagerkvist, B., Nordberg, G. F. and Vouk, V., Vanadium, in *Handbook on the Toxicology of Metals*, Friberg, L., Nordberg, G. F. and Vouk, V. (Eds.), Elsevier, Amsterdam, 1986, Chapter 27, pp. 638–664.
103. Rhoads, K. and Sanders, C. L., *Environ. Res.*, **36**, 359 (1985).
104. Paleologos, E. K., Koupparis, M. A., Karayannis, M. I. and Velsistas, P. G., *Anal. Chem.*, **73**, 4428 (2001).
105. Gao, J. Z., Zhang, X., Yang, W., Zhao, B. W., Hou, J. G. and Kang, J. W., *Talanta*, **51**, 447 (2000).
106. Gouthu, S., Weginwar, R., Arie, T., Ambe, S., Ozaki, T., Enomoto, S., Ambe, F. and Yamaguchi, I., *Environ. Toxicol. Chem.*, **18**, 2023 (1999).
107. Sabbioni, E. and Edel, E., *Sci. Total Environ.*, **133**, 139 (1993).
108. Miramand, P., Fowler, S. W. and Guary, J. C., *Mar. Biol.*, **114**, 349 (1992).
109. Nielsen, F. H., *J. Trace Elem. Exp. Med.*, **13**, 113 (2000).
110. Sakurai, H. and Tsuji, A., Antidiabetic action of vanadium complexes in animals: blood glucose normalizing effect, organ distribution of vanadium, and mechanism for insulin-mimetic action, in *Vanadium in the Environment: Health Effects, Part II*, Nriagu, J. O. (Ed.), John Wiley & Sons, New York, 1998, Chapter 15, pp. 297–316.
111. Barceloux, D. G., *Clin. Toxicol.*, **37**, 265 (1999).
112. Thompson, K. H., Battell, M. and McNeill, J. H., Toxicology of vanadium in mammals, in *Vanadium in the Environment: Health Effects, Part II*, Nriagu, J. O. (Ed.), John Wiley & Sons, New York, 1998, Chapter 2, pp. 21–38.
113. Corbella, J. and Domingo, J. L., Developmental and reproductive effects of aluminum, manganese, uranium and vanadium, in *Toxicology of Metals*, Chang, L. W., Magos, L. and Suzuki, T. (Eds.), CRC Press, New York, 1996, Chapter 67, pp. 1083–1096.
114. De Kimpe, J. *Chemical Speciation for the Study of Arsenate Metabolism*, Unpublished Ph.D. Dissertation, Ghent University, Ghent, Belgium, 1996.
115. Baran, E. J., Vanadium detoxification, in *Vanadium in the Environment: Health Effects, Part II*, Nriagu, J. O. (Ed.), John Wiley & Sons, New York, 1998, Chapter 16, pp. 317–346.
116. Naylor, G. J., Smith, A. H. W., Bryce-Smith, D. and Ward, N. I., *Biol. Psychiat.*, **19**, 759 (1984).
117. Naylor, G. J. and Smith, A. H. W., *Psychol. Med.*, **11**, 249 (1981).
118. Naylor, G. J., Corrigan, F. M., Smith, A. H. W., Conelly, P. and Ward, N. I., *Br. J. Psychiat.*, **150**, 656 (1987).
119. Sanchez, D. J., Colomina, M. T., Domingo, J. L. and Corbella, J., *Biol. Trace Elem. Res.*, **69**, 249 (1999).
120. Kay, D. S. G., Naylor, G. J., Smith, A. H. W. and Greenwood, C., *Psychol. Med.*, **14**, 533 (1984).
121. Etcheverry, S. B. and Cortizo, A. M., Bioactivity of vanadium compounds on cells in culture, in *Vanadium in the Environment: Chemistry and Biochemistry, Part I*, Nriagu, J. O. (Ed.), John Wiley & Sons, New York, 1998, Chapter 15, pp. 359–394.
122. Patterson, B. W., Hansard, S. L., Ammerman, C. B., Henry, P. R., Zech, L. A. and Fisher, W. R., II *Am. J. Physiol.*, **251**, R325 (1986).
123. Edel, J. and Sabbioni, E., *J. Trace Elem. Electrolytes Health Dis.*, **2**, 23 (1988).
124. Al-Bayati, M. A., Raabe, O. G., Giri, S. N. and Knaak, J. B., *J. Am. Coll. Toxicol.*, **10**, 233 (1991).
125. Setyawati, I. A., Thompson, K. H., Yuen, V. G., Sun, Y., Battell, M., Lyster, D. M., Vo, C., Ruth, T. J., Zeisler, S., McNeill, J. H. and Orvig, C., *J. Appl. Physiol.*, **84**, 569 (1998).
126. Adachi, A., Ogawa, K., Tsushi, Y., Nagao, N. and Okano, T., *J Health Sci.*, **46**, 59 (2000).
127. Tsukamoto, Y., Saka, S., Kumano, K., Iwanami, S., Ishida, O. and Marumo, F., *Nephron*, **56**, 368 (1990).
128. Hosokawa, S. and Yoshida, O., *Nephron*, **64**, 388 (1993).
129. Gallieni, M., Brancaccio, D., Cozzolino, M. and Sabbioni, E., *Nephrol. Dial. Transplant.*, **11**, 1232 (1996).
130. Kiss, T., Kiss, E., Garribba, E. and Sakurai, H., *J. Inorg. Biochem.*, **80**, 65 (2000).
131. Kiss, T., Jakusch, T., Kilyen, M., Kiss, E. and Lakatos, A., *Polyhedron*, **19**, 2389 (2000).
132. De Cremer, K., Van Hulle, M., Chéry, C. C., Cornelis, R., Strijckmans, K., Dams, R., Lameire, N. and Vanholder, R., *J. Biol. Inorg. Chem.*, **7**, 884 (2002).
133. Chasteen, N. D., *Struct. Bonding*, **53**, 105 (1983).

134. Macara, I. G., Kustin, K. and Cantley, L. C., *Biochem. Biophys. Acta*, **629**, 95 (1980).
135. Elberg, G., Li, J. and Shechter, Y., Mechanisms of actions of vanadium in mediating the biological effects of insulin, in *Vanadium in the Environment: Health Effects, Part II*, Nriagu, J. O. (Ed.), John Wiley & Sons, New York, 1998, Chapter 14, pp. 277–296.
136. Yasui, H., Takechi, K. and Sakurai, H., *J. Inorg. Biochem.*, **78**, 185 (2000).
137. Nakai, M., Watanabe, H., Fujiwara, C., Kakegawa, H., Satoh, T., Takada, J., Matsushita, R. and Sakurai, H., *Biol. Pharm. Bull.*, **18**, 719 (1995).
138. Sakurai, H., Tsuchiya, K., Nukatsuka, M., Sofue, M. and Kawada, J., *J. Endocinol.*, **126**, 451 (1990).
139. Sabbioni, E., Marafante, E., Amantini, L. and Ubertalli, L., *Bioinorg. Chem.*, **8**, 503 (1978).
140. Nechay, B. R., Nanninga, L. B., Nechay, P. S. E., Post, R. L., Grantham, J. J., Macara, I. G., Kubena, L. F., Philips, T. D. and Nielsen, F. H., *Fed. Proc.*, **45**, 123 (1986).
141. Kramer, H. J., Backer, A. and Meyer-Lehnert, H., *Am. J. Hypertens.*, **11**, 1208 (1998).
142. Kramer, H. J., Krampitz, G., Backer, A. and Meyer-Lehnert, H., *Clin. Exp. Hypertens.*, **20**, 557 (1998).
143. De Cremer, K., Cornelis, R., Strijckmans, K., Dams, R., Lameire, N. and Vanholder, R., *J. Inorg. Biochem.*, **90**, 71 (2002).
144. Kiviluoto, M., *Br. J. Ind. Med.*, **37**, 363 (1980).
145. Kiviluoto, M., Pyy, L. and Pakarinen, A., *Int. Arch. Occup. Environ. Health*, **48**, 251 (1981).
146. Sabbioni, E. and Maroni, M. *A study on Vanadium in Workers from Oil Fired Power Plants*, EUR 9005, Commission of the European Communities, Brussels, 1983.
147. Ide, C. W., *Int. J. Environ. Health Res.*, **5**, 269 (1995).
148. Hauser, R., Elreedy, S., Ryan, P. B. and Christiani, D. C., *Am. J. Ind. Med.*, **33**, 55 (1998).
149. Woodin, M. A., Liu, Y. C., Hauser, R., Smith, T. J. and Christiani, D. C., *J. Occup. Environ. Med.*, **41**, 973 (1999).
150. Woodin, M. A., Liu, Y. C., Neuberg, D., Hauser, R., Smith, T. J. and Christiani, D. C., *Am. J. Ind. Med.*, **37**, 353 (2000).
151. Hauser, R., Elreedy, S., Hoppin, J. A. and Christiani, D. C., *Am. J. Respir. Crit. Care*, **152**, 1478 (1995).
152. Kucera, J., Lener, J., Mnukova, J. and Bayerova, E., Vanadium exposure tests in humans: hair, nails, blood, and urine, in *Vanadium in the Environment: Health Effects, Part II*, Nriagu, J. O. (Ed.), John Wiley & Sons, New York, 1998, Chapter 4, pp. 55–73.

7 FURTHER READING

Chasteen, N. D. (Ed.), *Vanadium in Biological Systems, Physiology and Biochemistry*, Kluwer Academic Publishers, Dordrecht, The Netherlands, 1990.

Sigel, H. and Sigel, A. (Eds.), *Metal Ions in Biological Systems, Vanadium and its Role in Life*, Marcel Dekker, New York, United States, 1995.

Nriagu, J. O. (Ed.), *Vanadium in the Environment, Part I, Chemistry and Biochemistry*, John Wiley and Sons, New York, United States, 1998.

Nriagu, J. O. (Ed.), *Vanadium in the Environment, Part II, Health Effects*, John Wiley and Sons, New York, United States, 1998.

2.22 Speciation of Zinc

Klaus Günther and Bernd Kastenholz

Institute for Chemistry and Dynamics of the Geosphere, Institute III: Phytosphere, Research Center Juelich, Germany

1 ENVIRONMENT

1.1 Aquatic environment

Zinc species are predominantly determined in the aquatic environment and in soils and sediments. Speciation measurements in waters are necessary for an estimation of the toxicity, bioavailability and bioaccumulation of a particular element with respect to aquatic organisms and for an understanding of the trace-metal transport in rivers and estuaries [1]. Methods applied to differentiate between the various chemical forms of a metal in a natural water are discussed with special reference to zinc, cadmium, copper, and lead [2].

More recently, the speciation of zinc has been applied mainly to the different aqueous matrices such as sea [3, 4], estuarine [5, 6], lake [7–10], waste [11, 12], runoff [13], and river waters [14–18].

Two electrochemical methods, differential pulse cathodic stripping voltammetry (DPCSV) and differential pulse anodic stripping voltammetry (DPASV), were used to determine the zinc species in Northeast Pacific Ocean waters. By these procedures, it was found out that more than 95% of the dissolved zinc is organically complexed at two depths (60 and 150 m) at an open-ocean station. The results reported show that strong zinc complexes, formed with an organic ligand class existing at nanomolar concentrations, dominate zinc speciation in the North Pacific [3]. In the Northeastern Atlantic Ocean waters, zinc was complexed by a natural organic ligand that was found to be uniformly distributed throughout the water column even though zinc concentrations increased with depth. Organic ligand concentrations were similar to those published for the North Pacific. Free zinc ion concentrations were in the low picomolar range

Handbook of Elemental Speciation II: Species in the Environment, Food, Medicine & Occupational Health
Edited by R. Cornelis, H. Crews, J. Caruso and K. G. Heumann
 ISBN: 0-470-85598-3 (HB)

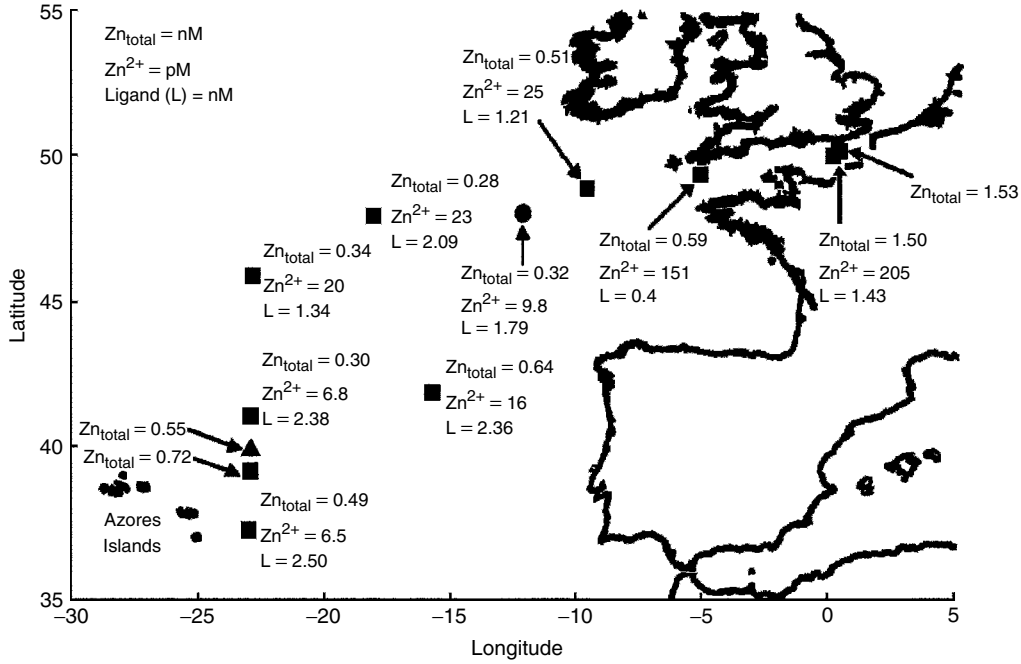

Figure 2.22.1. Surface concentrations of total zinc, zinc-complexing ligand and free Zn^{2+} for each sampling site in the Northeastern Atlantic Ocean. Zinc concentrations for the surface transect samples were low in open-ocean waters with a concentration of about 0.3 nM. Zinc levels increased landward to reach a value of 1.53 nM in the Channel. (Reprinted from *Mar. Chem.*, **68**, Ellwood, M. J. and Van den Berg, C. M. G., Organic complexation of zinc in the north eastern Atlantic, 295 (2000) with permission of Elsevier.)

in open-ocean waters but were not low enough to limit growth of a typical oceanic species of phytoplankton. The map including the sampling sites of the analyzed surface water samples in the Atlantic Ocean and the respective results of the concentrations of free zinc ions, total zinc and zinc ligands is represented in Figure 2.22.1 [4].

In estuarine water samples from a major United Kingdom estuary, dissolved zinc in the two major river inputs and low salinity zones appeared to be exclusively associated with naturally occurring organic complexing material. The results were obtained by a combination of complexation titration and DPCSV [5]. DPASV was used for the chemical speciation of dissolved zinc and other metals in the high-salinity region of the Narrangsett Bay estuary, Rhode Island. Speciation results show that organic chelates of the trace metals (Cu, Zn, Cd, Pb) examined were the dominant forms in conventionally filtered samples with ranges from 51 to 97% for zinc in these estuarine waters [6].

Ethylenediaminetetraacetic acid (EDTA) was used for the determination of zinc species and free zinc ion concentration in eutrophic lake water by DPASV. Thereby, a pretreatment or chromatographic separation of the samples was not necessary. The average fractions of dissolved zinc species in these lake water samples were 7.8% free zinc ions, 33.5% weak organic complexes, and 50.5% strong organic complexes [7]. Zinc speciation in the Lakes Manapouri and Hayes, New Zealand, revealed that zinc was mainly complexed by natural organic ligands in both lakes. The calculated free Zn^{2+} ion concentrations, which ranged from 5 to 48 pM, may limit the growth of some phytoplankton in both lakes [8]. A combination of different extraction methods and multielement techniques (inductively coupled plasma atomic emission spectrometry (ICP-AES),

inductively coupled plasma mass spectrometry (ICP-MS)) were applied to measure elemental concentrations in lake water polluted by mining activities. The aqueous speciation of Zn was followed by the use of two computer-supported speciation models for zinc. $ZnS(HS)^-$ was the predominant species at the sediment/water interface. In oxygenated waters, $ZnSO_4^0$, $Zn(OH)_2^0$, $ZnCO_3^0$, and other Zn species were mainly detected [9]. In another contaminated aquatic environment, the Zn-bearing particles in a lake were characterized by using electron microscopy techniques (analytical electron microscopy (AEM), transmission electron microscopy (TEM) and X-ray energy dispersive spectrometry (EDS)). Zinc, far from the source of contamination, was found primarily in sulfur moieties present in environmental samples [10].

Various species of Zn and Pb from mine wastewater in a lead-producing area were identified in the biotreatment system by a chemical equilibrium model named MINTEQ [11]. Computer modeling was also applied to predict the concentrations of dissolved metal species at the pH levels commonly seen in toxicity test vessels [12]. In runoff waters collected immediately after release from various commercial zinc-based surfaces, the element (>95%) was suggested to be present predominantly as hydrated Zn^{2+} ions, the most bioavailable form. The chemical speciation of zinc in these matrices could be predicted using the water ligand model MINTEQA2 and the humic aqueous model WHAM [13].

Shiller and Boyle found that, in relatively undisturbed river systems, dissolved zinc concentrations typically ranged from 10^{-9} to 10^{-8} mol kg^{-1}, with some dependence of concentration on pH. In industrially influenced systems, however, zinc concentrations can be 1 to 2 orders of magnitude higher [14]. In European river water samples, the total zinc concentrations ranged from 0.09 to 4.76 μmol L^{-1}. Voltammetric experiments on these matrices revealed the presence of labile zinc(II) complexes. The distribution of zinc(II) over free metal and complexed species was found to be roughly 30 and 70%, respectively. These results are supposed to affect the operational bioavailability of zinc(II) for aquatic organisms [15]. By voltammetry on a gel-integrated microelectrode array (GIME), the simultaneous determination and speciation of Zn, Cd, Pb, and Cu in natural water was performed. The separation technique was applied to the quantitative discrimination between mobile and colloidal metal species in aqueous matrices. As a result, in river water samples, for example, the mobile metal species were largely composed of aquo metal ions and inorganic metal complexes, in particular, the carbonate complexes [16].

In order to study the kinetic speciation of zinc in unpolluted river water, the Chelex-100 batch technique was carried out in combination with ICP-MS and graphite furnace atomic absorption spectrometry (GFAAS), respectively [17]. A schematic diagram of the reactor for the Chelex-100 batch experiment is presented in Figure 2.22.2. The procedure consisted of adding pretreated Chelex resin to a pretreated river water sample, the mixture then being stirred. The sample solution was delivered through a filter. As an example, the results of the experimental data from the ICP-MS detection of Zn are represented in Figure 2.22.3 [17]. Herein, the signal versus time for ultrapure water (a) and the respective plot for the Rideau River water (c) examined serve as blanks. Curve b shows the uptake of Zn in Rideau River water by the Chelex resin at pH 5. At the starting point of this experiment, the Zn concentration in the sample was about 0.08 μM, while after 500 s, most of the zinc species were taken up by the Chelex resin. Using these experimental values, the *iterative convolution method* was applied to the analysis of kinetic data for speciation of Zn in river water. As a result of the calculations, three kinetically distinguishable components of Zn were observed in Rideau River surface water [17].

1.2 Soil and soil solutions

A semiempirical model of Suwannee River fulvic acid based on experimental evidence has been used as a basis for determining the structural characteristics of divalent metal-ion binding. The structures of 1 : 1 and 2 : 1 metal-ion–fulvic acid complexes have been determined for Zn^{2+}, Cd^{2+},

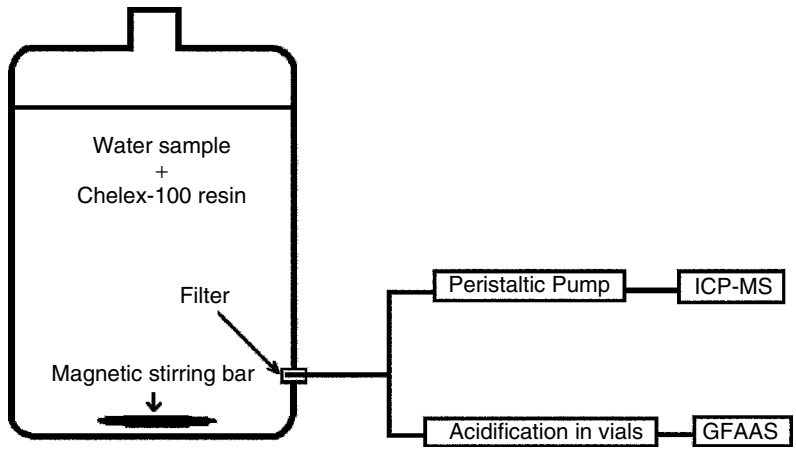

Figure 2.22.2. Schematic diagram of the apparatus for the Chelex-100 batch experiment investigating the speciation of zinc in river surface water samples, followed by ICP-MS and GFAAS detection. (Reprinted from *Anal. Chim. Acta*, **293**, Lu, Y., Chakrabarti, C. L., Back, M. H., Gregoire, D. C. and Schroeder, W. H., 95 Kinetic studies of aluminum and zinc speciation in river water and snow (1994) with permission of Elsevier [17].)

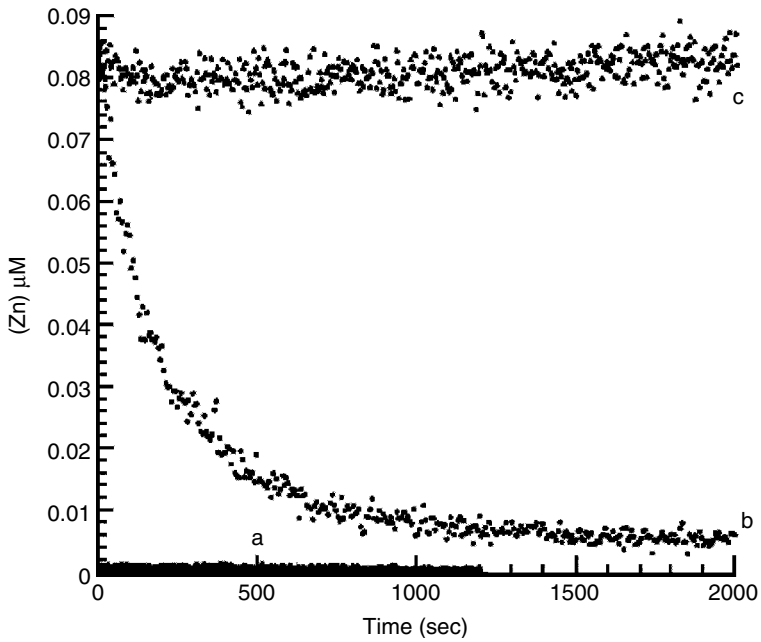

Figure 2.22.3. Zinc remaining in the sample of Rideau River surface water, as a function of time after uptake of zinc by the Chelex-100 resin in the Chelex batch technique as shown in Figure 2.22.2, determined by ICP-MS pH 5.0. (a) Ultrapure water without the Chelex resin; (b) [Chelex] = 1% (w/w); (c) the sample without Chelex resin. The resulted curve (b) shows that zinc concentrations of the sample decrease fast with increasing time. (Reprinted from *Anal. Chim. Acta*, **293**, Lu, Y., Chakrabarti, C. L., Back, M. H., Gregoire, D. C. and Schroeder, W. H., 95 Kinetic studies of aluminum and zinc speciation in river water and snow (1994) with permission of Elsevier [17].)

and other metal ions bound to pairs of carboxylate groups in the three low-energy configurations of fulvic acid [18].

A novel continuous-flow sequential extraction procedure for metal speciation in soils and other solids was developed. The extracts were collected in a number of subfractions for subsequent flame atomic absorption analysis. Some advantages of this system were that there was no need for pH adjustment during extraction and no cross contamination between extraction steps was to be expected [19]. Samples from different early Tertiary paleosols were extracted using a selective dissolution procedure. The specificity of each extracting solution for the different adsorption components was examined and the most important phases for the dispersion of Zn, Cu, and other metals were identified [20]. The trace-metal speciation was determined in two standard reference soils by using the *Commission of European Communities Bureau of Reference* (*BCR*) sequential extraction procedure. All leachate analyses were performed with flame atomic absorption spectrometry (FAAS). The results from the *BCR* extraction of two *National Institute of Standards and Technology* (*NIST*) soils were found to agree for the most part with those of the *Tessier* method with respect to the elements zinc, copper, and cadmium [21].

The activity of free Zn^{2+} and other metal ions in soil solutions was determined using a combination of the Donnan equilibrium cell and graphite furnace atomic absorption spectrometry (DE/GFAAS). The principal metal species in these matrices was free metal ions and hydrolyzed ions. Soil pH displayed a pronounced effect on the activity of free Zn^{2+}, Cd^{2+}, Cu^{2+}, and Pb^{2+} ions. The total Zn content of the soil hardly had any effect on the activity of Zn^{2+} [22]. X-ray absorption spectroscopy was employed to identify and quantify Zn species in soil cores collected from a contaminated wetland soil that undergoes seasonal flooding. As a result, zinc was associated with (hydr)oxide phases in dry, oxidized soils and with sulfides and carbonates in flooded systems. Data obtained indicate that Zn sorption is a dynamic process influenced by environmental changes [23]. The use of anodic stripping voltammetry, atomic absorption spectroscopy, and equilibration with Chelex-100 exchange resin has been applied to study the forms of zinc and copper in the soil solution of a sandy loam. Most of the zinc in soil solutions occurred as either free metal ions or labile complexes. The zinc availability decreased with increasing soil pH, whereas copper availability showed little dependence on pH [24]. Another technique, capacitively coupled plasma atomic emission spectrometry, was applied to the speciation of zinc and other metals in sedimented dust and soil from a heavily polluted area by use of selective dissolution of the samples in acids and ammonium salts [25].

Australian Vertisols used for cereal cropping were incubated with ultrapure distilled water and the soil solutions were extracted by centrifugation under nitric acid conditions followed by washes with double-distilled water. Zinc in the soil solutions was analyzed by GFAAS using *Gelman* polypropylene separators. The available zinc species in the same matrices were determined by applying cation-exchange techniques. The distribution of various zinc species in the examined soil solutions was calculated with the aid of the computer program GEOCHEM. Figure 2.22.4

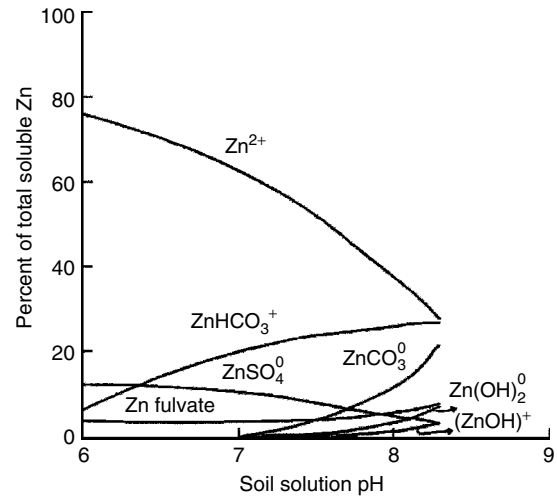

Figure 2.22.4. Calculated zinc species present in the soil solutions extracted from unfertilized and fertilized Vertisols, as a function of soil solution pH over the range 6.0 to 8.2. (Reproduced from the *Australian Journal of Soil Research*, **34**, 369–383 (Y. P. Dang, K. G. Tiller, R. C. Dalal, & D. G. Edwards, 1996) by permission of CSIRO PUBLISHING [26].)

shows an example of these calculations as a function of soil solution pH. It is obvious that zinc in the soil solution exists mainly as free Zn^{2+} ions in the investigated soils. This fact is important because divalent Zn^{2+} is probably the most available form of zinc to plants. Dominant inorganic zinc complexes, $ZnHCO_3^+$ and $ZnCO_3$, which increased with increasing soil solution pH, constituted 60 to 75% of the total inorganic Zn complexes. The organo-zinc complexes constituted a minor fraction of the total zinc species as shown in Figure 2.22.4 [26].

1.3 Plant extracts

Weber and Messerschmidt determined the metal-binding carbohydrates in plant extracts. For that purpose, plant roots were sequentially extracted at several pH (9 to 4), which represent the range of natural pH inside the plants (e.g. pH 8) and the lower pH at the soil–root interface. After ultrafiltration (<10,000 Da) of the collected extracts, aliquots of the low molecular mass (LMM) ultrafiltrate were used directly for FIA and HPLC analyses with pulsed amperometric detection (PAD) and also for corresponding metal determinations applying flame AAS. By high-performance liquid chromatography (HPLC) analysis of both the pH 8.7 and pH 5.0 extracts, zinc was exclusively found in the carbohydrate peak. In Figure 2.22.5, the results for zinc for the FIA-PAD experiments are shown. A direct correlation of zinc and carbohydrates is not reflected, probably because of the high excess of carbohydrate compared with the relatively low zinc content of the extracts. In this figure, it is also revealed that below pH 5 zinc complexes could have dissociated under the acidic conditions, otherwise the solubility of certain carbohydrate–zinc complexes may have increased. The results for sodium and potassium, however, show that a strong correlation exists with the carbohydrate content as measured by FIA-PAD. Conclusively, the existence of real metal binding to carbohydrates in plant root can only be proved by the proposed flow-injection analysis (FIA) method when limited to well-characterized samples [27].

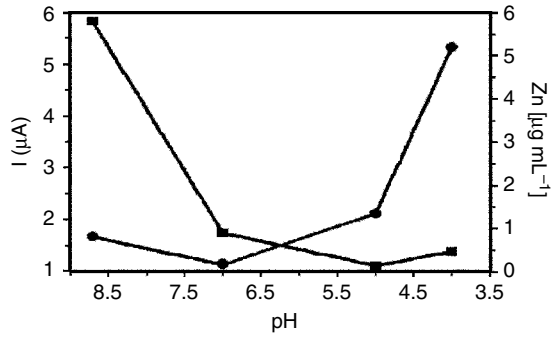

Figure 2.22.5. FIA-PAD and zinc content of root extracts as a function of extraction pH. ■: Peak current of FIA–PAD signals in μA, equivalent to the carbohydrate content. ●: Corresponding zinc concentration in $\mu g\,mL^{-1}$ measured by flame AAS. (Reproduced from *Fresenius' J. Anal. Chem.*, Weber, G. and Messerschmidt, J., **367**, 356, Figure 2, 2000 by permission of Springer-Verlag GmbH & Co KG [27].)

2 FOOD

The first evidence of the essential effect of Zn was reported in 1896. The first Zn-containing enzyme investigated by Keilin and Mann was carbonic anhydrase. Since then, more than 160 different enzymes containing Zn have been found. In the first half of the last century, indications of effects of the Zn deficiency became public [28]. Therefore, it is very important to determine total amounts of this element in the diet. In a book from Pfannhauser, the content of many trace elements, including As, Co, Cr, Cu, Fe, I, Li, Mn, Mb, Ni, Se, Si, Sn, V, and Zn, in foodstuffs are reviewed and their uptake, metabolism, and bioavailability discussed. In the literature, it is generally accepted that the uptake of essential trace elements from food is dependent on the kind of chemical compound in which the trace element is present [28]. To estimate the bioavailability of zinc in different foodstuffs, an extraction with simulated digestive fluids was applied. The compounds extracted *in vitro* were separated by ion-exchange procedures, followed by AAS and DPASV [29], to determine the zinc species and total zinc contents in these matrices. The results of this strategy of analysis showed that the low bioavailability of zinc in flour correlated with the relatively strong bonds between Zn and its binding partner and also with a

high concentration of competitive elements Fe and Cu detected in corn [29].

2.1 Fruit and vegetables

Fruits and vegetables are important sources of trace elements in the human diet. For example, the separation of a high molar mass polysaccharide fraction (>50,000 Da) containing Pb, Ba, Sr, Ce, and B in these matrices was performed by a combination of size-exclusion HPLC with parallel refractrometric and ICP-MS detection. Following application of this method to aqueous leachates of apple and carrot samples, Zn, Cu, and Mg eluted as complexes with low molar mass non-carbohydrate compounds in the water-soluble fraction of the investigated samples [30]. A LMM zinc-containing fraction was partly purified from lettuce leaf by using a combination of ultrafiltration, gel-permeation, and ion-exchange chromatography. The major zinc-binding fraction had a molecular mass of about 1250 Da. The isolated LMM fractions contained 73% of the total soluble zinc, indicating that they may have nutritional importance [31].

The distribution of metals between the soluble and insoluble cell fractions of vegetable food was investigated using a multielement analytical procedure [32–34]. Sample preparation was applied according to two different methods. For cell fractionation, either freeze-dried vegetables were mortared in the presence of fine-grain quartz and extracted with a buffer solution [32] or the examined plants were subjected to liquid shearing by treatment with an electrical dispersant (ultra-turrax) in a buffer [33, 34]. The resultant suspensions and plant homogenates, respectively, were separated in supernatants (cytosols) and pellets by centrifugation. The zinc contents of these fractions were determined by using total reflection X-ray fluorescence spectrometry (TXRF) with one internal standard after an acid digestion. Thus, the zinc distribution between the cytosol phase and the insoluble components of the plant cell was revealed [32–34]. These investigations show that a large fraction of Zn, for example, in the different plant cytosols, is directly accessible to further analytical separation procedures.

Subsequently, more than 20 vegetable and fruit samples were homogenized in the buffer by ultra-turrax treatment, and the homogenates were centrifuged and separated in cytosol and pellet. The resultant fractions were analyzed for zinc, cadmium, iron, manganese, copper, calcium, potassium, and many other elements using TXRF and GFAAS [35]. In Figure 2.22.6, the percentages of zinc in the cytosols of different commercially available vegetables and fruits are shown. The zinc amounts range between 31 and 87%. In most plants, the cytosol parts range from 51 to 87%. About 90% of the total zinc of iceberg lettuce 1 was found in the cytosol of the foodstuff. Thus, nearly the whole zinc content of this vegetable plant can be submitted to a further characterization of the available zinc species using a combination of gel permeation chromatography (GPC) and an element-specific detection method [35].

By conducting a GPC–AAS method, it was revealed that zinc is predominantly bound as species with a molecular mass of smaller than 5000 Da in all examined plant cytosols shown in Figure 2.22.7. Small amounts of zinc with ranges from 1 to 34% were found as species of greater than 30,000 Da in nearly all plants analyzed. In banana, chicory, Chinese cabbage, cucumber, and paprika, 100% of the zinc species eluted in the molecular mass range of smaller than 5000 Da [35, 36].

In Figure 2.22.8, the chromatograms from an investigation of commercial celery and spinach are presented. In contrast to cadmium, in both plants, zinc is eluted mainly in the LMM range (<5000 Da) by a combination of GPC and electrothermal AAS [36, 37]. A further characterization of the LMM zinc species in spinach and five other plants revealed that the examined zinc complexes had a very similar elution behavior in GPC and anion-exchange chromatography. Therefore, a great resemblance in structure between the species from these vegetables can be supposed [38]. The elucidation of the structure of the LMM zinc species from kohlrabi and Chinese cabbage showed that neither phytochelatins nor other

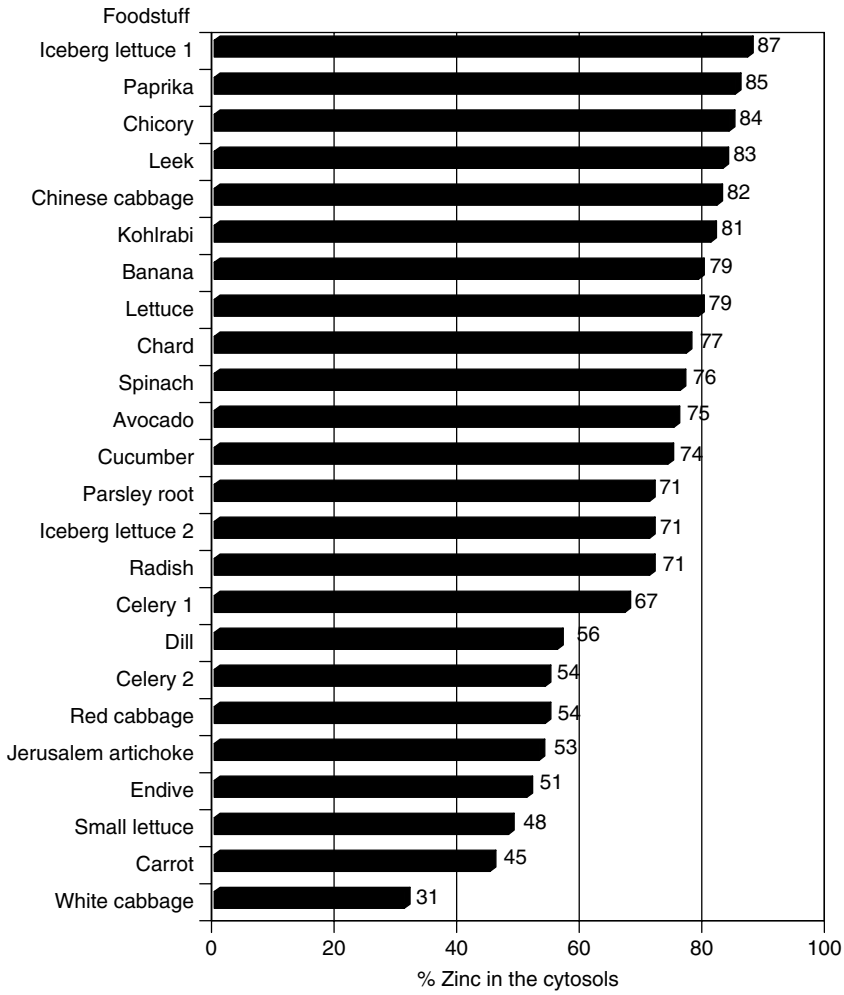

Figure 2.22.6. Percentual zinc in the cytosols (supernatants) of commercial vegetable foodstuffs after ultra-turrax treatment in buffer and centrifugation of the homogenates received. The soluble parts are now available for further speciation analysis. (Reproduced from Reference [35] by permission of Forschungszentrum Juelich GmbH.)

zinc-binding factors as described in the literature, do describe the zinc ligands found in the edible parts of the investigated plants. It is supposed that zinc is bound to an unknown glutamic acid derivative, possibly a malic acid ester [38].

The uptake of Zn is not only affected by the amounts of total zinc and the available zinc species in the diet but also by other elements (e.g. Cd, Ca, As, Cr, Ni, Mn, Co, Fe, Pb, and Cu) and their form present in food. To evaluate the physiological meaning of an element in a certain food matrix, multielement speciation analysis applied to these samples is absolutely necessary [28, 35]. For example, multielement speciation in vegetable foodstuffs was performed by a combination of GPC and TXRF in the off-line mode. It was revealed that this system is a very useful tool for a first characterization of element species in solution. Cytosols of lamb's lettuce and cauliflower were separated by a Sephadex G-50 column, and a screening analysis of the fractions by TXRF with an internal Co-standard was carried out [39]. Total reflection X-ray fluorescence analyses are rapid and easy and require only minute samples. No

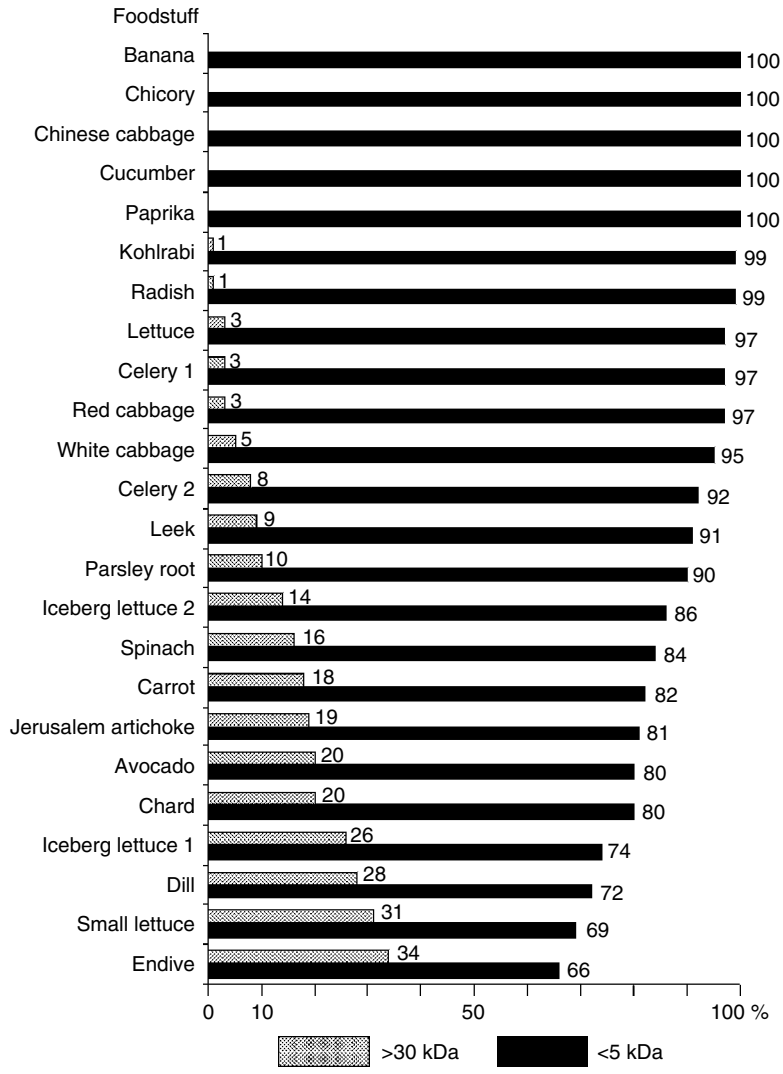

Figure 2.22.7. Distribution of the zinc recovered on low-molecular-mass (<5000 Da) and high-molecular-mass (>30,000 Da) species in the cytosols of vegetable foodstuffs after cell breakdown, centrifugation, and gel permeation chromatography on Sephadex G-50. (Reproduced from Reference [35, 36] by permission of Forschungszentrum Juelich GmbH.)

chemical pretreatment of the samples is demanded. By this technique, the distributions of the elements P, S, Cl, Br, K, Ca, Fe, Cu, Zn, Rb, Mn, and Sr were investigated in the different fractions of the separated plant cytosols. For example, at least three Zn-species were detected in the cytosols of both lamb's lettuce and cauliflower, two Fe-species in lamb's lettuce and three Fe-species in cauliflower, and two Cu-species in cauliflower. K, Ca, Rb, and Sr are present only in the LMM fraction, where free hydrated ions elute [39].

2.2 Cereals

In corn from wheat, rye, oats, and maize, an average 35% of the zinc-containing compounds were extracted by neutral buffer with high ionic strength. The separation of these extracts by

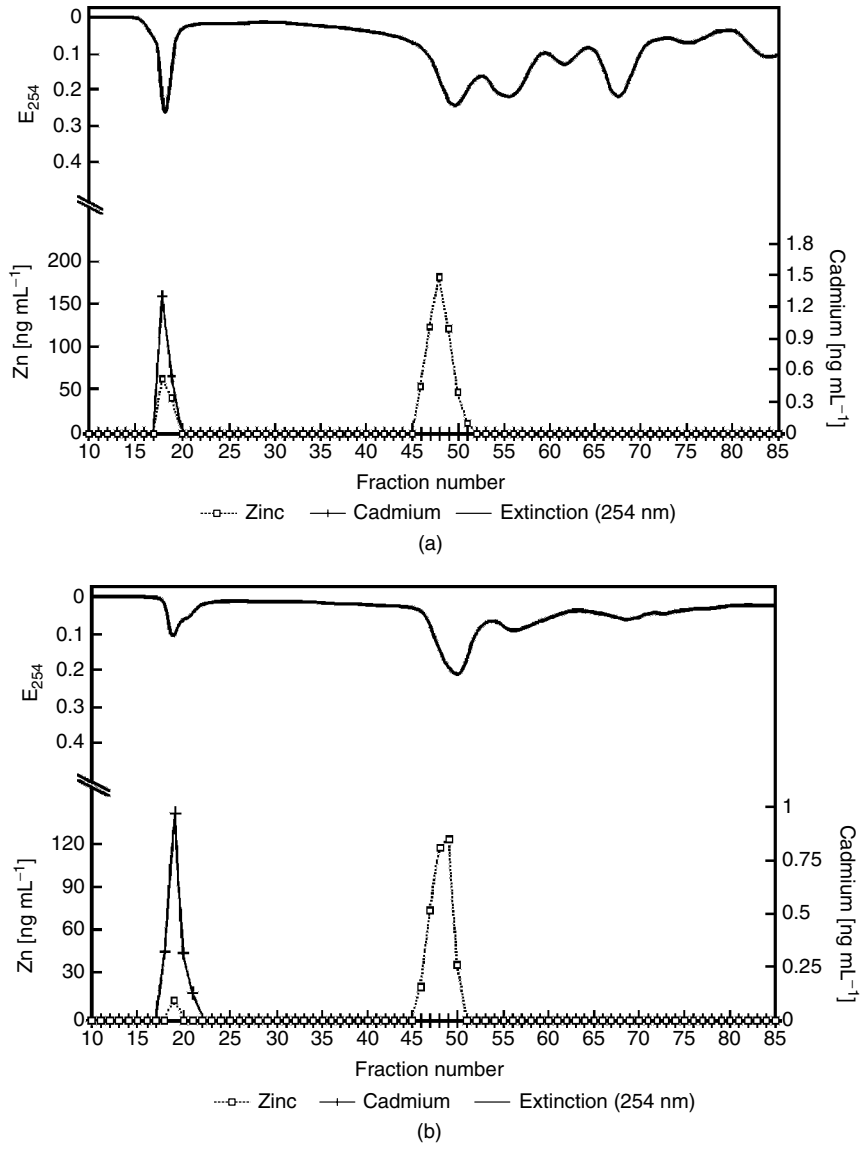

Figure 2.22.8. Gel permeation chromatograms of spinach cytosol (a) and celery cytosol (b) with off-line determination of zinc and cadmium by electrothermal atomic absorption spectrometry (ET-AAS) without decomposition. The results received reveal the different binding properties of both elements present in vegetable food. The highest percentages of zinc are found in the LMM range (<5000 Da, fraction 46 to 50). Contrary to zinc, cadmium is eluted exclusively in the range of the void volume (>30,000 Da, fraction 18 to 21) of the Sephadex G-50 column. (Reproduced from *Analytiker-Taschenbuch*, Element speciation analysis: an overview, Guenther, K. and Weber, G., Vol. 20, pp. 71–103, Figures 11a and 11b, 1998, © Springer-Verlag.)

GPC mainly showed LMM compounds of smaller than 5000 Da. However, by using buffer solutions of a low ionic strength, high molecular mass (HMM) Zn-containing substances of greater than 100,000 Da were detected in wheat and oats. Under the latter conditions, zinc phytate could not be observed [40]. Gradient gel electrophoresis and isoelectric focusing were applied to the separation of metal species in soybean flour extracts. The separated substances were electrophoretically

eluted, followed by the determination of Zn, Ni, and Cu via flame AAS [41]. As a result, zinc was mainly eluted with protein fractions in the molecular mass range of 18,000 to 20,000 Da after chromatographic separation of the extracts [41, 42] and was also detected in the molecular mass range of 18,000 to 21,000 Da by using electrophoretic techniques as comparative method [41].

2.3 Shellfish

The Zn, Cd, and Cu binding forms in the mussel *Mytilus edulis* were studied by using Sephadex G-75 chromatography. The distribution of zinc and copper in homogenates of these matrices showed that the two metals were principally associated with HMM proteins [43]. The accumulation and elimination of zinc and cadmium by the common mussel in the natural environment was investigated in combination with a study about the speciation of these elements in this aquatic organism [44].

Natural mussel populations from a wild, uncontaminated coast and an industrialized, contaminated coastal area in Spain were used to study multielement distributions in different fractions of the cytosols of mussels. For the separation of the cytosolic extracts, size-exclusion chromatography was applied, followed by double focusing ICP-MS detection for the determination of 18 trace metals in the fractions. As a result, the speciation of zinc, cadmium, copper, and many other elements showed a similar distribution pattern among cytosolic ligands for all the studied samples. In Figure 2.22.9, the elution profiles show that zinc and copper were predominantly

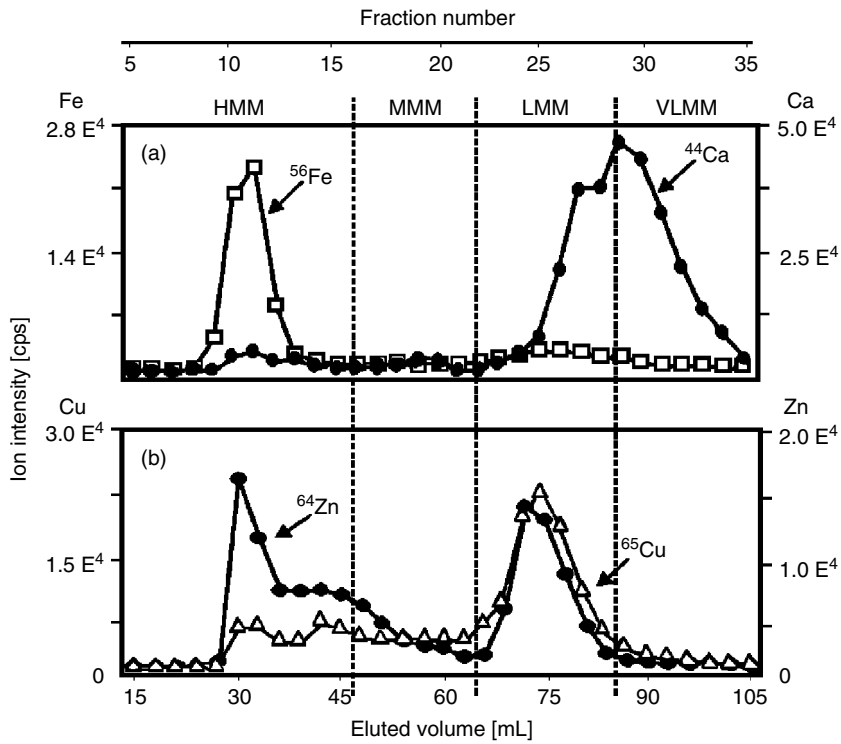

Figure 2.22.9. Levels of iron and calcium (a) and copper and zinc (b) in diluted fractions of mussel cytosol after size-exclusion chromatography (SEC) measured by double focusing ICP-MS at medium resolving power (R = 3000). The fractions received are distributed over very low molecular mass (VLMM), low molecular (LMM), medium molecular (MMM), and high molecular mass ranges (HMM). (Reproduced from Nestor Ferrarello, C., del Rosario Fernandez de la Campa, M., Sariego Muniz, C. and Sanz-Medel, A., *Analyst*, **125**, 2223 (2000) by permission of The Royal Society of Chemistry [45].)

bound to metallothionein-like proteins (fractions 22–28, 12–4 kDa, LMM), but also that significant amounts of Zn (and Cu to a lesser extent) were associated to high molecular mass (HMM > 30 kDa) and medium molecular mass (MMM 30–12 kDa) pools following chromatographic separation of mussel cytosols derived from the industrialized area [45].

2.4 Meat

Beef, lamb, pork, and chicken leg muscles were extracted with distilled water and the soluble zinc and iron compounds separated by gel filtration and dialysis. Zinc was present mainly in the insoluble fraction of these matrices. The soluble zinc was distributed between five main components. Over 70% of soluble zinc was associated with two components having molecular masses of 65,000 and 35,000 Da [46].

2.5 Yeast

Other zinc species were detected in yeast. For example, a natural yeast enzyme had a molecular mass of 140,000 Da and contained four zinc ions [47]. In baker's yeast, DNA-dependent RNA polymerase is a zinc protein with a 1 : 1 stoichiometry [48]. The uptake and cellular distribution of zinc in *Saccharomyces cerevisiae* was investigated by White and Gadd. Zn^{2+} was compartmented within the yeast cell as follows: 56% of the total intracellular pool was in the soluble vacuolar fraction, 39% was bound to insoluble components and only 5% was found in the cytosol [49].

2.6 Milk

In the last three decades, the speciation of zinc in milk was an important field of nutritional science with respect to human health. Symptoms of *Acrodermatitis enteropathica* (AE) occur especially when infants with an inherited disorder of zinc resorption are weaned from human breast milk to cow's milk. The two milk matrices were defatted and separated by gel filtration. The fractions obtained after this procedure were assayed for protein and analyzed for zinc by means of atomic absorption spectrophotometry. Gel chromatography indicated that most of the zinc in cow's milk was associated with HMM fractions, whereas zinc in human milk was associated with LMM fractions. A species difference in zinc-binding ligands may explain why symptoms of AE can be alleviated by feeding human but not cow's milk [50, 51]. These studies initiated several investigations on the binding ligands of zinc and other elements in human or bovine milk [52–65], infant formula based on cow's milk [63], and in different biological fluids [66, 67].

During a study in the early "1990s," human milk was pooled and separated into fat, proteins, and LMM substances by centrifugation. The LMM and the protein fractions were further separated by size-exclusion chromatography and analyzed for Zn. Among milk proteins, zinc was associated with casein, albumin, lactoferrin, and metallothionein, whereas among LMM substances, a Zn peak could be observed exclusively with citrate. The authors concluded that in human milk, zinc is primarily bound to citrate, and only about 5% of the total amount of zinc is attached to proteins [68].

For the speciation of zinc, iron, and selenium in human milk whey, a combination of chromatographic separation (HPLC), followed by instrumental neutron activation analysis (INAA) and ICP-AES was used [69]. In human milk and in commercial cow's milk-based formulas, the zinc-containing species were separated by means of size-exclusion chromatography combined with flame atomic absorption spectroscopy detection. Protein profiles and Zn distribution in an infant formula sample and in breast milk are shown in Figure 2.22.10. From this data, it appears that in breast milk whey, zinc is normally distributed among different protein fractions. However, in infant formula milk whey, zinc was detected only in the fractions with molecular masses of smaller than 5,000 Da and of greater than 158,000 Da. These differences in zinc distribution can be important for the bioavailability [70].

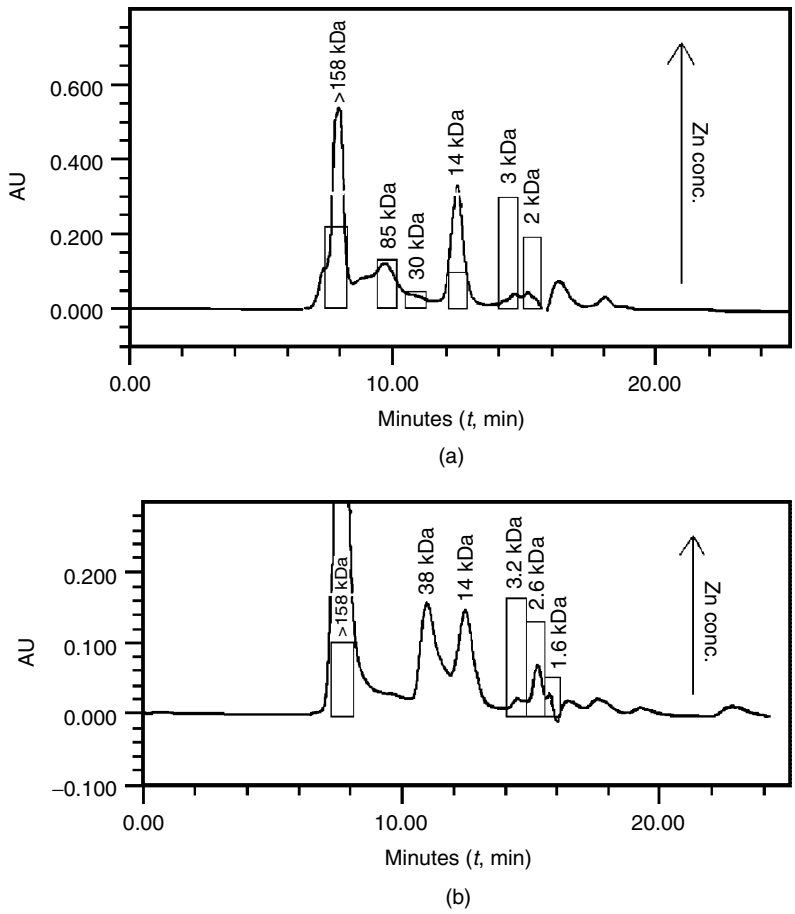

Figure 2.22.10. UV profiles at 254 nm and Zn distribution on a broad molecular mass spectrum ranging from high molecular (>158,000 Da) to low molecular (<5000 Da) mass species in: (a) breast milk sample; (b) infant formula sample, after the application of SEC and flame AAS detection. (Reprinted from *J. AOAC Int.* (2001), **84**, 847–852, Copyright 2001, by AOAC INTERNATIONAL [70].)

3 CLINICAL

Zinc is a cofactor for over 200 biologically important enzymes, particularly enzymes involved in protein synthesis. Other cellular processes affected by this element are, for example, DNA synthesis, reproduction, bone formation, growth, and wound healing [71]. The effects of zinc deficiency and toxicity are reviewed with respect to specific organs, immunological and reproductive function, and genotoxicity and carcinogenicity [72].

For example, zinc-binding factors were analyzed in different organs and tissues such as kidney [73], placenta [74], and brain [75]. However, the most important clinical matrices investigated with respect to Zn speciation analysis are biofluids [76–95] from human beings and animals, with special regard to blood serum and plasma [76–87].

3.1 Blood, serum, and plasma

Human serum proteins from blood donors and dialysis patients were separated by means of gel filtration chromatography, and zinc and copper in the resulting fractions were determined by GFAAS. The separation resulted in three zinc peaks with molecular mass of about 700,000,

300,000, and 75,000 Da, respectively, coeluting with α_2-macroglobulin in the first peak and with albumin in the third peak. The zinc protein(s) of the second peak remained unidentified [76]. By using a combination of gel filtration with Sephadex G-100, ET-AAS, and immunonephelometry, to the speciation of protein-bound zinc and copper in human blood serum, the known association of Zn with α_2-macroglobulin and albumin was confirmed. However, association with other proteins was also found [77].

Berthon, May, and Williams revealed that the most important LMM zinc complexes in blood plasma were $[Zn(CysO)_2]^{2-}$ and $[Zn(CysO)(HisO)]^{-}$ (CysO = cysteinate, HisO = histidinate) by applying computer simulation of metal-ion equilibria in biofluids [78]. The intrinsic stoichiometric equilibrium constants for the binding of zinc(II) and copper(II) to the high-affinity site of human and bovine serum albumin were obtained by conducting equilibrium dialysis experiments. Results indicated, for example, that histidyl residues alone were sufficient for zinc binding in both matrices [79].

A hyphenated technique consisting of HPLC (SEC) and inductively coupled plasma optical emission spectroscopy (ICP-OES) was applied for the characterization of metal and nonmetal species in human serum and food extracts. Zn in serum was reported to be bound to macroglobulin (720,000 Da) and albumin (66,500 Da) whereas Cu was bound to ceruloplasmin (160,000 Da) and albumin (66,500 Da) [80]. These results are very interesting with respect to the mutual antagonism between zinc and copper, which has been regarded as a prime example of competitive biological interactions between metals with similar chemical and physical properties [81]. By the use of a SEC-ICP-MS system, it was shown that albumin-zinc and albumin-copper (loosely bound species) could be selectively removed from human blood serum by adsorption on to Chelex-100 resin (after pretreatment of the chelating resin) while α_2-macroglobulin-zinc and ceruloplasmin-copper (firmly bound species) remained in the serum [82].

A suitable procedure was developed for the separation of metalloprotein complexes of Zn, Fe, and Ca in serum by using SEC directly coupled to an element-specific detector. Two column matrices used for SEC were investigated with respect to the recovery and retention behavior for these compounds. Optimization of the separation parameters (buffer type, concentration, pH) in serum was achieved by means of metalloprotein complexes marked with radiotracers *in vitro* [83].

A combination of SEC coupled to ICP-MS was used to study zinc speciation in human plasma. In blood plasma from a child exhibiting symptoms of severe zinc deficiency, the element was not associated with the albumin fraction. Instead, the zinc was predominantly associated to an unidentified HMM protein and was therefore depleted at the normal site of action. This result helped to explain how a child with abnormally high levels of plasma zinc could exhibit symptoms of severe zinc depletion [84]. In another case of human disease, a combination of HPLC and ICP-MS was successfully applied to the simultaneous speciation of elements and characterization of metallothionein in blood serum of an epileptic child who developed valproate-associated hepatotoxicity. The investigations showed that at the beginning of the hepatic coma, metallothionein appeared in the serum mainly in the form of zinc–thionein, which altered the zinc distribution pattern of the serum in a characteristic manner [85].

Zinc and copper protein complexes in blood plasma were identified and determined after chromatographic separation on a diethylaminoethyl cellulose (DEAE)-Sepharose column. The identities of proteins in individual fractions were determined by radial immunodiffusion, UV absorbance, and the use of purified protein 'markers'. Zn and Cu concentrations were determined by atomic absorption spectroscopy. In the investigated matrices, zinc was bound mainly to albumin (80–90%) and α_2-macroglobulin (10–20%). The remainder (<3%) was associated with the retinol-binding protein complex and with a LMM fraction [86].

In pooled human plasma, the zinc species were separated by fast protein liquid chromatography (FPLC) and the Zn in the resultant fractions was determined by using on-line coupled FAAS. For that purpose, an interesting interface for

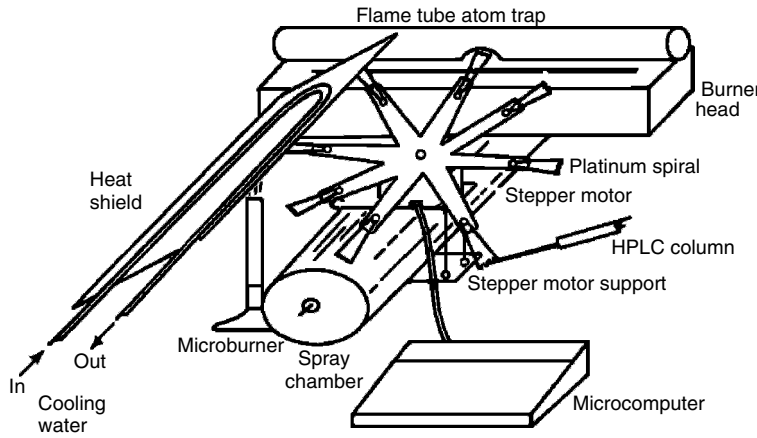

Figure 2.22.11. Interface used for the speciation of zinc in blood plasma by direct coupling of high-performance liquid chromatography with flame atomic absorption spectrometry detection. (Reproduced from Ebdon, L., Hill, S. and Jones, P., *Analyst*, **112**, 437 (1987) by permission of The Royal Society of Chemistry [87].)

direct coupling of HPLC with FAAS was used and is represented in Figure 2.22.11. The plasma components were first separated using FPLC and the eluate then being transported as a series of discrete aliquots directly to the flame. The interface consisted of eight platinum wire spirals mounted at 45° to each other on a rotating disc. The disc was turned to a number of predefined positions by a stepper motor. One of the advantages of this system, controlled by a microcomputer, was that it allowed complete compatibility between the interface and a wide range of eluate flow rates [87]. Using this method, zinc in blood plasma was readily seen to be associated with the albumin and α_2-macroglobulin fractions although resolution between the two is poor. In Figure 2.22.12, α_2-macroglobulin was eluted in the leading edge of the albumin peak in the UV scan, and is seen as a smaller shoulder in the lower trace for zinc. Ebdon *et al.* concluded that the use of FPLC greatly reduced the time required to separate many clinical samples and allowed comparative analysis during therapy [87].

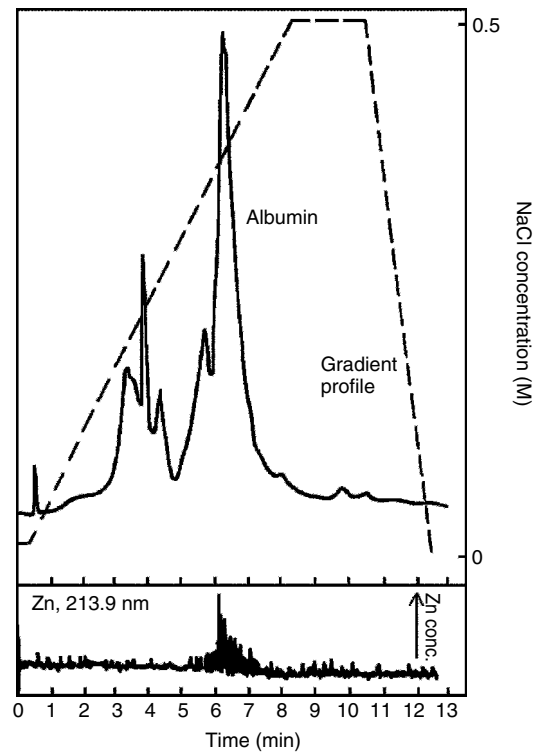

Figure 2.22.12. Chromatogram (UV profile at 280 nm) of pooled human plasma showing associated zinc after the application of FPLC and flame AAS detection, by using a linear gradient of NaCl to 0.5 M and an interface as represented in Figure 2.22.11. (Reproduced from Ebdon, L., Hill, S. and Jones, P., *Analyst*, **112**, 437 (1987) by permission of The Royal Society of Chemistry [87].)

3.2 Biofluids other than blood

Human duodenal secretions were investigated with regard to a comparison of the zinc binding in duodenal secretions derived from healthy adults with

Table 2.22.1. The effect of pH on the speciation profile of zinc(II), expressed as a percentage of the total zinc, in resting human saliva [95].

Zn(II) Complex	Charge	% of total zinc at pH					
		4.00	5.00	6.00	6.75	7.00	7.50
Bis(Protonated) cysteinate $[ZnH_2Cys]^{2+}$	+2	77	76	70	23	8	1
Free metal ion $Zn^{2+}{}_{aq}$	+2	12	12	11	4	1	0
Protonated alanate $[ZnHAla]^{2+}$	+2	6	6	6	2	1	0
Chloride $[ZnCl]^{+}$	+1	3	3	2	1	0	0
bis(Protonated) phosphate $[ZnH_2PO_4]^{+}$	+1	1	1	0	0	0	0
bis(Protonated) citrate $[ZnH_2Cit]^{+}$	+1	1	0	0	0	0	0
Citrate $[ZnCit]^{-}$	−1	2	5	2	1	1	0
Protonated cysteinate phosphate $[ZnHCysPO_4]^{2-}$	−2	0	0	2	54	75	88
Cysteinate citrate $[ZnCysCit]^{3-}$	−3	0	0	1	7	9	10
Protonated phosphate $[ZnHPO_4]^{0}$	0	0	0	1	1	1	0
Histidinate $[ZnHis]^{+}$	+1	0	0	1	4	3	1
Hydroxide $[Zn(OH)_2]^{0}$	0	0	0	1	1	1	0

Source: Reproduced from *Chemical Speciation and Bioavailability* by permission of Science Reviews

that from patients with *A. enteropathica* [88]. Rat prostate fluid was subjected to a purification procedure, based on gel filtration and cationic exchange chromatography. As result, a protein with a molecular mass of about 66,000 Da was separated from free zinc ions and other secretory components. Two zinc ions were estimated to be associated with one molecule of isolated protein [89]. Rat seminal plasma holds zinc both as free ion and as protein-bound forms. Isolated Zn–protein complexes, as well as the Zn-free ions, bind *in vitro* to rat epididymal spermatozoa [90]. A combined application of potentiometric stripping analysis (PSA) and computer simulation of speciation analysis has been used to determine the total element concentrations and the proportions of the different chemical species of zinc, copper, and manganese in human wound fluids [91]. The prevailing chemical forms of zinc and copper amongst the LMM ligands in samples of fluid obtained from surgical wounds were investigated by computer modeling using the *J*oint *E*xpert *S*peciation *S*ystem named *JESS*. The model predicted that Zn would occur predominantly as charged species, $[ZnCysCitric]^{3-}$ (53.1%) and $[ZnHCysPO_4]^{2-}$ (23.3%), in wound fluid at pH 7.4 [92].

A zinc protein with a molecular mass of 37,000 Da was isolated and purified to apparent homogeneity from human parotid saliva of subjects with normal taste acuity by using gel filtration and ion-exchange chromatography. It was composed of 8% histidine residues and had two moles of Zn per mole of protein [93]. The chemical speciation of Zn- and Sn(II)–containing dentifrices and of the reaction between saliva and such toothpastes has been researched using computer simulation. It was concluded that, at a single pH value, there cannot be maximal availability of antimicrobial salts of $Zn^{2+}{}_{(aq)}$ and soluble tin(II) species added for the provision of clinical efficacy for hard and soft tissue diseases and in breath protection [94].

An investigation into the effectiveness of treating common colds with zinc gluconate lozenges revealed that there was a significant correlation between the biological response of the volunteers and the concentration of free $Zn^{2+}{}_{aq}$ ions in their saliva at pH 5.5 or pH 6.75. The oral administration of zinc gluconate lozenges enhanced the levels of salivary concentrations of free $Zn^{2+}{}_{aq}$ for those formulations that were reported to reduce the symptoms of the common cold [95]. In Table 2.22.1, the percentage distribution of zinc amongst the LMM complexes in resting saliva between pH 4.00 and 7.50 is shown. At pH 6.75, the pH of resting saliva, the quaternary $[ZnHCysPO_4]^{2-}$ (54%), and ternary $[ZnH_2Cis]^{2+}$ (23%) and $[ZnCysCit]^{3-}$ (7%) complexes predominate. Less than 4% of the total zinc in saliva exists as free $Zn^{2+}{}_{aq}$ at neutral pH. The speciation was assessed using the *JESS* computer simulation of speciation in a saliva model [95].

3.3 Cells

The complex mechanism of intracellular transport in mammalian cells is regulated by free calcium in different ways. Another ion necessary for the function of factors involved in vesicular transport is zinc. One of the zinc-dependent factors is probably a protein with a cysteine-rich region that coordinates zinc and binds phorbolesters [96]. A major zinc-binding protein from the renal brush border membrane (BBM) of rat, which could be involved in the translocation of the element across the BBM, was identified and purified by a combination of chromatographic methods, sodium dodecyl sulfate polyacrylamide gel electrophoresis (SDS-PAGE) and other techniques. The identified zinc-binding transmembrane glycoprotein had a molecular mass of 40,000 Da and was exclusively localized in the proximal convoluted tubules in kidney sections detected by immunofluorescence. It was found that only Cd^{2+} could displace the zinc bound to this protein. It was concluded that the purified protein was highly specific with a high affinity for zinc [73].

3.4 Cytosols

By applying a combination of chromatographic methods, SDS-polyacrylamide gel electrophoresis and amino acid analysis, a LMM, native zinc binding cytosolic protein with a molecular mass of 6000 Da was isolated, purified, and characterized from human normal term placenta [74]. This placental metal-binding protein bound only 1 mole of zinc per mole of protein and it was proposed that it could play a role in homeostatic control or transport of essential elements like zinc from placenta to fetus [74]. This proposition might be very important as zinc is an essential element for normal fetal growth and development [71].

3.5 Brain tissue

Using GPC, three major zinc-binding species were resolved in the hippocampus of rat. One of the species was a metallothionein-like protein. The other species may be a zinc–glutathione complex. Cytosolic zinc-binding proteins could be responsible for the sequestration of zinc observed in the hippocampus [97, 98].

An acidic zinc- and heme-containing protein with a molecular mass of 31,200 Da was isolated from the soluble fraction of bovine brain. The monomeric globular protein, as determined by electrospray ionization mass spectrometry (ESI-MS), was purified to homogeneity using a combination of several anion-exchange and gel permeation chromatographic steps [75].

4 OCCUPATIONAL HEALTH

Zinc or zinc compounds are not listed as suspected carcinogens. Limited data exist on the incidence of cancer in workers exposed to zinc. Zinc compounds can produce irritation and corrosion of the gastrointestinal tract, along with acute renal tubular necrosis and interstitial nephritis. In the occupational setting, inhalation of fumes from zinc oxide is the most common cause of metal fume fever, which is characterized by leukocytosis, fever, thirst, metallic taste, salivation, and many other symptoms [71].

Epidemiological studies of occupational diseases in human beings exposed to Zn or Zn compounds, or to other metals and their compounds, were statistically evaluated with respect to lung cancer mortality among workers making Pb chromate and Zn chromate pigments [99], and to the risk of Parkinson's disease [100]. It is assumed that Zn can cause occupational asthma [101]. The relationship between neuropsychiatric syndromes and occupational exposure to the pesticide zinc phosphide was investigated in Egyptian workers [102]. For example, urinary zinc, cadmium, lead and copper concentrations were analyzed in steel production workers by using DPASV [103].

Only a few studies in the field of occupational medicine deal with the speciation analysis of zinc in human matrices derived from workers who suffer from an occupational disease or who are exposed to work materials.

In the erythrocytes of patients with lead intoxication or with iron deficiency anemia, the fluorescent protoporphyrin is chelated with zinc. Zinc protoporphyrin (ZnPP) in these matrices is bound to globin moieties, probably at heme binding sites [104]. From a group of referents, it has been established that the normal mean ZnPP concentration is in the region of 25 μg per 100 mL blood. Women have higher ZnPP values than men. Measurements of ZnPP on a group of people exposed to Pb in a storage battery factory revealed that the mean ZnPP concentration of the group throughout a certain period was 70.9 μg per 100 mL blood [105].

The separation of metalloporphyrins in blood derived from a lead-poisoned person with elevated blood lead levels was performed by a combination of liquid chromatography and ICP-MS. The detection limits obtained were in the nanogram range for ZnPP as shown in Table 2.22.2. ZnPP in whole blood was extracted and the mixture consisting of extraction solution and blood was centrifuged. The resulting supernatant was dried in a rotary evaporator at 40 °C and the residue obtained was dissolved in methanol. The chromatographic separation of the ZnPP in this methanolic sample and the subsequent element analysis by ICP-MS revealed that zinc was present as two species in the examined matrix [106]. In Figure 2.22.13, the elution profile obtained for ZnPP by monitoring m/z 64 is shown. The amount of ZnPP found was estimated to be approximately 2.3 μg per 1 mL of whole blood analyzed. Another zinc peak around 4 min in this chromatogram was identified to be from free metal ion present in the extracted solution [106]. In Table 2.22.2, the detection limits and the reproducibilities of peak areas for those porphyrin compounds that were used to find the optimal chromatographic conditions for metalloporphyrin separations are shown. Reproducibilities of peak areas were determined using 10 replicate injections of a mixture of cobalt protoporphyrin CoPP, hemin (Fe-protoporphyrin), and ZnPP. The results are listed in Table 2.22.2 and presented as relative standard deviations. They were within 5% for all porphyrin compounds studied [106].

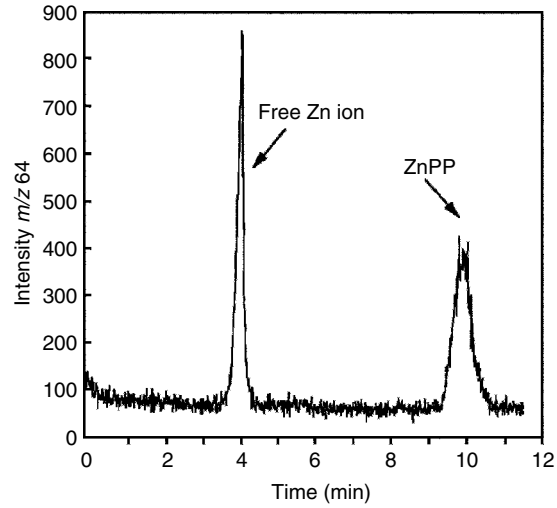

Figure 2.22.13. Liquid chromatographic separation of the extracted solution from blood sample of a lead-poisoned patient and subsequent ICP-MS detection of Zn. (Reproduced from the *Journal of Chromatographic Science* by permission of Preston Publications. A Division of Preston Industries, Inc. [106].)

Table 2.22.2. Figures of merit [106].

Porphyrin	Reproducibility of peak area[a]	Detection limits[b]	LDR (order of magnitude)[c]
CoPP	2.2	0.1 ng	3
Hemin	3.3	5.8 μg	1.5
ZnPP	3.7	4.6 ng	3

[a] % relative standard deviation.

[b] Detection limit $= \dfrac{3 \times \text{standard deviation of background}}{\text{slope of calibration curve}}$.

[c] LDR = linear dynamic range.

Source: Reproduced from the *Journal of Chromatographic Science* by permission of Preston Publications. A Division of Preston Industries, Inc.

In the future, for example, cancerous and normal human tissues have to be investigated with respect to the binding factors of important trace elements (e.g. Zn or Se) in healthy and degenerated cells to obtain first evidence of a changed elemental metabolism in diseased tissues [107]. Because of the interdependencies of elements in the different physiological and environmentally relevant processes, multielement speciation analysis is a very useful and absolutely necessary means to evaluate the effects and the biochemical behavior of many elements and their chemical forms in biological organisms [35, 37]. For example, combined procedures and coupled techniques,

preferentially consisting of chromatographic systems with multielement analytical methods, can be used for elemental speciation in the different matrices [35, 37, 108].

5 REFERENCES

1. Florence, T. M., *Talanta*, **29**, 345 (1982).
2. Florence, T. M. and Batley, G. E., *Talanta*, **24**, 151 (1977).
3. Donat, J. R. and Bruland, K. W., *Mar. Chem.*, **28**, 301 (1990).
4. Ellwood, M. J. and Van den Berg, C. M. G., *Mar. Chem.*, **68**, 295 (2000).
5. Gardner, M., *Chemosphere*, **38**, 2117 (1999).
6. Kozelka, P. B. and Bruland, K. W., *Mar. Chem.*, **60**, 267 (1998).
7. Xue, H. B. and Sigg, L., *Anal. Chim. Acta*, **284**, 505 (1994).
8. Ellwood, M. J., Hunter, K. A. and Kim, J. P., *Mar. Freshw. Res.*, **52**, 217 (2001).
9. Evans, L. J., *Water Air Soil Pollut.*, **122**, 299 (2000).
10. Webb, S. M., Leppard, G. G. and Gaillard, J.-F., *Environ. Sci. Technol.*, **34**, 1926 (2000).
11. Erten-Unal, M. and Wixson, B. G., *Water Air Soil Pollut.*, **116**, 501 (1999).
12. Erten-Unal, M., Wixson, B. G., Gale, N. and Pitt, J. L., *Chem. Spec. Bioavail.*, **10**, 37 (1998).
13. Wallinder, I. O., Leygraf, C., Karlen, C., Heijerick, D. and Janssen, C. R., *Corros. Sci.*, **43**, 809 (2001).
14. Shiller, A. M. and Boyle, E., *Nature*, **317**, 49 (1985).
15. Jansen, R. A. G., Van Leeuwen, H. P., Cleven, R. F. M. J. and Van Den Hoop, M. A. G. T., *Environ. Sci. Technol.*, **32**, 3882 (1998).
16. Pei, J., Tercier-Waeber, M.-L. and Buffle, J., *Anal. Chem.*, **72**, 161 (2000).
17. Lu, Y., Chakrabarti, C. L., Back, M. H., Gregoire, D. C. and Schroeder, W. H., *Anal. Chim. Acta*, **293**, 95 (1994).
18. Nantsis, E. A. and Carper, W. R., *J. Mol. Struct. (Theochem)*, **423**, 203 (1998).
19. Shiowatana, J., Tantidanai, N., Nookabkaew, S. and Nacapricha, D., *J. Environ. Qual.*, **30**, 1195 (2001).
20. McAlister, J. J. and Smith, B. J., *Microchem. J.*, **63**, 415 (1999).
21. Ho, M. D. and Evans, G. J., *Anal. Commun.*, **34**, 363 (1997).
22. Wu, Q., Hendershot, W. H., Marshall, W. D. and Ge, Y., *Commun. Soil Sci. Plant Anal.*, **31**, 1129 (2000).
23. Bostick, B. C., Hansel, C. M., La Force, M. J. and Fendorf, S., *Environ. Sci. Technol.*, **35**, 3823 (2001).
24. Jeffery, J. J. and Uren, N. C., *Aust. J. Soil Res.*, **21**, 479 (1983).
25. Cordos, E. A., Frentiu, T., Rusu, A.-M. and Vatca, G., *Analyst*, **120**, 725 (1995).
26. Dang, Y. P., Tiller, K. G., Dalal, R. C. and Edwards, D. G., *Aust. J. Soil Res.*, **34**, 369 (1996).
27. Weber, G. and Messerschmidt, J., *Fresenius' J. Anal. Chem.*, **367**, 356 (2000).
28. Pfannhauser, W., *Essential Trace Elements in the Diet*, Springer-Verlag, Berlin, Heidelberg, New York, London, Paris, Tokyo, 1988.
29. Schwedt, G., Tawali, A. B. and Koch, K., *Fresenius' J. Anal. Chem.*, **360**, 589 (1998).
30. Szpunar, J., Pellerin, P., Makarov, A., Doco, T., Williams, P. and Lobinski, R., *J. Anal. At. Spectrom.*, **14**, 639 (1999).
31. Walker, C. D. and Welch, R. M., *J. Agric. Food Chem.*, **35**, 721 (1987).
32. Guenther, K. and von Bohlen, A., *Z. Lebensm.-Unters.-Forsch.*, **190**, 331 (1990).
33. Guenther, K., von Bohlen, A. and Waldner, H., *Fresenius' J. Anal. Chem.*, **345**, 533 (1993).
34. Guenther, K., von Bohlen, A. and Strompen, C., *Anal. Chim. Acta*, **309**, 327 (1995).
35. Guenther, K., *Contributions to Multielemental Speciation Analysis in Vegetable Food: Investigations on the Binding Forms of Many Elements with Special Regard to Zinc and Cadmium*, Reports of the Research Centre Juelich 3358, ISSN 0944–2952, Publishing House of the Research Center Juelich' Juelich, 1997.
36. Guenther, K. and Waldner, H., *Anal. Chim. Acta*, **259**, 165 (1992).
37. Guenther, K. and Weber, G., Element speciation analysis: an overview, in *Analytiker-Taschenbuch*, Vol. 20, Guenzler, H., Bahadir, A. M., Danzer, K., Fresenius, W., Galensa, R., Huber, W., Linscheid, M., Schwedt, G. and Toelg, G. (Eds.), Springer-Verlag, Berlin, Heidelberg, New York, 1998, pp. 71–103.
38. Waldner, H. and Guenther, K., *Z. Lebensm.-Unters.-Forsch.*, **202**, 256 (1996).
39. Guenther, K. and von Bohlen, A., *Spectrochim. Acta*, **46B**, 1413 (1991).
40. Ditters, H., Brueggemann, J., Ocker, H.-D. and Thier, H.-P., *Getr. Mehl Brot*, **45**, 294 (1991).
41. Dunemann, L. and Reinecke, H., *Fresenius' Z. Anal. Chem.*, **334**, 743 (1989).
42. Reinecke, H. and Dunemann, L., *Fresenius' J. Anal. Chem.*, **338**, 630 (1990).
43. Noel-Lambot, F., *Experientia*, **32**, 324 (1976).
44. Luten, J. B., Bouquet, W., Burggraaf, M. M. and Rus, J., *Bull. Environ. Contam. Toxicol.*, **37**, 579 (1986).
45. Nestor Ferrarello, C., del Rosario Fernandez de la Campa, M., Sariego Muniz, C. and Sanz-Medel, A., *Analyst*, **125**, 2223 (2000).
46. Hazell, T., *J. Sci. Food Agric.*, **33**, 1049 (1982).
47. Sadler, P. J., *Nature*, **262**, 258 (1976).
48. Lattke, H. and Weser, U., *FEBS Lett.*, **65**, 288 (1976).
49. White, C. and Gadd, G. M., *J. Gen. Microbiol.*, **133**, 727 (1987).
50. Eckhert, C. D., Sloan, M. V., Duncan, J. R. and Hurley, L. S., *Science*, **195**, 789 (1977).

51. Hurley, L. S., Duncan, J. R., Sloan, M. V. and Eckhert, C. D., *Proc. Natl. Acad. Sci. U.S.A.*, **74**, 3547 (1977).
52. Piletz, J. E. and Ganschow, R. E., *Am. J. Clin. Nutr.*, **32**, 275 (1979).
53. Loennerdal, B., Stanislowski, A. and Hurley, L. S., *J. Inorg. Biochem.*, **12**, 71 (1980).
54. Evans, G. W. and Johnson, P. E., *Pediatr. Res.*, **14**, 876 (1980).
55. Martin, M. T., Licklider, K. F., Brushmiller, J. G. and Jacobs, F. A., *J. Inorg. Biochem.*, **15**, 55 (1981).
56. Harzer, G. and Kauer, H., *Am. J. Clin. Nutr.*, **35**, 981 (1982).
57. Loennerdal, B., Hoffman, B. and Hurley, L. S., *Am. J. Clin. Nutr.*, **36**, 1170 (1982).
58. Hurley, L. S. and Loennerdal, B., *Nutr. Rev.*, **40**, 65 (1982).
59. Blakeborough, P., Salter, D. N. and Gurr, M. I., *Biochem. J.*, **209**, 505 (1983).
60. Fransson, G.-B. and Loennerdal, B., *Pediatr. Res.*, **17**, 912 (1983).
61. Martin, M. T., Jacobs, F. A. and Brushmiller, J. G., *J. Nutr.*, **114**, 869 (1984).
62. Nelson, L. S. Jr., Jacobs, F. A., Brushmiller, J. G. and Ames, R. W., *J. Inorg. Biochem.*, **26**, 153 (1986).
63. Braetter, P., Gercken, B., Roesick, U. and Tomiak, A., Speciation of trace elements in human milk and milk formulas, in *Trace Element Analytical Chemistry in Medicine and Biology*, Vol. 5, Braetter, P. and Schramel, P. (Eds.), Walter de Gruyter, Berlin, 1988, pp. 145–156.
64. Singh, H., Flynn, A. and Fox, P. F., *J. Dairy Res.*, **56**, 249 (1989).
65. Singh, H., Flynn, A. and Fox, P. F., *J. Dairy Res.*, **56**, 235 (1989).
66. Christie, G. L., Duffield, J. R. and Williams, D. R., *Proc. Summer Comput. Simul. Conf.*, 405 (1986).
67. Evans, G. W., Johnson, P. E., Brushmiller, J. G. and Ames, R. W., *Anal. Chem.*, **51**, 839 (1979).
68. Michalke, B., Muench, D. C. and Schramel, P., *J. Trace Elem. Electrolytes Health Dis.*, **5**, 251 (1991).
69. Negretti de Braetter, V. E., Recknagel, S. and Gawlik, D., *Fresenius' J. Anal. Chem.*, **353**, 137 (1995).
70. Bermejo, P., Pena, E. M., Fompedrina, D., Dominguez, R., Bermejo, A., Cocho, J. A., Fernandez, J. R. and Fraga, J. M., *J. AOAC Int.*, **84**, 847 (2001).
71. Barceloux, D. G., *J. Toxicol. Clin. Toxicol.*, **37**, 279 (1999).
72. Walsh, C. T., Sandstead, H. H., Prasad, A. S., Newberne, P. M. and Fraker, P. J., *Environ. Health Perspect.*, **102**, 5 (1994).
73. Kumar, R. and Prasad, R., *Biochim. Biophys. Acta*, **1419**, 23 (1999).
74. Honey, S., Dhall, G. I. and Nath, R., *Mol. Cell. Biochem.*, **136**, 77 (1994).
75. Fundel, S. M., Pountney, D. L., Bogumil, R., Gehrig, P. M., Hasler, D. W., Faller, P. and Vasak, M., *FEBS Lett.*, **395**, 33 (1996).
76. Gless, U., Schmitt, Y., Ziegler, S. and Kruse-Jarres, J. D., *J. Trace Elem. Electrolytes Health Dis.*, **6**, 245 (1992).
77. Gardiner, P. E., Ottaway, J. M., Fell, G. S. and Burns, R. R., *Anal. Chim. Acta*, **124**, 281 (1981).
78. Berthon, G., May, P. M. and Williams, D. R., *J. Chem. Soc. Dalton*, **11**, 1433 (1978).
79. Masuoka, J., Hegenauer, J., Van Dyke, B. R. and Saltman, P., *J. Biol. Chem.*, **268**, 21533 (1993).
80. Schoeppenthau, J. and Dunemann, L., *Fresenius' J. Anal. Chem.*, **349**, 794 (1994).
81. Bremner, I. and Beattie, J. H., *Proc. Nutr. Soc.*, **54**, 489 (1995).
82. Inagaki, K., Mikuriya, N., Morita, S., Haraguchi, H., Nakahara, Y., Hattori, M., Kinosita, T. and Saito, H., *Analyst*, **125**, 197 (2000).
83. Raab, A. and Braetter, P., *J. Chromatogr., B*, **707**, 17 (1998).
84. Owen, L. M. W., Rauschert, A. M., Fairweather-Tait, S. J. and Crews, H. M., *Biochem. Mass Spectrom.*, **24**, 947 (1996).
85. Braetter, P., Brunetto, R., Gramm, H.-J., Recknagel, S. and Siemes, H., *J. Trace Elem. Electrolytes Health Dis.*, **6**, 251 (1992).
86. Chilvers, D. C., Dawson, J. B., Bahreyni-Toosi, M.-H. and Hodgkinson, A., *Analyst*, **109**, 871 (1984).
87. Ebdon, L., Hill, S. and Jones, P., *Analyst*, **112**, 437 (1987).
88. Casey, C. E., Hambidge, K. M. and Walravens, P. A., *J. Pediatr.*, **95**, 1008 (1979).
89. Sansone, G. and Abrescia, P., *J. Exp. Zool.*, **259**, 379 (1991).
90. Sansone, G., Martino, M. and Abrescia, P., *Comp. Biochem. Physiol.*, **99C**, 113 (1991).
91. Taylor, D. M., Liyanage, J. A., Williams, D. R. and Harding, K. G., *Appl. Radiat. Isot.*, **49**, 677 (1998).
92. Jones, P. W., Taylor, D. M. and Williams, D. R., *J. Inorg. Biochem.*, **81**, 1 (2000).
93. Henkin, R. I., Lippoldt, R. E., Bilstad, J. and Edelhoch, H., *Proc. Natl. Acad. Sci. U.S.A.*, **72**, 488 (1975).
94. Coombes, C. C., Laing, M. E., Taylor, D. M., Vesey, J. A. and Williams, D. R., *Chem. Spec. Bioavail.*, **6**, 33 (1994).
95. Bakar, N. K. A., Taylor, D. M. and Williams, D. R., *Chem. Spec. Bioavail.*, **11**, 95 (1999).
96. Aballay, A., Arenas, G. N. and Mayorga, L. S., *Biocell*, **20**, 339 (1996).
97. Sato, S. M., Frazier, J. M. and Goldberg, A. M., *J. Neurosci.*, **4**, 1662 (1984).
98. Sato, S. M., Frazier, J. M. and Goldberg, A. M., *J. Neurosci.*, **4**, 1671 (1984).

99. Davies, J. M., *Br. J. Ind. Med.*, **41**, 158 (1984).
100. Gorell, J. M., Rybicki, B. A., Cole Johnson, C. and Peterson, E. L., *Neuroepidemiol.*, **18**, 303 (1999).
101. Malo, J.-L., Cartier, A. and Dolovich, J., *Eur. Respir. J.*, **6**, 447 (1993).
102. Amr, M. M., Abbas, E. Z., El-Samra, G. M., El Batanuoni, M. and Osman, A. M., *Environ. Res.*, **73**, 200 (1997).
103. Horng, C.-J., *Analyst*, **121**, 1511 (1996).
104. Lamola, A. A. and Yamane, T., *Science*, **186**, 936 (1974).
105. Wildt, K., Berlin, M. and Isberg, P. E., *Am. J. Ind. Med.*, **12**, 385 (1987).
106. Kumar, U., Dorsey, J. G., Caruso, J. A. and Evans, E. H., *J. Chromatogr. Sci.*, **32**, 282 (1994).
107. von Czarnowski, D., Denkhaus, E. and Lemke, K., *Spectrochim, Acta, Part B*, **52**, 1047 (1997).
108. Lobinski, R., *Appl. **Spectrosc.***, **51**, 260A (1997).

2.23 Speciation of Actinides

Gerhard Geipel
Institute of Radiochemistry, Dresden, Germany

1 OUTLINE

Actinides are the 14 elements that follow the element actinium in the periodic table of the elements. The first three actinides, thorium, protactinium and uranium, can be found in nature, whereas the others are artificial elements. Most speciation studies have been carried out with the actinides thorium to curium. The elements uranium, neptunium and plutonium show a wide variety of

Handbook of Elemental Speciation II: Species in the Environment, Food, Medicine & Occupational Health
Edited by R. Cornelis, H. Crews, J. Caruso and K. G. Heumann
 ISBN: 0-470-85598-3 (HB)

oxidation states. In the tetravalent oxidation state, the solubility is very low. In this oxidation state, hydrolysis is the most important reaction.

As all these elements are radioactive, special laboratories are necessary to handle them. The concentration range for speciation studies with actinides is below 1×10^{-5} M. Therefore, several speciation techniques, mostly based on laser-induced methods, have been developed. A short overview of these methods will be given.

For thorium and protactinium, only few data are available. Thorium only exists in the tetravalent oxidation state. Hydrolysis and phosphate speciation will be described. Protactinium exists in the pentavalent oxidation state and forms a dioxy-cation.

Most data are available for uranium speciation. Uranium exists in four oxidation states. Uranium(III) is only stable in nonaqueous environments and therefore plays no role in speciation studies. Under reducing conditions, uranium(IV) is formed. Speciation examples for hydrolysis, sulfate, phosphate and arsenate binding will be given. In aqueous solutions, uranium(V) disproportionates into uranium(IV) and uranium(VI). Hexavalent uranium exists only as dioxy-cation.

In a next section, environmental aspects of the uranium(VI) speciation will be dealt with. Uranium is found in more or less high concentrations anywhere in the environment. Speciation examples from mining and milling will be given.

Uranium speciation in plants (as an example for the food chain) will be described.

Neptunium forms oxidation states from +3 to +7. Np(III) is slightly oxidized to Np(IV). The most stable oxidation states are Np(IV) and Np(V). The latter also forms a dioxy-cation. As an example for environmental speciation, the speciation of Np(V) with humic substances will be quoted.

Plutonium has oxidation states from +3 to +6. The redox potentials between these oxidation states are similar, so one can often find several oxidation states existing together. Examples for speciation in the environment (here the special case of the Oklo mine in Gabun and the results of bomb tests will be included) will be shown, and clinical and health aspects will be discussed (Pu is one of the most toxic elements).

Americium and curium form trivalent ions in solution. These elements are important in waste repositories. Speciation in concentrated salt solutions and in mineral (calcite) phases are important examples for speciation in natural environments.

Most of the actinides higher than curium have short half-lives. The only long-living isotopes are berkelium 247 (1400 y), californium 251 (900 y) and einsteinium 252 (1.24 y). Fermium, mendelevium, nobelium and lawrencium, as well as the transactinide elements, have half-lifes less than 1 y. Because of their very low production rates, most of these elements are less relevant in speciation chemistry. Berkelium is found to have two oxidation states (+3 and +5). Only few data on chloride and sulfate speciation are available.

2 INTRODUCTION

Actinides are the 14 elements that follow actinium in the periodic table of the elements. The first three actinides, thorium, protactinium and uranium, can be found in nature, and the others are artificial elements. Sources of these elements are nuclear reactions. In nuclear power plants most of the transuranium elements are generated in weighable amounts. Other sources of these elements are nuclear explosions and the bombardment of targets made of lower elements with accelerated protons and ions.

The amounts of the natural actinides on the earth are in the range of 3×10^{23} g for thorium and 3×10^{22} g for uranium. It is estimated that the accumulation of the human made element plutonium until 1982 has reached about 3×10^{8} g. The yearly production of this element in nuclear power plants is about 2×10^{7} g. The isotopes curium-242 (half-life 162.8 d) and curium-244 (half-life 18.1 y) are available in gram quantities. From the isotope californium-252 (half-life 2.65 y), about 63 mg were produced until 1975.

All actinide elements are radioactive. Therefore, special laboratories are necessary to handle these elements. Actinides show a wide variety of

isotopes. The concentration range for speciation studies with actinides is mostly below 1×10^{-5} M. At high concentrations, the radioactivity of these elements can cause radiolysis of actinide species in the environment.

Most speciation studies are carried out with the actinides from thorium to curium. In analogy to the lanthanides, most of the actinide elements exist as trivalent ions. Tetravalent ions are formed from thorium to americium. The element thorium exists only in the tetravalent oxidation state. In this oxidation state, the solubility generally is very low and hydrolysis is the most important reaction. Pentavalent ions are known from the elements protactinium to americium. However, only protactinium and neptunium are stable in this oxidation state under normal atmospheric conditions. Except protactinium in the pentavalent oxidation state, oxo-cations are formed. The elements uranium, neptunium and plutonium show a wide variety of oxidation states. Uranium, neptunium and plutonium are stable in the oxidation state +6. A stable form of a heptavalent ion is known from neptunium, and plutonium also can be oxidized to the heptavalent oxidation state. Mendelevium and nobelium form divalent ions in solution. A detailed overview on the several oxidation states of actinides is given by Choppin [1]. Eh-pH diagrams illustrate the ranges of the stability of the several oxidation states of an element [2].

Most early studies on transuranium elements were done to develop efficient strategies for the separation of these elements. Stary [3] refers to the use of specially developed and highly selective organic ligands, and therefore this part is not reflected here.

Speciation studies of radionuclides in the environment can be performed in three main areas: atmosphere, hydrosphere and lithosphere. Actinides in the atmosphere can only exist in forms that are bond to aerosols. Airborne actinides result from the following sources: nuclear weapon tests, uranium mining and nuclear fuel cycle, coal burning and resuspension from soil and surface waters (sea) by wind. Ions, ion pairs, molecules, colloids and particulate matter characterize the variety of actinide speciation in aquatic systems. In solid systems, the actinides can be adsorbed to a surface, precipitated or coprecipitated and incorporated into crystal lattices.

The solubility of actinides and the speciation in an aquatic environment are main factors for their transportation. The chemistry at the interface solution-surface may strongly influence the migration of actinides in aquatic systems. In the series of the actinides, a general trend from high to low mobility depending on the oxidation state can be expected as: $5+ > 6+ > 3+ > 4+$. K_d models describe only concentration/activity ratios. Newer studies use the surface complexation model to describe the interaction between metal ions and the surface [4].

The increase in publications on speciation of actinides over the last years shows the importance of knowledge in this field. This is connected to the high international and public interest in this field and to the worldwide search for safe repositories of radioactive and nuclear waste. At least seven international conference series deal more or less with the speciation of these elements. Therefore, it is not possible to give a complete overview on the speciation chemistry of actinides. The restricted length of this contribution allows only a relatively small and personally influenced selection. The focus of this contribution is mainly on the speciation of actinides in aquatic systems. Soils and rocks species of actinides are also present in the atmosphere and in sediments. Modern databases for surface and sorption thermodynamics are under development [5]. For the speciation of actinides in other compartments as sediments, colloids and atmospheric systems (aerosols), additional reviews may be consulted [6–9].

Most important reactions of actinides in aquatic systems are hydrolysis and complexation with inorganic ligands as carbonate, sulfate, phosphate and chloride, and organic ligands as well as humic substances. The solubility of these species determines the migration of actinides in environmental compartments.

The actinides can exist in different oxidation states; therefore, redox reactions have also to be taken into consideration. The chemistry of actinides includes the formation of colloids and interactions with living matter like bacteria and plants.

In a review of the actinide chemistry [10], data on the hydrolysis of the actinides neptunium to californium are summarized. The stability constants for the first hydrolysis step of the trivalent actinides increase in the sequence of the ordinal numbers. Nevertheless, these data may be subject to change because of better experimental conditions. For example, the first hydrolysis constant given for Cm(III) was $\log \beta_{11} = 7.9$. Experiments done by Wimmer *et al.* [11] resulted in a lower constant of $\log \beta_{11} = 6.67$. These differences are often caused by problems due to the low solubility of the actinide compounds under study.

The most important reactions under aquatic conditions are precipitation, complex formation, sorption and colloid formation. Silva *et al.* [12] emphasize the prediction of the release and the transportation rates of actinides. Furthermore, this paper summarizes nuclear properties and electronic configurations of these elements, which should therefore not be repeated here.

Several authors tried to explain the change in the stability constants and other properties of actinides by the change in the ionic radii. For comparison, available data are summarized in Table 2.23.1. The database on calculations has been published by Choppin [1].

For the determination of actinide species, the knowledge on the hydration number is important. Several methods can be used for their determination. Beside fluorescence spectroscopic methods [16], extended X-ray adsorption fine structure (EXAFS) studies may also be exploited. As an example for usage of EXAFS measurements, the Bk^{4+}/Bk^{3+} redox couple should be named. For these studies, a specially designed spectroelectrochemical cell was used [17]. Besides these methods, calculations were also carried out [18].

Available hydration numbers are summarized in Table 2.23.2.

Table 2.23.2. Hydration numbers of actinide ions [17, 19–24].

Element	Oxidation state			
	3+	4+	5+	6+
Ac				
Th		11		
Pa		11	5	5
U	9	≤11	5	5
Np	9	11	4–5	5
Pu	8–10	9–11	5	4–5
Am	8		4–5	5
Cm	9			
Bk	9	8		
Cf				
Es				

Table 2.23.1. Atomic radii [13] and effective ionic radii [1, 13, 14, 15] of actinide elements.

Element	Atomic radius[a]	Ionic radius[b]			
		Radius in nm			
		+3	+4	+5	+6
Ac	0.188	0.111			
Th	0.180		0.094		
Pa	0.163	0.104	0.090	0.078	
U	0.154	0.1025	0.089	0.076	0.073
Np	0.150	0.101	0.087	0.075	0.072
Pu	0.164	0.100	0.086	0.074	0.071
Am	0.173	0.0975	0.085		
Cm	0.174	0.097	0.085		
Bk	0.170	0.096	0.083		
Cf	0.186	0.095	0.082		
Es	0.186				
Fm					
Md					
No		0.0894			
Lr					

[a] Metallic radii for coordination number 12.
[b] Calculated for coordination number 6.

3 SPECIATION TECHNIQUES FOR ACTINIDES

Several new techniques for the speciation of actinides have been developed during the past decades. Three requirements are of importance:

- License for handling of radioactive elements, especially for α-emitting actinides
- Availability of actinides, especially the higher actinides are generated in small amounts
- Speciation methods that cover the concentration range of actinides expected or found in nature.

Speciation analysis can be distinguished into two types: noninvasive and invasive methods. Among the first group, are spectroscopic methods (see also Chapters 6.1 and 6.2 of Volume 1 of the Handbook of Elemental Speciation). They are not restricted to the form of the species (solid, liquid, gas). Noninvasive methods need no treatment of the sample and allow the direct speciation of an element in its environment. Invasive methods in general are applicable to solids and solutions. They normally need a pretreatment and a separation of the sample. Sequential extraction can be used for the determination of species in solid systems. Besides, for the separation of actinides [25] extraction techniques are important for the determination of oxidation states of the actinides in solution. For example, the oxidation states of plutonium can be determined using α-thenoyltrifluoroacetone (TTA) at $pH = 0$. Tetravalent plutonium is extracted to the organic phase, whereas all other oxidation states and polymeric plutonium remain in the aqueous phase. This technique was used to detect the reduction of neptunium(V) to tetravalent neptunium and its retardation by drill cores from the ÄSPÖ site, Sweden [26]. The same extraction procedure after addition of chromate allows to separate plutonium(III) and plutonium(IV). Other common extraction agents are tributylphosphate (TPB) and bis(2-ethyl-hexyl)-hydrogen-phosphate (HDEHP).

Several overviews on the speciation of actinides can be found in the literature. Laser-induced photoacoustic spectroscopy (LPAS or LIPAS) and laser-induced thermal lensing spectroscopy were introduced in research on actinides in the eighties [10]. Notable progress was demonstrated especially in the spectroscopy of americium. Because of their good sensitivity, the new methods did allow speciation studies at lower concentration ranges.

The availability of tunable X-rays in synchrotron facilities has lead to the development of methods to obtain basic molecular-level information. X-ray absorption spectroscopy (XAS) has become a powerful technique for the study of the speciation of actinides in aquatic systems [27]. This is required for a better understanding of the mechanisms in radionuclide transportation.

In the following paragraphs, two methods are briefly discussed. There are, however, many more instrumental techniques, as well as chemical separation techniques. Very often, extraction and ion exchange methods are used for the determination of species. A review of several methods is given in the literature [28, 29].

Laser-induced spectroscopy: In the field of laser-induced spectroscopy, four main methods are used: LIPAS, Laser-induced Time-resolved Fluorescence Spectroscopy (TRLFS), Ultra-short Laser pulse-Induced Time-resolved Fluorescence Spectroscopy (fs-TRLFS), Laser-induced Breakdown Detection and Laser-Induced Breakdown Spectroscopy (LIBD/LIBS). All these methods have been developed intensively during the last decades [10, 29–35]. They became powerful tools to study interactions in solutions and at the solid–liquid interface. Both methods (LIPAS and TRLFS) complement each other with respect to optical properties.

These are noninvasive and nonintrusive methods and allow qualitative and quantitative *in situ* investigations. Compared to conventional spectroscopic methods, like UV-VIS spectroscopy, the detection limits are at least 2 orders of magnitude lower.

Laser-induced spectroscopic methods follow the same setup like conventional methods, however, they use several types of laser as excitation source and because of the high, applied light energy specially designed detectors are used.

In LPAS, a pulsed or chopped tunable laser is used as light source. This tunable laser can

be a so-called dye laser, where a laser dye is excited with a pump laser system and the dye itself generates a broad spectrum of laser light that is selected by a grating system [36]. The disadvantage of these laser systems is a relatively small light spectrum of about 30 nm for each dye, and therefore for scanning over longer wavelength ranges the dye has to be changed. In contrast to this, modern solid-state tunable laser systems are based on angle tuning of a nonlinear optical crystal. These laser systems are useful over wavelength ranges of several hundreds nanometer.

In LIPAS, the observed signal is directly proportional to the absorption of light by the sample and to the applied light power.

Setups of LIPAS system are described in the literature, for instance, by several authors [34, 35, 37, 38]. In Table 2.23.3, some sensitivities for speciation studies are summarized.

A special type of laser-induced absorption spectroscopy is the thermal lens spectroscopy. This method, however, is used only in a few cases because of the need for a second probe laser system, which has to be overlapped with the pump laser system [30].

The limiting factor in laser-induced absorption spectroscopy is water, which is usually present as a solvent. Nevertheless, the detection limits of laser-induced spectroscopic methods represent an improvement by a factor of 100 and more compared with conventional spectrophotometric techniques [30].

Fast Fourier Transformation has been used to distinguish the photoacoustic signal from noise.

Table 2.23.3. Sensitivity of LIPAS [10, 39].

Actinide	Medium	Sensitivity in M	
U(IV)			1×10^{-7}
U(VI)	0.1 M $HClO_4$	8×10^{-7}	1×10^{-6}
Np(V)			1×10^{-7}
Pu(III)			1×10^{-7}
Pu(IV)	1.0 M $HClO_4$	7×10^{-8}	1×10^{-7}
Pu(V)			5×10^{-7}
Pu(VI)	1.0 M $HClO_4$	3×10^{-8}	1×10^{-7}
Am(III)	0.1 M $HClO_4$	2×10^{-8}	1×10^{-8}

Source: Reprinted from *Radiochim. Acta*, (1995) **70/71** with permission of Oldenbourg and from Handbook of the Physics and Chemistry of the Actinides (1986), p. 413 with permission of Elsevier.

Applying this method to the spectroscopy of uranium, a detection limit of 6×10^{-6} M was estimated [40]. In this paper, the authors also report on the application of photoacoustic spectroscopy to precipitates. However, in the UV-VIS-NIR range, only a broad absorption below 500 nm is observed, and Fourier Transform Infrared (FT-IR) spectra gave much more information.

Fluorescence spectroscopy is a very sensitive type of absorption spectroscopy. This method can be used when the absorption of light is followed by the emission of photons. Normally, a setup is used, in which the emitted light is detected in a right angle to the incident laser beam. The decay process can be observed by time-resolving methods. Besides single-photon counting methods [41], mostly gated charge coupled device (CCD) cameras were used, which allow the spectral and time resolution within one step [42].

A short review on speciation of radionuclides is given by Moulin [43]. The authors compare some direct speciation methods for application toward actinides. As new method, the electro spray mass spectrometry (ES-MS) was used on speciation studies. However, this method is an invasive method, and the sensitivity is between laser-induced absorption and fluorescence measurements.

X-ray absorption spectroscopy: Synchrotron-based XAS has been used for studying the speciation of environmental samples during the past decade. Monochromatized synchrotron radiation is applied to the sample, and the absorption spectrum of a selected element is measured as function of the X-ray photon energy.

XAS is used for the determination of molecular-level information on the speciation of elements in solids and solutions [44, 45].

X-ray absorption near edge structure (XANES) exploits the detailed structure in the absorption intensities within the range of 20 eV below and above the absorption edge of the atomic shell. The structure in the absorption spectrum within 20–1000 eV above the absorption edge is assigned to the EXAFS.

XANES provides information about the electronic structure and local geometry of the absorbing atom.

Therefore, XANES can be used for the determination of the oxidation state of the absorbing atom. The weak modulations of the spectrum in the EXAFS region give information on the coordination number and the atomic distance between the absorbing atom and the surrounding backscatterer [46]. The coordination number can be determined within 15–25%, and the error of the inner-atomic distance is ±0.002 nm. EXAFS can provide structural information in amorphous solids and species in solution because this method is not dependent on the long-range order of the atoms. XAS became therefore an important tool to study radionuclides in environmental systems [44].

For use with radionuclides, specially dedicated experimental stations are necessary in which radioactive samples can be handled safely [27].

4 SPECIATION CALCULATIONS

Two basic requirements are needed for speciation calculations – a database including stability constants of the formed species and a computerized program for the real calculation. For the input, analytical data or theoretical concentrations of the basic species can be used.

Hydroxide and carbonate are two of the most important environmental ligands. Fuger [47] resumes many available data.

Up to now, several databases have been developed [48–52]. However, the most up-to-date and best-reviewed databases for the actinide elements uranium, neptunium, plutonium and americium are the NEA databases [50, 53, 12]. For speciation calculations, the listed data should be used, including the desired estimations for correction of the ionic strength. Two estimates are widely used:

1. an adapted SIT (Specific Ion-Interaction Theory) method [50]
2. Davies equation, including extension for high ionic strength [51].

On the basis of the database, several program codes can be used for calculation of the species distribution as a function of concentrations, pH, ionic strength. Which one will be selected depends on the experience of the user. The most important input in such calculations is the use of a correct and validated database.

A relatively early speciation program is HYDRAQL [54, 55]. As in all programs, it is necessary that the included database should be inspected carefully. This program does not do calculations of the charge balance of the calculated species. As a consequence, some results may not be correct.

In addition, the code RAMESES [56] runs under DOS. In this program, a table of the reactions to be included must be generated, and a feed of the equilibrium constants at the desired ionic strength is necessary.

The most useful program code is EQ 3/6 [57]. The estimation of the stability constants at the ionic strength of the solution to be calculated is included in this program. Reactions at the interphase gas/liquid can also be included.

A newer code is SPECIES [58]. The input is comfortable; also a program code for the estimation of formation constants at different ionic strength is available. However, and this is mentioned by the authors, the attached database (SC Database) should be used only after checking of the original literature. The program is not able to include reactions with gas phases (CO_2/CO_2 (a.)).

Also available on the web is the program MEDUSA [59]. In the program, a database is included, and there is also the possibility to correct the used stability constants.

Two other useful codes are PhreeqC and MinteqA2. Both of them have included surface complexation models, and with PhreeqC a linear transport model can be used.

Useful additional information can also be found on the web (http://www.fz-rossendorf.de/FWR/VB/modeling.shtml#speciation).

Some of the speciation program codes have not been developed any further (Hydraql, EQ 3/6). This may lead to some compatibility problems with modern operating system in the future.

In the literature, the compiled data are sometimes given in different forms. An instructive

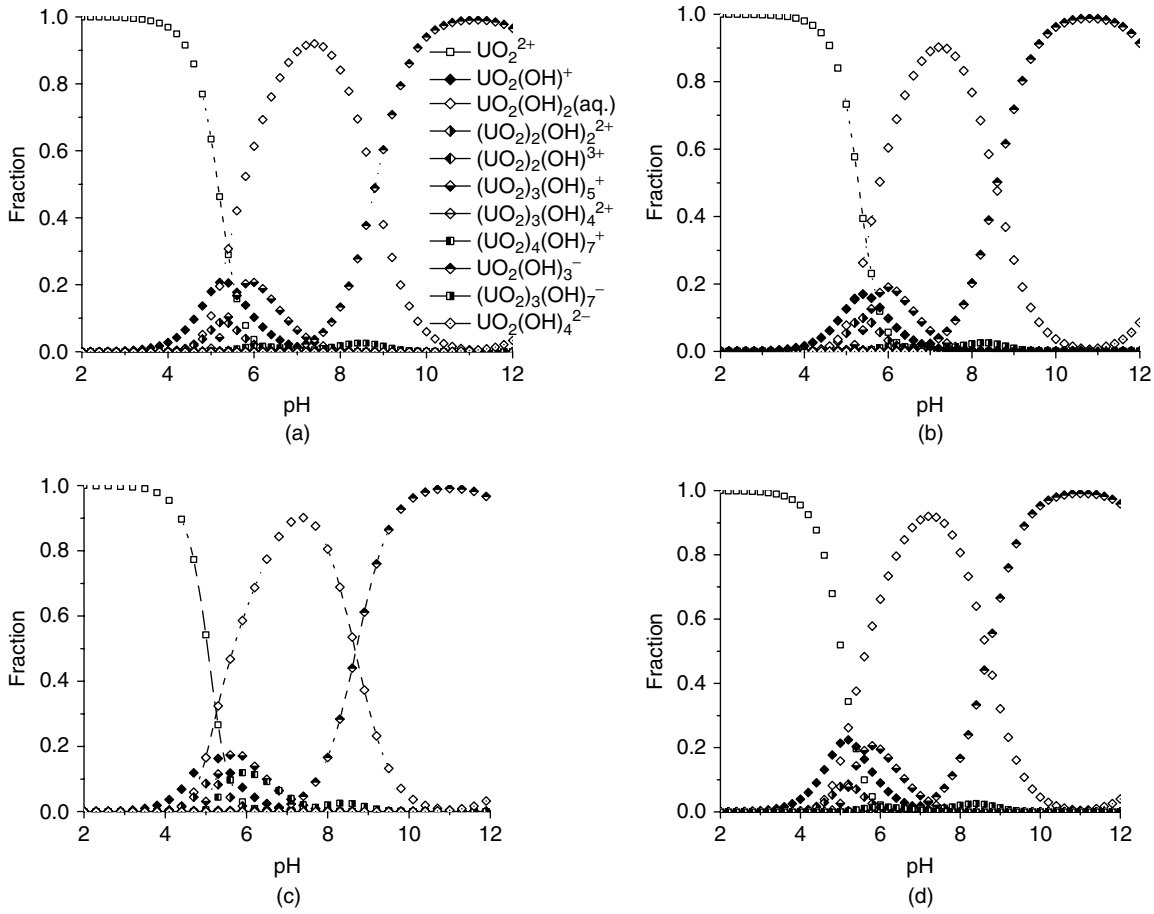

Figure 2.23.1. Comparison of several speciation program codes (visualized output): (a) EQ 3/6 [57], (b) MEDUSA (Ver. 31) [59], (c) Species (Academic software Ver. 1.2) [58], (d) RAMESES [56]; stability constants, see [50].

example can be found in Wimmer *et al*. [11]

$$Cm^{3+} + OH^- \rightleftarrows Cm(OH)^{2+}$$
$$\log \beta_{11} = 6.67 \pm 0.18 \quad (2.23.1)$$

Others like the review of uranium data [50] used a form that is closer to speciation calculations. Our example than would be compiled in the form

$$Cm^{3+} + H_2O \rightleftarrows Cm(OH)^{2+} + H^+$$
$$\log *\beta_{11} = -7.33 \pm 0.18 \quad (2.23.2)$$

To distinguish between both forms, an asterisk will be used, if the protonated form of the ligand is involved in the reaction.

In Figure 2.23.1, the output of several speciation program codes are compared. The uranium concentration was set in all cases to be 1.0×10^{-5} M and the ionic strength was set to be 0.1 M. No additional ligands were included; therefore, only hydroxo species are expected. The figure shows that the predominant species are the same in every case. However, some small differences can be observed. The causes for these differences cannot be discussed here. It may be connected to extrapolations in the ionic strength or to different database sets.

An important fact is that the uncertainties of the measurements have to be included in speciation observations and calculations [60, 61].

Most of the following speciation diagrams have been calculated with the computer code MEDUSA, because of the easy handling of this code. The use of EQ 3/6 will be noticed in the diagrams. In addition, if not noticed the ionic strength for these calculations was set to be 0.1 M.

5 ACTINIDE ELEMENTS

5.1 Actinium

A. Debierne in 1899 and F. Giesel in 1902 discovered actinium independently. The most stable isotope of actinium is Ac-227, a beta emitter, with a half-life of 21.6 years. Actinium is an element of group IIIb. It can be seen as the prototype of the actinide series of elements. The chemical behavior of actinium is similar to that of lanthanum.

Actinium undergoes coprecipitation with any quantitative lanthanum carrier [62]. On the solubility of the hydroxide, $Ac(OH)_3$ has been reported by Ziv and Shestakova in 1965 [63]. They mentioned an aging effect on the solubility of freshly prepared precipitates explained by radiolysis effects especially of absorbed ^{227}Th.

Stability constants of actinium toward complexing ligands are quite similar to that of lanthanum [64]. However, only few datasets can be found for the complex formation of actinium. At an ionic strength of 0.1 M $LiClO_4$, the formation constant of the first hydroxo species is given to be $\log *\beta_{11} = -8.5$ [65]. The solubility product was determined to be $\log K^{\circ}_{sp} = -18.68$ [58]. Up to now, carbonate data are not available.

Figure 2.23.2 shows the estimated species distribution for Ac^{3+} as function of pH ($[Ac^{3+}] = 1 \times 10^{-6}$ M; I = 0.1 M). Besides $Ac(OH)^{2+}$, the stability constants were estimated from the La^{3+} data. The formation of a solid phase was excluded because the solubility product probably is only valid for crystalline phases.

The phosphate complexation of actinium has been studied by use of a liquid cation exchanger [66]. The data were derived at an ionic strength of 0.5 M. The complex formation occurs between Ac^{3+} and $H_2PO_4^-$ at pH 2.0 and 3.0. The formation

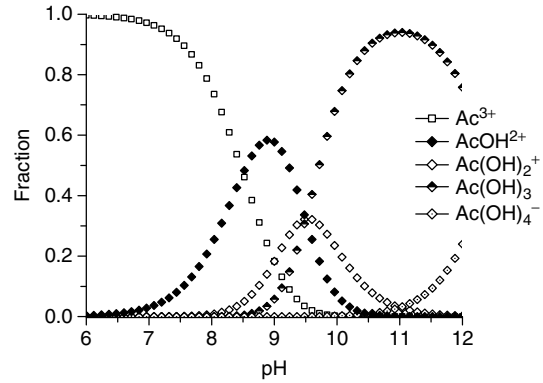

Figure 2.23.2. Estimated speciation of Ac^{3+}, stability constants [64].

of other phosphate complexes is negligible under these conditions. The formation constant for the 1 : 1 complex has been assigned to be $\log \beta_{11} = 38.8 \pm 5$.

5.2 Thorium

Thorium and the next actinide element protactinium occur naturally in association with uranium. J. Berzelius discovered the element thorium in 1828. Up to now, 25 isotopes of thorium are known. The atomic masses range from 212 to 236. It is one of the naturally occurring radioactive elements, and Th-232 has a half-life of 1.4×10^{10} years. Thorium does only exist in the tetravalent oxidation state.

Only thorium and uranium can be handled in the laboratory in weighable amounts (1000 Bq Th-232 with its natural decay products in equilibrium) without additional precautions [67]. This reflects in a large number of contributions in the literature to the complex formation of these two elements.

The hydration number of thorium(IV) was selected to be 10 ± 1 by considering previous structure information and results from EXAFS measurements [21].

5.2.1 Solubility and inorganic species

Thorium solubility has been studied under different atmospheric conditions [68]. On the basis

Table 2.23.4. Reaction constants of thorium dissolution equilibria [68].

Reaction	Equilibrium constant
$ThO_2 + 4H^+ \leftrightarrow Th^{4+} + 2H_2O$	Log $K^\circ_{sp} = 7.31 \pm 0.3$
$ThO_2 + H^+ + H_2O + CO_3^{2-} \leftrightarrow Th(OH)_3CO_3^-$	Log $\beta^\circ_{131} = 6.78 \pm 0.3$
$ThO_2 + 4H^+ + 5CO_3^{2-} \leftrightarrow Th(CO_3)_5^{6-} + 2H_2O$	Log $\beta^\circ_{105} = 39.64 \pm 0.4$

of the results from solubility measurements of microcrystalline ThO_2, the authors concluded that mixed hydroxo-carbonate species are formed in the solution. The data were extrapolated to infinite dilution. In Table 2.23.4, the constants are summarized.

The solubility products of actinides compounds are important thermodynamic data for understanding the solution chemistry of these elements. Several authors have studied precipitates of $Th(OH)_4$(am). However, the results vary over about 3 orders of magnitude if compared to ThO_2(cr). Various methods are used to obtain these data. Laser-induced breakdown detection is used to verify the solubility data of amorphous Th(IV)-hydroxide [69].

It could be shown by this method that earlier published data, which show a big discrepancy to the solubility of crystalline ThO_2, have included polynuclear species or very small Th(IV) colloids. The solubility product was calculated using the specific ion interaction theory (SIT) coefficients to be log $K^\circ_{sp} = -52.8 \pm 0.3$. It is based on equilibrium between dissolved Th(IV) and colloidal thorium dioxide particles. However, this value was changed later to log $K^\circ_{sp} = -47.8 \pm 0.3$ [70]. The authors give no explanation for this change. In the work published in 2002 [71], only the last dataset was used. A set of hydrolysis constants is also summarized in this work. Using these data for the system Th(IV)-hydroxide, a speciation diagram is shown, depicting the species distribution in a carbonate-free solution. Polynuclear species such as $Th_4(OH)_8^{8+}$ are also present in the solution.

In Figure 2.23.3, the species distribution of a 5×10^{-5} M Th^{4+} solution as function of pH is shown. Comparing this figure with the species distribution calculated for a 1×10^{-6} M Th^{4+} solution (Figure 2.23.13), the pH for the formation

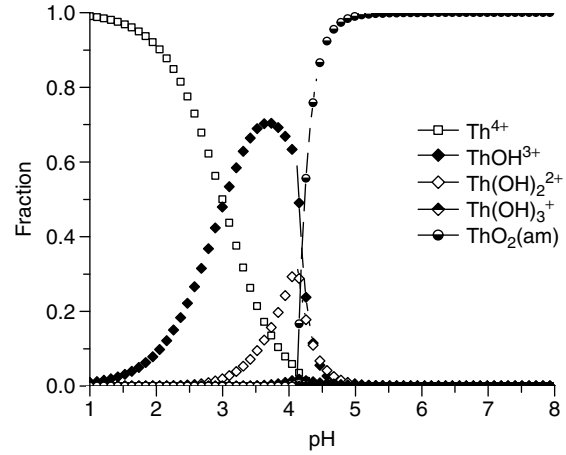

Figure 2.23.3. Species distribution of Th^{4+} as function of pH (5.0×10^{-5} M).

of amorphous ThO_2(am) is shifted by about 0.6 pH units. In addition, formation of the third hydroxo species is not expected at this higher concentration.

Several authors have studied the hydrolysis of thorium. Because of the tetravalent oxidation state of this element, the formation of hydrolyzed species starts already at low pH. The formation of colloidal species is known but not understood completely. Lieser and Hill [72] report on the formation of colloids in natural groundwater. It was found that silicic acid acts as a carrier for thorium. After removing of these colloids by ultrafiltration, new colloids and particles are formed, bearing Th. The concentration of colloids in these fractions depends on the salinity of the groundwater.

One problem in speciation calculations is the uncertainty of the available stability constants of the formed actinide complexes [61]. As an example, the speciation of Th^{4+} is used. Without inclusion of uncertainties, $ThOH_3^+$ and $Th(OH)_4$ dominate the speciation of Th^{4+} in the range pH 5 to 6.5. Including the uncertainty of the thermodynamic data for the hydrolysis of thorium, the species $Th(OH)_2^{2+}$ and $Th(OH)_3^+$ may become more important in the species distribution around pH 6.

The published data for the stability constants of the hydroxo species of tetravalent actinides

differ depending on the method of estimation. As an example in Table 2.23.12, the data from Neck and Kim [70] and Moriyama *et al*. [73] are summarized.

The carbonate speciation of thorium is not completely investigated up to now. There are only data published on the limiting complex formation of $Th(CO_3)_5^{6-}$ with $\log \beta_{15} = 26.3 \pm 0.2$ at an ionic strength of 2.5 M and $\log \beta_{15} = 26.2 \pm 0.2$ at an ionic strength of 1.0 M [68, 74].

Complex formation data with phosphate are provided by Elahyaoui *et al*. [75] and Moskvin [76]. Phosphate is besides hydroxide and carbonate one of the most important inorganic ligands in nature. Thorium forms several complexes with phosphate anions [75]. It is not possible to derive stability constants because of lack of information about the calculated ionic strength of the experiments. From their data, the authors claim the following species: $Th(H_2PO_4)_2^{2+}$; $Th(H_2PO_4)_4$; $Th(OH)(H_2PO_4)^{2+}$; $Th(OH)_2(H_2PO_4)^{+}$; $Th(OH)(H_2PO_4)_2^{+}$; $Th(OH)(H_2PO_4)_3$ and a seventh complex of unclear stoichiometry.

The study of the complex formation of tetravalent actinides with phosphates remains problematic because of the low solubility of the actinide phosphate compounds. By use of an extraction technique, the formation constants of Th(IV) with HPO_4^{2-} were obtained [77]. Because of experimental difficulties, the authors claim the formation of a $Th(HPO_4)_2$ precipitate; the data will be not repeated here.

5.2.2 Species with organic ligands

As citrate is expected among the organic ligands in the waste repository, waste isolation pilot plant (WIPP) studies of the complex formation of actinides with this ligand are necessary [78]. Three thorium-citrate complexes are determined. The data were obtained from solvent extraction studies at different ionic strength up to 5 M NaCl and 14 M $NaClO_4$. Using the recommended SIT formalism [50], the data were extrapolated to infinite dilution. The formation constants for $Th(Cit)^{+}$, $ThH(Cit)^{2+}$ and $ThH_2(Cit)_2$ are $\log \beta^\circ = 13.7$, $\log \beta^\circ = 16.6$ and $\log \beta^\circ = 31.9$, respectively. The errors are given to be ± 0.1 in all cases. The authors conclude that this complex formation may increase the concentration of Th(IV) in the solution.

The influence of the ionic strength on the stability constants has been studied in many cases. Erten *et al*. [79] studied the complex formation of oxalic acid Th(IV) at ionic strength between 1 and 9 M. The extended SIT analysis results in the following formation constants.

$$\begin{aligned} Th(HC_2O_2)^{3+} \quad & \log \beta_{111} = 11.0 \\ Th(C_2O_2)^{2+} \quad & \log \beta_{101} = 9.8 \\ Th(HC_2O_2)_2^{2+} \quad & \log \beta_{122} = 18.13 \\ Th(C_2O_2)_2 \quad & \log \beta_{102} = 17.5 \end{aligned}$$

A potentiometric investigation of the complex formation of malonic acid with thorium was performed at an ionic strength of 1 M [80]. The stability constants for the thorium species are $\log \beta_{11} = 7.47 \pm 0.03$, $\log \beta_{12} = 12.79 \pm 0.07$ and $\log \beta_{13} = 16.28 \pm 0.28$.

Cacheris and Choppin [81] have studied the thorium humate speciation. The authors conclude from their kinetic measurements that the thorium may be bond to at least seven different binding sites. These can be divided into two classes. In the first group are four pathways with rate constants that are invariant with the pH. These dissociation rate constants were found to be the largest in this system. The slower three components are characterized by rate constants that are dependent on pH.

An overview of some data on the complex formation of actinides with humic substances is given by Moulin [82]. Data are listed for the elements Th^{4+}, UO_2^{2+} and Am^{3+}. Some additional information on hydroxo and carbonato complexation is also included. Species distributions for these three actinide ions are given including both hydrolysis and carbonate complexation. It has to be noticed that competitive metal ions such as calcium and aluminum are included. Two models for description of the complexation behavior are used: a single-site model and Choppin's complexation model.

5.2.3 Thorium in the environment

As thorium belongs to the natural actinides, this element occurs in the geosphere in a large number of minerals. Frondel [83] gives a systematic overview of the mineralogy of thorium.

The geochemistry of thorium has been summarized in the EPA-report [84]. The authors used the program code MINTEQA2 and provide speciation diagrams for Th^{4+} assuming a water composition given by Hem [85]. For Th^{4+} depending on the pH, the free thorium fluoride, hydrogen phosphate and mixed hydroxo-carbonate species were found.

Data for modeling of the migration of thorium in clay minerals (bentonite) are provided by Torstenfelt [86]. As the diffusivity is found to be less than 7.7×10^{-15} $m^2\,s^{-1}$, the author concludes that the mobility is extremely slow, about 3 orders of magnitude lower than for fission products. The low mobility is explained by the fact that Th^{4+} is extensively hydrolyzed and does not form any carbonate complexes.

5.2.4 Thorium in biological systems

The tendency of actinides to form complexes controls the behavior of actinides in blood. Plasma has been found to be the main transport chain in blood [87]. The actinide element Th(IV) forms strong complexes with transferrin. However, the formation strength and probably the mechanism differ between the actinides. Studies have also shown that a second anion like bicarbonate is necessary for the formation of the transferrin species. Thorium has been found to form a di-Th-transferrin complex, where the two Th atoms are bond to two different sites. It is suggested that Th is bond as monohydroxide to the transferrin. Slight decrease of the pH changes the complex formation rapidly.

5.3 Protactinium

K. Fajans and O.H. Gohring describe the discovery of protactinium (Pa-234) in 1913. They gave the new element the name brevium. In 1918, O. Hahn and L. Meitner have isolated the longer living isotope Pa-231. Pa-231 has a half-life of 32,700 years and is an extremely rare naturally occurring element. Protactinium exists in the pentavalent and in the tetravalent oxidation state.

Only a few studies on protactinium speciation are published. This may be due to the extreme rareness of this element. In addition, protactinium has no importance in the nuclear fuel cycle.

5.3.1 Protactinium(IV)

Protactinium exists in solution in two oxidation states, Pa(IV) and Pa(V). In both oxidation states, protactinium hydrolyzes easily. Because of the tendency to oxidize in aqueous solution, studies of the speciation of Pa(IV) did not yield reproducible results. The hydrolysis is somewhat less dominant than for Pa(V). The species formed in solution are $Pa(OH)^{3+}$, $Pa(OH)_2{}^{2+}$, $Pa(OH)_3{}^{+}$, and $Pa(OH)_4$ (see Fig. 2.23.4). The formation constants at an ionic strength of 3 M are log $K_1 = -0.14$, -0.52 and -1.77, respectively [88].

However, there is a discussion of the stoichiometry of the second hydroxo species. The suggestions to its stoichiometry are $Pa(OH)_2{}^{2+}$ [89] and PaO^{2+} [90]. The stability constants estimated by a hard sphere model [73] are summarized in Table 2.23.12. In the series of tetravalent actinide ions, the data for the protactinium species show

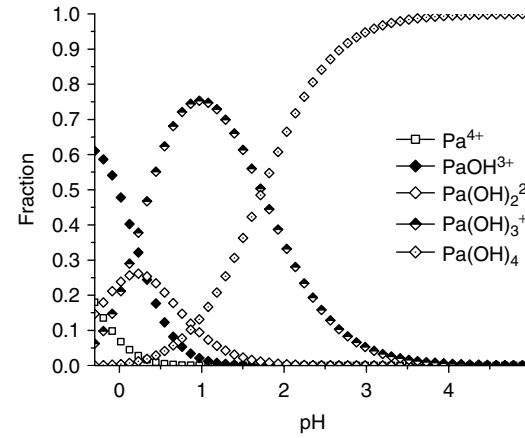

Figure 2.23.4. Species distribution of Pa^{4+} (1.0×10^{-6} M Pa^{4+}, I = 3.0 M) as a function of pH.

a deviation if they are compared to the analogous thorium and uranium species.

Only little information about complex formation is available. Data for the formation of $PaCl_2^{2+}$; $PaSO_4^{2+}$ $Pa(SO_4)_2$, PaF^{3+} and PaF_2^{2+} in 3 M solution are reported by Guillaumont [88].

5.3.2 *Protactinium(V)*

In solutions with >3 M H^+, the species PaO^{3+} is suggested. If the concentration of H^+ is decreased in a first hydrolytic reaction, $PaO(OH)^{2+}$ is formed. The next step of hydrolysis is the formation of $PaO(OH)_2^+$, starting at about 1 M H^+. This species dominates at pH ~3 the speciation of Pa. $Pa(OH)_5$ becomes important at pH around 5, but if the Pa concentration is close to the saturation limit polynuclear species are formed and precipitation occurs. In alkaline solutions, small amounts of $Pa(OH)_6^-$ are formed in solution.

It is important to notify that the hydrolysis of protactinium(V) is different from that of other pentavalent actinide ions. In the case of Pa, the usual form MO_2^+ could not be confirmed up to now. For the hydrolysis of this ion, the reactions are pointed out to be:

$$PaO(OH)^{2+} + H_2O \leftrightarrow PaO(OH)_2^+ + H^+ \quad (2.23.3)$$

$$PaO(OH)^{2+} + 3H_2O \leftrightarrow Pa(OH)_5 + 2H^+ \quad (2.23.4)$$

with formation constants of $\log \beta_{1,2} = -1.05$ (reaction 2.23.3) and $\log \beta_{1,5} = -5.55$ (reaction 2.23.4) at an ionic strength of 3 M [91, 92]. The calculated speciation is shown in Fig. 2.23.5.

Recently, D. Trubert and coworkers [93] published new results of studies on hydrolysis of Pa(V). The hydrolysis constants at 25 °C are found to be $\log \beta_{1,2} = -2.0 \pm 0.15$ and $\log \beta_{1,5} = -7.8 \pm 0.45$. The species distribution then results in a shift of the maximum concentration of the $PaO(OH)_2^+$ to about pH 4, and $Pa(OH)_5$ reaches a fraction of 1.0 at about pH 8.0. There is no explanation for the discrepancy

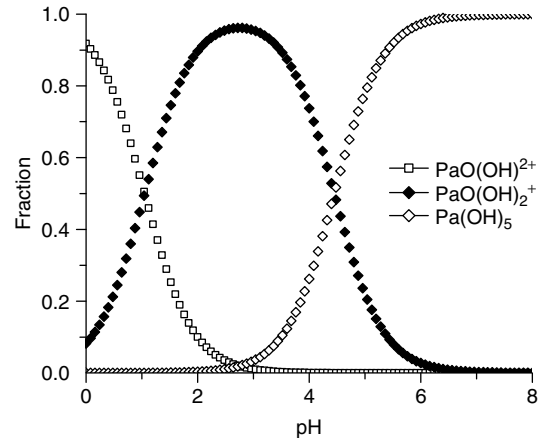

Figure 2.23.5. Hydroxo species of Pa^{5+} (1.0×10^{-6} M; I = 3 M), stability constants [91].

in the datasets at the moment. Besides this, experiments at elevated temperatures were also done to obtain thermodynamic data [94, 95].

Torstenfelt [86] performed a study on the migration of protactinium in clay. Pa adsorbs strongly onto bentonite with a K_d of 5 $m^3\,kg^{-1}$, which is in contrast to neptunium in the same oxidation state. The diffusivity D_a is assigned to be 6.3×10^{-13} $m^2\,s^{-1}$. However, this value implies that the mobility of this ion may be greater than its self-diffusion in water.

5.4 Uranium

Uranium was discovered first by Klaproth in 1789. Peligot isolated the pure metal in 1841. Naturally occurring uranium contains the isotopes ^{238}U (99.2830% by weight), ^{235}U(0.7110%), and ^{234}U(0.0054%). U-238 has a half-life of 4.51×10^9 years. Uranium forms many minerals in nature; most of them show bright yellow colors and have fluorescence properties. The abundance of uranium on earth is considered to be in the same order like molybdenum or arsenic [96].

Uranium exists in four oxidation states. Uranium(III) is only stable in nonaqueous environments and plays therefore no role in environmental speciation studies. Under reducing conditions, uranium(IV) is formed. In aqueous solutions, uranium(V) disproportionates rapidly into uranium(IV)

and uranium(VI). Hexavalent uranium exists only as dioxocation.

5.4.1 Uranium(IV)

A hydration number of 10 ± 1 for uranium(IV) was assigned considering structure information and results from EXAFS measurements [97, 21].

Uranium occurs in nature in primary deposits as UO_2, but nuclear fuel also consists of uranium oxide.

The solubility product of the amorphous hydroxide is determined to be $\log K^{\circ}_{sp} = -54.5 \pm 1.0$ [98]. The stability constants of the hydroxo species are summarized in Table 2.23.12.

The solubility of the actinide oxides is an important factor for the availability and transportation of actinide ions. The solubility product of UO_2xH_2O has been found to be $\log K^{\circ}_{sp} = -55.8 \pm 1.0$ [99]. The authors concluded that the measured value is lower than expected from theoretical calculations. However, the authors used a UV-VIS spectrophotometer for the detection of the uranium(IV) species in the solution.

The limiting carbonate complex is $U(CO_3)_5^{6-}$, its stability constant was assigned to be $\log \beta_{15} = 34.0 \pm 0.9$ [50].

The complex formation of uranium(IV) with arsenate and phosphate may become important only under reducing conditions. Such conditions may exist in a waste repository. The stability constants for the first complexation step have been studied [100]. In the system uranium(IV) – phosphoric acid, the stability constant for the formation of $U(H_2PO_4)^{3+}$ was assigned to be $\log \beta^{\circ}_{121} = 25.25 \pm 0.13$. For the arsenate system, the formation constant was derived to be $\log \beta^{\circ}_{121} = 23.94 \pm 0.08$. Speciation calculations show that under comparable solution conditions, the amount of the phosphate species is about 5% higher than the arsenate species.

The complexation constants of actinides are sometimes explained by use of a simple hard sphere model [101, 73]. In this model, the effective charges of the actinide central ion were used. By use of this model, the formation of carbonate species can be well described.

Laser-induced spectroscopic studies of uranium(IV) also showed fluorescence properties of this element in this oxidation state [102]. Because of the low detection limits of photon counting methods and despite the short fluorescence lifetime, an increase of speciation studies of this tetravalent ion can be expected.

5.4.2 Uranium(VI)

5.4.2.1 Solubility and inorganic species

A recent study of the hydrolysis of uranium(VI) has been performed by Brown [103] in 0.10 M $NaClO_4$ and KCl and in 1.0 M KNO_3 exploiting potentiometric measurements. In the solutions, the species UO_2OH^+, $(UO_2)_2(OH)_2^{2+}$, $(UO_2)_3(OH)_4^{2+}$ and $(UO_2)_3(OH)_5^{+}$ were determined. However, in the KNO_3-containing solutions, additionally the $(UO_2)_4(OH)_7^{+}$ species was observed. The formation constant for this species has been determined to be $\log \beta_{47} = -22.76$ in 0.1 M KNO_3 and the extrapolation to 1M KNO_3 results in $\log \beta^{\circ}_{47} = -21.9 \pm 1.0$. A species distribution at a total uranium concentration of 5×10^{-5} M is shown in Fig. 2.23.6. However, at high uranium concentrations the species distribution in the mid pH range is dominated by the $(UO_2)_4(OH)_7^{+}$ species [50].

The influence of the temperature on the hydrolysis of the uranylion was studied by Eliet [104]. Meinrath [60] gives an overview of the aquatic chemistry of uranium in the environment. This report reviews the hydrolytic behavior of uranium, mostly from UV-VIS spectroscopic data.

The hydroxo species of actinides often show the formation of ternary complexes. This is known from the carbonate system. The formation of ternary sulfate species of uranium(VI) was studies by Moll *et al.* [105]. By use of ^{17}O-NMR spectroscopy and potentiometric titration, the authors could confirm the formation of the species $(UO_2)_2(OH)_2(SO_4)_2^{4-}$, $(UO_2)_3(OH)_4(SO_4)_3^{4-}$, $(UO_2)_4(OH)_7(SO_4)_4^{7-}$ and $(UO_2)_5(OH)_8(SO_4)_6^{10-}$. These species exist at relatively high concentrations of uranium and sulfate in solution. Comarmond and

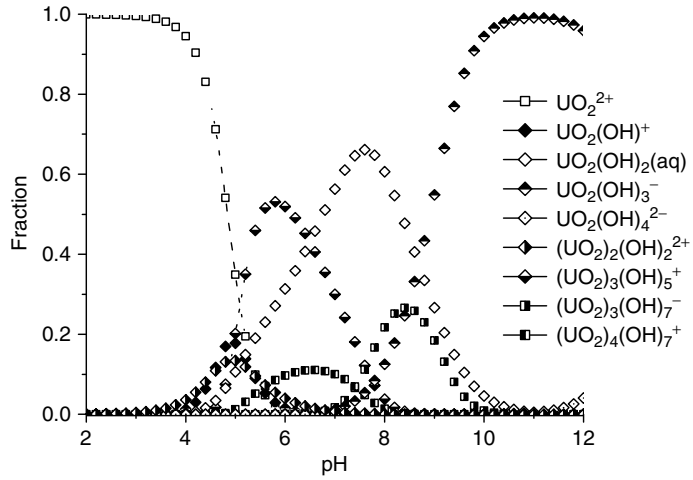

Figure 2.23.6. Species distribution of uranium(VI) ($[UO_2^{2+}{}_{tot}] = 5.0 \times 10^{-5}$ M, calc. with EQ 3/6), stability constants [50].

Brown [106] have given independent proof for the existence of these species.

The formation of uranium species has been studied in the temperature range up to 200 °C and pressures of 40 MPa [107]. It could be shown that the species distribution of the hydroxo compounds strongly changes with increasing temperature. For example, $UO_2(OH)^+$ is formed to about 10% in a 1×10^{-4} M uranium solution at pH 5. If the temperature is increased to 100 °C, the same species is formed to about 70%, and the pH at which the maximum occurs decreases to pH 4.3. In the sulfate system, a shift of the formation of the UO_2SO_4 species to lower SO_4^{2-} concentrations with increasing temperature was observed. The influence of the temperature on the formation of fluoride species is much less than for hydroxides and sulfates. Therefore, at higher temperatures and low fluoride concentrations the formation of hydroxo species occurs.

The advantages of laser-induced fluorescence spectroscopy have been demonstrated several times. The different spectra and fluorescence lifetimes of the uranium species make the determination of multicomponent systems possible. The most impressive example is the direct speciation of uranium(VI) at pH 4. The fluorescence spectrum of the first hydrolysis species is shifted by about 10 nm compared to the free uranyl ion. In addition, the fluorescence lifetime is more than 1 order of magnitude increased. Because of these properties, extremely low concentrations of the first hydrolysis species can be detected in a superior strength of free uranyl ions [108].

The single component fluorescence spectra of the hydrolysis species $(UO_2)_2(OH)_2^{2+}$, $(UO_2)_3(OH)_5^+$ and probably UO_2CO_3 have been described by Kato [109]. The fluorescence properties of some uranium(VI)-carbonate species are not known completely up to now. However, it is commonly accepted that the species $UO_2(CO_3)_2^{2-}$ and $UO_2(CO_3)_3^{4-}$ do not emit any fluorescence at room temperature. Therefore, only the absorption spectra can be used for the direct determination of these species in nature. The complex formation of uranium with carbonate at low uranium concentrations was confirmed by LPAS [35]. The formation constant was found to be in good agreement with the data reviewed in the NEA database [50]. The method was applied for the direct detection of such species in tailing water from a uranium-milling site. It could be shown that the $UO_2(CO_3)_3^{4-}$ species can be detected in a concentration range of about 2.5×10^{-5} M without any pretreatment. As in the original water, other absorbing species are present, like organic carbon with a concentration of 132 mg L^{-1}, and the result demonstrates the power of this method for direct speciation.

UV-VIS absorption spectra were recorded in the system $UO_2^{2+}/HCO_3^-/CO_3^{2-}/OH^-$. From the data, the single component spectra of the species UO_2CO_3, $UO_2(CO_3)_2^{2-}$, $UO_2(CO_3)_3^{4-}$ and $(UO_2)_2(OH)_2^{2-}$ were derived [110]. The obtained formation constants at an ionic strength of 0.1 M for the carbonate species are determined to be $\log \beta_{101} = 8.81 \pm 0.04$, $\log \beta_{102} = 15.5 \pm 0.4$ and $\log \beta_{103} = 21.74 \pm 0.22$, respectively. Comparing these data with the NEA database [50], it seems that there is a discrepancy for the species UO_2CO_3 and $UO_2(CO_3)_2^{2-}$. However, the authors mention that the exact determination of the formation constant of $UO_2(CO_3)_2^{2-}$ remains difficult because of its minor occurrence.

As carbonate can from strong complexes with several actinides, it may be possible that these complexes increase the solubility of oxides and hydrous oxides [111]. The solubility of UO_2(am) was studied in several alkaline- and carbonate-bearing solutions [112]. The species in the solution, being in equilibrium with the solid phase, were identified to be $U(CO_3)_5^{6-}$ and $U(OH)_2(CO_3)_2^{2-}$. By use of the solubility product of UO_2(am) ($\log K_s = -53.44$; [106]), the formation constants of these two species were assigned to be $\log \beta^\circ_{105} = 31.29$ and $\log \beta^\circ_{122} = 41.33$, respectively. However, the formation constant for $U(CO_3)_5^{6-}$ shows a large difference to the data reported in the NEA database [50]. The authors explain this by the thermodynamic models (Pitzer model vs SIT theory) used for the calculations.

In the nineties, first hints on as yet unknown aqueous species in natural systems can be found [113]. The stoichiometry of the species $Ca_2UO_2(CO_3)_3$(aq) was first described by Bernhard *et al.* [114]. The most important property of this species, the fluorescence emission of a tricarbonate species, made the detection of this species possible. Because of these properties, this species could be identified in the calcium- and carbonate-rich mining and seepage waters of the mining region of Schlema, Germany. However, the calculation of the formation constant is rather difficult because of problems in the determination of the fluorescence yield of this species. The formation constant of this species at infinite dilution has been estimated by Kalmykow and Choppin [115] to be $\log \beta^\circ_{213} = 29.8 \pm 0.7$. As the first data for the formation constant are quite erroneous, new series of fluorescence measurements and EXAFS studies was done [116]. They used two analytical approaches with time-resolved laser-induced fluorescence spectroscopy (TRLFS) species detection: i) titration of a nonfluorescent uranyl tricarbonate complex solution with calcium ions, and ii) variation of the calcium concentration in the complex by competitive calcium complexation with Na_2EDTA. The formation constants determined from the two independent methods are (i) $\log \beta^\circ_{213} = 25.26 \pm 0.71$ and (ii) $\log \beta^\circ_{213} = 25.57 \pm 0.37$. Kalmykow and Bernhard used for the estimation of the formation constants at infinite dilution different methods (SIT theory and Davies equation). This may explain the difference in the datasets. Fig. 2.23.7 shows the influence of this species on the species distribution of uranium(VI) in carbonate and calcium containing solutions.

A study of the complexation of uranium with phosphate at low concentrations was performed to avoid the problems of precipitation of uranylphosphates [117]. For $UO_2(HPO_4)$, the formation constant of $\log \beta^\circ = 19.53$ and 19.87 agrees with data obtained from the literature [118]. The obtained constant for $UO_2(H_2PO_4)^+$ is slightly lower and for $UO_2(H_2PO_4)_2$ a larger value was determined. A possible explanation for these differences may be the extrapolation procedure to infinite dilution.

Studies on the kinetics of the complex formation of actinides are very rare. The formation of uranium(VI)–diphosphonic acid species has been studied by stopped flow spectrophotometry [119]. Arsenazo(III) was used as indicator for the noncomplexed uranium(VI). In all experiments, a first-order rate law was found to describe the kinetics of the complex formation.

The solubility product of uranyl silicate (soddyite) was determined to be $\log K^\circ_{sp} = 6.03 \pm 0.45$ under N_2 atmosphere and $\log K^\circ_{sp} = 6.15 \pm 0.53$ in air [120]. In the solid phase, no change and no formation of a secondary phase was detected. The solution species were calculated to be UO_2^{2+} at pH 3, UO_2^{2+} and $(UO_2)_3(OH)_5^+$ at pH 4.6, $UO_2(OH)_2$ at pH 6 and 8 and $UO_2(OH)_3^-$ at pH 9.

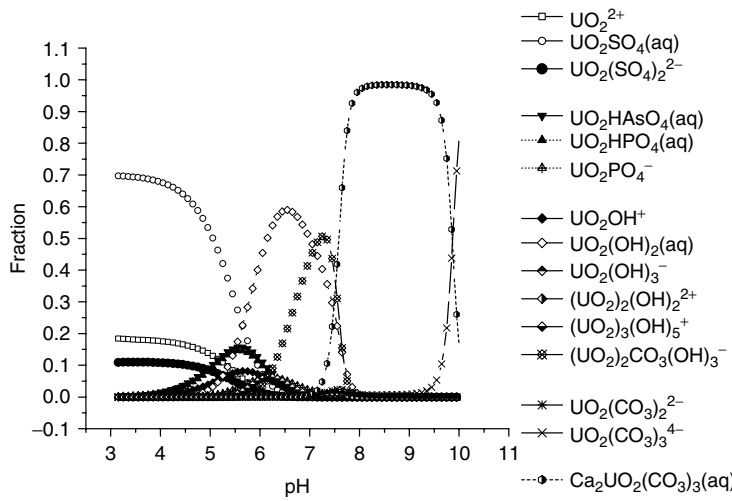

Figure 2.23.7. Species distribution of uranium(VI) in natural, mining related waters with Ca concentrations, calc. with program EQ 3/6, analytical data, see Table 2.23.6.

The formation of dissolved uranylsilicate species should be negligible. The fluorescence lifetimes obtained from TRLFS measurements have shown the existence of UO_2^{2+} at pH 3 and of hydrolysis products at higher pH.

Species of silicic acid are common in aqueous solutions. The formation of the $UO_2(OSi(OH)_3)^+$ was confirmed by spectrophotometry [121]. The formation constant for the reaction (2.23.5)

$$UO_2^{2+} + Si(OH)_4 = UO_2(OSi(OH)_3)^+ + H^+ \quad (2.23.5)$$

was assigned to be $\log K_1 = -2.92 \pm 0.06$. Calculations of the species distribution show a maximum amount of the formed species at pH 6 and under conditions for solution undersaturated with amorphous silica of 50%.

Satoh and Choppin [122] report on the interaction of uranium with silicic acid. By use of a solvent extraction technique, the formation constant $\log *\beta_{11} = -2.44 \pm 0.12$ was determined. From the evaluation of their data, the authors assume that polymeric silicate species are not formed in the solution or that they have the same binding strength toward uranium as the monomeric silicic acid.

As dissolved silica is an important ligand in natural systems, the formation of actinide complexes may contribute to the mobility of these elements. The formation constant of uranium(VI) was determined to be $\log \beta^\circ = (-1.67 \pm 0.20)$ [123]. Additional literature data are $\log \beta^\circ = (-2.25 \pm 0.13)$ [124] and $\log \beta^\circ = (-2.70 \pm 0.34)$ [125]. Compared to data in the literature [122, 124], this formation constant leads to a higher amount of silicate species in solution.

Chloride and nitrate show only a small tendency to complex with uranium. At highly concentrated salt solutions, this complexation may become remarkable. The formation of UO_2Cl^+ and $UO_2NO_3^+$ was studied at ionic strength of 3.0 to 9.0 M for the chloride system and 7.0 M for the nitrate system [125]. It was found that the derived formation constants in the nitrate system agree with predicted data from the SIT theory. The formation constants for the chloride complexation are smaller than expected for ionic strength higher than 6.5 M.

5.4.2.2 Species with organic ligands

The complex formation of oxalic acid toward U(VI) has been studied at ionic strength between 1 and 9 M [79]. The following formation constants result from extended SIT analysis.

$$UO_2(HC_2O_2)^+ \quad \log \beta = 5.60$$

$$UO_2(C_2O_2) \quad \log \beta = 5.60$$

To simulate the complexation of actinides with polyelectrolytes like humic substances, simple organic ligands were often used. Carboxylic and phenolic groups represent this functionality. The structure of humic substances contains aliphatic and aromatic functional groups. Malonic acid was used as an aliphatic carboxylic model ligand. The complexation of this ligand was studied by TRLFS [126]. The complex stability constants were assigned to be $\log \beta_{11}^{\circ} = 4.48 \pm 0.06$ and $\log \beta_{12}^{\circ} = 7.42 \pm 0.06$. The thermodynamic data for the formation of the 1 : 1 species are comparable to literature data, the stability constant of the 1 : 2 complex was found to be 1 order of magnitude lower. A possible explanation for this difference may be the higher uranium concentration used in the potentiometric studies.

The potentiometric investigation of the complex formation [80] was performed at an ionic strength of 1 M. The results are $\log \beta_{11} = 5.42 \pm 0.02$ and $\log \beta_{12} = 9.58 \pm 0.15$.

In nature, alpha-substituted carboxylic acids are present as degradation products of wood material. Such compounds are also often used for separation processes of 4f and 5f elements. In the uranyl-α-hydroxycarboxylate system, a strong quenching process occurs on the fluorescence of the uranyl [127]. By use of the Stern–Volmer equation, this process can be described and at least complex formation constants can be derived from the fluorescence intensity of the noncomplexed uranyl ion. Other systems like uranium(VI)–α-aminoisobutyrate show no fluorescence quenching, and the concentration of the species in the solution can be determined directly by deconvolution of the time-resolved fluorescence spectra. From the TRLFS measurements, the stability constants were derived, and EXAFS studies were used to get information on the structure of the complex. A summary of the obtained data is given in Table 2.23.5.

Malonate may be an interesting ligand for actinide complexation. Absorption spectroscopy was used to obtain the formation constants [128]. It was pointed out that the fluorescence did not show shifts with increasing temperature. However, the intensity was decreased by 10 times from 25 to 70°. The formation constants are obtained at an ionic strength of 1.05 M. From the dependence on the temperature, the formation enthalpy and entropy has been derived. From EXAFS spectroscopy, the structure of the 1 : 1 complex was found to consist in two monodentate coordinations.

Humic substances may play an important role in the transportation of actinides under natural conditions. Choppin and Allard [129] summarizes that organic macromolecules could dominate the speciation of trivalent and tetravalent actinides. One possibility to model the functionality of humic acids (HA) may be the synthesis of such compounds in the laboratory to obtain a more uniform product.

The formation of humate species has been studied in actinide chemistry in the past years by many authors. The formation of such species is seen to be important in the transportation of actinides with groundwater of a waste repository. Many models have been developed to understand these phenomena [130, 131].

The study of the complex formation of the synthetic product with uranium leads to a complexation constant of $\log \beta = 6.16 \pm 0.05$ (pH 3.90 ± 0.05; I = 0.1 M $NaClO_4$) [132]. The results lead to the conclusion that such synthetic products may model the functionality of natural HA.

Besides carboxylic groups, humic substances also have phenolic OH groups. The complex formation of these functional groups is not well understood yet. By blocking the phenolic groups in HA [133], it should be possible to study the influence of these groups. Two of the three used

Table 2.23.5. Stability constants and structural data of complexes of uranium(VI) with alpha-substituted carboxylic acids [127].

Ligand	Stoichiometry	Stability constant $\log \beta_{11}$	Distance U–O_{eq} nm	Coordination
Glycolic acid	1 : 1	2.52 ± 0.20	0.238–0.240	Monodentate
α-Hydroxyisobutyric acid	1 : 1	3.40 ± 0.21	0.240–0.243	Bidentate
α-Aminoisobutyric acid	1 : 1	1.30 ± 0.10	0.239–0.240	Bidentate
α-Aminoisobutyric acid	1 : 2	2.07 ± 0.25	0.239–0.240	Bidentate

HA with this partly blocked OH groups have significantly lower loading capacities. However, the derived formation constants, exploiting the metal ion charge neutralization model [130], are in any case comparable.

To understand the complex formation of humic substances with actinides, several different approaches were used. Saito *et al*. [134] used the combination of excitation and fluorescence spectroscopy to get multidimensional fluorescence spectra. They found two excitation/emission peaks in their spectra. These are located at 450/520 nm and 250/475 nm. Adding uranium to the humic acid solution, the fluorescence of the ligand is quenched. This is used for the determination of the formation constant, exploiting the multisite Ryan–Weber model in combination with SIMPLISMA, a computer code to decompose complex matrices into two smaller ones. From their experimental data, the authors derived two apparent complex formation constants ($\log K_{app1} = 5.07 \pm 0.09$ and $\log K_{app2} = 4.70 \pm 0.20$) as well as the accompanying ligand concentrations ($2.24 \pm 0.09) \times 10^{-6}$ M and $(1.28 \pm 0.04) \times 10^{-6}$ M.

From this it was concluded that humic acid forms two complexes with uranium that can be distinguished by the two fluorescence emissions.

5.4.2.3 Uranium in the environment

5.4.2.3.1 Uranium minerals A wide variety of uranium minerals are known up to know [83, 135]. Many of them show fluorescence properties. For the development of a fluorescence database of uranium species, about 120 uranium minerals were studied [136]. This dataset can be used to identify unknown solution species. Among the studied minerals are also uranium(VI)-arsenates such as troegerite. The fluorescence properties were used to assign fluorescence emissions in solution to a formed $UO_2HAsO_4(aq)$ species [137].

Studies on minerals can be used to obtain information on the formation of species during weathering processes of ores bearing actinides and the formation of secondary minerals [138]. The formation of the mineral bayleyite was found to occur only under relatively extreme natural conditions. The solubility of the mineral phase is very high (54.70 ± 0.05 g L^{-1}), and it cannot be excluded that dissociation processes form species in solution different from the mineral composition.

The solubility of becquerelite ($Ca(UO_2)_6O_4(OH)_6 \cdot 8H_2O$) has been studied using synthetic and natural samples. The solubility product of synthetic samples was found to be $\log K^\circ_{sp} = -41.4 \pm 0.2$ [139] according to the equation (2.23.6)

$$Ca(UO_2)_6O_4(OH)_6 \cdot 8H_2O + 14H^+ \leftrightarrows Ca^{2+} + 6UO_2^{2+} + 18H_2O \quad (2.23.6)$$

However, this value is by several orders of magnitude different from a value obtained in a natural sample [140]. At the time of writing, this difference cannot be explained.

Torrero *et al*. [141] has compared the solubility of UO_2 and schoepite. Schoepite $UO_2(OH)_2 \cdot H_2O(s) \rightarrow UO_3 \cdot 2H_2O(s)$ has been formed during solubility experiments on the surface of $UO_2(s)$ at neutral pH. The uranium concentration in the solution was then controlled by the schoepite solubility. The solubility constants for the reaction (2.23.7)

$$UO_3 \cdot 2H_2O(s) + 2H^+ \leftrightarrow UO_2^{2+} + 3H_2O \quad (2.23.7)$$

are $\log K^\circ_{sp} = 5.73 \pm 0.28$ and $\log K^\circ_{sp} = 5.38 \pm 0.20$ for schoepite on UO_2 and synthetic schoepite, respectively. The authors agree with Silva [142] and Choppin and Mathur [143] that the formation constant listed in the NEA database [50] for the formation of the species $UO_2(OH)_2$ of $\log \beta_{1,2} < -10.5$ may be overestimated. More useful data are $\log \beta_{1,2} = -11.5$ [142] or $\log \beta_{1,2} = -12$ [143].

Solid phases of the type schoepite $UO_3 \cdot 2H_2O(s)$ transform easily in calcium or potassium containing solutions in to the minerals bequerelite ($CaU_6O_{19} \cdot 11H_2O$) or compreignacite ($K_2U_6O_{19} \cdot 11H_2O$).

The solubility of the formed minerals has been determined according to the reaction (2.23.8)

$$M_xU_6O_{19} \cdot 11H_2O + 14H^+ \leftrightarrow xM^+ + 6UO_2^{2+} + 18H_2O \quad (2.23.8)$$

The solubility constants are assigned to be $41.9 < \log K^\circ_{sp} < 43.7$ for bequerelite and $36.8 <$

$\log K^{\circ}_{sp} < 39.2$. The values are obtained from two runs, and the difference between these two experiments is explained by differences in the crystallinity of the solid phase.

The values for bequerelite are in the same order as the data obtained by Vochten and van Haverbeke [144]. They found the solubility product to be $\log K^{\circ}_{sp} < 43.2$.

The interpretation of solubility products obtained from minerals taken from nature is quite difficult. Casas *et al*. [140] report for the solubility product from natural bequerelite the value $\log K^{\circ}_{sp} = 29 \pm 1$. This is much lower than the data obtained from synthetic material. It was concluded that at low calcium concentrations in the solution, the mineral is thermodynamically more stable than expected previously. However, the authors cannot exclude an incongruent dissolution, as the Ca/U ratio was different from that in the solid phase.

Uranium minerals schoepite ($UO_3 \cdot 2H_2O$) and rutherfordine (UO_2CO_3) are often expected to be solubility-limiting phases in natural systems. However, several studies have shown that under different conditions, the minerals can be transformed to other compounds.

It could be shown that silica-containing solutions retard the schoepite–bequerelite transformation [145]. In contact with solutions containing Ca^{2+} and phosphate, it was found that schoepite can be transformed in a rapid and complex reaction into autonite.

Other authors have also described such alterations [118].

5.4.2.3.2 Uranium mining and milling Transportation of radionuclides has often been studied by investigation of natural analoga. In these cases, the behavior of naturally occurring radionuclides like uranium and thorium has been studied.

Natural analogue studies are a very useful scientific methodology to understand the processes, which can occur in waste repositories on a long time scale [146]. However, often only sum parameters are given. The analyzed concentrations for thorium are within the predictions. Uranium concentrations are at least 2 orders of magnitude lower than predicted.

The European Commission gives an overview on uranium mining and milling activities in Europe in 1996 [147].

By use of TRLFS, new soluble species were detected [116]. These species are important in the understanding of leaching and weathering processes in uranium mining and milling. Besides, this the study of the fluorescence properties of uranium minerals [136] leads to the detection of new complex species and their quantitative description [137].

The speciation of actinides is an inherent part for the description of their environmental and geochemical processes [148]. Variations in temperature and pressure occur in geochemical processes. The knowledge on changes in the speciation caused by the physical properties is therefore essential. The aqueous chemistry of actinides has been reported in innumerable papers and many reviews are available. However, many aspects of the chemistry of actinide species remain uncertain or unknown.

In the Krunkelbach Mine (Germany), four types of mine water are found: surface waters with isotope ratios $^{234}U/^{238}U > 1$ and uranium concentrations below 1×10^{-8} M. The second group are waters in contact with the ore zone, characterized by isotope ratios $^{234}U/^{238}U \sim 1$ and uranium concentrations from 5×19^{-6} M to 2×10^{-5} M. The speciation of these waters is mainly influenced by carbonate complexation. However, the majority of marine waters is dominated by phosphate species with uranium concentrations around 1×10^{-7} M and isotope ratios less than 1. The highest isotope ratios of about 1.2 were found in granite equilibrated mine waters with uranium concentrations of 3×10^{-7} M [149].

A study of mining related waters in Saxony and Thuringia (Germany) has shown several types of speciation in the waters [113, 114, 150]. Table 2.23.6 gives analytical data of four mining-related waters in Saxony. On the basis of the analytical data and by laser-induced spectroscopic measurements, the speciation of natural uranium-containing waters from mining areas was studied.

Table 2.23.6. Typical selected analytical element concentrations in mining-related waters [150].

Concentration 10^{-3} M	Seepage water Schlema	Mining water Schlema	Tailing water Helmsdorf	Mining water Königstein
Ca	7.8	6.9	0.3	5.9
Mg	17.1	11.6	0.9	0.7
Na	0.5	20.6	6.1	1663
U	0.009	0.021	0.025	0.073
As	0.01	0.03	0.52	0.01
SO_4^{2-}	25.6	20.7	35.6	23.9
PO_4^{3-}	<0.02	<0.02	0.29	<0.02
$CO_2/HCO_3^-/CO_3^{2-}$	0.45	3.9	10.3	<0.02
Cl^-	0.1	3.3	25.8	3.8
TOC/mg L^{-1}	1	6.2	13.2	3.5
PH	7.82	7.13	9.76	2.6

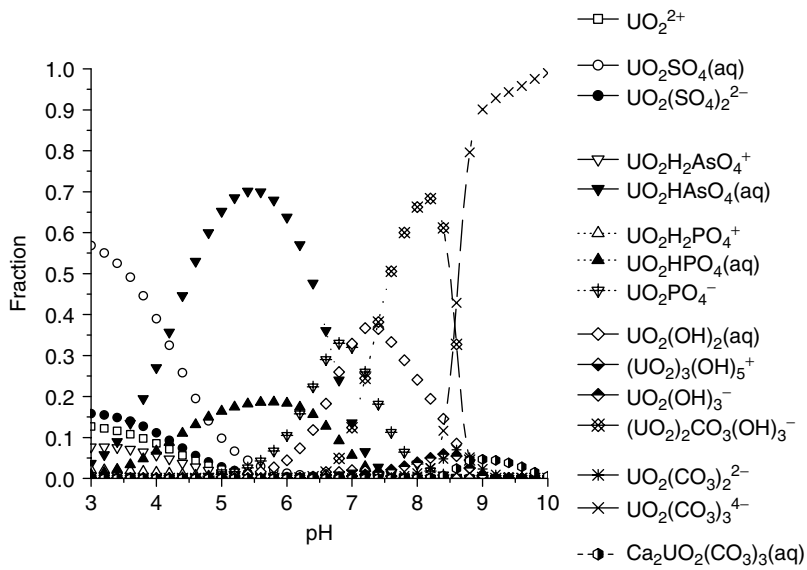

Figure 2.23.8. Calculated species distribution of uranium in surface water from a milling tailing (Helmsdorf), calc. with program EQ 3/6, stability constants [50, 116].

It is possible to distinguish among three types of uranium-contaminated waters:

1. Carbonate-rich waters with low calcium concentration; pH 9.8: main species $UO_2(CO_3)_3^{4-\bullet}$
2. Carbonate and calcium-rich waters at pH around 7: main species $Ca_2UO_2(CO_3)_3(aq)$.
3. Sulfate-rich waters at pH 2.6: main species $UO_2SO_4(aq)$.

These species are in agreement with calculated species distributions.

For confirmation of the species distribution as a function of pH, a series of fluorescence measurements has been carried out. Figure 2.23.8 shows the calculated species distribution of the tailing water. In Figure 2.23.9, the corresponding change in the fluorescence spectra are shown. Including the data for the complexation of uranium with arsenate [137], the calculated species distribution could be confirmed by deconvolution of the measured spectra.

In natural water, carbonate species are dominant. If the pH decreases, arsenate and phosphate

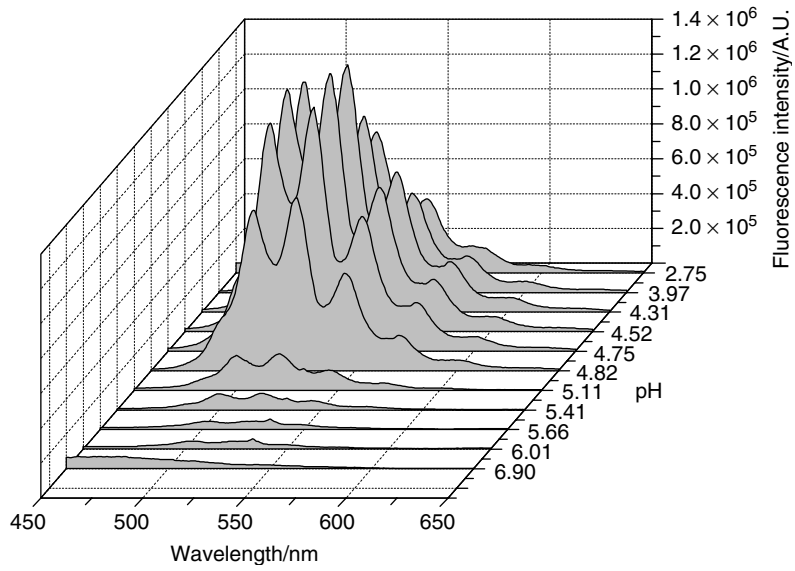

Figure 2.23.9. Fluorescence spectra of uranium(VI) species in the tailing water Helmsdorf as function of pH.

complexes play an important role in the species distribution. In the acid pH range sulfate species of uranium(VI) dominate.

Groundwaters show often redox potentials that assume the reduction of higher oxidation state of actinides. Uranium can be found in the oxidation states U(IV) and U(VI). Under reducing conditions, the uranium concentration in groundwater is very low, because of the low solubility of U(IV) compounds. In the natural system of the Palmottu site, several drill holes for groundwater sampling exist [152]. The measured redox potentials in waters from these boreholes are between -92 and $+55$ mV and the pH was found to be between 9.05 and 6.87. It was found that at redox potentials between -70 and $+55$ mV, the uranium is mainly in the oxidation state $+6$ (93 . . . 97%) and if the redox potential decreases a change in this ratio occurs. At -92 mV, 97% of the uranium exists in the oxidation state $+4$. Addition of acid or base to the original waters has shown that the observed Eh-pH relationship agrees very well with the theoretical behavior of the U(IV)/U(VI) redox pair. The redox potential of the $U(OH)_4(aq)/UO_2(CO_3)_3^{4-}$ couple can be expressed as given in equation (2.23.9).

$$\mathrm{Eh} = 0.410 - \frac{3 - 0.059\ \mathrm{pH}}{2} + \frac{0.059}{2} \times \log \frac{[UO_2(CO_3)_3{}^{4-}]}{[U(OH)_4(aq)]\bullet[HCO_3{}^-]^3} \quad (2.23.9)$$

In northern Australia in the Ranger Uranium Mine, contaminated excess water is sprayed on a 33 ha region [153]. This water contains about 1.3 mg L^{-1} uranium together with alkaline earth ions and sulfate. The pH of this water is about 8.0. Unfortunately, no carbonate content is listed in this paper. Adsorption experiments have shown that the uranium is retained in the top of the soil profile. The groundwater samples from this site have uranium concentration of about 7.8 μg L^{-1}.

The mine water chemistry is very complex. For the Ronneburg mining district (Thuringia, Germany), predictions for the contaminants have been made [154]. By use of a geochemical model (STEADYQL), the uranium concentration was estimated to be in the order of 2×10^{-6} M.

Laboratory studies were often used to characterize the formation of species and to test their mobility under environmental conditions. In these experiments, materials of natural origin were used. In a

study of the sediments of the Snake River (Idaho, USA), the uranium species were analyzed [155]. As predicted from calculations in carbonate-rich solutions, mainly $UO_2(CO_3)_3^{4-}$ and in carbonate poor waters $UO_2(OH)_2$ and $UO_2(OH)_3^-$ was found. The speciation of uranium strongly influences the transportation of this element. In the case of the Snake River sediment, the hydroxo species have retardation factors of about 300 compared to 5 to 10 for carbonate species.

However, using newer data [116] for calculation of the species distribution under the given conditions shows that uranium may be bond in a carbonate-bearing species. The main species under these conditions are $UO_2(CO_3)_3^{4-}$ (51%) and $Ca_2UO_2(CO_3)_3(aq)$ (41%). The residue of about 8% is assigned to other minor species.

Several radionuclides were detected in the seepage waters from the Ellweiler Uranium Mill, among them uranium and its decay products and ^{237}Np [156]. In the groundwater maximum concentrations of 460 Bq L^{-1} uranium and 2 Bq L^{-1} ^{237}Np were found. The groundwater was modeled by use of a simple surface complexation model. It could be shown that very low uranium concentrations are caused by the phosphate concentration. The Np found in the groundwater comes from a nuclear reaction (2.23.10) in uranium deposits

$$^{238}U(n, 2n)^{237}U \longrightarrow ^{237}Np + \beta^- \qquad (2.23.10)$$

In natural pitchblende, about 0.05 neutrons $g^{-1}s^{-1}$ are generated because of spontaneous fission of ^{238}U and (α,n) reactions of light elements [157].

A wide variety of uranium minerals have been described recently from an actual point of view [158]. The authors state that about 5% of all known minerals contain uranium. Because of their chemical diversity, uranium minerals are indicators for geochemical environments. However, there is a lack of thermodynamic data on uranium minerals. This is because uranium minerals in nature are rarely pure and that they are often finely grained. Besides this, variations in the composition, including the number of hydration water, often occur. Nevertheless, stability diagrams in the systems CO_2–CaO–UO_3–H_2O and SiO_2–CaO–UO_3–H_2O are established.

Studies of the speciation of actinides on mineral surfaces have shown major improvements during the last years. Waite *et al.* [159] have studied the interaction of uranium with ferrihydrite. The results of this study were interpreted by use of the two-site surface complexation model, where a strong and a weak affinity site were defined at the surface of ferrihydrite. Each of these sites forms only one species with uranium. This species is assigned to be a bidentate, mononuclear inner sphere complex. EXAFS spectroscopy has been used to confirm the structure of the species. In alkaline, carbonate-containing solutions, a third species has been used to describe the behavior of uranium. The carbonate-containing surface species was assigned to be $\equiv FeOH_2^+ - UO_2(CO_3)_3^{4-}$.

The derived surface complex stabilities are summarized in Table 2.23.7.

As Waite *et al.* [159] have shown, complex formation in the aqueous phase may change the surface complexation by forming new surface species or by prevention of surface complexation. Beneš *et al.* [160] have studied the influence of humic acid in the sorption of uranium to clay minerals. However, the results could only be interpreted qualitatively. The adsorption of uranium on clay shows broad minima in the pH range around 8. By adding humic substances, the pH range of these minima is enlarged. At higher amounts of clay concentration, this effect is smaller and can only be explained by carbonate in the solution. As carbonate forms strong solution complexes with uranium in this pH range, a decrease in the sorption can be expected. In general at low pH values the added humic acid increases the sorption of uranium on clay. This is explained by formation of a uranium-humate-clay complex. The suppression of the absorption at higher pH is explained by precipitation or sorption of humate on the clay. In

Table 2.23.7. Surface complexation constants of uranium ferrihydrite [159].

Species type	Species	Log K (I = 0.1 M)
Strong site	$\equiv Fe_sO_2 - UO_2$	−2.57
Weak site	$\equiv Fe_wO_2 - UO_2$	−6.28
Strong site	$\equiv Fe_sOH^+{}_2 - UO_2(CO_3)_3^{4-}$	−3.67
Weak site	$\equiv Fe_wOH^+{}_2 - UO_2(CO_3)_3^{4-}$	−0.42

the pH range 8–12, the formation of uranium humate complexes is used as one explanation for the lower adsorption. As there is no information on the atmospheric conditions, it can also be suggested that the formation of the uranium(VI)-carbonate complexes in the solution suppresses the adsorption.

Uranium sorbs poorly onto bentonite [86]. Three diffusivities for uranium were obtained. They are in the same order as for neptunium. The fastest fraction has a mobility equal to that of the waterfront. The two others are connected to the formation of complexes. Many of the other actinides are also discussed.

5.4.2.3.3 Uranium in biological systems Several data on the uptake and biological effects of uranium in biological systems have been reviewed [161]. However, the speciation of uranium is not treated extensively. The use of sequential extraction techniques leads only to rough estimates of the formed species.

Adenosine triphosphate (ATP) is an important enzymatic compound, which is able to transfer phosphate groups between molecules. Metals bond to adenosine phosphates can be transported into living cells and then deposited. The complex formation of adenosine phosphate was studied with uranium [162] and neptunium [163]. Because of the strong dynamic quench processes in the uranium system, only observing the fluorescence of the formed complex can be used for the examination of this system. The obtained data suggest a strong dependence of the complex formation on pH, indicating that protons are involved in the chemical equilibrium. From the analysis of the fluorescence data, it was concluded that a 1-to-1 complex would be formed. The formation constant was found to be $\log K = -3.80 \pm 0.44$.

Speciation studies for the interaction of actinides in plants are very rare. Most publications deal with the transfer factor from soil to plants.

Uptake of radionuclides by plants should be seen in comparison to their speciation in soil [164]. Also in this review it is mentioned that the uptake is generally dependent on the concentration of radionuclides in the soil. Plants (black spruce) were found, which contained more uranium than the natural background [165].

Tomato plants were grown in uranium-contaminated soil to study the uptake of these plants [166]. The soil was contaminated with several concentrations of uranium. Because of the lack of exact experimental details, no transfer factors can be calculated. Therefore, only two qualitative conclusions can be drawn as follows.

1. The concentration of uranium decreases in the plants in the order root > stem > leaf.
2. The uranium concentration in the roots is relatively high compared to that in the lesser contaminated soil.

Conclusion 1 was, however, not confirmed by Singh nine years later [167].

Soil to plant transfer factors for uranium can be found in the publication by Frindik [168]. They range from 7.2×10^{-5} to 1×10^{-3}. Transfer factors for uranium into vegetables are reported recently [169]. The obtained data are somewhat higher than those published by Frindik [168].

Because of the chemical behavior of the actinides, a different plant uptake can be expected. Ibrahim and Whicker [170] have compared thorium and uranium uptake. The plant uptake of elements of the uranium series was studied at a mine mill. It was observed that the plants growing on weathered tailings show the highest uptake for uranium followed by thorium. The data are not comparable to others, as mixed groups of plants were used in this study.

Instrumental neutron activation analysis has been used to determine uranium in plants from a milling site at Köprübasi in Turkey [171].

Because of the fact that organic acids form soluble complexes with the actinides, the uptake by plants may increase if such species are present in the soil. It was found that in soil containing acetic, malic and citric acid, the plant uptake for uranium was increased [172]. The concentration of uranium in shoots from *Brassica juncea* and *Brassica chinensis* increases from 5 mg kg^{-1} to more than 5000 mg kg^{-1} when the soil is treated with citric acid. The authors explain this extremely high uptake by the biodegradation of the citric acid.

The first study dealing with the speciation of uranium during growing of plants was done in 1998 [173]. Plants of peas *Pisum sativum* were investigated. The speciation of uranium in the hydroponics solution (modified Johnson's nutrient solution) was modeled with the program code GEOCHEM-PC. The plants were pretreated in a phosphate-containing solution without uranium for 10 days. After that, the plants were transferred to nutrient solutions without phosphate but including uranium(VI) ions and given an additional seven days of growing before harvesting. The roots and shoots were rinsed and dried before digesting with nitric acid. The uranium uptake was influenced by pH. At pH 5, when uranium was present as free uranyl cation, the root concentration was generally higher than that in the shoots. Among other species, *Phaseolus acutifolius* and *Beta vulgaris* have shown the greatest uranium uptake. Information on the speciation of uranium in these plants is not available.

Speciation of uranium in plants can only be determined after uptake of the radionuclide. The application of laser-induced spectroscopic techniques and XAS has shown differences in the speciation from that in the initial solution, that is, hydroponics solution or pore water of the soil, and from that of lupine plants. However, the uranium speciation of the different parts of the plant was found to be the same. This speciation was independent of the species present in the original solution. From spectroscopic data, it was relevant that the uranium is bound to phosphoryl groups [174].

The fraction of an ingested radioactive element in blood (fl) and the residence time within the different parts of the gastrointestinal tract control the doses delivered to the different target tissues. This can be altered by many factors. For uranium transfer, factors are found in the order of 2×10^{-2} [87]. For the other actinides, values of 5×10^{-4} were found. In the case of pentavalent Np and Pu, the factor fl depends on the mass of the ingested radionuclide.

Laser-induced fluorescence spectroscopy has been used for the detection of uranium in human urine samples [175]. Human urine is a complex matrix and the measurement of uranium at very low concentrations may be strongly influenced by matrix effects. Therefore, original samples were diluted and the uranium was determined as its phosphate complex. The detection limit was determined to be 1.3×10^{-8} M [175].

The uptake of uranium by bacteria has also been studied [176]. *Thiobacillus ferrooxidans* isolated from a uranium mine had shown a slightly higher capability to accumulate uranium than a strain recovered from a coal mine. Reducing bacteria such as *Desulfovibrio desulfuricans* are able to reduce most of the U(VI) within 24 h. The rate depends on the pH. Sulfate-reducing bacteria were also isolated from a uranium waste pile.

EXAFS investigation was used to examine the interaction of uranium with two types of bacteria [177]. The two bacteria *Bacillus cereus* and *Bacillus sphaericus* were taken from the uranium waste pile 'Haberlandhalde' in Johanngeorgenstadt in Saxony, Germany. Two reference strains of these bacteria were analyzed as well. A cell culture was treated with a sodium chloride solution containing 10^{-4} M uranium(VI). It could be shown that the uranium was bond via oxygen to a phosphorus atom. The average atomic distance between uranium and phosphorus was estimated at 0.362 nm. The distances are in good agreement to the U–P distance in meta-autunite, which has been found to be 0.360 nm [178].

Laser-induced fluorescence measurements are used to study the interactions of metal ions with living matter [179]. The interaction of U(VI) with vegetative cells, heat-killed cells, spores, and decomposed cells of *B. sphaericus* was studied by Panak *et al*. [179]. The cells were decomposed to study the speciation of uranium, and U(VI) was precipitated as $UO_2(H_2PO_4)_2$. The decomposed bacterial suspension showed the same fluorescence spectrum as $UO_2(H_2PO_4)_2$. This spectrum differed significantly from that of the bacterial U(VI) surface complexes. The authors attribute their results to the formation of inner sphere complexes with organo-phosphate groups on the cell surface.

Several authors studied the influences of uranium on the metabolism of bacteria. The biotransformation of the uranium citrate complex by *Clostridium sphenoides* was studied recently [180].

It was found that uranium was reduced to uranium(IV) only when citric acid was present in excess or when glucose was added. These results are in good agreement with data for *Pseudomonas fluorescens* [181].

Acidithiobacillus ferrooxidans were isolated from uranium waste piles [182] and their interaction with uranium was compared with those of the bacteria *Pseudomonas stutzeri* and *Pseudomonas migulae*. Studies show that these bacteria accumulate uranium(VI) and transform it to phosphate complexes with different structural parameters.

One of the most studied types of bacteria is the *Acidithiobacillus ferrooxidans*. The interaction of this bacterium with uranium(VI) was studied by Merroun *et al*. [183]. It was found that by measurement of the fluorescence of the bond uranium, three fluorescence lifetimes were obtained. From these measurements, it was concluded that one complex is stronger than the others. However, no structural differences could by observed by EXAFS spectroscopy. The interpretation of these findings point to the fact that the same functional groups are implicated in the complex formation.

5.5 Neptunium

McMillan and Abelson have produced Np-239 by bombarding uranium with neutrons in 1940. Neptunium is the first synthetic transuranium element. Np-237 has a half-life of 2.14×10^6 years. Trace quantities of the element can be found in nature because of nuclear reactions in uranium ores.

Neptunium forms oxidation states from +3 to +7. Np(III) is easily oxidized to Np(IV). The most stable oxidation states are Np(IV) and Np(V), the latter also forms a dioxocation.

In solution, neptunium can be stabilized in four ionic oxidation states: Np^{3+} (pale purple), Np^{4+} (yellow green), NpO_2^+ (green blue) and NpO_2^{2+} (pale pink).

Changes in the oxidation state may also change the complex formation and at least also the transportation of actinides in the environment. Neptunium is found to be bond to colloidal humic species, which can be transported in a column somewhat faster than the water flow [184]. It was found that with the reduction of Np(V) to Np(IV), the interaction of neptunium with the humic substances becomes much stronger.

5.5.1 Neptunium(IV)

The lower actinides form tetravalent ions in aqueous solution. These ions undergo strong hydrolysis reactions and also form colloids even at low pH. The evaluation of thermodynamic data of the tetravalent actinide ions becomes more complicated because of low solubility of the hydroxides or hydrous oxides [185]. Spectroscopic studies often fail as the concentrations of the actinide ion are above the solubility limit. It has been observed [69, 186] that colloids are formed when the concentration exceeds the solubility limit of the corresponding hydroxide. The data for the Np(IV) system are $\log K^\circ_{sp} = -56.5 \pm 0.4$.

The NEA database (reaction type B) lists only the first hydrolysis constant for Np(IV) to be $\log *\beta_1^\circ = -0.29 \pm 1.00$. Neck and Kim [70] estimated from the data of Duplessis and Guillaumont [187] the formation constants of the other hydroxide species to be $\log *\beta_{11}^\circ = 0.5 \pm 0.2$; $\log *\beta_{12}^\circ = 0.3 \pm 0.3$, $\log *\beta_{13}^\circ = -2.8 \pm 1.0$ and $\log *\beta_{14}^\circ = -8.3 \pm 1.1$.

The difficulties with speciation calculations are demonstrated in Figure 2.23.10. Figure 2.23.10(a) shows the calculated species distribution of Np(IV) using the estimates from the NEA database that are included in the database for MEDUSA [53, 59], Figure 2.23.10(b) uses the estimates of Neck and Kim [70]. Both calculations were made using the speciation code MEDUSA.

In agreement with the other tetravalent actinides, it appears that the limiting carbonate complex is determined to be $Np(CO_3)_5^{6-}$. The stability constant has been found to be $\log \beta_5 = 38.98 \pm 1.97$ [53].

5.5.2 Neptunium(V) and neptunium(VI)

5.5.2.1 Solubility and inorganic species

In the literature [188], the solubility of actinide hydroxides at different oxidation states in natural

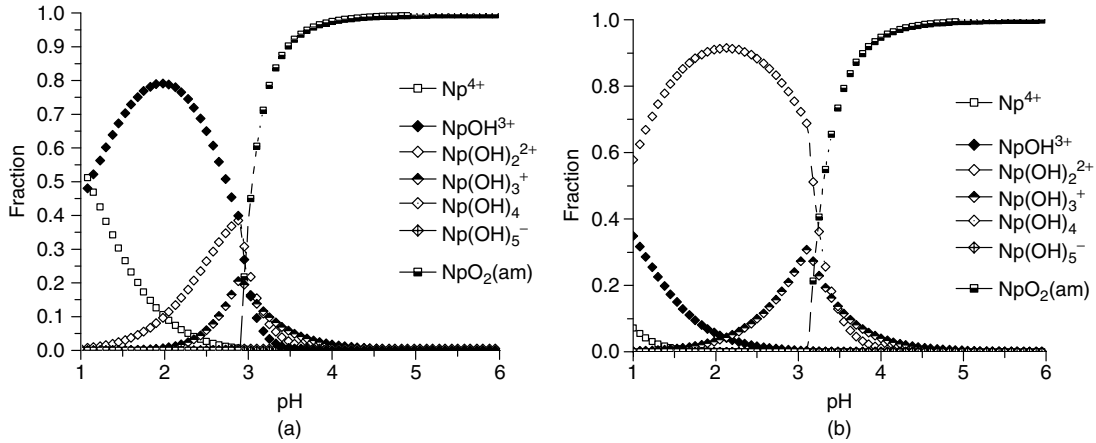

Figure 2.23.10. Influence of datasets on species distribution (1.0×10^{-6} M Np(IV) I = 0.1 M), ((a) stability constants [53], (b) estimated constants [70], see text).

water systems has been compared. The solubility of $NpO_2(OH)$ is nearly the same in groundwater as in seawater.

The solubility of neptunium(V) hydroxide was studied in a CO_2-free atmosphere in the pH range from 7 to 13.5 [189]. Under these conditions only neptunium and its hydrolysis species are expected in solution. Their experiments were performed at several ionic strengths to extrapolate the obtained constants for infinite dilution. At infinite dilution, the solubility product is assigned to be log $K^\circ_{sp} = -8.68 \pm 0.26$. The two derived hydrolysis constants are log $\beta^\circ_{11} = 3.30 \pm 0.35$ and log $\beta^\circ_{12} = 5.58 \pm 0.31$.

Under natural conditions, carbonate is a complexing agent, which is ubiquitous. The safety assessment for nuclear waste repositories needs solubility data on all relevant actinides under the chemical terms relevant to the proposed waste management. Reducing conditions can often be expected. Kitamura and Kohara [190] as well as Rai *et al*. [191, 192] provide data on the solubility of neptunium(IV) in these media. The species expected in solution are $Np(CO_3)_2(OH)_2^{2-}$ and $Np(CO_3)_2(OH)_4^{4-}$.

The solubility product for NpO_2CO_3 was determined to be log $K_s = -14.04 \pm 0.07$ [193]. The solution species are NpO_2CO_3, $NpO_2(CO_3)_2^{2-}$ and $NpO_2(CO_3)_3^{4-}$ depending on the concentration of carbonate. The formation constants for NpO_2CO_3 and $NpO_2(CO_3)_3^{4-}$ were assigned to be log $\beta^\circ_{101} = 9.02 \pm 0.10$ and log $\beta^\circ_{103} = 20.41 \pm 0.09$, respectively. The formation constant for the intermediate complex could only be estimated to be log $\beta^\circ_{102} < 14.2$. In addition, the formation constant for the first hydrolyzed species $NpO_2(OH)^+$ was assigned to be log $\beta^\circ_{110} < 9.0$. The concentration of the Np(VI) species was detected using photoacoustic spectroscopy in the near infrared region (NIR) [193]. Neck *et al*. [194] has also investigated the Np(V) complexation by carbonate.

As the same data are available for uranium(VI) and plutonium(VI), a comparison of the datasets can be envisaged. The given solubility product is about 0.6 orders of magnitude higher than previously published data [195]. This is explained by differences in the crystallite size of the solid phase. However, the given solubility product is in good agreement with data for uranium(VI)-carbonate and plutonium(VI)-carbonate. The formation constants for the solution species were compared at an ionic strength of 0.1 M $NaClO_4$. They follow the order U(VI) > Np(VI) > Pu(VI).

A comparison of the species distribution is shown in Figure 2.23.11. For the calculation, the data of the NEA database [53] were used. The total concentration of neptunium was 1.0×10^{-6} M. The maximum of the carbonate concentration was set to 1.0×10^{-2} M.

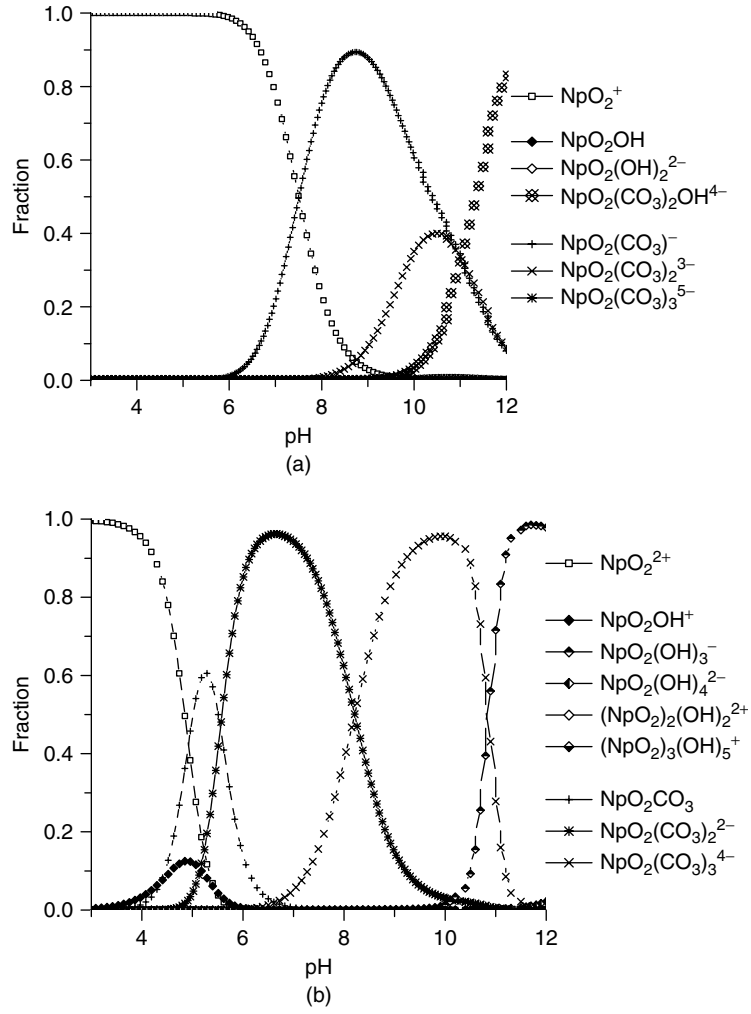

Figure 2.23.11. Species distribution of Np(V) and Np(VI) in carbonate media, stability constants [53].

Mixed hydroxo-carbonate species of uranium are well known. The evidence for such species of neptunium(V) was very unclear. However, the absorption spectra of neptunium(V) at 1010 nm [196–198] were interpreted on the basis of the existence of a mixed hydroxo-carbonate species. The stoichiometry and the formation constants of these mixed species could be determined recently [198]. Two complexes, $NpO_2(OH)(CO_3)_2^{4-}$ and $NpO_2(OH)_2(CO_3)^{3-}$, were identified. The derived formation constants are $\log \beta_{112} = 10.06 \pm 0.11$ and $\log \beta_{121} = 9.56 \pm 0.15$, respectively. It was expected that a complex $NpO_2(OH)(CO_3)^{2-}$ should also be formed [199]. The formation constant of this complex was estimated to be $\log \beta_{111} = 7.6 \pm 0.3$. The ionic strength of the solutions used in this study was set to 3.0 M. Speciation calculations show that these complexes become dominant in highly alkaline solutions (pH > 12) and carbonate concentrations $> 1 \times 10^{-4}$ M.

Groundwaters normally show a pH around 7.0. The pH of waters sampled at Yucca Mountain is also in this range. The solubility of several actinides in different oxidation states was

studied [200]. Besides the composition of the solid phase, the authors also give information on the expected species in the solution. In the case of Np(V), the solid phase is of the stoichiometry $Na_xNpO_2(CO_3)_y \cdot zH_2O$, where x and y have values up to 1.0 and z ranges from 2.0 to 3.5. In the solution at pH 6 and 7, the main species are free Np(V) together with hydroxo and carbonate complexes. At pH 8.5, the amount of noncomplexed Np(V) becomes less or, if the carbonate concentration is higher, no free Np(V) is obtained.

5.5.2.2 Species with organic ligands

Studies to model the functionality of polyelectrolytes were often used to get more precise data for the complex formation of actinides. In these efforts also studies of the neptunium(V) complexation by dicarboxylic acids can be included. Jensen and Nash [201] have assigned the stability constants for the 1 : 1 complexes of oxydiacetic acid and iminodiacetic acid. Malonic acid forms 1 : 1 and 1 : 2 complexes. To study the speciation in these systems, several methods such as UV-VIS spectrometry, potentiometry and calorimetry have been used. The assigned formation constants are summarized in Table 2.23.8.

Moriyama *et al*. [202] have used a two-site model to describe the complex formation of neptunium(V) with humic acid. The two functional groups, carboxylic and phenolic, are expected to participate in the complex formation. Therefore, the dissociation constants of both groups were determined. The stability constants were found to be independent on pH. Nevertheless, a dependence on ionic strength was observed. The formation constants are summarized in Table 2.23.9.

Table 2.23.8. Stability constants of some Np(V)-dicarboxylic acids [201].

Ligand	Complex	Log β (1 M $NaClO_4$)
Malonate	$NpO_2(C_3O_4)^-$	2.63 ± 0.01
Malonate	$NpO_2(C_3O_4)_2^{3-}$	4.28 ± 0.02
Oxydiacetate	$NpO_2(C_4O_5)^-$	3.79 ± 0.01
Iminodiacetate	$NpO_2(C_4O_4\ NH)s^-$	5.88 ± 0.01

The neptunium(V) ion forms in aquatic systems a 1 : 1 complex with humic and fulvic acids (FAs).

The complex formation of neptunium(V) with humic acid has been studied several times. Kim and Sekine [203] have found only a 1 : 1 complex by interpretation of spectroscopic data. In this early report, the loading capacity has been introduced as the value for the ligand concentration. The formation constant was then derived to be log $\beta_{11} = 3.66 \pm 0.02$. The concentration range for neptunium was in the order of 2×10^{-4} M. The UV-VIS spectra show a clear isosbestic point, indicating a chemical reaction between two dependent components. Isosbestic points were found in spectra of reacting mixtures, if they were repeatedly scanned over the wavelength range of interest. It can be found that several spectra intersect at one or more wavelength. The points of the intersection are named *isosbestic points* [204].

In 1999, Kim [205] and Marquardt have published data on the complexation of Np(V) by HA from Gorleben groundwater. In this study, neptunium concentrations of 1.5×10^{-5} to 1.2×10^{-4} M were used. To avoid influences of carbonate complexation, all experiments were carried out under argon atmosphere. The average of the derived complex formation constant is given to be log $\beta_1 = 3.39 \pm 0.11$. This is in good agreement with data from purified HA.

In contrast to the charge neutralization model, in which the loading capacity is included, other models use only the dissociation of the HA as parameter for the description of the properties of the ligand. In this way, pH independent

Table 2.23.9. Dissociation and complexation constants of carboxylate and phenolate groups of humic acid [202].

Ionic strength/M	Log β_{COOH}	Log β_{OH}	Log $\beta_{1,COOH}$	Log $\beta_{1,OH}$
0.01	5.94 ± 0.15	9.37 ± 0.82	2.89 ± 0.05	4.26 ± 0.11
0.1	6.06 ± 0.16	9.20 ± 0.23	2.69 ± 0.08	4.11 ± 0.11
0.5	5.25 ± 0.38	8.32 ± 0.21	2.56 ± 0.08	4.09 ± 0.14

binding constants were derived, which show small differences depending on the origin and the molecular mass of the humic acid [206]. The data are in a range from $\log \beta_1 = 2.15$ to $\log \beta_1 = 2.44$.

The first study to obtain speciation of neptunium with humic acid at very low concentrations was published in 1996 [207]. By use of electrophoretic ion focusing and anion exchange, chromatography in combination with radiometric detection methods neptunium concentrations down to 10^{-13} M could be studied. As known from other studies, a 1 : 1 metal humate species was observed. After correction of the dissociation of the humic acid, a stability constant for the neptunium(V)–Aldrich humate of $\log \beta = 4.2 \pm 0.15$ was observed at 10^{-13} M neptunium(V). The values for the Gorleben humic acid range between $\log \beta = 3.6$ and $\log \beta = 4.4$. However, increasing metal concentration in the solution varies the formation constant by a factor of up to 2.5. The effect is explained by the complicated structure of polyelectrolyte humic acid. It was also observed that under anaerobic conditions neptunium(V) could be reduced to neptunium(IV) by humic acid.

A more recent study [208] has shown that the complexation of neptunium(V) with humic acid is possibly not yet completely understood. In this paper, the authors report on a study of the complex formation of neptunium(V) with humic acid in a wide range of neptunium concentrations (10^{-14} to 10^{-7} M), which is very close to environmental conditions. To study this wide range of neptunium concentration, several methods have been used. For data evaluation, the charge neutralization model was exploited. For this case, the derived formation constants vary with the metal ion concentration. The formation constant was assigned to be $\log \beta = 5.0 \pm 0.3$ in the concentration range below 10^{-11} M and in the concentration range 10^{-8} to 10^{-6} M the value decreases and reaches at least $\log \beta = 3.7 \pm 0.4$. The latter value is in good agreement with other literature data.

Marquardt and Kim [209] have studied the FA system. The formation constant for the complex is assigned to be $\log \beta_1 = 3.53 \pm 0.04$. The stability constant was derived using NIR absorption spectroscopy and the charge neutralization model was used for data handling. The authors mention that the formation constant was independent of the metal ion concentration.

5.5.2.3 *Neptunium in the environment*

In natural uranium minerals, a small amount of neutrons is generated. The neutron generation in natural uranium minerals is 5×10^{-2} neutrons $g^{-1}\,s^{-1}$. Two processes contribute to this: spontaneous fission of ^{238}U and (α, n) reactions. By a $(n, 2n)$ reaction, ^{237}U is generated. The formed ^{237}U undergoes a β^- decay to ^{237}Np. A ^{237}Np : ^{238}U ratio of 1.8×10^{-12} was found in natural pitchblende [157].

Small amounts of this isotope were found in groundwater samples from the Ellweiler mining site [156].

Most of transuranium elements in the environment originate from nuclear accidents (Chernobyl), bomb tests (Nevada, Semipalatinsk, Mururoa), nuclear bombing (Hiroshima and Nagasaki) and waste storage (Hanford, Tomsk, Krasnoyarsk).

One of the most problematic elements in the nuclear waste is probably the element neptunium. The element forms stable pentavalent dioxocations and it is expected that the solubility under typical groundwater conditions is relatively high. Because of the chemical properties, it is also expected that neptunium tends only to have a low sorption on common minerals. However, neptunium will be present in large quantities in spent fuel. Neptunium carbonate complexes may play an important role in the migration behavior of this element. Three carbonate complexes are known. The NIR spectra of these complexes show significant differences, which allow their deconvolution [210]. EXAFS studies on these complexes show a coordination number of five for the complexes $NpO_2(CO_3)^-$ and $NpO_2(CO_3)_2{}^{3-}$. The third complex $NpO_2(CO_3)_3{}^{5-}$ has a coordination number of 6.

The description of sorption phenomena is an important element in modeling of the transport of actinides in the geosphere. The sorption is strongly influenced by pH and any ligands in the aquifer because of hydrolysis and complex formation. The influence of pH and carbonate onto the sorption

behavior of neptunium(V) on hydrargilite has been studied [211]. A nonelectrostatic model was used for the description of the surface complexation. Within a concentration range of 10^{-13} to 10^{-7} M neptunium, a linear relationship between the neptunium concentration at the mineral surface and in the solution was found for carbonate-free media at pH 7.45. However, the concentration on the surface is strongly dependent on the pH of the solution. If carbonate was added to the system, a decrease of the neptunium uptake was found for the alkaline pH region. This is due to the carbonate complexation of NpO_2^+ in the solution. The surface complexation model results in a surface complexation constant of log ${}^cK_{SONpO_2} = -3.6 \pm 0.2$ at an ionic strength of 0.1 M for the reaction (2.23.11)

$$SOH + NpO_2^+ \leftrightarrow SONpO_2 + H^+ \qquad (2.23.11)$$

In combination with the stability constants for the neptunium(V) carbonate and hydroxide species, an accurate description of the sorption behavior was possible.

The interaction of neptunium(V) with the three adenosine phosphates has been studied by Rizkalla *et al*. [163]. It has been found that two species were formed in the solution: NpO_2L and NpO_2HL, where L means adenosine monophosphate (AMP), adenosine diphosphate (ADP) and ATP. The stability constants decrease in the order

$$ATP^{4-} > ADP^{3-} > AMP^{2-}$$

The data were obtained by potentiometric titration and the stability constants at an ionic strength of 0.1 M are listed in the Table 2.23.10.

Using the data of the Np-ATP complexes for calculation of a species distribution, it was found that at pH 4.5 a 2 times negatively charged complex should be formed and that the NpO_2ATP^{3-} complex becomes dominant at pH $\sim$ 7.0.

For comparison, the uranium data [162] have to be transformed. The necessary protonation constants for ATP are given in the literature [212]. In the pH range 2.0 to 3.5, the ATP exists in the solution mainly as ${}^+H_2ATP^{3-}$. If a 1 : 1 complex with a release of two protons is assumed, the stability constant can be estimated to be log $\beta_{(UO_2HATP^-)} = 7.44 \pm 0.44$.

The species distribution for both metal ions (1×10^{-2} M ATP, I = 0.1 M) is shown in Figure 2.23.12.

The figure shows that the UO2–ATP interaction is much stronger than that of the neptunium(V) complex.

An overview on neptunium in environmental systems is given by Coughtrey *et al*. [213, 214]. However, the authors refer only to concentration data.

Neptunium seems to be transferred into a cell as metal ion, when it is transported to the cell wall by transferrin. Inside the cell, Np is bound first to a cytosolic protein. However, this is not a stable form, and Np is then transferred to so-called high mass molecular compounds [87].

The interaction of *D. desulfuricans* with neptunium shows no dependence on pH [215], but for anaerobic bacteria an increase of the distribution coefficient K_d was found. The results of this study were compared to the interaction of Np(V) with humic acid that increases with pH. The interpretation was that the complexing sites should predominantly be deprotonated functional groups. The K_d values for the humic acid were found to be 100-fold higher than for *D. desulfuricans*.

Table 2.23.10. Stability constants for the formation of NpO_2^+ –adenosine phosphate complexes [163].

Equilibrium	Log β
$NpO_2^+ + AMP^{2-} \leftrightarrow NpO_2AMP^-$	2.51 ± 0.02
$NpO_2^+ + ADP^{3-} \leftrightarrow NpO_2ADP^{2-}$	2.97 ± 0.04
$NpO_2^+ + H^+ + ADP^{3-} \leftrightarrow NpO_2HADP^-$	7.48 ± 0.12
$NpO_2^+ + ATP^{4-} \leftrightarrow NpO_2ATP^{3-}$	3.52 ± 0.04
$NpO_2^+ + H^+ + ATP^{4-} \leftrightarrow NpO_2HATP^{2-}$	8.87 ± 0.06

5.6 Plutonium

Plutonium was discovered in 1940 by Seaborg, McMillan, Kennedy and Wahl. The isotope ^{238}Pu was produced by deuteron bombardment of uranium in the 60-inch cyclotron at Berkeley, California. Plutonium can also be found in trace amounts in uranium ores.

The most stable isotope is Pu-244 with a half-life of 8.01×10^9 years. However, the most important isotope is Pu-239. Its half-life is 24.100 years.

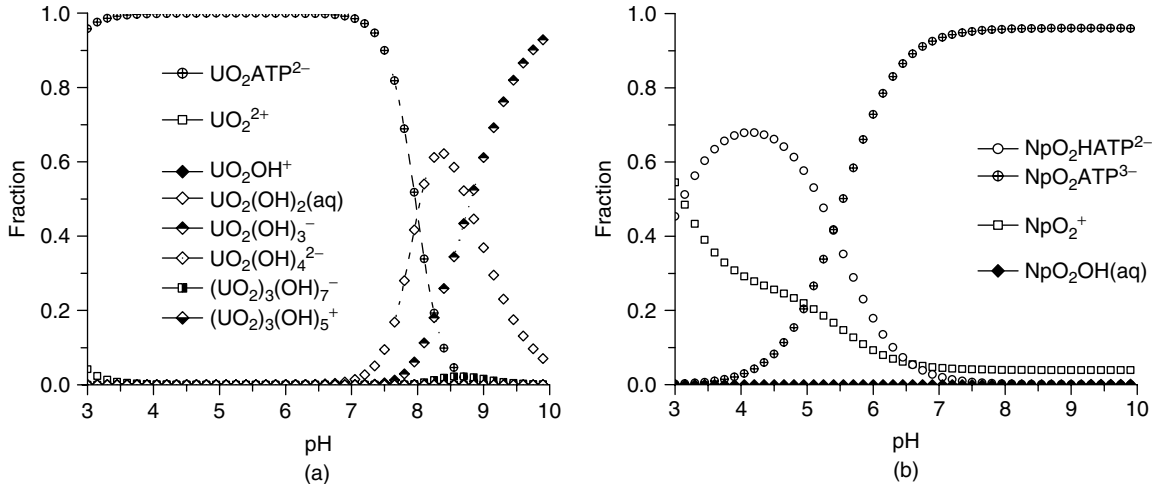

Figure 2.23.12. Species distribution of uranium(VI) and neptunium(V) ATP complexes as a function of pH (calc. with EQ 3/6), stability constants [162, 163, 212].

Plutonium has oxidation states from +3 to +6. The redox potentials between these oxidation states are close together, so one can often find several oxidation states existing together. Plutonium is one of the most toxic elements.

Plutonium exhibits four ionic valence states in aqueous solutions: Pu^{+3} (blue lavender), Pu^{+4} (yellow brown), PuO_2^{+} (pink) and PuO_2^{2+} (pink-orange). The pentavalent ion PuO_2^{+} is unstable in aqueous solutions, it disproportionates into Pu^{+4} and PuO_2^{2+}. The Pu^{4+} then oxidizes the PuO_2^{+} into PuO_2^{2+}, itself being reduced to Pu^{3+}. The final products are Pu^{3+} and PuO_2^{2+}. Plutonium is a very dangerous radiological and hazardous material. Precautions must be taken to prevent the unintentional formulation of a critical mass.

The redox potentials of plutonium are very close together. Therefore, several oxidation states can often exist in solution together. The stability of the several oxidation states under different solution conditions is therefore an important factor in speciation calculations. Capdevila *et al*. have studied the disproportionation of the pentavalent plutonium [216]. In perchloric media, the disproportionation constant was determined to be log $K^{\circ}_{V} = 2.6 \pm 0.5$. It was also found that PuO_2^{+} is less stable at elevated temperatures. The data obtained agree very well with those published earlier. A Pourbaix diagram (Eh-pH diagram) was established, showing that PuO_2^{+} is stable only in a small range around pH 6 and at redox potentials of 800 mV.

Only a few data are available about interaction of Pu(III) with natural complexing ligands. This may be due to the fact that the Pu(III) chemistry does not play such an important role as that of plutonium in the other oxidation states. However, the reducing properties of HA are well known [217]. Solvent extraction has been used to obtain the formation constant with humic acid at pH 2.9 and 5.0 in 0.5 M $NaClO_4$ [218]. In this publication, no error for the stability constants is given. Therefore, the slight increase in log β_1 is negligible and only an average value of log $\beta_1 = 2.95$ is cited.

5.6.1 Plutonium(IV)

The data on the solubility product of tetravalent Pu hydroxide show great discrepancies. This may be due to the fact that the chemical speciation in solution was taken into account only in three studies [219]. From spectrophotometric data, a log $K^{\circ}_{sp} = 58.3 \pm 0.5$ was derived. The other published data are log $K^{\circ}_{sp} = 56.85 \pm 0.36$ [220] and log $K^{\circ}_{sp} = 57.85 \pm 0.05$ [221]. The corresponding species in solution are determined by the redox

reaction of the dissolved Pu^{4+} to Pu^{3+}, PuO_2^{+} and PuO_2^{2+}.

The solubility product for the Pu(IV) system is assigned to be $\log K^{\circ}_{sp} = -57.97 \pm 0.24$ [222]. The data were obtained by performing oversaturation experiments followed by an undersaturation study of the formed solid sample. Exploiting the SIT algorithm, the solubility product at infinite dilution was extrapolated. A comparison of the available data shows a clear dependence of the solubility product on the radius of the tetravalent actinides. However, it should be noted that the authors mention that for the use of the relationship on the inverse square of the ionic radii [223] more data are necessary.

For comparison, the latest available results on the solubility products of tetravalent actinide hydroxides are summarized in Table 2.23.11.

The increase of the hydrolysis in the series of the tetravalent actinides can be seen in Figure 2.23.13. For this comparison, the data provided by Neck and Kim [70] were used. The inset of the formation of the amorphous hydroxides at lower pH in the series Th > U ~ Np > Pu can be clearly detected. The existence of a crystalline actinide(IV)-oxide was excluded in these calculations. A change in the main species can be found if the species distribution is compared at constant pH.

Table 2.23.11. Solubility products of amorphous hydroxides of tetravalent actinides.

Element	Ionic radii/nm	Solubility product $\log K^{\circ}_{sp}$
Th	0.094	-47.0 ± 0.8
Pa	0.090	–
U	0.089	-54.5 ± 1.0
Np	0.087	-56.5 ± 0.4
Pu	0.086	-57.97 ± 0.24

Nevertheless, it should be pointed out that the calculated species distributions should be seen as an example. Other databases may result in slightly different species distributions. As an example, the data derived by the hard shell model [73] and the estimated data [70] are summarized in Table 2.23.12.

There are only few data published about the complex formation of tetravalent actinides with carbonate. The dissociation of plutonium carbonate was studied by Capdevila *et al.* [224]. An isosbestic point was found in spectrophotometric investigations, indicating two species connected by a complex formation reaction. The two species detected in solution were assigned to be $Pu(CO_3)_4^{4-}$ and $Pu(CO_3)_5^{6-}$. The formation constant was

Table 2.23.12. Comparison of stability constants of An(IV) hydroxo species.

Actinide	Species				
	$An(OH)^{3+}$	$An(OH)_2^{2+}$	$An(OH)_3^{+}$	$An(OH)_4$	$An(OH)_5^{-}$
Th	-2.73 ± 1.14	-5.57 ± 1.74	-8.59 ± 4.18	-15.06 ± 4.65	–
Pa	0.83 ± 0.03	0.51 ± 0.91	0.44	-1.29 ± 2.67	–
U	-0.54 ± 0.06	-1.88	1.69	-2.37	>-16
Np	-0.74 ± 1.00	0.79 ± 1.48	–	-5.91	–
Pu	-0.62 ± 0.51	-0.54 ± 1.65	-3.1 ± 2.03	-6.32 ± 2.78	–

Note: Data listed by Moriyama *et al.* [73]

Actinide	Species					Solubility product $An(OH)_4(am)$
	$An(OH)^{3+}$	$An(OH)_2^{2+}$	$An(OH)_3^{+}$	$An(OH)_4$	$An(OH)_5^{-}$	
Th	-2.2 ± 0.2	-6.0 ± 0.6	-11.0 ± 1.0	-17.5 ± 1.0	>-30.5	-47.0 ± 0.8
Pa	–	–	–	–	–	–
U	-0.4 ± 0.2	-1.1 ± 1.0	-4.7 ± 1.0	-10.0 ± 1.4	>-23	-54.5 ± 1.0
Np	0.5 ± 0.2	0.3 ± 0.3	-2.8 ± 1.0	-8.3 ± 1.1	>-21.5	-56.7 ± 0.5
Pu	0.6 ± 0.2	0.6 ± 0.3	-2.3 ± 0.4	-7.9 ± 0.9	>-21	-58.5 ± 0.7

Note: Data estimated by Neck and Kim [70].
The data provided by Moriyama are averages of data taken from the literature.
Source: Reproduced from References [70 and 73] by permission of The Atomic Energy Society of Chemistry.

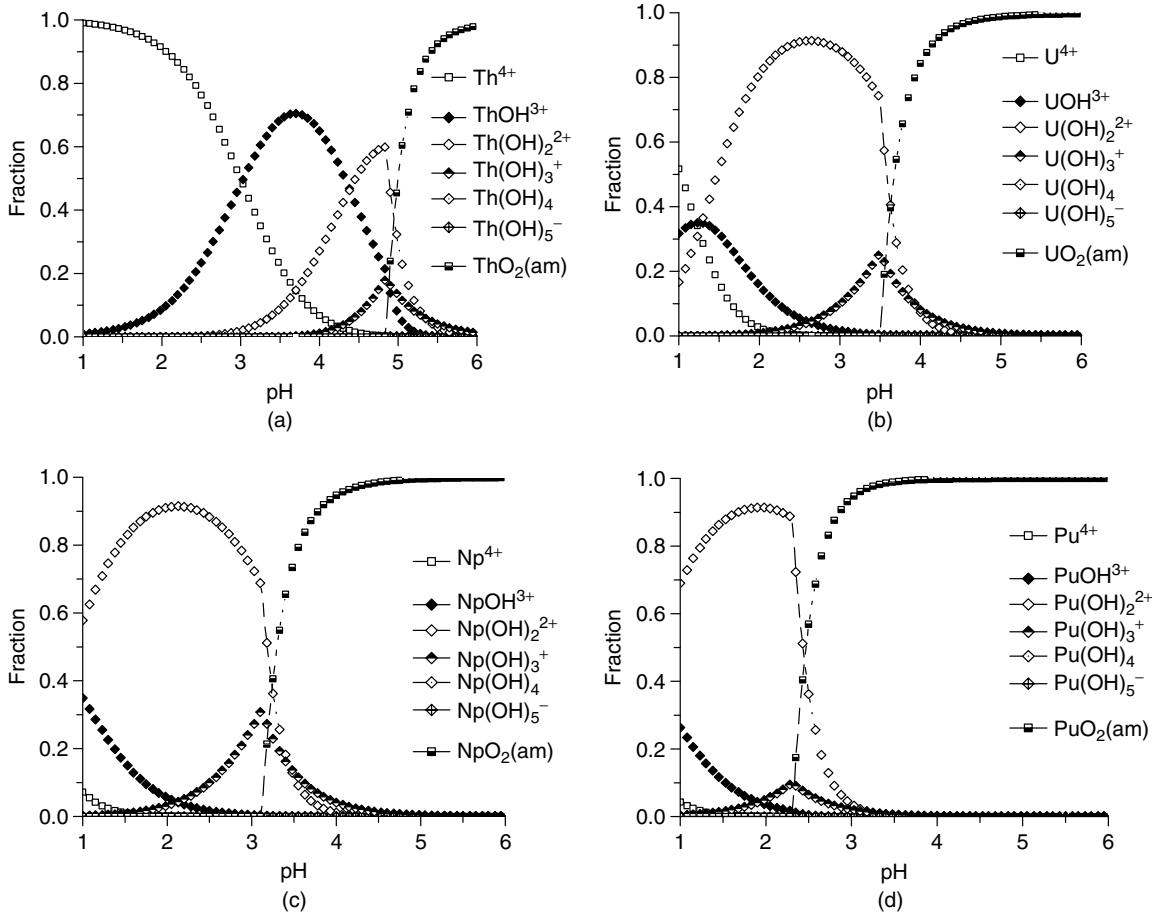

Figure 2.23.13. Comparison of the species distribution of tetravalent actinide (An) hydroxo species (1.0×10^{-6} M An^{4+}, I = 0.1 M), stability constants [70].

estimated for infinite dilution to be $\log \beta^{\circ}_{15} = -1.36 \pm 0.09$. Comparing this with the data for uranium(IV) [50, 225] and neptunium(IV) [226, 227] systems, these results are very similar. By use of EXAFS, Clark *et al.* [228] and Rai and Felmy *et al.* [111, 229, 230] have shown by EXAFS measurements that the limiting complex has a $M(CO_3)_5^{6-}$ stoichiometry.

As $An(CO_3)_5^{-}$ can be expected to be the limiting complex of the tetravalent actinides, a comparison between the actinides thorium through plutonium can be made.

For the reactions of the actinides (2.23.12–2.23.15), the following data are found in the literature.

$$Th^{4+} + 5CO_3^{2-} \leftrightarrow Th(CO_3)_5^{6-}$$
$$\log \beta^{\circ}_{15} = 32.33 \pm 0.7 \quad [68] \qquad (2.23.12)$$

$$U^{4+} + 5CO_3^{2-} \leftrightarrow U(CO_3)_5^{6-}$$
$$\log \beta^{\circ}_{15} = 34.0 \pm 0.9 \quad [50] \qquad (2.23.13)$$

$$Np^{4+} + 5CO_3^{2-} \leftrightarrow Np(CO_3)_5^{6-}$$
$$\log \beta^{\circ}_{15} = 38.98 \pm 1.97 \quad [53] \qquad (2.23.14)$$

$$Pu^{4+} + 5CO_3^{2-} \leftrightarrow Pu(CO_3)_5^{6-}$$
$$\log \beta^{\circ}_{15} = 32.2 \pm 2.0 \quad [226] \qquad (2.23.15)$$

However, these data are mostly estimates, which may explain the differences between them.

The formation and structure of nitrate complexes was confirmed in solutions with nitrate concentrations up to 13 M using EXAFS spectroscopy [231, 232].

Several studies have shown that water-soluble polymers are able to bind actinides quantitatively and selectively. Some of these compounds have been used to investigate the interactions with plutonium(IV) and plutonium(VI) [233]. It has been found that polyacrylic acid forms complexes with both Pu(IV) and Pu(VI). The formation constants of the Pu(IV) complexes are comparable to acetate complexation ($\log \beta_1 = 5.23 \pm 0.20$; $\log \beta_2 = 10.5 \pm 0.4$; $\log \beta_3 = 14.9 \pm 0.6$ and $\log \beta_4 = 18.3 \pm 0.8$; I = 0.5 M). For plutonium(VI), the formation constants are $\log \beta_1 = 2.68 \pm 0.08$; $\log \beta_2 = 5.75 \pm 0.10$ and $\log \beta_3 = 8.31 \pm 0.08$ at an ionic strength of 0.1 M ClO_4^-. However, the data derived from ultrafiltration are somewhat different, especially the $\log \beta_1$ value differs by 1 order of magnitude. An explanation by electrostatic forces is given for this.

Absorption spectroscopy has also been used to study hydrolysis, acetate and carbonate speciation of plutonium(IV) [234]. In this study, a plutonium concentration of 1.3×10^{-4} M was used. From the spectra, the stability constants of the first carbonate species is assigned to be $\log \beta_{11} < 12.3$ at an ionic strength of 0.5 M.

5.6.2 *Plutonium(V) and plutonium(VI)*

The disproportionation reaction of PuO_2^+ makes it difficulty to obtain data for this oxidation state. However, to predict the plutonium behavior for all oxidation states, thermodynamic data are necessary. Rai *et al*. [235] have studied the solubility of PuO_2(am) in slightly acidic media to get information on plutonium(V). As expected, the data for Pu(V) were very close to those of Np(V).

Photoacoustic spectroscopy has been used to study the complex formation between plutonium(V) and carbonate [234]. For the detection of the absorption spectra by this method, concentrations of 1.0×10^{-5} M Pu and less were used. To estimate the formation constants at infinite dilution, the SIT approach was applied. The formation constants are assigned to be $\log *\beta_{11} = -9.73 \pm 0.10$ for the first hydrolysis step and $\log \beta_{11} = 5.12 \pm 0.07$ for the carbonate complexation. A species distribution of PuO_2^{2+} in carbonate media is shown in fig. 2.23.14.

5.6.3 *Plutonium in the environment*

According to the same mechanisms as for the generation of ^{237}Np, ^{239}Pu can also be found in natural uranium minerals (16).

$$^{238}U(n,\gamma)^{239}U \xrightarrow{\beta^-} {}^{239}Np \xrightarrow{\beta^-} {}^{239}Pu \qquad (2.23.16)$$

The highest ratio $^{239}Pu/^{238}U$ found in the nature was 15×10^{-12} [157].

The distribution of plutonium as a function of the geographic latitude has been studied by several expeditions [236]. Samples of seawater were taken and analyzed for the plutonium isotope ratios. The origin of the artic plutonium is mainly from nuclear tests. The concentration range is from about less than 1 m Bq m^{-3} to a few hundred m Bq m^{-3}.

It was concluded from the measurements of the isotopic composition of plutonium taken during an expedition in 1980 that most of the plutonium in Greenland and the Barents Sea originates from European reprocessing facilities. The expedition in 1991 has shown lower activity concentrations. From this decrease, an ecological half-life for Pu was calculated to be 17 years. This is twice the amount observed in other parts of the North and South Atlantic Ocean. This difference is explained among others by an influence of ice formation with redox-sensitive elements.

Up to now, about 4.2 tons of anthropogenic plutonium have been released into the environment [237]. The concentration of the element in aquatic systems is relatively constant and found to be less than 2×10^{-5} Bq L^{-1} in lake waters and 4×10^{-5} Bq L^{-1} in ocean waters. Assuming that this plutonium comes only from radioactive fallout with a $^{240}Pu/^{239}Pu$ ratio of 0.18, the chemical concentration of this element can be estimated to be in the order of 4×10^{-17} M. Lake sediments and soils contain plutonium in the order of 2×10^{-16} to 4×10^{-15} mol g^{-1}. However, speciation

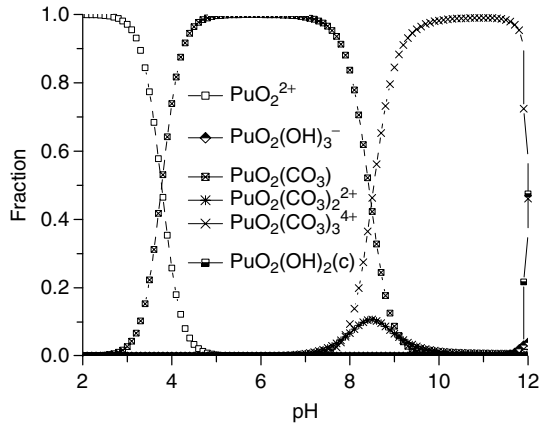

Figure 2.23.14. Species distribution of plutonium(VI) in carbonate media.

techniques for such extremely low concentrations have not been developed yet. Starting from this point, Guillaumont and Adloff [238] discuss possible speciation of the element plutonium in the environment. At first, they assume three basic types of reactions: complexation with inorganic ligands, dimerization of the plutonium and disproportionation of Pu(V). Including natural organic matter like HA, they expect the following main species in solution: Pu(IV): $Pu(OH)_4$; Pu(V): PuO_2^+ at pH < 8 and $PuO_2CO_3^-$ at pH > 8; Pu(VI): PuO_2A^+ at pH < 7.8, $PuO_2(CO_3)_2^{2-}$ at pH < 8.6 and $PuO_2(CO_3)_3^{4-}$ at pH > 8.6. However, Guillaumont concludes that it is not possible to confirm this assumption by experiments.

It has been argued that plutonium in a subsurface environment is relatively immobile because of its low solubility in ground water [239] and strong sorption onto rocks [240].

Recently, it has been reported that plutonium observed in groundwater samples from aquifers at the Nevada Test Site is associated with the colloidal fraction. From the $^{240}Pu/^{239}Pu$ isotope ratio of the samples, it was concluded that the origin of the plutonium is an underground nuclear test site 1.3 km north of the sample site. Therefore, colloidal groundwater migration must have played an important role in the migration of the plutonium [241].

The geochemistry of some actinides has been reviewed in the EPA-report [84]. For speciation calculations, the program code MINTEQA2 was used. The authors provide speciation diagrams for Th^{4+}, the system Pu^{3+}, Pu^{4+} and PuO_2^+ and UO_2^{2+}. For their calculations, the authors assume a water composition given by Hem [85].

The main species in the plutonium system under these water conditions at low pH are PuF_2^{2+} and PuO_2^+; PuO_2^+ exists in the pH range below 6 and in alkaline solutions $Pu(OH)_2(CO_3)_2^{2-}$ is found to be the main species. Other species as $Pu(HPO_4)_4^{4-}$ and $Pu(OH)_4$ are only of minor importance.

Resonance ionization mass spectrometry has been used to analyze the content of Pu in environmental samples [242]. This method allows to detect very small amounts of actinides in the environment and to study the isotopic distribution in a shorter time than conventional α-spectrometry. The isotopic ratio of Pu in sea sediment at the Mururoa atoll was determined to be 97% ^{239}Pu and 3% ^{240}Pu at a specific content of 31 mBq g^{-1}.

For waste management scenarios, the estimation of the dissolved species is important. Synthetic and WIPP brines have been used to study the stability of dissolved Pu(VI) species [243]. It was found that in carbonate-rich synthetic solutions, the formed Pu(VI) carbonate species are very stable over long periods. If carbonate is absent, hydrolytic species are formed in the solution. These species tend to be partly reduced to Pu(V) species. In original WIPP brines, the stability of Pu(VI) is significantly lessened. Pu(VI) concentrations of $\sim 10^{-4}$ M were reduced within a few hours. The reduced species were not identified.

The solubility of plutonium in waters from Yucca Mountain area in different oxidation states was studied [200]. In the plutonium measurements, the oxidation state has to be taken into account. It was found that most of the plutonium remains in the pentavalent oxidation state. At pH 8.5, the patterns for the oxidation state depend on the origin of the ground water. In the carbonate-rich solution with a redox potential of 360 mV, the Pu(IV) content increases. The second water studied had a redox potential of 700 mV. Here, the Pu(VI) cannot be neglected.

An important fact in the speciation of the first transuranium elements in natural environments is their ability to undergo redox reactions. In a study using water conditions comparable to that of a groundwater from the Yucca mountain project site, Nitsche [244] has shown that oxidation states of neptunium, plutonium and americium become stable over time. The experiments were done under supersaturated conditions so that the precipitates could be studied by X-ray powder diffraction measurements. Neptunium was found in steady state always in the +5 oxidation state. Americium did not undergo any change in the oxidation state +3. The situation for plutonium is much more complex. The soluble plutonium was converted to the oxidation state +5 and +6. Starting the experiment from the tetravalent, pentavalent or hexavalent oxidation state, a ratio of 2 : 1 between PuO_2^+ and PuO_2^{2+} was found under steady state conditions. In the case of Pu^{4+} as initial oxidation state, this ratio was 1 : 1 for the original water from the test site.

Complex formation of actinides toward chelating ligands as nitrilotriacetic acid (NTA) and ethylenediaminetetraacetic acid (EDTA) may stabilize these elements in a soluble form. Such ligands have been identified to be contaminants in the mixed organic-radionuclide waste. In the case of plutonium, several oxidation states can exist simultaneously. The complexation behavior of Pu(III), Pu(IV), Pu(V) and Pu(VI) in the presence of NTA and EDTA has been studied by AlMahamid *et al*. [245]. It could be demonstrated that at pH 5 to 8 Pu(IV) is the predominant oxidation state. The other oxidation states of plutonium will either be oxidized or reduced. The stability constant of the Pu(V)-NTA complex is found to be $\log \beta = 6.75$ [246]. In both the NTA and the EDTA system, Pu(IV) will be stabilized, whereas the kinetics in the EDTA system is faster.

Oklo in Gabon is well known as the site of historic natural reactors. Therefore, data for the migration of actinides obtained from this site may be useful for the prediction in a waste repository. The first of the present 16 reactors was discovered in 1972 and was active about 2 billion years ago [247]. This site is the only one known in the world where large amounts of actinides and fission products have been generated in the geosphere. The uranium dioxide concentration here can reach up 17%. It is mentioned that carbonate fissures played an important role in the transport pathway, especially for such elements, which can substitute calcium.

Besides the nuclear reactors at Oklo, one reactor was found at Bagombé, about 20 km from Oklo.

Natural analogue studies at present times resume only the distribution and nonequilibrium effects of isotopic ratios of actinides. The depleted uranium, which was found outside the reactor zone, gives strong evidence for actinide migration. The composition of uranium minerals at Oklo has been studied intensively. The phenomenon of the natural reactor is connected with the age of the uranium deposit, and it has been calculated that the deposit in Oklo is about 2 Ga old. [248, 249].

The radioactive fallout from the Nagasaki bomb explosion was measured as a function of the distance from the hypocenter [250]. The estimated level of distributed activity was 3.49×10^{13} Bq. The highest levels of $^{239+240}$Pu (181 mBq cm^{-2}) were found about 2.8 km east from the center of the explosion. From the data, local fallout of 9.48×10^{10} Bq in an area of 264 km^2 was calculated. With the newest analytical technologies, an ice core from the Ellesmer Island, Canada was investigated. In the zone from 1945, an amount of 0.16 μBq cm^{-2} $^{239+240}$Pu was found. Important information about the transportation of radionuclides during atmospheric testing could, however, be obtained from later zones. The highest amounts of $^{239+240}$Pu were found to be 800 μBq cm^{-2}.

Myasoedov reports about actinide release into natural environment at the site Mayak (Russia) [251]. Two nuclear accidents occurred in 1957 and 1967, respectively. In the first period of operation, about 2.56 MCi of waste were released into the river Techa, creating a contamination of 0.025 p Ci ^{239}Pu/kg sediment. It could be shown that the most mobile actinide is neptunium. The mobility of americium and plutonium remains lower. Studies have shown that the transport of Np and Am is increased because of the formation of FA compounds. The low transportation of

Pu is explained by the formation of insoluble Pu-hydroxo-humic acid complexes.

Nuclear waste of the fabrication of plutonium has been injected in deep boreholes in Tomsk-7 and Krasnoyarsk-26 (Russia) [252]. The study of these sites gives information about the transportation of actinides with groundwater flow in the deep underground. As a result of this study, it was stated that the actinide would reach nearby rivers with the groundwater stream. This occurs for ^{235}U as decay product of ^{239}Pu after 60,000 years and for ^{231}Pa, the decay product of ^{235}U, after 75,000 years. The study predicts polymeric species in the subsurface waters for the actinides thorium, plutonium and americium. The calculations assume a K_d based model. In a newer study [253], possible interactions of the actinides with bacteria were assumed. An important step in the knowledge about the transportation of actinides was the identification of the types of bacteria involved.

Measurements of the plutonium were done near the Semipalatinsk site (Kazakhstan) [254]. It could be shown that the contamination ranges from 140 to 9700 Bq m^{-2} for $^{239/240}$Pu. Depth profiles were taken to study the migration of the plutonium into the underground. The results revealed that most of the fallout plutonium was not leached and should therefore be bound to fused silicates, which are connected to the fallout.

5.6.4 Plutonium in biological systems

Plant uptake of plutonium has been much less studied than that of uranium [255]. Two ways of assimilation are known: direct deposition from radioactive fallout on leafs or by roots. In contrast to other radionuclides, most of the plutonium distributed by the radioactive fallout is found in the topsoil and may be resuspended in the air with dust. The plutonium may be resorbed by the plant via leafs. The transfer factor is estimated to be 0.02 [256, 257]. The transfer factor via roots should be several orders of magnitude lower. Values of 0.0005 are estimated [257]. These values are comparable to those of Haunold [258]. The estimates of transfer factor range from 1×10^{-7} to 2×10^{-4}.

Pimpl [259] gave a sequence for the soil plant transfer of actinides in the following order, Np $\gg$ Am $\sim$ Cm $>$ Pu. These studies were performed inside a greenhouse over seven vegetation periods. The soil was artificially contaminated with ^{237}Np, ^{238}Pu, ^{241}Am and ^{244}Cm. The concentration of the radionuclides in the soil was 1–20 Bq g^{-1} dry mass. The highest transfer factors are measured for grass and corn. It could be shown that the transfer of the actinides from the soil to the plants depends not only on the chemical properties of the actinide ion but are also influenced by properties of the soil.

A critical overview on the distribution of plutonium in soil and plants as well as in organism and animals is given by Coughtrey *et al.* [214].

The conditional stability constant for the Pu(IV)-transferrin complex was determined to be log $\beta = 21.25 \pm 0.75$ [87]. Studies have shown that the Pu-transferrin complex is not able to facilitate the transport of Pu into the cell. The complex dissociates near the cell wall.

Microorganisms may play an important role in the mobility of actinides. Studies of the interaction of this living matter often start with the determination of the uptake of actinides by microorganisms. The association of uranium and plutonium to several bacteria has been studied [260]. It was found that the uptake of uranium is higher than for plutonium. However, there the oxidation state of Pu was not determined, so that the data are not comparable.

Besides studies on the interaction of bacteria with uranium, the uptake of other actinides is also of interest for distribution calculations. It could be shown that some types of bacteria are able to accumulate high amounts of Pu(VI). *P. stutzeri* and *B. sphaericus*, as representatives for aerobic bacteria, have been stressed with hexavalent plutonium [261]. During the study lower oxidation states of Pu were also formed. The authors develop a model to explain these results. In the first step, Pu(VI) interacts with the biomass. This reaction has a fast kinetics and depends on the concentration of the biomass in the suspension.

Using EXAFS, earlier results on the interaction of uranium with biomass confirmed that the actinide metal ion is bound to organo-phosphate

groups. In a second step a slow reduction of the bound Pu(VI) occurs. As the formed Pu(V) shows a much lesser tendency to interact with the biomass, most of it was found in solution. In a third step, this Pu(V) disproportionates into Pu(VI) and Pu(IV). Both oxidation states react with the bacterial cells.

In this way, it could be demonstrated clearly that the formed plutonium(IV) is a result of the disproportionation of Pu(V) and is not caused by the interaction with the biomass.

5.7 Americium

Seaborg, James, Morgan and Ghiorso identified the isotope ^{241}Am late in 1944 after repeated neutron capture reactions by plutonium isotopes in a nuclear reactor. ^{243}Am has the longest half-life of the americium isotopes (8.8×10^3 years as compared to 470 years for ^{241}Am). Americium must be handled with great care to avoid personal contamination. As little as 0.03 μCi of ^{241}Am is the maximum permissible total body burden.

Americium and Curium form trivalent ions in solution. These elements are important in waste repositories.

Laser-induced spectroscopic methods are mostly used for the determination of complex formation constants of Am(III) and Cm(III) in aqueous systems. Low concentration of americium can be detected by LPAS, and laser-induced fluorescence spectroscopy is widely used in curium chemistry [32].

The inner sphere hydration number for Am(III) has been reported to be 9. An equation, similar to Cm (equation 2.23.18), has been derived to correlate the fluorescence decay constant with the number of water molecules in the hydration shell (equation 2.23.17) [16, 326].

$$N_{H_2O} = 2.56 \times 10^{-7} k_{obs}(Am) - 1.43 k_{obs} \text{ in } (s^{-1}) \quad (2.23.17)$$

5.7.1 Solubility and inorganic species

Kulyako *et al*. [188] have compared the solubility of actinide hydroxides at different oxidation states in natural water systems. The authors found that in the series pentavalent Np > hexavalent uranium > trivalent Am > tetravalent Pu decreases and also the origin of the used solvent influences also the solubility. The solubility of $Am(OH)_3$ is nearly the same in groundwater and seawater. For $Pu(OH)_4$, a higher solubility in seawater was found and $UO_2(OH)_2$ was better dissolved in groundwater. However, thermodynamic data were not derived and the species in the solution (pH 6–11) were also not determined.

Runde has studied the solubility of americium carbonate [262]. The solubility product for $AmOHCO_3$ is given to be $\log K_{sp} = -18.70 \pm 0.12$ under a CO_2 partial pressure of 0.03% and for $Am_2(CO_3)_3$ to be $\log K_{sp} = -29.45 \pm 0.18$ for pure CO_2 atmosphere. The ionic strength was 0.1 M, and no extrapolation to infinite dilution has been made.

The NEA database of americium [12] lists only carbonate, cyanide and thiocyanate in the carbon-bearing complexes. The oxalate system has been studied by Choppin and Chen [263] by solvent extraction in $NaClO_4$ solution up to an ionic strength of 9 M. The stability constants were estimated for infinite dilution by use of the Pitzer approach. The first hydrolysis constant was derived to be $\log *\beta_{11} = -7.78 \pm 0.1$ at I = 1 M, $\log *\beta_{11} = -7.83 \pm 0.10$ at I = 3 M and $\log *\beta_{11} = -8.00 \pm 0.12$ at I = 5 M. For the hydrolysis, no data for infinite dilution were estimated. The stability constants with oxalate were also listed as a function of the ionic strength.

To obtain thermodynamic data, temperature-dependent studies are required. The use of LPAS for deriving such data is complicated because of the temperature dependence of the photoacoustic signal. As an example, the americium carbonate system has been studied [37]. In Table 2.23.13, the data for the formation constants as a function of the temperature are summarized. The derived formation constants show the expected temperature dependence. The enthalpy of formation of $AmCO_3^+$ was determined first to be $\Delta H = 37 \pm 11$ kJ mol^{-1} at an ionic strength of 0.1 M.

Experiments on the release of radionuclides are needed as input date for modeling of radioactive

Table 2.23.13. Formation constants of $AmCO_3^+$ at I = 0.1 M [37].

T/K	Log β_{11}
298.2	6.26 ± 0.12
323.2	6.68 ± 0.12
348.2	7.54 ± 0.43

waste disposals. Lysimeter studies can simulate the transportation of contaminants. ^{241}Am was used as tracer for experiments to obtain quantitative datasets [264]. Reducing conditions were reached rapidly in the columns. It was assumed that $AmOHCO_3$ is the solubility-limiting phase. The observed maximum concentration of Am was 3×10^{-9} M, which is below the predicted concentration of 10^{-8} M. The species in solution for neutral pH range are carbonate species.

5.7.2 Species with organic ligands

Several authors have studied the interaction of water from well J-13 (Yucca Mountain Project) with actinides. This water also contains humic material, which was isolated and then studied by Minai *et al*. [265]. The concentration of carboxylic groups has been determined to be 2.7 meq g^{-1} and 4.6 meq g^{-1} for fulvic and humic acid, respectively. The interaction of this material with americium has been studied, and the binding constants were found to be similar to other humic materials. The binding constants were given as function of the degree of ionization α. Thus, unfortunately these data cannot be compared with those of other authors. It is mentioned that in contrast to the uranium(VI) system the formation of americium humate is not negligible, if carbonate is present.

The interaction of the Am^{3+} with humic, fulvic and citric acid (HA, FA and Cit) was studied as a function of ionic strength (NaCl). It was found that at high ionic strength, the binding constants are comparable to log β_1(AmCit) $\approx$ log β_1(AmFA) $\approx$ log β_1(AmHA) [266].

Formation constants for the Am(III) humate complexation are determined by laser-induced photoacoustic spectroscopy (LIPAS) [267]. For speciation measurements, the absorption of Am^{3+} at 503.2 nm and of the formed complex at 506 nm was used. The study was performed at an initial americium concentration of 9×10^{-7} M. For normal UV-VIS spectroscopy, americium concentrations between 2×10^{-5} and 1×10^{-4} M have been used. This also demonstrates the advantage of LIPAS. As also found later for the curium speciation, the stability constants show no dependency on the ionic strength. For Aldrich humic acid and Bradford HA formation, measured constants are log $\beta_{An(III)-HA} = 6.27 \pm 0.04$ and log $\beta_{An(III)-HA} = 6.36 \pm 0.14$, respectively. For Gorleben humic acid, the stability constant was assigned to be log $\beta_{An(III)-HA} = 6.44 \pm 0.15$ [268]. In this paper, a slightly higher value of log $\beta_{An(III)-HA} = 6.39 \pm 0.14$ for Aldrich HA is given, but both data agree within the error limits.

By spectrophotometry and size exclusion chromatography (SEC), Moulin *et al*. [269] determined the interaction of americium with humic material. It was assumed that a 1 : 1 complex formation occurs. However, it is mentioned that the comparison of the data with other authors is problematic because of the use of nonconsistent systems of units. By this, it was tried to recalculate all available data to a system based on the $L^* g^{-1}$ scale. The data obtained by SEC are somewhat higher than the spectrophotometric data. Most of the data are in a range from log $\beta = 3.1$ to log $\beta = 4.8$. Because of the assumed 1 : 1 model, the authors admit the limitations of these determinations.

Czerwinski *et al*. [131] have applied the charge neutralization model to the trivalent actinides. Ternary complexes are not included in this study. A relatively small effect of the ionic strength on the complexation constants was ascertained. Because of the model, the averaged formation constant was determined to be log $\beta_{An(III)-HA} = 6.24 \pm 0.14$. By extrapolation to infinite dilution, the formation constant was assigned to be log $\beta_{An(III)-HA} = 6.52 \pm 0.06$. However, these data are only valid at pH > 6 because of the possible formation of ternary species.

The interaction of humic acid with actinides has been studied intensively. The complexation of americium with humic acid at very low concentrations [270] shows no significant difference to data

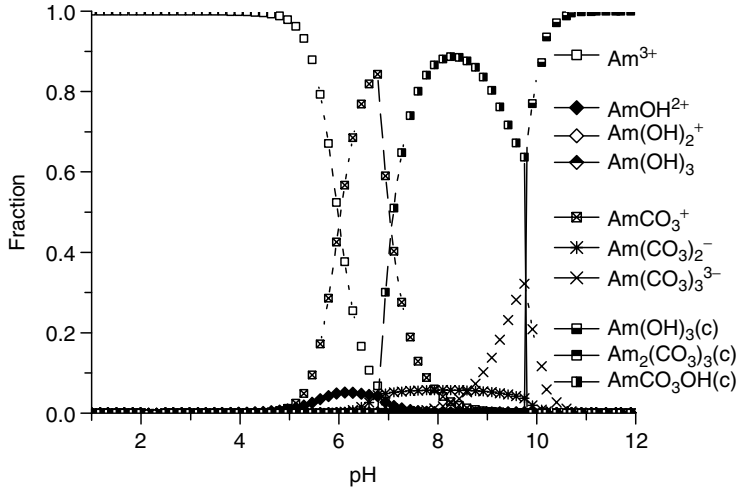

Figure 2.23.15. Species distribution of Am^{3+}, see text, stability constants [12].

obtained at higher concentrations. In a 1×10^{-11} M solution, the formation constant was derived to be $\log \beta = 6.6 \pm 0.2$. Data obtained at higher americium concentrations are $\log \beta = 6.41 \pm 0.14$ at 1×10^{-5} M Am [268], $\log \beta = 6.31 \pm 0.09$ at 7×10^{-7} M Am [267] and $\log \beta = 6.44 \pm 0.12$ at 1×10^{-6} M Am [130].

A calculation of the species distribution of actinide humate complexes has been published by Andersson [271]. For modeling the computer code, PHREEQE was used. As phosphate ions were included in these calculations, it was found that the humate complexes are present only in very small amounts in the thorium, uranium, neptunium and plutonium system. In contrast to this in the americium system, which was used as an example for trivalent actinides, americium humate species were formed, which are more stable than the phosphate species. Figure 2.23.15 shows the species distribution of Am. The total Am^{3+} concentration was set to be 1.0×10^{-6} M and the maximum total carbonate concentration was 0.01 M.

The available data for speciation of the higher actinide elements are mostly limited to studies for the separation of these elements during the production cycle. The stability constants of the trivalent actinides americium, curium, californium fermium and mendelevium with 1,2-diaminocyclohexane tetraacetic acid range from $\log \beta = 18.7$ to $\log \beta = 19.7$ [272]. The increase of the stability constants in this series is explained by the decrease of the ionic radii of the trivalent actinides.

As mentioned already for neptunium and plutonium, very little information on the speciation of americium in biological systems can be found. Some information on soil and uptake by plants are summarized in the literature [214].

5.8 Curium

As a result of helium-ion bombardment of ^{239}Pu, curium was discovered by Seaborg, James and Ghiorso in 1944. The most stable isotope is ^{247}Cm, with a half-life of 16 million years. The presence of natural curium, however, has never been detected.

Only a few papers on the absorption spectra of transuranium elements has been published. This may be due to the problems involved in the handling of highly concentrated radioactive solutions. Especially, the generation of decomposition products of the solvent by the radiation caused a lot of problems in observing these spectra [273]. For curium, three absorption bands have been reported. In perchloric acid solutions, they are located at 375.4 nm, 381.1 nm and 396.4 nm.

Similar to Am, the correlation between the number of water molecules in the hydration shell and the fluorescence decay constant is: (equation 2.23.18) [326].

$$N_{H_2O} = 0.65 \times 10^{-4}\ k_{obs}(Cm) - 0.48\ k_{obs}(s^{-1}) \qquad (2.23.18)$$

5.8.1 Solubility and inorganic species

The hydrolysis of curium has been studied exploiting several techniques. The most applicable method to study the chemistry of curium at low concentration is the laser-induced fluorescence spectroscopy. Wimmer *et al.* [274] report the hydrolysis constants in 0.1 M $NaClO_4$ solution to be $\log \beta_{11} = 6.67 \pm 0.18$ and $\log \beta_{12} = 12.06 \pm 0.28$. These data differ significantly from those reported earlier by other authors, who exploited conventional techniques such as extraction and electromigration. When the data were compared to those of the neighboring element americium, a much better agreement was found.

Emission spectra of the hydrolysis products of curium have been obtained by deconvolution [275]. The emission maxima for $Cm(OH)^{2+}$ and $Cm(OH)_2{}^{+}$ are 598.7 nm and 603.5 nm, respectively. From the fluorescence intensities, the formation constants are derived to be $\log \beta_{11}^{\circ} = 6.38 \pm 0.09$ and $\log \beta_{12}^{\circ} = 12.3 \pm 0.2$.

The chemistry of curium with carbonate has been studied intensively because of the excellent fluorescence properties of this actinide ion in solution. By use of this method, the species $CmCO_3{}^{+}$, $Cm(CO_3)_2{}^{-}$ and $Cm(CO_3)_3{}^{3-}$ can be quantified by peak deconvolution. However, there is evidence for species formed with hydrogencarbonate ions [276, 277]. The formation constant was assigned to be $\log \beta_{111}^{\circ} = 1.9 \pm 0.2$ for the $Cm(HCO_3)^{2+}$. The formation constants for the other carbonate species $CmCO_3{}^{+}$, $Cm(CO_3)_2{}^{-}$, $Cm(CO_3)_3{}^{3-}$ and $Cm(CO_3)_4{}^{5-}$ are $\log \beta_{101}^{\circ} = 5.9 \pm 0.1$, $\log \beta_{102}^{\circ} = 10.27 \pm 0.3$, $\log \beta_{103}^{\circ} = 13.18 \pm 0.45$ and $\log \beta_{103}^{\circ} = 14.18 \pm 0.65$, respectively. The data show that hydrogencarbonate complex is formed to a small extent. As the study is performed in 1 mol kg^{-1} NaCl, a direct comparison to other data is not possible; the formation of mixed hydroxo-carbonate species also cannot be confirmed.

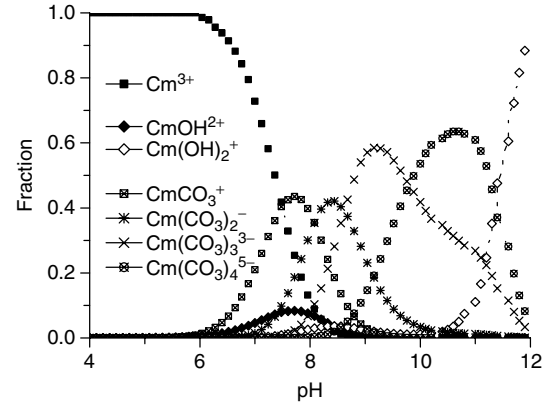

Figure 2.23.16. Species distribution of 1.0×10^{-8} M Cm^{3+} in carbonate water, stability constants [277].

The species distribution of a solution containing 1.0×10^{-8} M Cm^{3+} and 0.01 M CO_2(aq)/$HCO_3{}^{-}$/$CO_3{}^{2-}$ is shown in Figure 2.23.16.

Three curium-sulfate species could be identified spectroscopically [278]. These species are $Cm(SO_4)^{+}$, $Cm(SO_4)_2{}^{-}$ and $Cm(SO_4)_3{}^{3+}$. The fluorescence emission maxima of these species are 596.2, 599.5 and 602.2 nm, respectively. The formation constants are given for an ionic strength of 3 mol kg^{-1} to be $\log \beta_1 = 0.93 \pm 0.08$ and $\beta_2 = 0.61 \pm 0.08$. The formation of the third species is estimated only at a high sulfate concentration above 1 mol kg^{-1} sulfate.

Brine solutions contain several potential inorganic ligands such as OH^{-}, $CO_3{}^{2-}$, $H_2PO_4{}^{-}$, $HSiO_4{}^{-}$ F^{-}, $HCO_3{}^{-}$ $SO_4{}^{2-}$ and Cl^{-}. Fanghänel and Kim [279] give an overview on the complex formation of Cm(III) with inorganic ligands. Included in this summary are the ion-interaction coefficients to estimate the formation constants according to the Pitzer equation. This model can be used up to high salt concentrations of 6 mol kg^{-1}.

5.8.2 Species with organic ligands

Fluorescence studies with organic ligands may be accompanied by energy transfer reactions

from the excited metal ion and *vice versa*. An intramolecular energy transfer in Cm^{3+} complexes is reported [280]. It was found that at an excitation wavelength of 308 nm, the fluorescence yield was increased by 77% for the phthalate and by 30% for the salicylate complex. In contrast to this, humate and fulvate complexes show only an increase of 2.3% and less.

The speciation of curium(III) in Gorleben groundwater was studied directly by time-resolved laser-induced fluorescence spectroscopy [274]. The curium concentration added to the groundwater was 7.8×10^{-9} M to 6.3×10^{-8} M. For deconvolution of the measured spectra, those of the individual species were used. The result was compared to a thermodynamic calculation of the species distribution. The predominant speciation of curium was assigned to be humate and carbonate species. Hydrolysis species are present in negligible concentrations. The direct measurements have demonstrated that the humate speciation is underrepresented in the thermodynamic calculation. Possible explanations for this behavior are the formation of ternary species and the formation of pseudocolloids.

Time-resolved laser-induced fluorescence spectroscopy was used to determine the speciation of curium in groundwater from the Gorleben site that is rich in HA. Ternary species of curium were postulated because of a stronger interaction of this actinide element than predicted using known humate complexation constants. The species expected in the solution are Cm(OH)HA, $Cm(OH)_2HA$ and $Cm(CO_3)HA$ [281]. A strong interaction of humic acid with curium has been reported. The stability of these complexes can only be explained by the assumption of ternary hydroxo or carbonato species. Fluorescence measurements confirm this assumption. The stability constants are given to be $\log \beta_{Cm(CO_3)HA} = 12.4 \pm 0.2$, $\log \beta_{Cm(OH)HA} = 13.1 \pm 0.2$ and $\log \beta_{Cm(OH)_2HA} = 17.0 \pm 0.3$. Calculations of species distribution including these ternary complexes and 1% CO_2 show at pH 6.6 up to 20% of the Cm(OH)HA complex and at pH 7.8 up to 85% $Cm(CO_3)HA$. It was concluded that stability constants obtained at low pH cannot be extrapolated to natural systems with pH > 6. It can be expected that under groundwater conditions both binary and ternary complexes be formed. An important result of this study is that results obtained below pH 6 may not be extrapolated to higher pH values.

To model the functionality of humic substances, several organic ligands have been used. Klenze *et al*. [282] have studied the complex formation of 5-sulfosulfuric acid (H_3SSA) with Cm(III). The formation constants are obtained at ionic strengths of 0.15 M and 0.3 M. The formation constants did not show a dependence on the ionic strength of the solution. Two complexes are detected, Cm(SSA) and $Cm(SSA)_2^{3-}$, the formation constants are derived to be $\log \beta_{101} = 6.44 \pm 0.03$ and $\log \beta_{101} = 11.99 \pm 0.04$.

The metal charge ion neutralization model was developed to obtain the stability constants for humate complexes, which are independent on pH, concentration of the metal and the concentration of the organic ligand [130]. This is due to the diverse origins of HA. By introducing the loading capacity as concentration term for the humic acid, for example, the trivalent actinides show a stability constant between $\log \beta = 6.10 \pm 0.12$ and $\log \beta = 6.42 \pm 0.14$.

The stability constants for fulvate species of americium and curium are $\log \beta = 5.78 \pm 0.07$ and $\log \beta = 5.90 \pm 0.11$, respectively [283].

Stumpf *et al*. [284] report on the sorption of curium onto smectite and kaolinite. However, it could be also shown that curium is incorporated into the crystal lattice of calcite [285]. The authors came to this conclusion by studying the spectral shift of the fluorescence signal and the increase of the fluorescence decay time of the formed curium species.

5.8.3 Curium in biological systems

From studies of the Nd(III)- and Sm(III)-transferrin complexes [87], the formation constants of Am(III) and Cm(III) were estimated to be $\log K_1 = 6.3 \pm 0.7$ and $\log K_1 = 6.5 \pm 0.8$.

Curium shows one of the highest fluorescence efficiency of f-elements. Therefore, this property

can be used to study the interaction of curium species with bacteria. The interaction of Cm(III) with *Bacillus subtilis* and *Halobacterium salinarum* shows K_d values from 1000 to 10,000 in the pH range 3.0–5.0 [286]. These data are comparable to those obtained by Kobuta *et al.* [215] for neptunium(V) and *D. desulfuricans*. From the fluorescence lifetime a change in the number of water molecules in the coordination sphere was derived. In case of *B. subtilis*, a decrease was found with increasing pH, and in case of *H. salinarum* an increase of the number of water molecules with increasing pH was shown. The authors conclude that the sorption on *H. salinarum* occurs on a more outer sphere than for *B. subtilis*.

5.9 Transcurium elements

5.9.1 Berkelium

Thompson, Ghiorso and Seaborg discovered berkelium in 1949. It was synthesized by cyclotron bombardment of Am-241 with helium ions. Bk-247 has the longest half-life of 1380 years. Berkelium should be soluble in dilute mineral acids. Up to now, berkelium is found to have the oxidation states +III and +IV. Bk(IV) can be generated only by strong oxidizing agents.

Bk(III) shows emission lines at 15,349 cm^{-1} and 13,475 cm^{-1} [287]. The intensity ratio between these two bands depends on the intensity of the exciting light source and the temperature of the sample.

Antonio *et al.* [17] have studied the coordination environment of Bk^{3+} and Bk^{4+}. They describe the redox reaction between both oxidation states as follows (equation 2.23.19).

$$[Bk(OH_2)_8]^{4+} + H_2O + e^- \leftrightarrow [Bk(OH_2)_9]^{3+} \quad (2.23.19)$$

They conclude that the change in the hydration number is predominantly influenced by steric factors, namely the difference in the ionic radii.

Désiré and H. Hussonois *et al.* report on the hydrolysis of some trivalent actinides [288–290]. At an ionic strength of 0.1 M, the following data were derived using solvent extraction

Table 2.23.14. Stability constants of complexes of some trivalent transplutonium elements with 1,2-diaminocyclohexanetetraacetic acid [292].

Element	Log β_{11}
Am^{3+}	18.79
Cm^{3+}	18.81
Bk^{3+}	19.16
Cf^{3+}	19.42
Es^{3+}	19.44
Fm^{3+}	19.56

$\log *\beta_{11} = -5.92$ (Am^{3+} and Cm^{3+}), $\log *\beta_{11} = -5.10$ (Bk^{3+}), $\log *\beta_{11} = -5.62$ (Cf^{3+}). However, Ahrland [291] assumes that the used method gives much to high values. The speciation distribution in Fig. 2.23.17 was calculated using the data of Désiré [288–290].

To compare complex formation of the transplutonium elements, only some publications on element separations can be used. Bybarz [292] lists the stability constants of several complexes with 1,2-diaminocyclohexanetetraacetic acid in 0.1 M NH_4ClO_4. These data (Table. 2.23.14) may give an impression about the systematic in the formation constants of trivalent transplutonium elements. The data are derived from ion exchange experiments.

An important ligand used in such separation studies is di(2-ethylhexyl)orthophosphoric acid (HDEHP), [293]. However, the stability constants

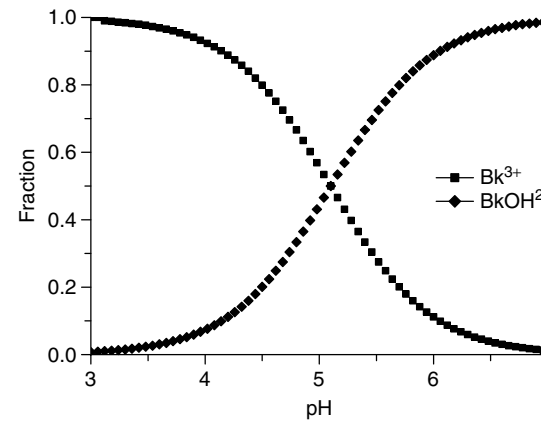

Figure 2.23.17. Formation of the first hydrolysis product of Bk^{3+} (1.0×10^{-8} M, I = 0.1 M), stability constants [288].

were not derived from these extremely fast and sensitive separations.

Several complex formation constants of berkelium are known and summarized in [294].

Recently, the production of organometallic ions of berkelium has been reported [295]. These ions were generated by laser ablation of Bk_2O_3 and are characterized by an actinide-carbon bond.

5.9.2 Californium

Thompson, Street, Ghiorso and Seaborg have discovered the element californium in 1950 by bombarding ^{242}Cm with helium nuclei. The half-life of ^{251}Cf Californium is estimated to be 899 y. All isotopes of californium known from the literature are artificial.

It is possible to produce weighable amounts of Cf, especially of the isotope ^{252}Cf in the high flux isotope reactor at Oak Ridge National Laboratory (ORNL). Up to now, there are four main uses as follows for ^{252}Cf.

1. As neutron source, because of its spontaneous fission
2. As target material for the production of transcalifornium elements
3. For work with Cf tracers and
4. As source for the production of ^{248} Cm, which is mainly used in basic Cm studies.

In aqueous solutions, californium(III) is the normally stable ion. The highest reported oxidation state is the tetravalent oxidation state.

The tendency of actinides to form complexes controls the behavior of actinides in blood. Plasma has been found to be the main transport chain in blood. The bond of trivalent actinides, like Ac(III), Am(III), Cm(III) and Cf(III), to transferrin appears to be weaker [87]. However, the formation strength and probably also the mechanism differ between the actinides. Studies have also shown that a second anion like bicarbonate is necessary for the formation of the transferrin species. It should be noted that carbonate and citrate anions might influence the speciation of U(VI) and Pu(IV), respectively.

Similar to berkelium organometallic ions could be produced for californium [295].

5.9.3 Einsteinium

Ghiorso and coworkers in 1952 discovered the element einsteinium together with the element fermium in the debris from a thermonuclear explosion in the Pacific. This element was generated from uranium-238 by capturing a large number of neutrons. The neutron-rich nuclei then undergo several β decays, leading to ^{253}Es. ^{252}Es has the longest half-life of 1.29 y.

In solution, einsteinium is only stable in the trivalent state. The properties vary only slowly within the series of trivalent actinides. Therefore, the stability constants can be estimated from data of other trivalent actinides.

Basic research on the excited states of einsteinium show emission spectra if Es^{3+} in LaF_3 and $LaCl_3$ matrices [296]. Data for the fluorescence lifetime of the $^5F_5$ state of Es^{3+} are 1.05 μs in aqueous systems and 3 μs in D_2O.

Complex formation of einsteinium has been studied with several inorganic and organic ligands. Hydrolysis of einsteinium occurs at medium pH. The first hydrolysis constant was found to be $\log *K_1 = -5.14$ [290]. Also, the chloride [297] and sulfate complexes [298] are described in the literature. However, there are some discrepancies in the referred data [299, 58].

Divalent einsteinium is only stable under strong reducing conditions. The reduction potential was first estimated to be -1.6 [300]. Es^{2+} in solution was detected by cocrystallization with $SmCl_2$ in ethanol [301, 302].

5.9.4 Fermium

The element fermium was discovered together with einsteinium in the residues of a thermonuclear test. The isotope ^{257}Fm has a half-life of 101 d.

The chemical properties of fermium have been studied with tracer amounts. Under normal conditions in aqueous media, only the oxidation state Fm^{3+} exist. Under strong reducing conditions, Fm also forms a divalent species [303–305].

Complex formation of fermium with several ligands has been reported already. Most of them are important for the separation of fermium from other actinide elements.

Reported organic ligands are β-diketones [289], hydroxycarboxylic acids [306–310] and organophosphorous esters [311, 312, 293]. Lactic acid [308] and α-hydroxyisobutyric acid have also been used for separation of the trivalent actinides by cation exchange chromatography. Using di-2-ethylhexylorthophosphoric acid [293], the separation can be done by solvent extraction chromatography.

Two types of 1 : 2 complexes are reported for citric acid. They differ only by one proton bond to the ligand. The formation constants differ by more than 4 orders of magnitude [313]. For the reaction (2.23.20),

$$Fm^{3+} + 2\ C_6H_8O_7 \leftrightarrow Fm(C_6H_2O_7)_2{}^{3-} + 6H^+ \quad (2.23.20)$$

a formation constant of $\log K = 13.76$ was assigned. The second reaction (2.23.21) is given as

$$Fm^{3+} + 2C_6H_8O_7 \leftrightarrow Fm(C_6H_3O_7)_2{}^{3-} + 5H^+ \quad (2.23.21)$$

with a formation constant of $\log K = 9.15$.

Diethylenetriamine-pentaethanoic acid forms a 1 : 1 complex, the formation constant is assigned to be $\log K_1 = 22.7$ [292]. The formation constant with trans-1,2-Diaminocyclohexane-*N*,*N*,*N*′,*N*′-tetraethanoic acid is found to be the same as for mendelevium [272].

The first hydrolysis constant of fermium(III) has been determined to be $\log *\beta_1 = -3.8 \pm 0.2$ [289]. For the determination, a solvent extraction method was used. Fermium can be reduced under acidic conditions. The polarographic half wave potential of the redox couple Fm^{3+}/Fm^{2+} has been determined to be -1.45 V versus NHE [304].

5.9.5 Mendelevium

Mendelevium is the ninth transuranium element of the actinide series. Ghiorso, Harvey, Choppin, Thompson and Seaborg first identified it in 1955. The isotope ^{253}Es was bombarded with helium ions in the Berkeley 60-inch cyclotron. ^{258}Md has a half-life of 55 d.

Mendelevium forms ions in the tripositive (III) oxidation state, which is characteristic for most of the actinide elements. However, it also possesses a moderately stable dipositive (II) oxidation state.

First experiments with mendelevium confirmed a trivalent oxidation state, as this element is quantitatively coprecipitated with trivalent lanthanides [314]. Data from cation exchange and solvent extraction are also consistent with this assumption.

Under reducing conditions, Md can be coprecipitated with $BaSO_4$. These and also solvent extraction experiments under reducing conditions show that Md can be reduced easily to the divalent oxidation state.

The reported monovalent oxidation state [315] could not be confirmed independently [316–318].

Experiments to oxidize Md^{3+} to Md^{4+} were also unsuccessful [319].

Complex formation of mendelevium is only reported with trans-1,2-Diaminocyclohexane-*N*,*N*,*N*′,*N*′-tetraethanoic acid [272]. The formation constant for the 1 : 1 complex is assigned to be $\log K_1 = 19.7$.

5.9.6 Nobelium

In April 1958, A. Ghiorso, T. Sikkeland, J.R. Walton and G.T. Seaborg discovered and identified a new element. However, the name nobelium was assigned and accepted by the IUPAC on the basis of an experiment performed by a team of workers from US, Britain and Sweden in 1957. The half-life of the longest-living isotope ^{255}No is 3.1 min. As nobelium is an element of the actinide series, it was expected to form a trivalent ion. Seaborg predicted in 1949 that a relatively stable 2+ state might exist. Using cation exchange and coprecipitation, this prediction was confirmed [320].

The standard oxidation potential for the redox couple No^{2+}/No^{3+} has been estimated from tracer experiments to be -1.4 to -1.5 V [321].

The complexing ability of this element toward chloride can be compared to that of divalent transition metals and weakly complexed alkaline earth

elements [322]. The formation of complexes with citrate oxalate and acetate was studied employing solvent extraction techniques [298, 323]. The stability of the 1 : 1 complexes was found to be comparable to that of Ba and Sr. The formation constants in 0.5 M NH_4NO_3 are reported to be log $K_1 = 2.2 \pm 1.3$; 1.7 ± 0.8 and 0.7 ± 0.7 for citrate, oxalate and acetate, respectively. This behavior is more like that of strontium.

5.9.7 Lawrencium

A. Ghiorso, T. Sikkeland, A.E. Larsh and R.M. Latimer discovered the last member of the 5f transition elements in 1961. Lr-261 has a half-life of 3.9 min.

By use of very rapid solvent extraction techniques, Silva and coworkers [324] extracted lawrencium ions from a buffered aqueous solution into an organic solvent, completing each extraction in about 30 s. They were able to study the oxidation behavior of this element at only a few atoms of the isotope Lw-256.

The chemistry of Lw is like the tripositive elements of the actinide and lanthanide series. Up to now, detailed information about the solution chemistry of this element is not available.

6 OUTLOOK

New developments toward speciation of actinides are seen in two ways:

1. *Synthesis and structural studies of complexes with bioactive ligands* – Natural complexing ligands often show a nonhomogeneous structure. The determination of stability constants with these ligands is often accompanied by several problems, as the discussion of the humate speciation has shown. The synthesis of substances to model the functionality of natural ligands and the study of the complex formation [132, 133] can be seen as one way for a better understanding of speciation in the environment. The role of biological activity in the migration of radionuclides in the biosphere at a molecular basis can be better understood if basic studies on the interaction of actinides with species of biological relevance are performed. The design of new, effective pharmaceutical agents for the removal of radiotoxic elements from contaminated individuals is an important goal for the protection of our environment [325].

2. *Development and application of new methods* – The combination of excitation and emission spectroscopy in a two-dimensional fluorescence spectroscopy provides a lot of information on the spectroscopic change during complex formation of multifunctional ligands such as humic acids [134]. A second interesting way is the direct study of the spectroscopic properties of organic ligands and their change by complex formation. This needs a spectrometer, which is dedicated to the spectroscopic properties of the ligand with short fluorescence lifetimes. Also, the discovery of new properties of actinides [102] leads to the application of modern speciation techniques for the direct determination of species.

7 ACKNOWLEDGMENT

The author gratefully acknowledges the help of many colleagues at the Institute of Radiochemistry. Prof. G. Bernhard gave many hints during the preparation of the manuscript. V. Brendler and D. Vulpius have performed speciation calculations. A. Günther, S. Hübener, H. Moll, C. Nebelung and S. Sachs provided support during the selection of the literature.

8 REFERENCES

1. Choppin, G. R., *Radiochim. Acta*, **43**, 43 (1983).
2. Brookins, D. G., *Eh-pH Diagrams for Geochemistry*, Springer-Verlag, Berlin, Heidelberg, New York, London, Paris, Tokyo, 1988.
3. J. Stary and H. Freiser, *Equilibrium Constants of Liquid-Liquid Distribution Reactions*, Part 4, Chelating Extractants, IUPAC Chemical Data Series No. 18, Pergamon Press, Oxford, 1978.
4. Arnold, Th., Zorn, T., Zänker, H., Bernhard, G. and Nitsche, H., *J. Contam. Hydrol.*, **47**, 219 (2001).
5. Brendler, V., Vahle, A., Arnold, Th., Bernhard, G. and Fanghänel, Th., *J. Contam. Hydrol.*, **61**, 281 (2003).
6. Kim, J. I., *Radiochim. Acta*, **53/53**, 71 (1991).

7. von Gunten, H. R. and Benes, P., *Speciation of Radionuclides in the Environment*, Report PSI No. 94–03, 1994.
8. Kim, J. I., *MRS Bull.*, **19**, 47 (1994).
9. von Gunten, H. R. and Benes, P., *Radiochim. Acta*, **69**, 1 (1995).
10. Kim, J. I., in *Handbook of the Physics and Chemistry of the Actinides*, Vol. 4, Freeman, A. J. and Keller, C. (Eds.), Elsevier Science Publishers B.V., 1986, Chapter 8, p. 413.
11. Wimmer, H., Klenze, R. and Kim, J. I., *Radiochim. Acta*, **56**, 79 (1991).
12. Silva, R. J., Bidoglio, G., Rand, M. H., Robouch, P., Wanner, H. and Puigdomenech, I., *Chemical Thermodynamics of Americium*, Chemical Thermodynamics Vol. 2, NEA-OECD, Elsevier, Amsterdam, Lausanne, New York, Oxford, Shannon, Tokyo, 1995.
13. d'Ans, J. and Lax, E., in *Taschenbuch für Chemiker und Physiker*, Vol. 3, 4th ed., Blachnik, R. (Ed.), Springer-Verlag, Berlin, Heidelberg, New York, Barcelona, Budapest, Hong Kong, London, Mailand, Paris, Santa, Clara, Singapore, Tokio, 1998, p. 259.
14. Cotton, F. A. and Wilkinson, G., *Anorganische Chemie*, 3rd ed., translated by Fritz, H. P., VEB Deutscher Verlag der Wissenschaften, Berlin, 1970, p. 1007.
15. Bilewicz, A. and Wlodzimirska, B., *Determination of the Ionic Radius of No3+*, Department of Radiochemistry, INCT, Warsaw, 1996.
16. Kimura, T. and Kato, Y., *J. Alloys Compd.*, **271–273**, 867 (1998).
17. Antonio, M. R., Williams, C. W. and Soderholm, L., *Radiochim. Acta*, **90**, 851 (2002).
18. Mauerhofer, W. and Rösch, F., *Primary hydration numbers of actinyl ions*, Annual report, Inst. F. Kernchemie, Johannes Gutenberg-Universität Mainz, 2001.
19. Antonio, M. R., Soderholm, L., Williams, C. W., Blaudeau, J. P. and Bursten, B. E., *Radiochim. Acta*, **89**, 17 (2001).
20. Bolvin, H., Wahlgren, U., Moll, H., Reich, T., Geipel, G., Fanghänel, Th. and Grenthe, I., *J. Phys. Chem. A*, **105**, 11441 (2001).
21. Moll, H., Denecke, M. A., Jelilehvand, F., Sandström, M. and Grenthe, I., *Inorg. Chem.*, **38**, 1795 (1999).
22. Allen, P. G., Bucher, J. J., Shuh, D. K., Edelstein, N. M. and Reich, T., *Inorg. Chem.*, **36**, 4676 (1997).
23. Reich, T., Geipel, G., Funke, H., Hennig, C., Rossberg, A. and Bernhard, G., *XANES and EXAFS Measurements of Plutonium Hydrates*, Project Group ESRF Beamline (CRG ROBL) – Bi-Annual Report 1999/2000, FZR-322 27, 2001.
24. Spencer, S., Gagliardi, L., Handy, N. C., Ioannou, A. G., Skylaris, Ch.-K., Willetts, A. and Simper, A. M., *J. Phys. Chem. A*, **103**, 1831 (1999).
25. Lieser, K. H., *Einführung in die Kernchemie*, 3. Auflage, VCH Verlagsgesellschaft, Weinheim, New York, Basel, Cambridge, MA, 1991, p. 48.
26. Römer, J., Kienzler, B., Vejmelka, P., Soballa, E., Görtzen, A. and Fuß, M., *Actinide Migration Experiment in the HRL ÄSPÖ*, Results of Laboratory and *In situ* Experiments (Part II), Report FZKA 6770, Sweden, 2002.
27. Reich, T., Bernhard, G., Geipel, G., Funke, H., Hennig, C., Rossberg, A., Matz, W., Schell, N. and Nitsche, H., *Radiochim. Acta*, **88**, 633 (2000).
28. Brown, R. M., Hislop, J. S. and Pickford, C. J., in *Speciation of Fission and Activation Products in the Environment*, Bulman, R. A. and Cooper, J. R. (Eds.), Elsevier Applied Science Publishers, London, 1985, p. 1.
29. Nitsche, H., Silva, R. J., Brendler, V., Geipel, G., Reich, T., Teterin, Y. A., Thieme, M., Baraniak, L. and Bernhard, G., in *Actinide Speciation in High Ionic Strength Media*, Reed, D. T., Clark S. B. and Rai, L. (Eds.), Kluwer Academic/Plenum Press, New York, Boston, Dordrecht, London, Moscow, 1999, pp. 11–138.
30. Beitz, J. V. and Hessler, J. P., *Nucl. Technol.*, **51**, 169 (1980).
31. Schrepp, W., Stumpe, R., Kim, J. I. and Walther, H., *Appl. Phys. B*, **32**, 207 (1993).
32. Beitz, J. V., Bowers, D. L., Doxtander, M. M., Maroni, V. A. and Reed, D. T., *Radiochim. Acta*, **44/45**, 87 (1988).
33. Kim, J. I., Stumpe, R. and Klenze, R., *Top. Curr. Chem.*, **157**, 129 (1990).
34. Klenze, R., Kim, J. I. and Wimmer, H., *Radiochim. Acta*, **52/53**, 97 (1991).
35. Geipel, G., Bernhard, G., Brendler, V. and Nitsche, H., *Radiochim. Acta*, **82**, 59 (1998).
36. Demtröder, W., *Laserspektroskopie*, 2nd ed., Springer-Verlag, Berlin, Heidelberg, New York, London, Paris, Tokyo, Hong Kong, Barcelona, Budapest, 1991.
37. Wruck, D. A., Palmer, C. E. A. and Silva, R. J., *A Study of Americium(III) Carbonate Complexation at Elevated Temperatures by Pulsed Laser Photoacoustic Spectroscopy*, Report UCRL-JC-125198, 1996.
38. Sekine, T., Naito, S., Kino, Y. and Kudo, H., *Radiochim. Acta*, **82**, 135 (1998).
39. Silva, R. J. and Nitsche, H., *Radiochim. Acta*, **70/71**, 377 (1995).
40. Kimura, T., Serrano, J. G., Nakayama, S., Takahashi, K. and Takeishi, H., *Radiochim. Acta*, **58/59**, 173 (1992).
41. Valeur, B., *Molecular Fluorescence*, Wiley-VCH, Weinheim, New York, Chichester, Brisbane, Singapore, Toronto, 2002.
42. Kim, J. I., Wimmer, H. and Klenze, R., *Radiochim. Acta*, **54**, 35 (1991).
43. Moulin, V. and Moulin, C., *Radiochim. Acta*, **89**, 773 (2001).
44. Nitsche, H., *J. Alloys Compd.*, **223**, 274 (1995).
45. Conradson, S. D., *Appl. Spectrosc.*, **52**, 252A (1998).
46. Koningsberger, D. C. and Prins, R., *X-Ray Absorption, Principles, Application Techniques of EXAFS, SEXAFS and XANES*, John Wiley & Sons, New York, 1988.

47. Fuger, J., *Radiochim. Acta*, **58/59**, 81 (1991).
48. Pearsons, F. J. and Berner, U., *NAGRA Thermochemical Data Base I. Core Data*, Technical report 91-17, NAGRA, Wettingen, Switzerland, 1991.
49. Pearsons, F. J., Berner, U. and Hummel, W., *NAGRA Thermochemical Data Base II. Supplemental Data 05/92*, Technical report 91-18, 1992.
50. Grenthe, I., Fuger, J., Konings, R. J. M., Lemire, R. J., Muller, A. B., Nguyen-Tung Cregu, Ch. and Wanner, H., *Chemical Thermodynamics of Uranium*, Chemical Thermodynamics Vol. 1, NEA-OECD, North-Holland, Amsterdam, London, New York, Tokyo, 1992.
51. Falck, W. E., Read, D. and Thomas, J. B., *Chemval 2: Thermodynamic Database*, Report EUR 16897, 1996.
52. J. Fuger, *The Chemical Thermodynamics of the Actinide Elements and Compounds, Part 12, the Actinide Aqueous Complexes*, International Atomic Energy Agency, Vienna, 1992.
53. Fuger, J., Nitsche, H., Pooter, P., Rand, M., Rydberg, J., Spahiu, K., Sullivan, J. C., Ullman, W. J., Vitorge, P. and Wanner, H., *Chemical Thermodynamics of Neptunium and Plutonium*, Chemical Thermodynamics Vol. 4, NEA-OECD, Elsevier, Amsterdam, London, New York, Oxford, Paris, Shannon, Tokyo, 2001.
54. Papelis, C., Hayes, K. F. and Leckie, J. O., *A Program for the Computation of Chemical Equilibrium Composition of Aqueous Batch Systems Including Surface-Complexation Modeling of Ion Adsorption at the Oxide/Solution Interface*, Environmental Engineering and Science, Department of Civil Engineering, Stanford University, Stanford, CA 1988, p. 94305.
55. Redden, G., Hydraql, http://eep.stanford.edu/SEEPWeb/hydraql/hydraql.html, 1997.
56. Leung, V. W. H., Darvell, B. W. and Chan, A. P. C., *Talanta*, **35**, 713 (1988).
57. Wolery, T. J., *EQ 3/6, A Software Package for the Geochemical Modeling of Aqueous Systems*, UCRL-MA-110662 Part I, Lawrence Livermore National Laboratory, Livermore, CA, 1992.
58. Pettit, L. D. and Powell, K. J., *Stability Constants Database (SC-Database)*, Academic Software, Sourby Old Farm, Timble, Otley, 2001, http://www.acadsoft.co.uk.
59. Puigdomenech, I., *MEDUSA: Make Equilibrium Diagrams Using Sophisticated Algorithms*, Inorganic Chemistry Royal Institute of Technology, (KTH)SE-100 44, Stockholm, 2001, http://w1.156.telia.com/%7 Eu15651596/.
60. G. Meinrath, *Aquatic chemistry of uranium*, Geoscience Vol. 1, Freiberg on-line, 1998, http://www.geo.tu-freiberg/fog.
61. Ekberg, C., in *Uranium in the Aquatic Environment*, Merkel, B. J., Planer-Friedrich, B. and Wolkersdorfer, C. (Eds.), Springer-Verlag Berlin, Heidelberg, New York, 2002, p. 343.
62. Kahn, M., in *Radioactivity Applied to Chemistry*, Wahl, A. C. and Bonner, N. A. (Eds.), Wiley, New York, 1951, pp. 403–433.
63. Ziv, D. M. and Shestakova, I. A., *Radiokhim*, **7**, 175 (1965) (russ.).
64. Kirby, H. W., in *The Chemistry of the Actinide Elements*, Vol. 1, 2nd ed., Katz, J. J., Seaborg, G. T. and Morss, L. R. (Eds.), Chapman & Hall, London, New York, 1986, pp. 30–34.
65. Moutte, A. and Guillaumont, R., *Rev. Chim. Miner.*, **6**, 603 (1969).
66. Rao, V. K., Shahani, C. J. and Rao, C. L., *Radiochim. Acta*, **14**, 31 (1969).
67. Strahlenschutzverordnung, *Verordnung Über den Schutz vor Schäden Durch Ionisierende Strahlen, Vom 20*, (BGBl. I S. 1714), Carl Heymanns Verlag KG Köln, Berlin, Bonn, München, Juli 2001.
68. Östholz, E., Bruno, J. and Grenthe, I., *Geochim. Cosmochim. Acta*, **58**, 613 (1994).
69. Bundschuh, T., Knopp, R., Müller, R., Kim, K. I., Neck, V. and Fanghänel, Th., *Radiochim. Acta*, **88**, 625 (2000).
70. Neck, V. and Kim, J. I., *Radiochim. Acta*, **89**, 1 (2001).
71. Neck, V., Müller, R., Bouby, M., Altmaier, M., Rothe, J., Denecke, M. A. and Kim, J. I., *Radiochim. Acta*, **90**, 485 (2002).
72. Lieser, K. H. and Hill, R., *Radiochim. Acta*, **56**, 37 (1992).
73. Moriyama, H., Fujiwara, K. and Yamana, H., *J. Nucl. Sci. Technol., Suppl.*, **3**, 246 (2002).
74. Joâo, A., Bigot, S. and Fromage, F. *Bull. Soc. Chim. Fr.*, 42 (1986).
75. Elyahyaoui, A., Brillard, L., Boulhassa, S., Hussonnois, M. and Guillaumont, R., *Radiochim. Acta*, **49**, 39 (1990).
76. Moskvin, A. I., Essen, L. N. and Bukhtiyarova, T. N., *Russ. J. Inorg. Chem.*, **12**, 1794–1795 (1967).
77. Engkvist, I. and Albinson, Y., *Radiochim. Acta*, **66/67**, 139 (1994).
78. Choppin, G. R., Erten, H. N. and Xia, Y., *Radiochim. Acta*, **74**, 123 (1996).
79. Erten, H. N., Mohammed, A. K. and Choppin, G. R., *Radiochim. Acta*, **66/67**, 133 (1994).
80. di Bernardo, P., di Napoli, V., Cassol, A. and Magon, L., *J. Inorg. Nucl. Chem.*, **38**, 1659 (1976).
81. Cacheris, W. P. and Choppin, G. R., *Radiochim. Acta*, **42**, 185 (1987).
82. Moulin, V., Tits, J. and Ouzounian, G., *Radiochim. Acta*, **58/59**, 179 (1992).
83. Frondel, C., *Systematic Mineralogy of Uranium and Thorium*, Geological Survey Bulletin 1064, Washington, 1958.
84. Wilhelm, R. G. and Beam, P., *Understanding Variation in Partition Coefficient, K_d, Values*, Vol. 1 and Vol. 2, EPA 402-R-99-004B, 1999.

85. Hem, J. D., *Study and Interpretation of the Chemical Characteristics of Natural Water*, Water Supply Paper 2254, U. S. Geological Survey, Alexandria, VA, 1985.
86. Torstenfelt, B., *Radiochim. Acta*, **39**, 105 (1986).
87. Taylor, D. M., *J. Alloys Compd.*, **271–273**, 6 (1998).
88. Guillaumont, R., *Rev. Chim. Miner.*, **3**, 339 (1966).
89. Mitsuji, T., *Bull. Chem. Soc. Jpn.*, **41**, 115 (1968).
90. Lundqvist, R., *Proceedings International Solvent Extraction Conference*, Lyon, Sept. 8–14, Paper No. 143 1974.
91. Bouissières, G. in Born, H. J. (Ed.), *Tagungsber. 3*rd *Int. Pa-Konf.*, Report BMBW-FBK 71-17, Paper No. 26, German, 1971.
92. Guillaumont, R., Bouissières, G. and Mauxart, M., *Actin. Rev.*, **1**, 135 (1968).
93. Trubert, D., Le Naour, C. and Jaussaud, C., *J. Solution Chem.*, **31**, 261–277 (2002).
94. Le Naour, C., Trubert, D. and Jaussaud, C., *J. Solution Chem.*, **32**, 489–504 (2003).
95. Trubert, D., Le Naour, C. and Jaussaud, C., *J. Solution Chem.*, **32**, 505–526 (2003).
96. Rössler, H. J., *Lehrbuch der Mineralogie*, 5th ed., Deutscher Verlag für Grundstoffindustrie, Leipzig, 1991, p. 184.
97. Allen, P. G., Shuh, D. K., Bucher, J. J., Edelstein, N. M., Reich, T., Denecke, M. A. and Nitsche, H., *Inorg. Chem.*, **35**, 784 (1996).
98. Rai, D., Swanson, J. L. and Ryan, J. L., *Radiochim. Acta*, **42**, 35 (1987).
99. Fujiwara, K., Yamana, H., Fujii, T. and Moriyama, H., *J. Nucl. Sci. Technol., Suppl.*, **3**, 290 (2002).
100. Geipel, G., Bernhard, G. and Brendler, V., in *Uranium in the Aquatic Environment*, Merkel, B. J., Planer-Friedrich, B. and Wolkersdorfer, C. (Eds.), Springer-Verlag, Berlin, Heidelberg, New York, 2002, p. 369.
101. Moriyama, H., Kitamura, A., Fujiwara, K. and Yamana, H., *Radiochim. Acta*, **87**, 97 (1999).
102. Kirishima, A., Kimura, T., Tochiyama, O. and Yoshida, Z. *Chem. Comm.*, 910 (2003).
103. Brown, P. L., *Radiochim. Acta*, **90**, 589 (2002).
104. Eliet, V., Grenthe, I. and Bidoglio, G., *Appl. Spectrosc.*, **54**, 99 (2000).
105. Moll, H., Reich, T., Hennig, C., Rossberg, A., Szabo, Z. and Grenthe, I., *Radiochim. Acta*, **88**, 559 (2000).
106. Comarmond, H. J. and Brown, P. L., *Radiochim. Acta*, **88**, 573 (2000).
107. Kimura, T., Nagashi, R., Ozaki, T., Arisaka, M. and Yoshida, Z., *J. Nucl. Sci. Technol., Suppl.*, **3**, 233 (2002).
108. Moulin, C., Decambox, P., Moulin, V. and Decaillon, J. G., *Anal. Chem.*, **67**, 348 (1995).
109. Kato, Y., Meinrath, G., Kimura, T. and Yoshida, Z., *Radiochim. Acta*, **64**, 107 (1994).
110. Meinrath, G., Klenze, R. and Kim, J. I., *Radiochim. Acta*, **74**, 81 (1996).
111. Rai, D., Felmy, A. R., Hess, H. J., Moore, D. A. and Yui, M., *Radiochim. Acta*, **82**, 17 (1998).
112. Rai, D., Felmy, A. R. and Ryan, J. L., *Inorg. Chem.*, **29**, 260 (1990).
113. Geipel, G., Bernhard, G., Brachmann, A., Brendler, V. and Nitsche, H., in *Uranium-Mining and Hydrology*, Merkel, B., Hurst, S., Löhnert, E. P. and Struckmeier, W. (Eds.), Verlag Sven von Loga Köln, 1995, p. 167 (in German).
114. Bernhard, G., Geipel, G., Brendler, V. and Nitsche, H., *Radiochim. Acta*, **74**, 87 (1996).
115. Kalmykow, S. N. and Choppin, G. R., *Radiochim. Acta*, **88**, 603 (2000).
116. Bernhard, G., Geipel, G., Reich, T., Brendler, V., Amayri, S. and Nitsche, H., *Radiochim. Acta*, **89**, 511 (2001).
117. Brendler, V., Geipel, G., Bernhard, G. and Nitsche, H., *Radiochim. Acta*, **74**, 75 (1996).
118. Sandino, M. C. A. and Grambow, B., *Radiochim. Acta*, **66/67**, 37 (1994).
119. Hines, M. A., Sullivan, J. C. and Nash, K. L., *Inorg. Chem.*, **32**, 1820 (1993).
120. Moll, H., Geipel, G., Bernhard, G. and Nitsche, H., *Radiochim. Acta*, **74**, 3 (1996).
121. Jensen, M. P. and Choppin, G. R., *Radiochim. Acta*, **82**, 83 (1998).
122. Satoh, I. and Choppin, G. R., *Radiochim. Acta*, **56**, 85 (1992).
123. Moll, H., Geipel, G., Brendler, V., Bernhard, G. and Nitsche, H., *J. Alloys Compd.*, **271–273**, 765 (1998).
124. Porter, R. A. and Weber, W. J., *J. Inorg. Nucl. Chem.*, **33**, 2443 (1971).
125. Choppin, G. R. and Du, M., *Radiochim. Acta*, **58/59**, 101 (1991).
126. Brachmann, A., Geipel, G., Bernhard, G. and Nitsche, H., *Radiochim. Acta*, **90**, 147 (2002).
127. Moll, H., Geipel, G., Reich, T., Bernhard, G., Fanghänel, T. and Grenthe, I., *Radiochim. Acta*, **91**, 11 (2003).
128. Rao, L., Jiang, J., Zanonato, P.-L., di Bernardo, P., Bismondo, A. and Garnov, A. Y., *Radiochim. Acta*, **90**, 581 (2002).
129. Choppin, G. R. and Allard, B., in *Handbook of the Physics and Chemistry of the Actinides*, Vol. 3, Freeman, A. J. and Keller, C. (Eds.), Elsevier Science Publishers, Amsterdam, 1986, pp. 407–429.
130. Kim, J. I. and Czerwinski, K. R., *Radiochim. Acta*, **73**, 5 (1996).
131. Czerwinski, K., Kim, J. I., Rhee, D. S. and Buckau, G., *Radiochim. Acta*, **72**, 179 (1996).
132. Pompe, S., Brachmann, A., Bubner, M., Geipel, G., Heise, K. H., Bernhard, G. and Nitsche, H., *Radiochim. Acta*, **82**, 89 (1998).
133. Pompe, S., Schmeide, K., Bubner, M., Geipel, G., Heise, K. H., Bernhard, G. and Nitsche, H., *Radiochim. Acta*, **88**, 553 (2000).
134. Saito, T., Nagasaki, S. and Tanaka, S., *Radiochim. Acta*, **90**, 27 (2002).
135. Katz, J. J., Seaborg, G. T. and Morss, L. R., *The Chemistry of Actinide Elements*, Vol. 1, 2nd ed., Chapman & Hall, London, New York, 1986.

136. Geipel, G., Bernhard, G., Rutsch, M., Brendler, V. and Nitsche, H., *Radiochim. Acta*, **88**, 757 (2000).
137. Rutsch, M., Geipel, G., Brendler, V., Bernhard, G. and Nitsche, H., *Radiochim. Acta*, **86**, 135 (1999).
138. Amayri, S., Geipel, G., Reich, T., Matz, W. and Bernhard, G. *NRC5, 5th International Conference on Nuclear and Radiochemistry*, Extended Abstracts, Pontresina, September 3–8, 2000, p. 404.
139. Rai, D., Felmy, A. R., Hess, N. J., LeGore, V. L. and McCready, D. E., *Radiochim. Acta*, **90**, 495 (2002).
140. Casas, I., Bruno, J., Cera, E., Finch, R. J. and Ewing, R. C., *Geochim. Cosmochim. Acta*, **61**, 3879 (1997).
141. Torrero, M. E., Casas, I., de Pablo, J., Sandino, M. C. A. and Grambow, B., *Radiochim. Acta*, **66/67**, 29 (1994).
142. Silva, R. J., *Mater. Res. Soc. Symp. Proc.*, **257**, 323 (1992).
143. Choppin, G. R. and Mathur, J. N., *Radiochim. Acta*, **52/53**, 25 (1991).
144. Vochten, R. and van Haverbeke, L., *Miner. Petrol.*, **43**, 65 (1990).
145. Sowder, A. G., Clark, S. B. and Field, R. A., *Radiochim. Acta*, **74**, 45 (1996).
146. Smellie, J. A. T., Karlson, F. and Alexander, W. R., *J. Contam. Hydrol.*, **26**, 3 (1997).
147. Hebert, J. P., Daroussin, J. L., Michel, P., Perih, Ch., Martinez, F. L., Romero, A. L., Fietz, J., Langer, L., Kahn, A., Litvin, V. and Nitsche, H., *Decommissioning of Old Uranium Ore Extraction and Treatment Installations*, European Commission, Nuclear science and technology, Contract No. FI2D/CT93/0083, Final Report, EUR 16885, 1996.
148. Murphy, W. M. and Shock, E. L. in *Uranium: Mineralogy, Geochemistry and the Environment*, Reviews in Mineralogy, Vol. 38, Burns, P. C. and Finch, R. (Eds.), Mineralogical Society of America, Washington, DC, 1999, pp. 221–253.
149. Dearlove, J. P. L., Green, D. C. and Ivanovich, M., *Mater. Res. Soc. Symp. Proc.*, **127**, 927 (1989); *12th International Symposium Scientific Basis for Nuclear Waste Management*, Berlin, Germany.
150. Bernhard, G., Geipel, G., Brendler, V. and Nitsche, H., *J. Alloys Compd.*, **271–273**, 201 (1998).
151. Geipel, G., Bernhard, G., Rutsch, M., Brendler, V. and Nitsche, H., in *The Environmental Challenges of Nuclear Disarmament*, Baca, T. E. and Florkowski, T. (Eds.), Kluwer Academic Publishers, 2000, pp. 323–332.
152. Ahonen, L., Ervanne, H., Jaakola, T. and Blomquist, R., *Radiochim. Acta*, **66/67**, 125 (1994).
153. Brown, P. L., Guerin, M., Hankin, S. I. and Lowson, R. T., *J. Contam. Hydrol.*, **35**, 295 (1998).
154. Brown, P. L. and Lowson, R. T., *J. Contam. Hydrol.*, **26**, 27 (1997).
155. Field, R. A., Cotes, J. T., Elzerman, A. W. and Navratil, J. D. in *Uranium in the Aquatic Environment*, Merkel, B. J., Planer-Friedrich, B. and Wolkersdorfer, C. (Eds.), Springer-Verlag, Berlin, Heidelberg, New York, 2002, p. 293.
156. Koß, V., Winkler, A. and Bütow, E., *Radiochim. Acta*, **58/59**, 447 (1991).
157. McKay, H. A. C., *Principles of Radiochemistry*, CRC Press, Cleveland, 1971, p. 232.
158. Finch, R. and Murakami, T., in *Uranium: Mineralogy, Geochemistry and the Environment*, Reviews in Mineralogy, Vol. 38, Burns, P. C. and Finch, R. (Eds.), Mineralogical Society of America, Washington, DC, 1999, pp. 91–179.
159. Waite, T. D., Davis, J. A., Payne, T. E., Waychunan, G. A. and Xu, N., *Geochim. Cosmochim. Acta*, **58**, 5465 (1994).
160. Beneš, P., Kratzer, K., VlŠkova,. and Šebestova, E., *Radiochim. Acta*, **82**, 367 (1998).
161. Ribera, D., Labrot, F., Tisnerat, T. and Narbonne, J. F., *Rev. Environ. Contam. Toxicol.*, **146**, 53 (1996).
162. Geipel, G., Bernhard, G., Brendler, V. and Reich, T., *NRC5, 5th International Conference on Nuclear and Radiochemistry*, Extended Abstracts, Pontresina, Sept. 3–8, 2000, p. 473.
163. Rizkalla, E. N., Netoux, F., Dabod-Seignon, M. and Pages, M., *J. Inorg. Biochem.*, **51**, 701 (1993).
164. Mortvedt, J. J., *J. Environ. Qual.*, **23**, 643 (1994).
165. Simon, L. S. and Ibrahim, S. A., *Radium in the Environment*, International Atomic Energy Agency, Vienna, 1988.
166. Kaur, A., Singh, S. and Virk, H. S., *Nucl. Tracks Radiat. Meas.*, **15**, 795 (1988).
167. Singh, K. P., *Curr. Sci.*, **73**, 532 (1997).
168. Frindik, O., *Landwirtschaftliche Forsch.*, **39**, 75 (1986) (in German).
169. Nalezinski, S. and Lux, D., Ermittlung von Transferfaktoren Boden-Pflanze für U-238 und Ra-226 in einer uranbergbaulich beeinflußten Kleingartenanlage in BfS Annual Report 1997, 1998, p. 37.
170. Ibrahim, S. A. and Whicker, F. W., *J. Radioanal. Nucl. Chem., Art.*, **156**, 253 (1991).
171. Yaprak, G., Cam, N. F. and Yener, G., *J. Radioanal. Nucl. Chem.*, **238**, 167 (1998).
172. Huang, J. W., Blaylock, M. J., Kapulnik, Y. and Ensley, B. D., *Environ. Sci. Technol.*, **32**, 2004 (1998).
173. Ebbs, S. D., Brady, D. J. and Kochian, L. V., *J. Exp. Bot.*, **49**, 1183 (1998).
174. Günther, A., Bernhard, G., Geipel, G., Reich, T., Rossberg, A. and Nitsche, H., *Radiochim. Acta*, **91**, 1 (2003).
175. Decambox, P., Mauchen, P. and Moulin, C., *Appl. Spectrosc.*, **45**, 116 (1991).
176. Panak, P., Hard, B. C., Pietzsch, K., Kutschke, S., Röske, K., Selenska-Pobell, S., Bernhard, G. and Nitsche, H., *J. Alloys Compd.*, **271–273**, 262 (1998).
177. Hennig, C., Panak, P. J., Reich, T., Rossberg, A., Raff, J., Selenska-Pobell, S., Matz, W., Bucher, J. J., Bernhard, G. and Nitsche, H., *Radiochim. Acta*, **89**, 625 (2001).

178. Thompson, H. A., Brown, G. E. and Parks, G. A., *Am. Mineral.*, **82**, 483 (1997).
179. Panak, P. J., Knopp, R., Booth, C. H. and Nitsche, H., *Radiochim. Acta*, **90**, 779 (2002).
180. Francis, A. C., Joshi-Tope, G. A., Dodge, C. J. and Gillow, J. B., *J. Nucl. Sci. Technol., Suppl.*, **3**, 935 (2002).
181. Joshi-Tope, G. A. and Francis, A. J., *J. Bacteriol.*, **177**, 1989 (1995).
182. Merroun, M., Hennig, C., Rossberg, A., Reich, T., Nicolai, R., Heise, K. H. and Selenska-Pobell, S., in *Uranium in the Aquatic Environment*, Merkel, B. J., Planer-Friedrich, B. and Wolkersdorfer, C. (Eds.), Springer-Verlag, Berlin, Heidelberg, New York, 2002, p. 505.
183. Merroun, M., Hennig, C., Rossberg, A., Geipel, G., Reich, T. and Selenska-Pobell, S., *Biochemical Society Transactions*, **30**, 669 (2002).
184. Artinger, R., Marquardt, C. M., Kim, J. I., Seibert, A., Trautmann, N. and Kratz, J. V., *Radiochim. Acta*, **88**, 609 (2000).
185. Neck, V., Kim, J. I., Seidel, B. S., Marquardt, C. M., Dardenne, K., Jensen, M. P. and Hauser, W., *Radiochim. Acta*, **89**, 439 (2001).
186. Knopp, R., Neck, V. and Kim, J. I., *Radiochim. Acta*, **86**, 101 (1999).
187. Duplessis, J. and Guillaumont, R., *Radiochem. Radioanal. Lett.*, **31**, 293 (1997).
188. Kulyako, Y., Fujiwara, A., Malikov, D., Perevalov, S., Suzuki, A., Tananaev, I., Tashiro, T., Trofimov, T., Tsushima, S. and Myasoedov, B., *J. Nucl. Sci. Technol., Suppl.*, **3**, 298 (2002).
189. Itagaki, H., Nakayama, S., Tanaka, S. and Yamawaki, M., *Radiochim. Acta*, **58/59**, 61 (1991).
190. Kitamura, A. and Kohara, Y., *J. Nucl. Sci. Technol., Suppl.*, **3**, 294 (2002).
191. Rai, D. and Ryan, J. L., *Inorg. Chem.*, **24**, 247 (1985).
192. Rai, D., Hess, N. J. and Felmy, A. R., *Radiochim. Acta*, **84**, 159 (1999).
193. Kato, Y., Kimura, T., Yoshida, Z. and Nitani, N., *Radiochim. Acta*, **82**, 63 (1998).
194. Neck, V., Runde, W. and Kim, J. I., *Radiochim. Acta*, **65**, 29 (1994).
195. Kato, Y., Kimura, T., Yoshida, Z. and Nitani, N., *Radiochim. Acta*, **74**, 21 (1996).
196. Cohen, D. and Fried, S., *Inorg. Nucl. Chem. Lett.*, **5**, 653 (1969).
197. Valashkin, P. G., Hobart, D. E., Begun, G. M. and Peterson, J. R., *Radiochim. Acta*, **31**, 91 (1984).
198. Riglet, C., *Chimie du Neptunium et Autres Actinides en Milieu Carbonate*, Rapport CEA-R-5535, CEN Fontenay aux Roses, France, 1990.
199. Neck, V., Fanghänel, Th. and Kim, J. I., *Radiochim. Acta*, **77**, 167 (1997).
200. Nitsche, H., Mueller, A., Standifer, E. M., Deinhammer, R. S., Becraft, K. A., Prussin, T. and Gatti, R. C., *Radiochim. Acta*, **58/59**, 27 (1992).
201. Jensen, M. P. and Nash, K. L., *Radiochim. Acta*, **89**, 557 (2001).
202. Moriyama, H., Nakata, Y. and Higashi, K., *Mater. Res. Soc. Symp. Proc.*, **353**, 1129 (1995); *18th International Symposium Scientific Basis for Nuclear Waste Management*, Kyoto, Japan.
203. Kim, J. I. and Sekine, T., *Radiochim. Acta*, **55**, 187 (1991).
204. Perkampus, H. H., *Encyclopedia of Spectroscopy*, VCH, Weinheim, New York, Basel, Cambridge, Tokyo, 1995, p. 303.
205. Kim, J. I. and Marquardt, C. M., *Radiochim. Acta*, **87**, 105 (1999).
206. Rao, L. and Choppin, G. R., *Radiochim. Acta*, **69**, 87 (1995).
207. Marquardt, C., Herrmann, G. and Trautmann, N., *Radiochim. Acta*, **73**, 119 (1996).
208. Seibert, A., Mansel, A., Marquardt, C. M., Keller, H., Kratz, J. V. and Trautmann, N., *Radiochim. Acta*, **89**, 505 (2001).
209. Marquardt, C. and Kim, J. I., *Radiochim. Acta*, **81**, 143 (1998).
210. Clark, D. L., Conradson, S. D., Ekberg, S. A., Hess, N. J., Janecky, D. R., Neu, M. P., Palmer, P. D. and Tait, C. D. *A multi method approach to actinide speciation applied to pentavalent neptunium carbonate complexation*, http://mwanal.lanl.gov/CST/101159101159P_1.html, (1995).
211. Del Nero, M., Said, K. B., Made, B., Clement, A. and Bontems, B., *Radiochim. Acta*, **81**, 133 (1998).
212. Oscarson, J. L., Wang, P., Gillespe, S. E., Izatt, R. M., Watt, G. D., Larsen, C. D. and Renuncio, J. A. R., *Thermodynamics of Protonation of AMP, ADP and ATP from 50 to 125°C*, Plenum Publishing, 1995, p. 171.
213. Coughtrey, P. J., Jackson, D. J., Jones, C. H., Kane, P. and Thorne, P., *Radionuclide Distribution and Transport in Terrestrial and Aquatic Ecosystems. A Critical Review of Data*, Vol. 4, Balkema, Rotterdam, Boston, 1984.
214. Coughtrey, P. J., Jackson, D. J., Jones, C. H., Kane, P. and Thorne, P., *Radionuclide Distribution and Transport in Terrestrial and Aquatic Ecosystems. A Critical Review of Data*, Vol. 5, Balkema, Rotterdam, Boston, 1984.
215. Kobuta, T., Sasaki, T., Tochiyama, O. and Kudo, A., *J. Nucl. Sci. Technol., Suppl.*, **3**, 946 (2002).
216. Capdevila, H., Vitorge, P. and Gifaut, E., *Radiochim. Acta*, **58/59**, 45 (1991).
217. Choppin, G. R. and Allard, B., in *Handbook on the Physics and Chemistry of the Actinides*, Freeman, A. J. and Keller, C. (Eds.), Elsevier Science, pp. 407–429.
218. Mahajan, G. R., Rao, V. K. and Natarajan, P. R., *J. Radioanal. Nucl. Chem. Lett.*, **137**, 219 (1989).
219. Capdevila, H. and Vitorge, P., *Radiochim. Acta*, **82**, 11 (1998).
220. Rai, D., *Radiochim. Acta*, **35**, 97 (1984).

221. Kim, J. I. and Kanellakopulus, B., *Radiochim. Acta*, **48**, 145 (1989).
222. Fujiwara, K., Yamana, H., Fujii, T. and Moriyama, H., *Radiochim. Acta*, **90**, 857 (2002).
223. Rai, D., Hess, N. J. and Felmy, A. R., *Radiochim. Acta*, **86**, 89 (1999).
224. Capdevila, H., Vitorge, P., Giffaut, E. and Delmau, L., *Radiochim. Acta*, **74**, 93 (1996).
225. Bruno, J., Grenthe, I. and Robouch, P., *Inorg. Chim. Acta*, **158**, 221 (1989).
226. Vitorge, P., *Neptunium en Solution Carbonate Concentrée Réductrice: Bibliographie Pour l'OECD-AEN-TDB*, Report CEABIB-246, Commissariat à l'énergie atomique, France, 1995.
227. Delmau, L., Vitorge, P. and Capdevila, H. *Np(V)/Np(IV) en Solutions Carbonate/Bicarbonate Concentrées*, Technical Report CEA-N-2807, CEA, France, 1996.
228. Clark, D. L., Conradson, S. D., Webster Keogh, D., Palmer, P. D., Scott, B. L. and Drew Tait, C., *Inorg. Chem.*, **37**, 2893 (1998).
229. Rai, D., Felmy, A. R., Moore, D. A., Masson, M. J., Murakami, T. and Ewing, R. C., *Mater. Res. Soc. Symp. Proc.*, **353**, 1143 (1995); *Scientific Basis for Nuclear Waste Management XVIII,* Kyoto, Japan.
230. Felmy, A. R., Rai, D., Sterner, S. R., Mason, M. J., Hess, N. J. and Conradson, S. D., *J. Solution Chem.*, **26**, 233 (1997).
231. Veirs, D. K., Smith, D. A., Berg, J. M., Zwick, B. D., Marsh, S. F., Allen, P. and Conradson, S. D., *J. Alloys Compd.*, **213/214**, 328 (1994).
232. Allen, P. G., Veirs, D. K., Conradson, S. D., Smith, C. A. and Marsh, S. F., *Inorg. Chem.*, **35**, 2841 (1996).
233. Gerstmann, U. C., Lierse, C. and Geckeler, K. E., *Radiochim. Acta*, **89**, 377 (2001).
234. Nitsche, H. and Silva, R. J., *Radiochim. Acta*, **72**, 65 (1996).
235. Rai, D., Moore, D. A., Felmy, A. R., Choppin, G. R. and Moore, R. C., *Radiochim. Acta*, **89**, 491 (2001).
236. Holm, E., Roos, P., Josefsson, D. and Persson, B., Radioactivity from the North pole to the Antarctic, in: Guéguéniat, P., Germain, P., Métivier, H. (Eds.), Radionuclides in the Oceans: Inputs and Inventories. Les Éditions de Physique, 1996, pp. 59–74.
237. Perkins, R. W. and Thomas, C. W., in *Transuranic Elements in the Environment*, Hansen, W. C. (Ed.), Technical Information Center, US Department of Energy, 1980, p. 53.
238. Guillaumont, R. and Adloff, J. P., *Radiochim. Acta*, **58/59**, 53 (1991).
239. Nitsche, H., *Radiochim. Acta*, **52/53**, 3 (1991).
240. Triay, I. R., Hobart, D. E., Mitchell, A. J., Newton, T. W., Ott, M. A., Palmer, P. D., Rundberg, R. S. and Thompson, J. L., *Radiochim. Acta*, **52/53**, 127 (1991).
241. Kersting, A. B., Efurd, D. W., Finnegan, D. L., Rokop, D. J., Smith, D. K. and Thompson, J., *Nature*, **397**, 56 Letters to Nature, 56–59 (1999).
242. Nunnemann, M., Erdmann, N., Hasse, H. U., Huber, G., Kratz, J. V., Kunz, P., Mansel, A., Passler, G., Stetzer, O., Trautmann, N. and Waldek, A., *J. Alloys Compd.*, **271–273**, 45 (1998).
243. Reed, D. T., Okajima, S. and Richmann, M. K., *Radiochim. Acta*, **66/67**, 105 (1994).
244. Nitsche, H. and Edelstein, N. M., *Radiochim. Acta*, **39**, 23 (1985).
245. AlMahamid, I., Becraft, K. A., Hakem, N. L., Gatti, R. C. and Nitsche, H., *Radiochim. Acta*, **74**, 129 (1996).
246. AlMahamid, I., Becraft, K. A. and Nitsche, H., *Radiochim. Acta*, **68**, 63 (1995).
247. Neuilly, M., Bussac, J., Frejacques, G., Nief, G., Vendryes, G. and Yvon, J., *C. R. Acad. Sci.*, **275D**, 1847 (1972).
248. Janeczek, J., in *Uranium: Mineralogy, Geochemistry and the Environment*, Reviews in Mineralogy, Vol. 38, Burns, P. C. and Finch, R. (Eds.), Mineralogical Society of America, Washington, DC, 1999, pp. 321–392.
249. Menet, C., Ménager, M. T. and Petit, J. C., *Radiochim. Acta*, **58/59**, 395 (1992).
250. Kudo, A., Kobuta, T., Zheng, J., Sasaki, T., Kauri, T. and Miyahara, S., *J. Nucl. Sci. Technol., Suppl.*, **3**, 537 (2002).
251. Myasoedov, B. F. and Drozhko, E. G., *J. Alloys Compd.*, **271–273**, 216 (1998).
252. Viehweg, M., Denecke, C., Neerdal, B., Marivoet, J., Meyus, Y., Sillen, X., Schneider, L., Herzog, C., Lopatin, V. V., Kamnev, E. N., Ribalchenko, A. I., Kurochkin, V. M., Okunkov, G., Sigaev, B., Zubkov, A. A., Pikaev, A. K., Kosareva, I. M., Zakharova, E. V., Rakov, N. A., Savushkina, M. K., Kaimin, E. P., Kuznetsov, Y. and Tichkov, V., *Evaluation of the Radiological Impact Resulting from Injection Operations in Tomsk-7 and Krasnoyarsk-26*, European Commission, Nuclear safety and the environment, Contract No. B7-5340/96/000757/MAR/C3, Final Report, EUR 18189, 1999.
253. Wickham, S., Sillen, X., Wang, L., Marivoet, J., Beaucaire, C., Bourgeois, M., Artinger, R., Kienzler, B., Klenze, R., Metz, V., Schuessler, W., Bernhard, G., Brendler, V., Geipel, G., Nedelkova, M., Selenska-Pobell, S., Kamnev, E., Okunkov, G., Rybalchenko, A., Zubkoy, A., Aranivich, L., Graphchikov, A., Kaimin, L., Zakharova, E., Casas, I., de Pablo, J., Rivira, M., Torras, J., Davison, J., Duerden, S., Galson, D., Wite, M., Baker, A., Jackson, P. and Knight, L. *Building Confidence in Deep Disposal: The Borehole Injection Sites at Krasnoyarsk-26 and Tomsk-7 (BORIS)*, European Commission Contract No. FIKW-CT-2000-00105, Final report, 2002.
254. Gastberger, M., Hubmer, A., Steinhäusler, F., Lettner, H., Spano, M., Stronati, L. and Testa, A., *Radiochim. Acta*, **89**, 371 (2001).
255. Auer, J., Knof, G., Augustus, J., Freytag, H. E., Merbach, W. and Toussaine, V., *ZALF Berichte*, 1993, p. 33, 45, (in German).

256. Bunzl, K. and Kracke, W., *Sci. Total Environ.*, **63**, 111 (1987).
257. Bunzl, K. and Kracke, W., *J. Radioanal. Nucl. Chem.*, **138**, 83 (1989).
258. Haunold, E., Horak, O. and Gerzabek, M., *Bodenkultur*, **38/2**, 95 (1987).
259. Pimpl, M., Untersuchungen zum Boden/Pflanzen Transfer von Np-237, Pu-238, Am-241 und Cm-244; Report KfK-4452, Kernforschungszentrum Karlsruhe, 1998.
260. Gillow, J. B., Dunn, M., Francis, A. J., Lucero, D. A. and Papanguth, H. W., *Radiochim. Acta*, **88**, 769 (2000).
261. Panak, P. J. and Nitsche, H., *Radiochim. Acta*, **89**, 499 (2001).
262. Runde, W., Meinrath, G. and Kim, J. I., *Radiochim. Acta*, **58/59**, 93 (1991).
263. Choppin, G. R. and Chen, J.-F., *Radiochim. Acta*, **74**, 105 (1996).
264. Kelly, E. J., Bell, D. I. and Johnstone, T. L., *J. Alloys Compd.*, **271–273**, 227 (1998).
265. Minai, Y., Choppin, G. R. and Sisson, D. H., *Radiochim. Acta*, **56**, 195 (1992).
266. Wall, N. A., Borkowski, M., Chen, J. and Choppin, G. R., *Radiochim. Acta*, **90**, 563 (2002).
267. Kim, J. I., Buckau, G., Bryant, E. and Klenze, R., *Radiochim. Acta*, **48**, 135 (1989).
268. Kim, J. I., Rhee, D. S. and Buckau, G., *Radiochim. Acta*, **52/53**, 49 (1991).
269. Moulin, V., Caceci, M. S. and Theyssier, M. J., in Bhattacharji, S., Neugebauer, H. J., Reitner, J. and Stüwe, K. (Eds.), *Lecture Notes in Earth Sciences*, Springer-Verlag, 1990, p. 305.
270. Franz, C., Herrmann, G. and Trautmann, N., *Radiochim. Acta*, **77**, 177 (1997).
271. Andersson, K., *Mater. Res. Soc. Symp. Proc.*, **127**, 693 (1989); *12th International Symposium Scientific Basis for Nuclear Waste Management*, Berlin, Germany.
272. Gorski, B., Buklanov, G. V., Dok, L. D., Gleisberg, B., Timokhin, S. N., Milek, A. and Salamatin, L. I., *Radiochim. Acta*, **51**, 59 (1990).
273. Carnall, W. T., Fields, P. R. and Stewart, D. C., *J. Inorg. Nucl. Chem.*, **6**, 213 (1958).
274. Wimmer, H., Kim, J. I. and Klenze, R., *Radiochim. Acta*, **58/59**, 165 (1992).
275. Fanghänel, Th., Kim, J. I., Paviet, P., Klenze, R. and Hauser, W., *Radiochim. Acta*, **66/67**, 91 (1994).
276. Fanghänel, Th., Weger, H. T., Könnecke, Th., Neck, V., Paviet-Hartmann, P., Steinle, E. and Kim, J. I., *Radiochim. Acta*, **82**, 47 (1998).
277. Fanghänel, Th., Weger, H. T., Schubert, G. and Kim, J. I., *Radiochim. Acta*, **82**, 55 (1998).
278. Paviet, P., Fanghänel, Th., Klenze, R. and Kim, J. I., *Radiochim. Acta*, **74**, 99 (1996).
279. Fanghänel, Th. and Kim, J. I., *J. Alloys Compd.*, **271–273**, 728 (1998).
280. Panak, P., Klenze, R., Kim, J. I. and Wimmer, H., *J. Alloys Compd.*, **225**, 261 (1995).
281. Panak, P., Klenze, R. and Kim, J. I., *Radiochim. Acta*, **74**, 141 (1996).
282. Klenze, R., Panak, P. and Kim, J. I., *J. Alloys Compd.*, **271–273**, 746 (1998).
283. Buckau, G., Kim, J. I., Klenze, R., Rhee, D. S. and Wimmer, H., *Radiochim. Acta*, **57**, 105 (1992).
284. Stumpf, Th., Bauer, A., Coppin, F. and Kim, J. I., *Environ. Sci. Technol.*, **35**, 3691 (2001).
285. Stumpf, Th. and Fanghänel, Th., *J. Colloid Interface Sci.*, **249**, 119 (2002).
286. Ozaki, T., Gillow, J. B., Francis, A. J., Kimura, T., Ohnuki, T. and Yoshida, Z., *J. Nucl. Sci. Technol., Suppl.*, **3**, 950 (2002).
287. Assefe, Z., Haire, R. G. and Stump, N. A., *J. Alloys Compd.*, **271–273**, 854 (1998).
288. Désiré, B., Hussonois, H. and Guillaumont, R., *C. R. Acad. Sci. Paris*, **269C**, 448–451 (1969).
289. Hussonois, H., Hubert, S., Aubin, L., Guillaumont, R. and Boussieres, G., *Radiochem. Radioanal. Lett.*, **10**, 231 (1972).
290. Hussonois, H., Hubert, S., Brillard, L. and Guillaumont, R., *Radiochem. Radioanal. Lett.*, **15**, 47 (1973).
291. Ahrland, S., in *The Chemistry of the Actinide Elements*, Vol. 2, 2nd ed., Katz, J. J., Seaborg, G. T. and Morss, L. R. (Eds.), Chapman & Hall, London, New York, 1986, p. 1483.
292. Bybarz, R. D., *J. Inorg. Nucl. Chem.*, **28**, 1055 (1965).
293. Horwitz, E. P. and Bloomquist, C. A. A., *J. Inorg. Nucl. Chem.*, **35**, 271 (1973).
294. Hobart, D. E. and Peterson, J. R. in *The Chemistry of the Actinide Elements*, Vol. 2, 2nd ed., Katz, J. J., Seaborg, G. T. and Morss, L. R. (Eds.), Chapman & Hall, London, New York, 1986, p. 1010.
295. Gibson, J. K. and Haire, R. G., *Radiochim. Acta*, **89**, 363 (2001).
296. Beitz, J. V., Williams, C. W. and Liu, G. K., *J. Alloys Compd.*, **271–273**, 850 (1998).
297. Harmon, H. D. and Peterson, J. R., *Inorg. Nucl. Chem.*, **8**, 57 (1972).
298. McDowell, W. J. and Coleman, C. F., *Inorg. Nucl. Chem.*, **34**, 2837 (1972).
299. Baes, C. F. and Messmer, R. E., *The Hydrolysis of Cations*, John Wiley & Sons, New York, 1976, p. 191.
300. Nugent, L. J., Bybarz, R. D. and Burret, J. L., *J. Phys. Chem.*, **73**, 1177–1178 (1969).
301. Mikheev, N. B., Spitsyn, V. I., Kamenskaja, A. N., Rosenkevitch, N. A., Rumer, I. A. and Auerman, L. N., *Sov. Radiochem.*, **14**, 494 (1972).
302. Mikheev, N. B. and Rumer, I. A., *Sov. Radiochem.*, **14**, 502 (1972).
303. Samhoun, K. and David, F., in *Transplutonium 1975*, Proceedings of the 4th International Symposium, Müller, W. and Lindner, R. (Eds.), North-Holland, Amsterdam, 1976, pp. 297–304.
304. David, F. and Hussonois, H., *Radiochem. Radioanal. Lett.*, **11**, 1 (1972).

305. Mikheev, N. B., Spitsyn, V. I., Kamenskaja, A. N., Konovalova, N. A., Rumer, I. A., Auerman, L. N. and Podorzhnyi, A. M., *Inorg. Nucl. Chem. Lett.*, **12**, 651 (1977).
306. Choppin, G. R., Harvey, B. G. and Thompson, S. G., *J. Inorg. Nucl. Chem.*, **2**, 66 (1956).
307. Thompson, S. G., Harvey, B. G., Choppin, G. R. and Seaborg, G. T., *J. Am. Chem. Soc.*, **76**, 6229 (1954).
308. Ermakov, V. A. and Stary, I., *Radiokhimya*, **9**, 197 (1967).
309. Baybarz, R. D., *J. Inorg. Nucl. Chem.*, **27**, 1831 (1965).
310. Baybarz, R. D., *J. Inorg. Nucl. Chem.*, **28**, 1055 (1966).
311. Baybarz, R. D., *Nucl. Sci. Eng.*, **17**, 463–467 (1963).
312. Stary, I., *Talanta*, **13**, 421–437 (1966).
313. Hubert, S., Hussonnois, M., Brillard, L., Goby, G. and Guillaumont, R., *J. Inorg. Nucl. Chem.*, **36**, 2361 (1974).
314. Hulet, E. K., Lougheed, R. W., Brady, J. D., Stone, R. E. and Coops, M. S., *Science*, **158**, 486 (1967).
315. Mikheev, N. B., Spitsyn, V. I., Kamenskaja, A. M., Rumer, I. A., Gvozdev, B. A., Rozenkevich, N. A. and Auerman, L. N., *Dokl. Akad. Nauk SSSR*, **208**, 1146 (1973).
316. Samhoun, K., David, F., Hahn, R. L., O'Kelley, G. D., Tarrant, J. R. and Hobart, D. E., *J. Inorg. Nucl. Chem.*, **41**, 1749 (1979).
317. David, F., Samhoun, K., Hulet, E. K., Baisden, P. A., Dougan, R., Landrum, J. H., Lougheed, R. W., Wild, J. F. and O'Kelley, G. D., *J. Inorg. Nucl. Chem.*, **43**, 2941 (1981).
318. Hulet, K., Lougheed, R. W., Baisden, P. A., Landrum, J. H., Wild, J. F. and Lundqvist, R. F. D., *J. Inorg. Nucl. Chem.*, **41**, 1743 (1979).
319. Hulet, E. K., Lougheed, R. W., Brady, J. D., Stone, R. E. and Coops, M. S., *Science*, **158**, 486 (1967).
320. Maly, J., Sikkeland, T., Silva, R. J. and Ghiorso, A., *Science*, **160**, 1114 (1968).
321. Silva, R. J., Sikkeland, T., Nurmia, M., Ghiorso, A. and Hulet, E. K., *J. Inorg. Nucl. Chem.*, **31**, 3405 (1969).
322. Silva, R. J., McDowell, W. J., Keller, O. L. Jr. and Tarrant, J. R., *J. Inorg. Chem.*, **13**, 2233 (1974).
323. McDowell, W. J., Keller, O. L. Jr., Dittner, P. E., Tarrant, J. R. and Case, G. N., *J. Inorg. Nucl. Chem.*, **38**, 1207 (1976).
324. Silva, R. J., Sikkeland, T., Nurmia, M. and Ghiorso, A., *Inorg. Nucl. Chem. Lett.*, **6**, 733 (1970).
325. Keramidas, A. D., Rikkou, M. P., Drouza, C., Raptopoulou, C. P., Terzis, A. and Pashalidis, I., *Radiochim. Acta*, **90**, 549 (2002).
326. Kimura, T., Nagaishi, R., Kato, Y. and Yoshida, Z., *Radiochim. Acta*, **89**, 125 (2001).

2.24 Speciation of Halogen Compounds

Rodolfo G. Wuilloud
University of Cincinnati, Cincinnati, Ohio, USA

Jorgelina C. Altamirano
Forensic Chemistry Center, Cincinnati, Ohio, USA

1 INTRODUCTION

Halogenated organic compounds have caused high public concern as organic pollutants. Compounds such as dichlorodiphenyltrichloroethane (DDT), polychlorinated biphenyls (PCBs) and chlorinated dioxins have become symbols of global environmental pollution. Scientific investigations of specific organohalogens have shown that many of them are toxic, persistent and subject to bioaccumulation in food chains. Additionally, the understanding of generation mechanisms and possible sources of halogenated volatile organic compounds have become fundamental for complete information on the different volatilization pathways into the atmosphere. As it is well known, the presence of halogens in the atmosphere is an issue of particular environmental concern because of their role in the deterioration of the ozone layer. On the other hand, the essential character of some halogens, such as iodine and the growing evidence for bromine, justify most of the research done on

Handbook of Elemental Speciation II: Species in the Environment, Food, Medicine & Occupational Health
Edited by R. Cornelis, H. Crews, J. Caruso and K. G. Heumann
 ISBN: 0-470-85598-3 (HB)

these elements in biological systems. For the same reason, determination of halogens in food is of importance to perform nutritional studies.

Consequently, the development of new analytical methodologies to perform speciation analysis for this group of elements and their compounds has been propelled by the increasing relevance that halogens have to environmental, biological and nutritional studies. Moreover, the application of highly sensitive detection techniques is important for speciation studies in which the individual amount of the species can be a minimal fraction of the total elemental concentration. Many analytical methodologies focused on determining halogenated species, particularly organohalogens, have been developed and proposed in the last few years. They mainly consist of an on-line coupling of a highly efficient separation technique such as chromatography or electrophoresis to an element-specific detector based on the use of plasmas as excitation and/or ionization sources. Consequently, the most recent advances in the development of analytical methodologies that involve the use of this type of hyphenated technique will be discussed.

2 SPECIATION ANALYSIS OF IODINE

2.1 Environmental concerns related to the presence of iodine species

During the last 20 years, the interest to speciate iodine in environmental samples, particularly in different types of waters, has increased appreciably [1–11]. Water is considered essential to establish proper nutritional conditions for nearly all biological systems. It plays a fundamental role, supplying a certain amount of nutrients, including minerals, salts and essential elements, such as iodine, which are required by biological systems.

The iodine species present in water depend on the nature of the water sample analyzed; thus mainly inorganic iodine species exist in seawater and treated waters. On the other hand, organoiodine species can be present in natural waters such as river waters. This fact has been already established in many publications related to iodine in these samples [2, 4, 6, 8, 9, 11–14]. Groundwaters comprise about 0.6% of the total global water. They are derived almost entirely from rainwater, although small amounts are 'relic waters' trapped during the emplacement or sedimentation of rocks. The concentration of iodide in groundwaters can vary within a wide range between 1 and 100 $\mu g\,L^{-1}$ depending on the region, age and season [15]. River water and lake water comprise only about 0.1% of the global-total. It arises from three main sources: (a) surface runoff, (b) shallow groundwater and (c) the disposal of sewage and other urban effluents. Iodine occurs in varying amounts in all these sources. The iodine concentration in noncontaminated water could be around 1–3 $\mu g\,L^{-1}$. However, in areas remote from centers of human population, the concentration of iodine could be increased because of the use of iodophor detergents and sterilizators on dairy farms. Therefore, concentrations of iodine as high as 20 $\mu g\,L^{-1}$ could be found in river waters. Recent evidence suggests that inorganic forms of iodine, particularly iodide, introduced into river and lake waters from the atmosphere or other sources, are subject to conversion to organic forms by microbiological activity and enzymatic oxidation. The concentration of iodine in seawater is of the order of 45–60 $\mu g\,L^{-1}$ where it is mainly present as iodate and iodide. The biological accumulation of iodine probably contributes largely to the iodine content of marine sediments, which is often in the range of 20–600 mg/kg.

The analytical methodologies developed to determine iodine species in environmental samples have involved almost exclusively inductively coupled plasma-mass spectrometry (ICP-MS) as detector of the chromatographic eluent of liquid chromatography (LC) and gas chromatography (GC) separation techniques. Liquid chromatographic separations have been developed in the reversed-phase mode involving aqueous solutions as the mobile phase in order to avoid the extinction of the plasma. Heumann *et al.* [16] developed a method for the determination of iodide, iodate and anionic organoiodine species in river water samples by using high performance liquid chromatography (HPLC) coupled to ICP-MS. An

isotopic dilution study was performed in order to obtain accurate results. The detection of organoiodine species was sequentially on-line performed using UV and ICP-MS detectors. Additionally, size-exclusion chromatography (SEC) studies were performed in order to fractionate iodine compounds associated to humic substances.

More recently, other studies involving SEC to separate iodine species have been used to determine the molecular mass distribution of iodine compounds bound to humic substances [17–19]. Although halogens do not exist in their elementary form in the environment, important amounts of these elements are present as inorganic substances. Moreover, iodine forms organoiodines that have a great affinity for and can be accumulated in humic substances. The iodinated humic substances dissolved in aquatic systems play an important role transporting iodine in the environment and are therefore responsible for the great mobility of iodine in the hydrogeochemical systems. Experiments have been performed to determine the distribution patterns of iodine among humic substances in different types of samples using the SEC-ICP-MS coupling [17–19]. Wastewater samples from several origins showed that iodine was mainly associated to the high molecular mass fractions. In those cases, the samples analyzed were groundwater, soil samples from municipal deposits and wastewater from industrial origin [16–19].

At present, there is little information about the binding of iodine to humic substances or the stability of these organoiodine species, neither possible transformations into other species by aging have been extensively studied. These topics are of high interest for the assessment of the transport of organohalogens in the environment, as well as to determine the possible toxicological effect of low molecular mass compounds generated by degradation of naturally formed halogenated organic matter. SEC-ICP-MS coupling has been applied to determine the aging of organoiodine compounds associated to humic substances [17, 19]. In these experiments, it was observed that microbiological activity had a strong influence on the aging process of halogenated humic substances. A significant modification of the iodine distribution was found after four and eight weeks of aging, showing a conversion of the organoiodine species into higher molecular weight fractions. (See Figure 2.24.1)

Another analytical strategy, which has been frequently used, is the application of the GC-ICP-MS [20–24]. Actually, GC has been coupled to plasma detectors since many years because of the sample introduction possibility for halogens analysis into several types of plasma spectrometers, such as ICP-MS, inductively coupled plasma-optical emission spectrometry (ICP-OES) and MIP-AES. GC is particularly useful to study volatile iodine species in environmental samples, especially for samples such as seawater in which volatile iodine species can be generated plus volatile iodinated alkyl compounds resulting from microbiological degradation of organic matter. In this sense, a recent development in GC coupling to different detectors has been proposed by Schwarz and Heumann [21]. A GC system was simultaneously coupled to electron capture detector (ECD) and then to ICP-MS for the determination of iodinated volatile organic compounds resulting from aquatic and air systems. A GC-ECD/ICP-MS coupling scheme is shown in Figure 2.24.2. The GC-ECD/ICP-MS system provided high selectivity and sensitivity for the individual detection of volatile organic compounds (VOCs) under fast chromatographic conditions. An absolute detection limit of 0.5 pg iodine was obtained with this system, which is comparable with that typically obtained with the GC-ICP-MS. The two-dimensional GC-ECD/ICP-MS instrumentation was compared with electron ionization mass spectrometry (EI-MS) and microwave-induced plasma-atomic emission detector (MIP-AED). It can be concluded that the main advantage of the GC-ECD/ICP-MS coupling was the possibility of identifying coeluting compounds.

A more recent application of the GC-ICP-MS coupling has been illustrated by Wuilloud and coworkers [20] for the determination of iodophenols compounds used as disinfecting byproducts (DBPs). The use of iodine as a drinking water disinfectant is well established [25, 26]. The National Aeronautic and Space Administration (NASA) has

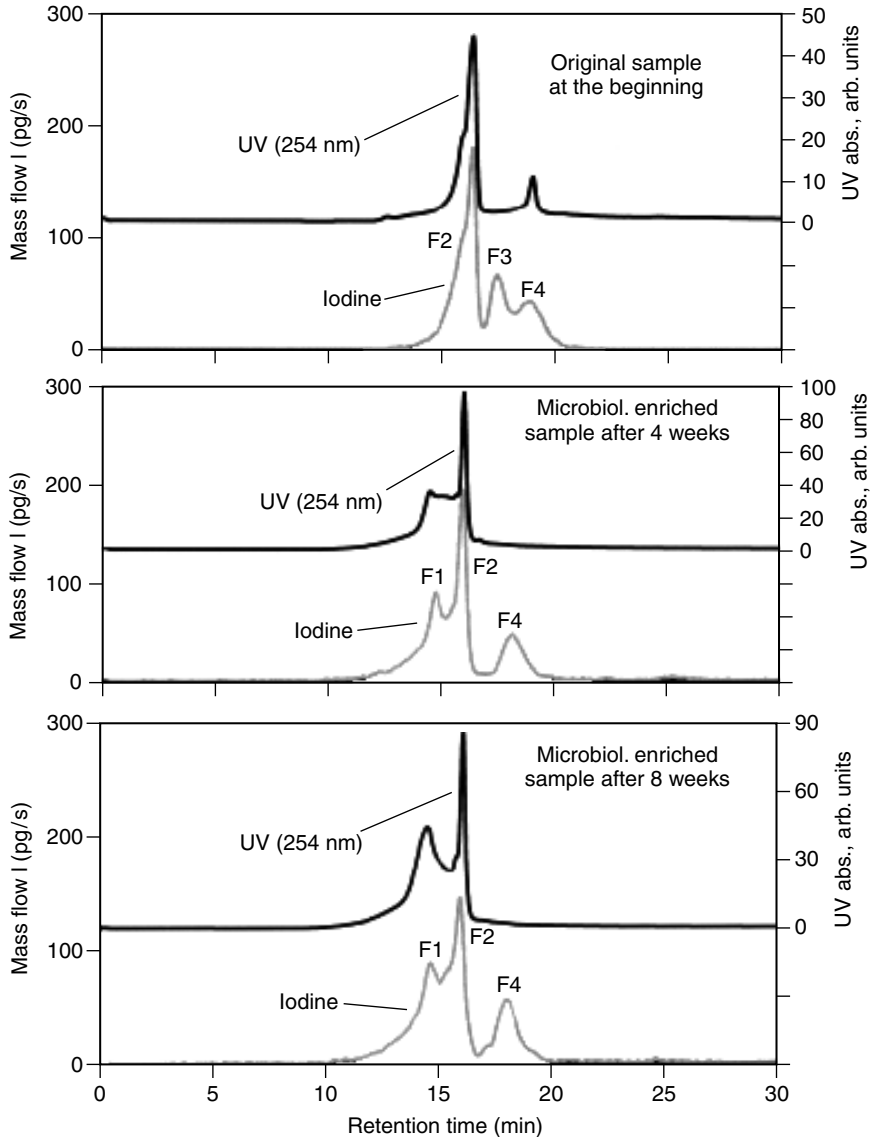

Figure 2.24.1. SEC-ICP-IDMS chromatogram of iodine for a microbiologically enriched sewage water sample after four and eight weeks of aging in comparison with the original sample at the beginning. (Reproduced from Reference [19] by permission of Wiley-VCH.)

chosen iodine to disinfect recycled water on long-duration manned space missions. However, the chemistry and toxicology of iodinated DBPs are not well known [27]. On the other hand, research has been done by the NASA space program in order to evaluate the odor properties of phenolic iodinated DBPs in drinking water [28]. Odor evaluations indicated that the iodophenols have much lower odor threshold concentration (OTC) values than phenol itself. Additionally, it has been observed that the iodophenols impart a slight medicinal odor to water even at low concentrations (1 to 500 $\mu g\,L^{-1}$), and this is not desirable [28]. Other researchers have shown that the halogenated

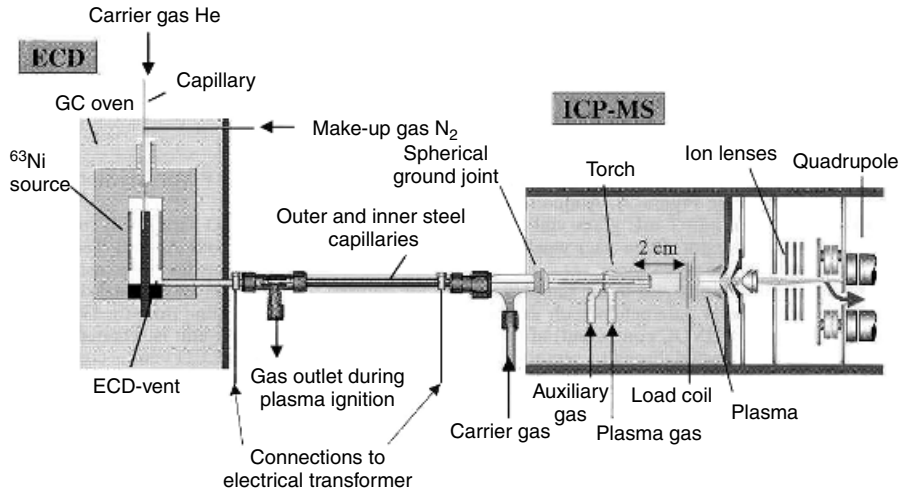

Figure 2.24.2. Schematic figure of the transfer line used for coupling GC-ECD with ICP-MS. (Reproduced from Two-dimensional on-line detection of brominated and iodinated volatile organic compounds by ECD and ICP-MS after GC separation *Anal Bioanal Chem*, Schwarz, A. and Heumann, K. G., **374**, 212–219, Figure 1 (2002) © Springer-Verlag.)

phenols can be formed from the phenols or phenolic compounds with the active halogens present in the sample at pH values lower than 7 [29]. Wuilloud *et al*. [20] developed an analytical method to determine iodophenols by GC-ICP-MS, with 2-iodophenol, 4-iodophenol and 2,4,6-triiodophenol as primary compounds which might be formed with the iodine used for recycled water disinfection [28]. The authors explored the use of optional gases added to the argon plasma as well as solid-phase microextraction (SPME) technique in order to obtain low limits of detection for the method. It was also observed that the use of oxygen as an optional gas increased the sensitivity by ca 50%, comparing with that obtained without the use of optional gases. The detection limits yielded were 0.07 ng L^{-1} (2-iodophenol), 0.12 ng L^{-1} (4-iodophenol) and 0.09 ng L^{-1} (2,4,6,triiodophenol). Therefore, the determination of iodophenol species at the low ng L^{-1} levels was reached in drinking, bottled and river waters.

In the last decade, volatile halogenated organic compounds have received considerable interest in atmospheric chemistry. This is because their contribution to the greenhouse effect as a source of halogen radicals. The radicals are formed by photodissociation, making halogenated compounds important for stratospheric photochemical reactions, such as ozone decomposition. One important source of halogen radicals are biogenic VOCs. The input of these compounds into the atmosphere is difficult to estimate, however, recent research has shown that oceans, marine algae, phytoplankton and forest soil are important sources of biogenic VOCs. An analytical technique proposing GC coupled to MIP-AES has been applied to the determination of volatile iodinated hydrocarbons in seawater samples [23]. The specific elemental detector was coupled to an automated purge and trap GC system for the determination of volatile halogenated hydrocarbons in environmental water samples. Complete separation of CH_3I, C_2H_5I, CH_2ClI and CH_2I_2 species was possible with GC-MIP-AES within 14 min. The use of the purge and trap system yielded absolute detection limits on the order of 11 to 257 pg. A comparison between atomic emission spectrometry (AES) and ECD of the GC eluent was necessary. It was pointed out that AES was advantageous compared to ECD regarding its higher selectivity. Because of the possibility of measuring the analyte at a specific wavelength, no selectivity problems occurred. However, using ECD, the measured signals were not element specific and therefore a deteriorated selectivity was obtained.

2.2 Importance and determination of iodine species in food

During the past few years, increasing interest has been accorded on the role of trace elements in human nutrition [30]. Essential elements contribute to the structure and functions of many metalloproteins and enzymes that play important biological roles. This is particularly the case during childhood because infants are more sensitive than adults to possible elemental deficiency or excess owing to their higher metabolic rate. As a result, the scientific community has shown increasing interest in the determination of trace elements in food [31–37].

The bioavailability and toxicology of a given element depends strongly on the chemical form in which it occurs in the biological sample. Consequently, it justifies the necessity to carry out not only total determinations but also speciation studies to obtain complete information about trace elements in food for nutritional purposes. Generally, the iodine concentration in most foods is low. Despite this, about 90% of dietary iodine is derived from food and the remaining 10% from drinking water. The iodine content in grains, fruits and vegetables is generally determined by the environment in which they grow (soil, water, geographical location, use of fertilizers, etc.). The amount of iodine contained in marine foods is generally high and can vary on the basis of the amount of iodine that has been concentrated from the sea water.

From analyzing the data shown in Table 2.24.1, it can be rapidly concluded that most of the publications concerning the determination of iodine species in food have been developed exclusively in different types of milk samples [36, 38–40]. This can be justified because of the high importance that milk has in human nutrition. Milk plays an essential role in growth and development of the person. As a consequence, a correct administration of all macronutrients, including proteins, lipids, carbohydrates and micronutrients involving minerals, vitamins and enzymes, from milk is necessary to assure the health of children. Moreover, milk is considered as a basic food required in the daily diet of all mammals in the first stage of life. It is accepted worldwide that human milk provides the most adequate intake of nutrients for infants and thus human milk should be used as a nutritional reference to evaluate alternative milk formulas for feeding infants.

As it is possible to observe in Table 2.24.1, the speciation analysis of iodine in food has been carried out mostly using SEC coupled to ICP-MS. In a speciation study of several elements, including iodine present in several milk samples, Martino *et al*. [38] applied SEC-ICP-MS to evaluate the elemental fractionation patterns in whey. The molecular mass distribution was studied using a high-pressure column (SEC on a TSK G 2000 SWXL). Recovery studies were performed after chromatographic elution. Recovery values between 85 and 119% were obtained for all elements. After optimizing the analytical variables of the method, it was applied for the multielemental fractionation pattern study developed in four different samples of milk whey, including human, raw cow, ultra high temperature (UHT) cow and formula. The results showed substantial differences in the elements' binding depending on the type of milk analyzed. Figure 2.24.3 shows the results for iodine fractionation in milk whey analysis. 94 to 100% of iodine was found to be essentially associated to low molecular mass compounds (1.4 kDa). These results were similar to those previously reported by other authors [36]. The comparison of the distribution patterns of iodine among the several types of milk whey samples permitted to conclude that a more complex speciation seems to occur in human and formula milk.

Another method utilizing the SEC-ICP-MS technique for the determination of iodine species in different types of milk whey samples was proposed by Sanchez and Szpunar [40]. Iodine species were separated within 40 min using a 30 mmol L^{-1} Tris buffer solution. A systematic study of iodine species in milk samples, including

Table 2.24.1. Summary of publications about iodine speciation using plasma spectrometry detection.

Year	Sample	Species	Analytical technique	Detection limit	Comments	References
	Environmental samples					
2003	Drinking water; river water	2-iodophenol; 4-iodophenol; 2,4,6-triiodophenol	GC-ICP-MS	0.07–0.12 ng L^{-1}	Optimization of different optional gases. Extraction and preconcentration of iodophenols species by using the SPME technique.	20
2002	Seawater; air	CH_3I; C_2H_5I; 2-C_3H_7I; 1-C_3H_7I; CH_2ClI; 2-C_4H_9I; *i*-C_4H_9I; 1-C_4H_9I; CH_2I_2	GC-ECD-ICP-MS	0.5 pg	The coupling of GC to ECD and ICP-MS detectors is developed for the first time.	21
2000	Water; Seawater; Saltwater	I_2; I^-; IO_3^-	ICP-OES	–	Iodine generation using $NaNO_2$ in H_2SO_4 solution. Speciation analysis by selective reduction and oxidation of the iodine species.	41
2000	Wastewater; groundwater; wastewater from coal pyrolysis process	Iodine species associated to humic substances	SEC-ICP-MS	–	Information about the distribution of iodine among different humic substances fractions.	17
2000	Soil samples from municipal waste deposits	CH_3I	HG-LT-GC-ICP-MS	0.3 pg as I	Multielemental speciation was carried out using hydride generation followed by cooled trap preconcentration system before GC and ICP-MS	22
2000	Wastewaters of industrial and communal origin	Halogens (I, Cl, Br) species associated to humic substances	SEC-ICP-MS	–	Microbiological influence on the conversion of humic substances-iodine species was observed.	19
1999	Seawater	CH_3I; C_2H_5I; CH_2ClI; CH_2I_2	GC-MIP-AES	11–257 pg for compounds	A purge and trap system was coupled to GC-MIP-AES to preconcentrate haloorganic species.	23
1998	Sea crude oil; nickel refinery deposited sludge	Iodobenzene	GC-MP-MS	53 pg as I	A radio frequency plasma containing inside a silica capillary column was presented. Oxygen gas permitted to avoid carbon deposition.	24
1997	Sewage waters	Iodine/HS species	SEC-ICP-MS; SEC-ICP-IDMS	–	Observation of molecular size transformation of humic substances-iodine species after 4 weeks of aging.	18

Table 2.24.1. (*continued*)

Year	Sample	Species	Analytical technique	Detection limit	Comments	References
1996	Seawater; saltwater	I_2; I^-; IO_3^-	ICP-OES	0.04 mg L^{-1}	Determination of iodine species performed by I_2 generation and sequential oxidation.	42
1994	River water	I^-; IO_3^-; Anionic organo-iodine	HPLC-ICP-IDMS	pg as I	Comparison of ICP-IDMS and UV chromatogram confirmed the association of iodine with organic matter.	16
1992	Drinking water	I^-; IO_3^-	HPLC-ICP-MS	25 pg	A gel permeation column was used to separate I^- and IO_3^- species in a very short time, in the order of 5 min.	43
	Food samples					
2002	Cow, formula and human milk whey	Iodine associated with different fractions	SEC-ICP-MS	–	Iodine resulted to be associated to low molecular mass compounds and mainly under the form of iodide.	38
2001	Cow milk	I^-; IO_3^-	HPLC-ICP-MS	0.03 pg as I	Small proportion of iodine was found to be associated with the organic matter.	39
1999	Cow, formula and human milk whey	I^-	SEC-ICP-MS	0.1 ng as I	More than 50% of iodine was observed to be associated to an unidentified macromolecular compound.	40
1998	Soy-based formula; cow milk-based formula; breast milk	I^-; organoiodine compounds	SEC-ICP-MS	–	Distribution of the elements changed depending on the type of milk analyzed.	36
	Biological samples					
2002	Synthetic thyroxine	Levothyroxine (T_4); Liothyroxine (T_3)	μLC-ICP-MS	5 pg as I	A DIHEN nebulizer was used to couple the μLC to the ICP-MS increasing the nebulization efficiency.	44
2002	Whole-body homogenates of Zebrafish and tadpoles of African clawed frog	I^- T_4; T_3; reverse T_3; monoiodothyrosine (MIT); diiodothyrosine (DIT)	HPLC-ICP-MS	–	Pronase E released the iodinated species from the transport proteins. Five additional iodinated compounds that were not identified.	45
2001	Pharmaceutical products	Iohexol; Iodixanol	HPLC-ICP-MS	0.4 ng as I	Analysis of iodinated X-ray reagents using normal phase chromatography and O_2 as an optional gas for ICP-OES.	46

(*continued overleaf*)

Table 2.24.1. (*continued*)

Year	Sample	Species	Analytical technique	Detection limit	Comments	References
2001	Zebrafish tissue	I^-; T_4; T_3; reverse T_3; MIT; DIT	HPLC-ICP-MS	–	Two unknown iodine species were found in the samples. The samples were previously digested in order to release the T_4 bonded to the proteins.	47
2000	Human blood serum	I^-; organoiodine species	HPLC-ICP-MS		Separation of different molecular weight compounds using surfacted-mediated HPLC.	48
2000	Human urine	I^-; T_4; T_3; reverse T_3; monoiodothyrosine (MIT); diiodothyrosine (DIT)	HPLC-ICP-MS	8–80 pg as the compounds	On-line addition of HNO_3 permitted to oxidize the species. Oxygen avoided the deposition of carbon on the cones of the ICP-MS.	49
2000	Human serum	I^-; T_4; T_3; reverse T_3; monoiodothyrosine (MIT); diiodothyrosine (DIT)	HPLC-ICP-MS	8–80 pg as the compounds	The content of bounded T_4 to globulin was determined by previous enzymatic hydrolysis of the proteins.	50
1999	Human milk	Low molecular iodine species; T_4; I^-; IO_3^-	CE-ICP-MS	0.04–1.2 $\mu g\,L^{-1}$ as I	Development of a homemade interface to connect the CE to ICP-MS detector. Total separation of the iodine species was obtained within 8 min.	51
1999	Human urine and serum	I^-; IO_3^-; T_3; T_4	CE-ICP-MS	0.08–3.5 $\mu g\,L^{-1}$ as I	Evaluation of TBG role in the bonding of T_4 and T_3 by adding those hormones on TBG.	52
1997	Human urine	I^-; IO_3^-	HPLC-ICP-MS	–	It was shown that the digestion conditions can strongly affect the species conversion, especially when oxidizing reagents are used.	53
1993	Bovine tyroglobulin	I^-; T_4; T_3; reverse T_3; MIT; DIT	HPLC-ICP-MS	35–130 pg as I	Proteolysis of thyroglobulin was carried out in order to release the iodine hormones.	54
1992	Human urine	I^-; IO_3^-	HPLC-ICP-MS	25 pg	Separation of I^- and IO_3^- species within 5 min using gel permeation chromatography.	43

Table 2.24.1. (*continued*)

Year	Sample	Species	Analytical technique	Detection limit	Comments	References
	Plasma studies					
2000		Iodobutane	GC-GD-TOFMS	4 pg	A controlled discharge was generated, permitting to switch between atomic and molecular ionization modes.	55
2000		Iodobenzene; Iodoheptane	GC-MP-MS	0.13 pg as I	The mechanisms of negative ion formation and breakdown were discussed.	56
1997		Iodobenzene	GC-LP-ICP-MS	140 pg	An LP-ICP source sustained at only 6 W and utilizing 6 mL min^{-1} helium was investigated as an ionization source for molecular and atomic MS.	57
1994		Iodobenzene	GC-RFP-AED	1.0–2.8 pg as I	The elimination of the makeup gas permitted to sustain a 350-kHz radio frequency plasma inside the end of a fused silica GC column.	58
1993		Iodobenzene	GC-MIP-MS	20–100 pg	Use of reduced-pressure water cooled MIP torch to interface a GC with the plasma-mass spectrometer.	59
1990		Iodobenzene	GC-LP-MIP-MS	0.1 pg as I	Utilization of GC to quantitatively introduce halogenated compounds to evaluate the overall system performance.	60
1990		1-Iodobutane	HPLC-MIP-MS	0.9 pg as I	Methanol, ethanol and 2-propanol were evaluated about their compatibility with the detector.	61
1989		Iodobenzene	GC-MIP-MS	0.16 pg	Significant improvement of detection limit in comparison with others' works.	62
1989		I^-; IO_3^-	HPLC-MIP-OES	3.4–4.5 ng as I	Use of a small-volume helium MIP operated at 100 W to measure the iodine signal at 206.24 nm.	63
1987		Iodopropane	GC-ICP-MS	1 pg as I	Atomization of injected compounds was nearly complete and independent of molecular structure.	64

(*continued overleaf*)

Table 2.24.1. (*continued*)

Year	Sample	Species	Analytical technique	Detection limit	Comments	References
1977		1-iodopropane; 2-iodopropane	GC-MIP-OES	0.46–0.56 ng	Initial studies were developed about the GC-MIP coupling. Characterization of the system in terms of linear response, sensitivity, etc.	65
1967		Diiodomethane; 2-iodochlorobenzene; 3-iodomethylbenzoate; 1-iododecane; 2-iodobiphenyl; 2,5-diiodomethylbenzoate; 2,3,5-triiodomethylbenzoate	GC-MIP-OES	–	Different emission lines in the spectra were evaluated. The iodine emission line selected for the determinations was 533.82 nm.	66

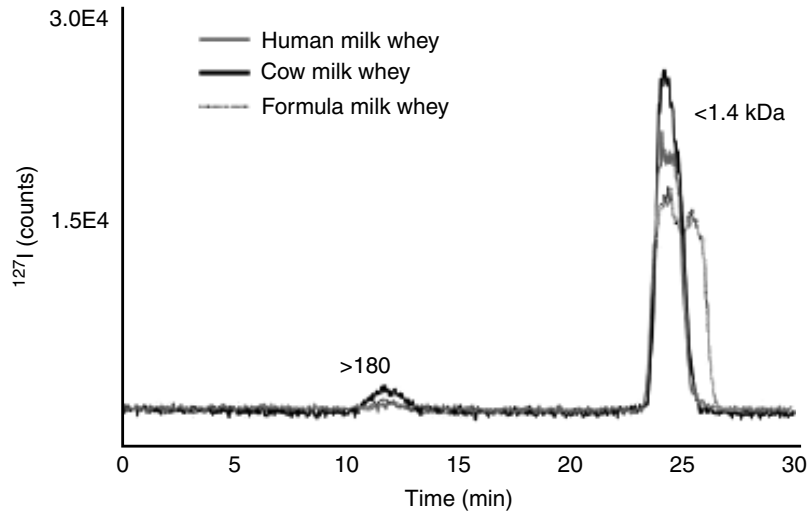

Figure 2.24.3. Examples of the binding patterns of iodine in cow, formula and human milk whey. (Reproduced from Reference [38] by permission of The Royal Society of Chemistry.)

different animals (cow, goat), humans of different geographic regions (several European countries) and infant formulas from different manufacturers was carried out. Comparable results were obtained for almost all samples. Ninety-five percent of the iodine initially present in the milk was found in the milk whey. Only in the milk whey of infant formula the iodine was 15–50% of the total one. The authors studied the effect of adding sodium dodecyl sulfonate (SDS) on the recovery of iodine on these samples. It was observed that the addition of SDS produced a significant improvement of the iodine recovery into milk whey. From this study, it is possible to conclude that iodine is primarily present as iodide in all the samples except infant formulas. It was also observed that more than half of the iodine was bound to a high molecular mass (>1000 kDa) species. Speciation studies of iodine in milk after enzymolysis was also performed in an effort to understand the cracking of macromolecular compound in this sample. The resulting changes in the distribution patterns of iodine were

monitored by SEC-ICP-MS. After enzymolysis, although a different molecular mass distribution was found, it turned out that the procedure was unsuitable for iodine species. A broad distribution was found for iodine species, indicating that iodine is associated to a complex mixture of macromolecular compounds. Therefore, the identification of the iodine species associated to high molecular mass fractions in milk samples is still unclear.

A different analytical methodology for the determination of iodine species in different kinds of milk samples was developed by Leiterer *et al.* [39] In this methodology, ion exchange chromatography was utilized for the separation of primarily inorganic iodine under the form of iodide and iodine associated to organic matter. A combination of HPLC and ICP-MS was used to determine iodine species in milk samples. Iodide was identified as the main iodine species in milk, but in a few samples traces of iodate and several unidentified species, presumably organoiodine compounds, were observed as well. In addition, the total iodine concentration in the samples was determined by ICP-MS and gives a general indication about the iodine species in milk.

From the analysis of the existing bibliography, it can be concluded that studies regarding speciation of iodine in foods are exclusively done in milk. Considering the importance that iodine has to assure a proper nutrition, the number of studies is scarce. Therefore, more research is required to reach a more complete knowledge about iodine in different food types.

2.3 Iodine species in biological systems

Iodine is an essential element for normal growth and development in humans and animals. The importance of iodine as an essential element in our diet arises from the fact that it is a major component of the thyroid hormone 3,5,3′-triiodothyronine (T_3) and 3,5,3′,5′-tetraiodothyronine (T_4) or thyroxine (see Figure 2.24.4). These hormones are essential for normal growth and physical as well as mental development. Iodine accounts for about 65% of the amount of the T_4 hormone and 49% of the amount of T_3 hormone. The most familiar iodine disorder is goiter, which is characterized by an enlargement of the thyroid gland. On the other hand, excessive intake of iodine (2 mg per day) can also have an antithyroid effect by impairing synthesis of the thyroid hormone. This in turn results in the enlargement of the thyroid gland, just as deficiency does. This goiterlike condition may be serious enough to block the airways in children and cause suffocation. An adequate control of the iodine concentration and its different species in biological systems should be performed

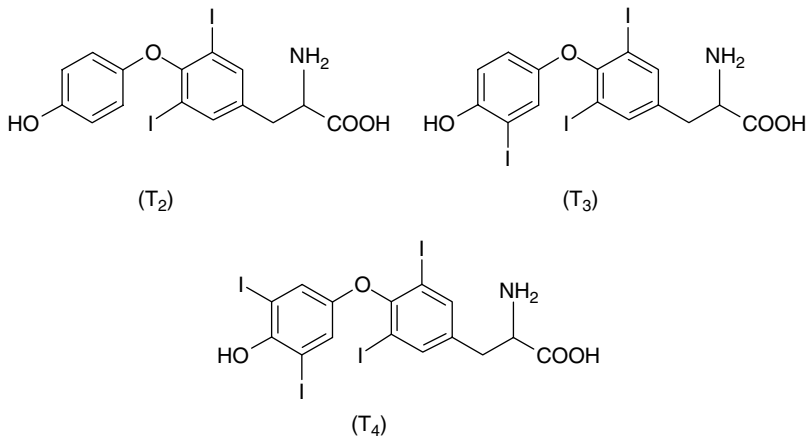

Figure 2.24.4. Structure of iodinated hormones involved in the functioning of the thyroid gland: 3,5-diiodothyronine (T_2); 3,5,3′-triiodothyronine (T_3) and 3,5,3′, 5′-tetraiodothyronine (T_4).

to assure correct nutrition and avoid disorders associated with excessive or insufficient iodine intake.

The great importance of the iodine presence in biological systems has been reflected in the number of publications involving determination of iodine species in biological samples as can be seen in Table 2.24.1 [43, 44, 46–54]. Because of the importance of the thyroid hormones T_4 and T_3, most of the work on iodine speciation has been focalized on the determination of these hormones in biological fluids, particularly urine and serum, which are specific indicators to test the thyroid function [43, 44, 46–54].

The analytical methodologies developed for the determination of iodine species in biological samples mainly use HPLC coupled to ICP-MS for the separation and detection of I^-, IO_3^-, T_4, T_3, reverse T_3, monoiodothyrosine (MIT) and diiodothyrosine (DIT). Wind *et al.* [44] coupled liquid chromatography of micro-scale (μLC) and ICP-MS to determine synthetic thyroxine and synthetic phospholipids. The experiment consisted of a direct injection into a high efficiency nebulizer (DIHEN) modified for μLC-ICP-MS coupling by inserting an additional internal capillary with o.d. 90 μm and i.d. 20 μm to minimize the interface dead volume. The modified DIHEN was compared with a conventional microflow nebulizer with regard to sensitivity, signal stability and organic modifier dependency at flow rates ranging from 0.5 to 5 mL per minute. Although the modified DIHEN presented slightly less sensitivity, it had the advantage of superior signal stability, less pronounced modifier dependency and better chromatographic resolution because of its small dead volume.

The potential use of ICP-MS as a chromatographic detector for HPLC to analyze organic pharmaceutical compounds has been evaluated by Axelsson *et al.* [46]. The analytical advantages of using ICP-MS were evaluated by comparing its efficiency with other possible chromatographic detectors such as UV, mass spectrometry (MS), refractive index (RI) and evaporative light-scattering detection (ELSD). The results showed that the best performance in terms of low detection limits and usability was obtained with ICP-MS detection. Normal phase chromatography with ICP-MS detection was applied to the separation and determination of iodinated impurities in two iodinated X-ray contrast reagents (Iohexol and Iodixanol). Three impurities were simultaneously quantified as iodine based with UV detection at 238 nm and ICP-MS (^{127}I). However, these impurities, which were lower than 0.1%, could not be identified or characterized by UV alone. The use of oxygen in the carrier argon gas flow permitted the introduction of an elevated amount of organic solvent into the plasma; therefore, these species could be analyzed by ICP-MS after LC separation.

Reversed-phase HPLC coupled to ICP-MS has been used on many occasions for the separation of iodine species in biological samples [44, 45, 47, 49, 50, 54]. Generally, a C_{18} column with a mobile phase containing a phosphate or TRIS buffer at pH = 6.5–8.0 was used to perform the I^-, IO_3^-, T_4, T_3, reverse T_3, MIT and DIT separation. Biological samples including, Zebrafish tissue [47], human urine [43, 49], human serum [50], and bovine thyroglobulin [54] were analyzed by these methodologies. It should be pointed out that the main differences among these methods were the separation conditions and the use of organic solvents. Michalke *et al.* [49] developed a methodology based on reversed-phase HPLC combined with ICP-MS detection. In that method, the determination of I^-, IO_3^-, T_4, T_3, reverse T_3, MIT and DIT species was accomplished by applying a methanol gradient in the chromatographic mobile face. The stability of the plasma under these conditions was obtained by diluting the chromatographic eluent with a HNO_3 solution making up a flow rate of 2 mL per minute. The addition of oxygen in the carrier argon gas flow helped to reduce the carbon residue from methanol pyrolysis on the torch. Investigations about the influence of buffer pH and column temperature on the separation efficiency were also carried out. After complete optimization, the mentioned iodine species were separated in 30 min.

Speciation analysis of iodine in human urine samples has also been carried out using ion exchange chromatography coupled to ICP-MS [53]. The determination of iodine in aqueous solutions suffers from several serious problems caused by the

formation of different iodine species, derived from the oxidative pretreatment of biological materials. Taking into account a possible conversion of the iodine species as a consequence of the medium pH, different eluent-column combinations were evaluated. The results using IC-ICP-MS showed that different iodine species were obtained depending on the sample composition and the sample preparation procedure. Iodide, iodate and in some cases unknown organic iodine-containing compounds were qualitatively determined in the sample solutions. The detection of I_2 itself was not successful. However, it was assumed that I_2 might have been formed in the final solutions after an oxidizing digestion by conversion of I^- into IO_3^- in the acid matrix. By addition of an ammonia solution prior to analysis, IO_3^- and I_2 were converted into I^-. In untreated and acidified/preserved urine samples, the simultaneous multielemental determination including iodine was possible by pneumatic nebulization ICP-MS using the method of standard addition.

In a different analytical study, HPLC-ICP-MS was applied to determine halogenated proteins in human blood serum [48]. In this work, a surfactant-mediated chromatographic separation system was developed, which allowed simultaneous multicomponent separation based on the mixed-mode separation properties such as size-exclusion, electrostatic and hydrophobic interactions. Large-molecular species (MM 6500–2,000,000) were eluted within 3 min, whereas small-molecule species (MM < 1000) were eluted after 3.5 min. Simultaneous detection of the different fractions was achieved by coupling a UV detector and an ICP-MS on-line to the HPLC system. Information about the human blood serum proteins regarding their iodine binding or nonbinding properties is given in this analysis. It was found that 90% of the iodine present in the serum samples was bonded to high molecular mass-compounds, suggesting the presence of iodinated proteins. The remaining 10% of iodine was present in the low molecular mass fraction. Identification and characterization of the iodinated proteins was not done in this study.

Recently, the first applications of capillary electrophoresis (CE) on-line coupling to ICP-MS for the determination of iodine species in biological samples have been published [51, 52]. Michalke and Schramel [52] developed an analytical methodology involving the hyphenation of CE to ICP-MS. The method includes a buffer of phosphate (pH 2.3), NaOH, SDS and borate (pH 8.3) for stacking purposes aiming the separation of sufficient amounts of I^-, IO_3^-, T_4 and T_3. Separation of the iodine species was accomplished within 15 min. The method was applied to speciation analysis of iodine in human serum and urine samples. A comparison between the iodine species levels in these samples was performed in healthy and thyroid-operated patients. It was observed that patients after being operated on showed similar concentrations of I^- and T_4 as healthy patients. Additionally, a study on the binding capacity of thyroid hormone binding globulin (TBG) for I^- and T_4 was carried out. It is known from the literature that free hormones are not found in serum because they are predominantly (>75%) attached to transport proteins, to TBG. To study this effect, the authors added thyroxine to the serum samples and enhanced the binding capacity of TBG. It was found that less than 50% of TBG in serum is saturated with hormones. Consequently, its binding capacity is rather high, producing the immediate complexing of T_4 or T_3 and increasing the levels of T_4-TBG and T_3-TBG in serum. Finally, human urine samples were analyzed to determine iodine species. Only the presence of I^- could be confirmed using CE-ICP-MS.

The capabilities of CE-ICP-MS were also demonstrated by Michalke [51] for iodine speciation in human milk samples. The hyphenation interface was characterized with respect to capillary position, gas flow rates and positioning of the interface to the ICP-MS. The system showed high separation capabilities, low detection limits and potentially wide applicability. Its capabilities were extended especially to iodine speciation. Detection limits of 0.04–1.2 mg L^{-1}, depending on the iodine species, were achieved. Retention of iodine species on the capillary surface because of nonoptimal separation conditions was also discussed. Adequate separation of the iodine species was obtained using a 25-mmol L^{-1} borate buffer at

pH 8.3 and two stacking electrolytes, 20 mmol L^{-1} NaOH and 10% SDS. To establish the applicability to real samples, the low molecular mass fraction of human milk was analyzed and peaks were identified by standard additions. The presence of I^- and T_4 was confirmed by matching the migration times. The concentration found for iodide was in the range of 14 ± 0.2 mg L^{-1} ($n = 3$) and for T_4 was 27.3 ± 3.0 mg L^{-1} ($n = 3$).

Most of the iodine speciation studies have been related to the thyroid gland. It can be expected that future iodine speciation studies will follow in this direction.

2.4 Development of hyphenated techniques using iodine species

There are a significant number of publications in which iodine species were determined using plasma spectrometry. Gas chromatography has been utilized to separate the iodine species, as well as a means for analyte introduction into the plasma. Normally, iodobenzene or iodobutane have been studied.

In a recent publication [55], a GC system was coupled to a direct-current gas sampling glow discharge (GSGD) ionization source for the mass spectrometric analysis of halogenated hydrocarbons. The continuous discharge was contained in the first vacuum stage of the differentially pumped spectrometer interface. The discharge was operated statically or rapidly switched between atomic and molecular ionization modes; both atomic and molecular spectra were generated in the helium-supported plasma. The ionization mode is selected by application of either a positive (molecular) or negative (atomic) potential to the sample introduction electrode, and the two kinds of spectra were sequentially collected by changing the voltage and current. The source was capable of generating mass spectra resembling those from an electron-impact source while it was operated in the molecular ionization mode (both static and dynamic). The best atomic detection limits (1–25 fg) were obtained when the plasma was operated in the static mode with single-channel gated ion counting. In this study, iodobutane was determined among other halogenated species.

In a different research work, a GC system was coupled to plasma MS with a microplasma ion source for negative ion detection (see Figure 2.24.5). The ion source was mounted within the high

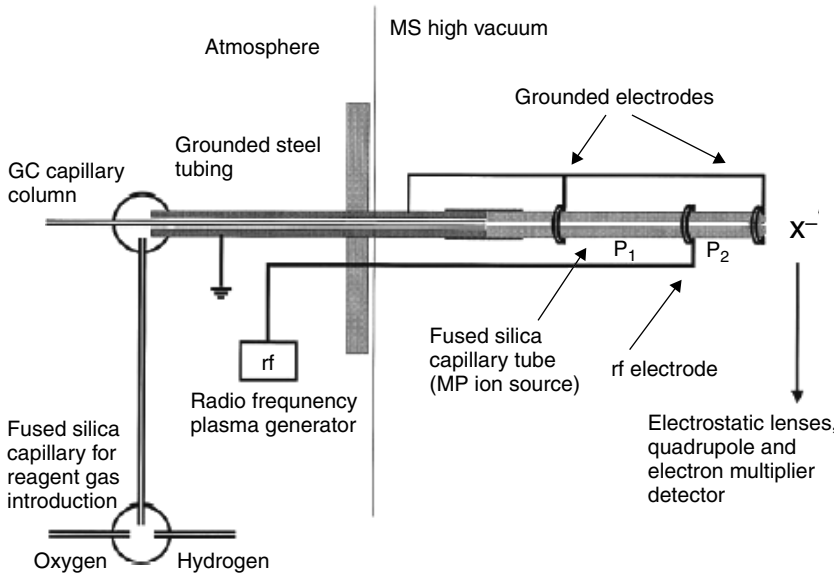

Figure 2.24.5. Schematic figure of the GC-MP-MS coupling interface and microplasma interface design. (Reproduced from Reference [56] by permission of The Royal Society of Chemistry.)

vacuum chamber of the mass spectrometer. It is a rigid fused silica capillary tube containing a capacitively coupled radio frequency helium plasma. This made the setup relatively simple, eliminating the sampler-skimmer pressure-reducing interface traditionally used in plasma MS. This study also describes the utilization of a halogen-selective negative ion detection. A highly sensitive detection for F, Cl, Br and I (0.13–12 pg s^{-1}) was obtained. The mechanisms of negative ion formation and breakdown were discussed in conjunction with the results. The iodine species utilized to do this study were iodobenzene and iodoheptane.

Many other studies and developments in plasma spectrometry have been carried out utilizing iodine species. Most of them involved the use of GC systems coupled to MIP-MS [59, 60, 62], while others coupled to MIP-AES [58, 65, 66] or ICP-MS [57, 64] detectors.

3 SPECIATION ANALYSIS OF BROMINE

3.1 The growing interest of bromine in environmental studies

An increasing number of publications have been dedicated to the analysis of bromine species in samples of environmental interest (Table 2.24.2). Particular attention has been given to the determination of (hydrocarbon volatile organic compounds) HVOCs in the environment, which can be generated as the product of microbiological degradation in the biota [67, 68]. The transfer of biogenic HVOCs from the earth surface into the atmosphere is difficult to estimate because the primary sources of these substances have not been totally explored. The brominated HVOCs are easily decomposed in the troposphere by photodissociation forming reactive halogen compounds such as BrO, which can cause decomposition of tropospheric ozone [69]. The determination of the distribution pattern of brominated VOCs in the tropospheric boundary layer relative to different potential sources is a great challenge. For example, Schwarz and Heumann [21] developed an analytical methodology using ECD and ICP-MS for the on-line monitoring of the GC eluent. The same coupling was applied for the determination of iodinated VOCs (Figure 2.24.2). The two-dimensional detection of 23 brominated VOCs was possible. A comparison of different other detectors, including MIP-AES and EI-MS, were also shown in this study. By using ECD as detector, it was possible to obtain better detection limits (0.08–2.1 pg as Br) than those obtained using ICP-MS (10 pg as Br) as a detector. The detection limits obtained when MIP-AED was used as detector for GC effluents were about 60 pg as Br. However, with EI-MS (0.5–7 pg as Br), detection limits were lower than ICP-MS but higher than ECD. Despite these differences in the detection limits obtained, ICP-MS permits determining those compounds that specifically contain halogens. The combined use of ECD and ICP-MS detectors for GC permitted the effective identification and quantification of brominated VOCs from aquatic and air samples. The halogenated compounds were previously preconcentrated by using stir bar sorptive extraction (SBSE) methodology. A 2-cm long stir bar coated with polydimethylsiloxane was used. The recoveries found for the first extraction step were in the range of 55 (2-C_3H_7Br) to 85% ($CHBr_3$).

Brominated flame retardants (BFRs) comprise approximately 25% of the volume of flame retardants (FR) used on a global scale and are used in applications that require high FR performance or in resins needing an FR active in the gas phase [83–86]. BFRs are a group of compounds such as aromatic diphenyl oxides (a.k.a. ethers), cyclic aliphatics, phenolic derivatives, aliphatics, phthalic anhydride derivatives and others. The bromine portion of the compound is responsible for FR activity of the molecule and is unique in its ability to provide flame retardancy in the gas phase. One of the major classes of compounds in this group is the polybrominated diphenyl ethers (PBDEs). BFRs have recently come under scrutiny because of their appearance in various substances. Several epidemiological studies have shown that these compounds pose a health risk. The PBDEs have structures similar to thyroid hormones; both consist of two phenyl rings and while PBDEs has 2 bromine substituents,

Table 2.24.2. Summary of publications related to bromine speciation using plasma spectrometry detection.

Year	Sample	Species	Analytical technique	Detection limit	Comments	Ref.
	Environmental samples					
2002	Sewage sludge	Polybrominated biphenyl ethers (BDE-28, BDE-47, BDE-85, BDE-99, BDE-100, BDE-128, BDE-153, BDE-154)	GC-ICP-MS	1–4 pg as Br	The best analytical performance was obtained when helium was used as an optional gas.	70
2002	Seawater	CH_3Br; C_2H_5Br; 2-CH_3H_7Br; CH_2Br_2; $CHBrCl_2$; $CHBr_2Cl$; CH_2BrI; $CHBr_3$	GC-ECD-ICP-MS	10 pg as Br	Simultaneous ECD-ICP-MS detection permitted to determine the association of halogens to organic matter.	21
2000	Surface water	Br^-; BrO_3^-	HPLC-ICP-MS	35–50 pg as Br	Use of ion exchange chromatography coupled to ICP-MS for the separation of inorganic bromine species in water samples.	71
2000	Sewage wastewater	HS/Br species	SEC-ICP-MS	–	Evaluation of an aging study of the humic substances-Br species and several effects such as microbiological activity on the distribution patterns.	19
1999	Gasolines	Bromoalkanes	GC-AED	300 pg as Br	Determination of alkanes after brominating them by using GC-AED.	72
1999	Seawater	CH_2BrCl; $C_2H_2Br_2$; $CHBrCl_2$; C_2H_4BrCl; $CHBr_2Cl$; 1,2-$C_2H_4Br_2$; $CHBr_3$	GC-MIP-AES	0.01–0.04 ng	Volatile halogenated organic compounds were determined using an automated purge and trap GC system.	23
1999	Drinking water	Br^-; BrO_3^-	HPLC-ICP-MS	1 ng as Br	Bromate was found to be the only bromine species present in disinfected water.	73
1998	Crude oil; sludge deposit	1,4-dibromobenzene	GC-MP-MS	37 pg as Br	Use of a microplasma ion source: a radio frequency plasma contained inside the last 4–5 cm of a 0.32-mm i.d. fused silica capillary column.	24
1997	Groundwater; seepage water from soil; brown water	HS/Br species	SEC-ICP-MS	–	Bromine was found to be associated to a single peak obtained by UV detection.	18
1997	Polluted ground water	Bromine-containing contaminants	GC-MIP-MS	–	Interfacing directly GC with a MIP torch and quadrupole MS provided information about elemental compositions.	74

Table 2.24.2. (*continued*)

Year	Sample	Species	Analytical technique	Detection limit	Comments	Ref.
1997	Crude oil; chimney soot	Polybrominated biphenyls	GC-RFP-AES	1–5 pg	A GC system with on-column radio frequency plasma AED was applied for the determination of PBDEs.	75
1990	Motor car exhaust gases	HBr; CH_3Br; C_2H_3Br; $C_2H_4Br_2$	GC-MIP-AES	–	Separation and determination of the bromine species within 10 min. The bromine detection was performed at 470.49 nm.	76
	Food samples					
2002	Cow; formula and human milk whey	Bromine associated with different molecular mass fractions	SEC-ICP-MS	–	Bromine was found to be attached to a low molecular mass fraction.	38
	Biological samples					
2002	Rat urine	Metabolites of 4-Bromoaniline	HPLC-UV-ICP-MS-TOF-MS	–	The use of reversed-phase chromatography coupled to UV, ICP-MS and TOFMS for the profiling and identification of metabolites in rat urine.	77
2002	Human and rat plasma	Metabolites of bradykinin	HPLC-UV-ICP-MS-TOF-MS	–	Detection of hormone and its metabolites by ICP-MS previous bromination.	78
2001	Rat urine	Metabolites of 2-bromo-4-trifluoromethyl-[^{13}C]-acetanilide	HPLC-UV-ICP-MS-TOF-MS	–	The metabolites were identified as sulfate and glucuronide conjugates of hydroxy-substituted metabolite, an *N*-sulfate, an *N*-hydroxylamine glucuronide and *N*- and *N*-hydroxyglucuronides.	79
1992	Human urine	Br^-; BrO_3^-	HPLC-ICP-MS	0.8 ng	Two unidentified bromine species were found to be present in human urine.	43
	Plasma studies					
2000		Bromobenzene; 1-bromoheptane; benzyl bromide	GC-LP/RP-ICP-MS	4.2–11 pg	Molecular ions for all three organobromine compounds were obtained, as well as some characteristic alkyl chain fragments for 1-bromoheptane.	80
2000		Bromoform; bromobenzene	GSGD-GC-ICP-TOF-MS	3–9 pg	Use of GC was coupled to a direct-current GSGD ionization source to analyze halogenated hydrocarbons by mass spectrometry.	55
2000		1,4-dibromobenzene	GC-MP-MS	0.50 pg	Elimination of the sampler-skimmer by keeping the ion source inside the high vacuum chamber of the mass spectrometer.	56
1997		Dibromobenzene	GC-LP-ICP-MS	229 pg	Enhancement of all the analyte molecular and fragment ion signals by adding isobutane.	57

(*continued overleaf*)

Table 2.24.2. (*continued*)

Year	Sample	Species	Analytical technique	Detection limit	Comments	Ref.
1994		Dibromobenzene	GC-ICP-AES	0.9–3.1 pg	The measuring of bromine was performed using 827.2; 863.9 and 889.8 nm spectral lines.	58
1993		1-bromononane	GC-LP-ICP-MS	–	Generation of a low-pressure Ar ICP-MS without modifying the torch box of a commercial ICP-MS instrument.	81
1990		$CHBrCl_2$; $CHBr_2Cl$; $CHBr_3$	GC-MIP-AES	4 pg	Coupling of GC system to MIP to determine traces of nonmetallic elements that are not traditionally determined by AES.	82

the thyroid hormones have iodine atoms are attached to the rings. General structural formulas of the most utilized BFRs are shown in Figure 2.24.6. In a study performed recently by Eriksson and coworkers [87], defects of the nervous system were observed in mice dosed in their early lives with 2,2′,4,4′-tetrabromodiphenyl ether (BDE-47) and 2,2′,4,4′, 5-pentabromodiphenyl ether (BDE-99). It is not precisely clear how these compounds affect the nervous system, but toxicologists suspect it may be in part the result of imbalance of thyroid hormones [88]. In general, data suggest that the PBDEs of lower bromination have a propensity to disrupt thyroid hormones, cause neurobehavioral deficits and possibly cancer [89]. Vonderheide *et al*. [70] developed a method for the analysis of these compounds involving the coupling of fast GC to ICP-MS detection. Eight different PDBEs were separated and determined using the GC-ICP-MS in a 10-min run. Different sewage sludge samples were analyzed, and

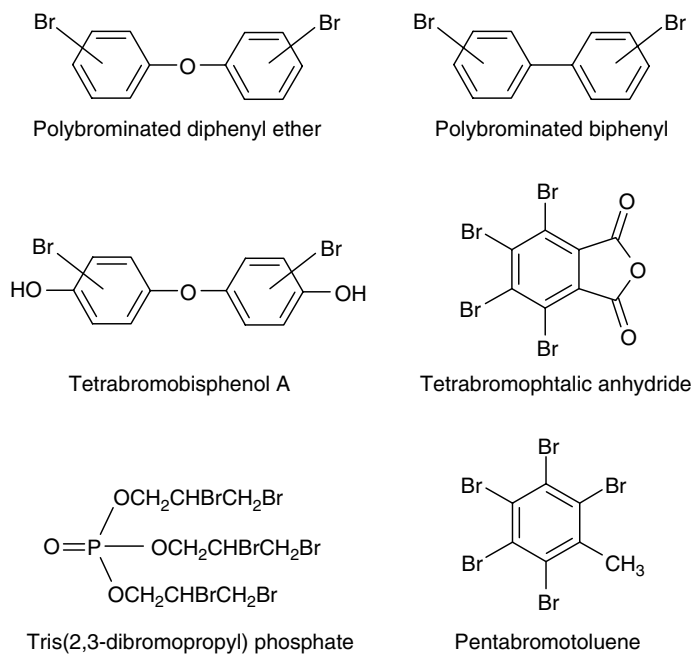

Figure 2.24.6. Structural formulas of some BFRs commonly used for different applications.

only the presence of BDE-47, BDE-99 and BDE-100 was confirmed. Concentrations of these contaminants were in the order of 7.11 to 28.6 $\mu g\,kg^{-1}$. Other BDEs were found at lower concentrations. Additionally, the authors explored the addition of different gases to the argon plasma in an effort to improve detection limits as a result of the high ionization potential of bromine. Detection limits of 0.5–2 $ng\,L^{-1}$ were achieved with the addition of approximately 4% nitrogen to the argon plasma.

Bromate is formed during the ozone water disinfection process. Bromate is recognized as a potential kidney carcinogen for rats and mice at $mg\,L^{-1}$ levels. Newer toxicological studies have led the International Agency for Research on Cancer (IARC) to classify bromate as a group 2B carcinogen for humans with renal risks at concentrations above 0.05 $\mu g\,L^{-1}$. Ion chromatography (IC) in combination with atmospheric pressure ionization-mass spectrometry (API-MS) as well as with ICP-MS had been compared for trace analysis of bromate by Seubert and coworkers [71]. The results indicated that both techniques yield comparable results and were in agreement with those obtained with standard methods for bromate determination. Because API-MS is a soft ionization technique, the determination of unfragmented bromate is possible, resulting in a highly selective detection with little background noise. On the other hand, ICP-MS operating at m/z 79 detects bromine and other molecular ions with similar masses, such as $^{39}K^{40}Ar^+$. Furthermore, high background counts can be expected from the molecular ion $^{38}Ar^{40}Ar^1H^+$ and by the strong nearby signal of $^{40}Ar_2{}^+$. Despite these differences, both techniques showed almost equal absolute detection limits, on the order of 50 pg as bromate. Additionally, the IC-ICP-MS coupling tolerated higher salt concentrations in the mobile phase when compared to IC-API-MS. Another analytical methodology for the speciation of bromine in water samples using IC-ICP-MS was proposed by Pantsar-Kallio and coworkers [73]. Eluent with potassium as counter ion cannot be used in the analysis of bromine by ICP-MS, because of the ArK^+ polyatomic interferences at the bromine isotope 79. NH_4NO_3 was an effective eluent and also avoided the interference problem at the m/z 79. Detection limits using the IC-ICP-MS system were in the 10 $\mu g\,L^{-1}$ range. On-line preconcentration of the bromine species prior to the chromatographic separation allowed the determination of bromate and bromide in the low $\mu g\,L^{-1}$.

There is a high interest in the study of humic substances since they may accumulate metals and halogens from the environment (Table 2.24.2). In the particular case of bromine distribution, Heumann *et al.* [19] studied the aging of dissolved brominated humic substances and the microbiological influence on that process. SEC-ICP-MS coupling was used, and a single peak distribution was assessed for bromine in sewage water samples. This halogen was associated to the low molecular mass fraction. No conversion effect on the bromine distribution was observed in the presence of different types of enzymes including esterase, aminopeptidase and β-glucosidase. Association of bromine to low molecular mass humic substances was also confirmed by the same authors in another study [18].

An interesting analytical method for the determination of alkenes in gasolines by bromination reactions has been proposed by Hardas and coworkers [72]. The authors used GC-AED for the analysis of several brominated alkenes. This enabled selective and quantitative bromination of alkenes without affecting aromatic and saturated compounds. Bromination was performed using a 17-component hydrocarbon mixture that contained 0.25% (v/v) of each hydrocarbon in carbon tetrachloride. Hydrocarbon solution was reacted with 1% (v/v) bromine in CCl_4. The detection limit for bromine was 300 pg. Bromine was measured at 478 nm.

3.2 Food samples

Determination of bromine species in food has not been extensively applied in speciation analysis (Table 2.24.2). The most recent application of SEC coupled to ICP-MS has been reported by Martino *et al.* [38] The authors analyzed different types of milk samples to evaluate the differences in the molecular mass distribution pattern of several elements including bromine in bovine, formula and human milk whey samples. It was found that 94–100% of the total bromine present in the

samples was associated to a low molecular mass fraction (<1.4 kDa). No differences in the distribution patterns for bromine were found among the milk samples, indicating a similar association of bromine in all samples. No information about the bromine species was given in this study.

3.3 Hyphenated techniques for metabolic studies of bromine-containing drugs

The article published by Nielsen in 1984 [30] supports the view that bromine is an essential nutrient. This evidence included: (a) bromide can be substituted for chloride in chicks; (b) bromide can alleviate growth retardation induced in chicks and mice by feeding iodinated casein; and (c) insomnia exhibited by some hemodialysis patients was associated with bromide deficit. Recently, it was reported that when goats are fed with a 0.8–20 mg bromide kg^{-1} diet, they exhibited depressed growth, fertility, hematocrit, hemoglobin and life expectancy but an increment of their milk fat and the number of abortions. Although these last findings give more credibility to the concept of bromine essentiality, the findings are still limited. The evidence presented to support essentiality of bromine does not provide much information about its possible biochemical role.

Determination of brominated inorganic species using hyphenated techniques has not been commonly done. However, Salov *et al.* [43] developed a method using HPLC-ICP-MS for the identification and determination of bromine species in human urine. Separation of bromine species was accomplished by utilizing a gel permeation column in order to avoid high retention times as observed when using an ion exchange column. The presence of bromide as the main species was confirmed in human urine samples. Bromate was also found be it in lower amounts compared that of bromide. The detection limit for bromine obtained with this coupling was 0.8 pg, which is sufficiently low for the determination of the bromine species in the urine samples. Besides the identification of bromide and bromate as the main bromine species in urine, an unknown bromine-containing compound was observed in these samples.

The interest for the application of HPLC-ICP-MS for speciation studies of bromine-containing pharmaceutical compounds is on the increase [77–79]. Studies of the possible metabolites of these drugs have been carried out with combined use of HPLC-ICP-MS and MS for the identification and characterization of all metabolites of those bromine-containing compounds. Abou-Shakra *et al.* [77] utilized HPLC-UV-ICP-MS and orthogonal acceleration TOFMS for the sequential detection and identification of metabolites of 4-bromoaniline in rat urine. Following the chromatographic separation and UV detection, the eluent was split, and the major portion of the eluent (90%) was infused directly into the ICP-MS detecting bromine and sulfur-containing metabolites. The remaining 10% of the eluent was introduced into the orthogonal acceleration TOFMS obtaining accurate mass spectral information for the identification of the metabolites. The main advantage of this type of coupling was the simultaneous identification of the bromine-containing metabolites and those that did not contain bromine. The identity of the major metabolite was confirmed to be a sulfate of a ring-hydroxylated metabolite. In addition, a number of peaks were identified as conjugated metabolites, including glucuronides, an *N*-oxanilic acid and an *N*-acetylcysteinyl conjugates.

In a different study, Marshall *et al.* [78] utilized the same techniques for the characterization and determination of bradykinin metabolites in human and rat urine. Bradykinin is a small peptide that acts mainly as a hormone by activating specific receptors that provide protection against the development of hypertension. The efficacy of bradykinin is affected by the activities of various kinases present in plasma and blood. The metabolic fate of bradykinin was measured by HPLC-ICP-MS and orthogonal acceleration TOFMS. The results obtained in that study showed marked differences in the metabolic mechanisms of bradykinin in human and rat plasma. Metabolism of bradykinin in rat plasma was much more aggressive than that observed in human plasma. The half-life of bromobradykinin incubated in

human plasma at 4 $\mu mol\,L^{-1}$ was calculated to be 3.8 times greater than that observed in rat plasma. Similarly, the half-life of bromobradykinin at 12.5 $\mu mol\,L^{-1}$ was 2.8 times greater in human plasma than in rat plasma. Additionally, the authors could identify new bradykinin metabolites in both rat and human plasma.

Another application of HPLC-ICP-MS and orthogonal acceleration TOFMS has been reported by Nicholson and coworkers [79]. In this case, the authors identified and determined metabolites of 2-bromo-4-trifluoromethylacetanilide in rat urine samples. A similar method described previously [77, 78] was utilized for simultaneously measuring the chromatographic eluent by UV, ICP-MS and TOFMS. The chromatographic separation of metabolites was done using a C_{18} column in the reversed-phase mode. The introduction of a helium–hydrogen mixture in the collision/reaction cell system of the ICP-MS permitted eliminating typical interferences produced by the molecular ions $ArAr^+$ and $ArArH^+$. The application of this technique permitted determining metabolites that were identified as sulfate and glucuronide conjugates of a ring hydroxyl-substituted metabolite, an *N*-sulfate, an *N*-hydroxylamine glucuronide and *N*-hydroxyglucuronides.

It can be concluded that in spite of the great importance of bromine in biological systems, the number of speciation studies is scarce. ICP-MS plays an important role in recent studies.

3.4 Developments in plasma spectrometry using bromine species

Many studies utilizing brominated species have been published (Table 2.24.2) [55–58, 80–82]. Most of these publications applied GC coupling to ICP-MS or MIP-AED to study and develop low power plasma sources. Among the different brominated species, the preferred were in general bromobenzene, dibromobenzene and bromoalkanes because of their high volatility and ease of separation. For example, Waggoner *et al*. [80] utilized a low power/reduced-pressure helium inductively coupled plasma (ICP) ionization source for the analysis of the brominated organo-compounds, bromobenzene, 1-bromoheptane and benzyl bromide. A plasma generator operated at 35 MHz and an estimated forward power of 12–15 W was used in that study. Characteristic fragments were obtained for each of the brominated compounds that increased the capabilities of low pressure/reduced pressure ICP-MS (LP/RP-ICP-MS) as a GC detector. Total elemental information was augmented because of this possibility of taking fragment spectra, thereby providing structural information. Absolute limits of detection for the brominated compounds were at the pg level.

In other recent instrumental developments, a GC system was coupled to plasma MS utilizing a microplasma ionization source for negative ion detection [56]. The ion source was kept inside the high vacuum chamber of the mass spectrometer and a rigid fused silica capillary tube contained the capacitively coupled radio frequency helium plasma. In an effort to obtain lower detection limits for halogens by MS, negative ion detection was studied. The halogen anion abundance was found to be largely affected by the power level, decreasing with an increase in the power value. Therefore, only 1–2 W of power were used, which was lower than the power levels of the optimum halogen signal in the positive ion detection mode (3–7 W). Bromine and halogens in general exhibited a 10-fold improvement of detection limits in the negative mode than in the positive mode. Detection limits in the range of 0.5 pg as Br were obtained.

Other applications to brominated compounds include GC-MIP-AES [82] and GC-LP-ICP-MS [55, 57, 80, 81]. Innovations have been directed to the design of new GC-plasma interfaces, use of low power plasmas to obtain structural molecular information of the surrounding chemical environment of the elements and the development of more sensitive and robust analytical methodologies.

4 SPECIATION ANALYSIS OF CHLORINE

4.1 Environmental studies of chlorinated compounds

The presence of halogenated substances in the natural environment has become an increasingly

contentious matter. Mounting public concern and recent heightened political awareness of environmental issues have arisen through the realization of the threat posed by chemicals to the quality of life. Industrial use of chlorine started shortly after the discovery of this element in 1744. The first interest was focused on the bleaching properties of chlorine. Relatively large quantities of elemental chlorine were also used in the manufacturing of artificial silk and as chlorine disinfection in the preparation of drinking water, particularly in the United States. The interwar period was also the time when many of the present organochlorine products were introduced. These products included solvents, grease-removers, dyestuffs, insecticides, fire-extinguishing liquids and anesthetics. Furthermore, an increasing fraction of the chlorine was used by the petrochemical industry to produce chloroorganic compounds, in particular, polyvinylchloride (PVC) and chlorinated solvents. In the last few years, strong efforts have been made to reduce the environmental load of chloroorganics, and consequently the production of chlorine is decreasing in both Europe and the United States.

During the last decade, polychlorinated dibenzo-p-dioxins and dibenzofurans (PCDDs and PCDFs) have received particular attention because of their extreme toxicity in certain bioassays. Although these compounds have not been intentionally produced and natural sources may exist, there is no doubt that the present levels in the environment primarily reflect human activities. This is demonstrated by the trends found in laminar lake sediments. DDT, PCBs, PCDDs and PCDFs are all semi-volatile, lipophilic organic compounds. Soil, sediments and the oceans represent the largest sinks of such compounds, and their vapor pressures are sufficiently high to allow substantial atmospheric transport. Volatile compounds, such as chlorofluorocarbons (CFCs), carbon tetrachloride, trichloroethene, tetrachloroethene and methyl chloroform are another group of industrially produced globally spread organohalogens. Measurable concentrations occur in the open sea but the large-scale distribution of these compounds are initially determined by atmospheric mixing within the northern and southern hemispheres and by the susceptibility of the different compounds to UV-induced reactions involving hydroxyl radicals [90, 91]. It is apparent that the anthropogenic contribution to the set of halogenated substances has had a major impact on the environment. However, this contribution should be measured against the background of natural abiotic and biotic production. An example of that is the biological contribution to atmospheric pollution by volatile halohydrocarbons. Natural organisms capable of metabolizing a wide range of haloaromatic and aliphatic substrates have been isolated to study mobility and conversion into other halogenated substances in the environment.

Analytical methodologies to determine chlorinated species in samples of environmental interest have involved, in most of the cases, the use of GC as high-efficiency separation technique coupled to different plasma MS detectors. A recent analytical approach for the determination of chlorinated VOCs has been proposed by Schwarz and Heumann [21]. The sequential detection of halogenated species was performed by using the GC-ECD-ICP-MS. The authors compared the detection limits obtained by using different detectors such as ECD, ICP-MS, MIP-AED and EI-MS. The best results were obtained with the ECD detector. A schematic diagram of the instrumental setup can be observed in Figure 2.24.2.

Halogenated VOCs have been determined by using GC-MIP-AES detection in seawater samples [23]. Chlorinated VOCs were studied among other kinds of halogenated compounds using a purge and trap preconcentration systems. Additionally, the effect of different scavenger gases on the MIP-AES detector was considered. It was found that oxygen was necessary to increase the sensitivity in the determination of chlorine. The monitoring of chlorine was performed at 479 nm. Detection limits were between 0.03 and 0.14 ng. A different approach has been proposed by Brede and coworkers [24]. Basically, a microplasma ion source was designed by locating a radio frequency plasma directly inside of the GC column. Detection limits obtained were at the low pg level. Analyte reactions with the silica of the GC column were

avoided by addition of hydrogen and oxygen to diminish peak tailing.

Correlations between halogenated compounds and total organic carbon concentrations have been observed in some surveys of surface water quality, indicating that halogenated species can be bound to one of the main groups of organic matter in the environment. The role of humic substances in the occurrence of halogenated substances in unpolluted waters has been verified by isolation of humic substances and determination of the organochlorine content of the fractions. The analysis of the structures requires sophisticated methods, and recently the first chlorinated structures in humic substances were identified [92]. Figure 2.24.7 shows the chlorinated aromatic structures that have been identified in naturally occurring aquatic fulvic acids after ethylation of the phenolic groups followed by oxidative degradation and methylation of the carboxylic acids. Moreover, brominated aromatic structures have been found in samples of marine origin [93]. The data showed that 10% of the aromatic rings in freshwater fulvic acid can be mono- or dichlorinated. Despite this progress, considerable work is necessary to determine the bonding of halogenated species in waters and the environment in general. Plasma detection for speciation of halogenated humic substances does not have extensive applications. Initial studies have investigated the molecular distribution of halogens in humic substances utilizing ICP-MS for SEC separation of the different molecular mass fractions [18, 19]. Characteristics of the fractionation profiles depended on the types of samples analyzed. Differences in the bonding of chlorine to high or low molecular mass fractions were observed. Chlorine was associated to a high molecular fraction in sewage water samples. The molecular mass of the chlorinated species monitored in groundwater samples was higher than that obtained from sewage samples. Additionally, aging studies demonstrated no influence of time on the fractionation profiles of chlorinated humic substances. Moreover, the effect of microbiological activity on the chlorine distribution in humic substances was studied, and the fractionation pattern did not vary even after eight weeks of storage in the presence of different microorganisms, including bacteria, yeast and fungi.

Another hot issue in environmental research comes from the presence of halogenated pesticides in different parts of the environment. Gas chromatography has been commonly used for the determination of halogenated pesticides. Plasma spectrometry sources have been utilized for GC eluent detection, and different instrumental approaches including GC-MIP-AES, GC-MIP-MS, GC-ICP-MS were used. A primary advantage in using GC with plasma detection is multielemental speciation analysis. Generally, the lowest detection limits for chlorine and other halogens

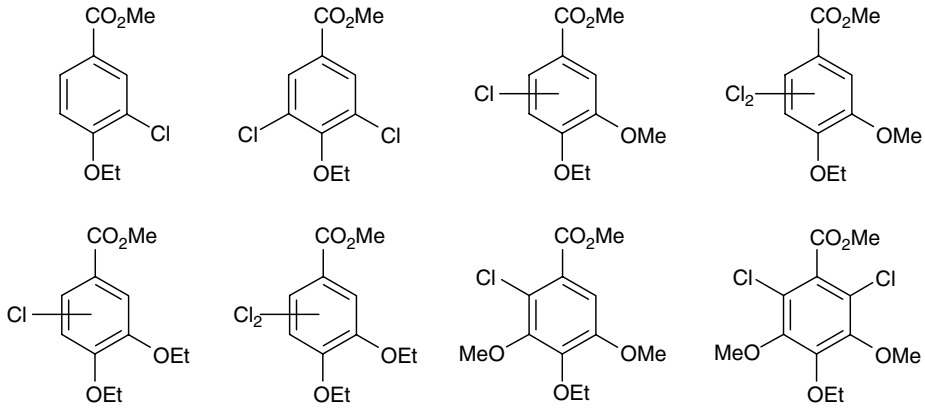

Figure 2.24.7. Chlorinated aromatic compounds identified in both naturally occurring fulvic acids and organic matter of bleached-kraft mill effluents after ethylation of phenolic groups, followed by oxidative degradation with permanganate and hydrogen peroxide and finally methylation of formed carboxylic acids.

have been obtained when MIP-AES was used as a GC detector. However, good figures of merit can be obtained with ICP-MS. For example, Zapata and Robbat [94] obtained better stability with GC-MIP-MS by optimizing power transfer to the cavity using a tunable coaxial microwave-induced plasma (MIP). The MIP was operated at atmospheric pressure with 30 mL/min He and 60 W of power. Detection limits were between 3 and 19 pg of Cl, seven times lower than the detection limits obtained with the nontunable MIP-MS. Analysis of pesticides containing sulfur atoms was also possible by placing the GC column at the plasma expansion stage. Molecular fragmentation of a mixture of volatile organic compounds was also observed. Determination of 16 organochlorine pesticides in a petroleum-contaminated reference soil was possible using the GC-MIP-MS system (Figure 2.24.8). Coupling of GC to MIP-MS has been also used for the analysis of 15 different halogenated pesticides present in the United States EPA method 505 mixture #1 [74]. Additionally, different PCBs were determined in that study. Chlorine was monitored utilizing the m/z 37 isotope. Polluted ground water samples were also analyzed and the presence of major chlorinated pollutants was confirmed. Polychlorinated biphenyl ethers have been determined using GC-RFP-AED in chimney soot samples [75]. Detection limits on the order of 1–5 pg were obtained in that study.

A summary of the different applications of hyphenated techniques that involve the use of plasma sources is detailed in Table 2.24.3.

4.2 The importance of chlorine speciation in biological and related samples

Diverse application of hyphenated techniques can be found concerning the presence of chlorinated compounds in biological systems. Recently, the application of HPLC-ICP-MS for the study of diclofenac and chlorpromazine has been reported [95]. Diclofenac is a nonsteroidal antiinflammatory drug, possessing two chlorine substituents, while chlorpromazine is an antipsychotic drug with two chlorine atoms in its structure. The study was an introduction to a larger study of the metabolism of pharmaceutical compounds in biological samples. The chromatographic separation was performed

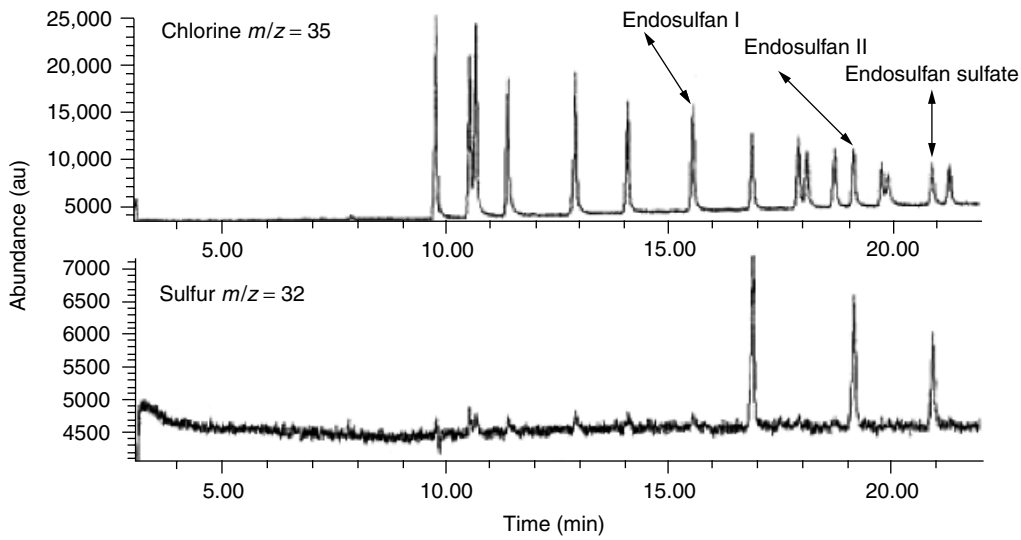

Figure 2.24.8. (a) GC/MS total ion current chromatogram. (b) GC-MIP-MS 35Cl chromatogram. The contaminated reference soil (IRM-105, Ultra Scientific) contained 8 chlorinated pesticides, 17 polycyclic aromatic hydrocarbons, pentachlorophenol, carbazole and dibenzofuran as well as an unknown mixture of petroleum contaminants. (Reprinted with permission from [94]. Copyright (2000) American Chemical Society.)

Table 2.24.3. Summary of publications related to chlorine speciation using plasma spectrometry detection.

Year	Sample	Species	Analytical technique	Detection limit	Comments	Ref.
	Environmental samples					
2002	Seawater	CH_2BrCl; $CHBrCl_2$; CH_2ClI; 1,2-C_2H_4BrCl; 2,1-C_3H_6BrCl; $CHBr_2Cl$; 1,3-C_3H_6BrCl	GC-ECD-ICP-MS	50 pg as Cl	Comparison of different detectors for the GC separation. The lowest detection limits were obtained with ECD.	21
2000	Sewage wastewater	HS/Cl species	SEC-ICP-MS	–	No changes were observed on molecular mass distribution when microbial activity in presence of chlorine was assayed, even after 8 weeks.	19
2000	Petroleum-contaminated reference soil	Endosulfan I; dieldrin; 4,4′-DDE; endrin; endosulfan II; 4,4′-DDD; 4,4′-DDT	GC-MIP-MS	30–190 pg as Cl	Molecular fragmentation of a mixture of VOCs was demonstrated by placing the GC column at the plasma expansion stage.	94
1999	Seawater	CH_2BrCl; 1,2-$C_2H_4Cl_2$; C_2HCl_3; $CHBrCl_2$; C_2H_4BrCl; C_2Cl_4; $CHBr_2Cl$	GC-MIP-AES	0.03–0.12 ng as Cl	Determination of coeluting halogenated alkanes using AES and ECD.	23
1998	North sea crude oil; sludge from nickel refinery	1,3,5-trichlorobenzene	GC-MP-MS	9.7 pg as Cl	An alternative ionization source to CI and EI is presented in this work.	24
1997	Groundwater; seepage water from soil; brown water	HS/Cl species	SEC-ICP-MS	–	Chlorine interacted with single peak high molecular mass fraction.	18
1997	Polluted ground water; pesticide mixture	PCBs; 15 chlorinated pesticides	GC-MIP-MS	1 ng as Cl	The design and application of the GC-MIP interface is comparatively simpler than the GC-ICP-MS one.	74
1997	Crude oil; chimney soot	Polychlorinated biphenyls	GC-RFP-AES	1–5 pg as Cl	The detection proved to be nonstructure-dependent. Arochlor 1260 was analyzed in this work.	75
1993	Supelco pesticide mixture	Chlorotoluene; chloronaphthalene	GC-RP-MIP-MS	2–10 pg as Cl	The systems presented good sensitivity for the determination of phosphorus, sulfur, chlorine and bromine in GC eluates.	59
	Biological samples					
2002	Pharmaceuticals products	Diclofenac; chlorpromazine	HPLC-ICP-MS	–	Reversed-phase chromatography (65 : 35 0.05% formic acid in H_2O/MeOH mobile phase and a C_2 column) was applied in the separative step of the analysis.	95

(*continued overleaf*)

Table 2.24.3. (*continued*)

Year	Sample	Species	Analytical technique	Detection limit	Comments	Ref.
2000	Human blood serum	Halogenated proteins	HPLC-ICP-MS	–	Chlorine showed a single peak in the small-molecule zone, which corresponded to a 35.5 kDa fraction.	48
2000	Rat urine	Diclofenac	HPLC/UV/ICP-MS/TOFMS	–	Metabolites of diclofenac drug were identified by using a simultaneous UV/ICP-MS/TOFMS detection.	96
1995	Freshwater fish; Cow bioptic fat	PCB 28; PCB 52; PCB 101; PCB 118; PCB 153; PCB 138; PCB 180	GC-MIP-AED	0.54 pg as Cl	Seven 'indicator' PCBs in biotic matrices were evaluated. Detection of chlorine was performed at 479 nm.	97
1992	Human urine	Cl^-; ClO_3^-	HPLC-ICP-MS	36 ng	Inorganic chloride was the only species present in human urine samples.	43
	Plasma studies					
2000		Hexachloroethane	GC-MP-MS	0.35 pg as Cl	The mechanisms of negative ion formation and breakdown were discussed.	56
2000		1-chloropentane; 1-chlorohexane; 1-chloroheptane; 1-chlorooctane; 1-chlorononane; 1-chlorodecane; chloroform	GSGD-GC-ICP-TOF-MS	5–24 pg	The elemental ratio ($^{35}Cl/^{12}C$) permitted to differentiate several chlorinated hydrocarbons.	55
1997		Chlorobenzene	GC-LP-ICP-MS	100 pg	Addition of nitrogen increased plasma stability and improved the detection limits of chlorobenzene molecular fragments.	57
1994		Trichlorobenzene	GC-RFP-AED	1.1 pg as Cl	Suppression of peak tailing and creation of high selectivity as well as repeatability by doping the RFP with oxygen.	58

with isocratic elution of the compounds using a 65 : 35 formic acid in H_2O/methanol solution as the mobile phase. Additionally, the effect of a solvent (methanol) gradient in the mobile phase was studied on the sensitivity of ICP-MS. No variation of the ^{35}Cl signal was observed when the methanol concentration was increased up to 50% (v/v) in the mobile phase. Chlorine was determined using the m/z 37 isotope. In a different study, determination and characterization of diclofenac metabolites in rat urine was reported by Corcoran and coworkers [96]. In that work, the authors utilized the application of HPLC coupled to ICP-MS and orthogonal acceleration TOFMS. The metabolites were separated by reversed-phase chromatography using UV monitoring, after which 90% of the eluent was introduced into the ICP-MS. The remaining 10% was directed to the orthogonal acceleration TOFMS. Information of the metabolites containing ^{35}Cl, ^{37}Cl and ^{32}S was obtained by specific detection with ICP-MS and identification by TOFMS. The metabolites detected and characterized were glucuronic acid and sulfate conjugates, mono- and dihydroxylated and free diclofenac. An *in vivo* metabolite of diclofenac, an *N*-acetylcysteinyl conjugate, was additionally characterized. The first application of this powerful hyphenated technique for the investigation of the

metabolic fate of chlorinated xenobiotics was reported in that paper.

The total concentrations of some trace elements in blood serum are considered important in medical diagnostics. Chemical species of trace elements are generally divided into two groups. The first category corresponds to protein-associated species, which play an important role in enzymatic activities, transportation and storage of elements in biological systems. The second one refers to nonprotein-associated species related to membrane transport or excretion of the elements. Determination of chlorine associated to different molecular mass fractions in human blood serum has been developed [48]. Fractionation of the chlorinated species was done using surfactant-mediated HPLC-ICP-MS. In this case, an octadecyl silane (C18) column dynamically coated with 3-[(3-cholamidopropyl) dimethylammonium]-1-propanesulfonate (CHAPS), zwitterionic bile acid derivative was utilized for the separation. A single peak fractionation profile was obtained for chlorine in human blood serum samples. Chlorine was found to be present as free chloride in the small-molecule zone (35.5 Da) of the chromatographic profile. However, retention times for Cl and other halogens were different because of ion-pair interactions between these elements and alkali and alkaline earth ions present initially in the sample.

Plasma source detection after GC separation of the chlorinated species has also been utilized for the determination of pollutants in biological samples. The aim was to achieve a better understanding of the toxicological mechanisms and metabolization pathways of this element in biological systems. The application of GC-MIP-AED has been documented by Hajslova *et al*. [97] for the determination of PCBs in biota. Basic parameters associated with the practical application of GC coupled to MIP-AED in the determination of seven 'indicator' PCBs were evaluated. The detection limits for chlorine was found to be 0.54 pg. The application to determine chlorinated pesticides and PCBs in synthetic samples and fat from animal origin was also shown in this study. The main advantage was the high selectivity obtained in the determination of chlorinated pesticides and PCBs as can be seen in Figure 2.24.9.

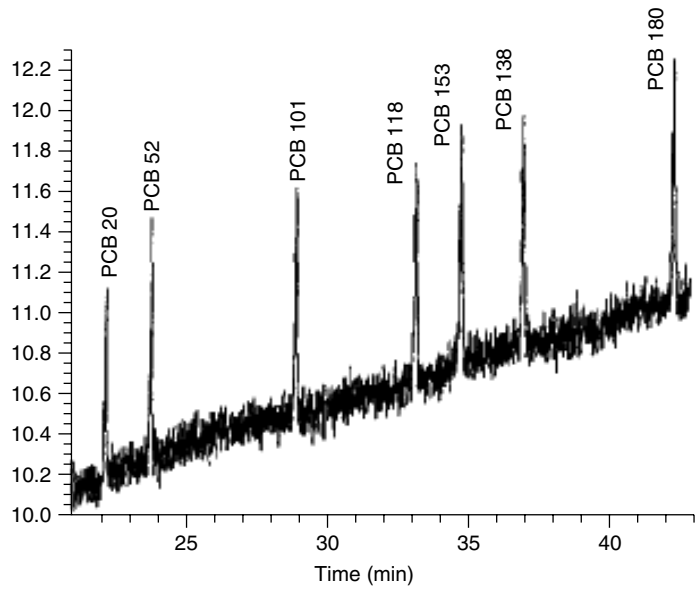

Figure 2.24.9. Chromatogram of seven indicator congeners obtained by GC-MIP-AED; 0.5 ng of each analyte injected. (Reprinted from determination of polychlorinated biphenyls in biotic matrices using gas chromatography-microwave-induced plasma atomic emission spectrometry, *J. Chromatogr. A*, **699**, Hajslova, J., Cuhra, P., Kempny, M., Poustka, J., Holadova, K. and Kocourek, V., 231–239 (1995), with permission from Elsevier.)

4.3 Determination of chlorine species in food samples

It is well known that determination of chlorine in food is of high importance. However, no recent publications on chlorine speciation in foods could be found in the literature. It may be because the overall high concentration levels of chlorine found in most matrices gave no incentive to develop methods with high sensitivity. In fact, chlorine is commonly determined by traditional precipitation methods that are relatively inexpensive.

4.4 Developments in plasma spectrometry using chlorine species

In Table 2.24.3, examples of chlorine species to perform plasma studies are shown. Most of the recent studies were described above [55–58]. Generally, halogenated compounds, particularly halogenated alkanes and aromatics, have been used because of their elevated volatility and easy separation by GC. Different plasma source detectors have been tested in order to obtain the best figures of merit for the determination of chlorinated compounds. The primary problem with some halogens by Ar ICP is the high ionization potentials. Consequently, MIP-AES is preferred for Cl. Halogenated compounds have been employed to study the effect of different optional gases, commonly known as *scavenger gases*, to increase the elemental ionization in plasmas and improve the sensitivity for the determination of chlorine.

5 SPECIATION ANALYSIS OF FLUORINE

5.1 Environmental interest in the determination of fluorine species

The presence of fluorine in the environment has received increasing attention in the last decade. Fluorine in the environment is mostly related to anthropogenic activities from applications of fluorine in manufacturing. A typical example is the presence of chlorofluorocarbons (CFCs) in the atmosphere. Prior to the 1930s, the common compounds used as refrigerants were ammonia, chloromethane, carbon tetrachloride, isobutane and propane. Concerns about their toxicity and flammability, particularly at home, led to chlorofluorocarbons as replacements.

Anthropogenic organofluorine compounds are widespread because of their application as refrigerants, propellants, agrochemicals, surfactants and lubricants. On the other hand, naturally produced organofluorine compounds are rare, even considering that fluorine is the most abundant halogen and the 13th most abundant element in the earth's crust. Only six different biologically produced organofluorine compounds have been identified in plant species growing mainly in tropical and semitropical regions and in two bacteria [98]. Natural organofluorine compounds that are formed abiotically have also been described, for example, CF_4 and CFCs in igneous and metamorphic rocks. The increasing interest in natural organofluorine compounds arises from some fundamental differences in the chemistry of fluorine. Fluorine has a relatively low bioavailability compared with the other halogens, since it is bound in a largely insoluble form, thus the concentration of fluoride in seawater (1.3 $mg\,L^{-1}$) is several orders of magnitude lower than that of chloride (19,000 $mg\,L^{-1}$). Additionally, because of its high hydration energy, the fluoride ion is a poor nucleophile in aqueous solution limiting its participation in displacement reactions. Finally, fluorine is not incorporated into organic compounds via the haloperoxidase reaction since the redox potential required for the oxidation of fluoride is much greater than that for the reduction of hydrogen peroxide. Consequently, the bonding of fluorine to carbon in a biological system is of considerable interest.

In spite of the great interest that fluorine has for environmental studies, the number of analytical methodologies for fluorine speciation analysis is scarce (Table 2.24.4). Because of the high ionization potential, F is readily ionized only in He plasmas. Brede *et al.* [24] developed a technique using GC-MP-MS for the determination of fluorine species present in crude oil samples.

Table 2.24.4. Summary of publications related to fluorine speciation using plasma spectrometry detection.

Year	Sample	Species	Analytical technique	Detection limit	Comments	Ref.
	Environmental samples					
2002	Coals	Fluoride	HPLC-ICP-MS	1 $mg\,kg^{-1}$	Use of ion-exchange chromatography to separate different halogens (Br, I, Cl and F).	99
1998	North sea crude oil	1-fluoronaphthalene	GC-MP-MS	6.1 pg as F	Difficulties in the selective determination of F were observed when the m/z 19 isotope was utilized.	24
	Biological samples					
1996	Leaves; milk powder; oyster tissue	Fluoride	HPLC-ICP-MS	100 $ng\,mL^{-1}$	Pyrohydrolysis of the samples and collection of the volatilized halogens in a receiver solution prior to analysis.	100
1983	Rat blood plasma	Metabolites of 2-(Heptadecafluoro-octyl)ethanol	GC-MIP-AES	–	An MIP-AES was interfaced to GC utilizing a dual column system resulting in parallel detection using FID or ECD to MIP-AES detection.	101
	Plasma studies					
2000		1-fluoronaphthalene	GC-MP-MS	12 pg as F	The interference at m/z 19 (H_3O^+) in the positive detection mode was diminished by using the negative mode.	56
1994		Trifluoronitrotoluene	GC-RFP-AED	13 pg as F	A $H_2 + O_2$ mixture was found to be efficient to avoid peak tailing for fluorine.	58
1994		Fluoroethers	GC-MIP-AED	0.82 ng as F	Fluorine and oxygen were simultaneously monitored in the plasma at 775 nm and 777 nm emission lines, respectively.	102

The microplasma ion source was a radio frequency plasma contained inside the last 4–5 cm of a 0.32-mm i.d. fused silica capillary column. Difficulties in the selective determination of F were observed since this is a monoisotopic element (m/z at 19) and H_3O^+ ion interference also occurred. Similar interference problems were observed by introducing a minimal amount (20 ng) of hydrocarbon compound (n-decane), since H_3O^+ was formed as well. The background signal was significantly reduced by increasing the power applied to the plasma. In spite of these problems, the detection limit for fluorine is 6.1 pg as 1-fluoronaphthalene. Matrix effects in the crude oil samples were studied by fortification with 1-fluoronaphthalene species.

5.2 Fluorine species in biological samples

In the early 1970s, experiments performed on mice indicated that low-fluoride diets (as low as 5 $ng\,g^{-1}$) compared to those supplemented with 50 $mg\,mL^{-1}$ of fluorinated drinking water showed anemia and infertility in mice [30]. Subsequently, it was found that these results were obtained with diets that were

iron-deficient and that high dietary fluoride could improve iron absorption or utilization. Therefore, mice fed with low-fluoride diets that contained sufficient iron did not exhibit anemia or infertility. Additionally, it has been observed that a relatively high fluoride supplement (2.5 to 7.5 mg g^{-1} diet) slightly improved the growth of rats fed with 0.04 to 0.46 mg g^{-1} F diet. Because the diet used in this study did not give optimal growth in rats, this effect was suggested as a result of a pharmacological effect of fluoride. High or pharmacological amounts of fluoride also depress lipid absorption, alleviate nephrocalcinosis induced by phosphorus feeding, alter soft tissue calcification caused by magnesium deprivation and perhaps prevent bone loss leading to osteoporosis [30]. A recent study indicated that a fluoride deficiency in goats, less than 0.3 mg kg^{-1} diet, decreases life expectancy and caused pathological histology in the kidney and endocrine organs. These findings should be confirmed with studies on nonruminant species before being accepted as evidence of essentiality for those animals. In general, fluoride is not considered as an essential element for humans. However, it still is considered a beneficial element because of its ability to protect against pathological demineralization of calcified tissues. In the United States, estimated safe and adequate daily dietary intakes (ESADDI) have been established for fluoride; infants aged 0 to 0.5 years: 0.1 to 0.5 mg and infants aged 0.5 to 1 years: 0.2 to 1.0 mg; children aged 1 to 3 years: 0.5 to 1.5 mg; children aged 4 to 6 years: 1.0 to 2.5 mg; children or adolescents aged 7 years and older: 1.5 to 2.5 mg and adults: 1.5 to 4.0 mg. These ESADDIs are based on amounts that will give protection against dental caries and do not generally result in any consequential mottling of teeth. Thus, the ESADDIs are much higher than any postulated need for fluoride to have an essential role, as such a need would most likely be much less than 1.0 mg per day [30].

Although considering the increasing importance of fluorine, the number of analytical methodologies for the determination of fluorine species in biological samples is scarce. Some of the few studies about fluorine speciation have not yet been reported. They will be discussed later in this chapter because of the importance of F determinations. For example, a method for determining iodine, bromine, chlorine and fluorine in geological and biological materials was described by Schnetger and coworkers [100]. The solid material was heated to 1100 °C under a wet oxygen flow. By this process, the halogens were released from the matrix and collected in a receiver solution. The following analysis of the fluorine content as fluoride was done utilizing HPLC coupled to ICP-MS. Fluorine content was determined in leaves, milk powder and marine tissue. Detection limits obtained for fluorine were typically in the mg kg^{-1} region. The separation of the halogen species was accomplished by ion-exchange chromatography of the anions in solution.

A different application for fluorine speciation was reported by Hagen and colleagues [101]. In this case, GC-MIP-AES was applied for the separation and determination of fluorine-containing metabolites in rat blood plasma samples. Metabolites of 2-(heptadecafluorooctyl)ethanol were determined utilizing reduced-pressure helium MIP-AES interfaced to a capillary GC column with a dual column system resulting in parallel detection by flame ionization detection (FID) or ECD. This system was also applied to the detection and quantitation of perfluorooctanoate in human blood plasma resulting from an industrial exposure to this compound. The use of MIP-AES element-specific detection permitted understanding the complicated ECD and FID chromatograms and allowed a straightforward quantitation of perfluorooctanoate. High inorganic fluoride levels in rat plasma and the presence of perfluorooctanoate confirmed that metabolic defluorination of the original alcohol occurred.

In the study developed by Brede *et al*., the ion source was kept inside the high vacuum chamber of the mass spectrometer [56]. The interference at m/z 19 was clearly present in the positive ion background mass spectrum. On the other hand, in the negative mode the same mass region contained less background ions and none at m/z 19. Actually, the whole negative background spectrum had ions only at m/z 1, 16, 17 and 32, which were assigned to H^-, O^-, OH^- and O_2^-, respectively (Figure 2.24.10). Considering

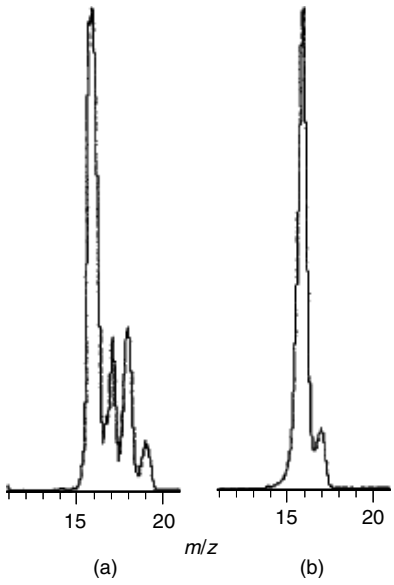

Figure 2.24.10. Background mass spectra (m/z 11–21) of the microplasma in (a) positive mode and (b) negative mode. (Reproduced from Reference [56] by permission of The Royal Society of Chemistry.)

these results, the authors applied negative ion detection to achieve a higher selectivity for fluorine determination in the presence of hydrocarbons and trying at the same time to increase the sensitivity of the determination of the halogens. In fact, some other studies have indicated that higher signal-to-noise ratios for fluorine and chlorine can be achieved when negative ionization is utilized [103]. Additionally, the effect of optional gases on the fluorine sensitivity was evaluated. It was observed that oxygen addition to the plasma enhanced the sensitivity that was attributed to a charge transfer mechanism for halogen anion formation by reaction with O^-. The addition of hydrogen to oxygen increased the fluorine signal probably as a result of the introduction of H^- ions, donating electrons in a charge transfer process.

6 CONCLUSIONS

The constant evolution of speciation techniques has permitted the speciation analysis of halogens and halogen-containing compounds in samples from different origins including, environmental, biological pharmacological, nutritional and food. The advances and design of more sensitive plasma spectrometers with particular devices such as reaction/collision cells have permitted the development of new analytical methodologies to determine halogens from gaseous samples utilizing GC as the sample introduction device and progressing to techniques such as LC or even CE.

A variety of analyte types, such as VOCs, pesticides, metabolites, and so on, can be determined. Moreover, several publications have demonstrated the applicability of speciation techniques as a tool for the analysis of drug metabolites, which are of high importance in pharmacological and toxicological areas. Additionally, the increasing number of studies about natural bio-accumulative substances, such as humic substances, renders the evaluation of the bioaccumulation of halogens an almost common analytical task.

7 FUTURE ANALYTICAL DEVELOPMENTS IN SPECIATION OF HALOGENS

Future advances in the speciation analysis of halogens will evolve together with the more sophisticated plasma spectrometers, which will not only permit the determination of halogens at lower concentration levels but also enable fast and simple analyses. The intrinsic importance of these halogenated species together with the improved analytical technology will result in a vast array of applications in environmental and biological sciences. The speciation of anthropogenic contaminants, such as FR, pesticides, PCBs, and so on, has been of great concern to evaluate environmental pollution and regulate their uses. Also, it is important to point out the applicability of speciation studies to food and biological samples to know their bioavailability and mechanism of action.

8 REFERENCES

1. Moran, J. E., Oktay, S. D. and Santschi, P. H., *Water Resour. Res.*, **38**, 1149 (2002).
2. Andersen, S., Petersen, S. B. and Laurberg, P., *Eur. J. Endocrinol.*, **147**, 663 (2002).

3. Wong, G. T. F. and Cheng, X. H., *Mar. Chem.*, **74**, 53 (2001).
4. Wong, G. T. F. and Cheng, X. H., *J. Environ. Monit.*, **3**, 257 (2001).
5. Yamada, H., Sugahara, M., Kosaka, H., Katayama, A., Takahashi, K. and Yonebayashi, K., *Soil Sci. Plant Nutr.*, **42**, 367 (1996).
6. Stipanicev, V. and Branica, M., *Sci. Total Environ.*, **182**, 1 (1996).
7. Fordyce, F. M., Johnson, C. C., Navaratna, U. R. B., Appleton, J. D. and Dissanayake, C. B., *Sci. Total Environ.*, **263**, 127 (2000).
8. Wong, G. T. F. and Cheng, X. H., *Mar. Chem.*, **59**, 271 (1998).
9. Luther, G. W. and Campbell, T., *Deep Sea Res. Part I Oceanogr. Res. Pap.*, **38**, S875 (1991).
10. Nakahara, T., Yamada, S. and Wasa, T., *Appl. Spectrosc.*, **45**, 1561 (1991).
11. Woittiez, J. R. W., Vandersloot, H. A., Wals, G. D., Nieuwendijk, B. J. T. and Zonderhuis, J., *Mar. Chem.*, **34**, 247 (1991).
12. Arafa, E. A., Beshewa, F. H., Saleh, A. I. and Das, H. A., *J. Trace Microprobe Tech.*, **18**, 137 (2000).
13. Zareba, G., Cernichiari, E., Goldsmith, L. A. and Clarkson, T. W., *Environ. Health Perspect.*, **103**, 1032 (1995).
14. Takaku, Y., Shimamura, T., Masuda, K. and Igarashi, Y., *Anal. Sci.*, **11**, 823 (1995).
15. Whitehead, D. C., *Environ. Int.*, **10**, 321 (1984).
16. Heumann, K. G., Rottmann, L. and Vogl, J., *J. Anal. At. Spectrom.*, **9**, 1351 (1994).
17. Radlinger, G. and Heumann, K. G., *Environ. Sci. Technol.*, **34**, 3932 (2000).
18. Radlinger, G. and Heumann, K. G., *Fresenius' J. Anal. Chem.*, **359**, 430 (1997).
19. Heumann, K. G., Radlinger, G., Erbes, M., Heiber, I., Obst, U., Filip, Z. and Claus, H., *Acta Hydroch. Hydrob.*, **28**, 193 (2000).
20. Wuilloud, R. G., Wuilloud, J. C. A., Vonderheide, A. P. and Caruso, J. A., *J. Anal. At. Spectrom.*, **18**, 1119 (2003).
21. Schwarz, A. and Heumann, K. G., *Anal Bioanal Chem*, **374**, 212 (2002).
22. Gruter, U. M., Kresimon, J. and Hirner, A. V., *Fresenius' J. Anal. Chem.*, **368**, 67 (2000).
23. Slaets, S., Laturnus, F. and Adams, F. C., *Fresenius' J. Anal. Chem.*, **364**, 133 (1999).
24. Brede, C., Lundanes, E., Greibrokk, Y. and Pedersen-Bjergaard, S., *J. High Resolut. Chromatogr.*, **21**, 633 (1998).
25. Fina, L. G., Hassouna, N., Horacek, G. L., Lambert, J. P. and Lambert, J. L., *Appl. Environ. Microbiol.*, **44**, 1370 (1982).
26. Fina, L. G. and Lambert, J. L., *Int. Water Res. Assoc.*, **2**, 53 (1975).
27. Means, E. G. and Krasner, S. W., *J. Am. Water Works Assoc.*, **85**, 68 (1993).
28. Dietrich, A. M., Mirlohi, S., DaCosta, W. F., Dodd, J. P., Sauer, R., Homan, M. and Schultz, J., *Water Sci. Technol.*, **40**, 45 (1999).
29. March, J., *Advanced Organic Chemistry*, 2nd ed., McGraw-Hill, New York, 1977.
30. Nielsen, F. H., *J. Trace Elem. Exp. Med.*, **11**, 251 (1998).
31. Arthur, J. R., *Proc. Nutr. Soc.*, **58**, 507 (1999).
32. Angeles-Agdeppa, I., *Asia Pac J Clin Nutr*, **11**, S335 (2002).
33. Ali, O., *Nutrition*, **11**, 517 (1995).
34. Abdulla, M., Reis, M. F., Schutz, A., Dashti, H. and Al-Mosawi, M., *J. Trace Elem. Exp. Med.*, **11**, 197 (1998).
35. Bhan, M. K., Sommerfelt, H. and Strand, T., *Br. J. Nutr.*, **85**, S199 (2001).
36. Bratter, P., Blasco, I. N., de Bratter, V. E. N. and Raab, A., *Analyst*, **123**, 821 (1998).
37. Chandra, R. K., *Am. J. Clin. Nutr.*, **66**, S460 (1997).
38. Martino, F. A. R., Sanchez, M. L. F. and Medel, A. S., *J. Anal. At. Spectrom.*, **17**, 1271 (2002).
39. Leiterer, M., Truckenbrodt, D. and Franke, K., *Eur. Food Res. Technol.*, **213**, 150 (2001).
40. Sanchez, L. F. and Szpunar, J., *J. Anal. At. Spectrom.*, **14**, 1697 (1999).
41. Anderson, K. A. and Markowski, P., *J. AOAC Int.*, **83**, 225 (2000).
42. Anderson, K. A., Casey, B., Diaz, E., Markowski, P. and Wright, B., *J. AOAC Int.*, **79**, 751 (1996).
43. Salov, V. V., Yoshinaga, J., Shibata, Y. and Morita, M., *Anal. Chem.*, **64**, 2425 (1992).
44. Wind, M., Eisenmenger, A. and Lehmann, W. D., *J. Anal. At. Spectrom.*, **17**, 21 (2002).
45. Simon, R., Tietge, J. E., Michalke, B., Degitz, S. and Schramm, K. W., *Anal. Bioanal. Chem.*, **372**, 481 (2002).
46. Axelsson, B. O., Jornten-Karlsson, M., Michelsen, P. and Abou-Shakra, F., *Rapid Commun. Mass Spectrom.*, **15**, 375 (2001).
47. Simon, R., Michalke, B. and Schramm, K. W., *Organohalogen compd.*, **52**, 120 (2001).
48. Inagaki, K., Umemura, T., Matsuura, H. and Haraguchi, H., *Anal. Sci.*, **16**, 787 (2000).
49. Michalke, B., Schramel, P. and Witte, H., *Biol. Trace Elem. Res.*, **78**, 67 (2000).
50. Michalke, B., Schramel, P. and Witte, H., *Biol. Trace Elem. Res.*, **78**, 81 (2000).
51. Michalke, B., *J. Anal. At. Spectrom.*, **14**, 1297 (1999).
52. Michalke, B. and Schramel, P., *Electrophoresis*, **20**, 2547 (1999).
53. Stark, H. J., Mattusch, J., Wennrich, R. and Mroczek, A., *Fresenius' J. Anal. Chem.*, **359**, 371 (1997).
54. Takatera, K. and Watanabe, T., *Anal. Chem.*, **65**, 759 (1993).
55. Guzowski, J. P. and Hieftje, G. M., *Anal. Chem.*, **72**, 3812 (2000).

56. Brede, C., Pedersen-Bjergaard, S., Lundanes, E. and Greibrokk, T., *J. Anal. At. Spectrom.*, **15**, 55 (2000).
57. Oconnor, G., Ebdon, L. and Evans, E. H., *J. Anal. At. Spectrom.*, **12**, 1263 (1997).
58. Pedersen-Bjergaard, S. and Greibrokk, T., *J. Microcolumn Sep.*, **6**, 11 (1994).
59. Story, W. C. and Caruso, J. A., *J. Anal. At. Spectrom.*, **8**, 571 (1993).
60. Creed, J. T., Davidson, T. M., Shen, W. L. and Caruso, J. A., *J. Anal. At. Spectrom.*, **5**, 109 (1990).
61. Heitkemper, D., Creed, J. and Caruso, J. A., *J. Chromatogr. Sci.*, **28**, 175 (1990).
62. Mohamad, A. H., Creed, J. T., Davidson, T. M. and Caruso, J. A., *Appl. Spectrosc.*, **43**, 1127 (1989).
63. Zhang, L. M., Carnahan, J. W., Winans, R. E. and Neill, P. H., *Anal. Chem.*, **61**, 895 (1989).
64. Chong, N. S. and Houk, R. S., *Appl. Spectrosc.*, **41**, 66 (1987).
65. van Dalen, J. P. J., de Lezenne Coulander, P. A. and de Galan, L., *Anal. Chim. Acta*, **94**, 1 (1977).
66. Bache, C. A. and Lisk, D. J., *Anal. Chem.*, **39**, 786 (1967).
67. Cicerone, R. J., Heidt, L. E. and Pollock, W. H., *J. Geophys. Res.-Atmos.*, **93**, 3745 (1988).
68. Schall, C., Laturnus, F. and Heumann, K. G., *Chemosphere*, **28**, 1315 (1994).
69. Wagner, T., Leue, C., Wenig, M., Pfeilsticker, K. and Platt, U., *J. Geophys. Res.-Atmos.*, **106**, 24225 (2001).
70. Vonderheide, A. P., Montes-Bayon, M. and Caruso, J. A., *J. Anal. At. Spectrom.*, **17**, 1480 (2002).
71. Seubert, A., Schminke, G., Nowak, M., Ahrer, W. and Buchberger, W., *J. Chromatogr. A*, **884**, 191 (2000).
72. Hardas, N. R., Adam, R. and Uden, P. C., *J. Chromatogr. A*, **844**, 249 (1999).
73. Pantsar-Kallio, M. and Manninen, P. K. G., *Int. J. Environ. Anal. Chem.*, **75**, 43 (1999).
74. Read, P., Beere, H., Ebdon, L., Leizers, M., Hetheridge, M. and Rowland, S., *Org. Geochem.*, **26**, 11 (1997).
75. Asp, T. N., Pedersen-Bjergaard, S. and Greibrokk, T., *J. High Resolut. Chromatogr.*, **20**, 201 (1997).
76. Baumann, H. and Heumann, K. G., *Fresenius' Z. Anal. Chem.*, **327**, 186 (1987).
77. Abou-Shakra, F. R., Sage, A. B., Castro-Perez, J., Nicholson, J. K., Lindon, J. C., Scarfe, G. B. and Wilson, I. D., *Chromatographia*, **55**, S9 (2002).
78. Marshall, P., Heudi, O., McKeown, S., Amour, A. and Abou-Shakra, F., *Rapid Commun. Mass Spectrom.*, **16**, 220 (2002).
79. Nicholson, J. K., Lindon, J. C., Scarfe, G. B., Wilson, I. D., Abou-Shakra, F., Sage, A. B. and Castro-Perez, J., *Anal. Chem.*, **73**, 1491 (2001).
80. Waggoner, J. W., Milstein, L. S., Belkin, M., Sutton, K. L., Caruso, J. A. and Fannin, H. B., *J. Anal. At. Spectrom.*, **15**, 13 (2000).
81. Evans, E. H. and Caruso, J. A., *J. Anal. At. Spectrom.*, **8**, 427 (1993).
82. Abdillahi, M. M., *J. Chromatogr. Sci.*, **28**, 613 (1990).
83. Hardy, M. L., *Chemosphere*, **46**, 717 (2002).
84. Hardy, M. L., *Chemosphere*, **46**, 757 (2002).
85. Hardy, M. L. and Smith, R. L., *Abstr. Pap. Am. Chem. Soc.*, **217**, 253-ENVR (1999).
86. Hardy, M. L., *Abstr. Pap. Am. Chem. Soc.*, **208**, 91-PMSE (1994).
87. Eriksson, P., Jakobsson, E. and Fredriksson, A., *Environ. Health Perspect.*, **109**, 903 (2001).
88. Zhou, T., Ross, D. G., DeVito, M. J. and Crofton, K. M., *Toxicol. Sci.*, **61**, 76 (2001).
89. McDonald, T. A., *Chemosphere*, **46**, 745 (2002).
90. Grimvall, A., Evidence of naturally produced and man-made organohalogens in water and sediments, in *Naturally-Produced Organohalogens*, Grimvall, A. and de Leer, E. W. B. (Eds.), Kluwer Academic Publishers, 1995.
91. Grimvall, A., Boren, H. and Asplund, G., *Abstr. Pap. Am. Chem. Soc.*, **199**, 170-ENVR (1990).
92. Dahlman, O., Morck, R., Ljungquist, P., Reimann, A., Johansson, C., Boren, H. and Grimvall, A., *Environ. Sci. Technol.*, **27**, 1616 (1993).
93. Johansson, C., Pavasars, I., Boren, H., Grimvall, A., Dahlman, O., Morck, R. and Reimann, A., *Environ. Int.*, **20**, 103 (1994).
94. Zapata, A. M. and Robbat, A., *Anal. Chem.*, **72**, 3102 (2000).
95. Duckett, C. J., Bailey, N. J. C., Walker, H., Abou-Shakra, F., Wilson, I. D., Lindon, J. C. and Nicholson, J. K., *Rapid Commun. Mass Spectrom.*, **16**, 245 (2002).
96. Corcoran, O., Nicholson, J. K., Lenz, E. M., Abou-Shakra, F., Castro-Perez, J., Sage, A. B. and Wilson, I. D., *Rapid Commun. Mass Spectrom.*, **14**, 2377 (2000).
97. Hajslova, J., Cuhra, P., Kempny, M., Poustka, J., Holadova, K. and Kocourek, V., *J. Chromatogr. A*, **699**, 231 (1995).
98. Murphy, C. D., Schaffrath, C. and O'Hagan, D., *Chemosphere*, **52**, 455 (2003).
99. Bettinelli, M., Spezia, S., Minoia, C. and Ronchi, A., *At. Spectrosc.*, **23**, 105 (2002).
100. Schnetger, B. and Muramatsu, Y., *Analyst*, **121**, 1627 (1996).
101. Hagen, D. F., Belisle, J. and Marhevka, J. S., *Spectrochim, Acta, Part B-At. Spectrosc.*, **38**, 377 (1983).
102. Slowick, J. J. and Uden, P. C., *J. Anal. At. Spectrom.*, **9**, 951 (1994).
103. Vickers, G. H., Wilson, D. A. and Hieftje, G. M., *Anal. Chem.*, **60**, 1808 (1988).

2.25 Volatile Metal Compounds of Biogenic Origin

Jörg Feldmann
University of Aberdeen, Old Aberdeen, UK

1 ABSTRACT

This chapter review will focus on the analytical methods available to determine volatile compounds from metals and metalloids (VMCs) in gaseous samples, but it will also cover some elements that are usually not covered by speciation analysis for volatile organic compounds, such as phosphorous and iodine. This chapter starts with some general considerations about the kind of VMCs, metal hydrides, volatile organometallic compounds and volatile inorganic species, their thermodynamic stability and their occurrence in the environment. It highlights how some VMCs can be generated: either by biological means (microorganisms in microcosms) or chemically as pure standards. This is followed by an introductory coverage of traditional analytical methods to determine specific volatile metal(loid) compounds in gas samples.

The analytical section focusses on spectroscopic methods, especially the modern hyphenated techniques, which are necessary to meet the requirements of challenges in environmental analytical chemistry. This section introduces sampling and separation strategies with consideration of the physicochemical behavior of the target molecules and the matrix. Limitations and advantages of different sampling techniques used for the different gas samples, for example, atmospheric gases, process gases to volcanic exhalations and their applicability to hyphenated techniques is discussed in detail before quantification strategies are given. The possibility of artifact formation is illustrated by way of case studies. An outlook on potential applications and possible future developments to

Handbook of Elemental Speciation II: Species in the Environment, Food, Medicine & Occupational Health
Edited by R. Cornelis, H. Crews, J. Caruso and K. G. Heumann
 ISBN: 0-470-85598-3 (HB)

master the analysis of volatile metal(loid) compounds is given at the end.

2 GENERAL ASPECTS

A number of compounds found in the earth crust and its atmospheric envelope undergo movement, transport and chemical changes that are of cyclical nature – that is, their chemical states and distribution may recur over time [1]. The cycles may vary over many time scales and for some substances cycles of short duration may be embedded within longer periodicities. Often, biological processes are important agents of chemical change, thus, many cycles are significantly affected by biological uptake, chemical transformation and release. Microorganisms can easily interact with the formation and alteration of minerals and many biogeochemical cycles are even driven by microbial energy and carbon requirements. Microorganisms affect the redistribution of metals by oxidation, reduction, methylation or by metal binding.

When attention is focused on a component that may be involved within such a cycle, the complexity of both the nature of the compartments (pools) and the exchanges between them (fluxes) emerges. Our current knowledge about the behavior of chemicals in the environment has arisen from the development of sophisticated analytical methodology and instrumentation [2]. To permit us to understand the processes that control the distribution and fate of material in the environment we must be able to identify changes that occur to the biogeochemical cycling of the elements. Geochemical cycles of long periods are strongly affected, and even regulated, by biological action on many compounds found near or at the earth's surface [3]. A better understanding of these cycles and their complex feedback mechanisms may help understand the global consequences of anthropogenic alterations of the earth's environment. It illustrates in a very simplified manner the possible interactions and the transfer and transformation processes between the different compartments in the environment. The role of microbiological activity within these cycles cannot be stressed enough. Only immediate microbiological processes can efficiently facilitate the compartmental interchange of species moving between the different spheres. The volatilization process through biomethylation can lead to an effective dispersion of the species in the atmosphere if the compounds of interest possess a sufficient stability. By obtaining information on the chemical structures of an element (speciation), it is possible to investigate the processes that influence the dispersal, toxicity and eventual fate of both natural and anthropogenic chemicals in the environment.

The scope of this review concentrates on the volatile metal and metalloid compounds (VMC). The volatility of a compound plays an important role in the cycling of the elements. Since these compounds exist either as gases or volatile liquids under prevailing natural conditions, their entrance into the earth's atmosphere and circulation therein are critical to the environmental cycles for the corresponding elements [4]. Whatever their origin, these volatile hydrido compounds affect the natural environment in many ways. It was during the 1960s that interest and concern about the global environment and the philosophy of sustainability arose and there is a lot more work to do to enable us to understand the problems and effects of chemicals globally. Nevertheless, as a matter of fact, metal cycles on a regional and global basis have been profoundly modified by human activity.

Here, the focus is on volatile compounds generated through a biogenic process in the environment and/or in microbiological experiments in the laboratory. Thus, the volatilization of metal compounds derived in high temperature processes such as incineration or volcanic exhalation is not covered. Therefore, volatile compounds should not only be generated at ambient temperature (which is subzero up to 100 °C) but they must also have a higher vapor pressure to volatilize (>0.01 mbar). Mercury occurs in the elemental form with a sufficiently high vapor pressure to have a significant flux from soil and surface water. Although the formation of Hg^0 can be biologically mediated, this is not covered in this review. I concentrate on organometallic compounds and some volatile inorganic species like the metal hydrides.

Metalloid hydrides and their methylated counterparts are gases or volatile liquids at ambient temperatures. Attachment of hydrogen or alkyl groups

directly to metal(loid) atoms usually substantially enhances volatility [1, 4]. The lack of strong intermolecular attractions such as hydrogen bonding or dipol–dipol interactions is the reason behind this phenomenon.

2.1 Volatile metal hydrides

Elements of mainly group 14 to 17 form volatile, rather stable hydrides, while hydrides of transition metals behave more like metallic-alloys than as distinct molecules. Table 2.25.1 gives an overview of many hydrides with M–H bond energies. With the increase of the metallic character of the element, the bond is more polarized and therefore less stable. For example, arsine (AsH_3) shows a higher stability than bismuthine (BiH_3). Limited information is available about the biological hydride transfer to metals. The chemical potential necessary for the formation of such compounds is very low. It is therefore apparent that anaerobic conditions must favor the hydride transfer. Methanogenic bacteria are known to generate these hydrides even including BiH_3. It has been speculated that the coenzyme F430, which is involved in the methane generation, might play a key role in the hydride transfer. NADH is an obvious H^- donor in biological systems, but to the author's knowledge no clear mechanism has been given for such a process. In addition, an electrochemical potential can be created in the galvanizing industry or when batteries are being charged. $H^\bullet$ (*in statu nascendi*) can be generated, which is able to reduce, for example, arsenic and antimony to their elemental form, eventually generating AsH_3 and SbH_3.

Table 2.25.1. Thermodynamic constants of selected volatile metal species, in particular, hydrides, methylated metal hydrides and permethylated species.

Element	Species	D (M–H) kJ mol^{-1}	E/EH$_x$ V	bp °C
As	AsH_3	332	−0.61	−55
	$MeAsH_2$			2
	Me_2AsH			36
	Me_3As			50
Sb	SbH_3	265	−0.51	−17
	$MeSbH_2$			41[a]
	Me_2SbH			61[a]
	Me_3Sb			82
Bi	BiH_3	217	<−0.8	17
	$MeBiH_2$			72[a]
	Me_2BiH			103[a]
	Me_3Bi			109
Ge	GeH_4	<322	−0.3	−88
	$MeGeH_3$			
	Me_2GeH_2			
	Me_3GeH			
	Me_4Ge			43.4
Sn	SnH_4	264		−52
	$MeSnH_3$			14
	Me_2SnH_2			35
	Me_3SnH			57
	Me_4Sn			78
Pb	PbH_4	176		−13[a]
	Me_4Pb			110
Se	SeH_2		−0.399	−41.5
	MeSeH			25.5
	Me_2Se			55
	Me_2Se_2			
Te	TeH_2		−0.72	−2
	MeTeH			57
	Me_2Te			94
Hg	MeHgH			
	Me_2Hg			92
Ni	$Ni(CO)_4$			42.7
Fe	$Fe(CO)_5$			104.7
Mo	$Mo(CO)_6$			156.3[a]
W	$W(CO)_6$			175.0[a]

[a] Extrapolated boiling points.

2.2 Volatile organometallic compounds

The same group of elements also form rather stable M–C bonds. Since the C_1 transformation is very common in biological systems, the methylation of elements in the environment does not come as a surprise. If the process is biologically mediated, it is called *biomethylation*, in contrast to transmethylation, which does not involve a biological system. The formation of volatile compounds by biological methylation has been described for various elements in the literature [5]. This biomethylation has been identified in natural system for the elements As, Se, Cd, Sn, Sb, Te and Hg and can be proven under laboratory conditions for Cr, Pd, Pt, Au and Tl [6, 7].

The polarization of the M–C bond and the empty low energy orbitals of the transition metals destabilize the bond to the extent that transition metals such as cobalt can only form a stable M–C bond if the metal ion is kinetically stabilized. Such a stabilization can, for example, be implemented by a bio-ligand such as tetrapyrrole in methyl-cobalamin. Therefore, if metal ions are fully saturated with either carbon, hydrogen or halides and form noncharged

molecules, their vapor pressure is high enough to sustain in the gas phase at ambient temperature. If, however, one of these nonpolar bonds is cleaved, the molecule's volatility vanishes because a nonpolar bond changes into a bond with higher polarity. This leads to an increase in hydrophilicity. For example, if an oxide is formed in water, H-bonds increase the solubility of the organometallic compounds and this means that the volatility decreases. A series of rather stable volatile metal compounds is listed in Table 2.25.1.

Bioalkylation such as ethylation is a subject of controversy. Although it is fully recognized that ethyliodine exists, the occurrence of ethylated arsenical or mercuric compounds is not fully established. Transethylation from industrial products (IPs) such as Et_4Pb is a possible source of an ethyl group at metal centers. The butylated compounds have their sources in the variety of butylated tin compounds that have been used for decades as additives for PVC and antifouling paints. Degradation products can occur in the environment and form VMCs. Reducing environments, in particular, are known to generate VMCs (Figure 2.25.1).

2.3 Volatile inorganic compounds

Transition metals do not form stable M–C bonds but form a strong synergistic bond with the CO ligand. If all the empty d-orbitals can be filled by several CO ligands, which donate electrons to strengthen the bond (d_π-p_π-bond), volatile neutral metal carbonyls can be formed. The best-known example is $Ni(CO)_4$, which is eventually a gas (bp: 42.7 °C) and has been used for decades to clean up nickel in the so-called Mond process. Other compounds are liquids like $Fe(CO)_5$ or even solids like $Mo(CO)_6$ that have a rather high vapor pressure at room temperature (28.3 mbar, 0.036 mbar). To bring this into perspective, the mobility of persistent organic compounds is considered to be high if compounds have a vapor pressure above 0.01 mbar.

Furthermore, some metal halides form nonpolar compounds that result in a higher vapor pressure (e.g. $SnCl_4$ has a boiling point of 114 °C). However, they do show tendencies to hydrolyze easily in moisturized air and eventually form ions that significantly reduce the volatility. Other compounds like methylmercury chloride have been shown to exist in the environment and should not be forgotten in the ensemble of volatile metal species. In addition, a few oxides form rather volatile compounds (e.g. OsO_4). Unlike most of the other inorganic species, maybe with the exception of the carbonyls, they have never been shown to be of biogenic origin.

2.4 Thermodynamic considerations

If we want to identify and quantify these compounds in environmental or biological samples,

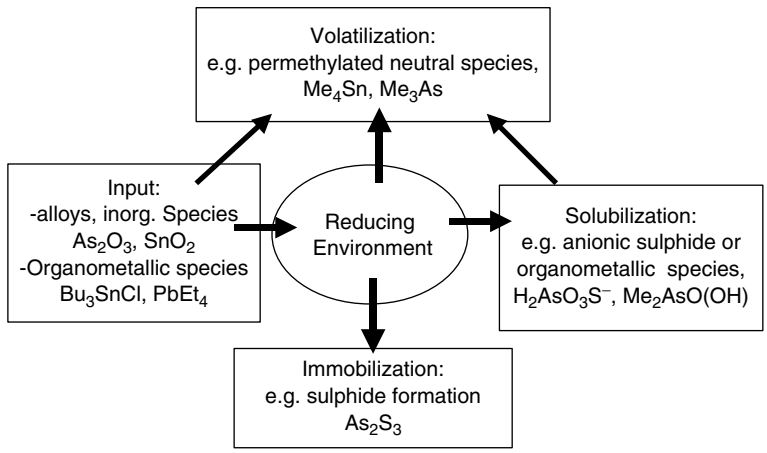

Figure 2.25.1. Simplified model of biogeochemical cycling of metal compounds in a reducing environment.

it is necessary to consider their physicochemical properties. Their mobility and especially the stability is heavily dependent on such fundamental data as boiling point, the strength of the metal-carbon bond (indicated by the bond dissociation energies) and their thermodynamic properties (mainly standard molar enthalpies of formation). Figure 2.25.2 shows the standard formation enthalpy of permethylated metal compounds versus the average dissociation energy of the M–C bond. The upper left area is characterized by species that are energetically high but low in stability, so that they tend to explode when exposed to air and in high concentrations, while species in the lower right corner are more stable so that more energy is necessary to cleave the M–C bond. Clearly, the latter compounds are much more likely to be found in the environment than the other species from a thermodynamic perspective. However, the occurrence of certain compounds such as Me_3Bi in large quantities in sewage or fermentation gas and landfill gas and the absence of Me_4Ge demonstrates that energetic considerations alone are not necessary for their occurrence in the environment. On the other hand, the metal–carbon bond energies do in fact lie within the normal range of chemical bond energies, so other scenarios must also be considered, namely, the kinetic stability or instability. Although intrinsically unstable, some of the compounds might be kinetically stabilized if there is a high energetic barrier to overcome for decomposition to a thermodynamically more favorable compound. It has been shown that the first M–C cleavage, which is significant for the volatility of the compounds, is often more stable. For example, Me_4Pb is rather stable and decomposes just above 265 °C. Its dissociation energy for the first M–C is 205 kJ mol^{-1}, while the average M–C bond energy is 155 kJ mol^{-1}. High enough activation energy allows the compounds to have a rather long atmospheric lifetime. On the other hand, most of the volatile organometallic compounds have a low enough activation barrier for the first M–C cleavage so that they are not persistent. The data in Figure 2.25.2 have to be interpreted with care because the definition of the formation energy involves the formation of the compounds out of the elements but that is not always the preferred mode of decomposition. Further, thermodynamic considerations, particularly for volatile permethylated compounds, are summarized by Craig in an excellent book chapter [5].

2.5 Occurrence of VMCs in the environment

Among the various volatile organometal(loid) compounds under debate, the group of hydrides, methylated hydrides and permethylated species is the

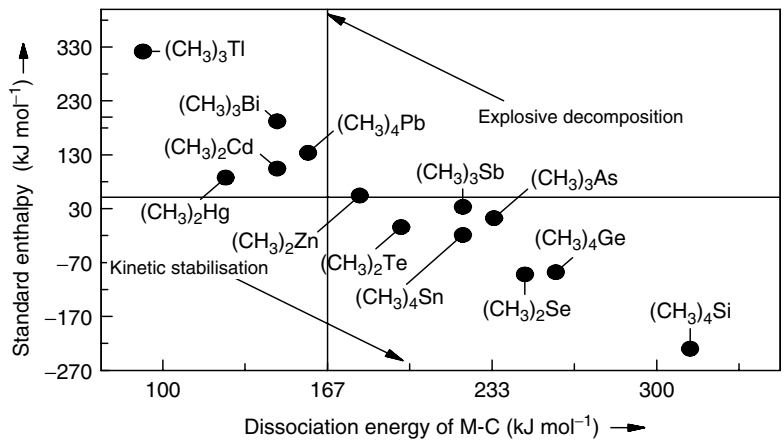

Figure 2.25.2. Standard enthalpy of formation ΔH_f^0 versus the average dissociation energy of the M–C bond in a selection of neutral permethylated metal(loid) compounds.

most important. The transfer from an ionic water-soluble compound to a hydride or permethylated VMC leads to a far less pronounced intermolecular attraction and thus increases the volatility to such an extent that the soil–air or water–air boundary can be crossed. Although some sources of VMCs in the environment have been identified, their potential hazardous health effects to humans are still unknown. In general, methylation increases the volatility, toxicity, lipid solubility and adsorptivity and possibly mobility in the environment. It is therefore important to identify potential sources and sinks of those volatile compounds. Apparently, their atmospheric half-life is not very long, so no considerable concentration has been established. Most of the studies are therefore focused on point sources in which those VMCs are likely to be found in higher concentrations. Parameters that characterize such environments are, for example, high concentration of bioavailable metal(loid)s and high microbiological activity and diversity. An anaerobic environment seemed to be beneficial for most of the compounds since methanogenic and sulfate-reducing bacteria are known to produce a number of VMCs from their inorganic precursors. However, the latter cannot be generalized, in particular, Me_2Se seemed to be linked to an aerobic environment; Me_2Se is one of the end-products of the selenium metabolism in mammals and can be detected in human breath, whereas Me_3As or Me_3Sb are more likely to be produced in an anaerobic environment (Figure 2.25.1) [8].

In this context, dozens of volatile organometal (loid) compounds have been found to occur in municipal waste deposits and in fermentation processes of sewage sludge (see Table 2.25.2). The

Table 2.25.2. Selected VMCs detected in the environment or generated in microbiological experiments.

Element	Species	Concentration ng m^{-3} (unless otherwise stated)	Environment	Analytical method	References
As	AsH_3			Filtration, absorption	17
	Me_xAsH_{3-x}			Chemofocusing	18
	Me_3As		Algal mats	P-CT-CF-GC-ICP-MS	13
		16,100–48,500[a]	L, S gas	CT-CF-GC-ICP-MS	19
Sn	SnH_4		Enteromorpha[b]	P-CT-GC-AAS	20
	Me_xSnH_{4-x}		Water samples (Chesapeake Bay)	GC-AAS	21
	Me_4Sn	0.002 ng L^{-1}	Sea water	P-CT-GC-ICP-MS	9
	Me_4Sn	8600–35,000	L, S gas	CT-CF-GC-ICP-MS	19
Pb	$PbMe_4$	23–55[2]	Landfill,	CT-CF-GC-ICP-MS	22
		0.004 ng L^{-1}	Sea water	P-CT-GC-ICP-MS	9
		0.09–95	Urban air	CT-CF-GC-ICP-MS	15
Bi	BiH_3		Methanogenic bacteria	CT-CF-GC-ICP-MS	23
	Me_3Bi	0.2–24,200	L, S gas	CT-CF-GC-ICP-MS	24
Ni	$Ni(CO)_4$	500–1000	S gas	CT-CF-GC-ICP-MS	25
Mo	$Mo(CO)_6$	200–3600	L, S gas	CT-CF-GC-ICP-MS	26
W	$W(CO)_6$	5–15	L, S gas		
Sb	SbH_3		L, S gas	CT-CF-GC-ICP-MS	19
	Me_3Sb		Algal mats	P-CT-CF-GC-ICP-MS	13
		618–71,600	L, S gas		19
Te	Me_2Te	<1–887	L, S gas		19
			Pseudomonas spp.	GC-MS, GC-F-ICL[a]	27
Se	Me_2Se	80–980	Breath,	CT-CF-GC-ICP-MS	8
		0.7–8.7	Urban air	CT-CF-GC-ICP-MS	15
			Wetlands		12
	Me_2Se_2	0.3 ng L^{-1}	Seawater	P-CT-GC-AFS	28
	Me_2SeS	0.08 ng L^{-1}	Seawater	P-Ct-GC-ICP-MS	
I	MeI		Macroalgae	GC-ECD	11
	CH_2I_2	0.7–58 ng g^{-1}	Macroalgae		
Hg	Me_2Hg	0.5 ng g^{-1}	Floodplain soils	Selective absorption	10
		12–130	L, S gas	CT-CF-GC-ICP-MS	19

[a] GC-F-ICL = GC-fluorine-induced chemiluminescence; CT = cryotrapping; CF = cryofocusing; P = purging, L = landfill, S = Sewage sludge
[b] Enteromorpha: marine seaweed.

concentrations are comparable with trace amounts of VOCs in waste incinerators (between ng m^{-3} and 100 $\mu g\,m^{-3}$) and therefore are considerable. However, not only methylated compounds of common elements such as arsenic or mercury were identified, large quantities of Me_3Bi, Me_3Sb and Me_2Te should be mentioned in addition to the neutral carbonyls of nickel, molybdenum and tungsten. Donard and coworkers have reported the generation of rather volatile methylated butyltins in polluted sediments (South-West France) and in the water column of the estuarines of the rivers Scheldt (Belgium/Netherlands) and Gironde (France) [9]. Although sediments are very good sinks for tributyltin, the methylated tributyltin (Bu_3SnMe) has a significantly lower affinity to this phase. It could easily be released to the water column and because of the high lipophilicity consequently released to the atmosphere. In addition to $BuSnMe_3$, Bu_2SnMe_2 traces of tin hydrides (SnH_4, $BuSnH_3$, Bu_2SnH_2) seemed to be generated. Other studies have determined the generation of Me_2Hg in the mudflats of the heavily polluted River Elbe in northern Germany [10]. Many volatile iodine compounds are known to be generated from marine macroalgae. Laturnus has shown that both methyl-iodine and ethyl-iodine, along with $CH_2Cl–I$, CH_2I_2, could be detected in seaweed [11]. Hansen *et al*. reported the volatilization of selenium from a constructed wetland that was purpose-built to clean up refinery process water containing 20–30 $\mu g\,L^{-1}$ selenium [12]. They have found that 10–30% of the selenium was volatilized, presumably as Me_2Se. The maximum flux was measured to be 190 μg of Se/m^2/day. In contrast to most previously mentioned sources (landfills and contaminated sediments), the volatilization of selenium is more pronounced for aerobic systems. Furthermore, it has been found that algal mats of geothermal waters in southern British Columbia generate volatile arsenic and antimony species besides a series of volatile iodine compounds [13]. The water contained up to 300 $\mu g\,L^{-1}$ arsenic and only 2 $\mu g\,L^{-1}$ antimony. A direct sampling of the algal mats using a flux chamber could demonstrate that AsH_3, $MeAsH_2$, Me_3As and Me_3Sb were generated from the algal mats. Phosphine, although not a metal or metalloid, is important too. Despite the fact that a very low chemical potential is necessary to produce PH_3, it has been identified in the environment from sediment to soil and animal manure in concentration up to 964 ng kg^{-1} [14]. However, the question of whether PH_3 is generated biologically has not been answered yet. Although not biologically generated, volatile siloxanes and alkyllead compounds should be mentioned here; Et_4Pb occurred in urban air [15], while L2-4 (linear siloxanes), D3-5 (cyclic siloxanes) are detectable in sewage and landfill gas [16]. However, their degradation, which might be catalyzed enzymatically, also produces a volatile compound: Me_3SiOH.

2.6 Generation of VMCs in microcosms and in pure microorganism cultures

The formation of VMCs from pure cultures of bacteria, fungi and algae has been intensively studied. Fifteen years ago, Donard and Weber published the generation of volatile tin compounds (SnH_4, Me_2SnH_2) from algae [20]. In the 90s, Richardson put forward the hypothesis of poisoning by arsines, phosphines and stibines generated by fungi from As, P and Sb compounds used as fire retardants in mattress material – as a primary cause for SIDS (sudden infant death syndrome) [29, 30]. This statement increased the interest of microbiologists and analytical chemists in the biovolatilization of metals. In the following years, a considerable amount of work was published particularly for antimony [31, 32]. Prior to that, the focus was on arsenic. Dozens of microorganisms were identified, which generated volatile arsines (AsH_3, $MeAsH_2$, Me_2AsH, Me_3As) from different inorganic and organic sources. Cullen and Reimer have covered arsenic very well in their exceptionally informative review [33], while Chasteen and Gadd have focused more on selenium and tellurium and their biotransformation [27, 34]. Besides the more common species, Me_2Te, Me_2Se and Me_2Se_2, mixed selenium and sulfur species have also been identified (e.g. Me_2Se-S) [9]. Most of these studies concern the identification of microbiological mediated biotransformations.

2.7 VMC standards

There are a limited number of volatile metal compounds commercially available as pure standards. Only neutral permethylated standards such as Me_4Sn, Me_3As, Me_2Hg and Me_2Sn or metal carbonyls such as $Mo(CO)_6$ are available off-the-shelf. Hydrides or methylated metal hydrides are not available but can easily be generated using hydride generation methodology. For example, methylated tin and arsenic compounds are readily obtainable, if they are subject to hydride generation using $NaBH_4$. Volatile products such as $Me_xSnH_{(4-x)}$, $Me_xAsH_{(3-x)}$ can be generated quantitatively. Antimony compounds are more problematic. Me_3SbCl_2 can easily be synthesized but not the precursor for the mono- and dimethylated stibines. If Me_3SbCl_2 is subject to hydride generation at pH 2 or below, significant demethylation can be observed and besides Me_3Sb, significant amounts of Me_2SbH, $MeSbH_2$ and SbH_3 are formed [35]. In addition to the hydrides, it has recently been shown that during hydride generation volatile arsenic halides such as $MeAsCl_2$ and Me_2AsCl are formed [36]. The importance of those compounds for the study of biovolatilization remains to be shown. However, most other compounds such as Me_2Te or Me_3Bi have to be synthesized conventionally (e.g. Grignard reactions).

Having those pure VMC standards in a temperature-controlled environment means that headspace samples can be taken directly from the vials. Knowing the vapor pressure allows the calculation of the exact amounts of VMCs to be handled and used for spiking. However, the volatility of those compounds is often so high that the amount (even if only μL gas have been withdrawn) is an order of magnitude higher than the expected amounts in environmental gas samples so further dilutions are inevitable. Despite this, however, it is not trivial to produce gas standards in concentrations that are comparable to those that are going to be analyzed, such as process gases from sewage treatment plants or the headspace from incubators in which concentrations between $ng\,L^{-1}$ and $mg\,L^{-1}$ are very common. Ready-made gas standards, however, are very difficult to find. To the author's knowledge, there are only two VMC gas standards in appropriate dilution available; PH_3 or AsH_3 in air or argon in concentration of about 50 ppm (v/v). This should not be mistaken by ppm usually used for mass of metal or metalloid in a volume of solutions (i.e. $50\,mg\,L^{-1}$). These gas standards are not very stable and very expensive but can directly be used for identification and/or for calibration purposes [37].

3 ANALYTICAL METHODOLOGY

The choice of any analytical technique, involving a sampling procedure to sample preparation, separation and detection, has to be based on the physico–chemical properties of the analytes. The character of the samples as a whole plays an important role as well. Any chemical or spectroscopic property on which the measurement principle is based could be counterbalanced by major matrix gases. The concentrations of most trace elements of concern in the natural samples are in μg per kg range and below. The challenge for the analytical chemist is to undertake speciation measurements without any losses, transformation or contamination. Analytical procedures are required to selectively respond to specific chemical forms. There are, however, few techniques that have this capability and more often than not some separation based on either physical or chemical properties is required before any measurements can be undertaken. Considerations about the occurrence of volatile metal(loid) compounds in the environment, where those compounds are generated at the concentration level to be expected, have a considerable impact on the choice of the analytical method used for identification and/or quantification of the volatile metal(loid) compounds. The analytical method of choice for environmental samples has to fulfill the following requirements and the technique should be characterized by the following.

- Preconcentration step (specific but not too specific)
- Limited transformation or loss of analyte (stabilization)

- Limited matrix effects
- High sensitivity
- High specificity
- Multielement capability
- Small interactions with chemicals and separation material
- Suitable for gas samples.

3.1 Traditional methods

Volatile organometallic compounds have a long lasting and notorious history. It is no surprise that in the early years analytical chemists developed methods that enabled them to analyze traces of those volatile compounds. Already in 1945, Challenger was able to identify a series of volatile arsenic, selenium, tellurium and antimony compounds generated by cultures of fungi and bacteria [18]. He used chemi-focusing methods to trap volatile metalloid species on a cellulose filter immersed with $AgNO_3$ or $Hg(NO_3)_2$ [38]. The metalloid with its lone-pairs binds to Hg^{2+} or Ag^+, respectively, according to a simple Lewis acid–base reaction. The color change was often used as an indication for the occurrence of volatile antimony or arsenic compounds, while others were able to determine the kind and amount of these elements trapped on the filter paper. The extent to which these methods are quantitative has not been ascertained. Most importantly, it should be remembered that these methods were not very sensitive (detection limits of staining was estimated to be approximately 1–2 μg Sb) and did not allow the determination of individual element species. Other investigators simply pump gases through membrane filters from which the gas is percolating through an absorption solution. The total metal concentration was measured, which per definition belongs to the class of volatile metal compounds. With the knowledge of the occurrence of one species per element, it was possible to use this crude method to identify the fraction of element occurring as a volatile species (e.g. in occupational hygiene for AsH_3) [17]. For the speciation of mercury in the atmosphere, Schroeder and Jackson [39] fractionated mercury species in a sequential sampling scheme using a sampling train consisting of four different traps in series. They put four different absorption tubes in series: the first one adsorbs $HgCl_2$ and was filled with Chromosorb-W/HCl, the second one adsorbs MeHgCl (Chromosorb-W/NaOH), while the third one was filled with silver-coated glass beads to adsorb Hg^0 and finally a cartridge filled with gold-coated glass beads traps Me_2Hg. This is a highly sophisticated fractionation that, however, does not identify any new species. Since there are four different reagents rather than continuously changing conditions (like in chromatography), little control is implemented to see if the sampling conditions or the matrix have an impact on the adsorption conditions. In contrast, if a chromatographic system had been employed, a slight change in retention time might have been instrumental in finding out.

3.2 Hyphenated techniques

Traditional methods are hardly used for the speciation analysis of VMC, with the exception of mercury. Conventional chromatographic separations are typically employed before sample introduction to an element-specific detector. For volatile compounds, GC has widely been used. There are a few detectors that are highly specialized for the determination of VMCs. Fluorine-induced chemiluminescence was employed to detect quite selectively volatile tellurium species [27]. Phosphine can be detected in small concentration (0.1 ppt (v/v) – here again not to be mistaken by ng P/L) using GC-NPD [14]. GC can be coupled to a variety of detectors, from nonspecific detectors (flame ionization detection (FID)) to highly specific detectors such as ICP-MS [2]. In the following paragraphs I will introduce different methods of sampling for the determination of VMCs in gas samples. These will be followed by the discussion of various separation and detection systems.

3.3 Sampling procedures

Sampling is the first step within an analytical investigation. Clearly the process of sampling

can have a strong influence on the correctness and quality of any analytical result. Factors such as representativeness, homogeneity and stability have to be considered [40]. The choice of the sampling technique depends on the physical and chemical nature of the material, on the analytical method being used and on the accuracy and speed required. In order to comply with all quality assurance features, care has to be taken to avoid any possible contamination that does not alter the analytical result. Volatile metal(loid) compounds (VMC) have been identified in various anthropogenic gases such as landfill gas and sewage sludge digester gas. In terms of their physical and chemical properties, volatile metal(loid) compounds and volatile organic compounds cannot be totally lumped together. Most of the VMCs are thermodynamically unstable and thus prone to degradation of any kind. This feature is important for the choice of an appropriate sampling technique. Possible phenomena causing analyte loss are diffusion, oxidation, hydrolysis, photodecomposition, adsorption, absorption and heterogeneous surface catalyzed break down.

It is of particular interest to know if the sampled environment is an anaerobic environment or an aerobic one. Not only is the amount of CO_2 very important but also the other trace organic compounds (e.g. aldehydes, ketones, organosulfur compounds) generated under anaerobic conditions as these can turn the sample into a messy chemical cocktail. There are hundreds of individual volatile organics that in turn may be potential interferences for the analysis of VMCs. Since the volatile metal compounds are reactive and not very stable, care has to be taken when gas samples are taken. It is necessary on the one hand, to separate the volatile metal compounds (VMCs) from matrix gases and consequently preconcentrate the compounds, on the other hand to keep the compounds less reactive in order to preserve them for analysis. Different approaches as follows have been applied to suit the analysis of these VMCs.

- Absorption solutions (oxidation, speciation not possible)
- Adsorption tubes (Tenax)
- Tedlar bags (Polyfluorinated plastic bags)
- Cryotrapping at different temperatures
- Solid phase micro-extraction (SPME).

Most of the listed methods are preconcentration methods except the method that uses Tedlar bags. In general, preconcentration methods are necessary for most analyses since the expected concentration of VMCs is rather small. However, if a preconcentration method is used, the disadvantages are that only one analysis can be done with one trapped sample and the approximate concentration range has to be known since further manipulations (dilutions or further preconcentrations) are not possible.

Absorption solutions like HNO_3 or H_2SO_4/$K_2Cr_2O_7$, in which gases are percolated via an impinger, oxidize most organometallic compounds to water-soluble element species [32]. The total element concentration is measured, and that gives a hint for the occurrence of any volatile compound in the gas sample, but no speciation analysis is possible. Contamination with generated aerosols cannot be excluded easily, so the trapped total elements are the sum of the 'true' volatile species and the species in the aerosol-phase. Other solvents or absorbing liquids cannot be used for the sampling of volatile metal(loid) compounds because the interactions needed for the analyte to be caught in the absorbent are far too high so that a change of the chemical form of the VMCs would be inevitable. For the same reason, adsorbents have been considered not suitable for such unstable compounds. Irreversible adsorption, degradation during the desorption process and buildup of artifacts may be underlying causes for possible negative results associated with the use of materials such as Tenax® and Porapak®, especially when the samples are stored at ambient temperatures [41, 42]. The US Environmental Protection Agency (EPA) method TO-17 is based on sampling onto solid adsorbents [43]. Adsorbents might be tailored for a small number of VMCs as, for example, sequential sampling for the determination of volatile Hg-species using a noble-metal trap in series with an activated-carbon trap [44]. Stainless-steel containers, however, are officially used in the United States EPA canister method TO-14 where

volatile organic compounds (VOCs) are monitored in urban air [45]. This method describes the use of the canisters in the passive mode (i.e. vacuum filling) to eliminate any introduction of contaminants originating from the pump. This approach has not been used for VMCs, but Tedlar bags have been shown to be useful, if the concentration of the target compound in a field study is not known [46]. Gas samples can easily be taken to the laboratory in which the analysis can be carried out but should be protected from UV light and kept at room temperature conditions. Many parallel analyses with necessary dilutions/preconcentrations can be performed. Tedlar bags have been described in the literature to be useful for sampling of various volatile organic compounds (VOC) [47]. They have also been used successfully for the generation of standard gaseous mixtures and their storage for studying gaseous media containing traces of analytes (lower ppb (v/v)) [48]. The results indicate the excellent reliability of Tedlar bags, whereas Teflon bags are seen to cause some problems.

On the other hand, critical reports underline possible complications and constraints of using Tedlar bags especially the evidence of significant VOC losses and adsorption of especially polar compounds. Lipari found methanol losses of over 70% in 6 h, while Andino and Butler also studied methanol vapor storage in Tedlar bags and they found only about 8% losses occurring in 60 L bags in 6 h [49, 50]. The adsorption seemed to be dependent on the humidity of the gas sample. In dry gas samples, the loss is higher than in humid samples.

Five static gaseous atmospheres with concentrations of 8–18 ng L^{-1} for the various compounds have been generated in Tedlar® bags and the stability of the VMCs, which are $Me_xAsH_{(3-x)}$, $Me_xSbH_{(3-x)}$, with $x = 0$–3, and $Me_xSn_{(4-x)}$ and $BuSnH_3$ with $x = 0$–4, have been monitored over a period of five weeks. After eight hours, the recovery rate of all the compounds in air was better than 95% at 20 and 50 °C, whereas the recovery after 24 hours was found to be between 81 and 99% for all VMCs at 20 and 50 °C except for Me_3Sb and Me_3As. These species show a loss between 48 and 73% at both temperatures, while the hydrides AsH_3, SnH_4, SbH_3 and $Me_xSnH_{(4-x)}$ with $x = 1$–3 are stable over many weeks [46]. The stability is not dramatically influenced by the temperature, but UV/VIS radiation does effect it. With increased grade of methylation, the effect becomes more important [51]. If UV/VIS radiation can be excluded, sampling of VMCs in the field using a Tedlar bag covered with a black bag can be employed successfully. Furthermore, it is relatively easy and inexpensive.

Recently, it has been shown in laboratory experiments that solid-phase micro-extraction (SPME) is a powerful tool to preconcentrate volatile species when coupled to an element-specific detection of volatile species. The volatile organomanganese compound MMT (methylcyclopentadienyl manganese tricarbonyl) can be preconcentrated on such a fiber and injected directly onto a column. SPME can be used for total volatiles (without any separation column) as well as for speciation [52]. The advantage of using no column is that one can check if there are any very unstable VMC in the gas sample, which would not elute from a GC column.

So far, the method mostly used for the sampling of VMCs has been cryotrapping. Feldmann *et al.* as well as Amouroux *et al.* used a chromatographic packing (SP2100 10% on Supelcoport (60/80 mesh) in a U-shaped glass tube immersed in liquid nitrogen as the cryogenic liquid, for the sampling of VMCs in human breath, in the headspace of a microbial culture, in landfill gas, in sewage gas, in urban air or in the water column of an estuarine [9, 19]. The cryotrapping was already the first step within a packed column GC-ICP-MS method. The strategy was to stabilize the analytes, which are thermodynamically labile, as well as air- and UV-sensitive. The cryotrapping tubes can easily be stored in liquid nitrogen and thus the sample is stabilized until the measurement is carried out. The transfer of analyte from the sampling point into an adequate analytical device must be achieved without loss, transformation or decomposition. Parameters like flow rate and temperature are dependent on each other in order to achieve high trapping efficiency. Often, only 1 to 2 L/min have been used as flow rates, which makes the preconcentration of dilute gas samples such as

urban air a time-consuming task. Practical experience unfortunately highlights plugging problems when sampling atmospheres with high levels of humidity. Cryotrapping can be performed with or without adsorbents being used. Depending on the trapping temperature, the use of adsorbents may not be necessary with the advantage that moderate volatilization temperatures can be applied, so that the labile compounds do not suffer the risk of thermal degradation. Of course, the choice of the trapping temperature has got an intrinsic influence on the trapping efficiency. Pecheyran *et al*. controlled trapping temperatures down to $-175\,^{\circ}C$ during the sampling of urban air, thereby avoiding the condensation of oxygen in the U-tubes (boiling point of oxygen is $-183\,^{\circ}C$) [15]. In order to remove matrix components from the gas samples, which are easy to trap (mainly CO_2 and water), different approaches have been taken. Cartridges filled with a drying agent $Mg(ClO_4)_2$, $CaCl_2$ or $CaSO_4$ have been used prior to cryotrapping in order to prevent clogging of the cryotrap. When those chemicals are used, interaction of the VMCs cannot be excluded. This is, however, not the case if a Nafion® is used for the removal of moisture. Donard and coworkers have successfully employed both these membranes and a cryogenic water trap set to $-20\,^{\circ}C$ in their sampling train prior to cryofocusing [20]. This is, however, subject to memory effects of less volatile compounds such as Hg^0. In addition to water, CO_2 can be a major matrix gas, especially in anaerobic environments. When cryotrapping is used for the preconcentration of VMCs, CO_2 has to be removed. For this purpose, NaOH pellets have been used successfully. The disadvantage of using NaOH is that unstable or slightly acidic compounds can react with the absorbants. However, good recovery rates have been identified for $Me_xAsH_{(3-x)}$, $x = 0–3$ (81–89%) and for $Me_xSnH_{(4-x)}$, $x = 0–4$ (85–98%), while methylated antimony compounds show lower recovery rates (52–69%) with SbH_3 being the worst (33%) [53].

For the determination of volatilization rates of metals and metalloids from biota in the terrestrial environment, flux chambers have to be used. The chambers are made out of Plexiglass, which can cover a well-defined area of soil or even vegetation. The volatile compounds produced in a certain period can be sampled when filtered air is allowed to enter the chamber so that the gas in the chamber can be trapped and whatever it is used to sample the gas is purged out. Having a well-defined area and collection time, a flux rate of target compounds mostly given in $ng/m^3/day$ can be calculated. This method can also be used for surface water. In this case, the flux chambers have to be mounted on a float. We have used these chambers to collect gas percolating through the water in a wetland. Another option for the determination of volatile metal compounds is to determine the supersaturation of the water column with the analyte by purging the water with helium and subsequent cryotrapping of VMCs. With the knowledge of the Henry constant, the flux of the volatile compound from the water column can be estimated. This *in situ* purge and cryotrapping method used by Donard and coworkers is illustrated in Figure 2.25.3 [54].

A promising approach as a new sample introduction method for volatile metal species has been described only recently by Mester *et al*. [55]. They coupled a solid phase micro-extraction (SPME) directly with an ICP-MS using a thermal desorption interface directly at the base of the torch. This allows to sample any volatile metal compound, even those that are very labile.

3.4 Separation

Sampling, sample preparation, separation and eventually the detection of individual species are four steps that need tuning. If one step is highly specific, the others do not have to be so specific. For example, if there is a highly specific detection system for one compound and this system does not show any matrix effect it is not necessary to have a very sophisticated separation step. On the other hand, if the detection is not very specific, a better separation step has to be developed in order to guarantee 'specific' detection. Having this simple concept in mind and considering the limited number of volatile compounds per element, it is

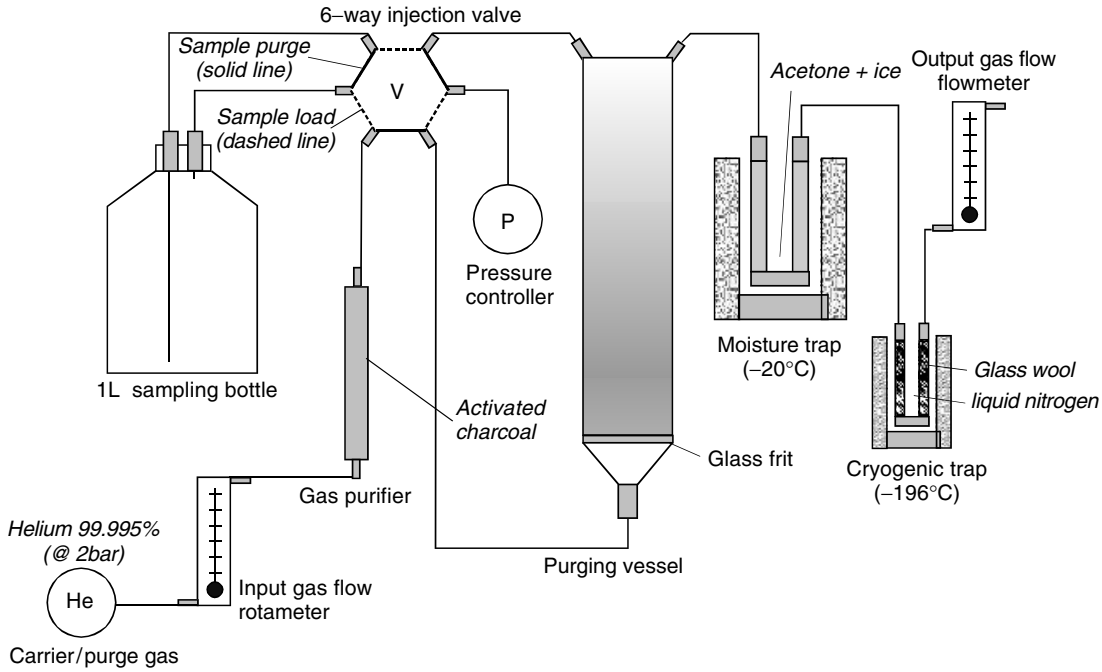

Figure 2.25.3. Purge and trap GC setup for dissolved VMCs in water samples. (Reprinted from *Anal. Chim. Acta*, **377**, Amouroux, D., Tessier, E., Pecheyran, C. and Donard, O. F. X., Sampling and probing volatile metal(loid) species in natural waters by in-situ purge and cryogenic trapping followed by gas chromatography and inductively coupled plasma mass spectrometry (P-CT-GC-ICP-MS), 241 (1998), with permission from Elsevier.)

not necessary in most cases to have a high performance separation technique if an element-specific detection can be employed.

In most cases, crude glass columns packed with nonpolar materials such as OV 101 or SP2100 on Chromosorb or Supelcoport materials have successfully separated volatile metal compounds. The separation of a few very volatile compounds like the volatile arsines was developed almost 30 years ago. Volatile arsines were separated with a U-tube filled with the above-mentioned material after they underwent the so-called hydride generation for the speciation of methylated arsenic compounds in water. The same system can be used for the separation of volatile compounds, only the sample injection differs slightly, since volatile compounds have to be analyzed directly in a gas sample. Some decades ago, these systems were used for many different applications, be it mostly for methylated arsenic, tin, mercury, germanium and antimony. Although the resolution with $R = 2 - 3$ is relatively small, the separation of the 3 to 5 different methylated hydrides (Me_xEH_y, $x + y =$ 2, 3 or 4) is sufficient. The big advantage of a packed column system is that it has a very high sample uptake capacity and is therefore perfectly suited for trapping and separation of gaseous samples. Traps are often used for those volatile compounds that are too volatile to be trapped on an adsorptive column. The traps can easily be submerged into liquid nitrogen or other solutions to cryotrap them on-column.

Another advantage is that this separation can be used for relatively unstable compounds since the compounds are injected (cryotrapping) and separated at relatively low temperatures and the interaction of the analyte with the stationary phase (mostly dimethylpolysiloxane) is relatively small. Recovery experiments in which the eluting compounds are injected again have shown that packed columns show higher recoveries for volatile metal compounds such as Me_3As, Me_3Sb, and Me_4Sn

than capillary columns with a similar stationary phase (see Table 2.25.3).

The gas flow of a packed column system (100–200 mL/min) fits very nicely to any atomizer like AAS, AFS, ICP-OES and ICP-MS. One of the first setups for volatile organometallic compounds in the atmosphere was already published two decades ago. Adams and coworkers have determined organolead compounds with GC-AAS [58]. Approximately, 100–300 mL helium per min is sufficient to transport the eluting analytes through a transfer line to the atomizer. This could easily mix with other gases to suit the atomization or ionization conditions. The hyphenation of the packed column system directly to a mass spectrometer is, however, challenging since a split of 1/100 does not guarantee representative sampling of the eluting gas.

The peak width of the species using a packed column system is acceptable (20 s) for the very volatile compounds (bp $< 100\,^{\circ}C$), but increases dramatically for the less volatile compounds such as $PbEt_4$ or Bu_3SnMe. They show peak widths of (1–3 min.) because these traps are usually electrothermally heated up to 150 – 180 °C, which is not sufficient for those compounds to elute in a very narrow band. Higher temperature up to 250 °C will narrow the peaks, but imposes the risk of species degradation during the separation process. In order to achieve sharper peaks, in particular, for the less volatile compounds, and gain better resolution, the length of the columns have to be increased from 0.1 m to 1 m. However, more importantly, a cryofocusing on a second column has been introduced to clean up the sample from matrix components and to condense the analyte on a short spot directly on-column. This setup has been used for the determination of VMCs in landfill gas as well as in purge gases from estuarines (see Table 2.25.4).

Capillary columns were also widely used. Improved resolution was not the only reason to switch from a packed column system to a capillary system; the sharper peaks could guarantee a better level of detection because of the better signal to noise ratio. Achievable levels of detection can be seen in Table 2.25.3. Undoubtedly, the higher resolution of the capillary column gives a better separation between the different compounds. This is only necessary, however, if many possible compounds from one element can be generated (see Figure 2.25.4). In addition to biomethylation, mankind generated perhaps too enthusiastically higher alkylated metal compounds such as tetraethyl lead (TEL) or tributyltin (TBT). These compounds and their degradation products increased the amount of mostly less volatile compounds enormously. Although capillary columns lack on sample capacity, they show better separation and can easily be heated externally, so that both extremely volatile and less volatile compounds can be separated and eluted in a narrow band (Figure 2.25.4). The resolution of capillary columns exceeds by far that from packed columns (R_{cap}19.26 compared to R_{packed}3.84). Less volatile compounds can easily be absorbed into a solvent or onto a fiber

Table 2.25.3. Recovery on the different separation systems and the detection limits.

Species	Capillary-GC compared to packed column[a] [56] (%)	Recovery experiment capillary-GC [56] (%)	Recovery experiment capillary-GC [51] (%)	Detection limits capillary-GC [57] (pg)	Detection limits capillary-GC [56] (pg)
Me_3SnH	72	–	92	–	–
Me_2AsH	61	–	86	–	0.18
Me_2SbH	39	–	21	–	–
Me_4Sn	–	92	91	0.200	0.071
Me_3As	57	62	82	–	0.22
Me_3Sb	69	46	75	–	0.045
Me_2Hg	–	66	–	0.810	0.335
Me_3Bi	–	78	–	–	0.028
Me_4Pb	–	–	–	0.06	–
Me_2Se	–	–	–	2.5	–

[a] Packed column (22 cm length, filled Supelcoport 10% SP2100) was set to 100%.

Table 2.25.4. Selected volatile alkylated compounds or hydrides, mostly of anthropogenic origin, which undergo methylation or hybridization in the environment.

Element	Volatile species	Original species	Environment	Analytical method	References
Sn	$BuSnH_3$	$Bu_nSn^{(4-n)+}$	Sediment	GC-ICP-MS	9
	Bu_2SnH_2	$Bu_nSn^{(4-n)+}$			
	Bu_3SnMe	$Bu_nSn^{(4-n)+}$			
	Bu_2SnMe_2	$Bu_nSn^{(4-n)+}$			
	$BuSnMe_3$	$Bu_nSn^{(4-n)+}$			
	Et_2SnMe_2	?	Landfill	GC-ICP-MS	59
	$EtSnMe_3$	?	Landfill		22
Pb	Et_3PbMe[a]	Et_4Pb/Et_3Pb^+	Sewage sludge tank	GC-ICP-MS	19
	Et_4Pb	I.P.[3] (US)	Urban air		15
	Et_xPbMe_{4-x}	I.P.[3] (Europe)	Urban air	GC-AAS	58
I	Et-I[b]	?	Macroalgae	GC-ECD	11
	Pr-I[b]	?	Macroalgae		11
As	$EtAsMe_2$	?	Natural gas	GC-MS	
	$EtAsMe_2$	?	Landfill gas	GC-ICP-MS	19
Mn	MMT/CMT[c]	I.P.[c]	Urban air	SPME-GC-AED	60
P	PH_3[b]	?	Manure, soil, sediments	GC-NPD	14
	PH_3	I.P.	Tobacco factory	GC-ICP-MS	61

[a] Main volatile Pb species in the gas can only be explained by methylation in the tank by methanogenic bacteria.
[b] Probably natural products.
[c] Volatile metal(loid) species as industrial product (IP), (MMT); cyclopentadienyl manganese tricarbonyl (CMT).

(SPME). They are ideal as sample introduction systems for the capillary columns. In particular, SPME can be applied, for example, for the measurement of volatile compounds in microcosm experiments in the laboratory. In those experiments, it is often necessary to determine VMCs at very low level in a very small gas volume.

If the separation is not satisfactory either because of a complex mixture of VMCs or matrix compounds such as natural gas condensates or process gases, a sample cleanup stage is necessary. Bouyssiere *et al.* [62] have shown that this concept has to be employed if volatile arsenic compounds have to be identified in natural gas condensates.

One aspect of using gas chromatography for the determination of volatile metal compounds should not be forgotten: very reactive and polar species will not elute from columns. Volatile compounds, which are not filterable, could include organometallic halides. These compounds hydrolyze quickly and do not necessarily elute with high recovery from the column. In Table 2.25.3, the recovery rate from a series of different volatile compounds was compared using packed column and capillary column GC both filled with the most nonpolar stationary phase (polydimethylsiloxanes (PDMS)) [56]. The higher interaction and higher temperature used for capillary-GC result in significantly lower recovery rates than those from packed column systems. Care has to be taken with the interpretation of gas analysis when GC has been used for the separation of volatile metal compounds. Since some species are very reactive, it cannot be taken for granted that the detected compounds are the only volatile metal species in the gas sample analyzed.

3.5 Detection systems

Many chromatographic separation techniques are available, and the hyphenation to another analytical technique having the appropriate sensitivity makes the identification and quantification of the separated species possible. Techniques such as liquid chromatography and gas chromatography, commercially available as integrated separation and detection systems, do not provide the necessary sensitivity if straightforward detectors such as UV, FID or TCD are used. An array of detection systems has been applied for the detection of the pg amounts of organometals from environmental samples. Among the more usual commercial detectors, electron capture (ECD) has been used for

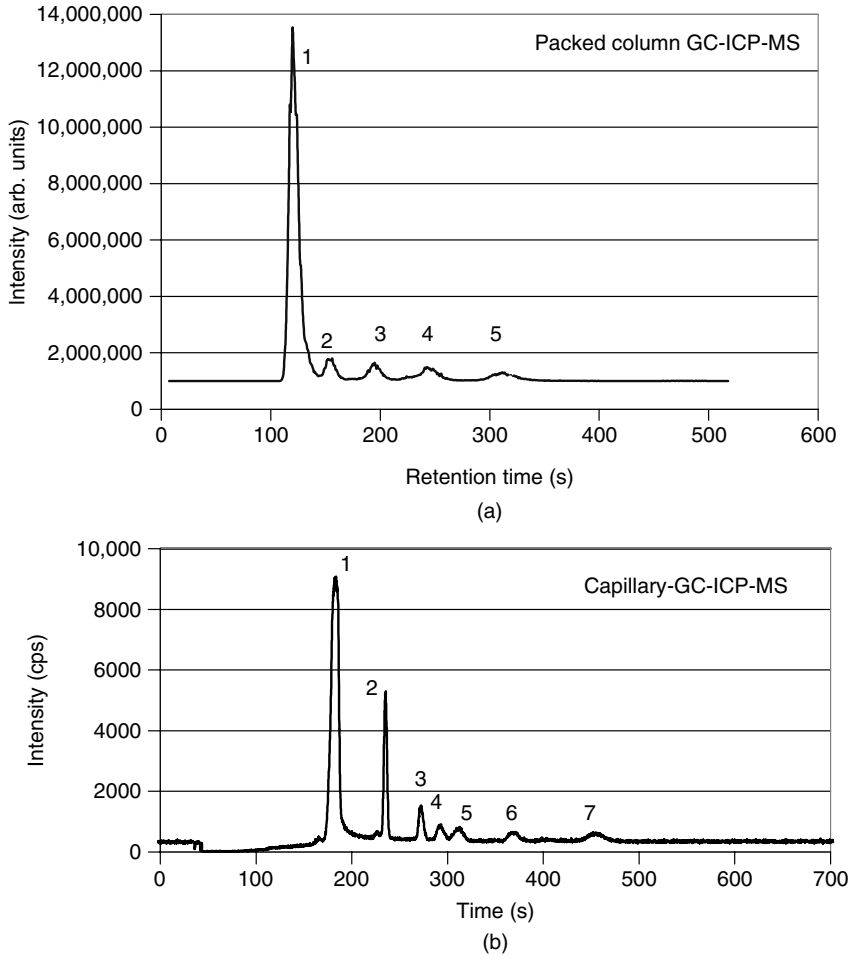

Figure 2.25.4. A comparison of two chromatograms (m/z 120, Sn) of two landfill gas samples; one was measured with a packed column separation and the other with a capillary column using cryofocusing and ICP-MS. Packed column: a U-shaped glass column filled with Supelcoport and 10% SP2100, capillary column and 25 m CP-Sil 5CB column was used. 1 is positively identified as Me_4Sn, whereas 2–8 are unknown volatile Sn species.

many compounds because of its high sensitivity to halogen atoms and polar functional groups. Despite their lack of specificity and susceptibility to contamination and changes in operating conditions, ECDs have been successfully used for organometallic compounds of tin, arsenic, selenium, lead and mercury. More widely used is the flame photometric detector (FPD), which has been specifically employed for organotin detection at the SnH emission wavelength. Moreover, an MIP-AES detector, commercially available since the mid 90s, has also been applicable especially for volatile halides. However, the small helium microwave plasma seemed to fail to deliver. It did not find broad use for the determination of volatile metal compounds in environmental gas samples, with the exception of halides. It was maybe not robust enough to deal with the quickly changing gas constituents, if environmental gas samples were introduced. Interfacing to ICP and other emission detectors is more complex, whereas mass spectrometric detectors such as ICP-MS are too expensive for routine laboratories to challenge the more commonly used systems. The use of inductively

coupled plasma-mass spectrometry (ICP-MS) as a detector for separation techniques such as gas chromatography (GC) has on the other side developed into a well-established technique in modern environmental research. A wealth of publications in the detection of organometallic compounds emerged. However, these compounds are generated in the lab by utilization of a derivatization step in order to determine organometallic nonvolatile species. Notwithstanding the possibilities of capillary-GC coupled to atomic emission detection (CGC-AED) for metal speciation, there are a number of features that make the hyphenation CGC-ICP-MS unique. State-of-the-art ICP-MS instrumentation provides sensitivities that no other technique can offer and allows multielement detection in a single run. The Ar ICP destroys the sample almost entirely, yielding atoms and ions efficiently. Generally, if organic solvents are used, carbon tends to deposit on the walls of the plasma containment tube and the cones unless a scavenger gas such as O_2 or N_2 is added to prevent these deposits and extend the lifetime of the various instrumental parts. Oxygen can also be added in a controlled way by adding a nebulized solution to the GC outlet and create wet plasma conditions. This is not to say that detrimental oxides of matrix elements do not interfere with the analyte. Detection limits vary depending on the degree of ionization of the element monitored and the background for that element. There are GC-ICP-MS systems commercially available that include temperature-controlled injector, column oven and interface in order to ensure the transport of volatile and less volatile compounds to the detector. The carrier gas from the GC was mixed with sufficient argon to add up to the 1 L/min flow necessary to carry the analyte to the plasma and eventually into the mass spectrometer of an ICP-MS.

The advantage of a GC-ICP-MS for the determination of volatile organometallic compounds in gaseous samples, often containing dozens of different volatile organic compounds, is that the powerful atomizer and ionizer almost completely destroys the matrix and so limits interferences. A further advantage is that an ICP-MS is a multielement detector although the detection is in a sequential mode. A quadrupole mass spectrometer can switch within μsec from one mass per charge ratio (m/z) to the next one. Therefore, signals of 3-second width can sufficiently be described if five different m/z are monitored using a quadrupole ICP-MS [22]. A spectral skew, however, can be noticed if more m/z need to be monitored and the peak widths are smaller (see Figure 2.25.5). Recently, Hieftje and coworkers developed a time-of-flight MS coupled to ICP [63]. This setup enables the monitoring of more than 40 m/z without losing time resolution. Figure 2.25.5 shows the direct comparison between the use of an ICP-QMS and the ICP-TOF-MS with the same time resolution per m/z.

3.6 Identification of compounds using GC-ICP-MS

The identification of volatile metal compounds is not different from other chromatographic systems. It is a combination of element-specific detection and retention time. The element-specificity of ICP-MS is often described. However, in particular when complex matrices are introduced to a chromatographic system, the matrix introduction into the plasma changes with time. This can influence the plasma and could generate interferences on the m/z of interest. Since the ICP-MS is a multichannel analyzer, it should be used in a similar way as it is used in routine solution analysis and all isotopes of the element of interest should be monitored. The isotopic fingerprint of the transient signal can reveal an interfering signal. This, however, cannot be used for mono-isotopic elements like arsenic or manganese. In order to check if any interference occurs for those elements, potential interfering ions can be monitored as well. For example, volatile organochlorine compounds could generate a transient signal on m/z 75 and 77 and would interfere with arsenic (m/z 75). More problems can be expected for elements with $m/z < 60$. It is particularly difficult to identify the interference if the element of interest is monoisotopic and no obvious interference can be allocated. In this case, it is beneficial to have a continuous internal standard

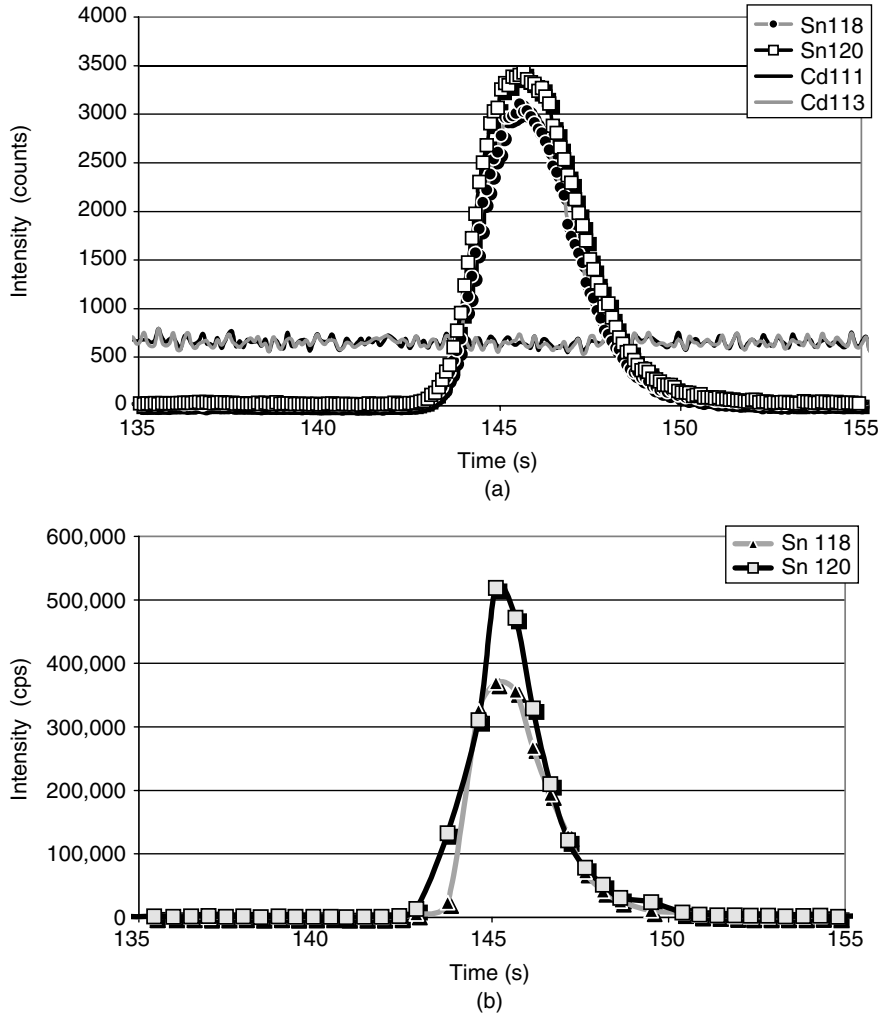

Figure 2.25.5. Spectral skew if many masses are measured with ICP-QMS in comparison to ICP-TOF-MS. The figure shows the peak of Me_2SnH_2 (measured 9 m/z if ICP-QMS was used or 30 m/z after ICP-TOF-MS). (Reproduced from *Fresenius' J. Anal. Chem.*, Species-specific isotope – ratio measurements of volatile tin and antimony compounds using capillary GC-ICP-time-of-flight MS, Haas, K., Feldmann, J., Wennrich, R. and Stärk, H. J., **370**, 587 (2001), © Springer-Verlag.)

that should produce a constant signal over the entire chromatographic run. Any plasma interference (introduction of matrix gases like CO_2 or CH_4 can significantly shift the ionization conditions) can generate positive and negative peaks of the baseline, and may be wrongly attributed to volatile metal compounds. Figure 2.25.6 shows the detection of a peak at 85 s on m/z 55 for manganese while rhodium, (m/z 103) used as an continuous internal standard, shows a fluctuation, and a peak at m/z 52 indicates the introduction of high amounts of any organic compound ($^{40}Ar^{12}C^+$ is formed in an argon plasma and shows up on m/z 52). In this setup, the GC was connected to ICP-MS via a tee-piece in which the GC-outlet was mixed with the nebulizer flow transporting the aerosol of a nebulized 10 ng Rh mL^{-1} solution that has been introduced continuously. The signal of the internal standard varies enormously, which points to a massive elution of a compound, which in turn has

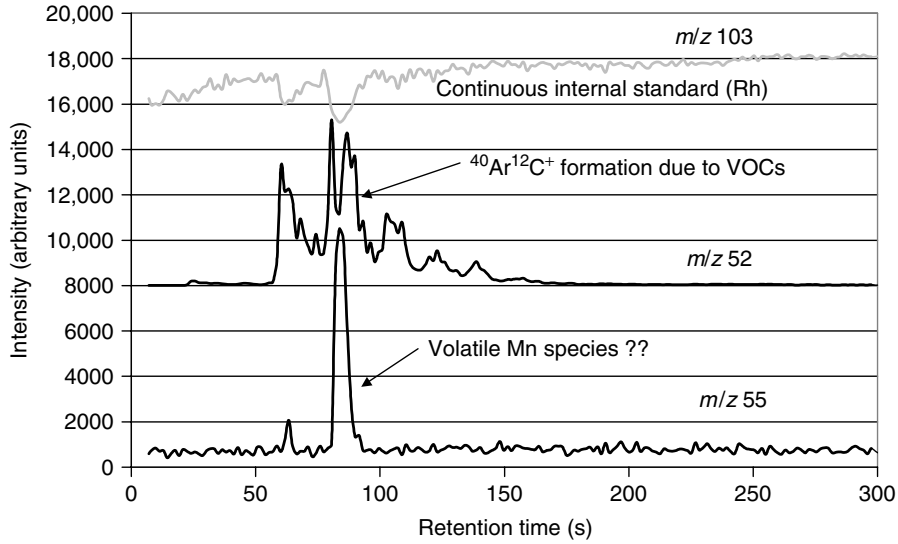

Figure 2.25.6. Chromatogram of an indoor gas sample that contained enormous amounts of VOCs (cigarette smoke). Besides m/z 55 for Mn, the m/z 103 for the internal standard Rh and m/z 52 for the Ar–C interference as an indicator for VOCs were also measured. The large variation of Rh, at the same time as the peak on m/z 55 appears, would suggest that it is probably an artifact and not a volatile Mn species.

a significant influence on the plasma conditions. It is common that volatile organic compounds, often in concentrations exceeding those of the VMCs by many orders of magnitude, can be generated in microcosms or in the environment. To summarize: in order to guarantee the element-specific detection, it is necessary to record the plasma performance simultaneously to the chromatographic run either by the introduction of a volatile gas such as Xe, which is added to the make-up gas, or by a postcolumn addition of a nebulized solution that contains Rh or In. Furthermore, the occurrence of possible interfering clusters should be monitored in addition to the monitoring of other isotopes of the element of interest: this practice guarantees element-specific detection.

For a clear identification, the retention time should be matched with those of a VMC standard. However, the real challenge is to get standards. Since most of the standards have to be synthesized, other approaches have often been used to identify unknown peaks using the Kovacs index approach of the retention time to boiling point correlation (see Figure 2.25.7). Since the number of possible species is limited for individual elements, it is relatively easy to assign certain compounds to the recorded peaks, in particular, for those that are very volatile. Care has to be taken for those compounds that interact in a different manner with the chromatographic material because they will show a different behavior that is not governed by the correlation curve (e.g. Hg^0). It is good analytical practice to spike the sample with the species to be identified, since the matrix can shift the retention time significantly. When no suitable standard is available, spiking with a different species-specific standard will give information about the retention time shift, when the sample is measured. We have successfully used $W(CO)_6$, as any shift of retention time has a significant effect on the elution of this compound [22].

However, it has been shown that spiking of standards does not always identify the compounds correctly since ICP-MS destroys any molecular information. Soft ionization like electron impact (EI) has to be employed to get a fragmentation pattern, which gives clues to their molecular structure. The concept of identification has been illustrated and described above (see also Figure 2.25.8). It

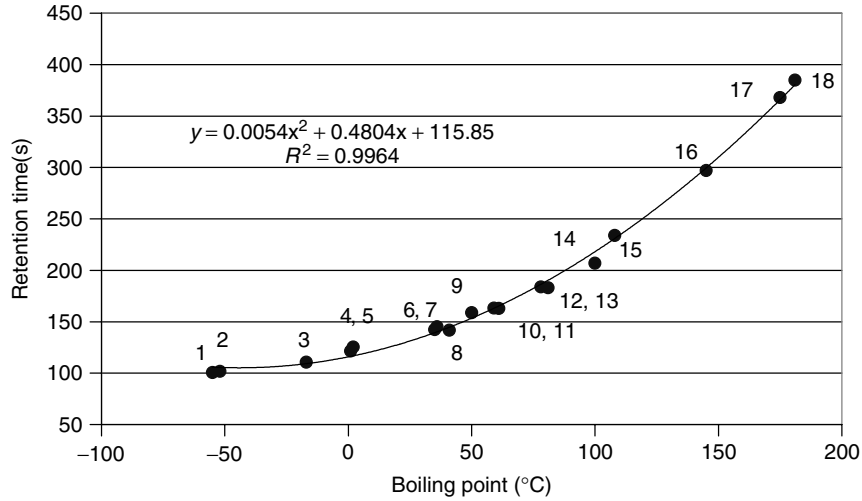

Figure 2.25.7. Correlation of retention time and boiling point is a useful instrument to characterize unknown peaks, and streamline the synthesis of VMC standards. 1: AsH_3, 2: SnH_4, 3: SbH_3, 4: $MeSnH_3$, 5: $MeAsH_2$, 6: $MeSbH_2$, 7: Me_2SnH_2, 8: Me_2AsH, 9: Me_3As, 10: Me_2SbH, 11: Me_3SnH, 12: Me_3Sb, 13: Me_3Sn, 14: $BuSnH_3$, 15: Me_3SnEt, 16: Me_2SnEt_2, 17: $W(CO)_6$, 18: Et_4Sn [51].

has been shown that for the identification of certain organometallic compounds in a gas sample gas chromatography-mass spectrometry (GC-MS) is necessary. EI ionization produces molecular fragments from which the molecular structure of the eluting species can be elucidated. The GC-MS is not very sensitive, therefore the analytes in the gas samples have to be significantly preconcentrated. If a complex matrix like landfill gas or headspace gas from microcosms has to be analyzed, an increase of VOCs is inevitable, and the interferences increase considerably because of the use of a non-element-specific detection. A cleanup using a packed column provides the opportunity to trap large amounts of gases on-column using cryogenic fluids and separates the compounds reasonably well. Small gas fractions that contain the species of interest besides a few other VOCs can be collected and injected onto a capillary column with a different stationary phase resulting in a different chromatographic separation. With this approach, it was possible to identify trace amounts of trimethylstibine (Me_3Sb), tetramethyl tin (Me_4Sn) and dimethyldiethyl tin (Me_2Et_2Sn) in landfill gas and trimethylbismuthine (Me_3Bi) in fermentation gas from a sewage treatment plant [59].

3.7 Quantification

There are many ways to achieve a quantitative answer if one determines the amount of volatile metal compounds in a gas sample. The most straightforward approach is the application of an external calibration using different gas standards (e.g. Me_4Sn, Me_2Se, etc.) [57]. This has been demonstrated to work for a number of compounds. The dynamic range of those calibrations varies (between 1 pg and 1000 pg for several volatile metal compounds (Me_4Pb, Et_4Pb, Me_4Sn, Et_4Sn, Hg^0, Me_2Hg, Et_2Hg, Me_2Se) and detection limits in the femtogram level were given except for Me_2Se (2.5 pg) [57]. Reproducibility of individual injections were measured between 1 and 10%. The problem with those standards, however, is that it is not easy to make up standards that are stable and can be reproducibly generated in concentrations, which are relevant to the samples. Another way is the generation of a dynamic atmosphere using penetration tubes, which has been demonstrated nicely by Gallus and Heumann for Me_2Se [64]. They added the isotopically labeled Me_2Se spike to the sample. This made it possible to do direct quantification using the isotope dilution technique

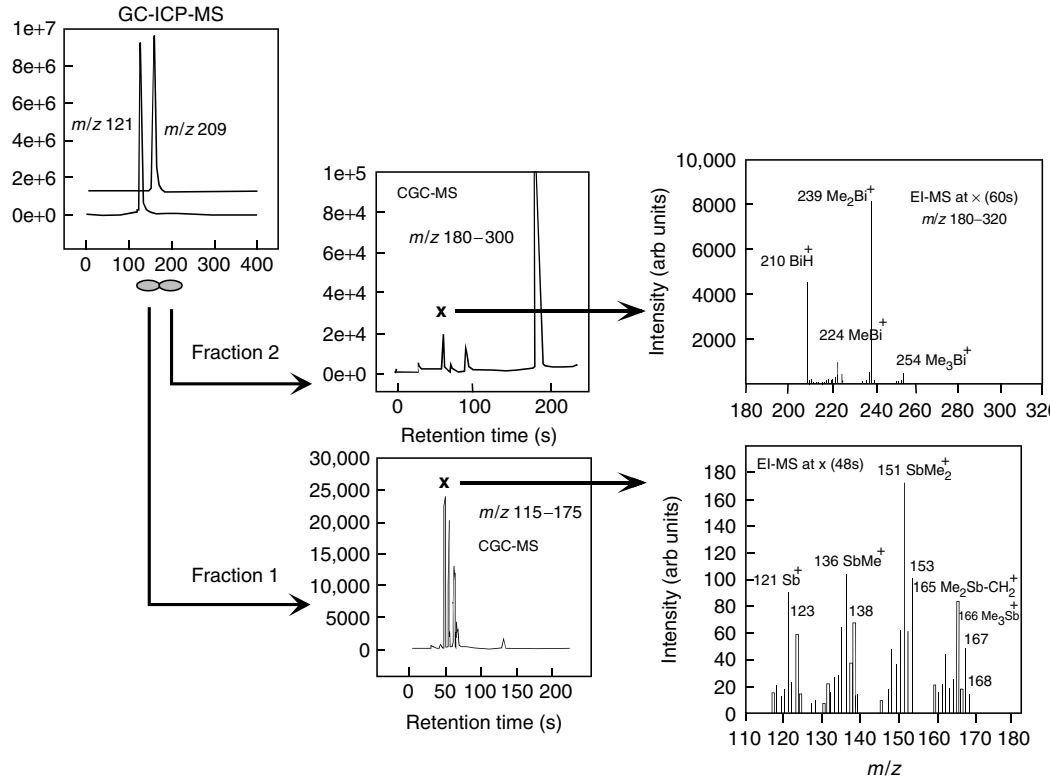

Figure 2.25.8. Two-dimensional GC-separation for the identification of VMCs in a very complex matrix of dozens of different VOCs using GC-MS. According to Feldmann *et al*. [59].

(ID-GC-ICP-MS). Accuracy of better than 1% and superb reproducibility was demonstrated. This approach excludes the above-mentioned problems of reproducibility but cannot be used for all VMCs. The other approach is the generation of a static gas standard in a matrix gas like air or nitrogen after utilization of a derivatization reaction [46]. If hydride generation is employed, such a purging step can be used to produce the matrix gas, and the purged gas can easily be collected in Tedlar bags. This approach has the advantage that it generates a gas standard that contains moisture and is therefore similar to the headspace of cultures or other environmental gas samples.

If, however, no stable volatile compound is available, the ICP-MS can be calibrated with a postcolumn addition of a solution. By knowing the nebulization efficiency of the solution and the assumption of a 100% elution efficiency from the GC column, the amount of the VMCs in the sample could be determined within ±30% [37]. The reason for the imprecision is that the technique is not a species-specific calibration. However, it is especially important if the species are not known or no stable standard of the metal species can be generated (e.g. Me_3Bi). This technique is sufficiently precise and accurate to use for environmental analysis of VMCs. In any case, the reproducibility of external calibration can be increased by using an internal standard like the continuously nebulized Rh solution.

4 FUTURE DEVELOPMENTS

The real challenge here is to identify small quantities of unknown VMCs in very complex matrices like landfill gas or natural gas condensates.

Tunable plasmas for GCs would take the determination of volatile metal compounds a step further. Unequivocal identification is possible if soft ionization conditions are employed, changing the ionization conditions in microseconds so that the eluting compounds can be fragmented to the elements and sufficiently ionized. The development of tunable plasma and their applications were reviewed recently [65]. This is also described in Chapter 5.5, Volume 1 [66]. So if VMCs are eluting, and the ionization changes from soft to hard in a few steps, it will produce a transient mass spectrum from one eluting peak. This means that at least three different mass spectra can be recorded within one run to give information about the molecular mass of the eluting compound, its structure and its element composition. Whether this technique can be used for real samples has to be investigated.

In order to increase the detection limits for the identification of VMCs, a promising approach was recently developed. A temperature-programmable injector for cryofocusing of volatile compounds was used for the preconcentration of less volatile compounds after a major cleanup procedure that would lower the detection limits of GC-ICP-MS dramatically. This has already been demonstrated for the detection of low levels of TBT after ethylation in open sea water samples (detection limits of TBT in water is estimated to be $0.1\ \mathrm{ng\,L^{-1}}$) [67].

Furthermore, there is currently a development to do isotope ratio measurements on small quantities of VMCs (e.g. Me_3Sb, Et_4Pb) in environmental samples or in microbiological experiments in which the role of VMCs in the biogeochemical cycle of metals is studied [68]. In most cases, a quadrupole ICP-MS gives sufficient precision to tackle the analytical problem, but if isotopic fractionation of metals are a focus of the investigations, ICP-TOF-MS or even multi collector magnetic sector ICP-MS have to be employed to give high-precision isotope ratio measurements on the individual VMCs. Recently, it has been shown, when GC-multi collector ICP-MS has been used for the determination of the isotope ratio of Sb (i.e. 121/123) in Me_3Sb, that the accurate measurement of the isotope ratio of these VMCs might suffer from isotopic fractionation during the chromatographic separation [69].

Finally, the biovolatilization of radioactive compounds such as $Me_2^{210}Po$ can be a focus of future research, since it has recently been proven that microorganisms are able to generate volatile polonium compounds [70].

5 REFERENCES

1. Merian, E., *Metals and their Compounds in the Environment: Occurrence, Analysis and Biological Relevance*, VCH Publishers, New York, 1991.
2. Batley, G. E., *Trace Element Speciation: Analytical Methods and Problems*, CRC Press, Boca Raton, FL, 1989.
3. Butcher, S. S., Charlson, R. J., Orians, G. H. and Wolfe, G. V., *Global Biogeochemical Cycles*, Academic Press, London, 1992.
4. Thayer, J. S., *Environmental Chemistry of the Heavy Metals: Hydrido and Organo Compounds*, VCH Publishers, New York, 1995.
5. Craig, P. J., *Organometallic Compounds in the Environment*, 2nd ed., Wiley, Chichester, 2003.
6. Craig, P. J. and Glockling, F., *The Biological Alkylation of Heavy Metals*, The Royal Society of Chemistry, 1988.
7. Irgolic, K. J., Determination of organometallic compounds in environmental samples with element-specific detectors, in *Trace Metal Analysis and Speciation*, Krull, I. S. (Ed.), Elsevier, 1991.
8. Feldmann, J., Riechmann, T. and Hirner, A. V., *Fresenius' J. Anal. Chem.*, **354**, 620 (1996).
9. Amouroux, D., Tessier, E. and Donard, O. F. X., *Environ. Sci. Technol.*, **34**, 988 (2000).
10. Wallschläger, D., Kock, H. H., Schroeder, W. H., Lindberg, S. E., Ebinghaus, R. and Wilken, R. D., *Atmos. Environ.*, **34**, 3745 (2000).
11. Laturnus, F., *Environ. Sci. Pollut. Res.*, **8**, 103 (2001).
12. Hansen, D., Duda, P. J., Zayed, A. and Terry, N., *Environ. Sci. Technol.*, **32**, 591 (1998).
13. Hirner, A. V., Feldmann, J., Krupp, E., Grümping, R., Goguel, R. and Cullen, W. R., *Org. Geochem.*, **29**, 1765 (1998).
14. Gassmann, G. and Glindemann, D., *Angew. Chem., Int. Ed. Engl.*, **32**, 761 (1993).
15. Pecheyran, C., Lalere, B. and Donard, O. F. X., *Environ. Sci. Technol.*, **34**, 27 (2000).
16. Schweigkofler, M. and Niessner, R., *Environ. Sci. Technol.*, **33**, 3680 (1999).
17. Peterson, B., *Ann. Occup. Hyg.*, **32**, 385 (1988).
18. Challenger, F., *Chem. Rev.*, **36**, 315 (1945).
19. Feldmann, J. and Hirner, A. V., *Int. J. Environ. Anal. Chem.*, **60**, 339 (1995).
20. Donard, O. F. X. and Weber, J. H., *Nature*, **332**, 339 (1988).

21. Jackson, J. A. A., Blair, W. R., Brinckman, F. E. and Iverson, W. P., *Environ. Sci. Technol.*, **16**, 1 (1982).
22. Haas, K., Feldmann, J., Wennrich, R. and Stärk, H. J., *Fresenius' J. Anal. Chem.*, **370**, 587 (2001).
23. Michalke, K., Meyer, J., Hirner, A. V. and Hensel, R., *Appl. Organomet. Chem.*, **16**, 221 (2002).
24. Feldmann, J., Krupp, E. M., Glindemann, D., Hirner, A. V. and Cullen, W. R., *Appl. Organomet. Chem.*, **13**, 739 (1999).
25. Feldmann, J., *J. Environ. Monit.*, **1**, 33 (1999).
26. Feldmann, J. and Cullen, W. R., *Environ. Sci. Technol.*, **31**, 2125 (1997).
27. Van Fleet-Stalder, V. and Chasteen, T. G., *J. Photochem. Photobiol. B: Biol.*, **43**, 193 (1998).
28. Pecheyran, C., Amouroux, D. and Donard, O. F. X., *J. Anal. At. Spectrom.*, **13**, 615 (1998).
29. Richardson, B. A., *Lancet*, **335**, 670 (1990).
30. Richardson, B. A., *J. Forensic Sci. Soc.*, **34**, 199 (1994).
31. Andrewes, P., Cullen, W. R., Feldmann, J., Koch, I., Polishchuk, E. and Reimer, K. J., *Appl. Organomet. Chem*, **12**, 827 (1998).
32. Jenkins, R. O., Craig, P. J., Goessler, W., Miller, D., Ostah, N. and Irgolic, K. J., *Environ. Sci. Technol.*, **32**, 882 (1998).
33. Cullen, W. R. and Reimer, K. J., *Chem. Rev.*, **89**, 713 (1989).
34. Gharieb, M. M., Kierans, M. and Gadd, G. M., *Mycol. Res.*, **103**, 299 (1999).
35. Koch, I., Feldmann, J., Lintschinger, J., Serves, S. V., Cullen, W. R. and Reimer, K. J., *Appl. Organomet. Chem.*, **12**, 129 (1998).
36. Mester, Z. and Sturgeon, R., *J. Anal. At. Spectrom.*, **16**, 470 (2001).
37. Feldmann, J., *J. Anal. At. Spectrom.*, **12**, 1069 (1997).
38. Gao, S. and Burau, R. G., *J. Environ. Qual.*, **26**, 753 (1997).
39. Schroeder, W. H. and Jackson, R. A., *Int. J. Environ. Anal. Chem.*, **22**, 1 (1985).
40. Osberghaus, U. and Helmers, E., in *Sampling and Sample Preparation: A Practical Guide for Analytical Chemists*, Stoeppler, M. (Ed.), Springer, Berlin, 1997.
41. Falter, R., *Chemosphere*, **39**, 1037 (1999).
42. Cao, X. L. and Hewitt, C. N., *J. Chromatogr. A*, **688**, 368 (1994).
43. McClenny, W. A. and Colon, M., *J. Chromatogr. A*, **813**, 101 (1998).
44. Sommar, J., Feng, X. B. and Lindqvist, O., *Appl. Organomet. Chem.*, **13**, 441 (1999).
45. Evans, G. F., Lumpkin, T. A., Smith, D. L. and Somerville, M. C., *J. Air Waste Manage. Assoc.*, **42**, 1319 (1992).
46. Haas, K. and Feldmann, J., *Anal. Chem.*, **72**, 4205 (2000).
47. Hoshika, Y., Nishikitani, M., Yokoyama, K. and Araki, S., *Anal. Sci.*, **13**, 505 (1997).
48. Fugit, J. L., Dutaur, L., Simon, V., Riba, M. L. and Torres, L., *Fresenius Environ. Bull.*, **5**, 682 (1996).
49. Lipari, F., *J. Chromatogr.*, **503**, 51 (1990).
50. Andino, J. M. and Butler, J. W., *Environ. Sci. Technol.*, **25**, 1644 (1991).
51. Haas, K. and Feldmann, J., unpublished results (2002).
52. Mester, Z., Sturgeon, R. and Pawliszyn, J., *Spectrochem, Acta, Part B*, **56**, 233 (2001).
53. Feldmann, J., Naëls, L. and Haas, K., *J. Anal. At. Spectrom.*, **16**, 1040 (2001).
54. Amouroux, D., Tessier, E., Pecheyran, C. and Donard, O. F. X., *Anal. Chim. Acta*, **377**, 241 (1998).
55. Mester, Z. N., Lam, J., Sturgeon, R. and Pawliszyn, J., *J. Anal. At. Spectrom.*, **15**, 837 (2000).
56. Krupp, E., Analytik umweltrelevanter Metall(oid)spezies mittels gaschromatographischer Trennmethoden, PhD thesis, University of Essen, Cuvillier, Göttingen, 1999.
57. Pecheyran, C., Quetel, C. R., Martin, F. M. and Donard, O. F. X., *Anal. Chem.*, **70**, 2639 (1998).
58. De Jonghe, W. R. A., Chakraborti, D. and Adams, F. C., *Anal. Chem.*, **52**, 1974 (1980).
59. Feldmann, J., Koch, I. and Cullen, W. R., Species-specific isotope – ratio measurements of volatile tin and antimony compounds using capillary GC-ICP-time-of-flight MS, *Analyst*, **123**, 1069 (1998).
60. Egyed, M. and Wood, G. C., *Sci. Total Environ.*, **190**, 11 (1996).
61. Pavageau, M. P., Pecheyran, C., Demange, M. and Donard, O. F. X., *J. Anal. At. Spectrom.*, **18**, 323 (2003).
62. Bouyssiere, B., Baco, F., Savary, L., Garraund, H., Gallup, D. L. and Lobinski, R., *J. Anal. At. Spectrom.*, **16**, 1329 (2001).
63. Myers, D. P. and Hieftje, G. M., *Microchem. J.*, **48**, 259 (1993).
64. Gallus, S. M. and Heumann, K. H., *J. Anal. At. Spectrom.*, **11**, 887 (1996).
65. Marcus, R. K., Evans, E. H. and Caruso, J. A., *J. Anal. At. Spectrom.*, **15**, 1 (2000).
66. Marcus, R. K., Glow discharge plasmas as tunable sources for element speciation, in *Handbook of Elemental Speciation: Techniques and Methodology*, Cornelis, R., Caruso, J., Crews, H. and Heumann, K. (Eds.), Wiley, Chichester, 2003, Chapter 5.5, pp. 335–355.
67. Rajendran, R. B., Tao, H., Miyazaki, A., Ramesh, R. and Ramachandran, S., *J. Environ. Monit.*, **3**, 627 (2001).
68. Krupp, E. M., Pecheyran, C., Pinaly, H., Motelica-Heino, M., Koller, D., Young, S. M. M., Brenner, I. B. and Donard, O. F. X., *Spectrochim, Acta, Part B*, **56**, 1233 (2001).
69. Wehmeier, S., Ellam, R. M. and Feldmann, J., *J. Anal. At. Spectrom.*, **18**, 1001 (2003).
70. Momoshima, N., Song, L. X., Osaki, S. and Maeda, Y., *Environ. Sci. Technol.*, **35**, 2956 (2001).

2.26 Metal Complexes of Humic Substances

Klaus G. Heumann
Johannes Gutenberg-University Mainz, Mainz, Germany

1 ABSTRACT

Humic substances (HS) with their polyelectrolytic functional groups are able to form HS–metal complexes with many metal ions. Because of the great diversity of the composition and structure of HS molecules, it is only possible to determine HS–metal fractions instead of individual molecules. Separation into different fractions by their molecular size, using ultrafiltration or size exclusion chromatography (SEC), is most often applied for the characterization of HS–metal complexes. Hyphenated techniques, such as coupling of liquid chromatographic methods with inductively coupled plasma mass spectrometry (HPLC-ICP-MS), are sensitive analytical methods for the characterization of HS–metal complexes at the usually low concentration level in environmental aquatic samples on the basis of an element-specific detection. On-line structural information can be obtained by a UV flow-through cell, but more detailed structural information is only available after preconcentration steps that often imply a risk of species transformation. Typical chromatograms by SEC-ICP-MS and SEC-ICP-AES (atomic emission spectrometry) are shown for HS–metal fractions of aquatic samples from different origin. In these cases, organic fractions can be, in general, identified by also measuring the carbon track with the corresponding mass or atom spectrometric method. Quantification of separated HS–metal fractions and its validation can be carried out best by isotope dilution mass spectrometric (IDMS) methods, which are also the only possibility, up to now, to receive 'real-time' concentrations of chromatographically separated HS–metal fractions. Specific interactions of HS with sulfur-containing functional groups were observed for Hg(II), and kinetically stable HS–Cr(III) and HS–Co(III) complexes were found in accordance with the classical theory of metal complexes.

2 INTRODUCTION

Natural aquatic systems contain dissolved organic carbon (DOC), which usually vary in the concentration range of 0.1–100 mg L^{-1} [1]. Depending on the geochemical composition of the environment,

Handbook of Elemental Speciation II: Species in the Environment, Food, Medicine & Occupational Health
Edited by R. Cornelis, H. Crews, J. Caruso and K. G. Heumann
 ISBN: 0-470-85598-3 (HB)

50% and more of this DOC are usually humic substances (HS). HS are heterogeneous polyelectrolytic macromolecules with a complex structure [2]. These HS are formed by microbiological processes with plant and animal residues and consist of molecular masses that can vary by several orders of magnitude. Using a standard method of the International Humic Substance Society, the dissolved organic matter in water is separated from particles by filtration with a 0.45-μm pore-sized filter. After adsorption at XAD-8 material, the nonhumic substances are first eluted and then humic acids (HA) are separated from fulvic acids (FA) by their different solubility in acids [3].

HS contain negatively charged and polar functional groups, such as phenolic, carboxylic, carbonyl, and amino groups, and it has long been recognized that HS are therefore able to complex metal ions [4]. Even if the HS–metal interaction depends strongly on the origin of the humic substance, which limits possible comparisons, stability constants of complexation have been published in the past, for example, in [5]. The complexation of metal ions by HS can strongly influence the mobility of metals in the environment [6, 7], which is one of the most important reasons to get a better knowledge about this type of elemental species.

One of the consequences of the complex structure of HS is the fact that there is not a great probability to find exactly identical molecules in the environment. This also means that all HS–metal complexes in an aquatic system differ, at least slightly, from each other in their structure and composition. It is therefore not possible to determine individual HS–metal species with any of the analytical methods available. Fractionation by using different separation methods is applied to characterize various groups of HS–metal species. The analysis of HS–metal complexes can therefore only be carried out for a fraction of HS similar in its behavior determined by the used separation method. One of the most frequently used fractionation methods for HS is SEC, which separates HS as well as HS–metal species by their molecular mass, or more correctly, by their molecular size [8, 9]. This separation method is limited by possible adsorptive interactions of HS with the SEC gel and by a lack of HS molecular mass standards. Nevertheless, this chromatographic method is suitable to determine possible fingerprints of HS fractions and their metal species of samples from different origin. On the other hand, other separation techniques have also been applied to HS and HS–metal complexes, such as metal-affinity chromatography [10], reversed-phase chromatography [11], capillary electrophoresis [12], and multistep ultrafiltration [13].

To follow the interaction of metal ions with HS, electroanalytical methods like anodic stripping voltammetry and ion-selective electrodes [14, 15], as well as spectrophotometric methods measuring the fluorescence quenching caused by metal complexation [16], have been used in the past. In principle, electroanalytical methods are able to differentiate between complex bonded and 'free' metal ions, so that the determination of the HS–metal species is always obtained by subtraction. More modern systems are hyphenated techniques where atom spectrometric methods for element-specific detection are coupled with corresponding procedures of high-performance liquid chromatography (HPLC). Because of the very well adapted liquid flow rate of HPLC with an inductively coupled plasma (ICP), coupling of atom emission spectrometry (ICP-AES) [17] and mass spectrometry (ICP-MS) [9, 18, 19] are powerful techniques for the determination of fractions of HS–metal species. These coupling systems allow extremely sensitive determinations of metals in HS fractions by transient signals. Usually, ICP-AES is a factor of 10–100 less sensitive than ICP-MS, where picogram amounts of metals per second can still be detected [18]. The organic ligand of the HS–metal species is not determined by these element-specific methods. A flow-through cell with UV detection is therefore usually integrated in the HPLC-ICP-AES and HPLC-ICP-MS system, respectively, which allow registration of organic ligands. A wavelength of 254 nm is often used to detect aromatic units in HS or those with conjugated double bonds. A SEC-ICP-AES chromatogram of different metals as well as the corresponding UV chromatogram for a seepage water from a harbor mud is shown in Figure 2.26.1 [17].

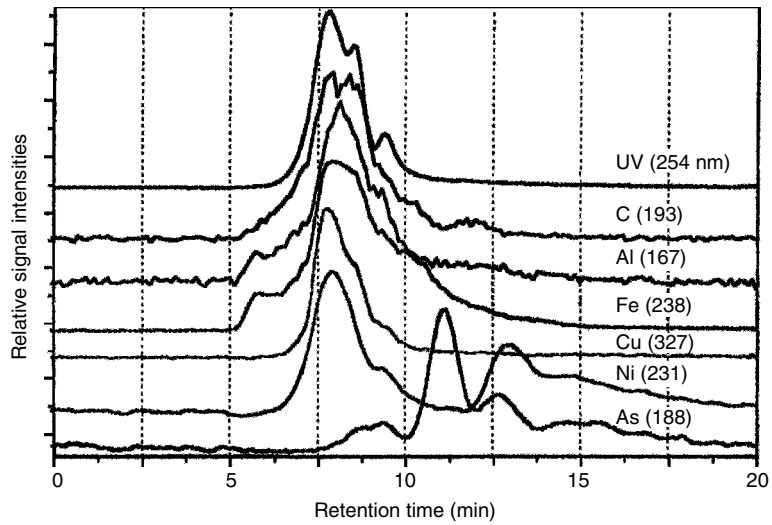

Figure 2.26.1. SEC-ICP-AES chromatogram of different elements in a seepage water from a harbor mud together with the corresponding UV absorption curve. For better representation, the different curves are parallely shifted upwards on the y-axis. (Reproduced from Reference [17] by permission of GIT – Verlag GmbH & Co KG.)

The chromatogram clearly shows that aluminum, iron, and copper are eluted at the same retention time as the UV absorbing HS material, whereas a substantial portion of the total nickel leaves the column distinctly later (at about 13 min retention time), which corresponds to free Ni^{2+} ions. Because of its anionic character, most of the arsenic does not interact with HS and therefore also elutes at higher retention times. A specific carbon emission line of the ICP-AES spectrum and the ^{12}C or ^{13}C mass chromatogram by ICP-MS, respectively, can also be used to identify organic material. This can be seen in Figure 2.26.1 by the carbon emission at 193 nm, which essentially follows the UV absorption curve. However, in many cases UV detection at 254 nm does not correlate with the amount of organic material, which can be seen from Figure 2.26.2, where the UV and the corresponding ^{12}C chromatogram by ICP-MS of a FA sample, isolated from brown water, are represented [9]. Whereas this figure clearly shows that copper and the major portion of molybdenum are eluted with the UV-absorbing fulvic acid fraction, it cannot be seen by the UV curve that additional organic material is eluted at about 12 min retention time together with the other molybdenum fraction. This becomes only obvious by simultaneous ICP-MS detection of the ^{12}C intensity. In addition, the peak areas of the different carbon peaks directly correlate with the DOC amount in these fractions.

The element-specific detection by ICP-MS is sensitive enough to determine metal mass flows in HS–metal fractions in the lowest picogram per second range. This enables determination of HS–metal species down to a level of less than $1\,\mu g\,L^{-1}$ (see Section 3). The DOC mass flow of SEC-separated brown water samples usually lies in the upper nanogram per second range (Section 3). This low mass flow of DOC limits the analytical methods that can be applied on-line for direct structural characterization of the HS ligands of the corresponding metal complexes. With respect to its sensitivity, UV absorption is therefore the only possible method that can be used in connection with a HPLC-ICP-AES or HPLC-ICP-MS system. The structural information of UV absorption curves is limited so that it will be an important challenge in the future to develop more sensitive nuclear magnetic resonance (NMR) or MS methods.

Structural elements of HS can be determined in isolated HS at higher concentrations by NMR [20], laser desorption MS [21], electrospray ionization

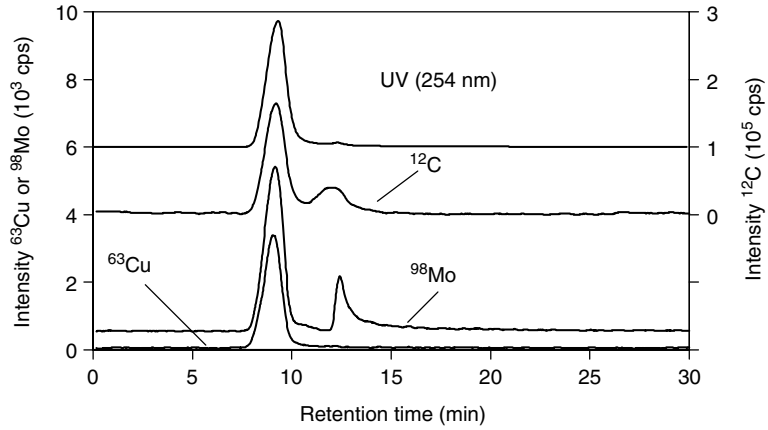

Figure 2.26.2. SEC-ICP-MS chromatogram of copper, molybdenum and carbon of an FA sample prepared from brown water together with the corresponding UV absorption curve [9]. For better representation, the different curves are parallely shifted upwards on the y-axis. (Reproduced from *Fresenius' J. Anal. Chem.*, Determination of heavy metal complexes with humic substances by HPLC/ICP-MS coupling using on-line isotope dilution technique, Vogl, J. and Heumann, K. G., **359**, 438, Figure 4 (1997), © Springer-Verlag.)

MS [22], and pyrolysis gas chromatography-mass spectrometry (GC-MS) [23]. None of these methods is able to totally characterize the HS molecules or ligands, but they enable the determination of characteristic functional groups, for example, typical fingerprints of spectra. However, if different sample preparation steps are involved before the characterization of HS–metal species, conversion of the original HS molecule can easily occur. On the other hand, the HS–metal complexes are part of a dynamic system in which ion exchange of metal ions can occur if the conditions are changed. With respect to these restrictions, direct analysis of the original sample by hyphenated techniques without or with only minimal sample pretreatment is the best choice to receive information on the real situation of HS–metal species in the environment. The discussed problems during sample preparation are also the reason why HS–metal speciation is best possible in aquatic samples and not, for example, in solid samples such as soil where additional extraction steps must be applied. The analytical methods available for direct determinations of elemental species in solid samples, for example, X-ray absorption methods like X-ray absorption near edge structure (XANES) or extended X-ray adsorption fine structure (EXAFS) (see Chapter 6 in Volume 1 of the Handbook), are not sensitive enough to analyze most of the environmental samples at their low concentration level.

3 QUANTIFICATION OF HS–METAL SPECIES AND ITS VALIDATION

Because separation of HS–metal species is not possible for an individual compound of exactly identical composition and structure, only fractions of metal complexes with HS can be quantified. Because of the limitation that a molecular mass of these fractions can therefore not be specified, it is also not possible to quantify the HS–metal species itself but only the metal concentration in the corresponding fraction. The most elegant way to receive such a result with high accuracy is application of the species-unspecific IDMS technique. A corresponding HPLC-ICP-IDMS system is described in Chapter 7.1 of Volume 1 of this Handbook (Figure 7.1.5). In this case, isotopically enriched spike solutions of the metals to be determined in the HS–metal complexes are totally mixed with the separated species fractions. The metal isotope ratio of the isotope-diluted fractions is then measured by ICP-MS. From the corresponding transient signals, the mass flow of the metal can be calculated under certain conditions by usually used IDMS equations [18].

A mass flow chromatogram of copper from a brown water sample together with the corresponding UV absorption curve of this sample is shown in Figure 2.26.3 by using SEC separation. In the case of this sample, the copper content directly follows the UV absorbing organic material, which means that only HS with aromatic structural units or conjugated double bonds interact with the copper ion. From the determined mass flow and the applied sample volume for separation, one can easily calculate the concentration of the metal ion in the corresponding HS fraction. HPLC-ICP-IDMS is the only possibility, up to now, which allows real-time determinations of chromatographically separated elemental species. In addition, the results for the different fractions are accurate as well under certain conditions because the measurement of only an isotope ratio is not limited by matrix effects, which is normally a problem in ICP-MS determinations. One precondition for accurate results is the necessity that no substance was lost during the separation process and that there is no discrimination in the isotope diluted sample between the (species-unspecific) spike compound and the separated HS–metal fraction by the ICP-MS system (see Chapter 7.1 of Volume 1 of the Handbook).

HPLC-ICP-IDMS is also a potential system to quantify the DOC content in separated HS–metal fractions by using, in addition to enriched metal isotopes, a ^{13}C-enriched organic compound in the spike solution, for example, ^{13}C-benzoic acid [24]. Figure 2.26.4 represents the DOC and copper SEC chromatogram of a brown water sample,

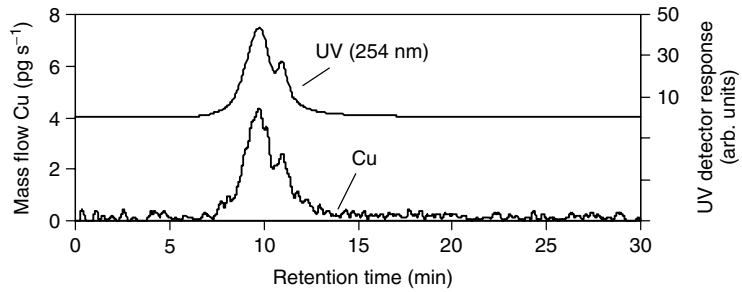

Figure 2.26.3. SEC-ICP-IDMS mass flow chromatogram of copper of a brown water sample together with the corresponding UV absorption curve. (Reproduced from *Fresenius' J. Anal. Chem.*, Determination of heavy metal complexes with humic substances by HPLC/ICP-MS coupling using on-line isotope dilution technique, Vogl, J. and Heumann, K. G., **359**, 438, Figure 4 (1997), © Springer-Verlag [9].)

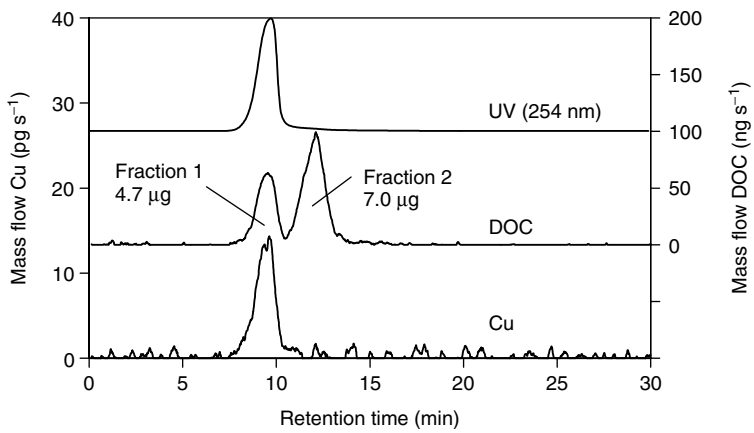

Figure 2.26.4. SEC-ICP-IDMS mass flow chromatogram of copper and DOC of a brown water sample together with the corresponding UV absorption curve [25].

which shows that copper only interacts with the first fraction of organic matter. This first fraction of higher molecular mass consists of UV absorbing HS, whereas the second DOC fraction does not show these properties. This again also demonstrates the importance of the carbon measurement by ICP-MS because only this type of detection and not the UV absorbance indicates a second fraction of organic material.

The best way to validate the quantitative results of HS–metal fractions is the determination of the total metal content in the nonseparated sample and comparison with the sum of the different separated HS–metal species. An example is given in Figure 2.26.5 for a SEC chromatogram of a river water sample by determining molybdenum and copper in different fractions with ICP-IDMS [18]. Molybdenum shows three sharp peaks but not baseline separated, which can be related to UV absorption peaks at corresponding retention times. Copper shows two well-separated fractions that correspond to the first and second UV absorption band. From the metal peak areas, the concentrations of these HS–metal species were calculated, and they are listed in Table 2.26.1. The total molybdenum and copper concentrations in the original nonseparated sample were also determined by ICP-IDMS, and they are also summarized in Table 2.26.1. The results show that the sum of concentrations of the different HS–metal fractions agree well with the total metal concentration of the corresponding metal in the original sample. The sum of the HS–Cu fraction fits the total concentration a little better than in the case of molybdenum. However, this is easy to understand by the much higher uncertainty in the determination of the peak area of the three molybdenum fractions not baseline resolved compared to the two well separated copper fractions. The example represented by Figure 2.26.5 also demonstrates that under the used SEC separation conditions (TSK 3000 column; eluant: pure water), all molybdenum and copper ions were eluted within the different fractions, which cannot be automatically assumed in SEC separation because sometimes adsorption effects may also result in a lack of eluted substances [19]. If this happens during SEC or other separation methods, validation of the results for eluted HS–metal fractions becomes a problem.

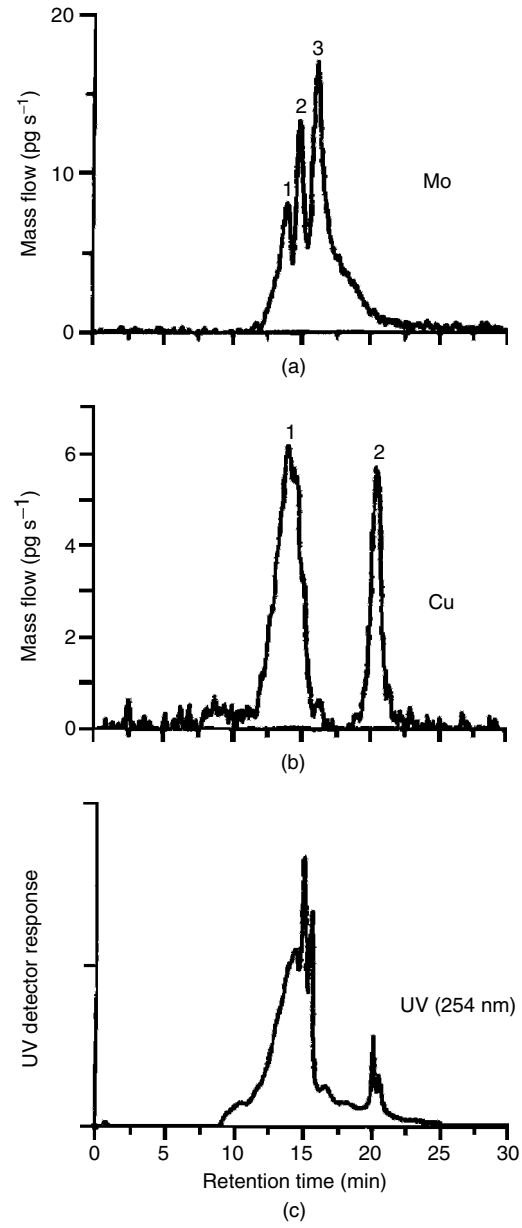

Figure 2.26.5. SEC-ICP-IDMS mass flow chromatogram of molybdenum and copper of a river water sample together with the corresponding UV absorption curve. (Reproduced from *Fresenius' J. Anal. Chem.*, Rottmann, L. and Heumann, K. G., **350**, 221, Figure 6 (1994), © Springer-Verlag [18].)

Table 2.26.1. Concentrations of different HS–Mo and HS–Cu fractions determined in a river water sample by SEC-ICP-IDMS compared with the total concentration of these metals in the original sample determined by ICP-IDMS [18].

Compound	Concentration ($\mu g\,L^{-1}$)
HS–Mo fraction 1	1.14
HS–Mo fraction 2	1.09
HS–Mo fraction 3	3.61
Total Mo in fractions 1–3	5.84
Total Mo in original sample	5.69 ± 0.04[a]
HS–Cu fraction 1	1.82
HS–Cu fraction 2	0.69
Total Cu in fractions 1–2	2.51
Total Cu in original sample	2.55 ± 0.05[a]

[a] Standard deviation was calculated from three parallel analyses.
Source: Reproduced from *Fresenius' J. Anal. Chem.*, Rottmann, L. and Heumann, K. G., **350**, 221, Figure 6 (1994), © Springer-Verlag [18].

4 CHARACTERISTIC FINGERPRINTS OF HS–METAL SPECIES

Depending on the origin of an aquatic system with dissolved HS, the portion of the different metal ions complexed by HS can vary strongly (Table 2.26.2). Different functional groups of HS, the pH value, and the concentration of other electrolytes are able to influence the amount of a HS–metal species formed. Cu^{2+} and Pb^{2+} ions are, for example, complexed by 100% of the HS from a sewage water sample, whereas only 19% of the Ni^{2+} ions are forming HS–Ni species [9]. On the other hand, a much higher Ni^{2+} portion of about 45% is complexed in a ground water sample, which is comparable with the HS–Cu species formation. All these data are only correct under the presupposition that separation by SEC does not change the HS–metal species distribution compared to the original sample.

Table 2.26.2. Degree of metal complexation by HS (in %) in different aquatic samples (calculated by the sum of all HS–metal fractions analyzed by SEC-ICP-IDMS and the corresponding total metal concentration in the samples by direct ICP-IDMS analysis).

Metal	Sewage sample	Seepage water	Ground water	Brown water
Cu	100	68	44	39
Ni	19	31	45	17
Pb	100	5	100	3
Zn	44	2	15	<0.3

No positive correlation could be found between the DOC content of the different water samples and the complexation probability. For example, the sewage sample with the highest degree of HS–metal species for copper, lead, and zinc (Table 2.26.2) has the lowest DOC content of all listed water samples of only 8.6 $mg\,L^{-1}$, whereas the seepage water is highest in its DOC content by 73 $mg\,L^{-1}$. A more significant correlation was found in connection with the different functional groups of HS determined by NMR spectroscopy [20]. The highest fraction of C–O groups (60%) and the lowest fraction of aromatic groups (24%) was determined for the sewage sample, which showed the highest complexation probability for most of the metals investigated [26].

Different water samples of comparable origin very often show similar distribution patterns of HS–metal species when SEC separation is used. For brown water samples, this pattern is usually relatively simple because most of the HS–metal species are associated with the high molecular UV absorbing fraction (at low retention times) of HS (see Figures 2.26.3 and 2.26.4 for copper). Another example of a brown water sample preconcentrated by ultrafiltration, in which simultaneous detection of four different metals was carried out by ICP-MS, is shown in Figure 2.26.6 [19]. In this case, the elution of metal ions takes place at identical retention times and the maxima of the metal peaks very well fit the corresponding maximum of the UV absorption curve (not shown in the figure).

A more miscellaneous distribution pattern than for brown water samples is usually observed for other aquatic samples. For example, Figure 2.26.7 represents the copper, zinc, and molybdenum chromatograms obtained by SEC-ICP-IDMS, together with the corresponding UV absorption curves, for two different sewage samples. From the UV absorption curves, it is apparent that a broad range of SEC-separated HS fractions with different molecular mass interacts with the metal ions detected. Significantly, different interactions of the three metals can be seen for both sewage samples. Whereas zinc forms preferably HS species with the high molecular fractions, copper interacts with the high as well as with the low molecular

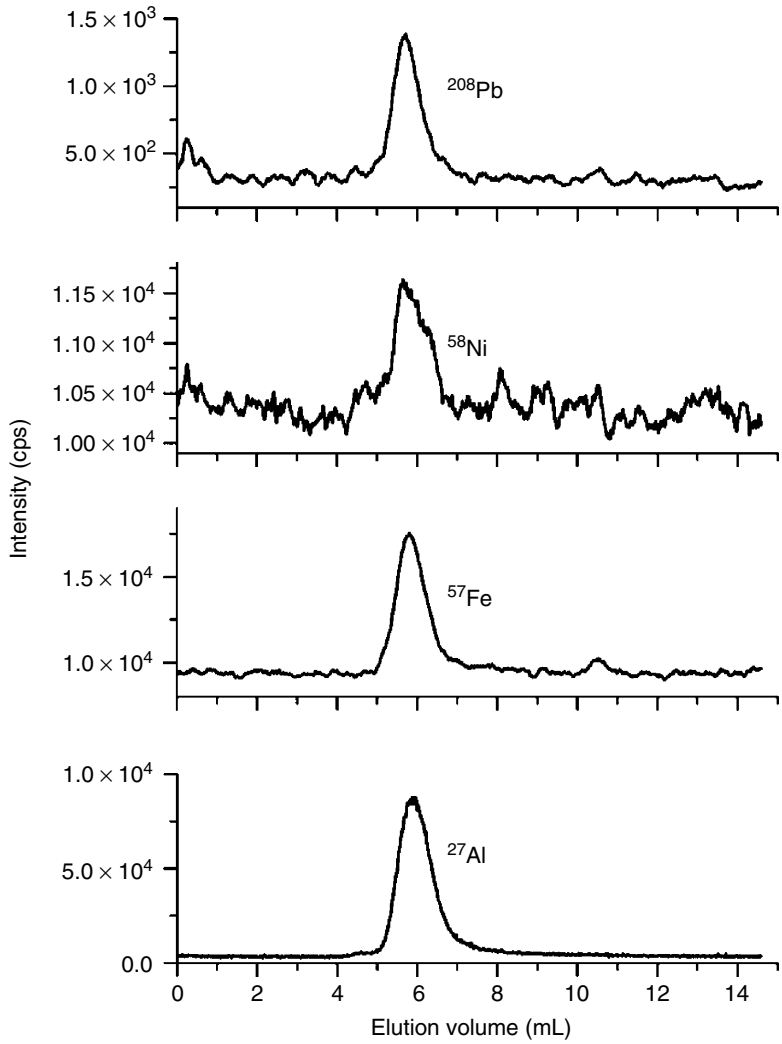

Figure 2.26.6. SEC-ICP-MS chromatogram of lead, nickel, iron, and aluminum of a brown water sample, preconcentrated by ultrafiltration. The UV absorption curve is not shown in this figure, but its maximum was found at the same retention time as the maxima of metals. (Reproduced from Reference [19] by permission of Wiley–VCH.)

HS compounds. Molybdenum is only found in a small UV-absorbing fraction of HS [26]. Other metals, not presented in Figure 2.26.7, can usually be compared with the distribution of one of the metals given in this figure. Lead, for example, fits best the zinc curve, whereas nickel shows good similarity with copper. From this, it follows that groups of metal ions have similar interactions with SEC-separated fractions, at least, in sewage samples. The different distribution pattern of HS–Cu species in three water samples of different origin (bog, river, lake) is demonstrated in Figure 2.26.8 [27].

It can also be assumed that similar HS–metal fractions analyzed in samples of different origin may consist of species with comparable HS structure. For example, seepage water as well as wastewater from a brown coal pyrolysis process were investigated by SEC-ICP-IDMS (Figure 2.26.9). Whereas the water from the

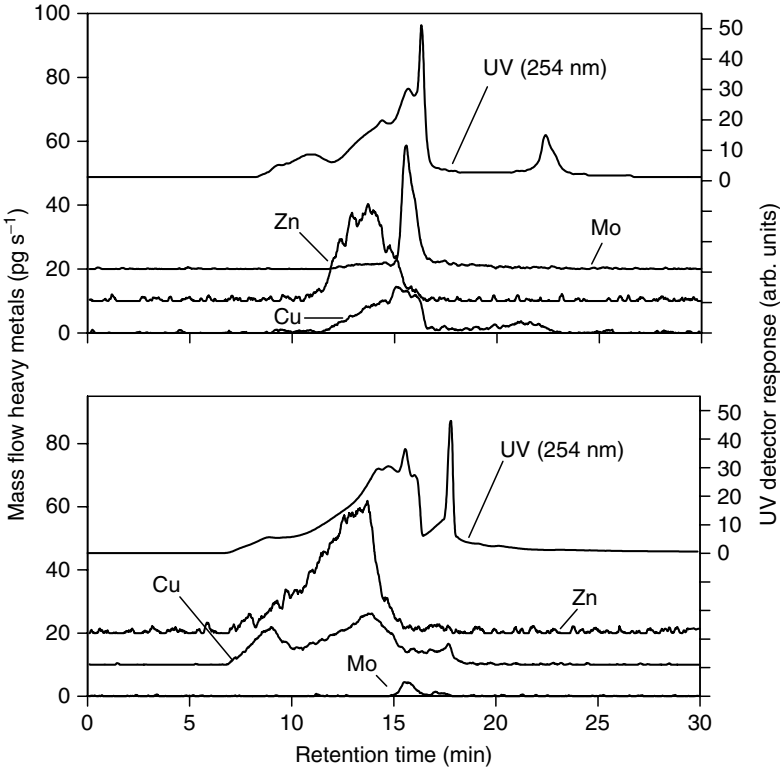

Figure 2.26.7. SEC-ICP-IDMS mass flow chromatogram of molybdenum, zinc, and copper of two different sewage samples together with the corresponding UV absorption curves. (Reproduced from Reference [26] by permission of Wiley–VCH.)

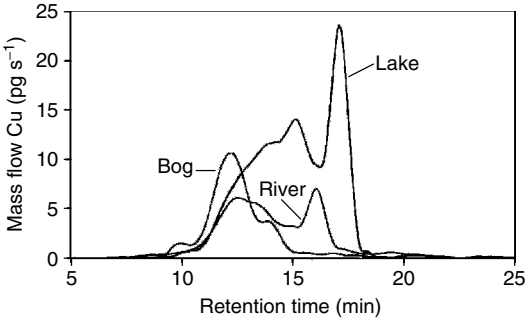

Figure 2.26.8. Dependence of the distribution of HS–copper species in HS fractions of samples of different origin. (Reprinted with permission from [27]. Copyright (1994) American Chemical Society.)

pyrolysis process shows a broad UV absorption band at high molecular masses, all measured metals are exclusively bound by the small UV absorbing fraction at lower molecular masses. It is interesting that this metal binding fraction is identical in its retention time with the only UV absorbing fraction of the seepage water sample that also forms HS–metal species.

5 SPECIFIC INTERACTIONS OF METALS WITH HUMIC SUBSTANCES

5.1 HS–Hg species

Because of the great importance of mercury in the environment, the influence of the mercury mobility on the formation of HS–Hg complexes is of special interest. The role of HS in the mobilization of mercury in aquatic systems was therefore subject of a number of investigations [28–30]. Because of the high chemical affinity of Hg^{2+} ions to sulfur in the oxidation state −2, it is assumed that mercury is preferably bound at HS fractions containing

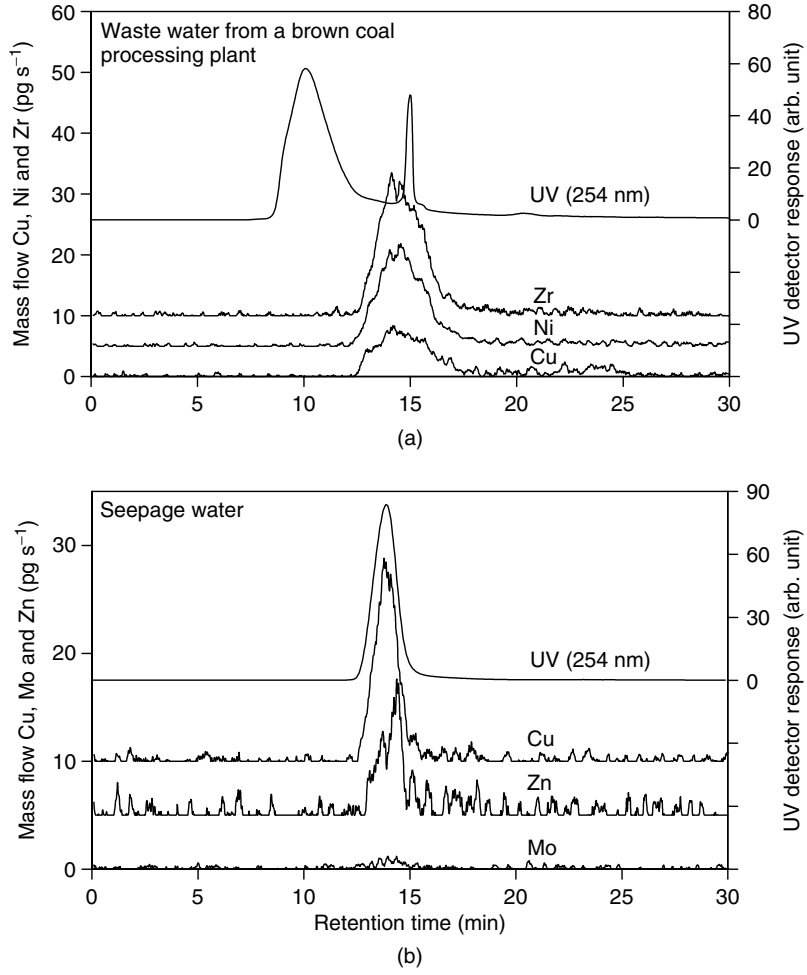

Figure 2.26.9. Comparison of the SEC-ICP-IDMS mass flow chromatograms of different heavy metals of a wastewater from a brown coal processing plant and a seepage water sample together with the corresponding UV absorption curves [25].

sulfur in this chemical form [31]. In principle, the sulfur content of online separated fractions can be determined by ICP-IDMS, as was first published for metallothioneins by CE-ICP-IDMS [32]. In the case of sulfur measurements, a mass resolution of 3000, which can be received by a sector-field ICP-MS, must be applied to resolve the sulfur isotopes ^{32}S and ^{34}S from the interfering molecular ions $^{16}O_2^+$ and $^{33}S^1H^+$, respectively. As an alternative, a reaction cell quadrupole ICP-MS can be used to eliminate the corresponding molecular ions.

Figure 2.26.10 represents the SEC-ICP-MS chromatogram of sulfur for a HA isolate from a wastewater of a brown coal processing plant. Relatively high sulfur contents of 9.3% were analyzed in this sample [3]. Because sulfate also elutes within the first fractions of SEC, three runs with the same HA solution but increasing sulfate amounts were carried out to identify the sulfate peak. As can clearly be seen from the chromatograms, the maximum of the sulfate peak appears at a retention time of 9.5 min.

The SEC-ICP-MS chromatograms of ^{12}C, ^{34}S, and ^{202}Hg of an original wastewater sample from a brown coal processing plant are shown in Figure 2.26.11 together with the corresponding

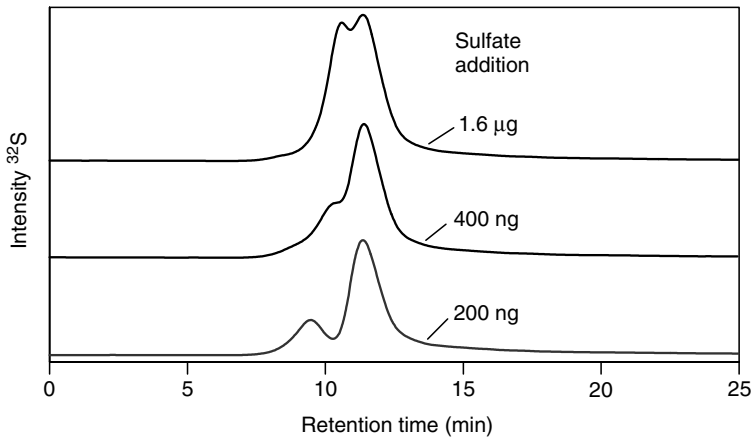

Figure 2.26.10. SEC-ICP-MS chromatograms of ^{32}S for a HA isolate from a wastewater sample of a brown coal processing plant in which different amounts of sulfate were added [31].

UV absorption curve [31]. The ^{12}C chromatogram indicates that only a small amount of the HS in this sample contains high molecular mass molecules at retention times of 11 min and 12 min, respectively. However, only these two fractions show a UV absorption, and they are also the only fractions in which sulfur as well as mercury could be detected. These chromatograms demonstrate, for the first time, that there is a special interaction of Hg^{2+} ions with sulfur-containing HS fractions. To check the mercury capacity of this sample, 15 ng Hg^{2+} were added to 500 µL of the original sample, and this mixture was again analyzed by SEC-ICP-MS. The result is represented by the ^{202}Hg chromatogram at the bottom of Figure 2.26.11. A significant increase of the mercury content in the HS fraction at 11 min is observed but also in an unidentified compound at the front of this sulfur-containing HS fraction.

A wastewater sample from a treatment plant of a community shows only one sulfur-containing HS fraction at the high molecular site of 11 min retention time (Figure 2.26.12). Similar to the sample from the brown coal processing plant, this fraction at 11 min retention time also absorbs UV irradiation at 254 nm and represents only a small portion of the total DOC content of the sample.

The ICP-MS measurements cannot identify the oxidation state of sulfur in HS fractions. A preferable binding of mercury at sulfur-containing HS fractions is expected for HS groups that contain sulfur in the oxidation state −2, whereas sulfonate groups (oxidation state +6) should not show a specific interaction with mercury ions. It is therefore of interest to also analyze the oxidation state of HS fractions. In principle, the difference of sulfur in the oxidation state −2 and +6 can be determined by XANES (see Chapter 6 in Volume 1 of the Handbook) or X-ray photoelectron spectroscopy. However, with respect to sensitivity problems, this is not possible in online separated SEC fractions. Using larger amounts of isolated HS, for example, FA or HA fractions, sulfur was determined in the reduced as well as in the oxidized form, where the different forms vary in the range of about 15–70% depending on the origin of the sample [33, 34].

5.2 Kinetic stability of HS–metal complexes

Thermodynamic complex stability constants of HS–metal species can best be determined by electroanalytical methods [35, 36]. The complex-formation capacity of HS is usually determined under thermodynamic equilibrium conditions by applying Cu^{2+} ions [37]. Even if the thermodynamic stability of HS–metal species was exclusively discussed in the past as the responsible parameter for

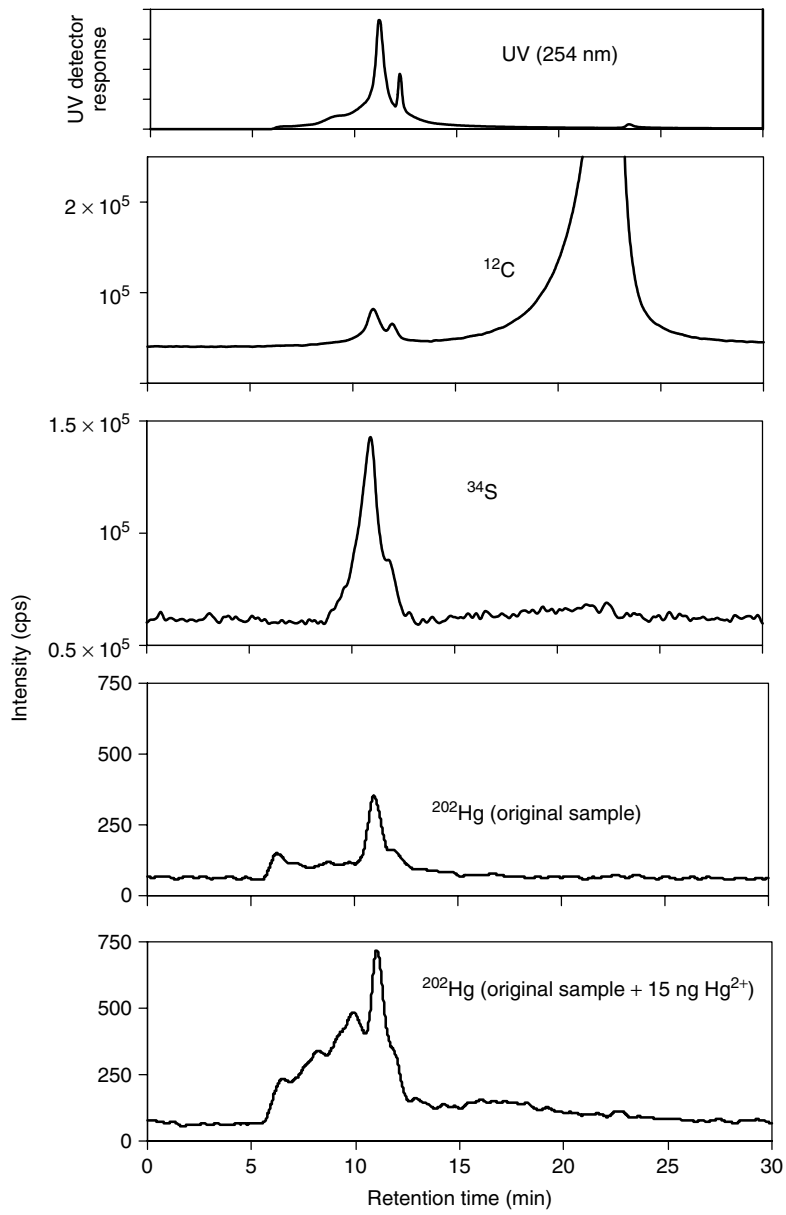

Figure 2.26.11. SEC-ICP-MS chromatograms of ^{12}C, ^{34}S, and ^{202}Hg of an original wastewater sample from a brown coal processing plant, together with the corresponding UV absorption curve. The chromatogram at the bottom shows the mercury distribution in the original sample after adding 15 ng Hg^{2+} [31].

their distribution in nature, the kinetic stability of such complexes may also strongly influence environmental processes.

It is well known for transition metal ions with d^3 (high spin) and d^6 (low spin) electron configuration that they are able to form kinetically stable complexes with classical ligands such as NH_3. Cr^{3+} and Co^{3+} ions are those that fulfill these electron configurations. A first indication for the presence of kinetically stable HS–Cr(III)

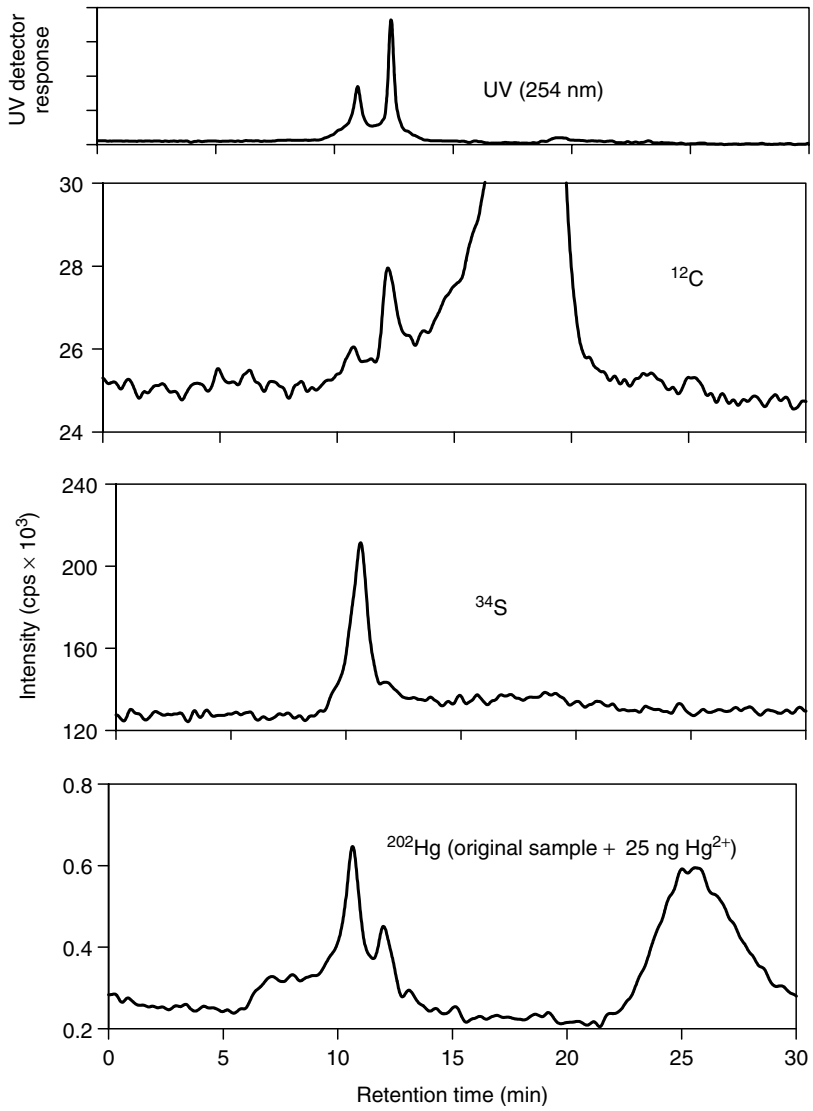

Figure 2.26.12. SEC-ICP-MS chromatograms of ^{12}C, ^{34}S, and ^{202}Hg of an original wastewater sample from a treatment plant of a community, together with the corresponding UV absorption curve. The chromatogram at the bottom shows the mercury distribution in the original sample after adding 25 ng Hg^{2+} [31].

complexes in natural aquatic systems was reported by Götz and Heumann [38]. Experiments with isotopically enriched spike solutions and subsequent measurements by SEC-ICP-MS can, in principle, easily identify kinetically labile and kinetically stable HS–metal species. After saturation of a HS solution with metal ions of natural isotopic composition, isotopically labeled ions of the same element are added. In the case of a kinetically labile HS–metal complex, equilibration of the isotopes will occur within a short time and all HS–metal fractions will then show identical isotope ratios. On the other hand, a kinetically stable HS–metal complex will not equilibrate with the spike isotopes so that different isotope ratios are measured in the various fractions.

HS–Cr(III) and HS–Cu(II) complexes of natural isotopic composition have first been formed in a water sample from a brown coal processing plant. After equilibration, ^{53}Cr(III) and ^{65}Cu(II) spike solutions were added and the SEC-ICP-MS chromatograms were registered about 1 h after spike addition [39]. Whereas the isotopic composition was found to be identical in all HS–Cu(II) fractions, the isotopic distribution was different in the various HS–Cr(III) fractions (Figure 2.26.13), which clearly shows the kinetic instability (within the experimental time scale) of all HS–Cu(II) and

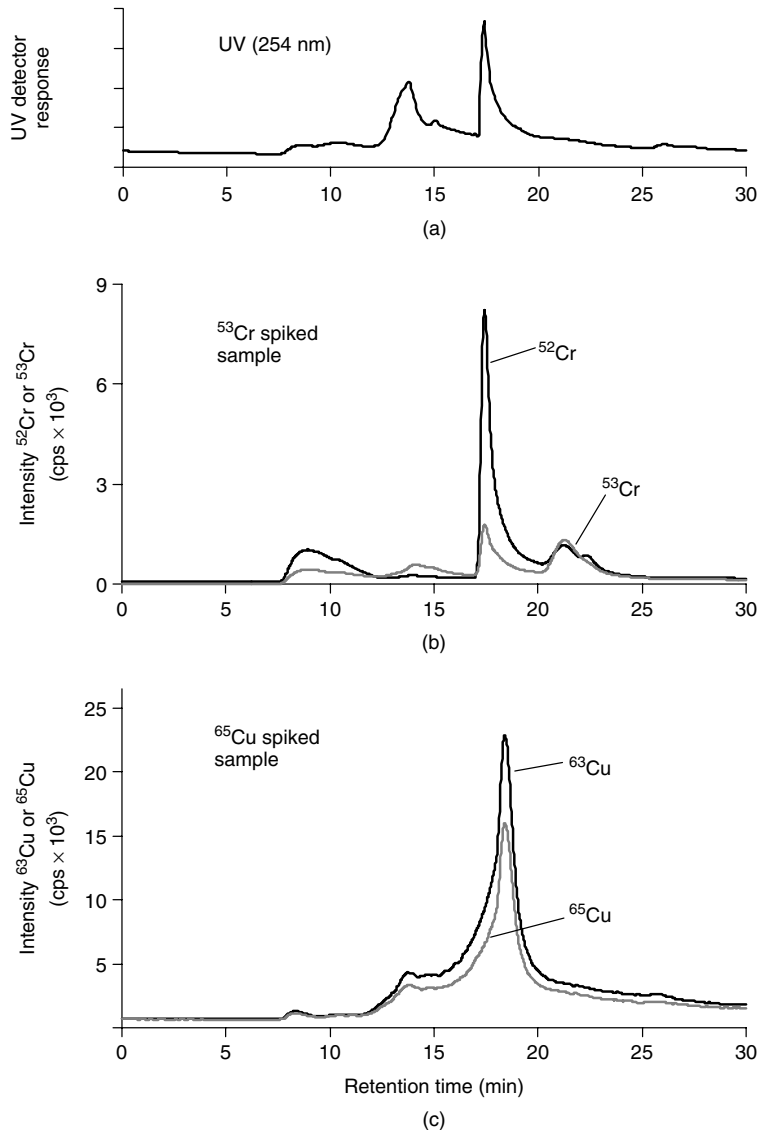

Figure 2.26.13. SEC-ICP-MS chromatograms of chromium and copper of a wastewater sample from a brown coal processing plant after isotope labeling experiments to determine the kinetic stability of corresponding HS–Cr(III) and HS–Cu(II) complexes. (Reproduced from Mass spectrometric investigations of the kinetic stability of chromium and copper complexes with humic substances by isotope-labeling experiments, *Fresenius' J. Anal. Chem.*, Marx, G. and Heumann, K. G., **364**, 489, Figure 3 (1999), © Springer-Verlag [39].)

the kinetic stability of some of the HS–Cr(III) species. The HS–Cr(III) complexes with the highest molecular mass at 8–12 min retention time and those at 17.5–20 min are distinctly enriched in the natural ^{52}Cr isotope, which indicates kinetic stability of these species. On the other hand, the HS–Cr(III) complexes eluted at about 14 min (represented also by one of the UV absorption maxima) and 21.5 min retention time show ^{53}Cr enrichments, which indicate isotope exchange reactions with the spike compound and therefore kinetically labile species. Differences in the functional groups and probably also in the conformation of the different HS fractions are obviously responsible for the different kinetic stability of HS–Cr(III) complexes.

A similar experiment as described for Cr(III) was carried out with radioactive ^{57}Co(III) after the wastewater sample from a brown coal processing plant was equilibrated with Co(III) of natural isotopic composition [31]. Because cobalt is a mono-isotopic element (^{59}Co), the radioactive γ-emitter ^{57}Co was used as spike compound. Fractions of a 1-min elution period were collected to measure their γ-activity, which resulted in a step-like ^{57}Co activity chromatogram (Figure 2.26.14). However, the distribution of ^{59}Co and ^{57}Co differ significantly in the various HS fractions, showing that Co(III) is able to form kinetically stable HS–Co(III) complexes in accordance with the theory for classical metal complexes.

Long-term experiments over 3–20 weeks with chromium have also confirmed the kinetic stability of HS–Cr(III) complexes. This means that transition metals with d^3 (high spin) or d^6 (low spin) electron configuration are able to form kinetically stable HS complexes, which will not remove or exchange their metal ions even under thermodynamically unstable conditions. An especially high mobility of such HS–metal species in the environment can therefore be predicted.

6 CONCLUSION

Whereas complexation of metals by HS was preferably investigated in the past by electroanalytical methods, more and more hyphenated techniques, using coupling of HPLC with ICP-MS or ICP-AES, are now applied to determine HS–metal interactions. A characterization of HS–metal species is limited by the fact that the probability to find exactly identical species in the environment is relatively low and, on the other hand, there is also a lack of highly sensitive methods that can provide structural information at the usually low natural concentration level of these compounds. Preconcentration procedures must therefore be applied before a structural

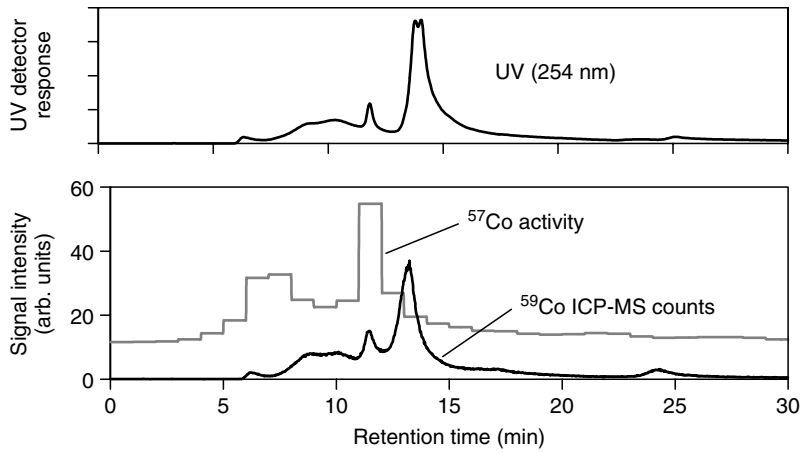

Figure 2.26.14. SEC-ICP-MS chromatograms of cobalt isotopes of a wastewater sample from a brown coal processing plant after isotope labeling experiments with radioactive ^{57}Co to determine the kinetic stability of HS–Co(III) complexes [31].

characterization, which always implies the risk of species transformation. It is therefore the 'state-of-the-art' in HS–metal speciation not to characterize single molecules but HS–metal fractions obtained after a suitable separation step. Because of the broad range of molecular masses of HS molecules in environmental systems, SEC or multistep ultrafiltration are methods often used to separate by the molecular size of the HS–metal species. However, reversed-phase or metal-affinity chromatography and capillary electrophoresis are also suitable procedures for the separation of HS–metal fractions of similar properties. Typical fingerprints for individual metals or groups of them can be observed for HS–metal complexes of HS from comparable origin, and specific interactions of some metals with individual functional groups of HS are possible, as has been demonstrated for the strong binding of Hg(II) at sulfur-containing HS groups.

7 REFERENCES

1. Artinger, R., Buckau, G., Kim, J. I., Geyer, S., Fritz, P. and Wolf, M., *Appl. Geochem.*, **15**, 81 (1999).
2. Aiken, G. R., McKnight, D. M., Wershaw, R. L. and MacCarthy, P. (Eds.), *Humic Substances in Soil, Sediment and Water*, John Wiley, New York, 1985.
3. Abbt-Braun, G. and Frimmel, F. H., The relevance of reference materials – isolation and general characterization, in *Refractory Organic Substances in the Environment*, Frimmel, F. H., Abbt-Braun, G., Heumann, K. G., Hock, B., Lüdemann, H.-D. and Spiteller, M. (Eds.), Wiley-VCH, Weinheim, 2002, p. 7.
4. Schnitzer, M. and Khan, S. W., *Humic Substances in the Environment*, Marcel Dekker, New York, 1972, p. 327.
5. Buffle, J., *Complexation Reactions in Aquatic Systems: An Analytical Approach*, Ellis Horwood, Chichester, 1988, p. 692.
6. Weber, J. H., Binding and transport of metals by humic materials, in *Humic Substances and Their Role in the Environment*, Frimmel, F. H. and Christman, R. F. (Eds.), John Wiley, Chichester, 1988, p. 165.
7. Frimmel, F. H. and Huber, L., *Environ. Int.*, **22**, 507 (1996).
8. Müller, M. B., Schmitt, D. and Frimmel, F. H., *Environ. Sci. Technol.*, **34**, 4867 (2000).
9. Vogl, J. and Heumann, K. G., *Fresenius' J. Anal. Chem.*, **359**, 438 (1997).
10. Burba, P., Jakubowski, B., Kuckuk, R., Küllmer, K. and Heumann, K. G., *Fresenius' J. Anal. Chem.*, **368**, 689 (2000).
11. Frimmel, F. H., Chromatographic characterisation of the acid-soluble part of humic substances, in *Progress in Hydrogeochemistry*, Matthess, G., Frimmel, F. H., Hirsch, P., Schulz, H. S. and Usdowski, E. (Eds.), Springer, Berlin, 1992, p. 24.
12. Schmitt, P., Kettrup, A., Freitag, D. and Garrison, A. W., *Fresenius' J. Anal. Chem.*, **354**, 915 (1996).
13. Burba, P., Shkinev, V. and Spivakov, B. Y., *Fresenius' J. Anal. Chem.*, **351**, 74 (1995).
14. Leita, L., De Nobili, M., Catalano, L. and Mori, A., Formation and voltammetric characterisation of iron-humate complexes of different molecular weight, in *Humic Substances II: Structures, Properties, and Uses*, Davies, G. and Ghabbour, E. A. (Eds.), The Royal Society of Chemistry, Cambridge, MA, 1998, p. 165.
15. Cabaniss, S. E. and Shuman, M. S., *Geochim. Cosmochim. Acta*, **52**, 185 (1988).
16. Waite, T. D. and Morel, F. M. M., *Anal. Chim. Acta*, **162**, 263 (1984).
17. Schmitt, D., Sembritzki, R. and Frimmel, F. H., *GIT Labor-Fachzeitschr.*, 447 (2002).
18. Rottmann, L. and Heumann, K. G., *Fresenius' J. Anal. Chem.*, **350**, 221 (1994).
19. Schmitt, D., Müller, M. B. and Frimmel, F. H., *Acta Hydrochim. Hydrobiol.*, **28**, 400 (2000).
20. Lankes, U. and Lüdemann, H.-D., Structural characterization of refractory organic substances by solid-state high-resolution ^{13}C and ^{15}N nuclear magnetic resonance, in *Refractory Organic Substances in the Environment*, Frimmel, F. H., Abbt-Braun, G., Heumann, K. G., Hock, B., Lüdemann, H.-D. and Spiteller, M. (Eds.), Wiley-VCH, Weinheim, 2002, p. 96.
21. Novotny, F. J., Rice, J. A. and Weil, D. A., *Environ. Sci. Technol.*, **29**, 2464 (1995).
22. Pfeifer, T., Klaus, U., Hoffmann, R. and Spiteller, M., *J. Chromatogr., A*, **926**, 151 (2001).
23. Schulten, H.-R., *J. Anal. Appl. Pyrolysis*, **49**, 385 (1999).
24. Vogl, J. and Heumann, K. G., *Anal. Chem.*, **70**, 2038 (1998).
25. Vogl, J., *Characterization and Quantification of Heavy Metal-Humic Substances Species by HPLC-ICP-MS*, PhD Thesis, University of Regensburg, Germany, 1997.
26. Heumann, K. G., Marx, G., Rädlinger, G. and Vogl, J., Heavy metal and halogen interactions with fractions of refractory organic substances separated by size-exclusion chromatography, in *Refractory Organic Substances in the Environment*, Frimmel, F. H., Abbt-Braun, G., Heumann, K. G., Hock, B., Lüdemann, H.-D. and Spiteller, M. (Eds.), Wiley-VCH, Weinheim, 2002, p. 55.
27. Rottmann, L. and Heumann, K. G., *Anal. Chem.*, **66**, 3709 (1994).
28. Wallschläger, D., Desai, M. V. M. and Wilken, R. D., *Water, Air, Soil Pollut.*, **90**, 507 (1996).
29. Wang, D. Y., Qing, C. L., Guo, T. Y. and Guo, Y. J., *Water, Air, Soil Pollut.*, **95**, 35 (1997).

30. Cai, Y., Jaffé, R. and Jones, R. D., *Appl. Geochem.*, **14**, 119 (1999).
31. Marx, G., *Element-Specific Interactions of Aquatic Humic Substances*, PhD Thesis, University of Mainz, Germany, 2000.
32. Schaumlöffel, D., Prange, A., Marx, G., Heumann, K. G. and Brätter, P., *Anal. Bioanal. Chem.*, **372**, 155 (2002).
33. Aiken, G. R., US Geological Survey, Boulder, CO, personal communication, 2000.
34. Bubert, H., Lambert, J. and Burba, P., *Fresenius' J. Anal. Chem.*, **368**, 274 (2000).
35. Fish, W. and Morel, F. M. M., *Can. J. Chem.*, **63**, 1185 (1985).
36. Soares, H. M. V. M. and Vasconcelos, M. T. S. D., *Anal. Chim. Acta*, **293**, 261 (1994).
37. Frimmel, F. H. and Geywitz, J., *Fresenius' J. Anal. Chem.*, **316**, 582 (1983).
38. Götz, A. and Heumann, K. G., *Fresenius' J. Anal. Chem.*, **325**, 24 (1986).
39. Marx, G. and Heumann, K. G., *Fresenius' J. Anal. Chem.*, **364**, 489 (1999).

2.27 Selected Examples of Important Metal–Protein Species

Douglas M. Templeton
University of Toronto, Toronto, Canada

1 INTRODUCTION

The IUPAC definition of 'speciation' refers to 'the specific form of an element defined as to... complex or molecular structure', including macromolecular compounds and complexes [1]. Among the macromolecular interactions of metals and metalloids, those involving proteins are perhaps the most diverse, and from a biological point of view the most significant. This chapter will deal with selected examples of metal–protein interactions of current importance in speciation analysis. Some important aspects of metal–protein biochemistry that are beyond the scope of this chapter are mentioned immediately below for completeness, but the focus is on complexes of sufficient stability and concentration to be detected in a robust manner by commonly used analytical techniques. Our intention is to give some background biochemistry on some metalloproteins that the analyst is likely to encounter in the literature of speciation analysis. We also note that 'fractionation' refers to classification of an analyte from a sample according to physical or chemical properties [1]. In some cases, a protein may represent a collection of related molecules, for example, with variable posttranslational modification or amino acid substitutions. In such cases, use of the terms 'species' or 'fraction' may reflect both protein heterogeneity and personal preference.

A full consideration of metal–protein interactions would include the rich chemistry of metalloenzymes, central to the field of bioinorganic chemistry. Many enzymes exploit metal ions for structural stability, thermodynamic effects (e.g. the entatic state [2], allostery), acid–base catalysis, and (or) redox properties [2–4]. In some instances, the same element can serve multiple roles in the same enzyme. An example is the occurrence of two Zn^{2+} ions in alcohol dehydrogenase, one of which stabilizes protein structure while the other serves as a Lewis acid polarizing the substrate oxygen atom [5]. Another important aspect of metal–protein interactions is the

Handbook of Elemental Speciation II: Species in the Environment, Food, Medicine & Occupational Health
Edited by R. Cornelis, H. Crews, J. Caruso and K. G. Heumann
 ISBN: 0-470-85598-3 (HB)

selective passage of ions such as Ca^{2+}, Na^{+}, and K^{+} through protein-based ion channels. Numerous excellent reviews exist [6–8]. In addition to passive conductance down a concentration gradient, energy-dependent protein transporters pump ions against gradients. Of numerous examples, the copper transporters ATP7A and ATP7B have been particularly well characterized [9–12]. These are the protein products of the genes mutated in Menkes and Wilson disease, respectively. Interaction of copper with thiol groups in the 'tail' of the protein delivers the ion to an ATP-dependent transport domain for export from the cell or delivery to intracellular organelles. A channel that conducts down a concentration gradient can nevertheless be energy-dependent, an example being the cystic fibrosis transmembrane conductance regulator, which uses ATP hydrolysis to regulate Cl^{-} channel opening [13].

Here we will not consider in detail the interactions of metals and metalloids with specific sites in enzymes, these usually being present in trace (catalytic) concentrations in biological samples. Nor will we discuss further interactions with channels, these interactions in general being transient in nature and not representing isolable complexes. Nor will we address the topic of interaction of metal ions with the abundant proteins of the cytoskeleton, reviewed recently [14]. We will instead present information on some major classes of metal- or metalloid-binding proteins that may be of interest to the analytical chemist. Even this is a daunting task, and only a few examples will be covered; the aim is to be illustrative rather than comprehensive.

Diferric transferrin, Cd/Zn/Cu-metallothioneins, and the copper protein ceruloplasmin are used frequently as standards in developing speciation methods. Thus, tissue iron speciation, the metallothioneins, and copper-binding proteins will be considered here. Zn^{2+} plays a central role in biology and serves as a particularly challenging example for speciation; present in $\mu g\,mL^{-1}$ concentrations in plasma (and higher in many tissues), and mainly protein-bound, its protein complexes are nevertheless of sufficiently low stability that its speciation profile is seldom well defined. Finally, selenoproteins and Ca^{2+}-binding proteins are presented as an interesting contrast. In the former, Se is covalently incorporated as the amino acids selenocysteine and selenomethionine, a permanent part of the protein's structure. In the latter, Ca^{2+} is often transiently associated with proteins that serve in more of a buffering capacity, but this very transience suits Ca^{2+} to a central role in rapid cellular signaling events, and well-conserved Ca^{2+}-binding motifs have evolved.

2 IRON PROTEINS

Iron is essential to practically all biology, and thus it is present in higher organisms as a macronutrient found in several major and many minor species. The flexible, ligand-dependent redox chemistry of the Fe^{2+}/Fe^{3+} couple suits it to a variety of catalytic and electron transport functions, in enzymes and in cytochromes of the mitochondrial electron transport chain. This chemistry also renders Fe potentially toxic via its role as a Fenton catalyst generating the harmful $HO^{\bullet}$ radical [15, 16], and so the speciation of Fe in higher organisms is dominated by the several proteins that have evolved to carry it safely to sites of utilization or storage. Differences in coordination requirements, hydrolysis properties, and kinetic lability between Fe(II) and Fe(III) species also govern Fe biology and Fe–protein interactions [17–19].

Iron interacts with proteins both directly and as part of the organometallic heme complex. In the latter, Fe coordinated in the porphyrin ring associates with various proteins, including globins (e.g. to carry O_2 on hemoglobin) and cytochromes. Hemoglobin accounts for about 65% of the total Fe in an adult human, and myoglobin in muscle cells for about another 4%. Iron–porphyrin chemistry will not be considered further here. Rather, we will describe the major nonheme Fe species in plasma and tissues, transferrin and ferritin. First, we will consider the iron–sulfur (Fe–S) proteins, an interesting case of Fe bound directly to ligands of the protein backbone (thiol groups of cysteine residues) that nevertheless can be separated from the protein as discrete polynuclear complexes.

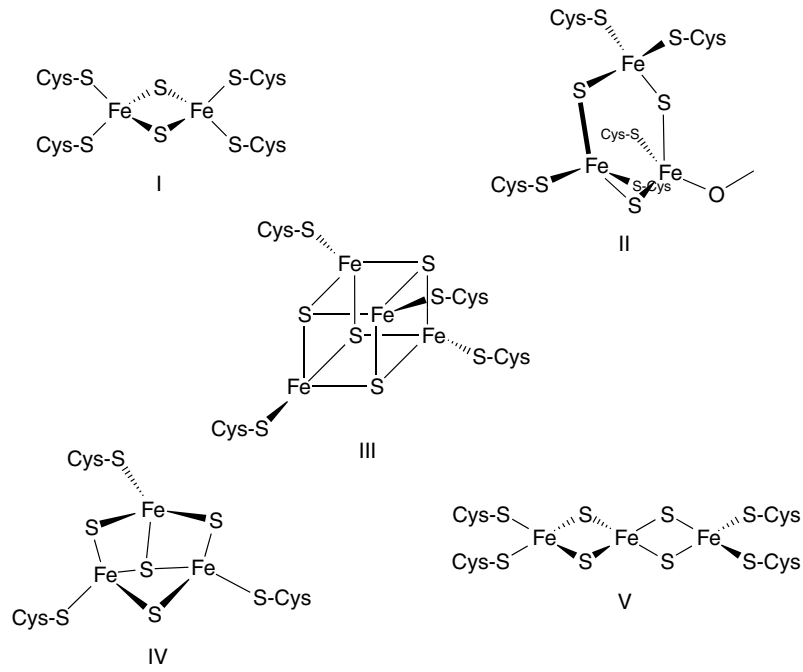

Figure 2.27.1. Some representative iron–sulfur clusters. I, a typical [2Fe–2S] cluster of plant ferredoxins. II, a [3Fe–3S] cluster of *A. vinelandii* ferredoxin. III, the cubane [4Fe–4S] cluster of aconitase. IV and V, two possible [3Fe–4S] cluster structures from inactivated aconitase. The linear structure may occur at high pH. Cys-S represents the sulfur atom of a peptide cysteine residue.

The Fe–S proteins contain several different types of clusters, with [2Fe–2S] (e.g. plant ferredoxin) [3Fe–3/4S], (e.g. *Azotobacter vinelandii* ferredoxin), and the cubane [4Fe–4S] (e.g. aconitase) being most common [20]. Here, the number of S ligands refers to elemental sulfur; Fe is typically tetracoordinated by sulfur, with the additional ligands supplied by thiol groups from cysteine residues of the protein. For example, in the 4Fe–4S cluster, four iron atoms and four sulfur atoms form a symmetrical cube with Fe at opposite corners, and each Fe bound to three S atoms. The fourth coordination site of each Fe atom is occupied by a cysteinyl sulfur, anchoring the cluster into the protein. In the presence of appropriate reductants, however, the cubane structure can be isolated intact. Some representative structures are shown in Figure 2.27.1.

Bacterial Fe–S clusters are formed by two proteins, IscU and IscS. IscS is a cysteine desulfurase that generates elemental sulfur from cysteine [21, 22] and transfers it to IscU, which acts as a scaffold for the assembly of $[2Fe–2S]^{2+}$ [23]. $[4Fe–4S]^{2+}$ clusters form on IscU, sequentially from $[2Fe–2S]^{2+}$ precursors [23]. Homologous enzymes have been identified in the cytosol and mitochondria of human cells [24].

Transferrin is the carrier protein that picks up newly absorbed iron in the gut and delivers it through the circulation to the various cells in the body. The transferrins of higher vertebrates are single polypeptide chains of about 80 kDa that have two Fe^{3+} binding sites, one at the N-terminus and one at the C-terminus; the N and C domains are homologous and bind Fe^{3+} in a similar manner. The transferrins have been extensively reviewed [25, 26], and a compilation of references to crystal structures is given in Table 1 of [25]. In each domain, Fe^{3+} is bound in a cleft between the faces of two antiparallel β sheets, with the requirement for an inorganic anion (typically carbonate) to complete coordination. For instance, the human transferrin N-terminal contributes Asp, Tyr, and His ligands from one

β sheet and an additional Tyr from the other. Two oxygen atoms to complete octahedral coordination of Fe^{3+} are supplied by carbonate.

Because of the high stability constants of the Fe-binding sites ($\sim 10^{22}$ M^{-1} [27]), the transferrins are frequently used as stable Fe–protein calibrators in speciation analyses. Species related to the serum transferrins that may also be encountered in testing analytical systems include ovotransferrin (found in avian egg white, encoded by the transferrin gene but differing in glycosylation pattern), lactoferrins (encoded by a discrete gene family and probably serving an antimicrobial function in human secretions such as milk, tears, saliva, and seminal fluid), and melanotransferrins (proteins of uncertain function, originally isolated from human melanoma cells, and binding only one iron atom at the N-terminal of the protein).

The major species of Fe in mammalian tissues is the storage protein ferritin. Ferritins from plants, animals, and bacteria have been reviewed recently [28–30]. Mammalian ferritins are roughly spherical particles that consist of 24 protein subunits, each about 20 kDa, that accommodate an Fe-rich core of up to 4000 Fe atoms [28, 30]. They are composed of H and L subunits that are structurally similar, encoded by different genes, and present in different ratios in different tissues. The individual subunits do not bind Fe; rather, they assemble into a structure with channels that guide Fe into a sequestered interior. The H chain has catalytic ferroxidase activity that assists in directing Fe^{2+} ions into the oxygen-rich mineral core. Ferritin Fe can be separated readily from other tissue Fe species by size or other chromatographic properties (see below).

In the core, Fe is found in an approximately ferrihydrite structure ($5Fe_2O_3 \cdot 9H_2O$) of variable crystallinity. Each Fe atom is surrounded by 5–6 O atoms, with some tetracoordination also likely [31]. Hydration, a disordered structure, and exposure of up to 40% of the Fe atoms on the surface of the core may all facilitate mobilization of Fe, consistent with a storage function for the protein [30]. Phosphate is also present in the ferritin Fe core, with tissue- and species-dependent variations in Fe:P ratios. Phosphate may further regulate the bioavailability of ferritin Fe, but its true role is not known.

2.1 Clinical aspects of iron–protein species

If plasma from a healthy individual is fractionated, all the Fe will be found associated with transferrin, and an excess capacity of transferrin binding sites of about 70% can be expected. Because of the high association constants, it is only in cases of moderate-to-severe Fe overload, as occurs for instance in hemochromatosis or transfusion-dependent thalassemia, that transferrin becomes saturated and the excess Fe then finds other binding sites. The nature of this nontransferrin-bound Fe (the so-called NTBI fraction) remains somewhat controversial, but most likely it is nonprotein bound. Ferric citrate is the most likely species [32]. Whatever the nature of NTBI, it is of great clinical significance insofar as it is almost certainly Fenton-active, and therefore toxic. The challenge to the analytical chemist is to distinguish transferrin-bound Fe from the much lesser amounts of nonprotein-bound Fe. Various approaches to this problem have yielded estimates of between 0 and >10 μM for the concentration of NTBI (reviewed in [33]). Probably NTBI concentrations of 1–10 μM do exist in the plasma of some Fe-overloaded patients, and we have proposed that specific transport mechanisms for uptake of NTBI into cells of the soft tissues may serve a protective function by clearing any NTBI in excess of this [34].

In tissues, Fe is found in three predominant forms, two of them protein-bound (transferrin and ferritin), and the other derived from ferritin. A method for fractionating tissue Fe on the basis of carboxymethyl cellulose ion exchange was developed by Selden and Peters [35], and we coupled it with ICP-MS detection to distinguish several Fe-containing fractions and species [36]. The small amount of transferrin cycling within the cell through receptor-mediated endocytosis can be distinguished from ferritin and other (mainly heme-containing) proteins. In healthy liver tissue, for example, about 75% of the iron is found in

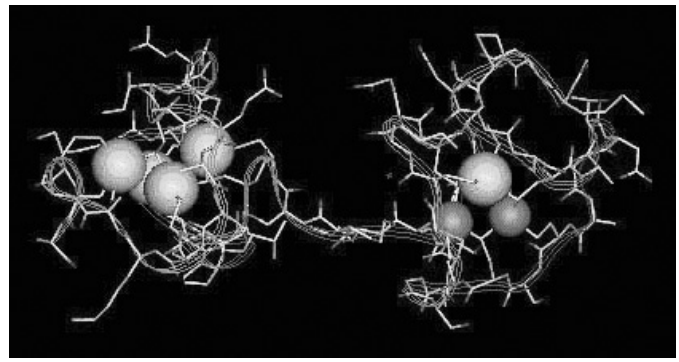

Figure 2.27.2. (Plate 1) Depiction of rat metallothionein-II in the Cd_5Zn_2 form. Cd^{2+} ions are in green, Zn^{2+} in purple. The C-terminal α-domain is to the left. The image was provided by John H. Beattie of the Rowett Institute, Aberdeen, and is used with permission.

ferritin, small amounts in transferrin, and traces in heme-protein fractions. The remainder is in an insoluble form that is eluted with 0.1 M NaOH after conversion to $Fe(OH)_4^-$. This siderophilic cellular Fe deposit is called 'hemosiderin'. Its exact nature is not well defined, but it probably derives from the iron core of ferritin after the protein chains are degraded, as it contains a mixture of ferrihydrite and noncrystalline ferric oxohydroxide structures [37].

In liver biopsies from patients with transfusion-dependent thalassemia and severe Fe overload, tissue concentrations of several times normal or higher are accompanied by a predominance of a hemosiderin-like fraction, which can account for up to 90% of the total [36]. Presumably the capacity of ferritin synthesis to keep up with the iron overload has been exceeded. Whether all this hemosiderin-like Fe has trafficked through ferritin or rather represents NTBI that has entered the cell and hydrolyzed before becoming protein-bound remains to be decided.

3 METALLOTHIONEINS

Isolated more than 40 years ago as a Cd^{2+}-binding protein from equine kidney [38], metallothionein remains one of the most extensively studied metalloproteins. The term 'metallothionein' has appeared in 6000 MedLine citations to date. It refers to a family of proteins with now nearly 200 sequences from a variety of organisms having been reported, but the most recent classification [39] still relies on structural similarity to the original equine Cd^{2+}-binding protein, the presence of multiple Cys–X–Cys sequences, and spectral features characteristic of metal-thiolate clusters. Comprehensive reviews of all aspects of metallothioneins can be found in reports of a series of international meetings on the protein, the most recent of which is [40].

The prototype mammalian metallothionein contains about 60 amino acid residues with 20 conserved cysteines, all reduced in the native protein. Thus, it is basically a polythiol adapted for metal binding, especially of soft metal ions. It has no aromatic residues and thus no hydrophobic interior; it is in essence a low molecular mass amino acid chain that wraps itself in a minimalist conformation around metal ions, most importantly, Cd^{2+}, Cu^+, and Zn^{2+}. (The charges here refer to the fact that copper binds as a Cu(I)-thiolate complex.) In the native protein, both Cd^{2+} and Zn^{2+} bind in a 7 : 1 stoichiometry with the protein, 4 atoms in a C-terminal α-domain and 3 atoms in an N-terminal β-domain (Figure 2.27.2), a structure that is preserved in mixed Cd–Zn metallothioneins [41]. To our knowledge, this is the first metalloprotein whose solution structure deduced by NMR spectroscopy [42, 43] and crystal structure [44, 45] was available for direct comparison. The comparison revealed an internal dynamic

ligand exchange process occurring in solution that was not representative of the most thermodynamically favorable structure found in the crystal [46]. Binding of copper, and other metals such as silver, cobalt, and mercury *in vitro*, is somewhat more complicated than the classic (4+3):1 binding of Cd^{2+} and Zn^{2+} (for instance, see [47]).

Despite extensive investigation into its chemistry, biochemistry, and biology, the precise function of metallothionein remains elusive [48–50]. Certainly, it decreases the toxicity of cadmium, plays a role in Cu^{2+} and Zn^{2+} homeostasis and metabolism, and can function as an antioxidant. It may be a source of Zn^{2+} [51, 52] (and possibly Cu^{2+}) for enzymes that require the metal as a cofactor, and it may serve as a sensor of cellular levels of those elements. The appearance of this nonsecreted, cytosolic protein in the nucleus in some circumstances [53–56] also hints at a role for this small protein in regulating gene expression. We have suggested that metal-binding might serve to maintain the abundant thiol groups of metallothionein in a reduced state [48]; rather than viewing the thiols as accommodating the metals, the metals might preserve the thiols for redox-based functions. Genetic studies with knockout mice have been disappointing in failing to reveal any essential function of this nevertheless widely conserved, inducible, and ubiquitous protein [57].

4 COPPER AND CERULOPLASMIN

Copper is one of the major metallic elements in plasma, being homeostatically regulated at a plasma concentration of about 1 $\mu g\,mL^{-1}$ in a healthy human being. While tissue copper storage is dominated by metallothionein, this protein is not secreted, and other forms account for circulating copper, predominant among them being ceruloplasmin. About 65% of circulating copper is essentially irreversibly bound to ceruloplasmin [58]. A lesser amount (ca 15%) is bound to the N-terminal aspartic acid-alanine-histidine tripeptide of albumin. Traditionally, ceruloplasmin has been viewed as a transport and storage form of copper, and albumin as the exchangeable form for delivery of Cu^{2+} to tissues. Both roles must now be reformulated. The true function of ceruloplasmin is considered below. Normal delivery of injected ^{67}Cu to the livers of analbuminemic rats [59] casts doubt on an essential role of albumin in delivery of Cu^{2+} to tissues, and suggests rather a role in buffering plasma Cu^{2+}.

While ceruloplasmin and albumin together account for about 80% of Cu in normal human plasma, the remainder is less well defined. Another protein fraction has been called 'transcuprein' [58], but has not been characterized in any detail. About 5% of plasma Cu^{2+} is bound in low molecular mass complexes. Stability constant-based modeling predicts that histidine and histidine-containing bis-peptide complexes will be important in this fraction [60]. In Wilson disease, ceruloplasmin levels are frequently decreased as a result of failure of the ATP7B protein to deliver Cu^{2+} to intrahepatocytic sites of ceruloplasmin synthesis. Plasma Cu^{2+} levels are also frequently increased as a consequence of increased tissue stores. The proportion of copper bound to noncaeruloplasmin fractions is therefore increased [61].

Ceruloplasmin is frequently used as a marker of macromolecular copper in fractionation and speciation analyses. Human ceruloplasmin is a 132-kDa glycoprotein of 1046 amino acids that was first isolated in 1948 [62]. Historical aspects of the recognition of the true function of ceruloplasmin as a ferroxidase enzyme essential for proper iron metabolism have been reviewed in an entertaining editorial comment by Harris [63]. Though a connection between copper status and iron utilization had long been known, the basis was elusive. The ability of ceruloplasmin to oxidize Fe^{2+} was not given much significance by most investigators, as it was generally believed that spontaneous oxidation of Fe^{2+} and subsequent association of Fe^{3+} with transferrin could explain iron transport and delivery. Normal iron metabolism in most patients with Wilson disease, despite decreased ceruloplasmin levels, did little to convince skeptics of a biological role for ceruloplasmin's ferroxidase activity. It is only over the past decade that the matter has been resolved. Molecular dissection of the role of the Fet3 protein, a homologue of mammalian ceruloplasmin, in iron acquisition by

Saccharomyces cerevisiae, provided a strong indication that parallel pathways would exist in higher animals [64]. Now, several families in Japan and the United States have been described with a gene defect in ceruloplasmin that leads to aceruloplasminemia [65–67]. These individuals suffer a fatal systemic hemosiderosis with dementia, diabetes, and cirrhosis secondary to excessive iron deposition in the central nervous system, pancreas, and liver, respectively. Presumably, patients with Wilson disease are spared because their diminished ceruloplasmin levels are nevertheless sufficient for catalytic efficiency. However, while it is now clear that ceruloplasmin functions as an essential ferroxidase in mammalian iron metabolism, specific mechanistic details remain to be elucidated, and additional multifunctional roles in copper transport and storage cannot be dismissed.

The copper-binding sites in ceruloplasmin encompass several structural aspects of copper–protein interactions. The protein is a so-called blue multicopper oxidase, and the only one found in humans. These enzymes require at least four copper atoms to function in the four-electron reduction of O_2 to $2H_2O$, via sequential one-electron oxidations of reduced substrates. Three types of copper sites occur in these proteins: T1 has an intense charge transfer band and imparts a sky-blue color to the protein (hence ceruloplasmin), T2 is without strong spectral perturbations, and T3 is an antiferromagnetically coupled copper ion pair. T1 accepts electrons sequentially from substrate, passing them on to T2 and T3. The latter form a trinuclear cluster that is the site of dioxygen reduction [68]. Ceruloplasmin has two additional copper atoms at T1 sites, for a total copper content of six atoms per protein molecule [69]. Each of the T1 sites in human ceruloplasmin has Cu^{2+} coordinated to a cysteine and two histidine residues, with the fourth coordination site occupied by either methionine (in two cases) or leucine (in the third T1 site). The trinuclear cluster is coordinated by four His–X–His pairs [69].

5 ZINC-BINDING PROTEINS

Like Cu^{2+}, Zn^{2+} is homeostatically regulated at a serum concentration of about 1 $\mu g\,mL^{-1}$, and is mainly protein-bound in plasma. As a relatively abundant essential element, its protein-based speciation is of interest. Albumin-bound Zn^{2+} is generally the major species in mammals, with α_2-macroglobulin accounting for about 30% of the metal. This indicates a lack of specific protein–binding interactions but rather nonspecific, concentration-dependent equilibria. Indeed, the N-terminus of albumin, containing the aspartic acid-alanine-histidine (ATCUN motif [70]; Figure 2.27.3) Cu^{2+}-binding site does not fully coordinate Zn^{2+}, and the ion binds with less specificity elsewhere throughout the molecule. Ternary complexes with small molecules (chiefly amino acids) and albumin also occur [71]. Modeling studies performed by May and colleagues [60] suggest that among low molecular mass species, bis-amino acid complexes that contain at least one cysteine molecule should predominate. Zinc and copper, as two essential divalent metals with comparable, homeostatically controlled concentrations in plasma, might be predicted to interact more strongly. Bremner and Beattie [72] have pointed out that several aspects of Zn^{2+}–Cu^{2+} protein–amino acid interactions limit potentially adverse competition. Cu^{2+} and Zn^{2+} do not share a common binding site on albumin, the major plasma protein. Ceruloplasmin does not bind Zn^{2+}; α_2-macroglobulin does not bind Cu^{2+}. Furthermore, in their amino acid and amino acid–protein ternary complexes, Cu^{2+} and Zn^{2+} have differential preference for cysteine (Zn^{2+}) and histidine (Cu^{2+}).

Particularly stable Zn^{2+}–protein interactions occur in the so-called zinc-finger transcription factors [73, 74]. The prototype is transcription factor IIIA, which contains nine zinc-binding loops. Each is about 30 amino acids long and contributes two histidine and two cysteine residues for tetrahedral coordination of Zn^{2+}. The tandem arrangement of the loops provides an elongated structure that recognizes specific sequences of DNA.

Additional insights into Zn^{2+}–protein interactions have come from studies of Zn^{2+} transport and resistance in both eukaryotic and prokaryotic organisms. Although not representing major components in speciation analyses, some examples are mentioned here as illustrative of the nature

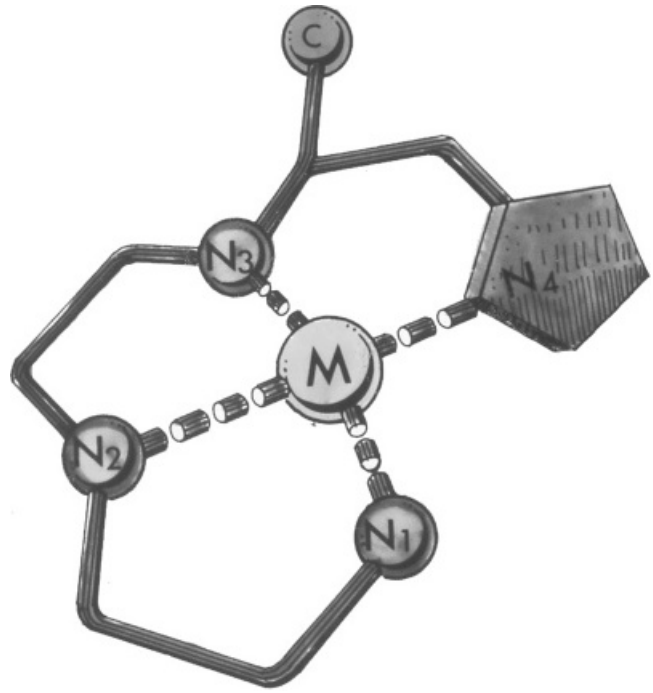

Figure 2.27.3. Schematic of the metal-binding ligands of the aspartate-alanine-histidine ATCUN motif. The drawing was prepared by Bibudhendra Sarkar, Hospital for Sick Children, Toronto, and is used with permission.

of Zn^{2+}–protein interactions. Zinc tolerance in Zn^{2+}-sensitive BHK cells (lacking metallothionein expression) is conferred by expression of two transporters, ZnT-1 and ZnT-2 [75, 76]. Each contains six membrane-spanning regions and a histidine-rich cytosolic loop that presumably binds Zn^{2+} for transport, perhaps analogous to the cysteine-rich domains of the ATP7A and ATP7B proteins. Repeating $(His–X)_n$ sequences occur in the ZIP family of Zn^{2+} transporters [77]. The involvement of histidine-rich domains in Zn^{2+} binding reaches an extreme in the peripheral zinc-binding protein (PZP1) homologue of *Hemophilus influenza*. This protein contains a central region of 31 amino acids of which every second one is histidine [78, 79].

6 SELENOPROTEINS

Selenium can substitute for sulfur in cysteine and methionine, thus incorporating into the permanent structure of proteins. We acquire various species of organic and inorganic Se in the diet, with different oxidation states, and biotransform them into selenocysteine and selenomethionine. In addition to selenomethionine, trimethylselenonium, selenite, selenate, and selenocholine, various selenoproteins have been separated from human urine [80]. Most Se in blood and plasma is in selenoproteins that have incorporated selenocysteine or selenomethionine. In the erythrocyte, most Se is in hemoglobin and glutathione peroxidase (GPX). In plasma, it is found in albumin, selenoprotein P, and GPX [81]. GPX is important in antioxidant defense. Selenoprotein P is a 50-kDa glycoprotein of unknown function containing 12 selenocysteine residues [82]. It may function as an antioxidant or in Se transport. A role in Hg^{2+} detoxification has also been proposed [83]. Other selenoproteins of unknown function are reviewed in [84].

Recently, Behne and Kyriakopoulos [84] have classified selenoproteins into three categories: specific selenoproteins result from transcription of

the TGA codon specific for selenocysteine; these include GPX and thioredoxin reductase, where the Se atom participates in a catalytic event, and presumably selenoprotein P. Nonspecific selenoproteins result from the incidental incorporation of selenomethionine in place of methionine; Se is not required for function. Hemoglobin and albumin are examples. Third, Se-binding proteins occur that bind the element specifically but in unknown chemical form. Little is known of the structure or function of these latter proteins [84].

Tracer studies, for example, with radioactive ^{75}Se and 2D-SDS-PAGE/IEF [84, 85], or the stable isotope ^{82}Se with HPLC-ICP-MS [86] have been used to show that most Se is protein-bound in animals, and to probe the ultimate distribution of dietary Se amongst plasma/serum and tissue proteins. For instance, Kobayashi *et al*. [86] have shown endogenous Se to be roughly equally distributed between GPX and selenoprotein P in rat serum before supplementation, and almost exclusively in GPX in the liver.

The protein destination of dietary Se depends on its chemical form in ways that are poorly understood and depends also on the animal species concerned. For example, in humans, intake of selenomethionine results in most erythrocyte Se incorporated into hemoglobin, whereas selenite deposits more erythrocyte Se in GPX. Selenate produces a roughly equal distribution. Comparing Se content in erythrocytes of two populations, Oregon residents had about three times the level of those from New Zealand, but functional GPX was similar in both populations [81]. Inconsequential incorporation into hemoglobin was higher in the Oregon population. In rats, both dietary selenite and selenomethionine distribute plasma Se into 50–60% selenoprotein P, 20–30% GPX, and 20–25% albumin [81].

7 CALCIUM-BINDING PROTEINS

Two aspects of Ca^{2+} chemistry dominate its interactions with proteins. First, on the Pearson scale of hardness/softness, Ca^{2+} is a hard ion (a Klopman hardness parameter of 2.33 eV is comparable to that of Fe^{3+} and Mg^{2+} [87]) and thus prefers oxygen ligands. Second, the ion is kinetically labile, with a water exchange rate of $5 \times 10^8\ s^{-1}$ [2]. This can be compared, for example, to Mg^{2+} ($10^5\ s^{-1}$) and Al^{3+} ($10\ s^{-1}$), the former being used by biological systems mainly in a structural role, and the latter so inert as to be without biological significance except as a toxic entity.

Calcium–protein interactions serve extracellular functions such as protease stabilization and coordination of biomineralization, binding equilibria being maintained by the high (mM) extracellular concentrations of Ca^{2+}. However, it is the intracellular coordination of Ca^{2+} by a superfamily of proteins known as the 'EF-hand' proteins that is most interesting. Over 200 Ca^{2+}-buffering or sensing proteins containing this motif are now known [88]. These include molecules such as parvalbumin, whose main function appears to be to buffer intracellular Ca^{2+}, and a second group, typified by troponin C and calmodulin (Figure 2.27.4), that undergo conformational changes upon Ca^{2+}-binding and then activate downstream targets [89]. These latter *Ca^{2+}-modulated* proteins are thus central to Ca^{2+}'s role as a signaling second messenger. Calmodulin typifies the Ca^{2+}-modulated signaling paradigm. On binding Ca^{2+}, calmodulin activates a family of downstream kinases that includes myosin light chain kinase, calcineurin, adenylyl cyclases, phosphodiesterase, and calcium/calmodulin-dependent protein kinases (the so-called CaMKs [90]) [89].

The EF-hand motif refers to a helix–loop–helix structure that is highly conserved in the family. Between two α-helices, a loop of 12 amino acids provides at least five oxygen ligands for Ca^{2+}. Together with water in the coordination sphere, these satisfy 6- or 7-fold coordination of Ca^{2+}, typically in a pentagonal bipyramidyl structure. The 'EF' designation is of no significance other than historically; the image is of an E-helix that represents an index finger and an F-helix that represents the thumb. Ca^{2+} sits in the notch between, hence the 'hand'. It is interesting to note that the closeness of the ionic radii of many different elements to that of Ca^{2+} (0.099 nm) correlates with the element's ability to activate calmodulin in an

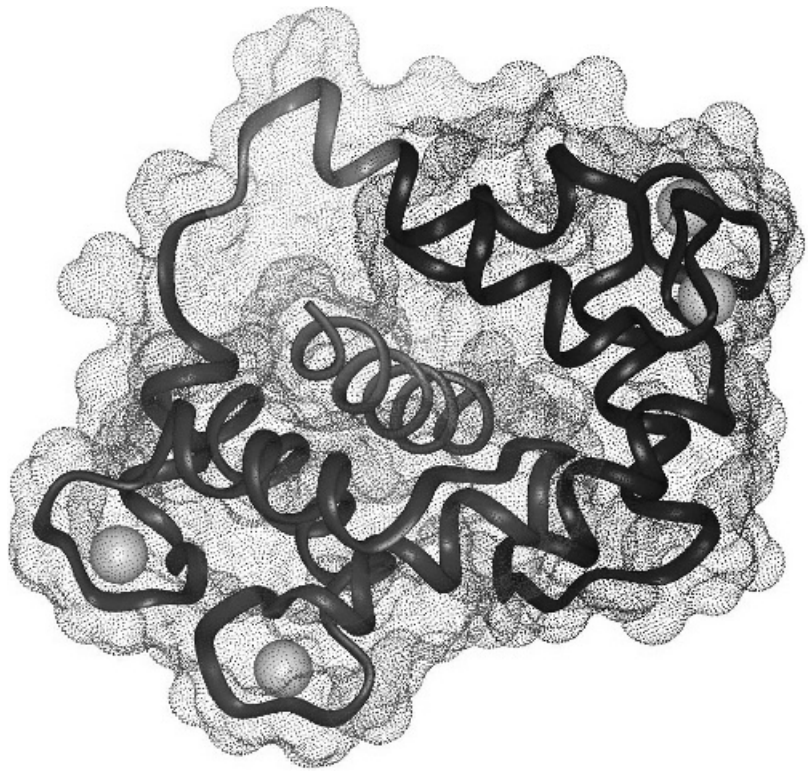

Figure 2.27.4. Calcium-loaded calmodulin in complex with a peptide derived from smooth-muscle myosin light chain kinase (PDB code 1CDL). The peptide and protein backbones are represented as ribbons along with their Conolly molecular surfaces and the calcium ions as spheres. The image appears in the Calcium Binding Proteins Database (http://structbio.vanderbilt.edu/chazin/cabp_database/cabp.html). It was prepared by Melanie R. Nelson in the laboratory of Walter J. Chazin and is used with permission.

in vitro assay [91]. This suggests that the desolvated ion is bound in a spatially well-defined pocket that, in addition to the obvious electrostatic interactions, obeys rigid geometrical constraints.

8 CONCLUSIONS

In biological systems, protein binding dominates macromolecular species of metal ions. Protein ligands including oxygen and carboxylates, amino and imidazole groups, and thiols provide a range from hard to soft ligands that can accommodate many metals in highly stable or readily exchangeable form, depending on the required function of the protein in transport, storage, or catalysis. In speciation analysis, some of the more abundant and stable metalloproteins like transferrin, metallothioneins, and ceruloplasmin have served as models for macromolecular separation techniques. As the proteome becomes defined, many more analytical protocols will be developed, with special challenges presented by the more labile metal–protein interactions.

9 REFERENCES

1. Templeton, D. M., Ariese, F., Cornelis, R., Danielsson, L.-G., Muntau, H., van Leeuwen, H. and Lobinski, L., *Pure Appl. Chem.*, **72**, 1453 (2000).
2. Williams, R. J. P., *Eur. J. Biochem.*, **150**, 231 (1985).
3. Williams, R. J. P., *Philos. Trans. R. Soc. London, Ser. B*, **294**, 57 (1981).
4. Nieboer, E. and Fletcher, G. G., Determinants of reactivity in metal toxicology, in *Toxicology of Metals*,

Chang, L. W. (Ed.), CRC Lewis Publishers, Boca Raton, FL, 1996, pp. 113–132.
5. Walsh, C., *Enzymatic Reaction Mechanisms*, W. H. Freeman, San Francisco, CA, 1979.
6. Catterall, W. A., *Annu. Rev. Biochem.*, **64**, 493 (1995).
7. Roden, D. M. and George, A. L. Jr., *Annu. Rev. Med.*, **47**, 135 (1996).
8. Catterall, W. A., *Annu. Rev. Cell Dev. Biol.*, **16**, 521 (2000).
9. Forbes, J. R., Hsi, G. and Cox, D. W., *J. Biol. Chem.*, **274**, 12408 (1999).
10. Iida, M., Terada, K., Sambongi, Y., Wakabayashi, T., Miura, N., Koyama, K., Futai, M. and Sugiyama, T., *FEBS Lett.*, **428**, 281 (1998).
11. La Fontaine, S., Firth, S. D., Lockhart, P. J., Brooks, H., Parton, R. G., Camakaris, J. and Mercer, J. F. B., *Hum. Mol. Genet.*, **7**, 1293 (1998).
12. Payne, A. S. and Gitlin, J. D., *J. Biol. Chem.*, **273**, 3765 (1998).
13. Riordan, J. R., CFTR function, in *Cystic Fibrosis – Current Topics*. Vol. I, Dodge, J. A., Brock, D. J. H. and Widdicombe, J. H. (Eds), John Wiley & Sons, 1993, pp. 157–173.
14. Templeton, D. M., Metal ions and the cytoskeleton, in *Molecular Biology and Toxicology of Metals*, Zalups, R. F. and Koropatnick, J. (Eds), Taylor and Francis, London, 2000, pp. 460–476.
15. Halliwell, B. and Gutteridge, J. M. C., *Methods Enzymol.*, **186**, 1 (1990).
16. Halliwell, B. and Gutteridge, J. M. C., *FEBS Lett.*, **307**, 108 (1992).
17. Raymond, K. N. and Carrano, C. J., *Acc. Chem. Res.*, **12**, 183 (1979).
18. Schneider, W., *Chimia*, **42**, 9 (1988).
19. Harris, W. R., Iron chemistry, in *Molecular and Cellular Iron Transport*, Templeton, D. M. (Ed.), Marcel Dekker, New York, 2002, pp. 1–40.
20. Beinert, H., Holm, R. H. and Münck, E., *Science*, **277**, 653 (1997).
21. Zheng, L., White, R. H., Cash, V. L. and Dean, R. R., *Biochemistry*, **33**, 4714 (1994).
22. Schwartz, C. J., Djaman, O., Imlay, J. A. and Kioley, P. J., *Proc. Natl. Acad. Sci. U.S.A.*, **97**, 9009 (2000).
23. Agar, J. N., Krebs, C., Frazzon, J., Huynh, B. H., Dean, D. R. and Johnson, M. K., *Biochemistry*, **39**, 7856 (2000).
24. Tong, W.-H. and Rouault, T., *EMBO J.*, **19**, 5692 (2000).
25. MacGillivray, R. T. and Mason, A. B., Transferrins, in *Molecular and Cellular Iron Transport*, Templeton, D. M. (Ed.), Marcel Dekker, New York, 2002, pp. 41–69.
26. He, Q.-Y. and Mason, A. B., Molecular aspects of release of iron from transferrin, in *Molecular and Cellular Iron Transport*, Templeton, D. M., (Ed.), Marcel Dekker, New York, 2002, pp. 95–123.
27. Aisen, P., Leibman, A. and Zweier, J., *J. Biol. Chem.*, **253**, 1930 (1978).
28. Harrison, P. M. and Arosio, P., *Biochim. Biophys. Acta*, **1275**, 161 (1996).
29. Ponka, P., Beaumont, C. and Richardson, D. R., *Semin. Hematol.*, **35**, 35 (1998).
30. Arosio, P. and Levi, S., Ferritins: structural and functional aspects, in *Molecular and Cellular Iron Transport*, Templeton, D. M. (Ed.), Marcel Dekker, New York, 2002, pp. 125–154.
31. Islam, Q. T., Sayers, D. E., Gorun, S. M. and Theil, E. C., *J. Inorg. Biochem*, **36**, 51 (1989).
32. Grootveld, M., Bell, J. D., Halliwell, B., Aruoma, O. I., Bomford, A. and Sadler, P. J., *J. Biol. Chem.*, **264**, 4417 (1989).
33. Parkes, J. G. and Templeton, D. M., Transport of non-transferrin-bound iron by hepatocytes, in *Molecular and Cellular Iron Transport*, Templeton, D. M. (Ed.), Marcel Dekker, New York, 2002, pp. 451–466.
34. Randell, E. W., Parkes, J. G., Olivieri, N. F. and Templeton, D. M., *J. Biol. Chem.*, **269**, 16046 (1994).
35. Selden, C. and Peters, T. J., *Clin. Chim. Acta*, **98**, 47 (1979).
36. Stuhne-Sekalec, L., Xu, S. X., Parkes, J. G., Olivieri, N. F. and Templeton, D. M., *Anal. Biochem.*, **205**, 278 (1992).
37. St Pierre, T. G., Chua-anusorn, W., Webb, J., Macey, D. and Pootrakul, P., *Biochim. Biophys. Acta*, **1407**, 51 (1998).
38. Kägi, J. H. R. and Vallee, B. L., *J. Biol. Chem.*, **235**, 3460 (1960).
39. Binz, P.-A. and Kägi, J. H. R., Metallothionein: molecular evolution and classification, in *Metallothionein IV*, Klaassen, C. D. (Ed.), Birkhäuser Verlag, Basel, 1999, pp. 7–13.
40. Klaassen, C. D. (Ed.), *Metallothionein IV*, Birkhäuser Verlag, Basel, 1999.
41. Öz, G., Pountney, D. L. and Armitage, I. M., Metallothionein structure update, in *Metallothionein IV*, Klaassen, C. D. (Ed.), Birkhäuser Verlag, Basel, 1999, pp. 37–43.
42. Schultze, P., Wörtgötter, E., Braun, W., Wagner, G., Vasák, M., Kägi, J. H. R. and Wüthrich, K., *J. Mol. Biol.*, **203**, 251 (1988).
43. Messerle, B. A., Schäffer, A., Vasák, M., Kägi, J. H. R. and Wüthrich, K., *J. Mol. Biol.*, **214**, 765 (1990).
44. Robbins, A. H., McRee, D. E., Williamson, M., Collett, S. A., Xuong, N. H., Furey, W. F., Wang, B. C. and Stout, C. D., *J. Mol. Biol.*, **221**, 1269 (1991).
45. Robbins, A. H. and Stout, C. D., *Methods Enzymol.*, **205**, 485 (1991).
46. Braun, W., Vasák, M., Robbins, A. H., Stout, C. D., Wagner, G., Kägi, J. H. R. and Wüthrich, K., *Proc. Natl. Acad. Sci. U.S.A.*, **89**, 10124 (1992).
47. Stillman, M. J., Green, A. R., Gui, Z., Fowle, D. and Presta, P. A., Circular dichroism, emission, and exafs studies of Ag(I), Cd(II), Cu(I), and Hg(II) binding to metallothioneins and modeling the metal binding site, in *Metallothionein IV*, Klaassen, C. D. (Ed.), Birkhäuser Verlag, Basel, 1999, pp. 23–35.
48. Templeton, D. M. and Cherian, M. G., *Methods Enzymol.*, **205**, 11 (1991).

49. Palmiter, R. D., *Proc. Natl. Acad. Sci. U.S.A.*, **95**, 8428 (1998).
50. Klaassen, C. D., Liu, J. and Choudhuri, S., *Annu. Rev. Pharmacol. Toxicol.*, **39**, 267 (1999).
51. Maret, W. and Vallee, B. L., *Proc. Natl. Acad. Sci. U.S.A.*, **95**, 3478 (1998).
52. Jacob, C., Maret, W. and Vallee, B. L., *Proc. Natl. Acad. Sci. U.S.A.*, **95**, 3489 (1998).
53. Panemangalore, M., Banerjee, D., Onosaka, S. and Cherian, M. G., *Dev. Biol.*, **97**, 95 (1983).
54. Templeton, D. M., Banerjee, D. and Cherian, M. G., *Can. J. Biochem. Cell Biol.*, **63**, 16 (1985).
55. Woo, E. S., Dellapiazza, D., Wang, A. S. and Lazo, J. S., *J. Cell. Physiol.*, **182**, 69 (2000).
56. Nagano, T., Itoh, N., Ebisutani, C., Takatani, T., Miyoshi, T., Nakanishi, T. and Tanaka, K., *J. Cell. Physiol.*, **185**, 440 (2000).
57. Palmiter, R. D., Metallothionein facts and frustrations, in *Metallothionein IV*, Klaassen, C. D. (Ed.), Birkhäuser Verlag, Basel, 1999, pp. 215–221.
58. Wirth, P. L. and Linder, M. C., *J. Natl. Cancer Inst.*, **75**, 277 (1985).
59. Vargas, E. J., Shoho, A. R. and Linder, M. C., *Am. J. Physiol.*, **267**, G259 (1994).
60. May, P., Modelling metal-ligand equilibria in blood plasma, in *Handbook of Metal-Ligand Interactions in Biological Fluids: Bioinorganic Chemistry*, Berthon, G. (Ed.), Marcel Dekker, New York, 1995, pp. 1184–1194.
61. Barrow, L. and Tanner, M. S., *Eur. J. Clin. Invest.*, **18**, 555 (1988).
62. Holmberg, C. G. and Laurell, C. B., *Acta Chem. Scand.*, **2**, 550 (1948).
63. Harris, E. D., *Nutrition*, **15**, 72 (1999).
64. Ardon, O., Kaplan, J. and Martin, B. D., Iron uptake in yeast, in *Molecular and Cellular Iron Transport*, Templeton, D. M. (Ed.), Marcel Dekker, New York, 2002, pp. 375–393.
65. Yoshida, K., Furihata, K., Takeda, S., Nakamura, A., Yamamoto, K., Morita, H., Hiyamuta, S., Ikeda, S., Shimizu, N. and Yanagisawa, N., *Nat. Genet.*, **9**, 267 (1995).
66. Harris, Z. L., Klomp, L. J. and Gitlin, J. D., *Am. J. Clin. Nutr.*, **67**(Suppl), 972S (1998).
67. Hellman, N. E. and Harris, Z. L., Aceruloplasminemia, in *Molecular and Cellular Iron Transport*, Templeton, D. M. (Ed.), Marcel Dekker, New York, 2002, pp. 749–760.
68. Farver, O. and Pecht, I., Electron transfer reactions in multi-copper oxidases, in *Multi-Copper Oxidases*, Messerschmidt, A. (Ed.), World Scientific Publishers, Singapore, 1997, pp. 355–389.
69. Zaitseva, I., Zaitsev, V., Card, G., Moshkov, K., Bax, B., Ralph, A. and Lindley, P., *J. Biol. Inorg. Chem.*, **1**, 15 (1996).
70. Harford, C. and Sarkar, B., *Acc. Chem. Res.*, **30**, 123 (1997).
71. Harford, C. and Sarkar, B., Main natural forms of metal ions in biofluids, in *Handbook of Metal-Ligand Interactions in Biological Fluids: Bioinorganic Medicine*, Berthon, G. (Ed.), Marcel Dekker, New York, 1995, pp. 62–70.
72. Bremner, I. and Beattie, J. H., *Proc. Nutr. Soc.*, **54**, 489 (1995).
73. Berg, J. M., *J. Biol. Chem.*, **265**, 6513 (1990).
74. Berg, J. M., *Acc. Chem. Res.*, **28**, 14 (1995).
75. Palmiter, R. D. and Findley, S. D., *EMBO J.*, **14**, 639 (1995).
76. Palmiter, R. D., Cole, T. B. and Findley, S. D., *EMBO J.*, **15**, 1784 (1996).
77. Eng, B. H., Guerinot, M. L., Eide, D. and Saier, M. H. Jr., *J. Membr. Biol.*, **166**, 1 (1998).
78. Lu, D., Boyd, B. and Lingwood, C. A., *J. Biol. Chem.*, **272**, 29033 (1997).
79. Lu, D., Boyd, B. and Lingwood, C. A., *FEMS Microbiol. Lett.*, **165**, 129 (1998).
80. Cornelis, R., *Ann. Clin. Lab. Sci.*, **26**, 252 (1996).
81. Whanger, P. D., Xia, Y. and Thomson, C. D., *J. Trace Elem. Electrolytes Health Dis.*, **8**, 1 (1994).
82. Saijoh, K., Saito, N., Lee, M. J., Fujii, M., Kobayashi, T. and Sumino, K., *Mol. Brain Res.*, **30**, 301 (1995).
83. Yoneda, S. and Suzuki, K. T., *Biochem. Biophys. Res. Commun.*, **231**, 7 (1997).
84. Behne, D. and Kyriakopoulos, A., *Annu. Rev. Nutr.*, **21**, 453 (2001).
85. Kyriakopoulos, A., Röthlein, D., Pfeifer, H., Bertelsmann, H., Kappler, S. and Behne, D., *J. Trace Elem. Med. Biol.*, **14**, 170 (2000).
86. Kobayashi, Y., Ogra, Y. and Suzuki, K. T., *J. Chromatogr.*, **B 760**, 73 (2001).
87. Klopman, G., Generalized perturbation theory of chemical reactivity, in *Chemical Reactivity and Reaction Paths*, Klopman, G. (Ed.), John Wiley, New York, 1974, pp. 55–165.
88. Yap, K. L., Ames, J. B., Swindells, M. B. and Ikura, M., *Proteins*, **37**, 499 (1999).
89. Strynadka, N. C. J. and James, M. N. G., *Annu. Rev. Biochem.*, **58**, 951 (1989).
90. Hook, S. S. and Means, A. R., *Annu. Rev. Pharmacol. Toxicol.*, **41**, 471 (2001).
91. Chao, S.-H., Suzuki, Y., Zysk, J. R. and Cheung, W. Y., *Mol. Pharmacol.*, **26**, 75 (1984).

CHAPTER 3

Modeling of Elemental Species

3.1 Thermodynamic Modeling of Trace Element Partitioning in the Environment: New Concepts and Outlook

Michael Kersten
Johannes Gutenberg-University, Mainz, Germany

Dmitrii A. Kulik
Paul Scherrer Institute, Villigen-PSI, Switzerland

1 INTRODUCTION

Partitioning and fate of trace elements in natural aquatic systems cannot be described without an understanding of chemical processes that determine the distribution of chemical elements between aqueous, gaseous, and solid phases and into different physicochemical forms (species) in

Handbook of Elemental Speciation II: Species in the Environment, Food, Medicine & Occupational Health
Edited by R. Cornelis, H. Crews, J. Caruso and K. G. Heumann
 ISBN: 0-470-85598-3 (HB)

these phases. Knowledge of such *speciation* is particularly important, for instance, in studies of the interaction of trace metals with aquatic organisms, where the free metal ion activity in aqueous solution appears to be a major indicator of metal toxicity or availability. Migration of metals in saturated and unsaturated zones in the subsurface is affected by their interaction with soil and sediment solids, which strongly depends on properties such as charge and associated ligand functionality of both the metal species and pore surfaces. In water–rock interaction, the precipitation or dissolution of trace element–bearing minerals occurs under a particular set of conditions such as temperature, pressure, redox potential, and pH of aqueous solution.

Advanced direct analytical speciation techniques (such as X-ray absorption spectroscopy) overcome sensitivity and heterogeneity problems and enable better species selectivity. However, it is still difficult to determine quantitatively the complete speciation in a heterogeneous system and the evolution of concentrations and fluxes of trace element species of interest under dynamic natural physicochemical conditions, because this would require labor-intensive multitechnique sampling and analytical approaches. Alternatively, the *numerical methods of trace element speciation modeling* using the concepts of chemical thermodynamics, developed since 1960s, can provide important parameters of species formation or rate constants for the (steady-state) system of interest. In particular, the computer-aided chemical thermodynamic models were successfully used (i) to *a priori* determine the possibility and conditions of a process or reaction to proceed; (ii) to quantitatively determine the equilibrium composition (speciation in phases) at the conditions of interest in a complex heterogeneous geochemical system; (iii) to investigate stability of mineral assemblages at such conditions where experimental studies are difficult or impossible (e.g. under extreme temperature, pressure, or very long equilibration times); and (iv) to visualize possible equilibrium states or reaction paths under selected physicochemical conditions in phase diagrams. Descriptions of the basic rationale of such diagrams (and the thermodynamic concepts behind them) can be found in many physicochemical textbooks for earth sciences, in particular, those dedicated to geochemistry in general [1, 2] or those more constrained to aquatic geochemistry [3–5] or chemical oceanography [6].

This chapter is neither intended to provide a complete overview of all chemical speciation modeling techniques nor to give a tutorial on a particular thermodynamic modeling program or database for inorganic or organic species of trace metals. Available modern program packages are in most cases share- or freeware, and many can be downloaded together with the built-in thermodynamic databases and the extensive HTML or PDF documentation files. As there are numerous reviews and several good textbooks on geochemical modeling already available [7–10], in our contribution we would like rather to emphasize less commonly described innovative issues in the aquatic geochemical modeling, namely, (i) the Gibbs energy minimization (GEM) method with a special reference to metastability and redox states of aquatic geochemical systems, (ii) the end-member stoichiometry and (non) ideal mixing in solid-solution aqueous-solution systems, further extended to sorption phases with surface complexation, (iii) the temperature corrections of standard thermodynamic data for aqueous and surface species, and (iv) the 'dual-thermodynamic' calculations. GEM-based models are emphasized here because they favorably adopt these issues and comprise a versatile approach capable of considering the whole range of chemical speciation in coexisting phases (i.e. multicomponent aqueous speciation + adsorption + ion exchange + solid solutions + minerals) simultaneously in one model run. In this way, hypotheses about the evolution pathways of the geochemical system can be tested, ultimately yielding a deeper understanding of the system of interest and its chemical mass-transfer processes within a framework of the available geochemical and experimental data.

Application of thermodynamic models to elucidate trace element speciation/partitioning is relatively easy in the close-to-equilibrium systems in which necessary thermodynamic input parameters are reasonably well known. However, modeling

of complex systems such as natural waters and sediments presents certain difficulties. The most serious limitation is that a uniform thermodynamic database for all components of interest in the environmental geochemistry has not yet been compiled so far, in particular, not for the overwhelming variety of organic species, ligands, and colloids, whose formation is mediated by living (micro) organisms, albeit much progress is currently done in filling out this gap [11–13]. Moreover, purely thermodynamic models can consider only stable initial and final states of the system, while metastability or reactivity of phases with transformation pathways can only be simulated using additional kinetic constraints. Nevertheless, thermodynamic speciation models often provide a significant contribution to our understanding of the dynamic environmental geochemical system [14] and thus complement analytical studies of trace metal partitioning and speciation reviewed recently, for example in [15, 16].

2 EQUILIBRIUM THERMODYNAMIC SPECIATION MODELING

2.1 Concepts

While it is widely recognized that kinetic factors may play an important role in trace element speciation, all thermodynamic modeling approaches commence with the problem of finding the phase speciation from the bulk chemical composition at an *equilibrium state*, where all the intensive (nonadditive) parameters such as temperature T, pressure P, chemical potential μ, and so on, are equal in all parts of the system of interest and do not change with time. Such a system, in principle, is a collection of material phases separated from their environment by a boundary chosen according to the objective of the study. *Phases* can have constant or variable chemical composition (expressed as single- or multicomponent phases, respectively) and exist in gaseous, aqueous, or solid aggregate state.

To describe chemical composition of the whole system, with all phases and their species, one first has to select the *independent components*, that is, individual chemical substances that, being taken in the smallest possible quantities (stoichiometry units), are sufficient to form all phases. A convenient and rigorous way is to take the chemical elements and electrical charge as independent components; however, other choices (aqueous ions, oxides like SiO_2) have also been in use. Now, all involved chemical species (*dependent components*, substances, chemical species) can be expressed using the independent components (with stoichiometry coefficients). In the case of elemental stoichiometry units, the composition of any species is just given by its chemical formula, such as $CaHCO_3^+$ or CH_4.

The choice of chemical species must be done in such a way that equilibrium properties of all phases can be described in a full range of their chemical composition. Natural waters, for example, contain species belonging to an aqueous electrolyte, a gas mixture, and several solid and sorption phases. By neglecting exchange of matter with the surroundings outside the chosen boundary, and assuming ideal mixing behavior in the multicomponent phases, the thermodynamic treatment of such a closed system becomes relatively straightforward.

The equilibrium composition of the system (i.e. phase assemblage and *speciation*) can be found by minimizing the total Gibbs energy of the system subject to the material balance constraints (referred to as the *GEM approach*). Alternatively, the equilibrium speciation can be calculated by minimizing the material balance deviations subject to the boundary conditions made of the law of mass action (LMA) expressions for the so-called 'product species' (referred to as the *LMA approach*). In the past, several mathematical algorithms and program codes have been developed to implement these two complementary approaches, but, so far, the latter (LMA) approach is mostly in use. Unlike the latter, the more general GEM approach considers only properties of thermodynamic phases and their species, but does not require writing of any explicit reactions between species [17, 18] because, at equilibrium, no reactions actually proceed.

Table 3.1.1. Generic tabular form of chemical speciation (used in GEM approach).

Components	H	O	e	x_j, mole amounts
H_2^0	2	0	0	x_1
O_2^0	0	2	0	x_2
OH^-	1	1	−1	x_3
H^+	1	0	1	x_4
H_2O	2	1	0	x_5
Vector $\boldsymbol{b}$	b_1	b_2	$b_3 = 0$	

In a more formal algebraic notation, one can write for a phase (indexed with α):

$$n_\alpha = \sum_j n_j; \quad j \in D_\alpha, \alpha \in \Phi \tag{3.1.1}$$

where D_α stands for a set of indices of species included into α^{th} phase (e.g. aqueous electrolyte), Φ is a set of all phases included into the system definition, n_α denotes total mole amount of this phase, and n_j stands for the mole amount of j^{th} species. Note that in geochemical literature (e.g. [17]), x or X characters are sometimes used for the number of moles to emphasize that mole amounts of species and phases are *mathematical unknowns* in a sense of equilibrium speciation calculations. Conversely, the bulk chemical composition of the system (given as input data) will be denoted by the b_i values (mole amount of i^{th} stoichiometry unit), with indices i belonging to a set of indices of *independent components*.

Any chemical system can be constrained by a set of equations expressing the mass conservation of independent components. Consider, for simplicity, that only one phase of variable composition is present – then equations like (3.1.1) can be avoided. There is one material balance equation per independent component:

$$\sum_j a_{ij} n_j = b_i; \quad i \in I_C, j \in D_C \tag{3.1.2}$$

where D_C is a set of indices of all dependent components, a_{ij} is a mole amount of i^{th} independent component in one mole of j^{th} species, and b_i is the total mole amount of i^{th} independent component in the bulk chemical composition of the system. The coefficients a_{ij} form a *stoichiometry matrix* $\boldsymbol{A} = \|a_{ij}\|, i \in I_C, j \in D_C$. For instance, the pure aquatic system, H–O–e (e stands for the electrical charge), has three independent components (H, O, and e) and consists of five species: H_2^0, O_2^0 (dissolved gases), OH^-, H^+ (ions), and H_2O (solvent). Hence, the $\boldsymbol{A}$ matrix (numbers in the box) will look like that shown in Table 3.1.1. Likewise, one can represent the system bulk composition as a vector-row $\boldsymbol{b} = \{b_i\}$, where $i \in I_C$, and the sought-for speciation as a column-vector $\boldsymbol{x} = \{x_j\}$, with $j \in D_C$ (Table 3.1.1, x is used here to emphasize that mole amounts n of individual chemical species in this vector are *unknowns*). In such a vector–matrix notation, the system of material balance equations (3.1.2) looks pretty simple:

$$\boldsymbol{A} \cdot \boldsymbol{x} = \boldsymbol{b} \tag{3.1.3}$$

Mathematical solution of equations (3.1.2) or (3.1.3) is straightforward only if the number of species does not exceed the number of independent components, that is, $N(D_C) \leq N(I_C)$. However, this trivial case is usually not interesting for geochemists because it implies that the calculation will not yield any new information about chemical speciation. Therefore, any practically important thermodynamic system formulation with $N(D_C) > N(I_C)$ requires more input information in the form of *thermodynamic data*.

The two (LMA and GEM) approaches to calculate equilibrium speciation differ mainly in what kind of input thermodynamic data is needed, and in which way these data are used. In the case of system formulation like that presented in Table 3.1.1, there is no dependent component of the same elemental composition as any independent component (chemical element or charge). Hence, in

Table 3.1.2. LMA tableau concept [4] exemplified for the pure water system: H^+ and H_2O are the master species; OH^- is a product species.

Species	H^+	H_2O	log K	n_j, mole amounts
OH^-	−1	1	−14	$1{\cdot}10^{-7}$
H^+	1	0	0	$1{\cdot}10^{-7}$
H_2O	0	1	0	$55.5084{-}1{\cdot}10^{7}$
Total, moles	0	55.5084		

order to decide how to split the bulk elemental composition between possible species, one needs to know the *standard molar chemical potential* μ^0 of each dependent component in order to find such a vector $\boldsymbol{x}$ that would provide a minimum of the total Gibbs energy of the whole system,

$$G = \sum_j x_j \left(\frac{\mu_j^0}{RT} + \ln c_j + \ln \gamma_j \right), \quad j \in D_C \tag{3.1.4}$$

where c_j stands for the *concentration*, γ_j is an *activity coefficient* of jth species in its phase, R is the universal gas constant, T is temperature, and x_j is subject to material balance constraints, as expressed in equation (3.1.2). The $\mu_j^0 = G_j^0$ values at reference temperature $T_r = 25\,^\circ\mathrm{C}$ and pressure $P_r = 1$ bar, representing the *standard molar Gibbs energy function* (of formation from elements), can be found in several published chemical thermodynamic databases such as SUPCRT92-98 [19] and can be corrected to temperature T and pressure P of interest (see below). The presence of logarithmic terms in equation (3.1.4) requires application of a nonlinear minimization iterative numerical algorithm to solve the problem directly, starting from a feasible initial guess of mole amounts of chemical species. This method of solution is the most straightforward and universal, though relatively difficult in computer code implementation and rather sensitive to inconsistencies in thermodynamic data. Declaration of independent components ('master species') identical to some dependent components can make some problems of equilibrium aqueous speciation much easier to solve. For instance, the water system can be described using the H^+ and H_2O master species, while the remaining OH^- ion (a 'product species') is constructed out of the master species in a formation reaction $H_2O - H^+ \leftrightharpoons OH^-$. Now (in Table 3.1.2), stoichiometry coefficients in each line are actually coefficients in the respective reaction of formation of the product species from the master species. For the H^+ and H_2O species, such reactions are trivial (e.g. $H^+ = H^+$ with *equilibrium constant* $K = 1$), but the OH^- product species is defined by the water dissociation reaction $H_2O - H^+ = OH^-$ with an equilibrium constant $K \approx 10^{-14}$ at 25 °C (in molal concentrations m, mol·[kg H_2O]$^{-1}$). Since the input total amount of charge (total H^+) is given zero, the activities of both OH^- and H^+ ions must be equal and their product must be close to 10^{-14} (the equilibrium constant of the water dissociation reaction), or $m(H^+){\cdot}\gamma(H^+) = m(OH^-){\cdot}\gamma(OH^-) = 10^{-7}$ molal. In this system, one can assume both activity coefficients $\gamma(H^+) = \gamma(OH^-) = 1$ because total concentration of charged ions ('ionic strength') is very low ($2{\cdot}10^{-7}$ m). Hence, $n(H^+) = n(OH^-) = 10^{-7}$ mol; the first mass-balance equation (3.1.2), $n(H^+) - n(OH^-) = 0$, is already fulfilled; substitution of the $n(H^+)$ and $n(OH^-)$ values into the second balance equation for H_2O master species yields $10^{-7} + 0 + n(H_2O) = 55.5084$, that is, $n(H_2O) = 55.5084 - 10^{-7}$ mol (see Table 3.1.2).

This very simple case can be solved by hand; however, more complex aqueous equilibria would require knowledge of activity coefficients and 'trial-and-error' iterative calculations – widely used since the pioneering work by Garrels [20, 21]. In a more general sense, introduction of the nonlinear LMA expressions for the 'product species' requires the application of computers using the Newton–Raphson (or similar) numerical algorithm to minimize deviations in the mass-balance equations (3.1.2). LMA expressions are used as boundary conditions to find the quantity

(molar amount or concentration) of a product species from current quantities of the master species, equilibrium constants, and activity coefficients. The most-widespread computer codes of this kind are MINEQL [22, 23], FITEQL [24], and PHREEQC [25]. The LMA codes use only equilibrium constants of reactions of formation of product species from the master species at given T, P as input thermodynamic data. Many of them also eliminate the water solvent from the material balance equations by considering, for example, molality concentrations directly, instead of mole amounts of master and product species [7–9].

Regardless of how the geochemical equilibrium speciation vector $\boldsymbol{x}$ has been found, it represents an *equilibrium state* completely defined by the system bulk composition $\boldsymbol{b}$, T, and P and, optionally, by a given set of the *metastability constraints*. Any change in this isobaric–isothermal state (e.g. change of the bulk composition) will drive the system toward a new (partial or local) equilibrium state via the mass transfer through some reactions (belonging to a set $\Re$) between species of some phases. In a general way, such a (irreversible) process can be expressed as

$$n_j = n_j^0 + \sum_k \nu_{jk}\xi_k,\ j \in D_C, k \in \Re \qquad (3.1.5)$$

where n_j^0 is the initial molar amount, ν_{jk} is a stoichiometry coefficient of jth species in kth reaction, ξ_k is a *reaction extent parameter*, and $\Re$ is the entire set of reactions. If no changes in $\boldsymbol{b}$, T, and P occur with time, then the process is purely *kinetic*, and $\mathrm{d}\xi_k/\mathrm{d}\tau$ can be considered as a k^{th} reaction rate. The system is constrained by the material balance equation (3.1.2) at constant bulk composition vector $\boldsymbol{b}$; thus, an increase in certain n_j amounts must be exactly compensated by a decrease in other n_j according to stoichiometry coefficients ν_{jk} of species in the kinetically controlled reactions. If all the relevant reactions between chemical species proceed much more rapidly than the parameters of state ($\boldsymbol{b}$, T, or P) change (*steady state*), then all the individual ν_{jk} and ξ_k parameters become obsolete because over a given time interval $\Delta\tau$, the equilibrium speciation vector $\boldsymbol{n}$ is determined only by the current parameters of state. Such a process can be fully described by applying the extent variables *directly* to the input T, P, or b_i values. The most common situation is an *irreversible change of the bulk composition*:

$$b_i = b_i^0 + \sum_k \nu_{ik}\xi_k,\ i \in I_C \qquad (3.1.6)$$

where ν_{ik} can be called a 'process stoichiometry coefficient', and ξ_k, a 'process extent variable'. Titration, mixing, and weathering are typical examples that can be simulated using equation (3.1.6) as a sequence of $N(Q)$ discrete equilibrium states set by

$$b_i^q = b_i^0 + \frac{q}{N(Q)}\sum_k \nu_{ik}\xi_{k,\max},\ i \in I_C,$$
$$q = 1, \ldots, N(Q) \qquad (3.1.7)$$

Here, $\xi_{k,\max}$ is a maximum possible process extent value. Equation (3.1.7) linearly increments the bulk composition vector; often, a logarithmic version of the process extent increment is used in chemical thermodynamic modeling, especially to simulate titration-induced reactions:

$$\log b_i^r = \log b_i^0 + \frac{q}{N(Q)}\sum_k \log(\nu_{ik}\xi_{k,\max}) \qquad (3.1.8)$$

For instance, titration of the aquatic system with Na_2CO_3 will require $\nu_O = 3\nu_C$, $\nu_{Na} = 2\nu_C$, and a common $\xi_{\max}$ value to increment b_O, b_C, and b_{Na}, leaving other elements of the stoichiometry vector $\boldsymbol{b}$ unchanged. Upon equilibration, concentrations of dissolved species of Na, C, pH, $f(CO_2)$, and other parameters will change; plotting those against the fractional reaction extent ξ yields *process-extent diagrams* – a common tool for depicting geochemical process models.

Slow heterogeneous reactions (mineral coprecipitation, dissolution, chemisorption) often control trace metal behavior in low-temperature geochemical environments. Simulation of such cases obviously requires a combination of the reaction-extent and process-extent models where rates in equations (3.1.5) and (3.1.6) may also be functions of time. With time, all reactions proceed toward equilibrium, causing a decrease in the total Gibbs energy function G of the system. A j^{th} species

contributes to this as given by equation (3.1.9):

$$\left(\frac{\partial G}{\partial \xi_j}\right)_{\xi_{k\neq j}} = \left(\frac{\partial G}{\partial n_j}\right)_{n_{k\neq j}} \left(\frac{\partial n_j}{\partial \xi_j}\right)_{\xi_{k\neq j}} \qquad (3.1.9)$$

The expression $\left(\frac{\partial G}{\partial n_j}\right)_{n_{k\neq j}} = \mu_j$ defines a chemical potential of the j^{th} species in the system at fixed T and P. At equilibrium (denoted by a roof symbol, e.g. $\hat{x}$), $\left(\frac{\partial G}{\partial \xi_j}\right)_{\xi_{k\neq j}} = 0$ for all species, so the total Gibbs energy $G(\hat{x})$ of the system is an additive function of chemical potentials: $G(\hat{x}) = \sum_j x_j \mu_j$, $j \in D_C$.

Any k^{th} reaction between chemical species can be characterized by a molar Gibbs energy effect (change) $\Delta_r G = \Delta_r \mu$, where $\Delta_r G$ is an algebraic sum of molar Gibbs energies of reactants (with negative stoichiometry coefficients ν_j) and products (with positive coefficients ν_j), all belonging to a set of reaction components $\Re_k$:

$$\Delta_r G = \sum_j \nu_j G_j, \quad j \in \Re_k \qquad (3.1.10)$$

According to the definition of standard state, the molar Gibbs energy of a jth species is $G_j = G^0 + RT \ln a$, where a stands for the *activity* (thermodynamic concentration) and $G^0 = \mu^0$ is a standard molar Gibbs energy (of formation from elements in their standard states) at unity activity. Substituting this expression into equation (3.1.10), one obtains

$$\sum_j \nu_j G_j^0 + RT \sum_j \nu_j \ln a_j = \Delta_r G,\ j \in \Re_k \qquad (3.1.11)$$

As the system approaches equilibrium, where for all species $\left(\frac{\partial G}{\partial \xi_j}\right)_{\xi_{k\neq j}} = 0$, $\Delta_r G$ approaches zero by changing activities of species involved into the reaction in such a way that, at equilibrium,

$$\Delta_r G^0 = \sum_j \nu_j G_j^0 = -RT \sum_j \nu_j \ln a_j = -RT \ln \prod_j a_j^{\nu_j} = -RT \ln K,\ j \in \Re_k \qquad (3.1.12)$$

where $\Delta_r G^0$ is the standard Gibbs energy change and $K = \prod_j a_j^{\nu_j}$ is an *equilibrium constant* for the reaction. The value of K depends on the choice of standard state and concentration scale for all the species [1]. Usually, the *pure substance* standard state and *mole fraction* concentration scale are applied to gases (at $P = 1$ bar), solids, nonelectrolyte liquids, and water-solvent; *unimolal* standard state and *molal* concentration scale (mol per 1 kg of H_2O) are used for aqueous electrolyte species and surface species at the mineral–water interfaces.

The fundamental equations (3.1.10) to (3.1.12) link equilibrium constants of reactions to activities and standard molar Gibbs energies of separate species and, in this sense, demonstrate a complementarity of the alternative GEM and LMA approaches to thermodynamic modeling. In GEM algorithms, the total Gibbs energy of the system (equation 3.1.4) is minimized by adjusting mole amounts of species subject to material balance constraints (equation 3.1.2). In LMA speciation algorithms, based on equation (3.1.12), the LMA expressions $\ln K = \sum_j \ln a_j^{\nu_j}$, $j \in \Re_k$ for the 'product species' are used for solving the system of mass balance equations for mole amounts (or concentrations) of the 'master species', and, via LMA expressions, 'product species'.

The LMA approach has been pioneered by geochemists since early 1960s; the history of this endeavor can be found, for example, in a recent review by Waite [8]. The majority of early modeling codes were based on the LMA concept and used the Newton–Raphson algorithm to iteratively minimize the difference between the input and the calculated total master species concentrations. The choice of master species is critical to the efficient solution of the problem. Improvements in algorithms based on the LMA approach have led to several 'second-generation' computer programs, capable of modeling sorption processes important in describing the speciation of trace elements in heterogeneous environmental systems. Modern LMA codes such as EQ3/6 [26], GWB [7], and PHREEQC-2 [25] are also capable of simulating reaction pathways and irreversible processes in batch calculations of series of aqueous equilibria (similar to equations 3.1.5

to 3.1.8). These computer codes are equipped with LMA thermodynamic databases maintained by relevant governmental organizations (USGS, DOE, or USEPA). Since its release in 1999, the public-domain code PHREEQC-2 has rapidly become a widespread standard for hydrogeochemical modeling, in particular, also because of its capability to deduce reaction pathways along the groundwater flow from the inverse modeling, and to include kinetics via the built-in Basic script editor and the powerful Runge–Kutta integrator. The PHREEQC-2 speciation solver has also been included into a number of coupled codes for transport modeling (for details, see [25]).

The LMA algorithms do have some clear advantages, in particular: (i) simple theory and mathematical definitions; (ii) very good mass balance precision and fast convergence of the numerical algorithms; (iii) simple, compact, and transparent program codes, already coupled with mass-transport programs for simulating pollutant transport in (sub)surface waters; (iv) no thermochemical data are needed for the master species, and only $\log K = f(T)$ for the product species are required as input thermodynamic data. At the same time, even though the convenience and the computational ease of the LMA approach are beyond dispute, its inherent mathematical structure poses certain limits to setting up the thermodynamic models, and these limits become severe when complex natural systems are to be considered. Only a predefined set of fixed-composition solid phases can be included into the mass balance, and only one multicomponent phase of variable composition (either aqueous or gaseous) can be directly considered without introducing new master species. This drawback is particularly painful when sorption- or solid-solution phases are to be considered together with aqueous electrolyte. In the case of surface complexation, this is circumvented by adding one or more master species called 'total number of sites'. Mineral solid solution phases can be taken into the LMA tableau as fixed-stoichiometry product species only, described by a single equilibrium solubility product constant assuming a unit activity. In other words, to calculate the aqueous speciation at equilibrium with the solid solution, one must know the composition of the solid solution, which itself depends on the composition of coexisting aqueous electrolyte – a logical circle... For binary solid solutions, the problem can be obviated by using supporting tools such as the Lippmann's diagrams and the MBSSAS code [27–29]. Moreover, different redox states of the same element (e.g. Fe^{2+}, Fe^{3+}) are usually assigned to separate master species and mass-balance constraints, which means that the redox state of the system must be known *before* speciation calculations and given as separate total concentrations of master species of the same element but different redox states. Alternatively, one can introduce an 'electron' master species and then provide an *a priori* known pe (or Eh) value as input data; but this is often something that we would rather model than guess!

The GEM approach is complementary to the LMA concept and it is free from the limitations mentioned above. In GEM formulation, the mole amounts of elements and charge can be given as the input bulk composition of the system (stoichiometry vector $\boldsymbol{b}$), and *all stoichiometrically feasible species* in all potentially existing phases can be taken with their chemical formulae into the mass balance. Species (dependent components) belong to either single- or multicomponent aqueous, gaseous, liquid, solid, or sorption phases, any number of which can be included into the system formulation and may (or may not) appear at the equilibrium state. A nonlinear minimization algorithm [17] iteratively finds such quantities of all relevant species and phases that minimize the convex total Gibbs energy function of the system, subject to the elemental mass balance constraints (equation 3.1.3) and optional metastability restrictions. An efficient mathematical approach to GEM formulation of chemical equilibria has been developed using a set-theoretical vector–matrix notation [17]. This 'third generation' of thermodynamic modeling concept (and potential applications thereof) is still less well known and will therefore be discussed in more detail, and also from a perspective of the more usual LMA approach where appropriate, in the following sections.

2.2 Gibbs energy minimization approach

The GEM approach is based on an explicit consideration of *independent components* (stoichiometry units, usually chemical elements and charge), from which the *dependent components* (chemical *species* of a definite stoichiometry) are built and then grouped into *multi- or single-component phases*. Stability of each j^{th} species is characterized by its molar Gibbs energy of formation G_j^0 from chemical elements in their respective standard states, available from thermochemical databases like SLOP98.DAT [19]. Dependent components are taken into the material balance (set by total mole quantities of independent components) using their elemental stoichiometries (formulae), each expanded into one line of the stoichiometry matrix $\boldsymbol{A}$ (see equation 3.1.2). An important difference between the LMA and the GEM algorithms is that in the latter, activities and concentrations of dependent components are treated separately in each phase, taking into account the appropriate standard and reference states, concentration scales, and mixing properties. Conversely, it is possible in the GEM approach to solve complex equilibria directly, even in systems containing simultaneously several multicomponent (non) ideal liquid or solid solutions, gas mixture, aqueous electrolyte, sorption phases, and more single-component condensed phases than allowed by the Gibbs phase rule. The input and output data sets required by the GEM technique are listed in Table 3.1.3.

Calculation of equilibrium and, hence, the full speciation in stable phases of the system is equivalent to solving a 'primal' Gibbs energy minimization problem: find such a vector $\boldsymbol{x}$ that

$$G(\boldsymbol{x}) \Rightarrow \text{ min}, \quad \text{subject to } \boldsymbol{A}\cdot\boldsymbol{x} = \boldsymbol{b} \qquad (3.1.13)$$

where $\boldsymbol{A} = \{a_{ij}, i \in I_C, j \in D_C\}$ is the stoichiometry matrix, $\boldsymbol{b} = \{b_i, i \in I_C\}$ is the input vector of the total bulk chemical composition of the system, and $\boldsymbol{x} = \{x_j, j \in D_C\}$ is a sought-for vector of molar amounts of dependent components in all phases (x_j is used instead of n_j here to emphasize that mole amounts of chemical species are *unknowns*). However, solving the primal minimization problem for the aquatic system routinely with the Newtonian algorithm (as it was done in early GEM computer codes, cf. [30]) may sometimes lead to numerical failures because of the extreme range (more than 20 orders of magnitude) of dissolved aqueous concentrations and hence values of the $\boldsymbol{x}$ vector. A far more advanced 'Interior Points Method' algorithm [17, 18] to solve numerically the problem (equation 3.1.13) is based on the so-called *Kuhn–Tucker duality theorem* of mathematical programming. This theorem includes an alternative vector $\boldsymbol{u}$ of unknowns – Lagrange multipliers – that allow one to solve the minimization problem iteratively in a space of much smaller dimensionality ($d(I_C)$ instead of $d(\Phi)$). Moreover, the u_i values vary only within 2–3 orders of magnitude – not in more than 20 orders as the x_j

Table 3.1.3. Input and output data sets and vectors in the GEM convex programming algorithm.

Input data	Output data
I_C – set of independent components	–
D_C – set of dependent components	$\boldsymbol{x}$ – vector of mole amounts of D_C at equilibrium (primal solution)
Φ – set of phases ($\Phi \geq I_C$)	$\boldsymbol{f}_\alpha$ – Karpov's stability criteria for phases
$\boldsymbol{A}$ – formula I_C stoichiometry matrix for D_C	–
$\boldsymbol{b}$ – bulk chemical composition (moles of I_C)	$\boldsymbol{u}$ – vector of chemical potentials of I_C at equilibrium state (dual solution)
T – temperature, P – pressure of interest	–
$\boldsymbol{g}_{T,P}$ – vector of partial molar Gibbs energy functions of D_Cs corrected to T, P	$\boldsymbol{\mu}$ – vector of chemical potentials of D_C's at equilibrium state
Parameters and equations for calculation of activity coefficients, kinetic restrictions	D_C activity coefficients $\boldsymbol{\gamma}$ (or SAT values for surface species)
Optional: specific surface area and surface free energy of solid sorbents, parameters of surface (site) types	Secondary: concentrations of species in phases, equilibrium pH, pe (Eh), partial pressures of gases, surface densities of sorbates, distribution coefficients, and so on

values. But, most important, the duality theorem leads to the Kuhn–Tucker necessary and sufficient conditions of the minimum that also show in which direction the minimum is located. For chemical equilibria (without additional metastability constraints), the Kuhn–Tucker conditions in vector–matrix form as introduced by Karpov *et al.* [17, 18, 30] are

$$\begin{aligned} \upsilon - A^{\mathrm{T}}u &\geq 0; \\ A\cdot\hat{x} = b;\ \hat{x} &\geq 0; \\ \hat{x}^{\mathrm{T}}(\upsilon - A^{\mathrm{T}}u) &= 0 \end{aligned} \qquad (3.1.14)$$

where $^{\mathrm{T}}$ is the transpose operator, and υ is a vector of chemical potential approximations,

$$\boldsymbol{\upsilon}_j = \mu_j^0/RT + \ln c_j + \ln \gamma_j + \text{const},\ j \in D_C. \qquad (3.1.15)$$

The first condition in (equation 3.1.14), if rewritten with indices, implies that for any species present at equilibrium concentration c_j in its phase, the *primal* chemical potential υ_j (calculated from the mole amount x_j and the standard potential μ_j^0/RT) numerically equals the *dual* chemical potential $\sum_i a_{ij}u_i$. Hence, the $u_j{\cdot}RT$ values are *chemical potentials of independent components* at the equilibrium state of interest. If the $G(\hat{x})$ minimum is not yet achieved, the primal chemical potential approximation will differ from the dual potential at least for some species present in positive mole quantities. The sign of the difference shows whether the respective x_j values should be decreased or increased at the next iteration of the minimization algorithm.

Solutions of both primal and its mirroring dual minimization problems coincide in a saddle point in the $(D_C + I_C)$ space, determined by the Kuhn–Tucker conditions of optimality [17] (equation 3.1.14). Since the scalar $G(x)$ function, defined in the D_C space of dependent components, is generally nonlinear and convex, this saddle point is a global minimum of $G(x)$. The dual function $G(u)$, defined in the coordinate space of independent components, approaches a global maximum at the same point, that is, there $G(\hat{x}) = G(u)$.

The 'interior points method' (IPM) algorithm [17] is a robust and efficient tool for calculation of complex chemical equilibria. The IPM is a 'numerical engine' of the Selektor family of computer codes [17, 18], of which GEM-Selektor v.2-PSI is the most recent user-friendly version [31, http://les.web.psi.ch/Software/GEMS-PSI/index.html].

For any species present at equilibrium, the first Kuhn–Tucker condition (equation 3.1.14) can be combined with equation (3.1.15) into a 'dual thermodynamic equation' [18, 32]:

$$\sum_i a_{ij}u_i = \frac{\mu_j^0}{RT} + \ln a_j = \frac{G_{j,T}^0}{RT} + \ln c_j + \ln \gamma_j + \text{const} \qquad (3.1.16)$$

This equation is used in the IPM module of GEM-Selektor to calculate (i) activities of aqueous, solid-solution and sorption species, (ii) fugacities of gases, (iii) saturation indices for single-component condensed phases, and (iv) functions of activity such as pH, pe, and Eh. Equation 3.1.16 also forms a basis of the 'dual thermodynamic' (DualTh) calculations – a new technique for retrieval of thermodynamic data from the information about the equilibrium partitioning of chemical elements between solid-solution, sorption, and aqueous phases. Since the DualTh concept appears to be an important innovation in thermodynamic data evaluation, it will be discussed briefly in the following sections.

2.3 Input chemical thermodynamic database

Results of thermodynamic speciation modeling cannot be better as the input $\log K$ or G_T^0 values. For this reason, the compilation of internally consistent chemical thermodynamic databases has long been an important priority topic. All recently developed modeling codes are distributed together with one or several thermodynamic data files. For instance, the LMA code PHREEQC version 2.6 comes with four databases (**`wateq.dat`**; **`phreeqc.dat`**; **`minteq.dat`** and **`llnl.dat`**) that can be used alternatively [25]. The ChemSage GEM code [33] has recently been merged into the integrated thermochemical databank system

F*A*C*T; the resulting (commercial) product is now called FactSage [34]. 'Stand-alone' chemical thermodynamic databases such as SUPCRT92 [19, 35] and Nagra-PSI 01/01 [36] were also integrated into modeling codes, for example, into GEM-Selektor. This trend is quite understandable because only a combination of the modeling algorithm with the appropriate database of species stoichiometries and thermodynamic properties will make both efficient. Even an excellent numerical code makes little sense alone because the compilation of a meaningful thermodynamic database requires years of highly qualified work.

Application of GEM to aquatic systems requires, in fact, more thermodynamic data of higher quality (G^0 values for all species in all phases) than that for the LMA algorithms ($\log K$ for the product species only); the data requirements become severe if the modeling has to be performed in a wide T–P range. While good thermochemical databases for solids and gases exist since 1950s ([37–41]; see also a list in [2]), the standard partial molal properties (Gibbs energy G^0, enthalpy H^0, entropy S^0, heat capacity C_P, volume V^0) of many aqueous ions and complexes remained unknown or inconsistent until 1980s, when Helgeson and coworkers developed the so-called revised HKF EoS (Helgeson–Kirkham–Flowers Equation of State) and used it to regress the standard properties of the majority of aqueous ions from experimental data [42, 43]. These authors have also established a set of correlation techniques to predict standard partial molal properties and HKF EoS parameters for a vast variety of aqueous ions, complexes, and organic species [19, 44]. Compilation of this database was also supported by a release of the SUPCRT92 program [35] capable of calculating standard partial molal properties of aqueous species up to 1000 °C and 5 kbar and their changes in any reaction between aqueous species in those T and P ranges. The SUPCRT92 source code was also available, which led to its incorporation in several thermodynamic modeling programs. Data for all major cations and anions with strong and weak aqueous complexes between them can now be based on the recent SLOP98.DAT data set [19, 44] for SUPCRT92. Extension of this data set for some aqueous complexes can be done using the PRONSPREP97 algorithm [19, 44] and/or temperature extrapolations of equilibrium constants of some isoelectric/isocoulombic reactions [45].

In a great variety of environmental case studies, many required trace metal species (especially metal–organic complexes) can be provided with their formation equilibrium constants known only at 25 °C. To accommodate such information for GEM modeling (which can only operate with G^0 values of chemical species but not with reaction $\log K$ values), the chemical thermodynamic database should be maintained in two complementary data formats: 'thermochemical' and 'reaction defined'. Not much attention has been paid so far to this issue, even though a clear-cut separation between the developer- and the user-provided data sets is critical for assessing final reliability of the models. Thermodynamic data of different quality, in fact, form a hierarchy, calling for a 'layered' database structure consisting of 'kernel data', 'uncertain data', and 'application-specific extensions' [46]. Moreover, the high-temperature and the low-temperature systems require different subsets of the kernel thermochemical data, especially for solids.

The present state of knowledge in physical chemistry does not yet allow the 'kernel' database to cover even inorganic chemical speciation of trace elements in many meaningful environmental geochemical systems. Therefore, the actual speciation modeling applications often require additional thermodynamic data of much greater uncertainty, for instance, for trace metal–humate/fulvate complexes or for surface complexes. Such values (mostly $\log K$ of complexation or dissolution reactions) are derived only from the ambient-conditions experimental data, or even just estimated from various linear free energy correlations. For many low-temperature mineral phases, the measured solubility products contradict with calorimetric properties obtained independently; sometimes, this can also cause discrepancies in thermodynamic data for some aqueous ions or complexes.

To the group of 'uncertain' thermodynamic data, many weak inorganic aqueous complexes can be

added because selection of these depends on the chosen model of ionic strength corrections (nonideal behavior), as discussed below. Until recently, there was a lot of controversy in establishing a consistent set of thermodynamic constants for the surface complexes on amphoteric oxide (and nonoxide) mineral surfaces. Much of the problems related to the 'uncertain data' layer correspond to the lack of parameters for temperature corrections, which may lead to accumulation of large modeling errors at elevated temperatures, even around 100–150 °C. This problem, however, can be circumvented by defining thermodynamic data for the 'uncertain' species via constructing isocoulombic/isoelectric reactions [45–47], at best enhanced with estimated entropy ΔS^0_{298} and heat capacity $\Delta C^0_{P,298}$ values to minimize the temperature extrapolation errors. The required set of the 'model reactions', not accessible directly for calculations of equilibrium speciation, can be constructed in many cases from 'kernel database' species.

Third in the hierarchy, the 'application-specific' part of the built-in modeling database is fully open to case-specific extensions. Data for missing species can be added in the reaction-defined or thermochemical format; threads of thermodynamic data can be created for 'exotic' chemical elements or dissolved species not present in the kernel database, as well as their minerals or solid-solution end-members needed for the specific modeling scenario; and some 'overriding' data can be inserted by the users who disagree with the choices provided by the developers of kernel database. Such application-specific data are to be represented mainly in the reaction-defined format. This kind of 'layered' extension from kernel to application database ensures compatibility between different modeling applications ('projects'), as it has been implemented in the database structure of GEM-Selektor v.2-PSI code [31].

2.4 Dual thermodynamic calculations

A new concept for evaluation of thermodynamic data is the DualTh equation. As follows from the Kuhn–Tucker necessary and sufficient conditions of chemical equilibrium (equation 3.1.14), the dual chemical potential of a jth species $\sum_i a_{ij}u_i$ is a function of chemical potentials u_i of chemical elements that, in turn, are functions mainly of the bulk chemical composition b. Therefore, if an external information about the species activity, concentration, or activity coefficient is available, and there is an evidence that this species coexists with the rest of the system at equilibrium, then one unknown or uncertain parameter on the right side of equation (3.1.16) can be restored [18, 32, 48]. The species of interest may not be included into the calculation of equilibrium state to obtain the u_i chemical potentials. It is only required that this species is stoichiometrically compatible with the rest of the system and known to exist at equilibrium in its phase. There are two practically important cases, both obtained by a simple rearrangement of equation (3.1.16).

1. Determination of the unknown molar Gibbs energy of formation from the experimentally known concentration or activity of a species and the bulk composition of the coexisting aqueous and/or gas phase (DualTG equation):

$$G^0_{j,T} = RT\left(\sum_i a_{ij}u_i - \ln c_j - \ln \gamma_j - \text{const}\right) \tag{3.1.17}$$

2. Determination of the unknown species activity coefficient (e.g. in solid solution) from its independently known concentration and bulk composition of the aqueous and/or gas phase:

$$\ln \gamma_j = \sum_i a_{ij}u_i - \frac{G^0_{j,T}}{RT} - \ln c_j - \text{const} \tag{3.1.18}$$

The absolute or 'true' values of chemical potentials of elements and species in any system cannot be determined, so the values of the $\boldsymbol{u}$ and $\boldsymbol{\upsilon}$ vectors are relative and refer to the same standard states of elements and species as the respective $G^0_{j,T}$ values. However, equations (3.1.16), (3.1.17) and (3.1.18) remain valid at any consistent choice of standard states or concentration units because these equations include only the *difference* between the

dual chemical potential $\sum_i a_{ij}u_i$ and the standard-state Gibbs energy function $G_j^0/(RT)$ of the species. These equations are general and remain the same regardless of the number of other species or phases (such as solid solutions, gas mixture, sorption phases, other single-component minerals, etc.). The only prerequisite is that at least a local/partial equilibrium state is achieved, which means equality of chemical potentials of elements in all stable phases and species involved. The latter may not be easy to prove, especially for the low-temperature environmental systems.

Application of the DualTG equation to the aquatic system first requires to define a *basis subsystem* L' [18] composed of the aqueous phase plus other equilibrated phases with known thermodynamic properties for all species, but *without* any phase or species having unknown thermodynamic properties. Next, the IPM algorithm is used for calculation of the equilibrium state in *the basis subsystem only* (at T and P of interest). The resulting dual $\boldsymbol{u}'$ vector of chemical potentials of chemical elements obtained from this calculation is then used at the third step in equation (3.1.17) to obtain the sought-for estimate of $G_{j,T}^0$ for the component(s) of interest that form a *nonbasis subsystem*. Later on, some nonbasic species can be added to the basis subsystem for 'fine-tuning' of their $G_{j,T}^0$ estimates. For sensitivity studies, the whole sequence can be repeated starting from the second step but with less species remaining in the nonbasis subsystem. If several experimental points are available in a solid solution–aqueous solution system (SSAS), then the DualTG equation (3.1.17) can be used for determining the optimal stoichiometries of solid solution end-members provided that their mixing model (e.g. ideal) is known [48].

Conversely, if stoichiometries and standard thermodynamic properties of the solid solution end-members are fixed, then the experimental solubility data can be applied in equation (3.1.18) to determine the end-member activity coefficients and convert them into estimates of mixing properties (e.g. Margules parameters) of the nonideal solid solution. This has been done, for instance, in our studies of authigenic formation of Ca–rhodochrosite in a complex marine porewater system of the Gotland Deep (Baltic Sea) to estimate parameters of the regular Margules model of a multicomponent carbonate solid solution [32].

DualTG determination of end-member stoichiometries and stability can be illustrated by an example of incorporation of the trace element europium into calcite using experimental data of Tits *et al.* [49, 50], who have shown that the coprecipitation mechanism (i.e. solid solution formation) is most probably responsible for the sorption of Eu by calcite $CaCO_3$ in the artificial cement water (ACW) in presence of portlandite $Ca(OH)_2$. The printout of equilibrium calculation for the artificial cement water with trace Eu at 1 bar and 25 °C (one of 36 experiments considered by Curti *et al.* [50]) is given in Table 3.1.4. We used the GEM-Selektor code and thermodynamic data from Nagra-PSI 01/01 database [36]. Chemical potentials of independent components (dual $\boldsymbol{u}$ vector) are listed in the two rightmost columns of Table 4-1, both in mol mol^{-1} ($\boldsymbol{u}$) and J mol^{-1} ($\boldsymbol{u}_e$) scales. From these values, the primal chemical potential μ_j^* of any dependent component in the system can be immediately estimated by summing up the formula stoichiometry coefficient times the chemical potential of the respective element. For example, let us calculate $\mu(CaCO_3) = u_e(Ca) + u_e(C) + 3u_e(O) = -638756.9 + -427273.3 + 3\cdot(-21048.5) = -1129176$ (in J mol^{-1}). The aqueous solution exists at equilibrium with calcite and portlandite, so the activity of solid calcite is unity and $\mu(CaCO_3) = G_{298}^0$(calcite), as expected. Now, we can go one step further and try to find the G^0 value of an Eu-containing end-member of the presumed ideal Eu(III)-Ca carbonate solid solution. Several possible end-member stoichiometries like $Eu_2(CO_3)_3$ (or $Eu(CO_3)_{1.5}$), $EuOHCO_3$, $EuNa(CO_3)_2$ and $Eu(OH)_3$ can be suggested right away because pure lanthanide solids of such stoichiometry are known to exist. We also need to know how much calcite (of total 0.5 g L^{-1}) has been recrystallized during experimental times, though this effective solid concentration is difficult to determine. From a minimum estimate of ca. 1.034 mg L^{-1} obtained from the interpretation of ^{45}Ca exchange data [50], the amount of total

Table 3.1.4. Example of a GEM-Selektor printout for the Eu-calcite system #12 (calculated using the Davies equation, text output file, modified).

```
GEM-Selektor v.2-PSI: Calculation of Equilibrium State in the System:
Eu-carb-T:G:TestFig10:12:0:1:25:0: 14/08/2003 13:08

Test for Eu speciation in ACW+calcite+portlandite system
Modeling data of Fig.10 from Tits et al., 2003

State variables: P(bar)= 1 T = 25(C) = 298.15(K) V(cm3) = 620727
Mass(kg)= 1.712234974 Min.potential (moles): G(x) = -5348.85484

                                                                Table 4-1

Parameters of Independent Components (IC, Stoichiometry Units)
=====|================|==============|============================
IC   |   Input bulk   |     Mass     |  Dual chemical potential
Name |  composition,  |    balance   |-----------|---------------
     |  moles total   |   residuals  |  mol/mol  |      J/mol
-----|----------------|--------------|-----------|---------------
     |       b        |      d_b     |     u     |       ue
=====|================|==============|===========|===============
Al         3.700849e-06         1.3e-18    −316.693       −785072.8
C         0.00012527253     −4.522e-17   −172.3591       −427273.3
Ca        0.00166468415     −2.989e-17   −257.6702       −638756.9
Eu             4.14e-10     −2.603e-17   −331.8341       −822607.1
H           110.9822845      2.501e-12   −43.59849       −108079.4
K           0.182045147      6.217e-15   −128.9202       −319589.4
N             1.242e-09      1.737e-23    −27.1407        −67281.0
Na          0.114028275     −2.151e-15   −121.1306       −300279.2
Nit                  50              0    −2.1e-08            −0.0
O           55.64122391      8.117e-13   −8.490834        −21048.5
Si         6.101615e-05      2.067e-19   −339.3221       −841169.8
Zz                    0      8.272e-15    12.92689         32045.4
=====|================|==============|===========|===============
Aqueous phase: I(molal)= 0.2665 pH = 13.3 pe = 7.304 Eh(V)= 0.4312
Nit is the atmospheric nitrogen; Zz denotes electric charge.

                                                               Table 4-1a

Total Dissolved Independent Components IC
=====|==============|=============|==============|===============
IC   |  Molality m  |     log     |   Molarity   | Concentration
Name |  (mol/kgH2O) |  molality   |              |  (g/kg-soln)
-----|--------------|-------------|--------------|---------------
     |      m_t     |   log m_t   |     log M    |      c_t
=====|==============|=============|==============|===============
Al         3.712e-06      −5.43039       −5.43181     9.86786e-05
C          0.00012565     −3.90084       −3.90225     0.001486903
Ca          0.0016697     −2.77736       −2.77878      0.06593145
Eu        4.15248e-10     −9.38169       −9.38311     6.21721e-08
H           0.2999436     −0.52296      −0.524376       0.2978699
K           0.1825937     −0.738514       −0.73993        7.033828
N         1.24574e-09      −8.90457       −8.90599     1.71914e-08
Na          0.1143719     −0.941681      −0.943096        2.590613
Nit       0.001285874       −2.8908       −2.89222      0.01774526
O           0.3005035     −0.52215      −0.523566        4.736978
Si           6.12e-05     −4.21325       −4.21466     0.001693486
Zz         −8.301e-15            0              0               0
=====|==============|=============|==============|===============
Eu-carb-T:G:TestFig10:12:0:1:25:0:
```

Table 3.1.4. (*continued*)

Table 4-2

Parameters of Dependent Components (DC, Species)

Species name	type	Amount in the system	Concen-tration	Activity coeff.	log activity	Chemical potential
		x (moles)		gamma	log a	mu(J/mol)
Aqueous phase (aq_gen)						
AlO2-	S	3.70082e-06	3.712e-06	0.7345	−5.564	−859215
AlO2H@	S	3.63481e-13	3.6458e-13	1	−12.44	−935249
AlSiO4-	S	2.71695e-11	2.7251e-11	0.7345	−10.7	−1742482
Ca(CO3)@	S	5.47447e-06	5.491e-06	1	−5.26	−1129176
Ca(HCO3)+	S	5.76904e-11	5.7864e-11	0.7345	−10.37	−1205210
Ca(OH)+	S	0.00101647	0.0010195	0.7345	−3.126	−735839
Ca(OH)2@	S	0.000110715	0.00011105	1	−3.954	−897013
Ca+2	S	0.000498574	0.00050008	0.2911	−3.837	−574666
Ca(HSiO3)+	S	1.85213e-08	1.8577e-08	0.7345	−7.865	−1619106
CaSiO3@	S	3.34311e-05	3.3532e-05	1	−4.475	−1543072
EuO+	S	1.08283e-15	1.0861e-15	0.7345	−15.1	−811610
EuO2H@	S	4.13796e-11	4.1504e-11	1	−10.38	−972784
EuO2-	S	3.72619e-10	3.7374e-10	0.7345	−9.561	−896749
K(OH)@	S	0.00912208	0.0091496	1	−2.039	−448717
K+	S	0.172923	0.17344	0.7345	−0.8948	−287544
Na(CO3)-	S	4.34288e-05	4.356e-05	0.7345	−4.495	−822744
Na(HCO3)@	S	9.82332e-10	9.8529e-10	1	−9.006	−898778
Na(OH)@	S	0.010411	0.010442	1	−1.981	−429407
Na+	S	0.103574	0.10389	0.7345	−1.117	−268234
HSiO3-	S	7.94559e-06	7.9695e-06	0.7345	−5.233	−1044440
SiO2@	S	1.81965e-09	1.8251e-09	1	−8.739	−883267
SiO3-2	S	1.96191e-05	1.9678e-05	0.2911	−5.242	−968406
CO2@	S	2.46024e-15	2.4677e-15	1	−14.61	−469370
CO3-2	S	7.63373e-05	7.6567e-05	0.2911	−4.652	−554510
HCO3-	S	3.08479e-08	3.0941e-08	0.7345	−7.643	−630544
NO3-	S	1.242e-09	1.2457e-09	0.7345	−9.039	−162472
Nit2@	S	0.000641006	0.00064294	1	−3.192	0
O2@	S	5.47045e-11	5.4869e-11	1	−10.26	−42097
OH-	S	0.278264	0.2791	0.7345	−0.6882	−161173
H+	S	6.42251e-14	6.4419e-14	0.7345	−13.32	−76034
H2O@	W	55.3416	0.98969	1	−0.004503	−237207
Gaseous phase (gas_gen)						
CO2	G	1.8042e-12	7.217e-14	1	−13.14	−469370
N2-atm	G	24.9994	1	1	−1.831e-08	−0
O2	G	1.05411e-06	4.2165e-08	1	−7.375	−42097
Solids						
calcite	O	0	1	1	−2.419e-06	−1129176
portlandite	O	0	1	1	−8.47e-06	−897013
Eu2(CO3)3	O	0	1	1	−32.2	−3116471
EuCO3OH(cr)	O	0	1	1	−10.26	−1442154
EuNa(CO3)2(cr)	O	0	1	1	−16.56	−2103724
Eu(OH)3(cr)	O	0	1	1	−1.582	−1209991

Concentration and activity are given for aqueous species 'S' in mol/(kgH2O),
for other species (gases 'G', water 'W') - in the mole fraction scale.
For single minerals 'O', log_a means log10 of the saturation index.
In aqueous and gaseous phases, only species with amounts x_j > 1e-20 mol are listed.

(*continued overleaf*)

Table 3.1.4. (*continued*)

```
                                                                    Table 4-3
Parameters of Phases at Equilibrium State
================|=======|=============|===========|===========|============
Phase           | Nr.of |  Amount in  |   Phase   |   Phase   |  Stability
name            | spec. | the system  |   mass    |  volume   |  criterion
----------------|  in   |-------------|-----------|-----------|------------
                | phase |  X (moles)  |    (g)    |   (cm3)   |    F_a
================|=======|=============|===========|===========|============
aq_gen          |    31 |     55.9184 |    1011.9 |    1000.3 | -1.333e-09
gas_gen         |     3 |     24.9994 |    700.32 | 6.197e+05 | -4.811e-12
Calcite         |     1 |           0 |         0 |         0 |          0
Portlandite     |     1 |           0 |         0 |         0 |          0
Eu-carbonate    |     1 |           0 |         0 |         0 |          0
EuOH-carbonate  |     1 |           0 |         0 |         0 |          0
EuNa(CO3)2_cr   |     1 |           0 |         0 |         0 |          0
Eu(OH)3cr       |     1 |           0 |         0 |         0 |          0
================|=======|=============|===========|===========|============
Use the L1 column (number of species per phase) to locate
  the species in Table 4-2. F_a is a value of Karpov's phase stability
  criterion (close to 0 for stable phases present in nonzero amounts).

Eu-carb-T:G:TestFig10:12:0:1:25:0:
--------
```

Table 3.1.5. Example DualTG calculations for the Eu-calcium carbonate solid solution system in ACW using Table 3.1.4 (experiment #12, full set of DualTh calculations for 36 experiments is considered in [50]).

End-member candidate	μ^*, DualT chem. potential, J mol^{-1}	Mole fraction χ in solid soln.	$RT \ln \chi$ J mol^{-1}	Estimate of G^*_{298}, J mol^{-1}	Mineral[a] G^0_{298}, J mol^{-1}	$W = G^*_{298} - G^0_{298}$ J mol^{-1}	$\alpha = \frac{W}{RT}$
$Eu_2(CO_3)_3$	−3116471	0.00975[c]	−11479	−3104992	−2932653	−172339	−69.52
$EuOHCO_3$	−1442154	0.0065[d]	−12484	−1429670	−1383580	−46090	−18.59
$EuNa(CO_3)_2$	−2103724	0.013[e]	−10766	−2092958	−2009208[b]	−83750	−33.78
$Eu(OH)_3$	−1209991	0.0065[d]	−12484	−1197507	−1200962	3455	+1.39
$EuOOHCaCO_3$	−2101984	0.013[e]	−10766	−2091218	−2101986[f]	10768	+4.34
$EuOCa(CO_3)_{1.5}$	−2218040	0.013[e]	−10766	−2207274	n.a.	n.a.	n.a.
$EuO(CO_3)_{0.5}$	−1088864	0.0065[d]	−12484	−1076380	n.a.	n.a.	n.a.

[a] Nagra-PSI database [36], 'n.a' means 'not available'.
[b] data from [50].
[c] Assuming $Ca_3(CO_3)_3$ end-member.
[d] Assuming $CaCO_3$ end-member.
[e] Assuming $Ca_2(CO_3)_2$ end-member.
[f] Assuming G^0_{298} of the pure solid equal to G^0_{298}(calcite) + G^0_{298}(Eu(OH)$_3$) − G^0_{298}(H_2O).

Eu(III) added in the experiment ($6.79 \cdot 10^{-8}$ M), and its partitioning ($4.14 \cdot 10^{-10}$ M remained dissolved, and $6.749 \cdot 10^{-8}$ M Eu(III) was incorporated into 1.034 mg = $1.038 \cdot 10^{-6}$ moles of calcite), one calculates the cationic mole fraction of Eu in calcite $6.749 \cdot 10^{-8} / 1.038 \cdot 10^{-5} = 6.50 \cdot 10^{-3}$, that is, 0.65%. Further conversion of cationic- to end-member mole fraction χ_j depends on the stoichiometry of Eu(III) end-member candidate and the assumed substitution mechanism (see Table 3.1.5). From the chemical potential of an ideal solid-solution end-member, $\mu_j = \mu^0_j + RT \ln \chi_j$, knowledge of the mole fraction χ_j from the experimental data and the chemical potential μ_j obtained from chemically equilibrated aqueous phase composition (vector $\boldsymbol{u}$ in Table 4-1), the estimate of standard state chemical potential G^*_j of any pure Eu-bearing ideal end-member

can be calculated by simple subtraction, $G_j^* = \mu_j - RT \ln \chi_j$. Results of these simple DualTG calculations for seven Eu-bearing end-member candidates were compiled in Table 3.1.5.

Solubility products and G_{298}^0 values of some solid (hydroxo)carbonates of Eu(III) are known and can now be used for performing the first feasibility check for four end-member candidates. For instance, the G_{298}^0 value of the $Eu_2(CO_3)_3$ phase is -2932.654 ± 2.85 kJ mol^{-1}. But the value calculated from the dual-thermodynamic equation for the experiment #12 is -3105 kJ mol^{-1} (Table 3.1.5), or 172.34 kJ mol^{-1} more negative. Where can this difference be attributed, assuming that the stoichiometry of this end-member is feasible, and its stability corresponds to that of the pure mineral?

From the theory of regular solid solutions [29], it follows that the activity coefficient of an end-member in the binary solid solution is $\ln \gamma_1 = \alpha \chi_2^2$ (and $\ln \gamma_2 = \alpha \chi_1^2$). If the first end-member is major with $\chi_1 > 0.99$ (calcite) and the second one is trace end-member ($\chi_2 < 0.01$), then $\ln \gamma_1 \approx 0$ and $\ln \gamma_2 \approx \alpha$, where $\alpha = W_G/(R_T)$ is the Margules interaction parameter; for carbonates, this is usually a positive number in the interval from 0 to 9 [29, 51]. Thus, the difference between the DualTG estimate for a trace end-member candidate and the respective G_{298}^0 value for the pure mineral analog can be directly attributed to the magnitude of interaction parameter (assuming the regular mixing behavior) as

$$W_G = \alpha RT = G_{298}^* - G_{298}^0 \qquad (3.1.19)$$

Estimates of the interaction parameter α are given in the last column of Table 3.1.5 for the first four candidates that exist as pure minerals. From these data, it becomes clear that only the $Eu(OH)_3$ stoichiometry shows a realistic value of $\alpha \approx 1.4$, whereas all other candidates result in quite large negative values, suggesting either not-yet-understood strong mixing effects or the structural state and stoichiometry of Eu end-member being quite different from any pure mineral analogs. Note, however, that it is not required that the solid-solution end-member exists as a pure substance. Another problem with the first four end-member stoichiometries is that neither of them can describe experiments from both high-pH and low-pH regions [50]. For those reasons, DualTG calculations were done for more end-member candidates that do not exist as pure minerals. In Table 3.1.5, three such examples are given. The $EuOOHCaCO_3$ stoichiometry results in a G_{298}^* estimate that still can be roughly compared with the sum of molar Gibbs energies for Eu hydroxide and carbonate; this results in somewhat greater apparent 'nonideality' than that for the $Eu(OH)_3$ end-member candidate. The remaining two end-members can be viewed as mixed oxide-carbonates of europium; it happens that they can fit both high- and low-pH experiments.

DualTG calculations can be repeated for many experimental points obtained at the same S/L ratio of calcite but different total Eu concentrations in the system, or even at different S/L and pH. The estimated G_{298}^* values for the same end-member stoichiometry can be compared between experiments by computing arithmetic means and standard deviation values. If the DualTG estimates exhibit a trend depending on total Eu concentration and the standard deviation of G_{298}^* is large (above 3–4 kJ mol^{-1}), then the end-member stoichiometry is considered as the inappropriate one. If the standard deviation is significantly less than 3 kJ mol^{-1}, then it can be can be taken as a good uncertainty estimate for a realistic end-member stoichiometry and DualT-determined G_{298}^* value. If the latter matches well with the independently measured solubility product of a solid of the same stoichiometry as the end-member, then the system can be described using the ideal solid solution model; moderate differences (5 to 15 kJ·mol^{-1}) point out that a nonideal mixing model is required. This approach has already been shown to be particularly useful in the determination of trace element end-member stoichiometries not only in the carbonate system [32], but in particular, also in the complex chemistry of hydrated cement, where multicomponent solid solutions exists, which are not accessible to conventional log K_{SP} determinations due to a severe phase characterization problem [48, 52].

3 NONIDEALITY AND TEMPERATURE CORRECTIONS

3.1 Ideal and nonideal mixing in multicomponent phases

The account for nonideal behavior of aqueous species, surface species, and solid solution end-members is the most complicated part and, hence, a 'know-how' of thermodynamic speciation modeling. Many alternative but nonequivalent models were published in the literature and implemented in computer codes. The need for introducing nonideality arises because, in most cases of interest, thermodynamic activities of chemical species in 'real' experimental or geochemical systems strongly deviate from concentrations due to molecular or electrostatic interactions at elevated pressure or ionic strength. Such deviation is described by introducing an activity coefficient of the chemical species – an essentially nonthermodynamic quantity defined as $\gamma_j = a_j/c_j$ (for jth species, where c_j is real concentration in the phase, and a_j is the activity or 'thermodynamic concentration'). From fundamental relations between activities and chemical potentials,

$$\mu_j = \mu_j^0 + RT \ln a_j \text{ or}$$
$$\mu_j = \mu_j^0 + RT \ln c_j + RT \ln \gamma_j \quad (3.1.20)$$

it follows that $RT \ln a_j$ is a difference between chemical potential at the state of interest (μ_j) and chemical potential at the standard state (μ_j^0), and activity equals concentration at the so-called reference state, where $\ln \gamma_j = 0$ (or $\gamma_j = 1$). Therefore, the whole concept of 'ideal' ($a_j = c_j$) and 'nonideal' ($a_j \neq c_j$) behavior depends on the choices of the species' stoichiometry, the standard state and concentration scale, and the reference state. On the grounds of practical convenience, such choices have been made differently for the solid, gaseous, and aqueous species in chemical thermodynamics (cf. [1, 2]. Regarding surface species, the situation remained very unclear until recently, when new definitions of standard and reference states have been proposed [53].

3.1.1 Nonideality in aqueous electrolytes

In thermodynamics of aqueous electrolytes, the standard state of dissolved species is preferentially taken as a unimolal ($m^0 = 1$ mol per 1 kg of H_2O-solvent) concentration at the reference state of (hypothetical) infinite dilution. Another standard state (pure substance with mole fraction $\chi^0 = 1$) and reference state (activity equals mole fraction, $a_w = \chi_w$) are used for the water-solvent. Note that in chemistry, the molar concentration scale (moles per liter of aqueous solution) is often used, but it is less convenient for thermodynamic calculations because the molarity M depends on the density of the aqueous solution and, hence, on its composition, T and P, whereas the molality m does not depend on them. The nonideal behavior of aqueous species is usually described in multicomponent chemical speciation models using a concept of effective ionic strength:

$$I = \frac{1}{2} \sum_j m_j z_j^2 \quad (3.1.21)$$

where z_j is the formula charge and m_j is the molal concentration of jth aqueous species. At very low $I < 5 \cdot 10^{-3}$ m, the activity coefficients of ions can be approximated by the Debye–Hückel limiting law: $\log \gamma_j = -1/2 z_j^2 \sqrt{I}$. At moderate ionic strength ($0.1 < I < 0.5$ m), activity coefficients can be calculated using the Davies equation

$$\log \gamma_j = -A_\gamma z_j^2 \left(\frac{\sqrt{I}}{1 + \sqrt{I}} + 0.3I \right) \quad (3.1.22)$$

At the ionic strength below 1.0 m, the extended Debye–Hückel equation with a common linear term $b_\gamma I$ (where b_γ is a parameter specific to the major electrolyte, for example, $b_\gamma = 0.064$ for NaCl at 25 °C) is the most versatile one to apply:

$$\log \gamma_j = \frac{-A_\gamma z_j^2 \sqrt{I}}{1 + B_\gamma a_\gamma^0 \sqrt{I}} + b_\gamma I \quad (3.1.23)$$

Here, a^0 is a Kielland's 'ion-size' parameter (in 10^{-8} cm) specific to aqueous ions; A_γ and B_γ are T-dependent parameters (at 25 °C, $A_\gamma \approx 0.51$

and $B_\gamma \approx 0.33$). More about the Debye–Hückel-type ionic strength corrections can be found in textbooks [1–3, 5]. Equations (3.1.22) or (3.1.23) are commonly used in the framework of the so-called 'ion-association' aqueous model, in which weak complexes between major cations and anions, or 'ion pairs', are considered as chemical species of definite stoichiometry and stability. For neutral aqueous species and dissolved gases, equation (3.1.23) reduces to the Sechenow equation, $\log \gamma_j = b_\gamma \boldsymbol{I}$; for dissolved gases, separate values $b_{\gamma j}$ of Setschenow (or salting-out) coefficients are known (e.g. [54]). However, at $I > 1\ m$, and even in seawater ($I \approx 0.65$), the 'ion association' aqueous models are not considered satisfactory; instead, the 'specific ion interaction' models must be used, where ion pairs are not considered, but activity coefficients of aqueous ions are computed using complex (e.g. Brönsted–Guggenheim or Pitzer) equations with empirical parameters specific to ion–ion interactions [6, 55, 56]. With these approaches to ionic strength corrections, inorganic speciation of the majority of elements can be modeled in seawater and in fresh surface and ground waters in a wide range of salinities and temperatures [6, 57–63].

3.1.2 Nonideality in solid solutions

The equilibrium solubility of a mineral solid ML (e.g. where M is the cation, L the anion) is governed by an equilibrium constant called 'ionic solubility product', $K_{SP} = \{M\}\cdot\{L\}/\{ML\}$ referred to a reaction like $CdCO_3(\text{solid}) \leftrightharpoons Cd^{+2} + CO_3^{-2}$ (here, braces {} denote activities in aqueous electrolyte, and $\{ML\} = 1$ for pure solids). Speciation modeling codes can account for nonideality of aqueous solution and calculate ion activities from total dissolved concentrations, assuming equilibrium when the calculated ion activity product $IAP = \{M\}\cdot\{L\}$ equals K_{SP}. Recall that a ratio $\Omega = IAP/K_{SP}$ is called *saturation index*, where, by definition, $\Omega = 1$ at equilibrium, $\Omega > 1$ at oversaturation, and $\Omega < 1$ at undersaturation of aqueous solution with respect to a given solid ML, and that in LMA speciation codes minerals are usually not included into mass balance, but have their saturation indices computed from the speciation in aqueous solution.

IAP values calculated from measured total concentrations of dissolved metals in sediment-water systems existing apparently very close to equilibrium are often much less than K_{SP} of the respective pure solid phases. This is mostly because trace metals do not form pure minerals, but instead are bound by other host minerals forming solid solution–aqueous solution equilibria. In host minerals, the activity of the trace metal end-member (by definition, $\{\text{solid TrL}\} = \chi_{TrL}$ in the simplest case of ideal mixing) is far less than unity, which decreases the dissolved trace metal activity {Tr} or concentration [Tr] at equilibrium far below that of the pure TrL end-member. For instance, if solubility products K_{SP} of trace and host end-members are equal, and $\chi_{TrL} = 0.001$, then {Tr} will be about 1000 times below that in presence of the pure TrL solid phase, while {M} will be almost the same as that of the pure ML host mineral. At a fixed total amount of trace metal in the system, χ_{TrL}, and thus {Tr}, becomes dependent on the effective host solid–liquid ratio. This dissolution property of solid solution systems is often erroneously neglected, in part because of the difficulties in determining the 'reacted' mass of the host mineral.

Solid solutions often display nonideal mixing behavior, which, together with differences in aqueous speciation and ion activity coefficients of the participating trace metals may produce quite complex nonlinear relationships between measurable bulk compositions of the coexisting aqueous solution and solid phases, even up to the miscibility gaps. In solid solution aquatic systems, the usual notion of 'solid solubility' controlled by a single solubility product K_{SP} is no more appropriate and must be replaced by a more general concept of 'partitioning equilibria' [64] that change in response to solid-to-liquid ratios, trace metal loadings, temperature and conditions in aqueous phase (pH, Eh), all of which, in turn, may be affected by solid solution composition and nonideality at higher solid-to-liquid ratios [27, 29, 32, 48, 65–67]. This kind of behavior makes aqueous solid solution systems similar to systems

involving adsorption on mineral–water interfaces. The difference, however, lies in that the essentially monolayer adsorption is controlled by the amount of solid sorbent and its effective specific surface area, which also may cause strong nonideal effects on 'strong' surface sites or at high sorbate concentrations (see below).

A relatively simple approach commonly used to quantify sorption or coprecipitation processes is based on the empirical partition (distribution) coefficients [68]. Partitioning of a trace element (Tr) between a mineral of a major element (M) and aqueous solution usually follows a power function [69]:

$$\left(\frac{\chi_{\mathrm{Tr}}}{\chi_{\mathrm{M}}}\right)^{n}\left(\frac{m_{\mathrm{M}}}{m_{\mathrm{Tr}}}\right)=D \tag{3.1.24}$$

where D is the empirical partitioning coefficient. In practice, aqueous molarity of trace element is also used instead of molality m, and mass concentration of trace metal in solid – instead of trace mole fractions χ_{Tr}; this yields an empirical distribution coefficient D in units $\mathrm{L\,kg^{-1}}$). In a Rayleigh-type fractionation (closed system conditions), the increase of the trace component in the solution is controlled by the exponent n of the power law expression in equation (3.1.22), while that of the solid depends on the exponent, the equilibrium constant, and the initial concentration of the trace component in the solution [69]. The Nernstian distribution law is a special case of equation (3.1.24) where the value of n approaches unity and the partitioning of the trace element follows a linear relationship controlled exclusively by the distribution coefficient D (usually at very low concentrations of the solute and/or sorbate).

In the partitioning coefficient (equation 3.1.24), the differences in aqueous speciation of both the trace and major elements are not considered because total dissolved concentrations are used. Equilibrium partitioning can be described using the thermodynamic partitioning constant, K_D, based on free aqueous ion activities. In logarithmic form, it can be expressed as the McIntire equation, for example for the case of divalent metal carbonates [70]:

$$\log K_D=\log\frac{K_{\mathrm{SP,MCO_3}}}{K_{\mathrm{SP,TrCO_3}}}+\log\frac{\gamma_{\mathrm{Tr}}}{\gamma_{\mathrm{M}}}+\frac{-\Delta\mu}{2.303RT} \tag{3.1.25}$$

where the first term on the right side is the ratio of thermodynamic solubility products, the second term is the ratio of the free ion activity coefficients in aqueous solution, and $\Delta\mu=-RT\ln a_{\mathrm{TrCO_3}}$ stands for a difference between the standard chemical potential, $\mu^0_{\mathrm{TrCO_3}}$, of $\mathrm{TrCO_3}$ in pure $\mathrm{TrCO_3}$, and the chemical potential, $\mu_{\mathrm{TrCO_3}}$ as a solid-solution end-member in the host carbonate phase $\mathrm{MCO_3}$. Therefore, it is possible to compute K_D of a trace element incorporated in the carbonate host phase whenever the solubility product of the end-member phases, the aqueous speciation, and the activity of the trace end-member in the host mineral are known. For binary (nonideal) SSAS systems, these data can be conveniently derived from Lippmann equations [27, 51, 71, 72], further facilitated by a MBSSAS code [28].

For a j^{th} solid phase end-member, the chemical potential can be written as usual:

$$\mu_j=g_{j.T.P}+RT\ln\chi_j+RT\ln\lambda_j,\quad j\in l_\alpha \tag{3.1.26}$$

where $g_{j.T.P}$ is the standard molar Gibbs energy of jth end-member recalculated at temperature T and pressure P of interest, χ_j is the mole fraction, and λ_j is the activity coefficient. While both χ_j and λ_j are conventionally unities for a single-component solid phase ($\ln\chi_\alpha=0$ and $\ln\lambda_\alpha=0$), for a solid solution end-member, both terms are nonzero. From equation (3.1.26):

$$\Delta\mu=\mu_{\mathrm{TrCO_3}}-G^0_{\mathrm{TrCO_3}}=RT(\ln\chi_{\mathrm{TrCO_3}}+\ln\lambda_{\mathrm{TrCO_3}}) \tag{3.1.27}$$

where $\lambda_{\mathrm{TrCO_3}}$ is the activity coefficient of trace end-member in the $(\mathrm{M,Tr})\mathrm{CO_3}$ solid solution. Note, however, that equation (3.1.27) is an approximation, true only if $\chi_{\mathrm{TrCO_3}}<0.01$ and $\chi_{\mathrm{MCO_3}}>0.99$. A more general equation is

$$\frac{-\Delta\mu}{2.303RT}=\log\frac{\chi_{\mathrm{MCO_3}}}{\chi_{\mathrm{TrCO_3}}}+\log\frac{\lambda_{\mathrm{MCO_3}}}{\lambda_{\mathrm{TrCO_3}}} \tag{3.1.28}$$

Comparison of equations (3.1.27) and (3.1.28) shows that in the nonideal cases when $\chi_{\mathrm{MCO_3}}<$

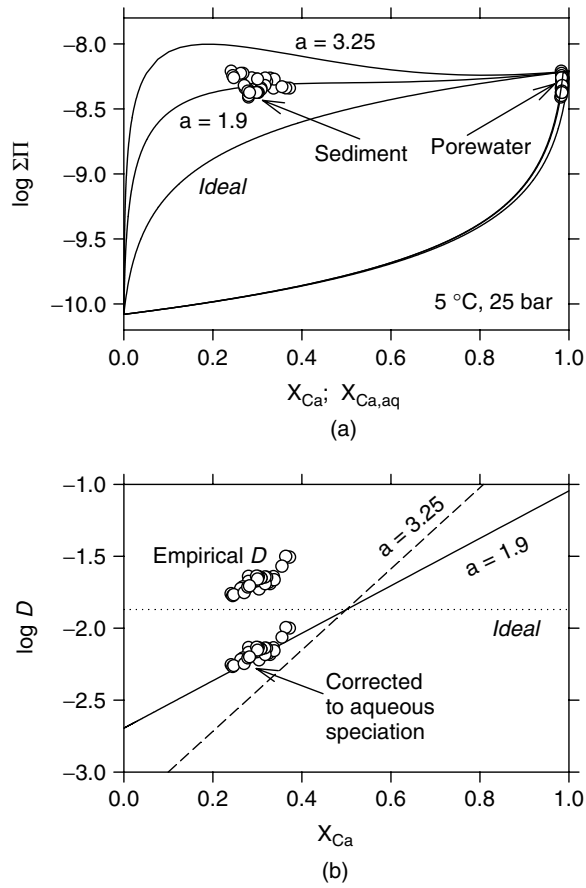

Figure 3.1.1. Lippmann diagram (a), and empirical log D versus thermodynamic log K_D partitioning coefficient plots (b) for the major $(Mn_XCa_{1-X})CO_3$ binary of the six-component (Ca, Mn, Mg, Sr, Fe, Ba) carbonate-anoxic porewater solid solution–aqueous solution equilibrium in Baltic Sea sediments from the Gotland Deep. (Reproduced from *Aquat. Geochem.*, **6** (2000), 147, Application of Gibbs Energy Minimization to Model Early-Diagenetic Solid-Solution Aqueous-Solution Equilibria Involving Authigenic Rhodochrosites in Anoxic Baltic Sea Sediments, Kulik, D. A., Kersten, M., Heiser, U. and Neumann, T., Figure 5© with kind permission of Springer Science and Business Media [32].)

0.99, and hence $\lambda_{MCO_3} \neq 1$, application of equation (3.1.27) may bias estimated values of K_D.

Description of thermodynamic properties of a nonideal solid solution, and hence of the solid-phase activity coefficients *versus* solid composition relations, requires knowledge of the respective parameters of Margules or Guggenheim equations for the relationship between solid end-member activity coefficients and solid-solution composition, $\lambda_j = f(\chi_i,\ \chi_j,\ \alpha_{ij}, \ldots)$. Values of interaction parameters α_{ij} in these equations can be predicted for simple ionic crystal structures (e.g. carbonates, sulfates) by using a Madelung–Vegard approach in calculating electrostatic excess energies of the mixed crystals [51, 73], or (in most cases) estimated semiempirically from experimental data [28, 29, 32]. As an example, both the theoretical and empirical distribution constants log K_D and log D were plotted with field data on Mn coprecipitation by $CaCO_3$ in anoxic sediment porewaters of the Baltic Sea (Figure 3.1.1) [32]. A theoretical curve for both an ideal solid solution (with a Margules interaction parameter $\alpha_0 = 0$) and a nonideal solid solution model with the same end-member pK_{SP} values, but with an interaction parameter $\alpha_0 = 1.9$, were

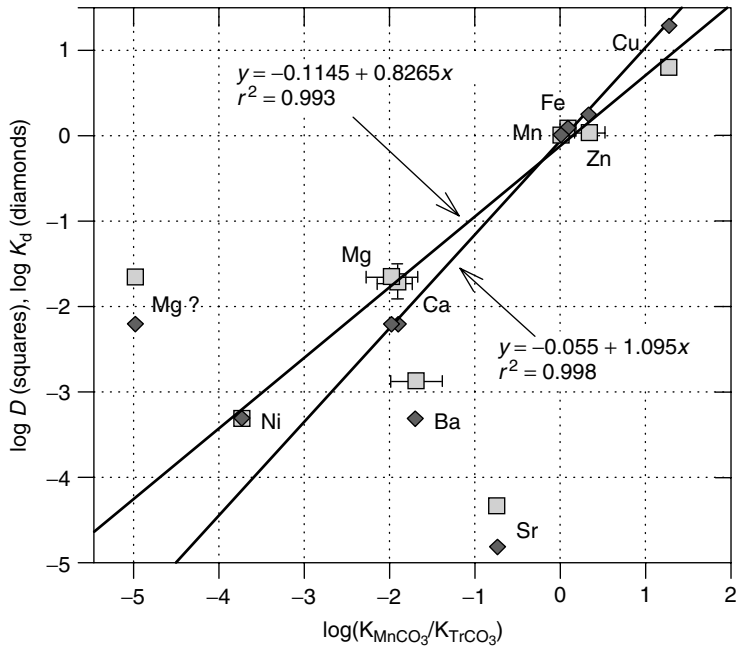

Figure 3.1.2. Plot of thermodynamic (K_D) and empirical (D) partitioning coefficients predicted or fitted for trace components ($TrCO_3$) in host authigenic rhodochrosite ($MnCO_3$) of Gotland Deep sediments (data from [32]).

added to the diagram. Another hypothetical model line was added based on a strongly nonlinear system involving even a mixing gap due to the higher interaction parameter $\alpha = 3.25$ predicted by using the Lippmann equations [51, 73]. The log D points display a slope consistent to the one predicted by the model line for a solid solution of moderate nonideality (i.e. no mixing gap between the end-members), but the points are shifted up from that line by about 0.5 log units. This shift can be attributed to the difference in aqueous complexation between Mn (strongly affected by HS^- complexes in the anoxic sediment porewater) and Ca (not affected). Addition of this difference to log D values results in a perfect match of theoretical and empirical distribution constants for the nonideal SSAS model.

The interaction parameters for trace carbonate end-members predicted on the basis of the theory of isomorphous miscibility allow calculation of interaction parameters α and Lippmann equations to predict concentrations of trace metals like Zn, Ni, and Cu in anoxic porewater, which were found below analytical detection limits [32]. These predictions, together with the D values obtained from available porewater field data using the GEM approach, permitted us to construct a $\log D - \log(K_{SP,MnCO_3}/K_{SP,TrCO_3})$ diagram for the authigenic rhodochrosite (Figure 3.1.2), where log D for Mg was plotted for the frequently reported $pK_{SP} = 5.1$, as well as for a more thermodynamically consistent $pK_{SP} = 8.1$. The data points for the various elements show a striking correlation ($r = 0.996$) with a positive linear regression slope of 0.83 and an intercept of -0.11, excluding for the Mg point based on the less reliable $pK_{SP} = 5.1$, and both the Ba and Sr points. The latter elements do not fit well to this regression because of the incompatibility of those larger cations with the rhombohedral carbonate lattice. This slope is greater than 0.6 found for calcite and siderite [70], but the latter can be readily explained by an improper choice of $MgCO_3$ solubility product by Rimstidt *et al.* [70], as shown on Figure 3.1.2. Another set of points included in Figure 3.1.2 (diamonds) correspond to (nonideal) thermodynamic

values of K_D obtained from Lippmann equations at respective mole fractions of trace end-members in Mn-Tr binaries [32]. Regression of the K_D points for Mn, Ca, Fe, Mg, Zn, and Cu results again in a very good correlation with an intercept of −0.055 and a slope of 1.095, that is, close to the theoretical unity slope for equilibrium distribution constants, evidencing near-equilibrium conditions for this complex natural carbonate SSAS system existing in reduced sapropelic marine sediments.

Solid phases, for example, pure minerals, can be considered in the LMA approach as fixed composition species, described by their stability constants and assuming unit activity in LMA equations. This makes modeling of solid solution–aqueous solution systems difficult using the LMA approach because of varying composition of solid solution(s) [29, 74, 75]. To express it, the knowledge of mole fractions of solid solution end-members (and weighted total solubility product of the solid solution) at equilibrium with aqueous electrolyte is required. The aqueous speciation, in turn, depends on the quantity and composition of solid solution phase, and both are, in principle, unknown at the beginning of speciation calculations. Moreover, Lippmann equations that support LMA-based SSAS modeling are not defined beyond a binary system. Higher-order SSAS can be solved only using the GEM approach, as exemplified recently for the six-component carbonate system [32], or for the zinc-doped C-S-H system [48].

3.1.3 Nonideality in surface complexation

Partitioning of many trace elements in water-sediment columns, soils and subsurface is dominated by surface binding on natural colloids, suspended mineral or organic particles, or clay mineral surfaces [4, 16, 76, 77]. For this reason, the account for surface complexation on mineral–water interfaces is an essential topic in environmental-geochemical thermodynamic speciation modeling, included in almost all recent modeling codes.

Surface complexes are traditionally treated in the LMA approach in the same way as aqueous complexes [78], formally – as part of the aqueous phase, but subject to additional balance constraints for the total number of surface sites and surface charge. All information about the sorbent, its quantity, stability, structure, composition, specific surface area, distribution of site types on surface, and so on, is hidden within the total number of surface sites, but not included in the explicit mathematical structure of the equilibrium speciation problem. The mass balance constraints are so strong that any calculated surface speciation is apparently successful. Such calculations seem to reflect our *a priori* guesses more than elucidate the relative (meta)stabilities of aqueous, gaseous, solid-solution, and sorption multicomponent phases potentially in equilibrium at a given bulk composition of the system. They must also not necessarily reflect how these relative stabilities would affect speciation in each of these phases and, consequently, metal partitioning in the overall system.

Most of the LMA-based surface speciation models (e.g. FITEQL-3 [24]) require intrinsic adsorption constants K_{int} for all surface complexes. Such constants may not always be directly compared between different surfaces of solid sorbents because of their hidden dependence on the total and maximum site density parameters [53, 79, 80], usually taken as the same, generic 'site density parameter' in LMA SCMs. However, fitting at a single value of the total site density is essential for obtaining a consistent set of the intrinsic surface constants for different trace metals even on the same oxide sorbent [77, 81]. Until recently, it remained unclear how K_{int} values fitted at different site densities can be consistently compared for different minerals, as it was attempted by some authors for the triple layer (TLM) surface complexation model (e.g. [82]). One of the particular shortcomings of LMA-based SCMs is that, in fact, separate mass-balance constrains are needed for each surface site type. The most severe shortcoming, however, is that nonideal behavior of surface complexes has not been seriously considered, except of Coulombic factors in the electrostatic SCMs [3, 83], albeit other nonideal effects have been recognized in a number of experiments [84, 85].

A more rigorous thermodynamic sorption modeling becomes possible if unequivocal definitions of the standard and reference states for surface species, the so-called 'surface activity coefficient terms' (SAT), and chemical elemental stoichiometry of surface functional groups and complexes are provided [53, 79]. From this, standard partial molal properties of the surface species can be determined, comparable between different sorbent phases and consistent to standard properties of solids, gases, and aqueous species. Once converted into thermodynamic equilibrium constants, they can be compiled into a uniform thermodynamic database [80]. This also creates a sound basis to reevaluation of nonideality effects on the solid–water interface (e.g. [84, 85]), leading to the treatment of surface complexation thermodynamically in a way similar to SSAS systems, using a 'sorption phase' concept [53].

The 'sorption phase' consists of (i) a mineral sorbent with known specific surface area A_α ($m^2\ g^{-1}$), (ii) covered with a monolayer of neutral amphoteric surface functional groups ('surface solvent') that (iii) can react with aqueous sorbates forming surface complexes on different surface patches (types). The standard state of surface species must then define a unique combination of conditions (i) to (iii), also compatible with the standard states chosen for minerals, water, and aqueous species. This is only possible if a unique value of reference density at standard state Γ_0 is fixed for all mineral–water interfaces; the standard state of a surface species occurs when one mole of it occupies all sites of reference density $\Gamma_0 = 20\ \mu mol\ m^{-2}$ on all the surface of one mole of the sorbent suspended in 1 kg of water at $P = 1$ bar and defined T in absence of external fields and at zero surface potential $\Psi = 0$ [53, 79].

So far, the LMA site balance constraints have also obscured the relations between the surface density, Γ_j ($mol\ m^{-2}$), and activity of surface species (taken as $RTa_j = \mu_j - \mu_j^0$), and did not let the surface concentration, activity, and activity coefficients be unequivocally defined. Formerly, the reference state of surface species used to be assumed similar to that of the aqueous species, that is, unimolal (unimolar) at a hypothetical infinite dilution (or at constant ionic strength) and at $\Psi = 0$ [77]. However, it is far more convenient to consider the asymmetric, complementary reference states for the 'surface solvent' $\equiv OH^0$ and the surface complex. The reference state of the neutral amphoteric functional group $\equiv OH^0$ is reached when all such groups are free (nonreacted) and occupy the sorbent surface in a monolayer of Γ_0 density, that is, one mole per 1 kg H_2O of $\equiv OH^0$ groups on a sorbent with reference total surface area $A^0 = 1/\Gamma_0 = 5{\cdot}10^5\ m^2\ mol^{-1}$. The hypothetical reference state of a surface complex (i.e. reacted functional group) is reached at infinitely low surface density and infinite dilution of the aqueous sorbate counterpart. These two reference states are reciprocal to each other, just as the states used for water solvent and solutes in the aqueous electrolyte phase.

The above definitions permit description of the *activities* and (electro)chemical potentials of surface-bound species at any state of interest for a multisite-surface sorption phase. It can be shown [53] that, if the concentration of a surface species is expressed as a surface density (mole) fraction Γ_j/Γ_0 then the a_j activity of jth surface species (at $\Psi = 0$) can be expressed as

$$a_j = \frac{\Gamma_j}{\Gamma_0}\Xi_j = \frac{A^0_{\alpha,v} n_j}{\phi_{\alpha,t} A_{\alpha,v} n_{\alpha,v}}\Xi_j \qquad (3.1.29)$$

where $A^0_{\alpha,v} = 1/(M_{\alpha,v}\Gamma_0)$ with the molar mass $M_{\alpha,v}$ of the αth sorbent, n_j is the mole amount of jth surface species, $n_{\alpha,v}$ is that of the sorbent part, $\phi_{\alpha,t}$ is a fraction of specific surface area $A_{\alpha,v}$ related to tth surface type, and $\Xi_j = f(n_j, \Gamma_{max})$ stands for a surface activity term (SAT). Using the common definition of electrochemical potential, $\mu = \mu^0 + RT \ln a + C_F$ (where C_F is the Coulombic factor defined by the electrostatic model of choice, see an overview in [86]), together with equation (3.1.29), an expression of the (electro)chemical potential of a jth surface species can be deduced [53]:

$$\upsilon_j = \frac{g^0_{j,T}}{RT} + \ln 55.5084 + \ln \frac{A^0_{\alpha,v}}{\phi_{\alpha,t} A_{\alpha,v}} + \ln \frac{n_j}{n_{\alpha,v}} + \ln \Xi_j + \frac{F}{RT} z_j \Psi_{\alpha,t} \qquad (3.1.30)$$

where z_j is the effective formula charge, F is Faraday's constant, $\Psi_{\alpha,t}$ is an electrostatic potential on tth surface type (at EDL plane), $g^0_{j,T}$ is the partial molal Gibbs energy function of jth surface species at temperature T of interest, $n_{\alpha,v}$ is the total molar amount of the sorbent part, and ln(55.5084) converts from molality to mole fraction scale.

Equation (3.1.30), used in the GEM approach, contains all the necessary conversions from the state of interest to the standard/reference states and fully reflects the 'interfacial' nature of surface species. The last two terms on the right side can be viewed together as an 'activity coefficient' providing corrections for a nonideal behavior of a surface complex, whereas the preceding three terms stand for its concentration (expressed as the surface mole fraction referenced to density at standard state, see equation 3.1.29). Note that this surface concentration, Γ_j/Γ_0, is not the same as the fractional surface coverage $\theta_j = \Gamma_j/\Gamma_{\max}$ used in the Langmuir isotherm equation. The difference lies in the denominator: while the Γ_0 is the reference density at standard state conventionally taken the same for all mineral surfaces, the $\Gamma_{\max}$ is a physically or geometrically limited, sample-surface-specific maximum attainable density of jth surface complex. As seen from equations (3.1.29) and (3.1.30), $\Gamma_{\max}$ does not appear as part of the expression for thermodynamic concentration of surface species; therefore, $\Gamma_{\max}$ must be a part of the surface activity term, $\ln \Xi_j$, that accounts for the nonideal behavior of surface complexes at zero Coulombic corrections (see below).

For SCMs used in the LMA approach, the total number of moles of reactive surface sites of tth surface is set by the $n_{t,s}$ balance constraint for the total mole amount of sites [87, 88]. Hence, in the multisite adsorption models, several $n_{t,s}$ values must be *a priori* fixed as input data. On the other hand, in SCMs in the GEM implementation (based on equations 3.1.29 and 3.1.30), any $n_{t,s}$ constraint can be avoided and replaced by a nonideal SAT Ξ_j equation that suppresses concentration of jth surface complex when, upon increasing activity of the aqueous sorbate, the density Γ_j approaches a 'geometrical' limit set by the $\Gamma_{\max}$ parameter. $\Gamma_{\max}$ can either be taken the same for species competing on tth surface type ($\Gamma_{t,\max}$ for *competitive adsorption*), or individual for certain species ($\Gamma_{j,t,\max}$ for *noncompetitive adsorption*).

It is important to realize that the reference site density Γ_0 is used in GEM SCMs only to compare surface concentrations between the state of interest and the standard state, whereas individual $\Gamma_{j,t,\max}$ or common $\Gamma_{t,\max}$ parameters can be used for the nonideality corrections by SAT. This distinction has not yet been done in LMA-based SCMs, where the site density parameter Γ_t (involved in the $n_{t,s}$ constraint) is a blend of a competitive maximum density $\Gamma_{\max}$ and a conditional total site density Γ_C (from 1 to 22 sites/nm^2), to which the fitted values of the K^{int} (for 2pK_A-type SCM) refer. From equations 3.1.29 and 3.1.30, it becomes clear why values of $g^0_{j,t}$(also a_j and K^{int}), fitted at different $\Gamma_{C_1} \neq \Gamma_{C_2}$, are not directly comparable and must be scaled down to the reference site density Γ_0 *before any comparison or correlation* even between different facets of the same mineral particle.

Let $\Gamma_0 = q\Gamma_C$, where $q \neq 1$. For 2pK_A-type reactions like the amphoteric surface group deprotonation ($>OH^0 = >O^- + H^+$), it follows that $K^{(0)}_j q = K^C_j$ because activity of 'surface solvent' $>OH^0$ group is bound to the activity of bulk water solvent, which is almost constant and close to unity (in mole fraction scale) at any given $\phi_{\alpha,t}$, $X_{\alpha,v}$, $M_{\alpha,v}$, and $A_{\alpha,v}$ values [53, 80]:

$$\log K_j = \log K^C_j + \log \frac{\Gamma_C}{\Gamma_0} \qquad (3.1.31)$$

This equation approximately converts K^{int} values (fitted at low surface coverages) to standard-state K constants, with less than 0.2 pK units deviation. The sign at the last term of equation (3.1.31) must be inverted if the $>OH^0$ group is shifted to the right side of the surface complexation reaction. However, it can be shown that the 1pK_A-based $K^{\text{int}} \approx K$ (e.g. at pH_{PPZC}) do not require conversions like equation (3.1.31) since Γ_C terms divide out from their LMA expressions.

The reference state of a surface complex, defined here as an infinitely low surface density at an infinite dilution of the aqueous sorbate counterpart,

occurs simultaneously with the 'full coverage at Γ_0' reference state of the 'surface solvent' (i.e. the $\equiv OH^0$ surface group). Consider two simple reciprocal surface-binding reactions, (Sorbate, aq) = (Surface-complex), and (H_2O, solvent) = ($\equiv OH^0$, surface), respectively. Upon increasing activity of the aqueous sorbate, the activity and density of the surface complex first increase both proportionally (in the linear adsorption region), consuming or eliminating the equivalent amount of $\equiv OH^0$ groups (of almost constant activity). When the maximum density $\Gamma_{j,t,\max}$ is approached closer, the activities of the sorbate and the surface complex both will continue to increase, while concentration (density) of the latter gets limited by the density of available sites ($\Gamma_{j,t,\max}$) as prescribed by the Langmuir isotherm [88, 89]. This isotherm, actually, contains an 'activity coefficient' $\Xi_j = \theta/(1-\theta)$, where $\theta = \Gamma_j/\Gamma_{j,\max}$ is the fractional surface coverage, $0 < \theta < 1$ at $\Xi_j \geq 1$. Coverage θ is the same as the surface concentration Γ_j/Γ_0 (equation 3.1.29) only when $\Gamma_{j,\max} = \Gamma_0$. If the sorbate binds to specific sites into a monodentate jth surface complex without lateral interactions with other surface complexes, then a noncompetitive SAT function can be applied [53]:

$$\ln \Xi_j^{(n)} = \left\{ \begin{array}{c} 0, x_j \leq 1/2\eta_{j,t,L}; \\ \ln x_j - \ln(\eta_{j,t,L} - x_j) \end{array} \right\} \qquad (3.1.32)$$

where $\eta_{j,t,L} = \phi_{\alpha,t} A_{\alpha,\nu} X_{\alpha,\nu} M_{\alpha,\nu} \Gamma_{j,t,\max}$ is an expected limiting mole quantity of jth surface complex on tth surface type. The SAT (equation 3.1.32) permits to assign *separate maximum densities* to reactive sites of different energy on the same surface without introduction of balance constraints on the total number of sites $n_{t,s}$. Calculated at GEM iterations, equation (3.1.32) reproduces in simple systems the shapes very similar to Langmuir isotherms, with linear part of 'ideal adsorption behavior' at low coverage ($\theta \leq 0.5$), bending asymptotically to $\Gamma_{j,t,\max}$ at higher coverage and thus exhibiting the nonideal adsorption behavior. The maximum density $\Gamma_{j,t,\max}$ is a nonthermodynamic, physical parameter, either fitted or obtained from crystallographic or spectroscopic data. If several sorbates compete for the same surface sites, then a competitive SAT function must be used, which has the same form as equation (3.1.32), with the only difference that $\eta_{j,t,L}$ is substituted by $\eta_{t,L}$ – a difference between the limiting mole quantity of available sites and the sum of all competing surface complexes on these sites but jth surface complex [53].

Accounting for the nonideality of surface complexation using SAT turns to be an efficient way to implement complex multisite-surface thermodynamic models involving adsorption on mineral–water interfaces, even that as complex as clays [80, 90], only in chemical elemental stoichiometry of the system. At the same time, the newly proposed standard and reference states permit us to start with a compilation of thermodynamic database for surface complexes [80], given that a proper electrostatic SCM is chosen.

GEM-based SCMs are calculated in the elemental (+charge) stoichiometries, pretty much in the same way as the SSAS systems, but with some more input information about specific surface area of the sorbent, surface types, assignment of surface complexes to EDL planes, and maximum surface densities, as discussed above. In terms of the 2pK_A-type SCMs for a triple layer (TLM), a double diffuse layer (DLM), or a constant capacitance (CCM), all assume that at nonreacted sites, the oxide surface exposes the *neutral amphoteric* $\equiv$OH *functional groups,* which can react with aqueous species via (de)protonation or ion binding into the outer- or inner-sphere surface complexes [77, 78, 88]. Hence, the standard partial molal properties (e.g. G^0_{298}) of surface complexes can be calculated via the respective adsorption reaction thermodynamic constants K if such properties and elemental stoichiometry of the $\equiv$OH group are known.

Several examples of GEM surface complexation modeling have already been published [53, 79, 80, 90]. The GEM technique can also conveniently model the multisite adsorption with surface precipitation, both occurring at relatively high metal loadings. This was demonstrated in [53] for Cr(III) sorption on amorphous silica SiO_2, am using experimental data of Fendorf *et al.* [91], who studied the uptake of dissolved Cr(III) by 0.25 g L^{-1} amorphous silica (with specific surface area of

Table 3.1.6. Maximum site densities and thermodynamic data for the sorption system Cr/SiO_2(am) as fitted by GEM modeling (data from [53]).

Species	Γ_{max}, sites nm^{-2}	Stoichiometry	G^0_{298}, kJ mol^{-1}
$>O_{0.5}H^0$	5.5	$O_{0.5}H$	−128.55
$>O_{0.5}^-$	5.5	$O_{0.5}$	−82.31
$w > O_{0.5}Cr(OH)_2{}^0$	5.5	$O_{0.5}Cr(OH)_2$	−740.12
$s > O_{0.5}Cr(OH)_2{}^0$	0.2	$O_{0.5}Cr(OH)_2$	−758.33
SiO_2(am) sorbent		SiO_2	−848.77
CrOOH,s phase		CrOOH	−623.49

221 m^2 g^{-1}) at pH between 3.5 and 6.5, and total chromium concentration 10^{-4} mol L^{-1} in 0.1 *M* $NaNO_3$ electrolyte. Using high-resolution spectroscopy and microscopy (EXAFS and HRTEM), these authors found surface clusters of a γ-CrOOH structure forming on the silica surface at pH > 5.5, while at lower pH, monodentate surface complexes of Cr(III) dominate. The shapes of pH edges of Cr(III) adsorption at 3.5 < pH < 5.5 also suggest binding of Cr(III) into 'strong' and 'weak' surface complexes. Hence, the sorption of Cr(III) on $SiO_{2,am}$ was modeled in the whole experimental pH interval using a simple two-site nonelectrostatic model (NEM) plus a separate CrOOH hydroxide phase. Two surface complexes of elemental stoichiometry $O_{0.5}Cr(OH)_2^0$ were defined via reactions:

$$>O_{0.5}H^0 + Cr^{3+} + 2H_2O \leftrightharpoons s > O_{0.5}Cr(OH)_2^0 + 3H^+ \quad (3.1.33)$$

and

$$>O_{0.5}H^0 + Cr^{3+} + 2H_2O \leftrightharpoons w > O_{0.5}Cr(OH)_2^0 + 3H^+ \quad (3.1.34)$$

where w > denotes the 'strong', and s > the 'weak' surface complex. Gibbs energies of the surface species and the maximum density parameter for 'strong' sites $\Gamma_{max,S}$ were fitted in GEM calculations; total maximum density of 5.5 sites/nm^2 as given in [91] was used for 'weak' species (Table 3.1.6). The modeling results [53] clearly show that the two-site GEM NEM with the separate Cr(III) hydroxide phase provides quite a good description of the experimental data. Up to pH = 5, the 'strong' $s > O_{0.5}Cr(OH)_2^0$ species dominates the adsorption (Figure 3.1.3). Beginning from pH = 4.5, 'strong' sites get saturated (manifested with SAT values $\Xi_S \gg 1$), and the $w > O_{0.5}Cr(OH)_2^0$ species accumulates to some extent up to a pH of 5.5. At this point, the CrOOH,s phase becomes stable, and its precipitation fixes ultimately the Cr(III) activity in aqueous solution and on surface at further increasing pH values. Consequently, the surface density of the $w > O_{0.5}Cr(OH)_2^0$ species remains constant without any SAT contribution. The SAT for the strong $s > O_{0.5}Cr(OH)_2^0$ species, however, strongly increases from $\ln \Xi_S \approx 0$ at a pH = 4 up to $\ln \Xi_S \approx 5.8$ at a pH ≈ 5.2, then remains more or less constant above that pH value (fluctuating around $\ln \Xi \approx 6$). This example of a sorption continuum modeling exemplifies how different sorption phases can be described simultaneously within a single GEM thermodynamic model, even without any electrostatic corrections for surface complexation. Such 'third-generation' models will narrow a gap between the increasing amount of microstructural information currently made available by the rapid progress with spectroscopic techniques like EXAFS and the ordinary LMA approach to merely fit the titration curves without much regard to any structural features of the surfaces. Within the GEM framework, multisite-surface SCMs can easily be enhanced by adding electrostatic interface models (TLM, BSM) as shown in [80].

3.2 Temperature corrections

3.2.1 Temperature correction methods

In most applications published so far in the field of environmental speciation modeling, the LMA approach has been used with $\log K_{298}$ values, assuming that the temperature effect is negligible

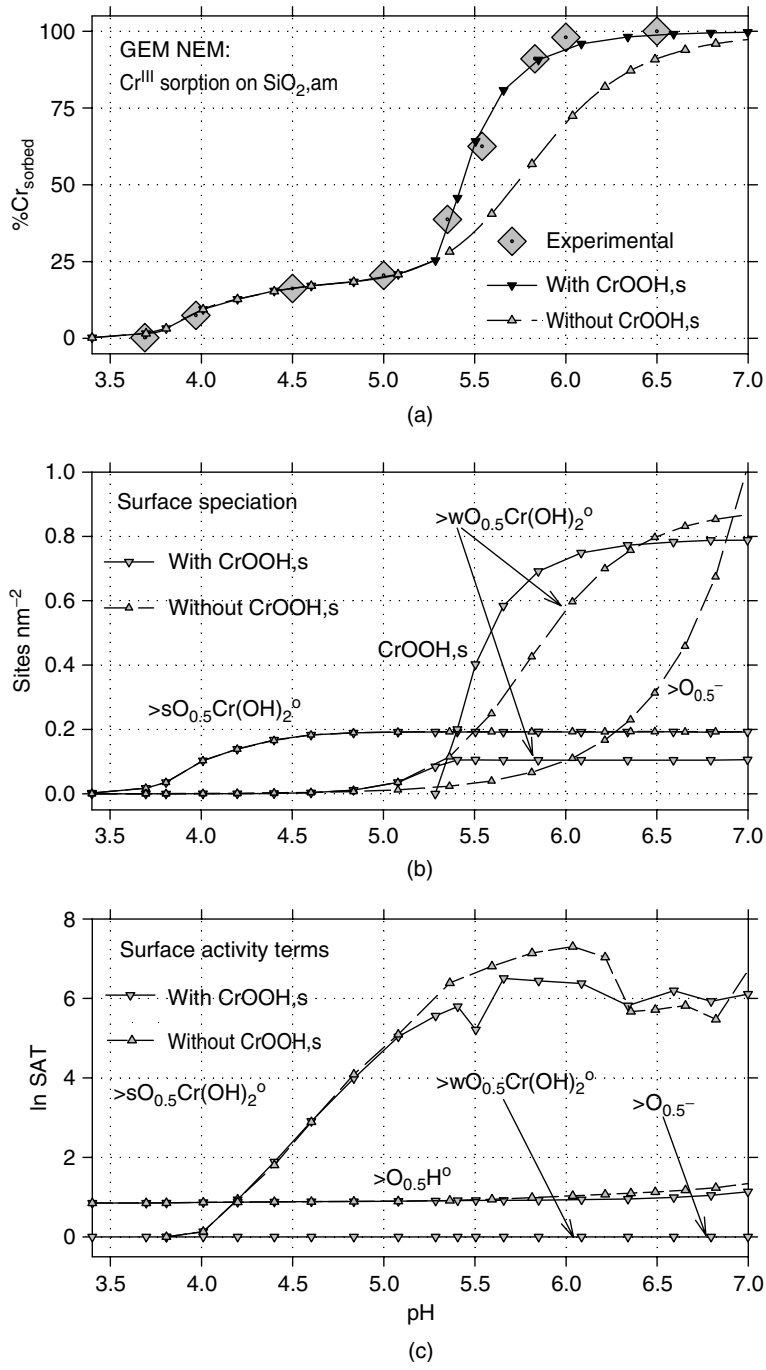

Figure 3.1.3. Model of the sorption of Cr onto the amorphous silica surface including monodentate $>O_{0.5}Cr(OH)_2^0$ surface complexes and CrOOH surface precipitation. (Reproduced from *Am. J. Sci.* **302** 2002 227, Gibbs energy minimization approach to modeling sorption equilibria at the mineral-water interface: Thermodynamic relations for multi-site-surface complexation, Kulik, D. A., Figure 7, copyright with kind permission of Yale University [53].)

Table 3.1.7. Simple temperature extrapolations and associated uncertainty propagation in $\log K(T)$ and $\Delta_r G^0(T)$ of reactions (from [46]).

N terms	Fixed parameters	Zero parameters	Other parameters	Comments, examples
One	$g^0(T) = \Delta G^0_{298}$	$\int_{298}^{T} \Delta S^0(T)dT = 0$	$-(T-298)\Delta S^0(298) = \int_{298}^{T}\int_{298}^{T} \frac{\Delta Cp(T)}{T} dTdT$	Not recommended, except for some aqueous complexes (e.g. $CaCO^0_3$ to 250 °C)
One[a]	$\ln K(T) = \ln K(298)$	$\Delta_r H^0(T) = 0$, $\Delta_r C_P(T) = 0$	$\Delta_r G^0(T) = -RT \ln K(298)$, $\Delta_r S^0(T) = R \ln K(298)$	Recommended for surface sorption modeling[33]
One[b]	$\Delta_r G^0(T) = \Delta_r G^0_{298}$	$\Delta_r S^0(T) = 0$, $\Delta_r C_P(T) = 0$	$\ln K(T) = -\Delta G^0_{298}/(RT)$ $\Delta_r H^0(T) = \Delta_r G^0_{298}$	For isocoulombic reactions only
Two[c]	$\Delta_r S^0(T) = \Delta_r S^0_{298}$	$\Delta_r C^0_P(T) = 0$	$\Delta_r H^0(T) = \Delta_r H^0_{298} = \Delta_r G^0_{298} + T\Delta_r S^0_{298}$ $\Delta_r G^0(T) = \Delta_r G^0_{298} - (T-298)\Delta_r S^0_{298}$	Good for isocoulombic and isoelectric reactions
Three[d]	$\Delta_r Cp(T) = \Delta_r Cp_{298}$	Second and higher $\Delta_r C_P = f(T)$ coefficients are zeros	$\Delta_r S^0(T) = \Delta_r S^0_{298} + \ln(T/298)\Delta_r C_{P,298}$ $\Delta_r H^0(T) = \Delta_r H^0_{298} + (T-298)\Delta_r C^0_{P,298}$ $\Delta_r G^0(T) = \Delta_r G^0_{298} - (T-298)\Delta_r S^0_{298} + (T - 298 - T\ln(T/298))\Delta_r C_{p,298}$	Best for isoelectric reactions, good for generic reactions up to 150 °C

[a] $\delta \log K(T) = \text{const}$, while $\delta\Delta_r G^0(T) = (T/298)\delta\Delta_r G^0_{298}$, where δ denotes the absolute uncertainty of the respective value.
[b] Valid for many kinds of isoelectric reactions; *decreasing* $\delta \log K(T) = (298/T)\delta \log K(T)$ error propagation; at $T = 596$ K, $\delta \log K(T) \approx 1/2\delta \log K(298)$, while $\delta\Delta_r G^0(T) = \text{const}$.
[c] $\delta \log K(T) = \delta \log K(298) + [(T-298)/(2.3RT)]\delta\Delta_r S^0_{298}$; this Van't Hoff extrapolation at 596 K and $\delta\Delta_r S^0_{298} = 10\ \text{K}^{-1}\ \text{mol}^{-1}$ results in $\delta\Delta_r G^0(T) \approx 3\ \text{kJ mol}^{-1}$, or $\delta \log K(T) \approx 0.3$.
[d] $\delta \log K(T) = \delta \log K(298) + [(T-298)/(2.3RT)]$; $\delta\Delta_r S^0_{298} + [(T - 298 - T\ln(T/298))/(2.303RT)]\delta\Delta_r C_{P,298}$; at $T = 596$ K, $\delta\Delta_r S^0_{298} = 0$ and $\delta\Delta_r C_{P,298} = 25\ \text{J K}^{-1}\ \text{mol}^{-1}$, one obtains again $\delta\Delta_r G^0(T) \approx 3\ \text{kJ mol}^{-1}$, or $\delta \log K(T) \approx 0.3$.

in the ambient temperature range between about 5 and 50 °C. It is known, however, that temperatures up to 90 °C may occur within landfills or underground repositories. The question of whether to consider temperature corrections, however, seems to be related more to pragmatic implementation issues than to scientific problems. Table 3.1.7 lists some simple temperature-correction methods in the order of increasing demand to the input data. Some of these techniques, based on measured or predicted thermochemical properties (molar enthalpy H, entropy S, heat capacity C_P), are routinely used in hydrothermal geochemistry, metamorphic or igneous petrology [2].

Advanced LMA-based speciation programs, for example, PHREEQC-2 [25], provide temperature corrections using the integrated Van't Hoff equation (i.e. the two-term $\log K_{298}$ and ΔH^0_{298} extrapolation at zero ΔC_P) for the formation reactions of product species (aqueous complexes, minerals, and gases), and allow also for polynomial $\log K = f(T)$ expressions (but without the possibility for refitting). When no data other than $\log K_{298}$ are available for some aqueous and surface species, or minerals, a common practice is to take $\log K(T) = \log K_{298} = \text{const}$ (the one-term approximation at $\Delta H^0_{298} = 0$), albeit a more reliable approximation would be $\Delta H^0_{298} = \Delta G^0_{298} = -RT \ln K_{298} = \text{const}$ (the one-term approximation at $\Delta S^0_{298} = 0$). One can also assume $\Delta G^0(T) = \Delta G^0_{298} = \text{const}$ in the absence of other parameter values if the GEM modeling code is used. The above three assumptions already define the simplest temperature extrapolations with associated uncertainties [46], sometimes justified, but more often inadequate, up to producing completely wrong temperature trends, in particular if the reactions are not written in an isoelectric/isocoulombic form. Here, we call 'isoelectric' such (aquatic) reactions that have an equal sum of positive and negative charges on both sides, for example hydrolysis reactions like $4\,Zn^{+2} + 2\,H_2O \leftrightharpoons Zn(OH)^0_2 + 2\,H^+$. An isocoulombic reaction, in addition, has only species of equal charge on both sides, like a cation-exchange reaction $Zn^{+2} + CaSO^0_4 \leftrightharpoons ZnSO^0_4 + Ca^{+2}$ or an anion-exchange reaction $ZnOH^+ + HS^- \leftrightharpoons ZnHS^+ + OH^-$. Such

reactions usually have small or negligible entropy, volume and heat capacity effects and therefore can be used even in the simplest, one-term extrapolations for temperature corrections up to 200–250 °C [45] when only an equilibrium constant K at 25 °C is known.

Many formation reactions used in LMA code databases (except isoelectric hydrolysis or gas dissolution reactions) are expected to have large entropy and heat capacity effects. Even the two-term (Van't Hoff) extrapolation may then accumulate significant errors at temperatures above 50–100 °C. In such cases, an approximation using polynomial $\log K = f(T)$ functions (such as provided in the PHREEQC-2 program) is to be preferred. There are also programs that use the SUPCRT92 code and database [35] developed for petrologic high-T, P applications for obtaining molar Gibbs energy functions $g_{T,P}$ for aqueous ions, complexes, gases, and minerals, in order to use them (i) directly in GEM equilibria calculations (as in GEM-Selektor), or (ii) to convert them into $\log K(T)$ values for product species used by LMA modeling codes (e.g. the LLNL.DAT database in PHREEQC-2, or utility programs like PMATCHC [50] for checking the internal consistency of thermodynamic data). The SUPCRT92 code itself uses temperature–pressure corrections (up to 1000 °C and 5 kbar) based on thermochemical and revised HKF-EoS data for calculation of $\log K$ of any possible reaction; at T, P of interest, the $g_{T,P}$ values of all involved species are calculated first and then $\log K(T, P)$ values can be found by algebraic summation [35].

If standard molar entropy (or enthalpy) and heat capacity of the reaction are available, they can be used together with $\log K_{298}$ values to calculate the coefficients of a three-term temperature extrapolation:

$$\log K(T) = a + \frac{b}{T} + c \ln T, \text{ where}$$
$$a = \frac{\Delta S^0_{T_0} - \Delta C_{P,T_0}(1 + \ln T_0)}{2.303R};$$
$$b = \frac{-\Delta H^0_{T_0} + \Delta C^0_{P,T_0} T_0}{2.303R}; c = \frac{\Delta C_{P,T_0}}{2.303R} \quad (3.1.35)$$

T_0, $\Delta S^0_{T_0}$, and $\Delta C_{P,T_0}$ denote reference temperature (298 K), changes in entropy and in heat capacity of the reaction at T_0, respectively. If standard molar properties are known for the reaction and all but one of its components, then the standard (partial) molar (molal) properties of this kth component can be calculated algebraically for any temperature of interest:

$$\Theta_k(T) = \left(-\Delta\Theta(T) + \sum_{j \neq k}^{L} \nu_j \Theta_j(T) \right) \Big/ \nu_k \quad (3.1.36)$$

where Θ represents one of the standard (partial) molar (molal) properties, that is, Gibbs energy G^0, enthalpy H^0, third-law entropy S^0, heat capacity C_P, or volume V^0 for individual species. $\Delta\Theta$ stands for their respective changes in the reaction involving L independent components with stoichiometry coefficients ν_j. For dissolution reactions, especially hydrolysis-type reactions for oxides, the three-term extrapolation (equations 3.1.35 and 3.1.36) produces up to 200 °C practically the same values of G^0 as the direct calculation based on $C_P = f(T)$ equation.

3.2.2 Error propagation in temperature corrections

Table 3.1.7 presents an assessment of error propagation in $\log K(T)$ for the various temperature-correction methods, provided that the respective extrapolation was appropriate. Any reliable temperature-correction method must avoid accumulation of errors in $\log K(T)$ or $g^0(T)$ considerably greater than the inherent uncertainties of the respective $\log K_{298}$ or ΔG^0_{298} values. For the generic three-term extrapolations, it follows that an error in $\Delta C_{P,298}$ 2–3 times larger than that in ΔS^0_{298} would lead to about the same magnitude of uncertainty at T, which is acceptable in practice if $\delta \log K(T) < \delta \log K_{298}$ in the whole temperature interval of interest. If parameters of three-term extrapolation are given (e.g. fitted from experimental data), then one can estimate how much uncertainty is introduced at T of interest by a less precise two- or one-term extrapolation by taking errors equal to zeroed-off $\Delta C_{P,298}$ and

ΔS^0_{298}, respectively. As these numbers for some formation or redox reactions may exceed 100 to 300 $J\,K^{-1}\,mol^{-1}$, one- and two-term extrapolations may in such cases produce large deviations $\delta \log K(T) > \delta \log K_{298}$ even within the relatively small temperature interval below 50–70 °C relevant for environmental studies. For the non-isocoulombic formation reactions, the estimated values of $\Delta C_{P,298} > 20\ J\,K^{-1}\,mol^{-1}$ and $\Delta S^0_{298} > 10\ J\,K^{-1}\,mol^{-1}$ must therefore always be used. Otherwise, these values must be predicted or the species described through an isoelectric reaction.

Generic formation reactions, taken in the three-term (3-t) extrapolation, can provide good fits up to 200 °C for the ion pairs of cationic trace elements with the common oxyanions carbonate, sulfate, and phosphate. As an example, consider the uranyl complexation reaction

$$UO_2^{+2} + CO_3^{-2} \leftrightharpoons UO_2CO_3^0(aq);\ \log K_1 \quad (3.1.37)$$

for which experimental $\log K(T)$ values up to 300 °C are available [47, 92]. By adding the carbonate ion formation reaction, $CO_2(aq) + H_2O = CO_3^{-2} + 2H^+$, the reaction (3.1.37) can be converted into an isoelectric form:

$$UO_2^{+2} + CO_2(aq) + H_2O \leftrightharpoons UO_2CO_3^0(aq) + 2H^+;\ \log K_2(ie) \quad (3.1.38)$$

The latter reaction (denoted in Figure 3.1.4 as 'ie'), if compared with experimental data, provides a good two-term extrapolation up to 300 °C. Many alternative reactions can be constructed in

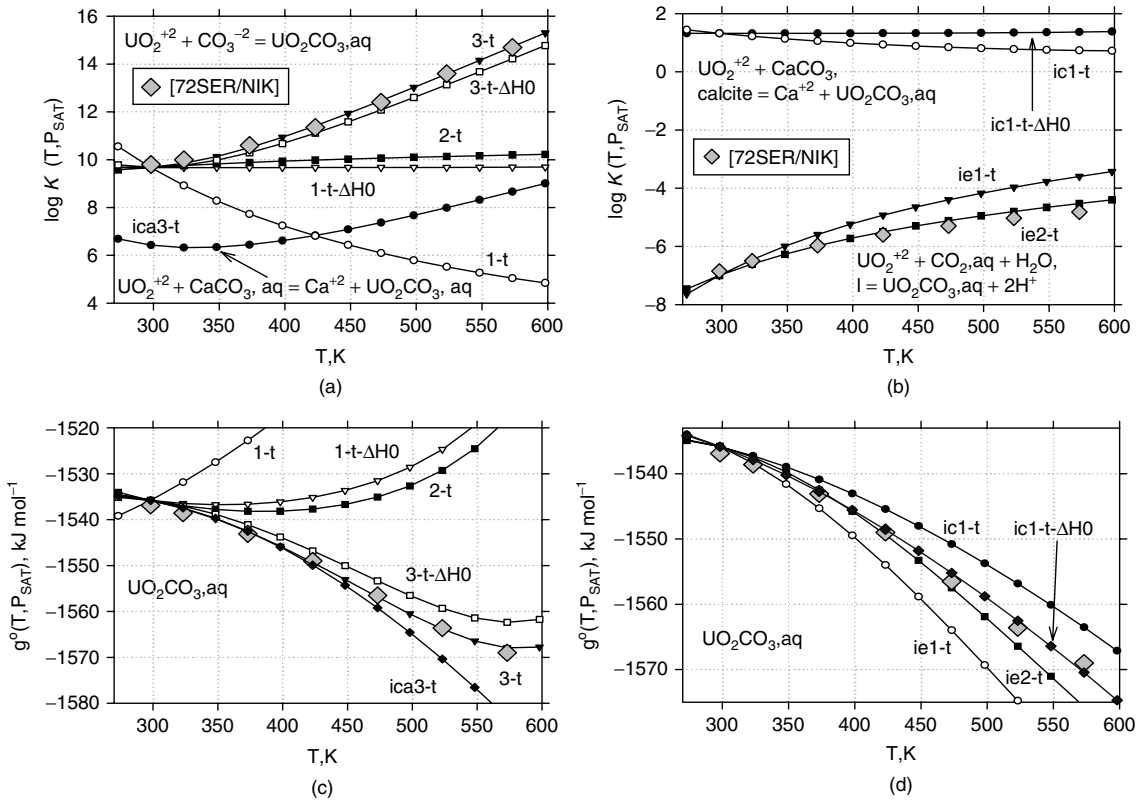

Figure 3.1.4. Various temperature extrapolations for the aqueous $UO_2CO_3^0$ complex ([46]). Data [72SER/NIK] are from Sergeeva and coworkers [94], for other abbreviations see text. Plotted using the GEM-Selektor 'RTParm' module and data from Tables 3.1.8 and 3.1.9.

order to describe thermodynamic properties of the $UO_2CO_3^0$(aq) species on the basis of available thermochemical or EoS data for other involved species [19, 44, 93]. For example, the following isocoulombic reactions can be formulated [46], see also Tables 3.1.8 and 3.1.9:

$$UO_2^{+2} + CaCO_3^0(aq) \leftrightharpoons UO_2CO_3^0(aq) + Ca^{+2}; \quad \log K_3(\text{ica}) \tag{3.1.39}$$

$$UO_2^{+2} + CaCO_3^0(s) \leftrightharpoons UO_2CO_3^0(aq) + Ca^{+2}; \quad \log K_4(\text{ic}) \tag{3.1.40}$$

A surprising result is that the one-term (1-t) extrapolation of reaction 'ic-1-t-DH0' for $\log K_4(T)$ at $\Delta H^0(T) = 0$ (equation 3.1.40) yields an excellent description of $g^0(T)$ for the $UO_2CO_3^0$(aq) species up to 300 °C (Figure 3.1.4). However, for $\log K_1(T)$, both one- and two-term extrapolations do not appear satisfactory.

Isoelectric reactions are also helpful in defining temperature corrections for surface complexes and pH of zero charge [79, 95]. At present, this seems to be the only possibility, because no EoS for surface species analogous to the HKF-EoS for aqueous species has been suggested so far. The elemental stoichiometry and standard partial molal properties of the oxide surface species, consistent to that for gases, minerals, and aqueous ions, can be conveniently determined on the basis of a reaction $0.5H_2O(\text{aqueous}) = O_{0.5}H(\text{surface})$ for the amphoteric neutral functional (group) $> O_{0.5}H^0$, considered as a 'surface solvent'. From this reaction, it follows that the activity $a(> O_{0.5}H^0) = K \cdot a(H_2O)^{0.5}$ is constant, as long as the aqueous electrolyte phase is stable and the ionic strength is constant. From a presumption that surface density of $>O_{0.5}H^0$ at the reference state is independent of temperature, it follows that $\log K(T) = 1.74436$, $\Delta G^0_{298} = -9.957$ kJ mol^{-1}, $\Delta H^0(T) = 0$, $\Delta C_p(T) = 0$, and $\Delta S^0(T) = 33.4$ J K^{-1} mol^{-1} for the above reaction [53]. From these numbers and standard molar properties of the H_2O solvent, $G^0_{298}(>O_{0.5}H^0) = -128.55$ kJ mol^{-1} and other standard partial molal properties of the $>O_{0.5}H^0$ 'surface solvent' can be determined at 298 K and other temperatures [79]. Next, the standard properties of the protonated surface species $>O_{0.5}H_2^+$ can be defined from an isoelectric reaction $>O_{0.5}H_2^+ \leftrightharpoons >O_{0.5}H^0 + H^+$, using one-term extrapolation at $\Delta S^0(T) = 0$, the $\log K_{298}$ of which can be predicted for different oxides together with pH point of zero charge [94]. Standard properties of deprotonated surface species can be found, for example, from the Schoonen's [95] reaction $>O_{0.5}H_2^+ + OH^- \leftrightharpoons >O_{0.5}H^0 + H^+ + H_2O$, or similar isoelectric reactions involving adsorbed cations or anions, provided that more hydrothermal adsorption data becomes available. Generic formation reactions for surface complexes on simple oxides such as rutile TiO_2 can provide good fits up to 200–300 °C, but only in three-term temperature extrapolation [79].

In determining the elemental stoichiometry of the 'surface solvent' that in any case must

Table 3.1.8. Standard properties of $UO_2CO_3^0$ (aq) species at 25 °C.

Parameter	From 3-t extrapolation, equation (3.1.37)	From ic1-t-$\Delta H0$ extrapolation, equation (3.1.40)
$\Delta G^0(298)$	−1535.85	−1535.86
$\Delta H^0(298)$	−1688.25	−1683.33
$S^0(298)$	57.12	75.13
$C_P(298)$	247.74	152.46

In kJ mol^{-1}; J K^{-1} mol^{-1}.
Source: Modified from [46].

Table 3.1.9. Parameters of temperature extrapolations (reactions 3.1.37–3.1.40) involving $UO_2CO_3^0$(aq) species.

Parameter of reaction	r.(37), 3-t	r.(37), 2-t	r.(37), 1-t	r.(37), 1-tΔH0	r.(39), ica3-t	r.(38), ie2-t	r.(38), ie1-t	r.(40), ic1-t	r.(40), ic1-t-ΔH0
$\log K(298)$	9.68 ± 0.04	9.68	9.68	9.68	6.424	−7.0 ± 0.05	−7.0	1.32	1.32
$\Delta_r H^0(298)$	6.0 ± 6.0	6.04	−55.196	0	−11.8	28.9 ± 2.0	39.96	−7.535	0
$\Delta_r S^0(298)$	205.44	205.44	0	185.13	83.4	−37.08	0	0	25.27
$\Delta_r Cp(298)$	499.0	0	0	0	355	0	0	0	0

In kJ mol^{-1}; J K^{-1} mol^{-1}.
Source: Modified from [46].

contain water at mineral–water interfaces, there is an ambiguity whether to include the sorbent atoms (e.g. for rutile surfaces, $TiO_{1.5}OH^0$ versus OH^0). To resolve this ambiguity, a cornerstone decision for the unified thermodynamic sorption database must be made. Involvement of the sorbent would make standard molal properties of surface species dependent on composition of the sorbent and comparable within a single mineral surface type only. Perhaps, this problem is more relevant for the GEM than for the LMA approach, because in the latter, the sorbent stoichiometry only identifies the $n_{t,s}$ balance constraint. Therefore, our choice *not to include* the stoichiometry of the sorbent into the elemental stoichiometry of surface species [53, 79] makes their standard thermodynamic properties comparable between different surfaces and minerals, consistent with that of aqueous sorbates, solids, and gases, and thus appears preferable.

4 SIMULATION OF IRREVERSIBLE CHEMICAL MASS TRANSFER

4.1 Process simulation

Most geochemical modeling problems require calculation of a series of equilibrium states to simulate irreversible mass transfer processes such as mixing, dissolution, titration, weathering, and so on, based on the principles of local and partial equilibrium. Performing such a batch computing manually, however, is time consuming, especially for the processes controlled by regular changes of bulk composition of (otherwise the same) system. To facilitate and automate this work, the 'batch simulator' functionality has been implemented in many geochemical codes, in particular, PHREEQC-2 [25], GWB [7], and GEMS (GEM-Selektor) [31]. In the latter, the 'Process Simulator' module generates a sequence of records, which are then used for calculating equilibrium states and storing the results to be sampled, plotted, and exported later on.

Theoretically, two types of irreversible process simulations are possible. A 'simultaneous' type implies that the next step of the process does not depend on the parameters of equilibrium (speciation, pH, Eh, activities, fugacities) calculated at the previous step. This is the case for P and/or T changes, direct titrations, and simple reaction progress models like an 'incongruent' dissolution of a given bulk rock composition. After all necessary input variants of the system have been generated, they, in principle, can be computed independently, for example, in parallel on a PC cluster. On the other hand, a 'sequential' type of the process simulation must be performed when the next step depends on some parameters unknown before the calculation of the present equilibrium state. Typical examples are sequential reactors, inverse titrations, kinetically dependent processes, or coupled reactive mass transport models. In the latter case, parallel calculations of local/partial equilibria in many nodes ('voxels') can still be performed, but only for the same time point.

In general, there is no way to predict and implement in a program all of the unlimited variety of meaningful process simulations that may be of interest to (geo)chemists. Hence, in codes like PHREEQC-2 [25] or GEMS [31], irreversible processes can be defined using the 'mathematical scripts', where the user can write in a simple basic- or C-like language what and where changes have to be made in the chemical system input data at the next step of the simulated sequence. User-defined scripts are also very helpful for sampling and plotting/exporting relevant results of the process simulation; this provides maximum freedom and flexibility to the user and makes the whole modeling effort far more efficient.

4.2 Metastability and redox state controls

In complex heterogeneous aquatic systems existing at near-to-ambient conditions of the Earth's surface, the complete equilibrium is almost never attained because of large differences in reactivity of the involved mineral phases, organic matter, and even some aqueous species and gases. For example, the surface seawater is oversaturated with respect to calcium and magnesium carbonates (calcite, aragonite, dolomite, magnesite),

precipitation of which is biologically mediated. Phosphates of calcium and magnesium, especially apatite, can be a thousand times oversaturated in the sediment porewater without any observable precipitation that occurs only during the diagenesis in a timescale of thousands to millions of years. Sediment porewaters are often very highly oversaturated with respect to pyrite FeS_2, but measured concentrations of dissolved iron are usually on the level of solubility of amorphous iron sulfides mackinawite FeS and greigite Fe_3S_4, even though pyrite is also present in sediments [32]. In weathering crusts and soils, many minerals of igneous rocks such as magnetite or garnets, thermodynamically unstable at surface conditions, may persist during millions of years because of nonreactive or passivated surfaces. Finally, the very existence of life depends on a fundamental disequilibrium between the atmospheric nitrogen N_2 and dissolved nitrate NO_3. The reaction between them proceeds only at high temperatures, for example, within a thunderstorm lightning. If these species would react according to their known thermodynamic properties, then the oceans would have been filled with nitric acid [4]. In thermodynamic calculations involving nitrogen gas, this reaction has therefore to be suppressed, as indicated by the abbreviation 'Nit' in Table 3.1.4.

There are many other redox processes in natural waters that are strongly affected by metastability or kinetic hindrances, for instance, oxidation of dissolved arsenite AsO_3^{-3} species to arsenate AsO_4^{-3}. For these reasons, thermodynamic modeling of element speciation and partitioning must clearly be able to account for certain metastability restrictions. This is done usually on the basis of 'partial equilibrium' principle, which tells that, if some phases or species are 'frozen' but the rest of the system is well mixed to be fully reacted within a timescale of interest, then the irreversible evolution of such a system can be represented as a sequence of partial equilibria at constant total bulk composition but varying quantities of the 'frozen' phases or species protected from equilibration. Mathematically, this can be represented using the 'process extent' variables (equations 3.1.5 to 3.1.8) that control the bulk composition of the equilibrating part of the system, and plotted in various kinds of the 'process extent' diagrams.

Characterization and modeling of redox-dependent chemical speciation is probably one of the most difficult tasks of environmental geochemistry, not to a least extent because of strong metastability of redox-controlling substances at low temperatures ([5, 96–98]; Chapter 7 in [10]). It is of critical importance to know which phases that can potentially affect redox speciation are reactive at the chosen timescales. In addition, LMA-based speciation models usually require total concentrations of different valence forms of elements (e.g. Fe^{II} and Fe^{III}) or, alternatively, pe or Eh or oxygen fugacity as input data, whereas often one wants to obtain these parameters from the modeling calculation. In the GEM approach, only the total bulk elemental composition of the chemical system (vector $\boldsymbol{b}$) must be supplied as input data (see Table 3.1.3); all the above-mentioned parameters will be calculated. The calculated values of pH, pe, fugacities of gases, and activities of redox-sensitive species will depend on the initial modeling assumptions about reactive and metastable solids; the complexity of chemical system plays no role. Note ultimately, that unlike in LMA-based modeling, the inverse titration method is the only possibility in GEM to fix the system at a given value of pH or pe. In the inverse titration modeling, a certain amount of titrant added (acid, base, oxidant, or reductant) should be found that brings the aquatic system to a predefined equilibrium pH (or pe, or both). This mode is needed because it is not possible to use activities, pH, and pe as master input variables in the GEM approach. To perform inverse titrations, a 'gold section' optimization procedure is implemented within the process simulator module of the GEMS code [31], which compares the calculated value (e.g. of pH) to the prescribed one, and makes a correction to the amount of titrant, until convergence with necessary precision is achieved.

4.3 The local equilibrium principle

Another restriction of the complete equilibrium concept requires that the system should be uniform in bulk composition, temperature, and pressure as

a whole and in any macroscopic part. Obviously, such cases in nature are very seldom, if they exist at all; natural waters, sediments, rocks, and soils are stratified and/or inhomogeneous in other respects. Also, the mass transport via diffusion and/or advection in the aqueous and/or gas phases can occur between different parts of a large spatially inhomogeneous system. Can thermodynamic modeling then be applied at all? The local equilibrium principle postulates that any macroscopically inhomogeneous system can be subdivided into parts ('nodes', 'voxels') small enough to be spatially homogeneous, where mixing and equilibration occurs within a time interval less than the time step of interest to consider the (steady state) mass transport between different parts. This local equilibrium principle, taken together with the partial equilibrium principle, forms a heuristic basis of the majority of coupled reactive transport modeling approaches (cf. also [10, 99, 100]).

The first degree in model sophistication is to include a spatial dimension by introducing a multibox model, where a number of individual process simulation boxes are stacked and coupled through diffusive or advective transport conservation equations, or (as the simplest case) by some steady-state fluxes with a general system of mass-balance equations within all boxes. The basic assumption here is that a steady state can be achieved in the whole system of internally well-mixed boxes. The boxes are limited in size as to reach local equilibrium within each box, that is, kinetically dependent reactions proceed more rapidly than the residence time of the aqueous phase inside of the box. Any temporal change of the equilibrium state inside of a single box is due to an increment of mass exchange across the box boundaries, modeled as a sequence of local/partial equilibrium states using the same chemical speciation thermodynamic data set. In the case of stratified marine or lacustrine water columns, the whole mass transport model can be reduced to a one-dimensional column of boxes, where each box represents a water layer with uniform density, temperature, and redox conditions [101, 102].

In principle, the models available can be differentiated again into a simultaneous and a sequential approach. The first approach is to insert all the interaction chemistry directly into the mass transport equations and to reduce the problem to one strongly nonlinear equation set [103, 104]. Because of this nonlinearity, only a simplified equilibrium chemistry and kinetics can be solved simultaneously with the transport equations using, for example, a finite-element method subject to concentration or flux boundary conditions and appropriate initial conditions. The HBGC123D code suitable for a 32 processor cluster is an example of such an approach [105]. Several such capable models have been found to give reliable results in even a multidirectional flow field, provided sufficiently small time and space increments together with fast mainframes are used for the calculations.

The concept behind the 'sequential coupling' approach is to pose the equilibrium chemical mass transfer independent of the mass transport equations, that is, to decouple hydraulic and geochemical simulations. This approach requires a nested two-step iteration over all nodes (chemical equilibration and mass transport), but the benefit is that an extensive geochemical model can be computed in parallel within a time step. There are several two-step models available, such as PHREEQC-2 [25], MCOTAC [106], or COTRAM [107]. Such codes provide for an elaborate speciation model part (e.g. based on PHREEQC [25]), including redox and various solid–solution interaction mechanisms, but are limited in their application to unidirectional groundwater flow regimes. A two-step mass transport model using the GEM approach is currently under development, which shall ultimately provide the capability to model trace metal and radionuclide transport forced by unidirectional water flow in the aquifer sorption continuum.

5 CONCLUSIONS AND OUTLOOK

In this chapter, an overview has been given of the thermodynamic modeling of chemical speciation with an emphasis on application to trace elements in natural waters. An attempt has been made to provide essential thermodynamic concepts with some

rigor. This rigor is of particular importance in complex natural systems, which benefit from the now available 'third-generation' models based on Gibbs energy minimization approach. This development has been made possible through the recent advance in compilation of relevant thermodynamic data, in particular also for aqueous species. It has been shown how the GEM approach allows easily for rigorous consideration of nonideality of all relevant phases (the aqueous, surface, and solid), as well as for the yet largely neglected temperature corrections. Using the GEM approach (implemented, for example, in the GEMS code [31]), the 'sorption continuum' involving trace elements on (hydr)oxide mineral–water interfaces can be modeled (similar to SSAS systems) only in chemical elemental stoichiometry, without additional balance constraints for surface sites. This is made possible by introducing (i) standard and reference states for surface species on a multisite-surface sorption phase involving a reference site density Γ_0, (ii) activity- concentration relations for surface species based on 'surface activity terms' as Langmuirian functions of maximum site densities Γ_{max}, and (iii) elemental stoichiometries of surface species that do not involve cations of the sorbent. Now, the standard partial molal properties of surface complexes become comparable between all mineral oxide surfaces and consistent to that for solids, gases and aqueous species. It is this sorption continuum modeling capability that makes the GEM approach now superior to the conventional equilibrium constant ($\log K$) approach, which do not consider items (i)–(iii) mentioned above. The proliferation of process- or mass transport-specific models based on the third generation GEM-approach is likely to continue as it is still done with the second generation $\log K$ approach. However, our inability to adequately describe the thermodynamic properties of naturally occurring organic materials and surfaces, or the mode of biogeochemical interaction of these complex moieties with trace elements, has not been overcome with the new modeling tools. This is not only a matter of still insufficient thermodynamic database but also of the many kinetic constraints involved in the biogeochemical processes. This gap severely limits our ability to reliably model natural water processes, though progress in this direction is actually being made with the increasing interest in biogeochemical processes.

6 ACKNOWLEDGMENTS

The authors thank Urs Berner, Enzo Curti, Igor K. Karpov, Vasilii A. Sinitsyn, and many other colleagues for stimulating discussions about thermodynamic modeling concepts. Partial financial support from DFG (German National Science Foundation grant Ke508/6) and Nagra (Swiss National Cooperative for the Disposal of Radioactive Waste) is gratefully appreciated.

7 REFERENCES

1. Anderson, G. M. and Crerar, D. A., *Thermodynamics in Geochemistry: The Equilibrium Model*, Oxford University Press, New York, 1993.
2. Nordstrom, D. K. and Munoz, J. L., *Geochemical Thermodynamics*, Blackwell Scientific, Palo Alto, CA, 1994.
3. Morel, F. M. M. and Hering, J. G., *Principles and Applications of Aquatic Chemistry*, Wiley Interscience, New York, 1993.
4. Stumm, W. and Morgan, J. J., *Aquatic Chemistry*, Wiley Interscience, New York, 1996.
5. Langmuir, D., *Aqueous Environmental Geochemistry*, Prentice Hall, 1997.
6. Millero, F. J., *Chemical Oceanography*, CRC Press, Boca Raton, FL, 1996.
7. Bethke, C. M., *Geochemical Reaction Modeling: Concepts and Applications*, Oxford University Press, New York, 1996.
8. Waite, T. D., Mathematical modeling of trace element speciation, in *Trace Element Speciation: Analytical Methods and Problems*, Batley, G. E. (Ed.), CRC Press, Boca Raton, FL, 1989, pp. 117–184.
9. Butler, J. N., *Ionic Equilibrium. Solubility and pH Calculations*, Wiley Interscience, New York, 1998.
10. Appelo, C. A. J. and Postma, D., *Geochemistry, Groundwater and Pollution*, Balkema, Rotterdam, 1993.
11. Schwarzenbach, R. P., Gschwend, P. M. and Imboden, D. M., *Environmental Organic Chemistry*, Wiley, New York, 1993.
12. Nelson, Y. M., Lion, L. W., Ghiorse, W. C. and Shuler, M. L., *Appl. Environ. Microbiol.*, **65**, 175 (1999).
13. Newman, D. K. and Banfield, J. F., *Science*, **296**, 1071 (2002).
14. Kersten, M. and Böttcher, M., *Geowissenschaften*, **15**, 34 (1997).

15. Town, R. M. and Filella, M., *Aquat. Sci.*, **62**, 252 (2000).
16. Brown, G. E. J. and Parks, G. A., *Int. Geol. Rev.*, **43**, 963 (2001).
17. Karpov, I. K., Chudnenko, K. V. and Kulik, D. A., *Am. J. Sci.*, **297**, 767 (1997).
18. Karpov, I. K., Chudnenko, K. V., Kulik, D. A., Avchenko, O. V. and Bychinskii, V. A., *Geochem. Int.*, **39**, 1108 (2001).
19. Shock, E. L., Sassani, D. C., Willis, M. and Sverjensky, D. A., *Geochim. Cosmochim. Acta*, **61**, 907 (1997).
20. Garrels, R. M. and Thompson, M. E., *Am. J. Sci.*, **260**, 57 (1962).
21. Garrels, R. M. and Christ, C. L., *Solutions, Minerals, and Equilibria*, Harper and Row, New York, 1965.
22. Morel, F. and Morgan, J., *Environ. Sci. Technol.*, **6**, 58 (1972).
23. Westall, J. C., Zachary, J. L. and Morel, F. M. M., *MINEQL: A Computer Program for the Calculation of Chemical Equilibrium Composition of Aqueous Systems*, Department of Civil Engineering, Massachusetts Institute of Technology, Cambridge, MA., 1976.
24. Herbelin, A. L. and Westall, J. C., *FITEQL: A Computer Program for Determination of Chemical Equilibrium Constants from Experimental Data*, Department of Chemistry, Oregon State University, Corvallis, OR, 1996.
25. Parkhurst, D. L. and Appelo, C. A. J., *User's Guide to PHREEQC (Version 2) - A Computer Program for Speciation, Batch-Reaction, One-Dimensional Transport, and Inverse Geochemical Calculations*, U.S.G.S. Water-Resources Investigations Report 99–4259, 1999, http://wwwbrr.cr.usgs.gov/projects/GWC_coupled/phreeqc/.
26. Wolery, T. J., Jackson, K. J., Bourcier, W. L., Bruton, C. J., Viani, B. E., Knauss, K. G. and Delany, J. M., Current status of the EQ3/6 software package for geochemical modeling, in *Chemical Modeling in Aqueous Systems II*, Bassett, R. L. and Melchior, D. C. (Eds.), American Chemical Society, Washington, DC, 1990, pp. 104–127.
27. Glynn, P. D. and Reardon, E. J., *Am. J. Sci.*, **290**, 164 (1990).
28. Glynn, P. D., *Comput. Geosci.*, **17**, 907 (1991).
29. Glynn, P., Solid solution solubilities and thermodynamics: sulfates, carbonates and halides, in *Sulfate Minerals: Crystallography, Geochemistry and Environmental Significance*, Reviews in Mineralogy and Geochemistry Vol. 40, Jambor, J. L. and Nordstrom, D. K. (Eds.), Mineralogical Society of America and Geochemical Society, Washington, DC, 2000, pp. 481–511.
30. Karpov, I. K., *Computer-Aided Physico-Chemical Modeling in Geochemistry*, Nauka Publishers, Novosibirsk, 1981, in Russian.
31. Kulik, D. A., Dmytriyeva, S. V., Rysin, A. V., Chudnenko, K. V. and Karpov, I. K., *GEM-Selektor (GEMS): A Research Program Package for Interactive Thermodynamic Modelling of Aquatic (Geo)Chemical Systems*, Waste Management Laboratory, Paul Scherrer Institute, 2003, http://les.web.psi.ch/Software/GEMS-PSI.
32. Kulik, D. A., Kersten, M., Heiser, U. and Neumann, T., *Aquat. Geochem.*, **6**, 147 (2000).
33. Eriksson, G. and Hack, K., *Metall. Trans.*, **b21**, 1013 (1990).
34. Bale, C. W., Chartrand, P., Degterov, S. A., Eriksson, G., Hack, K., Ben Mahfoud, R., Melancon, J., Pelton, A. D. and Petersen, S., *Calphad*, **26**, 189 (2002).
35. Johnson, J. W., Oelkers, E. H. and Helgeson, H. C., *Comput. Geosci.*, **18**, 899 (1992).
36. Hummel, W., Berner, U. R., Curti, E., Pearson, F. J. Jr. and Thoenen, T., *Nagra-PSI Chemical Thermodynamic Database, Version 01/01*, Universal Publishers (upublish.com), New York, 2002.
37. Cox, J. D., Wagman, D. D. and Medvedev, V. A., *CODATA Key Values for Thermodynamics*, Hemisphere Publishers, New York, 1989.
38. Wagman, D. D., Evans, W. H., Parker, V. B., Schumm, R. H., Halow, I., Bailey, S. M., Churney, K. L. and Nuttall, R. L., *J. Phys. Chem. Ref. Data*, **11**, 392 (1982).
39. Reid, R. C., Prausnitz, J. M. and Sherwood, T. K., *The Properties of Gases and Liquids*, McGraw Hill Book Company, New York, 1977.
40. Helgeson, H. C., Delany, J. M., Nesbitt, H. W. and Bird, D. K., *Am. J. Sci.*, **278-A**, 1 (1978).
41. Robie, R. A. and Hemingway, B. S., *US Geol. Survey Bull.*, **2131**, 1 (1995).
42. Helgeson, H. C., Kirkham, D. H. and Flowers, G. C., *Am. J. Sci.*, **281**, 1249 (1981).
43. Shock, E. and Helgeson, H. C., *Geochim. Cosmochim. Acta*, **52**, 2009 (1988).
44. Sverjensky, D. A., Shock, E. L. and Helgeson, H. C., *Geochim. Cosmochim. Acta*, **61**, 1359 (1997).
45. Gu, Y., Gammons, C. H. and Bloom, M. S., *Geochim. Cosmochim. Acta*, **58**, 3545 (1994).
46. Kulik, D. A., Minimizing uncertainty induced by temperature extrapolations of thermodynamic data: a pragmatic view on integration of thermodynamic databases into geochemical computer codes, *The Use of Thermodynamic Databases in Performance Assessment*, NEA OECD, Paris, 2002, pp. 125–137.
47. Puigdomenech, I., Rard, J. A., Plyasunov, A. V. and Grenthe, I., Temperature corrections to thermodynamic data and enthalpy calculations, in *Modelling in Aquatic Chemistry*, Grenthe, I. and Puigdomenech, I. (Eds.), OECD, Paris, 1997, Chapter X, pp. 427–493.
48. Kulik, D. A. and Kersten, M., *Environ. Sci. Technol.*, **36**, 2926 (2002).
49. Tits, J., Wieland, E., Bradbury, M. H., Eckert, P. and Schaible, A. *The Uptake of Eu(III) and Th(VI) by Calcite Under Hyperalkaline Conditions*, PSI Bericht 02–03, Paul Scherrer Institute, Villigen, 2002.
50. Curti, E., Kulik, D. and Tits, J. *Geochim. Cosmochim. Acta*, **69** (2005) in press.

51. Lippmann, F., *Neues Jahrb. Miner. Abh.*, **139**, 1 (1980).
52. Tommaseo, C. and Kersten, M., *Environ. Sci. Technol.*, **36**, 2919 (2002).
53. Kulik, D. A., *Am. J. Sci.*, **302**, 227 (2002).
54. Millero, F. J. and Schreiber, D. R., *Am. J. Sci.*, **282**, 1508 (1982).
55. Pitzer, K. S., Ion interaction approach: theory and data correlation, in *Activity Coefficients in Electrolyte Solutions*, Pitzer, K. S. (Ed.), CRC Press, Boca Raton, FL, 1991, pp. 75–154.
56. Pitzer, K. S., *Thermodynamics*, McGraw-Hill, 1995.
57. Millero, F. J. and Pierrot, D., *Aquat. Geochem.*, **4**, 153 (1998).
58. Millero, F. J., *Geochem. Trans.* **2**, 56 (2001).
59. Byrne, R. H., *Geochem. Trans.*, **3**, 11 (2002).
60. Turner, D. R., Whitfield, M. and Dickson, A. G., *Geochim. Cosmochim. Acta*, **45**, 855 (1981).
61. Turner, D. R. and Whitfield, M., *Geochim. Cosmochim. Acta*, **51**, 3231 (1987).
62. Whitfield, M., *Geochim. Cosmochim. Acta*, **39**, 1545 (1975).
63. Millero, F. J., *Mar. Chem.*, **30**, 205 (1990).
64. Turner, D. J., *Nucl. Energy*, **31**, 327 (1992).
65. Kurepin, V. A., Kulik, D. A., Hiltpold, A. and Nicolet, M., *Thermodynamic Modelling of Fe-Cr-Ni Spinel Formation at the Light-Water Reactor Conditions*, PSI Bericht 02–04, Paul Scherrer Institute, Villigen, 2002.
66. Kulik, D. A. and Kersten, M., *J. Am. Ceram. Soc.*, **84**, 3017 (2001).
67. Königsberger, E., Königsberger, L.-C. and Gamsjäger, H., *Geochim. Cosmochim. Acta*, **63**, 3105 (1999).
68. McIntire, W., *Geochim. Cosmochim. Acta*, **27**, 1209 (1963).
69. Dietzel, M. and Uzdowski, E., *Chem. Geol.*, **131**, 55 (1996).
70. Rimstidt, J. D., Balog, A. and Webb, J., *Geochim. Cosmochim. Acta*, **62**, 1851 (1998).
71. Lippmann, F., *Neues Jahrb. Miner. Abh.*, **130**, 243 (1977).
72. Lippmann, F., *Bull. Miner.*, **105**, 273 (1982).
73. Urusov, V. A., *Theory of Isomorphous Miscibility*, Moscow State University, Moscow, 1977, in Russian.
74. Glynn, P., Modeling solid-solution reactions in low-temperature aqueous systems, in *Chemical Modeling in Aqueous Systems II*, Bassett, R. L. and Melchior, D. C. (Eds.), American Chemical Society, Washington, DC, 1990, pp. 74–86.
75. Glynn, P. D. and Parkhurst, D. L., Modeling non-ideal solid-solution aqueous-solution reactions in mass-transfer computer codes, in *Water-Rock Interaction*, Kharaka, Y. K. and Maest, J. (Eds.), Balkema, Rotterdam, 1992, pp. 175–179.
76. Davis, J. A., Coston, J. A., Kent, D. B. and Fuller, C. C., *Environ. Sci. Technol.*, **32**, 2820 (1998).
77. Davis, J. A. and Kent, D. B., Surface complexation modeling in aqueous geochemistry, in *Mineral-Water Interface Chemistry*, Reviews in Mineralogy Vol. 23, Hochella, M. F. and White, A. F. (Eds.), Mineralogical Society of America, Washington, DC, 1990, pp. 177–260.
78. Banwart, S. A., Aqueous speciation at the interface between geological solids and groundwater, in *Modelling in Aquatic Chemistry*, Grenthe, I. and Puigdomenech, I. (Eds.), NEA OECD, Paris, 1997, pp. 245–287.
79. Kulik, D. A., *Geochim. Cosmochim. Acta*, **64**, 3161 (2000).
80. Kulik, D. A., *Radiochim. Acta*, **90**, 815 (2002).
81. Dzombak, D. A. and Morel, F. M. M., *Surface Complexation Modeling. Hydrous Ferric Oxide*, Wiley Interscience, New York, 1990.
82. Sahai, N. and Sverjensky, D. A., *Geochim. Cosmochim. Acta*, **61**, 2801 (1997).
83. Lützenkirchen, J., Surface complexation models of adsorption: a critical survey in the context of experimental data, in *Adsorption: Theory, Modeling, And Analysis*, Toth, J. (Ed.), Marcel Dekker, New York, 2002, pp. 631–710.
84. Becker, U., Rosso, K. and Hochella, M. F., Jr. *Geochim. Cosmochim. Acta*, **65**, 2641 (2001).
85. Honeyman, B. D. and Santschi, P. H., *Environ. Sci. Technol.*, **22**, 862 (1988).
86. Lützenkirchen, J., Surface complexation models of adsorption, *Encyclopedia of Surface and Colloid Science*, Hubbard, A. (Ed.), Marcel Dekker, New York, 2002, pp. 5028–5046.
87. Morel, F. M. M., Yeasted, J. G. and Westall, J. C., Adsorption models: a mathematical analysis in the framework of general equilibrium calculations, in *Adsorption of Inorganics at Solid-Liquid Interfaces*, Anderson, M. A. and Rubin, A. J. (Eds.), Ann Arbor Science, Ann Arbor, MI, 1981, pp. 263–294.
88. Zachara, J. M. and Westall, J. C., Chemical modeling of ion adsorption in soils, in *Soil Physical Chemistry*, 2nd ed., Sparks, D. L. (Ed.), CRC Press, Boca Raton, FL, 1999, pp. 47–95.
89. Adamson, A. W., *Physical Chemistry of Surfaces*, John Wiley & Sons, New York, 1990.
90. Kulik, D. A., Aja, S. U., Sinitsyn, V. A. and Wood, S. A., *Geochim. Cosmochim. Acta*, **64**, 195 (2000).
91. Fendorf, S. E., Lamble, G. M., Stepleton, M. G., Kelley, M. J. and Sparks, D. L., *Environ. Sci. Technol.*, **28**, 284 (1994).
92. Sergeeva, E. I., Devina, O. A. and Khodakovsky, I. L., *J. Alloys Compd.*, **213/214**, 125 (1994).
93. Shock, E. L., Sassani, D. C. and Betz, H., *Geochim. Cosmochim. Acta*, **61**, 4245 (1997).
94. Sergeeva, E. I., Nikitin, A. A., Khodakovskiy, I. L. and Naumov, G. B., *Geochem. Int.*, **4**, 900 (1972).
95. Schoonen, M. A. A., *Geochim. Cosmochim. Acta*, **58**, 2845 (1994).
96. Banwart, S., *Geochim. Cosmochim. Acta*, **63**, 2919 (1999).

97. Christensen, T. H., Bjerg, P. L., Banwart, S. A., Jakobsen, R., Heron, G. and Albrechtsen, H., *J. Contam. Hydrol.*, **45**, 165 (2000).
98. Davison, W., Philips, N. and Tabner, B. J., *Aquat. Sci.*, **61**, 23 (1999).
99. Lichtner, P. C., The quasi-stationary state approximation to fluid/rock reaction: local equilibrium revisited, in *Advances in Physical Geochemistry*, Ganguly, J (Ed.), Springer-Verlag, Berlin, 1991, pp. 454–562.
100. Boudreau, B. P., *Diagenetic Models and their Implementation: Modelling Transport and Reactions in Aquatic Sediments*, Springer-Verlag, Berlin, 1997.
101. Imboden, D. M. and Schwarzenbach, R. P., Spatial and temporal distribution of chemical substances in lakes: modeling concepts, in *Chemical Processes in Lakes*, Stumm, W. and Farrington, J. W. (Eds.), Wiley-Interscience, New York, 1985, pp. 1–30.
102. Johnson, C. A., Ulrich, H., Sigg, L. and Imboden, D. M., *Limnol. Oceanogr.*, **36**, 1415 (1991).
103. Lichtner, P. C., *Geochim. Cosmochim. Acta*, **49**, 779 (1985).
104. Lichtner, P. C., *Geochim. Cosmochim. Acta*, **52**, 143 (1988).
105. Gwo, J. P., D'Azevedo, E. F., Frenzel, H., Mayes, M., Yeh, G.-T., Jardine, P. M., Salvage, K. M. and Hoffman, F. M., *Comput. Geosci.*, **27**, 1231 (2001).
106. Pfingsten, W., *Nucl. Technol.*, **116**, 208 (1996).
107. Adler, M. A., Hensen, C., Kasten, S. and Schulz, H., *Int. J. Earth Sci.*, **88**, 641 (2000).

3.2 Modeling in Nutrition. The Metabolism of Selenium, Copper, Zinc and Calcium Using Stable Isotopes in Humans

Jack R. Dainty and Tom E. Fox
Institute of Food Research, Norwich, UK

1 INTRODUCTION TO STABLE ISOTOPES AND MODELING

Selenium, copper, zinc and calcium all have several naturally occurring stable isotopes. By artificially enriching one of their low abundance isotopes, they can be 'traced' in biological samples after oral ingestion and/or intravenous (IV) infusion. Although stable isotopes were the first tracers to be used in nutritional science [1],

Handbook of Elemental Speciation II: Species in the Environment, Food, Medicine & Occupational Health
Edited by R. Cornelis, H. Crews, J. Caruso and K. G. Heumann
 ISBN: 0-470-85598-3 (HB)

radioisotopes quickly became the standard amongst researchers after the Second World War. It was not until the 1960s that the first studies using calcium [2] were performed, and the late 1970s saw the first undertaking of zinc and copper stable isotope studies [3]. A combination of advances in mass spectrometry and concern about exposure to ionizing radiation led to a growing number of nutritional researchers switching to stable isotope tracers. Several reviews and guides have been written subsequently [4–8]. The stable isotopes used in nutrition studies are normally incorporated in food either intrinsically [9–11] or extrinsically [12–15]. An intrinsic label is one in which the stable isotope is incorporated biosynthetically into a plant or animal, whereas an extrinsic label is simply added to the food prior to ingestion. Comparative absorption data for intrinsically and extrinsically labeled foodstuffs is limited. However, the use of extrinsic labels in stable isotope absorption studies for nonheme Fe [16], Zn [17], Ca [18], Mg [19] and Cu [14] has been validated for a small range of foods in some studies, whereas other studies have reported differences in absorption between intrinsic and extrinsic labels, for example, zinc [9, 20]. Ideally, all studies should be performed with intrinsic labels, especially where different forms of a mineral exist within a food (e.g. organic vs inorganic selenium, heme vs nonheme iron). The cost of such studies is, however, often prohibitive so extrinsic labels are far more widely used.

Recent advances in mass spectrometry have been accompanied by a massive increase in computing power and software development. This has allowed complicated mathematical equations to be solved quickly. The use of mathematical modeling in nutrition has been advanced since the 1980s in conferences and workshops [21–26]. The vast majority of the work published from those meetings was concerned with compartmental modeling. This type of modeling is especially suited to mineral metabolism because the kinetics of such systems can be approximated by a small number of distinct compartments connected together to form a deterministic process. Important nutritional information can be provided in a well-designed kinetic study that uses stable isotope labels in conjunction with compartmental modeling.

Before describing why models might be useful in nutrition, some definitions must be given to clarify the terminology. A compartment is a theoretical construct that may well combine material from several different physical spaces. It is defined as an amount of material that acts as though it is well mixed and kinetically homogeneous and a compartmental model consists of a finite number of compartments with specified interconnections between them. The interconnections are a representation of the flux of material that is transported from one location to another. By defining a compartmental model in this way, the researcher can reduce a complex metabolic system into a small number of pathways and compartments. The outputs from such a model include the quantity of mineral stored in certain body pools, the rate and extent to which the mineral moves from one pool to another and how long it will remain in the body before being excreted. This can inform the approach of the nutritionist about status, daily requirements and mineral retention and only by doing modeling can this sort of information be obtained from humans in a noninvasive way. Consider the two-compartment model shown in Figure 3.2.1.

The circles represent compartments and the arrows are pathways that show the direction of transfer of material. Associated with each pathway is a rate constant that is conventionally written as k(i, j), which denotes transfer of material from compartment ‘j’ to compartment ‘i’ per unit time. The type of compartment models that are usually

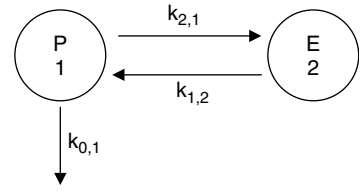

Figure 3.2.1. Example of a two-compartment model. Circles represent compartments, arrows the direction of transfer of material between compartments. Associated with each arrow is a rate constant in the form k(i, j) where transfer is from j to i.

found in nutrition is described by constant coefficient, ordinary, first-order differential equations. The basis of these equations are that the rate constants do not alter over the course of the experiment and by applying The Conservation Of Mass to the system under study one can solve the resultant series of equations. If we denote the mass of material in compartment 1 as P (for plasma) and that in compartment 2 as E (the 'rest' of the body), the system can be described as

$$\frac{dP}{dt} = k_{1,2}\cdot E - (k_{2,1} + k_{0,1})\cdot P$$

$$\frac{dE}{dt} = k_{2,1}\cdot P - k_{1,2}\cdot E$$

To solve these equations, we need to sample one of the two compartments so that the parameters ($k_{0,1}$, $k_{1,2}$ and $k_{2,1}$) can be fitted to the resultant data. It is often the case that the only compartment we can sample is the plasma. This limits the number of 'other' compartments we can use in our model because we will not be able to uniquely identify the parameters that make up the resultant equations. This is called *a priori* identifiability and is used to identify, given noise-free data, the number of compartments a model may have in order that all its parameters will have a single solution. Investigators often have an in-depth knowledge of the metabolism of a particular mineral and want to include many compartments to reflect this. Any model that is not *a priori* identifiable must be carefully evaluated and the results from it used cautiously. The fitted parameters from a model should always be quoted with their calculated precision so that an assessment of the quality of the model can be made. This is called *a posteriori* identifiability and plays an important part in drawing nutritional conclusions from the modeling of real data. The *a posteriori* identifiability is dependent on good quality data and the correct choice of model structure for the system under investigation. Our two-compartment model is *a priori* identifiable. If the data from the plasma samples are of sufficient quality and they support a two-compartment rather than, say, a one- or three-compartment structure, then the model should be *a posteriori* identifiable. A compartment model is, therefore, constrained by the type of data collected, the location it is collected from and the statistical considerations involved in fitting experimental data to models.

A comprehensive literature exists on compartmental modeling [27–35] and it is well grounded theoretically. Dedicated software tools such as SAAMII [36] allow nonmathematicians to set up compartmental models without the need to define the differential equations that underpin them.

This chapter focuses on the metabolism of copper, calcium, zinc and selenium and cites specific examples from the literature where modeling with stable isotopes has been carried out in human volunteers. Selenium is covered in more detail than the other three elements because its speciation in food has important metabolic consequences *in vivo*.

2 SELENIUM

2.1 Introduction

Selenium was first identified in 1817 by a Swedish chemist, Berzelius, who named it after the Greek moon goddess, Selene. It is a metalloid element classified in group 16 of the periodic table and shares similar chemical properties with sulfur and tellurium. There are six naturally occurring stable isotopes of selenium, Se-74, Se-76, Se-77, Se-78, Se-80, Se-82. Like sulfur, selenium reacts with metals and gains electrons to form ionic compounds that contain the selenide ion Se^{2-}. It will also form covalent compounds with most other substances. The inorganic forms exist naturally in several oxidation states, -2 (e.g. sodium selenide), 0 (elemental selenium) $+4$ (e.g. sodium selenite) and $+6$ (e.g. sodium selenate). It will form many inorganic compounds similar to sulfur, the important ones being the selenides, halides, oxides and oxy acids. Sodium selenite is a white crystalline substance with a molecular mass of 173.19, soluble in cold water but insoluble in alcohol. Sodium selenate is rhombic, colorless with a molecular mass of 189.19, less soluble in cold water (0.84 g mL^{-1}).

The organic compounds of selenium are similar but not identical to organosulfur compounds, and many different compounds exist. Of particular interest to nutrition are the selenoamino acids, selenium-containing peptides and selenium derivatives of nucleic acids. These compounds occur naturally in cells and tissue with selenomethionine and selenocysteine being incorporated into protein synthesis, including enzymes. Selenoamino acids result from the displacement of the sulfur atom by selenium in the corresponding amino acids. The metabolism of these selenium-containing compounds parallels sulfur metabolism as long as selenium is bound to carbon in an amino acid form with some important differences. The higher redox potentials of selenium compounds, compared with their sulfur analogues, cause selenium metabolism to be inclined toward reduction, whereas sulfur metabolism is generally oxidative [37, 38]. Selenocysteine has a higher acidity compared to cysteine (due to the difference in acid strength between the hydrides of the elements with H_2Se having a pK_a of 3.8 compared with H_2S with a pK_a of 8.25). This accounts for thiols like cysteine being protonated at physiological pH while the selenohydryl groups of selenoamino acids are largely dissociated [39]. The insertion of selenium into selenium-dependent enzymes is under the control of a specific UGA codon for selenocysteinyl RNA, making selenocysteine the 21st amino acid in terms of ribosome-mediated protein synthesis [40, 41].

2.2 Selenium in foods

The primary source of selenium in the food chain is soil, which has an uneven distribution of selenium worldwide, ranging from less than 0.1 $\mu g\,g^{-1}$ in some areas to more than 1 $mg\,g^{-1}$ in others. Apart from extremely selenium deficient or seleniferous areas, most soils will contain between 1.0 and 1.5 $\mu g\,g^{-1}$ [42]. Areas of highly siliceous rocks will produce soils low in selenium whilst areas that contain a high concentration of organic matter, peat, coal and shale will have soil with high levels of the element. The chemical form in soils is an important determinant of the availability of selenium to plants and hence the concentration found in the food chain. Selenites are the most important source available to plants and account for most of the selenium taken up by plants, though its solubility and hence its availability is affected by factors such as soil pH, redox potential and the presence of iron. Highly alkaline soils in low rainfall areas in which selenates accumulate can produce toxic levels in accumulator plants because of the readily available chemical form. Though not required for growth by higher plants [43], selenium accumulation in plants generally reflects the level of selenium in the soil and is directly responsible for the level of selenium that enters the food chain.

The wide variation in soil selenium content from one region to another means that the selenium concentration found within a single food type is very variable. Morris & Levander [44] reported wide fluctuations in the selenium content of different foods; cereals ranged from 0.105 to 0.676 $\mu g\,g^{-1}$, meat and sea foods from 0.106 to 0.681 $\mu g\,g^{-1}$ and fruit and vegetables from 0.002 to 0.023 $\mu g\,g^{-1}$. The problem of estimating selenium intake from the diet is further exacerbated by the fact that an important source of selenium is cereals, with wide variability between (and within) countries.

The predominant forms of selenium in food are organically bound, primarily selenomethionine [45], and other selenoamino acids and their methyl derivatives. A minor quantity of inorganic selenium is found in drinking water, the level depending on the selenium concentration of the soil and the soil type through which the water has passed. Larger intakes of inorganic selenium only occur when selenium supplements of selenate or selenite are taken.

Although several different selenium-containing proteins occur in higher animals, it is only the selenocysteine-containing proteins that are physiologically regulated, encoded by a UGA codon in mRNA [46]. These selenoproteins are strictly selenium dependent, and when dietary intake of the element is restricted, synthesis of the selenoproteins is reduced. Animals are able to synthesize selenocysteine [47]. The biological functions of selenium are mediated through at least 13

selenoproteins that contain selenium as selenocysteine [46, 48]. Selenomethionine-containing proteins are the principal dietary sources and are incorporated nonspecifically into proteins, there being no metabolic distinction between the sulfur and selenium amino acid analogues [37]. However, as yet, there are no known selenomethionine-containing proteins that have selenium-specific functions.

2.3 Absorption

There appears to be no homeostatic control of absorption of selenium from foods [49–52] and under normal feeding conditions absorption is not a limiting factor to bioavailability. The efficiency of absorption of the seleno amino acids and selenate is high and is remarkably consistent with very little variability within or between individuals reflecting the absence of homeostatic mechanisms controlling selenium absorption [51–53]. Selenite is more variable and affected by the food matrix with which it is consumed [13, 53–56]. Selenite is absorbed passively across the brush border and competes with inorganic sulfur compounds [57] having an apparent absorption, ranging from 30 to 60% [53, 58, 59]. Selenate absorption is assisted by a sodium pump [60], which explains the high absorption characteristics observed with a fractional absorption of over 90%, similar to selenomethionine [53, 61, 62]. Selenomethionine absorption is an active process that uses the same enzyme system as methionine in competition with its seleno analogue [60, 63]. Similarly, selenocysteine competes with cysteine for an active transport system [64], whilst it is thought that other selenoamino acids are absorbed passively. Thus, selenium does not form a common pool within the gut but several distinct pools with different absorption characteristics.

2.4 Metabolism of absorbed selenium

The systemic metabolism of absorbed selenium depends on the chemical form consumed. Selenomethionine is largely taken up by the liver [62], where it is used for general protein synthesis, there being no metabolic distinction between the sulfur and amino analogues [37]. Another group [65] found 50% of absorbed selenium associated with albumin from a diet in which selenomethionine was the main form of selenium. There is evidence that extensive recycling of selenium derived from absorbed selenomethionine occurs in which selenium is reutilized for protein synthesis after the catabolism of protein in which it was first incorporated [66–68]. Consequently, retention of selenomethionine has been observed to be more than twice the length of selenite [62, 67]. Selenomethionine can be converted to selenocysteine via the methionine transamination and trans-sulfuration enzymatic pathway, provided that adequate methionine is available [69–71], but the selenocysteine that is produced in this way cannot be used directly for selenoprotein synthesis but must first be changed into other forms of the element [72].

Although selenocysteine can be nonspecifically incorporated into general protein synthesis (but not into the active metabolic sites of selenoproteins) [46], it does not accumulate and the selenium released by selenocysteine β lyase [73] undergoes reduction similar to the inorganic sources of selenium to selenides, specifically hydrogen selenide. This means that whilst selenocysteine is a more available source of selenium for selenoprotein synthesis, it is less well retained in tissues compared with selenomethionine sources [74].

Only a minor fraction of absorbed selenite is removed from the hepatic portal circulation by the liver, and a larger fraction is excreted in the urine [75]. Selenite has been reported to undergo reduction in the erythrocytes to selenide, a form that is immediately available for selenocysteine synthesis [76]. Another group [77] reported that the main plasma carrier for selenite was albumin during the first four hours, with the majority incorporated into selenoprotein P by the liver after eight hours. It has been proposed that four different plasma pools exist from observations in an experiment in which six volunteers took oral doses of labeled selenite [75]. The appearance of selenium from absorbed selenite in a selenoprotein

after seven to eight hours is supported by a number of different workers [61, 75, 78]. Selenite is readily available for selenoprotein synthesis, whereas selenomethionine is available only after catabolism of the protein into which it was incorporated. There are differences between the metabolism of selenite and selenate in that the urinary clearance of absorbed selenate is much faster than selenite even when an allowance is made for the lower efficiency of absorption exhibited by selenite [50, 79, 80]. Inorganic selenium cannot be stored but is used directly in the liver for selenoprotein synthesis [76].

2.5 Speciation of selenium found in foods

2.5.1 Yeasts and selenium-enriched yeasts

Selenium-enriched yeasts are usually prepared by growing brewer's yeast (*Saccharomyces cerevisiae*) in a selenium-enriched nutrient medium. To increase the uptake and incorporation of selenium into the yeast cells, sulfur is limited in the nutrient medium composition, which encourages the formation of seleno analogues of organic compounds of amino acids [81]. The yeast is usually prepared by isolation, washing, freeze-drying and made into a tablet form. The chemical composition of selenium-enriched yeast preparations depends on the conditions of growth, nutrient medium, and chemical form of selenium used. They contain different amounts of a variety of different selenium compounds, including selenoamino acids, selenoproteins, selenosulfides and inorganic forms, particularly the form used in the nutrient medium. It was reported [82] that the major organic selenium species in a Finnish yeast was selenomethionine, which accounted for 50% of the total selenium in the preparation. Inorganic selenium made up 2% (as sodium selenite), with the remainder comprised of selenoglutathione, selenodiglutathione, selenocysteine and other unidentified selenocompounds. In contrast, the selenium yeast manufactured in the United States and used in studies in New Zealand [83] contains the major fraction (85%) as selenomethionine. Another group [84] also confirmed that the major form of selenium in yeast is selenomethionine or Se-methylselenomethionine. These differences are probably due to variations in the chemical form of selenium used in preparation as well as the method of yeast culturing and subsequent treatment. Other workers have reported more than 20 selenium compounds, including selenomethionine, methylselenocysteine and inorganic forms found in selenium-enriched yeasts [85]. An investigation by another group [86] into the chemical forms of selenium present in nine selenium supplements labeled as containing yeast, commercially available in Europe, found that selenomethionine was the major component with selenocysteine and other unknown selenocompounds in smaller amounts. Four of the supplements claiming to contain selenium-enriched yeast had only inorganic selenium compounds present, highlighting the need for care when culturing yeast for organic sources of selenium.

2.5.2 Garlic

Investigations into the selenium species present in garlic and yeast have been undertaken [84]. They found no major differences in the compounds of selenium analyzed by high performance liquid chromatography with inductively coupled plasma mass spectrometry using two different extraction methods (water and enzyme extracts). The major form of selenium in garlic was reported to be γ-glutamyl-*S*-methylselenocysteine, which they suggest serves as a carrier for Se-methylselenocysteine and is the major storage form in garlic samples that contain 300 $\mu g\, g^{-1}$ selenium or more. Earlier reports have confirmed the major form of selenium present in garlic that contained 1355 μg selenium per gram of tissue to be Se-methylselenocysteine [85, 87].

2.5.3 Fish

Studies suggest that the majority of selenium in fish is in the organic form selenomethionine [88, 89]. Fish may contain significant proportions of

other organic forms of selenium such as selenocystathionine, selenocysteine, metabolic intermediates (e.g. selenodiglutathione, selenodimethylselenide and selenotrimethylselenonium ion), selenoproteins and other organic forms such as 6-selenopurine and selenoprolyl-tRNA, as well as other organic compounds not yet characterized. A recent publication [89] could not detect the presence of selenocysteine in tuna muscle and accounted for 30% of the total selenium present as trimethylselenonium ion, selenomethionine and another selenoamino acid not identified. Hexavalent, water-soluble forms of selenium have been isolated from tuna fish [90], and another group [91] found that different selenium compounds were dominant in different species of fish. It is probable that different proportions of selenoorganic compounds do exist in different foods of animal origin between different species, as observed in plants, however, there is a paucity of data on the speciation of selenium in foods in general and there is still much work to be done.

2.5.4 Urine

The trimethylselenonium ion and dimethyl selenide are thought to be detoxified forms of metabolites of selenium that are excreted by the body either expired in air or present in urine [92, 93]. Speciation of selenium forms in urine has been carried out using high performance liquid chromatography with inductively coupled plasma mass spectrometry [94].

2.6 Evidence for the existence of different forms in foods

In a recent study [95] that investigated the absorption of selenium from biosynthetically labeled foods and selenite, the plasma appearance of absorbed label from cod, garlic, wheat and selenite were observed to have different characteristics. Although the time intervals used to assess plasma appearance were not comprehensive (plasma samples were taken at 8, 24 and 48 h after the test meal), the study was able to demonstrate different plasma appearance characteristics between cod, selenite, wheat and garlic. Selenium absorbed from cod had a much slower peak plasma appearance than from wheat or garlic, whereas wheat had a faster plasma clearance and earlier plasma peak compared with garlic selenium. The difference in the quantity of absorbed fraction appearing in the blood and the time difference in plasma peak appearance suggests that the forms of selenium present in garlic differ from those present in wheat as confirmed by another group [84].

2.7 Compartmental modeling of selenium in nutritional studies

Stable isotopes of selenium have been used in pharmacokinetic studies to measure the size and turnover of body selenium pools for the assessment of selenium status. The initial work [96] developed the concept of the selenite exchangeable metabolic pool for the assessment of selenium status in rats and then applied it to humans using Chinese subjects with varying selenium status [97]. The method depends on the dilution of a single intravenous dose of isotopically enriched selenite solution in the selenite exchangeable metabolic pool. This approach was first attempted using isotope dilution principles with radiolabeled selenium as the tracer [49]. It has been shown that when selenite is used as the tracer, the method measures an asymptotically increasing exchangeable pool with a magnitude approaching 10 mg at infinite time for North Americans [96]. The model is based on some known aspects of mammalian selenium metabolism and assumes that there are two distinct pools of selenium present in the body. One consists of selenium that is available for the synthesis of selenoproteins and that will also contain intermediate selenocompounds as well as end products such as GSHPx. It is this pool that exchanges with the selenite tracer and has been termed the selenite exchangeable metabolic pool (Se-EMP). The second pool consists mainly of selenomethionine-containing proteins in which selenomethionine has been incorporated into the amino acid sequence in

place of its amino acid analogue. The selenium present in this second pool cannot contribute to selenoprotein synthesis until degradation of the proteins has taken place. The turnover for selenium in this pool is very long and depends not only on the degradation of the protein but also its participation in the transamination and trans-sulfuration pathway to yield selenocysteine or breakdown of the amino acid and subsequent release of selenium. It is thought that the first pool does not contribute towards the second pool. Both pools are present in the plasma compartment.

Another study [75] fed 200 μg of enriched ^{74}Se as selenite and collected blood, urine and feces for 12 days thereafter. They developed a complicated model that included four plasma pools, a liver/pancreas pool and a tissue pool (Figure 3.2.2).

Multiple plasma pools were thought necessary since more than one peak was seen in volunteers' plasma and urine data. The model has 18 rate constants and is *a priori* unidentifiable. No information is given as to the uncertainty of the rate constants so it is not possible to speculate as to whether it is *a posteriori* identifiable. However, some interesting findings emerge from the model. The mean residence times (the average amount of time a molecule spends in a pool or system before irreversibly leaving) in the four plasma pools are 0.02, 0.18, 0.74 and 9.6 days (P1–P4). The authors speculate that the first plasma pool (P1) could either be newly absorbed selenium that has not been removed by the liver in the first-pass or a rapidly turning over pool in the liver. It is suggested that the second pool (P2) may be material absorbed from the enterocyte into the lymphatic system and transported in chylomicrons or very low density lipoproteins (VLDL). The kinetics of the third pool (P3) indicates that the selenium found here is probably contained in glutathione peroxidase and/or selenoprotein P. The selenium in the fourth compartment (P4) comes from the

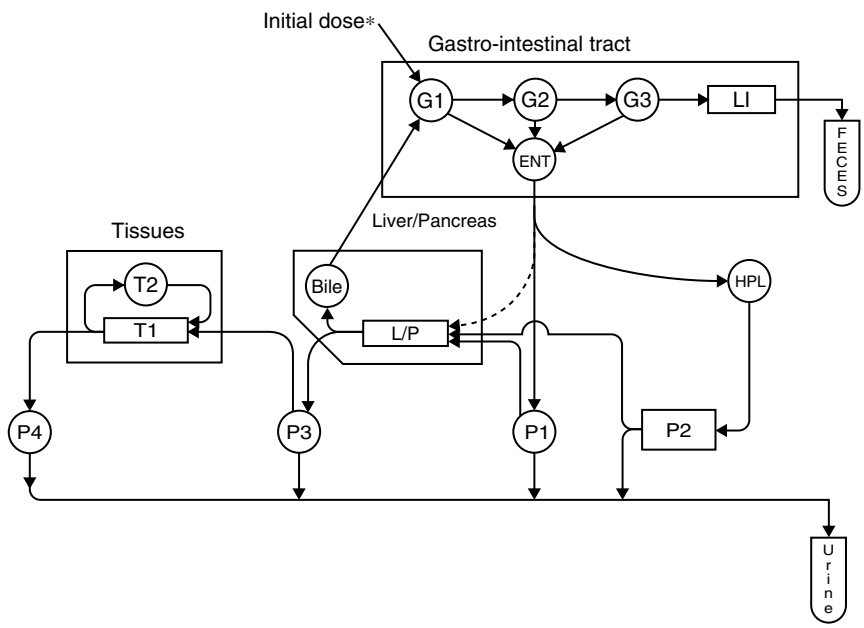

Figure 3.2.2. Model for selenite metabolism [75]. The arrow with an asterisk indicates the site of oral tracer administration. Arrows between compartments represent movement of selenium. Compartments drawn as rectangles represent delays. G1, G2, G3 are three gut compartments; ENT represents enterocytes; HPL is a compartment in the hepatopancreatic subsystem or lymphatic system; L/P is the liver and pancreas; LI, large intestine; T1, T2, peripheral tissues, largely skeletal muscle. P1–P4 are four kinetically distinct plasma compartments. (Reproduced from Reference [75] by permission of The American Physiological Society.)

large tissue pools. The mean residence time of the liver–pancreas subsystem was 20 days and that of the tissues was 221 days. The development of this model is examined in a paper [76] given as part of a symposium entitled The Application of Models to Determination of Nutrient Requirements.

A further study [77] gave an oral dose (100 μg) of labeled selenite (^{74}Se, 98.2% enriched) to three groups of women. All the volunteers lived in the same area and were divided into free-living elderly (aged 64–82 years), institutionalized elderly (aged 68–82 years) and a comparison group of young women aged 31–40 years. The aim of the study was to investigate whether age and/or lifestyle influenced selenium exchangeable pool size. Blood samples were taken periodically for six months and a two-compartment model was found to fit the resulting data. Compartment 1 had a mean pool size that ranged from 619 μg for the institutionalized elderly to 835 μg for the young adult. This first pool is approximately three times larger than the plasma pool (native selenium plasma concentration multiplied by plasma volume) and has a half-life in the region of one day. Compartment 2 had a mean pool size range of 1767 μg for the institutionalized elderly and 2473 μg for the young adult. The average half-life is approximately 30 days. Compartment 1 had similar kinetics to the third plasma pool identified in another paper [75]. As blood samples were only taken from one-hour post-dose, no pools could be identified that turn over in less than two hours. The second compartment had a much shorter turnover time than the tissue compartment identified in a different report [75]. The authors suggest that this compartment may represent label, with a slow turnover, released from the peripheral tissues. They conclude that aging has no effect on selenium status.

A selenomethionine (SeMet) model was published in 1991 [62] and was based on six adults consuming a 200 μg oral dose of ^{74}Se as L-selenomethionine. It was developed from the earlier selenite model [75] but contained some differences. A second tissue pool was connected between the third and fourth plasma pools. A pathway to the liver/pancreas system from the fourth plasma pool was also required and the first pass effect was much greater in comparison with the selenite model. The turnover times of both models are given in Table 3.2.1.

Table 3.2.1. Comparison of turnover times for models of selenite [75] and selenomethionine [62]. All values are in days.

	Selenite	SeMet
Plasma	2.0 ± 0.1	0.6 ± 0.1
Liver and pancreas	20 ± 5	2.4 ± 0.3
Tissues	221 ± 33	73 ± 3
Whole-body	147 ± 13	363 ± 21

Reference to Table 3.2.1 shows that organic selenium is metabolized quite differently from inorganic selenium. A major difference is that whole-body turnover is much slower with the SeMet form of selenium. This is attributed to reutilization of the organic form via the pathway from the fourth plasma pool to the liver-pancreas subsystem. This pathway does not exist in selenite metabolism and, consequently, the whole-body turnover time is faster. This is in contrast to the major storage areas of the body, where we find that the turnover of SeMet is much faster than that of selenite. In a paper that compared the two models [98], it was concluded that the ability to redistribute selenium is beneficial if the body's requirements change suddenly. They also comment, however, that at high dietary intakes, reutilization of SeMet could result in excessive tissue accumulation and toxicity.

2.8 Future work

The extent to which these models may be related to the real world has been limited because of a lack of studies incorporating intrinsic labels in the test meals. Even when intrinsic labels have been used, no speciation work has been carried out to determine what proportions of the different forms of selenium are present in the food.

The use of selenium exchangeable pool size, as a measure of status, merits further investigation through an intervention study. This would help determine whether changes in dietary intake were proportionately reflected in changes in the rapidly exchangeable pools.

3 COPPER

3.1 Introduction

Copper is essential for humans and is involved in many enzyme systems in the body [99]. The most abundant copper-containing enzyme is cytosolic superoxide dismutase that is concerned with disposal of superoxide anions. Adult humans contain about 110 mg of copper, and the highest concentrations are found in the kidney (12 $\mu g\,g^{-1}$) and nails (20 $\mu g\,g^{-1}$). In terms of mass, most copper is in the skeleton (46%), muscles (26%) and liver (10%) but it is found in all cells and tissues. It is a difficult element to study because it only has two stable isotopes (^{63}Cu (69.2%) and ^{65}Cu (30.8%)), which means that oral and intravenous (IV) labels cannot be given simultaneously. Endogenous losses play a significant role in copper metabolism [100] and are usually quantified by IV dose in conjunction with fecal monitoring [101]. Copper exists in two distinct forms in the plasma; the non-ceruloplasmin or albumin-bound fraction is the form in which the copper appears in the plasma following a meal [102]. Most of this is rapidly converted to the CP (ceruloplasmin) form in the liver. This creates a problem in modeling copper metabolism because it is difficult to separate and accurately measure the quantity of copper in the two forms [103]. The average UK diet contains approximately 1.5 mg of copper per day, but the last COMA report on Dietary Reference Values [104] stated that there were no adequate data on human copper requirements and they were unable to derive estimated average requirements (EARs) or lower reference nutrient intakes (LRNIs) with sufficient confidence.

3.2 Copper in foods

Good sources of copper include nuts (14.0 $\mu g\,g^{-1}$), condiments/spices (6.8 $\mu g\,g^{-1}$), brown rice (4.1 $\mu g\,g^{-1}$), eggs (4.1 $\mu g\,g^{-1}$) and meat (3.9 $\mu g\,g^{-1}$). Legumes, liver and shellfish are also good sources and the avocado has the highest concentration amongst fruits. It is least abundant in milk, dairy products and non-whole grain cereals [105]. As with many minerals, food concentrations are known to be affected by the soil copper levels where crops are grown or animals reared and the use of fertilizers or pesticides [106]. In addition, food processing such as milling or canning procedures may affect levels [99].

3.3 Absorption

Copper absorption from a mixed diet is in the range 30–60% and depends on the status of the individual. It is known to decrease with age, malnutrition [107] and in various disease states with malabsorption syndromes, for example, celiac disease [108], whilst a range of dietary factors have an adverse effect on absorption, for example, infant cow's milk formulas [109], zinc [110, 111], and antacids. In a recent EU study [112], a comparison was made between the absorption of intrinsic and extrinsic labels of copper in sunflower seeds. There was a significant difference ($P = 0.01$) between the absorption of the intrinsic copper label (37%) compared with the extrinsic (19%).

3.4 Metabolism of absorbed copper

Once the dietary copper is across the gut wall, it is transported on albumin to the liver where it is incorporated either into ceruloplasmin and specific liver proteins/enzymes or excreted via the bile. As much as 20% of the absorbed copper is excreted in this way within two weeks. This is under homeostatic control and is the body's main means of maintaining adequate supplies for normal cell function whilst avoiding a toxic buildup. Urinary excretion is very small and does not appear to change with different dietary intakes. Once the dietary copper has been packaged onto the ceruloplasmin, it can be released from the liver back into the plasma and then removed by cells for normal functions.

3.5 Compartmental modeling of copper in nutritional studies

Few papers have been published that attempt to model human copper metabolism using stable

isotopes, although work has been done using animal models [113, 114]. These were used as the basis for the human model [115] in which five young men took part in a 90-day intervention trial. The study was divided into three metabolic periods: adequate copper (1.68 mg day^{-1} for 24 days), low copper (0.785 mg day^{-1} for 42 days) and high copper (7.53 mg day^{-1} for 24 days), with the copper (as a $CuSO_4$ solution) added to the diet as an extrinsic label during all three metabolic periods. A solution that contained 392 μg of ^{65}Cu was infused on days 7, 49 and 73 of the study and an oral dose ingested on days 13 (1600 μg), 31/32 (1020 μg), 55/56 (1020 μg) and 79 (7660 μg). The model consists of five compartments, two delays and two excretion routes (Figure 3.2.3).

Only data from plasma samples were used to fit the rate constants in the compartment model. Although two plasma compartments were specified, no attempt was made to quantify the separate copper-containing plasma fractions. The model predicted that the half-life of copper in the compartment identified with the non-CP form was approximately 40 min. This value is higher than that found in the only other two studies that have attempted to measure the half-life of non-CP bound copper in humans. A research group [103] has reported lower half-lives (8.7 and 12.3 min) in two volunteers after IV infusion with a ^{65}Cu label. These values agreed with an earlier report [116] that found 8.5 and 10 min for the half-life of ^{64}Cu in two subjects after intravenous injection.

Although the Scott & Turnlund model [115] did not include urinary data in their model, this should not influence the accuracy since it is well known [117] that urinary excretion makes up a very small percentage of the total endogenous excretion and is relatively constant. The lack of any fecal data is a drawback. It is thought that as much as 4.5 mg day^{-1} of endogenous copper may be secreted into the GI (gastrointestinal) tract [102]. Since the average dietary intake is approximately 1 mg day^{-1}, it is evident that most of the secreted copper is reabsorbed to maintain overall balance. The Scott & Turnlund model [115] incorporates a biliary excretion path that predicts that about 0.15 mg day^{-1} will be excreted with moderate copper intake (1.68 mg day^{-1}) and another study [101] found a similar experimental value.

The route of administration was found to influence some of the rate constants. This is a clear indication that the body handles oral and IV copper differently and calls into question the use of IV tracers to quantify reexcretion of dietary copper.

There is only one other stable isotope paper that contains a compartmental model of human copper metabolism [118]. This model contains 10 compartments and 16 rate constants. The model

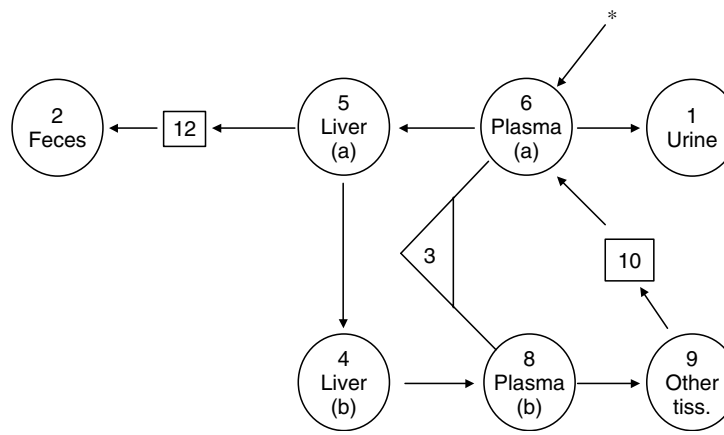

Figure 3.2.3. Compartmental model of copper metabolism in adult men [115]. Circles represent compartments, rectangles are delays, the triangle is the sum of the indicated compartments, * is the site of ^{65}Cu input. Plasma samples were taken from compartment 3. (Reprinted from *J. Nutr. Biochem.*, **5**, Scott, K. C. and Turnlund, J. R., Compartmental model of copper metabolism in adult men, 342, Copyright (1994), with permission from Elsevier.)

is used to simulate how different dietary levels of copper might influence endogenous excretion and, ultimately, copper levels in the liver, muscle and other tissues. It is very useful as a prediction tool, but no attempt has been made to validate it using real data.

3.6 Future work

Future work on designing models of copper metabolism should include the collection of fecal samples; a longer period of blood sampling and the separation of CP and non-CP-bound copper fractions in the plasma. An extended period of blood sampling will allow the appearance of labeled ceruloplasmin to be fully quantified. Also, the re-absorption pathway from the gut should be included; it must be present as the body reuses most of the very large amount of copper excreted in bile and pancreatic juices.

Care must also be exercised in the choice of route for label administration. Two possible reasons why IV copper may be metabolized differently are (a) the chemical form administered, and (b) the rate of administration. Both of these could cause the IV copper to be bound and transported differently in the plasma from copper in a meal. If it is demonstrated that IV and oral copper behave differently, the use of IV dosing must be restricted to studies where information on parenteral feeding is required.

Studies on mineral bioavailability should be carried out using intrinsically labeled foods in conjunction with a controlled copper diet. This has a dual purpose; firstly, that a physiological dose in the correct chemical form is consumed. Secondly, the volunteers will be in a steady state and any resultant model will relate directly to the quantity of copper they have received over several days. Transient, confounding effects will be minimized.

At present, dietary intervention studies are used to investigate mineral bioavailability. Used in conjunction with a compartmental model, intervention studies could yield much more information about the homeostatic control points in the body. It should be possible to see which body stores of copper are mobilized during a shortage of dietary copper and, conversely, where copper is stored and at what rate in times of plenty. Knowledge of this sort will enable more appropriate dietary recommendations to be made.

4 ZINC

4.1 Introduction

Zinc is one of the most abundant trace elements in man and is essential for the transmission of the genetic message, cell division, cell differentiation and growth. There is approximately 2 g of zinc in the human body and the majority is contained in muscle and bone. The whole blood zinc concentration is 9 $\mu g\,mL^{-1}$ and 80% of this is in red cell carbonic anhydrase and superoxide dismutase. Zinc has five stable isotopes (^{64}Zn 48.6%, ^{66}Zn 27.9%, ^{67}Zn 4.1%, ^{68}Zn 18.8%, ^{70}Zn 0.6%). ^{67}Zn and ^{70}Zn are usually chosen to artificially enrich because they have the lowest natural abundance. The use of stable isotopes in the study of human zinc metabolism began in the early 1980s [119]. Several reviews [120, 121] deal specifically with zinc metabolism, whereas others focus on status [122]. The driving force behind the use of modeling in zinc research is mainly due to the lack of a good biochemical status indicator. Zinc status has been estimated from the plasma zinc concentration, but this is known to vary markedly because of stress, infection and glucocorticoids [123]. Although erythrocyte metallothionein has been suggested as a useful status marker [124, 125], more studies are needed to evaluate it.

4.2 Zinc in foods

Good sources are meats, whole grains, seeds, nuts, eggs, root and leafy vegetables.

4.3 Absorption

Zinc absorption is in the range 20–40% in adults but is inhibited when phytate and fiber are prevalent in the diet. Status has an effect on absorption and is higher in deficiency. Dietary zinc has to compete

with endogenous secretions into the GI tract for absorption, and care must be taken when stable isotope studies are performed as there are reports that size of dose has an influence on fractional absorption [126]. Absorption of zinc is a two-step process: there is passive carrier-mediated diffusion into mucosal cells followed by partial transfer across the basolateral membrane to the circulatory system. This second step is regulated by dietary need [127] and is facilitated by the mucosal cells producing the metal-binding protein metallothionein. More of this protein is produced when the dietary intake is high, thereby trapping excess zinc that is then lost into the GI tract when the mucosal cells are sloughed off three or four days later.

Reports vary as to whether intrinsic and extrinsic zinc stable isotope labels are absorbed to the same extent. Two studies [9, 17] concluded that they were absorbed in the same way, whereas another two studies [12, 20] found that the absorption of an intrinsic zinc label was higher compared to an extrinsic equivalent.

4.4 Metabolism of absorbed zinc

Once the zinc is in the circulatory system, it is transported around the body bound to three carriers in the plasma that are in equilibrium with each other. Approximately 80% is bound to albumin and almost all the rest is on α_2-macroglobulin. The bone and muscles are a dynamic store of zinc, whereas the skin and hair are sinks from which there is no return back into the circulation. As much as 4–5 mg day^{-1} of zinc is excreted into the gut via pancreatic and intestinal fluids but almost all of this is reabsorbed. Excretion via the bile is homeostatically controlled and most zinc is not reabsorbed. Zinc has an important role in semen, and each ejaculation contains about 1 mg. Skin, hair and sweat also contribute to losses of about 1 mg day^{-1} on average.

4.5 Compartmental modeling of zinc in nutritional studies

There have been numerous compartmental models developed using radioisotopes, two of which [128, 129] were used as the basis of a stable isotope model [130]. They studied the effect of three different dietary levels of copper on zinc metabolism in five adult men. Figure 3.2.4 shows a schematic representation of their model.

Two liver compartments, two red blood cell (RBC) compartments and five other tissue compartments were required to fit the radioisotope data. It is unlikely that such a detailed model could be developed using stable isotope data. The experiment was conducted over 90 days and divided into three metabolic periods consisting, nominally, of medium (MP1), low (MP2) and high (MP3) copper intakes. Zinc intake was kept constant at approximately 11 mg day^{-1} over the study period. Oral ^{67}Zn was given on days 13, 31, 55 and 79. Intravenous ^{70}Zn was given on days 7, 49 and 73. Blood, urine and fecal samples were collected on the study days and for several days thereafter. On fitting the data, it was found that excretion into the GI tract (L(24,1)) depended on the route of administration and was lower after the IV dose than the oral. All other rate constants, however, showed no effect of route of administration. The main finding from the study was that only three of the rate constants were affected by the different levels of copper in the metabolic periods. These were L(1,24), L(12,1) and L(24,23). All other rate constants were not affected by dietary copper level, and their values did not differ by more than 4% from those found in an earlier study [129]. Compartment masses were also in agreement with earlier predictions [128, 129]. Total body zinc was calculated to be in the range 1800–2300 mg, of which 95% was found in the 'other tissues' compartments. Predictions for the total zinc in the liver compartments ranged from 66 to 80 mg and that in the red blood cells was estimated to be about 30 mg. It should be noted that half the predicted rate constants have coefficients of variation (CV) of more that 50%. Particularly, uncertain (CVs in excess of 1000%) are the predicted values for the rate of return of zinc from the other tissue compartments (3, 7 and 22) to the plasma. Since these compartments probably represent bone and skeletal muscle, an investigation of several months is needed to accurately predict the rate of return of label from these slowly

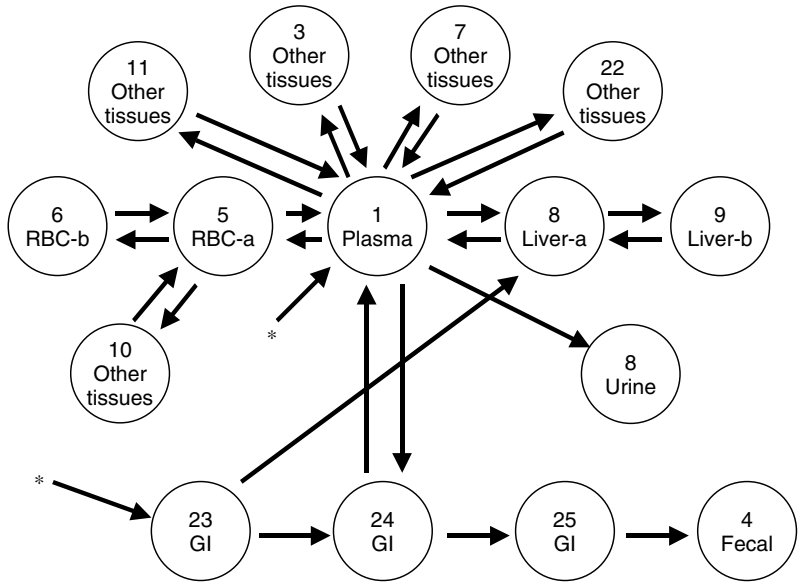

Figure 3.2.4. Compartmental model of zinc metabolism in adult men [130]. Compartments are represented by circles, sites of isotope input by *. Arrows represent direction of transfer between compartments. Although not shown in the diagram, a rate constant of the form L(i, j) (transfer from j to i), is associated with each arrow. The model was analyzed using the CONSAM program [131]. (Reproduced from Reference [130] by permission of The American Physiological Society.)

turning over compartments. This indicates that a simpler model would have been more appropriate for this study. Another shortcoming, as pointed out by the authors, was that only a few blood samples were taken after administration of the oral doses. This would not have allowed proper characterization of the initial appearance of the label in the plasma. It is, therefore, difficult to say whether the oral and IV doses are handled in the same way by the body. In a separate study [132], the same model structure as Figure 3.2.4 was used and it was found that a ^{70}Zn oral dose of 1.99 mg gave very similar kinetic results to an oral dose of ^{65}Zn (a radioisotope) given at the same time. This is an important finding since one of the criticisms of stable isotope research is that the dose sizes are too large and therefore they do not act as true tracers.

A subsequent stable isotope study [133] used a much simpler model (Figure 3.2.5).

Only six compartments are estimated from the stable isotope labels although a seventh is included (compartment 7) because it was calculated by another method. Six healthy women were recruited and placed on a constant zinc diet (7 mg day^{-1}) for seven days before the study day and seven days subsequent to it. Label administration was a simultaneous oral (^{67}Zn) and IV (^{70}Zn) dose followed by blood, urine and fecal sampling for up to 11 days afterwards. The model was developed on the basis of known physiology and the minimum number of compartments required to adequately fit the data. The resulting model was *a priori* identifiable according to the GLOBI program [134]. This means that all the parameters had a single possible solution. It was also *a posteriori* identifiable, meaning that all parameters were estimated with good precision from the experimental data. Compartments 2, 3 and 7 have not been named explicitly, but the authors speculate that compartments 2 and 3 are some combination of liver, erythrocytes and kidney. The mass of compartment 7 was estimated by assuming it contained zinc stored in the rest of the body (skeletal muscle and bone). This could not be calculated from the stable isotope data because the label was not returned from it within the seven-day study period. Previous radioisotope studies [128, 129] have estimated skeletal muscle and bone

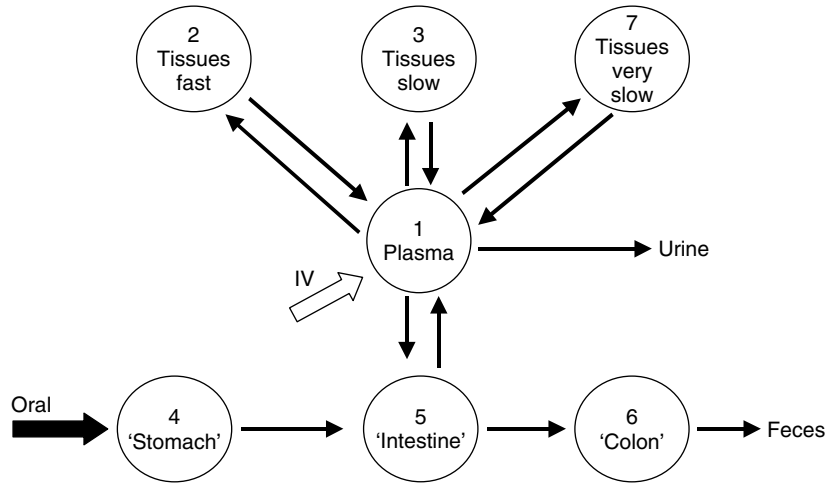

Figure 3.2.5. 'Tracer' compartmental model [133]. Although compartment 7 (tissues very slow) is indicated, the rate constant L (1, 7) and compartment mass (M_7) could not be resolved from the data and were estimated by other means (see text). (Reproduced with permission from the *American Journal of Clinical Nutrition*. © American Society for Clinical Nutrition.)

to contain approximately 95% of the body zinc. Another study [135] compared results from this model with those from the same model but with an added RBC compartment that exchanges with the plasma compartment. Body-weight corrected zinc pool masses were found to be significantly greater ($P < 0.05$) in children than in adults.

The most recent multi-compartmental model used two oral labels (^{67}Zn, ^{68}Zn) and one IV (^{70}Zn) label [136]. Blood, urine and feces were collected, and a constant daily diet was adhered to over the course of the experiment. As shown in Figure 3.2.6, 14 compartments were identified as contributing to zinc metabolism over the nine-day study period.

This structure was not shown to be *a priori* identifiable but was shown to be *a posteriori* identifiable. As well as the tracer data, use was made of information from the published literature on tracer excretion, absorption, circulation and storage. A large part of the paper is taken up with an in-depth explanation of the rationale behind the model. One volunteer's data is thoroughly examined, and the stages through which the experimenter must go in order to fit a model to the data are examined in detail. The compartments that are included as part of the rapidly exchanging zinc pool (EZP) are marked with an asterisk (*). The criterion for inclusion was defined as any compartment with IV label enrichment equal to that in the plasma (±25%) by 72 h after label administration. This readily exchangeable zinc accounts for only about 5% of the total body zinc but is thought to be involved in the known physiological functions of the element. An estimate of the EZP for subject 1, based on the compartmental model, was 141 mg. An alternative method [137], which uses a measure of the plasma or urine enrichment, calculated the EZP to be 180 mg, an overestimation of about 28%.

The rapidly exchanging zinc pools (EZP) can be calculated without the need for a full compartmental model [137]. This paper demonstrated that plasma or urine enrichment data could be used to estimate the EZP. By assuming that the pools that make up the EZP can be combined (after 48 h) into one 'EZP compartment', a single exponential function can be fitted to either plasma or urine enrichment data collected two days after IV or oral administration. An additional requirement with oral enrichment data is that the absorption of the dose must be known. Enrichment in this case is defined as follows.

$$\text{EZP enrichment} = \text{mass of isotope label in EZP} / \text{total EZP mass}$$

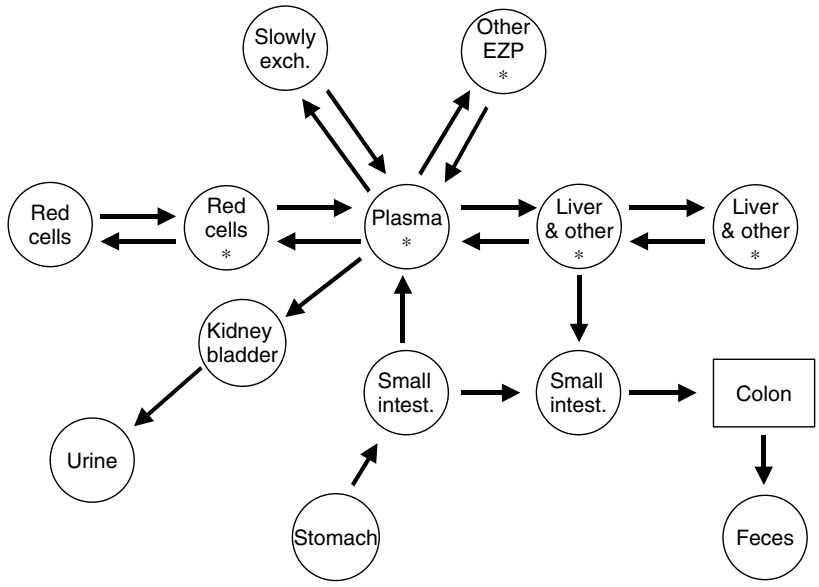

Figure 3.2.6. Zinc compartmental model [136]. Circles represent compartments, squares are delay elements. Compartments included in the exchangeable zinc pool (EZP) are indicated with an asterisk (*). (Reproduced from *Mathematical Modeling in Experimental Nutrition*, 1998, pp. 253–269, Human zinc metabolism: advances in the modeling of stable isotope data, Miller, L. V., Krebs, N. F. and Hambidge, K. M., Figure 5, Plenum Press, New York, © with kind permission of Kluwer Academic Publishers.)

By plotting the natural logarithm ($\log_e$) of the EZP enrichment against time (for data collected two days after oral dosing), a straight line is produced, which is an indication that labeled zinc is being cleared out of a single compartment (the EZP). By extrapolating the straight line back to the time of label administration, the size (mass) of the EZP can be calculated. Several assumptions are made in this type of modeling: (a) the loss of isotopic label from the EZP occurs at a mono-exponential rate from the time of label administration, and (b) the label is homogeneously mixed with the EZP during the measurement period. These two assumptions lead to an inherent overestimation of EZP (approximately 24% higher) when compared to a compartmental model [129]. The later paper [136] found an overestimation of about 28%. If this error is consistent, then it is not an impediment to the use of this type of calculation for predicting the EZP size. The method has been used by several investigators [138, 139]. Other workers have also calculated EZP size using compartmental modeling [140, 141].

4.6 Future work

Future work would benefit from a study design that incorporates a controlled diet before and during the experimental period. Studies using intrinsic labels of zinc should also be encouraged. There is no definitive evidence that oral and IV zinc are handled in the same way by the body. The effect of size of IV dose and rate of infusion should be examined in relation to the subsequent appearance in plasma, urine and feces. There is also some evidence that the size of the oral dose affects the quantity that is absorbed because of competition with endogenous zinc [126]. Care must be taken in study design to minimize the quantity of oral dose if it is to be given in a meal.

There have been few studies involving pregnant or lactating women. There is an increased need for zinc during these periods, and the results from one study led the researchers to suggest that the extra zinc comes from bone resorption of the mother [142]. Unfortunately, this study assumed that all the zinc in the skeleton was available for

resorption. In fact, only the trabecular bone can be broken down rapidly and this accounts for just 20% of the overall skeleton. Estimates of bone resorption, using stable isotopes, are prone to large error so future pregnancy/lactation studies must be well planned.

5 CALCIUM

5.1 Introduction

Calcium is a mineral with a long history of metabolic studies using radio and stable isotope tracers. This is hardly surprising, given its important role in human physiology in areas such as cell signaling and bone health. Almost 99% of the calcium in humans resides in the skeleton where bone is a dynamic part of the body and is in constant flux. Calcium homeostasis must be closely regulated because of the role of calcium in cell signaling. Thus, when the body is in need of calcium, bone is broken down and the calcium released into the circulation. Between the ages of 20 and 40 years, bone loss is approximately equal to bone growth so that net bone remains constant. The situation is somewhat different for postmenopausal women. Bone is lost at an increasing rate and may therefore result in osteoporosis. Bone density measurements and bone biomarkers cannot detect subtle changes in bone dynamics that might indicate the onset of osteoporosis [143]. Bone biomarkers are subject to high variability and are not a sensitive index of changes in calcium metabolism resulting from nutritional factors. Stable isotope tracers and mathematical modeling can provide an accurate picture of calcium kinetics and can give some estimation of bone turnover. The double isotope technique is useful for calcium absorption studies since the oral and IV forms of calcium have been shown to follow similar kinetics once in systemic circulation. When this technique is used in conjunction with balance studies, a wide range of calcium kinetics and body pool sizes can be determined. Precise blood sampling and complete urine and fecal collections need to be made and samples analyzed for the calcium from the naturally abundant source (both endogenous and dietary) and the oral and IV labels.

5.2 Calcium in foods

Good sources include milk and dairy products, especially cheese. Some plants have high calcium concentrations, but it may be largely unavailable for human absorption because of the oxalates and phytates in the plants that form water-insoluble salts.

5.3 Absorption

Approximately, 30–50% of calcium in the diet is absorbed by adults. Chelating agents promote the absorption of calcium by forming water-soluble salts. Examples include lactose, citrate and sucrose. It is known that tea inhibits calcium absorption because of oxalates. Absorption involves two major processes: (a) This is a saturable process and takes place in the duodenum and upper jejunum. It is subject to nutritional regulation via the vitamin D endocrine system. (b) Absorption takes place all along the intestine and is nonsaturable.

5.4 Metabolism of absorbed calcium

Calcium is found in three forms in the plasma: as the free ion (47%); in chelated nonprotein-bound form, primarily complexed with citrate and other organic acids (6.5%); and bound to proteins especially prealbumin (46%). The plasma concentration is tightly controlled by hormonal action and in adults is usually about 100 $\mathrm{mg\,L^{-1}}$. Transport is to all cells where it takes part in regulatory processes. Calcium in bone is very dynamic and is being released and taken up continuously in healthy adults. Urinary excretion tends to reflect levels of calcium in the diet and, alongside biliary excretion, is the main excretory route from the body.

5.5 Compartmental modeling of calcium in nutritional studies

A recent paper [144] examined the differences in calcium kinetics between adolescent girls and young women. Healthy adolescent ($n = 14$) and adult ($n = 11$) subjects were given a controlled diet with calcium intakes of approximately 1300 mg day^{-1} for seven days prior to receiving oral (^{44}Ca, 98.5% enrichment) and IV (^{42}Ca, 93.6% enrichment) doses. Blood was sampled at frequent intervals for the next few hours and then daily for 14 days. All urine and feces were also collected for two weeks. The model is shown in Figure 3.2.7.

Compartment 1 contains the vascular space and some of the extracellular fluid, compartment 2 is soft tissue and compartment 3 contains exchangeable calcium in bone. The rate constants between the three compartments were derived using the IV plasma data. One possible limitation of this work is that the initial volume of distribution in compartment 1 could not be well determined and was fixed at ten, one and five times vascular space in various volunteers. A much earlier study [146] found that the size of the sampled compartment (compartment 1) was approximately four times the vascular space. They speculated that this was due to calcium penetration of capillary walls and/or adsorption to endothelial surfaces.

The rate of endogenous fecal excretion (V_f) was calculated from the cumulative appearance of the IV dose in the feces. The rate of urinary excretion (V_u) and dietary fecal excretion (V_F) were both calculated from the appearance of naturally abundant calcium in the urine and feces, respectively. Knowledge of V_u and V_F, along with the daily intake of calcium (V_i), permits the calculation of calcium balance ($\Delta = V_i - (V_F + V_u)$). The rate of bone deposition of the IV label can be estimated by fitting the IV plasma data to this model. The rate of bone deposition of the naturally occurring calcium (V_{0+}) can then be calculated from knowledge of the mass of calcium in compartment 3. The rate of bone resorption (V_{0-}) cannot be measured directly from stable isotope data since it takes several months for dietary calcium laid down in the bone to be returned to the plasma. Instead, V_{0-} must be calculated by difference ($\Delta = V_{0+} - V_{0-}$). Calculations of this type indicate that, in comparison to adult women, adolescent girls resorb more calcium from their skeleton (1177 vs.

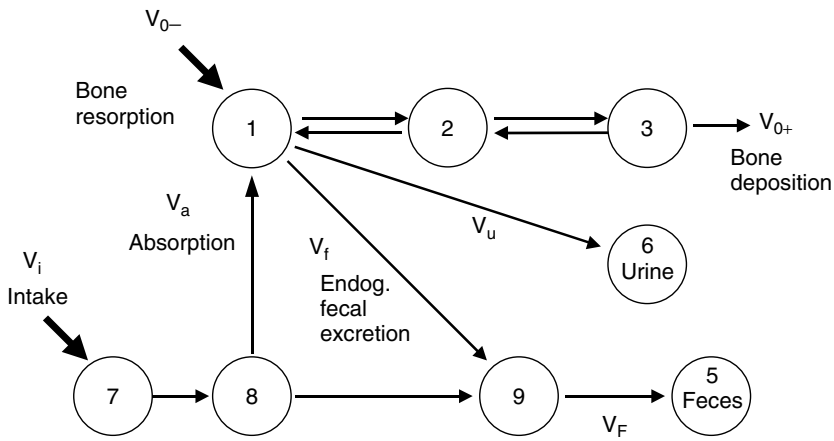

Figure 3.2.7. Model for calcium metabolism in women [144]. The notation of the transport rates are after that of an earlier paper [145]. Circles represent compartments, numbers in circles represent compartment number, thin arrows represent movement between compartments and thick arrows represent entry of calcium via the diet (V_i) or bone resorption (V_{0-}). V_a, rate of calcium absorption; V_{0+}, deposition in bone; V_u, urine excretion; V_f, endogenous fecal excretion; V_F, fecal excretion. (Reproduced from Reference [144] by permission of The American Physiological Society.)

542 mg day^{-1}), deposit more calcium in their bone (1459 vs. 501 mg day^{-1}) and therefore retain more calcium (282 vs. 41 mg day^{-1}). A loss of calcium of 41 mg day^{-1}, as estimated for women, would eventually lead to detrimental structural changes in the skeleton and increase the risk of fracture in later life. It is essential that the error or uncertainty is quoted with such calculations so that other investigators can evaluate the precision of the data.

A structurally identical model to Figure 3.2.7 was employed to calculate calcium kinetics [147]. On the basis of a similar sampling protocol to a previous study [144], but with the addition of saliva sampling and much smaller dose sizes, the study only used two volunteers (one male, one female) and did not include a controlled diet, either before or during the study. Therefore, balance could not be guaranteed and all results were based on an estimated daily calcium intake for both volunteers. It was shown that the small doses still gave measurable enrichment using high precision TIMS (thermal ionization mass spectrometry). This led to the conclusion that saliva samples could be used alongside blood samples to calculate calcium kinetics. Again, because no errors or uncertainties were quoted in the paper, the use of smaller doses cannot be properly evaluated.

Similar techniques have been used in two studies by Abrams *et al*., and the second study [148] found a very high bone calcium deposition rate (160 mg kg^{-1} day^{-1}) amongst 13 very-low-birthweight infants fed a high-calcium diet. The earlier paper [149] used an empirical model of calcium kinetics, in conjunction with urine and plasma data, to derive an equation containing three exponential terms.

The total exchangeable pool size (TEP) and the rate of bone absorption (V_{0+}) can be calculated from a combination of the parameters of the above equation and the rate of urinary (V_u) and endogenous fecal excretion (V_f).

Of the 13 volunteers, 10 were children (aged 10 months to 14 years) and 3 were adult women (aged 22–33 years). The three adult volunteers had a significantly lower V_{0+} (10 mg kg^{-1} day^{-1}) compared to the children (81 mg kg^{-1} day^{-1}) and a significantly lower TEP (76 mg kg^{-1}) compared to the children (279 mg kg^{-1}).

5.6 Future work

Calcium-41 is present naturally in minute quantities in nature (approximately 10^{-15}% of all calcium is ^{41}Ca). It has a half-life of 104,000 years and so is not a true stable isotope. Nor is it a radioisotope but instead is defined as a semi-stable or cosmogenic isotope. However, it can be used as a safe tracer in humans because its radiation risk is extremely low. The drawback to using it is that the resulting human samples must be analyzed on an accelerator mass spectrometer (AMS), which are not found in many centers in the world, and the cost per sample analysis is relatively high. Subjects need to consume the ^{41}Ca label a few months before any intervention study is contemplated so as to allow the ^{41}Ca to exchange completely with trabecular and cortical bone. Several papers have been published in this area [150–153]. The basic premise is that the rate of bone resorption can be measured from urine samples approximately 100 days after a ^{41}Ca dose. By this time, there should be a plateau in the ^{41}Ca urine concentration. This indicates that all the ^{41}Ca is coming exclusively from the skeleton and therefore gives a direct measurement of the rate of bone resorption. A dietary intervention at this point will reveal whether the ^{41}Ca concentration changes and therefore indicate if the intervention increases or decreases bone resorption. This technique obviously has potential for pharmaceutical companies manufacturing 'anti-osteoporosis' drugs but is particularly appropriate as a tool for investigating dietary interventions in which bone biomarkers are not sensitive enough and need to be monitored for lengthy periods. Another benefit of using ^{41}Ca is that all volunteers are labeled for life. A study with a combination of a stable isotope dose, a ^{41}Ca tracer and a controlled diet should be able to answer many of the interesting kinetic questions about calcium.

6 REFERENCES

1. Schoenheimer, R. and Rittenburg, D., *J. Biol. Chem.*, **111**, 163 (1935).

2. McPherson, G. D., *Acta Orthop. Scand.*, **78**, 1 (1965).
3. King, J. C., Raynolds, W. L. and Margen, S., *Am. J. Clin. Nutr.*, **31**, 1198 (1978).
4. Buckley, W. T., *Proc. Nutr. Soc.*, **47**, 407 (1988).
5. Turnlund, J. R., *J. Nutr.*, **119**, 7 (1989).
6. Turnlund, J. R., *Crit. Rev. Food Sci. Nutr.*, **30**, 387 (1991).
7. Turnlund, J. R., *J. Nutr.*, **124**, 1765S (1994).
8. Mellon, F. A. and Sandstrom, B. (Eds), *Stable Isotopes in Human Nutrition*, Academic Press, London, 1996.
9. Janghorbani, M., Ting, B. T. G., Young, V. R. and Steinke, F. H., *Br. J. Nutr.*, **46**, 395 (1981).
10. Weaver, C. M., *Crit. Rev. Food Sci. Nutr.*, **23**, 75 (1985).
11. Fox, T. E., Fairweather-Tait, S. J., Eagles, J. and Wharf, S. G., *Br. J. Nutr.*, **66**, 57 (1991).
12. Janghorbani, M., Istfan, N. W., Pagounes, J. O., Steinke, F. H. and Young, V. R., *Am. J. Clin. Nutr.*, **36**, 537 (1982).
13. Christensen, M. J., Janghorbani, M., Steinke, F. H., Istfan, N. and Young, V. R., *Br. J. Nutr.*, **50**, 43 (1983).
14. Johnson, P. E. and Lykken, G. I., *J. Agric. Food Chem.*, **36**, 537 (1988).
15. Weaver, C. M., Isotopic tracer methodology: potential in mineral nutrition, in *Trace Minerals in Foods*, Smith, K. T. (Ed.), Marcel Dekker, New York, 1988, pp. 429–454.
16. Boza, J. J., Fox, T. E., Eagles, J., Wilson, P. D. G. and Fairweather-Tait, S. J., *J. Nutr.*, **125**, 1611 (1995).
17. Egan, C. B., Smith, F. G., Houk, R. S. and Serfass, R., *Am. J. Clin. Nutr.*, **53**, 547 (1991).
18. Weaver, C. M., Heaney, R. O., Martin, B. R. and Fitzsimmons, M. L., *Am. J. Clin. Nutr.*, **55**, 451 (1992).
19. Liu, Y.-A., Neal, P., Ernst, J., Weaver, C., Rickard, K., Smith, D. L. and Lemons, J., *Pediatr. Res.*, **25**, 496 (1989).
20. Fairweather-Tait, S. J., Fox, T. E., Wharf, S. G., Eagles, J., Crews, H. M. and Massey, R., *Br. J. Nutr.*, **66**, 65 (1991).
21. Canolty, N. and Cain, T. P. (Eds), *Mathematical Models in Experimental Nutrition*, University of Georgia, Athens, GA, 1985.
22. Hoover-Plow, J. and Chandra, R. K., *Prog. Food Nutr. Sci.*, **12**, 211 (1988).
23. Abumrad, N., *J. Parenter. Enteral Nutr.*, **15**, 44S (1991).
24. Siva Subramanian, K. N. and Wastney, M. E. (Eds), *Kinetic Models of Trace Element and Mineral Metabolism During Development*, CRC Press, New York, 1995.
25. Coburn, S. P. and Townsend, D., *Adv. Food Nutr. Res.*, **40**, 1 (1996).
26. Clifford, A. J. and Muller, H.-G. (Eds), *Mathematical Modeling in Experimental Nutrition*, Plenum Press, New York, 1998.
27. Atkins, G. L., *Multicompartment Models in Biological Systems*, Methuen, London, 1969.
28. Shipley, R. A. and Clark, R. E., *Tracer Methods for in Vivo Kinetics*, Academic Press, New York, 1972.
29. Anderson, D. H., *Compartmental Modeling and Tracer Kinetics*, Springer-Verlag, Berlin, 1983.
30. Carson, E. R., Cobelli, C. and Finkelstein, L., *The Mathematical Modeling of Metabolic and Endocrine Systems: Model Formulation, Identification, and Validation*, John Wiley & Sons, New York, 1983.
31. Green, M. H. and Green, J. B., *Annu. Rev. Nutr.*, **10**, 41 (1990).
32. Wolfe, R. R., *Radioactive and Stable Isotope Tracers in Biomedicine*, Wiley-Liss, New York, 1992.
33. Jacquez, J. A., *Compartmental Analysis in Biology and Medicine*, 3rd ed., Biomedware, Ann Arbor, MI, 1996.
34. Wastney, M. E., Patterson, B. H., Linares, O. A., Greif, P. C. and Boston, R. C., *Investigating Biological Systems Using Modeling*, Academic Press, San Diego, CA, 1999.
35. Cobelli, C., Foster, D. and Toffolo, G., *Tracer Kinetics in Biomedical Research*, Kluwer Academic/Plenum Publishers, New York, 2000.
36. *SAAMII: A program for kinetic modelling. Resource Facility for Kinetic Analysis*, University of Washington, Seattle, WA, 1997.
37. Sunde, R. A., *J. Am. Oil Chem. Soc.*, **61**, 1891 (1984).
38. Magos, L. and Webb, M., *Crit. Rev. Toxicol.*, **8**, 1 (1980).
39. Huber, R. E. and Criddle, R. S., *Arch. Biochem. Biophys.*, **122**, 164 (1967).
40. Leinfelder, W., Zehelein, E., Mandrand-Berthelot, M. A. and Bock, A., *Nature*, **331**, 723 (1988).
41. Forchhammer, K., Leinfelder, W. and Bock, A., *Nature*, **342**, 453 (1989).
42. Berrow, M. L. and Ure, A. M., Geological materials and soils, in *Occurrence and Distribution of Selenium*, Ihnat, M. (Ed.), CRC press, Boca Raton, FL, 1989, pp. 226–228.
43. Terry, N., Zayed, A. M., de Sousa, M. P. and Tarum, A. S., *Ann. Rev. Plant Physiol. Plant Mol. Biol.*, **51**, 401 (2000).
44. Morris, V. C. and Levander, O. A., *J. Nutr.*, **100**, 1383 (1970).
45. World Health Organisation, *Environmental Health Criteria 58: Selenium, International Programme on Chemical Safety*, World Health Organisation, Geneva, 1987.
46. Burke, R. F. and Hill, K. E., *Ann. Rev. Nutr.*, **13**, 65 (1993).
47. Bock, A., Forchhammer, K., Heider, J. and Baron, C., *Trends Biochem. Sci.*, **16**, 463 (1991).
48. Behne, D., Weiss-Nowak, C., Kalcklosch, M., Westphal, C., Gessner, H. and Kyriakopoulos, A., *Analyst*, **120**, 823 (1995).
49. Stewart, R. D. H., Griffiths, N. M., Thomson, C. D. and Robinson, M. F., *Br. J. Nutr.*, **40**, 45 (1978).
50. Bopp, B. A., Sonders, R. C. and Kesterson, J. W., *Drug Metab. Rev.*, **13**, 271 (1982).
51. Mutanen, M., *Ann. Clin. Res.*, **18**, 48 (1986).
52. Diplock, A. T., *Am. J. Clin. Nutr.*, **45**, 1313 (1987).

53. Atherton, C., Fox, T., Fairweather-Tait, S., Dainty, J., Lewis, J., Baxter, M., Crews, H. and Langford, N., in *Trace Elements in Man and Animals – TEMA 10*, Favier, A., Anderson, R. A. and Roussel, A. M. (Eds), Plenum Publishing, New York, 2000.
54. Sirichakwal, P. P., Young, V. R. and Janghorbani, M., *Am. J. Clin. Nutr.*, **41**, 264 (1985).
55. Janghorbani, M. and Young, V. R., in *Proceedings of the 3rd International Symposium on Selenium in Biology and Medicine*, Combs, G. F. (Ed.), AVI Publishing, Westport, CT, 1987.
56. Martin, R. F., Janghorbani, M. and Young, V. R., *J. Parenter. Enteral Nutr.*, **12**, 351 (1988).
57. Oldfield, J. E., *Selenium in Fertilizers*, Selenium–Tellurium Development Association, Grimbergen, 1992.
58. Young, V. R., Nahapetian, A. and Janghorbani, M., *Am. J. Clin. Nutr.*, **35**, 1076 (1982).
59. Moser-Veillon, P. B., Mangels, A. R., Patterson, K. Y. and Veillon, C., *Analyst*, **117**, 559 (1992).
60. Wolffram, S., *Med. Klin.*, **90**, 1 (1995).
61. Thomson, C. D. and Stewart, R. D. H., *Br. J. Nutr.*, **32**, 47 (1974).
62. Swanson, C. A., Patterson, B. H., Levander, O. A., Veillon, C., Taylor, P. R., Helzlsouer, K., McAdam, P. A. and Zech, L. A., *Am. J. Clin. Nutr.*, **54**, 917 (1991).
63. McConnell, K. P. and Cho, G. J., *Am. J. Physiol.*, **208**, 1191 (1965).
64. Barbezat, G. B., Casey, C. E. and Reasbeck, P. G., Selenium, in *Absorption and Malabsorption of Mineral Nutrients*, Solomons, N. W. and Rosenberg, I. H. (Eds), Alan R Liss, New York, 1984, pp. 213–258.
65. Whanger, P., Xia, V. and Thomson, C., *J. Trace Elem. Elect. Health Dis.*, **7**, 121 (1993).
66. Waterlow, J. C., Garrow, J. S. and Millward, D. J., *Clin. Sci.*, **36**, 489 (1969).
67. Griffiths, N. M., Stewart, R. D. H. and Robinson, M. F., *Br. J. Nutr.*, **35**, 373 (1976).
68. Veillon, C., Patterson, K. Y., Button, L. N. and Sytkowski, A., *Am. J. Clin. Nutr.*, **52**, 155 (1990).
69. Combs, G. F. Jr. and Combs, S. B., *Ann. Rev. Nutr.*, **4**, 257 (1984).
70. Sunde, R. A., *Ann. Rev. Nutr.*, **10**, 451 (1990).
71. Burke, R. F., *FASEB J.*, **5**, 2274 (1991).
72. Esaki, N., Nakamura, T., Tanaka, H., Suzuki, T., Morino, Y. and Soda, K., *Biochem.*, **205**, 955 (1981).
73. Esaki, N., Nakamura, T., Tanaka, H. and Sada, K., *J. Biol. Chem.*, **257**, 4386 (1982).
74. Combs, G. F., *Br. J. Nutr.*, **85**, 517 (2001).
75. Patterson, B. H., Levander, O. A., Helzlsouer, K., McAdam, P. A., Lewis, S. A., Taylor, P. R., Veillon, C. and Zech, L. A., *Am. J. Physiol.*, **257**, R556 (1989).
76. Patterson, B. H. and Zech, L. A., *J. Nutr.*, **122**, 709 (1992).
77. Ducros, V., Faure, P., Ferry, M., Couzy, F., Biajoux, I. and Favier, A., *Br. J. Nutr.*, **78**, 379 (1997).
78. Janghorbani, M., Christensen, M. J., Nahapetian, A. and Young, V. R., *Am. J. Clin. Nutr.*, **35**, 647 (1982).
79. Thomson, C. D. and Robinson, M. F., *Am. J. Clin. Nutr.*, **44**, 659 (1986).
80. Van Dael, P., Davidsson, L., Munoz-Box, R., Fay, L. B. and Barclay, D., *Br. J. Nutr.*, **85**, 157 (2001).
81. Power, R., *Proceedings of the Selenium–Tellurium Development Association's Fifth International Symposium*, Selenium Tellurium Development Association, Grimbergen, 1995.
82. Korhola, M., Vainio, A. and Edelmann, K., *Ann. Clin. Res.*, **18**, 65 (1986).
83. Thomson, C. D., Robinson, M. F., Butler, J. A. and Whanger, P. D., *Br. J. Nutr.*, **69**, 577 (1993).
84. Ip, C., Birringer, M., Block, E., Kotrebai, M., Tyson, J. F., Uden, P. C. and Lisk, D. J., *J. Agric. Food Chem.*, **48**, 2062 (2000).
85. Bird, S. M., Uden, P. C., Tyson, J. F., Block, E. and Denoyer, E., *J. Anal. At. Spectrom.*, **12**, 785 (1997).
86. Zheng, J., Goessler, W. and Kosmus, W., *Trace Elem. Elect.*, **15**, 70 (1998).
87. Cai, X., Block, E., Uden, P., Zhang, Z., Quimby, B. D. and Sullivan, J. J., *J. Agric. Food Chem.*, **43**, 1754 (1995).
88. Akesson, B. and Srikumar, T. S., *Food Chem.*, **51**, 45 (1994).
89. Quijano, M. A., Moreno, P., Gutierrez, A. M., Concepcion, M., Perez-Conde, M. C. and Camara, C., *J. Mass Spectrom.*, **35**, 878 (2000).
90. Cappon, C. J. and Smith, J. C., *J. Appl. Toxicol.*, **2**, 181 (1982).
91. Onning, G. and Bergdahl, I. A., *Analyst*, **124**, 1435 (1999).
92. Ip, C., Hayes, C., Budnick, R. M. and Ganther, H. E., *Cancer Res.*, **51**, 595 (1991).
93. Vadhanavikit, S., Ip, C. and Ganther, H. E., *Xenobiotica*, **23**, 731 (1993).
94. Quijano, M. A., Gutierrez, A. M., Perez-Conde, M. C. and Camara, C., *Talanta*, **50**, 165 (1999).
95. Fox, T. E., *The Use of Stable Isotopes to Study Selenium Metabolism in Humans*, PhD Thesis, University of East Anglia, 2003.
96. Janghorbani, M., Kasper, L. J. and Young, V. R., *Am. J. Clin. Nutr.*, **40**, 208 (1984).
97. Janghorbani, M., Martin, R. F., Kasper, L. J., Sun, X. F. and Young, V. R., *Am. J. Clin. Nutr.*, **51**, 670 (1990).
98. Patterson, B. H., Zech, L. A., Swanson, C. A. and Levander, O. A., *J. Trace Elem. Elect. Health Dis.*, **7**, 117 (1993).
99. Linder, M. C., *The Biochemistry of Copper*, Plenum Publishing, New York, 1991.
100. Turnlund, J. R., *Am. J. Clin. Nutr.*, **67**, 960S (1998).
101. Turnlund, J. R., Keyes, W. R., Peiffer, G. L. and Scott, K. C., *Am. J. Clin. Nutr.*, **67**, 1219 (1998).
102. Linder, M. C., *Am. J. Clin. Nutr.*, **67**, 965S (1998).
103. Buckley, W. T., Vanderpool, R. A., Godfrey, D. V. and Johnson, P. E., *J. Nutr. Biochem.*, **7**, 488 (1996).

104. Department of Health, *Dietary Reference Values for Food Energy and Nutrients for the United Kingdom*, HMSO, London, 1991.
105. McCance, R. A. and Widdowson, E. M., *The Composition of Foods*, Royal Society of Chemistry and MAFF, London, 1991.
106. Pennington, J. T. and Calloway, D. H., *J. Am. Diet. Assoc.*, **63**, 143 (1973).
107. Cordano, A., Baertl, J. M. and Graham, G. G., *Paediatr.*, **34**, 324 (1964).
108. Goyens, P., Brasseur, D. and Cadranel, S., *J. Paediatr. Gastroenterol. Nutr.*, **4**, 677 (1985).
109. Dorner, K., Dziadzka, S., Hohn, A., Sievers, E., Oldigs, H. D., Schulz-Lell, G. and Schaub, J., *Br. J. Nutr.*, **61**, 559 (1989).
110. August, D., Janghorbani, M. and Young, V. R., *Am. J. Clin. Nutr.*, **50**, 1457 (1989).
111. Turnlund, J. R., Wada, L., King, J. C., Keyes, W. R. and Acord, L. L., *Biol. Trace Elem. Res.*, **17**, 31 (1988).
112. FAIR CT95-0813. *Effect of Copper in the Food Chain on Human Health (FOODCUE)*, 1999.
113. Dunn, M. A., Green, M. H. and Leach, R. M., *Am. J. Physiol.*, **261**, E115 (1991).
114. Buckley, W. T., *Can. J. Anim. Sci.*, **71**, 155 (1991).
115. Scott, K. C. and Turnlund, J. R., *J. Nutr. Biochem.*, **5**, 342 (1994).
116. D' Addabbo, A., Germinario, L., Campanella, G., Damato, V. D. and Boccuni, N., *Acta. Neurol.*, **26**, 436 (1971).
117. Turnlund, J. R., Keen, C. L. and Smith, R. G., *Am. J. Clin. Nutr.*, **51**, 658 (1990).
118. Buckley, W. T., *J. Nutr.*, **126**, 2312S (1996).
119. Jackson, M. J., Jones, D. A., Edwards, R. H. T., Swainbank, I. G. and Coleman, M. L., *Br. J. Nutr.*, **51**, 199 (1984).
120. Krebs, N. F., Miller, L. V., Naake, V. L., Lei, S., Westcott, J. E., Fennessey, P. V. and Hambidge, K. M., *Nutr. Biochem.*, **6**, 292 (1995).
121. Wastney, M. E., House, W. A., Barnes, R. M. and Subramanian, K. N. S., *J. Nutr.*, **130**, 1355S (2000).
122. King, J. C., *J. Nutr.*, **120**, 1474 (1990).
123. Cousins, R. J., Systemic Transport of Zinc, in *Zinc in Human Biology*, Mills, C. F. (Ed.), Springer-Verlag, Berlin, Heidelberg, 1989, pp. 79–85.
124. Grider, A., Bailey, L. B. and Cousins, R. J., *Proc. Natl. Acad. Sci. U.S.A.*, **87**, 1259 (1990).
125. Sullivan, V. K., Burnett, F. R. and Cousins, R. J., *J. Nutr.*, **128**, 707 (1998).
126. Sian, L., Hambidge, K. M., Westcott, J. L., Miller, L. V. and Fennessey, P. V., *Am. J. Clin. Nutr.*, **58**, 533 (1993).
127. Solomons, N. W., in *Modern Nutrition in Health and Disease*, Shils, M. and Young, V. (Eds.), Lea & Febiger, Philadelphia, PA, 1988, pp. 238.
128. Foster, D. M., Aamodt, R. L., Henkin, R. I. and Berman, M., *Am. J. Physiol.*, **237**, R340 (1979).
129. Wastney, M. E., Aamodt, R. L., Rumble, W. F. and Henkin, R. I., *Am. J. Physiol.*, **251**, R398 (1986).
130. Scott, K. C. and Turnlund, J. R., *Am. J. Physiol.*, **267**, E165 (1994).
131. Foster, D. M., Boston, R. C., Jacquez, J. A. and Zech, L. A., *The SAAM Tutorials: An Introduction to Using Conversational SAAM (Version 30)*, Resource Facility for Kinetic Analysis, Seattle, WA, 1989.
132. Wastney, M. E., Gokmen, I. G., Aamodt, R. L., Rumble, W. F., Gordon, G. E. and Henkin, R. I., *Am. J. Physiol.*, **260**, R134 (1991).
133. Lowe, N. M., Shames, D. M., Woodhouse, L. R., Matel, J. S., Roehl, R., Saccomani, M. P., Toffolo, G., Cobelli, C. and King, J. C., *Am. J. Clin. Nutr.*, **65**, 1810 (1997).
134. Saccomani, M. P., Audolym, S., Angio, L. D., Sattier, R. and Cobelli, C., Pride: a program to test a priori global identifiability of linear compartmental models, in *Proceedings of the 10th IFAC Symposium on System Identification*, Blanke, M. and Soderstrom, T. (Eds), Danish Automation Society, Copenhagen, 1994.
135. Griffin, I. J., King, J. C. and Abrams, S. A., *J. Nutr.*, **130**, 2607 (2000).
136. Miller, L. V., Krebs, N. F. and Hambidge, K. M., Human zinc metabolism: advances in the modeling of stable isotope data, in *Mathematical Modeling in Experimental Nutrition*, Clifford, A. J. and Muller, H.-G. (Eds), Plenum Publishing, New York, 1998, pp. 253–269.
137. Miller, L. V., Hambidge, K. M., Naake, V. L., Hong, Z., Westcott, J. L. and Fennessey, P. V., *J. Nutr.*, **124**, 268 (1994).
138. Sian, L., Xiang, M. Y., Miller, L. V., Tong, L., Krebs, N. F. and Hambidge, K. M., *Am. J. Clin. Nutr.*, **63**, 348 (1996).
139. Watson, W. S., Mitchell, K. G., Lyon, T. D. B. and Kerr, N., *J. Trace Elem. Med. Biol.*, **13**, 141 (1999).
140. Fairweather-Tait, S. J., Jackson, M. L., Fox, T. E., Wharf, S. G., Eagles, J. and Croghan, P. C., *Br. J. Nutr.*, **70**, 221 (1993).
141. Lowe, N. M., Green, A., Rhodes, J. M., Lombard, M., Jalan, R. and Jackson, M. L., *Clin. Sci.*, **84**, 113 (1993).
142. Moser-Veillon, P. B., *Analyst*, **120**, 895 (1995).
143. Marcus, R., Holloway, L., Wells, B., Greendale, G., James, M. K., Wasilauskas, C. and Kelaghan, J., *J. Bone Miner. Res.*, **14**, 1583 (1999).
144. Wastney, M. E., Ng, J., Smith, D., Martin, B. R., Peacock, M. and Weaver, C. M., *Am. J. Physiol.*, **271**, R208 (1996).
145. Aubert, J.-P., Bronner, F. and Richelle, L. J., *J. Clin. Invest.*, **42**, 885 (1963).
146. Neer, R., Berman, M., Fisher, L. and Rosenberg, L. E., *J. Clin. Invest.*, **46**, 1364 (1967).
147. Smith, S. M., Wastney, M. E., Nyquist, L. E., Shih, C. Y., Wiesmann, H., Nillen, J. L. and Lane, H. W., *J. Mass Spectrom.*, **31**, 1265 (1996).
148. Abrams, S. A., Schanler, R. J., Yergey, A. L., Vieira, N. E. and Bronner, F., *Pediatr. Res.*, **36**, 424 (1994).
149. Abrams, S. A., Esteban, N. V., Vieira, N. E., Sidbury, J. B., Specker, B. L. and Yergey, A. L., *J. Bone Miner. Res.*, **7**, 287 (1992).

150. Elmore, D., Bhattacharyya, M. H., Sacco-Gibson, N. and Peterson, D. P., *Nucl. Instrum. Methods B*, **52**, 531 (1990).
151. Freeman, S. P. H. T., Serfass, R. E., King, J. C., Southon, J. R., Fang, Y., Woodhouse, L. R., Bench, G. S. and McAninch, J. E., *Nucl. Instrum. Methods B*, **99**, 557 (1995).
152. Freeman, S. P. H. T., King, J. C., Vieira, N. E., Woodhouse, L. R. and Yergey, A. L., *Nucl. Instrum. Methods B*, **123**, 266 (1997).
153. Freeman, S. P. H. T., Beck, B., Bierman, J. M., Caffee, M. W., Heaney, R. P., Holloway, L., Marcus, R., Southon, J. R. and Vogel, J. S., *Nucl. Instrum. Methods B*, **172**, 930 (2000).

3.3 Modeling of Trace Element Species in Health and Disease

Janusz Z. Byczkowski
JZB Consulting, Fairborn, Ohio, USA

The atoms of transition metals have valence electron shells incompletely filled in at least one of their oxidation states. Thus, they can accept or donate one electron at a time. The one-electron mechanism can overcome spin restrictions on accepting electrons by the ground-state molecular oxygen. This implies that transition metals, in general, are good catalysts, especially for redox reactions. Several transition metals are found at the catalytic centers of many enzymes, for instance, oxidases and oxygenases. Therefore, at low concentrations these metals are required by the living organisms as essential trace elements, and they must be supplied in a diet. At higher concentrations, however, they may become detrimental and toxic [1].

Typically, the physiological concentrations of free trace metal ions in animal tissues are extremely low (e.g. 10^{-23} M Fe^{2+}, 10^{-18} M Cu^{2+}, 10^{-12} M Mn^{2+}) and generally all the measurable amounts of metals exist as complexes or chelates of metal ions with biological ligands. On the other hand, high concentrations of various transition metal derivatives, mostly in the form of oxides and salts, may appear in the environment and the workplace. Therefore, under conditions of environmental or occupational exposure, the target tissue must cope with a local concentration of transition metal ions often exceeding several thousand or even million times the normal physiological levels [2].

Because of this dual role of the majority of transition metals, beneficial at low concentrations and toxic at high concentrations, it would be appropriate to call them 'essential at trace concentrations'. Their dose-response curves are U-, or more exactly, J-shaped, which represents the so-called hormetic effect [3]. On the other hand, some metals (e.g. Pb, Hg, Cd) are nonessential even at trace concentrations and in the target tissues their internal dose-response curves are typically S-shaped.

This is why the abilities of modeling and predicting absorption, distribution, ligand binding, metabolism and elimination of trace metals in the organism are crucial for understanding their nutritional and therapeutic effects and are indispensable in toxicity and risk assessment. Since most of the pharmacokinetic experiments were performed in animals treated with massive doses of trace metals so their tissue distributions could be measured with sufficient precision, these experiments should be supplemented by the studies of binding with biological ligands in the target sites at feasible concentrations. Only this approach can provide a complete picture, which is necessary for understanding the biological role, pharmacotherapeutic effects and toxicity of trace metals.

In this chapter, these two kinds of the trace metal modeling endeavor, pharmacokinetics and biological ligand binding, will be reviewed separately,

Handbook of Elemental Speciation II: Species in the Environment, Food, Medicine & Occupational Health
Edited by R. Cornelis, H. Crews, J. Caruso and K. G. Heumann
 ISBN: 0-470-85598-3 (HB)

using examples of the best-researched trace metals. These reviews were not thought to be exhaustive. Rather, they just illustrate the approach used in some selected successful models, the modeling methodology, and they point to gaps in our understanding of absorption, distribution, ligand binding, metabolism and elimination of these few of the best-researched trace metals.

3.3.1 Pharmacokinetic Approach and Mathematical Modeling

Janusz Z. Byczkowski
JZB Consulting, Fairborn, Ohio, USA

The goal of pharmacokinetic (PK) modeling of trace metals is to describe quantitatively the relationship between the external dose or exposure concentration of a metal compound (exposure level as input) and the effective internal dose or local concentration of the metal or its active complex in the target organ (internal dose or its surrogate, ID_s) as output.

$$ID_s = f(F \times ED, t) \qquad (3.3.1.1)$$

where F is bioavailability, ED is external dose or exposure concentration, t is time. A general concept of PK modeling of trace metals is depicted schematically in Figure 3.3.1.1.

The PK models are useful for both exposure and dose-response assessments, bioavailability estimate, route-to-route extrapolation, interspecies extrapolation, derivation of recommended daily intakes (RDI and Percentage of Daily Value, PDV) and toxicity values (Acceptable Daily Intake, ADI; Benchmark Dose, BMD; Reference Dose, RfD; Threshold Limit Value, TLV; etc.). Since biological responses of tissues and organs are mechanistically linked to the local concentration of the active form of trace metal, the internal dose of the metal that reached a particular physiological compartment should be used for any meaningful risk or benefit characterization [4].

1 PK MODELING METHODS

Several modeling and computing methods have been used for analysis and presentation of PK data, estimation of PK parameters, extrapolation between the experimental data points and simulation of disposition of metals (absorption, distribution, metabolism and excretion; ADME). Mathematical methods used in pharmacokinetic modeling can be subdivided into (a) descriptive and (b) predictive [4].

1. *Descriptive PK models* – Descriptive PK models that simulate metal concentration in the tissue over time may be valuable for extrapolating the system variables between the experimental data points, but they often fail in extrapolations beyond the range of experimental calibrations.

A nonlinear regression analysis is an example of the descriptive mathematical method, in which

Handbook of Elemental Speciation II: Species in the Environment, Food, Medicine & Occupational Health
Edited by R. Cornelis, H. Crews, J. Caruso and K. G. Heumann
 ISBN: 0-470-85598-3 (HB)

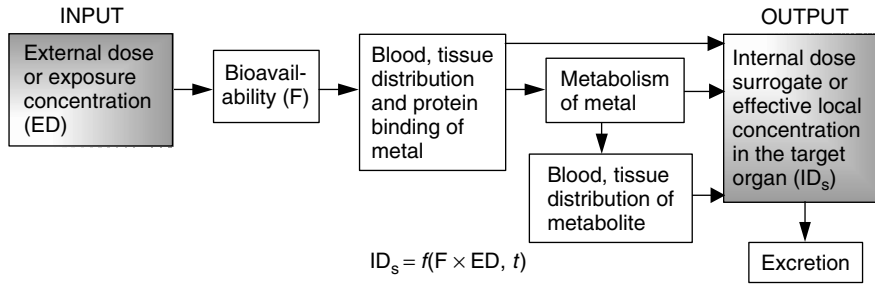

Figure 3.3.1.1. A general concept of the pharmacokinetic (PK) modeling of trace metals, where t is time.

parameters of the equation for a continuous curve of metal concentration in the tissue over time are fit into the experimental data points. The pitfall of such a curve-fitting is that even if one succeeds in finding equations that duplicate the behavior of the PK system, their internal workings may be very different from the internal mechanism of the real biological system. The simulations only 'mimic' kinetic behavior of the metal and do not provide insight into the quantitative or mechanistic relations between the internal components of the real system. Parameters of the fitted equations are often artificial and arbitrary, without physicochemical and/or physiological meaning.

Calculations of PK parameters based on phenomenological data analysis, such as curve fitting, curve stripping or feathering, area under the curve (AUC) estimate, and so on, are sometimes called 'model-independent' because they are apparently free of any assumption about underlying compartmental model that the chemical obeys. Examples of some computerized software useful for curve fitting, descriptive modeling and noncompartmental phenomenological PK data analysis include (a) Curve-fitting and statistical programs (e.g. MS Excel, Crystal Ball, TopFit, SigmaStat, SAS), and (b) Noncompartmental programs (e.g. PK Solutions, NCOMP, WinNonlin, NONMEM) [4].

In contrast to the above, classical compartmental PK models describe linear systems in which the rate of transfer of the chemical from one compartment to another is directly proportional to the total mass of the chemical in this compartment. For the multicompartment linear system, the concentration in the 'i-th' compartment ($C_{i(t)}$ in $\mathrm{mg\,L^{-1}}$) is a sum of exponential terms of the form

$$C_{i(t)} = A_i \times e^{-\alpha t} + B_i \times e^{-\beta t} + \cdots + N_i \times e^{-\gamma t} \quad (3.3.1.2)$$

where each term represents a partial contribution to the total concentration in the 'i-th' compartment. A, B, N are proportionality constants (macroconstants in $\mathrm{mg\,L^{-1}}$), α, β, γ are rate constants (microconstants in $\mathrm{l\,h^{-1}}$) and t is time (h). Equations of this type may be fitted to the data with nonlinear regression programs or resolved into two or three or more linear components using a method of residuals or curve stripping or feathering [5].

Examples of the computerized software useful for classical multicompartmental PK modeling include Simulation Analysis and Modeling (SAAM) and Conversational SAAM (CONSAAM), with updates WinSAAM and SAAM II; XLMEM for up to three-compartment systems, and so on. As an example, a relatively simple classical compartmental model, developed for PK of nickel in human volunteers [6], is described below (Section 2). More elaborated linear multicompartmental model was developed to simulate PK of cadmium in humans [7].

However, in reality, ADME of metals in biological systems are usually nonlinear and thus cannot be accurately described by a single elimination rate constant in each compartment for a wide range of concentrations. These nonlinearities are well handled by physiologically based pharmacokinetic (PBPK) models but not by classical compartmental PK models.

2. *Predictive PBPK models* – The PBPK models exemplify a predictive method, in which parameters of the PBPK model quantitatively

describe relations between the internal workings and correspond to the physicochemical and physiological properties of the PK system. The PBPK model provides insight into the mechanisms of ADME of the chemical within the biological system, and reflects as well as describes the real physiological phenomena of interaction between the chemical and the organism, usually expressed by nonlinear relationships [8].

In PBPK modeling, there is no need for assumptions of a steady state or first-order kinetics. These predictive models, when properly calibrated and validated, may be used beyond the range of experimental data points, and thus they can still reliably predict the behavior of trace metals in PK systems in regions where no information is available. This is often impossible with classical PK models that are data-based and easily fail in extrapolations. Examples of the computerized software useful for predictive PBPK simulations include Simulation Control Program (SCOP); Advanced Continuous Simulation Language (ACSL, ACSL Math, ACSL Optimize, ACSL Tox, etc.). As an example, a relatively complex PBPK model of chromium, developed by O'Flaherty *et al*. [9], is described below (Section 3). An even more elaborated PBPK model had to be developed to simulate accurately PK of methylmercury in pregnant and developing humans [10, 11].

2 DESCRIPTIVE PK MODELS OF NICKEL AND CADMIUM

1. *Nickel*

a. *Noncompartmental approach* – In the simplest, noncompartmental approach, the nickel (total nickel, Ni) retention in the human body can be estimated from the following equations [12].

$$A = R \times C \times V \times T \qquad (3.3.1.3)$$

where A is amount of Ni accumulated in the respiratory tract (μg); R is a percentage of Ni retention in the respiratory tract (75%); C is concentration of Ni in the inhaled air ($\mu g\,m^{-3}$); V is pulmonary ventilation (for 8 h sleep $-0.0075\ m^3\,min^{-1}$; for 8 h active $-0.02\ m^3\,min^{-1}$; for 8 h work $-0.03\ m^3\,min^{-1}$); and T is duration of exposure (min). The formula (3.3.1.3) was calibrated by comparing the measured concentration of Ni in urine of occupationally exposed workers ($C = 7\ \mu g\,m^{-3}$) and nonexposed adults from the industrial region (Zawiercie, Poland; $C = 0.0253\ \mu g\,m^{-3}$) with the estimated concentration. The concentration of Ni in urine was linked to the amount retained in the body using the following formula [12].

$$Y = (0.25A + Z + P) \times 0.7/1.4 \qquad (3.3.1.4)$$

where Y is estimated Ni concentration in urine ($\mu g\,L^{-1}$); A is amount of Ni accumulated in the respiratory tract (μg); 0.25 is coefficient of Ni permeation from the lung to the blood stream; Z is amount of Ni in blood (μg) from dietary intake, assuming 3% absorption from the gastrointestinal tract; P is amount of Ni in blood (μg) from complimentary mineral water (provided to workers); 0.7 is coefficient of the relationship between Ni content in urine and blood; 1.4 is volume of daily urine (L). Finally, on the basis of statistical fit (correlation coefficient $r = 0.973$) of the modeled estimates to the Ni amounts calculated from mass balance of the measured data, the following relationship was developed between Ni concentration in urine (Y) and the amount of Ni absorbed (internal dose, D in μg).

$$D = 3.07Y - 12.56 \qquad (3.3.1.5)$$

where 3.07 is the proportionality coefficient; and 12.56 is the constant value [12].

In the above example, a linear relationship was assumed between exposure concentration of Ni in the air (C) and its internal dose (D). While this simple quantitative model cannot be directly validated in the exposed humans, the concentration of Ni in urine (Y) representing the internal dose surrogate may serve as a biomarker of exposure as it is available for experimental measurement. The obvious deficiency of this model was that the internal dose has no physiological meaning because Ni may be distributed between blood and many other tissues or body compartments. Also, time after exposure was not considered as a variable in this model, which implies a steady

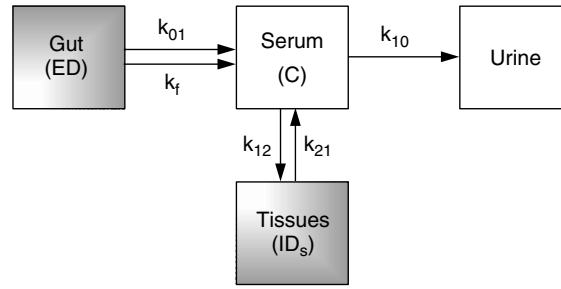

Figure 3.3.1.2. Schematic diagram of compartmental PK model of soluble nickel in humans, after Sunderman [6], where C is concentration of nickel in serum ($\mu g\,L^{-1}$), k_{01}, k_{10}, k_{12}, k_{21} are intercompartmental mass transfer first-order rate constants ($1\ h^{-1}$), k_f is pseudo-zero-order rate constant ($\mu g\,h^{-1}$).

state (a state of equilibrium between external and internal Ni concentrations). A comprehensive dosimetry model of inhaled Ni compounds, that included Ni speciation, has been developed by Yu *et al*. [13].

b. *Compartmental model* – Both time and body compartments were crucial features of the tri-compartment model of soluble nickel (Ni^{2+}) developed in human volunteers [6]. The rudimentary compartments included gut, blood serum and body tissues (Figure 3.3.1.2.). Concentrations of Ni^{2+} in the blood serum compartment (C in $\mu g\,L^{-1}$) as well as its cumulative amount in the urine evolved over time according to the following equation.

$$C = C_0 + F \times ED \times k_{01} \times (A_1 \times e^{-L1t} + A_2 \times e^{-L2t} + A_3 \times e^{-k01t})/V_1 \qquad (3.3.1.6)$$

where C_0 is baseline concentration of Ni^{2+} in serum ($\mu g\,L^{-1}$), calculated from pseudo-zero-order rate constant for intestinal absorption, k_f ($0.1\ \mu g\,h^{-1}$); F is bioavailability, defined as the mass fraction of Ni^{2+} absorbed from the oral dose of Ni_2SO_4 in water (27%) or food (0.7%); ED is dose of Ni_2SO_4 ingested (μg); k_{01} is first-order rate constant of Ni^{2+} absorption from GI tract ($0.3\ h^{-1}$); A_1 is algebraic macroconstant derived for the first exponential term as $(L_1 - k_{21})/(k_{01} - L_1)(L_1 - L_2)$; L_1, L_2 are hybrid microconstants calculated from rate constants k_{10} ($0.2\ h^{-1}$), k_{12} ($0.4\ h^{-1}$), and k_{21} ($0.08\ h^{-1}$); A_2 is algebraic macroconstant derived for the second exponential term as $(k_{21} - L_2)/(k_{01} - L_2)(L_1 - L_2)$; A_3 is algebraic macroconstant derived for the third exponential term as $-(A_1 + A_2)$; V_1 is plasma volume (L). The numerical values of parameters, which bore substantial standard deviations, are rounded-up numbers from Sunderman [6].

This kinetic model assumed uniform distribution of Ni^{2+} between all body tissues, did not address biliary excretion and the following enterohepatic recirculation of Ni^{2+}, and actually, only the concentrations of Ni^{2+} in blood serum and urine were calibrated with experimental data. Even though Menzel [14] has proposed to develop a PBPK model for nickel that would address the enterohepatic recirculation and some target tissues (spleen, lymph nodes, testes, kidney, etc.), this comprehensive model has not been published in its final form yet.

2. *Cadmium* – Kjellström and Nordberg [7, 15] developed a multicompartmental model for cadmium (Cd) in humans, based on the linear one-compartment PK model of Friberg *et al*. [16]. Their model accounted for age-dependent changes in the rate of Cd transfer from blood to urine and changes in the caloric intake. The model, schematically shown in Figure 3.3.1.3, also includes quantitative description of the deposition and clearance of cadmium in the lung after Oberdörster [17] (KNOB model). The KNOB Kjellström, Nordberg and Oberdörster model for cadmium was encoded in the Advanced Continuous Simulation Language (ACSL) [4]; and its codes and numerical values of all parameters are available on-line [18]. The model parameters were from Kjellström and

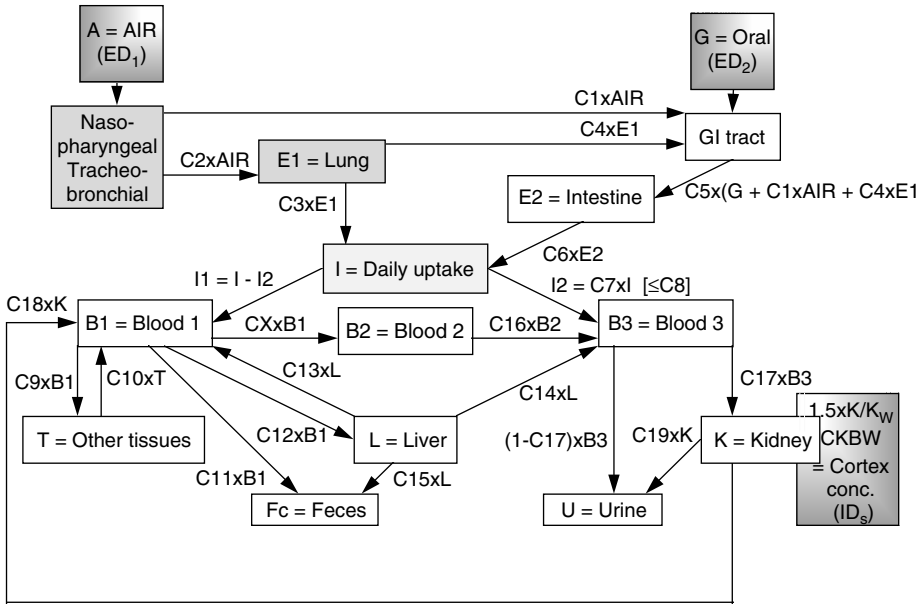

Figure 3.3.1.3. Schematic diagram of compartmental linear PK model of cadmium in humans, after Kjellström and Nordberg [7, 15]. The dotted area depicts description of the deposition and clearance of cadmium in the lung after Oberdörster [17]. C1–C19 are coefficients (rate constants and ratios); A and G are external dose rates (ED_1 and ED_2, respectively, in μg Cd/day); E1, E2, B1, B2, B3, T, L, K represent linear rates of change of Cd in body compartments (μg Cd/day); I is estimate of internal daily uptake (μg Cd/day); Fc and U are excretion rates (μg Cd/day), and CKBW is kidney cortex concentration (ID_s in μg/g of tissue); arrows show direction of Cd mass flow.

Nordberg [7, 15] and Oberdörster [17]. Parameters C17 decreased linearly by 33% from age 30 to age 80; C19 increased each year from age 30 with a rate constant 1.1×10^{-6} per day [15].

The KNOB model accepted an input of air cadmium concentration and total oral intake ($\mu g\ day^{-1}$) but did not have parameters for specific media (e.g. drinking water, food, soil), although it can be modified to accommodate such input. The KNOB model simulated the uptake, accumulation and elimination of cadmium in eight compartments that represented the lung, gastrointestinal tract, blood (three compartments), liver, kidney and 'other tissues'. The KNOB model was calibrated with data collected from humans and was intended for human risk assessment applications.

An example of simulation by the KNOB model is shown in Figure 3.3.1.4. The simulation was for renal cortical Cd concentrations ($\mu g\ g^{-1}$), at various ages, that result from a chronic cadmium intake of 20 μg Cd/day (age-adjusted based on age-specific caloric intake) to yield an average lifetime Cd intake of approximately 0.3 $\mu g\ kg^{-1}\ day^{-1}$. The major contributors to the nonlinearity of the renal cortical cadmium concentration are the age-related caloric intake changes and the aging kidneys. The gradual drop in cadmium concentration after age 50 years paralleled the decline in caloric intake over this age range and reflected age-related changes in kidney function. The same trend was seen in similar simulations reported by Kjellström and Nordberg [7]. Estimates of dietary Cd intake in areas of 'normal' exposure in Europe, New Zealand and United States are 10–41 $\mu g\ day^{-1}$ (0.14–0.59 μg Cd/kg/day); thus, the simulation shown in Figure 3.3.1.4 represents the midpoint in the range of reported estimates [19]. Peak renal cortical Cd concentrations associated with 10 μg Cd/day and 40 μg Cd/day (0.1–0.6 μg Cd/kg/day) were 7 μg Cd/g and 27 μg Cd/g,

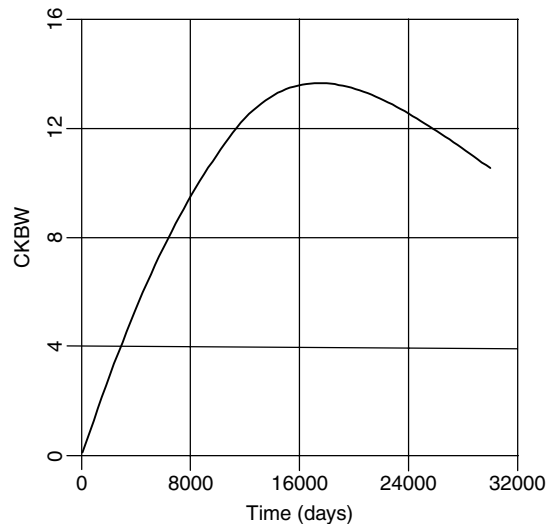

Figure 3.3.1.4. An example of computer-aided simulation of normal age-dependent renal cortical concentration of Cd (CKBW in $\mu g\, g^{-1}$ tissue wet weight) resulting from lifetime (82 years) continuous oral exposure to midpoint of 20 μg Cd/kg day. The simulation was performed by KNOB model encoded in ACSL [4], and equations were solved simultaneously with the ACSL Tox software using a personal computer.

respectively, and also occurred between the ages of 45 and 55 years.

This descriptive model did not address any potential for interspecies extrapolations. In general, the phenomenological approach does not allow inclusion of biological variability into the model to address the interspecies extrapolations or the population distributions of internal dose metric. Moreover, simulation of the deposition and elimination of cadmium in the respiratory tract used parameter values for adults (ages 20–75 yrs; e.g. an estimate of the adult breathing volume (day-volume) of 20 $m^3\, day^{-1}$). Although it would be possible to modify the KNOB model to simulate these parameters in young children, this was not attempted. Even though Frazier [20] has proposed to develop a PBPK model for Cd that could be allometrically scaled and address the growing child as well as an adult, this comprehensive model has not been published in its final form yet.

3 PREDICTIVE PBPK MODEL OF CHROMIUM

O'Flaherty [21] developed a predictive PBPK model for chromium (Cr) in rats. This model was based in part on the earlier model of lead, expanded for the redox metabolism of Cr in tissues and calibrated with experimental data for intravenous, oral and inhalation exposures to Cr^{3+} and Cr^{6+}. The model, schematically shown in Figure 3.3.1.5, included quantitative description of the deposition and clearance of Cr in the lung. In the model, inhaled Cr is deposited into bioavailable pool (A) in the lung, from which it can be absorbed into circulating blood, cleared into the gastrointestinal tract, and/or deposited into nonbioavailable lung pool (B). From the pool B, Cr can move only to the gastrointestinal tract. About 85% of Cr^{+6} entering gastrointestinal tract *per os* was reduced to Cr^{+3} before it could reach intestinal absorption sites. Distribution of Cr^{+6} into tissues was modeled as a rapid, plasma flow-limited process, whereas tissue distribution of Cr^{3+} depended on a slower diffusion through the cellular membranes. Important feature of this model was the attempt to describe quantitatively incorporation of Cr into bone [21]. The pharmacokinetic model parameters and intracompartmental Cr clearance values have been listed by the Agency for Toxic Substances and Disease Registry (ATSDR) and are available on the World Wide Web [22].

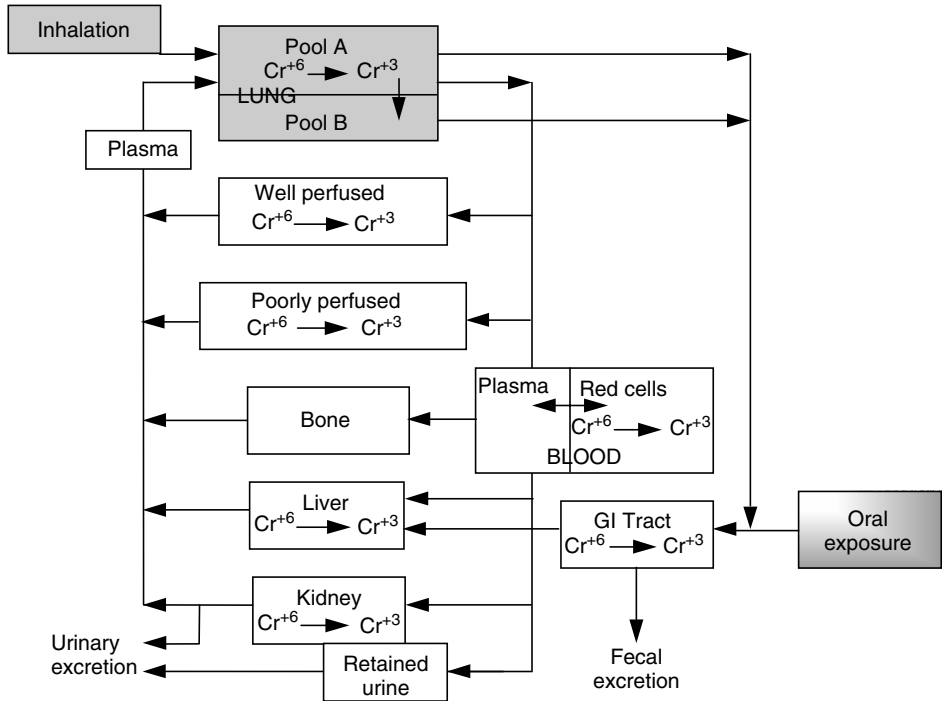

Figure 3.3.1.5. Schematic diagram of predictive PBPK model of chromium, after O'Flaherty [21]. This model was adapted to simulate metabolism and disposition of ingested Cr in humans [9]. In the PBPK model for humans, the dotted area was omitted. Rectangles depict separate tissue compartments, arrows show direction of Cr mass flow. In all tissue compartments, except blood plasma and bone, Cr^{+6} is reduced to Cr^{+3}.

The O'Flaherty PBPK model of Cr was adapted to allow kinetic description of ADME of ingested Cr^{+6} and Cr^{+3} in humans [9]. The lung compartment was not included in this PBPK model, as the calibration was performed with data from blood and urine of adult human volunteers drinking solutions of chromic or dichromate salts at varying concentrations and did not involve inhalation. The model accounted for age-dependent changes in body weight and volumes of tissue compartments, including the rate of bone formation. The complete model codes, written in ACSL, along with physiological parameters and body growth functions are given in the appendix to the publication by O'Flaherty *et al*. [9].

The kinetics of distribution, metabolism and excretion of Cr was not affected by the oxidation state of the ingested Cr, in contrast to the amount absorbed. The fraction absorbed from the orally administered salts of Cr^{+6} was highly variable, depending on the stomach content. In general, metals are better absorbed in fasted than fed individuals [23].

However, quantification of nutritional status was not included in this PBPK model. It remains virtually unknown how the diet containing exclusively milk may affect the bioavailability and absorption of Cr in the nursing infant.

4 OTHER SUCCESSFUL PBPK MODELS OF METALS

1. *PBPK model of methylmercury in human gestation and development* – Byczkowski and Lipscomb [11] developed a comprehensive predictive PBPK model for lactational transfer of methylmercury (MeHg) to the newborn exclusively breast-fed infant. The model was built as an extension of the PBPK description of

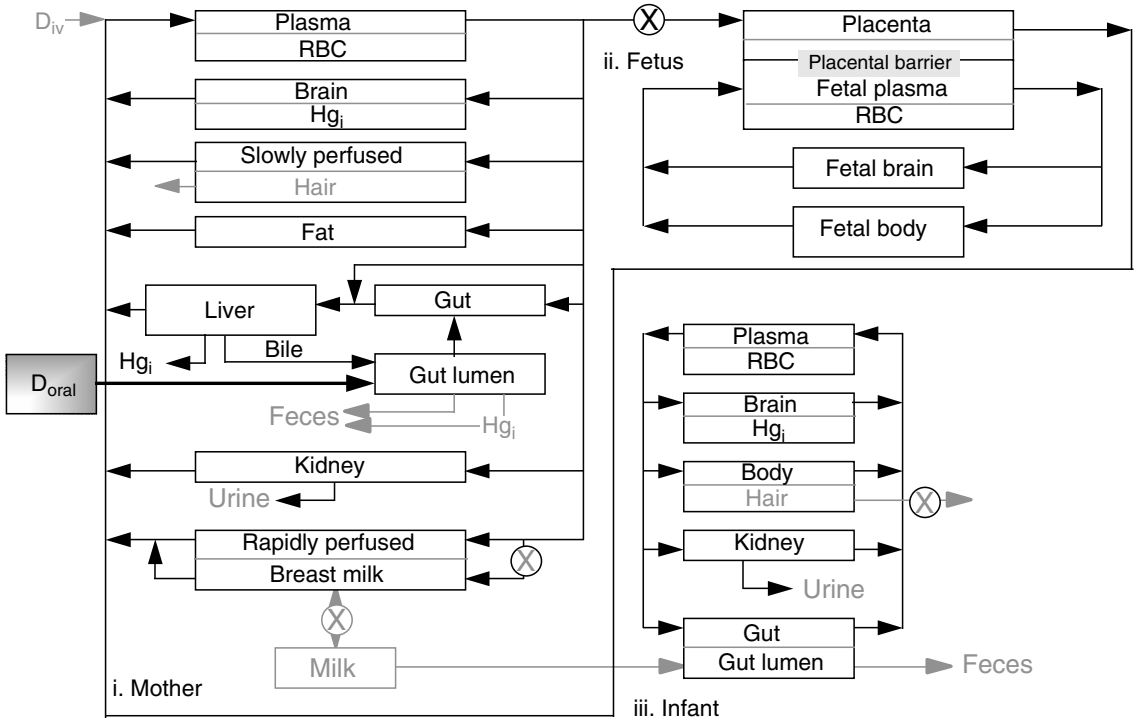

Figure 3.3.1.6. Schematic diagram of predictive PBPK model of methylmercury in mother and developing child, after Byczkowski and Lipscomb [11]. ⊗ – time-dependent *on/off* switches; D_{oral} – oral dose of MeHg (mg kg^{-1} day^{-1}); D_{iv} – intravenous dose of MeHg (mg h^{-1}); Hg_i – inorganic mercury; RBC – red blood cells. The model source codes for breast-milk compartment, logical switches and infant module are available on the World Wide Web [27].

MeHg in pregnant mother and her fetus [10]. A schematic diagram of this model is shown in Figure 3.3.1.6. The PBPK model of MeHg consisted of three modules for (a) mother, (b) fetus, and (c) infant (Figure 3.3.1.6). The first two modules were adopted from Gearhart *et al*. [24] with modifications and parameters as listed by Clewell *et al*. [10] A breast-milk compartment was added to the mothers' module, according to Byczkowski [25], and the third module for a nursing infant was built by analogy to a previously published PBPK model for lactational transfer of perchloroethylene in rats [26].

The PBPK model of MeHg was encoded in ACSL [11]. Governing algorithms of the lactational module included time-dependent logical switches, turning *on* and *off* fetus or infant modules. The lactation (milk yield, OUTI in L h^{-1}) was turned *on/off* along with the infant module by the following procedural statements.

$$\text{IF(.NOT.LAC)OUTI} = 0. \tag{3.3.1.7}$$

$$\text{IF(LAC)OUTI} = \text{INTAKE} \times \{[\text{PNO} \times (\text{WBODY} - \text{VFeA})]^{0.2}\}/(1.15 \times 24) \tag{3.3.1.8}$$

where LAC is logical constant (either. TRUE. or. FALSE.), INTAKE is fraction of the breast milk yield that is ingested by infant (default = 1), VFeA is initial body weight of infant (BWP = 2.5 kg), PNO is number of simultaneously breast-fed infants and WBODY is growing infant body weight. Infant body weight increased according to the growth function described by O'Flaherty *et al*. [9]. Time-dependent *on/off* switch (SWTCH) was turned *off* during the pregnancy and *on* during

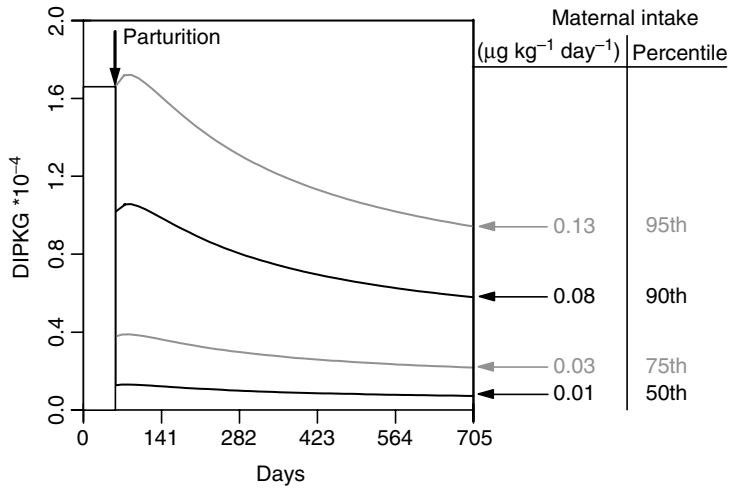

Figure 3.3.1.7. Examples of computer-aided simulations of age-dependent daily intakes of MeHg (DIPkg in mg kg^{-1} day^{-1}) by normal, exclusively breast-fed female infant whose mother was exposed to either 50^{th}, 75^{th}, 90^{th} or 95^{th} percentile of the US average MeHg nutritional intake (ADDmat in μg kg^{-1} day^{-1}), according to the NHANES III survey tables. The PBPK simulations included growth functions for both physiological infant body growth and increased intake of breast milk. Simulations were performed by MeHg model encoded in ACSL [11], and equations were solved simultaneously with the ACSL Tox software using a personal computer.

the lactation period:

$$\text{IF(T.LT.TLac)SWTCH} = 0. \quad (3.3.1.9)$$

$$\text{IF(T.GE.TLac)SWTCH} = 1. \quad (3.3.1.10)$$

where T is time from starting simulation (h), TLac equals time of conception from start *plus* length of pregnancy (h).

The rate of change of the MeHg amount in milk (RMAT in mg h^{-1}) was described as follows.

$$\text{RMAT} = \text{fQMT} \times \text{SWTCH} \times \text{QR} \times (\text{CP} - \text{CVMT}) - \text{RPUP} \quad (3.3.1.11)$$

where fQMT is fraction of rapid plasma flow that goes to mammary tissue (defaulted at 0.1) if time-dependent *on/off* switch SWTCH = 1, CP is MeHg concentration in plasma (mg L^{-1}), CVMT is MeHg concentration in mammary venous blood equilibrated with milk, QR is plasma flow through rapidly perfused tissues (L h^{-1}) allometrically scaled to the maternal body weight (BW in kg):

$$\text{QR} = \text{QCC} \times (\text{BW}^{0.75}) \times (1 - \text{HCT}) \quad (3.3.1.12)$$

where QCC is cardiac output (20 L/h/$kg^{0.75}$) and HCT is a hematocrit. Elimination rate of MeHg from milk to infant (RPUP in mg h^{-1}) was described as follows.

$$\text{RPUP} = \text{SWTCH} \times \text{OUTX} \times \text{CMAT} \quad (3.3.1.13)$$

and was equal to dose rate of MeHg ingestion by infant, where OUTX is milk intake = milk yield (OUTI) from equation (3.3.1.7) or (3.3.1.8), CMAT is MeHg concentration in breast milk (mg L^{-1}). The complete ACSL source codes and parameters of the lactational module are available on the World Wide Web [27].

Examples of simulations by the MeHg model are shown in Figure 3.3.1.7. These simulations were for daily intake of MeHg with milk by exclusively breast-fed 'average' female infant of the mother exposed to MeHg in food (mainly fish). The PBPK simulations, shown in Figure 3.3.1.7, were performed for the 50^{th}, 75^{th}, 90^{th} and 95^{th} percentile of the United States average MeHg nutritional intake (ADDmat in μg kg^{-1} day^{-1}), according to the NHANES III survey tables, assuming a normal age-dependent body growth and intake of breast milk. The major contributors to the nonlinearity of the infant MeHg daily intake (expressed per kg of body weight) were

these growth-related physiological changes in body weight and breast-milk intake.

2. *Biokinetic model of lead (IEUBK)* – The US EPA Technical Review Workgroup for Lead (TRW) [28] developed an integrated exposure uptake biokinetic (IEUBK) model for lead (Pb) in children. The IEUBK model may be used to estimate, for a hypothetical child or population of children, a plausible distribution of blood Pb levels, centered on a geometric mean blood Pb concentration, which depends, in turn, on exposure concentrations of Pb in different environmental media. The model relates blood Pb levels in children from 6 month to 7 years of age to environmental Pb concentrations in air, diet, dust, paint, soil, and water [29]. A schematic diagram of this model is shown in Figure 3.3.1.8. The IEUBK model of Pb consisted of three modules for (a) exposure, (b) uptake, and (c) biokinetics (Figure 3.3.1.8). The fourth component, the probability distribution module, estimated the probability of a certain outcome (e.g. the health-based blood Pb level of concern, assumed to be 10 μg dL^{-1}) in an exposed child, on the basis of the parameters used in the model. The calibration of IEUBK model was based on extensive epidemiological data, the model has been well documented, thoroughly peer-reviewed, and partially validated with empirical data [30].

Examples of IEUBK model simulations of probability distributions of blood Pb exceeding the specified level in a hypothetical population of children (from 6 month to 7 years of age), exposed to specified range of Pb concentrations in soil (200–400 mg Pb/kg), are shown in Figure 3.3.1.9. These predictions may be considered as distribution of the likely risk to children to suffer adverse health effects caused by the elevated blood Pb concentration resulting from the exposure to Pb in soil.

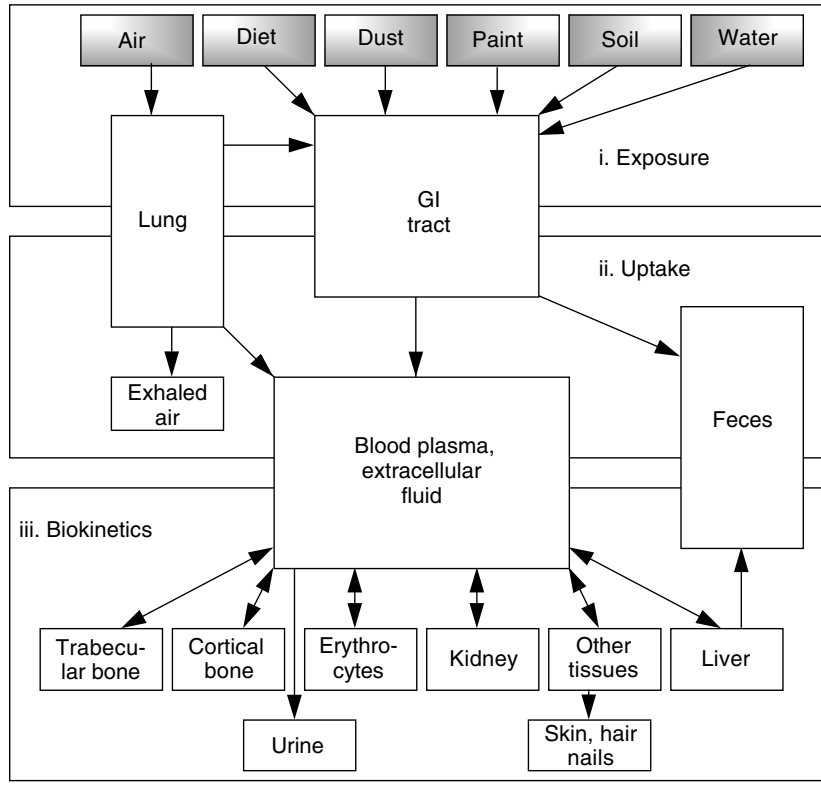

Figure 3.3.1.8. Schematic diagram of integrated exposure uptake biokinetic (IEUBK) model of lead in developing children, after US EPA – TRW [28].

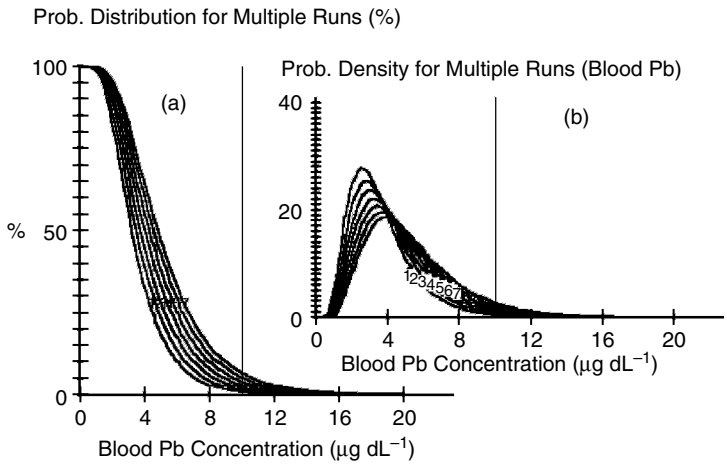

Figure 3.3.1.9. Examples of computer-aided simulations of probability distributions of the excess of blood Pb levels (presented on the x-axis in $\mu g\ dL^{-1}$) in children from 6 months to 7 years of age, exposed to 200–400 mg Pb/kg of soil. The range of geometric mean blood Pb concentrations was from 3.4 to 5.1 $\mu g\ dL^{-1}$; the health-based blood Pb level of concern is 10 $\mu g\ dL^{-1}$ (cutoff represented by thin vertical lines). (a) Cumulative distributions of probabilities. (b) Probability densities. Simulations were performed with the IEUBK model for Windows, available from US EPA – TRW [28], using a personal computer.

While the IEUBK model simulations may serve as a reasonably good predictor of community blood Pb levels, the accurate estimate for a specific individual or a specific group of children would require a site-specific input data, instead of the IEUBK defaults and adjustments to the geometric standard deviation. Collection of such a site-specific information may be very expensive, time-consuming and in some cases not feasible. Because the IEUBK model has been based on population data, any site-specific unique features (e.g. bioavailability of a site-specific Pb compound) may cause lack of agreement between observed and predicted blood Pb concentrations. This model does not address acute exposures to Pb and cannot be used in cases of Pb poisoning.

5 CONCLUSIONS

Pharmacokinetic modeling of trace metals represents a multidisciplinary challenge, involving necessary understanding of biology, physiology, pathology and biochemistry of the organism on one hand, and physical chemistry and metabolism of the metal compounds on the other. In addition, the development of a useful model requires from a modeler a rigorous mathematical approach and some experience in computer programming. In return, successful PK models have enormous potential to organize a variety of sometimes inconsistent experimental data into a coherent system. This is crucial for derivation of dose-response relationships of trace metals and helpful for planning additional experiments designed to fill any gaps in the current knowledge. Quantitative modeling of PK is by nature an interactive process in which the level of detail in the model depends on the available experimental data, and the developing model points out to any missing datum, necessary to increase the agreement between observed and predicted variables.

For many applications, a rudimentary quantification of the trace metal disposition using a nonlinear regression algorithm is all that is needed to reconcile the experimental data and to simulate the ADME of a trace metal. The noncompartmental model of Ni retention in the human body may serve as an example of such a case. On the other hand, for applications to complicated PK systems, such as a pregnant woman or a mother nursing her infant, as well as for cases of trace metals that undergo a complex metabolism (e.g. multiple changes of valency, alkylation/dealkylation,

protein binding, etc.) much more elaborated PK models are needed. The PBPK models, which reflect both the internal working of the PK system and the metabolic complexity of the trace metal, are best suited to solve these complicated cases. Moreover, in the PBPK model the predicted concentration of a trace metal within the target tissue may be interlinked with the kinetics of binding to the macromolecular ligands or other cellular receptors, giving the possibility of constructing biologically based dose-response or pharmacodynamic models that could predict the biological effects of trace metals.

The utility of PBPK models was demonstrated by O'Flaherty [31] using three major problems in metal PK as examples: (a) bioavailability of lead, (b) factoring of total chromium disposition into separate contributions of Cr^{+3} and Cr^{+6}, and (c) inconsistency in experimental PK data of uranium. Unfortunately, the progress in developing the PBPK models of trace metals is slow. In 1998, O'Flaherty [23] was able to list only three metals, chromium, mercury and lead, and one metalloid, arsenic, whose PKs have been modeled with some degree of completeness. To date, this list remains unchanged. This points out to the necessity of future research, aimed at resolving the kinetic behavior of trace metals and to the importance of gathering experimental data supporting further development and refinement of quantitative PK models of trace metals.

A statement, attributed to Box [32], claims that 'all models are wrong but some are useful'. Among those useful models, the PBPK description of the trace metal ADME is the most useful one because of its completeness, quantification of the internal mechanistic workings of the biological system and the metal chemistry and, finally yet importantly, its predictive power.

6 REFERENCES

1. Kulkarni, A. P. and Byczkowski, J. Z., Effects of transition metals on biological oxidations, in *Environmental Oxidants, Advances in Environmental Sciences and Technology*, Nriagu, J. O. (Ed.), John Wiley & Sons, New York, 1994, Chapter 16, pp. 475–496.
2. Byczkowski, J. Z. and Sorenson, J. R. J., *Sci. Total Environ.*, **37**, 133 (1984).
3. Menzie, C. A., *Belle Newslett.*, **10**(1), 7 (2001). Also available on the World Wide Web: http://www.belleonline.com/n7v101.html
4. Byczkowski, J. Z., Pharmacokinetic/dynamic modeling, in *Standard Handbook of Environmental Science, Health and Technology*, Lehr, J. (Ed.), McGraw-Hill, New York, 2000, Chapter 8.6.
5. Gibaldi, M. and Perrier, D., *Pharmacokinetics*, 2nd ed., Marcel Dekker, New York, 1982.
6. Sunderman, F. W. Jr., Toxicokinetics of nickel in humans, in *Nickel and Human Health, Current Perspectives*, Advances in Environmental Sciences and Technology, Nieboer, E. and Nriagu, J. O. (Eds.), John Wiley & Sons, New York, 1992, Chapter 5, pp. 69–76.
7. Kjellström, T. and Nordberg, G. F., *Environ. Res.*, **16**, 248 (1978).
8. Yang, S. H. and Andersen, M. E., Pharmacokinetics, in *Introduction to Biochemical Toxicology*, 2nd ed., Hodgson, E. and Levi, P. E. (Eds.), Appleton & Lange, Norwalk, CT, 1994, Chapter 3, pp. 49–73.
9. O'Flaherty, E. J., Kerger, B. D., Hays, S. M. and Paustenbach, D. J., *Toxicol. Sci.*, **60**, 196 (2001).
10. Clewell, H. J., Gearhart, J. M., Gentry, P. R., Covington, T. R., VanLandingham, C. B., Crump, K. S. and Shipp, A. M., *Risk Anal.*, **19**, 547 (1999).
11. Byczkowski, J. Z. and Lipscomb, J. C., *Risk Anal.*, **21**, 869 (2001).
12. Rozanska, R., Baranowska-Dutkiewicz, B. and Dutkiewicz, T., *Int. J. Occupat. Med. Environ. Health*, **9**, 37 (1996).
13. Yu, C. P., Hsieh, T. H., Oller, A. R. and Oberdörster, G., *Regul. Toxicol. Pharmacol.*, **33**, 165 (2001).
14. Menzel, D. B., *Toxicol. Lett.*, **43**, 67 (1988).
15. Kjellström, T. and Nordberg, G., Kinetic model of cadmium metabolism, *Cadmium and Health: A Toxicologic and Epidemiological Appraisal*, *Exposure, Dose and Metabolism, Vol. I*, CRC Press, Boca Raton, FL, 1985, pp. 179–197.
16. Friberg, L., Piscator, M., Nordberg, G. F. and Kjellström, T., *Cadmium in the Environment*, CRC Press, Cleveland, OH, 1974, pp. 79–89.
17. Oberdörster, G., Deposition and retention modeling of inhaled cadmium in rat and human lung: an example for extrapolation of effects and risk estimation, *Extrapolation of Dosimetric Relationships for Inhaled Particles and Gases*, Academic Press, New York, 1989, pp. 345–370.
18. Byczkowski, J. Z., *Linear PK Model for Cadmium Inhalation – KNOB, Codes and Parameters*, available on the World Wide Web: http://members.aol.com/januszb/knob.htm, 2004.
19. ATSDR (Agency for Toxic Substances and Disease Registry), *Toxicological Profile for Cadmium*, U.S. Department of Health and Human Services, Public Health Service, Atlanta, GA, 1999. Also available on the World Wide Web: http://www.atsdr.cdc.gov/toxprofiles/tp5.html

20. Frazier, J. M., Need for physiologically based toxicokinetic models estimating target organ dosage following oral ingestion of cadmium, in *Water Contamination and Health*, Wang, R. G. M. (Ed.), Marcel Dekker, New York, 1994, pp. 281–304.
21. O'Flaherty, E. J., *Toxicol. Appl. Pharmacol.*, **138**, 54 (1996).
22. ATSDR (Agency for Toxic Substances and Disease Registry), *Toxicological Profile for Chromium*, U.S. Department of Health and Human Services, Public Health Service, Atlanta, GA, 2000. Also available on the World Wide Web: http://www.atsdr.cdc.gov/toxprofiles/tp7.html
23. O'Flaherty, E. J., *Crit. Rev. Toxicol.*, **28**, 271 (1998).
24. Gearhart, J. M., Clewell, H. J. III, Crump, K. S., Shipp, A. M. and Silvers, A., *Water, Air, Soil Pollut.*, **80**, 49 (1995).
25. Byczkowski, J. Z., *Drug Inf. J.*, **30**, 401 (1996).
26. Byczkowski, J. Z., Kinkead, E. R., Leahy, H. F., Randall, G. M. and Fisher, J. W., *Toxicol. Appl. Pharmacol.*, **125**, 228 (1994).
27. Byczkowski, J. Z., *Codes of a PBPK Model for Lactational Transfer of Methylmercury*, available on the World Wide Web: http://members.aol.com/januszb/MeHgLac.htm, 2004.
28. U.S. EPA – TRW (U.S. Environmental Protection Agency – Technical Review Workgroup for Lead), *The Integrated Exposure Uptake Biokinetic (IEUBK) Model for Lead in Children*, Build 244 posted on October 15, 2001, available on the World Wide Web: http://www.epa.gov/superfund/programs/lead/prods.htm
29. White, P., Van Leeuwen, P., Davis, B., Maddaloni, M., Hogan, K., Marcus, A. and Elias, R., *Environ. Health Perspect.*, **106**(Suppl. 6), 1513 (1998).
30. Zaragoza, L. and Hogan, K., *Environ. Health Perspect.*, **106**(Suppl. 6), 1555 (1998).
31. O'Flaherty, E. J., *Toxicol. Lett.*, **82/83**, 367 (1995).
32. Box, G. E. P., Robustness is the strategy of scientific model building, in *Robustness in Statistics*, Launer, R. L. and Wilkinson, G. N. (Eds.), Academic Press, New York, 1979, p. 202.

3.3.2 Modeling of Biological Ligand Binding

Wojciech Bal

Institute of Biochemistry and Biophysics, Polish Academy of Sciences, Warsaw, Poland

Kazimierz Kasprzak

National Cancer Institute at Frederick, Frederick, Maryland, USA

The general approach in modeling interactions of trace elements within the body at the molecular level ideally consists of identification of potential tissue and cellular target molecules, their isolation or synthesis, followed by *in vitro* binding/reactivity studies under conditions most closely mimicking the 'native' situation. In reality, essential problems have to be overcome at each of these steps, and it is often necessary to use simplified models. These issues will be illustrated briefly with examples of studies of several metal ions relevant for toxicology.

1 IDENTIFICATION OF TARGETS FOR METAL IONS AS STUDY OBJECTS

There are two approaches possible for identification of biological ligands for a given metal ion. One, apparently straightforward, is based on isolation of species containing metal ions directly from biological material. This approach works fine for very strong and relatively inert complexes, like those in metalloenzymes or storage proteins, if they are present in the biological material at sufficiently high concentrations. These requirements stem from usually harsh conditions during standard tissue extraction procedures, with varying pH, concentrated buffers, and so on, which may cause metal loss directly or via protein denaturation. Positive examples include ceruloplasmin and albumin that transport copper in blood serum, metallothionein complexes with zinc, copper and cadmium, zinc finger proteins, hemoglobin and a number of essential enzymes. The modeling work is then focused on analysis of the structure of such isolated (or resynthesized) complexes and reproduction of their interactions with other molecules, like DNA, proteins, enzyme substrates and inhibitors, and so on. Such protein studies provide the main body of inorganic biochemistry and are described in standard textbooks. Even a vague discussion of

Handbook of Elemental Speciation II: Species in the Environment, Food, Medicine & Occupational Health
Edited by R. Cornelis, H. Crews, J. Caruso and K. G. Heumann
 ISBN: 0-470-85598-3 (HB)

this huge body of data would go beyond the scope of this chapter.

The above 'whole molecule' approach fails when molecules of interest are present in the biological material only in minute quantities. For proteins, in some cases, specific sequence motifs can be recognized. Then, homology searches of sequence databases can help identify target proteins. This option is reserved mainly for essential metal ions, and zinc finger motifs provide a good example here. Another interesting example, discussed below, is the N-terminal Cu(II)-binding site, discovered first in human serum albumin, which is also relevant for Ni(II). In cases where binding motifs are unique or adventitious (as for toxic metals), and for non-polymeric molecules, such as low-molecular-mass (LMM) ligands, no sequence data can be helpful. The isolation of such molecules from biological material in a metal-complexed form may pose difficulties, for example, due to inherent lability of such complexes. For such situations, the logical order of the study must be reversed. First, the assessment of binding properties of a given bioligand is done using coordination chemistry expertise. Then, the binding properties are studied *in vitro*, followed by reactivity studies. Such data can be used afterward for verification of relevance of the system studied, for example, by comparing stabilities or reactivity patterns. A further step may be necessary when the potential target molecule is complicated and/or difficult to handle experimentally. This regards, for example, a protein or a multiprotein complex with more than one metal binding site. In such instances, it is often possible to propose a simplified version of the target, for example, an oligopeptide mimicking the binding abilities of the whole protein. This approach is discussed below for studies of nickel interactions with histones and human protamine HP2.

2 FROM ALBUMIN TO PROTAMINE: THE N-TERMINAL XAA-YAA-HIS MOTIF FOR Cu(II) AND Ni(II) BINDING

Serum albumin is the most abundant serum protein in mammals, including humans, at a concentration of 0.63 mM [1]. It is a universal carrier for small molecules, including fatty acids, bilirubin, aromatic amino acids, hormones, drugs, and so on. It also participates in blood transport of many divalent metal ions, both essential [Ca(II), Zn(II), Co(II), Cu(II)] and toxic [Cd(II), Ni(II)], which bind at various sites on the albumin surface, often shared by more than one metal [2–4]. The best characterized, and also the most unique of them, is provided by the N-terminal Asp-Ala-His sequence, which exhibits specificity for Cu(II) and Ni(II) ions [5]. Studies of albumins from various species and synthetic and natural peptides reproducing their N-terminal sequences revealed that the essence of specificity is provided by the histidine residue at position three, in conjunction with the free amine at the N-terminus [4–8]. The precise nature of the first two amino acid residues is not critical for the formation of the specific metal complex because the binding of the metal ion is exerted by their amine and peptide amide nitrogens, rather than by side chain donors. This feature has been further confirmed by solid state and solution structures of several peptide analogs, which demonstrate an essentially identical metal binding core [9, 10]. The scheme of coordination and structures of complexes obtained by X-ray-guided NMR analysis are presented in Figure 3.3.2.1. Therefore, the binding motif can be named Xaa-Yaa-His. The alternative label, introduced by Sarkar, is ATCUN (Amino Terminal Cu and Ni) motif [5]. The metal-assisted deprotonation of peptide nitrogens, such as that observed in this motif, is extremely rare in proteins (at least for physiological metals) but is a common feature of simple, otherwise unstructured peptides. Earlier studies on amide coordination are summarized in the landmark review by Sigel and Martin [11], while the studies on coordination of His-containing peptides in the 1980s and the 1990s have been reviewed more recently [12].

The apparent simplicity of the metal-binding motif of albumins, limited just to three N-terminal amino acid residues, led to the usage of small peptides for modeling the coordination and reactivity of Cu(II) and Ni(II) with such motifs. The simplest possible, and thus the most

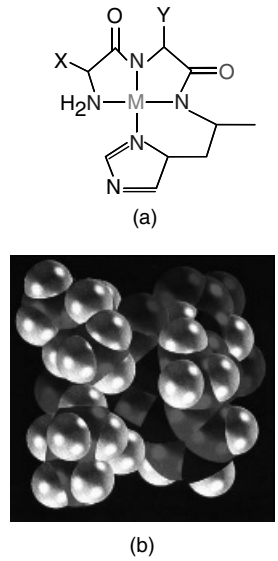

Figure 3.3.2.1. (Plate 2) (a) Scheme of coordination in a Xaa-Yaa-His- complexes of M = Cu(II) or Ni(II). (b) NMR structure of the Ni(II) complex of Val-Ile-His-Asn. (Reprinted with permission from Reference [10]. Copyright (1996), American Chemical Society.)

widely used, is tripeptide Gly-Gly-His. It has been used as a model for investigating stability of albumin complexes, kinetics of metal exchange reactions, and, following the discovery of easy formation of Ni(III) in Ni(II)-peptide complexes, for investigations of catalysis of redox processes (with an intention of reproducing the *in vivo* reactivity of toxic nickel) [13, 14]. These studies established that the Ni(II)-Gly-Gly-His complex could generate radical species, which were capable of damaging biological targets under air even in the absence of other oxidants/reductants. Also the analogous Cu(II) complex was studied in this respect, with an aim of providing a DNA cleaving agent that might be used therapeutically [15].

However, more detailed studies of the mechanism of reaction of the Gly-Gly-His complexes have revealed specific features of their redox reactivity that essentially disqualify them as model catalysts for oxidation of anything but themselves. Namely, the tripeptide complexes undergo oxidative decarboxylation, irreversibly transforming the His residue into hydroxyhistamine or dehydrohistidine, depending on conditions [9]. The Cu(II) and Ni(II) complexes of tripeptide amides or longer peptides (with any Xaa-Yaa-His- sequence; a dash following His indicates that the peptide chain goes on) are free of this deleterious process. Unlike Gly-Gly-His, they do not react with molecular oxygen but only with strong oxidants, such as hydrogen peroxide, oxone, or monoperoxyphthalate [14–16].

A considerable limitation for usage of the Xaa-Yaa-His- model is the complex stability. There is a wide variation of binding constants among the complexes of both Cu(II) and Ni(II), up to 6 log units in terms of β constants and 4 log units in terms of apparent binding constants at pH 7.4 [17]. The most stable ones known to date are those that contain nonprotein hydroxymethylserine residues [18], while the weakest ones include Gly-Gly-His and its histamine analog. Such an enormous spread of the binding constants within the same coordination mode has been explained by alterations of basicities of coordinating nitrogens, caused by the different side chains (with a fair linear correlation) [18], but it seems likely that steric/hydrophobic effects may also play some role [10, 17]. It is noteworthy that the binding constants estimated for albumin are at the low end of the range of all Xaa-Yaa-His- complexes for both Cu(II) and Ni(II). They are similar to those of Gly-Gly-His but are ca two orders of magnitude lower from those of Asp-Ala-His-am and Asp-Ala-His-Lys-am, the two short peptides with the metal-binding sequences identical with that of the human serum albumin N-terminus. In addition, kinetic aspects of Cu(II) and Ni(II) binding to albumin could not be reproduced using short peptides [17]. Therefore, it must be stated that for the Xaa-Yaa-His- sequences, the modeling should be limited only to general, qualitative features.

Still, such modeling has some merits, if done cautiously. For example, we have studied Cu(II) and Ni(II) binding to the N-terminal peptides of human protamine 2 (HP2), a small DNA-binding protein in the sperm, having the potential metal binding sequence Arg-Thr-His-. The body of preceding evidence, summarized above, has led us to propose that complexation would be strong and site-specific, the complex structures

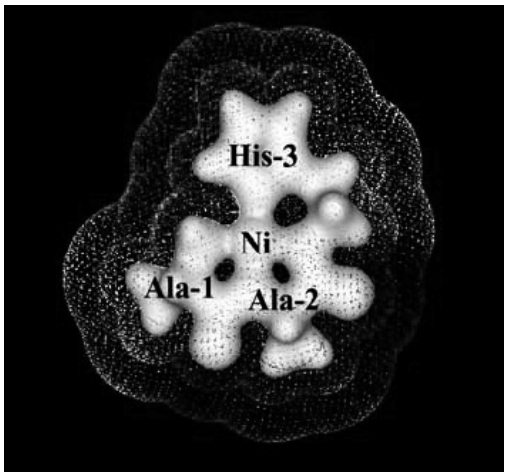

Figure 3.3.2.2. (Plate 3) Distribution of electrostatic potential (positive, red; negative, blue) in the chelate plane of the Xaa-Yaa-His- complex, calculated for the simulated structure of Ala-Ala-His for the sake of simplicity. (Reprinted with permission from Reference [22]. Copyright (2000), American Chemical Society.)

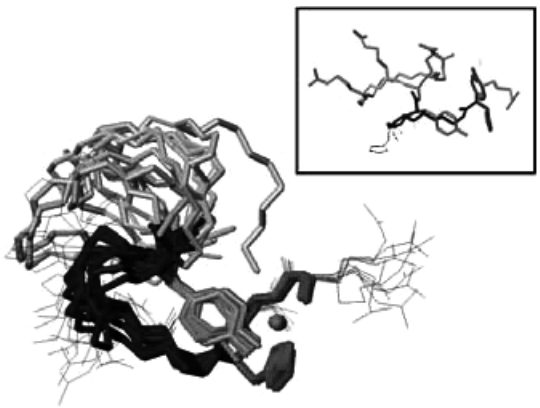

Figure 3.3.2.3. (Plate 4) One of the lowest energy structural families of Ni(II) complex with the pentadecapeptide modeling the N-terminal amino acid sequence of protamine HP2, illustrating the long-range structuring effects of metal ion coordinated by the terminal Xaa-Yaa-His- motif. The inset shows the position of the Arg side chains in a representative conformer of this structural family. (Reprinted with permission from Reference [22]. Copyright (2000), American Chemical Society.)

would be analogous to those known for other Xaa-Yaa-His- systems, and that complexes should be capable of generating reactive oxygen species (ROS) from H_2O_2. We have been able to demonstrate all these features, using a 15-mer peptide to represent the 57-amino acids long protein [19–21]. A rather safe assumption that, qualitatively, the reactivity would be retained in the whole protein led us to propose a novel physiological function for HP2, as a Cu(II) chelator and an ROS suicide inhibitor. A further NMR study of the isostructural Ni(II) complex of the 15-mer peptide provided structural basis for long-range effects, revealing the existence of interaction of the chelate plane with the Tyr^8 residue, fueled by a specific spatial distribution of electronic charge in the chelate plane [22]. These interesting features are presented in Figures 3.3.2.2 and 3.3.2.3. Altogether, our recent studies set clear limitations on applicability of short albumin mimics but do not disqualify them if appropriate caution is exerted in such studies.

3 MODELING IN NICKEL CARCINOGENESIS: LOW-MOLECULAR-MASS TARGETS AND HISTONES

Nickel is an established human carcinogen. The major route of exposure is via inhalation of dusts of various nickel compounds, especially the water-insoluble sulfides and oxides, in an occupational environment [23]. This fact evoked a considerable interest in establishing mechanisms of interactions of nickel compounds *in vivo*, strengthened recently by reports on potential environmental emergence of nickel carcinogens [24]. It has been established that insoluble crystals of nickel compounds of micrometer granulation enter the bronchia and lungs and penetrate into cells through phagocytosis. Subsequently, the crystals are transported actively toward the outer membrane of the cell nucleus [25]. Further steps of the carcinogenic process are a matter of debate. It seems clear that dissolution of the crystals is a prerequisite of any further activity, and thus soluble Ni(II) entities are actually ultimate carcinogens. The resulting intracellular Ni(II) concentrations are high, perhaps even millimolar. However, Ni^{2+} ions alone do not promote DNA damage [26]. Several concepts have been proposed to account for

further events leading to neoplastic transformation of the exposed cells. The oxidative damage hypothesis deals with nickel-catalyzed generation of ROS as a basis for genotoxicity [27], the repair hypothesis concentrates on nickel inhibition of DNA repair [28], and a number of epigenetic concepts are centered on indirect actions of nickel, such as impairment of DNA condensation or histone acetylation [29]. Among these concepts, the majority of model studies was performed within the oxidative theory. Inspired by the pioneering studies of the Margerum group [14], the earlier works were aimed at finding biogenic LMM ligands (amino acids and oligopeptides) that might form catalytic Ni(II) complexes, capable of generating DNA-damaging oxygen radicals. Several potential biogenic ligands, most notably histidine and several His-containing peptides, were established as such catalysts [15, 30, 31]. Interesting facts were provided by these studies, including the bell-shaped pH dependencies of catalytic activities, which indicated the presence of species specificity of catalysis [30, 31]. An example is provided in Figure 3.3.2.4. Also, the likelihood of formation of ternary catalytic complexes *in vivo* was speculated upon [31]. The further development of such models was, however, hampered by the absence of direct evidence and lack of essential knowledge on the formation of such complexes *in vivo*.

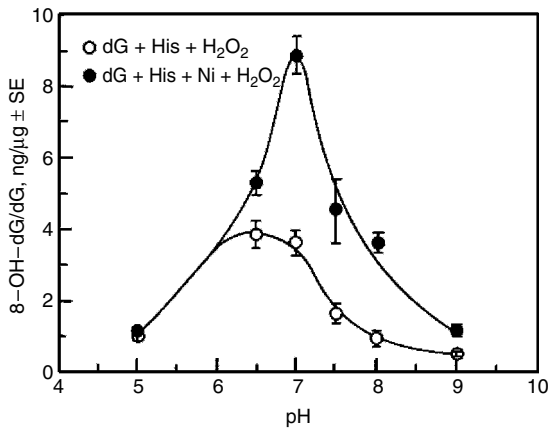

Figure 3.3.2.4. Dependence of 2′-deoxyguanosine (dG) oxidation to 7,8-dihydro-8-oxo−2′-deoxyguanosine (8-OH-dG) by H_2O_2 on pH in the presence of Ni(II) and His at 1 : 2 molar ratio [30].

A further step in modeling, still under the auspices of the oxidative theory, has been inspired by the finding that Ni(II) becomes an oxidative damage-mediating agent in the presence of the histone complex [32]. Histone octamer is by far the most abundant assembly of nuclear proteins, composed of two molecules of each of histone H3, H4, H2A, and H2B, providing molecular scaffold for all DNA in the nuclei of somatic cells [33]. Therefore, on the basis of the fundamental mass action law, histones should be the primary protein targets for interactions with metal ions in the nucleus, if appropriate binding sites are present. The direct, *in vitro* physicochemical studies of such interactions with the whole histone octamer, or nucleosome (histone-DNA complex), are, however, rather difficult to conduct because of limitations caused by poor solubility and stability of the protein assembly and also because of its complexity. To reduce these mostly technical difficulties, in a novel approach we used models provided by short peptides representing potential Ni(II) binding sequences, proposed on the basis of general coordination-chemical information. This approach, in contrast with previous studies, allows for accounting of the thermodynamic aspect of the interactions, by performing parallel potentiometric and spectroscopic studies of the complex formation process in a broad pH range. Such methodology provides the means for structure/activity correlations in LMM complexes. It should also be noted that concentrations of both Ni(II) and histones in the cell nucleus can be expected as millimolar. This fact facilitates interaction modeling.

A tetrapeptide -Cys-Ala-Ile-His- was used as a model for coordination and reactivity of histone H3 [34]. The data obtained showed effective binding at high Ni(II) concentrations, and a very high ability of the complexes to oxidize 2′-deoxyguanosine, which was interpreted as indication of DNA base-damaging potential *in vivo*. The coordination aspect of -Cys-Ala-Ile-His- was tested in a subsequent study, using a core histone tetramer $(H3\text{-}H4)_2$ as a more realistic model [35]. This study revealed the limitations of the tetrapeptide model, which reproduced Ni(II) binding through Cys residues fairly well but

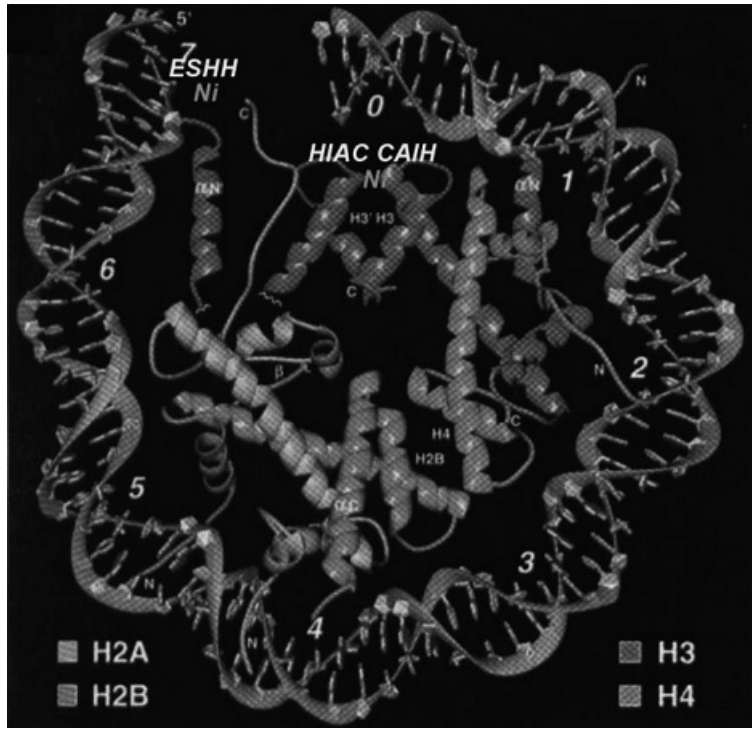

Figure 3.3.2.5. (Plate 5) Structure of the nucleosome core particle with Ni(II) binding sites marked as the respective amino acid motifs in histones H3 (CAIH, -Cys^{110}-Ala-Ile-His-) and H2A (ESHH, -Glu^{121}-Ser-His-His-). (Reprinted with permission from Nature [33]. Copyright (1997), Macmillan Publishers Ltd.)

underestimated the strength of the binding by ca 2 orders of magnitude. Another potential Ni(II)-binding site in the histone octamer could be located in histone H2A's unstructured C-terminal 'tail', represented in part by the peptide -Thr-Glu-Ser-His-His-Lys-. Ni(II) complex stability and reactivity were also studied for this simple model [36]. A novel reaction of Ni(II)-assisted (neither redox nor catalytic) peptide bond hydrolysis was found for this hexapeptide and for larger peptide models, including the whole 34 amino acid long C-terminal 'tail' of histone H2A, as well as for the entire molecule of this histone [37]. Most interestingly, the octapeptidic product of the Ni(II)-assisted hydrolysis, Ser-His-His-Lys-Ala-Lys-Gly-Lys, forms with Ni(II) a square-planar complex belonging to the Xaa-Yaa-His-Ni(II) family described in the preceding section. As expected, this complex mediates DNA oxidation [37]. The expected locations of Ni(II) binding sites in the nucleosome, derived from the oligopeptide modeling, are presented in Figure 3.3.2.5.

The model of interactions obtained from the above 'reductionist' studies, performed largely on small peptides, needs to be validated by *in vivo* experiments, through either interpretation of previous or prediction of novel experimental results. The thermodynamic data obtained from peptide studies enabled us to tentatively predict speciation of Ni(II) in the cell nucleus in a simulated competition with likely LMM ligands. We have attempted such calculations several times, improving our models upon obtaining new input data [35, 38, 39]. Selected results of these calculations are presented in Figure 3.3.2.6. Initially, reduced glutathione (GSH) emerged as the major Ni(II) chelator under physiological conditions, with significant histone binding only at GSH concentrations of 1 mM or less [35, 38]. In an apparent convergence, several previous independent studies have

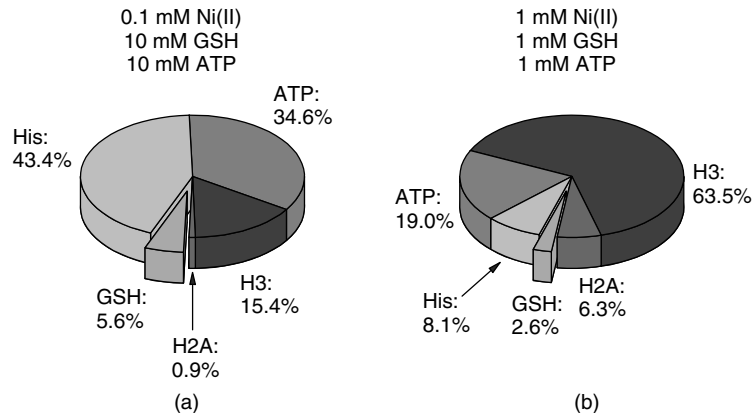

Figure 3.3.2.6. Calculated distribution of Ni(II) among histones and major low-molecular-mass cellular competitors at different concentrations, data taken from Reference [39].

demonstrated that exposure of cells to nickel carcinogens results in GSH depletion and that neoplastic transformation of cells occurs only at low, millimolar GSH levels [40]. Our new results, however, negate this simple picture, because in the presence of physiological concentrations of ATP, GSH can no longer be considered as the major Ni(II) chelator *in vivo*, although GSH-Ni(II) reactivity may contribute to Ni(II) toxicity [39].

Regarding specific reactivity of Ni(II) complexes, we have been recently able to demonstrate the hydrolysis of histone H2A in cultured cells [41]. In conclusion, simple-peptide models can provide valuable clues and guidelines for further *in vivo* research of adventitious metal–protein interactions in the mechanisms of metal-induced carcinogenesis.

4 CHROMIUM: LOW-MOLECULAR-MASS TARGETS

The uniqueness of chromium is due to a strict distinction between the carcinogenic Cr(VI) [23] and the physiologically essential, although still enigmatic Cr(III) [42]. The model studies performed until 1997 were extensively reviewed [43, 44] and are summarized below. The Cr(VI) oxyanion is a molecular mimic of sulfate and phosphate anions, sharing similar tetrahedral shape, size, and a negative two-electron charge at physiological pH. It enters cells through general anion-exchange channels and also by phagocytosis of poorly water-soluble particles, similar to that of Ni(II), that may result in millimolar intracellular concentrations of the metal species. However, not being capable of interacting with DNA or proteins, the chromate by itself would be an innocent anion if it were not redox active. Early studies demonstrated the involvement of chromate reduction as the process underlying chromium carcinogenesis. It should be noted here that involvement of the P450 enzymatic system in chromate reduction was excluded experimentally. The subsequent modeling efforts have been aimed at finding redox partners for chromate and outlining reaction pathways leading to DNA damage patterns, like those observed in relevant bioassays involving the induction by chromium of animal tumors. Such patterns included DNA strand breaks, cross-links, and other effects of oxidative assault on DNA. The recognition of the involvement of ROS in DNA damage induced by chromate directed the *in vitro* studies toward the detection of ROS generation.

The reactions between chromate and reductants are spontaneous and do not require other cellular components to occur, thus simplifying the modeling task to studies of respective chemical reactions. Also, the selection of primary targets becomes simple, while, again by means of the mass action law, the reactions with those reductants present at highest concentrations should be preferred *in vivo*. Two

such reductants are ascorbate and GSH. The relevance of chemical modeling was further strengthened by the presence of all major participants at millimolar concentrations *in vivo* (similarly to Ni(II)-histone studies), which are preferred by physicochemical experimental techniques.

GSH was originally thought to be the prime target for chromate, due to its higher concentration, and the fast 'trapping' of chromate by formation of a thioester, followed by slower redox processes. However, further *in vitro* works demonstrated that ascorbate reacted with chromate much faster than GSH, and that it might complement, or even dominate, chromate reduction under certain conditions. This picture was subsequently confirmed *in vivo* for various tissues. The first product of one-electron Cr(VI) reduction with GSH is a Cr(V) species, which can be easily studied using electron paramagnetic resonance (EPR). However, Cr(V) complexes are efficiently reduced by excess GSH to Cr(IV) and further to Cr(III). In the presence of high GSH concentrations and dioxygen (such conditions are justified physiologically), H_2O_2 is also formed as a by-product of chromium interactions with GSH. The emergence of H_2O_2 results in parallel two-electron redox processes. Formation of ROS and other radical species accompanies these processes, as demonstrated in many studies. Ascorbate is generally a two-electron reductant, but with Cr(VI) it may undergo one-electron reductions as well, yielding Cr(V)-stabilized radical species. Initially, the formation of hydroxyl radicals and related types of DNA damage were questionable, but later studies seem to have confirmed their formation as well [43–46]. The proposed scheme of chromium-mediated formation of hydroxyl radicals is presented in Figure 3.3.2.7.

The involvement of the Cr(III)/Cr(V) and even Cr(II)/Cr(III) redox systems in the processes of biological reduction of Cr(VI) has also been postulated [47–49]. These and similar modeling studies help unveil the complex mechanistic pathways of chromium metabolism and pathogenicity that would otherwise be impossible to decipher. It seems that further progress in chromate carcinogenesis studies will depend on the 'consumption'

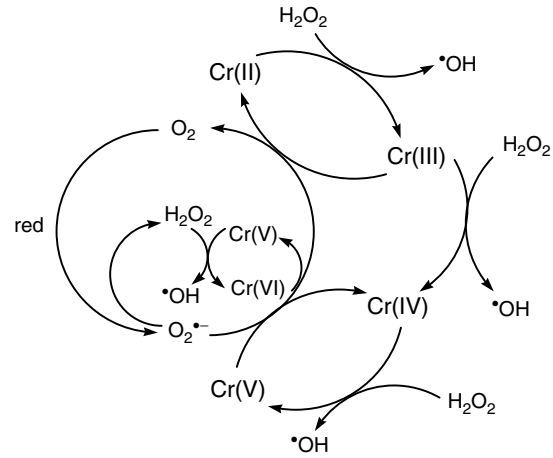

Figure 3.3.2.7. Scheme of chromium redox reactions leading to the formation of oxygen radicals [45].

and validation of the many available models of interactions, offered by *in vitro* studies, in cell culture and animal experiments. For example, mutagenicity assays using the Drosophila model suggest that Cr(IV) and hydroxyl radicals are the ultimate DNA-damaging species [50].

5 CONCLUSION

Let us conclude the above brief account of three 'modeling stories' by taking up the line from the preceding section that 'all models are wrong, but some are useful'. Our examples have been aimed at demonstrating that some models are, indeed, more useful than the others. Still, if the modeling studies are planned and performed in a way allowing for their validation and subsequent modification as work progresses, most models can, in fact, be helpful in directing and/or explaining biological experiments.

6 REFERENCES

1. Carter, D. C. and Ho, J. X., *Adv. Protein Chem.*, **45**, 153 (1994).
2. He, X.-M. and Carter, D. C., *Nature*, **358**, 209 (1992).
3. Sadler, P. J. and Viles, J. H., *Inorg. Chem.*, **35**, 4490 (1996).
4. Bal, W., Christodoulou, J., Sadler, P. J. and Tucker, A., *J. Inorg. Biochem.*, **70**, 33 (1998).

5. Predki, P. F., Harford, C., Brar, P. and Sarkar, B., *Biochem. J.*, **287**, 211 (1992).
6. Patel, S. U., Sadler, P. J., Tucker, A. and Viles, J. H., *J. Am. Chem. Soc.*, **115**, 9285 (1993).
7. Peters, T. Jr. and Blumenstock, F. A., *J. Biol. Chem.*, **242**, 1574 (1967).
8. Harford, C. and Sarkar, B., *Biochem. Biophys. Res. Commun.*, **209**, 877 (1995).
9. Bal, W., Djuran, M. I., Margerum, D. W., Gray, E. T., Mazid, M. A., Tom, R. T., Nieboer, E. and Sadler, P. J., *J. Chem. Soc., Chem. Commun.*, 1889 (1994).
10. Bal, W., Chmurny, G. N., Hilton, B. D., Sadler, P. J. and Tucker, A., *J. Am. Chem. Soc.*, **118**, 4727 (1996).
11. Sigel, H. and Martin, R. B., *Coord. Rev.*, **82**, 385 (1982).
12. Kozlowski, H., Bal, W., Dyba, M. and Kowalik-Jankowska, T., *Coord. Chem. Rev.*, **184**, 319 (1999).
13. Hay, R. W., Hassan, M. M. and Quay, C. Y., *J. Inorg. Biochem.*, **52**, 17 (1993).
14. Bossu, F. P., Paniago, E. B., Margerum, D. W., Kirksey, S. T. Jr. and Kurtz, J. L., *Inorg. Chem.*, **17**, 1034 (1978).
15. Cotelle, N., Tremolieres, E., Bernier, J. L., Catteau, J. P. and Henichart, J. P., *J. Inorg. Biochem.*, **46**, 7 (1992).
16. Harford, C., Narindrasorasak, S. and Sarkar, B., *Biochemistry*, **35**, 4271 (1996).
17. Sokolowska, M., Krezel, A., Dyba, M., Szewczuk, Z. and Bal, W., *Eur. J. Biochem.*, **269**, 1323 (2002).
18. Mlynarz, P., Valensin, D., Kociolek, H., Zabrocki, J., Olejnik, J. and Kozlowski, H., *New J. Chem.*, **26**, 264 (2002).
19. Bal, W., Jezowska-Bojczuk, M. and Kasprzak, K. S., *Chem. Res. Toxicol.*, **10**, 906 (1997).
20. Bal, W., Lukszo, J. and Kasprzak, K. S., *Chem. Res. Toxicol.*, **10**, 915 (1997).
21. Liang, R., Senturker, S., Shi, X., Bal, W., Dizdaroglu, M. and Kasprzak, K. S., *Carcinogenesis*, **20**, 893 (1999).
22. Bal, W., Wójcik, J., Maciejczyk, M., Grochowski, P. and Kasprzak, K. S., *Chem. Res. Toxicol.*, **13**, 823 (2000).
23. IARC Monographs on the Evaluation of Carcinogenic Risk to Humans, Vol. 49, Chromium, Nickel and Welding, IARC, Lyon, 1990.
24. Prahalad, A. K., Inmon, J., Daily, L. A., Madden, M. C., Ghio, A. J. and Gallagher, J. E., *Chem. Res. Toxicol.*, **14**, 879 (2001).
25. Costa, M., Simmons-Hansen, J., Bedrossian, C. W. M., Bonura, J. and Caprioli, R. M., *Cancer Res.*, **41**, 2868 (1981).
26. Lee, J. E., Cicareli, R. B. and Wetterhahn Jennette, K., *Biochemistry*, **21**, 771 (1982).
27. Bal, W. and Kasprzak, K. S., *Toxicol. Lett.*, **127**, 55 (2002).
28. Hartwig, A. and Schwerdtle, T., *Toxicol. Lett.*, **127**, 47 (2002).
29. Cangul, H., Broday, L., Salnikow, K., Sutherland, J., Peng, W., Zhang, Q., Poltaratsky, V., Yee, H., Zoroddu, M. A. and Costa, M., *Toxicol. Lett.*, **127**, 69 (2002).
30. Datta, A. K., Misra, M., North, S. L. and Kasprzak, K. S., *Carcinogenesis*, **13**, 283 (1992).
31. Datta, A. K., Shi, X. and Kasprzak, K. S., *Carcinogenesis*, **14**, 417 (1993).
32. Kasprzak, K. S. and Bare, R. M., *Carcinogenesis*, **10**, 621 (1989).
33. Luger, K., Mader, A. W., Richmond, R. K., Sargent, D. F. and Richmond, T. J., *Nature*, **389**, 251 (1997).
34. Bal, W. and Kasprzak, K. S., in *Cytotoxic, Mutagenic and Carcinogenic Potential of Heavy Metals Related to Human Environment*, NATO ASI Series, Hadjiliadis, N. (Ed.), Kluwer Academic Publishers, Dordrecht/Boston/London, 1997, pp. 107–121.
35. Bal, W., Karantza, V., Moudrianakis, E. N. and Kasprzak, K. S., *Arch. Biochem. Biophys.*, **364**, 161 (1999).
36. Bal, W., Liang, R., Lukszo, J., Lee, S. H., Dizdaroglu, M. and Kasprzak, K. S., *Chem. Res. Toxicol.*, **13**, 616 (2000).
37. Bal, W., Lukszo, J., Bialkowski, K. and Kasprzak, K. S., *Chem. Res. Toxicol.*, **11**, 1014 (1998).
38. Bal, W., Kozlowski, H. and Kasprzak, K. S., *J. Inorg. Biochem.*, **79**, 213 (2000).
39. Krezel, A., Szczepanik, W., Sokolowska, M., Jezowska-Bojczuk, M. and Bal, W., *Chem. Res. Toxicol.*, **16**, 855 (2003).
40. Lynn, S., Yew, F. H., Hwang, J.-W., Tseng, M. J. and Jan, K. Y., *Carcinogenesis*, **15**, 2811 (1994).
41. Karaczyn, A. A., Bal, W., North, S. L., Bare, R. M., Hoang, V. M., Fisher, R. J. and Kasprzak, K. S., *Chem. Res. Toxicol*, **16**, 1555 (2003).
42. Vincent, J. B., *J. Am. Coll. Nutr.*, **17**, 548 (1999).
43. Stearns, D. and Wetterhahn, K. E., The mechanisms of metal carcinogenicity. Chromium(VI)–induced genotoxicity: direct and indirect pathways, in *Cytotoxic, Mutagenic and Carcinogenic Potential of Heavy Metals Related to Human Environment*, NATO ASI Series, Ser 2, 26, Hadjiliadis, N. (Ed.), Kluwer Academic Publishers, Dordrecht/Boston/London, 1997, pp 55–72.
44. Kortenkamp, A., Casadevall, M., Da Cruz Fresco, P. and Shayer, R. O. J., Pathways in the chromium(VI)–mediated formation of DNA lesions: a review, in *Cytotoxic, Mutagenic and Carcinogenic Potential of Heavy Metals Related to Human Environment*, NATO ASI Series, Ser 2, 26, Hadjiliadis, N. (Ed.), Kluwer Academic Publishers, Dordrecht/Boston/London, 1997, pp 15–34.
45. Shi, X., Chiu, A., Chen, C. T., Halliwell, B., Castranova, V. and Vallyathan, V., *J. Toxicol. Environ. Health B.*, **2**, 87 (1999).
46. Wang, S. and Shi, X., *Mol. Cell. Biochem.*, **222**, 3 (2001).
47. Dillon, C. T., Lay, P. A., Bonin, A. M., Cholewa, M. and Legge, G. J. F., *Chem. Res. Toxicol.*, **13**, 742 (2000).
48. Speetjens, J. K., Collins, R. A., Vincent, J. B. and Woski, S. A., *Chem. Res. Toxicol.*, **12**, 483 (1999).
49. Sugden, K. D. and Stearns, D. M., *J. Environ. Pathol. Toxicol. Oncol.*, **19**, 215 (2000).
50. Katz, A. J., Chiu, A., Beaubier, J. and Shi, X., *Mol. Cell. Biochem.*, **222**, 61 (2001).

CHAPTER 4
Speciation and the Emerging Legislation

Nicole Proust
THALES Research and Technology France, Orsay, France

Wolfgang Buscher
University of Münster, Münster, Germany

Michael Sperling
University of Münster, Münster, Germany

1 INTRODUCTION

Undoubtedly, the most important practical application of elemental speciation is to be found in the area of toxicology. In turn, more refined toxicological knowledge leads to better, more specific legislation of hazardous substances.

Legislators are becoming increasingly aware of the importance of elemental speciation, but chances for widespread implementation remain remote, mainly because of a lack of reliable, detailed toxicological data. The prerequisite for setting maximum limits for each elemental species is a review of the relevant chemistry, toxicology (from toxicodynamics to toxicokinetics), providing information about concentration level-toxic effect relations in the appropriate media (biological fluids, air, soil, water, food, etc.). In food- and environment-related matters, the European Commission (EC) sponsors reviews called '*Position Papers*'. These are documents that summarize all the available information on the chemistry, toxicology, human intake or exposure, risk assessment for a given element. Papers on cadmium (CX/FAC 98/22 The Hague), on arsenic (CX/FAC 98/23 The Hague) and on tin (CX/FAC 98/24/The Hague) in food have been prepared and proposed in 1998 at the Codex Alimentarius. A position

Handbook of Elemental Speciation II: Species in the Environment, Food, Medicine & Occupational Health
Edited by R. Cornelis, H. Crews, J. Caruso and K. G. Heumann
 ISBN: 0-470-85598-3 (HB)

paper on 'Ambient air pollution by As, Cd and Ni compounds' has been published by the EC in 2001, and another one on 'Ambient air pollution by mercury (Hg)' is available since 2002 from the EC.

Some trace elements classified as harmful or even toxic have been found to be essential to life when they form part of biomolecules that play an important role in different biochemical processes. It is the chemical form of the element, together with the amount the organism has to cope with, that dictates whether essential elements such as Co, Cr, Cu, Mn, Ni, Se, Zn constitute a hazard or a benefit. Their assessment constitutes a big challenge for elemental speciation analysts, as the road toward possible solutions is full of obstacles. First, there is the often extremely low concentration at which they are present (often $<10^{-12}$ g L^{-1}). To measure such concentrations is already demanding when related to total element concentrations, even in expert laboratories. There is, however, a major second difficulty, linked to the stability of the species. Especially, the noncovalently bound elements are easily disrupted during sampling and sample preparation. In order to maintain the original species intact, all parameters (pH, redox conditions, temperature, inert atmosphere, etc.) should be kept unchanged or controlled within appropriate limits. The analyses should be fast, with minimal contact with reactive surfaces. Besides the danger of disruption, there is the opposite effect of capturing trace element impurities by the ligands of molecules acting as scavengers. All reagents, column fillings, the inner walls of the apparatus and many other sources may act as donors. These difficulties could be avoided by measuring the species *in situ*, for example, in the cell or the particle itself. This technique has, so far, only seldom been possible.

2 ELEMENTAL SPECIATION, TOXICOLOGY AND LEGISLATION

Without extensive and reliable toxicological data, legislators lack the tools to set maximum limits. A further prerequisite is the availability of validated, sufficiently simple and reliable analytical methods.

2.1 Environmental issues

When discussing the toxicity of chemical substances, it is important to remember that behind a given toxicity value for any toxicant (e.g. a chemical species) there is always a comprehensive toxicological investigation. Toxicologists try to predict a certain concentration of a toxicant that has a well-defined impact on well-defined organisms in well-defined ecosystems in a given environment. The main difficulty of this discipline becomes obvious: *How can comparability of toxicological data be achieved?*

Minor differences between test populations or parameters may cause considerable deviations in the results. This makes toxicological investigations difficult and time consuming.

It is estimated that only about 10% of all chemicals on the market have undergone full and stringent testing, even though many of these occur in everyday household products. The procedure to put chemicals on the market is regulated in many countries. At the European level, the procedure for '***R****EGISTRATION,* ***E****VALUATION AND* ***A****UTHORIZATION OF* ***CH****EMICALS*' (REACH) has recently been established and has to be implemented in the Member States.

REACH will require companies manufacturing or importing chemicals to assess the risks arising from their use and to take the necessary measures to manage any risk they identify. REACH will also reverse the burden of proof from public authorities to industry for ensuring the safety of chemicals on the market. An underlying aim of REACH is to phase out 'substances of very high concern', that is, those that may cause cancer or damage genetic material and to replace them with safer alternatives.

Industry has to follow the regulations but is not obliged to do more. Economical reasons still make the chemical industry prefer quick toxicological investigations rather than comprehensive studies about the short-, medium-, and long-term impact of newly developed compounds. That such a strategy cannot always prevent the massive marketing of hazardous substances is a lesson that can be learned from history. Organolead gasoline additives (first introduced in the 1930s) and

organotin compounds (e.g. tributyltin (TBT), first introduced in the 1950s) are historical examples for which the long-term effects were insufficiently investigated at the time of their introduction. Long-term studies of the negative effects of organolead additives have caused their gradual worldwide withdrawal from the market. More recent is the case of the organotin compounds, toxic for most organisms that cause damage to boats, textiles and many other materials. Unfortunately, these compounds also act as endocrine disruptors. In the case of TBT, dramatic effects on fertility are threatening entire populations of marine mollusks. It is to be anticipated that the concentration of these chemicals in seafood will continue to increase. It has been claimed that organotin compounds in food pose only negligible risk to humans, but there is absolutely no convincing scientific basis for such a statement.

Such long-term hazards are usually recognized only decades after the introduction and worldwide distribution of a new product. Therefore, it is absolutely necessary to use stringent risk management each time a new product is launched. Risk management is environmental issues has been extensively dealt by Duffus in Volume 1 of this Handbook [1]. Accordingly, three key steps lead to comprehensive risk assessment: hazard identification, dose-response assessment and exposure assessment, followed by evaluation and risk characterization. The data will be collected first in the form of dose-response assessments with microorganisms and/or biological species and of LC_{50} values. Further toxicological tests are decisive but are scientifically extremely difficult investigations with respect to comparability, repeatability and trueness. The principles by which toxicologists try to predict those concentrations of the chemical species that are expected to have no effect on ecosystems are well-documented [1]. The risk is calculated on the basis of the concepts PNEC (Predicted No Effect Concentration) and PEC (Predicted Environmental Concentration). Exposure assessment from scientific experiments, rather than from unwanted human exposure, needs, however, careful evaluation. All risks that may be discovered will have to be characterized in detail. These investigations will result in a more or less reliable risk assessment of potentially toxic chemicals. The aim of such an environmental risk assessment is the estimation of an acceptable environmental concentration at and below which there will be no harm to any exposed ecosystem or individual.

One key word is most important in the discussion of toxicity values: 'bioavailability'. Bioavailability strongly depends on many parameters of the environment under investigation. In watery media, for example, a small change of pH often causes a dramatic change in many chemical species and thus in their bioavailability. Aluminum is a good example. At pH 7, it is not bioavailable and at pH 5.5 it is a poison for fish. Furthermore, chemical transformations, redox potential, water hardness, total organic carbon (TOC) and the presence of complexing agents may heavily influence the effective concentrations of an investigated species. Only what can be taken up by organisms can have a toxic impact. In this context, it must be reemphasized that most established monitoring and control systems are based on the wrong assumption that elements other than carbon give the generic properties to their derivatives. They rely on total element content determinations instead of on elemental speciation.

The US Environmental Protection Agency (US-EPA) meanwhile applies the promising approach of the water quality criteria (WQC), which is comparable with the PNEC. It takes many aspects into account and is intended to protect 95% of the genera. However, this approach also has weak spots for which US-EPA applies certain correction factors. The water effect ratio procedure, for example, ($WER = LC_{50\,site}/LC_{50\,lab}$), is used to adjust the WQC to site-specific conditions in which a high organic carbon content may reduce the effective concentration of toxic species, for example, by complexing free ions and thus reducing their concentration.

To take such effects into account, the biotic ligand model (BLM) has been developed in which the real uptake of elemental species by organisms becomes the key to the use of toxicological test data. It is a computerized approach, which takes into account all available information for a given chemical species and a given environment and calculates the effective equilibrium concentrations. It is currently the most

suitable method for the reliable prediction of WQC and LC_{50} values for sweet water. Initial steps have already been taken for its application also to marine media. The BLM approach is currently under review by the US-EPA Science Advisory Board and considered for use in USA, Europe, South America and other areas worldwide.

2.2 Food issues

Food is of course the most important source for the uptake of elemental species by human beings. Accordingly, the legislation for food is extremely strict, and maximum limits for substances that are proven to be hazardous are extremely low.

As outlined by Berg in Volume 1 of this Handbook, in principle two different sources play a role when discussing elemental species in food. On the one hand, there are unwanted contaminants and toxins, on the other hand there are the additives claiming to improve the food quality [2].

At the international level, the United Nations agreed to create a special commission that is responsible for the development of international food legislation: the Codex Alimentarius Commission (CAC) under the FAO/WHO Food Standards Programme. Since 1962, the CAC has developed two types of specific standards: (a) for individual foods (vertical standards) and (b) for groups of foods (commodity standards). During the last decade, a trend has developed toward general (or horizontal) standards dedicated to consumer protection. The Codex Committee for Food Additives and Contaminants (CCFAC) has developed two main fields of concern: 'General Standard for Contaminants and Toxins in Food' and 'General Standard for Food Additives'.

The Codex Alimentarius General Standard for Contaminants and Toxins in Food is the legislative framework that is waiting for input to define further maximum levels to be added to the current legislative norms. A number of elements are already included (e.g. lead in orange juice), and even methylmercury occurs with explicit values for the maximum limit (Codex guideline level 1991: 0.5 $mg\,kg^{-1}$ in all fish except predatory ones for which it is 1.0 $mg\,kg^{-1}$). Unfortunately, for many elemental species there remains the need for more substantial and precise scientific data. Another hurdle is the translation of international legislation into national legislation.

At the international level, there also exists a Joint Expert Committee on Food Additives (JECFA) of the Food and Agriculture Organization/World Health Organization (FAO/WHO) to provide advice to the CAC. In July 2003, a JECFA recommendation on methylmercury in fish was issued: a Provisional Tolerable Weekly Intake (PTWI) of 1.6 μg methylmercury per kg of body weight per week has been recommended in order to sufficiently protect the developing fetus [3]. The fetus is exposed to methylmercury through contaminated food eaten by the pregnant mother. This new recommendation changes the prior recommendation for a dietary limit of 3.3 μg per kg body weight per week.

At the European level, the Commission Regulation EC 466/2001 is setting maximum levels for certain contaminants in food (lead, cadmium, mercury, etc.). There is an introduction on the methylmercury toxicity in this document, which is a first step toward speciation even though the Hg level for fishery products is still related to total mercury. Hg limits are set at 0.5 and 1 $mg\,kg^{-1}$ wet weight, the latter value being for predatory or fat fish listed in the document.

Information on EU regulations (decisions or directives) can be found on the website EUROPA – Gateway to the European Union [4].

In 2002, the Commission Regulation EC 221/2002 amended the Section 3.3.1 (metals: Pb, Cd, Hg) of annex I of the Regulation EC 466/2001). For mercury in fishery products, the maximum concentrations are the same: total Hg of 0.5 $mg\,kg^{-1}$ wet weight except for some species for which 1 $mg\,kg^{-1}$ wet weight is accepted (here there is only a different fish list for 1 $mg\,kg^{-1}$). This legislation does not take speciation into account. Methylmercury has been estimated to represent 84% of the total mercury, however, this value can fluctuate according to the fishing zone (ASFA-2002-SA-0014) and depends heavily on the fish species, with carnivore fish having the highest methylmercury content.

For food additives, the total trace element content is also the guiding principle in the EC directives. Unfortunately, bioavailability and biological efficacy are parameters of minor importance for the list of substances permitted as sources for the essential elements to be added to food. Accordingly, the EC directive imposes no need to look at the chemical species in food additives, which allows the marketing of thousands of dietary products that contain '*highly valuable trace elements*', unfortunately without or with negligible physiological efficacy. The example in the previous chapter that shows a different degree of toxicity of Al species in water depending on slight changes in pH is indicative for the great importance of this issue. Berg elaborates along these lines in Volume 1 of this Handbook [2]. He gives examples (As, Se, Fe, Cr) of important chemical properties of elements that highlight the necessity to distinguish between the different chemical species whenever their efficacy in food or their toxicity is discussed.

2.3 Occupational health issues

In all working places where metals (or metalloid) materials are processed or handled, elemental species exposure is a very important issue to ensure occupational health and hygiene. Materials are treated physically and/or chemically, emitting particles or gaseous species into the air to which unprotected operators can be exposed through respiration. In each country, there exists national occupational legislation related to at least 300 chemical species. Most of the Occupational Exposure Levels (OEL) are related to gaseous compounds or vapors.

We have to bear in mind that the different compounds have different chemical, physical and toxicological properties. Toxicokinetics and toxicodynamics will be specific for each compound as it is clearly demonstrated in the case of arsenic. To perform a suitable risk evaluation, speciation is a very important parameter to take into account when someone has to deal with exposure, metabolization and biological monitoring at work. Arsenic speciation in urine has been available since many years, but not all occupational doctors use it.

Size and shape of particles

The size, shape, composition and nature (amorphous or crystalline) of particles in dusts, fumes, filings, and so on, is decisive for their possible health effects because the uptake by humans first depends on physical size and shape. In such a case, inhalation is the major exposure route. The formation of particles takes place in many different processes (welding, rasping, filing, melting, etc.). The potential to inhale such particles depends strongly on size and aerodynamic form. Even in the nonoccupational environment, these characteristics are now intensively discussed, for example, in connection with the emission of soot from diesel cars in urban areas. The car industry succeeded in reducing the soot particle size, claiming 'clean' exhausts. Unfortunately, the remaining particles from modern diesel engines now are much smaller (<3 μm). As a consequence, they can now be inhaled into the deepest part of the lung (alveolar regions). In these circumstances, the toxic impact of the carried PAHs (polycyclic aromatic hydrocarbons) becomes even more important.

Chemical form

Sometimes the particles in the working place carry a mixture of chemically modified elements of the processed material. The chemical form of an element is determinant for the health effects. A number of examples can be found in [5, 6], and additional information on nickel species has been described in Section 2.14 of this volume [7]. The facts for nickel are representative for many other elements.

Nickel exposure can occur in many different industrial activities. The most harmful are the inhalable particles (between 5 and 1 μm diameter). The size, composition and nature (amorphous or crystalline) of the particles has to be determined, and it is common practice to classify them as soluble, insoluble or mixed (the EC Scientific Committee on Occupational Exposure Limits (SCOEL) classification). A sample collected at a workstation can also be a mixture of different compounds. Besides metallic nickel, there can occur different Ni-based compounds such as insoluble NiO, insoluble sulfur compounds (NiS is very toxic if

crystallized and nontoxic if amorphous, nickel subsulfide crystallized and toxic) and water-soluble compounds such as nickel sulfate, nickel chloride, nickel acetate, and so on.

The International Association for Research on Cancer (IARC) has classified insoluble compounds (oxide and sulfur) and one water-soluble compound (Ni sulfate) in list 1 as human carcinogens. The European legislation shows at the moment a different classification. The SCOEL has declared Ni as one of the priority substances, which have been discussed in 2003–2004 and for which a regulation including speciation is under preparation at the EC level.

Epidemiological and toxicological studies still remain the most important methods for studying occupational diseases. This can, however, be only one part of the puzzle. Simplified and harmonized methods for measuring species in workplace air and in body fluids are urgently needed to complement data obtained from traditional methods of occupational health research. Unfortunately, the different species of nickel and many other elements are often not well described, and total element concentrations are measured mostly for occupational health purposes, if at all. The estimation of adverse effects of elements in the working places is complicated and challenging. Besides the collection of information about the workplace exposures and the relation of the respective dose to adverse health effects, it is mandatory to consider two further aspects complicating the issue as follows.

1. All elements are ubiquitous and their species are often distributed in the environment as natural background concentrations or have been introduced as a result of anthropogenic activities. Environmental and workplace origins are clearly to be distinguished.
2. Chemical species can already be transformed during the sampling process, for example, Cr(VI) can be reduced by inappropriate filter materials or co-collected substances.

The solution for such problems lies in the development of test procedures measuring a substance that is unique to an individual's occupational exposure to a given species of the element. This seems to be possible, since exposure to different species will often be followed by different interactions in the body, leading to the production of different metabolites. An example for such an approach is the differentiation of exposure to harmful inorganic arsenic compounds from the intake of arsenic through seafood. While in case of exposure to inorganic species, arsenic will show up in the urine of workers as arsenate, arsenite, monomethylarsonic acid and dimethylarsinic acid, in the second case the main species are the non-metabolised species originating directly from the seafood, such as arsenobetaine, arsenocholine and arsenosugars. It is then sufficient to separate the different As-containing species in urine to identify the cause of exposure. These aspects clearly show that element speciation plays a crucial role in occupational health monitoring.

To improve health protection and consumer safety, substances classified as carcinogenic, mutagenic or toxic to reproduction (CMR), and preparations containing them must not be placed on the market for use by the public. The Directives related to CMR legislation take speciation into account as substances when these have been unequivocally identified. Council Directive 76/769/EEC lays down restrictions on the marketing and use of certain dangerous substances and preparations. Annex I to Directive 76/769/EEC contains a list of substances classified as carcinogenic, mutagenic or toxic to reproduction of category 1 or 2.

Commission Directive 2001/59/EC, which adapted to technical progress for the 28th time the Council Directive 67/548/EEC, lists:

- two substances newly classified as carcinogenic category 1;
- 19 substances newly classified as carcinogenic category 2;
- five substances newly classified as mutagenic category 2;
- one substance newly classified as toxic to reproduction category 1 and,
- 16 substances newly classified as toxic to reproduction category 2.

Those substances are added to the list in the appendix to Annex I to Directive 76/769/EEC.

The Directive 2003/36/EC is amending for the 26th time the Council Directive 76/769/EEC:

Article 29 on carcinogens and Article 30 on mutagens of the Appendix to Annexe I to Directive 76/769/EEC have been modified according the Annexe of Directive 2003/36/EC.

Speciation related to chromium species and sodium chromate will be now placed in carcinogen category 2 and in mutagen category 2.

From the data given in this chapter, it can be seen that speciation is now being introduced into legislation especially for the chromium species, mainly in the fields of Industrial Hygiene and Environment for Waste. This is due to the high toxicity of Cr(VI) species.

3 CURRENT LEGAL SITUATION

In several respects, legislators are waiting for input. Existing and new legislation containing maximum concentration levels of harmful substances has to be improved through new knowledge and the availability of suitable analytical techniques.

International legislation concerning food safety, environment and occupational health is mostly based on total element concentrations, frequently expressed as maximum limits or guideline levels. Only a few regulations refer to molecular species. The main reason is the lack of relevant speciation data (toxicology and available analytical procedure). Most often, only specific contaminants 'and their compounds' are mentioned without distinction and clear definitions, leaving a lot of room for interpretation.

The field of environment can be illustrated by examples from the water and the waste areas. The EU Water Framework Directive (WFD) (2000/60/EC), finally adopted on 23 October 2000, is a case in point. It sets ambitious objectives that should ensure that all water meet 'good status' by the year 2015. It also requires cross-border cooperation, which makes it a promising initiative. To achieve the objectives, pollution reduction and control have to be ensured. Article 16 of the WFD 2000/60/EC sets out a 'Strategy against pollution of water'. The first step of the strategy is the establishment of a list of priority substances, which shall become Annex X of the Directive. The list was adopted by a Decision 2455/2001/EC of the European Parliament and of the Council of 20 November 2001, establishing the list of priority substances in the field of water policy and amending Directive 2000/60/EC [Official Journal L331 of 15.12.2001]. This list with 33 substances shall become the Annexe X of WFD (2000/60/EC). Within this list, 11 substances have been identified as Priority Hazardous substances. Substances of interest are specified as follows: Cd and its compounds, Hg and its compounds, Pb and its compounds, Ni and its compounds and TBT (organotin). Only in case of TBT, speciation is requested.

Further WFD policy development has to be done and daughter directives are or will be proposed by the Commission (e.g. groundwater, priority substances, etc.). In the directive on mineral waters and spring waters (2003/40/EC), elements are mentioned as follows: antimony, arsenic, barium, boron, cadmium, chromium, copper, lead, manganese, mercury, nickel, selenium. Speciation is not mentioned. There is only a specification for arsenic, as it has to be measured as total arsenic. In the proposed directive on protection of ground water against pollution COM (2003) 550 final 2003/0210 (COD), speciation is not mentioned, arsenic, cadmium, lead and mercury have to be measured. In the waste field, some regulations have been adopted and others are waiting for final decision, they are related to 'heavy' metal and toxic substances. Between brackets, the term 'heavy metals' is meaningless and misleading, it has never been defined and should not be used [8]. Speciation is taken into account for chromium as Cr(VI) is clearly indicated for vehicle industry and for electronic and electric equipment.

The annexe II of the EC Directive 2000/53/EC is amended by the Decision 2002/525/EC. To minimize the impact of the end of life vehicles on environment, the use of Cr(VI) is forbidden except for corrosion preventing coatings of key components (a maximum of 2 g of Cr(VI) per vehicle).

The Council and Parliament Directive 2002/95/EC (RoHS (Restriction of the use of certain hazardous substances) directive) on the restriction of use of certain hazardous substances in electrical and electronic equipment takes speciation into account for chromium. The new equipment put on the market from 1 July 2006 has to be

free of Cr(VI). Cr(VI) is forbidden except as an anticorrosion of the carbon steel cooling system in absorption refrigerators (RoSH Annex).

The WEEE (Waste from electrical and electronic equipment) directive (2002/96/EC) related to electric and electronic equipment waste takes also Cr(VI) into account and speciation as a consequence.

In the Industrial hygiene field, the SCOEL is the expert group that has prepared recommendations for approximately 110 chemicals. There are about 60 OELs included in various Directives, but it will take time (maybe years) before being transposed and introduced by the Member States.

In summary, very few elemental species are included in EU legislation.

- Barium, soluble compounds as Ba (DIR 91/322)
- Diphosphorus pentoxide (DIR 91/322)
- Diphosphorus pentasulfide (DIR 91/322)
- Hydrogen selenide (DIR 96/94)
- Lithium hydride (DIR 91/322)
- Platinum, metallic (DIR 91/322)
- Silver, soluble compounds as Ag (DIR 91/322)
- Tin, inorganic compounds as Sn (DIR 91/322)
- Lead (DIR 82/605).

In various Member States, some speciation has been partly introduced many years ago for elements such as arsenic (arsine AsH_3, di-arsenic trioxide), phosphorus (phosphine PH_3, white phosphorus, di-phosphorous pentoxide, etc.), silicon (silane, silicon), and so on.

Speciation will probably be incorporated in EU legislation under preparation for chromium, nickel and tin.

Cr(VI) has been also introduced in regulations for the cement and leather industries. The Directive 2003/53/EC amending for the 26th time the Council Directive 76/769/EEC is in part dedicated to cement and Cr(VI) (point 47 to be added to the 76/769/EEC directive). As from 17 January 2005, cements used in processes, which are not totally automated, should not contain more than 2 mg kg^{-1} of Cr(VI).

In food legislation at the international level, methylmercury has been mentioned clearly by the Codex Alimentarius in 1991. At the EU level, the methylmercury problem is not clearly regulated (221/2002/EC), but this topic is under discussion at different levels.

At the international level, there are JECFA recommendations for weekly intake (PTWI) related to methylmercury (in 2003) and inorganic arsenic. The recently created European Food Safety Authority (EFSA) has started its activity in 2003. A priority substance list has been established, including arsenic, cadmium, lead, mercury, organotins.

DISCLAIMER

The authors do not warrant or assume any legal liability or responsibility for the accuracy, completeness, or usefulness of the information and advice written in this chapter.

4 REFERENCES

1. Duffus, J. H., Environmental Risk assessment and the bioavailability of elemental species, risk assessments/regulations, in *Handbook of Elemental Speciation: Techniques and Methodology*, Cornelis, R., Crews, H., Caruso, J. and Heumann, K. (Eds.), John Wiley & Sons, Chichester, 2003, Chapter 9.1, pp. 605–628.
2. Berg, T., Speciation and legislation, in *Handbook of Elemental Speciation: Techniques and Methodology*, Cornelis, R., Crews, H., Caruso, J. and Heumann, K. (Eds.), John Wiley & Sons, Chichester, 2003, Chapter 9.2, pp. 629–634.
3. http://www.who.int/mediacentre/news/notes/2003/np20/en/print.html, 2005.
4. http://www.europa.eu.int/index_en.htm, 2005, (followed by Documents, then EUR-Lex, the portal to European Union Law).
5. Ortner, H., Characterization of individual aerosol particles with special reference to speciation techniques, in *Handbook of Elemental Speciation: Techniques and Methodology*, Cornelis, R., Crews, H., Caruso, J. and Heumann, K. (Eds.), John Wiley & Sons, Chichester, 2003, Chapter 6.1, pp. 505–525.
6. Williams, S. P., Occupational health and speciation using nickel and nickel compounds as an example, in *Trace Element Speciation for Environment, Food and Health*, Ebdon, L., Pitts, L., Cornelis, R., Crews, H., Donard, O. F. X. and Quevauviller, Ph. (Eds.), Royal Society of Chemistry, Cambridge, MA, 2001, Chapter 20, pp. 297–307.
7. Schaumlöffel, D., Speciation of nickel, in *Handbook of Elemental Speciation: Species in the Environment, Food, Medicine and Occupational Health*, Cornelis, R., Crews, H., Caruso, J. and Heumann, K. (Eds.), John Wiley & Sons, Chichester, 2005, Chapter 2.14, pp. 310–326.
8. Duffus, J. H., *Pure Appl. Chem.*, **74**, 793 (2002).

Index

Note: Figures and Tables are indicated by *italic* page numbers.

Handbook of Elemental Speciation II: Species in the Environment, Food, Medicine & Occupational Health
Edited by R. Cornelis, H. Crews, J. Caruso and K. G. Heumann

 ISBN: 0-470-85598-3 (HB)